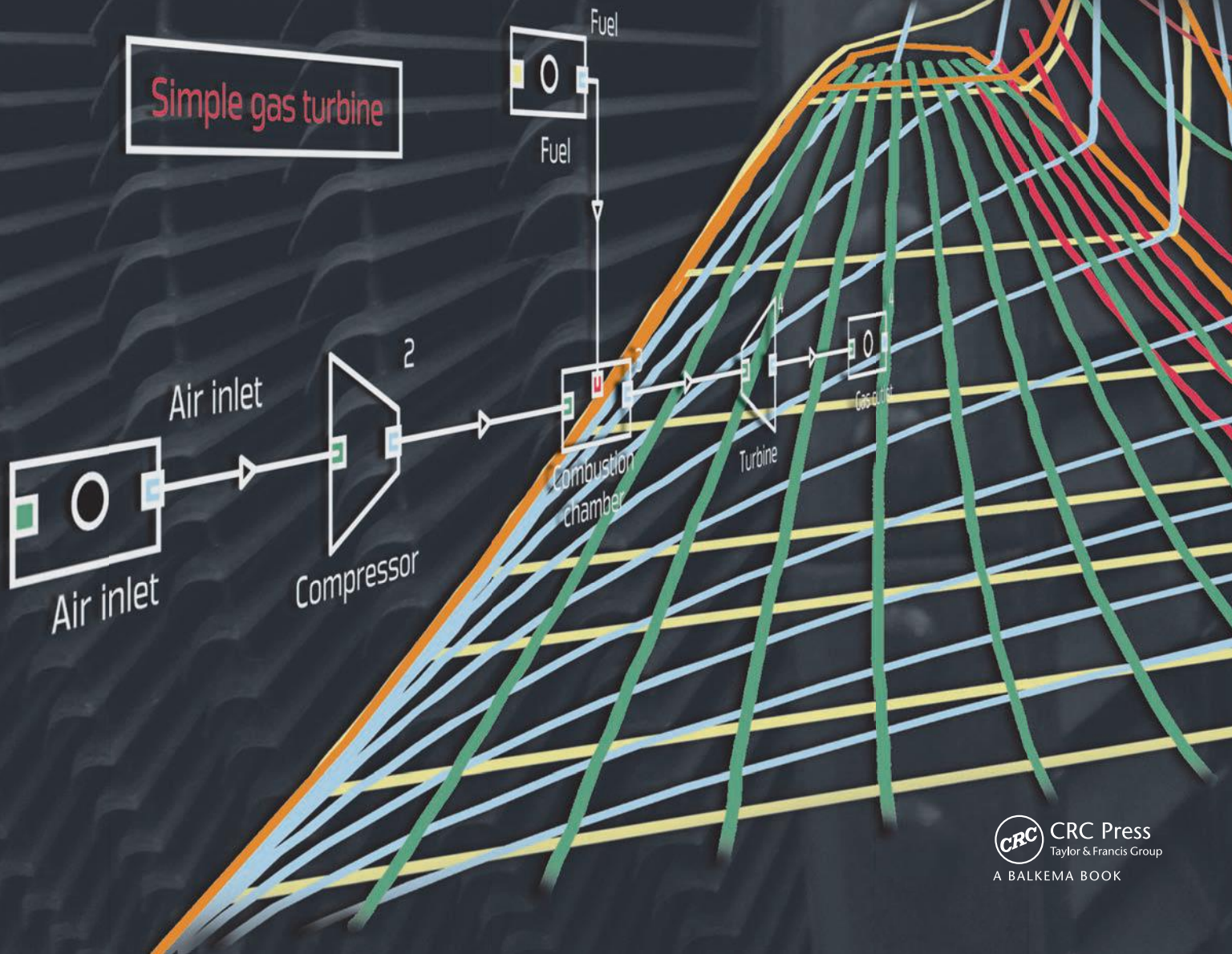


Renaud Gicquel

ENERGY SYSTEMS

A New Approach to Engineering Thermodynamics

With access to the ThermoOptim™ Software



ENERGY SYSTEMS

This page intentionally left blank

ENERGY SYSTEMS

A NEW APPROACH TO ENGINEERING THERMODYNAMICS

RENAUD GICQUEL

École des Mines de Paris, MINES ParisTech, France

THOPT

www.thermoptim.org



CRC Press

Taylor & Francis Group

Boca Raton London New York Leiden

CRC Press is an imprint of the
Taylor & Francis Group, an **informa** business

A BALKEMA BOOK

CRC Press
Taylor & Francis Group
6000 Broken Sound Parkway NW, Suite 300
Boca Raton, FL 33487-2742

© 2011 by Taylor & Francis Group, LLC
CRC Press is an imprint of Taylor & Francis Group, an Informa business

No claim to original U.S. Government works
Version Date: 20111214

International Standard Book Number-13: 978-1-4665-1538-3 (eBook - PDF)

This book contains information obtained from authentic and highly regarded sources. Reasonable efforts have been made to publish reliable data and information, but the author and publisher cannot assume responsibility for the validity of all materials or the consequences of their use. The authors and publishers have attempted to trace the copyright holders of all material reproduced in this publication and apologize to copyright holders if permission to publish in this form has not been obtained. If any copyright material has not been acknowledged please write and let us know so we may rectify in any future reprint.

Except as permitted under U.S. Copyright Law, no part of this book may be reprinted, reproduced, transmitted, or utilized in any form by any electronic, mechanical, or other means, now known or hereafter invented, including photocopying, microfilming, and recording, or in any information storage or retrieval system, without written permission from the publishers.

For permission to photocopy or use material electronically from this work, please access www.copyright.com (<http://www.copyright.com/>) or contact the Copyright Clearance Center, Inc. (CCC), 222 Rosewood Drive, Danvers, MA 01923, 978-750-8400. CCC is a not-for-profit organization that provides licenses and registration for a variety of users. For organizations that have been granted a photocopy license by the CCC, a separate system of payment has been arranged.

Trademark Notice: Product or corporate names may be trademarks or registered trademarks, and are used only for identification and explanation without intent to infringe.

Visit the Taylor & Francis Web site at
<http://www.taylorandfrancis.com>

and the CRC Press Web site at
<http://www.crcpress.com>

To my wife and companion,
To our three daughters

This page intentionally left blank

Contents

<i>Searching References in the ThermoOptim Unit</i>	<i>xxiv</i>
<i>Foreword by John W. Mitchell</i>	<i>xxv</i>
<i>Foreword by Alain Lambotte</i>	<i>xxvii</i>
<i>About the Author</i>	<i>xxix</i>
<i>General introduction</i>	<i>xxxi</i>
<i>Structure of the book</i>	<i>xxxii</i>
<i>Objectives of this book</i>	<i>xxxiii</i>
<i>A working tool on many levels</i>	<i>xxxiv</i>
<i>Mind Maps</i>	<i>xxxv</i>
<i>List of Symbols</i>	<i>xli</i>
<i>Conversion Factors</i>	<i>xlix</i>

I First Steps in Engineering Thermodynamics **I**

I A New Educational Paradigm **3**



1.1 Introduction	3
1.2 General remarks on the evolution of training specifications	4
1.3 Specifics of applied thermodynamics teaching	4
1.4 A new educational paradigm	5
1.5 Diapason modules	7
1.6 A three-step progressive approach	9
1.7 Main pedagogic innovations brought by ThermoOptim	10
1.8 Digital resources of the ThermoOptim-UNIT portal	10
1.9 Comparison with other tools with teaching potential	11
1.10 Conclusion	12
References	12




2 First Steps in Thermodynamics: Absolute Beginners **13**

2.1 Architecture of the machines studied	13
2.1.1 Steam power plant	13
2.1.2 Gas turbine	14
2.1.3 Refrigeration machine	15
2.2 Four basic functions	16
2.3 Notions of thermodynamic system and state	17
2.4 Energy exchange between a thermodynamic system and its surroundings	17
2.5 Conservation of energy: first law of thermodynamics	17
2.6 Application to the four basic functions previously identified	18
2.6.1 Compression and expansion with work	18
2.6.2 Expansion without work: valves, filters	19
2.6.3 Heat exchange	19
2.6.4 Combustion chambers, boilers	19
2.7 Reference processes	19
2.7.1 Compression and expansion with work	19
2.7.2 Expansion without work: valves, filters	20
2.7.3 Heat exchange	20
2.7.4 Combustion chambers, boilers	20

2.8	Summary reminders on pure substance properties	20
2.9	Return to the concept of state and choice of state variables to consider	21
2.10	Thermodynamic charts	21
2.10.1	Different types of charts	22
2.10.2	(h, ln(P)) chart	22
2.11	Plot of cycles in the (h, ln(P)) chart	23
2.11.1	Steam power plant	24
2.11.2	Refrigeration machine	26
2.12	Modeling cycles with Thermoptim	29
2.12.1	Steam power plant	30
2.12.2	Gas turbine	31
2.12.3	Refrigeration machine	31
2.13	Conclusion	32
3	First Steps in Thermodynamics: Entropy and the Second Law	35
3.1	Heat in thermodynamic systems	35
3.2	Introduction of entropy	36
3.3	Second law of thermodynamics	37
3.3.1	Limits of the first law of thermodynamics	37
3.3.2	Concept of irreversibility	37
3.3.3	Heat transfer inside an isolated system, conversion of heat into work	37
3.3.4	Statement of the second law	38
3.4	(T, s) Entropy chart	38
3.5	Carnot effectiveness of heat engines	40
3.6	Irreversibilities in industrial processes	41
3.6.1	Heat exchangers	41
3.6.2	Compressors and turbines	41
3.7	Plot of cycles in the entropy chart, qualitative comparison with the carnot cycle	41
3.7.1	Steam power plant	41
3.7.2	Gas turbine	43
3.7.3	Refrigeration machine	44
3.8	Conclusion	45
2	Methodology, Thermodynamics Fundamentals, Thermoptim, Components	47
4	Introduction	49
4.1	A two-level methodology	49
4.1.1	Physical phenomena taking place in a gas turbine	49
4.1.2	Energy technologies: component assemblies	50
4.1.3	Generalities about numerical models	51
4.2	Practical implementation of the double analytical-systems approach	52
4.3	Methodology	54
4.3.1	Systems modeling: the General System	54
4.3.2	Systems-analysis of energy technologies	55
4.3.3	Component modeling	56
4.3.4	Thermoptim primitive types	57
4.3.5	Thermoptim assets	62
	References	62

5	Thermodynamics Fundamentals	63
5.1	Basic concepts, definitions	63
5.1.1	Open and closed systems	64
5.1.2	State of a system, intensive and extensive quantities	65
5.1.3	Phase, pure substances, mixtures	66
5.1.4	Equilibrium, reversible process	66
5.1.5	Temperature	66
5.1.6	Symbols	67
5.2	Energy exchanges in a process	67
5.2.1	Work δW of external forces on a closed system	67
5.2.2	Heat transfer	68
5.3	First law of thermodynamics	69
5.3.1	Definition of internal energy U (closed system)	70
5.3.2	Application to a fluid mass	70
5.3.3	Work provided, shaft work τ	71
5.3.4	Shaft work and enthalpy (open systems)	73
5.3.5	Establishment of enthalpy balance	74
5.3.6	Application to industrial processes	75
5.4	Second law of thermodynamics	76
5.4.1	Definition of entropy	77
5.4.2	Irreversibility	78
5.4.3	Carnot effectiveness of heat engines	79
5.4.4	Fundamental relations for a phase	81
5.4.5	Thermodynamic potentials	82
5.5	Exergy	83
5.5.1	Presentation of exergy for a monotherm open system in steady state	84
5.5.2	Multithermal open steady-state system	85
5.5.3	Application to a two-source reversible machine	86
5.5.4	Special case: heat exchange without work production	86
5.5.5	Exergy efficiency	86
5.6	Representation of substance properties	87
5.6.1	Solid, liquid, gaseous phases	87
5.6.2	Perfect and ideal gases	88
5.6.3	Ideal gas mixtures	93
5.6.4	Liquids and solids	95
5.6.5	Liquid-vapor equilibrium of a pure substance	96
5.6.6	Representations of real fluids	97
5.6.7	Moist mixtures	117
5.6.8	Real fluid mixtures	124
	References	136
	Further reading	136
6	Presentation of ThermoOptim	137
6.1	General	137
6.1.1	Initiation applets	138
6.1.2	Interactive charts	139
6.1.3	ThermoOptim's five working environments	139
6.2	Diagram editor	142
6.2.1	Presentation of the editor	142

6.2.2	Graphical component properties	142
6.2.3	Links between the simulator and the diagrams	144
6.3	Simulation environment	146
6.3.1	Main project screen	146
6.3.2	Main menus	148
6.3.3	Export of the results in the form of text file	149
6.3.4	Point screen	149
6.3.5	Point moist properties calculations	153
6.3.6	Node screen	155
6.4	Extension of Thermoptim by external classes	157
6.4.1	Extension system for Thermoptim by adding external classes	157
6.4.2	Software implementation	158
6.4.3	Viewing available external classes	159
6.4.4	Representation of an external component in the diagram editor	160
6.4.5	Loading an external class	160
6.4.6	Practical realization of an external class	160
6.5	Different versions of Thermoptim	161
7	Basic Components and Processes	163
7.1	Compressions	163
7.1.1	Thermodynamics of compression	164
7.1.2	Reference compression	164
7.1.3	Actual compressions	166
7.1.4	Staged compression	174
7.1.5	Calculation of a compression  in Thermoptim	175
7.2	Displacement compressors	177
7.2.1	Piston compressors	177
7.2.2	Screw compressors	182
7.2.3	Criteria for the choice between displacement compressors	185
7.3	Dynamic compressors	185
7.3.1	General	185
7.3.2	Thermodynamics of permanent flow	186
7.3.3	Similarity and performance of turbomachines	192
7.3.4	Practical calculation of dynamic compressors	197
7.3.5	Pumps and fans	199
7.4	Comparison of the various types of compressors	199
7.4.1	Comparison of dynamic and displacement compressors	199
7.4.2	Comparison between dynamic compressors	200
7.5	Expansion	201
7.5.1	Thermodynamics of expansion	201
7.5.2	Calculation of an expansion  in Thermoptim	203
7.5.3	Turbines	203
7.5.4	Turbine performance maps	204
7.5.5	Degree of reaction of a stage	205
7.6	Combustion	206
7.6.1	Combustion phenomena, basic mechanisms	206
7.6.2	Study of complete combustion	213
7.6.3	Study of incomplete combustion	216

7.6.4	Energy properties of combustion reactions	225
7.6.5	Emissions of gaseous pollutants	234
7.6.6	Calculation of combustion  in Thermoptim	235
7.6.7	Technological aspects	239
7.7	Throttling or flash	241
7.8	Water vapor/gas mixtures processes	242
7.8.1	Moist process screens	242
7.8.2	Moist mixers	243
7.8.3	Heating a moist mixture	245
7.8.4	Cooling of moist mix	245
7.8.5	Humidification of a gas	248
7.8.6	Dehumidification of a mix by desiccation	251
7.8.7	Determination of supply conditions	253
7.8.8	Air conditioning processes in a psychrometric chart	255
7.9	Examples of components represented by external classes	256
7.9.1	Nozzles	256
7.9.2	Diffusers	260
7.9.3	Ejectors	264
	References	268
	Further reading	269
8	Heat Exchangers	271
8.1	Principles of operation of a heat exchanger	271
8.1.1	Heat flux exchanged	273
8.1.2	Heat exchange coefficient U	274
8.1.3	Fin effectiveness	275
8.1.4	Values of convection coefficients h	275
8.2	Phenomenological models for the calculation of heat exchangers	276
8.2.1	Number of transfer units method	276
8.2.2	Relationship between NTU and ϵ	278
8.2.3	Matrix formulation	282
8.2.4	Heat exchanger assemblies	283
8.2.5	Relationship with the LMTD method	287
8.2.6	Heat exchanger pinch	287
8.3	Calculation of heat exchangers in Thermoptim	288
8.3.1	“Exchange”   processes	288
8.3.2	Creation of a heat exchanger in the diagram editor	289
8.3.3	Heat exchanger screen	290
8.3.4	Simple heat exchanger design	290
8.3.5	Generic liquid	292
8.3.6	Off-design calculation of heat exchangers	292
8.3.7	Thermocouplers	294
8.4	Technological aspects	296
8.4.1	Tube exchangers	296
8.4.2	Plate heat exchangers	297
8.4.3	Other types of heat exchangers	298
8.5	Summary	299
	References	299
	Further reading	299

9	Examples of Applications	301
9.1	Steam power plant cycle	301
9.1.1	Principle of the machine and problem data	301
9.1.2	Creation of the diagram	302
9.1.3	Creation of simulator elements	306
9.1.4	Setting points	307
9.1.5	Setting of processes	308
9.1.6	Plotting the cycle on thermodynamic chart	309
9.1.7	Design of condenser	311
9.1.8	Cycle improvements	315
9.1.9	Modification of the model	316
9.2	Single stage compression refrigeration cycle	318
9.2.1	Principle of the machine and problem data	318
9.2.2	Creation of the diagram	319
9.2.3	Creation of simulator elements	323
9.2.4	Setting points	324
9.2.5	Setting of processes	325
9.3	Gas turbine cycle	327
9.3.1	Principle of the machine and problem data	327
9.3.2	Creation of the diagram	327
9.3.3	Creation of simulator elements	330
9.3.4	Setting points	331
9.3.5	Setting of processes	331
9.4	Air conditioning installation	335
9.4.1	Principle of installation and problem data	335
9.4.2	Supply conditions	336
9.4.3	Properties of the mix (outdoor air/recycled air)	337
9.4.4	Air treatment	338
9.4.5	Plot on the psychrometric chart	339
10	General Issues on Cycles, Energy and Exergy Balances	341
10.1	General issues on cycles, notations	341
10.1.1	Motor cycles	342
10.1.2	Refrigeration cycles	342
10.1.3	Carnot cycle	343
10.1.4	Regeneration cycles	343
10.1.5	Theoretical and real cycles	344
10.1.6	Notions of efficiency and effectiveness	344
10.2	Energy and exergy balance	345
10.2.1	Energy balances	345
10.2.2	Exergy balances	346
10.2.3	Practical implementation in a spreadsheet	347
10.2.4	Exergy balances of complex cycles	350
10.3	Productive structures	350
10.3.1	Establishment of a productive structure	350
10.3.2	Relationship between the diagram and the productive structure	351
10.3.3	Implementation in Thermoptim	353
10.3.4	Automation of the creation of the productive structure	355
10.3.5	Examples	357
10.3.6	Conclusion	365
	References	365

3	Main Conventional Cycles	367
11	Introduction: Changing Technologies	369
11.1	Limitation of fossil resources and geopolitical constraints	370
11.2	Local and global environmental impact of energy	373
11.2.1	Increase in global greenhouse effect	373
11.2.2	Reduction of the ozone layer	375
11.2.3	Urban pollution and acid rain	376
11.3	Technology transfer from other sectors	379
11.4	Technological innovation key to energy future	380
	References	381
	Further reading	381
12	Internal Combustion Turbomotors	383
12.1	Gas turbines	383
12.1.1	Operating principles	383
12.1.2	Examples of gas turbines	385
12.1.3	Major technological constraints	386
12.1.4	Basic cycles	390
12.1.5	Cycle improvements	398
12.1.6	Mechanical configurations	405
12.1.7	Emissions of pollutants	411
12.1.8	Outlook for gas turbines	411
12.2	Aircraft engines	413
12.2.1	Turbojet and turboprop engines	413
12.2.2	Reaction engines without rotating machine	431
	References	436
	Further reading	437
13	Reciprocating Internal Combustion Engines	439
13.1	General operation mode	440
13.1.1	Four- and two-stroke cycles	443
13.1.2	Methods of cooling	445
13.2	Analysis of theoretical cycles of reciprocating engines	446
13.2.1	Beau de Rochas ideal cycle	446
13.2.2	Diesel cycle	448
13.2.3	Mixed cycle	449
13.2.4	Theoretical associated cycles	451
13.3	Characteristic curves of piston engines	452
13.3.1	Effective performance, MEP and power factor	453
13.3.2	Influence of the rotation speed	453
13.3.3	Indicated performance, IMEP	455
13.3.4	Effective performance, MEP	457
13.3.5	Specific consumption of an engine	458
13.4	Gasoline engine	461
13.4.1	Limits of knocking and octane number	461
13.4.2	Strengthening of turbulence	462
13.4.3	Formation of fuel mix, fuel injection electronic systems	463
13.4.4	Real cycles of gasoline engines	465
13.5	Diesel engines	470
13.5.1	Compression ignition conditions	470

13.5.2	Ignition and combustion delays	470
13.5.3	Air utilization factor	472
13.5.4	Thermal and mechanical fatigue	473
13.5.5	Cooling of walls	474
13.5.6	Fuels burnt in diesel engines	474
13.5.7	Real cycles of diesel engines	474
13.6	Design of reciprocating engines	476
13.7	Supercharging	478
13.7.1	General	478
13.7.2	Basic principles	478
13.7.3	Conditions of autonomy of a turbocharger	480
13.7.4	Adaptation of the turbocharger	480
13.7.5	Conclusions on supercharging	482
13.8	Engine and pollutant emission control	482
13.8.1	Emissions of pollutants: Mechanisms involved	482
13.8.2	Combustion optimization	483
13.8.3	Catalytic purification converters	486
13.8.4	Case of diesel engines	489
13.9	Technological prospects	491
13.9.1	Traction engines	491
13.9.2	Large gas and diesel engines	495
	References	496
	Further reading	496
14	Stirling Engines	499
14.1	Principle of operation	500
14.2	Piston drive	502
14.3	Thermodynamic analysis of Stirling engines	503
14.3.1	Theoretical cycle	503
14.3.2	Ideal Stirling cycle	504
14.3.3	Paraisothermal Stirling cycle	506
14.4	Influence of the pressure	508
14.5	Choice of the working fluid	508
14.6	Heat exchangers	509
14.6.1	Cooler	509
14.6.2	Regenerator	509
14.6.3	Boiler	509
14.7	Characteristics of a Stirling engine	510
14.8	Simplified Stirling engine Thermoptim model	512
	References	513
	Further reading	513
15	Steam Facilities (General)	515
15.1	Introduction	515
15.2	Steam enthalpy and exergy	515
15.3	General configuration of steam facilities	517
15.4	Water deaeration	518
15.4.1	Chemical deaeration	518
15.4.2	Thermal deaeration	519
15.5	Blowdown	519

15.6	Boiler and steam generators	520
15.6.1	Boilers	520
15.6.2	Steam generators	522
15.6.3	Boiler operation	523
15.6.4	Optimization of pressure level	524
15.7	Steam turbines	525
15.7.1	Different types of steam turbines	525
15.7.2	Behavior in off-design mode	527
15.7.3	Degradation of expansion efficiency function of steam quality	528
15.7.4	Temperature control by desuperheating	529
15.8	Condensers, cooling towers	529
15.8.1	Principle of operation of cooling towers	530
15.8.2	Phenomenological model	530
15.8.3	Behaviour models	533
15.8.4	Modeling a direct contact cooling tower in Thermoptim	539
	References	539
	Further reading	540
16	Classical Steam Power Cycles	541
16.1	Conventional flame power cycles	541
16.1.1	Basic Hirn or Rankine cycle with superheating	541
16.1.2	Energy and exergy balance	545
16.1.3	Thermodynamic limits of simple Hirn cycle	546
16.1.4	Cycle with reheat	547
16.1.5	Cycle with extraction	548
16.1.6	Supercritical cycles	550
16.1.7	Binary cycles	551
16.2	Technology of flame plants	553
16.2.1	General technological constraints	554
16.2.2	Main coal power plants	555
16.2.3	Emissions of pollutants	557
16.3	Nuclear power plant cycles	557
16.3.1	Primary circuit	558
16.3.2	Steam generator	559
16.3.3	Secondary circuit	561
16.3.4	Industrial PWR evolution	564
	Reference	564
	Further reading	564
17	Combined Cycle Power Plants	567
17.1	Combined cycle without afterburner	568
17.1.1	Overall performance	568
17.1.2	Reduced efficiency and power	569
17.2	Combined cycle with afterburner	570
17.3	Combined cycle optimization	570
17.4	Gas turbine and combined cycles variations	575
17.5	Diesel combined cycle	575
17.6	Conclusions and outlook	575
	References	576
	Further reading	576

18	Cogeneration and Trigeration	577
18.1	Performance indicators	578
18.2	Boilers and steam turbines	579
18.3	Internal combustion engines	580
18.3.1	Reciprocating engines	580
18.3.2	Gas turbines	581
18.4	Criteria for selection	583
18.5	Examples of industrial plants	583
18.5.1	Micro-gas turbine cogeneration	583
18.5.2	Industrial gas turbine cogeneration	584
18.6	Trigeration	589
18.6.1	Production of central heating and cooling for a supermarket	589
18.6.2	Trigeration by micro turbine and absorption cycle	589
	References	595
	Further reading	595
19	Compression Refrigeration Cycles, Heat Pumps	597
19.1	Principles of operation	597
19.2	Current issues	598
19.2.1	Stopping CFC production	598
19.2.2	Substitution of fluids	599
19.3	Basic refrigeration cycle	601
19.3.1	Principle of operation	601
19.3.2	Energy and exergy balances	603
19.4	Superheated and sub-cooled cycle	606
19.4.1	Single-stage cycle without heat exchanger	606
19.4.2	Single-stage cycle with exchanger	606
19.5	Two-stage cycles	607
19.5.1	Two-stage compression cycle with intermediate cooling	607
19.5.2	Compression and expansion multistage cycles	608
19.6	Special cycles	614
19.6.1	Cascade cycles	614
19.6.2	Cycles using blends	615
19.6.3	Cycles using ejectors	617
19.6.4	Reverse Brayton cycles	622
19.7	Heat pumps	624
19.7.1	Basic cycle	625
19.7.2	Exergy balance	626
19.8	Technological aspects	627
19.8.1	Desirable properties for fluids	627
19.8.2	Refrigeration compressors	628
19.8.3	Expansion valves	631
19.8.4	Heat exchangers	631
19.8.5	Auxiliary devices	633
19.8.6	Variable speed	633
	References	633
	Further reading	634
20	Liquid Absorption Refrigeration Cycles	635
20.1	Introduction	635
20.2	Study of a $\text{NH}_3\text{-H}_2\text{O}$ absorption cycle	636

20.3	Modeling LiBr-H ₂ O absorption cycle in ThermoOptim	642
	References	643
21	Air Conditioning	645
21.1	Basics of an air conditioning system	645
21.2	Examples of cycles	647
21.2.1	Summer air conditioning	648
21.2.2	Winter air conditioning	649
	References	652
	Further reading	652
22	Optimization by Systems Integration	653
22.1	Basic principles	654
22.1.1	Pinch point	654
22.1.2	Integration of complex heat system	655
22.2	Design of exchanger networks	658
22.3	Minimizing the pinch	659
22.3.1	Implementation of the algorithm	660
22.3.2	Establishment of actual composite curves	663
22.3.3	Plot of the Carnot factor difference curve (CFDC)	663
22.3.4	Matching exchange streams	665
22.3.5	Thermal machines and heat integration	670
22.4	Optimization by irreversibility analysis	671
22.4.1	Component irreversibility and systemic irreversibility	671
22.4.2	Optimization method	674
22.5	Implementation in ThermoOptim	676
22.5.1	Principle	676
22.5.2	Optimization frame	677
22.6	Example	682
22.6.1	Determination of HP and LP flow rates	683
22.6.2	Matching fluids in heat exchangers	684
	References	690
	Further reading	690
4	Innovative Advanced Cycles, including Low Environmental Impact	691
23	External Class Development	693
23.1	General, external substances	693
23.1.1	Introducing custom components	693
23.1.2	Simple substance: example of DowTherm A	696
23.1.3	Coupling to a thermodynamic properties server	697
23.2	Flat plate solar collectors	699
23.2.1	Design of the external component	699
23.3	Calculation of moist mixtures in external classes	702
23.3.1	Introduction	702
23.3.2	Methods available in the external classes	703
23.4	External combustion	707
23.4.1	Model of biomass combustion	707
23.4.2	Presentation of the external class	710

23.5	Cooling coil with condensation	710
23.5.1	Modeling a cooling coil with condensation in Thermoptim	711
23.5.2	Study of the external class DehumidifyingCoil	712
23.6	Cooling towers	715
23.6.1	Modeling of a direct contact cooling tower in Thermoptim	716
23.6.2	Study of external class DirectCoolingTower	719
23.7	External drivers	721
23.7.1	Stirling engine driver	721
23.7.2	Creation of the class: visual interface	722
23.7.3	Recognition of component names	723
23.7.4	Calculations and display	723
23.8	External class manager	724
24	Advanced Gas Turbines Cycles	727
24.1	Humid air gas turbine	727
24.2	Supercritical CO ₂ cycles	732
24.2.1	Simple regeneration cycle	732
24.2.2	Pre-compression cycle	733
24.2.3	Recompression cycle	734
24.2.4	Partial cooling cycle	736
24.3	Advanced combined cycles	737
24.3.1	Air combined cycle	737
24.3.2	Steam flash combined cycle	739
24.3.3	Steam recompression combined cycle	741
24.3.4	Kalina cycle	741
	References	750
25	Evaporation, Mechanical Vapor Compression, Desalination, Drying by Hot Gas	751
25.1	Evaporation	751
25.1.1	Single-effect cycle	751
25.1.2	Multi-effect cycle	752
25.1.3	Boiling point elevation	753
25.2	Mechanical vapor compression	754
25.2.1	Evaporative mechanical vapor compression cycle	754
25.2.2	Types of compressors used	755
25.2.3	Design parameters of a VC	755
25.3	Desalination	757
25.3.1	Simple effect distillation	757
25.3.2	Double effect desalination cycle	758
25.3.3	Mechanical vapor compression desalination cycle	758
25.3.4	Desalination ejector cycle	758
25.3.5	Multi-stage flash desalination cycle	759
25.3.6	Reverse osmosis desalination	761
25.4	Drying by hot gas	764
	References	766
26	Cryogenic Cycles	767
26.1	Joule-Thomson isenthalpic expansion process	767
26.1.1	Basic cycle	767
26.1.2	Linde cycle	769
26.1.3	Linde cycles for nitrogen liquefaction	770

26.2	Reverse Brayton cycle	772
26.3	Mixed processes: Claude cycle	773
26.4	Cascade cycles	774
	References	775
27	Electrochemical Converters	777
27.1	Fuel cells	777
27.1.1	SOFC modeling	780
27.1.2	Improving the cell model	782
27.1.3	Model with a thermocoupler	784
27.1.4	Coupling SOFC fuel cell with a gas turbine	784
27.1.5	Change in the model to replace H ₂ by CH ₄	786
27.2	Reforming	789
27.2.1	Modeling of a reformer in Thermooptim	789
27.2.2	Results	792
27.3	Electrolysers	792
27.3.1	Modeling of a high temperature electrolyser in Thermooptim	793
27.3.2	Results	794
	References	795
28	Global Warming and Capture and Sequestration of CO₂	797
28.1	Problem data	797
28.2	Carbon capture and storage	798
28.2.1	Introduction	798
28.2.2	Capture strategies	800
28.3	Techniques implemented	801
28.3.1	Post-combustion techniques	801
28.3.2	Pre-combustion techniques	804
28.3.3	Oxycombustion techniques	814
	References	825
29	Future Nuclear Reactors	827
29.1	Introduction	827
29.2	Reactors coupled to Hirn cycles	829
29.2.1	Sodium cooled fast neutron reactors	829
29.2.2	Supercritical water reactors	830
29.3	Reactors coupled to Brayton cycles	830
29.3.1	Small capacity modular reactor PBMR	831
29.3.2	GT-MHR reactors	832
29.3.3	Very high temperature reactors	833
29.3.4	Gas cooled fast neutron reactors	834
29.3.5	Lead cooled fast reactors	834
29.3.6	Molten salt reactors	834
29.3.7	Thermodynamic cycles of high temperature reactors	835
29.4	Summary	840
	References	840
30	Solar Thermodynamic Cycles	841
30.1	Direct conversion of solar energy	841
30.1.1	Introduction	841

30.1.2	Thermal conversion of solar energy	842
30.1.2	Thermodynamic cycles considered	844
30.2	Performance of solar collectors	845
30.2.1	Low temperature solar collectors	845
30.2.2	Low temperature flat plate solar collector model	846
30.2.3	High temperature solar collectors	847
30.2.4	Modeling high temperature concentration collectors	847
30.3	Parabolic trough plants	849
30.3.1	Optimization of the collector temperature	849
30.3.2	Plant model	850
30.4	Parabolic dish systems	851
30.5	Power towers	852
30.6	Hybrid systems	853
	References	854
31	Other than Solar NRE cycles	855
31.1	Solar ponds	855
31.1.1	Analysis of the problem	856
31.1.2	Plot of the cycle in the entropy chart	857
31.1.3	Exergy balance	857
31.1.4	Auxiliary consumption	857
31.2	Ocean thermal energy conversion (OTEC)	858
31.2.1	OTEC closed cycle	859
31.2.2	OTEC open cycle	861
31.2.3	Uehara cycle	862
31.3	Geothermal cycles	864
31.3.1	Direct-steam plants	865
31.3.2	Simple flash plant	865
31.3.3	Double flash plant	867
31.3.4	Binary cycle plants	868
31.3.5	Kalina cycle	869
31.3.6	Combined cycles	870
31.3.7	Mixed cycle	872
31.4	Use of biomass energy	873
31.4.1	Introduction	873
31.4.2	Modeling thermochemical conversion	875
	References	878
32	Heat and Compressed Air Storage	879
32.1	Introduction	879
32.2	Methodological aspects	880
32.3	Cold storage in phase change nodules	881
32.4	Project Sether (electricity storage as high temperature heat)	881
32.5	Compressed air storage devices	883
32.5.1	CAES (Compressed Air Energy Storage) concept	883
32.5.2	Peaker concept of Electricite de Marseille Company	884
32.5.3	Hydropneumatic energy storage HPES	884
	References	887

33	Calculation of Thermodynamic Solar Installations	889
33.1	Specific solar problems	889
33.2	Estimation of the solar radiation received by a solar collector	891
33.3	Cumulative frequency curves of irradiation	893
33.3.1	Curve construction	894
33.3.2	Curve smoothing	894
33.3.3	Estimation of CFCS from empirical formulas	895
33.3.4	Interpolation on tilt	896
33.4	Hourly simulation models	896
33.5	Simplified design methods	897
33.5.1	Principle of methods	897
33.5.2	Usability curves	897
	References	899
5	Technological Design and Off-design Operation	901
34	Technological Design and Off-design Operation, Model Reduction	903
34.1	Introduction	903
34.2	Component technological design	905
34.2.1	Heat exchangers	906
34.2.2	Displacement compressors	908
34.2.3	Expansion valves	909
34.2.4	Practical example: design of a cycle	909
34.3	Off-design calculations	914
34.3.1	Principle of computing coupled systems in Thermoptim	914
34.3.2	Off-design equations of the refrigerator	915
34.3.3	After processing of simulation results	916
34.3.4	Effect of change in UA	917
34.4	Development of simplified models of systems studied	919
34.4.1	Model reduction principle	919
34.4.2	Model reduction example	920
34.5	Methodological difficulties	921
	References	922
35	Technological Design and Off-design Behavior of Heat Exchangers	923
35.1	Introduction	923
35.1.1	General	923
35.1.2	Reminders on the NTU method	924
35.2	Modeling of heat transfer	925
35.2.1	Extended surfaces	925
35.2.2	Calculation of Reynolds and Prandtl numbers	926
35.2.3	Calculation of the Nusselt number	927
35.2.4	Calculation of multi-zone exchangers	929
35.3	Pressure drop calculation	933
35.3.1	Gas or liquid state pressure drop	933
35.3.2	Two-phase pressure drop	934
35.4	Heat exchanger technological screen	935
35.4.1	Heat exchanger technological screen	935
35.4.2	Correlations used in Thermoptim	935
35.5	Model parameter estimation	937

35.5.1	Direct setting from geometric data	937
35.5.2	Identification of exchanger parameters	940
	References	941
36	Modeling and Setting of Displacement Compressors	943
36.1	Behavior models	943
36.1.1	Operation at rated speed and full load	945
36.1.2	Operation at partial load and speed	947
36.2	Practical modeling problems	948
36.2.1	Technological screen of displacement compressors	948
36.2.3	Identification of compressor parameters	949
36.2.4	Calculation in design mode	949
36.2.5	Calculation in off-design mode	949
36.2.6	Fixed V_i screw compressors	949
	References	950
37	Modeling and Setting of Dynamic Compressors and Turbines	951
37.1	Supplements on turbomachinery	952
37.1.1	Analysis of the velocity triangle	952
37.1.2	Degree of reaction of one stage	953
37.1.3	Theoretical characteristics of turbomachinery	954
37.1.4	Real characteristics of turbomachinery	956
37.1.5	Factors of similarity	959
37.2	Pumps and fans	961
37.3	Dynamic compressors	963
37.3.1	Performance maps of dynamic compressors	963
37.3.2	Analysis of performance maps of dynamic compressors	965
37.3.3	Technological screen of dynamic compressors	970
37.4	Turbines	971
37.4.1	Performance maps of turbines	972
37.4.2	Isentropic efficiency law	973
37.4.3	Stodola's cone rule	975
37.4.4	Baumann rule	977
37.4.5	Loss by residual velocity	978
37.4.6	Technological screen of turbines	979
37.4.8	Identification of turbine parameters	979
37.5	Nozzles	979
	References	980
38	Case Studies	981
38.1	Introduction	981
38.2	Compressor filling a storage of compressed air	982
38.2.1	Modeling of the heat exchanger	982
38.2.2	Design of the driver	984
38.2.3	Analysis of the cooled compressor	985
38.2.4	Use of the model to simulate the filling of a compressed air storage	989
38.3	Steam power plant	990
38.3.1	Introduction, results	990

38.4	Refrigeration machine	995
38.4.1	Introduction, results	995
38.4.2	Principle of resolution	996
38.5	Single flow turbojet	998
38.5.1	Introduction, results	999
38.5.2	Presentation of the external class	1003
	Index	1005

SEARCHING REFERENCES IN THE THERMOPTIM-UNIT PORTAL (www.thermoptim.org)



[CRC_In_0]

“In order to facilitate the use of the portal in relation with this book, we have adopted the following convention:

The small Thermoptim logo that appears in the margin of this page is used when a reference is made to the portal.

Just below is written a code which can be entered in the portal search engine to find the resource quoted.

The codes are of the kind “CRC_we_8” for a worked example, “CRC_pa_5” for a practical application, or “CRC_ln_9” for a simple link.

If you enter “CRC_*”, the search engine lists all the resources which are referenced in the book.

This way of doing is much simpler than entering the full URL of the resource you are looking for.”

Foreword by John W. Mitchell

This is an ambitious book that presents a new approach to teaching energy systems. The author, Renaud Gicquel, has introduced two new paradigms to teaching the subject. The first is that the study of energy systems is initiated at the system level rather than the mechanism level. The second paradigm is the use of software that is integral to the study of systems and, ultimately, to learning the underlying thermodynamic principles. The success of these paradigms is demonstrated through the adoption of this approach by over 120 institutions of higher education in France and worldwide.

The book is divided into five main sections. The first section, titled *First Steps in Engineering Thermodynamics*, covers the entire subject of energy systems, with the first chapter describing the pedagogic approach used in the rest of the book. The second chapter focuses on the system level and illustrates the teaching philosophy. This chapter gives students exposure to those components that comprise a complete energy systems such as a steam power plant, and what each component does. The emphasis is on understanding the concepts underlying the operation of each component, such as the change of phase from liquid to vapor in the boiler. Process diagrams are introduced to further understanding. Complete system models are created and the performance determined using the software Thermoptim. By starting at the system level students early on become familiar with the vocabulary, components, and performance of a system before they become enmeshed in the thermodynamic relations used to compute properties and energy flows. Stressing conceptual understanding rather than calculation reinforces the important basic ideas.

The pedagogical approach is a significant departure from the typical methods used in teaching thermodynamics. Traditionally, one starts with basic conservation equations and property relations, with calculations geared toward determining values for a process rather than for the performance of a system as a whole. Emphasis is on a detailed understanding of the relations that govern thermodynamic behavior. Typically, applications to system follow late in the study after all the underpinning has been developed.

While traditional approaches have been used successfully for many years, educational research has established that alternate approaches can improve learning. Context is one key driver for student learning, and the book's approach wherein students start with models of actual systems commonly used for power and refrigeration establishes relevance to engineering practice. Ideas from problem-based learning, in which students are confronted with a problem to solve and then learn what is needed to obtain a solution, are also incorporated. Student motivation and conceptual understanding are important to mastering thermodynamic fundamentals that underlie performance.

The second paradigm is that the learning of thermodynamics is intertwined with the software. Thermoptim allows students to quickly create realistic system models and explore a number of "What if" questions, such as what is the effect on power if the steam temperature in the boiler is raised a certain number of degrees. The component models are built on the fundamental relations, and the familiarity students gain working with models and observing behavior aids them in their later study of thermodynamics. Further, using simulation models from the start provides a bridge to engineering practice in which realistic situations require software for solution. It is essential that the student and practitioner understand the thermodynamic relations necessary to form a model, as is covered in later sections of the book, but it is not necessary to develop a model from basic relations each time. This intimately linking of software to content is in the vanguard of modern books on engineering topics.

The second section of the book is *Methodology, Thermodynamics Fundamentals, Thermoptim, Components*. With the background in systems, thermodynamics, and Thermoptim from the first

section, the rigorous study of thermodynamics proceeds rapidly. The first law, second law and property relations are introduced, following traditional approaches to teaching thermodynamics, except that now the context of the material is clear, motivating the student. The coverage extends to a number of real property effects that are often not emphasized in traditional thermodynamic books; there are sections on the property relations for moist air, solutions, and mixtures. The Thermoptim framework allows real property variations to be included in system analysis.

Models are constructed in Thermoptim analogous to the way they are in a real system, and a chapter is devoted to discussing model building. Conduits connect components through fluid transport, carrying information from one component to the next. In the steam power plant, for example, the pipe transporting steam from the turbine exhaust to the condenser carries with it all of the state information on the steam that the actual pipe would. Information is transported automatically, which reduces the need for the student to keep track of all properties at every point. Evaluation of the state of fluids throughout the system is accomplished analogous to measurement stations in a real system. The natural analog between the simulation and the real system facilitates learning.

The remaining chapters in this section cover a number of more advanced topics, such as different types of compression processes, complete and incomplete combustion, psychrometrics, heat exchangers, and second law topics (exergy/availability). As with the earlier thermodynamic material, the presentation is rigorous and includes effects that are often not taught in first courses, but that are included in the Thermoptim components available for simulation. Worked examples are included so that students can explore the subject using the available models.

The last three sections of the book are devoted to different heating, cooling, and power systems. The first of these is a strong and detailed exposition of conventional cycles. Gas turbine, internal combustion engine (spark ignition and diesel), steam power and co-generation plants, mechanical and absorption refrigeration systems are discussed from both thermodynamic and practical points of view. The last two sections deal with innovative cycles, with an emphasis on low environmental impact. Such topics as the Kalina cycle, desalinization, cryogenics, fuel cells, solar power, and sequestering carbon dioxide are discussed. These last three sections are beyond what would be covered in undergraduate courses, but the combination of references and Thermoptim components make these sections valuable for research projects and advanced study. As with the beginning chapters, the emphasis is always on conceptual understanding, with the implementation incorporated into Thermoptim.

This is a comprehensive book on energy systems with an almost encyclopedic coverage of the details of the equipment and systems involved in power production, refrigeration, and air-conditioning. The integration of technical content with advanced software allows a range of users from students who are beginning their study to those involved in research on promising cycles. From a teaching perspective, the initial focus on the system level combined with the simulation tool Thermoptim serves to quickly bring students up to speed on applications, and provides motivation for further study. This book promises to be one that engineers will keep on their desks for ready reference and study.

John W. Mitchell

Kaiser Chair Professor of Mechanical Engineering, Emeritus
University of Wisconsin-Madison
Madison, Wisconsin, USA

Foreword by Alain Lambotte

By an innovative approach to thermodynamics and a progressive study of systems – ranging from the simplest to the most complex – *Energy Systems* comprises three books in one: a guide for beginners, a reference book for advanced learners, and a support for development for professionals. I have been using the French version for several years personally, to develop training content and validate skill levels in the electricity utility company where I am engaged with.

My target audience consists of two groups: officials who have left university or the Haute École for some years and therefore have a certain ‘distance’ towards mathematics, and of fresh graduates, for whom ‘thermodynamics is math’, and who have little evocative image of the underlying physical reality.

This book, by its content and its character, is an encouraging and stylish manifesto of a new teaching practice of engineering thermodynamics. In contrast to existing teaching methods on the matter, it spares the reader mathematical contingencies, the aggregation of knowledge, and the immutable laws of thermodynamics in the first steps. Instead, learning by reflection has priority over the memorization of scientific knowledge that is not immediately essential. Mathematical relationships illustrate the point, but are not the heart of the matter. This is ideal for the technicians and engineers we train, who often have a much lower accurate mathematical level at their disposal than when they were still students.

The approach is fully systems-oriented. It allows both basic learning and the development of innovative thought. After the author has explained the setup, quite naturally and visually, there is place for reflection and numerous applications. Technologies are presented simply at first, and subsequently with increasing detail. This makes the adequacy of the author’s approach multiple: beginners, professionals and experts will all find answers to their questions.

In combination with the www.thermoptim.org portal and the possibilities this offers *Energy Systems* is an appealing textbook and developing tool for students, teachers, researchers and practitioners. The exhaustive character, through the given systems and models and through the enormous amount of tools in the Thermoptim portal and simulator, allows the reader to easily self-develop new models to fulfil his or her needs. These can range from basic notions to the most advanced concepts in energy systems. All factors together make this set a very powerful reference that allows easier implementation into practice than any existing books on the subject.

Although I use *Energy Systems & Thermoptim*, and even over-indulge in it, I am far from having been around the concept. Usage has changed my approach to thermodynamics, both in my engineering work and in preparing course content. The development of a much more accessible and user-friendly approach than encountered earlier made using it a pleasure, both personally and in training. Last but not least, it widely opens the doors to creativity, which is a major requirement for our energy future.

Alain Lambotte
Content Manager, Competence and Training Center
Electricity Utility, Belgium

This page intentionally left blank

About the Author



Active as a full professor since 1986, Dr Renaud Gicquel has taught a wide variety of energy subjects, such as applied thermodynamics and global energy issues and energy system modeling. His current research activities are focused on the optimization of complex thermodynamic plants (heat exchanger networks, cogeneration, combined cycles) and on the use of information and communication technologies for scientific instruction.

Renaud's special interest and passion is the combination of thermodynamics and energy-powered system education with modern information technology tools. To this end, he has developed various software packages to facilitate the teaching and learning of applied thermodynam-

ics and the simulation of energy systems:

- *Thermoptim (Thermo-Calc)* professional software, 2000
- *Interactive Thermodynamic Charts*, 2000
- *Diapason* e-learning modules, 2004, www.thermoptim.org

The origin of this book comes from earlier works, *Introduction to Global Energy Problems* (1992, Economica, in French) and the original *Energy Systems* (2 volumes, 2001, Presses de l'École des Mines in French). These have formed the basis for refinement of the Thermoptim Software and a 3 volume 2nd edition of *Energy Systems* in French. The latter was very well received by more than a hundred higher education institutes in France, and this current English edition was prepared. The three volumes were merged and melted together and reorganized into 5 major parts. More tools and directions were further added to make it suited and attractive for classroom use anywhere in the world, in combination with Thermoptim.

With a new approach to teaching and learning applied thermodynamics, including a large number of educational resources, Renaud Gicquel has made a major tour de force to significantly ease the learning of engineering thermodynamics. Together with the wealth of information, e-learning modules, examples and exercises of the Thermoptim portal, this work will provide any student and professional working on this subject with excellent tools to master the subject up to advanced level.

Career

Renaud Gicquel is Professor at the École des Mines de Paris (Mines ParisTech). He was trained as a mining engineer at the École des Mines and got his Ph.D. degree in engineering from the Paris VI University. He started his career as a Special Assistant to the Secretary General of the United Nations Conference on New and Renewable Sources of Energy in 1980 in New York. He then became the Deputy Director in charge of Dwellings at the Energy Division of the Marcoussis Laboratories of the Compagnie Générale d'Electricité until January 1982, and was in charge of multilateral issues in the International Affairs Service of the Ministry for Research and Technology in Paris in 1982. From 1983 to 1985, he was Adviser for International Issues of the National Center of Scientific Research (CNRS). In 1986, he founded with Michel Grenon the Mediterranean Energy Observatory (OME), based in Sophia Antipolis. In 1990, Dr Gicquel created the ARTEMIS group, a research body for thermal energy research, together with the University of Nantes and ISITEM (now Polytech) in Nantes. He acted as a coordinator while fulfilling the position of Deputy Director at the École des Mines de Nantes (EMN) from 1991 as well. In 1987 he was appointed head of the Centre of Energy Studies of the École des Mines de Paris.

This page intentionally left blank

General Introduction

As indicated by its title, this book deals with energy systems, i.e. energy conversion technologies (ECTs) considered as systems based on sets of elementary components coupled together. Although it mainly addresses thermodynamic energy conversion, it covers a very large field, including a variety of cycles: conventional as well as innovative power plants, gas turbines, reciprocating engines, Stirling engines, combined cycles, cogeneration, refrigeration cycles, new and renewable energy conversion, combustion, Generation I to IV nuclear energy conversion, evaporation, desalination, fuel cells, CO₂ capture and sequestration, air conditioning etc.

We have developed over the past twenty-five years a new way of teaching thermodynamics applied to energy conversion now used in more than one hundred and twenty higher education institutions, at both undergraduate and graduate levels (engineering schools, universities) as well as in vocational training.

The change in the education paradigm we have introduced is based on a shift of knowledge acquired by students. The writing of equations describing changes undergone by fluids is drastically reduced, the calculations being performed by a simulator such as Thermoptim (www.thermoptim.org) without learners needing to know the details. They devote most of the time on the one hand learning technologies, and secondly reflecting on the architecture of both conventional and innovative thermodynamic cycles, graphically building and setting models of various energy technologies.

The new teaching method has the distinction of being at the same time much simpler than conventional approaches for the introduction to the discipline, and much more useful for confirmed students who can go further in their studies thanks to a powerful and open modeling environment. They can work on real-world complex innovative cycles currently being studied in laboratories and companies.

This book seeks to meet the expectations that students may have throughout their training. Therefore:

- first, it allows beginners, whether in initial or vocational training, to easily understand design principles of energy systems, to get an overview of the different technologies available for their achievement, and to conduct by themselves realistic calculations using computerized tools;
- secondly, it provides its advanced readers with a statement as complete as possible of the whole discipline, with advanced methods allowing them to analyze these systems, as well as guidance in choosing equations if they wish to build their own models.

This book must then conciliate simple explanations for beginners and in-depth analyses for advanced readers, which may appear paradoxical:

- it offers a profound break in the implementation of methodological tools, while essentially retaining a conventional presentation of the discipline;
- it says that it is possible to learn thermodynamics without writing a single equation or programming a single line of code, yet is full of examples of equations and computer models.

It follows that the structure of the book is not entirely conventional.

STRUCTURE OF THE BOOK

Given the width of the field covered, it was decided to split the book into five main Parts.

Moreover, the goals we set ourselves have led us to identify three major transverse themes that are found throughout the presentations:

- theoretical foundations (whose presentation has been simplified as much as possible);
- an original modeling approach;
- a detailed presentation of technologies.

Part 1, especially dedicated to beginners and fellow teachers, introduces in a very simple way basic concepts necessary to understand elementary thermodynamic cycles (steam power plants, gas turbines, refrigerators).

For the simplest mono-functional components such as compression, expansion, heat exchange etc., the foundations of the first two themes are presented in Part 2 and implemented in Part 3, in addition to the presentation of technologies, to which we decided to devote a significant account given the ignorance of a large number of students in this subject.

Part 4, which complements the two previous ones by introducing advanced cycles, including low environmental impact ones, addresses in addition a new issue related to the study of systems operating under varied conditions: time management of energy use with thermal and pneumatic storage and time (e.g. hourly) simulation of systems (including solar).

Finally, Part 5 is devoted to a particularly difficult topic: the study of technological design and off-design operation. Specific features have been implemented in the Thermoptim software, mainly through the mechanism of external classes, which allows users to customize models as they wish. Some indications are also given on model reduction techniques which allow us to derive simplified models (e.g. polynomials) from a Thermoptim project.

Specifically, the overall structure of the book is:

- Part 1 is mainly dedicated to beginners and vocational trainees, and may also provide guidance to fellow teachers who wish to change their pedagogy. It is divided into three chapters. The first one introduces the new educational paradigm and software tools allowing us to implement it, while the other two, titled First Steps in Thermodynamics (Absolute beginners and Second law), provide an illustration in the form of a lightweight educational presentation of thermodynamic basic cycles, initially without resorting to entropy and then by introducing it in a simple manner;
- After recalling thermodynamics fundamentals, Part 2 establishes the main equations allowing one to calculate the behavior of basic components used in most energy technologies (compressors, turbines, combustion chambers, throttling devices, heat exchangers etc.). A structured approach to energy conversion technologies (ECTs) modeling with Thermoptim is given, followed by the presentation of the main features of the software and by four practical worked examples. Part 2 contains the essential elements for understanding how components that come into play in ECTs can be modeled. It also explains how to approach cycle studies and establish exergy balances;
- Part 3 discusses how the foundations laid in the first Part can be applied to the main conventional cycles. Classical ECTs are reviewed, analyzed as systems implementing the components whose operation has been studied previously. The link is made between knowledge and technological achievements, which are presented in more details than in the other parts;
- Part 4 is intended primarily for confirmed readers who wish to perform advanced modeling. After explaining how to design external classes, it completes Part 3 by addressing innovative advanced cycles, including low environmental impact ones, most of them involving such external classes. Two chapters are then devoted to time management of energy;
- Part 5 deals with Thermoptim extensions that have been introduced to conduct technological design and off-design operation studies.

The whole book is illustrated by numerous examples (about 135) of cycles modeled with Thermoptim, which provide the reader with models whose structure or settings he may customize

as he wishes to perform various simulations. The files of these examples are available for teachers, but not for their students.

The list of these examples, of varying difficulty, is given in a portal called ThermoOptim-UNIT (www.thermoOptim.org) with some comments and suggestions on ways in which they can be used educationally, depending on the context and the objectives pursued by teachers.

More generally, many digital resources for teaching energy systems have been gradually collected into this portal whose content is freely accessible, with few exceptions, including solutions of some exercises and problems, among which are those presented in this book. A brief presentation of these resources is given in Chapter 1 of Part I.

OBJECTIVES OF THIS BOOK

For beginners, the major interest of ThermoOptim is that it can help them to model complex energy systems simply, without having to write an equation or program. It discharges its users of many problems, including computational ones, and enables them to make analyses that they could not pursue otherwise, especially when starting out. It becomes possible, when learning the discipline, to focus on a qualitative approach, the calculations required for quantitative studies being performed by the software. Note that the name of this tool has a double meaning: it does allow one to optimize thermodynamic systems, but above all it allows one to learn this discipline with optimism...

Under these conditions, energy systems operation can be studied using a completely new pedagogy, where only a small number of elements must be considered: firstly those used to describe the systems studied, and secondly those used to set the simulator components.

If done this way, it is not necessary, at least initially, to take into account the details of the equations allowing calculation of the process involved: ThermoOptim automatically does this. Learning the discipline is limited to these basic concepts and their implementation in the package. The memorization effort and cognitive load required for beginners are greatly reduced, allowing them to focus their attention on understanding the basic phenomenological concepts and their practical implementation.

Thus ThermoOptim permits, without writing a single line of code, to calculate energy systems from simple to complex.

However, the ambition of this work does not end there: it is also to provide its readers with enough information so they can make custom models, either by introducing specific component models not available in the ThermoOptim core, which involves showing them how to derive their equations, or by using the software advanced features.

In summary, we pursue four objectives:

- allow students firstly to understand the functioning of various components at stake in energy systems and how they are assembled, emphasizing the technological aspects;
- show how it is possible through the use of ThermoOptim to model and calculate them very simply but with great precision, and make the reader familiar with this working environment;
- establish the constitutive equations representing the operation of key technologies, and provide readers who want to model these for themselves with sufficient evidence for them to do, including using the external class mechanism that allows them to add to ThermoOptim their own components or sets of algorithms for controlling complex projects;
- provide the reader with methodological guidance, simple or advanced, for analyzing the systems he studies. In this spirit, a significant place is devoted to exergy methods that are increasingly regarded as among the best suited to perform optimization studies, as they can take into account both the amount of energy put into play and its quality.

A WORKING TOOL ON MANY LEVELS

This book can be read and used as a working tool on several levels:

- for an introduction to the discipline with an illustration of its implementation in Thermoptim: you can then simply understand the different technologies, the physical phenomena that are involved and the methodologies recommended, possibly using the package somewhat blindly;
- for a deepening of the field, it presents not only the calculation principles and the basic equations, but also explains how to build exergy balance-sheets, by hand or automatically, implement the pinch method, perform technological design and off-design operation analyses etc.;
- for software users, this book is a scientific complement to the documentation provided with the tool, allowing those interested to better understand how the calculations are made and even to personalize it.

It follows that the book is deliberately composed of a series of sections that are on different planes, some more theoretical, others more applied and technological, and others methodological, concerning in particular the use of Thermoptim.

In this way, readers wishing to do an overview of the book will be guided through the research of basic concepts needed, especially to use the software properly, while those who wish to invest further in the discipline will benefit from a consistent and progressive presentation.

Pedagogically, this book and Thermoptim can be used in various contexts, under both a traditional approach (neo-behaviorist or objectivist) and a more recent constructivist approach. We hope it will help colleagues to overcome difficulties that they may face in their practice.

For supporters of a conventional approach, Thermoptim allows them particularly to enrich the classical presentation by accurate simulations and to make students study multiple and realistic examples. In a constructivist approach, the book and the software are in addition tools allowing students to work independently to explore a wide field and analyze very open topics:

- for beginners, it is a structured environment that reduces the cognitive load while acquiring the vocabulary and basic concepts encapsulated in the screens. Once this vocabulary is learned, cooperative learning with peers and teachers is strengthened;
- very quickly, it becomes possible to work on realistic problems and not caricatures (as conventionally internal combustion engines with perfect air as working fluid). In addition, during internships, students using Thermoptim are fully operational in the company where they work, which is very exciting for them and leads them to engage more thoroughly;
- for experienced users, Thermoptim allows them to study very complex systems (for example, Areva Framatome used Thermoptim to optimize combined cycles and cogeneration thermodynamic cycles coupled with high temperature nuclear reactors, see Section 29.3.7.3 of Part 4).

The reader will understand that we seek above all to make as accessible as possible the study of energy systems, demonstrating very concretely how realistic models can be developed to represent them. This bias has led us to voluntarily limit our discussion of scientific issues to key points, especially regarding the fundamentals of thermodynamics and heat transfer. As a result, the book loses in generality what it gains in ease of use: know-how is privileged compared to knowledge itself. Readers interested in further developments may if they wish refer to documents given in the bibliography.

Experienced engineers will find a coherent body of theory and practice through which they can become quickly operational, without having to get personally involved in solving equations or in the development of a computer modeling environment.

Explanation of icons (see table of contents for icons used). Discuss with author how to best explain.

Mind Maps

This book includes seven mind maps whose role is to help readers easily find information on a given topic.

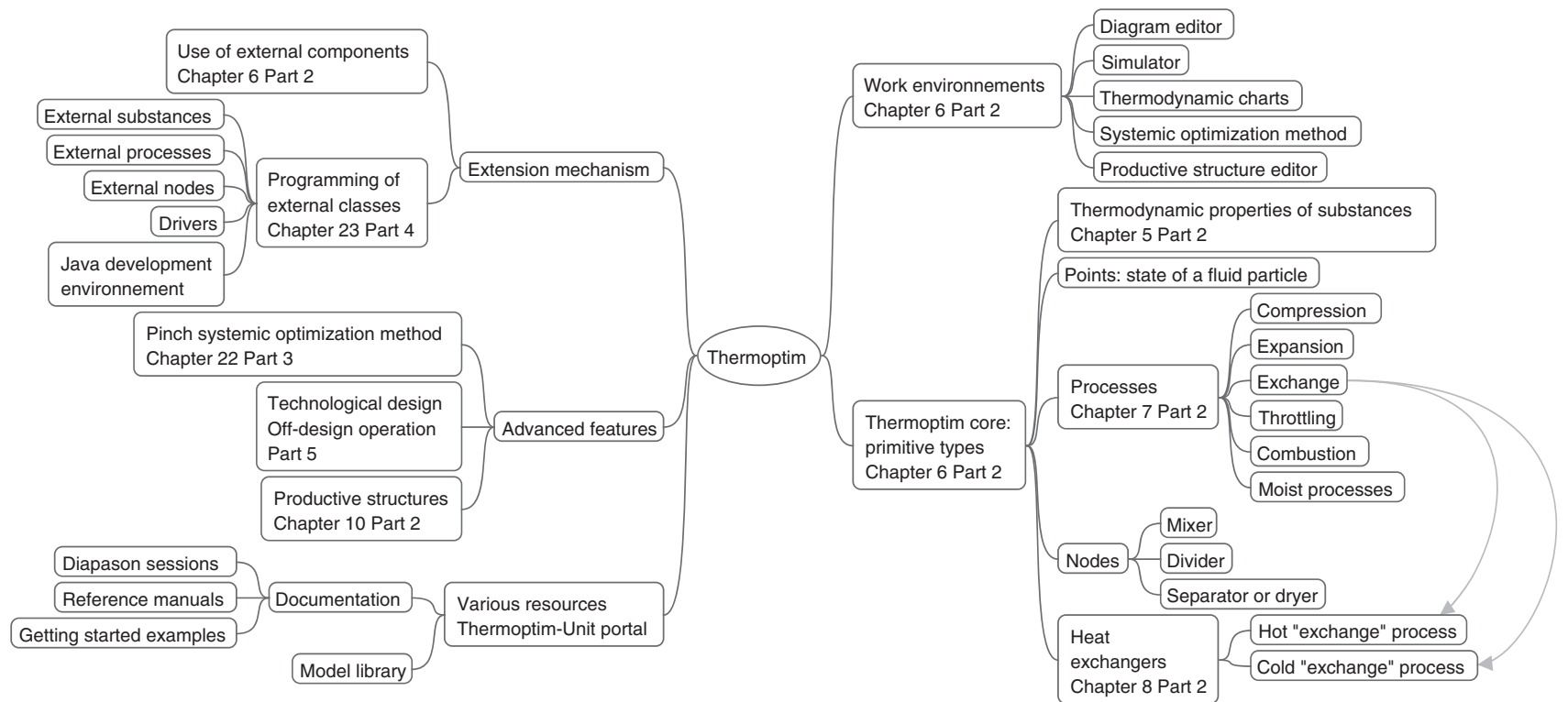
These knowledge maps are explanatory figures which summarize in a graphical way the main issues pertaining to the topic, with the indication of the chapter(s) of the book where they are dealt with.

After the General introduction, you will find a first map presenting the main features of the Thermoptim software, and four ones devoted to thermodynamic cycles:

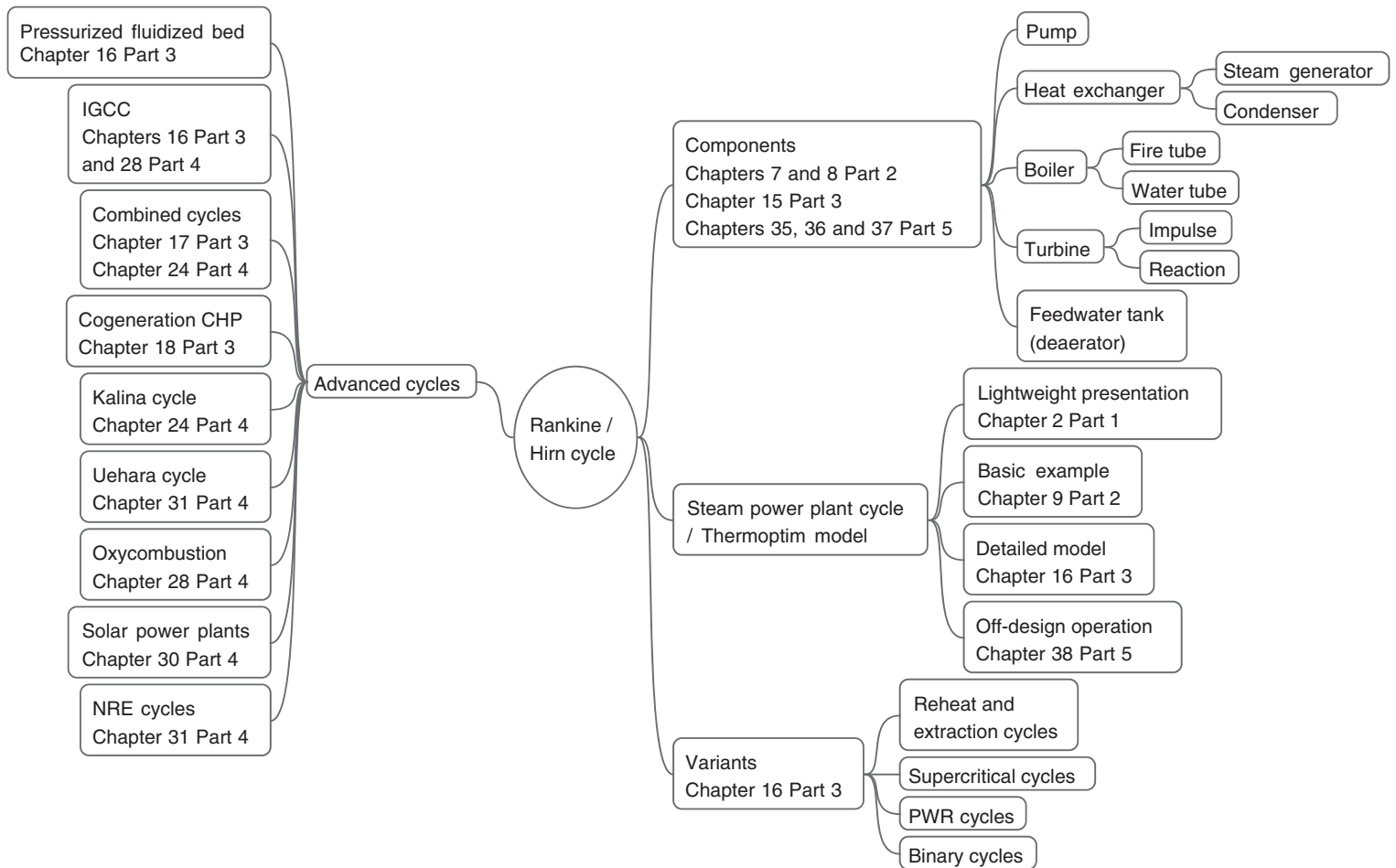
- Rankine cycles for steam power plants;
- Refrigeration cycles;
- Gas turbine cycles
- New and renewable energy cycles.

At the end of Chapters 2 and 3 of Part 1, two other maps summarize the different steps of the light-weight educational presentation of thermodynamic cycles.

Thermoptim



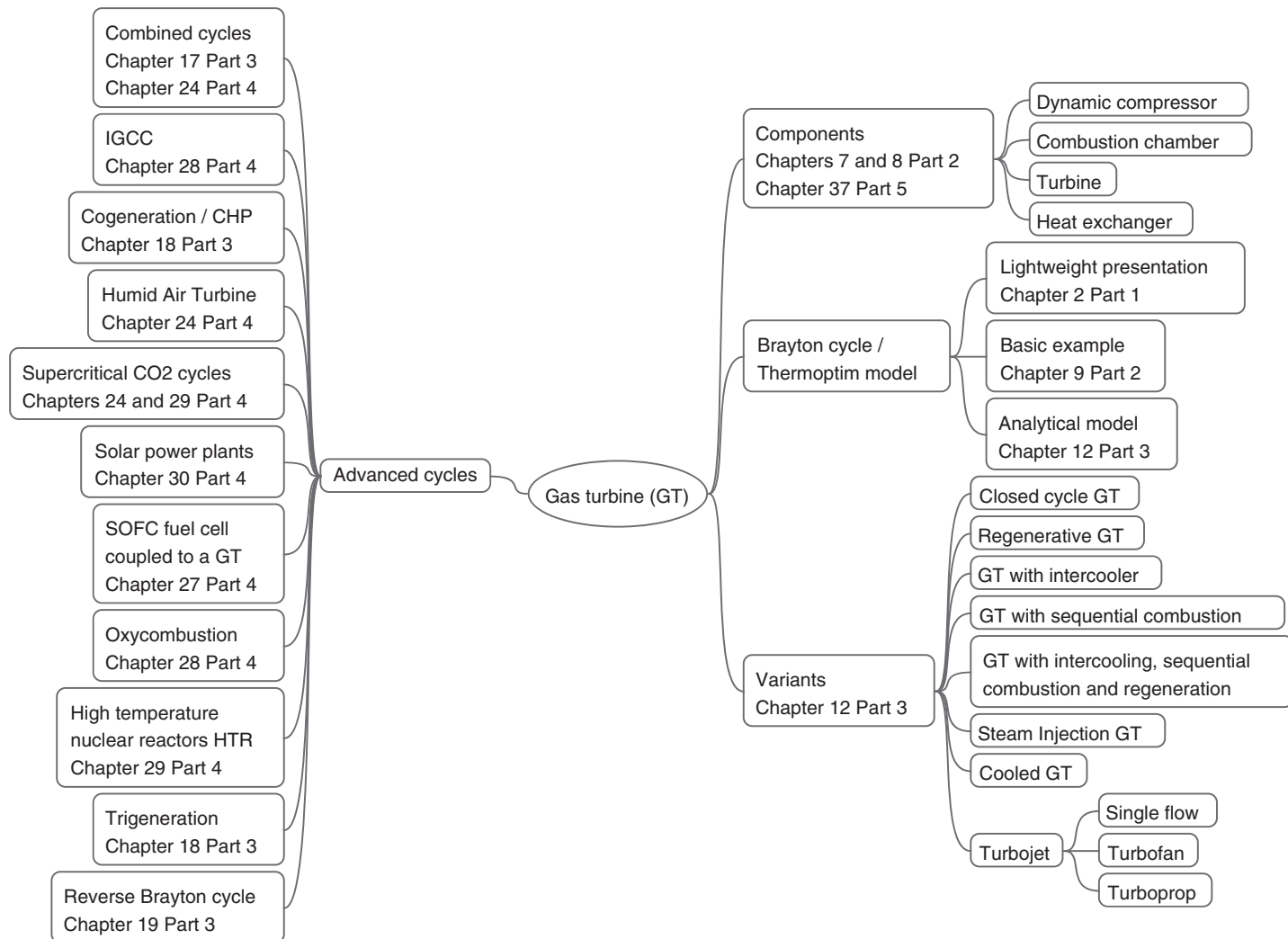
Rankine cycles for steam power plants



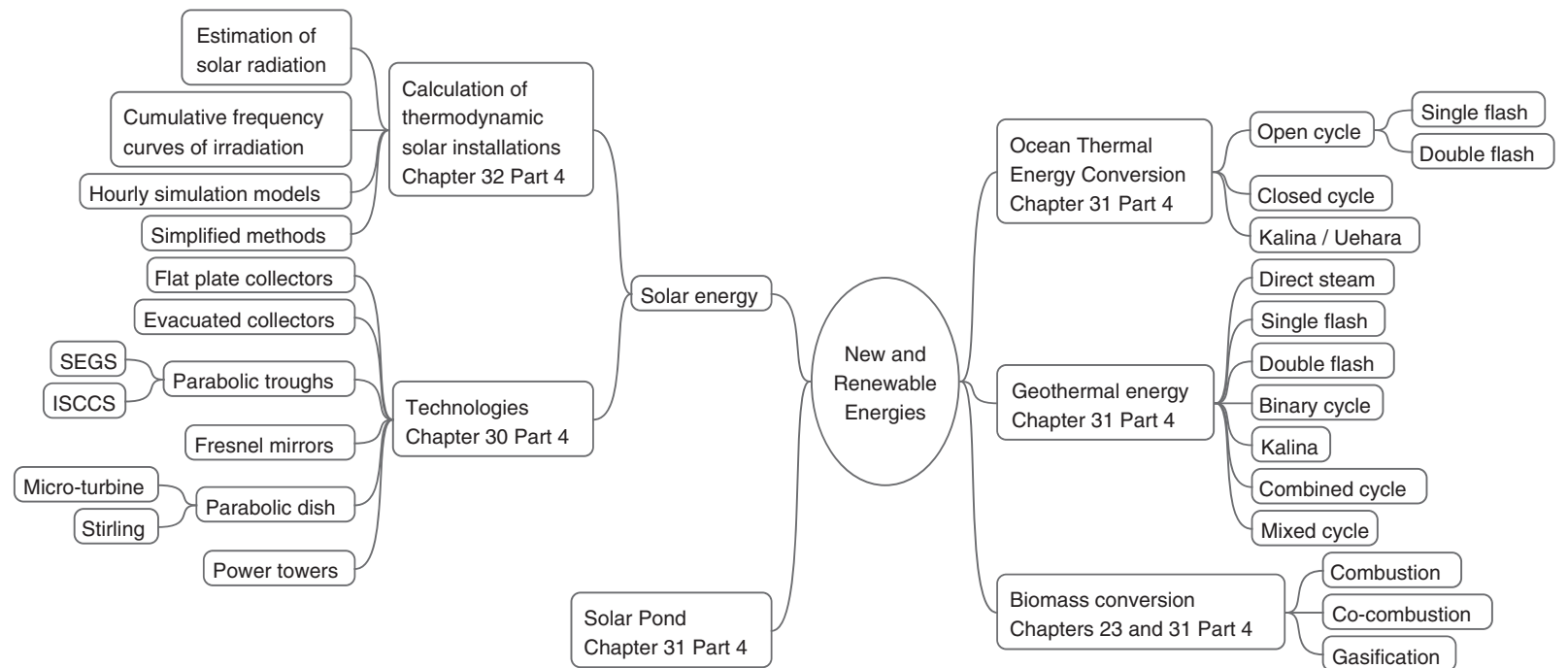
Vapor compression refrigeration cycles



Gas turbine cycles



New and renewable energy cycles



List of Symbols

A	area	m^2
a	hydrogen available for combustion	
A_c	free flow area	m^2
Bo	Boiling number	
C	concentration	
C	speed	$m\ s^{-1}$
C	fluid velocity	$m\ s^{-1}$
C	concentration factor	
C_s	speed of sound	$m\ s^{-1}$
C_r	volumetric efficiency	
C_p	molar heat capacity at constant pressure	$J\ mol^{-1}\ K^{-1}$
c_p	specific heat capacity at constant pressure	$J\ kg^{-1}\ K^{-1}$
C_r	Volumetric efficiency	
C_v	molar heat capacity at constant volume	$J\ mol^{-1}\ K^{-1}$
c_v	specific heat at constant volume	$J\ kg^{-1}\ K^{-1}$
D	diameter	m
D	diffuse irradiation	$W\ m^{-2}$
D/V	blowdown rate	
d_h	hydraulic diameter	m
e	excess air	
e	thickness	m
f	friction coefficient	
f	surface factor	
F	thrust	N
F	molar flow rate	$mol\ s^{-1}$
F	molar Helmholtz energy	$J\ mol^{-1}$
f	mass Helmholtz energy	$J\ kg^{-1}$
f	fugacity	Pa
f	annual leakage of refrigerant	%
f	residual gas rate	
G	molar Gibbs energy	$J\ mol^{-1}$
g	mass Gibbs energy	$J\ kg^{-1}$
g	acceleration due to gravity	$m\ s^{-2}$
Gh	global irradiation	$W\ m^{-2}$
H	molar enthalpy	$J\ mol^{-1}$
h	mass enthalpy	$J\ kg^{-1}$
h	heat transfer coefficient	$J\ K^{-1}\ m^{-2}$
h	calorimetric coefficient	$J\ kg^{-1}\ bar^{-1}$
h	height difference	m
h_f	enthalpy of formation	$J\ mol^{-1}$
i	octane number	
i	intermittency factor	
i	van't Hoff factor of the solute	
I	current density	A
I	direct irradiation	$W\ m^{-2}$

Is	specific impulse	s
k	polytropic coefficient	
k	dissociation rate	
k	interaction coefficient	
k_m	mixing entropy	$\text{J mol}^{-1} \text{K}^{-1}$
K	kinetic energy	J kg^{-1}
K_{eb}	ebullioscopy constant	K kg mol^{-1}
K_p	equilibrium constant	
K_0	cone or Stodola constant	
l	calorimetric coefficient	J m^{-3}
L	enthalpy of evaporation	J kg^{-1}
L	length	m
Le	Lewis number	
M	molar mass	kg mol^{-1}
m	mass	kg
Ma	Mach number	
m_c	specific fuel consumption	g kWh^{-1}
n	number of moles	
n	life expectancy	year
N	rotation speed	rpm
n_c	number of cylinders	
N_0	Avogadro's number	$6 \cdot 10^{23} \text{ mol/g}$
N_u	Nusselt number	
NTU	number of transfer units	
P	pressure	Pa or bar
Pr	Prandtl number	
p	wetted perimeter	m
P	power	W
Q	heat	J kg^{-1}
q'	specific enthalpy (moist gas)	J kg^{-1}
R	universal constant	$8,314 \text{ J mol}^{-1} \text{K}^{-1}$
R	ratio of heat capacity rates of a heat exchanger	
r	ideal gas constant	J K^{-1}
r	compression ratio	
R	richness	
RR	relative roughness	
Re	Reynolds number	
R/P	ratio reserves/annual production	year
S	molar entropy	$\text{J mol}^{-1} \text{K}^{-1}$
s	mass entropy	$\text{J kg}^{-1} \text{K}^{-1}$
S	surface	m^2
Sb	salt concentration in the feedwater tank	mg/l or °f
Sc	salt concentration in the boiler	mg/l or °f
Sc	Schmidt number	
s	volumetric efficiency	
T	thermodynamic temperature	K
t	temperature	°C or K
t	dry bulb temperature	°C
t'	wet bulb temperature	°C
t_r	dew point	°C

TA	total alkali	°f
TAC	total alkali	°f
TH	total hardness	°f
Toe	ton of oil equivalent	t
u	specific internal energy	J kg ⁻¹
U	molar internal energy	J mol ⁻¹
U	peripheral speed	m s ⁻¹
U	heat transfer coefficient	W K ⁻¹ m ⁻²
v	volume	m ³
v	specific volume	m ³ kg ⁻¹
V	volume	m ³
V	molar volume	m ³ mol ⁻¹
V	voltage	V
v _{spec}	specific volume	m ³ kg ⁻¹
V _{an}	airflow required or neutral air volume	m ³ kg ⁻¹
V _{fn}	smoke developed or neutral volume of smoke	m ³ kg ⁻¹
W	specific mechanical energy	J kg ⁻¹
w	specific humidity	kg water kg ⁻¹ of dry air
W	power density	W kg ⁻¹
x	length	m
x	vapor quality	
x	mole fraction	
x	mole fraction in liquid phase (mixtures)	
x _h	specific exergy	J kg ⁻¹
x _q	specific heat-exergy	J kg ⁻¹
y	mass fraction	
y	mole fraction in vapor phase (mixtures)	
z	global mole fraction (mixtures)	
Z	compressibility factor	
z	altitude	m
d	exact differential	
δ	differential form	
Δ	variation	

Indices

a	related to admission
c	related to the critical point
c	corrected
c	related to compressor
c	cold
cc	related to combined cycle
d	related to availability
d	related to expansion
dg	related to the dry gas
f	related to fuel
g	related to the gas turbine
g	related to the gas phase
h	hot

i	related to inlet
l	related to the liquid phase
mm	related to the moist mixture
p	related to polytropic
p	related to products
r	reduced (relative to the critical value)
r	related to discharge
r	related to reactants
s	related to saturation
s	related to isentropic
s	related to the output
sat	related to saturation
t	total
t	related to the turbine
v	related to the steam cycle
vap	related to the vapor

Greek symbols

α	recycling factor	
α	Baumann coefficient	
β	annual CO ₂ emissions per electric kWh	kg kWh ⁻¹
δ	Rateau coefficient	
Δ	specific diameter	
ε	degree of reaction	
ε	relative humidity RH	
ε	effectiveness	
ε	steam fraction	
ε	volume ratio at the end and start of combustion	
ε	initial expansion ratio	
ε	roughness	m
ϕ	heat flux	J kg ⁻¹
γ	ratio of thermal capacities	
η	efficiency, effectiveness	
φ	flow factor	
λ	calorimetric coefficient	J m ⁻³
λ	volumetric efficiency	
λ	air factor	
λ	thermal conductivity	W K ⁻¹ m ⁻¹
λ	ratio of the combustion pressure to the compression pressure	
Λ	power factor	
μ	calorimetric coefficient	J bar ⁻¹
μ	Rateau coefficient	
μ	viscosity	kg s ⁻¹ m ⁻¹
μ_i	molar chemical potential	J mol ⁻¹
ω	acentric factor	
ω	rotation speed	rd s ⁻¹
π	heat created by irreversibilities	J kg ⁻¹
π_i	internal pressure ratio	

π	osmotic pressure	Pa or bar
θ	Carnot factor	
θ	ratio of the turbine inlet temperature to the compressor inlet temperature	
ρ	density	kg m^{-3}
ρ	volumetric compression ratio	
τ	specific shaft work	J kg^{-1}
τ	hydrogen utilization rate	
τ	optical efficiency	
τ	recirculation rate	
Ω	coefficient of work	
ξ	mass fraction of fuel burned	
ξ	temperature ratio in a Stirling engine	
ψ	enthalpy factor	

Acronyms

AACAES	Advanced Adiabatic Compressed Air Energy Storage
AATE	Affordable Advanced Turbine Engines
AFC	Alkaline Fuel Cell
AFR	air fuel ratio
AICVF	Association des Ingénieurs en Chauffage et Ventilation de France
API	American Petroleum Institute
ASHRAE	American Society of Heating Refrigeration and Air conditioning Engineers
AZEP	Advanced Zero Emission Process
BDC	bottom dead center
BWR	Boiling Water Reactor
CAES	Compressed Air Energy Storage
CC	combined cycle
CC	composite curve
CCHP	combined, cooling, heating, and power generation
CCS	Carbon capture and storage
CFB	circulating fluidized bed
CFDC	Carnot factor difference curve
CF	heat-power ratio
CFC	chlorofluorocarbons
CFC	cumulative frequency curves
CFR	Cooperative Fuel Research Committee
CHAT	Cascaded Humidified Advanced Turbine
CHP	Combined Heat and Power
CI	component irreversibilities
CLC	Chemical Looping Combustion
COP	Coefficient of Performance
CSTB	Centre Scientifique et Technique du Bâtiment
CT	combustion turbine
CTI	Cooling Technology Institute
DCS	distillation and condensation system
deNO _x	destructive nitrogen oxides
ECT	energy conversion technology
EGR	exhaust gas recirculation

EPC	main cryogenic stage
EPR	European Pressurized Reactor
GCC	grand composite curve
GDP	gross domestic product
GFR	gas cooled fast neutron reactor
GIF	Generation IV International Forum
GT	gas turbine
GT-MHR	Gas Turbine-Modular Helium cooled Reactor
GWP	Global Warming Potential
HAT	humid air turbine
HCFC	hydrochlorofluorocarbon
HFC	hydrofluorocarbons
HHV	higher heating value
HP	High pressure
HPES	hydro pneumatic energy storage
HRSG	Heat Recovery Steam generator
HT	high temperature
HTR	high temperature reactor
HX	heat exchanger
ICE	internal combustion engine
IGCC	integrated coal gasification combined cycle
IPCC	Intergovernmental Panel on Climate Change
IHX	intermediate heat exchanger
IMEP	indicated mean effective pressure
IP	intermediate pressure
IHPDET	Integrated High Performance Turbine Engine Technology
ISCCS	Integrated Solar Combined Cycle System
LFR	lead cooled fast neutron reactor
LPM	locus of minimum pinches
LHV	lower heating value
LMTD	logarithmic mean temperature difference
LNG	Liquefied Natural Gas
LP	low pressure
LT	low temperature
MCFC	Molten Carbonate Fuel Cell
MED	multi-effect desalination
MEP	mean effective pressure
MFP	mean friction pressure
MIEC	Mixed ionic-electronic conducting membrane
MIT	Massachusetts Institute of Technology
MON	motor octane number
MP	mean pressure
MPP	mean pumping pressure
MPS	solid rocket motor
MSF	Multi-stage flash desalination
MSR	moisture separator reheater
MSR	molten salt reactor
MSWI	Municipal Solid Waste Incinerator
MVC	mechanical vapor compression
NCG	non-condensable gases

NO _x	nitrogen oxides
NPSHR	Net Positive Suction Head Required
NRE	new and renewable energies
NTU	Number of Transfer Units
OECD	Organization for Economic Cooperation and Development
ODP	ozone depletion potential
WMO	World Meteorological Organization
OPEC	Organization of Petroleum Exporting Countries
ORC	Organic Rankine Cycle
OTEC	Ocean Thermal Energy Conversion
PAFC	Phosphoric Acid Fuel Cell
PBMR	Pebble Bed Modular Reactor
PC	pulverized coal
PC	parabolic collectors
PDU	productive and dissipative unit
PFBC	Pressurized fluidized bed circulating
PEMFC	Proton Exchange Membrane Fuel Cell
PF	pulverized fuel
PT	power towers
PT	parabolic trough
PWR	Pressurized Water Reactor
RO	reverse osmosis
PURPA	Public Utility Regulatory Policies Act
UNEP	United Nations Environment
R&D	research and development
RH	relative humidity
RON	research octane number
SCWR	supercritical water reactors
SEGS	Solar Electric Generating Systems
SFR	sodium cooled fast neutron reactor
SG	Steam Generator
SHF	sensible heat factor
SHR	sensible heat ratio
SI	systemic irreversibilities
SO _x	sulfur oxides
SOFC	Solid Oxide Fuel Cell
SRBC	steam recompression bottoming cycle
ST	steam turbine
STIG	steam injection gas turbine
STL	latent heat storage
TDC	top dead center
TEWI	total equivalent warming impact
THESE	Thermal Energy Storage of Electricity
THI	time horizon of integration
UHC	Unburned hydrocarbons
VHTR	very high temperature reactor
VOC	volatile organic compounds
WFBC	water flashing bottoming cycle

This page intentionally left blank

Conversion Factors

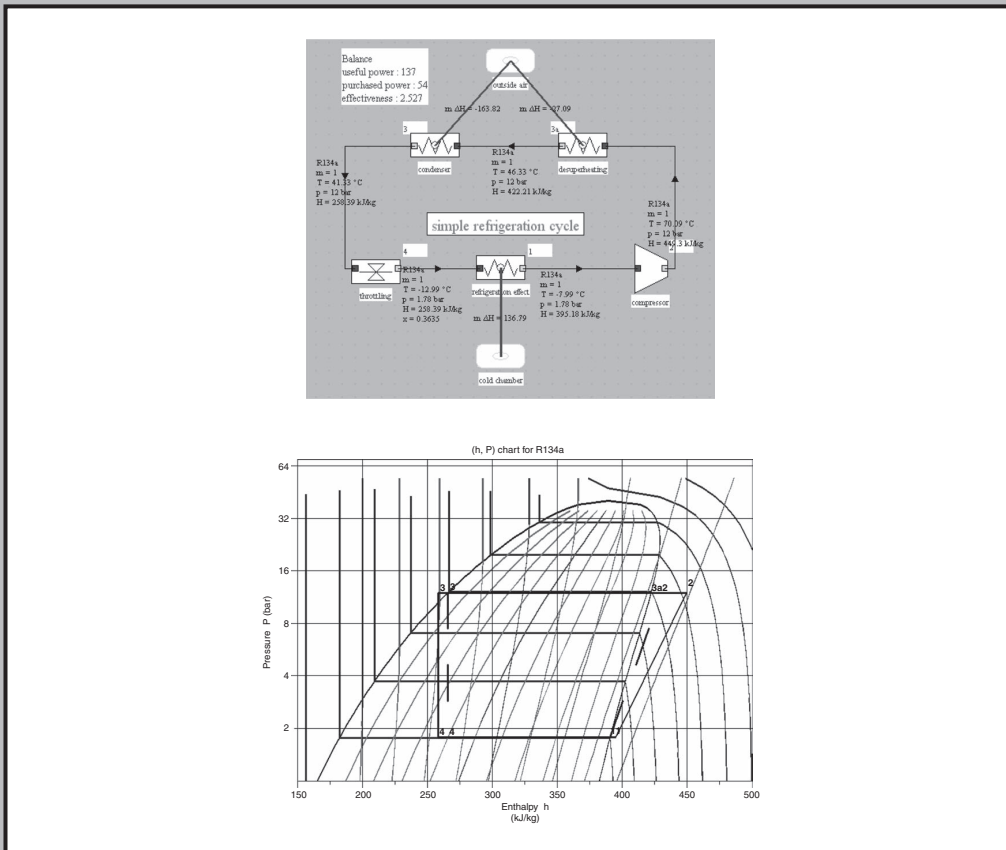
To obtain	Multiply	by	reverse factor
meter (m)	inch (in)	2.540000E-02	3.937008E+01
centimeter (cm)	inch (in)	2.540000E+00	3.937008E-01
meter (m)	foot (ft)	3.048000E-01	3.280840E+00
square meter (m ²)	square inch (in ²)	6.451600E-04	1.550003E+03
square centimeter (cm ²)	square inch (in ²)	6.451600E+00	1.550003E-01
cubic meter (m ³)	cubic foot (ft ³)	2.831685E-02	3.531466E+01
cubic meter (m ³)	cubic inch (in ³)	1.638706E-05	6.102376E+04
meter per second (m/s)	foot per second (ft/s)	3.048000E-01	3.280840E+00
meter per second (m/s)	inch per second (in/s)	2.540000E-02	3.937008E+01
meter per second (m/s)	kilometer per hour (km/h)	2.777778E-01	3.600000E+00
meter per second (m/s)	mile per hour (mi/h)	4.470400E-01	2.236936E+00
kilometer per hour (km/h)	mile per hour (mi/h)	1.609344E+00	6.213712E-01
radian per second (rad/s)	rpm (revolution per minute) (r/min)	1.047198E-01	9.549292E+00
gram (g)	ounce (oz)	2.834952E+01	3.527397E-02
kilogram (kg)	pound (lb)	4.535924E-01	2.204622E+00
kilogram per cubic meter (kg/m ³)	pound per cubic foot (lb/ft ³)	1.601846E+01	6.242797E-02
kilogram per cubic meter (kg/m ³)	pound per cubic inch (lb/in ³)	2.767990E+04	3.612730E-05
pascal (Pa)	pound-force per square foot (lbf/ft ²)	4.788026E+01	2.088543E-02
pascal (Pa)	pound-force per square inch (psi) (lbf/in ²)	6.894757E+03	1.450377E-04
pascal (Pa)	bar (bar)	1.000000E+05	1.000000E-05
pascal (Pa)	atmosphere, standard (atm)	1.013250E+05	9.869233E-06
watt (W)	British thermal unit per hour (Btu/h)	2.930711E-01	3.412141E+00
watt (W)	British thermal unit per second (Btu/s)	1.055056E+03	9.478170E-04
watt (W)	ton of refrigeration (12 000 Btu/h)	3.516853E+03	2.843451E-04
joule per kilogram kelvin [J/(kg · K)]	British thermal unit per pound degree Fahrenheit [Btu/(lb · °F)]	4.186800E+03	2.388459E-04
watt per square meter (W/m ²)	British thermal unit per square foot hour [Btu/(ft ² · h)]	3.154591E+00	3.169983E-01
watt per square meter (W/m ²)	British thermal unit per square foot second [Btu/(ft ² · s)]	1.135653E+04	8.805507E-05
joule per square meter (J/m ²)	British thermal unit per square foot (Btu/ft ²)	1.135653E+04	8.805507E-05

To obtain	Multiply	by	reverse factor
joule per cubic meter (J/m ³)	British thermal unit per cubic foot (Btu/ft ³)	3.725895E+04	2.683919E-05
joule per kilogram (J/kg)	British thermal unit per pound (Btu/lb)	2.326000E+03	4.299226E-04
joule per kelvin (J/K)	British thermal unit per degree Fahrenheit (Btu/°F)	1.899101E+03	5.265649E-04
watt per square meter kelvin [W/(m ² ·K)]	British thermal unit per hour square foot degree Fahrenheit [Btu/(h·ft ² ·°F)]	5.678263E+00	1.761102E-01
watt per square meter kelvin [W/(m ² ·K)]	British thermal unit per second square foot degree Fahrenheit [Btu/(s·ft ² ·°F)]	2.044175E+04	4.891949E-05
joule (J)	watt hour (W·h)	3.600000E+03	2.777778E-04
joule (J)	British thermal unit (Btu)	1.055056E+03	9.478170E-04
joule (J)	foot pound-force (ft·lbf)	1.355818E+00	7.375621E-01
kelvin (K)	degree Celsius (°C)	$T_K = t_{°C} + 273.15$	$t_{°C} = T - 273.15$
degree Celsius (°C)	degree Fahrenheit (°F)	$t_{°C} = \frac{t_{°F} - 32}{1.8}$	$t_{°F} = 1.8 t_{°C} + 32$
kelvin (K)	degree Fahrenheit (°F)	$T_K = \frac{t_{°F} + 459.67}{1.8}$	$T_{°F} = 1.8 T_K - 459.67$
kelvin (K)	degree Rankine (°R)	$T_K = \frac{T_{°R}}{1.8}$	$T_{°R} = 1.8 T_K$
degree Celsius (°C)	kelvin (K)	$t_{°C} = T_K - 273.15$	$T_K = t_{°C} + 273.15$

These values have been obtained from NIST Guide to the SI¹

¹ <http://physics.nist.gov/Pubs/SP811/appenB9.html>

First Steps in Engineering Thermodynamics



Part I, especially dedicated to beginners and fellow teachers, introduces in a very simple way basic concepts necessary to understand elementary thermodynamic cycles (steam power plants, gas turbines, refrigerators).

This page intentionally left blank



A New Educational Paradigm

Abstract: The change in education paradigm we have introduced is based on a shift of knowledge acquired by students. The writing of equations describing changes undergone by fluids is drastically reduced, the calculations being performed by a simulator such as ThermoOptim (www.thermooptim.org) without learners needing to know the details. They devote most of the time on the one hand learning technologies, and secondly reflecting on the architecture of both conventional and innovative thermodynamic cycles, graphically building and setting models of various energy technologies. This chapter introduces this new educational paradigm and software tools allowing one to implement it. The main pedagogic innovations brought by ThermoOptim are listed and a short comparison with other tools with teaching potential is made.

Keywords: education paradigm, ICT, initial training, vocational training, simulators.

1.1 INTRODUCTION

The teaching of applied thermodynamics has always been considered difficult, and recent developments have resulted in making this task even harder if one is content to use traditional approaches in this field.

We are indeed facing a new challenge, especially if we aim at making our students capable of handling today's problems that are more complex than those that their predecessors faced:

- initial training: to teach students with a lighter scientific background due to the evolution of programs, in a reduced number of hours;
- vocational training: this represents a growing stream of enrolled students, learners often do not have all the basics of mathematics and physics that are considered pre-requisites, and they do not have enough time to acquire them.

The classical approach being increasingly difficult to put into practice, many teachers try to change their teaching methods, but the task is difficult.

The educational use of Information and Communication Technology (ICT) including simulators may be the solution to this problem, insofar as it meets a number of rules, but it is not enough: we must also reconsider the content taught, especially for beginners.

We have developed over the past twenty-five years a new way of teaching thermodynamics applied to energy conversion, now used in more than one hundred and twenty higher education institutions, at both undergraduate and graduate levels (engineering schools, universities) or in vocational training.

This educational method has been gradually developed by the author when teaching at Mines ParisTech (École des Mines de Paris). As such, it stems in direct continuity from the courses offered by his predecessors, namely MM. Georges Brun, Professor from 1942 to 1968, and Paul Reboux, Professor from 1972 to 1992. It keeps in several places the presentational logic they found to be the most relevant, and which still remains valid.

However the proposed approach, which uses the ThermoOptim software, is original compared to the pedagogy that was in use in their time, and which obviously did not use the opportunities offered by ICT.

I.2 GENERAL REMARKS ON THE EVOLUTION OF TRAINING SPECIFICATIONS

The academic classical teaching in higher education is based on a disciplinary generalist deductive approach, which is to present a whole field of science and then to decline the applications of the discipline. Its advantage is that students thus trained are able, at the end of the course, to handle many problems and adapt to different situations, but such training requires a fairly long time and its cost is high.

It does not generally respond well to the needs of vocational training where a learner seeks to acquire as quickly as possible and at minimum cost a knowledge allowing him to solve a specific real-world problem without necessarily having any knowledge of the discipline. He is generally more reluctant to plunge into the theory, either because he has forgotten his studies dating back a while, or because he acquired his skills in the field without extensive scientific training.

What he seeks is a teaching method that goes to the essentials and provides him only with the answers to questions that interest him, minimizing the knowledge which has to be acquired, namely theoretical. He is often put off by the detours involved by the traditional disciplinary approach, which in any case his professional constraints do not allow him to follow.

Over the years, due to various changes both in society and more specifically in the energy sector, particularly related to its environmental impact and oil crises, the vocational training needs in the field of energy conversion have much increased.

The context of the initial training of engineers has also evolved considerably in recent years. Although their scientific and technical knowledge and ability to mobilize it to solve concrete problems are still among the features that continue to distinguish them most from other executives, like the latter they need more and more to pay attention to the non-technical dimensions of their job, i.e. people management, project economics, product marketing, environmental impact of technologies etc. In these circumstances, the time available to invest in technology and their motivation for doing so are now smaller than before. Moreover, the time devoted to technical subjects in the initial training programs of engineers is also declining gradually, practical work and projects being often the first sacrificed.

This evolution of the training specifications forces us to renew the pedagogies that we are implementing, but fortunately we also have new assets because of the existence of virtual environments, even if all these developments strongly challenge teachers and raise questions about their teaching in an area where they are most often almost completely self-taught.

I.3 SPECIFICS OF APPLIED THERMODYNAMICS TEACHING

The general remarks we have just made become particularly acute when considering the particular case of thermodynamics applied to energy.

Our approach has in fact originated in the difficulties we encountered when we began teaching the discipline: we found ourselves in a situation of failure against targets that we set and which traditional teaching approaches could not achieve, namely to make our students capable, at the end of the course, to address the current energy challenges: reducing the environmental impact of technology, improving efficiencies in acceptable economic conditions . . .

In caricature, one could say that traditional approaches are faced with a dilemma: the models which they lead to being either unrealistic, or incalculable. Given the difficulties in accurately estimating the thermodynamic properties of fluids, they usually lead to either making too simplistic assumptions, or adopting methods cumbersome to implement. This has two pitfalls that have the effect of demotivating students:

- the assumptions being too simplistic, they do not understand the practical relevance of the models they develop, these being very far from reality;
- the precise calculations of cycles being tedious, they are put off by the discipline.

Moreover, the time spent on the development of equations describing fluid properties and behavior of elementary components represents the bulk of the course, so that students can ultimately work only on basic discipline examples, without approaching the study of innovative cycles, for which they are not equipped in terms of methodology.

Conventional methods thus lead to many failures, whether in initial or vocational training, and our experience has shown that the approach we recommend, and which will be developed in this book, achieves much better results.

I.4 A NEW EDUCATIONAL PARADIGM

The change in education paradigm we have introduced is based on a shift in the knowledge acquired by students. The writing of equations describing changes undergone by fluids is drastically reduced, the calculations being performed by a simulator such as Thermoptim without learners needing to know the details. They devote most of the time on the one hand learning technologies, and secondly reflecting on the architecture of both conventional and innovative thermodynamic cycles, graphically building and setting models of various energy technologies.

A tool like Thermoptim can supplement the traditional teaching of thermodynamics in a wide variety of educational activities, which can be grouped into two main categories: those of discovery and initiation, including exploration of predefined models, and those of model building which relate to students seeking to learn how to model energy systems by themselves. Depending on the objectives and especially the time available, teachers can focus on either of these.

The screen of Figure 1.4.1 shows the 22 main equations which must be introduced in order to study, with reasonable accuracy, the performance of the simplest gas turbine in a conventional curriculum. It is of course possible to simplify, but the model becomes a caricature.

Equations describing the compression appear at the top left, and those for expansion in the upper right. These are the simplest.

The more complicated ones are at the bottom left: they determine the composition of exhaust gases at the combustion chamber outlet.

And yet, for simplicity, we have firstly considered here a very simple fuel and secondly have omitted to give the equation for calculating the end of combustion temperature, which is an implicit equation including an integral, one of the bounds of which is unknown.

In all cases, the gas properties require equations of the kind presented at the bottom of the figure. They are needed to calculate the energy properties of fluids put in.

All things considered, at least forty equations must be taken into account to obtain a realistic model of the gas turbine.

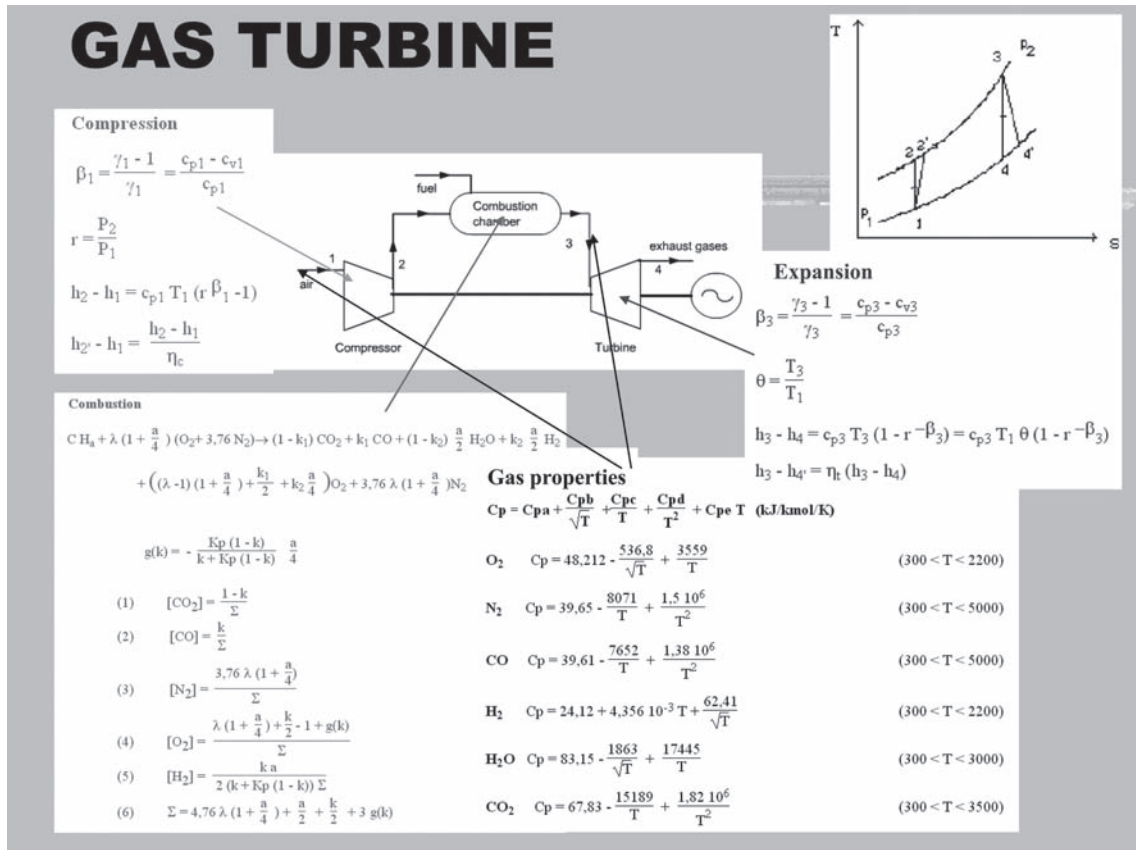


FIGURE 1.4.1
Conventional modeling of a gas turbine

Of course, even if each of the equations is known, the risks of error are numerous in the development of the model and its resolution, especially since they are interconnected and the resolution of some of them must be done iteratively.

Building a gas turbine model with Thermoptim is radically different from that which was traditionally implemented: we favor as we said a qualitative approach of phenomena, the calculations required for quantitative studies being conducted by software tools in a transparent manner for the learners, i.e. they have no need, at least initially, to know the details.

The use of equations is reduced to a minimum when introducing the discipline, the cognitive effort being mainly devoted to understanding concepts and technologies as well as their implementation, and it is only once the student has acquired sufficient knowledge of the discipline that we consider the writing of equations becomes possible and relevant.

Specifically, as shown in Figure 1.4.2, the model is constructed by assembling icons placed on a diagram editor working plan, the machine architecture being very close to its physical sketch.

Each component is then set with a small number of characteristic values. The thermodynamic properties of fluids being encapsulated in the software, computing performance presents no difficulty, giving much greater precision than with the traditional approach.

Using a tool like Thermoptim, the time to calculate a thermodynamic cycle is reduced to one-fifth or one-sixth of before, and once the model established it is possible to perform sensitivity analysis and resolve in minutes what would take hours by conventional methods.

In addition, there is no risk of programming error or incorrect reading of properties. This results in considerable time savings on one aspect of things not essential at the educational level, namely solving computational problems. Besides the time saved, the arduous nature of the work is greatly

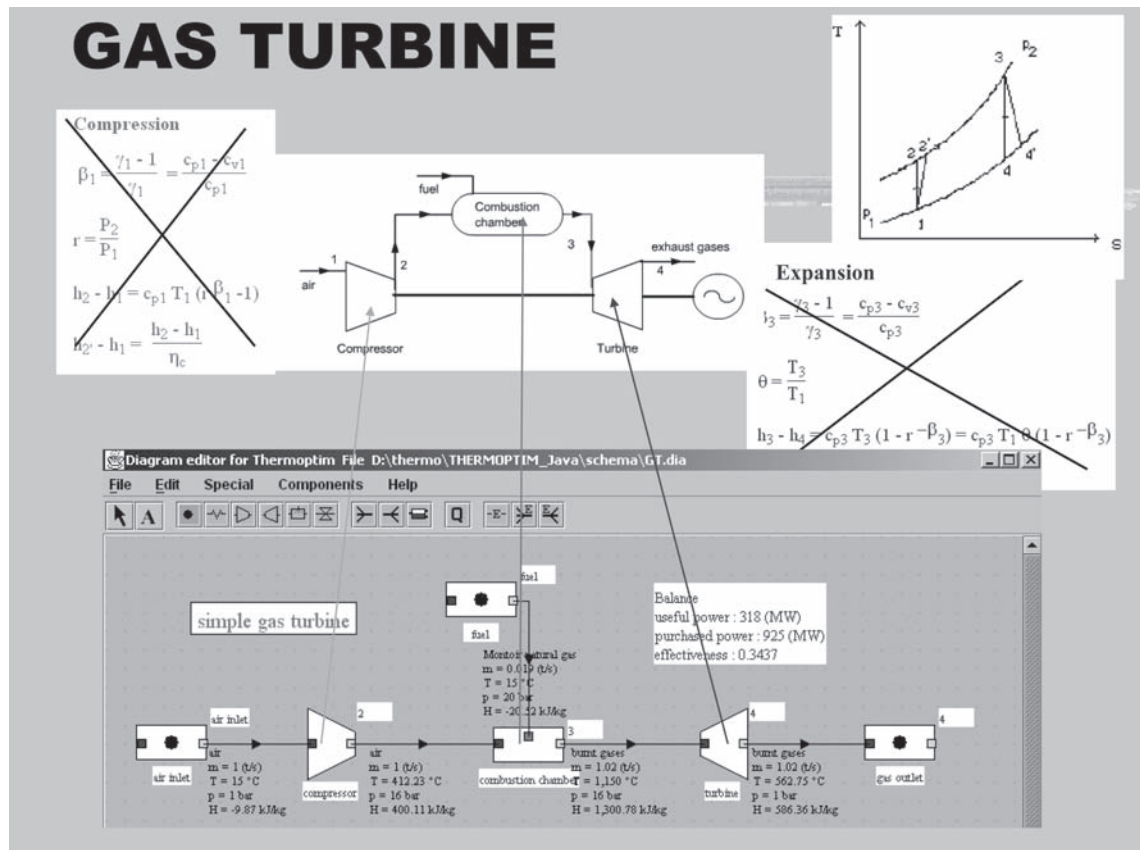


FIGURE I.4.2

Modeling with the new teaching method

reduced, resulting in a significant gain in student motivation, as they are no longer put off by cumbersome and tedious calculations.

Moreover, considerable gains in precision are obtained and thus in calculation likelihood: there is no need to resort to oversimplifying assumptions for the sole purpose of making possible the calculations. A typical example is the study of internal combustion engines, which to our knowledge are ultimately considered, in almost all lessons taught in undergraduate and graduate courses in the world, to be traversed by air assumed to be a perfect gas. How with such assumptions could we hope motivating students who today are concerned about the environmental impact of these technologies: an air engine has never polluted and will never pollute!

I.5 DIAPASON MODULES

Feedback from the ThermoOptim educational development showed there was an interest in complementing the simulator with other tools, in particular to introduce students to technology, which they largely ignore in their early learning.

Thus, since September 2004, ThermoOptim is supplemented by the Diapason modules (for Diaporamas Pédagogiques Animés et Sonorisés in French).

The Diapason modules (Figure 1.5.1) are educational animated slide shows, each provided with a soundtrack. This is Information and Communication Technology (ICT) applied to education. Using this ICT application, you may make presentations of theories, methodologies or technologies.

Copyright R. Gicquel 2004-2006

listen 1 mn 30 s pause

Session S26 Exercise simple steam cycle / Author : R. Gicquel / Date : 05/07/05

Steps

- Presentation of the exercise
- Steam power plant principle
- Steam power plants
- Steam power plant exercise
- Opening of ThermoOptim
- Creation of the model
- Creation of the economiser
- Creation of the first connexion
- Preliminary diagram
- Full diagram
- Diagram-simulator interface
- Diagram-simulator interface
- Setting model parameters
- Setting a point in the simulator
- Setting a process in the simulator
- Setting the parameters of a point
- Energy type choice in process
- Balance and synoptic
- Interface charts-simulator
- Setting an entropic chart
- Interface charts-simulator
- Cycle on (T,s) chart
- Cycle editor
- Final cycle on (T,s) chart
- Cycle on (h,P) chart
- Cycle on (h,s) chart
- Final summary

Steam power plants

Basic cycle (Rankine):

- compression 1-2 up to 80- 300 bars
- Heating up to about 560 °C
 - economiser 2-3a
 - evaporator 3a-3b
 - superheater 3b-3
- expansion 3-4'
- condensation 4'-1 at about 25 °C

FIGURE 1.5.1

Diapason module

These modules allow students to work by themselves at their own pace, alone or in groups, and access online at any time:

- the oral explanations given by the teacher in addition to written materials available to them;
- exercises using the simulator, which gives them the opportunity to familiarize themselves with the various cycles and their analysis methods.

These modules are structured in steps and sessions as well as in courses and programs. This gives rise to great possibilities in the conception of rich educational environments. Their specificity is the association of one soundtrack to the displayed slide. Thus, students may get audio explanations relative to the study context; these explanations may be about theory, or technology or even the practical use of the ThermoOptim simulator. Hyperlinks may give access to various documents such as spreadsheets or files in pdf format.

Based on double xml structure, these modules use as visual display a freeware Flash execution application supported by almost all recent Web navigators, which makes it possible to synchronize varied multi-media resources (images, sound tracks, pdf documents, swf animations, spreadsheets, hyperlinks, ThermoOptim etc.)

The principal interest of the Diapason modules is their excellent teaching effectiveness:

- When using these modules, students are more active than in the course room, in the sense that they regulate for themselves their rhythm of listening, but especially they choose for themselves the moments when they study, and are thus available when they do it; they learn better, more especially as they have any leisure to recap or to supplement information which is presented to them while resorting to the written documents;
- The sound tracks having an average duration of less than one minute, their attention can be constant when they study a step, and they pass to the following only after a rest period;

- The teacher can chain educational activities in a very flexible way, combining at best procedural and declarative knowledge so that the latter is provided contextually at the time when the student needs it;
- The students can work at their own rhythm, alone or in groups, and they have access constantly to the oral explanations given by the teacher; in case of doubt or if they missed anything, they can refer to it without any difficulty.

Although the simulator and the Diapason modules are used differently by different training institutions, their implementation usually results in the adoption of hybrid methods alternating presentational and online training sessions. The organization and conduct of training of this type induces an evolution in the role of the teacher towards more tutoring.

1.6 A THREE-STEP PROGRESSIVE APPROACH

This new method can in practice be divided into three main steps corresponding to a progression starting with a primarily qualitative and phenomenological approach, and finally leading some students to write complex equations:

1. The learning of basic concepts and tools, dedicated to reviewing basic thermodynamics concepts, to study basic thermodynamic cycles, to discover technologies and to learn how to use Thermoptim;
2. The reinforcement of the concepts viewed in step one, with theoretical complements concerning heat-exchangers and exergy, and the study of variations of basic cycles, combined cycles and cogeneration;
3. The in-depth analysis and personal practice regarding the study of innovative cycles, and some thoughts about the future of these technologies. These deep analyses and personal practice will concern mini-projects followed alone or within a group.

The first step is to enable students to acquire the basic vocabulary and understand the essential operating concepts, allowing them to implement these in simple cases; they become familiar with the new domain and start putting into practice available tools such as Thermoptim. In doing so, they get confidence in their ability to master the knowledge that they begin to acquire, thereby creating a virtuous circle in terms of motivation. Given the reputation of thermodynamics, this psychological aspect is far from negligible.

The second step enables them to anchor their knowledge by putting it into practice on the variants of elementary cycles, which allows them to make judgments about the performance criteria of real machines.

This leads to favor intuitive rather than axiomatic presentation of these concepts, with greater emphasis on qualitative and phenomenological understanding rather than on equations. This bias is all the more justified because rigid definitions require many precautions of language that may seem very cryptic to a beginner.

The first two steps are almost standard, even if their contents can vary slightly depending on the profile and prior knowledge of students: they allow students to acquire the basics of the discipline. They consist mainly of Diapason sessions that guide students step by step through the first lessons.

Gradually, as their understanding of the discipline grows, students gain autonomy and can use complementary digital resources, such as those of the Thermoptim-UNIT portal presented in the next section.

During the third step, students can customize their curriculum based on their interests and aspirations, and access methodology guides explaining how to tackle more difficult subjects. While previously they had very little interest in the internal functioning of components and in their

behavioral equations, they can if they wish start developing their own models by customizing the basic components available, or creating others.

I.7 MAIN PEDAGOGIC INNOVATIONS BROUGHT BY THERMOPTIM

The main pedagogic innovations brought by ThermoOptim are the following:

- First of all, as long and dull calculations are cancelled and most of the quantitative aspects are transferred to the computer, students have more time to train in essential thermodynamic qualitative and phenomenological notions and in technology;
- ThermoOptim is based on the distinction of some elementary concepts, called primitive types, whose structure helps the students to clearly understand inter-relationships;
- Using ThermoOptim, beginners learn the vocabulary and the basic concepts encapsulated in the displayed screens whose design has been very carefully developed making sure that their content is as simple as possible. Once the vocabulary is known, cooperative learning with other students and the teacher is intensified;
- The diagram editor gathers in a synthetic manner, on one screen, all the pertinent information about one thermodynamic cycle. The synoptic view displays the graphic structure of the system, the inter-connections between the components, the values of the thermodynamic state variables, the global energy balance of the system etc.;
- ThermoOptim is not only a very good courseware: it is also a powerful and professional simulator used by manufacturers such as EDF, CEA, Total or Areva-Framatome;
- ThermoOptim puts students' minds on a superior conceptual and methodological level as compared to traditional teaching. Therefore, there is not only a reduction of the cognitive load, but also a significant increase of the capacity to solve problems;
- Lastly, ThermoOptim makes students truly operational. This is an important element in their motivation and consequently in their attention.

I.8 DIGITAL RESOURCES OF THE THERMOPTIM-UNIT PORTAL

The success of our new teaching approach has attracted institutional support from first the Grande École Virtuelle project of the Group of Schools of Mines (<http://gemgev.industrie.gouv.fr/>), and then from the UNIT consortium (www.unit.eu), which helped develop many freely available digital resources for teaching energy issues. We wish to express our sincere thanks for their help thus provided.

With this support, in parallel with traditional book writing, we were able to develop multimedia presentations of some of the content of this work, dedicated for both training and scientific and technical information.

The set of digital resources for teaching energy we could muster was gradually integrated into a portal whose content is freely available, called ThermoOptim-UNIT (Figure 1.8.1). Its URL is: www.thermooptim.org.

These resources comprise seven main categories:

- thematic pages presenting theoretical or technological syntheses, which firstly are brief introductions to the discipline, and also refer to different learning activities (online courses, exercises etc.);
- methodological guides whose main objective is to sensitize the reader to the various issues raised and suggest some ways to find appropriate solutions;
- about seventy-five Diapason sessions, which represent a set of approximately 1,200 screens (85% with sound-track, i.e. 12 h of listening);

The screenshot shows the ThermoOptim-UNIT portal interface. At the top, there is a header with a circuit diagram and the text "unit universitè nationale ingènierie et technologie" and "La Thermodynamique appliquée aux systèmes énergétiques". Below the header is a navigation menu with items: "Thermodynamics basis", "Methodological guides", "Technologies", "Global issues", "Education", "Software", and "Glossary". On the right side of the header, there is a search bar and a "Login" button. The main content area is divided into several sections: "Last news" with a list of recent updates, "You are student?" with links for "Starting up", "FAQ, Glossary", "Self-learning modules (free access)", and "Sessions Diapason available"; "Teaching?" with links for "Discovery", "UNIT community", "ALET Club", and "Available resources"; "Other?" with links for "Simple guest", "Manufacturer", "Available documentation", and "Suggestions..."; and a large "Welcome to the ThermoOptim-UNIT portal!" section. The welcome section contains a detailed introductory text about the project's goals and the resources available.

FIGURE I.8.1

Portal welcome window

- written freely downloadable media (often excerpts from this book);
- guidance pages for practical works, which is a new educational resource type particularly interesting for two reasons: firstly they can provide students with personal activities of tutorials, exercises or projects, and secondly they help teachers to adapt and customize resources already developed;
- substance and component models, which allow us to represent substances or components not available in the ThermoOptim core, in order to simulate innovative energy systems, including low environmental impact, such as fuel cells, concentration solar power plants etc.;
- some papers relative to pedagogy in applied thermodynamics, including a number of references or web links that have been helpful in our own thinking. They are far from exhaustive but can provide an introduction to the subject for a number of fellow teachers.

Compared to the previous ones, this new 2011 edition thus presents the particularity to rely on all the ThermoOptim-UNIT portal digital resources, which we strongly recommend you to refer to (more specific references will be made in the text, as explained page xxiv of the preliminary pages).

I.9 COMPARISON WITH OTHER TOOLS WITH TEACHING POTENTIAL

To our knowledge, and apart from our own developments, the only currently available tools with teaching potential in this field with which ThermoOptim can be compared are as follows, and only the first two have been developed with a view to changing educational paradigms in applied thermodynamics:

- instructional software called CyclePad developed like an application of Qualitative Physics (Forbus & Whalley, 1994) to the teaching of thermodynamics, which has the advantage of being

- able to assist students in their training in thermodynamic cycles, thanks to an inference engine written in Lisp that is able to guide modeling and to make diagnosis of errors, but which has on the other hand significant limitations in its potential for application;
- instructional software called TEST (The Expert System for Thermodynamics), which is a collection of Java applets developed by S. Bhattacharjee (2003), of the California State University at San Diego;
 - software called Pinch (Favrat & Staine 1991), intended to illustrate thermal integration methods (see Chapter 22 of Part 3), developed at EPFL in Lausanne (Switzerland);
 - an equation solver intended for energy engineering (Klein & Alvarado, 1993, Mitchell & Braun, 2012), named EES (Engineering Equation Solver). It supposes, however, that the user is able to describe all the equations of the system which is to be studied, i.e. users are assumed to be able to quantify their problems as well as qualify them, which is seldom the case for a beginning student;
 - Cycle-Tempo, a computer program developed by TU Delft (Delft University of Technology) as a modern tool for the thermodynamic analysis and optimization of systems for the production of electricity, heat and refrigeration (<http://www.tudelft.nl>).

I.10 CONCLUSION

Thermoptim and the new teaching approach that it enables have been more and more adopted in higher education in France and worldwide: it has been estimated that in 2008 more than 120 institutions and more than 7000 students have used it for a total of approximately 57,000 student-hours.

This book will give numerous examples of the practical implementation of this new instructional paradigm.

Chapters 2 and 3 of this Part, titled First Steps in Thermodynamics (Absolute Beginners and Second Law), provide an illustration in the form of a lightweight educational presentation of thermodynamic basic cycles, initially without resorting to entropy and then by introducing entropy in a simple manner.

Their purpose is to discuss key concepts which should be presented to students in order to enable them to understand and study cycles of three basic energy technologies: steam power plant, gas turbine and refrigerating machine.

The idea is to minimize the background in mathematics and physics necessary for understanding these cycles, in order to make them accessible to readers unfamiliar with the language of specialists in thermodynamics. We show in particular that the essential concepts can be presented without resorting to a function that can be difficult to master (entropy), which is then introduced in the last chapter.

REFERENCES

- Mitchell J. W. & Braun J. E., Principles of HVAC in Buildings, John Wiley and Sons, Inc, January 2012.
- Forbus, K. & Whalley, P. (1994). Using Qualitative Physics to Build Articulate Software for Thermodynamics Education. Proceedings of AAAI-94. 1175–1182.
- Favrat, D. & Staine, F. (1991). “An Interactive Approach to the Energy Integration of Thermal Processes” CALISCE '91, EPFL.
- Klein, S.A. & Alvarado, F.L. (1993). EES Engineering Equation Solver, F-Chart Software, 4406 Fox Bluff Road, Middleton, Wisconsin 53562.
- Bhattacharjee S. (2003). The Expert System for Thermodynamics, A visual tour, Pearson Education Inc., Upper Saddle River, N. J., U.S.A., ISBN 0-13-009235-5.

2

First Steps in Thermodynamics: Absolute Beginners

Abstract: The purpose of this chapter is to discuss key concepts which should be presented to absolute beginners in order to enable them to understand and study the cycles of three basic energy technologies: steam power plant, gas turbine and refrigerating machine.

We are talking of lightweight educational presentation as we seek to minimize the background in mathematics and physics necessary for understanding these cycles, our goal being to make them accessible to readers unfamiliar with the language of specialists in thermodynamics. We show in particular that essential concepts can be presented without resorting to a function that can be difficult to master, entropy, which will be introduced only in the second part of this presentation.

The steam power plant and gas turbine are engines intended to convert heat into mechanical power, while the third cycle is a machine designed to extract heat at a temperature lower than the atmosphere thanks to a mechanical energy input.

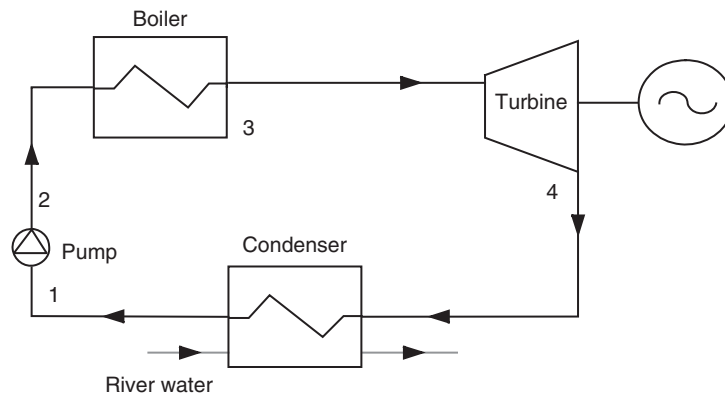
Keywords: lightweight educational presentation, steam power plant, gas turbine and refrigerating machine, thermodynamics work, heat exchange, enthalpy, first law of thermodynamics.

2.1 ARCHITECTURE OF THE MACHINES STUDIED

Let us begin with a brief description of the operation and architecture of these machines.

2.1.1 Steam power plant

The basic cycle of a steam power plant is essentially a boiler where the fuel (solid, liquid or gas) is burned for generating steam (usually superheated) which is then expanded in a steam turbine whose shaft provides the motor work (Figure 2.1.1).

**FIGURE 2.1.1**

Sketch of a steam power plant

The steam leaving the turbine is completely liquefied (water) in a condenser before a pump restores the boiler pressure. Since water is compressed in the liquid state, the compression work is almost negligible compared to the work recovered on the turbine shaft.

The condenser cooling is provided by an external cold source, usually the outside air or water from a river as shown in Figure 2.1.1.

The pump is generally centrifugal, multistage as it must provide a significant compression ratio.

The boiler has three successive functions and behaves thus like a triple heat exchanger. It must:

- heat pressurized feedwater (in the economizer) to the vaporization temperature corresponding to the pressure;
- vaporize steam;
- and finally superheat steam at the desired temperature.

Steam turbines are mostly multistage axial turbines.

The condenser is a heat exchanger whose particularity is to work at a pressure lower than the atmosphere, given the low vapor pressure of water at room temperature.

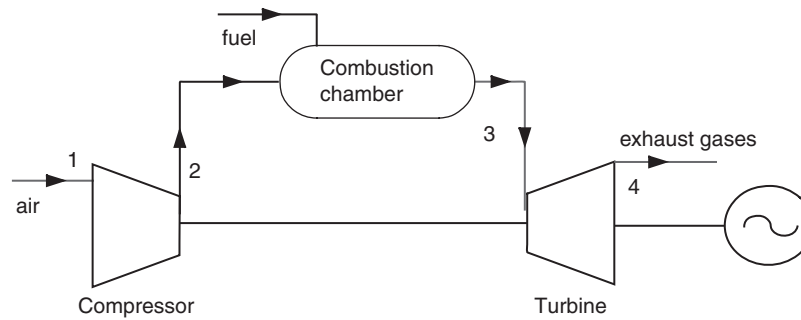
We speak of cycle because, going through the four successive plant components, the working fluid undergoes a series of processes that lead it to return in its original state.

More specifically, it is an external combustion cycle, allowing use of a variety of fuels (including uranium). In most countries, over 90% of the stock of thermal power plants until recently was composed of such plants.

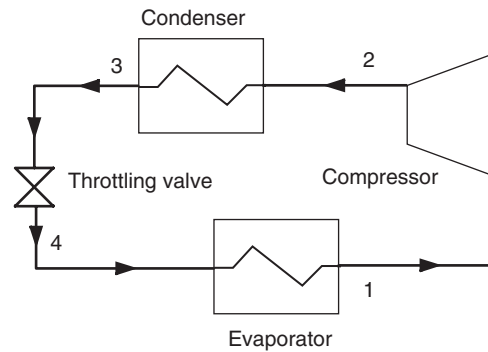
2.1.2 Gas turbine

In its simplest and most common form (Figure 2.1.2), a gas turbine is composed of three elements:

- a compressor, usually centrifugal or axial, which is used to compress the intake air at a pressure between 10 and 30 bar in modern machines;
- a combustion chamber in which fuel is injected under pressure, combusted with air previously compressed (the latter in large excess in order to limit the burnt gases temperature at the turbine inlet);
- a turbine, usually axial, in which are expanded the high temperature gases exiting the combustion chamber. A significant proportion (60–70%) of the recovered work on the turbine shaft is used to drive the compressor.

**FIGURE 2.1.2**

Sketch of a gas turbine

**FIGURE 2.1.3**

Sketch of a compression refrigeration cycle

In this form the gas turbine is a continuous stream internal combustion engine. Note that the gas turbine term comes from the status of the working fluid, which remains gaseous, and not the fuel used, which can be both gaseous and liquid (gas turbines typically use natural gas or light petroleum distillates).

To achieve compression ratios of 20 to 30, the compressor is multistage, with sometimes intermediate cooling to reduce the work consumed.

The combustion chamber is normally constructed of refractory alloy.

There are major technological constraints at the first stages of the expansion turbine, which are subject to the flow of burnt gas at high temperature. The parts most at risk are especially the rotor blades, which are very difficult to cool and in addition particularly sensitive to abrasion. It is therefore important to use a very clean fuel (no particles and chemicals that may form acids), and limit the temperature depending on the mechanical characteristics of the blades.

Exhaust gases being released into the atmosphere, it is inappropriate to speak of a cycle. However we do say it, in everyday language.

2.1.3 Refrigeration machine

In a refrigeration system (Figure 2.1.3), one seeks to maintain a cold chamber at a temperature below ambient. The idea is to evaporate a refrigerant at low pressure (and therefore low temperature) in a heat exchanger in contact with the cold chamber. For this, we need the refrigerant temperature to be lower than that of the cold chamber. The fluid is then compressed at a pressure such that its condensation temperature is greater than the ambient temperature. It is then possible to cool

the fluid by heat exchange with ambient air until it becomes liquid. The liquid is then expanded by isenthalpic throttling at low pressure and directed into the evaporator. The cycle is thus closed.

In a domestic refrigerator, the evaporator usually consists of two corrugated flat plates welded against each other, the refrigerant flowing in the channels formed by the corrugations. It generally lines the “freezing” compartment of the refrigerator (the frost layer forms on it). The plate between the flow channels operates as a fin to increase the thermal contact between the refrigerant and the cold compartment. This evaporator is connected to the rest of the machine by two tubes that cross the insulated wall. One of them is connected to the compressor suction, the other to the expansion valve.

The condenser is the black grill located on the refrigerator backside, consisting of coiled tubing supported by metal plates which firstly increase the heat exchange with the air, and secondly reinforce the mechanical rigidity. It is connected to the compressor outlet and expansion valve.

In most cases, the compressor is not directly visible because it is contained in a metal block mounted on rubber cushions to prevent vibrations, out of which exit an electric wire and two input and output fluid pipes. Such a compressor, generally of piston type, is called a hermetic compressor, which has the advantage that the engine is directly cooled and lubricated by the working fluid, without need for oil.

The expansion valve usually consists of a single capillary tube, and sometimes is a thermostatic valve.

2.2 FOUR BASIC FUNCTIONS

All three of these machines are crossed by thermodynamic fluids, steam or liquid water in the first, air and flue gases in the second, a refrigerant in the third.

What is particularly remarkable is that even if the technical solutions implemented are varied, as we have seen, these fluids are subjected to only four different types of processes:

- compression;
- expansion with work production;
- expansion without work production;
- temperature change (heating and cooling).

Therefore four functions are sufficient to describe the operation of these machines:

- compression can occur with the fluid being liquid or gaseous. In the first case the component is a pump, in the second a compressor;
- expansion with work production is generally made through turbines;
- expansion without work production in valves;
- heating can be generated either in combustion chambers or boilers, or in heat exchangers. Cooling is usually done in heat exchangers.

This finding has a very broad bearing: in all engines, the fluid is always successively compressed, heated, expanded and cooled, and, in all refrigeration cycles, it is compressed, cooled, expanded and heated.

Note finally, and this is very important in practice, that the flow of fluids through these components is either cyclical (in turbines, pumps and compressors), or continuous (in others).

In what follows, we will show how to characterize these processes in terms of thermodynamics. To do this we will focus on a small amount of fluid and we will seek to determine the evolution of its thermodynamic properties in these processes. In practical terms, it suffices to know what is called its state at the component inlet and outlet in order to calculate the performance of the entire machine.

2.3 NOTIONS OF THERMODYNAMIC SYSTEM AND STATE

It is necessary at this stage to introduce the concept of **thermodynamic system**, which represents a quantity of matter isolated from what we call the **surroundings** by a real or fictitious **boundary**. This system concept is very general in physics and is found especially in mechanics.

The notion of **state of a system** represents “the minimum information necessary to determine its future behavior”. This state is defined by what is called a set of state variables allowing us to completely characterize the system at a given moment.

In mechanics, the position coordinates and speed determine the state of a system.

In thermodynamics, there are obviously several sets that meet this definition. The ones most used in the literature are the following pairs: (pressure, temperature), (pressure, volume), (temperature, volume).

A **state function** is a quantity whose value depends only on the state of the system, not its history.

In thermodynamics, we are led to distinguish two types of systems: **closed systems** that do not exchange matter with the surroundings, and **open systems** that do exchange.

The presentation made earlier of the operation of components involved in the machines we want to study has shown that they operate in open systems, as fluids pass through them.

This distinction is important because thermodynamic properties are expressed differently in closed and open systems.

2.4 ENERGY EXCHANGE BETWEEN A THERMODYNAMIC SYSTEM AND ITS SURROUNDINGS

It is essential to note that thermodynamic systems involved in the components we are interested in, only exchange energy with the surroundings in **two** distinct forms:

- heat by heat exchange on the system boundaries. It is usually denoted by Q ;
- work, by action of pressure forces on the boundaries, the work of gravity forces being neglected.

This work is usually denoted W in closed and τ in open systems.

One can also easily show that in an open system, for an infinitely small change, τ and Q are given by the following equations:

$$\delta\tau = v dP \quad 2.4.1$$

$$\delta Q = C_p dT - v dP \quad 2.4.2$$

The latter expression simply expresses an experimental fact, which is an essential basis of compressible fluid thermodynamics: heat δQ exchanged with the surroundings is reflected in a linear change in the thermodynamic state of the system.

2.5 CONSERVATION OF ENERGY: FIRST LAW OF THERMODYNAMICS

The fundamental law that governs the behavior of thermodynamic systems is the conservation of energy, known as the first law.

For a closed system, it can be stated as follows: the energy contained in a system which is isolated, or evolving in a closed cycle, remains constant whatever processes it undergoes. The various forms that the energy of a system can take: mechanical energy, heat energy, potential energy, kinetic energy, are all equivalent under the first law. Let us recall that, in our case, only heat and work are taken into account.

Calling W the work of external pressure forces and Q the heat exchanged with the surroundings, and neglecting the kinetic energies brought into play, the first law can be written for a closed system in the form:

$$\Delta u = W + Q \quad 2.5.1$$

u is an extensive quantity called the internal energy of the system. It is a state function.

In this form, this law is very intuitive and readily accepted: it is a conservation law which states that energy (like mass) is neither lost nor created.

The internal energy, however, has meaning only if the system is closed, and needs to be generalized when considering a system in which matter enters and/or out of which it flows.

The work W exerted on a closed system can indeed be broken into two parts: one that is exerted on the mobile walls of the system if any, called shaft work τ , and one that is exerted on boundaries crossed by fluid coming out of the system and entering it. For open system components, which is the case for those that we are studying, this work, called transfer work, equals $-\Delta(Pv)$.

We therefore have: $W = \tau - \Delta(Pv)$

Introducing a function called enthalpy h , such as $\Delta h = \Delta u + \Delta(Pv)$, the first law is written in open systems:

$$\Delta h = \tau + Q$$

The first law is expressed as follows in open systems: the enthalpy change of an open system is equal to the amount of shaft work exerted on the moving walls and heat exchanged with the surroundings.

Enthalpy thus appears simply as a generalization in open systems of the internal energy of closed systems. In practical terms, just consider this state function as the energy associated with the system under consideration, neither more nor less.

2.6 APPLICATION TO THE FOUR BASIC FUNCTIONS PREVIOUSLY IDENTIFIED

We will show in this section that the enthalpy variation of the fluid flowing through them is sufficient to determine the energy involved in these four elementary processes.

2.6.1 Compression and expansion with work

Expansion can be made with and without work. In the first case, the machine most commonly used is the turbine. In the second case, it is a simple valve or a filter (see section 2.6.2).

Machines doing the compression or expansion of a fluid have a very compact design for reasons of weight, size and cost. For similar reasons, they rotate very fast (several thousand revolutions per minute). Each parcel of fluid remains there very briefly.

Moreover, fluids brought into play in compressors and turbines are often gas whose heat exchange coefficients have low values.

Short residence time, small areas of fluid-wall contact, and low exchange coefficients imply that the heat exchange is minimal and that **the operation of these machines is nearly adiabatic: $Q = 0$.**

In a compression or expansion adiabatic machine, shaft work τ is thus equal to the change in enthalpy of the fluid Δh .

2.6.2 Expansion without work: valves, filters

There is a class of devices, such as the expansion valve of the refrigeration machine, where τ and Q are both zero, i.e. $\Delta h = 0$: they are static expanders such as valves and filters. The corresponding process is called an **isenthalpic throttling** or a **flash expansion**.

2.6.3 Heat exchange

Components which transfer heat from one fluid to another require large exchange areas, their heat fluxes being proportional to these areas. Technical and economic considerations lead to the adoption of purely static devices. For example, large bundles of tubes in parallel, traversed internally by one fluid while the other flows outside.

τ is zero because of the absence of movable walls.

In a heat exchanger, heat Q transferred or provided by one fluid to another is equal to its enthalpy change Δh .

2.6.4 Combustion chambers, boilers

In a combustion chamber or boiler, there are no movable walls either, and $\tau = 0$.

Heat Q transferred to the fluid passing through is equal to the enthalpy change Δh .

2.7 REFERENCE PROCESSES

The previous section showed that the determination of the enthalpy change of the fluid flowing through them is enough to calculate the energy involved in these four elementary processes.

But this information is not sufficient to characterize them completely. The physical analysis of their behavior helps to highlight the **reference processes** corresponding to the operation of components that would be ideal.

It is then possible to characterize the actual process by introducing an imperfection factor, often called effectiveness or efficiency, which expresses its performance referred to that of the reference process. This way makes it much easier to understand the processes undergone by the fluid.

The choice of reference processes is based on analysis of physical phenomena that take place in the components: **it is an absolutely essential modeling choice.**

Lastly, as we shall see, the reference process is very useful when trying to plot the cycle studied on a thermodynamic chart.

2.7.1 Compression and expansion with work

In section 2.6.1 we saw that the compressors and turbines are machines in which heat exchanges with the outside are usually negligible; this is referred to as adiabatic. The reference process for compression or expansion with work is the perfect or reversible adiabatic. Its equation can be obtained by integrating the differential equation expressing that the heat exchanged is zero at any

time, i.e. $0 = C_p dT - v dP$. For a perfect gas, for which $Pv = rT$, the corresponding curve is easily obtained. It is given by law $Pv^\gamma = \text{Const.}$ with $\gamma = C_p/C_v$.

2.7.2 Expansion without work: valves, filters

For throttling or expansion without work conserving enthalpy ($\Delta h = 0$), the reference process is isenthalpic.

2.7.3 Heat exchange

As a first approximation, as the pressure drops are relatively low, heat exchange can be assumed to be isobaric. The reference process is thus isobaric.

2.7.4 Combustion chambers, boilers

Similarly, combustion chambers and boilers can usually be regarded as isobaric. Combustion takes place at constant pressure, therefore, which still surprises a number of students, who believe that the combustion raises pressure, even in open systems.

To illustrate this, consider a fairly common example of boiler: a wall-mounted gas boiler in an apartment. The pressure will remain the same in both fluids, whether the hot water circuit at a pressure of 1 to 3 bar, or air circuit and smoke, at atmospheric pressure of course.

2.8 SUMMARY REMINDERS ON PURE SUBSTANCE PROPERTIES

Let us recall that a pure substance can be in one or more of three phases: solid, liquid or gaseous. When heating a liquid it turns to vapor, and we talk of vaporization. The temperature at which this change is realized depends on the pressure exerted on the substance considered. It remains **constant** as long as the vaporization is not complete, i.e. while its quality x is between 0 and 1. Let us recall that x is defined for a pure substance two-phase mixture as the ratio of vapor mass to total mass (vapor + liquid).

For this phase change to happen, it is necessary to provide or absorb energy, called **latent heat of change of state**. During the change of state, there are significant variations in the specific volume, the vapor being about 600 to 1000 times less dense than the liquid. This change in specific volume occurs at **constant pressure and temperature**.

The **critical point** represents the state where the phase of pure vapor has the same properties as the pure liquid phase. At higher temperatures and pressures (supercritical), it is not possible to observe a separation between liquid and gas phases: the disk surface which separates the liquid and vapor phases disappears at the critical point.

We call an ideal gas a gas whose internal energy and enthalpy depend only on the temperature, which simplifies the modeling: its equation of state is $Pv = RT$.

Many thermodynamic fluids in the vapor phase may be treated as ideal gases in a wide range of temperatures and pressures. This requires that the temperature-pressure combination deviates from the condensation zone as much possible (that is to say that the pressure is not “too” high or the temperature “too” low). Such conditions are commonly the case for gases known as “permanent”

at ambient temperature and pressure, as hydrogen, oxygen, nitrogen, the oxygen-nitrogen mixture that is dry air etc.

2.9 RETURN TO THE CONCEPT OF STATE AND CHOICE OF STATE VARIABLES TO CONSIDER

Now that we have introduced the first law, established its equation for open systems and showed just how it applies to the four basic changes experienced by fluids in machines that interest us, we can discuss the advantages and disadvantages of different state variables that one can consider using.

We have seen that several sets of state variables can be used to characterize a thermodynamic system. The most “natural” are temperature, pressure and volume, but there are others, like the enthalpy just defined, and secondly they are not fully satisfactory for our goals, as we shall show.

Pressure P is essential, both because it directly determines the mechanical stress of components, and because, as we have seen, the reference process for fluid heating and cooling is isobaric.

Temperature T is also essential, but, unlike its predecessor, the isothermic process does not correspond to any process that concerns us.

Moreover, the pair **(P , T)** is not sufficient to represent the process experienced by a fluid as it changes state, the two variables being linked by the saturation pressure or temperature law: it lacks the vapor quality x .

Volume v intervenes very little in the analysis of interest, even in a closed system, because volume varies due to the existence of movable walls. In fact, its main practical interest is in the sizing of flow sections.

Enthalpy h is a fundamental variable too, because it is directly related to energy exchanges that take place in the machines. For an ideal gas, it is a linear function of temperature, very easily deduced, and in the liquid-vapor equilibrium zone, it provides additional information on the quality. Finally, remember that the isenthalpic process is the reference process for an expansion without work.

For our purposes, as part of this lightweight educational presentation, these remarks are sufficient to allow us to conclude that the pair **(P , h)** is a set of state variables of particular interest. We shall see the implications when we seek to plot the cycles of the machines we are studying in thermodynamic charts.

The analysis of processes undergone by fluids during compression and expansion with work showed that their reference process is reversible adiabatic. We indicated that for a perfect gas it follows law $Pv^\gamma = \text{Const}$.

Let us note, but incidentally given our focus for simplicity, that this law is that of the **isentrope**. **Entropy s** is also a state function widely used in thermodynamics, especially because the isentrope is the reference process for compression and expansion.

2.10 THERMODYNAMIC CHARTS

Thermodynamic systems which we consider can be characterized by two state variables; they are called bivariant. This means that their thermodynamic properties can be plotted in a plane in the form of a thermodynamic chart.

By highlighting the reference process of changes undergone by fluids and allowing us to calculate them, at least approximately, charts are among the basic tools of thermodynamics. Their interest is twofold:

- to help plot the cycles;
- to facilitate the estimation of the thermodynamic state of the various cycle points.

Because of the possibilities offered by software packages for calculating fluid properties that are increasingly common, the second interest tends to decline while the former retains its relevance. The display on a chart of a cycle calculated using a computerized tool helps ensure that it does not contain an abnormal point due to an error when entering data.

A chart is presented in a graphical map with the plot of a number of remarkable curves, including families of state function iso-values.

2.10.1 Different types of charts

In practical terms, the main processes that can occur in industrial processes involving pure fluids are, as we have seen, compression, expansion, heat exchange and throttling.

It is clear that the temperature T , pressure P and the steam quality x are state variables whose knowledge is necessary to study these processes and equipment design.

The above remarks show that the enthalpy h is also very important. Finally, knowledge of the specific volume v is necessary to size the pipes, since it allows us to convert mass flow rate into volume rate.

In conclusion, the most interesting quantities are in practice T , P , h , and additional information on x and v may be necessary. So the abscissas and ordinates of the charts that we can consider should be chosen among them (recall that we exclude here the entropy).

The pair (T, h) is rarely retained because the isobaric and reversible adiabatic are represented by curves with inflection points that make their use difficult. In addition, variations of T and h are proportional when the fluid follows the ideal gas law.

Except for permanent gases, i.e. whose state is very far from their saturation conditions, the pair (T, P) is insufficient, because T and P are bound by the saturation law in the liquid-vapor equilibrium zone. It would however be quite suitable to represent gas turbine cycles.

The pair (P, h) is increasingly used, usually with a logarithmic scale for pressures. Its widespread use has been promoted by refrigeration engineers, and it will be studied further.

Finally, the pair (P, v) , Clapeyron chart, has a certain educational value, especially for the study of changes in closed systems. Its main drawback is its low visibility, the area of vapors being reduced and energy functions not appearing directly.

In conclusion, as this lightweight educational presentation does not include entropy, the pair (P, h) appears the best suited.

2.10.2 $(h, \ln(P))$ chart

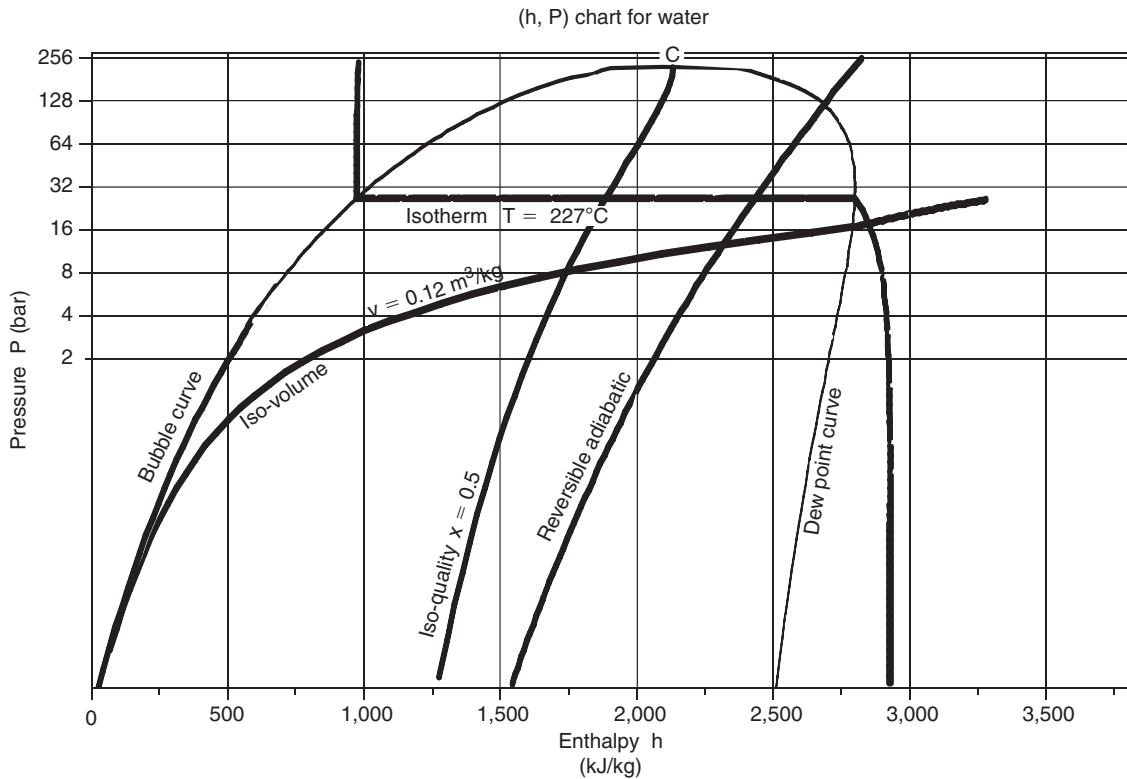
In the $(h, \ln(P))$ chart (Figure 2.10.1) the enthalpy is the abscissa and pressure the ordinate, usually on a logarithmic scale.

The saturation curve separates the plane in several zones. Its summit is the critical point C , the left side, bottom, representing the incipient boiling (bubble curve), and its right side down, the saturated vapor (dew point curve). Under this curve is the two-phase liquid-vapor equilibrium zone, and in the rest of the plan, that of simple fluid.

For this chart to be used, it is equipped with reversible adiabatic curves, isotherms, isovolumes, and in the mixed zone, iso-quality curves.

In the “liquid” zone on the left of the chart, isotherms have a very strong negative slope: the compression of a liquid involves a very small work.

In the two-phase zone, pressure and temperature are related by the law of saturation pressure, and isotherms are horizontal. The enthalpy increases enormously, corresponding to the heat of vaporization that must be supplied to the fluid.

**FIGURE 2.10.1**

Water (h, ln(P)) chart

In the zone to the right of the saturation curve, the isotherms are curved downward, close to vertical for values of low pressure. Indeed, the behavior of vapor then approaches that of an ideal gas, whose enthalpy depends only on temperature.

Heating or cooling (isobars) are reflected in this chart by a horizontal segment, an expansion without work (isenthalpic) by a vertical segment.

A reversible adiabat is an upward curve with a slope equal to the inverse of specific volume. They are much less inclined in the vapor zone than in the liquid zone.

Iso-quality curves are contained inside the liquid-vapor equilibrium zone. They intersect at the critical point.

Iso-volume curves converge in the liquid zone where they become independent of pressure.

2.11 PLOT OF CYCLES IN THE (h, ln(P)) CHART

We will now explain how to draw in the (h, ln(P)) chart the steam power plant and refrigerating machine cycles. We assume initially that the compressions and expansions are perfect, that is to say they follow the reversible adiabat, then we shall explain how to take into account the irreversibilities in these machines.

In practical terms, students should do the proposed activities in this section by hand, with diagrams on paper. These can either be printed directly from Thermoptim, but their accuracy is not great, or obtained commercially or in literature.

We have not yet specified the numerical data for these cycles. We shall do it now, selecting values which can be easily plotted, and build them step by step in this chart.

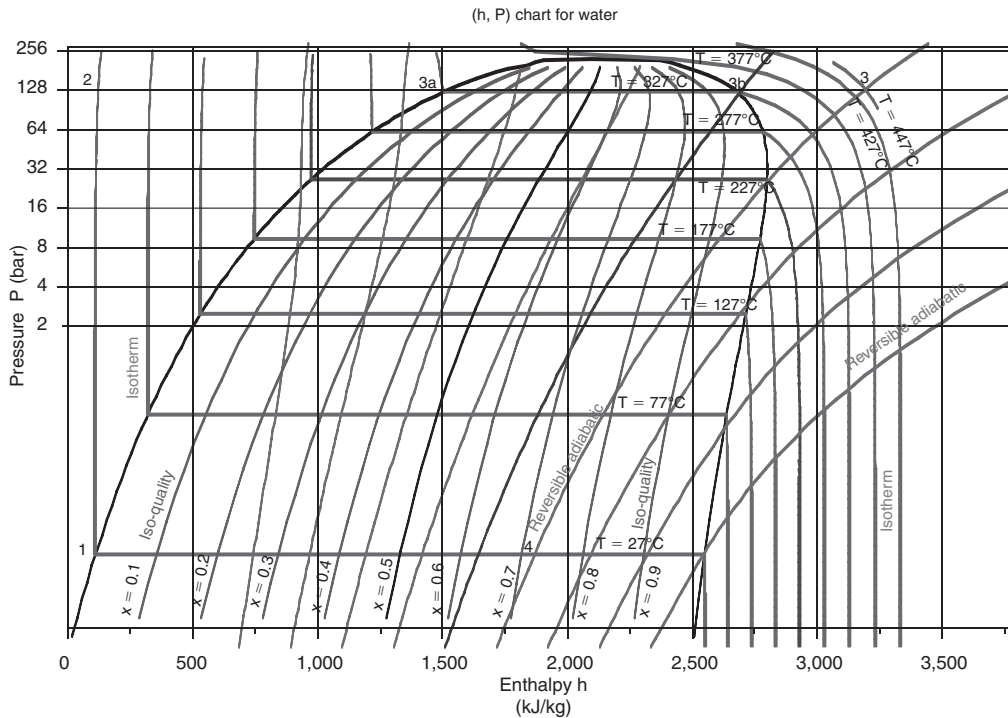


FIGURE 2.11.1
Construction of the steam power plant cycle

We will not seek to represent the gas turbine cycle for two reasons: firstly because the gas ($h, \ln(P)$) charts are little used in practice, and secondly because to estimate the thermodynamic properties of combustion products requires special care. In our opinion it is much easier for a beginner to directly model the machine with a tool such as Thermoptim as shown section 2.12, and the plot of the cycle in a chart is not always needed.

2.11.1 Steam power plant

At the condenser outlet (point 1, Figure 2.1.1), water is in the liquid state at a temperature of about 27°C , under low pressure (0.0356 bar). In Figure 2.11.1, the point is easy to find, at the intersection of the isotherm $T = 27^\circ\text{C}$ and the saturation curve.

The pump compresses water at about 128 bar, which represents a significant compression ratio (around 3600).

The temperature T remaining approximately constant during compression (1-2), point 2 is located at the intersection of the isotherm $T = 27^\circ\text{C}$ and the isobar $P = 128$ bar (ordinate 128 bar).

The pressurized water is then heated at high temperature in the boiler, heating comprising the following three steps:

- liquid heating from 27°C to about 330°C boiling point at 128 bar, just above isotherm $T = 327^\circ\text{C}$: process (2-3a). Point 3a lies on the vaporization curve at the same isobar;
- vaporization at constant temperature 330°C : process (3a-3b). Vaporization being carried out at constant pressure and temperature, it results on the chart in a horizontal segment 3a-3b. Point 3b is therefore on the descending branch of the vaporization curve, or dew point curve, at its intersection with the horizontal line of pressure 128 bar;

TABLE 2.11.1
ENTHALPY BALANCE OF SIMPLE STEAM CYCLE

Point	Flow-rate (kg/s)	h (kJ/kg)	
1	1	113	
2	1	126	
3a	1	1524	
3b	1	2672	
3	1	3189	
4'	1	1870	
Process	τ (kW)	Q (kW)	Δh (kW)
(1-2)	13		13
(2-3a)		1398	1398
(3a-3b)		1148	1148
(3b-3)		517	517
(3-4)	-1319		-1319
(4-1)		-1757	-1757
cycle	-1306	1306	
energy efficiency		42.64%	

- superheating from 330°C to 447°C, process (3b-3). Point 3 is still assumed to be the same pressure, but at a temperature T_3 of 447°C. It is thus at the intersection of the horizontal $P = 128$ bar and the isotherm $T = 447^\circ\text{C}$ (only partially shown in the figure).

Point 3 is also on an inclined downwards concave curve corresponding to a reversible adiabatic.

Process (3-4) is a reversible adiabatic expansion from 128 bar to 0.0356 bar. The point being in the mixed zone, the latter is within isotherm $T = 27^\circ\text{C}$. Point 4 is at the intersection of the inclined downwards concave curve and this isotherm. Quality x is between 0.7 and 0.8. Linear interpolation allows us to estimate its value, equal to 0.72.

The enthalpies of the points can be read directly by projecting these points on the x-axis, and the energies involved can be easily deduced. This allows us in particular to determine the cycle efficiency. Table 2.11.1 provides these values.

Note that reading the compression work in this chart is very imprecise and it is best estimated from the integration of $\delta\tau = v dP$, very easy to make, v being constant. It is therefore $\Delta h = v \Delta P$, P being expressed in Pa, v in m^3/kg and h in J.

As shown in this example, the representation of the cycle in the $(h, \ln(P))$ chart is very easy to understand: the heat exchanges, almost isobaric, correspond to horizontal segments, and the compression and expansion are reversible adiabatic, less steep as they are located far from the liquid zone. Figure 2.11.2 shows the cycle in the chart, the points being connected.

The efficiency here is the ratio of the mechanical work produced to the heat supplied by the boiler.

In reality, the turbine is not perfect, and expansion follows an irreversible adiabatic. It is customary to characterize the actual process by its isentropic efficiency η defined in the case of a turbine as the ratio of actual work to the reversible expansion work. Its value is typically about 0.85 to 0.9 in current applications.

To find the real point 4', we first determine the value of the perfect machine work τ_s , then we multiply it by η , which gives the value of real work τ .

The enthalpy of point 4 is equal to that of point 3 minus τ .

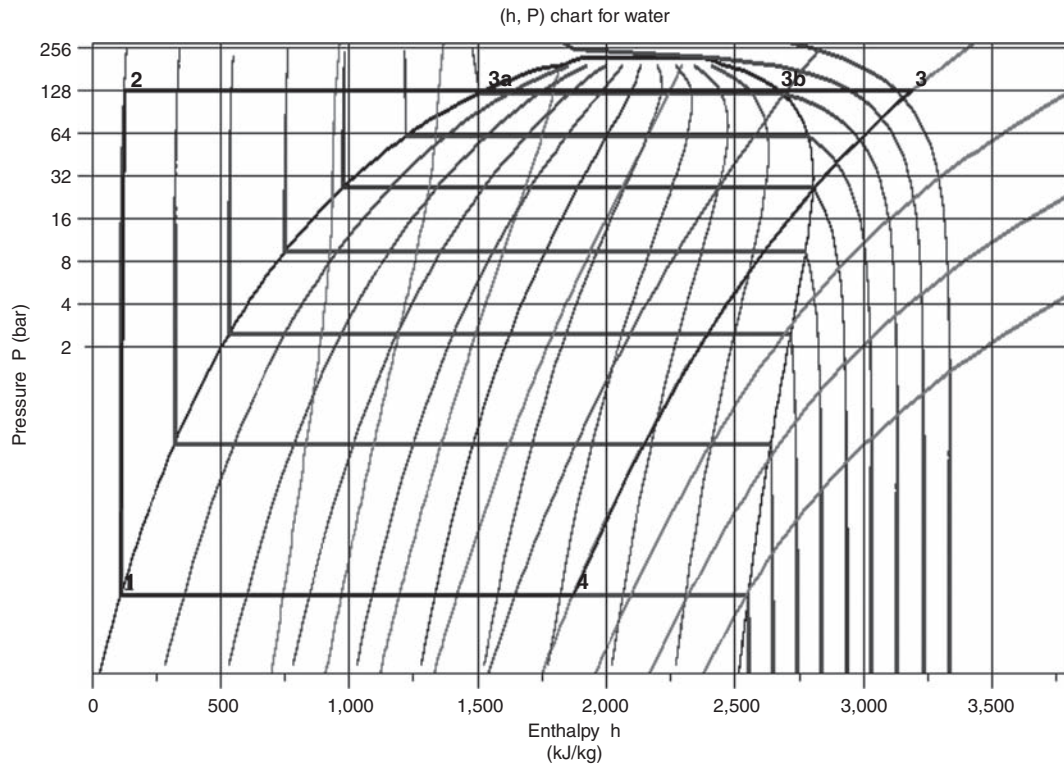


FIGURE 2.11.2
Steam power plant cycle in the $(h, \ln(P))$ chart

In this case, taking $\eta = 0.9$, we have:

$$\begin{aligned} \tau_s &= h_3 - h_4 = 1319 \text{ kJ/kg/K} \\ \tau &= \eta \tau_s = 0.9 \times 1319 = 1187 \\ h_{4'} &= 3199 - 1187 = 2002 \text{ kJ/kg/K} \end{aligned}$$

Point 4', which is still in the liquid-vapor equilibrium zone, is thus on isobar $P = 0.0356$ bar, i.e. on isotherm $T = 27^\circ\text{C}$ with abscissa $h = 2002$ kJ/kg/K. Figure 2.11.3 shows the new look of the cycle (the previous cycle is plotted in dashed line).

Here we have not considered the pressure drops in heat exchangers. It would of course be possible to do so by operating on the same principle as described, and changing the pressure between the inlets and outlets of heat exchangers.

2.11.2 Refrigeration machine

The R134a compression refrigeration cycle operates between a suction pressure of 1.78 bar and a condenser pressure of 12 bar.

At the evaporator outlet, the fluid is fully vaporized and thus point 1 (see Figure 2.11.4) is located at the intersection of the saturation curve and the isobar $P = 1.78$ bar, or, equivalently, the isotherm $T = -13^\circ\text{C}$.

It is then compressed at 12 bar along a reversible adiabatic. Point 1 being located approximately one third of the distance between two reversible adiabats on the chart, it is possible, by linear interpolation, to determine point 2 on isobar $P = 12$ bar, between these two curves.

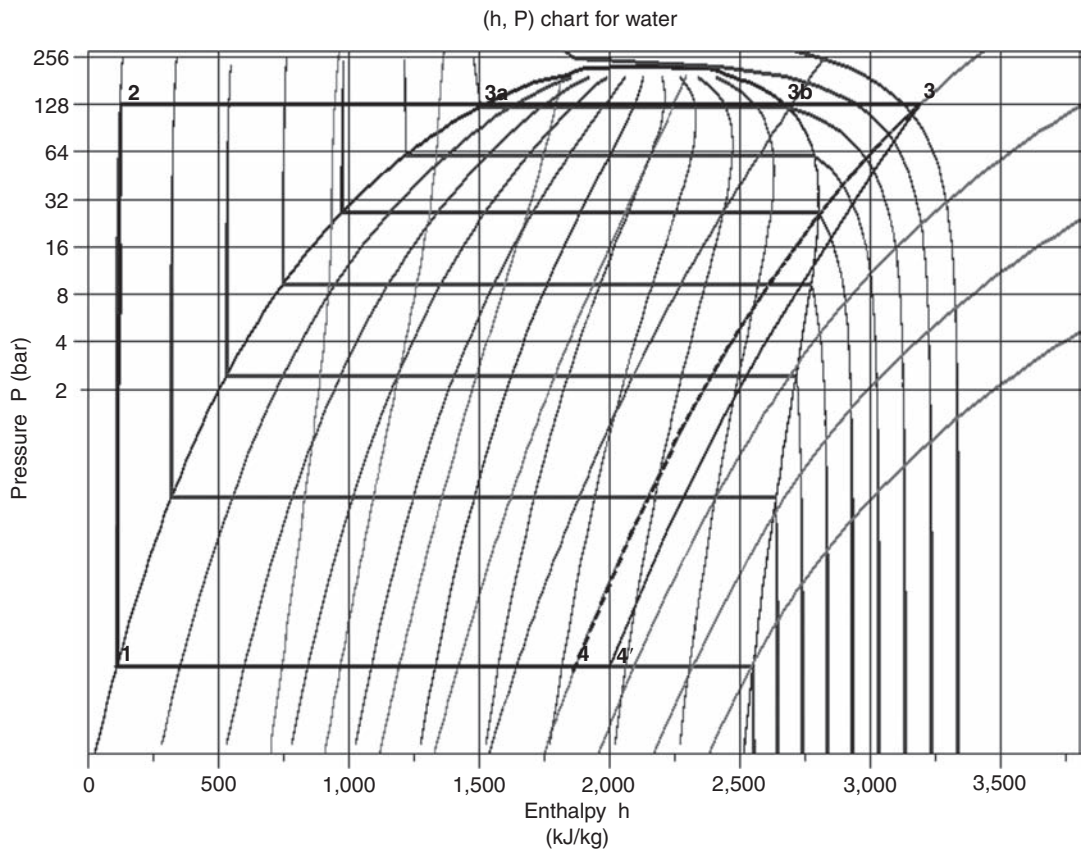


FIGURE 2.11.3
Steam power plant cycle with irreversible expansion

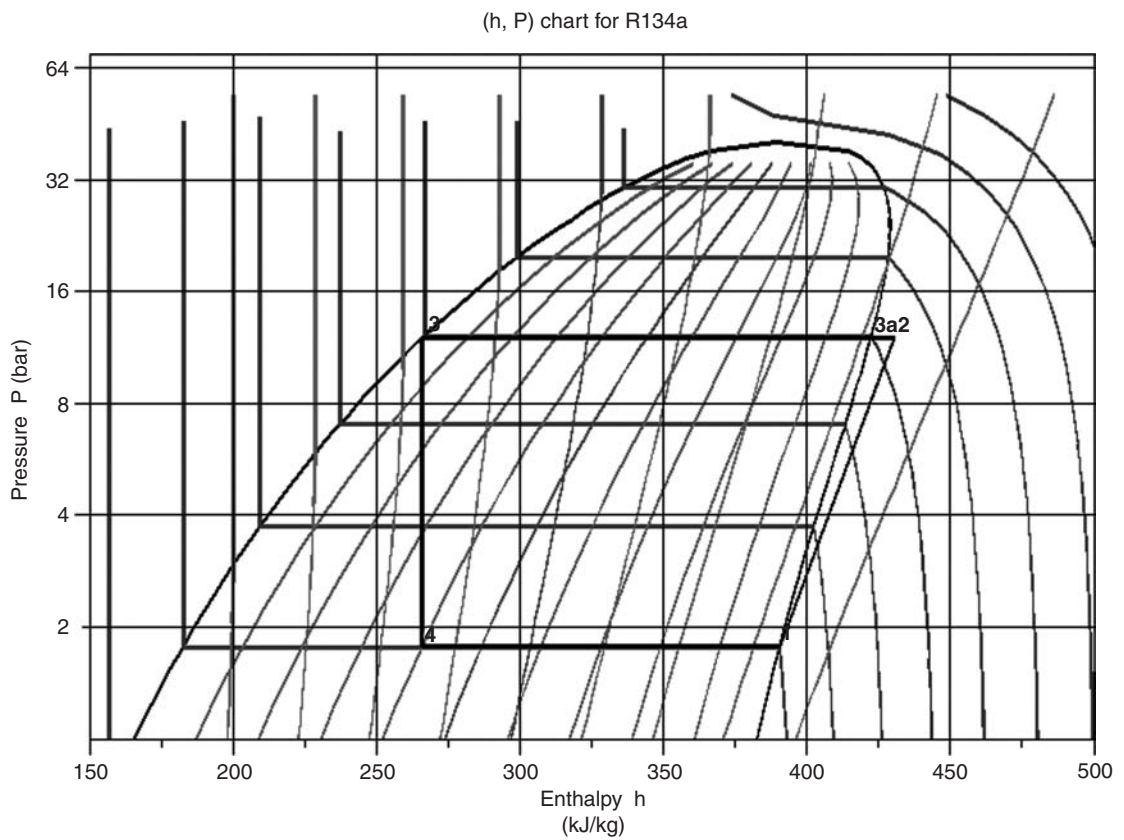


FIGURE 2.11.4
Refrigeration machine simplified cycle

TABLE 2.11.2

SIMPLE REFRIGERATION CYCLE ENTHALPY BALANCE

Point	Flow rate (kg/s)	h (kJ/kg)	
1	1.00	391	
2	1.00	430	
3a	1.00	422	
3	1.00	266	
4	1.00	266	
Process	τ (kW)	Q (kW)	Δh (kW)
(1-2)	40		40
(2-3a)		-8	-8
(3a-3)		-157	-157
(3-4)			
(4-1)		125	125
cycle	40	-40	
Coefficient of Performance			3.14

The refrigerant cooling in the condenser by exchange with outside air comprises two stages: de-superheating (2-3a) in the vapor zone followed by condensation along the horizontal line segment (3a-3). Points 3a and 3 lie at the intersection of the saturation curve and the isobar $P = 12$ bar, or, equivalently, the isotherm $T = 47^\circ\text{C}$. Point 3a is located on the right, at the limit of the vapor zone, and point 3 on the left, at the limit of the liquid zone.

Expansion without work, and therefore an isenthalpic process, corresponds to the vertical segment (3-4), point 4 being located on the isobar $P = 1.78$ bar, or, equivalently, the isotherm $T = -13^\circ\text{C}$, at abscissa $h = h_3$. Its quality reads directly from the corresponding iso-quality: it is $x = 0.4$.

The energies involved can easily be determined by projecting these points on the x-axis. This allows us in particular to calculate the coefficient of performance COP of the cycle, defined as the ratio of useful effect (the heat extracted at the evaporator) to the purchased energy (here the compressor work). Table 2.11.2 provides these values.

This cycle differs from that of a real machine on several points:

- the actual compression is not perfect, so that the compression work is higher than that which would lead to reversible adiabatic;
- to prevent aspiration of liquid into the compressor, which could deteriorate it as the liquid is incompressible, the gas is superheated by a few degrees (typically 5 K) above the saturation temperature before entering the compressor;
- before entering the valve, the liquid is sub-cooled by a few degrees (typically 5 K), this first ensures that this device is not supplied with vapor, and second increases the refrigerator performance.

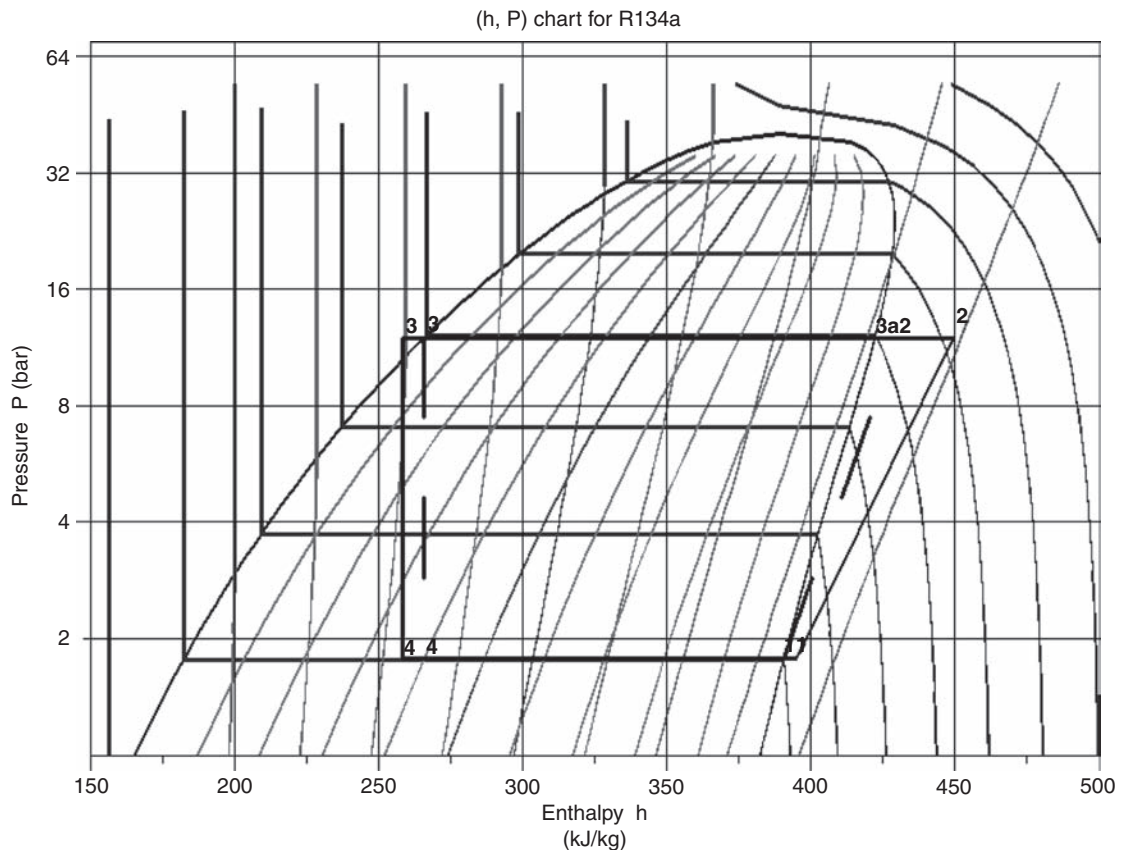
Here we can also characterize the actual compression by an isentropic efficiency, defined this time as the ratio of the work of the reversible compression to real work. Its value is typically around 0.7 to 0.85 in current applications.

To find the real point 2', we determine the value of work τ_s in the perfect machine, then divide it by η , which gives the value of real work τ .

The enthalpy of point 2' is equal to that of point 1 plus τ .

In this case, taking $\eta = 0.75$, we have:

$$\begin{aligned}\tau_s &= h_2 - h_1 = 40 \text{ kJ/kg/K} \\ \tau &= \tau_s / \eta = 40 / 0.75 = 53 \\ h_{2'} &= 391 + 53 = 444 \text{ kJ/kg/K}\end{aligned}$$

**FIGURE 2.11.5**

Refrigeration machine with superheating and sub-cooling

The cycle changed to reflect superheating, subcooling and compressor irreversibilities is shown in Figure 2.11.5 (the previous cycle is plotted in dashed line).

The COP of the machine is of course changed: it drops to 2.57 because of the compressor irreversibilities.

The relevance of sub-cooling can easily be shown in the $(h, \ln(P))$ chart because, for the same compression work, the effectiveness increases as the magnitude of the sub-cooling grows. It is however limited by the need for a coolant.

We did not consider the pressure drops in the exchangers. It would of course be possible to do so.

2.12 MODELING CYCLES WITH THERMOPTIM

At this point, all the notions allowing us to model these cycles with ThermoOptim have been presented, and examples in Chapter 9 of Part 2 can be treated by changing the settings, which have been chosen slightly differently so that they can be easily hand-drawn in charts. Before you start entering models in ThermoOptim, we recommend you to study Diapason initiation session S07En_init which introduces all the software concepts needed. The synoptic views that are obtained are given in Figures 2.12.1 to 2.12.3.

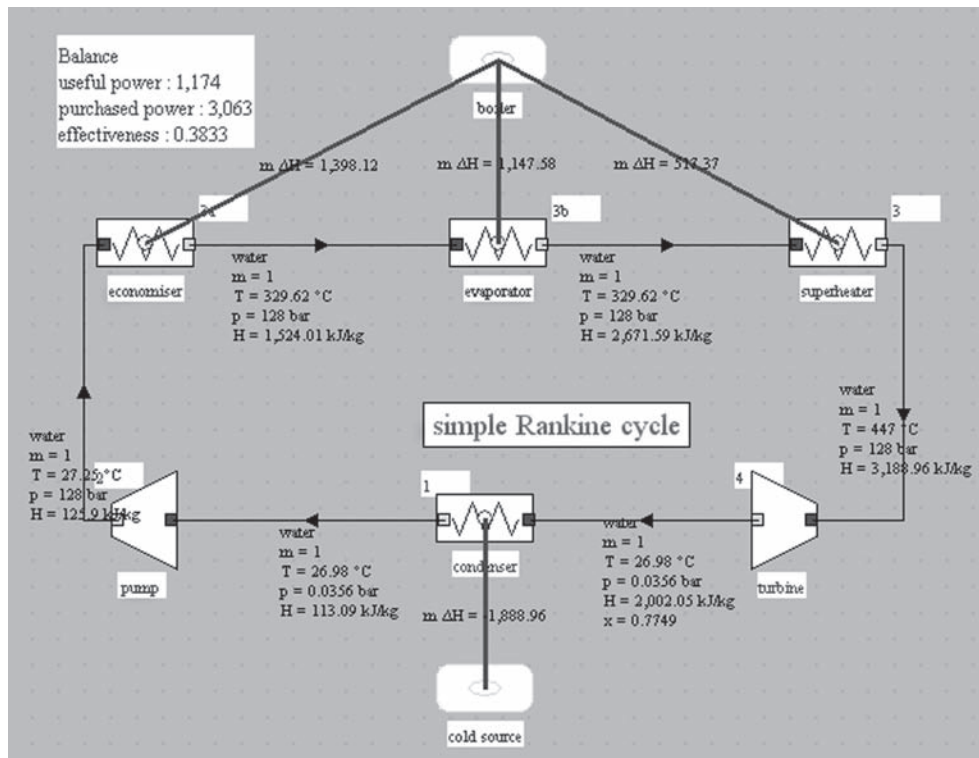


FIGURE 2.12.1
 Synoptic view of the steam power plant

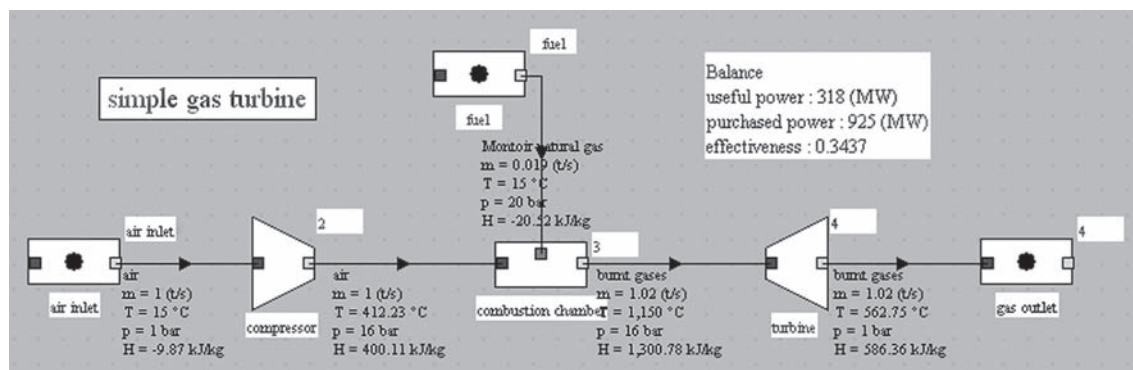


FIGURE 2.12.2
 Synoptic view of the gas turbine

2.12.1 Steam power plant

WORKED EXAMPLE

Modeling of a steam power plant with ThermoOptim

The basic cycle of a steam power plant is essentially a boiler where the fuel is burned for generating steam (usually superheated) which is then expanded in a steam turbine whose shaft provides the motor work. The expanded steam is subsequently condensed and compressed by a pump before returning to the boiler.

The modeling of this cycle in ThermoOptim is presented step by step in sections 9.1.1 to 9.1.5 of Part 2, with slightly different settings.



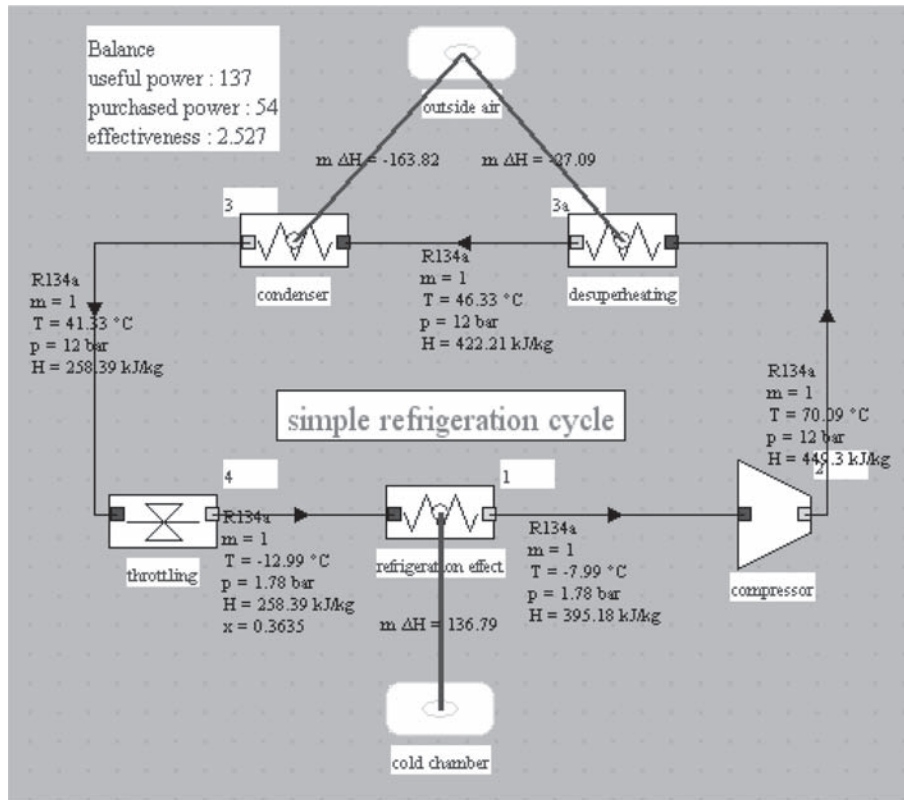


FIGURE 2.12.3

Synoptic view of the refrigeration machine with superheating and sub-cooling

2.12.2 Gas turbine

WORKED EXAMPLE

Modeling of a gas turbine with ThermoOptim

A gas turbine is composed of three elements: a compressor, a combustion chamber and a turbine, in which are expanded the high temperature gases.

The setup that we will retain is: a gas turbine burning natural gas without dissociation sucks 1 t/s of air at 15°C and 1 bar, compresses it at 16 bar in a 0.85 isentropic efficiency compressor, and expands the burnt gases in a 0.85 isentropic efficiency turbine. The temperature of the gases at the turbine inlet is 1150°C.

The modeling of this cycle in ThermoOptim is presented step by step in sections 9.3 of Part 2.

THOPT

[CRC_we_2]

2.12.3 Refrigeration machine

WORKED EXAMPLE

Modeling of a refrigeration machine with ThermoOptim

In a refrigeration machine a refrigerant is evaporated at low pressure, then compressed at a pressure such that it is then possible to cool it by heat exchange with ambient air until it becomes liquid. The liquid is then expanded by isenthalpic throttling at low pressure and directed into the evaporator.

The modeling of this cycle in ThermoOptim is presented step by step in sections 9.2 of Part 2, with slightly different settings.

THOPT

[CRC_we_3]

2.13 CONCLUSION

The essentially qualitative and phenomenological approach used in this presentation proves that it is possible to introduce thermal machine cycles to students with a limited number of thermodynamic concepts, especially not including entropy.

To sum up, the foundations of a lightweight educational presentation of thermodynamic cycles (Figure 2.13.1) appear to be the following (we have indicated in parentheses sections of Part 2 of

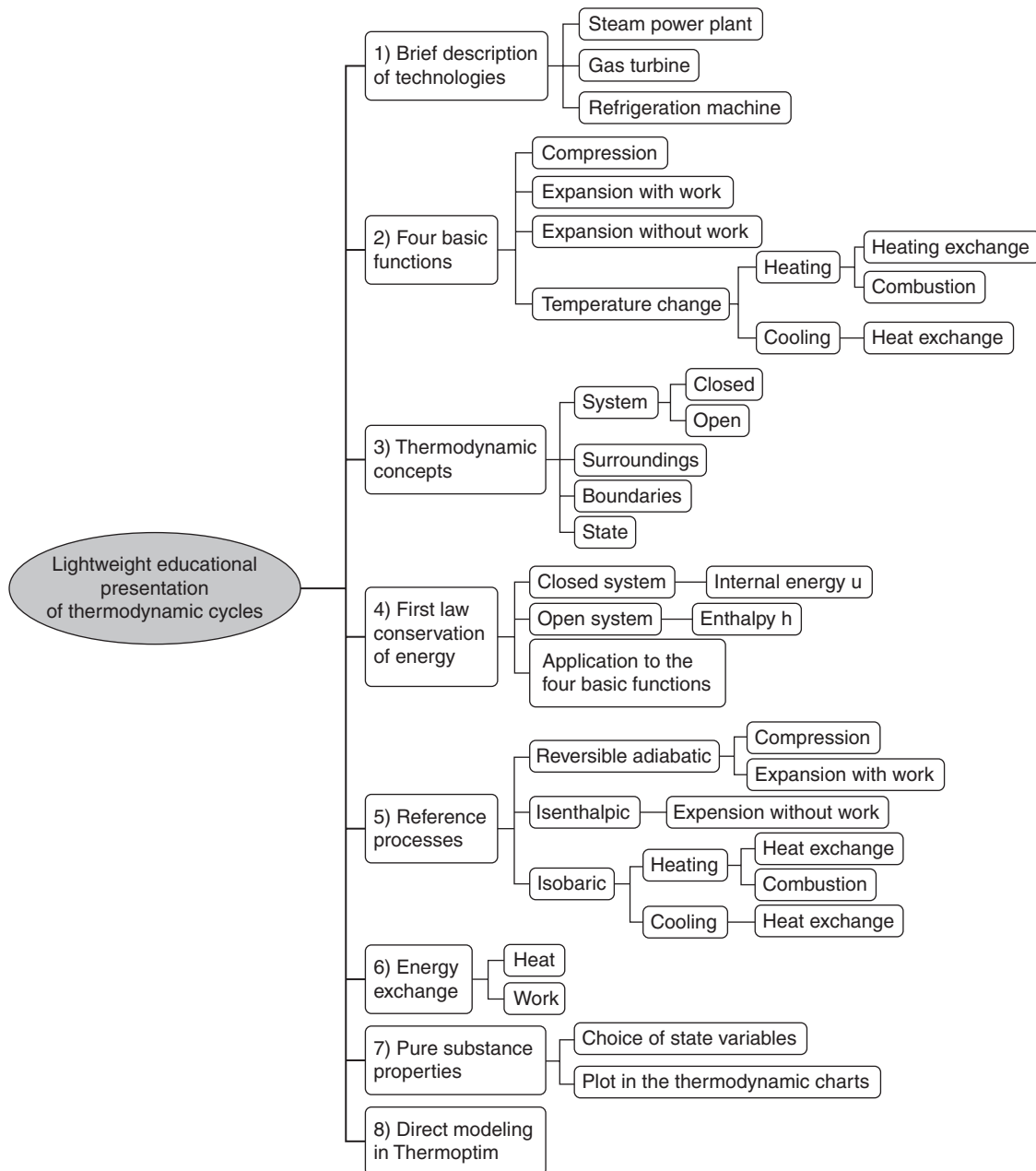


FIGURE 2.13.1

Map of the lightweight educational presentation milestones Part I

the book where these points are developed in order to facilitate a further deepening of concepts discussed):

- Brief description of technologies, with their architecture (sections 9.1.1, 9.2.1 and 9.3.1);
- Highlighting the four basic functions: compression, expansion with work production, expansion without work production, heat exchange (section 5.3.6);
- Introduction of the concepts of thermodynamic system and state, distinction between closed systems and open systems (sections 5.1.1, 5.1.2);
- The thermodynamic systems we are interested in only exchange energy with their surroundings in two distinct forms: heat and work (Section 5.2);
- The fundamental law that governs the behavior of thermodynamic systems is that of conservation of energy, known as the first law (sections 5.3.1 to 5.3.4);
- Its application to the four basic processes shows that the determination of the enthalpy change of the fluid flowing through them is enough to calculate the energy they bring into play, whether work or heat (section 5.3.6);
- Brief reminders on pure substance properties and their graphic representation in thermodynamic charts (sections 5.6.1 and 5.6.6.1);
- Highlighting reference processes relevant to these functions for perfect machines (sections 7.1.2, 7.5, 7.7);
- Reflecting on the choice of state variables most appropriate for students with a light background in mathematics and physics, showing the educational potential of the $(h, \ln(P))$ chart;
- Representation of the steam power plant and refrigeration machine cycles in these charts;
- Direct modeling of the cycles in Thermoptim (sections 9.1, 9.2 and 9.3).

All these milestones, with the exception of the two penultimate ones, are valid whether or not we use entropy.

It is not for us to minimize the relevance of this state function: we consider only that it may be preferable not to introduce it at the beginning of training when students do not have the required culture. If they do, we of course have no objection to use it, quite the contrary.

Without speaking of entropy, we insist instead on the adiabatic character of compressors and turbines, and the importance of the reversible adiabatic process as a reference for these machines. Without needing to say its name, the value of the entropy for cycle studies underlies therefore our approach, and its formal introduction at a later stage (e.g. in the second part of this presentation) is facilitated when the students have become familiar with all the new concepts presented here.

This page intentionally left blank

First Steps in Thermodynamics: Entropy and the Second Law

Abstract: The purpose of this chapter is to discuss key concepts which should be presented to absolute beginners in order to enable them to understand and study the cycles of three basic energy technologies: steam power plant, gas turbine and refrigerating machine.

We are talking of lightweight educational presentation as we seek to minimize the background in mathematics and physics necessary for understanding these cycles, our goal being to make them accessible to readers unfamiliar with the language of specialists in thermodynamics.

In the first part of this presentation (Chapter 2), we introduced the basic concepts of thermodynamics without resorting to the notion of entropy, which can be difficult to master for some students. In this second part, we introduce it as simply as possible, and discuss the main implications of the second law of thermodynamics.

Keywords: lightweight educational presentation, steam power plant, gas turbine and refrigerating machine, heat exchange, enthalpy, entropy, second law of thermodynamics.

3.1 HEAT IN THERMODYNAMIC SYSTEMS

In the first part, we indicated that the heat exchanged by a system with the surroundings is, for an infinitesimal process, given by the following expression:

$$\delta Q = C_p dT - v dP \quad 3.1.1$$

It expresses an experimental fact, the essential basis of the thermodynamics of compressible fluids: heat δQ exchanged with the surroundings is a linear function of the thermodynamic state of the system.

This equation is however valid only if there is no irreversibility inside or at the boundary of the fluid mass. If any, the relationship becomes:

$$\delta Q < C_p dT - v dP \quad 3.1.2$$

We can then write:

$$\delta Q = C_p dT - v dP - \delta \pi \quad 3.1.3$$

$\delta\pi$, essentially a positive term, has a very simple physical meaning: it is the heat generated by mechanical friction within the fluid. A straightforward interpretation for isobaric heating is that the fluid temperature rise dT is greater than $\delta Q/C_p$ because of irreversibilities.

Although it differs profoundly from heat received from the surroundings, it changes the thermodynamic state of the system in the same way.

δQ is the **heat exchanged with the surroundings**, counted positively if it is received by the system and negatively otherwise, and $\delta\pi$ the **heat dissipated by internal friction and shocks** if any. It is always positive or zero.

In practice, it is important to distinguish these two forms of heat, otherwise serious errors of reasoning can be made. In particular, processes without heat exchange with the surroundings, called adiabatic, are such that $\delta Q = 0$, whether the seat of irreversibility or not, that is to say whether $\delta\pi$ is zero or not.

3.2 INTRODUCTION OF ENTROPY

In the first part, we stressed how important in practice are **reference processes** corresponding to the processes that fluids would undergo in perfect machines.

We have also shown that, for compressors and turbines, the reference process is the reversible adiabatic, the corresponding law for a perfect gas being given by $Pv^\gamma = \text{Const.}$ with $\gamma = C_p/C_v$.

It is obtained by solving the differential equation $\delta Q = 0 = C_p dT - v dP$, which is quite simple replacing v by rT/P .

Given the importance of this law, it is interesting to try to generalize it to find a formulation that is valid on the one hand for all fluids and not only perfect gases, and secondly for all the processes, whether or not they bring into play irreversibilities.

Let us come back to the equation:

$$\delta Q = C_p dT - v dP - \delta\pi \quad 3.2.1$$

which is also written:

$$\delta Q + \delta\pi = C_p dT - v dP \quad 3.2.2$$

This equation is an inexact differential and not an exact differential. We call an integrating factor an expression by which one multiplies an inexact differential in order to turn it into an exact differential.

We can show that in the general case as for a perfect gas, $1/T$ is one of the simplest integrating factors for this equation. For the perfect gas, this integral expression is written:

$$s = s_0 + c_p \ln \frac{T}{T_0} - r \ln \frac{P}{P_0} \quad 3.2.3$$

As can be seen, function s is a state function formally very close to the calorimetric equation providing heat exchanged by a system with its surroundings, as it can be deduced by using as integrating factor $I = 1/T$. It is called the **entropy of the system**.

In the $(h, \ln(P))$ charts that we presented in the first part, the iso-value curves of the reversible adiabatic are those for which $ds = 0$. They are called **isentropic**.

The concept of entropy is thus introduced naturally, entropy being the state function closest to heat. There is no evidence in this approach, however, that this concept remains valid for non-perfect gases. With the more axiomatic definition we will give by introducing the second law, a perfect gas becomes a special case of the general theory.

3.3 SECOND LAW OF THERMODYNAMICS

3.3.1 Limits of the first law of thermodynamics

A major limitation of the first law of thermodynamics is the failure to take into account the quality of energy: indeed different forms of energy expressed in kWh are equivalent, but the possibilities of converting one form of energy into another are not.

Thus, work can still be fully converted into heat, but the converse is not true. The work is one form of energy whose quality is among the best, and which can therefore be taken as a reference.

We can rephrase this by saying that a possible indicator of the energy quality is its **ability to be converted into work**.

The first law postulates the equivalence of different forms of energy, but it does not take into account an essential experimental fact, which is that when a system interacts with its surroundings, the energy processes that it undergoes can only take place in a privileged sense, that cannot be reversed without a qualitative change in the system.

3.3.2 Concept of irreversibility

One can convert electricity into work using an electric motor of efficiency over 98%, or conversely convert mechanical work into electricity through a generator of equivalent efficiency, which means that these two forms of energy are about the same quality.

In the example of power conversion work we have just given, we stated that the machines used had excellent efficiencies, close to but slightly lower than 1: experience indeed shows that, whatever precautions are taken, some energy is degraded. The first law teaches us that the total energy is conserved, but some of its quality declines and ultimately ends up as heat, because of friction, Joule losses etc.

These losses are called irreversibilities, because the process work \rightarrow electricity \rightarrow work is not completely reversible: part of the initial work is converted into heat.

Irreversibilities encountered in energy facilities that interest us, except those taking place in combustion reactions, can be grouped into two broad classes that we discuss briefly a little later:

- irreversibilities stemming from temperature heterogeneity;
- mechanical irreversibilities due to viscosity.

3.3.3 Heat transfer inside an isolated system, conversion of heat into work

In the particular case of heat, it is always experimentally verified without exception, that the transfer of heat between two media at different temperatures is from the warmer body (the one whose temperature is higher), to the colder (whose temperature is lower).

Also a heterogeneous system composed of two media at different temperatures not isolated from each other always evolves towards a homogeneous state at intermediate temperature.

Moreover, when attempting to convert heat into work, experience proves that it is first necessary to have two heat sources, one at high temperature, and the other at low temperature (Figure 3.3.1).

Moreover, the larger the temperature difference between the sources, the greater the amount of work that can be converted from one kWh of heat. Temperature thus also appears as a possible indicator of the heat quality.

A further remark can be made at this stage: it is the existence of a temperature difference between two bodies that allows for work production.

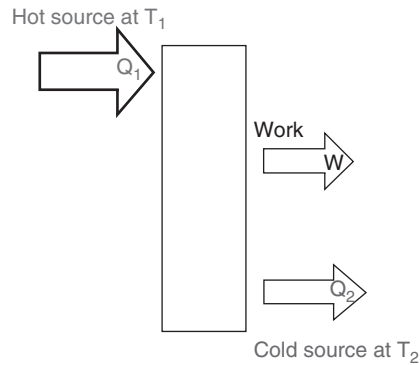


FIGURE 3.3.1
Conversion of heat into work

3.3.4 Statement of the second law

The second law complements the first by introducing a function called entropy, which is used to quantitatively characterize the effects of irreversibilities taking place in a system and explain the phenomena we have just discussed.

A rigorous and comprehensive presentation of the second law requires significant developments due to the precautions that must be taken first in writing assumptions and explanations of their connection with experience, and second in demonstrations which must be made.

Given our objectives, this is not justified here, especially as for applied thermodynamic calculations of practical interest, the main advantage of this second law can be summarized in two points:

- first, entropy is, as we have shown, the state function most closely related to the heat Q exchanged with the surroundings. It thus intervenes implicitly or explicitly in many equations governing the operation of energy components;
- second, the generation of entropy alone allows us to quantify all the irreversibilities taking place in these components and their boundaries, which is fundamental.

The second law states that entropy s has the following properties:

- s is a function of the system state variables;
- in any elementary process involving heat exchange δQ with the surroundings we have $\delta Q \leq T ds$, equality being satisfied if and only if the process is perfect (not irreversible).

Writing:

$$ds = \frac{\delta Q}{T} + d_i s \quad 3.3.1$$

$d_i s$, positive or zero, is called “entropy generation”.

This relationship can also be written, as we mentioned above:

$$\delta Q + \delta \pi = T ds \quad 3.3.2$$

$\delta \pi$ is called “uncompensated work” or “uncompensated heat”. It is positive for an irreversible process and zero otherwise.

3.4 (T, s) ENTROPY CHART

In the first part of this lightweight presentation, we excluded entropy from variables we have considered to represent the fluid properties. Now that we have introduced this state function, it is natural to question its relevance in this regard.

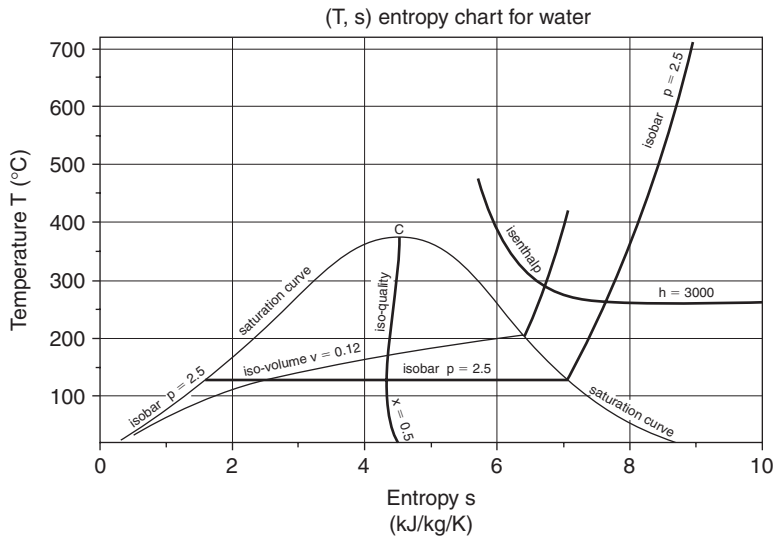


FIGURE 3.4.1
Water (T, s) entropy chart

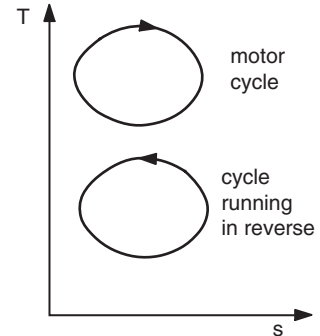


FIGURE 3.4.2
Types of cycles in the entropy chart

Experience shows that the entropy and Mollier charts, which use as coordinates pairs (T, s) and (h, s) , are particularly interesting, especially the first, to which we limit our analysis here.

In the entropy chart (Figure 3.4.1) entropy is the abscissa and temperature the ordinate. The vaporization curve again separates the plane into two areas, defining the two-phase zone and the zone of simple fluid. The critical point C is still at its maximum.

One of the advantages of such a chart (see Figure 3.4.2) is that any perfect cyclic process is reflected in the plane (T, s) by a contour (Γ), whose area A measures, depending on the sign, either the amount of heat Q brought into play, or the work provided or received τ .

Indeed, $Q = \int T ds$ by definition. As the cycle is closed, $Q + \tau = 0$, and $|\tau| = A$.

The rule of signs is as follows:

- if the cycle is described clockwise, work is negative, thus transferred by the fluid to the surroundings: we talk of a motor cycle or of a cycle running forward;
- if the cycle is described counterclockwise it is the opposite: we talk of a refrigeration cycle, or of a cycle running in reverse.

Form of isobars

To the left of the incipient boiling curve, liquid isobars are curved upward. Liquid isentropic compression having almost no effect on the temperature, liquid isobars are virtually merged with the ascending branch of the vaporization curve. The chart is very imprecise in this area and it is preferable to use a table or a program giving the thermodynamic properties along the vaporization curve.

Inside the two-phase zone, temperature and pressure are bound by the saturated pressure law, and isobars are horizontal.

Right of the vaporization curve, isobars are rising and, for an ideal gas, become exponential. They can be deduced from each other by horizontal translation.

If the pressure exceeds the critical pressure, isobars are strictly ascending curves, which do not intersect the vaporization curve.

Form of isenthalps

In the vicinity of the saturation curve, isenthalps are curved downward, with a strong negative slope.

Gradually as the distance from the vaporization curve increases, the gas approaches the corresponding ideal gas, and isenthalps become horizontal, as enthalpy is a sole function of temperature. Of course, the plot of an isentropic process is very simple in this chart: it is a vertical segment.

3.5 CARNOT EFFECTIVENESS OF HEAT ENGINES

Motor thermal machines are designed to transform heat into mechanical energy. Let us assume that heat to transform is provided by an external source, said heat source, whose temperature T_1 is set. A second source, known as cold, is required to evacuate part of the heat. Its temperature T_2 is necessarily lower than T_1 .

The second law is due to S. Carnot, who in 1824 showed that the efficiency of an ideal heat engine cycle is given by: $\eta = 1 - T_2/T_1$.

Carnot has shown that this efficiency does not depend on the nature of the machine and fluids used, but only T_1 and T_2 .

In the (T, s) entropy chart, it is represented by the rectangle ABCD, described clockwise (Figure 3.5.1).

- AB is a segment of isotherm T_1 described from left to right. The fluid receives heat (isothermal expansion in the case of a perfect gas);
- CD is a segment of isotherm T_2 described from right to left. The fluid releases heat (isothermal compression in the case of a perfect gas);
- BC is a segment of isentropic S_2 described from top to bottom (reversible adiabatic expansion in all cases);
- DA is a segment of isentropic S_1 described from bottom to top (reversible adiabatic compression in all cases).

This relation is probably rightly one of the best known in thermodynamics. It is of great practical importance, given its implications:

- First, with the assumptions made (reverse cycle without friction and heat transfer without temperature differences), it is easy to show that this effectiveness is the highest that can be achieved by a simple fluid heat engine operating between the two sources at T_1 and T_2 . It is therefore a maximum limit and real cycles generally have much lower efficiencies;
- Secondly, the Carnot effectiveness of all reversible machines operating between the two sources at T_1 and T_2 is the same and only depends on their temperatures, not on the working fluid used.

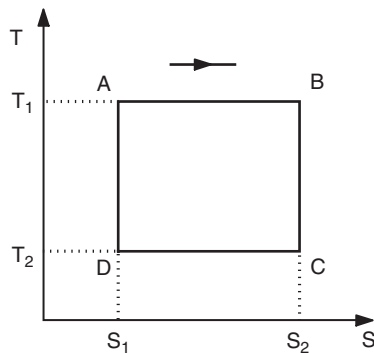


FIGURE 3.5.1
Carnot cycle

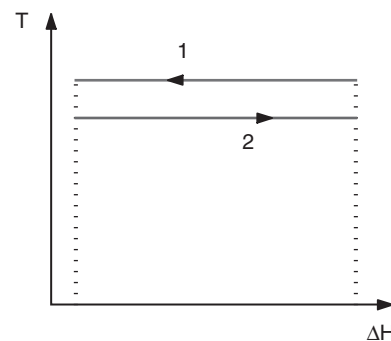


FIGURE 3.6.1
Constant temperature heat exchanger

3.6 IRREVERSIBILITIES IN INDUSTRIAL PROCESSES

3.6.1 Heat exchangers

In a heat exchanger, heat can only be transferred between two streams if a certain temperature difference exists between them. Indeed, for both technical and economic reasons, the exchange surfaces between these fluids are necessarily finite. It is then possible to show that the heat exchange is accompanied by an increase in entropy at the boundary between the two streams (at temperatures T_1 and T_2 , Figure 3.6.1), given by:

$$d_{i,s} = \left(\frac{T_1 - T_2}{T_1 T_2} \right) \delta Q$$

δQ being the heat absorbed by fluid 2. These irreversibilities are often described as external, because they take place at the boundary of the system.

The larger the temperature difference between the fluids, the greater the entropy creation. In a heat exchanger, the energy (enthalpy) transferred by the hot fluid to the cold fluid is conserved, but because the transfer is taking place with temperature decrease, entropy increases.

In energy systems, the temperature difference that must exist between two fluids that exchange heat generally constitutes an important source of irreversibility.

3.6.2 Compressors and turbines

We stated above that the compression and expansion devices are generally adiabatic ($\delta Q = 0$).

In an adiabatic reversible compressor or turbine, there is no creation of entropy. We say that evolution is **isentropic**, a very important concept in practice because it involves the reference process against which actual changes are characterized.

In real machines, as we saw in the first part of this presentation, we can take into account irreversibilities by introducing what we called an isentropic efficiency, equal to the ratio of isentropic work to real work for compressors, and the reverse for turbines, i.e. the ratio of actual work to isentropic work.

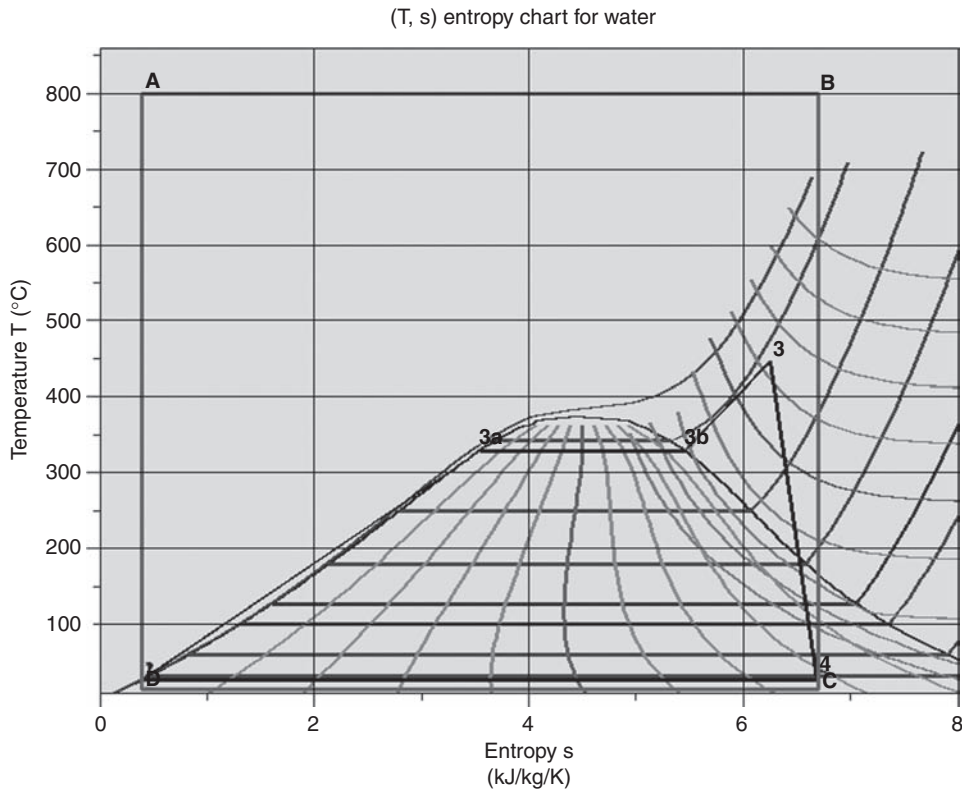
3.7 PLOT OF CYCLES IN THE ENTROPY CHART, QUALITATIVE COMPARISON WITH THE CARNOT CYCLE

The Carnot cycle being the one that leads to the best effectiveness, it is almost always interesting to compare actual cycles to it. In this section, we perform such a comparison for each of the cycles that we studied in the first part of this presentation.

3.7.1 Steam power plant

In the entropy chart (Figure 3.7.1), to increase readability, we have not shown iso-volumes. Points 1 and 2 showing compression in the liquid state are almost superimposed, and heating in the liquid state almost coincides with the liquid saturation curve. Vaporization is done in a horizontal line segment.

The isobaric superheating (3) is the maximum peak of the cycle and the irreversible expansion is reflected by an increase of entropy, the point 4 being located within the vapor-liquid equilibrium zone (quality equal to 0.775).

**FIGURE 3.7.1**

Steam power plant and Carnot cycles in the entropy chart

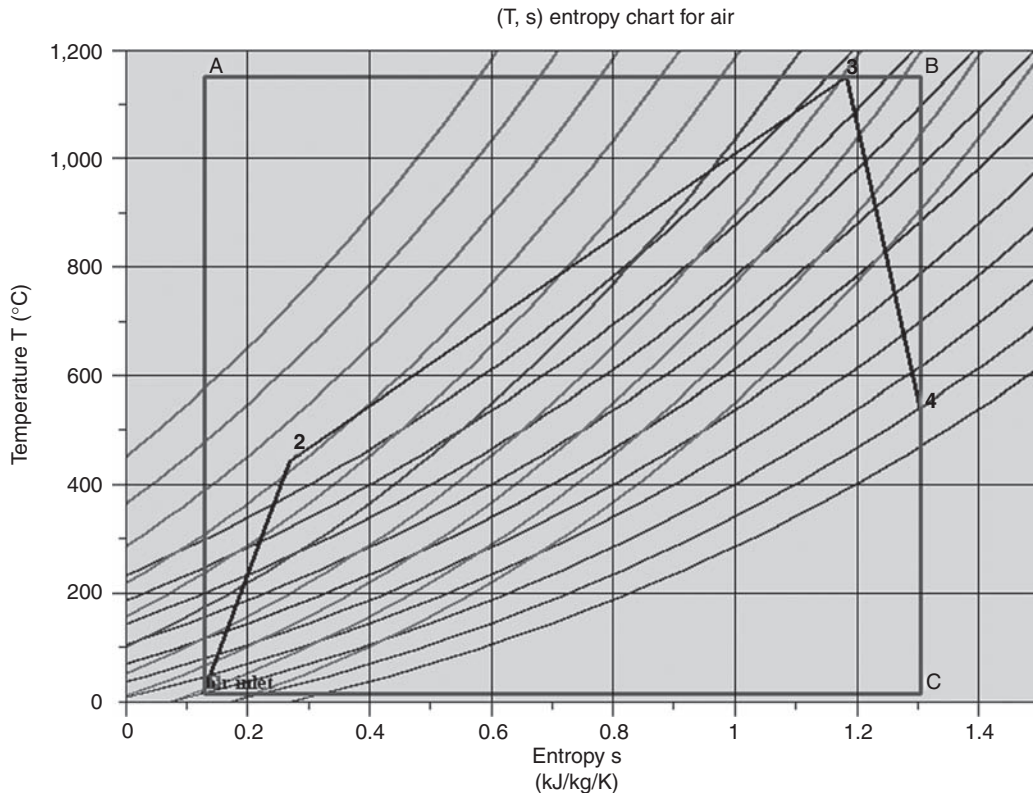
In order to plot the Carnot cycle (A-B-C-D), we have assumed that $T_1 = 800^\circ\text{C}$ and $T_2 = 15^\circ\text{C}$ (in practice T_1 is higher). The comparison of both cycles leads to the following comments:

1. the condenser (process 4-1) being a heat exchanger of finite size, condensing water cannot be at the same temperature as the cold source, which is a first difference with the Carnot cycle. However, we can consider that the heat exchange is nearly isothermal and irreversibilities are small;
2. compression (process 1-2) in the pump may at first approximation be assumed isentropic, its irreversibilities being low. However it deviates significantly from the Carnot cycle because the compression end temperature is about the same as that of the cold source, rather than that of the hot one;
3. we have seen that the isobaric pressurized water heating is done in three steps:
 - liquid heating in the economizer up to the saturation temperature at the pressure considered (process 2-3a);
 - vaporization at constant temperature in the vaporizer (process 3a-3b);
 - superheating up to maximum temperature in the boiler cycle (process 3b-3).

Given the shape of isobars in the entropy chart, this isobaric heating process deviates much from the Carnot cycle which states that the heat engine exchanges heat at constant temperature with the hot source. In particular the temperature difference with the hot source is maximum in the economizer: heat at high temperature is used to warm water below 100°C .

4. turbine (process 3-4) has an isentropic efficiency close to 0.85. Again the difference with the Carnot cycle is significant.

As illustrated in the figure, the shape of the steam power plant differs appreciably from that of the Carnot cycle: it looks rather like a triangle than a rectangle, and its surface is much smaller. There is room for improvement by conducting reheats that lead to so-called para-isothermal expansion, and extractions which allow to perform a partial regeneration.

**FIGURE 3.7.2**

Gas turbine and Carnot cycles in the entropy chart

3.7.2 Gas turbine

In the entropy chart (Figure 3.7.2), irreversible compression and expansion result in an increase of entropy (air inlet-2, and 3-4). Heating in the combustion chamber is isobaric. However, as the working fluid composition changes during the combustion, the properties of the burnt gases are not exactly the same as those of air and we should not in principle plot points 3 and 4 on the same chart as points 1 and 2. There is indeed a change in entropy due to the combustion which explains why points 2 and 3 and points air inlet and 4 seem not to be on the same isobar.

In order to plot the Carnot cycle (A-B-C-D), we have assumed that $T_1 = 1150^\circ\text{C}$ and $T_2 = 15^\circ\text{C}$. The comparison of both cycles leads to the following comments:

1. compression (process 1-2) cannot be assumed to be isentropic, due to irreversibilities taking place in the compressor. It departs from the Carnot cycle;
2. combustion (process 2-3) takes place at constant pressure. Given the shape of the isobars on an entropy chart (similar to exponential), the difference is important between this process and the Carnot cycle which states that the heat engine exchanges heat at constant temperature with the hot source.
3. turbine (process 3-4) has an isentropic efficiency close to 0.9. Again the difference with the Carnot cycle is significant.
4. hot gases leaving the turbine are then discharged directly into the atmosphere, which is an important form of irreversibility, since their heat is lost.

As illustrated in the figure, the shape of the gas turbine cycle differs appreciably from that of the Carnot cycle: it looks rather like a diamond than a rectangle, and its surface is much smaller. Improvements can be obtained by conducting cooled staged compression, staged expansion with reheats, regeneration and combined cycle arrangement.

3.7.3 Refrigeration machine

In the entropy chart (Figure 3.7.3), to increase readability, we have not shown the isovolumes. Point 1 (partly masked by point C), slightly superheated, is placed on isobar 1.8 bar right of the saturated vapor curve. Irreversible compression results in an increase of entropy. Cooling with outside air has three stages: de-superheating (2-3a) in the vapor phase, condensation along the horizontal segment (3a-3b), and a slight sub-cooling (3b-3) which almost coincides with the liquid saturation curve.

Isenthalpic throttling (3-4) leads to an increase of entropy, point 4 being located within the zone of vapor-liquid equilibrium (quality equal to 0.363).

In order to plot the reverse Carnot cycle (A-B-C-D), we have assumed that $T_1 = 40^\circ\text{C}$ and $T_2 = -8^\circ\text{C}$. The comparison of both cycles leads to the following comments:

1. the evaporator being a heat exchanger of finite size, the refrigerant cannot be at the same temperature as the cold chamber, which is a first difference with the reverse Carnot cycle. However, we can consider that the heat exchange is nearly isothermal;
2. compression cannot be assumed to be isentropic, due to irreversibilities taking place in the compressor, which induces a new gap with the reverse Carnot cycle;
3. cooling and condensation of the refrigerant by heat exchange with ambient air generally cannot be isothermal, given the thermodynamic properties of refrigerants: you must first desuperheat the vapor, then condense it. Given the shape of isobars on an entropy chart, the difference with the reverse Carnot cycle is very important here;
4. the expansion of the condensed refrigerant could theoretically be close to isentropic, but the technological reality is different, and this for three reasons: firstly the expansion of a two-phase

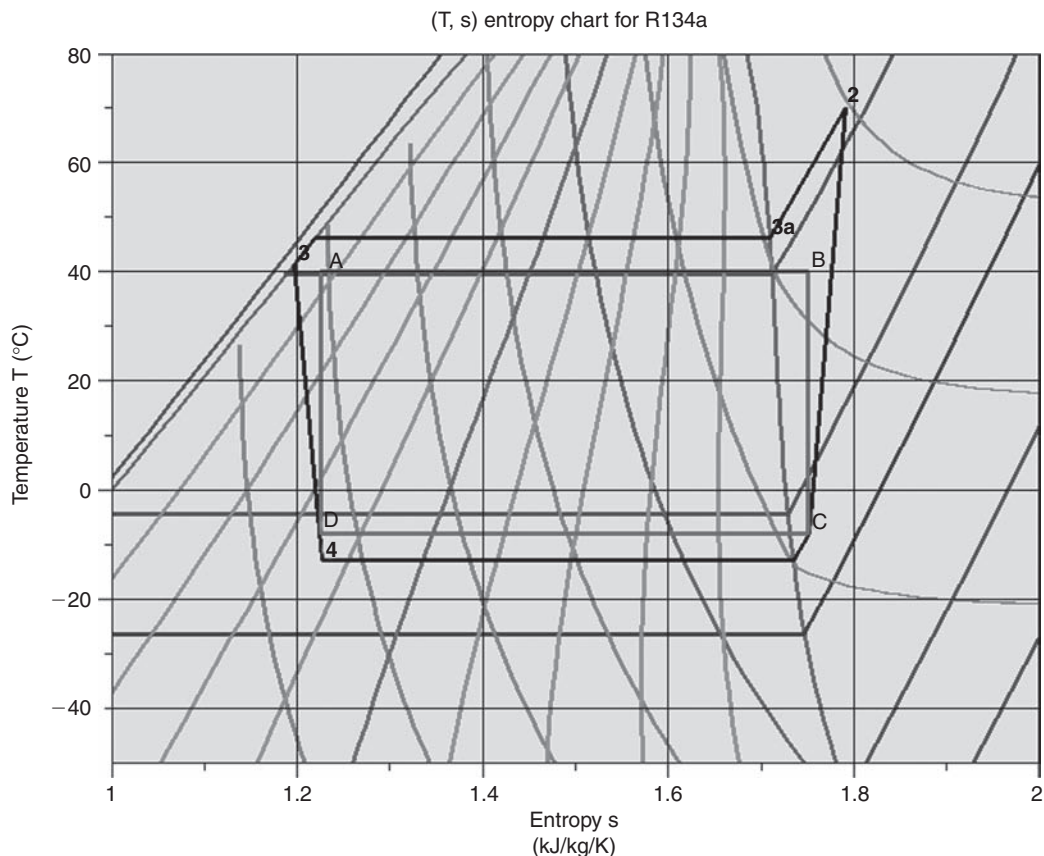


FIGURE 3.7.3

Refrigeration machine and reverse Carnot cycles in the entropy chart

mixture is done, unless special precautions are taken, with low isentropic efficiency; second, the work at stake is very low; and finally, especially for low-capacity refrigerators, there is no — suitable and cheap expansion machine. Therefore in practice one resorts to expansion valves or even simple capillary static devices that perform isenthalpic throttling. Again the gap with the reverse Carnot cycle is significant.

As illustrated in the figure, the reverse Carnot cycle appears inside the actual refrigeration cycle. The main difference is the compression curve (1-2-3a) due to the shape of isobars in the vapor zone. The surface of the actual cycle is larger.

3.8 CONCLUSION

In the first part of this presentation, we have shown that it is possible to introduce thermal machine cycles to students without referring to entropy. In this second part, we have shown that this notion is particularly interesting because it allows us to take into account irreversibilities that take place in actual processes.

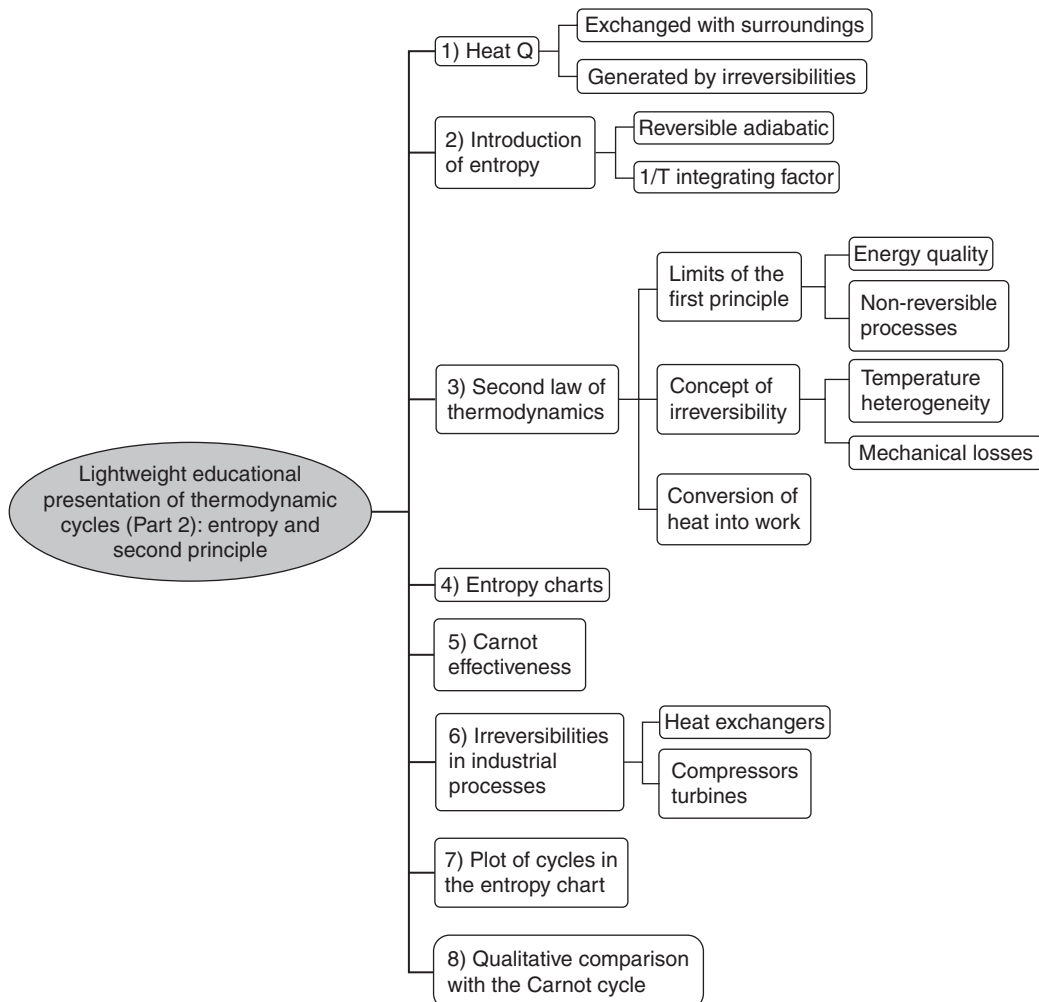


FIGURE 3.8.1

Map of the lightweight educational presentation milestones (Part 2)

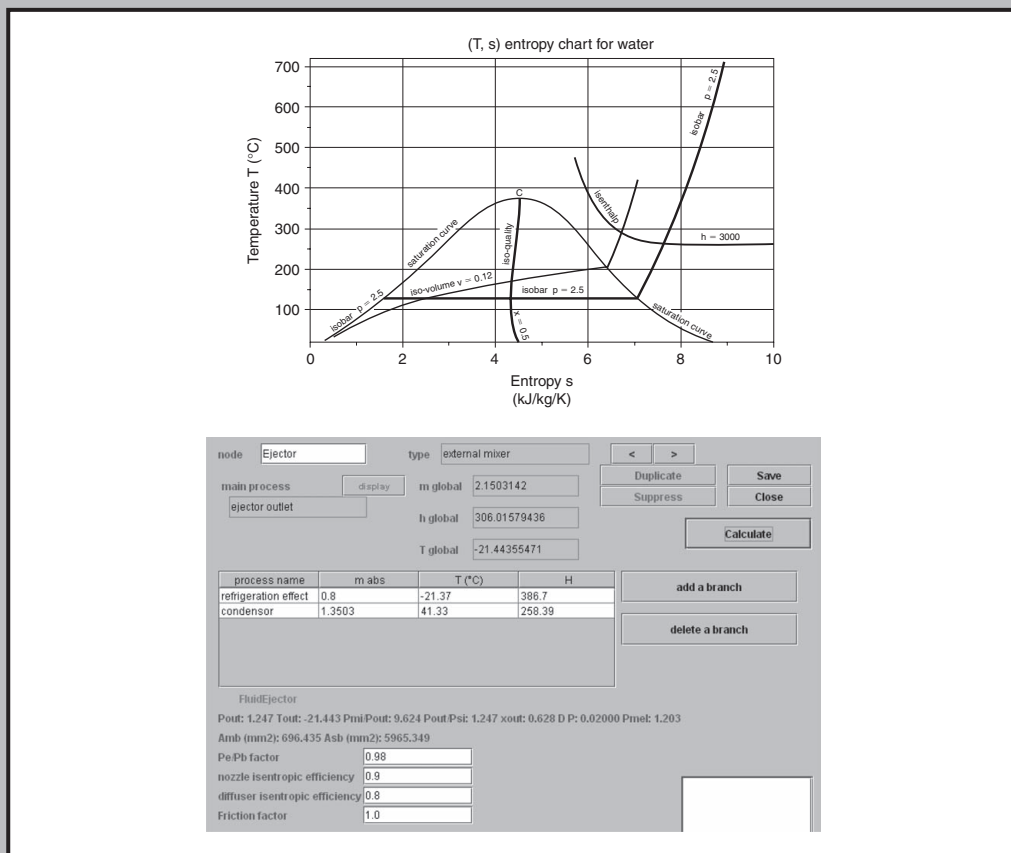
Qualitative comparison with the Carnot cycle can be made in the (T, s) entropy chart and provide guidance on possible improvements.

The different steps that we recommend (Figure 3.8.1) are the following (we have indicated in parentheses sections of Part 2 of the book where these points are developed in order to facilitate a further deepening of concepts discussed):

- Heat in thermodynamic systems (section 5.2.2);
- Limits of the first law of thermodynamics (beginning of section 5.4);
- Concept of irreversibility (section 5.4.2);
- Heat transfer inside an isolated system, conversion of heat into work;
- Statement of the second law (section 5.4.1);
- Presentation of the (T, s) entropy chart (section 5.6.6.1);
- Carnot effectiveness of heat engines (section 5.4.3);
- Irreversibilities in industrial processes (section 5.4.2);
- Plot of cycles in the entropy chart (sections 9.1, 9.2 and 9.3);
- Qualitative comparison with the Carnot cycle.

2

Methodology, Thermodynamics Fundamentals, Thermoptim, Components



Part 2 establishes the main equations allowing one to calculate the behavior of basic components used in most energy technologies (compressors, turbines, combustion chambers, throttling devices, heat exchangers etc.). A structured approach to energy conversion technologies (ECTs) modeling with Thermoptim is given, followed by the presentation of the main features of the software and by four practical worked examples

This page intentionally left blank

Introduction

Abstract: The approach proposed in this book is based on the observation that thermodynamics is much simpler in qualitative than in quantitative terms.

To explain it, we first briefly introduce the operation of a gas turbine¹, an engine whose principle is among the simplest. This will allow us to enter the heart of the matter by introducing a number of concepts needed for studying energy technologies: the fluids involved, the processes they undergo and the corresponding components, and finally assemblies of these components. This will show the relevance of a twofold methodological approach.

We then show that this methodology involves two complementary approaches, the analytical approach used to represent each component, and the systems approach as regards the definition of the internal architecture of the system.

The subsequent sections explain how the methodology proposed can be put in practice and present Thermoptim primitive types allowing one to model energy technologies according to it.

Keywords: Analytical modeling, systems modeling, energy technologies, primitive types, Thermoptim.

4.1 A TWO-LEVEL METHODOLOGY

4.1.1 Physical phenomena taking place in a gas turbine

The gas turbine, also called combustion turbine, is a heat engine which is currently very popular, given its excellent performance (efficiency greater than 35% when used alone, and 55% in combined cycle).

As we have seen Section 2.1.2 of Part 1, this machine is composed of three elements (Figure 2.1.2 of Part 1), a compressor, a combustion chamber and a turbine.

This very simple example is not representative, by far, of the operation of all internal combustion engines. It can however give a first idea of the complexity of the phenomena that take place, and therefore the knowledge necessary to calculate them:

- the various components of the machine are coupled. Their couplings come on the one hand from the fluid passing through them, and on the second hand from the mechanical connection between the compressor and turbine shafts;

¹We content ourselves here with a brief introduction of this technology, Chapter 12 of Part 3 being dedicated to it.

- working fluids are here gas mixtures: firstly the air and fuel and then burnt gases. They can in each case be considered as ideal gases, whose thermodynamic energy properties depend only on temperature;
- in other power plants such as steam power plants, the working fluid passes alternately from the liquid state to vapor. The ideal gas model is no longer sufficient and must be replaced by much more complex real fluids models, the energy properties depending on both pressure and temperature;
- the compression and expansion phases are of crucial importance in the functioning of the engine, because conversions of energy between the fluid and the drive shaft take place during them;
- combustion reaction is highly complex, currently still imperfectly known, but may nevertheless be approached by different methods, which calculate the energies involved and give an idea of the origin of pollutants;
- finally, the working fluids pass through the various engine components, and understanding their flow conditions requires advanced concepts in fluid mechanics (which are not discussed in this book).

4.1.2 Energy technologies: component assemblies

Like the gas turbine, energy technologies are assemblies of components through which flow thermodynamic working fluids which undergo changes of varying complexity. In some cases, such as in reciprocating diesel or gasoline engines, the same organ (cylinder and piston assembly) is brought successively to play the role of the compressor, combustor and expansion device.

In summary, the study of an energy technology such as a gas turbine faces a double challenge:

- fluids that pass through its various components follow behavior laws that are relatively complex and undergo basic processes whose analysis can be difficult (non-linear laws, combustion, etc.);
- components are coupled together, so they cannot be calculated independently.

Note however that in the example shown the connections between components are very simple: the outlet of the compressor is the inlet of the combustion chamber and the output of the latter the entrance to the turbine. This simplicity of the interconnection network is general and suggests adopting a dual approach in the study of energy technologies, separating on the one hand the description of the interconnection network between components, and on the other hand the internal behavior analysis thereof. This procedure has many advantages as discussed later in this book.

The approach proposed in the five parts of this book is thus based on the observation that thermodynamics is much simpler in the qualitative than quantitative terms.

Energy technologies being assemblies of components through which flow thermodynamic fluids which undergo various processes, we greatly simplify things if we adopt a dual approach, starting by separating the representation of the overall system, usually quite simple, from the study of its components taken individually.

The overall representation is very useful at the qualitative level: it is visual and helps us to understand the role played by each component in the complete system. When learning the subject, it is essential to fully assimilate the design principles of these technologies. Once one has in mind the internal structure of an engine or refrigerator, the study of the behavior of one of its components is made easier because we understand its place in the whole and how it contributes to the overall performance.

If one has a proper graphical environment such as the ThermoOptim diagram editor (Figure 2.12.2 of Part 1), the internal structure of the system can be described very easily. This gives a qualitative representation, very meaningful for the engineer, which can be quantified by setting the thermodynamic properties of the different components and then calculating them. This qualitative representation has furthermore the distinction of being largely independent of assumptions that are

adopted for the calculation of the various components: it is an invariant of the system. Thus, a given system architecture can be calculated with various component models.

This double modeling approach involves two approaches often presented as exclusive but which are in this case complementary and mutually enriching:

- the analytical approach used to represent each component by a number of characteristic parameters, coupling variables and a set of appropriate equations;
- the systems approach as regards the definition of the internal architecture of the system (choice of components, description of their relationships).

Not only does such an approach significantly simplify the modeling process and facilitate subsequent use and maintenance of the model, but mostly it secures its construction by automating the establishment of linkages between the various component elements and ensuring consistency. This point is especially important when the system under study comprises a large number of components.

This approach is moreover the only way to focus efforts on innovative study of cycles, which is now a research field both fascinating and essential for the future.

The many interesting ideas that have been proposed recently, for example to develop cycles without CO₂ emissions, are there to witness for the fruitfulness of this area of investigation, which it is essential to educate our students.

4.1.3 Generalities about numerical models

It seems particularly important to proceed in this manner as, due to the development of information technology, the way the engineer mobilizes his scientific knowledge has evolved in recent years. The time when he started from the fundamental equations and resolved them himself is now pretty much gone.

Increasingly, he uses models that encapsulate the equations needed, and implements them in modeling environments to facilitate their assembly. Modeling thus playing an increasing role in his activity, it is important that he is able to choose wisely the models he uses and evaluates well their limitations. Developing a strong culture in modeling should increasingly emerge as an inevitable necessity in engineering education².

Beyond the immediate resolution of a given problem, modeling, if it is to be effective, must be economical, safe and reusable. Based on work in this field in recent decades, it appears that this implies that it is modular (note that the etymology of both words is the same), and the assembly of complex models is facilitated by appropriate tools: modeling environments.

An environment for modeling energy technologies should if possible allow one to combine a systemic approach for global modeling, and an analytical or empirical thought process for developing component models. These two approaches turn out to be very complementary to model some technical systems. This requires:

- first identifying all the basic concepts necessary to solve a given class of problems. This raises the question of genericity: how, from a few basic primitive types, can we generate a large number of cases, what are the basic features that should be available, etc. The answer to this question is primarily a systems modeling one;
- second, primitive types being identified, establishing the corresponding models. The approach here is essentially analytical or empirical, connections and interrelationships between the modules being performed by coupling well-chosen variables.

²For further details, the reader may refer to the document “Numerical models and modeling environments: tools to effectively mobilize scientific knowledge” available at: <http://www.thermoptim.org/sections/base-methodologique/modelisation-systemes/modeles-numeriques>, or to (Hagin, 2000).

A good modeling environment thus consists on the one hand of a set of primitive types, forming a sufficient basis for the generation of as many projects as possible, and on the other hand an interface allowing one to easily link these primitives to represent studied objects, and having additional features, including archival material.

Numerical models are perhaps the most powerful basic tools to study complex systems. Modeling is a necessity and it does not supplant the experiment: it complements it by lowering the cost of studies and allowing one to understand operation modes otherwise inaccessible to direct observation. A numerical model is a simplified mathematical representation (or approximate abstract representation) of the studied system, which allows its behavior to be investigated. This is an operational tool developed by the engineer or physicist to solve the various problems they face.

It is important to note that a model is false by definition. Thus, it can have behaviors that are specific and distinct from those of the studied system. However, it may fail to represent some system behaviors. What is important is that these approximations do not influence the interpretations we make.

We can define on the one hand a phenomenological, or analytic, modeling based on a decomposition of the problem and the application of physical laws, and on the other hand a empirical modeling, based on correlations or laws derived from experimental data (especially when the complexity or the random nature of the problem studied prevents a phenomenological approach). In fact, the models used are often the result of a compromise between these two modes of operation.

In a deductive or analytical approach, most of the parameters introduced in the model have a physical meaning. These parameters may have been measured and some are known accurately, others are known in a range that is too large or impossible to measure. Finally, the more the model takes liberties with phenomenology, the more parameters appear having no physical meaning, sometimes known as calibration parameters. Ultimately, in a purely empirical or inductive approach parameters often have no direct physical meaning.

When the degree of complexity of the system is very high, the number of components, interactions and descriptive parameters does not always make possible a deductive approach. In this case, there are techniques which, from experimental data (Input-Output), can be used to derive simplified mathematical models called behavior models.

This non-phenomenological modeling approach does not allow us to improve or optimize the system studied. It can be used to characterize an existing system, to simulate it, or to control it. The methods used are borrowed mostly from control science and statistical sciences (regressions, correlations, parameter identification etc.).

Among these, identification opens up particularly attractive prospects because a black-box type study may allow, by analyzing only inputs and outputs of a system, good models to be obtained, even in the absence of equations set beforehand on the basis of the laws of physics. Identification methods therefore provide further insight into the traditional physics approach. In the broadest sense, identification is the phase that allows one to determine the numerical values of parameters used in the model, the selection criterion being to minimize the error between the calculated quantities and magnitudes observed experimentally.

4.2 PRACTICAL IMPLEMENTATION OF THE DOUBLE ANALYTICAL-SYSTEMS APPROACH

Incidentally, we have to use the term model in two different meanings, that the context will usually distinguish without difficulty: component models, which will be discussed in section 4.4.3, are used to calculate or analyze the internal behavior of a component, and system models (see Section 4.4.6), which are in the form of an assembly of previous models.

The Thermoptim core was built to help represent the most common components: compressors, turbines, combustion chambers, expansion valves and heat exchangers. Their thermodynamic models being almost universally accepted, it was possible to program them once and for all.

The software includes a second family of components, which take the form of external Java classes. These components (e.g. solar collectors, cooling coils, cooling towers, fuel cells, chemical reactors etc.) are easily customizable by users, who thus have the opportunity to define themselves the phenomenological and behavior models they wish to retain.

To implement the dual systems/analytical approach that we advocate, we must operate in two stages:

- begin by building models of system components;
- assemble them to create the model of the overall system.

The first step is essential and a prerequisite so that the systemic approach can be implemented. For a user, the problem is different depending on whether a realistic enough model is available or not in Thermoptim core or among external classes:

- when all required components are already available, the modeling approach is essentially limited to the systemic phase: it consists of assembling models of pre-built components, and then set them;
- when it is necessary to develop some component models, the external classes development environment allows one to create these models and make them compatible with the software.

Once the component models are available, building the model of a thermodynamic system with Thermoptim is very simple:

- we first make a qualitative description by representing it graphically as a set of components connected by links representing the fluid pipes or heat exchangers;
- the model defined is then quantified by setting the various primitive types that are involved, in order to calculate its performance, making use of the predefined templates.

The diagram editor allows for the qualitative stage: the user provides in a first step only the minimum information necessary for the logical definition of the project he builds (implicitly the types of components that he selects and explicitly their name and exit point and the substance associated with them, as well as the value of the flow through them). Then, when he interconnects these components, some of this information is automatically propagated from upstream to downstream (for example, the inlet point of the downstream component becomes the same as the one at the upstream component outlet). This small number of basic information provided to the graphical modeler corresponds to the systemic description of the technology studied.

When this step is complete, it becomes possible to transfer in the simulator the diagram components to create the primitive types required, with a default setting of their thermodynamic properties. Quantification of the desired model can then be made by refining this setting, each element of the simulator being easily displayed by double-clicking either on the corresponding component in the diagram editor, or on a table line of the main simulator project screen.

Once the element parameters are set and calculated, the results can be directly displayed in the diagram editor, which thus becomes a true synopsis of the installation, or plotted as a cycle in one interactive chart.

The objective of this book is to enable readers to understand the design principles of energy systems and to have an overview of the different technologies available for their realization.

We try to show how a structured approach to the study of energy technologies can be implemented based on these principles by relying on Thermoptim software, which was specifically designed for that purpose.

This book will have achieved its objectives if the dual approach it offers is able to show readers that it is now perfectly possible to reconcile facilitated study of energy systems and accurate calculations, when you have an appropriate modeling environment.

We believe that it is only if they are truly convinced that many students and engineers will be motivated for the discipline and desire to invest in it, when so many have so far been repelled by the heaviness of the mathematical formalism and calculations.

PRACTICAL APPLICATION

Modeling basic thermodynamic cycles with ThermoOptim

Three examples of practical application of the methodology presented in this section are presented Chapter 9: steam power plant, gas turbine and refrigeration machine.

The steam power plant and the gas turbine are engines intended to convert heat into mechanical power, while the third cycle is a machine designed to extract heat at a temperature lower than the atmosphere thanks to a mechanical energy input.

4.3 METHODOLOGY

When analyzing the most common energy technologies, we see that the number of elements which they are composed of is relatively limited, and that in most cases each component for a given phase of operation may be called mono-functional, as it exchanges energy according to a preferred mode, either as purely thermal (heat transfer) or by converting mechanical energy into heat energy or vice versa.

Consequently, functions that the various components are required to complete can be grouped into relatively few categories and calculated independently from each other, forming what one might call the primitive types basis which constitutes the core of ThermoOptim. It is sufficient to represent a large number of energy technologies, including those used in most conventional cycles. As we have already indicated, and as we will have the opportunity to show repeatedly in this work, the external class mechanism allows us to supplement this basis by adding to the software other components, particularly multi-functional ones.

The case of heat exchangers is somewhat unusual because it is clear that the calculations of the cooling of one fluid and the heating of the other must be conducted in a coupled manner. A special treatment will be reserved as discussed below.

When interconnected, these components are systems to which it is fruitful to apply the techniques of systems modeling, which we outline in the next section.

4.3.1 Systems modeling: the General System

The systems approach is the best available theoretical basis for understanding devices incorporating a set of components, each relatively complex, interconnected by a network of relationships also complex, organized according to a goal, and such that the behavior of each component can be explained only by that of the whole, while no one can derive *a priori* simple behavioral laws.

Introducing a systems modeling approach is even less easy as it is an evolving theory, which still lacks a universally recognized theoretical framework. One of the best summaries is probably the General System Theory of J. L. Le Moigne (1984), which defines itself as a systems modeling theory, to which the interested reader may refer.

A special feature of this presentation is to build an artificial General System, having all core systems characteristics. It is a sort of a model of models, which provides an analytical framework for all real systems, whose main interest is to provide guidance for operational modeling.

Without going into details, it is important to note that the systemic approach focuses on the functions of each of the elements which compose the system, which distinguishes it from the conventional Cartesian approach, which emphasizes the analytical description of phenomenological laws.

To describe a component, the conventional analytical approach has indeed to resort to describing all the relationships that explain its internal behavior (development of knowledge models). A purely functional approach does not necessarily have that luxury of detail. Where it is possible to establish a pattern of behavior based on analysis of only component inputs/outputs, without any assumptions about its physical or abstract content, we talk about a “black box” model or empirical model. This concept has proven very powerful, including in control science, where it is often not necessary to know the detailed inner workings of a process in order to control it.

In some cases, we only know partly the content or structure of the component. It then becomes possible to establish more accurate models or of a wider range of validity by using this information to guide the model choice. This is known as a gray box or adapted or semi-empirical model. It is precisely this type of representation we use to model the components involved in energy technologies.

The advantage of using systems analysis is that, to a very large extent, the structure of a system is independent of the degree of fineness of the modeling (the contents of the boxes). This organizational structure, which is a characteristic of the system in question, may therefore be subject to particular analyses, which remain valid if some process models are changed. This property allows one to operate in an iterative manner, while maintaining the gains of the previous phases, which is very efficient and economical.

Two of the main tasks of the systems modeler in these conditions are identifying the system components and building their network of interrelationships.

To accomplish the first task, the modeler must be able to separate the entire system by judicious choice of the separation points, the “natural joints” of the system and the coupling variables. This act carries a high level of subjectivity and explains that a given system may be modeled in several ways, even by the same modeler.

The analysis is facilitated if one has a catalog describing all the *functional elements* that may appear in the systems studied (for large systems, it is precisely the General System of Le Moigne). It is sufficient to identify the objects studied and then link them to define the structure of the system.

These elements can be grouped by classes of primitive types. When several primitive types form a core necessary and sufficient to represent a wide variety of systems, we say they form a basis. As such, they play a major role in the modeling process and their choice must be made with great care.

It is important to note that, given the emphasis that the systems approach gives to functions, these primitives represent the basic functionalities of the system, not for example its geometry. To illustrate this, let us take the case of internal combustion reciprocating engines (gasoline or diesel), where the same set of parts (cylinder and piston) plays successively in an engine cycle the role of the compressor, combustor and expansion device. Systems modeling of such a system leads us to interconnect the three primitive types representing these different functions.

For this reason, we are led to speak of primitive types and functional elements and not just basic components: firstly a component in the technological or geometric sense sometimes needs to be modeled by several primitive types, and secondly a given function may lead to different technological solutions.

4.3.2 Systems-analysis of energy technologies

Given what has been said, the systems analysis of an energy technology can be broken down into four basic steps:

- analysis of the structure (or architecture) of the technology in question, which highlights its main functional elements and their connections. This task can prove trickier than it seems because some components sometimes provide different functions in different phases of operation. It is facilitated

- if one has a basis of well chosen primitives. The structure of the system thus demonstrated is an invariant almost independent of the fineness retained for the modeling of components;
- for each element, identification of the thermodynamic fluids that come into play: for example, the fluid compressed in a gas turbine is air, which burns a fuel in the combustion chamber to form burnt gases themselves expanded in the turbine. In this case it is necessary to consider three thermodynamic fluids: in the compressor, air which may possibly be moist, in the combustion chamber, air, fuel, and burnt gases, and in the turbine the exhaust gases;
 - for each element, accurate determination of processes undergone by the various fluids identified, and calculation of their changes. The degree of fineness of modeling depends on the desired accuracy and available data. In this work, we will only quantitatively model overall component behavior, using parameters to characterize it (characteristics), and limit to qualitative considerations the analyses of the specifics of what happens internally;
 - establishing the overall model of the system considered by assembly of the different types of functional elements. When the previous steps have been taken with care, it is usually not of particular difficulty. At most we should take care to define the types of energy that come into play, to be sure to count them properly, particularly when one wishes to calculate a cycle effectiveness, which is often the case³.

Once these steps are undertaken, all the elements are available to pass to the system optimization phase, which can be made on the one hand by making sensitivity studies around key design parameters, and on the other hand by using specialized tools.

4.3.3 Component modeling

The second Part of this book is mainly devoted to the presentation of component models, which we have grouped into three types:

- phenomenological models constructed on the basis of an analysis of the physical functioning of the component. Their parameters have then a physical sense. Their goal is the study of thermodynamic cycles;
- empirical or behavior models, often of the black box type, which have the advantage of representing the overall input/output component behavior, and can especially be used to study its operation in off-design mode. Their parameters have usually no physical sense;
- technological design models which provide access to detailed internal design of the components. The most accurate of these models are specific tools that take into account both theoretical aspects (mechanics, thermodynamics, fluid mechanics and heat transfer⁴), and technological (manufacturing processes, surface treatments, material selection) or economic (costs) ones or environmental constraints. They are multidisciplinary sophisticated tools which can only equip manufacturers.

A compromise must be found between the desired accuracy and complexity (and cost) of modeling. Given the objective of this book, we limit ourselves to a steady-state representation of phenomena, and we do not generally seek, at least in the first four Parts, to get detailed models of how a particular component works, which can be extremely complex. Only in the fifth Part do we give some guidance on how to approach the technological design and off-design study of components.

³This issue will be discussed in Chapter 10.

⁴See sections 2 and 3 of (Kreith, 2000).

As we shall see, the models we use are often mixed, being partly phenomenological, and partly empirical.

For example, the study of heat exchangers (see Section 8.2) shows that a model of type (ϵ, NTU) is quite sufficient to study the insertion of such a component in a system, but it only gives access to the product UA of the heat transfer coefficient U by the exchange area A : it is therefore an incomplete phenomenological model. If it is associated with an empirical law giving the evolution of the value of UA as a function of the two fluid flows through the exchanger, it can be used as a model for analyzing the response of a specific exchanger to changes in its conditions of use. It can also become a technological design model if it is completed by the set of functions for determining the value of U , as explained in Part 5.

Some additional definitions relating to models deserve to be made. The models we are interested in involve four different concepts:

- parameters characterizing the component: some are purely geometric, as a free flow area or an exchange area, while others have a thermodynamic sense, as an isentropic efficiency. The thermodynamic properties of fluids are a special category of parameters;
- input variables represent the constraints set on the component, such as flow, temperature or pressure. These are exogenous, determined outside the component;
- internal variables are used to determine the component state. These will often be state variables in the thermodynamic sense of the term;
- output variables are the model results, such as temperatures, compositions etc.

To study the insertion of a component in a system, it is usually not necessary to know the details of its inner workings. In most cases, and this is the case with most technologies that interest us here, a phenomenological model may represent a given component by a small number of characteristics and its coupling variables (inputs and outputs). These characteristics depend on the type of component and the technology.

For example, a displacement compressor will be characterized by a volumetric compression ratio, a volumetric efficiency and an isentropic or polytropic efficiency, and a heat exchanger by a number of transfer units etc. The coupling variables are pressures, temperatures, flow rates etc.

We will focus on understanding the overall performance of components, sufficient for our purpose, committing ourselves to identify expressions of characteristics representative of their operation. By limiting our discussion to models which are as simple as possible while remaining thermodynamically relevant, we will not achieve completeness. Readers interested in further developments will find them in the literature.

4.3.4 Thermoptim primitive types

To determine the performance of energy technologies, we have seen that it suffices to have a tool to describe, assemble and calculate the various elements that compose them in a form as convenient as possible. Many solutions are of course possible at this level. For our part, we will illustrate this approach using the Thermoptim software, which was specifically designed for this purpose.

The list of functional elements that may appear in the main energy conversion technologies corresponds to the concepts that are implemented in Thermoptim and which are detailed below. This package is thus a General System in the sense of Le Moigne for energy technologies systems modeling: to build the model of a given energy technology is to build a representation as accurate as possible by assembling together different objects chosen from those that the software offers. We give several examples in this book that illustrate this approach.

The following list is a basis of primitives sufficient for studying a large number of energy technologies:

- We must first be able to represent the intensive properties of fluids used, and calculate their state for various values of pressure, temperature etc. The concepts of *substances* and *points* allow us to do this;
- these fluids undergo changes (*processes*) that can be grouped into several major categories, the most common being: compression, expansion, throttling or flashes, combustion and heat exchanges. It is in processes that the mass flow rates involved are specified, and therefore here that extensive properties can be calculated;
- fluids pass through components, forming more or less complex networks that we must be able to describe. The processes above are a portion of these circuits. To complement these, we must make use of *nodes* (dividers, mixers and separators);
- when two fluids exchange heat together, they form *heat exchangers*, components coupled with two processes which cannot be calculated separately.

4.3.4.1 Substance thermodynamic properties

The representation of thermodynamic properties of substances is of course a necessity. It requires firstly adequate fluid models, and secondly data to represent the fluids used.

Every substance is in at least one of the three phases solid, liquid or gaseous. When the pressure is sufficiently low and the temperature sufficiently high, it is reasonable to consider that the substance behaves like an ideal gas whose heat capacity, internal energy and enthalpy depend only on the temperature (not on pressure).

ThermoOptim includes all data needed to calculate the thermophysical state of fluids, which can be either pure or gas mixtures. Their composition can change, because of either mixing or combustion reactions.

It defines three categories of substances: pure ideal gases, compound ideal gases and condensable vapors or real fluids (without mixtures). The perfect gas corresponds to the particular case of ideal gases whose heat capacity is temperature independent.

The principles of calculating the properties of substances are outlined in Chapter 5.

4.3.4.2 States of fluids: points

Once you have a representation of substance properties, it becomes possible to calculate the state of a fluid as a function of relevant variables, such as pressure, temperature, enthalpy etc.

For this ThermoOptim defines points. A point represents a substance particle and determines its intensive state variables: pressure, temperature, heat capacity, enthalpy, entropy, internal energy, exergy, quality, absolute or relative humidity etc. A point is identified by a name and that of the substance associated with it.

To calculate it, you must:

- either enter at least two of its state variables, typically pressure and temperature for open systems, or specific volume and temperature for closed systems;
- or automatically determine it by using one of the processes defined below.

The calculation screens of substances and points are presented in Chapter 6.

4.3.4.3 Processes

Processes correspond to thermodynamic changes undergone by a substance between two states. A process associates therefore two points as defined previously, an inlet point and an outlet point. In addition, it indicates the mass flow rate involved, and allows one therefore to calculate extensive state variables, and notably to determine the variation of energy involved in the course of the process.

The most common evolutions have been modeled and are directly accessible. Knowing the state of the fluid at the process inlet, ThermoOptim may solve either the direct problem, or the

reverse problem. In the first case, knowing the characteristics of the process, it computes the state at the end of evolution and the energies involved, and updates the outlet point. In the second case, it identifies the parameters of the process selected that allow it to lead to the defined outlet point state.

Processes can be of several types: compression, expansion, combustion, throttling or flash (pressure drop without work production, as in a valve or a filter), heat exchange, and water vapor/gas mixtures (the latter includes six different categories of evolutions). They are presented in detail in Chapter 7.

According to each case, various characteristics of the process have to be specified, for example, in compression, its isentropic or polytropic efficiency, as well as the type of calculation which is required (open or closed system, direct or inverse calculation etc.).

A cycle can thus be described as a set of points connected by processes. To the extent that the mass flow rate fluid is the same in all the evolutions, processes and points are sufficient. If this is not the case, it may be necessary to describe at least partially the network of involved fluids using the nodes defined below.

4.3.4.4 Nodes

Nodes can describe the network elements which make up mixture, division or separation of fluids. In a node, several fluid branches are interconnected to form a single vein (Figure 4.3.1).

If this is a mixer, the various branches join to form a single vein. The mass flow of the main vein is equal to the sum of those of branches, and the enthalpy balance is used to calculate the enthalpy and temperature of the mixture.

If it is a divider, the main vein is divided into several branches which must of course specify the flow-rates. Temperature and enthalpy are conserved.

In Thermoptim, you can mix together several different fluids, provided that the mixture is a gas. This means that if there are condensable vapors (or real fluids) among the branches of a node mixing together several distinct fluids, it is assumed that at the outlet they find themselves in a gaseous state and follow an ideal gas behavior. Remember that mixtures of vapors are not modeled in the software.

The logical definition of a node is by $(1 - n)$ association of processes: a process is the main vein, and n processes correspond to the branches. The processes themselves being connected to points, and the latter to substances, updates of the fluid state are made automatically.

A third type of node also exists: the separator, which is a somewhat special divider, which receives as input a vapor in two-phase state, and separates the liquid and gas phases. Nodes are discussed in Chapter 6.

4.3.4.5 Heat exchangers

Heat exchangers are components that combine two streams, one that warms up, the other that cools, whose evolutions are coupled and cannot be computed independently. The simplest definition of a heat exchanger would ask that you indicate what are the two processes that it matches.

Thermoptim can design a heat exchanger, that is to say calculate the value of the UA product of its exchange surface by its heat exchange coefficient, if you indicate what constraints are set on the flow rates and temperatures (for instance minimum pinch, set value effectiveness).

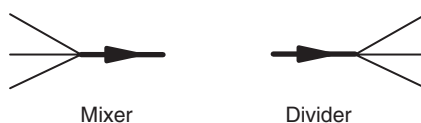


FIGURE 4.3.1

Nodes

The software can also, once the design is completed (i.e. for a given value of the UA product) calculate, for off-design operating conditions of the flow-rates or inlet temperatures, what is the exchanger behavior, that is to say what are the outlet temperature values. Exchangers are discussed in Chapter 8.

4.3.4.6 Components of the diagram editor

ThermoOptim is equipped with a diagram editor (Figure 4.3.2) which can qualitatively describe the system studied. It has a palette with the various components available (heat exchangers, compressors, turbines, combustion chambers, mixers, dividers etc.), and a working panel where these components are placed and interconnected by links. This environment offers a particularly interesting user-friendliness to view and control the connections of large systems.

If we remark firstly that a point is always associated with a process, and a substance to a point, and secondly that a heat exchanger does in fact define a coupling between two exchange type processes, we see that the description of a system can be made solely from processes, nodes and their interactions.

It is this property that is used in the diagram editor, whose palette includes only processes and nodes, which are then connected using two types of links: oriented links representing a fluid line i.e. essentially a point and a flow-rate, and non-oriented links symbolizing exchanger connections.

The great usefulness of the diagram editor is that you can build a visual representation of the systems studied from a very small number of elements, that it is sufficient to understand and know in order to model many energy technologies. Once this description is made, you just have to appropriately set the ThermoOptim primitive types that are put in. The modeling work is thus divided into two distinct and complementary phases, the qualitative and quantitative. We will see later that the tight coupling between the diagram editor and ThermoOptim simulator makes it easy to set the parameters and quantify the model.

When the elements are configured and their calculation is performed, the results can be directly displayed in the diagram editor (Figure 4.3.3), which behaves like a synopsis of the system, and represented as a cycle in the interactive charts (Figure 4.3.4).

4.3.4.7 Projects

The set of primitive types for describing an energy technology (substances, points, processes, nodes, heat exchangers) is known as a project in the package. A project can be easily manipulated through appropriate interfaces. All results can be exported to a text file and can be after-processed by a word processor or a spreadsheet.

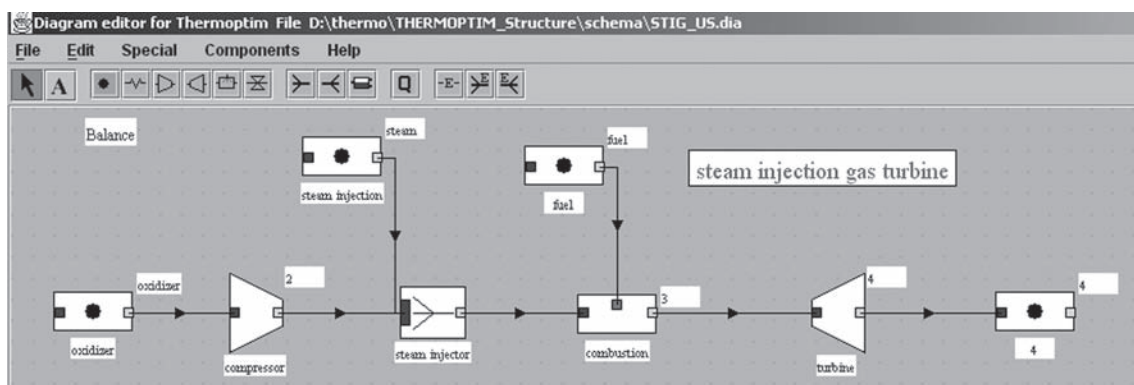


FIGURE 4.3.2
ThermoOptim diagram editor

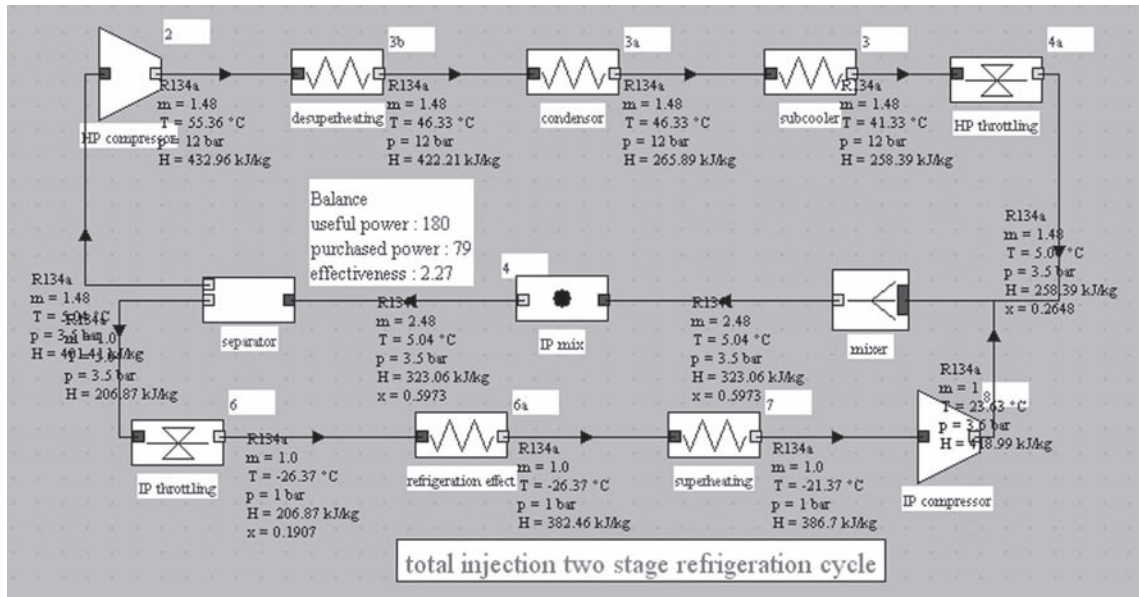


FIGURE 4.3.3
Viewing cycle point states

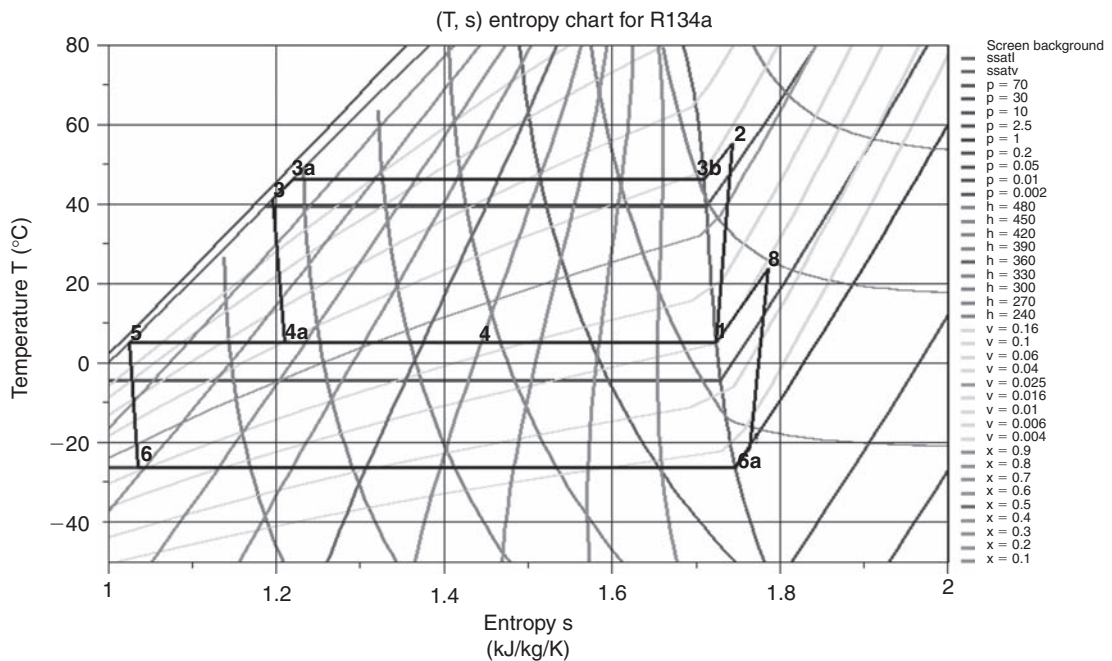


FIGURE 4.3.4
Two-stage R134a refrigeration cycle in the entropy chart

To facilitate archiving and reuse of different projects generated, a number of rules and project management tools have been defined. In particular, a project can receive a name and description to describe it succinctly. Then, as it is clear that the same diagram can match several projects, each with a different setting, and that a project cannot in principle have several diagrams, it is possible to associate a diagram name to a project.

In this way, when a diagram is displayed in the graphical modeler, you can search among the list of projects associated with it, and display it in a private library of the above type.

4.3.5 ThermoOptim assets

The preceding lines allowed us to introduce the main ThermoOptim primitive types. We will show throughout this book that this very small number of elements is sufficient to model a wide range of energy technologies. It is very remarkable that a dozen widgets (including links) are sufficient to represent so many. The modeling of these technologies, which is generally considered difficult, can be greatly simplified when you have a tool like ThermoOptim, the diagram editor allowing one to obtain a qualitative description of the model particularly meaningful for an engineer, that it is then relatively easy to quantify.

ThermoOptim appears as an applied thermodynamics package whose main assets are:

- it provides a coherent analytical and systems modeling environment. For a relatively small initial investment in understanding the underlying logic, itself quite natural and intuitive, it allows for a rigorous analysis process leading to significant productivity gains. The models developed can easily be documented, archived and re-used or modified;
- its primitive type basis is an analytical grid of energy technologies allowing one to highlight the components interrelationship graph. With a little experience, the modeler obtains a representation that is both faithful to reality and calculable by the software. This step is greatly facilitated by the graphical editor;
- the description of the problem is made using natural concepts of the engineer or physicist, primitive types having a very clear physical meaning. The modeler can concentrate on the physical analysis of phenomena, the mathematical translation, digital and computer generated models being provided by the tool in a transparent manner;
- the modeler does not himself write a single line of code or solve an equation, ThermoOptim processing the project description submitted to it. The user is thus guaranteed to get realistic results quickly without the risk of programming errors. If he wants to make calculations not provided in the tool, he can process (e.g. with macros) the text file of his project results;
- since fluid properties are calculated automatically, the modeler can obtain very accurate results while being relieved of many computational problems that would otherwise be avoided only by resorting to caricature simplifying assumptions;
- the package is an open environment, written in Java. If necessary, the basis of primitive types can be extended to represent additional components.

REFERENCES

- J.L. Le Moigne, *Théorie du système général*, PUF, 1984.
- F. Hagin, *Numerical analysis and computational tools*, in: *The CRC handbook of thermal engineering*, (Edited by F. Kreith), CRC Press, Boca Raton, 2000, ISBN 0-8493-9581-X.
- F. Kreith, Ed., *The CRC handbook of thermal engineering*, CRC Press, Boca Raton, 2000, ISBN 0-8493-9581-X.

Thermodynamics Fundamentals

Abstract: In this chapter which in particular extends some questions already introduced in Chapters 2 and 3 of Part 1, we present the basic thermodynamics knowledge needed to study energy technologies.

One ambition of this book, as we have said, is to propose a learning method of applied thermodynamics much simpler than that which is traditionally taught. This bias for simplicity has led us to limit our presentation of thermodynamics to the sole foundation required for our purpose.

After showing how to express the energy exchanges during a process, a reminder of the first two laws of thermodynamics provides the theoretical basis for conducting most of the subsequent calculations. The concept of exergy is then introduced, and the end of the chapter is devoted to studying substance properties. It shows how they can be represented by a cascade of nested models: perfect gases, ideal gases, real condensable fluids.

We give in these sections definitions of many concepts which it is important to understand in order to calculate energy technologies, even if one uses Thermoptim. Examples are state functions such as internal energy, enthalpy and entropy (Sections 5.3 and 5.4), the properties of matter and the various models used to represent fluids (Section 5.6).

Keywords: Fundamentals, thermodynamic systems, variables and equations of state, reversible and irreversible processes, fluid properties, charts, moist mixtures, absorption.

5.1 BASIC CONCEPTS, DEFINITIONS

Thermodynamics can be defined as the science of energy transformations, which can take four forms: mechanical, thermal, chemical or electrical.

We understand that exposing thermodynamics in a general way is particularly difficult, since the set of definitions, postulates and demonstrations should apply to all these forms of energy.

However, for the study of energy systems discussed in this book, we can in practice limit ourselves to the first two in this list, mechanics and heat transfer, except as regards moist mixtures and combustion reactions.

Accordingly, and except for calculating the moist mixtures and combustion, which will each be given special treatment, we always assume that the substances involved are of unvarying

composition. We thus will not show chemical variables, which significantly simplifies the formalism. Moreover, the systems we study will always be non-electrified.

This way of proceeding, which is common practice in power engineering, will lead us at times to move away from strict thermodynamics formalism, and we shall draw attention to this when it happens. As we have already mentioned in the general introduction, what we lose in generality will be offset by the gains in ease of use of the book.

At this stage of our study, it is best to define or recall a number of fundamental concepts that we will need later in the presentation: thermodynamic systems, variables and equations of state, phase equilibrium, reversible and irreversible processes. These concepts are necessary to compute the evolutions experienced by thermodynamic fluids. It is indeed necessary to introduce variables and functions connected by equations that can only be determined if the environment is considered continuous and homogeneous, that is to say if these functions are sufficiently regular in the mathematical term. In particular, we will focus only on macroscopic quantities.

5.1.1 Open and closed systems

A thermodynamic system means a quantity of matter isolated from its surroundings by a fictional or real boundary. This system is called closed if it does not exchange matter with the outside through its boundaries, otherwise it is called open. Note that this notion of system is not the same as the one we introduced above to characterize an energy technology as an assembly of components. There is a difficulty of vocabulary that we cannot avoid having regard to practice, but the context generally makes it not difficult to distinguish the two meanings of the term.

Beginners are often confused by the distinction between closed systems and open systems, the latter corresponding to a new concept for them, because during their undergraduate tuition they generally considered only closed systems (to avoid taking account the exchange of matter at boundaries).

In a diesel or gasoline engine, the valves are closed during compression, combustion and expansion, isolating from outside the mass of gas found between the piston, the jacket and head. The processes that take place inside the engine must be calculated in closed systems. In the case of a gas turbine, compressor, combustor and turbine, these are driven by a continuous flow of gas. At the entrance and exit of each of these components, matter is transferred. The changes must then be calculated in open systems.

There is a certain paradox in the fact that the calculations are generally easier to make for open systems than for closed systems, although these do not involve exchange of matter with the outside. The reason is that the pressure is usually given in the calculations in an open system, although it depends on many factors in a closed system.

For example, combustion in a gas turbine (open system) takes place at constant pressure, neglecting small pressure drops, whereas in a diesel or gasoline engine (closed system), the pressure varies greatly during the process, so it is preferable if one wants to stick to reality, to break it down into several stages: for example, first at constant volume, then constant pressure, and finally constant temperature.

To complete complicating things, it is natural (but fatal) to confuse the concepts of open and closed systems in thermodynamic sense that we just introduced and its meaning when considering the whole cycle swept by the fluids in a thermal machine.

For example a refrigerator compression cycle is a closed cycle Figure 2.1.3 of Part 1 otherwise the refrigerant would be lost to the atmosphere, which would be both costly and harmful to the environment, while each of its components taken separately (except optionally if the compressor is displacement type) is an open system, through which passes a steady-state flow of refrigerant.

The machine operates as a closed cycle involving several components, each working in open systems.

5.1.2 State of a system, intensive and extensive quantities

The notion of state of a system represents “the minimum information necessary to determine its future behavior”. State variables (temperature, pressure, etc.) are all physical quantities (or thermodynamic properties) necessary and sufficient to fully characterize a system at a given moment. There are usually several sets that meet this definition. We will see later that for a phase of unit mass, two quantities are sufficient to determine all the others. These results ensure the existence of equations relating each state variable to two of them independently: $v = f(P, T)$... We call such relationships equations of state, which are fundamental in practice.

Depending on the problem, the following pairs are generally retained: (pressure, volume), (pressure, temperature), (temperature, volume). A state function is a quantity whose value depends only on the state of the system, not its history.

A physical model involves variables representing the state of a system, which is *a priori* a function of time and position of the point considered. These quantities can be grouped into two broad classes:

- **intensive quantities** such as pressure, temperature or specific enthalpy, which are independent of the amount of matter considered;
- **extensive quantities** such as mass, enthalpy or entropy, which depend on the mass of the system.

An intensive quantity links the condition provided at a point of the medium to a reference condition at another point or another medium. For example, the temperature is defined relative to zero or to the triple point of water.

An extensive quantity is additive: if a system is composed of several phases, extensive quantities that characterize it are equal to the sum of those of its component phases. Mass or total enthalpy are extensive quantities.

Note that by multiplying the phase mass by certain intensive quantities such as specific enthalpy or entropy, extensive quantities are obtained as enthalpy or entropy.

Recall that a control volume is a region of space with real or fictitious boundaries, thus defining the system of interest (thermodynamic in this case). An example of a control volume is given in Figure 5.3.1. It is bounded by the walls of the fixed and mobile machine M and two immaterial geometric surfaces named A_1 and A_2 at the initial instant t_0 , and B_1 and B_2 at $t_0 + dt$.

In the example in Figure 5.3.1, the control volume is considered a closed system, which is followed in its movement over time, from A_1 to B_1 and A_2 to B_2 . In other cases, the control volumes can define open systems. The masses they isolate may then vary depending on mass flow rates crossing their boundaries.

In general, the component models we use are established by writing the laws of continuity and conservation of extensive variables: mass, energy, entropy, etc., balance sheets being established for well-chosen control volumes.

Conservation laws are written in the general form:

$$\left\{ \begin{array}{l} \text{accumulation in the} \\ \text{control volume} \end{array} \right\} = \left\{ \begin{array}{l} \text{inward transport} \\ \text{by the surface} \end{array} \right\} - \left\{ \begin{array}{l} \text{outward transport} \\ \text{by the surface} \end{array} \right\} \\ + \left\{ \begin{array}{l} \text{transfer through} \\ \text{the surface} \end{array} \right\} + \left\{ \begin{array}{l} \text{generation} \\ \text{in the volume} \end{array} \right\} - \left\{ \begin{array}{l} \text{consumption} \\ \text{in the volume} \end{array} \right\} \quad (5.1.1)$$

For the conservative quantities, such as mass, internal energy and enthalpy, the last two terms in the equation vanish. For non-conservative quantities, such as entropy or the number of moles of chemical species in reaction, it may be necessary to introduce one or the other.

Building a model is to translate that expression into a set of semantic equations and set the initial and boundary conditions.

5.1.3 Phase, pure substances, mixtures

A phase is a continuous medium having the following three properties:

- it is homogeneous (which implies a uniform temperature);
- speed in each point is zero in a suitable reference frame;
- it is subject to no external force at distance (uniform pressure).

As is known, matter exists in three phases: solid, liquid and gas. A thermodynamic system may consist of a single pure substance, or have several. In the latter case, the mixture is characterized by its molar or mass composition. Each of the components of the mixture may be present in one or more phases. If the components and their phases are uniformly distributed throughout the volume defined by the system boundaries, the mixture is homogeneous, otherwise it is heterogeneous. The properties of a mixture depend obviously on its homogeneity.

The concept of phase plays a very important role in practice, because we always assume in what follows that any physical system is decomposed into a set of phases.

5.1.4 Equilibrium, reversible process

A phase is said to be in static equilibrium, or simply in equilibrium, if:

- pressure and temperature are uniform in space;
- all state variables are constant over time.

We call a reversible process between two equilibrium states 1 and 2 a fictitious process which has the following two properties:

- it is slow enough at all points of view (speed, heat and matter transfer, etc.) so it can be likened to a continuous state of equilibrium;
- it is the common boundary of two families of real processes, one of which leads from 1 to 2, and the other from 2 to 1.

A process is said to be irreversible in the following two cases:

- the reverse process is not feasible without substantial modification of equipment (mixing, combustion, etc.);
- it contains a cause of irreversibility of the friction or viscosity type.

5.1.5 Temperature

The concept of temperature can be introduced in several different ways. We content ourselves here with the operational definition given by F. Fer (1970), which is based on two propositions:

- we know how to construct a thermometer device, of which all physical properties are, under well defined operating conditions, function of a single variable called temperature;
- we know how to get a physical system such that when a thermometer is immersed in it, its indication remains constant over time and independent of its orientation and its place.

It is said the temperature of the medium is equal to that of the thermometer and that the medium is in thermal equilibrium.

It is possible to link this presentation with the axiomatic definitions of the temperature deduced for example from the second law. A rigorous and comprehensive presentation of this notion, however, is beyond the limits we have set for this book. Furthermore this introduction is quite intuitive and its practical use does not generally pose a particular problem.

5.1.6 Symbols

We shall generally write state variables in lowercase (except the temperature in Kelvin and pressure) as well as intensive state functions (referred to the mass unit), and capitalize the extensive quantities (referred to the total mass).

Following established practice, however, an exception will be made for the kinetic energy K , the work of external forces W and the heat exchanged with the outside Q , which are written in capitals, even if expressed in mass units, and for the useful work τ , which is always written in lowercase.

We pass from one to another by multiplying the first by the mass m (for closed systems), or the mass flow \dot{m} (for open systems).

$$\begin{aligned} \text{volume } v &= \frac{V}{m} = \frac{\dot{V}}{\dot{m}} \quad (\text{m}^3 \text{ kg}^{-1}) & \text{internal energy } u &= \frac{U}{m} = \frac{\dot{U}}{\dot{m}} \quad (\text{J kg}^{-1}) \\ \text{entropy } s &= \frac{S}{m} = \frac{\dot{S}}{\dot{m}} \quad (\text{J kg}^{-1} \text{ K}^{-1}) & \text{enthalpy } h &= \frac{H}{m} = \frac{\dot{H}}{\dot{m}} \quad (\text{J kg}^{-1}) \end{aligned} \quad 5.1.2$$

For convenience, we will refer, whenever possible, to the unit mass of fluid.

In this book, as we will use extensive quantities only very rarely, to avoid burdening the notation, we take the liberty to also use capital letters for the molar quantities, which we sometimes use. When this is the case, we will say so.

Remember also that the kilomol (1 kmol) is the amount of a substance whose mass is equal to its molar mass M in kilograms: 1 kmol of O_2 has a mass of 32 kg.

If M^* is the mass of a molecule, $M^* = M/N_0$, N_0 being the Avogadro number:

$$N_0 = 6 \times 10^{23} \text{ molecules/g.}$$

In the normal state (0°C , 1 bar), the volume occupied by 1 kmol is equal to 22.414 m^3 .

5.2 ENERGY EXCHANGES IN A PROCESS

Thermal machine components are traversed by fluids that are most often gaseous or liquid. Over the processes that they undergo, these fluids exchange energy with the outside or between themselves in two forms: mechanical, traditionally denoted W , and thermal, denoted Q . Given their practical importance, we will first study the energy exchanges.

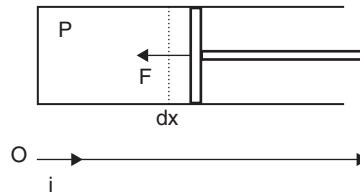
Consistent with our bias to favor as simple as possible a presentation of the thermodynamics fundamentals, we limit ourselves in what follows to steady state systems, because even if the results we establish generalize quite easily, it is necessary to adopt a heavier formalism if we want to be rigorous.

5.2.1 Work δW of external forces on a closed system

Consider a closed system phase. External forces acting on it are usually limited on the one hand in the action of gravity on the fluid mass, and on the other hand of pressure on its boundaries.

In heat engines, the work of gravity is in most cases negligible compared to that of actions called “contact”. To fix these ideas, the work provided by a mass of 1 kg of water falling from a height of 100 m is equal to 980 J, while that of the same mass of steam at 500°C isentropically expanded from 100 bar to 1 bar is equal to 983 kJ, or 1,000 times greater.

Consequently, in thermal machines, the work of mass forces will most often be negligible compared to that of pressure.


FIGURE 5.2.1

Sketch of a cylinder-piston assembly

Consider a fluid at rest (Figure 5.2.1), at uniform pressure P enclosed in a cylinder whose walls are all fixed except a piston capable of moving in one direction. Now exert a force \vec{F} on the piston to move it slowly enough (so that at any time the system can be likened to a phase).

Let us consider an axis (O, \vec{i}) directed from the bottom of the cylinder ($x = 0 \Rightarrow V = 0$). The force being exerted by the system outside, $\vec{F} = -\|F\| \vec{i}$

Call A the piston section, and $d\vec{x} = dx \vec{i}$ its motion.

Obviously $\|F\| = PA$, and work $m \delta W_A$ received by the mass m of fluid is:

$$m \delta W_A = \vec{F} \cdot d\vec{x} = -\|F\| dx \vec{i} \cdot \vec{i} = -PA dx = -P dV.$$

dV being the volume change of the mass, equal to $m dv$, and:

$$\delta W_A = -P dv \quad (5.2.1)$$

In case of compression, the volume change is negative and the work received is positive. We note this work with index A , to indicate it is exercised on the surface of the system considered.

This expression, which generalizes easily to a closed system of any form, is valid only if the system remains in static equilibrium, i.e. if the following assumptions are true:

- the pressure remains uniform across the system;
- the fluid remains at rest.

Note that formula (5.2.1) implies that the work received by the system is positive, and that the work it provides is negative. By convention, we generalize this result by counting positively the energy received by a system, and negatively the energy it provides to the outside.

During a reversible process making a closed phase pass from state 1 to state 2, the mass work of contact actions has the value:

$$W_A = -\int_1^2 P dv \quad (5.2.2)$$

In case the gravity work is not negligible, one can easily show that it is expressed as:

$$dW_v = -g dz \quad (5.2.3)$$

$g > 0$ is the acceleration of gravity, and z the altitude of the point, counted positively upwards. We note such work with index v , to indicate it is exercised in the volume of the system considered.

We have then:

$$W = W_A + W_v \quad (5.2.4)$$

5.2.2 Heat transfer

Consider a simple fluid mass, within which no friction occurs. δQ is the quantity of heat exchanged with the outside and received by the unit of fluid mass in an infinitely small process.

An important experimental fact, the basis of compressible fluid thermodynamics, is that δQ is a differential form of the fluid mass state, called a calorimetric equation.

For example, in the case of a mono-variant system (equilibrium between phases during a change of state), the calorimetric equation depends only on the quality x , ratio of vapor mass to total mass (liquid + vapor) in the case of vaporization or condensation: $\delta Q = L dx$

L is the change of state enthalpy.

More generally, the calorimetric equation that connects δQ to the simple fluid (bi-variant) state variables can take three well known equivalent canonical forms:

$$\begin{aligned}\delta Q &= c_p dT + h dP \\ \delta Q &= c_v dT + l dv \\ \delta Q &= \mu dP + \lambda dv\end{aligned}\tag{5.2.5}$$

Coefficients c_p , c_v , h , l , μ and λ are called equilibrium fluid calorimetric coefficients (note that h is **not** enthalpy, which will be introduced later). They are linked by differential relations that can be obtained without significant difficulty, but which do not interest us. Just know that the calorimetric properties of a fluid are determined by knowing two of these six coefficients.

Subsequently, we will use only coefficients c_p and c_v , which are respectively called specific heat capacity at constant pressure, and specific heat capacity at constant volume, whose former name was “specific heat”.

For a solid or a liquid, $c_p \approx c_v$, and $\delta Q \approx c dT$

For an ideal gas, depending on whether we are dealing with an open system operating at constant pressure, or a closed one operating at constant volume, $\delta Q = c_p dT$ or $\delta Q = c_v dT$. For a real gas, use one of the canonical forms above.

The above equations are however valid only if certain conditions are met:

- Firstly, the mass of fluid must be completely homogeneous, i.e. comparable to a phase;
- Secondly, we assumed that there was no irreversibility inside or at the boundary of the fluid mass. If any, the relationship becomes:

$$\delta Q < c_p dT + h dP$$

We will then write:

$$\delta Q = c_p dT + h dP - \delta \pi\tag{5.2.6}$$

$\delta \pi$, essentially a positive term, has a very simple physical meaning: it is the heat generated by mechanical friction within the fluid. Although it differs profoundly, it produces the same effect as heat received from the outside. Its meaning will be clarified during the presentation of the second law of thermodynamics (Section 5.4).

By convention, therefore, we denote δQ the heat exchanged with the outside, and counted positively if received by the system, and $\delta \pi$ the heat dissipated by internal friction if any. In practice, it is important to distinguish these two forms of heat, otherwise serious reasoning errors can be made. In particular, the processes without heat exchange with the outside, called adiabatic, are such that $\delta Q = 0$, whether or not the seat of irreversibility, that is to say $\delta \pi$ being either zero or not.

5.3 FIRST LAW OF THERMODYNAMICS

Now that we have established expressions for calculating the mechanical and thermal energy exchange of a fluid mass with its surroundings, we can recall the first law of thermodynamics. As usual, we start with the expression for closed systems, well known to all, and we generalize for open systems.

The first law, also known as the equivalence principle or the energy conservation principle, says that the energy contained in an isolated system or evolving in a closed cycle, remains constant, whatever the processes it undergoes. The various forms that can take the energy of a system: mechanical energy, heat energy, potential energy, kinetic energy etc. are all equivalent to each other under the first law.

5.3.1 Definition of internal energy U (closed system)

Any closed physical system is characterized by a scalar U , based exclusively on state variables, and such that for any real process:

$$\Delta U + \Delta K = W + Q \quad (5.3.1)$$

K being the kinetic energy of the system, W the work of external forces, expressed for the total mass of the system and given by relation (5.2.4) $W = W_A + W_v$, and Q the heat exchanged by the system with outside for the process considered.

U is an extensive quantity called the internal energy of the system, $U + K$ is sometimes called the system total energy. For a phase of mass m , $U = mu$, u being the specific internal energy.

Let us recall that the state variables that define, in the most general case, a physical system, fall into four broad categories:

- mechanical variables, position or deformation;
- temperature;
- chemical variables;
- electric variables.

Only the first two will be considered in most applications we have to deal with, and the third will be used for fluid mixtures and combustion reactions. As for the fourth, it will not intervene in the context of this book except in Chapter 27 of Part 4 dealing with electrochemical converters.

Note that many authors distinguish in the expression of the first law the work of gravity (W_v) and pressure forces (W_A), and therefore express it under the equivalent form:

$$\Delta U + \Delta K + mg\Delta z = W_A + Q$$

For an infinitely small control volume, Equation (5.3.1) becomes:

$$dU + dK = \delta W + \delta Q \quad (5.3.2)$$

Physically, the first law derives from the experimental evidence that, whatever the processes undergone by a given system, the sum $W + Q$ depends only on the initial state and final state. It follows therefore that $W + Q$ is a state function of the system.

Mathematically, the first law states that, while δW and δQ are not exact differentials, their sum is one, and is equal to the sum of kinetic energy changes and a function state, the internal energy.

5.3.2 Application to a fluid mass

We will see later that in the case of a single fluid phase, the physical state of the system, expressed in mass quantities, is characterized by variables P , v , T , connected by the equation of state. u is a function of these variables, or more precisely two of them.

Let us apply the first law to a fluid infinitesimal reversible process, neglecting the action of gravity. During this process, the kinetic energy remains constant equal to zero, which implies $dK = 0$. Moreover $\delta W = -P dv$ and δQ is expressed as:

$$\delta Q = du + P dv \quad (5.3.3)$$

By identification with the calorimetric equation (5.2.5), we get: $c_v = (\partial u / \partial T)_v$, which is often used as a definition of c_v .

The previous equation shows that for a constant volume heating without mechanical friction, the heat exchanged with the outside is equal to the change in the fluid internal energy:

$$Q_1^2 = u_2 - u_1$$

This relationship is the basis for calorimetric determinations of u .

5.3.3 Work provided, shaft work τ

Industrial operations generally take place continuously, each component (turbine, pump, valve, etc.) permanently receiving and evacuating matter. When, as it is often the case, their operating conditions are stabilized, possibly periodically, it is called “permanent” or “steady-state”. As mentioned previously, the calculation of these devices must be done in an open system, and the previous expression, valid only in a closed system, must be generalized.

The reasoning principle is to follow the evolution of a closed control volume, and calculate the work of external forces on all its boundaries, distinguishing between cross sections of the fluid, fixed walls, which obviously neither produce nor receive work, and moving walls like blades, in which some work τ is exerted, called “shaft work”.

In the most frequent case (Figure 5.3.1) we can assume that the component operates between two chambers of large dimensions, where the fluid is in equilibrium. The upstream (1) and downstream (2) states are defined by their pressure and temperature, assumed to be uniform despite the extractions and contributions due to the suction and discharge. For example, a gas turbine compressor sucks in air and discharges into the combustion chamber where the pressure is substantially uniform.

In its passage from (1) to (2), each unit mass of fluid receives from the moving walls the shaft work τ , whose knowledge is fundamental, since its product by the mass flow \dot{m} , gives the power involved (neglecting mechanical losses in bearings and transmission).

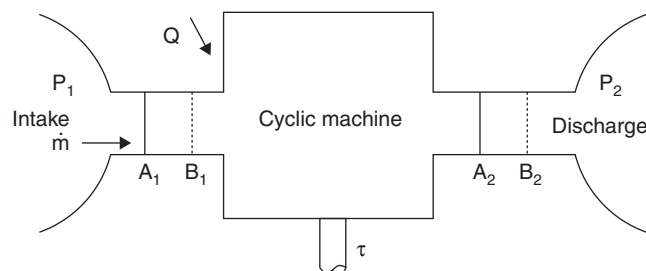


FIGURE 5.3.1

Periodic machine

One can easily show that, per unit mass, a component performing any kind of processing provides work τ algebraically equal to the work of pressure forces calculated in a closed system W_A , increased by the transfer work, that is to say the variation of product Pv :

$$\tau = W_A + P_2v_2 - P_1v_1 = W_A + \Delta(Pv) \quad (5.3.4)$$

In general, $P_2v_2 - P_1v_1 \neq 0$, and τ differs from W_A .

5.3.3.1 Demonstration

The machine, traversed by a flow rate \dot{m} , works in unsteady, but periodic, state that is to say all its components, including the fluid mass in it, are periodically in the same state (note that the steady-state operation is deduced from the periodic regime by letting the period tend to 0). Consider the closed system consisting of the fluid mass contained in the initial state in the control volume limited by the fixed and movable walls and sections A_1 and A_2 respectively located in the entry and exit chambers.

After a period dt , the control volume has been moved and is now limited by sections B_1 and B_2 , themselves in the entry and exit chambers. The machine has been traversed by the fluid mass $\dot{m} dt$, common mass of sections A_1B_1 and A_2B_2 (conservation of mass flow), and has provided work on the fluid $\tau \dot{m} dt$ (by definition).

The work of external forces $W \dot{m} dt$ is equal to the sum of the work of gravity and the work of pressure forces exerted on the various boundaries of the machine, four in number: A_1 , A_2 , moving walls and fixed walls.

On these, $\delta W_{A4} = 0$.

On A_1 , a reasoning similar to that in Section 5.2.1 (the machine cannot be treated as a single phase) shows that:

$$\delta W_{A1} = -P_1 dV_1 = -P_1(-\dot{m} dt)v_1 = P_1v_1\dot{m} dt$$

On A_2 , in the same way, $\delta W_{A2} = -P_2v_2\dot{m} dt$.

By definition, the shaft work is that of pressure forces on the moving walls,

$$\tau \dot{m} dt = \delta W_{A3}$$

We have thus

$$\delta W = \delta W_A + dW_v = \delta W_{A1} + \delta W_{A2} + \delta W_{A3} + \delta W_{A4} + dW_v$$

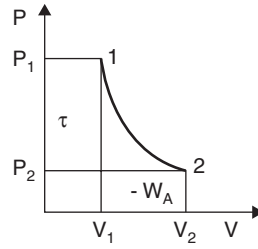
$$\delta W = W dt = P_1v_1\dot{m} dt - P_2v_2\dot{m} dt + \tau \dot{m} dt + dW_v$$

$$\tau = W_A + P_2v_2 - P_1v_1 = W_A + \Delta(Pv)$$

This notion of shaft work is far from trivial. In practical terms however, it poses no particular problem. In all the open system compressions and expansions, it is the shaft work that must be considered in the calculations.

We will later introduce another concept, that of useful energy, used to distinguish it from the purchased energy in calculating machine effectiveness.

Note that in the previous demonstration, we made no assumption on the restrictive nature of the processes in the machine itself. We simply recognized that the pressure was uniform and constant in the course of time at the inlet and outlet of the machine. The relationship obtained thus applies only in this condition, whatever the intermediate processes, whether reversible or not.

**FIGURE 5.3.2**Compression process in a (P, v) chart**5.3.3.2 Special case of a reversible process**

If the process is reversible, $W_A = -\int_1^2 P \, dv$

$$\tau = -\int_1^2 P \, dv + P_2 v_2 - P_1 v_1$$

We recognize the expression of integration by parts, hence:

$$\tau = -\int_1^2 v \, dP \quad (5.3.5)$$

All of these relationships can be represented graphically in the Clapeyron diagram, which corresponds to the plane (v, P) , v x-axis, P y-axis (Figure 5.3.2). The area between the curve $1 \rightarrow 2$ showing the process and the x-axis is equal to the opposite of the work of external forces W_A , while the area between the curve and the y-axis is equal to shaft work τ .

Note that these surfaces depend on the route of the curve $1 \rightarrow 2$, and therefore that mere knowledge of the initial and final states is not sufficient to determine W_A and τ .

Mathematically, this follows from the important fact that the differential expressions $-P \, dv$ and $v \, dP$ are not exact differentials. Physically, it is explained by the intervention of one form of energy other than mechanical work, i.e. thermal energy.

If two different reversible processes starting from the same initial state 1 and ending at the same final state 2 do not correspond to the same shaft work, this is because the fluid does not exchange the same amount of heat with the outside during these two processes.

It is for this reason that we note the differential forms with a small δ (δW_A , $\delta \tau$) and exact differentials by d .

5.3.4 Shaft work and enthalpy (open systems)

Let us come back to equation (5.3.1) and express it according to τ instead of W , for the total mass of the system. It comes:

$$\Delta U + \Delta K = W + Q = W_A + W_v + Q = \tau - \Delta(PV) - mg\Delta z + Q$$

which can be written:

$$\Delta(U + PV) + \Delta K + mg\Delta z = \tau + Q$$

Let us call enthalpy the state function $H = U + PV$ and specific enthalpy function $h = u + Pv$.

The enthalpic form of the first law is therefore written in mass variables (note that K , τ and Q are now expressed in mass quantities):

$$\Delta h + \Delta K + g\Delta z = \tau + Q \quad (5.3.6)$$

For an infinitely small control volume, this equation becomes:

$$dh + dK + gdz = \delta\tau + \delta Q \quad (5.3.7)$$

Transposing the reasoning of Section 5.3.2, we find that the calorimetric equation writes as:

$$\delta Q = dh - v dP \quad (5.3.8)$$

and $c_p = (\partial h / \partial T)_p$, which is often used as a definition of c_p .

5.3.5 Establishment of enthalpy balance

We have seen that, in industrial processes, operations usually take place continuously, i.e. in open systems. It is therefore the enthalpy first law expressions that apply most often.

Although it is known to almost everyone, experience shows that its implementation may pose some difficulties. It suffices, however, to be able to apply the conservation law of extensive energy quantities (shaft work, heat exchanged with the outside Q , enthalpy flow of the fluids involved) to an appropriate control volume, which most often is none other than the system defined by the boundaries of the component studied. Given the first law, enthalpy is a conservative quantity, and equation (5.1.1) is simplified, terms of generation and consumption disappearing, to become:

$$\left\{ \begin{array}{l} \text{accumulation in the} \\ \text{control volume} \end{array} \right\} = \left\{ \begin{array}{l} \text{inward transport} \\ \text{by the surface} \end{array} \right\} - \left\{ \begin{array}{l} \text{outward transport} \\ \text{by the surface} \end{array} \right\} + \left\{ \begin{array}{l} \text{transfer through} \\ \text{the surface} \end{array} \right\}$$

If we assume that the system operates in steady-state mode, which is usually the case, there is no net accumulation in the control volume, and this equation results in:

$$\left\{ \begin{array}{l} \text{inward transport} \\ \text{by the surface} \end{array} \right\} - \left\{ \begin{array}{l} \text{outward transport} \\ \text{by the surface} \end{array} \right\} + \left\{ \begin{array}{l} \text{transfer through} \\ \text{the surface} \end{array} \right\} = 0$$

In most cases, the enthalpy balance is determined when you know the boundary flows of heat, useful work and enthalpy.

Consider for example the case of an adiabatic gas turbine axial compressor, which will be calculated in more detail Section 9.3, sucking air at rest in the atmosphere, and discharging into the combustion chamber of the machine.

The control volume in this case corresponds to the geometry of the compressor, bounded upstream and downstream by its connecting flanges.

The mass balance is very simple to set up, because, noting with index 1 the compressor inlet, and 2 the outlet:

$$\dot{m}_2 = \dot{m}_1 \quad \text{in steady-state}$$

The machine being adiabatic, there is no heat exchange with the outside, and therefore $Q = 0$. At suction as well as at discharge, the air velocity is low and its kinetic energy negligible. The enthalpy

balance of this machine is very simple: $\Delta h = \tau$. The enthalpy communicated to the fluid is equal to the work received on the shaft.

If the compressor is cooled, the balance is slightly more difficult. If the heat exchanged with outside is $Q < 0$, we have: $\Delta h = \tau + Q$. The enthalpy communicated to the fluid is equal (in absolute value) to the difference between work received on the shaft and heat extracted.

Now let us consider a slightly more complex example, on closed systems. This is the combustion in a diesel engine, modeled as a succession of two elementary combustions (called mixed cycle): first at constant volume, then at constant pressure.

Mass balance is this time a little more complicated, m_c being the mass of fuel injected during each phase of combustion:

$$m_2 = m_1 + m_c$$

The control volume is in this case the whole set: head, cylinder and piston. The engine being cooled by water, the combustion is not adiabatic.

The first combustion phase taking place at constant volume, it does not involve any work ($W = 0$), and energy balance should be written here $\sum \Delta U_i = Q$, the summation being performed on all species present, assumed to be ideal gases. A first problem exists here, because this equation assumes that the calculation of the internal energy of gases present in the chamber is done taking into account the state of the combustion reaction, i.e. considering the changes in chemical variables.

However it is very rare in industrial practice that we operate as indicated previously: the internal energy (or enthalpy) of an ideal gas is generally defined in relation to the standard reference of 1 bar and 298 K for a given composition (see Section 7.6.4.2).

To overcome this difficulty, it is customary, although it is formally inconsistent with the first law, to reintroduce, rather artificially, in the balance equations a term of power generation in the volume, which corresponds to heat $Q_r (>0)$ released by the combustion reaction. As we indicated earlier in this chapter, this approach allows us to ignore the chemical variables, and thus significantly simplifies the formalism.

For combustion phase at constant pressure, the piston is in motion and produces a shaft work W that must also be included in the balance. We give in the section on combustion some guidance on how these calculations can be conducted.

5.3.6 Application to industrial processes

C being the velocity of the fluid, the first law applied to a component through which passes a fluid, of unit flow-rate, can be expressed in mass units in the form:

$$\tau + Q = h_2 - h_1 + \Delta K + g\Delta z = h_2 + h_1 + \frac{C_2^2 - C_1^2}{2} \quad (5.3.9)$$

We have already indicated that, for most heat engines, the term $g\Delta z$ is negligible. In many cases, the variation of kinetic energy is low vis-à-vis other changes (except of course in special cases such as jet engines, some turbomachinery blades or expansion devices).

Under these conditions, the amount of work received or provided and the heat exchanged with the outside by the component is equal to the change in enthalpy of the fluid passing through it.

This fundamental relationship explains why, in industrial devices, it is virtually impossible to implement both great mechanical work and a significant heat flux.

- Components which transfer heat from one fluid to another require large exchange areas, their heat fluxes being proportional to them. Technical and economic considerations lead to the adoption of purely static devices, for example, large bundles of tubes in parallel, traversed internally by a fluid while the other flows outside. τ is zero because of the absence of movable walls.
- Machines doing the compression or expansion of a fluid have a very compact design for reasons of weight, size and cost. For similar reasons, they rotate very fast (several thousand revolutions per minute). Each parcel of fluid remains there very shortly. Moreover, the heat exchange coefficients of gases have low values. Short residence time, small areas of fluid-wall contact, and low exchange coefficients imply that the heat exchange is minimal and that the operation of these machines is nearly adiabatic.
- There is a class of devices where τ and Q are both zero: they are static expanders such as valves, filters etc. The corresponding process is called an isenthalpic throttling or a flash expansion.

PRACTICAL APPLICATION

Practical modeling of industrial processes

The developments presented in this section are of paramount importance in practice, as they result in major simplifications in the modeling of industrial processes:

- in a heat exchanger, heat Q transferred or provided by one fluid to another is equal to its enthalpy change Δh (see Chapter 8);
- similarly, the heat Q released in a combustion chamber or boiler is equal to the enthalpy change Δh of the gases that flow through it (see section 7.6);
- in an adiabatic machine, shaft work τ is equal to the change in enthalpy of the fluid Δh (see sections 7.1 to 7.5);
- throttling conserves enthalpy ($\Delta h = 0$, see section 7.7).

For the calculation of processes, these findings are very important in practice since they indicate that in most components of industrial machinery, mechanical and thermal exchanges are decoupled. They also explain why the enthalpy is a state function widely used in open system processes: the change in enthalpy of the fluid represents the mechanical or thermal energy put in.

5.4 SECOND LAW OF THERMODYNAMICS

The first law postulates the equivalence of the different forms of energy, but it does not take into account an essential experimental fact, which is that when a system interacts with its surroundings, the energy processes it undergoes can take place only in a particular direction, that cannot be reversed without changing the system qualitatively.

Thus, heat flows naturally from one high temperature substance to a low temperature substance, but the reverse can only be achieved by using a complex thermal machine called a refrigeration machine or heat pump, or using a Peltier electrical component.

The second law complements the first by introducing a function called entropy, which is used to quantitatively characterize the effects of irreversibilities taking place in a system and explain the phenomena we have just discussed.

A rigorous and comprehensive presentation of the second law requires significant developments due on the one hand to the precautions that must be taken in writing assumptions and in explaining their connection with experience, and on the other hand to the demonstrations which must be performed.

Given the objectives of this book, it is not justified here, especially as for the calculations of applied thermodynamics we are considering here, the main practical advantages presented by this second law can be summarized in two points:

- First entropy is as we will show the state function most closely related to heat Q exchanged with the outside (by the simple relation $\delta Q = T ds$). It therefore appears in many formal equations governing the energy components operation;
- Secondly generation of entropy allows one to quantify all the irreversibilities taking place in these components and on their boundaries, which is fundamental.

That is why we selected the presentation below, sufficient for our purposes, which has the advantage of being short enough to set out and easy to understand. Readers interested in a comprehensive presentation of the subject may refer to the bibliography at the end of this chapter.

5.4.1 Definition of entropy

At any phase are attached two quantities T and s , respectively called “thermodynamic temperature” and entropy, having the following properties:

- T is a function of temperature alone, independent of the system considered;
- s is a function of the system state variables;
- in any elementary process involving heat exchange δQ with the outside $\delta Q \leq T ds$, equality being satisfied if and only if the process is perfect (not irreversible).

$$ds = \frac{\delta Q}{T} + d_i s \quad (5.4.1)$$

$d_i s$, positive or zero, is called “entropy generation”.

(5.4.1) can be rewritten:

$$\delta Q + \delta \pi = T ds \quad (5.4.2)$$

$\delta \pi$ is called “uncompensated work” or “uncompensated heat”. It is positive for an irreversible process, and zero otherwise.

The *ex abrupto* introduction of entropy can surprise and appear arbitrary. To try to explain it more gradually, we will study the case of a perfect gas, whose equation of state is written, as we shall see below:

$$Pv = rT$$

r being a constant depending on the gas ($r = 287 \text{ J/kg}$ for air), v is the specific volume, and T is temperature in Kelvin.

This equation stems from the laws of Gay-Lussac (in a given volume $P/T = \text{Const.}$) and Mariotte ($Pv = \text{Const}$ at a given temperature).

The thermal properties of perfect gases result from Joule’s laws, which can be stated as follows:

- First Law: the internal energy of a perfect gas depends only on its temperature;
- Second Law: the heat capacity at constant volume c_v is a constant.

$$c_v = \left(\frac{\partial u}{\partial T} \right)_v = \frac{du}{dT}$$

As $\delta Q = du + P dv$, we have: $\delta Q = c_v dT + P dv$,

By replacing P by its value from the equation of state, we get:

$$\delta Q = c_v dT + rT \frac{dv}{v}$$

In this form, we see immediately that $1/T$ is an integrating factor, and that is obviously the simplest possible. Let us recall that multiplying all the terms of a differential form δy by an integrating factor I turns it into an exact differential.

$$\text{Let } ds = \frac{\delta Q}{T} = c_v \frac{dT}{T} + r \frac{dv}{v}$$

ds being an exact differential, we get:

$$s = c_v \ln(T) + r \ln(v) + \text{Const.}$$

The concepts of thermodynamic temperature and entropy are thus introduced naturally, entropy being the state function closest to heat. There is no evidence in this approach, however, that these concepts retain their relevance for real gases. The advantage of the axiomatic approach at the beginning of this section is that you can then retrieve the perfect gas properties as a special case of the general theory.

5.4.2 Irreversibility

Irreversibilities encountered in energy devices that we consider in this book, except those taking place in combustion reactions, can be grouped into two broad classes which we present succinctly:

- mechanical irreversibilities due to the viscosity;
- irreversibilities by temperature heterogeneity.

5.4.2.1 Mechanical irreversibility

Relations 5.2.2 and 5.3.5 allow us to calculate the mechanical energy received by an open or closed system in the absence of irreversibility. When the processes are not reversible, they are no longer valid, and in the general case, there are no simple differential relations to determine the energy exchange mechanisms involved.

The first law of thermodynamics allows us to solve this problem, however, as we shall see now.

Consider an open system in which takes place an irreversible adiabatic compression, from state 1 to state 2', and such as the variations of kinetic energy can be neglected (Figure 5.4.1). Given the first law, as $Q = 0$, we have:

$$\tau = h_{2'} - h_1$$

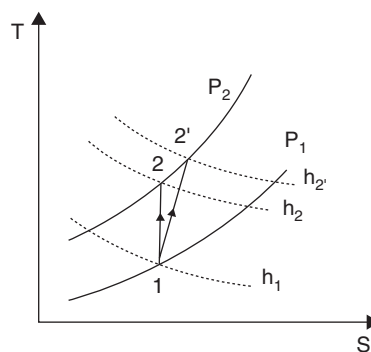


FIGURE 5.4.1

Irreversible compression

h being a state function, it is reasonable to decompose the change in enthalpy of the irreversible compression as the succession of the two changes corresponding to the following processes:

- isentropic compression from 1 to 2 involving work $\tau_s = \int_1^2 v dP$;
- fictitious isobaric heating from 2 to 2' of value π corresponding to irreversibilities.

$$h_{2'} - h_1 = h_{2'} - h_2 + h_2 - h_1 = \tau_s + \pi = \int_1^2 v dP + \pi$$

In conclusion

$$\tau = \tau_s + \pi \quad (5.4.3)$$

$$\delta\tau = v dP + \delta\pi \quad (5.4.4)$$

The reasoning can be transposed easily to irreversible expansion, as well as for closed systems, for which we have:

$$W = W_s + \pi \quad (5.4.5)$$

$$\delta W = -P dv + \delta\pi \quad (5.4.6)$$

These relations can be generalized to the case where the kinetic energy or mass forces must be taken into account:

$$\delta\tau + \delta Q = dh + dK$$

$$\delta\tau = dh + dK - \delta Q$$

$$\delta\tau = dh + dK - (dh - v dP) = v dP + dK$$

$$\text{If the kinetic energies are not negligible: } \delta\tau = v dP + dK$$

$$\text{If the mass forces are not negligible: } \delta\tau = v dP + dK + g dz$$

$$\text{In the presence of irreversibilities: } \delta\tau = v dP + dK + g dz + \delta\pi \quad (5.4.7)$$

These internal irreversibilities result in an increase of entropy, which can be calculated by applying the second law.

5.4.2.2 Irreversibility by temperature heterogeneity

The second major source of irreversibilities encountered in energy systems considered here comes from the temperature difference that must exist in practice between two bodies when they exchange heat. Indeed, for both technical and economic reasons, the exchange surfaces between these bodies are necessarily finite. It is then possible to show that the heat exchange is accompanied by an increase in entropy at the boundary between the two bodies (at temperatures T_1 and T_2), given by the following equation:

$$d_i s = \left(\frac{T_1 - T_2}{T_1 T_2} \right) \delta Q \quad (5.4.8)$$

δQ being the heat absorbed by body 2. These irreversibilities are often described as external, because they take place at the boundary of the system considered.

5.4.3 Carnot effectiveness of heat engines

Thermal engines are designed to transform heat into mechanical energy. Let us assume that heat to transform is provided from an external source, the said hot source, whose temperature T_1 is fixed.

A second source, known as cold, is necessary to evacuate the heat generated. Its temperature T_2 is necessarily lower than T_1 .

A heat engine connected between these two sources works as follows: a fluid mass describes a simple closed process or cycle, in which it exchanges heat Q_1 with the hot source, and heat Q_2 with the cold source, and receives shaft work τ .

Under the first law, we have: $\tau + Q_1 + Q_2 = 0$ or $\tau = -Q_1 - Q_2$

The effectiveness η of the machine (often called thermal efficiency) is defined as the (less than 1) ratio of the work produced to the heat from the hot source:

$$\eta = \frac{|\tau|}{Q_1}$$

For the cycle to be fully reversible, it is necessary firstly that the process takes place without friction, and secondly that the heat exchange between the fluid and the external sources is reversible, and therefore is made with no temperature difference.

Therefore, during the process phase where the fluid receives heat from the hot source, it will be at temperature T_1 , and during the phase where it yields heat to the cold source, it will be at temperature T_2 .

During the intermediate phases, where the fluid evolves between these two temperatures, it must not receive any heat from the sources, and if no exchange occurs internally, which we assume, the process must be adiabatic and reversible, that is to say, isentropic.

This leads to the Carnot cycle (named after its inventor). In the entropy diagram (T, s) (for details, see 5.6.6.1), it is represented by rectangle ABCD, described in the clockwise direction (Figure 5.4.2).

- AB is a segment of isotherm T_1 described from left to right. The fluid receives heat (isothermal expansion in the case of a perfect gas);
- CD is a segment of isotherm T_2 described from right to left. The fluid releases heat (isothermal compression in the case of a perfect gas);
- BC is a segment of isentropic S_2 described from top to bottom (reversible adiabatic expansion in all cases);
- DA is a segment of the isentropic S_1 described from bottom to top (reversible adiabatic compression in all cases).
- The calculation of Q_1 , Q_2 and η is immediate for the cycle. Indeed, for an isotherm:

$$Q = \int T ds = T \Delta s$$

It becomes:

$$Q_{AB} = Q_1 = T_1(S_2 - S_1) \quad \text{and} \quad Q_{CD} = Q_2 = T_2(S_1 - S_2)$$

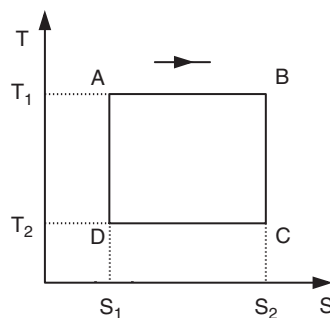


FIGURE 5.4.2

Carnot cycle

It will be noted in passing that these two equations combine to give the Carnot-Clausius relation (5.4.9), which shows that the measurement of thermodynamic temperatures can be reduced to that of heat:

$$\frac{Q_1}{T_1} + \frac{Q_2}{T_2} = 0 \quad (5.4.9)$$

Returning to calculate the performance of our cycle:

$$\begin{aligned} \tau &= -Q_1 - Q_2 = (T_2 - T_1)(S_2 - S_1) \\ \eta &= \frac{|\tau|}{Q_1} = \frac{T_1 - T_2}{T_1} = 1 - \frac{T_2}{T_1} \\ \eta &= 1 - \frac{T_2}{T_1} \end{aligned} \quad (5.4.10)$$

Relation (5.4.10), established by Carnot in 1824, is probably rightly one of the best known in thermodynamics. It is of great practical importance, given its implications:

- First, with the assumptions made (reversible cycle without friction and heat transfer without temperature differences), it is easy to show that this effectiveness is the highest that can be achieved by a simple fluid heat engine operating between the two sources at T_1 and T_2 . It is therefore a maximum limit and real cycles generally have much lower efficiencies;
- Secondly, the effectiveness of all reversible machines operating between the two sources at T_1 and T_2 is the same and only depends on their temperatures, not on the thermodynamic fluid used.

For these reasons we have preferred to speak of effectiveness, some authors considering that the efficiency term generally used to describe this limit cycle is not the most appropriate, and it is better to keep it to describe the performance of a real machine compared to that of an ideal machine.

In the foregoing, we were interested in motor heat engines. A second class of heat engines is used in reverse cycles to transfer heat from a cold source to a hot one, thanks to a mechanical power input. This is called a refrigeration cycle, or heat pump.

The above reasoning can be transposed to the case of these reverse cycles, and it can be shown that the maximum effectiveness of these cycles (also known as coefficient of performance) is equal to that of the reverse cycle, given by equations 5.4.11 or 5.4.12, depending on whether one looks at the heat exchanged with the cold source (refrigeration cycle) or with the hot one (heat pumps):

$$\eta = \frac{Q_2}{\tau} = \frac{T_2}{T_1 - T_2} \quad (5.4.11)$$

$$\eta = \frac{Q_1}{\tau} = \frac{T_1}{T_1 - T_2} \quad (5.4.12)$$

5.4.4 Fundamental relations for a phase

Given (5.4.4) and (5.4.6) and neglecting the kinetic energies put into play, the written expressions of the first law are:

$$\begin{aligned} du &= \delta W + \delta Q = -P dv + \delta Q + \delta \pi \\ dh &= \delta \tau + \delta Q = v dP + \delta Q + \delta \pi \end{aligned}$$

Substituting $(\delta Q + \delta \pi)$ by $T ds$ in these equations, we immediately obtain the following identities, which are fundamental in practical applications:

$$du = -P dv + T ds \quad (5.4.13)$$

$$dh = v dP + T ds \quad (5.4.14)$$

5.4.5 Thermodynamic potentials

The more general study of the behavior of a system requires that we know two of its state functions, for example u and s , or h and s , but it may be interesting to gather in a single well-chosen state function all the thermodynamic knowledge about it.

5.4.5.1 Free energy and free enthalpy

We are led to define two functions, either being sufficient for this, called respectively the free energy f or Helmholtz function and the free energy g or Gibbs function:

$$f(v, T) = u - Ts \quad (5.4.15)$$

$$g(P, T) = h - Ts \quad (5.4.16)$$

For example, let us show that, for a substance of constant composition, knowledge of f is sufficient to determine its behavior.

We have:

$$df = du - T ds - s dT, \quad \text{and} \quad du = -P dv + T ds,$$

which gives:

$$df = -P dv - s dT,$$

which involves:

$$P = -\frac{\partial f}{\partial v}, \quad s = -\frac{\partial f}{\partial T}, \quad u = f - T \frac{\partial f}{\partial T}$$

$$c_v = \frac{\partial u}{\partial T} = -T \frac{\partial^2 f}{\partial T^2}$$

Knowledge of the free energy or enthalpy is sufficient to fully characterize a thermodynamic system. In practice however, these state functions are little used by specialists because their physical meaning is less directly accessible.

5.4.5.2 Equilibrium relationship for chemical reactions

The second law of thermodynamics provides the fundamentals for the study of chemical equilibrium relationships.

Equation (5.4.1) can be written $dQ \leq T ds$.

Since, according to (5.3.3) $dQ = du + P dv$, we have:

$$du + P dv - T ds \leq 0 \quad (5.4.17)$$

We can rewrite inequality (5.4.15) by showing the free energy or enthalpy differential form:

$$df = du - T ds - s dT$$

$$dg = du + P dv + v dP - T ds - s dT$$

we get:

$$df + s dT + P dv \leq 0 \quad (5.4.18)$$

At constant temperature ($dT = 0$) and constant volume ($dv = 0$), a process can only evolve in the direction of a decrease of its free energy, and a stable equilibrium must be a minimum of free energy:

$$df \leq 0 \quad (5.4.19)$$

Furthermore:

$$dg + s dT - v dP \leq 0 \quad (5.4.20)$$

At constant temperature ($dT = 0$) and at constant pressure ($dP = 0$), a process can only evolve in the direction of a reduction of its Gibbs free energy, and a stable equilibrium must be a minimum of Gibbs energy:

$$dg \leq 0 \quad (5.4.21)$$

A classic example of this law concerns the equilibrium between phases in a system composed of a liquid and its vapor. It will be discussed in Section 5.6.5.3.

When looking at a mixture of several components, the constant temperature and pressure equilibrium equation becomes, expressed in molar quantities (Gibbs–Duhem relation):

$$dG_{T,p} = \sum n_i d\mu_i = 0 \quad (5.4.22)$$

n_i being the number of moles of i th component, and μ_i its chemical potential, equal for an ideal gas, to its partial molar free enthalpy:

$$\mu_i = G(T, P_i) \quad (5.4.23)$$

Equation (5.4.22) is the basis for calculating the equilibrium of chemical reactions. We will use it in paragraph 4.6.1.4 to establish the law of Mass Action.

5.5 EXERGY

The theory of exergy aims to develop an integrated analysis method that includes the first two laws of thermodynamics, and thus allows us to take into account both the amount of energy put into play and its quality, which the first law cannot do. Its interest is that it provides a quite rigorous thermodynamic framework to quantify the quality of any system, open or closed, in steady-state or not.

The first to introduce this concept was G. Gouy, who late in the nineteenth century, defined the concept of usable energy, now renamed exergy by many authors. The basic idea is to consider that a thermodynamic system interacts with what is called its environment, which behaves like an infinite reservoir at constant temperature and pressure and fixed composition, meaning that the system studied is small enough not to disturb this environment.

The environment will serve for example as a cold source for a power cycle, or hot source for a refrigeration cycle. Since the environment state determines the performance of the system studied, the theory of exergy can take it into account implicitly.

In the framework of this book, we content ourselves with a brief and steady state (and therefore not rigorous) presentation of exergy analysis. Readers wishing to engage further in this direction will find especially in the work of L. Borel and D. Favrat (2005) a comprehensive theory of the subject.

The practical implementation of the concepts introduced here will be presented in section 10.2.2 which explains how to build exergy balances.

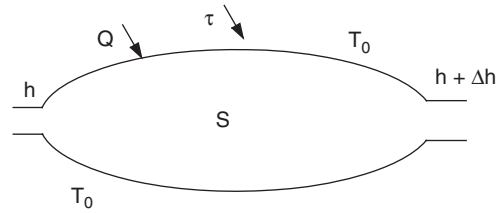


FIGURE 5.5.1
Monothermal system

5.5.1 Presentation of exergy for a monotherm open system in steady state

Let us consider a steady-state open system exchanging energy with its environment assumed to be at uniform temperature T_0 (Figure 5.5.1).

The energy equation is given by the first law (5.3.6):

$$\Delta h + \Delta K = \tau + Q$$

and the entropy production by the second law:

$$Q + \pi = T_0 \Delta s \quad 0 \leq \pi$$

$$\Delta s - \frac{Q}{T_0} \geq 0$$

If we assume that all the heat is provided by the environment, and T_0 is the temperature at the boundary of the open system, Q can be eliminated by combining these two equations, giving:

$$\begin{aligned} \tau &= \Delta h + \Delta K - Q \geq \Delta h + \Delta K - T_0 \Delta s \\ -\tau &\leq -(\Delta h + \Delta K - T_0 \Delta s) \end{aligned}$$

In most cases, we can neglect the kinetic energy changes ΔK .

For an open system, function $x_h = h - T_0 s$ is usually called **exergy**.

The maximum work that the system can provide is equal to the reduction of its exergy.

In practice, the actual work provided by the system may be less than this value. We define the exergy loss Δx_{hi} as being equal to the difference between the maximum work possible and the actual work provided:

$$\begin{aligned} \Delta x_{hi} &= (-\tau_{\max}) - (-\tau_{\text{real}}) = (-\Delta x_h) - (-\tau_{\text{real}}) \\ \Delta x_{hi} &= T_0 \Delta s - \Delta h - (-\tau_{\text{real}}) \end{aligned}$$

If the process is furthermore adiabatic:

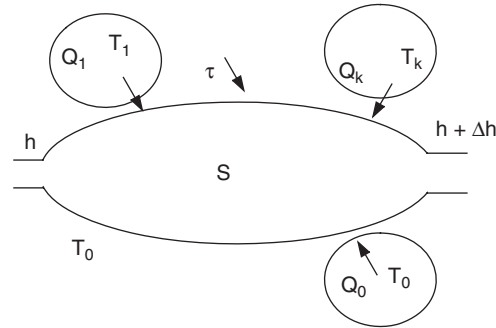
$$(-\tau_{\text{real}}) = -\Delta h \quad \text{and} \quad \Delta x_{hi} = -\Delta x_h + \Delta h = T_0 \Delta s$$

Note that this description is not entirely satisfactory because it is clear that for a closed system, the definition of exergy leads us to consider function $u - T_0 s$, so that there is some ambiguity.

Therefore L. Borel was moved to speak rather of co-enthalpy and co-energy.

Given the success of the concept of usable energy introduced by G. Gouy, largely used in the Anglo-Saxon world under the name availability, we could also speak of usable enthalpy or usable energy, depending on whether one considers an open or closed system.

Beyond the question of vocabulary, we note that this new function is characterized by the introduction of a variable outside the system, T_0 . As such, it is no longer a state function in the strict

**FIGURE 5.5.2**

Multithermal open system

sense. However, as T_0 is generally assumed to be constant, the exergy is sometimes presented as a linear combination of state functions.

Another remark can be made at this stage: exergy allows us, through the product of entropy by the environment temperature, to express variations of this state function in one dimension and by orders of magnitude similar to those usually encountered by the engineer in energy calculations, which facilitates the understanding of physical phenomena.

Finally, as discussed below, by this artifice we manage to formally eliminate from the calculations the “free” heat source represented by the environment.

Exergy can be used to evaluate the quality of the changes made in real processes, compared to ideal reversible ones.

5.5.2 Multithermal open steady-state system

Let us consider an open system that exchanges work and heat with n external sources at constant temperatures T_k , and environment taken at temperature T_0 (Figure 5.5.2).

Applying the first law gives here:

$$\Delta h + \Delta K = \tau + Q_0 + \sum_{k=1}^n Q_k$$

and entropy production is given by the second law:

$$\Delta s = \frac{Q_0}{T_0} + \sum_{k=1}^n \frac{Q_k}{T_k} + \Delta s_i$$

Δs_i , positive or zero, being the entropy generation. Neglecting kinetic energy changes, we get:

$$\Delta x_h = \Delta(h - T_0 s) = \tau + \sum_{k=1}^n \left(1 - \frac{T_0}{T_k}\right) Q_k - T_0 \Delta s_i \quad (5.5.1)$$

or, with $\Delta x_{hi} = T_0 \Delta s_i \geq 0$:

$$\tau + \sum_{k=1}^n \left(1 - \frac{T_0}{T_k}\right) Q_k - \Delta x_h - \Delta x_{hi} = 0 \quad (5.5.2)$$

τ is the work received by the system, Δx_h the exergy variation of the fluid passing through it, and Δx_{hi} the exergy dissipation resulting from irreversibilities. We call the Carnot factor the term $\theta = 1 - T_0/T$. This is the factor by which we must multiply a quantity Q of heat available at

temperature T to obtain the value of its exergy. If we call useful heat (or heat-exergy as per Borel) the quantity $x_q = \theta Q$, equation (5.5.2) gets the form:

$$\begin{aligned} \tau + \sum_{k=1}^n \theta_k Q_k - \Delta x_h - \Delta x_{hi} &= 0 \\ -\tau + \sum_{k=1}^n x_{qk} - \Delta x_h - \Delta x_{hi} & \end{aligned} \quad (5.5.3)$$

The maximum engine work that can provide an open system is equal to the sum of heat-exergies of the sources with which it exchanges heat, less the change in exergy of the fluid passing through it and the exergy destroyed because of irreversibilities.

5.5.3 Application to a two-source reversible machine

Let us consider a cyclic two-source reversible machine operating between a source at temperature T_1 and environment at temperature T_0 .

On a cycle, we have: $\Delta x_h = 0$, $\Delta x_{hi} = 0$ (reversible machine).

Applying formula (5.5.3) gives:

$$-\tau = x_{q1} = \left(1 - \frac{T_0}{T_1}\right) Q_1$$

If $T_0 < T_1$, $x_{q1} \geq 0$: the system receives heat-exergy from the hot source at T_1 , and converts it into work τ .

Here we find the Carnot cycle, whose effectiveness is $\eta = 1 - T_0/T_1$.

If $T_0 > T_1$, $x_{q1} \leq 0$: the system gives heat-exergy to the cold source at T_1 , taking it from the hot source at T_0 . For this, we must provide work τ . It is then a refrigeration cycle or heat pump.

5.5.4 Special case: heat exchange without work production

In the special case where there is no work produced, equation (5.5.3) can be rewritten as:

$$\Delta x_{hi} = \sum_{k=1}^n x_{qk} - \Delta x_h \quad (5.5.4)$$

The exergy destroyed in the process is equal to the sum of the heat-exergies of the various sources, minus the change in exergy of the fluid passing through the system.

5.5.5 Exergy efficiency

Exergy allows us to rigorously define the concept of system efficiency, and therefore to quantify its thermodynamic quality: it is the ratio of exergy uses to exergy resources. It is always between 0 and 1, and so is much greater than the irreversibilities are lower. Exergy resources is the sum of all exergies provided to the cycle from outside. Exergy uses represents the net balance of the cycle, i.e. the algebraic sum of exergy produced and consumed within it.

$$\eta = \frac{\text{exergy uses}}{\text{exergy resources}} \quad (5.5.5)$$

5.6 REPRESENTATION OF SUBSTANCE PROPERTIES

5.6.1 Solid, liquid, gaseous phases

A pure substance can be in one or more of three phases: solid, liquid or gaseous. Solid state may even include several varieties known as allotropic, which reflect the different possible arrangements of the crystal lattice.

These three phases are distinguished, at the microscopic level, by the intensity of intermolecular forces. In the solid state, they allow atoms only to oscillate around fixed positions randomly distributed or ordered (crystal).

Their intensity decreases in liquids, which have no proper form, but remain slightly compressible. This is called a short distance order and disorder at long range. In a gas, intermolecular forces are very weak and the molecules move in an erratic motion.

When heating a solid at a well chosen constant pressure, it turns into liquid, and we talk of fusion. If we continue to provide heat, the liquid turns to vapor, and we talk of vaporization. It is also possible that a solid turns directly into vapor, which is called sublimation. The temperature at which these changes are realized depends on the pressure exerted on the substance considered. For example at atmospheric pressure, the CO_2 sublimates, that is to say, goes directly from solid to gaseous state, while water boils at 100°C .

When a given mass of a pure substance is present in a single phase, its state is defined by two variables, for example its pressure and temperature. In the (P, T) plane, the three phases correspond to three areas, separated by three saturation curves (sublimation, vaporization and fusion) joining at the triple point T (Figure 5.6.1).

Each curve corresponds to a two-phase equilibrium. For example, the rightmost curve is the set of points representing the equilibrium of a liquid with its vapor. The two-phase equilibrium assumes that the pressure and temperature satisfy a relationship characteristic of the nature of the fluid.

For each of these phase changes to happen, it is necessary to provide or absorb energy, called latent heat of change of state. During the change of state, there are significant variations in the specific volume, except for fusion-solidification. This is particularly the case during vaporization, vapor being about 600 to 1,000 times less dense than the liquid. This change in specific volume occurs at constant pressure and temperature.

Let us give some examples illustrating either the practical use of phase changes, or the constraints induced by the presence of a liquid-vapor equilibrium:

- When adding ice cubes to a warm drink, we provide heat which melts them, which cools it. As the latent heat of fusion of ice is much larger than the heat capacity of the drink, we get the desired cooling effect without bringing too much water dilution;

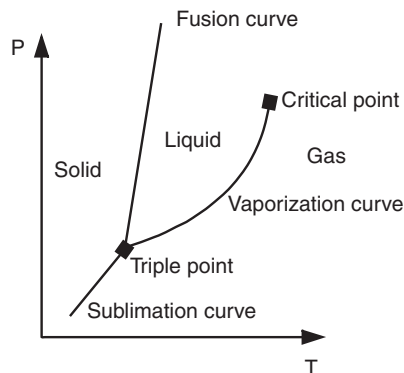


FIGURE 5.6.1

Phases of a substance

- To transport methane over long distances by sea, it is liquefied at a temperature of -160°C , reducing its specific volume 600 times with respect to gas. It is thus possible to maintain atmospheric pressure in the tanks of the LNG ship. Although these tanks are very well insulated, you cannot avoid some heat exchange with the surroundings, which has the effect of vaporizing a small amount of gas which is used for propulsion;
- In contrast, butane or propane gas distributed for culinary purposes is confined in a liquid state at room temperature in thick metal cylinders, in order to resist the inside pressure of a few hundred psi or tens of bar;
- All cooking done in boiling water takes place at 100°C if the pressure is equal to 1 atmosphere, and this irrespective of the thermal heat supplied to the cooking. Thus we can define the precise duration for cooking a recipe, for example, a boiled egg;
- The principle of the pressure cooker is to overcome this limit of 100°C by doing the cooking in a chamber at a pressure exceeding 1 atm. It can reach 110°C and 120°C , in order to cook food more quickly;
- An example of condensation is that which is deposited on cold surfaces in contact with moist air, like mist on a window, or the morning dew on leaves.

The triple point corresponds to the state where it is possible to simultaneously maintain equilibrium between all three phases. The critical point represents the state where the phase of pure steam has the same properties as the pure liquid phase. At higher temperatures and pressures (supercritical), it is not possible to observe a separation between liquid and gas phases: the disk surface which separates the liquid and vapor phases disappears at the critical point.

In practice, in heat engines, the working fluid is most often in the gaseous or liquid state, or as a mixture of gaseous and liquid phases. To calculate their properties, one is led to distinguish two broad categories of fluids: the ideal gas, which can be pure or compound, which includes the perfect gas, and condensable real fluids, which can also be pure or compound.

In Thermooption all these types of fluids are represented, with the exception of mixtures of real fluids, which can however be taken into account through external mixtures, as explained in Chapter 23 of Part 4. In what follows, we will successively deal with ideal gases, their mixtures, liquids and solids, properties of a mixture of phases in liquid-vapor equilibrium and condensable real fluids. We conclude with the study of moist mixtures of dry gas with water vapor, of real fluid mixtures and of charts used in absorption cycles.

5.6.2 Perfect and ideal gases

Many thermodynamic fluids in the vapor phase may be treated as ideal gases in a wide range of temperatures and pressures. This requires that the temperature-pressure combination deviates from the condensation zone as much as possible (that is to say that the pressure is not “too” high or the temperature “too” low). Such conditions are commonly the case for gases known as “permanent” at ambient temperature and pressure, such as hydrogen, oxygen, nitrogen, the oxygen-nitrogen mixture that is dry air etc. Even the water vapor in the atmosphere behaves almost like an ideal gas as its partial pressure remains moderate.

The ideal gas model is based on the assumption that the molecular interactions in the gas can be neglected, except for collisions between them. The kinetic theory of gases can then explain the gas macroscopic behavior from mechanical considerations, and statistics on the movements of its molecules.

The fundamental assumption of ideal gases is that their internal energy (and their enthalpy) is independent of pressure. Given that all real gases can be liquefied, there is rigorously no ideal or perfect gas. These concepts are fundamental, however, because the practical determination of the

state of a real fluid is always made by reference to the corresponding ideal or perfect gas, which approximates the behavior at very low pressure and/or high temperature.

Specifically, to represent the state of a fluid, a cascade of increasingly complex models is used depending on the desired accuracy, the simplest being that of the ideal gas, the most elaborate corresponding to real fluids.

5.6.2.1 Equation of state of ideal gases

The equations of perfect and ideal gases are very close, the first being in fact a special case of the latter. The equation of state of an ideal gas can be written:

$$Pv = rT \quad (5.6.1)$$

with $r = R/M$ ($\text{kJ kg}^{-1} \text{K}^{-1}$)

R is the universal constant = 8.314 ($\text{kJ kmol}^{-1} \text{K}^{-1}$)

M is the molar mass of the gas (kg kmol^{-1})

According to the units used, equation (5.6.1) takes different forms:

$$\text{in mass units: } Pv = rT$$

$$\text{in molar units: } Pv_m = RT$$

Based on the total volume V occupied by the fluid, n being the number of kilomol:

$$\text{in mass units: } PV = mrT$$

$$\text{in molar units: } PV = nRT$$

We can prove that equation (5.6.1) implies in particular that the internal energy and enthalpy of an ideal gas depend only on its temperature, and that

$$r = c_p - c_v$$

We thus have:

$$c_v = \frac{du}{dT} \quad (\text{J kg}^{-1} \text{K}^{-1})$$

and

$$c_p = \frac{dh}{dT} \quad (\text{J kg}^{-1} \text{K}^{-1})$$

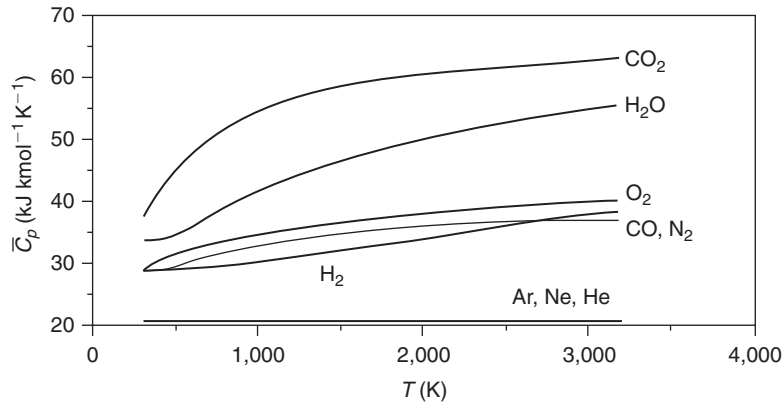
We call a “perfect” gas an ideal gas whose specific heat capacities c_p and c_v are constant. For such a gas, the internal energy and enthalpy are linear functions of temperature. Note that other authors call perfect gas what we call an ideal gas. In this case, they must each time tell whether the heat capacity of gas depends or not on the temperature.

The assumption of perfect gas (c_p and c_v constant) is rigorously met for monatomic gases (which have no rotation or molecular vibration mode). The larger the number of atoms in the gas molecule (and thus possible vibration modes), the less this assumption is valid.

Statistical thermodynamics allows us to determine the values of molar heat capacity of monatomic and diatomic gases.

For the former, we get:

$$C_p = \frac{5}{2}R = 20.785 \text{ kJ/kmol} \quad C_v = \frac{3}{2}R = 12.471 \text{ kJ/kmol}$$

**FIGURE 5.6.2**

Molar heat capacity of some gases

For diatomic gases usually, at room temperature, we obtain:

$$C_p = \frac{7}{2}R = 29.1 \text{ kJ/kmol} \quad C_v = \frac{5}{2}R = 20.785 \text{ kJ/kmol}$$

Figure 5.6.2 shows the changes in C_p for some typical mono-, bi- and tri-atomic gases.

5.6.2.2 Practical determination of the state of a perfect gas

Two parameters are sufficient to define an ideal gas: either its heat capacities at constant pressure and volume, or one of them and the value of its molar mass M , or the values of M and γ , the ratio of c_p to c_v .

Under the assumptions, $Pv = rT$, $c_p - c_v = r$, and constant c_p and c_v , we can easily calculate the internal energy u , enthalpy h of the gas from any reference state T_0 .

$$u = u_0 + c_v (T - T_0) \quad \text{and} \quad h = h_0 + c_p (T - T_0) \quad (5.6.2)$$

$$Tds = du + Pd v \Rightarrow ds = \frac{1}{T} du + \frac{P}{T} dv$$

which allows us to easily calculate the entropy of the fluid:

$$\begin{aligned} ds &= \frac{c_p}{T} dT + \frac{r}{v} dv \\ s &= s_0 + c_p \ln \frac{P}{P_0} + c_v \ln \frac{v}{v_0} \\ s &= s_0 + c_v \ln \frac{T}{T_0} + r \ln \frac{v}{v_0} \\ s &= s_0 + c_p \ln \frac{T}{T_0} - r \ln \frac{P}{P_0} \end{aligned} \quad (5.6.3)$$

The choice of the reference point is arbitrary and depends on conventions.

The characteristics (M , c_p , c_v , r , γ) of some substances are given in Table 5.6.1.

TABLE 5.6.1
CHARACTERISTICS OF SOME SUBSTANCES

	M kg/kmol	c_p J/kg/K	c_v J/kg/K	r J/kg/K	γ
Air	28.97	1005	718	287.1	1.40
Hydrogen (H ₂)	2.016	14320	10170	4127	1.41
Helium (He)	4.003	5234	3140	2078	1.66
Methane (CH ₄)	16.04	2227	1687	518.7	1.32
Steam (H ₂ O)	18.02	1867	1406	461.4	1.33
Neon (Ne)	20.18	1030	618	411.9	1.67
Acetylene (C ₂ H ₂)	26.04	1712	1394	319.6	1.23
Carbon monoxide (CO)	28.01	1043	745	296.6	1.40
Nitrogen (N ₂)	28.02	1038	741	296.6	1.40
Ethylene (C ₂ H ₄)	28.05	1548	1252	296.4	1.24
Ethane (C ₂ H ₆)	30.07	1767	1495	276	1.18
Oxygen (O ₂)	32.00	917	653	259.6	1.40
Argon (Ar)	39.94	515	310	208	1.67
Carbon dioxide (CO ₂)	44.01	846	653	188.9	1.30
Propane (C ₃ H ₈)	44.09	1692	1507	188.3	1.12
Isobutane (C ₄ H ₁₀)	58.12	1758	1620	143.1	1.09
Octane (C ₈ H ₁₈)	114.23	1711	1638	72.8	1.04

5.6.2.3 Practical determination of the state of an ideal gas

An ideal gas differs from a perfect gas because its thermal capacity is not constant, but depends solely on temperature.

Most often, C_p is represented by a polynomial fit of order n in T , as (either in molar units, as below, or in mass units):

$$C_p = \sum_{i=0}^n C_{p_i} T^i \quad (5.6.4)$$

The solution chosen in Thermoptim is a 7-term development of the following type:

$$C_p = A + BT + CT^2 + DT^3 + ET^4 + \frac{G}{T^2} + \frac{K}{T}$$

Data from Janaf Tables have been used to identify the parameters (Chase et al., 1985).

In order to reduce the number of terms while maintaining good accuracy, a polynomial fit of non-integer exponents can also be used, which leads to expressions like the following (Holman, 1988). T is in Kelvin.

$$C_p = C_{pa} + \frac{C_{pb}}{\sqrt{T}} + \frac{C_{pc}}{T} + \frac{C_{pd}}{T^2} + C_{pe} T \quad (\text{kJ/kmol/K})$$

$$\text{O}_2 \quad C_p = 48.212 - \frac{536.8}{\sqrt{T}} + \frac{3559}{T} \quad (300 < T < 2200)$$

$$C_p = 48.212 - \frac{536.8}{\sqrt{T}} + \frac{3559}{T} + 3.768 \cdot 10^{-4} (T - 2222) \quad (2200 < T < 5000)$$

$$\text{N}_2 \quad C_p = 39.65 - \frac{8071}{T} + \frac{1.5 \cdot 10^6}{T^2} \quad (300 < T < 5000)$$

$$\text{CO} \quad C_p = 39.61 - \frac{7652}{T} + \frac{1.38 \cdot 10^6}{T^2} \quad (300 < T < 5000)$$

$$\text{H}_2 \quad C_p = 24.12 + 4.356 \cdot 10^{-3} T + \frac{62.41}{\sqrt{T}} \quad (300 < T < 2200)$$

$$C_p = 24.12 + 4.356 \cdot 10^{-3} T + \frac{62.41}{\sqrt{T}} - 5.94 \cdot 10^{-4} (T - 2222) \quad (2200 < T < 5000)$$

$$\text{H}_2\text{O} \quad C_p = 83.15 - \frac{1863}{\sqrt{T}} + \frac{17445}{T} \quad (300 < T < 3000)$$

$$\text{CO}_2 \quad C_p = 67.83 - \frac{15189}{T} + \frac{1.82 \cdot 10^6}{T^2} \quad (300 < T < 3500)$$

$$\text{SO}_2 \quad C_p = 65.09 - \frac{11759}{T} + \frac{1.26 \cdot 10^6}{T^2} \quad (300 < T < 3500)$$

C_v is deduced by $C_v = C_p - R$, and specific variables c_p and c_v are obtained by dividing these values by the molar mass of the substance.

In practice, if we do not have a software application to calculate the properties of substances, and if we intend to determine the evolution of an ideal gas over a limited range of temperature, it is possible to assimilate it to a perfect gas, which enables us to use all the results established for them, provided its specific heat capacity is calculated at the mean temperature of the process. Of course, this is only valid in first approximation, but the loss of accuracy is compensated by a simplification of the calculations.

From a polynomial c_p or $c_v = f(T)$, it is easy to calculate u , h or s by integrating their differential relations, which leads to:

$$u - u_0 = \int_{T_0}^T c_v(t) dt \quad (5.6.5)$$

$$h - h_0 = \int_{T_0}^T c_p(t) dt \quad (5.6.6)$$

$$s = s_0 + \int_{T_0}^T \frac{c_v(t)}{t} dt + r \ln \frac{v}{v_0} \quad \text{or} \quad s = s_0 + \int_{T_0}^T \frac{c_p(t)}{t} dt - r \ln \frac{P}{P_0} \quad (5.6.7)$$

With the non-integer polynomial development proposed above, we obtain, as an integral for these functions, in molar variables:

$$u = (C_{pa} - R) T + 2 C_{pb} \sqrt{T} + C_{pc} \ln(T) - \frac{C_{pd}}{T} + \frac{C_{pe}}{2} T^2$$

$$h = C_{pa} T + 2 C_{pb} \sqrt{T} + C_{pc} \ln(T) - \frac{C_{pd}}{T} + \frac{C_{pe}}{2} T^2$$

$$s = C_{pa} \ln(T) - 2 \frac{C_{pb}}{\sqrt{T}} - \frac{C_{pc}}{T} - \frac{C_{pd}}{2T^2} + C_{pe} T - R \ln(P)$$

5.6.2.4 Equation of isentropic process

In many compressors or turbines, the fluid undergoes an evolution close to the isentropic, which forms the reference against which the actual process is calculated. The isentropic equations are therefore of particular importance. By posing $s = s_0 = \text{Const.}$, we find, for perfect gas:

$$Pv^\gamma = \text{Const.}, \quad \text{or} \quad Tv^{\gamma-1} = \text{Const.}, \quad \text{or} \quad PT^{\gamma/(1-\gamma)} = \text{Const.} \quad (5.6.8)$$

or, in differential form:

$$\frac{dP}{P} + \gamma \frac{dv}{v} = 0 \quad (5.6.9)$$

For an ideal gas, the isentropic equation does not take as simple a form as for a perfect gas. The formalism is more complex, but it remains quite usable in practice, as the pressure and temperature variables can be separated.

According to (5.6.7) we obtain

$$\ln \frac{P}{P_0} = \int_{T_0}^T \frac{c_p(t)}{rt} dt$$

which is similar to the corresponding expression for an ideal gas:

$$PT^{\gamma/(1-\gamma)} = \text{Const.} \quad \text{where} \quad \frac{\gamma}{\gamma-1} = \frac{c_p}{r}$$

5.6.3 Ideal gas mixtures

In many practical applications, we are dealing not with pure gases, but gas mixtures, whose composition may vary. This is particularly the case in an internal combustion engine cylinder: the composition of flue gas is evolving gradually as the combustion unfolds.

Dalton's law states an important result: a mixture of ideal gases behaves itself as an ideal gas.

The composition of a mixture is usually determined from either mole fractions or mass fractions of the constituents. In this section we establish the expressions for various usual thermodynamic properties in terms of these quantities.

5.6.3.1 Mole fractions and mass fractions

The total number of moles n of the mixture equals the sum of the numbers of moles of each component:

$$n = n_1 + n_2 + n_3 + \dots + n_n = \sum n_i$$

The mole fraction of a component is defined as the ratio of the number of moles of this constituent to the total number of moles in the mixture:

$$x_i = \frac{n_i}{n} \quad \text{and} \quad \sum x_i = 1$$

Moreover, the law of mass conservation implies that the total mass is equal to the sum of the masses of the constituents:

$$m = m_1 + m_2 + m_3 + \dots + m_n = \sum m_i$$

The mass fraction of a component is defined as the ratio of the mass of the component to the total mass of the mixture:

$$y_i = \frac{m_i}{m} \quad \text{and} \quad \sum y_i = 1$$

5.6.3.2 Dalton law of ideal gases

We define the partial pressure P_i of a component as the pressure exerted by this component if it occupied alone the volume V of the mixture, its temperature being equal to that of the mixture.

Dalton's law postulates that the pressure, internal energy, enthalpy and entropy of a mixture of ideal gases at temperature T and pressure P are respectively the sum of the pressures, internal energies, enthalpies and partial entropies of gas constituents, that is to say taken separately at temperature T and their partial pressures.

Each component behaves as if it existed at the temperature T of the mixture and was alone in the volume V .

Physically, this means that the fields of molecular forces of the individual components do not interfere with each other.

Mathematically, Dalton's law translates into the following two laws, the total pressure being P :

$$P_i = x_i P \quad (5.6.10)$$

$$c_p = \frac{1}{m} \sum c_{pi} m_i = \sum y_i c_{pi} \quad (5.6.11)$$

The mixture heat capacity at constant pressure equals the sum of the products of the specific heat capacity of the constituents by their mass fractions.

Dalton's law means that a mixture of ideal gases behaves itself as an ideal gas, whose fictitious mole molar mass would be $M = \sum x_i M_i$

This means that the results established for ideal gases can be used to calculate the evolution of mixtures of these gases, which is of paramount importance in practice.

We have: $y_i = x_i \frac{M_i}{M}$

We can also define an equivalent ideal gas constant by:

$$r = \frac{R}{M} \quad (\text{kJ kg}^{-1} \text{K}^{-1})$$

In mass notations, the ideal gas constant of the mixture is expressed in a very simple form:

$$r = \sum y_i r_i \quad (5.6.12)$$

Moreover,

$$H = \sum H_i \quad \text{and} \quad mc_p T = \sum c_{pi} m_i T$$

We deduce (5.6.11).

In molar notations (5.6.11) becomes:

$$C_p = \sum x_i C_{pi} \quad (5.6.13)$$

5.6.3.3 Energy properties of ideal gas mixtures

Enthalpy of a mixture

According to Dalton's law, the enthalpy of a mixture of ideal gases is equal to the sum of the enthalpies of each component.

In practice, we use relations (5.6.14) or (5.6.15):

$$\text{mass notations: } h = \sum y_i h_i \quad (5.6.14)$$

$$\text{molar notations: } H = \sum x_i H_i \quad (5.6.15)$$

The calculation of internal energy would be done in the same way.

Entropy of a mixture

It is when calculating the entropy of the mixture that the profound significance of Dalton's law appears, i.e. that the value of the entropy of the mixture shall be calculated by summing the entropies of the constituents taken at temperature T and **their partial pressures P_i** .

Indeed, the entropy of the mixture is greater than the sum of the entropies of the constituents before mixing by a value $k_m = -r \sum x_i \ln x_i > 0$. Physically, this is explained by the irreversibility of the mixing operation. It is important to note that the k_m gap remains constant (independent of T and P) as long as the concentrations do not vary. This gap must be taken into account once and for all when calculating the entropy of reference, but then, the mixture behaving itself as an ideal gas, we no longer need to worry about it.

Of course, this does not remain true if the composition of the mixture comes to vary during the process, in which case it is necessary to calculate the different values of k_m to determine the variations of entropy.

Thermoptim uses two types of ideal gases:

- pure gases, whose properties are predetermined in the software, not user-modifiable; they number about 20;
- compound gases, constructed by the user at will from pure gases included in the database. Their properties are calculated by the software by applying Dalton's law.

5.6.4 Liquids and solids

Liquids and solids are described as ideal when compressibility is negligible ($v = \text{Const.}$).

Since an "ideal" liquid or solid cannot be subjected to any form of reversible work, a well chosen single variable is enough to represent its thermodynamic state.

One can indeed consider that the internal energy of an ideal liquid or solid depends only on its temperature:

$$\frac{du}{dT} = c, \quad \text{as for an ideal gas.}$$

However the enthalpy of the ideal liquid (that of the solid has no physical sense) is still a function of pressure:

$$dh = c dT + v dP$$

We can still define the entropy $ds = (1/T)du + (P/T)dv$, which gives:

$$ds = \frac{cdT}{T}$$

As for gas, a liquid or solid whose heat capacity does not vary significantly is called "perfect": $c \approx \text{Const.}$

Then:

$$\begin{aligned}u - u_0 &= c(T - T_0) \\h - h_0 &= c(T - T_0) + v(P - P_0) \\s - s_0 &= c \ln \frac{T}{T_0}\end{aligned}$$

In practice, characteristics of liquids are often identified at the saturation pressure. However, as the correction $v(P - P_0)$ is generally small, this convention has little importance.

For an isobaric evolution, the calculation of thermodynamic properties of liquids involves only their heat capacity. Therefore, in Thermoptim, we introduce a particular substance, called generic liquid, specific heat capacity equal to unity, which is used to calculate the exchange in ways that will be explained in section 8.3.5.

5.6.5 Liquid-vapor equilibrium of a pure substance

In compressible fluid machines it is often necessary to study the processes bringing the fluid into the liquid state. The ideal gas to zero does not exist, all fluids being condensable, and it is necessary to know their properties in the liquid state.

The study of vapor-liquid equilibrium is based on the law of phase mixture or lever rule that merely reflects the extensiveness of state functions with the assumption that the interfacial energy is negligible, which reads: volume, internal energy, enthalpy, entropy of a phase mixture, at pressure P and temperature T , are respectively the sums of these properties in the different phases constituting the mixture, taken in isolation at the same pressure and at the same temperature.

On various thermodynamic charts presented below, the vaporization or vapor-liquid equilibrium area is evident for temperatures and pressures lower than the critical point. This area is bounded on the left by the saturated liquid curve, and on the right by the dry saturated vapor curve. These two curves define the saturation curve, whose shape is characteristic. Between these two curves, pressure and temperature are no longer independent: they are connected by a relationship known as saturation pressure law or vapor pressure law, and the system is mono-variant.

5.6.5.1 Saturation pressure law

Many formulas have been proposed to algebraically represent the saturation pressure law. One of the most used is that of Antoine:

$$\ln(P_s) = A - \frac{B}{C + T}$$

where A , B and C are characteristic parameters of the fluid, and P_s the saturated vapor pressure. With P_s in bar and T in K, for example for water:

$$A = 11.783 \quad B = 3895.65 \quad C = -42.1387$$

This however is not very precise, and in Thermoptim, the following development was selected:

$$\ln(P_s) = AT + \frac{B}{T} + C \ln(T) + DT^E$$

5.6.5.2 Vapor quality

In the middle part of the vapor-liquid equilibrium zone, fluid is present in both liquid and vapor phases. In this central zone, isobars and isotherms are combined, the liquid-vapor change taking

place at constant temperature and pressure. The composition of the mixture is defined by its quality x , ratio of vapor mass m_g to the total mass (m_g plus the mass of liquid m_l).

$$x = \frac{m_g}{m_g + m_l} \quad (5.6.16)$$

5.6.5.3 Enthalpy of vaporization

The length of the vaporization line gives the enthalpy (or heat) of vaporization L for the fluid conditions P and T considered. It is proportional to it in the entropy (s , T) and Mollier (s , h) charts, and equal to it in the (h , $\ln(P)$) chart:

$$\begin{aligned} h_g - h_l &= L \\ s_g - s_l &= \frac{L}{T} \end{aligned}$$

The above relationships can be demonstrated from relationship 5.4.20 expressing that the free energy is minimal at equilibrium: during the vaporization process, the Gibbs energy evolves from g_l to g_g .

If evolution is reversible, we have: $dg = 0$, or $g_l = g_g$:

$$h_l - Ts_l = h_g - Ts_g$$

We thus find the relationship $h_{lg} = (h_g - h_l) = T(s_g - s_l) = Ts_{lg}$.

L is a decreasing function of temperature, zero for T above the critical temperature. A formula due to Clapeyron allows us to estimate L from the saturation pressure law:

$$L = T(v_g - v_l) \frac{dPs}{dT}$$

In this formula, the gas specific volume v_g is obtained from the vapor equation of state, and the liquid specific volume v_l from a proper relationship.

In Thermoptim, we opted for a direct relationship giving L as a function of reduced temperature $Tr = T/T_c$:

$$L = A(1 - Tr)(B + C Tr + D Tr^2 + E Tr^3)$$

5.6.5.4 Calculation of pure two-phase substance properties

By applying the law of phase mixture, we have:

$$\begin{aligned} v &= (1 - x)v_l + xv_g \\ u &= (1 - x)u_l + xu_g \\ h &= (1 - x)h_l + xh_g = h_l + xL \\ s &= (1 - x)s_l + xs_g = s_l + x \frac{L}{T} \end{aligned} \quad (5.6.17)$$

Values of critical points and vaporization enthalpies for some common substances are given in Table 5.6.2.

5.6.6 Representations of real fluids

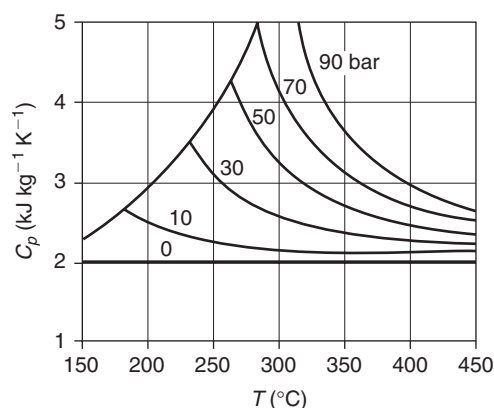
The increase in pressure and/or lowering of the temperature can justify a reconsideration of the ideal gas equation (5.6.1). This is especially the case near the liquid-vapor equilibrium zone.

When the fluid no longer satisfies the ideal gas equation, its internal energy and enthalpy are no longer based solely on temperature.

TABLE 5.6.2

CRITICAL AND VAPORIZATION PROPERTIES

	Ts (1bar) K	ρ at Ts kg/liter	L MJ/kg/K	c_p (Ts) kJ/kg/K	Pc bar	Tc K
air	80.2	0.860			37.70	132.6
oxygen	90.2	1.120	0.211	1.699	50.40	154.4
nitrogen	77.4	0.812	0.197	2.038	33.96	126.3
CO ₂ (sublimation)	194.7	0.793	0.369		73.50	304.2
CO	81.7	0.799	0.215		34.90	133.0
water	373.2	0.958	2.260	4.185	221.00	620.4
hydrogen	20.4	0.070	0.467	9.794	12.96	33.3
helium	4.3	0.122	0.023	4.604	2.28	5.3
argon	87.3	1.420	0.163	1.130	48.59	150.8
methane	111.5	0.424	0.503	3.474	46.27	190.7
ethane	184.6	0.546	0.489	2.427	49.80	305.4
ethylene	169.7	0.610	0.467	2.637	51.33	282.7
propane	230.6	0.582	0.410	2.511	42.52	370.0

**FIGURE 5.6.3**

Influence of pressure on steam heat capacity

This behavior is shown in Figure 5.6.3, for superheated steam. It is clear that the heat capacity c_p of this substance is the more affected by the pressure as it is higher and the temperature is lower (that is to say, especially in the immediate vicinity of the saturation curve).

To determine the state of a real fluid, we use most often a thermodynamic chart, a table of thermodynamic property values, or a set of equations of state covering the various zones necessary.

Traditionally, thermodynamic charts are the most used. There has however been a marked evolution of the practice, the development of micro-computers making possible the direct calculation of fluid thermodynamic properties in a wide range of variation of state variables. Thermoptim allows us to make such calculations precisely.

However, even if one has a fluid properties computer, charts retain a strong interest to provide education, because they can easily view the real gas properties, including the liquid-vapor zone. We therefore begin by presenting them.

Moreover, the usual diagrams are increasingly computerized, which allows us to conciliate ease of use due to graphical display and numerical accuracy. Interactive charts of the Thermoptim family, based on the same equations as the software, are one example. These diagrams, shown in Figures 5.6.7, 5.6.8, 5.6.11 and 5.6.12 are available from the demo version of Thermoptim, their

interactivity being deactivated. The reader interested in their construction may in particular display only some of the isovalue curves, by selecting them in the View menu.

5.6.6.1 Thermodynamic charts of pure substances

A pure substance of given mass being a bivariant system, its state can be represented on a 2 axes chart, on which are plotted a number of iso-values or “contours”.

Among the many possible coordinate systems, we will retain four:

- the Clapeyron chart (P, v) which gives the most direct image of the mechanical processes, but is little used for the study of industrial projects, because it does not allow one to accurately read the usual energy quantities, including entropy and enthalpy;
- the entropy chart (T, s) that directly visualizes the reversible heat transfers ($\int T ds$) and the various possible irreversibilities;
- the Mollier chart (h, s), which is a change of the former, intended to directly show the energy transfers in an open system, which has the advantage that the enthalpy involved can be read without difficulty;
- the ($h, \ln(P)$) chart, with enthalpy as abscissa and pressure as ordinate (usually with a logarithmic scale to cover a wide range of values). This chart is traditionally used in the study of cycles running in reverse (heat pumps or refrigeration). Its interest is to combine the essential mechanical constraint (P) of compressors to the energy variable (h);
- exergy charts (or usable enthalpy charts) (h, x_h) and (s, x_h), with the enthalpy or entropy as abscissa and exergy as ordinate, allow one to view exergy brought into play in processes, and therefore lend themselves well to the study of irreversibilities taking place in cycles.

Thermoptim provides electronic versions of these charts, called interactive charts, which can be set at leisure and on which we can represent the cycles.

Presentation of thermodynamic charts

Clapeyron chart

The Clapeyron chart (Figure 5.6.4) represents the fluid properties with specific volume v as abscissa and pressure P as ordinate. In this plane, one curve is of particular importance: the saturation curve.

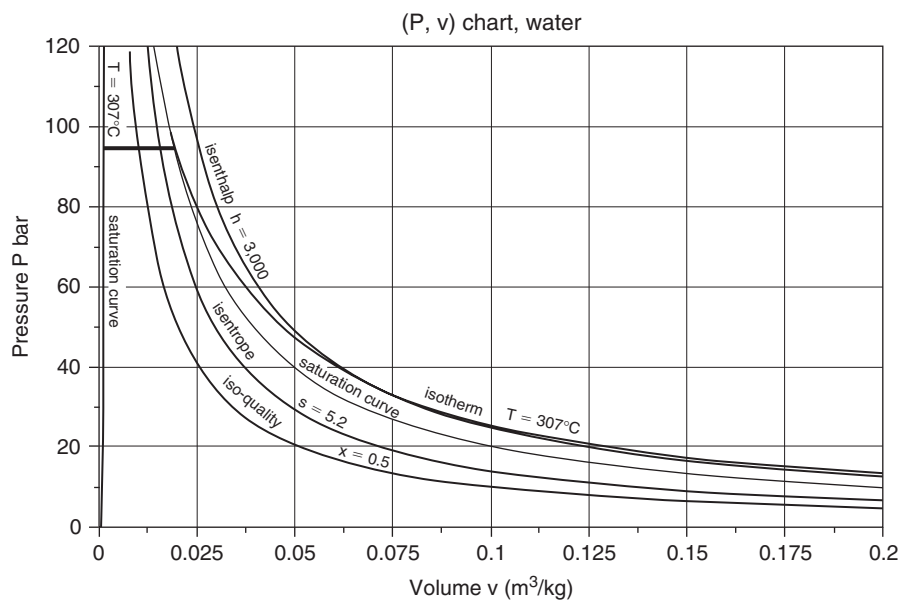


FIGURE 5.6.4

Clapeyron chart

Its summit is the critical point (not shown on the figure as its pressure is about twice that of the ordinate scale). The left side, upslope, represents the beginning of the boiling process (boiling curve), and its right side, down slope, the saturated vapor (dew point curve). Under this curve is the two-phase liquid-vapor equilibrium zone, and in the rest of the plane, that of simple fluid.

Form of isotherms

In the “liquid” zone on the left of the chart, isotherms have a very strong negative slope: the liquids are generally not compressible.

In the two-phase domain, pressure and temperature are linked by the saturated pressure law, and isotherms are horizontal. The volume increases enormously, since the density of the gas is much lower than that of the liquid (in the chart of Figure 5.6.4, the abscissa scale is logarithmic).

In the zone to the right of the vaporization curve, isotherms are curved downward. Gradually as the distance from the vaporization curve increases, the gas approaches the corresponding ideal gas, and isotherms are recovering to approach the equilateral hyperbolas of equation $Pv = \text{Const}$. We have shown an isotherm for $T = 307^\circ\text{C} < T_c$ in Figure 5.6.4.

Other iso-value curves

The main drawback of the Clapeyron chart is that it does not contain the usual thermodynamic quantities like enthalpy and entropy, and that if we equip it with isenthalpic and isentropic curves, it becomes very imprecise, as shown in the figure: the useful area of the chart is very narrow, and isentropic, isenthalpic and iso-quality curves have very similar shapes, so that determining their intersections is difficult.

Entropy chart

In the entropy chart (Figure 3.4.2 of Part 1), entropy is the abscissa and temperature the ordinate. The vaporization curve again separates the plane into two parts, defining the two-phase zone and the simple fluid zone. The critical point is still at its maximum (C in the figure).

For some substances, the right branch of the vaporization curve (saturated vapor), presents a point of maximum entropy. This is particularly the case for certain hydrocarbons and certain chlorofluorocarbons (CFCs).

One of the advantages of such a chart (see Figure 3.4.3 of Part 1) is that any perfect cyclic process results in the (T, s) plane by a contour (Γ), whose area A measures the absolute value of the amount of heat Q put into play (or the work provided or received τ).

Indeed, $Q = \int T ds$ by definition. As the cycle is closed, $Q + \tau = 0$, and $|\tau| = A$.

The rule of signs is as follows:

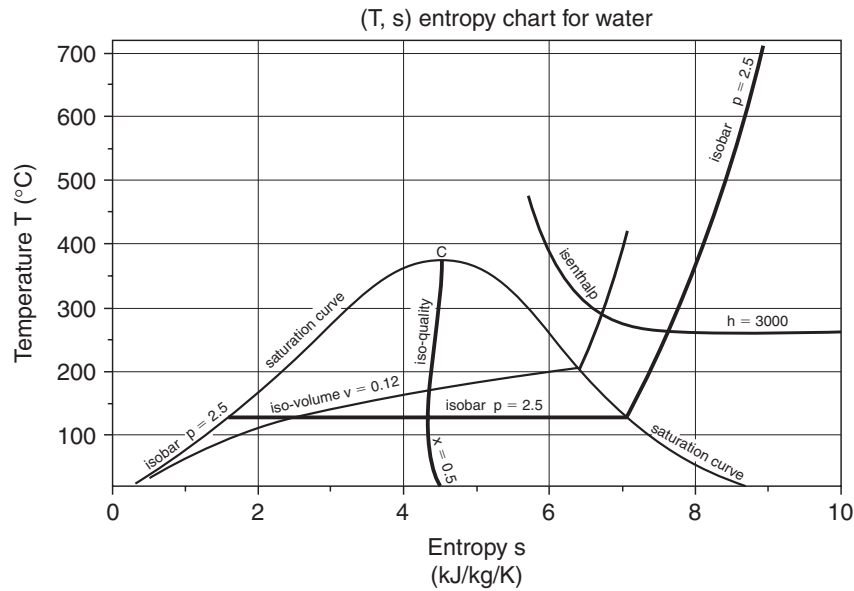
- if the cycle is described clockwise, the work is negative, thus transferred by the fluid to the surroundings: we talk of a motor cycle or of a cycle running forward;
- if the cycle is described counterclockwise it is the opposite: we talk of a refrigeration cycle, or of a cycle running in reverse.

Form of isobars

Left of the saturation curve, isobars are curved upward. Liquid isentropic compression having almost no effect on its temperature, liquid isobars are virtually merged with the ascending branch of the vaporization curve.

The chart is very imprecise in this area and it is preferable to use a table or a program giving the thermodynamic properties along the vaporization curve.

Inside the two-phase zone, temperature and pressure are bound by the saturated pressure law, and isobars are horizontal.

**FIGURE 5.6.5**

Helium entropy chart

Right of the vaporization curve, curves are rising and, for ideal gas, become exponential. They can be deduced from each other by horizontal translation.

If the pressure exceeds the critical pressure, isobars are strictly ascending curves, which do not intersect the vaporization curve.

Form of isenthalps

In the vicinity of the saturation curve, isenthalps are curved downward, with a strong negative slope.

Gradually as the distance from the vaporization curve increases, the gas approaches the corresponding ideal gas, and isenthalps become horizontal, as enthalpy is a sole function of temperature.

In an entropy chart, a Carnot cycle consisting of two isentropic and two isothermal processes is a rectangle.

Figures 5.6.5 and 5.6.6 give two examples of entropy charts available in Thermoptim, one for helium and the other for water. The abscissa unit (entropy s) is $\text{kJ kg}^{-1} \text{K}^{-1}$.

Mollier chart

In the Mollier chart (Figure 5.6.7), entropy is the abscissa, and enthalpy the ordinate. The advantage is that one can directly measure on the axis enthalpies put in. The critical point C is here at the left of the vaporization curve maximum.

Form of isobars

We have: $dh = v dP + T ds$ and therefore $(\partial h / \partial s)_p = T$. The slope of the isobars is at each point equal to the absolute temperature, and therefore presents no angular point. These curves are strictly ascending.

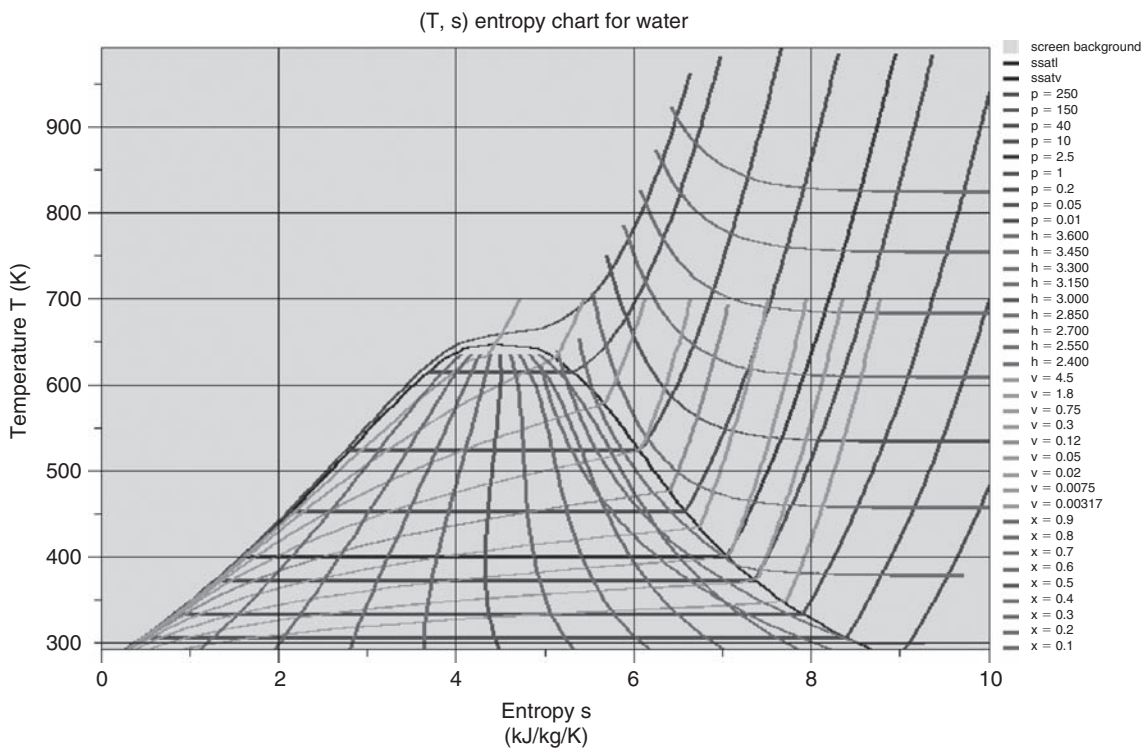


FIGURE 5.6.6
Water entropy chart

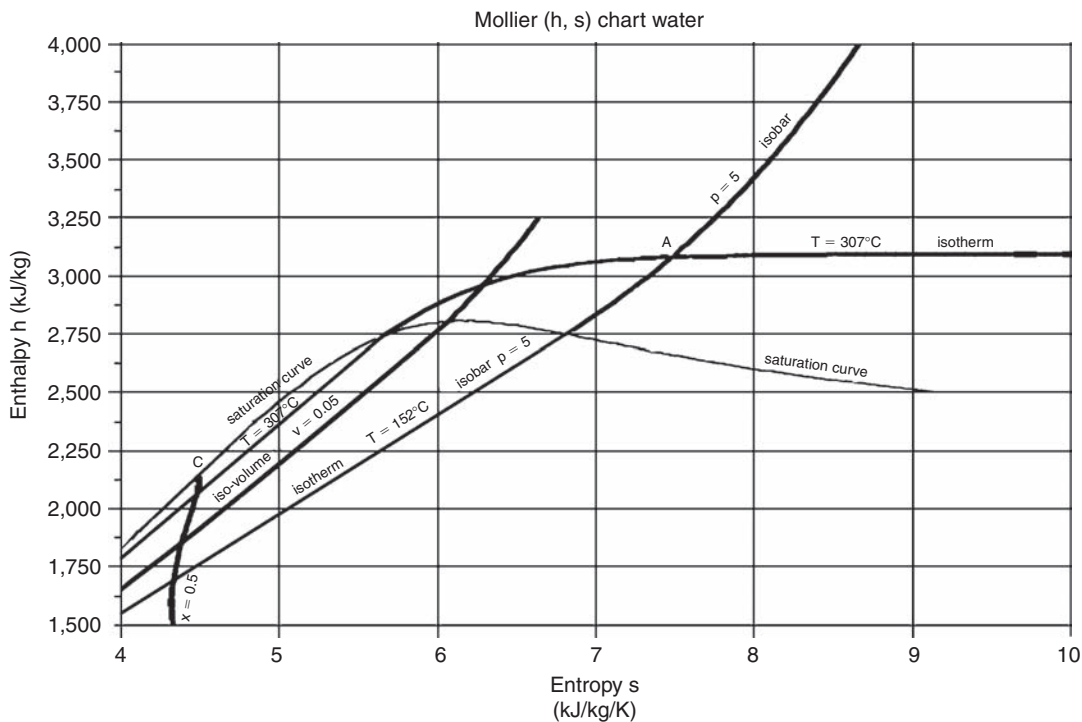


FIGURE 5.6.7
Mollier chart

In the liquid zone, they are practically merged with the vaporization curve, for the reasons outlined above. In the mixed zone, pressure and temperature being linked by the saturation pressure law, isobars are straight line segments of the slope T . As a first approximation, they are tangent to the boiling curve at the point corresponding to the start of boiling (not shown on the figure). In the gas zone, isobars escape tangentially to this straight line, and progressively approach the exponential corresponding to the ideal gas.

The critical isobaric curve starts tangentially to the vaporization curve in C.

Form of isotherms

In the mixed zone, isotherms are coincident with isobars. They then present an abrupt decrease in slope to move gradually toward the horizontal, since for the corresponding ideal gas, enthalpies depend only on temperature. In the vapor zone, we see that isotherms (low slope) and isobars (high slope) intersect with appreciable angles, which gives a very accurate reading (point A on Figure 5.6.7).

Form of isovolumes

It is possible to show that the slope of isovolumes is slightly larger than that of isobars.

Moreover, exergy is defined by relation $x_h = h - T_0s$, which can be written $h = T_0s + x_h$.

Once environment reference conditions (temperature and pressure) are defined, it is very easy to equip a (h, s) chart with iso-exergy curves, which are lines of slope T_0 .

Figures 5.6.8 and 5.6.9 show two examples of Mollier charts, one for water, and the second for R 134a.

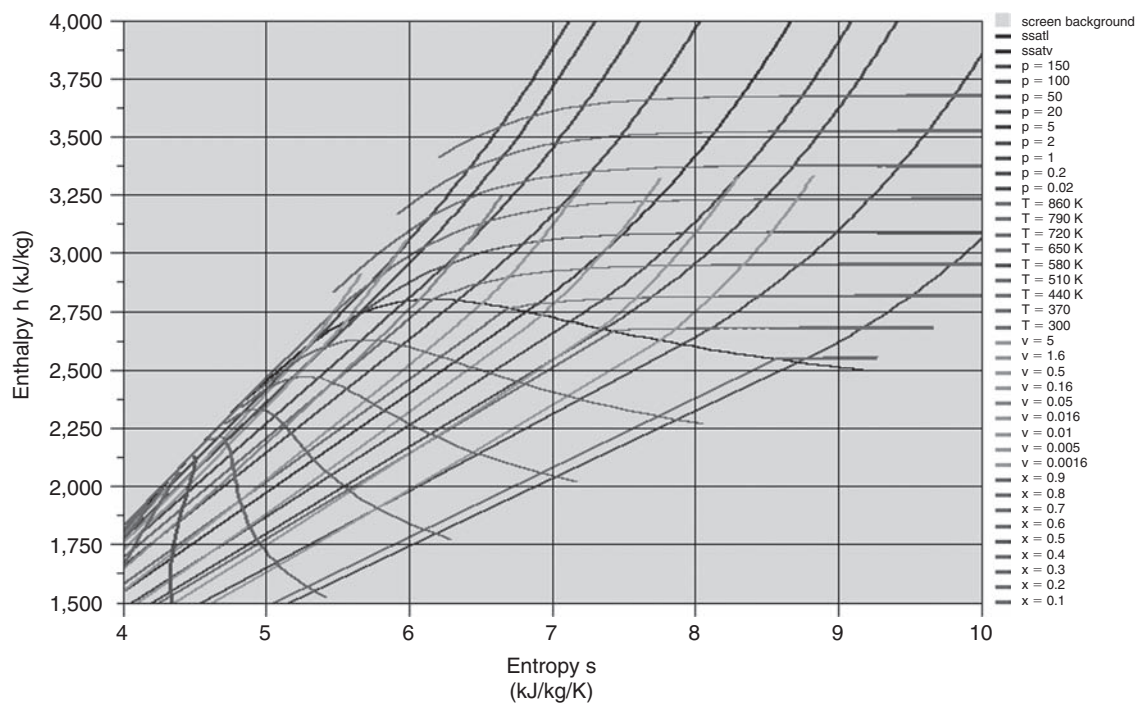
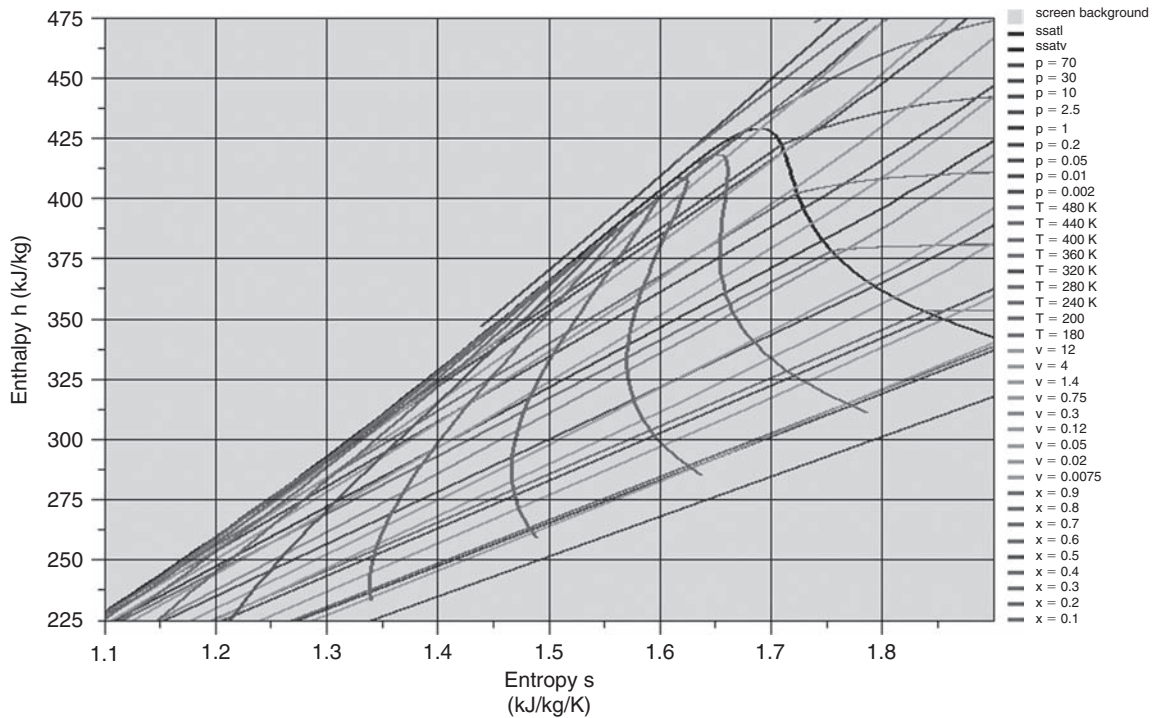


FIGURE 5.6.8

Mollier chart (h, s) for water


FIGURE 5.6.9

Mollier chart (h, s) for R134a

(h, ln(P)) chart

In the (h, ln(P)) chart (Figure 2.10.1 of Part 1), the abscissa is enthalpy, and the ordinate is pressure, usually on a logarithmic scale. This chart is equipped with isentropic, isothermal, isovolume curves, and in the mixed zone, equal quality curves.

The critical point C is here at vaporization curve maximum.

Form of isotherms

In the liquid region, isotherms are practically vertical, the enthalpy of the liquid being almost independent of pressure.

In the mixed zone, pressure and temperature being linked by the saturation pressure law, isotherms are horizontal.

In the vapor zone, the curves are decreasing with vertical asymptotes, the enthalpy of the corresponding ideal gas being independent of pressure.

Form of isentropes

The slope of isentropes is v , as $dh = v dP + T ds$, and thus $(\partial h / \partial P)_s = v$. They do not have angular points, and are almost vertical in the liquid zone, v being very small.

Figures 5.6.10 and 5.6.11 give two examples of (h, ln(P)) charts, the first for refrigerant R134a, and the second for ammonia. The ordinate unit (pressure P) is the bar, the abscissa (enthalpy h) is the kJ kg^{-1} .

Exergy enthalpy chart (h, ex_h)

In the exergy enthalpy chart (h, ex_h) (Figures 5.6.12 to 5.6.14), enthalpy is the abscissa and exergy the ordinate.

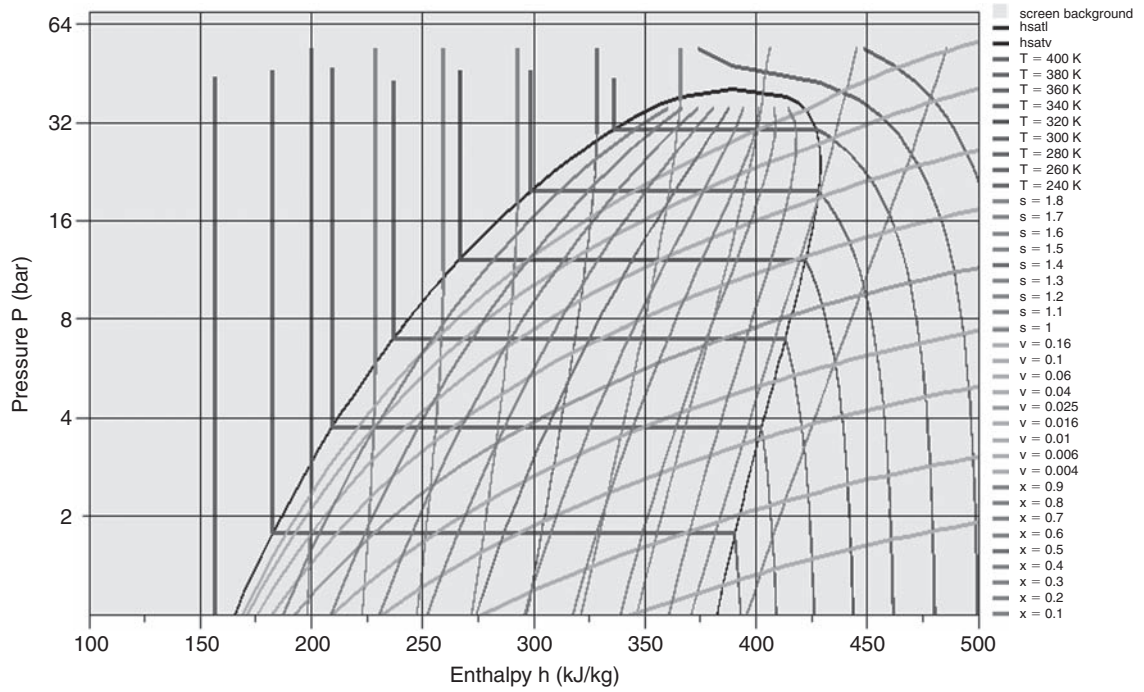


FIGURE 5.6.10
($h, \ln(P)$) chart for R134a

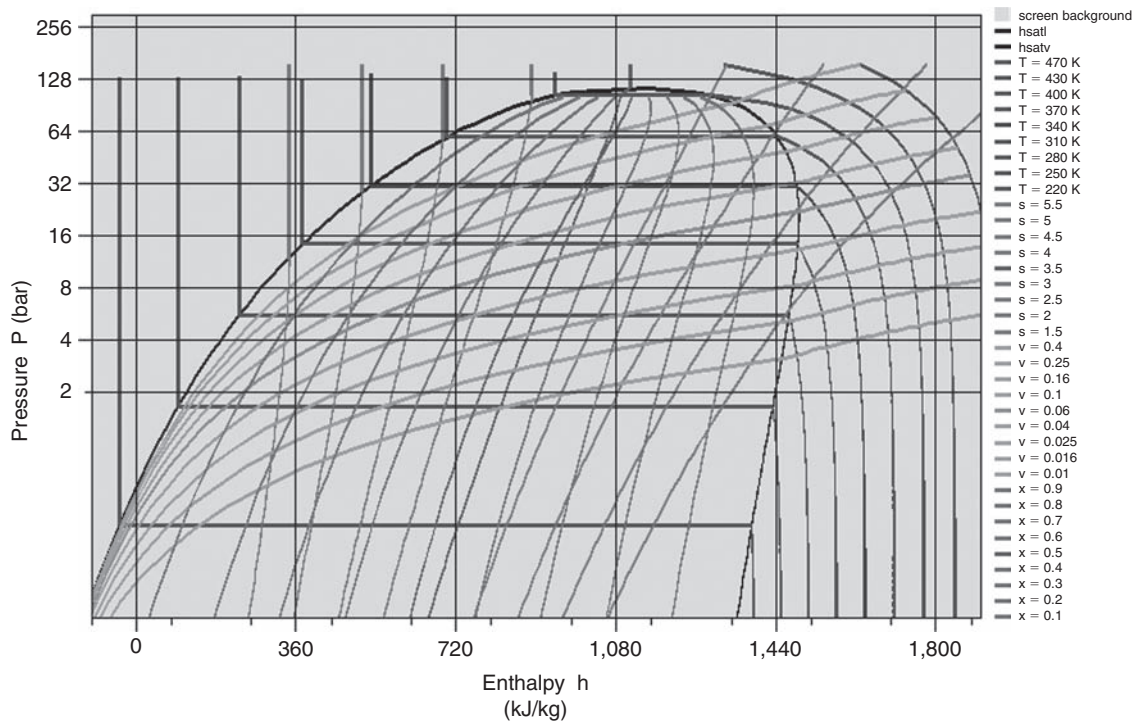


FIGURE 5.6.11
($h, \ln(P)$) chart for ammonia

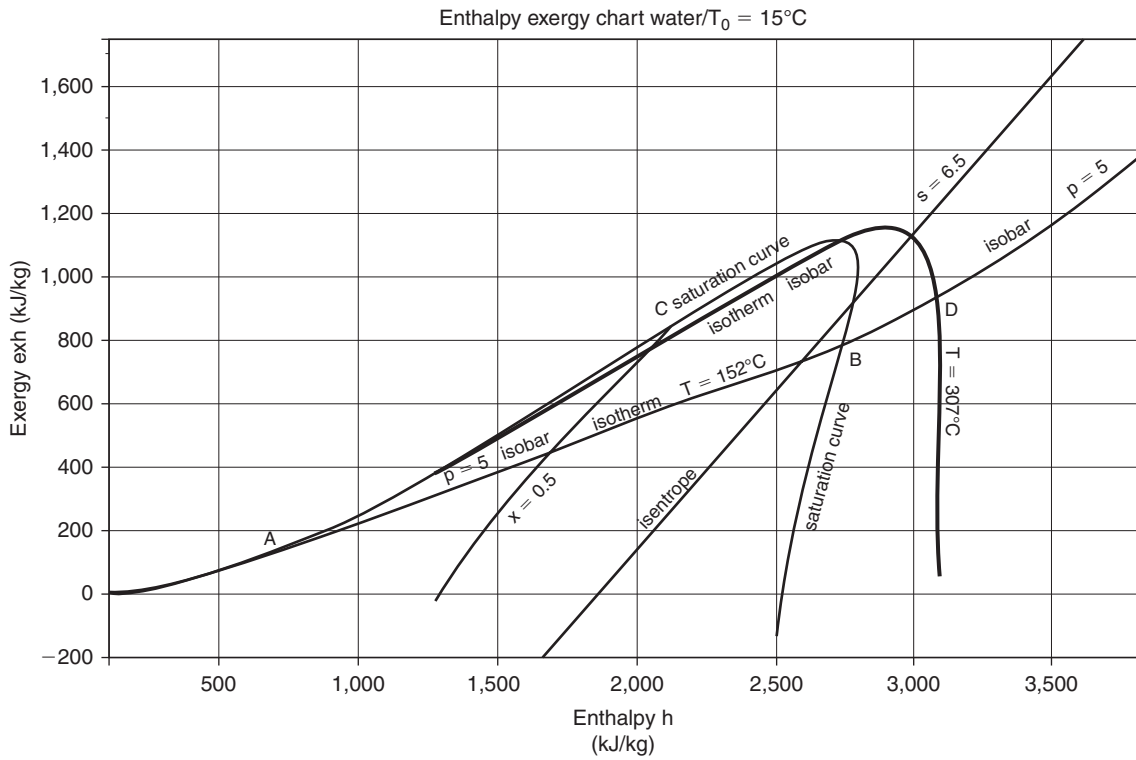


FIGURE 5.6.12
(h, xh) chart

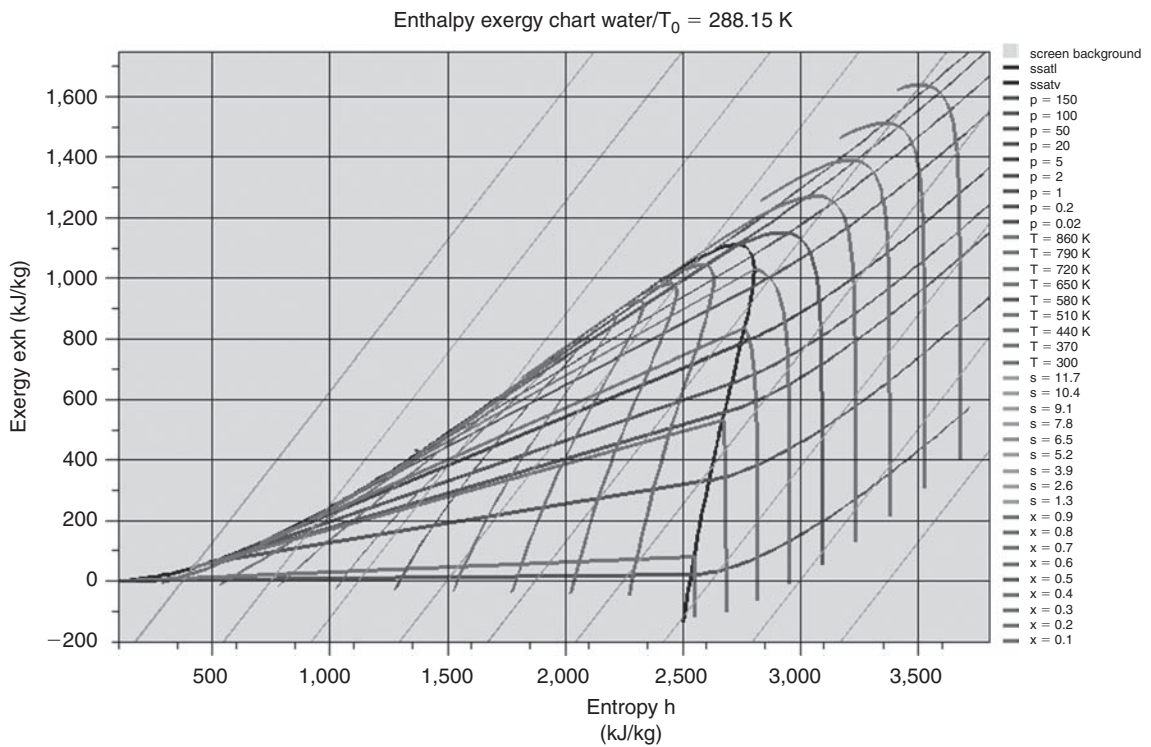


FIGURE 5.6.13
(h, x_h) exergy chart for water

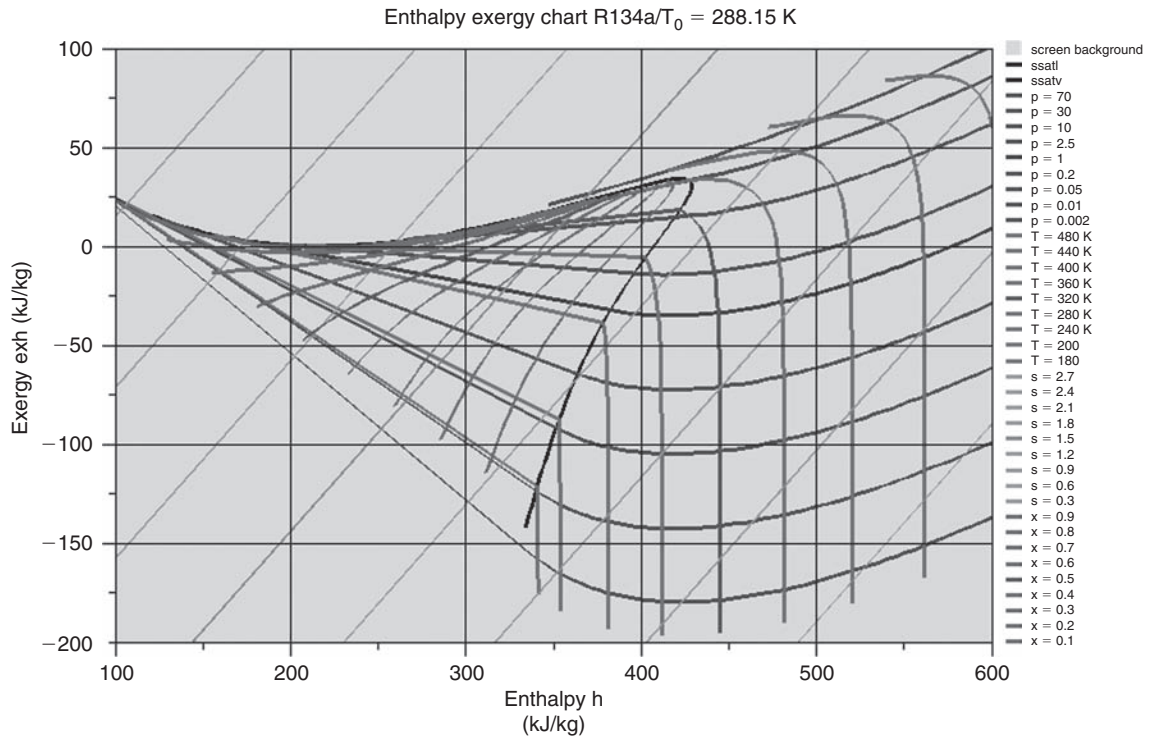


FIGURE 5.6.14

(h, x_h) exergy chart for R134a

As $x_h = h - T_0 s$, this chart is easily constructed from the Mollier chart by linear combination of axes once you know the reference temperature T_0 . Given this setting, it would be more accurate to speak, for a given substance, of an exergy charts family.

As for the Mollier chart (Fig. 5.6.9), one advantage is that we can measure directly on the x-axis the enthalpies put in. The critical point here is to the left of the maximum vaporization curve.

Form of isobars

We have: $dh = v dP + T ds$, and $dex_h = dh - T_0 ds$, hence

$$dex_h = \left(1 - \frac{T_0}{T}\right) dh - \frac{T_0}{T} v dP, \quad \text{and} \quad \left(\frac{\partial ex_h}{\partial h}\right)_P = \left(1 - \frac{T_0}{T}\right)$$

The slope of isobars at each point is equal to the Carnot factor $\theta = 1 - T_0/T$, and therefore presents no angular point. It becomes zero for $T = T_0$, which corresponds to the minimum exergy of the isobar chosen.

In the liquid zone, they are practically merged with the vaporization curve, for the reasons given for the Mollier chart. In the mixed zone, pressure and temperature being linked by saturation pressure law, isobars are straight line segments AB of slope $\theta = 1 - T_0/T$. As a first approximation, they are tangent to the boiling curve at point A corresponding to the start of boiling. In the gas zone, isobars escape tangentially to AB (blue dashed curve). At high temperatures, θ tends to 1, and they progressively approach straight lines parallel to isentropes.

The critical isobaric curve starts tangentially to the vaporization curve in C.

Form of isotherms

In the mixed zone, isotherms are coincident with isobars. Depending on the value of T_0 and temperature, they then pass through a maximum or have a sudden decrease in slope to gradually tend towards the vertical since for the corresponding ideal gas, enthalpies depend only on temperature. In the vapor zone, as can be seen in Figure 5.6.13, isotherms (high slope) and isobars (low slope) intersect with large angles (point D), which gives a very accurate reading.

The isothermal temperature T_0 is horizontal and tangent to the minimum of the saturation curve. Generally, it is chosen as the zero scale of ordinates.

Form of isovolumes

It is possible to show that the slope of the isovolumes is slightly higher than that of the isobars.

Form of isentropes

As $dx_h = dh - T_0 ds$, $(\partial x_h / \partial h)_s = 1$, the slope of isentropes is equal to unity: the isentropes are straight lines of slope 45° in a vertical rectangular frame. In the example given in Figure 5.6.13, whose axes do not have the same scale, they have a slightly lower angle.

As shown in this figure, it is very easy to identify on an exergy chart, for a given fluid temperature, pressure leading to the maximum exergy: it is that which passes through the maximum of the corresponding isotherm.

Figures 5.6.13 and 5.6.14 show two examples of enthalpy exergy charts, one for water, and the second for R 134a, prepared for $T_0 = 15^\circ\text{C} = 288.15\text{K}$.

Exergy entropy chart (s, ex_h)

In the entropy exergy chart (Figures 5.6.15 to 5.6.17), entropy is the abscissa and exergy the ordinate.

Like its predecessor, this chart is easily constructed from the Mollier chart once we know the reference temperature T_0 .

The critical point here is still to the left of the vaporization curve maximum.

Form of isobars

We have: $dh = v dP + T ds$, and $dex_h = dh - T_0 ds$, hence $dex_h = v dP + (T - T_0) ds$, and $(\partial ex_h / \partial h)_p = (T - T_0)$. The slope of isobars is at each point equal to $(T - T_0)$, and therefore presents no angular point. It becomes zero for $T = T_0$, which corresponds to the minimum exergy of the isobar chosen.

In the liquid zone, isobars are practically merged with the vaporization curve, for the reasons stated previously. In the mixed zone, pressure and temperature being linked by saturation pressure law, isobars are straight line segments AB of slope $(T - T_0)$. As a first approximation, they are tangent to the boiling curve at point A corresponding to the start of boiling. In the gas zone, isobars escape tangentially to AB (blue dashed curve). At high temperatures, they have a paraboloid look.

The critical isobaric curve starts tangentially to the vaporization curve in C.

Form of isenthalps

As $dex_h = dh - T_0 ds$, $(\partial ex_h / \partial s)_h = -T_0$, the isenthalp slope is equal to $-T_0$: isenthalps are the straight lines of negative slope. Given the difference in scale, their apparent slope is close to 45° .

Form of isotherms

In the mixed zone, isotherms are coincident with isobars. Depending on the value of T_0 and temperature, they then pass through a maximum or have a sudden decrease in slope to move gradually towards a straight negative slope parallel to isenthalps since for the corresponding ideal gas,

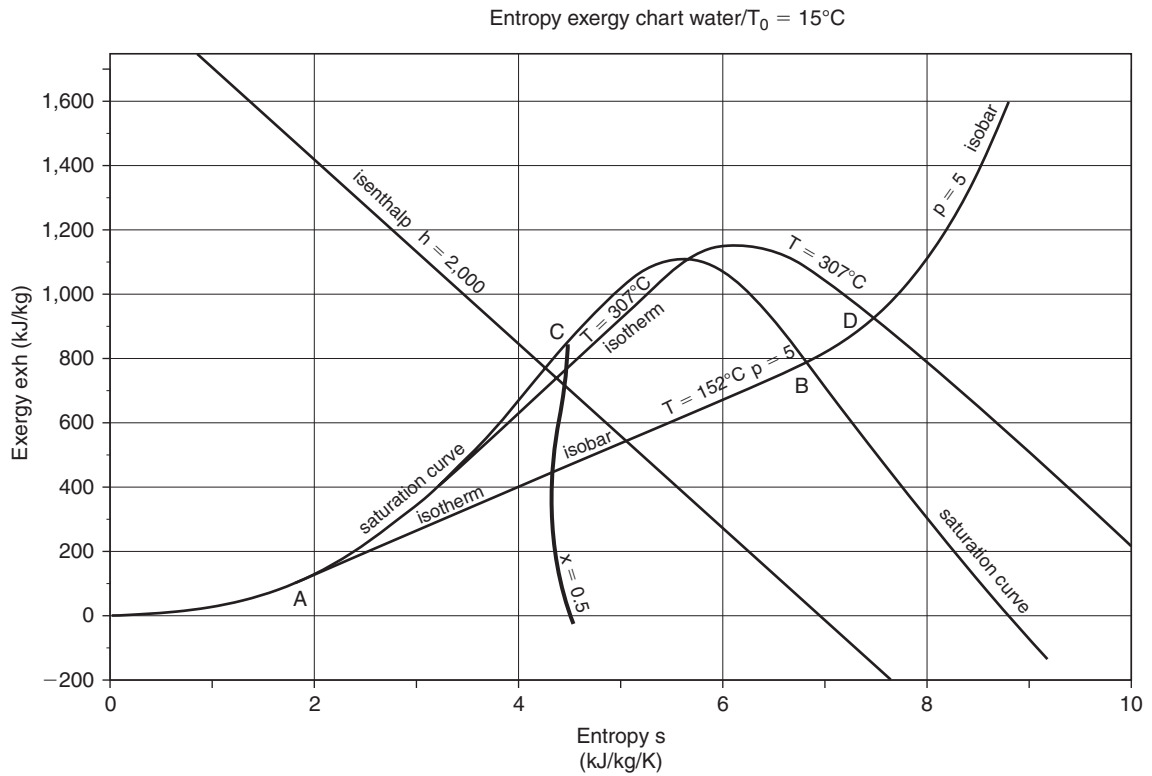


FIGURE 5.6.15

(s , x_h) chart

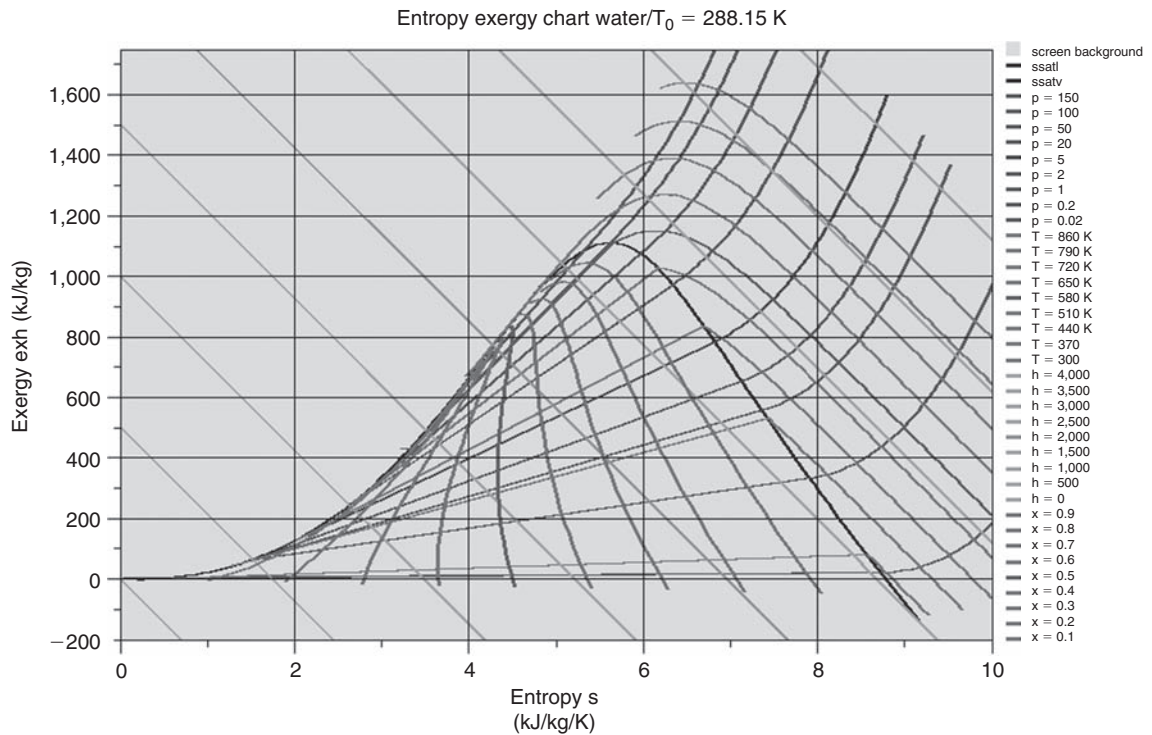


FIGURE 5.6.16

(s , x_h) exergy chart for water

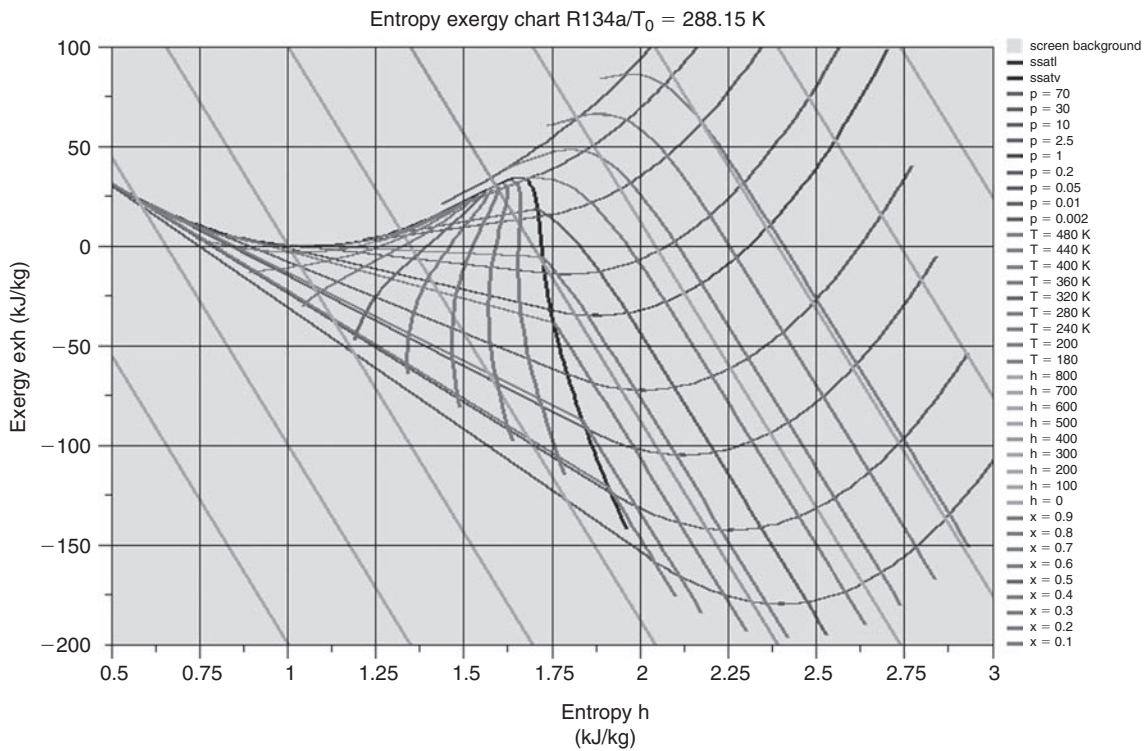


FIGURE 5.6.17

(s, x_h) exergy chart for R134a

enthalpies depend only on the temperature. In the vapor zone, as can be seen on figure 5.6.16, isotherms (high slope) and isobars (low slope) intersect with large angles, which gives a very accurate reading.

As shown in this figure, it is very easy to identify on a exergy chart, for a given fluid temperature, the pressure leading to the maximum exergy: it is that which passes through the maximum of the corresponding isotherm.

The isothermal temperature T_0 is horizontal and tangent to the minimum of the saturation curve. Generally, it is chosen as the zero scale of ordinates.

Form of isovolumes

It is possible to show that the slope of isovolumes is slightly higher than that of isobars.

Compared to the enthalpy exergy chart (h, ex_h), the value of the exergy entropy chart (s, ex_h) is the ability to directly visualize isentropic changes. However reading the enthalpy values is less easy.

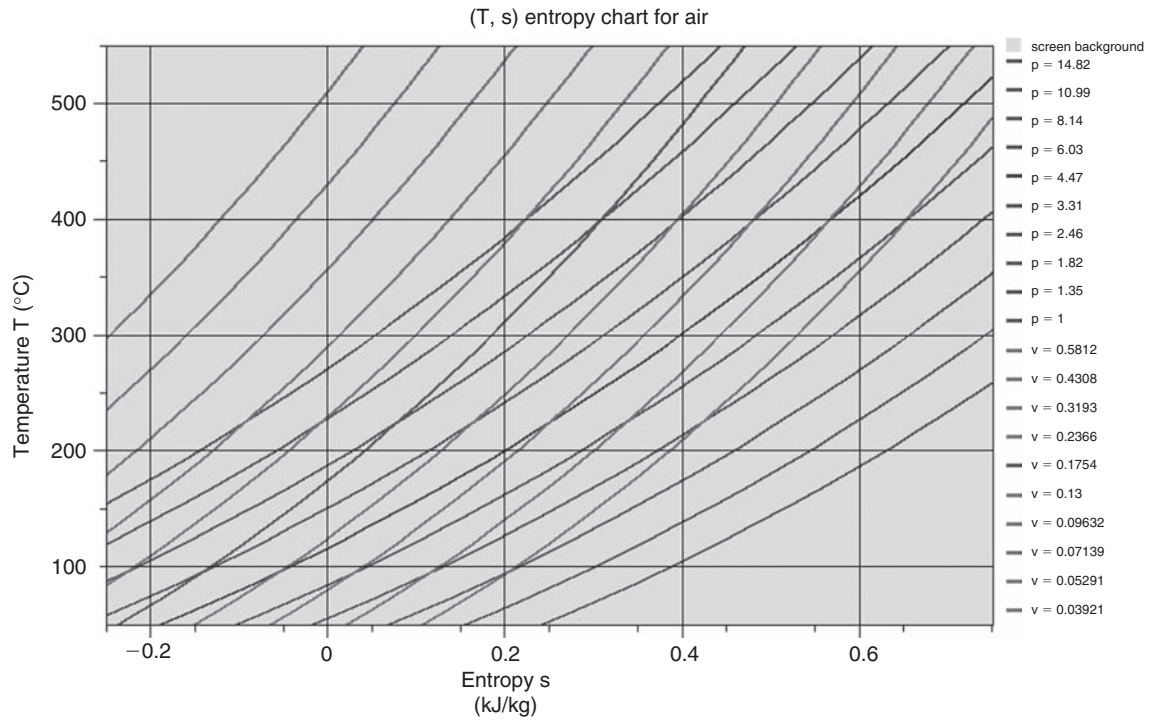
Figures 5.6.16 and 5.6.17 show two examples of entropic exergy charts, one for water, and the second for R134a, prepared for $T_0 = 15^\circ\text{C} = 288.15\text{ K}$.

Ideal gas charts

The charts above are well suited to the representation of real fluids. When the assumption of ideal gas is valid, most of them lose their interest however, as isotherms or isobars are much simpler.

In practice, the entropy chart is sufficient for most applications. Indeed, the Mollier chart is for an ideal gas, an entropy chart whose ordinate scale has undergone an affine transform, since $\Delta h = c_p \Delta T$. Exergy charts may be deduced by recombination of axes, like the ($h, \ln(P)$) chart.

Traditionally, computational difficulties were such that the charts were established for a generic ideal gas, which is no longer necessary since the availability of computers. The interactive charts

**FIGURE 5.6.18**

Air (T, s) entropy chart

that have been mentioned above allow one to build the entropy chart of a very large number of gases from pure gases available in the databases (see Figure 5.6.18).

5.6.6.2 Equations of real fluids

Law of van der Waals

General formulations of the equations of state that can account for the non-ideality of real gases have been sought for a long time. One of the oldest is the equation of van der Waals:

$$\left(P + \frac{a}{v^2}\right)(v - b) = rT \quad (5.6.18)$$

Today, its interest is primarily historical. It has the advantage of containing only two parameters a and b , which can be expressed simply in terms of the coordinates of the critical point, P_c , v_c , T_c , characterized by the existence of an inflection point on the critical isotherm:

$$\frac{\partial P}{\partial v} = 0 \quad \frac{\partial^2 P}{\partial v^2} = 0 \quad \text{for } T = T_c$$

In the case of the van der Waals equation, we obtain:

$$a = \frac{9}{8} rT_c v_c = 3P_c v_c^2 \quad b = \frac{rT_c}{8P_c} = \frac{v_c}{3}$$

We can also define the **compressibility factor Z**:

$$Z = \frac{Pv}{rT} \quad (5.6.19)$$

Obviously, $Z = 1$ for an ideal gas.

At the critical point, we have, as you may check:

$$Z_c = \frac{P_c v_c}{rT_c} = \frac{3}{8} = 0.375$$

A simple formulation, the equation of van der Waals has the disadvantage that it can sometimes deviate significantly from experimental results. It is seen that, if $v < v_c/3$, the pressures become negative, which is obviously absurd. Moreover, without even getting to such low specific volume values, we can test the accuracy of the van der Waals equation by calculating for a given substance, factor Z_c , since we know its critical coordinates.

For example, for water, we get $Z_c = 0.233$, which is very different from what gives this equation.

Other formulations have been sought and are still under study. Some examples of currently used equations of state are given below. Refer for further development to the literature, including the work of Reid, Prausnitz and Poling (1987): "Properties of gases and liquids" cited in the bibliography. Their great interest is that they can now be resolved automatically by computers, which offer an attractive alternative to thermodynamic charts.

Law of corresponding states

Most currently used equations of state can be expressed universally in terms of reduced variables:

$$P_r = \frac{P}{P_c} \quad T_r = \frac{T}{T_c} \quad v_r = \frac{v}{v_c}$$

For example, the equation of van der Waals can be written:

$$\left[P_r P_c + \frac{3P_c v_c^2}{v_r^2 v_c^2} \right] \left(v_r v_c - \frac{v_c}{3} \right) = r T_r T_c,$$

Which gives:

$$\left(P_r + \frac{3}{v_r^2} \right) \left(v_r - \frac{1}{3} \right) = \frac{8}{3} T_r$$

Note that this formulation is completely independent of fluid properties and is therefore general.

The **law of corresponding states** indicates that if there was an equation of state with two parameters reflecting the behavior of real fluids, we could, even without knowing that law, predict the properties of any fluid from those of a known fluid provided we know its critical state.

Such a universal law unfortunately does not exist. However, there are equations of state with a good approximation valid for groups of corresponding substances, such as a series of hydrocarbons, and this is where the principle of corresponding states can be useful.

The ideal gas equation of state is insufficient to represent the behavior of a vapor. However, since it constitutes the limit to which state functions must tend at high temperatures and low pressures, it is used to add simple correction terms to represent the non-ideality behavior of pure substances.

Under this law, we may assume that the compressibility factor Z can be expressed independently of the equation of state chosen:

$$Z = \frac{Pv}{rT} = Z_0(P_r, T_r) \quad (5.6.20)$$

This equation is called the simple fluid law of corresponding states. It is the basis of most currently used equations of state for real gases.

Many equations have been proposed and continue to be proposed to represent fluid properties. They differ in the number of parameters they require and their mathematical formulation. We will limit ourselves to presenting a few, then we will establish relations for calculating the thermodynamic properties of substances for that which is retained in Thermoptim (Peng-Robinson).

Equation of Beattie–Bridgeman

A rather accurate and widely used equation is the Beattie–Bridgeman equation:

$$P = \frac{rT}{v^2} (1 - e)(v + B) - \frac{A}{v^2} \quad (5.6.21)$$

or:

$$Z = \frac{Pv}{rT} = \frac{1}{v} (1 - e)(v + B) - \frac{A}{v}$$

where:

$$A = A_0 \left(1 - \frac{a}{v} \right) \quad B = B_0 \left(1 - \frac{b}{v} \right) \quad \text{and} \quad e = \frac{c}{vT^3}$$

There are five constants to be determined experimentally, which can be expressed in terms of reduced variables.

Virial equation

The virial equation is based on the fact that, at a given temperature, the Pv product tends to rT when P tends to 0, whatever the fluid. One writes:

$$Pv = rT (1 + B P + C P^2 + D P^3 + \dots) \quad (5.6.22)$$

or:

$$Z = \frac{Pv}{rT} = 1 + B P + C P^2 + D P^3 + \dots$$

The virial coefficients B , C , D , are functions of T only. Depending on the number of coefficients taken into account, the representation is valid for a more or less extensive range. The difficulty is to determine these coefficients. The only one for which empirical formulas exist today is B .

Another form of the virial equation is given as a Taylor expansion in $1/v$:

$$P = \frac{rT}{v} \left(1 + \frac{B'}{v} + \frac{C'}{v^2} + \dots \right) \quad (5.6.23)$$

or:

$$Z = \frac{Pv}{rT} = 1 + \frac{B'}{v} + \frac{C'}{v^2} + \dots$$

Cubic equations

Another family of equations commonly used is that of cubics. We saw an example with that of van der Waals. The interest of cubics is that they can be solved analytically, which is an undeniable asset for their calculation.

One of them, well known, is the Redlich Kwong equation which is written:

$$P = rT \left(\frac{1}{v-b} - \frac{a}{v(v+b)} \right) \quad (5.6.24)$$

or:

$$Z = \frac{Pv}{rT} = \frac{v}{v-b} - \frac{a}{(v+b)}$$

with

$$b = 0.08664 \frac{rT_c}{P_c}$$

$$a = 0.42748 \frac{rT_c^{2.5}}{P_c} T^{-1.5}$$

Much more accurate than the van der Waals equation, it likewise requires knowledge of the fluid critical coordinates. It is therefore very general, but does not apply to all fluids with the same precision. Various variants using an additional fluid parameter, the acentric factor ω , have been proposed in the literature (Wilson, Soave, Peng-Robinson, etc.)

We give in section 5.6.6.4 an example of the Peng-Robinson equation used in ThermoOptim to analytically determine the state of a real fluid.

5.6.6.3 Thermodynamic tables

It is also possible to represent the state of a real fluid by building tables giving, for various pressures and temperatures, the values of other state functions: enthalpy, entropy and specific volume.

These tables are generally composed of two parts:

- First, the table of the saturated vapor properties, which allows us to know with great accuracy the state of the fluid on both sides of the saturation curve;
- Secondly, the vapor table for the gas and vapor zone.

Given the existence of ThermoOptim, these tables are of no particular relevance in this book.

5.6.6.4 Equations of state retained in ThermoOptim

In ThermoOptim, we made the following choices.

The equation of state used for all condensable vapors except water is that of Peng-Robinson:

$$P = \frac{RT}{V-b} - \frac{a}{V^2 - 2bV - b^2} \quad (5.6.25)$$

with

$$b = 0.0778 \frac{RT_c}{P_c}$$

$$a = 0.45724 \frac{R^2 T_c^2}{P_c} [1 + (0.37464 + 1.54226\omega - 0.26992\omega^2) (1 - T_r^{0.5})]^2$$

Posing

$$f\omega = 0.37464 + 1.54226\omega - 0.26992\omega^2 \quad (5.6.26)$$

we get

$$a = \Omega_a \frac{R^2 T_c^2}{P_c} [1 + f\omega(1 - T_r^{0.5})]^2 = \Omega_a \frac{R^2 T_c^2}{P_c} \lambda(\omega, T_r)$$

This equation represents a good compromise between accuracy, number of parameters and resolution complexity. Expressed in terms of the compressibility factor Z , it leads to a cubic which can be solved analytically. However, a problem may arise for low values of Z_c , since this equation does not allow values of Z below 0.3214 in the vicinity of the critical point. We therefore slightly amended it to correct this limitation.

With this equation, the data required to characterize a fluid are its critical values T_c , P_c , the acentric factor ω and its molar mass M . The corrections that we introduced have led us to take into account two additional parameters numerically adjusted by comparison with more accurate equations of state.

To represent very accurately the liquid-vapor equilibrium zone, specific treatment is dedicated to it from regressions with many parameters. The liquid zone is treated in turn with other sets of equations.

For water, we chose the equations proposed by the International Committee for Formulation of the Sixth Conference on Properties of Steam in 1967, which involve many parameters, but are extremely accurate. It is therefore subject to special treatment (Grigull & Schmidt, 1982). The reason for this choice is to accurately study complex electricity generation cycles.

The precision is paid for by a very much greater complexity in solving the equations, which comes mainly from the fact that for part of the supercritical and circumcritical zone, they are given as a function of temperature and volume instead of temperature and pressure.

Calculation of energy state functions (enthalpy and entropy) for the equation of Peng-Robinson

The calculation of state functions is based on estimating the departure functions of the real gas relative to the ideal gas. In this section, we will examine the molar quantities.

The ideal gas is represented by a constant pressure molar heat capacity C_p given by a polynomial equation with integer or non-integer coefficients (see 5.6.2.3):

$$C_p = \sum_{i=1}^n C_{pi} T^i$$

The departure functions correspond to the differences ($S^* - S$) and ($H^* - H$) compared to ideal gas S and H given by (5.6.6) and (5.6.7) expressed in molar variables. They can take into account the variation of the molar heat capacity C_p with pressure, not considered in the ideal gas.

The estimation of these departure functions is done thanks to the free energy $F = U - TS$, one of the two thermodynamic potentials (Section 5.4.5).

These are calculated at constant temperature, relative to a reference pressure P_0 , usually taken as the pressure P of the system, or, equivalently, a reference molar volume V_0 ($V_0 = RT/P$ for an ideal gas).

At constant temperature and without heat exchange with the outside, the change of free energy is given by:

$$\begin{aligned} dF &= dU - TdS - SdT = -PdV + TdS - TdS - SdT \\ dT &= 0 \quad dF = -PdV \end{aligned}$$

Let us call F^* the free energy of the real gas, and F that of the considered ideal gas. Let us integrate this differential, at constant temperature, between an initial volume V_{in} and the final volume (V for the real gas, and V_0 for the ideal gas).

For the real gas:

$$F^* - F_{in}^* = - \int_{V_{in}}^V P dV$$

For the ideal gas:

$$F - F_{in} = - \int_{V_{in}}^{V_0} \frac{RT}{V} dV$$

At very low pressures, we know that a real fluid behaves like an ideal gas
We have then:

$$\lim_{V_{in} \rightarrow \infty} (F_{in}^* - F_{in}) = 0$$

Or, subtracting the two previous equations:

$$F^* - F = - \int_{\infty}^V P dV - \int_{V_0}^{\infty} \frac{RT}{V} dV = - \int_{\infty}^V P dV - \int_{V_0}^V \frac{RT}{V} dV - \int_{V_0}^{\infty} \frac{RT}{V} dV$$

We eliminate the infinite terminal of the last integral by grouping the first and last summations, RT/V being P for the ideal gas:

$$F^* - F = - \int_{\infty}^V \left(P - \frac{RT}{V} \right) dV - \int_{V_0}^V \frac{RT}{V} dV$$

$$F^* - F = - \int_{\infty}^V \left(P - \frac{RT}{V} \right) dV - RT \ln \frac{V}{V_0} \quad (5.6.27)$$

From this relation, we deduce the other departure functions:

$$S^* - S = - \frac{\partial}{\partial T} (F^* - F) \quad (5.6.28)$$

$$H = U + PV = F + TS + PV$$

$$H^* - H = F^* - F + T(S^* - S) + PV - RT \quad \text{with } Z = \frac{PV}{RT}, \text{ we get:}$$

$$H^* - H = F^* - F - T \frac{\partial}{\partial T} (F^* - F) + RT(Z - 1) \quad (5.6.29)$$

For the Peng-Robinson equation, we obtain the following results:
with

$$b = \Omega_b \frac{RT_c}{P_c}$$

$$a = \Omega_a \frac{R^2 T_c^2}{P_c} [1 + f\omega(1 - T_r^{0.5})]^2 = \Omega_a \frac{R^2 T_c^2}{P_c} \lambda(\omega, T_r)$$

and

$$\Omega_a = 0.45724 \quad \Omega_b = 0.0778$$

The calculation of the departure functions gives for the free energy, with $V_0 = RT/P$:

$$F^* - F = - \int_{\infty}^V \left[RT \left(\frac{1}{V-b} - \frac{1}{V} \right) - \frac{a}{(V+b(1+\sqrt{2}))(V+b(1-\sqrt{2}))} \right] dV - RT \ln \frac{V}{V_0}$$

At constant temperature, a is constant and we obtain $(F^* - F)$ in analytical form:

$$\begin{aligned} F^* - F &= RT \ln \frac{V_0}{V-b} - \frac{a}{2b\sqrt{2}} \ln \frac{V+b(1-\sqrt{2})}{V+b(1+\sqrt{2})} \\ F^* - F &= RT \ln \frac{V_0}{V-b} + \frac{RT_c \Omega_a}{2\sqrt{2}\Omega_b} [1 + f\omega(1 - T_r^{0.5})]^2 \ln \frac{V+b(1-\sqrt{2})}{V+b(1+\sqrt{2})} \\ F^* - F &= RT \ln \frac{V_0}{V-b} + \frac{RT_c \Omega_a}{2\sqrt{2}\Omega_b} \ln \frac{V+b(1-\sqrt{2})}{V+b(1+\sqrt{2})} \lambda(\omega, T_r) \end{aligned} \quad (5.6.30)$$

For entropy, the derivation of this expression with respect to T leads to:

$$S^* - S = - \frac{\partial}{\partial T} (F^* - F) \Rightarrow S^* - S = R \ln \frac{V-b}{V_0} - \frac{1}{2b\sqrt{2}} \ln \frac{V+b(1-\sqrt{2})}{V+b(1+\sqrt{2})} \frac{d(a)}{dT}$$

Let

$$\mu(\omega, T_r) = \frac{d(\lambda)}{dT} = \left[\frac{(f\omega)^2}{T_c} - \frac{f\omega}{\sqrt{T_c}} \frac{(1+f\omega)}{\sqrt{T}} \right] = \frac{(f\omega)}{T_c} [f\omega - (1+f\omega)T_r^{0.5}]$$

It comes:

$$\begin{aligned} \frac{1}{2b\sqrt{2}} \frac{d(a)}{dT} &= \frac{RT_c \Omega_a}{2\sqrt{2}\Omega_b} \mu(\omega, T_r) \\ S^* - S &= R \ln \frac{V-b}{V_0} - \frac{RT_c \Omega_a}{2\sqrt{2}\Omega_b} \ln \frac{V+b(1-\sqrt{2})}{V+b(1+\sqrt{2})} \mu(\omega, T_r) \end{aligned} \quad (5.6.31)$$

Finally, the relative departure in the enthalpy is obtained easily:

$$\begin{aligned} H^* - H &= F^* - F + T(S^* - S) + PV - RT \\ H^* - H &= \left[\frac{bRT}{V-b} - \frac{aV}{V^2 + 2bV - b^2} \right] \\ &\quad + \frac{RT_c \Omega_a}{2\sqrt{2}\Omega_b} \ln \frac{V+b(1-\sqrt{2})}{V+b(1+\sqrt{2})} [\lambda(\omega, T_r) - T\mu(\omega, T_r)] \end{aligned} \quad (5.6.32)$$

5.6.7 Moist mixtures

A number of commonly used gases are mixtures whose composition may vary due to condensation or vaporization of one of their components. In practice, the component that changes state is mostly water, which justifies that a special section in this book is dedicated to mixtures of gases and water vapor, hereinafter referred to as moist mixtures.

Dry air in particular is hardly ever found: it almost always includes water, in the form of gas, liquid or ice crystals. Controlling the air humidity determines the comfort conditions and the preservation of food and many products. It is obtained by air conditioning techniques that will be presented in Chapter 21 of Part 3.

In this section we limit ourselves to the calculation principles of thermodynamic properties of moist mixtures. While it is certain that the most numerous practical applications regard air, our presentation will cover all gases for which our assumptions are valid, that is to say the vast majority of cases. For example, the humidity properties of combustion products, which almost always contain water, may be determined by the methods presented here.

5.6.7.1 Definitions and conventions

When looking at a moist mix, we are dealing with a mixture of a gas that does not condense, which we call the dry gas, and water that could condense. Note that we will not discuss mist here; we can assume that the volume occupied by any condensed water is still very small compared to that occupied by the gas phase. We will therefore neglect mist. Under these conditions, for a given volume, the total mass of the gas phase can vary, while the mass of non-condensable constituents remains constant. Therefore it is customary to refer to the invariant mass which is the dry gas, all the thermodynamic properties of the mixture comprising the gas phase.

Everything happens as if somehow the moist mix was a mixture of two substances: the dry gas, whose composition is fixed, and water that may be present in one or more phases. As discussed later, it is essential, in order to carry out calculations, to clearly specify which substance the thermodynamic quantities used relate to, and what are the reference units and origin. The notations will be chosen accordingly.

We call **specific humidity** w the ratio of the mass of water contained in a given volume of moist mixture to the mass of dry gas contained in this volume.

The water in a moist mixture can be characterized in various ways: through its specific humidity, which we just introduced, but more typically by its mole or mass fraction, or by its partial pressure which is of particular interest here. As long as the partial pressure of water remains below its saturation pressure at the gas temperature, the water is in the form of vapor. Otherwise it exists at least partly in the condensed liquid or solid state. There is therefore an upper limit to the amount of water vapor that may be contained in a moist mixture. It depends on the temperature and pressure. When, at a given pressure, the temperature drops below the saturated vapor temperature of water, water vapor begins to condense as a mist or on cold walls that define the system if they exist.

Given its practical importance, the saturated state is the reference, and we call **relative humidity** ϵ the ratio of the partial pressure of water vapor divided by its saturation vapor pressure at the temperature of the mixture. This ratio is equal to 1 (or 100%) when the vapor begins to condense. Otherwise, it is less than 1.

We call respectively **specific enthalpy** q' and **specific volume** v_{spec} the enthalpy and the volume of moist mixture referred to 1 kg of dry gas.

5.6.7.2 Principles of calculation

We have seen that a condensable fluid remains comparable to an ideal gas at the immediate vicinity of the liquid state when its pressure is lower than its critical pressure. When this fluid is a mixture component, this rule applies taking into account the partial pressure.

As long as the liquid state does not appear, the mixture behaves like an ideal gas. When the mixture temperature drops below the condensation temperature corresponding to the partial pressure of the condensable component in the dry gas, liquid begins to appear. In most cases, although this is not strictly true, it is reasonable to consider that this liquid phase is pure, made up exclusively of the condensable component.

At that time, provided that equilibrium is established, experience shows that the situation is as follows:

- the vapor-liquid equilibrium relationship is met by the condensable component, as if the other constituents did not exist. Its saturated vapor (index sv) partial pressure, given by the law of saturation pressure, is therefore $P_{sv} = P_s(T)$;
- Dalton's law applies to the calculation of thermodynamic functions of the gas phase;
- the law of phase mixture applies to the calculation of thermodynamic functions of the liquid and gas phases (assuming that the interfacial tensions are negligible).

To calculate the thermodynamic properties of the mixture in the presence of a liquid phase, the procedure is thus as follows:

- knowing the temperature of the medium, one can determine the partial pressure of the condensable component. We deduce the sum of partial pressures ($P - P_{sv}$) of the other constituents. As we know their relative molar fractions, we can completely determine the composition of the gas phase, and the number of moles of the condensable component in the gaseous state. By difference, we know the number of moles liquefied;
- The Dalton and phase mixture laws are then used to calculate all the properties of the mixture. It is obvious that in this case the composition of the mixture changes as a function of the quality of the condensable component, and this must be taken into account in the calculation of thermodynamic properties.

In Thermoptim the calculation of moist mixtures is performed using this method. It is thus possible to study the behavior of a vapor and gas mixture of any composition.

5.6.7.3 Key Relationships

We will use indices dg to describe the dry gas, and mm for the moist mixture.

Case where the moist mixture composition is known

By definition of the partial pressure of water:

$$P_{\text{vap}} = x_{\text{H}_2\text{O}} \cdot P \quad (5.6.33)$$

The molar mass of the dry gas is:

$$M_{\text{dg}} = \frac{1}{1 - x_{\text{H}_2\text{O}}} \sum M_{\text{nc}} x_{\text{nc}} \quad (5.6.34)$$

nc representing the various noncondensable constituents.

The specific humidity is then by definition:

$$w = \frac{y_{\text{H}_2\text{O}}}{y_{\text{dg}}} = \frac{M_{\text{H}_2\text{O}} x_{\text{H}_2\text{O}}}{M_{\text{dg}} x_{\text{dg}}} \quad (5.6.35)$$

If P_{sv} is the saturation vapor pressure of water:

If $P_{\text{vap}} \leq P_{sv}$ $\varepsilon = P_{\text{vap}}/P_{sv}$

$$w = \frac{M_{\text{H}_2\text{O}}}{M_{\text{dg}}} \frac{P_{\text{vap}}}{P - P_{\text{vap}}} \quad (5.6.36)$$

If $P_{\text{vap}} > P_{sv}$ $\varepsilon = 1$

$$w = w_{\text{sat}} = \frac{M_{\text{H}_2\text{O}}}{M_{\text{dg}}} \frac{P_{sv}}{P - P_{sv}} \quad (5.6.37)$$

$$w - w_{\text{sat}} = \text{condensate} = \frac{M_{\text{H}_2\text{O}}}{M_{\text{dg}}} \left[\frac{P_{\text{vap}}}{P - P_{\text{vap}}} - \frac{P_{\text{sv}}}{P - P_{\text{sv}}} \right] \quad (5.6.38)$$

The values of specific volume v_{spec} and specific enthalpy q' can then be determined, the latter being calculated with an enthalpy zero at 0°C .

Generally (and this is the case in Thermooption) the reference state for calculating the gas enthalpies is taken at the standard value of 298 K. Now, HVAC engineers by custom choose 0°C as the reference state for dry air, and 0°C for saturated liquid water. The result is a mismatch between the enthalpies of moist gas as they are **usually calculated and those represented on the usual psychrometric charts**. This difference varies depending on the specific humidity.

In practice, as the enthalpies can be referred to three different references, you need to know how to distinguish them in order to avoid making mistakes. In what follows, we will use as appropriate:

- the moist mixture enthalpy h_{mm} ($h_{\text{mm}} = 0$ at $T = 298$ K)
- the dry gas enthalpy h_{dg} ($h_{\text{dg}} = 0$ at $T = 298$ K)
- the moist mixture specific enthalpy q' ($q' = 0$ at $T = 0^\circ\text{C}$, liquid water).

In general, unless otherwise indicated, the first is used by default, whereas in the calculations specific to moist mixtures, it is usually the third form that is used.

In what follows, the index water indicates that the calculation is performed with the equations of water as a real fluid, and the index H_2O that it is conducted with the equations of water treated as an ideal gas. h_{vwater} is the enthalpy of water in the vapor state, and $L_{0\text{water}}$ represents the enthalpy of vaporization of water at 0°C .

$$q'(t, w) = h_{\text{dg}}(t) - h_{\text{dg}}(0^\circ\text{C}) + w h_{\text{vwater}}(t, P_{\text{vap}}) \quad (5.6.39)$$

or by making the approximation that water vapor behaves like an ideal gas:

$$q'(t, w) = h_{\text{dg}}(t) - h_{\text{dg}}(0^\circ\text{C}) + w [h_{\text{H}_2\text{O}}(t) - h_{\text{H}_2\text{O}}(0^\circ\text{C})] + w L_{0\text{water}} \quad (5.6.40)$$

By introducing h_{mm} , enthalpy of the (ideal) moist mixture:

$$h_{\text{mm}}(t) = \frac{h_{\text{dg}}(t) + w h_{\text{H}_2\text{O}}(t)}{1 + w}$$

we get:

$$q'(t, w) = (h_{\text{mm}}(t) - h_{\text{mm}}(0^\circ\text{C})) (1 + w) + w L_{0\text{water}} \quad (5.6.41)$$

Similarly, $v_{\text{spec}} = v_{\text{mm}} (1 + w)$

In the supersaturated zone, the gas is saturated with water in the vapor state, the rest being water in the liquid state. The specific enthalpy is then given by:

$$q'(t, w) = h_{\text{dg}}(t) - h_{\text{dg}}(0^\circ\text{C}) + w h_{\text{vwater}}(t, P_{\text{sv}})$$

Case where the dry gas composition is known

When we know the dry gas composition, the calculations are done slightly differently, because w is then given.

We deduce, M_{dg} being the dry gas molar mass:

$$P_{vap} = P \frac{w \frac{M_{dg}}{M_{H_2O}}}{1 + w \frac{M_{dg}}{M_{H_2O}}} \quad (5.6.42)$$

$$\varepsilon = \frac{P_{vap}}{P_{vs}} \quad (5.6.43)$$

Other calculations are carried out as before.

5.6.7.4 Temperatures used for moist mixtures

The study of moist mixtures leads us to introduce several temperatures, whose definition it is important to know, because for a given state of the gas, their values may be substantially different.

We call **dry-bulb temperature** t ($^{\circ}\text{C}$) or T (K), the temperature indicated by a thermometer whose sensing portion is completely dry, and is placed into the moist mixture. This is the temperature in the usual sense.

We call **dew point** tr ($^{\circ}\text{C}$) or Tr (K) the temperature at which the first drops begin to appear when the moist mixture is cooled at constant humidity and pressure. If water condenses as ice, it is also known as ice temperature. This is the saturation temperature of the water at partial pressure P_{vap} .

With the previous notations, $T_r = T_{sat}(P_{vap})$ if $P_{vap} \leq P_{sv}$, and $T_r = T_{sat}(P_{sv}) = T$, otherwise.

We call **wet-bulb temperature** t' ($^{\circ}\text{C}$) or T' (K), the temperature indicated by a thermometer whose sensing element is covered with a thin film of water being evaporated due to strong mixing of the gas. In practice, the bulb of the thermometer is covered with a wick soaked with water. If measured in good conditions, this temperature is substantially equal to the adiabatic saturation temperature that would be obtained by moistening the gas to saturation in an adiabatic device, by spraying water at the temperature equilibrium.

One can show that its value is given by the following equation:

$$\begin{aligned} & \text{enthalpy of liquid water at } t' \text{ (saturated moisture at } t' \text{ - initial moisture)} \\ & = \text{enthalpy of saturated mixture at } t' \text{ - enthalpy of the initial mixture at } t. \end{aligned}$$

Relative to the dry gas, the equation is:

$$h_{lwater}(t')(w_{sat} - w) = h_{dg}(t') - h_{dg}(t) + w_{sat} h_{vwater}(t') - w h_{vwater}(t) \quad (5.6.44)$$

Relative to the specific units, it becomes:

$$q'(t', w_{sat}) - q'(t, w) = (w_{sat} - w) h_{lwater}(t') \quad (5.6.45)$$

This is an implicit equation in t' , involving the mixture formed in part by the dry gas, and secondly by water. It can be reversed in a temperature range between a value close to the dew point as a minimum, and the dry bulb temperature as the maximum.

As stated above, we must take care that the reference values of enthalpies are consistent. Moreover, when t or t' falls below 0°C , the equations of liquid water must be replaced by those of solid water (ice).

5.6.7.5 Moist mixture charts (Psychrometric charts)

The main thermodynamic relations that we have given show that moist mixture variables and state functions are connected by relatively complex equations, which justify seeking an easy to use graphical presentation.

Two broad families of charts exist: the charts derived from that proposed by Carrier, with the dry-bulb temperature as the abscissa and the specific humidity as the ordinate (Figures 5.6.19 and 5.6.21), and Mollier charts (Figures 5.6.20 and 5.6.22), with specific humidity as abscissa and the specific enthalpy as ordinate.

The gas water saturation curve is the smooth concave curve upwards in the Carrier chart (Figure 5.6.19) and downwards in the Mollier chart (Figure 5.6.20).

In the Carrier chart, the area above the saturation curve corresponds to cases where water is in excess and exists as a condensed liquid or solid: the gas is supersaturated. In the Mollier chart, the reverse is true: this zone is located below the saturation curve.

Charts in Figures 5.6.19 and 5.6.21 relate to air at atmospheric pressure. They are equipped with different iso-value curves:

- curves of equal relative humidity ϵ concave upward;
- isenthalpic curves are very close to straight lines and moist isotherm* curves are almost parallel to them* (usually not shown);
- isovolume curves are very close to straight negative lines of slope* stronger than the previous.

The Mollier chart in Figures 5.6.20 and 5.6.22 also relates to air at atmospheric pressure. It is equipped with different isovalues:

- curves of equal relative humidity ϵ are curves with concavity facing downwards;
- dry bulb temperature curves are very close to straight lines* and wet bulb temperature* curves are almost parallel to the x-axis;
- isovolume curves are very close to straight lines* of positive slope.

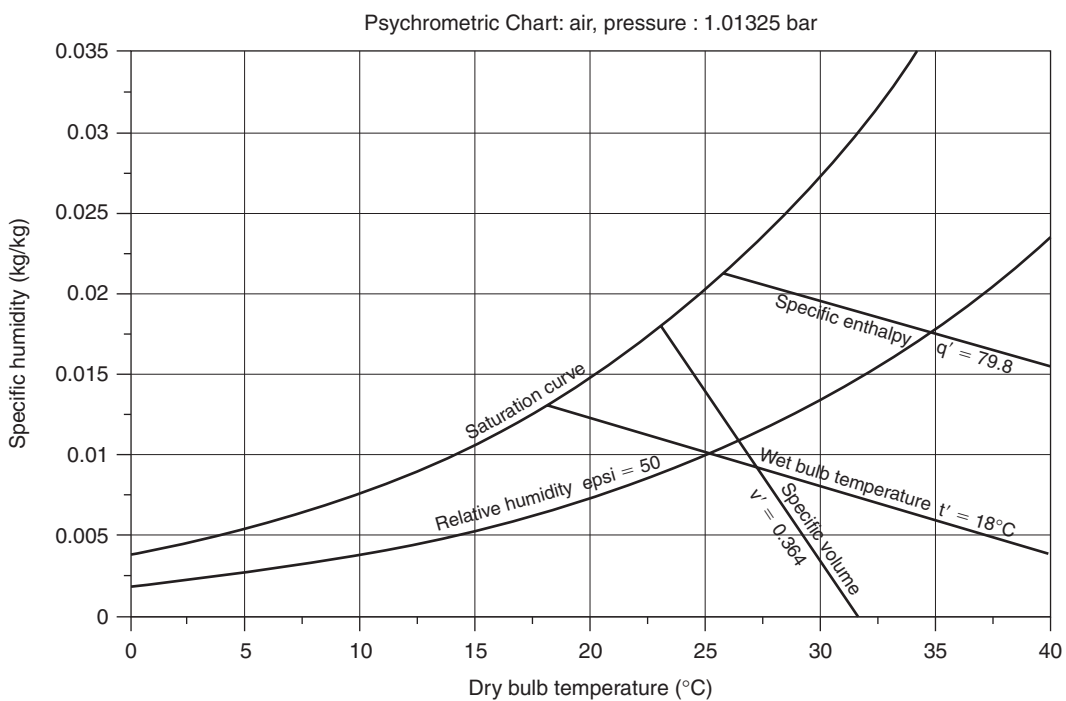


FIGURE 5.6.19

Carrier chart

*By equating the dry gas to an ideal gas and neglecting in some cases the contribution of water vapor, these expressions are simplified and correspond to those of straight lines.

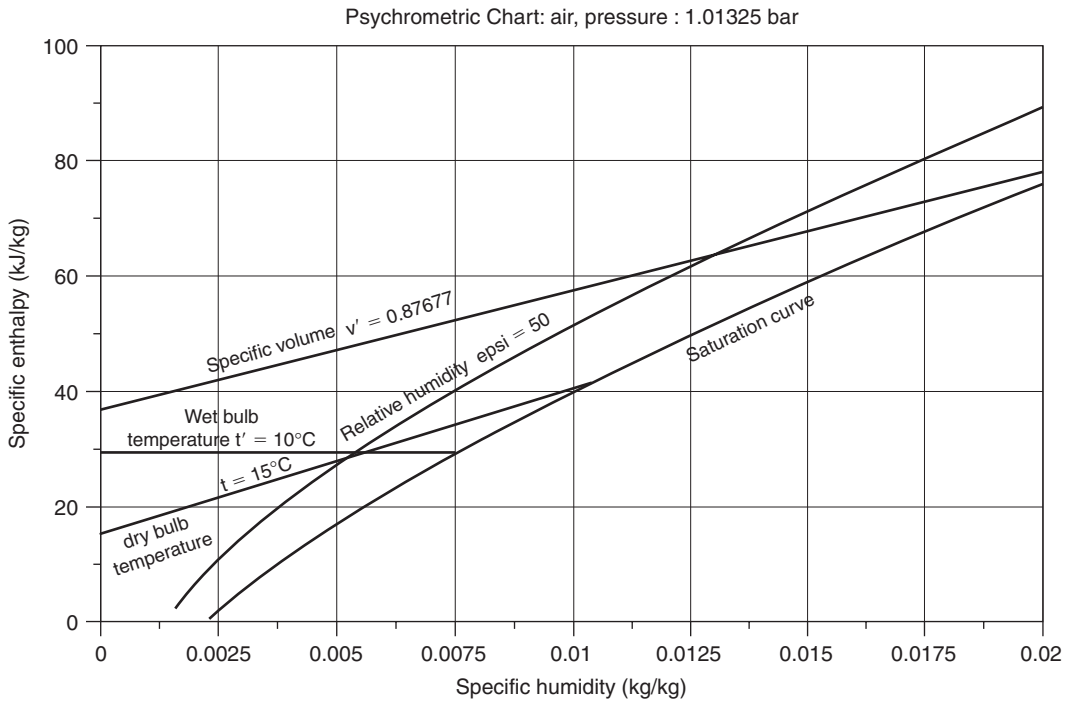


FIGURE 5.6.20
Mollier chart

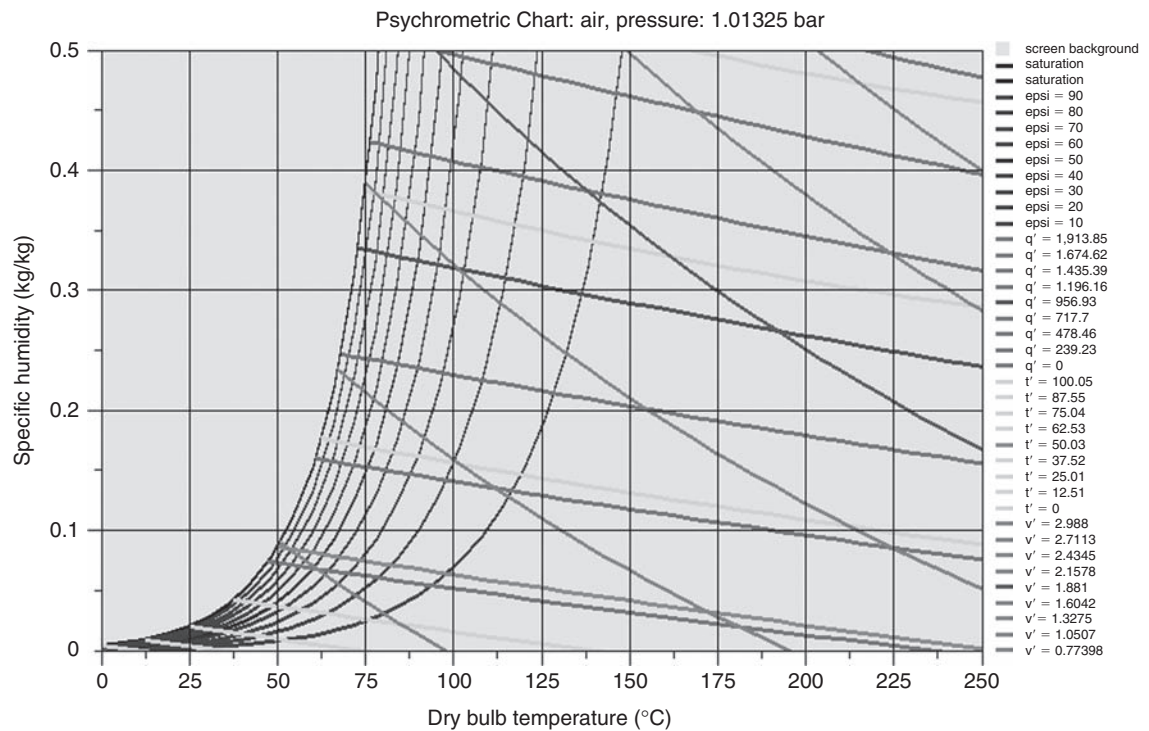
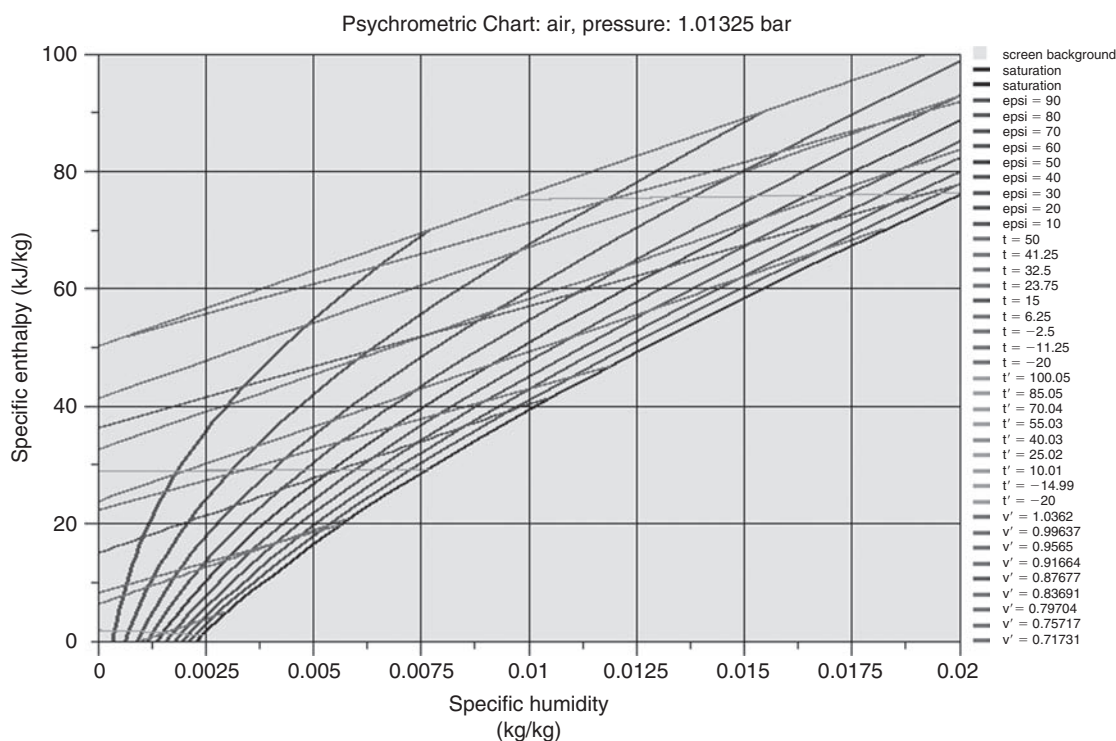


FIGURE 5.6.21
Moist air psychrometric chart

**FIGURE 5.6.22**

Moist air Mollier chart

At atmospheric pressure and above 100°C, it is impossible to condense water. On the Carrier chart, this translates into an almost vertical tangent on the saturation curve for 100°C, and on the Mollier chart by an asymptote to the saturation curve, corresponding to dry isotherm 100°C.

5.6.8 Real fluid mixtures

In the previous section, we considered moist mixtures for which the dry gas could be assumed to behave as an ideal gas, which allowed us to simplify the modeling. This section deals with real fluid mixtures which cannot be modeled as ideal gases.

Because of interactions between the molecules of the various constituents, the estimation of thermodynamic properties of real fluid mixtures is much more difficult than that of pure ones, whose principles were given Section 5.6.6. In the general case, it relates to chemical engineering and is outside the scope of this book. However we give below some guidance on how to proceed, so that the reader can get an idea of the problems posed.

5.6.8.1 Physical phenomena brought into play

The behavior of mixtures in liquid-vapor equilibrium is generally different from that of pure substances, the molar or mass fraction of each component moving between limits that depend on pressure and temperature, due to the distillation that takes place. In the presence of several components, the phase change is more complex than for a pure substance. Its graphical representation in a chart is simple if the mixture is binary, the case to which we will restrict ourselves in this introduction.

To understand the phenomena that occur, consider the behavior of a binary mixture of propane and butane. Some properties of pure components (critical pressure and temperature, boiling

TABLE 5.6.3
PURE COMPONENT PROPERTIES

	P_c (bar)	T_c (°C)	T_s (1 bar) (°C)	T_s (2 bar) (°C)
propane	42.48	96.7	-42.4	-25.4
butane	37.98	152.01	-0.7	18.8

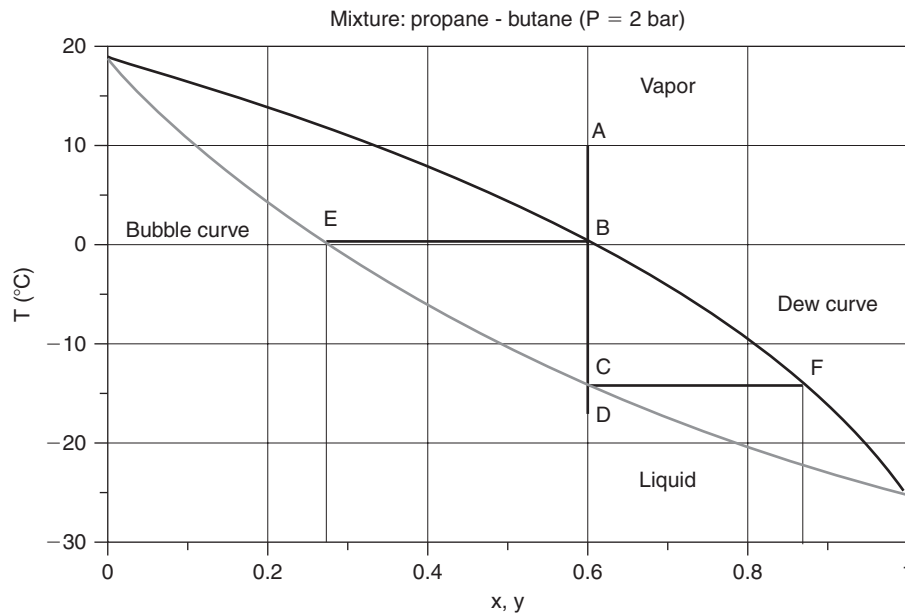


FIGURE 5.6.23
Isobaric equilibrium lens

temperature at 1 bar and 2 bar) are shown in Table 5.6.3. They show that propane is much more volatile than butane, as at 1 bar, respectively, they evaporate at -42.4°C and -0.7°C .

Consider a mixture of these two substances, and examine how it behaves at constant pressure when its temperature changes. Figure 5.6.23, called “equilibrium isobaric lens”, shows the phase chart of this mixture at a pressure of 2 bar.

The vapor zone is at the upper right of the chart, the liquid zone at the bottom left, and the liquid-vapor equilibrium in the lens delimited by the dew and bubble curves. The horizontal axis represents the mole fraction of propane, which means that the value 0 corresponds to pure butane ($T_s = 18.8^{\circ}\text{C}$), and the value 1 pure propane ($T_s = -25.4^{\circ}\text{C}$). As is usual when studying vapor mixtures, x represents the mole fractions in liquid phase, y the mole fractions in vapor phase, and z , the overall mole fractions. The vertical axis is temperature, in $^{\circ}\text{C}$.

Consider a mixture of given composition (here $z_1 = 0.6$ for propane, $z_2 = 1 - z_1 = 0.4$ for butane) in the vapor state, corresponding to point A at temperature 10°C . If the mixture is cooled at constant pressure (e.g. in a heat exchanger), the characteristic point moves along the vertical segment AB as it remains in the vapor state.

In B, at around 0°C , distillation begins on the dew curve (or drop curve), so named because the first drop of liquid appears. The two components are liquefied together, but since butane is less volatile than propane, it condenses more, so that the first drop composition differs from average z . The mole fraction x in the liquid state of component 1 (here propane) is given by the abscissa of point E on the bubble curve, so called because in a reverse process of temperature change it is on

this curve that the first bubbles appear (here $x_1 = 0.28$), and the mole fraction of liquid butane is $x_2 = 1 - x_1 = 0.72$.

Gradually, as the cooling continues, the composition of the liquid phase evolves, the mole fraction of propane being given by the abscissa of the intersection of the bubble curve and the corresponding isotherm, the figurative point moving from E to C, while that of the gas phase moves from B to F. At point C, there is only liquid, except for one last bubble of gas, whose composition is $y_1 = 0.85$ in propane and $y_2 = 1 - y_1 = 0.15$ in butane. Beyond, the mixture remains in liquid state, with its original composition.

In other words, at a given pressure, the state change of the mixture is not at constant temperature, but with a temperature “glide” (distillation range) that can be more or less important depending on the mixture. For example, for the above mixture, and the pressure of 2 bar, the temperature glide is 14 K.

Now consider an evolution of the mixture at constant temperature and variable pressure. On the chart of Figure 5.6.24, called equilibrium isotherm lens, the abscissa represents the propane quality and the ordinate the pressure in bar. Let us still assume that the mixture has as overall composition ($z_1 = 0.6$ and $z_2 = 0.4$). If the pressure is lower than 2.78 bar, the mixture is entirely in the vapor state, and if it exceeds 4.3 bar, it is entirely liquid. Between these two pressures, it is in liquid-vapor equilibrium, and the mixture composition changes continuously in the liquid and vapor phases. For $P = 2.78$ bar, the liquid phase has a composition ($x_1 = 0.28, x_2 = 0.72$). For $P = 3.7$ bar, it is ($x_1 = 0.48, x_2 = 0.52$), and for $P = 4.3$ bar it corresponds to the overall composition. Vapor phase compositions are as follows: ($y_1 = 0.6, y_2 = 0.4$) for $P = 2.78$ bar, ($y_1 = 0.77, y_2 = 0.33$) for $P = 3.7$ bar, and ($y_1 = 0.85, y_2 = 0.15$) for $P = 4.3$ bar.

A special case is the so-called azeotropic mixtures where the bubble and dew curves meet for a given overall composition. One can show that an azeotropic mixture is a pressure extremum at constant temperature, or temperature extremum at constant pressure. Such a mixture behaves in practice as a pure substance. Finally, when the temperature glide is small (< 1 K), the error being

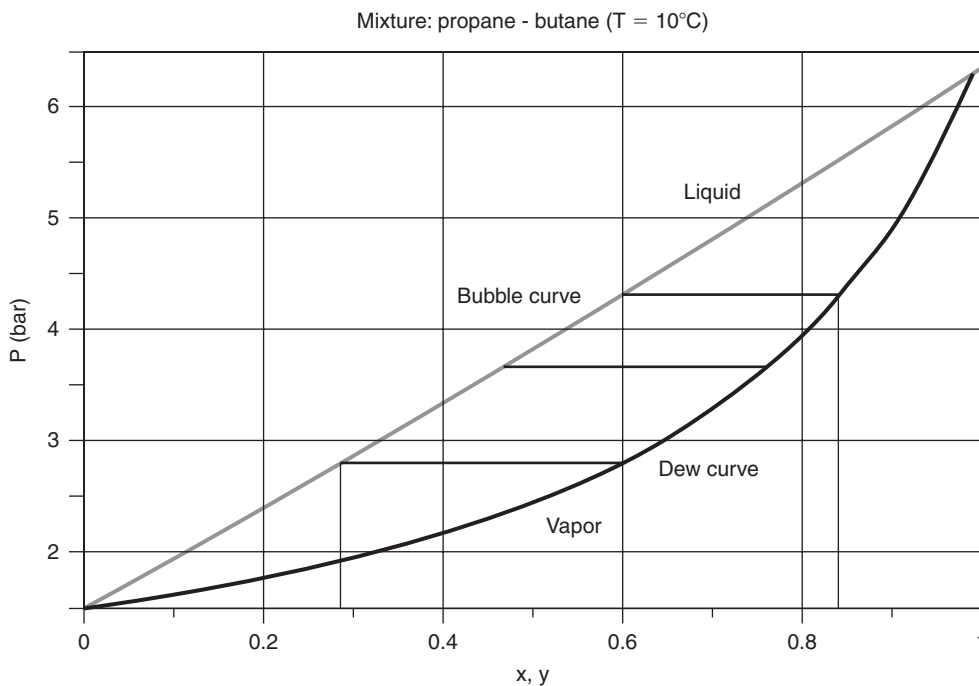


FIGURE 5.6.24
Isotherm equilibrium lens

committed by neglecting the distillation is very low. This is called quasi-azeotropic mixture. We chose here the propane/butane system because the glide is important and helps to demonstrate the phenomena peculiar to mixtures.

We introduced above two charts, binary mixture equilibrium isothermal and isobaric lenses, very useful for qualitatively understanding the phenomena involved. However, quantitatively, they are only valid for a single pressure or temperature, and above all they contain no information on the enthalpies put in. They are not of much interest for applications in power engineering.

5.6.8.2 Principles of calculation of vapor mixtures

The calculation of vapor mixtures is made using, for each of the pure components, a well-chosen representation, such as an equation of state, and appropriately modeling interactions between molecules of different components, often through empirical correlations. The equation of the mixture is thus distinct from that of pure substances by the existence of “mixing rules” allowing one to calculate the coefficients.

To illustrate, recall that we introduced in Section 5.6.6.2 the Peng-Robinson equation for a pure substance, which in molar units writes:

$$P = \frac{RT}{V-b} - \frac{a}{V^2 + 2bV - b^2} \quad (5.6.25)$$

with

$$b = 0.0778 \frac{RT_c}{P_c}$$

$$a(T) = 0.45724 \frac{R^2 T_c^2}{P_c} [1 + (0.37464 + 1.54226 \omega - 0.26992 \omega^2)(1 - T_r^{0.5})]^2$$

With this equation, four data are sufficient to characterize a pure substance: the critical coordinates T_c , P_c , the acentric factor ω , and the molar mass M to move to mass quantities.

For the equation (5.6.25) to be representative of a mixture, it is necessary to estimate the values of the mixture coefficients $a_m(T)$ and b_m , which is possible by using the following type of relations, indices i and j corresponding the various constituents:

$$a_m(T) = \sum_{i=1}^n \sum_{j=1}^n (x_i x_j a_{ij}(T)) \quad (5.6.46)$$

with

$$a_{ij} = (1 - k_{ij}) \sqrt{a_i(T) a_j(T)} \quad \text{if } i \neq j \quad (5.6.47)$$

$$b_m = \sum_{i=1}^n (x_i b_i) \quad (5.6.48)$$

The coefficients k_{ij} must be either determined experimentally or estimated. It is generally assumed that the binary coefficients can be used even for mixtures of order higher than two, thus implicitly assuming that the interactions of ternary and higher order are negligible.

For example, an equation giving k_{ij} is the following, V_c being the critical volume:

$$k_{ij} = 1 - \frac{8\sqrt{V_{ci} V_{cj}}}{(\sqrt[3]{V_{ci}} + \sqrt[3]{V_{cj}})^3} \quad (5.6.49)$$

It is important to know that an error in the determination of these interaction coefficients can lead to completely wrong results. It is strongly recommended to validate the models on the basis of

reference values, obtained experimentally if possible, and if not by comparison with validated software. The great danger in building models of fluids from equations of state and mixing rules is that one almost always gets results. In the absence of reference values, we may be tempted to have too much confidence in them... It is in this case recommended to try and build different models based on data from different sources, and compare their results to remove the doubt.

When the equation of state of the mixture is determined, the calculation of vapor-liquid equilibrium is done by writing the equality of fugacities of each species in each phase, that is to say, for each component:

$$f_{li}(P, T, x) = f_{vi}(P, T, y) \quad (5.6.50)$$

Without going into details, let us recall that fugacities are related to the departure of the chemical potential of a real fluid from that of the ideal gas. Equation (5.6.50) is thus derived from the Gibbs free enthalpy minimum at equilibrium.

This system of equations results in generally complicated expressions, the resolution of which can be quite difficult numerically. In addition, the accuracy of the model obtained depends of course on that of the equation of state retained. For example, the main interest of the Peng-Robinson is that it is a cubic equation whose solutions can be calculated formally, but it is generally not very good in the liquid phase, for which the methods based on activity coefficients are more accurate. In practice, therefore, it is necessary to retain much more complicated models for pure components and the estimation of the mixture properties becomes even more difficult.

In conclusion, the calculation of mixtures is often difficult to achieve and does not lend itself to simple graphical representations.

However, it is usually possible for applications in power engineering to simplify things by introducing a number of assumptions chosen wisely and well justified experimentally. The solutions adopted depend on the applications as we shall see.

5.6.8.3 Charts for refrigerants with temperature glide

For example, for refrigeration applications, the composition of a refrigerant blend remains constant in the vapor and liquid phases (if we neglect the influence of lubricating oil). In the liquid-vapor equilibrium zone, it is not strictly true, but almost always one does not require a precise calculation of the exact composition of the gas phase and liquid phase at the outlet of the expansion valve and the evaporator. By analogy with pure substances, we generalize the concept of vapor quality by that of mean quality, equal to the mass of the vapor phase, all components combined, relative to the total mass of liquid and vapor phases. We can then content ourselves with a fixed composition mixture model, much simpler. An equation numerically adjusted to the experimental values of a given mixture will thus be both more accurate and easier to calculate than the general formulation we have just seen. Furthermore, equations of state having been developed specifically for these applications, the reader will find references in the literature.

We give below the charts of two blends, R404A and R407C (Figures 5.6.27 and 5.6.28). In what follows, we shall only point out the differences introduced by the temperature glide, smaller for R404A than for R407C.

Refrigerant blend charts

Essentially, at a given pressure, the differences between the component saturation temperatures introduce a temperature glide in the liquid-vapor equilibrium zone: when boiling starts the temperature (bubble temperature) is lower than when boiling ends (dew point), while they are equal for pure substances. Thus, the pressure and temperature do not remain constant during boiling or condensation. In Clapeyron (P, v), entropy (T, s), and ($h, \ln(P)$) charts isobars or isotherms are not horizontal in the vapor-liquid equilibrium zone (Figures 5.6.25 and 5.6.26).

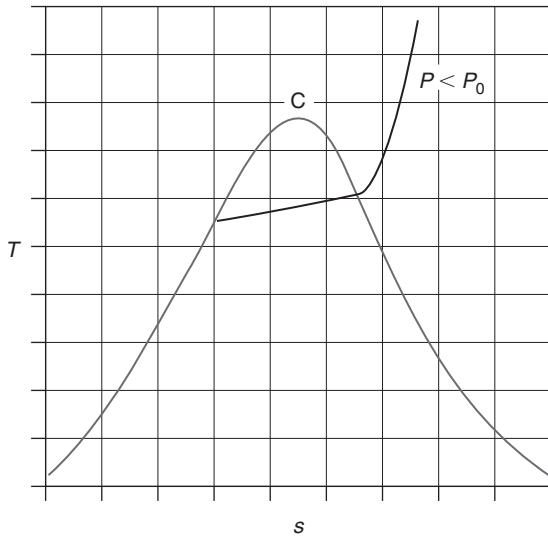


FIGURE 5.6.25
Entropy chart

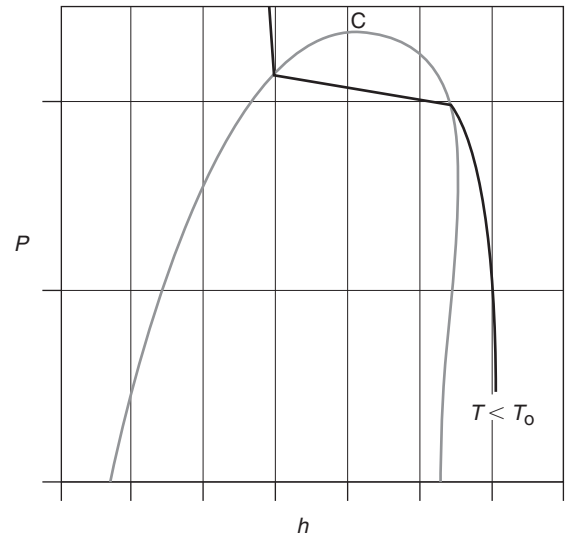


FIGURE 5.6.26
($h, \ln(P)$) chart

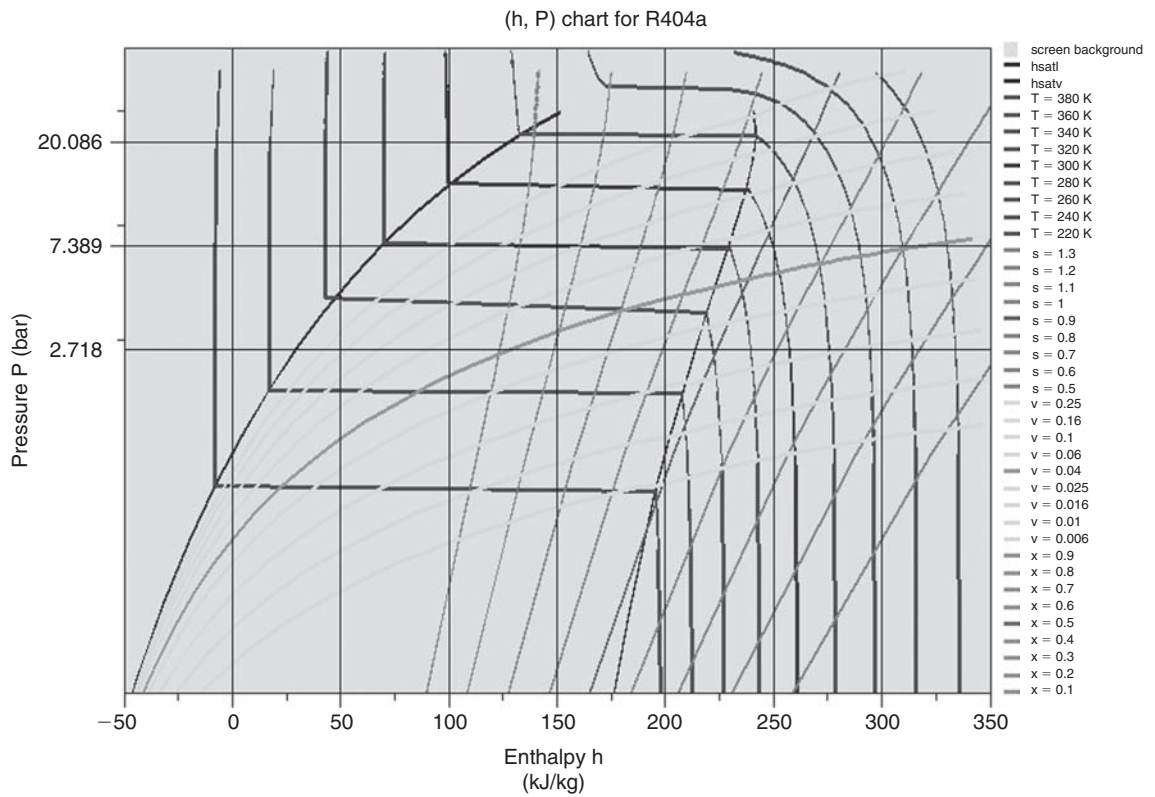


FIGURE 5.6.27
($h, \ln(P)$) chart for R404a

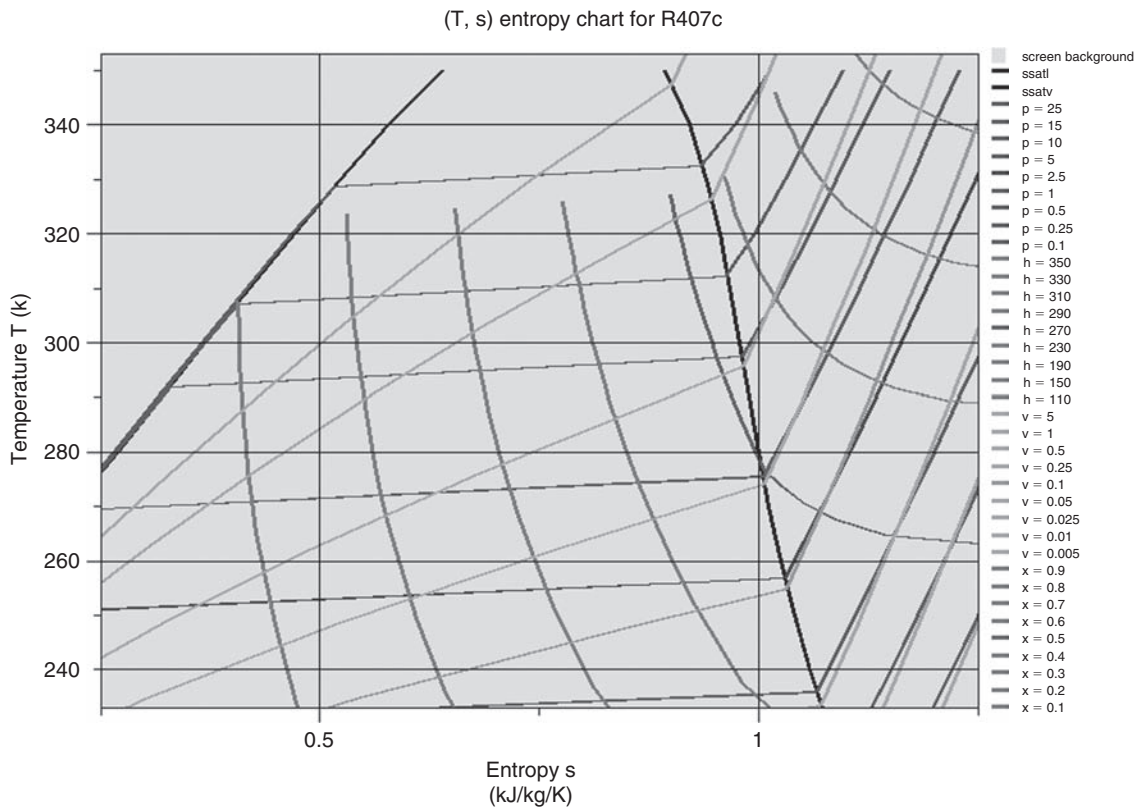


FIGURE 5.6.28

Entropy chart for R407c

As shown in Figures 5.6.25 to 5.6.28, an isobar is now represented in this area by an ascending line segment in the entropy chart, and an isotherm by a straight down slope line in the $(h, \ln(P))$ chart. In the vapor-liquid equilibrium zone of Mollier (h, s) , or exergy charts the difference is much smaller: isobars are little more ascending than isotherms.

The existence of a temperature glide has a direct impact on the design of heat exchangers used in refrigeration cycles. In first approximation, these can be considered as isobaric, so that differences in temperature between the coolant and other fluids are not the same as that observed in machinery using a pure fluid. Generally speaking, for blends with temperature glide, heat exchangers should be of the counter-flow type, which was not imperative with pure fluids.

Figures 5.6.27 and 5.6.28 correspond to $(h, \ln(P))$ chart for R404A, and entropy (T, s) chart for R407C.

5.6.8.4 Charts used in absorption refrigeration cycles

The main interest of liquid absorption refrigeration cycles, which will be presented in Chapter 20 of Part 3, is that they require only low power compared to their counterparts in vapor compression cycles (less than 1%). Using a tri-thermal thermodynamic cycle, they can directly make use of heat at medium or high temperatures to produce cooling, requiring no or little mechanical energy input. As such, they theoretically have total efficiencies in terms of primary energy greater than vapor compression cycles.

Liquid absorption cycles involve at least two fluids: a solvent and a solute (the coolant). While other pairs are studied, the only ones used in practice for almost all applications are the two

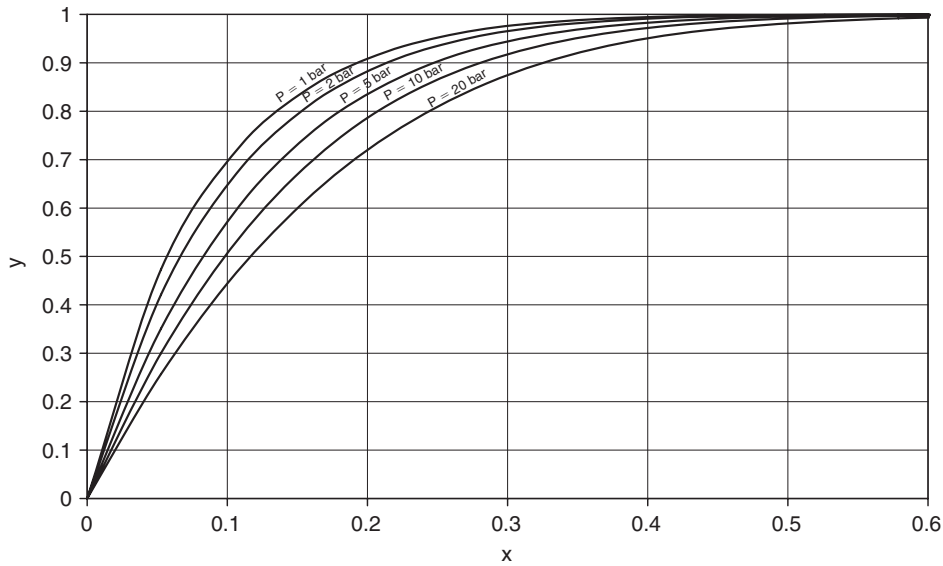


FIGURE 5.6.29

Vapor composition function of liquid $\text{NH}_3\text{-H}_2\text{O}$ composition

$\text{LiBr-H}_2\text{O}$ and $\text{H}_2\text{O-NH}_3$ pairs. Among the requirements for the prospective pair be appropriate, the solvent should firstly have a high affinity towards the solute, and secondly the latter should be much more volatile than the solvent so that the separation of the two components is optimal. The curve in Figure 5.6.29 shows, for water-ammonia pair, the relationship between the mass fraction of the ammonia liquid and vapor at different pressures (1, 2, 5, 10 and 20 bar). It clearly shows that, as soon as the liquid mass fraction of solute x exceeds 0.4, the ammonia content of the vapor exceeds 0.95. For lithium bromide-water mixture the separation is even stronger, so that one can legitimately assume that water vapor is pure.

With the $\text{LiBr-H}_2\text{O}$ pair, water is the refrigerant, which imposes two constraints: first working pressures are very low given the saturation pressure law of water, and secondly the minimum cycle temperature must be greater than 0°C . Machines using the lithium bromide-water pair are only used for air conditioning.

Oldham chart

The Oldham chart can view the saturation pressure curves of the mixture in question, for different values of its composition (mass fraction of solute or solvent, as appropriate). Pressure appears as the ordinate, with a logarithmic scale, while the abscissa corresponds to the bubble temperature T_b . It is also possible to show the curves corresponding to the dew point, but this is of less interest.

If one chooses $(-1/T_b)$ as temperature scale, the iso-quality curves are very close to straight lines (see Section 5.6.5.1). The extremes correspond to the vapor-liquid equilibrium of pure substances. An evolution of the rich or weak solution corresponds to a line segment tilted parallel to the nearest iso-quality curve. As the general shape of cycles in this chart is close to a parallelogram, scientists are used to illustrating the architectures of the machines in the form of diamond (Figure 5.6.32).

In machines using $\text{LiBr-H}_2\text{O}$ mixture, the difference in vapor pressure of the solvent (LiBr) and solute (H_2O) is such that we can neglect the mass fraction of solvent vapor, thereby simplifying calculations: the equilibrium chart can then be directly calibrated as a function of the solution temperature. Incidentally, it is customary to set the $\text{LiBr-H}_2\text{O}$ pair chart as a function of solvent (LiBr) mass

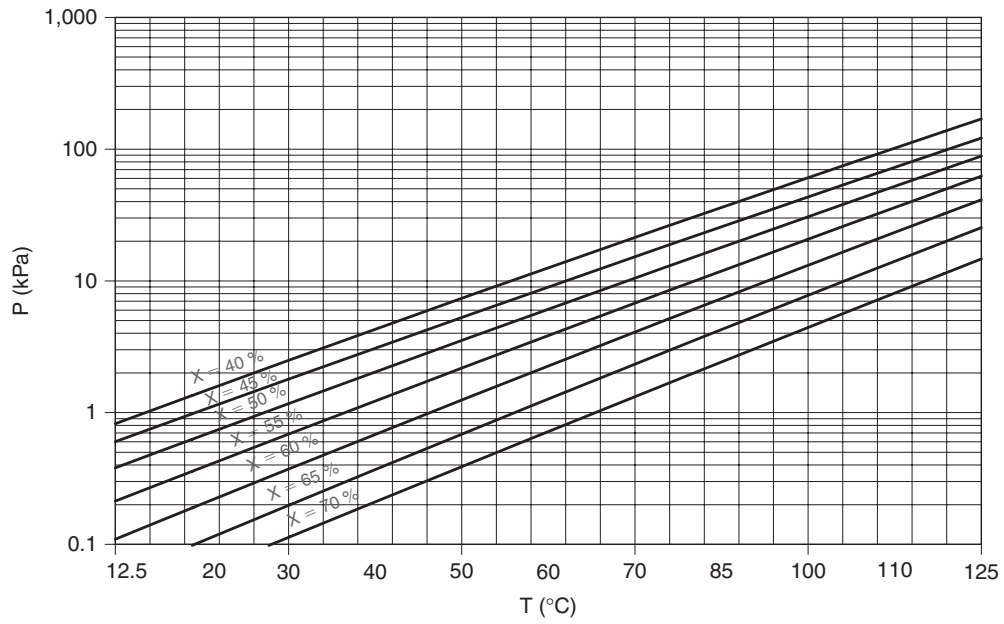


FIGURE 5.6.30
Oldham chart for LiBr-H₂O

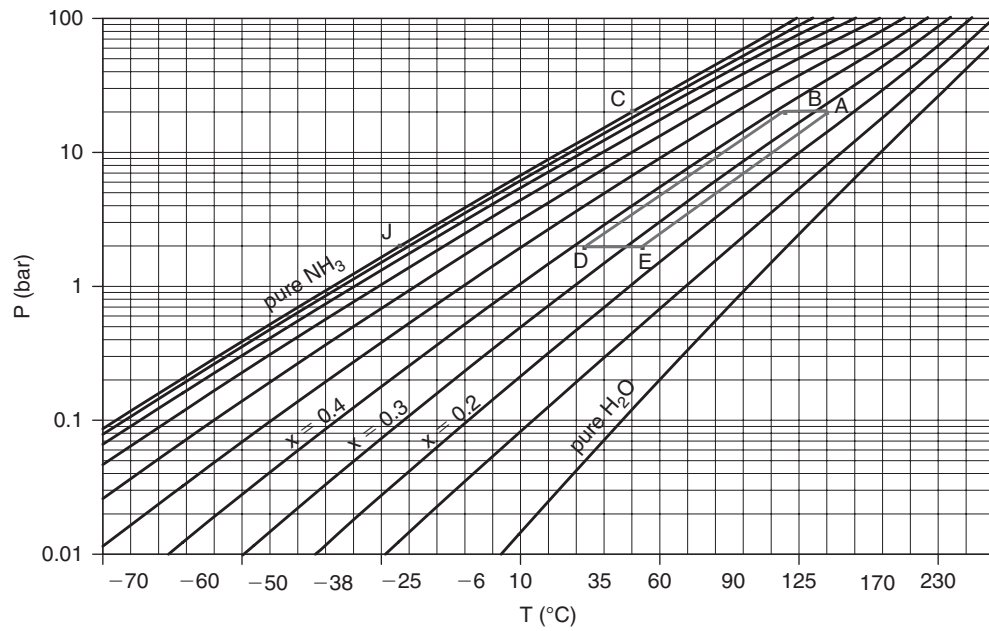


FIGURE 5.6.31
Cycle representation in the Oldham NH₃-H₂O chart

TABLE 5.6.4
COEFFICIENTS OF EQUATIONS 5.6.51 AND 5.6.52

A_0	-2.00755	B_0	124.937	C	7.05
A_1	0.16976	B_1	-7.71649	D	-1596.49
A_2	-3.13E-03	B_2	0.152286	E	-104095.5
A_3	1.98E-05	B_3	-7.95E-04		

fraction and not of solute. Water being likely to crystallize at low temperatures, the crystallization curve of the mixture often appears on the chart, which corresponds to the lower operating limit of machines.

For this pair, ASHRAE (2001) provides equations (5.6.51) and (5.6.52), established by generalizing the mixture saturation law of the coolant (water) pressure, in which the water temperature t' (°C) is replaced by a linear function of the solution temperature T (°C). P , expressed from the decimal logarithm, is the pressure in kPa, and X the mass fraction of LiBr mixture (Table 5.6.4).

These equations, which were used to prepare the chart in Figure 5.6.30 are valid in the ranges of values:

$$-15 < t' < 110^\circ\text{C}, \quad 5 < t < 175^\circ\text{C}, \quad 45 < X < 70\%.$$

$$\log(P) = C + \frac{D}{t' + 273.15} + \frac{E}{(t' + 273.15)^2} \quad (5.6.51)$$

$$t' = \frac{t - \sum_{i=0}^3 B_i X^i}{\sum_{i=0}^3 A_i X^i} \quad (5.6.52)$$

Figures 5.6.30 and 5.6.31 provide Oldham charts for LiBr-H₂O and H₂O-NH₃ pairs.

PRACTICAL APPLICATION

Modeling of the pair LiBr-H₂O

These equations, together with equation (5.6.53) giving the enthalpy of the pair LiBr-H₂O, have been implemented in ThermoOptim as an external substance.

It is thus possible to model absorption refrigeration machines using this pair.

Results obtained are given in several sections of this book and the associated models are available on the portal:

- Trigeneration by micro-turbine and absorption cycle, section 18.6.2 of Part 3, whose absorber is presented in section 8.3.7 of this Part as an example of thermocoupler;
- Single effect LiBr-H₂O absorption cycle, section 20.3 of Part 3.



[CRC_pa_1]

Merkel chart

The Oldham chart is easy to understand and use as discussed below, but, like isobar or isotherm equilibrium lenses, it has the disadvantage of not providing any information about the energies involved.

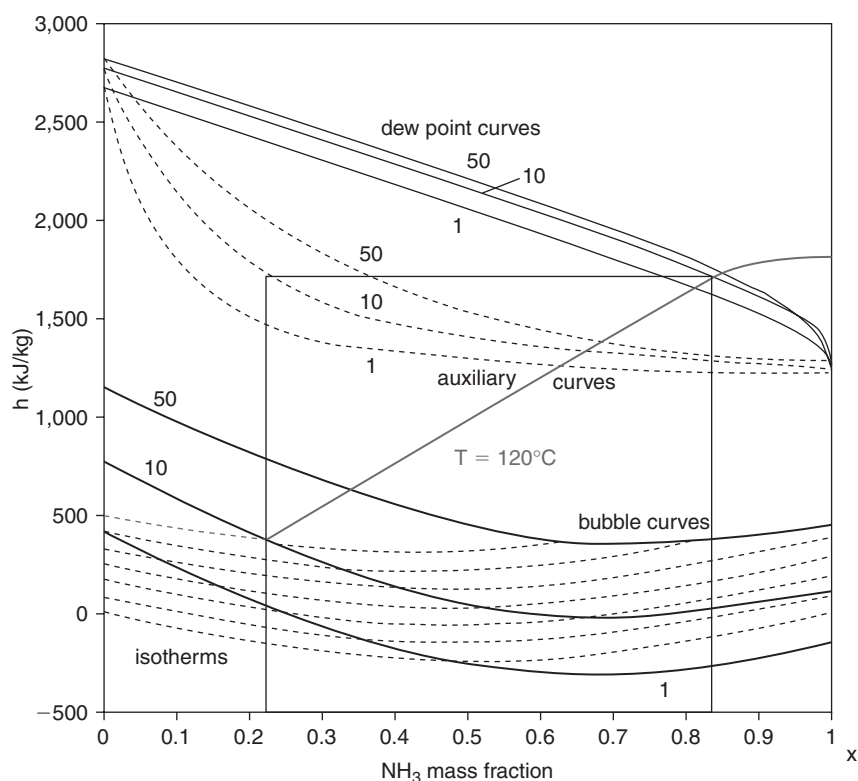


FIGURE 5.6.32

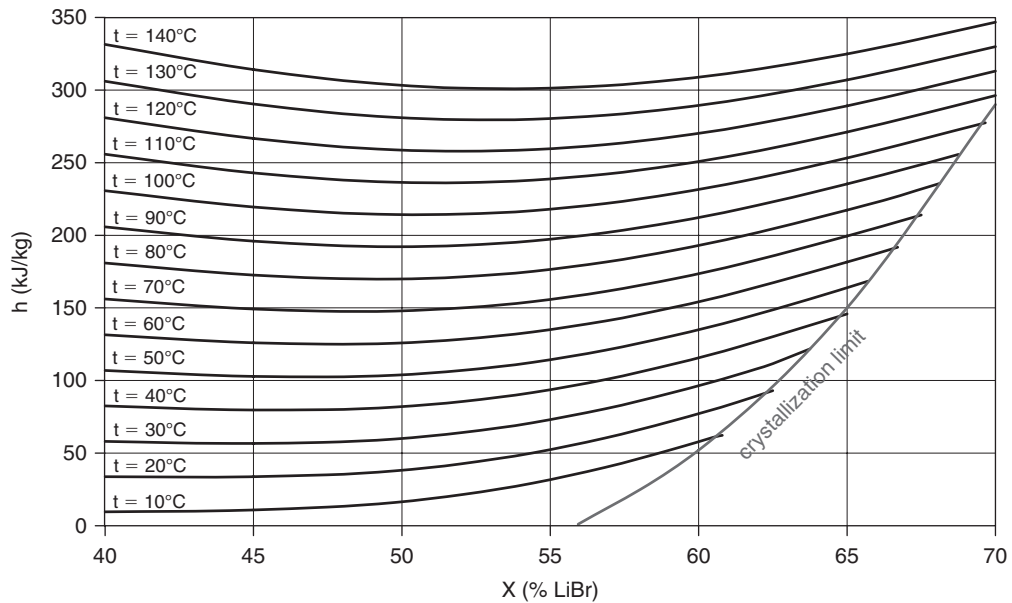
Isotherms in the Merkel chart

The Merkel chart (or enthalpy-concentration chart) is constructed with the enthalpy as ordinate, and the mass fraction of solute (or often the solvent for the LiBr-H₂O pair) as abscissa. It allows us to superimpose information from multiple isobar equilibrium lenses while showing enthalpies. Figure 5.6.32 gives the Merkel ammonia-water mixture chart. There are five types of curves:

- a set of bubble curves at $P = \text{Const.}$, continuous lines with the concavity turned upwards;
- a set of dew curves for the same pressures, solid lines with the concavity turned downwards
- a set of liquid zone isotherms, dashed in the lower part of the chart, which is valid whatever the pressure, the influence of pressure on the enthalpy of the liquid being negligible in first approximation (for example the difference in enthalpy of the liquid solution and 30% ammonia by weight is only 5 kJ/kg at 0°C when pressure increases from 0.5 to 50 bar, while the useful part of the chart covers more than 1000 kJ/kg in the liquid zone);
- a set of curves called auxiliary or construction, dashed in the upper part of the chart, which, for a given pressure, knowing the solute liquid mass fraction x , determine the solute vapor mass fraction y ;
- a set of refrigerant iso-quality curves in the vapor phase, which, for a given pressure, provide the mass fraction of liquid corresponding to the chosen vapor iso-quality (the latter set of curves is sometimes omitted from the Merkel chart, as in this example).

However, isotherms in the vapor zone do not appear in the Merkel chart, because they depend on pressure and the chart would become unreadable.

Notice that this chart superimposes two kinds of curves: liquid-vapor equilibrium and isotherm curves in the liquid state. There may be difficulties in interpreting the cycle points if you do not specify whether they are or not in liquid-vapor equilibrium.

**FIGURE 5.6.33**Merkel chart of LiBr-H₂O mixture**TABLE 5.6.5**

COEFFICIENTS FOR EQUATION 5.6.53

A ₀	-2024.33	B ₀	18.2829	C ₀	-0.037008214
A ₁	163.309	B ₁	-1.1691757	C ₁	2.89E-03
A ₂	-4.88161	B ₂	0.03248041	C ₂	-8.13E-05
A ₃	0.06302948	B ₃	-4.03E-04	C ₃	9.91E-07
A ₄	-2.91E-04	B ₄	1.85E-06	C ₄	-4.44E-09

In the NH₃-H₂O pair chart of Figure 5.6.31, the saturation pressure for $x = 0.22$ and $T = 120^\circ\text{C}$ is 10 bar. To know the mass fraction value y of the vapor we draw the vertical segment passing by $x = 0.22$ to the auxiliary curve corresponding to 10 bar, then the horizontal segment from that point until the dew isobar for 10 bar and then we draw the vertical to the horizontal axis, which gives $y = 0.83$.

We have already reported that for LiBr-H₂O pair we can neglect the mass fraction of solvent vapor, that is to say, consider that the refrigerant vapor behaves like pure water. The Merkel chart is thus simplified, and we generally content ourselves to build it by making only the liquid zone isotherms appear, bounded on the lower right by the crystallization curve (Figure 5.6.33).

Given this simplification, it is possible to determine the LiBr-H₂O mixture enthalpy through a simple equation, as proposed by ASHRAE (5.6.53) (Table 5.6.5, ASRAE 2001), where t is the temperature of the solution in $^\circ\text{C}$, h its specific enthalpy in kJ/kg, and X the LiBr mass fraction of the mixture. This equation, which was used to establish the chart of Figure 5.6.33, is valid within the ranges of values: $5 < t < 165^\circ\text{C}$, $40 < X < 70\%$. If this equation is chosen, the origin of the water vapor enthalpy is chosen at 0°C in the liquid state (which corresponds to the usual conventions for pure water charts).

$$h = \sum_{i=0}^4 A_i X^i + t \sum_{i=0}^4 B_i X^i + t^2 \sum_{i=0}^4 C_i X^i \quad (5.6.53)$$

These are the equations that are used in the external substance model of the LiBr-H₂O pair introduced Section 23.1.2.2 of Part 4.

REFERENCES

- Ashrae, *Fundamentals Handbook* (SI), Thermophysical properties of refrigerants, 2001.
- L. Borel, D. Favrat, *Thermodynamique and énergétique*, Presses Polytechniques Romandes, Lausanne, Vol. 1 (De l'énergie à l'exergie), 2005, Vol. 2 (Exercices corrigés), 1987.
- Chase et al., *Janaf thermochemical tables*, J. Phys. Chem. Ref. Data, Vol 14 Suppl. 1, 1985.
- U. Grigull, E. Schmidt, *Properties of water and steam in SI units 0-800°C, 0-1000 bar*, 3rd Ed., Springer-Verlag, Berlin Heidelberg, R. Oldenbourg, München, 1982.
- J.P. Holman, *Thermodynamics*, 4th Edition, Mc Graw-Hill, 1988.
- M. Moran, *Exergy analysis, The CRC handbook of thermal engineering*, (Edited by F. Kreith), CRC Press, Boca Raton, 2000, ISBN 0-8493-9581-X.
- R.C. Reid, J.M. Prausnitz, B.E. Poling, *The properties of gases and liquids*, 4th Edition, Mc Graw-Hill, 1987.
- S. K. Wang, Z. Lavan P. Norton, *Air Conditioning and Refrigeration Engineering*, CRC Press, Boca Raton, 2000, ISBN 0-8493-0057-6.

FURTHER READING

- R. Benelmir, A. Lallemand, M. Feidt, *Analyse exergetique*, Techniques de l'Ingénieur, Traité Génie énergétique, BE 8 015.
- G. Brun, *Thermodynamique des machines à fluide compressible*, Ed. Sennac, Paris, 1959.
- R. Coquelet, D. Richon, *Propriétés thermodynamiques, Détermination pour les fluides purs*, Techniques de l'Ingénieur, Traité Génie énergétique, BE 8 030.
- R. Coquelet, D. Richon, *Propriétés thermodynamiques, Détermination pour les mélanges*, Techniques de l'Ingénieur, Traité Génie énergétique, BE 8 031.
- D. Fargue, *Aide mémoire de thermodynamique*, Presses de l'Ecole des Mines de Paris, 1999.
- F. Fer, *Thermodynamique macroscopique*, Tome 1 Systèmes fermés, Gordon & Breach Science Publ., 1970.
- F. Fer, *Thermodynamique macroscopique*, Tome 2 Systèmes ouverts, Gordon & Breach Science Publ., 1971.
- A. Lallemand, *Thermodynamique appliquée: Premier principe. Énergie. Enthalpie*, Techniques de l'Ingénieur, Traité Génie énergétique, BE 8 005.
- A. Lallemand, *Thermodynamique appliquée: Deuxième principe. Entropie*, Techniques de l'Ingénieur, Traité Génie énergétique, BE 8 007.
- J. Lebrun, *Thermodynamique appliquée, introduction aux machines thermiques*, Polycopiés de l'Université de Liège
- S. Sandler, *Chemical and engineering thermodynamics*, 3rd edition, J. Wiley and Sons, New York, 1999.
- J. W. Tester, M. Modell, *Thermodynamics and its applications*, Prentice Hall PTR, Upper Saddle River, New Jersey, 1997.
- R. Vichnievsky, *Thermodynamique appliquée aux machines*, Ed. Masson & Cie, Paris, 1967.
- M. De Vlaminck, P. Wauters, *Thermodynamique et turbines*, CIACO, Louvain-la-Neuve, 1988.
- W. Wagner, A. Kruse *Properties of water and steam*, Springer, 1998.
- P. Wauters, *Thermodynamique*, Polycopié de l'Université de Louvain la Neuve, MECA 2190, 1990.
- M. W. Zemansky, R. H. Dittman, *Heat and thermodynamics, an intermediate textbook*, International Series in Pure and Applied Physics, McGraw Hill College Div, dec. 1996.

Presentation of ThermoOptim

Abstract: The ThermoOptim software package aims to enable easy calculation of relatively complex thermodynamic cycles without being obliged to resort to oversimplification, or engage in tedious calculations. It is composed of five interconnected complementary working environments: a diagram editor (or graphical modeler), a simulator; interactive thermodynamic charts, an optimization method and a productive structure editor.

Since energy conversion technologies are assemblies of interconnected components, the modeling environment combines a systemic approach and an analytical and/or empirical classical approach:

- each functional element is represented by an appropriate ThermoOptim primitive type (substance, point, process, node, heat exchanger) whose characteristics can be modified, and coupling variables;
- the complete system is modeled by assembling these types in an interactive interface, the diagram editor;
- simulation of the complete system is then managed by an automatic recalculation engine which exploits the inherent properties implicitly described in the model.

In this section we present the main ThermoOptim screens you need to know in order to use the tool. Since those corresponding to the processes and heat exchangers are detailed in Chapters 7 and 8, we do not analyze them here.

Keywords: ThermoOptim primitive types, software features.

6.1 GENERAL

ThermoOptim was developed to help resolve some difficulties in learning applied thermodynamics and getting expertise in it. Its objectives are:

- motivate beginners by preventing them from being deterred by the computational difficulties while allowing them to work on real-world examples;
- facilitate users getting started with the software thanks on the one hand to a major effort at designing the interface, and on the other hand to the integration in the tool of maximum functionality;
- offering advanced users a powerful and user-friendly computing environment enabling them to increase their productivity.

Applied thermodynamics is actually relatively complex as physical laws are highly nonlinear. Thermodynamic fluids are either ideal gases or condensable real fluids. The former are relatively simple to model compared to the latter, which are governed by much more complex laws.

Property	Value	Property	Value
M (kg/kmol)	18.015	T (K)	453.034
Pc (bar)	221.2	h (kJ/kg)	2512.079
Tc (K)	647.3	u (kJ/kg)	2343.122
Vc (m ³ /kg)	0.00317	s (kJ/kg/K)	6
quality x	0.868838	v (m ³ /kg)	0.168957

FIGURE 6.1.1

Calculator inverter

These fluids undergo processes, also nonlinear, from simple compressions or expansions to the most complex leading to variations in their composition, as is the case for combustion or moist mixture condensation. Depending on circumstances, these changes must be calculated in open or closed systems, the equations involved being different.

ThermoOptim is part of a family of tools bearing its name, a set of software tools for learning applied thermodynamics and getting expertise in it, including initiation applets, very easy to use interactive charts and a calculation package available in several versions.

These tools are intended for both graduate students and professionals. They allow the former to explore realistic cycles without being stopped by the computational difficulties that too often put off beginners. As for the latter, they bring them comfort of work now missing, which may encourage them to deepen their work in studying alternatives they would otherwise sometimes not do, not having a proper work environment. The terms of access to these various tools are specified on the ThermoOptim-Unit portal (www.thermoOptim.org).

6.1.1 Initiation applets

The lightest tools in the ThermoOptim family are small applets that can be run in most web browsers, such as the substance thermodynamic property calculator¹ shown in Figure 6.1.1. Although its capabilities are limited, it is already very useful to quickly obtain the properties of various ideal gases and real fluids. It offers the possibility to choose from among the following sets of independent variables: pressure, temperature (K or °C) and quality, enthalpy and pressure or even pressure and entropy. It can be used to easily calculate adiabatic compression and expansion, or even isenthalpic throttling, as discussed in studies of motor and vapor refrigeration cycles in sections 16.1.1 and 19.3.1 of Part 3.

¹ <http://www.thermoOptim.org/sections/logiciels/thermoOptim/ressources/applet-calculateur>

WORKED EXAMPLES

Vapor cycles modeling with the substance thermodynamic property calculator

Sections 16.1.1.2 and 19.3.1.2 of Part 3 present the detailed calculations that can be made with the substance thermodynamic property calculator in order to fully calculate two cycles:

- The Hirn or Rankine cycle of a steam power plant;
- A R134a refrigeration cycle.

They show how its features can be used to determine the state of all points.

Another combustion initiation applet² is available, and the development of other tools of this type is considered. Their goal is to be a bridge between classical education based on equations and more elaborate simulation tools as Thermoptim.

6.1.2 Interactive charts

The interactive charts have been developed with a view to replacing classical paper thermodynamic charts. Indeed, whatever care is taken by editors in the choice of color sets for distinguishing the various curves shown on the classical charts, it is always difficult to read them, and interpolation may lead to significant errors. Thermoptim interactive charts allow the user, by a simple mouse click, to display all relevant thermodynamic properties of the fluid, thus providing better accuracy.

Their main asset is to be very easy to use: the thermodynamic properties are immediately displayed on the screen, a user-friendly point editor allowing significant productivity gains for users.

At present, the following charts are available:

- vapor charts (Figures 5.6.4 to 5.6.17), which cover, namely in (T, s) , (h, P) , (h, s) , (h, x_h) and (s, x_h) coordinates, the liquid, liquid-vapor equilibrium and vapor zones, for fourteen pure substances, including steam. Vapor charts for external mixtures can also be partially plotted in (T, s) and (h, P) coordinates (see section 23.1.3.3 of Part 4);
- ideal gas pressure/specific volume (P, v) or temperature/entropy (T, s) charts, similar to the vapor charts (Figure 5.6.18), allowing one to make the gas composition vary (pure or compound);
- Carrier or Mollier psychrometric charts (Figures 5.6.19 to 5.6.22) in which one can modify either the pressure or the dry gas composition (for air as well as pure or compound gases, such as combustion flue gases).

6.1.3 Thermoptim's five working environments

We have seen that Thermoptim is composed of five interconnected complementary working environments: a diagram editor (or graphical modeler), a simulator, interactive thermodynamic charts, an optimization method and a productive structure editor.

²<http://www.thermoptim.org/sections/logiciels/thermoptim/ressources/applet-calc-comb>

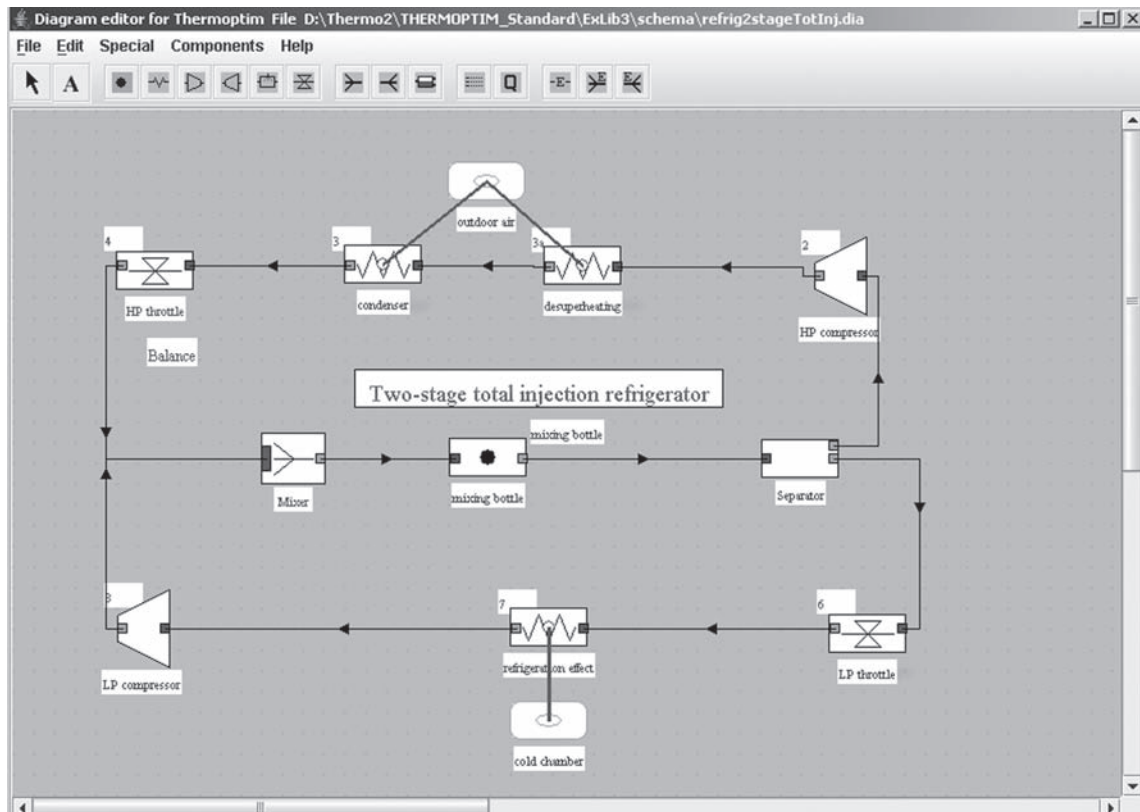


FIGURE 6.1.2

Diagram editor

The **diagram editor** (Figure 6.1.2) allows the user to graphically describe the system studied.

It includes a palette comprised of the various ThermoOptim components (process-points, heat exchanges, compressors, turbines, combustion chambers, expansion valves, mixers, dividers, separators). They can be displayed on a working panel in which the components are located and connected by links. This graphical environment provides a user-friendliness of great interest for viewing large projects and controlling internal linkages. Furthermore, as we shall see later, it allows for simpler data entry when creating a new project.

The **simulator** (Figure 6.1.3) allows one to quantify and solve the model described previously in the diagram editor. Its main screen gives access to the frames in which are set the logical and thermodynamic properties of the various model components (ThermoOptim primitive types).

The simulator calculates step by step the different elements of the project. This is a sequential calculation mode differing from that used in other (matricial) modeling environments, in which the whole set of equations of the problem is solved at the same time. It is much easier to successively calculate the elements than to solve the whole system simultaneously. This way of doing things however induces two difficulties: first it may be necessary to iterate several times to get the right solution when the project is comprised of loops, and second it may be difficult, for large and complex projects, to know in which order the calculations are to be done.

To solve the latter problem, a set of algorithms has been implemented. Named ThermoOptim *automatic recalculation engine*, it represents a key element of the software. A specific tool has been designed in order to follow the recalculation steps and thus be able to check the model consistency.

In addition, if a large project has been created, it may involve many elements such as points, processes and nodes. Using the diagram editor ensures that the connections between them are adequate, but not that their parameters are accurately set. A *diagnosis tool* has been developed to allow one to

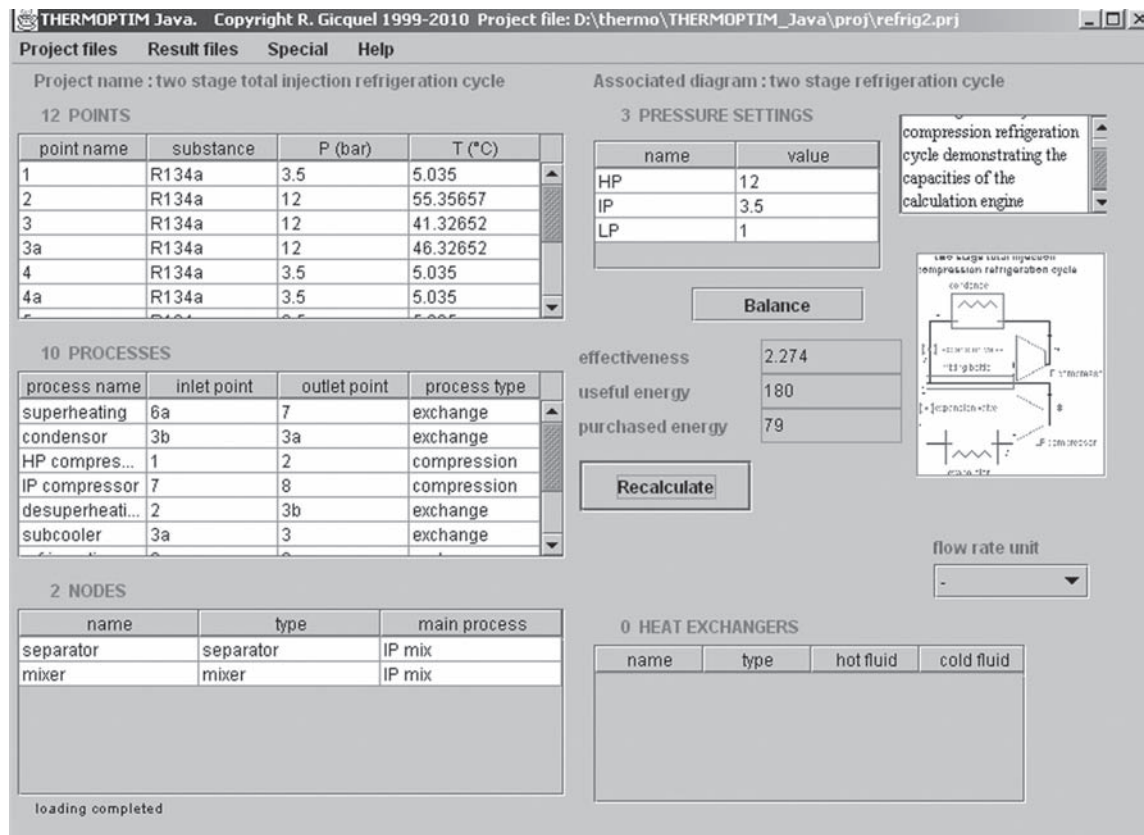


FIGURE 6.1.3

Two-stage refrigeration cycle in Thermoptim simulator screen

search and display the points or processes that share some characteristics, such as to be calculated in open or closed system, to have their flow rate set etc. It is thus possible to selectively display the various model elements in order to check their settings.

Lastly the simulator allows one to make simple *sensitivity analyses* with regard to flow rates, pressures or temperatures.

The thermodynamic interactive charts presented above are directly accessible in Thermoptim. They can be used to visualize the thermodynamic cycles calculated by the simulator.

Thermoptim fourth working environment is its **optimization method based on systemic integration**, which is an extension for energy systems (electricity power plants, cogeneration units etc.) of the Pinch method developed for Process Engineering in order to optimize large heat exchanger networks such as those existing in refineries.

This method, which distinguishes the irreversibilities specific to components from those that come from their arrangement within the system itself, allows, physically speaking, visualization of system critical areas, and highlights the irreparable systemic irreversibilities. By putting pinches in evidence, it identifies the locations of the system whose design must be done with special care, and is a valuable guide where heuristics were previously employed, sometimes requiring many iterations. It is presented in Chapter 22 of Part 3.

The fifth working environment is the **productive structure editor**, which will be discussed in Section 10.2.4 dealing with exergy balances.

In Thermoptim, these five environments are coupled by specific interfaces, the closest integration being realized on the one hand between the diagram editor and the simulator and on the other hand between the optimization tools and the simulator.

6.2 DIAGRAM EDITOR

6.2.1 Presentation of the editor

The editor looks like that shown above in Figures 4.3.2 and 6.1.2. To open it, select the line “Diagram editor” in the “Special” menu of the main project window. It includes a menu bar with three menus, a palette comprising ThermoOptim components which can be displayed (process-points, heat exchanges, compressors, expansion devices, combustion chambers, expansion valves, mixers, dividers, separators), and a working panel on which these components are placed and connected by links.

Note that, for now, the widgets corresponding to processes specific to moist mixtures have not yet been developed.

A diagram can be given a name and description to describe it succinctly. You can access these properties by the line “Description” in the editor File menu.

6.2.2 Graphical component properties

6.2.2.1 Property editor

Diagram component properties allow one to define only the minimum for creating a ThermoOptim project, the detailed characteristics of the various primitive types being subsequently entered through the simulator screens.

Diagram component properties are thus mainly the component name, those of the inlet and outlet port points and substances, as well as the value of the flow-rate.

More precisely, it is generally sufficient to define the component by its name, and for its outlet port, the name of the point and the corresponding substance as well as the value of the flow-rate through this port. The inlet port properties are subsequently automatically updated when an upstream component is connected. If in addition the component does not introduce a new substance, the outlet port substance is also updated. Properties are mainly accessed through a tab editor, either from the Edit menu, or by typing F4.

6.2.2.2 Placement of a component

In order to place a component in the editor, select it on the palette by clicking on it, then direct the crosshair cursor at the chosen location, and click. The property editor is automatically opened. For all processes but process-points³, it looks as shown in Figure 6.2.1.

Name the component, then click on the tab “outlet port”, and enter the point name. To enter the substance name, you may either type it if you know it, or get it from the list of available substances which can be displayed by double-clicking in the substance name field. Finally enter the flow-rate value, then click on “Apply” to directly validate all the tabs and exit the editor.

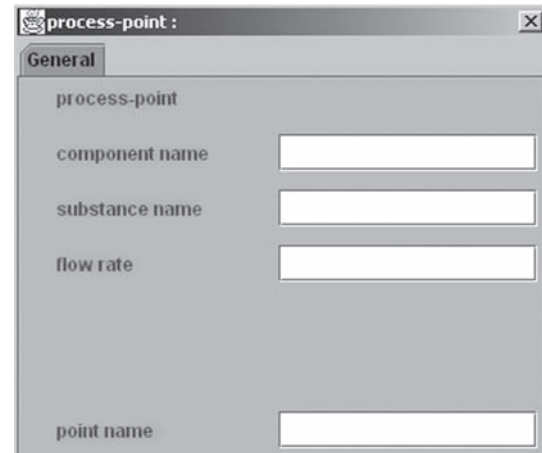
The number of tabs depends on the component selected. For ThermoOptim nodes, the name is sufficient, the other properties being defined by the connections. For process-points, there is but one tab, to enter its name and that of the point as well as the substance and the flow-rate (Figure 6.2.2). If the point name field is empty, the point name is that of the process.

Once you exit the property editor, the component is displayed with its name below it and that of the outlet point above on the right (Figure 6.2.3).

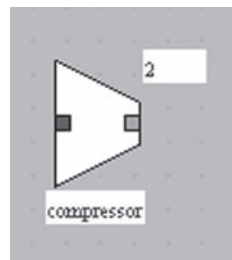
³This is an exchange process whose inlet and outlet points are the same, which is used to represent a small pipe, usually an entry or exit of fluid.

**FIGURE 6.2.1**

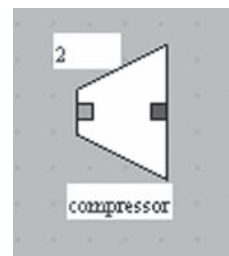
Property editor

**FIGURE 6.2.2**

Process point

**FIGURE 6.2.3**

Component oriented to the right

**FIGURE 6.2.4**

Component oriented to the left

By default, all components are oriented from the left to the right, but it is possible to orient them from the right to the left by selecting the item “flip vertical” on the Edit menu or typing F1 (Figure 6.2.4).

The name of the outlet point is then displayed above on the left. If you flip it again, the component is oriented as initially.

Once the component is created, you have access to all its properties by selecting the item “Show properties” on the View menu or typing F4. All the available tabs for this component are then available, including those which have been automatically updated during connections.

6.2.2.3 Connecting components

You can create links of two different types.

The first one corresponds to pipes connecting components, through which flow thermodynamic fluids. Their orientation is marked by an arrow.

Each component is equipped with small colored rectangles which are connection ports between which links can be set. Inlet ports are colored in blue (or red for the fuel of a combustion chamber), and outlet ones are green. The small rectangles (in practice squares) allow the user to graphically set

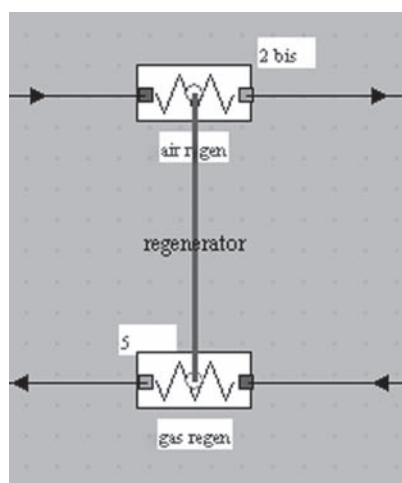


FIGURE 6.2.5

Heat exchanger

up one graphical connection (however several can be set programmatically), whereas the large ones, used for mixers and dividers, allow one to make multiple connections.

To connect two components, click on an outlet port (green) and drag the mouse to an available inlet port (blue), and then release the button. If the connection is allowed a link is created.

For instance, the diagram given in Figure 4.3.2 shows several such links: the process-point “oxidizer” is connected to the compressor by a single link, while the mixer has two input links, coming from the compressor and from the process-point “steam injection”.

The second type of link is used to represent heat exchangers. It is not oriented and connects two “exchange” components. In this book, we shall talk of exchanger connection to refer to this type of link.

An “exchange” component has in its center a small maskable exchanger connection port, which appears (as a small blue or red circle) only when the mouse is located above it, or when it is connected with another such component to represent a heat exchanger.

To make the connection, click on this port of one component and drag the mouse to the same port of another component and then release the button. During the connection the name of the exchanger is asked for. Once the heat exchanger settings are entered, the port is blue for the cold fluid, and red for the hot one (Figure 6.2.5).

6.2.3 Links between the simulator and the diagrams

The links between the simulator and the diagrams can be made either directly through the editor, by double-clicking on a sufficiently defined existing component, or through a specific interface. In both cases, the elements to be transferred are updated in the other environment, those not concerned by the transfer being unchanged. Thus, if some points or links are no longer useful, they are not deleted.

6.2.3.1 Creation and update of the simulator elements

To create the elements of the simulator, the easiest way is to use the diagram/simulator interface that can be opened from the Special menu. Then click the button “Update the element table”. The screen is shown in Figure 6.2.6.

The list of transferable elements is displayed in a table, and the user can select those he wishes to create or update. In front of each, an “X” marks the box “Diagram”, while the box “simulator”

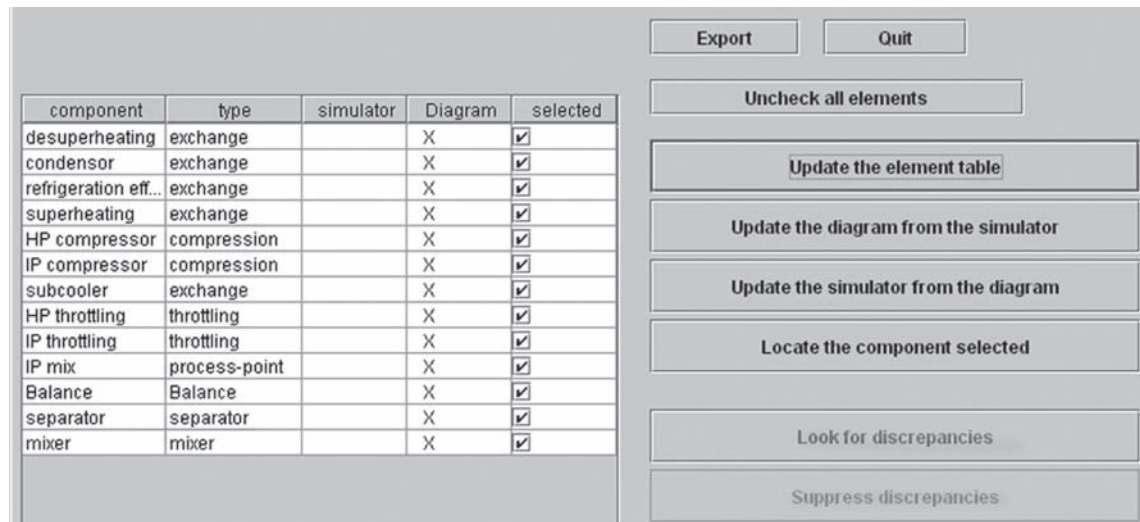
**FIGURE 6.2.6**

Diagram simulator interface

is empty. The right column shows which components are selected, that is to say which should be taken into account during operations conducted from the interface. By default, all components are selected, but a button allows you to deselect them all if you wish. Otherwise, by double-clicking a row in the table, you select it or not.

To transfer all components in the simulator, click the button “Update the simulator from the diagram”. In order for this operation to be possible, the component must be sufficiently defined, which means that its name and those of its port points and substances must have been defined. Otherwise, the component is colored in yellow, so that it can easily be identified. Show then its properties, and enter the missing values, and try again to create the simulator element.

A heat exchanger is created in the simulator when an exchanger connection exists in the diagram and that the two “exchange” components that it connects correspond to two “exchange” processes of the simulator sufficiently well defined (it is particularly necessary that their inlet and outlet temperatures are different, and that one is warming up while the other cools). By default, the exchanger is initialized with a “counter-flow” type.

Once the types are created, their characteristics must be entered in the regular simulator screens, and saved in a project file. When an element already exists, e.g. when exists in the simulator an element of the same name and the same type, a double-click on the component displays it. Similarly, double-clicking on a link opens the corresponding point screen.

The structure modifications (addition of new components, connection changes etc.) made in the diagram editor are transferred in the simulator when one double-clicks on a component or makes an update from the Diagram/Simulator interface.

Generally speaking, it therefore appears preferable to make all structure modifications from the diagram editor, and to set the simulator element parameters by displaying them from their graphical component. This way one takes full advantage of the visual interface, and one avoids on the one hand placement problems occurring with components created from the simulator, and on the other hand the automatic creation of physically meaningless links if some points are shared by several processes, as it is often the case for complex systems.

6.2.3.2 Creation of a diagram from the simulator

If the project only exists in the simulator, it is possible to automatically generate a diagram that matches it. However, the interface cannot know exactly where to position the components created.

For convenience, the convention is that their location is defined by the last rectangle selected in the editor. It is thus possible to progressively transfer elements at various locations of the diagram by choosing the destination zone on the working panel.

By default, all the elements are selected when the list is updated, but a button allows one to deselect all of them for a progressive transfer.

The links between the components are made on the basis of the points shared by the processes, and of existing connections for the mixers, dividers and separators.

The diagram is created as follows:

- during a first phase, the components are created if they do not already exist, and those corresponding to processes are initialized (names of points, substances, flow-rates etc.); for mixers, dividers and separators, there is no need for an initialization, their definition being made when the links are set up;
- during a second phase, the links are created. For the processes, a link is created each time a point is shared by two diagram components. When a given point is used by several processes, it is therefore possible for multiple links to be created. It is then up to the user to delete by hand those which have no physical meaning, as this operation cannot be automated. For mixers, dividers and separators, the connections are made in two steps: creation of the link with the main process, then of those with the branches. For separators, the upper outlet port is used for the vapor, the lower one for the liquid (more dense);
- when a heat exchanger exists in the simulator, both exchange components are linked by an exchanger connection named after the heat exchanger if both components exist and if at least one of them is selected.

6.2.3.3 Connections between two nodes

As it is impossible to directly connect two nodes, a process-point is automatically inserted between them if you try to do so. You then just have to set its parameters.

6.2.3.4 Note concerning process-points

The case of process-points merits further discussion. These processes are in particular useful when one creates large projects. They allow one to define fluid inputs or outputs, to connect nodes etc. As for the simulator, a process-point is an “exchange” process whose inlet and outlet points are the same and whose name is the same as that of these points; it is only when these conditions are met that a diagram editor component of the type “process-point” is created by transfer from the simulator.

6.3 SIMULATION ENVIRONMENT

6.3.1 Main project screen

The simulator screen (Figure 6.3.1) provides access to key Thermoptim primitives to define and modify projects.

It includes five tables, three on the left correspond to points, processes and nodes, and two on the right to the set pressures and heat exchangers. Each table is equipped with a label giving the number of existing elements. A comment field is located in the upper right of the screen. It helps to document the project with a short description displayed in the project library.

At the top of the screen are shown the name of the project and the associated diagram if there is one. To change these names, double-click in the appropriate field, and enter the new string.

In the right part the button labeled “Balance” allows one to calculate the overall balance with the following conventions. In each process, the energy type allows one to distinguish between purchased

Project name : regenerative gas turbine

Associated diagram : regenerative gas turbine

15 POINTS

point name	substance	P (bar)	T (°C)
1	air	1	20.85
2	air	16	238.85099
2 bis	air	16	610.47285
fuel	US mean nat ...	20	25
1a	air	4	187.83623
1i	air	4	54.24725

17 PROCESSES

process name	inlet point	outlet point	process type
air outlet	cooled air	cooled air	exchange
air inlet	air inlet	air inlet	exchange
1	1	1	exchange
1	1	1	exchange
fuel 2	fuel 2	fuel 2	exchange
exhaust gases	5	5	exchange

0 PRESSURE SETTINGS

name	value

effectiveness: 0.4239
useful energy: 531
purchased energy: 1,254

2 HEAT EXCHANGERS

name	type	hot fluid	cold fluid
intercooler	mixed cros...	air cooling	cooler
regenerator	mixed cros...	gas regen	air regen

loading completed

FIGURE 6.3.1

Simulator screen

Project files	Result files	S
New project		Ctrl+N
Load a project		Ctrl+O
Save ...		Ctrl+S
Save as ...		
Project library		
Example library		
Example catalog		Ctrl+E
Quit		Ctrl+Q

FIGURE 6.3.2

Project files menu

Result files	Special	Help
Export results		
Export cycle file		
Export pinch method fluids		
Export exergy calculations		

FIGURE 6.3.3

Result files menu

energy, useful energy, and other energy. The purchased energy generally represents the sum of all the energies that must be supplied to the cycle from outside. The useful energy is the net energy output of the cycle, e.g. the algebraic sum of the energies internally produced and spent.

These two energy types are those that appear in the definition of the cycle effectiveness⁴:

$$\eta = \frac{\text{useful energy}}{\text{purchased energy}} \quad (6.3.1)$$

⁴The concept of cycle efficiency is discussed in Section 10.1.6.

For example, in a Rankine cycle, the purchased energy is the heat supplied to the boiler and the useful energy is the net work output, i.e. the work produced by the turbine minus the work provided to the pump. The other energy is that used by the condenser. For a refrigeration cycle, the purchased energy is the input power of the compressor, the useful energy is the refrigeration effect (heat removed at the evaporator level), and the other energy is that removed at the desuperheater and condenser levels.

In the right part of the screen appears a thumbnail of a block diagram representing the project studied if an image has been associated with it, or an empty frame otherwise. If you double-click in the frame, a maximized window is opened where it can be displayed full size, with a menu allowing one to load or suppress the block diagram.

As already mentioned in Section 5.2.2 on the energy exchange in processes, it is noted that the concept of useful energy is not the same as the shaft work of a machine, even if sometimes it is the shaft work that is reported useful energy. The concept of useful energy is essentially economic, while the shaft work has a precise thermodynamic sense: the work produced or received by the shaft of the machine.

Just below, the button labeled “Recalculate” allows one to start the recalculation process.

6.3.2 Main menus

The “Project files” menu allows one to create a new project or to open an existing one, and save it. It also gives access to two libraries, the current projects, placed in an unprotected directory, and the examples, placed in a protected directory.

The “Result files” menu allows one to export the simulator results in text structured format (see Section 9.3.3), to export a cycle file that can be read by an interactive chart (see the charts manual in the software documentation), to export a pinch method problem or thermal exergy calculations.

The “Special” menu provides access to a number of tools:

- the diagram editor allows one to graphically define a project;
- interactive charts;
- thermal integration optimization tools;
- tools for automatic recalculation which were mentioned above;
- diagnosis tools allowing one to check the consistency of a model;
- a screen allowing one to perform sensitivity analysis on an existing project;
- the substance manager to make changes to a substance in the diagram editor and simulator;
- the screen giving access to drivers;
- the external class viewer.

Special	Help
Diagram editor	Ctrl+D
Interactive Charts	Ctrl+C
Optimization Tools	Ctrl+M
Automatic recalculation tools	Ctrl+R
Diagnosis tools	
Sensitivity analyses	
Substance manager	
Driver frame	
External class viewer	

FIGURE 6.3.4

Special menu

Help
Reference manuals
Quick Reference
About THERMOPTIM
License
Global settings

FIGURE 6.3.5

Help menu

	A	B	C	D	E	F	G	H	I	J	K	L	M
1	THERMOPTIM	Copyright R. Gicquel 1999-2010											
2	EXPORTATION	December 8, 2010 9:33:34 o'clock PM CET											
3	lang=en												
4	Project name	TAG cogén											
5													
6	Balance												
7	effectiveness:	purchased e	useful energy	TO exergy									
8	0.358	890	318	288.15									
9													
10													
11	POINTS	8											
12	name	substance n:	T (K)	P (bar)	quality	h (kJ/kg)	s (kJ/kg/K)	V (m3/kg)	u (kJ/kg)	xh (kJ/kg)	Cp	Cv	gamma
13	fuel	Montoir nat:	288.15	20	1	-20.52071	-1.195399	0.0650615	-16.07264	323.93349	2069.9404	1618.36	1.2790358
14	air inlet	air	288.15	1	1	-9.870371	0.1280112	0.8273012	-7.042359	-46.75679	1001.8778	714.77	1.4016786
15	2	air	715.77148	16	1	432.84313	0.2684783	0.1284397	312.89767	355.48111	1080.1978	793.09	1.3620116
16	3	flue gas	1423.15	16	1	1298.6633	1.1841042	0.2585817	971.56552	957.46368	1265.1348	974.42	1.2983465
17	4	flue gas	565.23678	1	1	282.3008	0.9091315	1.6432271	204.6111	20.334561	1086.2748	795.56	1.3654216
18	3 bis	flue gas	806.22559	1	1	551.37978	1.3050094	2.3438173	403.63107	175.34132	1146.5248	855.81	1.3396955
19	cold water	water	373.15	20	0	420.5154	1.3055338	0.0010427	418.42997	44.325837	0	0	0
20	hot steam	water	632.99214	20	1	3160.4562	6.9945587	0.1410613	2878.3336	1144.9741	0	0	0
21													
22	PROCESSES	10											
23	name	inlet point	outlet point	type	Delta_H	Delta_Xh	type_ener	flow rate					
24	hot steam	hot steam	hot steam	exchange	0	0	other	0.1					
25	HRSG water	cold water	hot steam	exchange	273.99408	110.06482	other	0.1					
26	cold water	cold water	cold water	exchange	0	0	other	0.1					
27	HRSG gas	3 bis	4	exchange	-273.9947	-157.8385	other	1.0182686					
28	exhaust gas	4	4	exchange	0	0	other	1.0287306					
29	air inlet	air inlet	air inlet	exchange	0	0	other	1					

FIGURE 6.3.6

Result file

The Help menu opens the “Quick Reference” screen, which provides a summary of the main concepts used in the software, displays the license text, and finally gives access to global parameters (definition of the working directory, selection of the temperature unit and the reference temperature for exergy calculations etc.).

6.3.3 Export of the results in the form of text file

All the results corresponding to a project can be gathered in a text file which can be processed either by a word processor or by a spreadsheet. For that, select the line “Export the results” on the “Result files” menu, A Save window is opened so that you can choose the backup file. Once it is created, open it with a spreadsheet. You obtain the result of Figure 6.3.6.

This file comprises the overall balance and the main computation results of the various primitive types which make your project: state of the various points, energies brought into play in the processes, compositions of the project gases etc.

6.3.4 Point screen

The “point screen” (Figure 6.3.7) allows one to define a point and to calculate and display values taken by all its state functions. A good understanding of the options it provides is necessary for the calculations to have the desired meaning. As was stated at the beginning of the book, only intensive values can be obtained at one point, extensive values requiring the mass flow, which is done in the processes.

Three tabs allow you to select the appropriate calculation method: first, by default, for open systems, enterable values are pressure and temperature or enthalpy, the second deals with closed systems, for which one enters the specific volume and temperature or internal energy, and finally the third applies to moist systems, mixtures of dry gas and water vapor, which will be detailed further.

FIGURE 6.3.7

Point screen

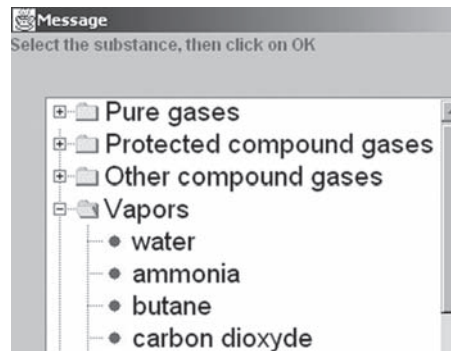
For condensable real fluids, the software does not calculate the values of specific heats C_p and C_v except in the liquid zone, nor their ratio γ .

6.3.4.1 Open systems

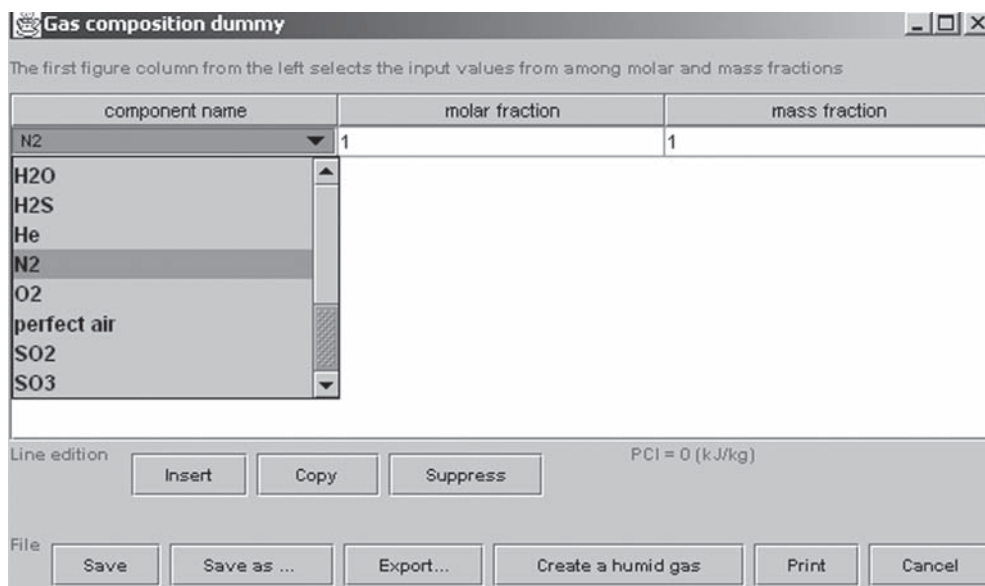
For open systems, the knowledge of the pressure and the temperature allows for the calculation of all the other state functions directly by clicking the checkbox labeled “P and T known” (the temperature must be entered in the unit chosen in the Global properties editor, but it is also displayed in the other unit when the point is calculated). Exergy is calculated on the basis of the reference temperature entered in the Global properties editor. If the pressure and enthalpy are known, select “P and h known”. If the pressure and entropy are known, select “P and s known” (see Figure 6.3.7).

For condensable vapors the following are displayed:

- two checkboxes, «set the saturation pressure» and «set the saturation temperature» whose meaning is obvious;
- the quality x of the mix which must be entered in the case when the point is located in the liquid-vapor zone;

**FIGURE 6.3.8**

Substance list

**FIGURE 6.3.9**

Gas composition editor

- a field labeled “Tsat approach” which, used in conjunction with “set the saturation temperature”, allows one to shift the value of the temperatures at a fixed value relative to the saturation temperature.

When the associated substance is defined, its name appears in the upper left side. To select the substance, you may:

- either double-click in the substance field located in the right side of the screen and expand the substance type folder (Figure 6.3.8), then click on the chosen substance (here “Vapors” and then «water »), and finally click on “OK”;
- or enter the requested name in the field and type the “Enter” key. ThermoOptim browses through all the existing substances looking for that name. If it exists, it is selected. Otherwise, it assumes you want to create a new compound gas and initializes it with nitrogen (N₂). By clicking the “display” button just to the left of the name, you open a gas editor which enables you to select the gas composition from among the existing pure gases (which are shown in a combo-box when you click on a cell of the “component name” column) (Figure 6.3.9).

Substance properties

substance: water H2O

Vapor

M (kg/kmol)	18.0153	Pmaxi (bar)	1,000
Pc (bar)	221.2	Tmaxi (K)	1,073.15
Tc (K)	647.3	Tmini (K)	273.15
Vc (m ³ /kg)	0.00317		

OK

FIGURE 6.3.10

Pure substance information screen

Open system (T,P,h) Closed system (T,v,u) Water vapor/gas mixtures

V (m³/kg) 0.00173902948 v and T known

u (kJ/kg) 1,641.82600266 v and u known

s (kJ/kg.K) 3.77802741 v and s known

T (°C) 349.82707 unconstrained

T (K) 622.98 set the saturation pressure

quality 0 set the saturation temperature

FIGURE 6.3.11

Closed system tab

Thermoptim considers that the first column of numbers on the left contains the data to take into account, the others being derived from them (you can easily move the columns by clicking on their name and dragging it sideways). Obviously, the sum of mole or mass fractions must be equal to 1.

If the substance is pure (real condensable fluid), the screen is slightly different (Figure 6.3.10). It provides the main features of the substance and the limits of validity of models used in Thermoptim.

6.3.4.2 Closed systems

To get access to the closed system screen, click on the middle tab. A slightly different screen is displayed (Figure 6.3.11).

For closed systems, the specific volume can be entered, as well as the internal energy or entropy, and one can set these two values to determine the other state functions by checking box “v and u known” or “v and s known”.

component name	molar fraction	mass fraction
O2	0.2068688	0.2307367
N2	0.7782206	0.7599001
H2O	0.01491061	0.009363201

FIGURE 6.3.12

Moist gas initial composition

Open system (T,P,h)		Closed system (T,v,u)		Water vapor/gas mixtures	
set w		set epsi		specific values (relative to 1 kg of dry gas)	
set the gas humidity				q' (kJ/kg)	0
w (kg/kg)	0.00945169907			v (m ³ /kg)	0
epsi	0			t' (°C)	0
condensation	0			tr (°C)	0
p (bar)	1.01325				
T (°C)	35				

FIGURE 6.3.13

Moist gas tab

6.3.5 Point moist properties calculations

Select the tab “Water vapor/gas mixtures” of the screen points to calculate the properties of moist mixtures.

6.3.5.1 Representation by a moist mix

When the substance is a moist mix, the latter may have been mixed in a mixer, generated from a dry gas and a specific humidity, or set directly by the user, in which case care must be taken that the water be entered as a gas (H₂O). Take, for example moist air whose composition is given Figure 6.3.12.

Construct a point using this substance, at the pressure of 1 atmosphere and temperature of 35°C, and click the tab labeled “Water vapor/gas mixtures”. The screen in Figure 6.3.13 appears.

At left are the data at the point considered: specific humidity w automatically calculated by the software from the mixture composition, relative humidity epsi . To the right are fields giving the specific values (that is to say relative to 1 kg of dry gas) of the enthalpy, volume, and the moist bulb temperature and dew point temperature. Possible condensate is displayed on the left under the relative humidity.

6.3.5.2 Moist properties calculations

To calculate all the moist properties of the point, click on the button “set w ”. The results of Figure 6.3.14 are displayed.

6.3.5.3 Setting the relative humidity

It is also possible to set the relative humidity to a particular value, by entering the value in the corresponding field, and then by clicking button “set epsi ”. Suppose now that one sets a relative humidity equal to 0.5: you get the screen shown in Figure 6.3.15.

Open system (T,P,h)		Closed system (T,v,u)		Water vapor/gas mixtures	
set w		set epsi		specific values (relative to 1 kg of dry gas)	
set the gas humidity				q' (kJ/kg)	59.5533
w (kg/kg)	0.00945169907	v (m ³ /kg)	0.8896703	t' (°C)	20.7218
epsi	0.268753928	tr (°C)	13.145		
condensation	0				
p (bar)	1.01325				
T (°C)	35				

FIGURE 6.3.14

Moist gas properties

Open system (T,P,h)		Closed system (T,v,u)		Water vapor/gas mixtures	
set w		set epsi		specific values (relative to 1 kg of dry gas)	
set the gas humidity				q' (kJ/kg)	81.0238
w (kg/kg)	0.0178163366	v (m ³ /kg)	0.9014101	t' (°C)	26.1419
epsi	0.499999999	tr (°C)	23.018		
condensation	0				
p (bar)	1.01325				
T (°C)	35				

FIGURE 6.3.15

Setting the relative humidity

component name	molar fraction	mass fraction
O2	0.2041745	0.2288404
N2	0.7680852	0.7536551
H2O	0.02774027	0.01750447

FIGURE 6.3.16

Moist gas new composition

It is possible to change the water content of the moist mix by clicking button “set the gas humidity”. The software prompts you to enter the desired humidity, offering by default the value of w. The gas composition is then modified as shown in Figure 6.3.16.

If the quantity of water present in the mix exceeds the saturation content, the relative humidity has the value 1, the specific humidity becomes equal to the saturation humidity, and the quantity of water in excess appears in the field titled “condensation”.

6.3.5.4 Representation by a dry gas

As the composition of the dry gas is most often invariant, we have seen in section 5.6.7 that it is interesting to define a moist mix by referring to its dry gas. Derogating from the general rule used in the package, ThermoOptim can do so by constructing points defined by the dry gas and the value of specific humidity.

Open system (T,P,h)		Closed system (T,v,u)		Water vapor/gas mixtures	
set w		set epsi		specific values (relative to 1 kg of dry gas)	
set the gas humidity				q' (kJ/kg)	81.0346
w (kg/kg)	0.0178187981	v (m3/kg)	0.9015347	t' (°C)	26.1418
epsi	0.499999999	tr (°C)	23.018		
condensation	0				
p (bar)	1.01325				
T (°C)	35				

FIGURE 6.3.17

Moist gas properties

process name	m abs	T (°C)	H
compression 1	0.85	19.75	85.69
extraction	0.15	318.54	3,041.83

FIGURE 6.3.18

Mixer screen

For example, create a point at pressure 1 atmosphere and temperature 35°C, associated with substance “atmospheric air”, then click the “Water vapor/gas mixtures” tab, and as before set a relative humidity of 0.5. The result you get is that of Figure 6.3.17, about the same as in Figure 6.3.15.

6.3.6 NODE SCREEN

A node screen is roughly divided in three parts:

- the upper left displays information relative to the node main process (the outlet one for a mixer, and the inlet one for a divider or a separator). To connect it from the node (if not already done in the diagram editor), double-click in the main process field, and choose from among the list of processes which is proposed in a combo box;
- the lower left one shows the branches of the node and buttons to add or delete branches from the node;
- the right part shows the actions which can be taken for building and calculating the node.

6.3.6.1 Mixer

When the mixer (Figure 6.3.18) is constructed, the “Calculate” button performs the mass and enthalpy balances of the branches and calculates the outlet temperature. The inlet point of the downstream process is recalculated.

node: extraction type: divider

main process: HP turbine display: [button] m global: 1

iso-pressure h global: 3,041.82915953

set flow: [red text] T global: 318.53986483

process name	m abs	m rel	T (°C)	H
reheat	0.85	0.85	318.54	3,041.83
extraction	0.15	0.15	318.54	3,041.83

Buttons: Duplicate, Suppress, Save, Close, Calculate, add a branch, delete a branch, flow setting

FIGURE 6.3.19

Divider screen

node: separator type: separator

main process: IP mix display: [button] m global: 2.48318

iso-pressure h global: 323.06

effectiveness: 1 T global: 5.04

process name	m abs	T (°C)	H
HP compressor	1.4832	5.04	401.41
IP throttling	1.0	5.04	206.87

Buttons: Duplicate, Suppress, Save, Close, Calculate, add a branch, delete a branch

FIGURE 6.3.20

Separator screen

6.3.6.2 Divider

The divider screen (Figure 6.3.19) has an additional button called “flow setting”.

It is used to define flow factors that are used in calculating the distribution of flow between the branches. The basic idea is the following: as a divider must conserve the mass flow rate, it is not possible to set the value in the different branches if that of the main branch varies. Therefore the user defines in each branch a “flow factor” which represents the share of the given branch in the global flow rate.

ThermoOptim then adds the different flow factors and distributes the main flow-rate between the branches proportionally to their “flow-rate factors”. In the example presented figure 6.3.19, 15% of the flow rate goes to the extraction process, and 85% to the reheat one.

There is however an exception: it is possible to set the flow rate in a process at the outlet of a divider, provided that this node has but two branches, the one with the set flow rate, and another one. In this case the flow rate of the second process is set equal to the flow rate of the main vein, minus that of the branch with the set flow rate, and the flow-rate factors are recalculated accordingly, while a label “set flow” is displayed in red below the name of the main vein, as in the example in Figure 6.3.19.

6.3.6.3 Separator (or dryer)

As its name indicates, its role is to separate a fluid in a liquid-vapor equilibrium, characterized by its temperature, pressure and quality. This is done by dividing its flow rate into two parts, liquid and vapor. It is therefore a type of divider (Figure 6.3.20).

You may set a separator effectiveness which must be in the range 0 to 1. It is defined as the ratio of the real liquid flow rate to the maximum theoretical one, and thus represents a drying effectiveness. If it is lower than one, the value of the quality of the vapor exiting the separator is less than 1.

To create a separator, select the process that represents the two-phase fluid. The outlet point of this process has to be in two-phase state, which means that its quality has to be strictly between 0 and 1. If this is not the case, the separator cannot be calculated and a message warns the user.

Select then the two outlet processes, which must have inlet points whose substance is the same as that of the main process outlet point. Furthermore one of these two processes must have its inlet point quality set to 0 so that ThermoOptim may identify it as being the liquid vein.

In the example above, the two-phase fluid is called “IP mix”. The total flow rate of 2.48 kg/s is separated into 1 kg/s liquid and 1.48 kg/s vapor, feeding respectively processes “IP throttling” and “HP compressor”.

6.4 EXTENSION OF THERMOPTIM BY EXTERNAL CLASSES

6.4.1 Extension system for ThermoOptim by adding external classes

One great advantage of ThermoOptim is that its graphic environment can be used to visually build models for a large number of energy systems, from the simplest refrigerator to complex integrated gasification combined cycle electric power plants using several hundred elements.

Not only does this greatly simplify the modeling process and facilitate subsequent use and maintenance of the model, but it also makes the models more reliable. The connections between the different elements are made automatically, thus ensuring consistency.

Until 2002, only the components available in ThermoOptim primitive type set could be assembled in this manner, which limited the potential of the software. A number of users wished to be able to define their own elements and/or their own substances.

ThermoOptim interface with external classes (Java code elements) provides the solution and facilitates the interoperability of the software with the outside world, especially with other applications developed in Java.

The benefits are two-fold:

- create ThermoOptim extensions from the common primitive type set, by adding external modules that define the elements that automatically appear on the screens in a seamless fashion. Thus users can add their own substances or components not available in the basic set. Examples are given Section 7.9 of this Part;
- drive ThermoOptim from another application, either to guide a user (smart tutorial) or to check the code (driver or regulation, access to thermodynamic libraries). A first example will be given section 12.2.1.10 of Part 3 for the modeling of a turbojet, but it is especially in Part 5 that external drivers are used because they allow one to solve off-design equation sets.

Figures 6.4.1 and 6.4.2 show how external substances are added to the list of ThermoOptim substances, then replace an internal substance in the point screen, making their use as easy for users as if they were part of the core.

Figure 6.4.3 shows how an external component representing a solar collector appears in the diagram editor, and Figure 6.4.4 shows the screen of the same process, composed partly by the internal ThermoOptim code, and partly by external code (right lower part).

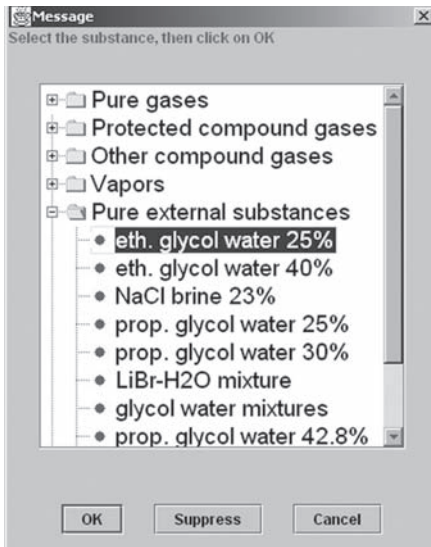


FIGURE 6.4.1

Substance list

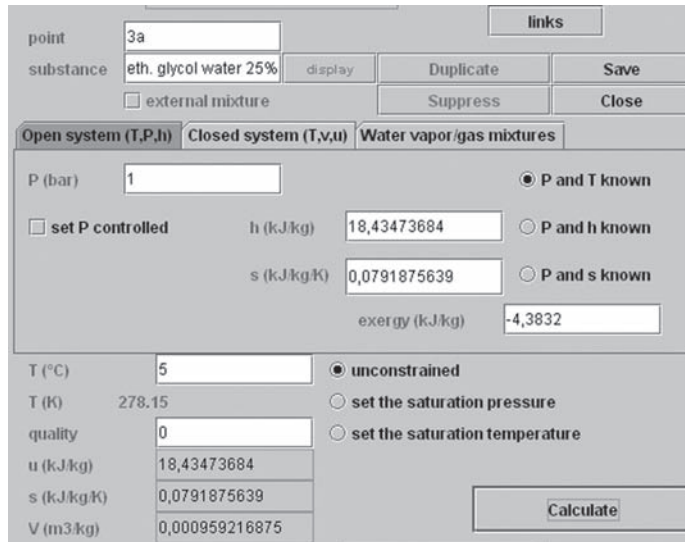


FIGURE 6.4.2

Substance screen

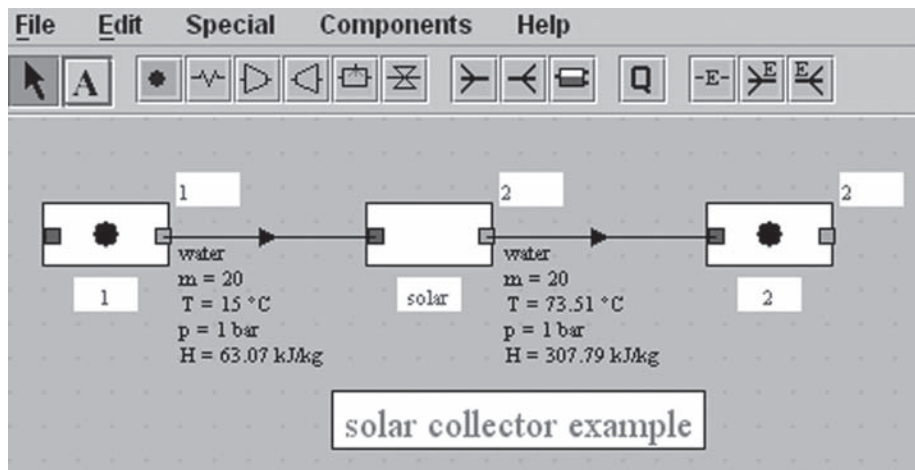


FIGURE 6.4.3

External process

6.4.2 Software implementation

Practically speaking, adding a new external process is quite easy. Simply create a specific class, which inherits from the abstract parent class `extThopt.ExtProcess`. The interaction with ThermoOptim is ensured on two levels:

- by general methods for performing the required calculations;
- by a `JPanel` that is built into the external process screen. Thus, the class designer can create his own graphic interface, which is then inserted into the ThermoOptim screen. It defines its own graphical elements (buttons, fields, labels etc.), and processes the user actions to convenience. Specific methods even allow one to save settings in the ThermoOptim project file, then reread them when loading the project.

FIGURE 6.4.4

External process screen

Loading external classes is dynamically ensured by ThermoOptim as follows: during its launch, the software analyzes archives extThopt.zip and extUser.zip, which contain, among others, all external classes.

It finds thus all classes added by users, which are sorted according to their parent class, and loaded into tables, adding external components to ThermoOptim lists so that they are transparently accessible to the user. Later, if any of these elements is selected, ThermoOptim transmits its class to the appropriate constructor, which instantiates it.

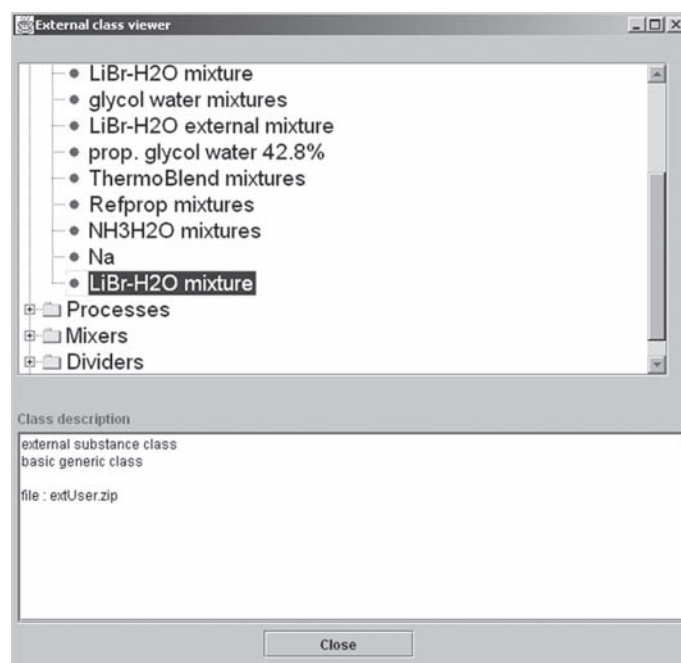
Classes that are involved in ThermoOptim and extThopt.zip and extUser.zip archives define the interface methods, which fall into three complementary categories:

- internal ThermoOptim methods not accessible from outside;
- internal methods that are accessible from outside, directly used by external classes: they can execute ThermoOptim methods with external settings, and **should not be overloaded**. Their signature must be scrupulously observed: in particular, the structure of Vectors or Objects passed as arguments must exactly match that expected by ThermoOptim, otherwise exceptions are cast;
- external methods corresponding to ThermoOptim methods not accessible from the outside: they allow one to execute external methods from ThermoOptim, and **must always be overloaded**.

6.4.3 Viewing available external classes

To help you use and manage external classes, line External Class Viewer on the Special menu displays all of the external classes available (Figure 6.4.5). They are sorted by type (substances, processes, mixers, dividers, drivers) with a short description of the class selected and where it comes from (extThopt.zip and extUser.zip archives as well as classes under development).

This screen can be consulted while you are developing your model.

**FIGURE 6.4.5**

External class viewer

6.4.4 Representation of an external component in the diagram editor

Specific icons were added to represent the external components (for processes, for mixers, and for dividers). The external component is then selected when the simulator is updated from the diagram as indicated below.

6.4.5 Loading an external class

To load an external process (for an external node, the process is the same), you can either:

- click in the simulator screen on the column header of the process table, then choose External and finally select the type of external process you want from the list;
- or, in the diagram editor, build the external component graphically then update the simulator from the diagram. An external process is by default of the “heat source/sink” type, as shown in the screen of Figure 6.4.6.

Once this default process is created, double click on the label “source/sink” to access the list of all external processes available. Choose the one you want and it is loaded.

6.4.6 Practical realization of an external class

Various examples of practical realization of external classes, with explanations on how to encode them, are given in Part 4 of this work, especially in Chapter 23.

The screenshot shows the 'Default screen an external process' in ThermoOptim. The interface includes the following elements:

- Process Information:** process: solar, type: external.
- Energy and Flow Settings:** energy type: other, set flow, flow rate: 1.
- System Configuration:** closed system, open system, observed.
- Inlet Point (1):** T (°C): 15, P (bar): 1, h (kJ/kg): 63.07, quality: 0.
- Outlet Point (2):** T (°C): 16, P (bar): 1, h (kJ/kg): 67.26, quality: 0.
- Other Parameters:** m Δh: 0, source / sink, reference: source / sink, Power generated or extracted: 1.
- Buttons:** Save, <, >, Suppress, Close, Calculate, display (for inlet and outlet points).

FIGURE 6.4.6

Default screen an external process

In addition, volume 3 of ThermoOptim reference manual is dedicated to external classes. We recommend that you refer to it for a full explanation of this powerful mechanism.

Finally, the ThermoOptim-UNIT portal model library includes many external classes annotated with their Java code.

THOPT
[CRC_In_14]

6.5 DIFFERENT VERSIONS OF THERMOPTIM

“ThermoOptim versions are firstly characterized by a label that defines the features (Demo, Education Classroom, Standard, Professional and Industrial) and secondly by a serial number (1.3, 1.4, 1.5, 1.6, 1.7 or 2.5, 2.6 or 2.7), which represents the chronological development of the software.

Numbers 1.3 to 1.7 are ThermoOptim versions using old Java libraries (JRE or JDK 1.1.8) while numbers 2.5 to 2.7 are ThermoOptim versions requiring Java 2 libraries (JRE or JDK 1.3 to 1.6). At the time of publication of this book, the latter are still under development.

The demo version is freely distributed to allow you to view existing projects and diagrams, and to build small ones in order to familiarize yourselves with the tools. Of course it does not provide access to all the software features. In particular, it does not allow you to save projects or diagrams, nor the output result files.

You will find details on these versions in the portal as well as links to the download pages.

THOPT
[CRC_In_20,
CRC_In_21]

This page intentionally left blank

Basic Components and Processes

Abstract: In the introduction to this book, we showed that energy technologies can be considered as assemblies of components through which pass thermodynamic fluids which undergo changes of varying complexity. In this chapter we will present the main types of components encountered in practice and the physical phenomena that govern them, and examine how they can be assembled and calculated in the ThermoOptim modeling environment.

Let us recall that, given our purposes, we limit ourselves to a steady-state representation of phenomena, and we will not try to model the fine detail of how a particular component behaves, which can be extremely complex. Supplements on the technological design of these components will be presented in Part 5.

For technologies that interest us, a component can be represented with sufficient accuracy when are given on the one hand the variables defining the coupling with other system components, and on the other hand a small number of characteristics, whose physical sense must be well understood. These characteristics depend on the type of component and the technology.

At first, we examine the components available in ThermoOptim core, i.e. compressions, expansions, combustions, and throttling or flash, and finally the various processes that can undergo a moist mixture. In a second step we present some examples of external components: nozzles, diffusers and ejectors. The presentation of principles for calculating each process will be followed by a presentation of the different technologies available, themselves supported by examples calculated with ThermoOptim.

Keywords: compression, expansion, volumetric efficiency, isentropic efficiency, polytropic efficiency, combustion, quenching, stoichiometry, excess air, richness, unburned hydrocarbons, law of mass action, throttling, flash, moist mixture processes, nozzle, diffuser, ejector, displacement compressor, dynamic compressor, turbine, Biard, Ostwald, HHV, LHV, airflow required, smoke developed, combustion chamber, boiler, moist mixture processes, humidification, condition line, supply conditions.

7.1 COMPRESSIONS

In this chapter we will mainly deal with compressors, which can be grouped into two broad classes: displacement compressors and dynamic compressors. The most common are the displacement

compressors, in which the fluid is trapped in a closed volume which is gradually reduced to achieve compression. Dynamic compressors use a different principle: the compression is achieved by converting into pressure the kinetic energy communicated to the fluid by moving blades.

Compressors are used for many industrial applications: refrigeration, air conditioning, transportation of natural gas etc. A special mention must be made of air compressors, used as a source of power for public and building works as well as in factories, pneumatic tools having many benefits.

In this section, having established the theoretical basis of compression, valid for all types of compressors, we will consider initially the displacement compressors (reciprocating and screw), then in a second stage dynamic compressors (centrifugal and axial) and pumps and fans. A comparison between different types of compressors is finally presented.

The fundamentals you have to make sure you understand are: isentropic, polytropic compression, adiabatic, isentropic or polytropic efficiency, polytropic exponent (7.1.3) and volumetric efficiency (7.2.1.3).

7.1.1 Thermodynamics of compression

Compressing a fluid is to raise it from the suction pressure P_a to the discharge pressure P_r (above P_a). The process involves some work, called “compression”.

The fluid initial state “a” before compression is known: pressure P_a , temperature T_a and specific volume v_a . However, of state “r” after compression, only the discharge pressure P_r is determined. The final temperature depends on heat exchanges with the outside. It is the same for all functions referred to the “r” thermodynamic state, including the compression work.

Assuming the process (a–r) is known, the compression work τ is given by (5.3.6) which is written here:

$$h_r - h_a + \Delta K = \tau + Q_a^r \quad (7.1.1)$$

Assuming that the fluid velocities are low, which is legitimate if we consider state in the discharge tank, we get:

$$\tau = h_r - h_a - Q_a^r \quad (7.1.2)$$

7.1.2 Reference compression

Compressors are compact machines, through which pass a gaseous fluid that stays there very briefly. Exchange surfaces are reduced and heat exchange coefficients are low. As a result, generally heat transfer between the working fluid and the outside is negligible compared to the compression work: the reference compression is therefore an adiabatic compression. If it is reversible, it is an isentropic.

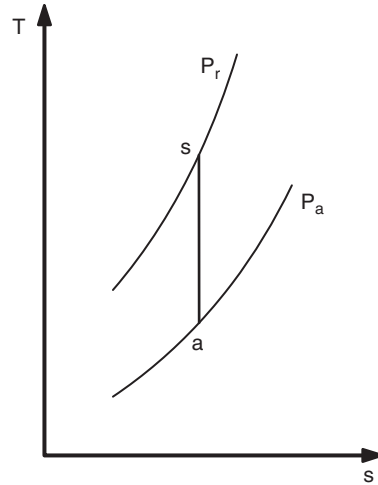
A second type of compression is of interest, at least in theory: it is the isothermal compression, which would be realized if we were able to cool the working fluid, which receives heat because of compression, so that its temperature remains constant.

The advantage of such a compression is that it would minimize the work required. Although generally not feasible in practice as we have seen, it may be advantageous to cool the fluid between two compression stages when you need to achieve a multi-stage compression. The process that is then performed approaches an isotherm and is called para-isothermal.

7.1.2.1 Reversible isothermal compression

Knowing the equation of state, it is easy to calculate τ_i by integration:

$$\delta\tau_i = v dP$$

**FIGURE 7.1.1**

Isentropic compression

For example, for an ideal gas:

$$Pv = rT, \quad \text{and} \quad \delta\tau_i = rT \frac{dP}{P}$$

As $T = T_a$ is constant:

$$\tau_i = r T_a \ln \left(\frac{P_r}{P_a} \right) = P_a v_a \ln \left(\frac{P_r}{P_a} \right) \quad (7.1.3)$$

7.1.2.2 Reversible adiabatic compression

The second law gives $s = \text{Const.}$, and, in the entropy chart, the process is represented by a vertical segment (a-s) (Figure 7.1.1). The corresponding work is called isentropic or sometimes adiabatic work. We denote it by τ_s .

Relationship (7.1.2) gives here:

$$\tau_s = h_s - h_a \quad (7.1.4)$$

For perfect gases whose heat capacity is independent of temperature, the isentropic process law reads:

$$Pv^\gamma = \text{Const} \quad \text{or} \quad v_r = v_a \left(\frac{P_r}{P_a} \right)^{-1/\gamma}$$

The integration of the vdP term gives the expression of the isentropic work:

$$\tau_s = \frac{\gamma}{\gamma-1} P_a v_a \left[\left(\frac{P_r}{P_a} \right)^{(\gamma-1)/\gamma} - 1 \right] \quad (7.1.5)$$

Given the equation of state and relations between r and the heat capacity, the above equality can be written as:

$$\tau_s = c_p T_a \left[\left(\frac{P_r}{P_a} \right)^{(\gamma-1)/\gamma} - 1 \right] \quad (7.1.6)$$

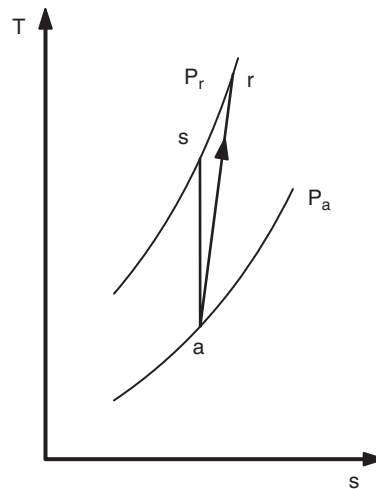


FIGURE 7.1.2

Real compression

For ideal or real gases integration of vdP term is not so simple. The calculation must be done by solving the equations of state. In all cases, we know the pressure and suction temperature, which determine the entropy and enthalpy at the suction. So we know the discharge pressure and entropy, thereby determining the temperature and corresponding enthalpy. Work τ is deduced by (7.1.4).

7.1.3 Actual compressions

7.1.3.1 Actual adiabatic

We have already established in section 5.4.2 the equations to be used when the compression, still adiabatic, is no longer reversible. Irreversibilities (friction, impact etc.) cause an entropy generation and, in the entropy chart (Figure 7.1.2), adiabatic compression is represented by a real curve ($a-r$) located to the right of the theoretical vertical ($a-s$). The temperature at the end of the compression is greater than that which would result in a reversible adiabatic compression.

Formula (7.1.2) follows directly from the first law, which does not involve any assumptions about the reversibility of the processes. The one that interests us being adiabatic $Q = 0$, we get:

$$\tau = h_r - h_a$$

It is clearly greater than the isentropic work τ_s .

If the gas can be regarded as perfect:

$$\tau = c_p (T_r - T_a)$$

Isentropic efficiency, or adiabatic efficiency, is defined as the ratio of isentropic work to real work:

$$\eta_s = \frac{\tau_s}{\tau} = \frac{h_s - h_a}{h_r - h_a} \quad (7.1.7)$$

This efficiency measures the imperfection of the process from the reversible adiabatic. It is important to note that the adiabatic efficiency η_s is thus the main characteristic of an irreversible adiabatic process, but its determination also presents the greatest difficulties.

When the machine considered is conventional, that is to say, has no major innovations as compared to machines made and tested, we take as a provisional value the one which results from

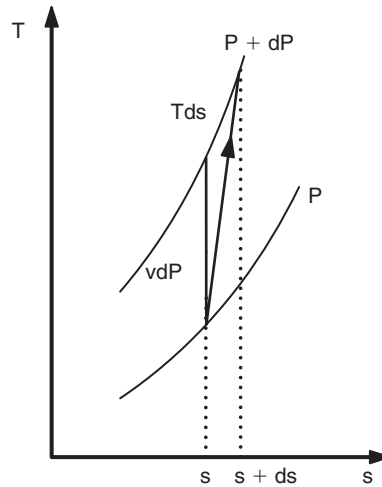


FIGURE 7.1.3

Elementary compression

testing these machines. Where no such data are available, or if they are not satisfactory, the preliminary evaluation of η_s is always very difficult. It is the result of the detailed study of losses and is only possible if one has numerous basic experimental data. The problem thus posed (calculation of losses, leaks, wall friction etc.) falls within the field of experimental fluid mechanics, not thermodynamics.

7.1.3.2 Polytropic adiabatic compression

Note that knowing the isentropic efficiency η_s provides no guidance on the law followed by the fluid during an irreversible compression, so that we cannot integrate the vdP term. To do so, we must make additional assumptions. One of the most common assumptions leads to the widely used concept of a polytropic process, which may cover slightly different definitions according to the authors. For some it is an irreversible process, while for others it is inherently reversible. We begin by presenting the first way of seeing things, which is justified for adiabatic compression, then we will show how the second is well suited to the study of non-adiabatic compressions. In addition, we will discuss this concept with two approaches often given as equivalent, whereas they are strictly so for perfect gas only, that is to say, for gases following to law $Pv = rT$, and whose specific heat capacity is constant (see 5.6.2.1).

7.1.3.2.1 Differential approach of the polytropic

The assumption that we make here is to consider that the irreversibilities are uniformly distributed throughout the compression, which is to assume that during any infinitesimal process stage, the isentropic efficiency keeps a constant value, equal by definition to the polytropic efficiency η_p (Figure 7.1.3).

For multi-stage machines, this efficiency has a clear physical meaning: it is the basic stage efficiency.

An infinitely small compression leads to state functions variations dP , dT , dh and ds .

The process being adiabatic, the actual work $\delta\tau$ is equal to dh , while the reversible work is $\delta\tau_s = vdP$.

By definition:

$$\eta_p = \frac{\delta\tau_s}{\delta\tau}$$

The assumption η_p constant thus results in the differential equation:

$$\eta_p = \frac{vdP}{vdP + Tds} = \frac{dh - Tds}{dh} = \text{Const.}$$

which can be written in different equivalent forms, such as:

$$\frac{Tds}{dh} = 1 - \eta_p = \text{Const} \quad \text{or} \quad \frac{1 - \eta_p}{\eta_p} vdP - T ds = 0 \quad (7.1.8)$$

Note that all these equations express the existence of a proportionality between the enthalpy change of the fluid and the work or the heat dissipated by the irreversibilities.

7.1.3.2.2 Integral approach of the polytropic

The assumption that we make here is to apply the law followed by the fluid between the compressor inlet and outlet, which is of type:

$$Pv^k = \text{Const.} \quad (7.1.9)$$

k is called the polytropic coefficient of the process.

One of the great interests of the polytropic concept lies in the simplicity of equation (7.1.9), which generalizes that of isentropic $Pv^\gamma = \text{Const.}$ By varying k , it generates a large number of elementary thermodynamic processes:

$k = 0$	$P = \text{Const.}$	isobaric
$k = 1$	$Pv = \text{Const.}$	isotherm for an ideal gas
$k = \gamma$	$Pv^\gamma = \text{Const.}$	isentropic for a perfect gas
$k = \infty$	$v = \text{Const.}$	isovolume (isochoric)

7.1.3.2.3 Equivalence between the two approaches for the perfect gas

Although different in the general case, these two approaches are equivalent for the perfect gas.

For an ideal gas, the first form of equation (7.1.8) gives:

$$Tds = (1 - \eta_p)c_p dT \quad \text{or} \quad ds = (1 - \eta_p)c_p \frac{dT}{T}$$

Moreover as $ds = c_p (dT/T) - r (dP/P)$, we have $\eta_p c_p dT/T - r dP/P = 0$ whose integration is straightforward and gives, if $c_p = \text{Const}$:

$$\frac{T}{P^\beta} = \text{Const.} \quad \text{with} \quad \beta = \frac{r}{c_p \eta_p} = \frac{\gamma - 1}{\gamma \eta_p}$$

With $(k-1)/k = \beta$, we find all calculations done:

$$Pv^k = \text{Const.}$$

or

$$Tv^{k-1} = \text{Const.} \quad \text{or} \quad TP^{(1-k)/k} = \text{Const.} \quad (7.1.10)$$

We thus find the form postulated by the integral approach, the polytropic coefficient k and efficiency η_p being linked by relationship:

$$\frac{k-1}{k} = \frac{\gamma-1}{\gamma\eta_p} \quad (7.1.11)$$

For adiabatic compression, the polytropic coefficient k is always greater than γ , especially since the process is irreversible.

Keep in mind that the equivalence between these two approaches is only valid for perfect gases. If the heat capacity of a gas depends on temperature, and even more on pressure, the differential form and integral form are not equivalent: if one assumes that the polytropic law is defined by the equation $Pv^k = \text{Const.}$, it is no longer true that irreversibilities are uniformly distributed. Conversely, relation (7.1.11) involving $c_p(T)$, k is no longer a constant.

PRACTICAL APPLICATION

Practical Difference Between Isentropic and Polytropic Approaches

Although they can be to a large extent considered as equivalent in a large number of cases, the polytropic approach is generally preferred to model the compression or the expansion in a multistage turbomachine, and the isentropic approach in displacement compressors, as the polytropic efficiency can be considered as an elementary stage isentropic efficiency.

It is particularly appropriate to do so if you make sensitivity analyses varying the compression or expansion ratio.

This is why gas turbine compressors and turbines are generally modeled using the polytropic reference in the examples provided with this book (Chapters 12, 13 and 16 of Part 3), and refrigeration machines using the isentropic reference (Chapter 19 of Part 3).

Differences generally exist at this level between the presentations made by authors. However, it is true that in most cases they do use in practice the polytropic under the assumption of perfect gas, so it loses some of its importance.

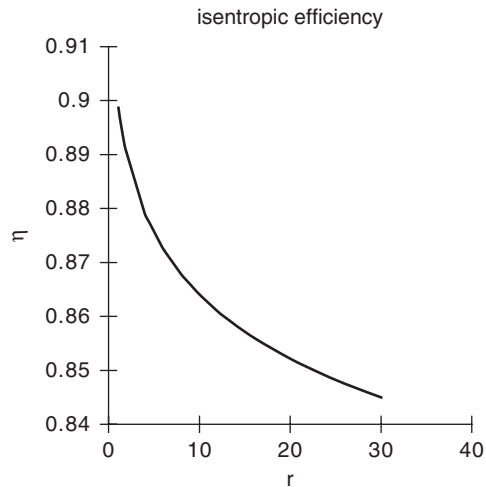
Knowing the polytropic coefficient k , it is easy to calculate the final state of adiabatic compression, and therefore the increase in enthalpy and the compression work.

For open systems, and, remember, for the perfect gas, we get:

$$\begin{aligned} \tau &= \Delta h = c_p(T_r - T_a) \\ \tau &= c_p T_a \left[\left(\frac{P_r}{P_a} \right)^{(k-1)/k} - 1 \right] = \frac{\gamma}{\gamma-1} P_a v_a \left[\left(\frac{P_r}{P_a} \right)^{(k-1)/k} - 1 \right] \end{aligned} \quad (7.1.12)$$

Note that:

$$\begin{aligned} \int_{P_a}^{P_r} v \, dP &= \frac{k}{k-1} P_a v_a \left[\left(\frac{P_r}{P_a} \right)^{(k-1)/k} - 1 \right] = \eta_p \frac{\gamma}{\gamma-1} P_a v_a \left[\left(\frac{P_r}{P_a} \right)^{(k-1)/k} - 1 \right] \\ \int_{P_a}^{P_r} v \, dP &= \eta_p \tau \end{aligned} \quad (7.1.13)$$


FIGURE 7.1.4

Isentropic efficiency function of compression ratio

The integration of vdP along the polytropic provides what might be called the “reversible polytropic work” ($\tau_p = \eta_p \tau$) of the reversible non-adiabatic process in which heat $Q = T\Delta s$ would be provided to the fluid.

Knowing the polytropic compression work, one can calculate the isentropic efficiency of the process, since we know the isentropic work τ_s . For a perfect gas:

$$\eta_s = \frac{\left(\frac{P_r}{P_a}\right)^{(\gamma-1)/\gamma} - 1}{\left(\frac{P_r}{P_a}\right)^{(k-1)/k} - 1}$$

Figure 7.1.4 shows that for a constant polytropic efficiency (here equal to 0.9), the compression isentropic efficiency decreases as the compression ratio increases.

7.1.3.2.4 Formulations for ideal gases

For an ideal gas, if one starts from differential equation (7.1.8), the calculation can be done as follows:

$$Tds = (1 - \eta_p)dh \text{ or, for closed systems, } Tds = (1 - \eta_p)du$$

$$dh = c_p dT, ds = (1 - \eta_p)c_p dT/T$$

$$\text{But as } ds = c_p(dT/T) - r(dP/P), \eta_p c_p(dT/T) - r(dP/P) = 0$$

$$ds = (1 - \eta_p) \frac{r}{\eta_p} \frac{dP}{P} = \frac{r(1 - \eta_p)}{\eta_p} \frac{dP}{P}$$

$$\int_{T_a}^{T_r} ds(t)dt = \frac{r(1 - \eta_p)}{\eta_p} \int_{P_a}^{P_r} \frac{dP}{P} \quad (7.1.14)$$

The difference in entropy is independent of c_p and T for a polytropic compression and can be expressed as

open systems:

$$\Delta s = \frac{1 - \eta_p}{\eta_p} r \ln \left(\frac{P_r}{P_a} \right) \quad (7.1.15)$$

or

closed systems:

$$\Delta s = \frac{1 - \eta_p}{\eta_p} r \ln \left(\frac{v_a}{v_r} \right) \quad (7.1.16)$$

The calculation of the outlet compression temperature T_r can be done by reversing the entropy function at discharge pressure for the value $s = s_a + \Delta s$. Knowing the inlet and outlet point states, k can then be identified by reversing $Pv^k = \text{Const}$.

If one starts from the polytropic law $Pv^k = \text{Const}$, T_r is calculated by:

$$T_r = T_a \left(\frac{P_r}{P_a} \right)^{(k-1)/k}$$

η_p is then given by:

$$\eta_p = \frac{r \ln \left(\frac{P_r}{P_a} \right)}{s_r - s_a + r \ln \left(\frac{P_r}{P_a} \right)} \quad (7.1.17)$$

These relations, which generalize equation (7.1.11) for ideal gases, are valid for any polytropic, and allow us to get k from η_p , and vice versa. They are even more interesting that, as they do not explicitly call for the $c_p(T)$ law, they can be used as a first approximation to study real gases, even if they are not strictly applicable.

To calculate the complete process, they must be completed by the equation providing the compression work. In the case of an adiabatic compression ($Q = 0$), it is very simple:

$$\tau = \Delta h$$

We will see in the next section what they become for non-adiabatic compressions.

For closed systems, we write:

$$\delta W_s = -P dv = du - T ds = \eta_p du \quad W_s = \eta_p \Delta u$$

7.1.3.3 Nonadiabatic polytropic compression

As mentioned above, it is also possible to present a polytropic process as (non-adiabatic) reversible by definition, verifying law $Pv^k = \text{Const}$., which passes through the points corresponding to the inlet and outlet.

The reversible compression work τ_r put into play in this evolution can be directly calculated from the differential equation of the polytropic, noting that, η_p being constant:

$$\delta \tau_p = v dP = dh - T ds = \eta_p dh \quad \text{which integrates directly to give } \tau_r = \eta_p \Delta h$$

Since the actual compression work $\tau = \Delta h$ is equal to τ_r/η_p , it is reasonable to assume that the polytropic law $Pv^k = \text{Const}$ is a reversible evolution. The real process is derived by taking into account the polytropic efficiency η_p . This way of putting it thus leads, for adiabatic compression, to a formalism similar to that obtained by considering the polytropic as irreversible.

If now we consider non-adiabatic compression, it appears clearly in the differential equations (7.1.8) defining the polytropic, that parameter η_p can be considered an elementary isentropic efficiency.

Using the term efficiency to describe it is confusing, and it seems better to rename it and consider it simply as a parameter α characterizing the polytropic, representative of the distribution of enthalpy between the compression work on the one hand, and the irreversibilities and the heat exchanged on the other hand.

$$\alpha = \frac{vdP}{vdP + Tds} \quad (7.1.18)$$

For the ideal gas, the non-adiabatic reversible polytropic law $Pv^k = \text{Const}$ implies the following equality:

$$\alpha = \frac{\tau_r}{\tau_r + Q_r} \text{ with } \tau_r + Q_r = \Delta h \text{ and, as we have seen above,}$$

$$\tau_r = \alpha \Delta h$$

By introducing an efficiency η to characterize real compression irreversibilities as compared to the reversible polytropic:

$$\eta = \frac{\tau_r}{\tau_r + \pi} = \frac{\tau_r}{\tau} \quad (7.1.19)$$

with $\tau + Q = \Delta h$ and π uncompensated work.

Knowing α and η , it is possible to calculate the compression work and to deduce heat Q exchanged with the outside.

We easily get:

$$\tau = \frac{\alpha}{\eta} \Delta h$$

and

$$Q = \left(1 - \frac{\alpha}{\eta}\right) \Delta h \quad (7.1.20)$$

The relevance of considering a polytropic process as reversible by definition and of characterizing the actual compression in relation to it by its polytropic efficiency η is clear.

One might criticize this approach by noting that the physical meaning of the polytropic efficiency η is not proven and in fact that it is perhaps just an arbitrary coefficient. To answer this, note first that one verifies that if the process is adiabatic $\alpha = \eta$, and we find the previous result. We will show later that in the case of isothermal compression, which is the limit of cooled compression, η still retains the sense of an efficiency.

If the fluid is a non perfect ideal gas, the differential approach and the integral approach are not exactly the same here, but the above relations can still be used as a first approximation, provided that α varies slightly if k is constant, and vice versa.

7.1.3.3.1 Practical calculation

Direct problem

If we know the polytropic coefficient k of the process, T_r is calculated by:

$$T_r = T_a \left(\frac{P_r}{P_a} \right)^{(k-1)/k}$$

We obtain the characteristic α of the reference reversible polytropic passing by the inlet and outlet points by:

$$\alpha = \frac{r \ln \left(\frac{P_r}{P_a} \right)}{s_r - s_a + r \ln \left(\frac{P_r}{P_a} \right)} \quad (7.1.21)$$

The work of the reversible polytropic is then:

$$\tau_r = \alpha(h_r - h_a) \quad (7.1.22)$$

Knowing the polytropic efficiency η of the real process from the reversible polytropic, we can deduce the actual compression work:

$$\tau = \frac{\alpha}{\eta}(h_r - h_a) \quad (7.1.23)$$

The heat exchanged with the outside is:

$$Q = h_r - h_a - \tau = \left(1 - \frac{\alpha}{\eta}(h_r - h_a) \right) \quad (7.1.24)$$

Inverse problem

Knowing T_r , we calculate the polytropic coefficient k of the process by:

$$T_r = T_a \left(\frac{P_r}{P_a} \right)^{(k-1)/k}$$

We obtain the characteristic α of the reversible polytropic reference through the inlet and outlet relationship 7.1.21.

Knowing the heat exchanged with the outside Q , η is determined by:

$$\eta = \frac{\alpha(h_r - h_a)}{h_r - h_a + Q} \quad (7.1.25)$$

We deduce $\tau = \alpha/\eta(h_r - h_a)$.

These results generalize easily to closed systems.

Since they do not explicitly involve the $c_p(T)$ law, they can be used as a first approximation to study real gases, even if they do not strictly apply.

7.1.3.3.2 Limiting case of isothermal compression

Isothermal compression is the limiting case of a cooled compression. The gas temperature at the compressor outlet being the same as at the input, the polytropic law comes down to the ideal gas law $Pv = \text{const.}$, and $k = 1$.

By taking equations written for non-adiabatic open system compressions, we have, for ideal gas:

$$\tau_r = \alpha(h_r - h_a) = \alpha c_p T_a \left[\left(\frac{P_r}{P_a} \right)^{(k-1)/k} - 1 \right]$$

$$\text{If } k \rightarrow 1, \frac{k-1}{k} \rightarrow 0 \quad \text{and} \quad \left[\left(\frac{P_r}{P_a} \right)^{(k-1)/k} - 1 \right] \rightarrow \frac{k-1}{k} \ln \left(\frac{P_r}{P_a} \right)$$

$$\tau_r = \alpha c_p T_a \frac{k-1}{k} \ln \left(\frac{P_r}{P_a} \right)$$

$$\text{As } \frac{k-1}{k} = \frac{\gamma-1}{\gamma\alpha} \quad \text{and} \quad c_p \frac{\gamma-1}{\gamma} = r$$

We get:

$$\tau_r = r T_a \ln \left(\frac{P_r}{P_a} \right)$$

What we called non-adiabatic polytropic reversible compression work does correspond to the work obtained by direct integration of vdP with $Pv = \text{Const}$. The polytropic efficiency η is then also an efficiency in the usual sense.

7.1.4 Staged compression

In turbomachines, one often makes use of dimensionless parameters, whose values must be within relatively narrow ranges. One in particular defines the power factor

$$\mu = \frac{\tau}{U^2} \tag{7.1.26}$$

where U is the peripheral velocity of the impeller. This factor cannot exceed certain values if we want a proper functioning (in the range 0.4 to 0.5 for a centrifugal impeller, much less an axial ring).

To obtain a high discharge pressure, it would theoretically be sufficient to increase the peripheral velocity U . But the stresses induced in the metal by centrifugal force being proportional to U^2 , we are led in actual devices to limit the peripheral velocity to around 200 to 300 m/s. As the elementary compression ratio cannot exceed a certain value, achieving high compression ratios requires putting several stages in series.

By analogy with hydraulic pumps, another quantity is also sometimes used to characterize a compressor: its pressure head, $H = \tau/g$, g being the acceleration of gravity.

In positive displacement or piston compressors, this problem does not arise, and one can theoretically achieve in one section very important compression ratios. In fact, other technological problems (dead space, leaks) arise, that become predominant at high compression ratios, as will be discussed later.

Relationship (7.1.6) shows that the isentropic compression work is proportional to the suction absolute temperature. When compression is to be staged, it is interesting in terms of thermodynamics (but not necessarily economically) to cool the working fluid in a heat exchanger between two stages, by reducing its temperature to a value close to that of suction. In this case, the compression is called para-isothermal. As the number of compression stages increases, the overall process gets closer to the isotherm. Assuming that the gas is perfect, that the fluid is cooled at its initial temperature and that the isentropic efficiencies of the n stages of compression are all equal, it is possible to

show that the total compression work is minimal if the intermediate pressures are a geometrical progression of ratio equal to the overall compression n th root:

$$\frac{P_{i+1}}{P_i} = \sqrt[n]{\frac{P_r}{P_a}} \quad (7.1.27)$$

When the above assumptions are not verified, the calculation of intermediate pressures must be done iteratively, but they often differ slightly from the values given by equation 7.1.27.

PRACTICAL APPLICATION

Improvement of a Gas Turbine Performance Thanks to Intercooling

It is possible to increase the performance of a gas turbine by staging the compression and placing an intercooler between the compressors. An example is given in section 12.1.5.2 of Part 3. In this example, the main improvement is in capacity (about 30%), as the reduction of the air temperature at the compressor outlet is compensated by an increase of fuel consumption. A variant using a regenerator would allow the efficiency to be improved.

7.1.5 Calculation of a compression in Thermoptim

The definition and calculation of processes involves a series of screens that differ by the type of process in question, but which nevertheless share certain characteristics (Figure 7.1.5):

- the name of the process is set at the top left;
- at the top right are a number of options and fields used to configure the process: “open” or “closed” system, “set flow” process, “observed” process (the latter two concepts are used to drive the automatic recalculation of a project);
- the left part is used to define the inlet and outlet points. To connect a point from this screen (if not already done from the diagram editor), double-click in the corresponding name field, and select it from the list. Generally, these points are distinct, but they can be the same, for example in the case of process-points;
- Buttons such as “Calculate”, “Save,” “Close”, “Delete” and “links” are also common. The latter, displayed only if requested in the Thermoptim Global settings screen, gives access to link browsers;
- energy type can be changed by double-clicking in the corresponding field;
- the value of the mass flow is by default initialized to 1. Its unit is deliberately not specified, so the user can choose in the simulator screen to work in mg/s in g/s or kg/s depending on the problem studied, while keeping a high readability. Obviously, the results of calculations on the energies or enthalpies (respectively on powers) put into play depends on the unit selected for the flow, and can be expressed in mJ, J or kJ (respectively mW, W or kW);
- finally, a text field can document the process.

For compressions and expansions (Figure 7.1.5), the calculation options available are:

- calculations can be performed either in an open system, in which case the input variables are temperature, pressure and enthalpy, or closed system, in which case it is the temperature, volume and the internal energy;
- the compression ratio ρ can be set, in which case the outlet point pressure (or volume) is determined from that of the inlet point and the value of ρ chosen, or calculated, in which case the

FIGURE 7.1.5

Compression screen

value of ρ is evaluated from pressures or volumes of inlet and outlet points, considered as given. Whether for a compression or expansion, ρ is greater than unity;

- the process can be adiabatic or not.

When adiabatic, it can be calculated using an isentropic or polytropic reference, and is characterized by an isentropic or polytropic efficiency η_s or η_p , as defined above, between 0 and 1. In this case, the polytropic exponent k appearing in the law $Pv^k = \text{Const.}$ is calculated by ThermoOptim.

When it is non-adiabatic, the process is necessarily of the polytropic type and is based on the principles outlined section 7.1.3.3. It is characterized by the polytropic exponent k and the polytropic efficiency η_p (for compression, it is the ratio of reversible work to real work, and for an expansion it is the reverse). The heat exchanged with the outside Q is displayed in the field under the compression or expansion work ΔH or ΔU .

Take care not to confuse the polytropic efficiency η_p with the polytropic exponent k . For an ideal gas, equations connecting them are 7.1.11 or 7.5.2 depending on whether compression or expansion are involved.

Two complementary calculation methods can be selected, depending on the option which is checked at the bottom right of the screen:

- “Set the efficiency and calculate the process” causes a search of the outlet point state from the inlet point and the characteristics of the compression or expansion. If the process is non-adiabatic, the input parameters are the polytropic exponent k and the polytropic efficiency η_p . Heat exchanged Q , work put into play ΔH and the outlet point state are calculated.
- “Calculate the efficiency, the outlet point being known” identifies the value of the compression or expansion efficiency leading to the outlet state. If the process is non-adiabatic, the input parameters are the adiabatic exponent k and heat exchanged Q . The work put into play ΔH and the polytropic efficiency η_p are calculated.

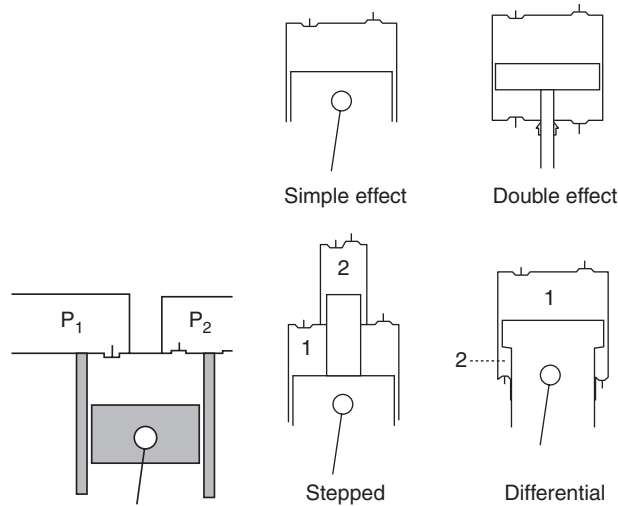


FIGURE 7.2.1
Sketch of a piston compressor

FIGURE 7.2.2
Various piston compressors (courtesy Techniques de l'Ingénieur — Génie mécanique)

7.2 DISPLACEMENT COMPRESSORS

A displacement compressor is characterized by encapsulation of the flow passing through it in a closed volume which is gradually reduced. A return of this fluid in the direction of decreasing pressure is prevented by the presence of one or more movable walls. In this type of machine, the kinetic energy imparted to the fluid usually does not play any useful role, unlike that which happens in turbomachinery.

By design, the displacement compressors are particularly suitable for processing relatively low fluid flow rates, possibly highly variable, and under relatively high pressure ratios.

Their operating principle is: a fixed mass of gas at suction pressure P_1 is trapped in a chamber of variable volume. To increase pressure, the volume is gradually reduced in a manner which differs according to the technique used. Generally, the process follows a law close to a polytropic $Pv^k = \text{Const}$.

By the end of compression, the chamber is in communication with the discharge circuit so that the compressed gas at pressure P_2 can emerge.

A new mass of gas at pressure P_1 is then sucked into the inlet pipe, and so on, the operation of the machine is cyclical. The cycle is represented on the “Watt chart” which gives the fluid pressure as the function of the chamber volume (Figure 7.2.3).

7.2.1 Piston compressors

The chamber is the volume defined by a cylinder, one of its bases being fixed and the other being a movable piston in the cylinder bore, driven by a connecting rod system (Figure 7.2.1).

The organs that control the discharge or admission are, in piston compressors, valves operated automatically by pressure differences between the chamber and the discharge or admission manifold.

One denotes V_s the volume swept by the piston between its two extreme positions, and “dead space” εV_s the minimum volume of the compression chamber. In the current achievements, ε is the order of 3 – 5%.

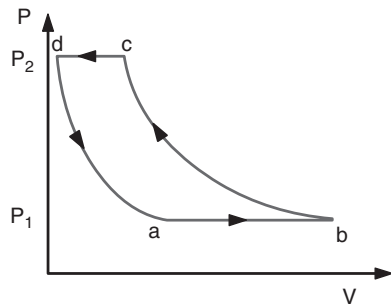


FIGURE 7.2.3
Theoretical Watt diagram

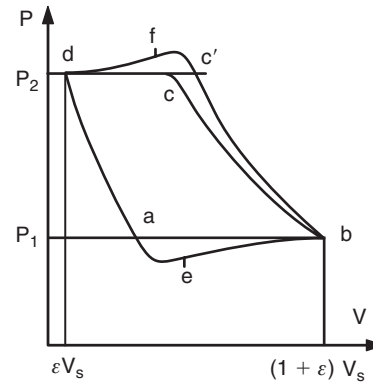


FIGURE 7.2.4
Real Watt diagram

Pistons may be of different types depending on the application. We distinguish generally (Figure 7.2.2):

- single-acting pistons, which work only on one side. Simple in mechanical terms, they have the disadvantage of having an irregular torque because there is only one compression per revolution;
- double-acting pistons, whose both faces produce useful work. The volume is twice the previous, torque is smoother, but the connecting rod system must include a piston rod in a sliding seal, which raises sealing problems;
- staged pistons contain elements of different diameters, moving in concentric cylinders. This system is very well suited for high-pressure compressors with two stages. However, the mechanical stresses are important and the torque irregular;
- differential pistons are double acting pistons of different diameters to obtain a staged compression with a high pressure cell ring. Their main disadvantage is that it is difficult to obtain a good seal at high pressure.

7.2.1.1 Theoretical energy balance

On its stroke of length L , the piston displacement sweeps V_s . If A is the cross-sectional area of the cylinder, one clearly has: $V_s = AL$.

The chart in Figure 7.2.3 is used to describe the machine cycle by four processes:

- a – b: intake of fluid mass (Δm), which mixes with that (Δm_0) already contained in the dead volume;
- b – c: isentropic compression of fluid mass ($\Delta m + \Delta m_0$) to state 2;
- c – d: expulsion of mass Δm ;
- d – a: isentropic expansion of mass Δm_0 to state 1.

Note that the mass of fluid in the chamber is not the same in the four phases of the cycle and that this will have to be taken into account when setting balances.

In the theoretical cycle we assume that the fluid undergoes no change of state during the intake (a – b) and discharge (c – d) phases. Another major simplification is to admit that the two evolutions (b – c) and (d – a) are isentropic.

Under these conditions, the thermodynamic cycle undergone by mass Δm_0 trapped in the dead volume is limited to one round trip between isentropic states 1 and 2, which does not involve any net work.

The assimilation of the fluid to a perfect gas leads to the law $Pv^\gamma = \text{Const.}$ and allows integration of the cycle work on the evolution 1–2. Expression (7.1.5) becomes:

$$\tau_s = P_1 v_1 \frac{\gamma}{\gamma-1} \left(\left(\frac{P_2}{P_1} \right)^{(\gamma-1)/\gamma} - 1 \right) \quad (7.2.1)$$

Note that it is this expression that must be used, even if the compression is done in a closed system, because of the existence of the intake and discharge phases, occurring in open systems, and involving transfer work $\Delta(Pv)$.

7.2.1.2 Actual piston compressor cycle

Compared to the theoretical cycle just described, the actual Watt chart has a number of differences (Figure 7.2.4).

- valves do not maneuver instantly and only at points marked e and f are they at their maximum aperture, and even then they create throttling. It follows that the pressure is less than P_1 during the intake stroke, and greater than P_2 for the discharge stroke;
- the compression curve (b-c') does not follow the perfect adiabatic. Irreversibilities increase the entropy of the gas, and, for a given pressure, its specific volume. Point c' is at the right of the theoretical c. It is characterized either by a polytropic law of exponent k, or by an isentropic efficiency η .

For all these reasons, the actual work is greater than the theoretical work. There are also other losses not mentioned above: they are due to wall thermal actions, where the temperature stabilizes at a value intermediate between that of the suction and discharge T_1 and T_2 , creating a “thermal shunt” that allows heat to pass from the heated fluid (on discharge) to the cold fluid (on admission), which is an additional irreversibility.

7.2.1.3 Determination of work per cycle

Relation (7.2.1) is not sufficient to calculate the efficiency of a real machine, and it is necessary to rely on experimental results. Lacking a theory capable of determining the quantitative impact of all irreversibilities, one can just generally define the real internal compressor work τ compared to the isentropic work τ_s calculated from the technological reference magnitude: the swept volume V_s (displacement).

If the phenomena were reversible, a compressor of swept volume V_s would contain, in the absence of any dead volume, useful mass V_s/v_1 . But mass $\Delta m_0 = \varepsilon V_s/v_2$ is recirculated due to the presence of dead space, and the useful mass becomes:

$$\begin{aligned} \Delta m_{\text{th}} &= (1 + \varepsilon) \frac{V_s}{v_1} - \Delta m_0 = \frac{V_s}{v_1} \left(1 - \varepsilon \left(\frac{v_1}{v_2} - 1 \right) \right) \\ \Delta m_{\text{th}} &= \frac{V_s}{v_1} \left(1 - \varepsilon \left(\frac{P_2}{P_1} \right)^{1/\gamma} - 1 \right) \end{aligned} \quad (7.2.2)$$

This relation shows that the more the compression ratio increases, the more important is the mass that recirculates and the more the useful mass decreases. There is therefore a maximum compression ratio beyond which the compressor runs without effect. Piston compressors have the advantage of working with variable compression ratios, and even automatically adjust over wide operating ranges, but at the cost of a decrease in their efficiency when the compression ratio exceeds a certain limit.

In fact, the useful mass is less than the value given by equation 7.2.2, due to many technological imperfections. To characterize it, we introduce the concept of volumetric efficiency λ , defined as the ratio of the mass flow actually discharged to the theoretical mass flow, the latter being referred either to the swept volume, or to Δm_{th} depending on the authors. We retain here the first definition, which leads to:

$$\Delta m = \lambda \frac{V_s}{v_1} \quad (7.2.3)$$

Introducing the isentropic efficiency η_c (often called compression efficiency or indicated efficiency) and the mechanical efficiency η_m , characteristic of friction in the compressor, the specific compression work is usually written:

$$\tau = \frac{\tau_s}{\eta_c \eta_m}$$

and the compression work per cycle is:

$$\Omega = \Delta m \tau = \frac{V_s}{v_1} \frac{\lambda}{\eta_c \eta_m} \tau_s \quad (7.2.4)$$

If N is the rotation speed (expressed in revolutions per minute), the compression power (assuming one cycle per revolution) is given by:

$$P_c = \frac{N\Omega}{60} = \frac{N}{60} \frac{V_s}{v_1} \frac{\lambda}{\eta_c \eta_m} \tau_s \quad (7.2.5)$$

The compression power is expressed as a function of volumetric efficiency λ , representing the compressor filling losses, compression efficiency η_c , characteristic of the deviation of actual process compared to the isentropic, and mechanical efficiency η_m .

7.2.1.4 Volumetric efficiency λ

Note that λ differs from the other efficiencies, since it appears in the numerator of relations 7.2.4 and 7.2.5. Although one is used to calling it volumetric efficiency, its meaning is very different: it represents the fraction of the displacement that produces a useful effect. Low volumetric efficiency is not inherently disadvantageous in terms of energy: it simply means that the mass flow passing through the compressor is less than that theoretically corresponding to the displacement. However, it is economically disadvantageous, since for a given specification, it leads to oversizing of the cylinder, and thus to a higher investment.

Analysis and experimentation (see section 36.1 of Part 5) have shown that λ corresponds to losses due to various origins: dead space, pressure drop in the intake and discharge manifolds, wall effects (thermal shunt), sealing defects (at the piston rings), and finally pressure drop in the inlet and outlet valves.

Overall, these losses combine to make the volumetric efficiency decrease substantially linearly with the compression ratio:

$$\lambda = 1 - \alpha \frac{P_2}{P_1} \quad (7.2.6)$$

α value is between 0.02 and 0.07.

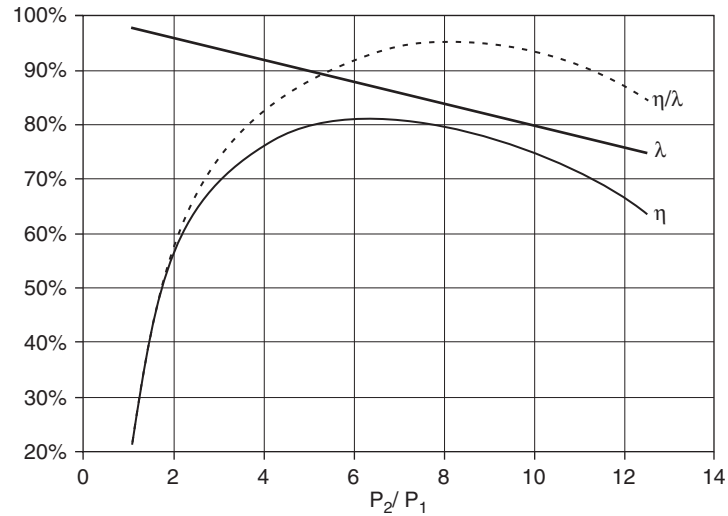


FIGURE 7.2.5

Volumetric and compression efficiencies

7.2.1.5 Compression efficiency η

The norm in the profession is to call compression efficiency the usual isentropic efficiency.

In a piston compressor, three sources of losses, connected to the previous ones, mainly affect the compression efficiency (see section 36.1 of Part 5). Wall effects are very disadvantageous because, as illustrated by the Watt chart in Figure 7.2.4, they seriously increase the compression work by twisting to the right (b-c') the isentropic (b-c). Pressure drop in valves are next, followed by losses due to sealing leakages.

At a given speed the shape of the compression efficiency as a function of the compression ratio shows the existence of a maximum around a rather low compression ratio (3-5). A relation of the Dehause type can be used when no constructor data are available:

$$\eta = 0.9 - 0.004 \left(\frac{P_2}{P_1} - 5 \right)^2 - \frac{0.5}{\frac{P_2}{P_1} - 0.3} \quad (7.2.7)$$

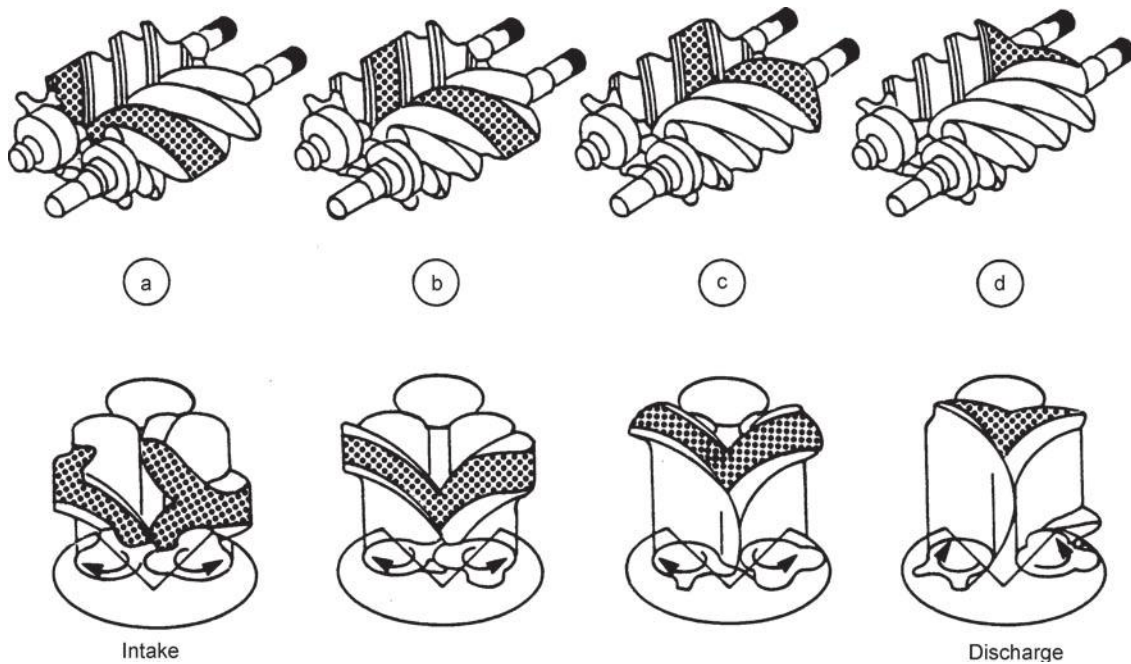
Volumetric and compression efficiencies intervening only by their ratios in the expression of work per cycle Ω , we can represent η/λ according to the compression ratio. We get for a given range of compressors a set of relatively grouped curves, each curve corresponding to a suction temperature. Figure 7.2.5 shows the curves giving volumetric efficiency λ (thin lines), compression efficiency η (bold line), and their ratio η/λ (dashed).

7.2.1.6 Practical calculation of a piston compressor

We first determine the inlet conditions (P_1, v_1) and the fluid mass flow \dot{m} . We deduce the theoretical volume flow $\dot{V}_{th} = \dot{m}v$ which must enter the compressor.

The pressure ratio r being known, manufacturer's charts provide the values of η_c and λ . We deduce the actual volume flow rate to be transferred:

$$\dot{V} = \frac{\dot{V}_{th}}{\lambda} \quad (7.2.8)$$

**FIGURE 7.2.6**

Screw compressors (courtesy Techniques de l'Ingénieur — Génie mécanique)

Knowing the swept volume V_s of each compression unit and the compressor rotation speed, we can select the most appropriate machine in the range.

The compression power is equal to the product of specific work $\tau = \tau_s/\eta_c$ by the mass flow, τ_s , being determined by application of an appropriate equation of state, or by a reading on a thermodynamic chart, or from ThermoOptim.

The mechanical losses are then added to the compression power, to provide the total power consumption. These mechanical losses are taken into account either by a mechanical efficiency, or by a fixed value equal to the unloaded drive power.

7.2.2 Screw compressors

In screw compressors, compression is achieved by varying the volume between two rotors of appropriate shape, enclosed in a particular cylinder (Figure 7.2.6).

The two rotors, or mobiles, have mating profiles, one forming lobes (male rotor), and the other cells (female rotor). These profiles are developed along the axis with a fixed pitch screw. The cylinder has a section formed by two intersecting circles. It surrounds the rotors with a very small clearance to minimize leakage. Ports are arranged at the inlet and outlet to allow transfer of fluid. There is no valve here.

The number of lobes and alveoli not being the same, both screws rotate at different speeds, which has the effect of moving axially their line of contact by pushing the enclosed fluid. After aspiration (end of phase a in Figure 7.2.6), the cell volume of trapped gas is gradually reduced (phases b and c) until the rotation of the rotor discovers the exhaust hole. The discharge then continues to complete drain (phase d).

In this type of compressor rotors are synchronized either by gears or by mutual mechanical drive. In the latter case, it is imperative to carefully lubricate the contact line between the male and female

lobes, which is done by injecting a liquid that can be oil or water, or, for refrigeration applications, the refrigerant in the liquid state. This injection, performed in relatively large quantities (about ten liters of oil per m^3 of gas sucked), is also used to seal and cool the compression to approach an isothermal operation, better in energy terms as we have seen in section 7.1.2.1. However, it is then necessary to separate the liquid from the compressed gas, which requires special equipment and leads to additional pressure drop.

7.2.2.1 Compression efficiency

In screw compressors, as also in the vane or lobe compressors, the compression ratio is determined by the geometry of the machine, which determines the internal volume ratio $V_i = V_1/V_{2c}$, construction volumetric ratio that can only be modified by acting on the shape of the exhaust opening (the index c refers to the constructional structural characteristics).

It follows that their compression ratio is fixed and the machine does not automatically adjust to different compression ratios, as do reciprocating compressors with valves. However, the absence of valves is an advantage in terms of maintenance, the latter being mechanically highly stressed parts.

If the discharge pressure P_r is less than the constructive pressure P_{2c} , rapid expansion from P_{2c} to P_r occurs at the opening of the exhaust port. Otherwise, there is sudden compression of the gas cell from P_r to P_{2c} , then discharge at this pressure.

In both cases, this induces a loss, which can be evaluated as follows.

The compression work is equal to the sum of the transfer work $\Delta(Pv)$ and external forces $W_A = -\int_1^2 P dv$:

$$\tau = \int_{v_1}^{v_{2c}} P dv + P_r v_{2c} - P_1 v_1$$

Introducing the internal pressure ratio π_i , given by:

$$\pi_i = V_i^k \quad (7.2.9)$$

k being the compression polytropic exponent, and with $\rho = P_r/P_1$, we get:

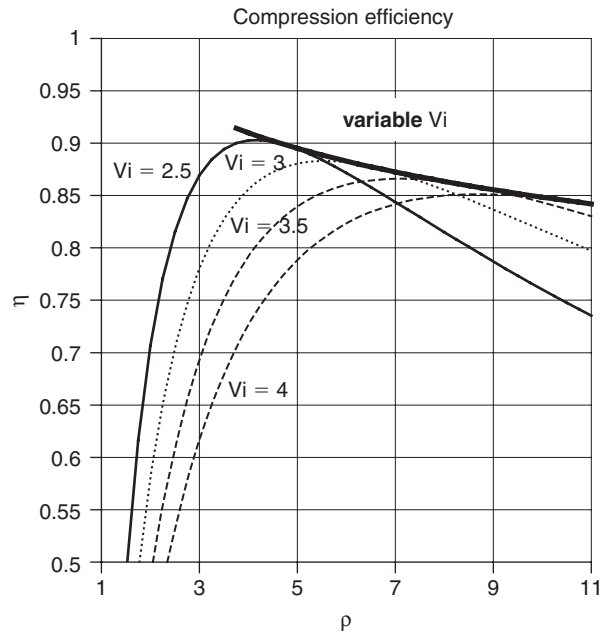
$$\tau = \frac{P_1 v_1}{k-1} \left[\pi_i^{(k-1)/k} + \frac{\rho}{V_i} (k-1) - k \right]$$

The compression efficiency is then:

$$\eta_s = \frac{\frac{\gamma}{\gamma-1} P_1 v_1 [\rho^{(\gamma-1)/\gamma} - 1]}{\frac{P_1 v_1}{k-1} \left[\pi_i^{(k-1)/k} + \frac{\rho}{V_i} (k-1) - k \right]}$$

$$\eta_s = \frac{\frac{(k-1)\gamma}{\gamma-1} [\rho^{(\gamma-1)/\gamma} - 1]}{\left[\pi_i^{(k-1)/k} + \frac{\rho}{V_i} (k-1) - k \right]} \quad (7.2.10)$$

However screw compressors have the advantage of being able to vary the internal volume ratio V_i , through a sliding drawer, which alters the discharge port. The “ V_i ” can thus vary continuously within a range of values around 2.2 to 5, depending on the power and the pressure ratio required.

**FIGURE 7.2.7**

Compression efficiency

Figure 7.2.7 gives the compression efficiency curves for fixed and variable V_i compressors. It shows that for a given internal pressure ratio π_i , the compression efficiency varies slightly with the operating compression ratio, with a maximum at $P_2/P_1 = \pi_i$.

However, the curve is fairly flat, so that a screw compressor maintains a proper efficiency even for compression ratios well above the nominal value. Given the shape of the curve, much steeper on the left than on the right, the operating point is chosen slightly right of the optimum, to maintain good efficiency even in case of disturbance of the operating regime.

Figure 7.2.7 also shows the efficiency gain that can be expected if one adopts a variable V_i . The counterpart is an increased compressor cost, due to the presence of the sliding drawer. For refrigeration installations where power control drawers already exist, the addition of a V_i variation drawer is generally justified.

7.2.2.2 Volumetric efficiency

The volumetric efficiency λ of screw compressors is much better than that of piston engines, for the following reasons:

- The expansion loss due to the dead space is very low because it is small;
- the pressure drop at suction and discharge is low due to the absence of valves;
- there is no thermal bridge: in steady state, the machine temperatures remain stable;
- conversely, losses due to sealing defects may be more important because of the length of the section leakage and difficulties of sealing the ends.

The volumetric efficiency depends on the compression ratio and the internal pressure ratio π_i . It varies almost linearly with the compression ratio, from a value of 0.98 or 0.99 for a compression ratio equal to 1, to values of 0.75 or 0.8 for compression ratios up to 20. With a variable V_i , excellent volumetric efficiencies are obtained over a very wide range.

The practical calculation of a screw compressor is done similarly to that of a piston compressor. Once the design V_i is determined, a comparison is made between the performance of variable V_i

and the machine in the manufacturer's range with the nearest V_i . The choice is then made according to the extra cost of the sliding drawer and its control.

7.2.3 Criteria for the choice between displacement compressors

Since the communication with the compression chamber is done through the automatic valve whose opening is triggered by the pressure difference on their faces, piston compressors can work at variable pressures. They can therefore operate through self-adaptation according to inlet and outlet conditions on a wide compression range.

Screw compressors however generally perform better than reciprocating compressors, if they are provided with a sliding drawer.

However, each of them corresponds to rather different capacity ranges.

In general, reciprocating compressors are suitable for low capacity (less than 75 kW mechanical drive), while screw compressors can match compression power of the order of 1 MW or greater.

Screw compressors are more expensive because they are more difficult to manufacture and the cost also increases with the sliding drawer and its control.

Reciprocating compressors are limited in pressure ratio, as we have seen, and do not tolerate the presence of liquid at the suction. On these two points, screw compressors have advantages.

7.3 DYNAMIC COMPRESSORS

7.3.1 General

Unlike positive displacement machines where the fluid is enclosed in a closed volume, in a dynamic compressor, a continuous flow of fluid takes place to which energy is communicated through moving blades driven by a rotor.

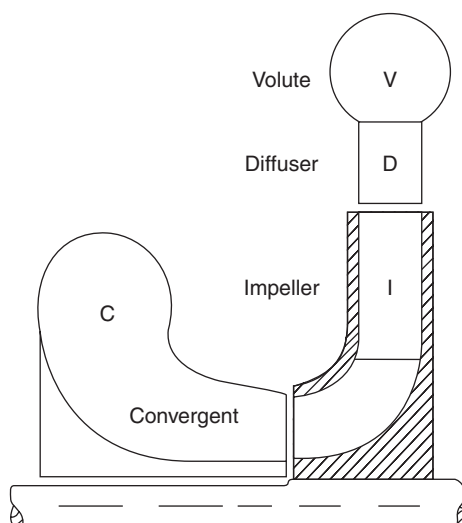
In this chapter we limit our ambition to establish the main results that are needed to understand the operation of dynamic compressors, and, given that the operation of the expansion turbines is quite similar to that of dynamic compressors, we will directly put up a number of results valid for all turbomachinery.

There are two main types of fluid flow relative to the rotor of a turbomachine: axial flow, almost always performed in turbojet dynamic compressors, and radial flow which is widely used for centrifugal dynamic compressors, including for refrigeration or automobile engine supercharging.

We will always consider the technical fluid to be compressible, either an ideal gas or a condensable real fluid. Consequently, the phenomena are governed by the fundamental laws of steady compressible flows which we begin by establishing in section 7.3.2. We will show that by varying the velocity of a gas, it is possible to change its pressure.

In general, a turbomachine consists of four elements in series (Figure 7.3.1).

- an inlet convergent C, or distributor, which is a fixed part whose function is to properly orient the fluid veins entering the impeller, and accelerate them slightly;
- the impeller I, or rotor, driven by a rotational movement around an axis. This wheel has vanes defining channels between which the fluid flow is distributed. It communicates to the fluid the mechanical energy of the blades in the form of kinetic, heat and pressure energy;
- the diffuser D is a fixed component that serves to transform in pressure part of the kinetic energy gained by the fluid when passing through the wheel. Depending on circumstances, the diffuser may or not involve blades. It is said to be partitioned or smooth;
- a volute V, also fixed, corrects the fluid lines on the periphery of the wheel, and guides them to the device outlet.

**FIGURE 7.3.1**

Sketch of a centrifugal compressor

For the reasons discussed in section 7.1.4, turbomachinery frequently has several stages, each having a limited pressure head. This is called multistage turbomachinery.

In axial turbomachinery, successive stages are juxtaposed by compact groups in which the volute is no longer necessary, and where the convergent and the diffuser situated between two moving wheels can be combined to form a single crown whose role is to straighten the fluid lines so they appear correctly on the input of the second impeller. Under such conditions, the middle stages have only two components.

It also happens that, for reasons of simplicity, a turbomachine even single staged may be composed of but two components, one fixed and one mobile.

In a turbine, it is essential to have expansion and guide nozzles at the inlet of the impeller, while the diffuser plays a secondary role and may eventually disappear.

In a dynamic compressor, conversely, the wheel inlet guide plays a secondary role in the recovery of the outlet kinetic energy. We can possibly suppress the inlet distributor.

7.3.2 Thermodynamics of permanent flow

In the previous sections, we assumed the kinetic energy variations of fluids undergoing processes were negligible, which allowed us to eliminate dK in our calculations. In dynamic compressors, this assumption is no longer valid, the practical effect being obtained by converting into pressure the kinetic energy of the fluid.

7.3.2.1 Compressible perfect fluid in steady-state

We restrict ourselves initially to the case of steady flows where the absolute pressure and the three velocity components are assumed to be constant over time. The flow occurs in fixed pipes, which implies the absence of moving walls. These conditions are obtained in the convergent and the diffuser of a turbomachine.

We assume initially the fluid is perfect from the hydrodynamic point of view, that is to say without viscosity (note that an ideal gas is not necessarily a perfect fluid from this point of view).

We obtain the law of a compressible fluid flow applying the first law of thermodynamics to a stream tube, taking into account the forces of gravity in calculating the enthalpy.

According to (5.4.7), we have: $\delta\tau = v dP + dK + g dz + \delta\pi$

The walls being fixed, $\delta\tau = 0$, and the fluid being perfect, $\delta\pi = 0$.

We have thus: $dK + v dP + g dz = 0$

which, in integral form, reads:

$$\frac{C^2}{2} + \int v dP + g z = \text{Const.} \quad (7.3.1)$$

This relationship is a generalization of the Bernoulli's equation of incompressible flows, which corresponds to the particular case when $v = \text{Const.}$

$$\frac{C^2}{2} + \frac{P}{\rho} + g z = \text{Const.}$$

In the form (7.3.1), it shows that even in the case of a reversible process, the flow law is complex because it depends on many factors (the initial state of the fluid, the final pressure, the external heat exchange).

Relationship (7.3.1) has been established in the case of an absolute steady flow. It can be generalized in the case of a relative steady flow, where the pressure and velocity values are fixed at every point of a system driven by a uniform movement. These are the conditions encountered in the impeller of a turbomachine.

This requires us to express that the useful work is equal to 0 (fixed walls), plus the work of inertial forces corresponding to the driving acceleration. These are the following laws:

- system driven by a uniform translation motion (axial turbomachinery case): driving acceleration is zero, equation (7.3.1) remains valid;
- system driven by a uniform rotation (centrifugal turbomachinery case): the acceleration drive is radial, and the work of the corresponding centrifugal inertia force is $\Delta \omega^2 R^2/2$. Posing $U = \omega R$, drive velocity, equation (7.3.1) becomes:

$$\frac{C^2 - U^2}{2} + \int v dP + g z = \text{Const.} \quad (7.3.2)$$

7.3.2.2 Viscous steady compressible fluid

Viscosity changes the above relations only slightly. The useful work remains zero, the walls being stationary, and the work of viscous forces is zero, if one applies the first law to a vein extending to the wall, because the velocity of a viscous fluid is always zero at the wall.

According to (5.4.7), we have: $\delta\tau = 0 = v dP + dK + g dz + \delta\pi$

We deduce:

$$\frac{C^2}{2} + \int v dP + g z + \int \delta\pi = \text{Const.} \quad (7.3.3)$$

The effect of friction is ultimately a decrease in the head. We thus find the concept of "pressure drop" π .

$$\pi = \int \delta\pi$$

In the present state of our knowledge, as we do not *a priori* know how to compute π , it is experimentally determined.

7.3.2.3 Adiabatic Flows

Basic law

In the foregoing, no assumption was made on the heat exchange of the flow with the outside, which may vary from the perfect isolation (adiabatic process), to the infinitely developed contact with a source (isothermal process).

The real changes are always very close to the adiabatic since the gases are very poor heat conductors (see 5.3.6). Therefore it is assumed that the processes are always adiabatic, the actual process being irreversible, while the theoretical reference is isentropic.

In what follows, we neglect the potential energy gz , which is perfectly legitimate, given the relatively low altitude variations of the fluid, compared to the variations of kinetic energy and enthalpy (see 5.2.1).

The fundamental law of adiabatic flow in a fixed reference follows directly from (7.3.3). It reflects the conservation of total enthalpy $h + K$, and is written along a stream tube:

$$h + \frac{C^2}{2} = \text{Const.} \quad (7.3.4)$$

Assuming further that the flow is reversible adiabatic ($ds = 0$) then:

$$\begin{aligned} dh &= v dP, \quad \text{and} \\ v dP + C dC &= 0 \end{aligned} \quad (7.3.5)$$

It is possible to change the fluid pressure acting on its velocity and vice versa.

In the case where the reference is no longer fixed, but driven by a relative permanent rotation movement of drive velocity $U = \omega R$, the relation is written:

$$\frac{C^2 - U^2}{2} + h = \text{Const.} \quad (7.3.6)$$

or

$$v dP + C dC - U dU = 0 \quad (7.3.7)$$

This relation shows that in a dynamic compressor rotor, compression can be achieved by reducing the fluid velocity C or increasing the driving velocity U . In an axial compressor, the diameter of the wheel is approximately constant, and the first effect is dominant, while a centrifugal compressor is able to combine both, which allows it to provide much higher compression ratios in one stage.

Stagnation properties

We have already introduced in the previous section the total enthalpy $h + K$, and in section 5.3.1 the total energy $u + K$. We call stagnation pressure the pressure P_i indicated by a Pitot tube placed in an perfect gas flow, and stagnation temperature the isentropic temperature T_i measured by a thermometer placed in a flow so that the process bringing the flow to rest in front of the thermometer would be isentropic.

Given (7.3.4),

$\Delta h = C^2/2$ and the gas being perfect, we have: $\Delta h = c_p \Delta T$

The total or stagnation temperature is given by:

$$T_i = T + \frac{C^2}{2c_p} \quad (7.3.8)$$

The isentropic equation (5.6.8) gives the stagnation or total pressure:

$$PT^{\gamma/(\gamma-1)} = \text{Const.} \quad \text{or} \quad P_i = P \left(\frac{T_i}{T} \right)^{\gamma/(\gamma-1)}$$

Introducing the flow Mach number:

$$\text{Ma} = \frac{C}{\sqrt{\gamma r T}} \quad \text{and noticing that: } c_p = \frac{\gamma r}{\gamma - 1}$$

we get:

$$P_i = P \left(1 + \frac{\gamma - 1}{2} \text{Ma}^2 \right)^{\gamma/(\gamma-1)} \quad (7.3.9)$$

These two relationships are interpreted as follows: in any isentropic flow of a perfect gas in a tube with fixed walls, the stagnation temperature and pressure are conservative.

In addition, the value of the stagnation properties is that they allow us to write the equations governing the flow by formally removing the velocity C , which greatly simplifies the expression.

Varying the section of a vein

Let us study what should be the section variation of a fluid stream undergoing an adiabatic expansion or compression in a reversible manner. In what follows, we assume that the fluid is a perfect gas.

In order for the flow to be reversible and adiabatic, three equations must simultaneously be verified:

- the continuity equation, which indicates that the flow is constant in any section of the flow;
- If S is the section, \dot{m} being the fluid flow, we get $SC/v = \dot{m}$;
It comes: $dS/S + dC/C = dv/v$
- the isentropic equation $Pv^\gamma = \text{Const.}$;

Combined, and introducing the Mach number Ma , the first two equations lead to:

$$\frac{dS}{S} = \frac{v dP}{C^2} (1 - \text{Ma}_a^2) \quad (7.3.10)$$

- the kinetic equation (7.3.5) $v dP + C dC = 0$.

These last two equations, for various sonic operation modes, allow one to simply analyze the changes in pressure and velocity in the convergent and divergent, as shown in Figure 7.3.2.

This shows that, for subsonic flow, compression corresponds to a deceleration of the fluid, and expansion corresponds to an acceleration, while the reverse is true for supersonic regimes.

We find a well-known result of fluid mechanics: a sonic nozzle must be comprised at the throat inlet by a convergent of decreasing section, and at the throat outlet by a diverging increasing section. We call such a converging-diverging nozzle configuration a Laval nozzle (Figure 7.9.1).

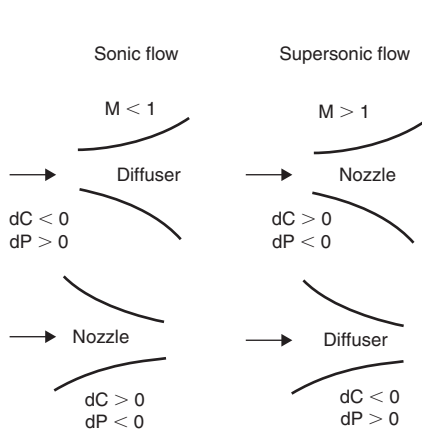


FIGURE 7.3.2
Adiabatic flow geometries

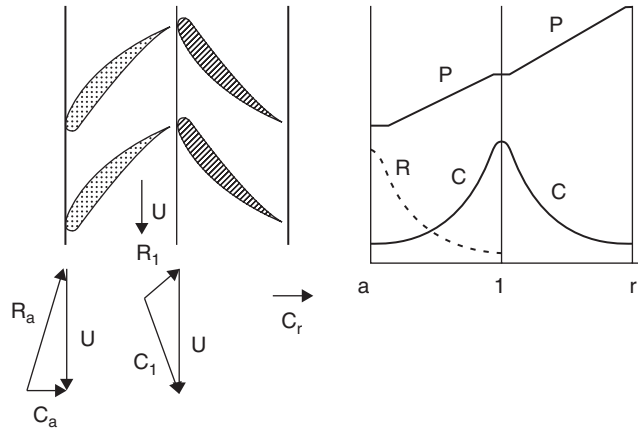


FIGURE 7.3.3
Velocity profile in an axial compressor

7.3.2.4 Changes in pressure and fluid velocity in a compressor

In a dynamic compressor, the evolution of the fluid is increased pressure, which, for a subsonic regime, requires that the section of the vein is increasing, while the velocity decreases. Evolution is a two time process (Figure 7.3.3): in the impeller, the relative velocity drops sharply, while the absolute velocity increases. The stator (diffuser) then slows the absolute velocity down.

To analyze in detail the operation of dynamic compressors, it would be necessary to make a detailed kinematic study of the evolution of fluid through the various organs.

Developments that would require such an analysis do not seem justified given our approach, oriented rather on systems than components, so we content ourselves at this stage to present the principle of these calculations, before considering the overall performance of compressors, based on dimensionless analysis. Further analysis will be provided in Chapter 37 of Part 5. We refer interested readers to the books of L. Vivier (1965) and M. de Vlaminck & P. Wauters (1988) cited in the bibliography.

We denote with index a the fluid suction, r the discharge, 1 the rotor output, and R is the relative velocity.

In the impeller, the application of (7.3.6) gives:

$$2(h_1 - h_a) = (U_1^2 - U_a^2) + (R_a^2 - R_1^2)$$

In the diffuser:

$$2(h_r - h_1) = C_1^2 - C_a^2$$

Summing, we get:

$$2(h_r - h_a) = (U_1^2 - U_a^2) + (R_a^2 - R_1^2) + (C_1^2 - C_a^2)$$

Since C_r is somewhat equal to C_a , one can write:

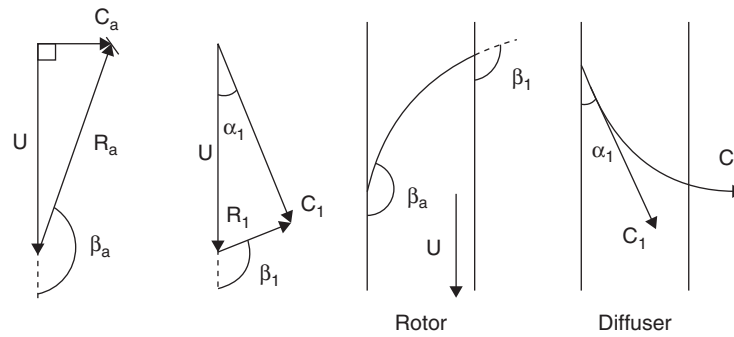
$$2(h_r - h_a) = U_1^2 + C_1^2 - R_1^2 - (U_a^2 + C_a^2 - R_a^2)$$

However, as shown in the velocity triangle (Figure 7.3.3):

$$\vec{R} = \vec{C} - \vec{U} \quad \text{and} \quad R^2 = C^2 + U^2 - 2\vec{U} \cdot \vec{C}$$

$$\tau = h_r - h_a = \vec{U}_1 \cdot \vec{C}_1 - \vec{U}_a \cdot \vec{C}_a \quad (7.3.11)$$

This relationship is Euler's theorem, which connects the enthalpy change and thus the useful work to the velocity profile in the compressor.

**FIGURE 7.3.4**

Velocity triangle

In an axial compressor, the drive velocity being substantially the same at the inlet and outlet of the wheel, this relationship is simplified, and yields:

$$\tau = h_r - h_a = \vec{U} \cdot (\vec{C}_1 - \vec{C}_a) \quad (7.3.12)$$

Generally one makes sure that \vec{C}_a be perpendicular to \vec{U} at the inlet of dynamic compressors, so that these relations become simpler yet:

$$\tau = \vec{U}_1 \cdot \vec{C}_1 \quad (7.3.13)$$

Velocity triangle and shape of the blades

Euler's relation is used to define the profile of the blades: in order for the fluid to flow in the rotor with the least possible irreversibilities, shocks must be avoided, whether from discontinuities in the fluid streams or from shock waves which can propagate if the velocity is too high. The thermodynamics of flows finds here one of its limits: the exact shape of the blade profile calls upon fluid mechanics and is thus outside the scope of this presentation. We will just give some indication of the results, only for axial compressors.

Given the Euler relationship, we seek to maximize the scalar product $\vec{U}_1 \cdot \vec{C}_1 = UC_1 \cos \alpha_1$. Therefore angle α_1 must be as small as possible.

Suppose the drive velocity U is known. To avoid shock in the blades, the relative velocity vector \vec{R} must at all times be parallel to blades, which sets its angle β with the drive velocity \vec{U} .

Entry speed C_a being perpendicular to \vec{U} , the inlet velocity triangle immediately gives angle β_a and defines vector \vec{R}_a .

At the outlet we obtain similarly β_1 and \vec{R}_1 , knowing that the absolute velocity \vec{C}_1 must generally remain subsonic to avoid shock in the diffuser vanes.

By continuity the blade profile can be plotted (Figure 7.3.4).

However as discussed later, technological issues lead manufacturers to choose the type of wheel and to set some reduced design parameters. We do not, therefore, generally know U as has been assumed here, but a number of relationships exist between the velocity triangle quantities, so that it is determined by reasoning similar to that which was just presented.

To determine the blade thickness, whose distance between them defines the cross-section available for the fluid, we must give, in addition to the Euler relation, the equation of continuity. Moreover, even more than for the profile of nozzles, it is necessary to reduce the curvature to prevent detachment of the fluid streams along the compressor blades, because the pressure gradient

exerted here is unfavorable, both in the rotor and in the diffuser. This constraint is much stronger for dynamic compressors than for turbines.

7.3.3 Similarity and performance of turbomachines

When the dynamic compressor is not working at its design conditions, performance generally suffers in larger proportion than in the case of positive displacement compressors. The reason is that dynamic irreversibilities (shock, detachment of fluid streams, etc.) are rising quite rapidly once the flow no longer corresponds to the geometry of the blades.

We will now further analyze the characteristics of turbomachinery, and the adaptation of a machine at different operating regimes. These regimes depend not only on basic variables considered in the design (N , \dot{V} , Δh), but also on the characteristic parameters of the fluid passing through the machine.

In the most common conditions, 7 independent physical variables may affect the efficiency of a turbomachine: a characteristic dimension (e.g. wheel diameter D), the rotation speed N , the fluid mass flow, the stagnation pressures at the inlet and outlet P_a and P_r and the total enthalpy at the entrance h_a and exit h_r .

As mentioned in section 7.3.2.3, we choose the stagnation properties to eliminate from the equations the fluid velocity at the entrance and exit of the machine.

Among these 7 variables are involved three basic units (M , L , T). The application of the Vaschy-Buckingham theorem reduces to $7 - 3 = 4$ the number of dimensionless variables characteristic of the operation of the machine.

The variables most commonly chosen are:

- * a flow velocity C_f Mach number:

$$(M_a)_c = \frac{C_f}{C_s}$$

with

$$C_f = \frac{\dot{m}v_a}{A} = \frac{4\dot{m}v_a}{\pi D^2} = \frac{4\dot{m}rT_a}{\pi D^2 P_a}$$

and C_s speed of sound in the fluid ($C_s = \sqrt{\gamma r T_a}$ by equating the fluid to a perfect gas), thus:

$$(M_a)_c = \frac{4\dot{m}\sqrt{rT_a}}{\pi D^2 P_a \sqrt{\gamma}} \quad (7.3.14)$$

- * a wheel Mach number

$$(M_a)_u = \frac{U}{C_s} \quad \text{with } U = \frac{\pi D N}{60}$$

$$(M_a)_u = \frac{\pi D N}{60 \sqrt{\gamma r T_a}} \quad (7.3.15)$$

- the ratio of inlet and outlet stagnation pressures:

$$\frac{P_r}{P_a}$$

- the isentropic efficiency of the stage:

$$\eta_s = \frac{(h_r)_s - h_a}{h_r - h_a} \quad \text{or} \quad \eta_s = \frac{h_r - h_a}{(h_r)_s - h_a}$$

depending on whether a compressor or a turbine.

When choosing a given machine and a particular fluid, the dimensionless numbers $(M_a)_c$ and $(M_a)_u$ become proportional to reduced variables of simpler expressions:

$$(M_a)_c \div \frac{\dot{m} \sqrt{T_a}}{P_a} = (\text{corrected mass flow } \dot{m}_c) \quad (7.3.16)$$

$$(M_a)_u \div \frac{N}{\sqrt{T_a}} = (\text{corrected rotation speed } N_c) \quad (7.3.17)$$

Other dimensionless quantities are also commonly used by manufacturers: flow factor φ and enthalpy factor ψ , or Rateau coefficients μ and δ .

The flow factor φ

It is natural to look at both Mach numbers representative of flows in the machines, $(Ma)_c$ and $(Ma)_u$. The ratio of these two quantities, independent of fluid properties, determines the shape of the velocity triangle, and corresponds to a first dimensionless property: the flow factor φ which ensures kinematic similarity over the entire flow boundaries.

$$\varphi = \frac{(M_a)_c}{(M_a)_u} = \frac{4\dot{m}\sqrt{rT_a}}{\pi D^2 P_a \sqrt{\gamma}} \frac{60\sqrt{\gamma r T_a}}{\pi D N}$$

$$\varphi = \frac{C_f}{U} = \frac{240 \dot{V}}{\pi^2 N D^3} = \frac{240}{\pi} \delta \quad (7.3.18)$$

This factor φ is proportional to another widely used dimensionless quantity: the second Rateau coefficient δ .

The enthalpy factor ψ

Turbomachinery is used either to expand a fluid to produce energy or to provide energy to a fluid. The flow being, as we noted earlier, close to adiabatic, because of low exchange surfaces and velocities, it is logical to take as a reference energy the expansion or compression isentropic work $|\Delta h_s|$.

We have:

$$|\Delta h_s| = \frac{\gamma}{\gamma - 1} P_a v_a \left[\left(\frac{P_r}{P_a} \right)^{(\gamma-1)/\gamma} - 1 \right] \quad (7.3.19)$$

The ratio of the reference energy to a well chosen kinetic energy is a dimensionless quantity of interest. A first idea is to use the speed of sound C_s . We get:

$$\frac{|\Delta h_s|}{1/2 C_s^2} = \frac{2}{\gamma - 1} \left[\left(\frac{P_r}{P_a} \right)^{(\gamma-1)/\gamma} - 1 \right] = \Omega \quad (7.3.20)$$

Usually this kinetic energy is taken equal to $1/2 U^2$, corresponding to the maximum kinetic energy in the rotor. This way of doing is equivalent to multiplying Ω by (M_a) . This defines the enthalpy factor ψ , equal to twice the first Rateau coefficient μ (itself equal to the power factor introduced in section 7.1.4).

In practice, the performance of a machine is usually given in the form of characteristic curves for constant values of the corrected rotation speed N_c :

$$\frac{P_r}{P_a} = f(\dot{m}_c) \quad \eta_s = f\left(\frac{P_r}{P_a}\right) \quad \text{or} \quad f(\dot{m}_c)$$

Curves of equal efficiency can be directly plotted on charts:

$$\frac{P_r}{P_a} = f(\dot{m}_c)$$

Sometimes, the curves are presented in relation to reference values of the corrected mass flow rate or corrected speed.

Note that the performance maps of turbomachinery (as well as displacement machines) play a unique role in that they constrain intensive variables with extensive variables, whereas usually they are independent: the flow affects the compression ratio.

Examples of experimental results are presented in the following pages, corrected flows and corrected speeds being reported to their nominal values.

7.3.3.1 Performance maps of dynamic compressors

We content ourselves in this section to present some general results concerning the performance maps of dynamic compressors, which will be completed in Chapter 37 of Part 5 on the off-design behavior of these machines.

For dynamic compressors (Figures 7.3.5 to 7.3.7) the corrected mass flow is used as abscissa. The ordinate is the pressure ratio or the isentropic efficiency. The corrected rotation speed is still used as parameter.

They have the same shape as diffuser characteristics, for different rotation speeds.

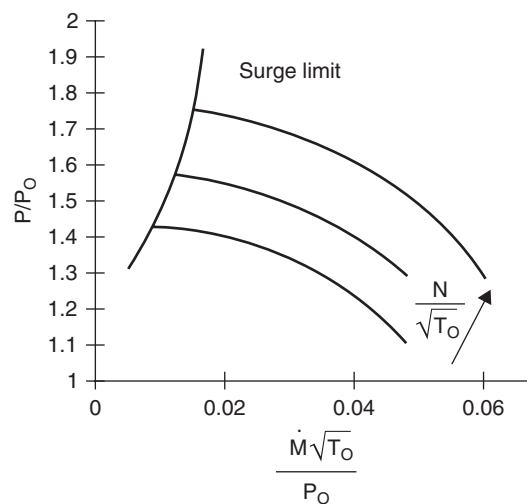


FIGURE 7.3.5

Dynamic compressor performance map

The corrected rotation speed strongly influences the performance of dynamic compressors. This is easily explained considering that in such a machine, energy is transmitted to the fluid by the rotor in the form of kinetic energy. At most, this energy is $1/2 U^2$, that is to say, is proportional to N^2 . It is therefore natural that the sensitivity of these machines to regime change is dramatic.

In addition, fluid mechanics tells us that the fluid flow in the blades is destabilized here by the pressure gradient. As soon as one deviates too much from the nominal operating conditions, there is a significant risk of stream separation along the blades. Besides a strong sensitivity of isentropic efficiency, this results in a double limitation of range of use of the machine: the risk of surge at low flow (which depends on the network in which the compressor discharges, cf. next section), and stalling on the side of higher flow rates. Some flexibility is indeed possible in this type of machine only if you can freely adjust the rotation speed and possibly the angle of incidence of certain rows of blades (guide vanes).

Axial compressors

The compression ratios per stage that can provide axial compressors are relatively low, generally between 1.2 and 2.

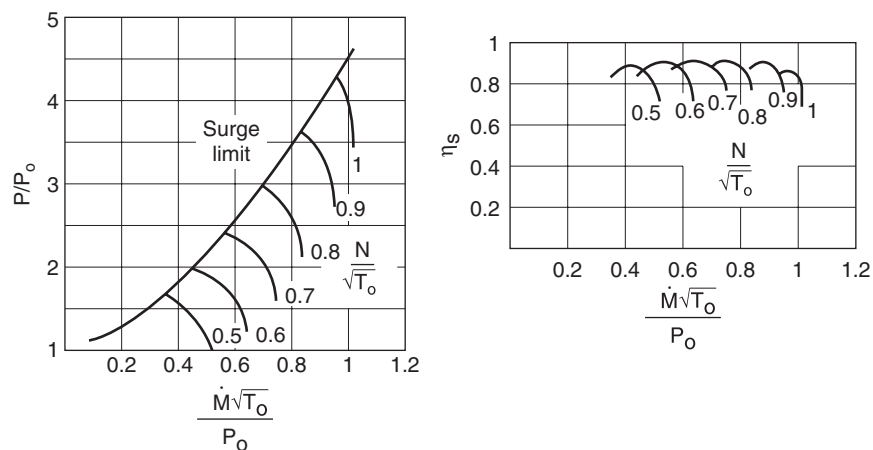


FIGURE 7.3.6

Axial compressor performance map

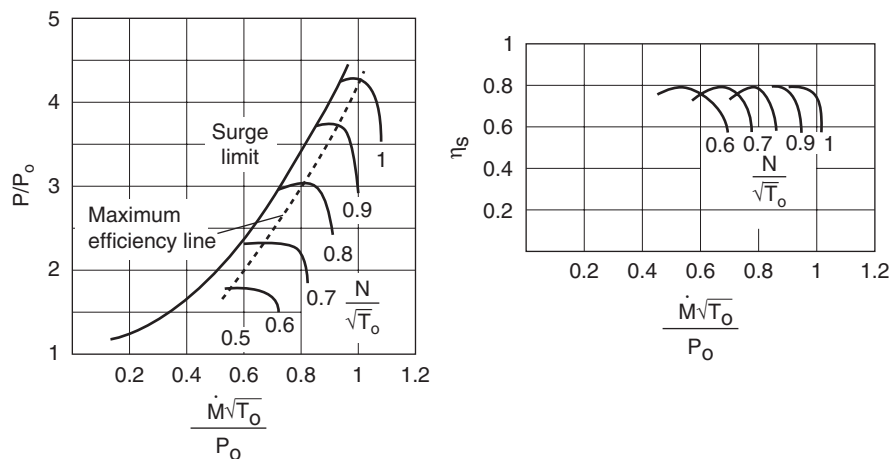


FIGURE 7.3.7

Centrifugal compressor performance map

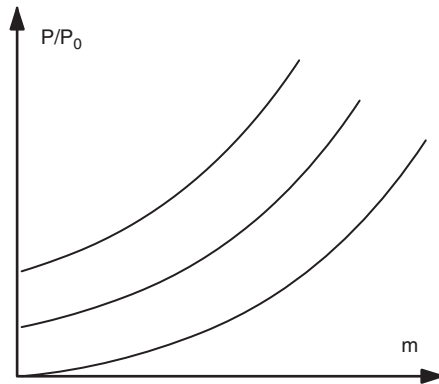


FIGURE 7.3.8
Circuit losses

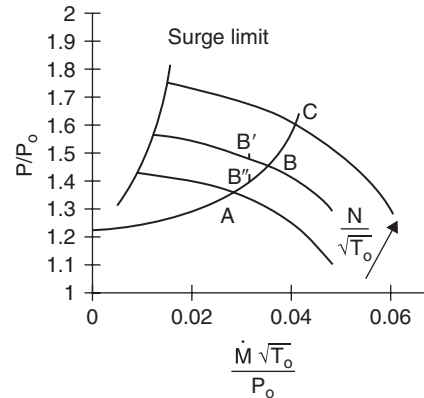


FIGURE 7.3.9
Stable operation point

Centrifugal compressors

Characteristics of centrifugal compressors are steeper than those of axial compressors, making them more stable. Due to the acceleration that the fluid receives during its passage through the rotor, the compression ratio per stage they can provide is much more important, between 2.5 and 9.

It will be noted on the characteristic of Figure 7.3.11 that we can equip the (pressure – flow) performance map by including the iso-isentropic efficiency η lines. The locus of these values corresponds substantially to portions of ellipses. They are commonly called efficiency islands.

7.3.3.2 Surge in dynamic compressors

When a dynamic compressor delivers in a receiver circuit, its operating point is determined by the intersection of its characteristic curve and that of the circuit.

The losses of the circuit being in first approximation proportional to the square of flow rate, the shape of the circuit characteristic is given in Figure 7.3.8. The ordinate intercept, sometimes called static load, corresponds to terms independent of flow in the generalized Bernoulli equation (7.3.3).

The operating point of a compressor evolves thus according to its rotation speed, so that at any time, the power dissipated in the circuit equals the shaft power of the machine, and passes from A to C when the rotation speed increases (Figure 7.3.9).

Things do not always happen as simply, as a zone of unstable operation may appear in the left part of the dynamic compressor performance map maximum for the reasons explained below.

Let us first check that a point such as B is stable (Figure 7.3.9). Suppose that the machine being in nominal operation at point B at constant speed, the flow drops suddenly. Given the shape of the characteristic of the machine, its operating point tends to move to B', while the resistance of the circuit drops to B''.

It follows that the compressor has more power (B' – B'') than that required by the resistance of the circuit, which has the effect of increasing the flow through it, and thus brings the point to B. The system is naturally stable.

If the operating point lies to the left of the compressor characteristic maximum, two cases may arise:

- if the slope of the characteristic of the circuit is greater than that of the machine, a reasoning similar to the previous shows that the system is stable.
- if, as in the chart of Figure 7.3.10 it is the compressor characteristic which is the steepest, we see that any flow-rate reduction translates into a reduction of the power of the machine faster than circuit resistance. So there is amplification of the initial disturbance, and the system is unstable. Complex phenomena occur then, depending on the mechanical inertia of the entire system. The flow rate decreases very rapidly (20 to 80 milliseconds) and may even reverse.

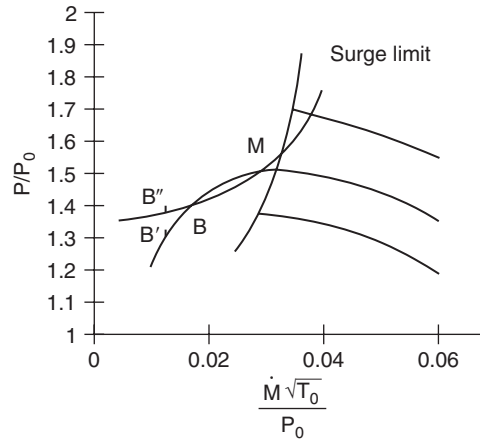


FIGURE 7.3.10

Unstable operation point

Circuit resistance falls accordingly, the discharge manifold empties and the compressor available power becomes surplus, which leads to a very rapid increase in flow. Very quickly, the point of functioning returns to the right of B' . The discharge pipe is filled, the pressure rises, and flow lowers again: cyclic conditions are met. We call this instability a surge cycle, whose period varies between 0.5 and 5 seconds. Surge is generally very detrimental to the mechanical compressor, which is subjected to intense vibration that can put rotor and stator in touch.

The phenomena involved are very complex because of the inertial effects associated with filling and emptying the collector network. They are still poorly known. So manufacturers recommend users to avoid operating in the left of the performance map maximum of their machines, bounded by the surge limit called surge line.

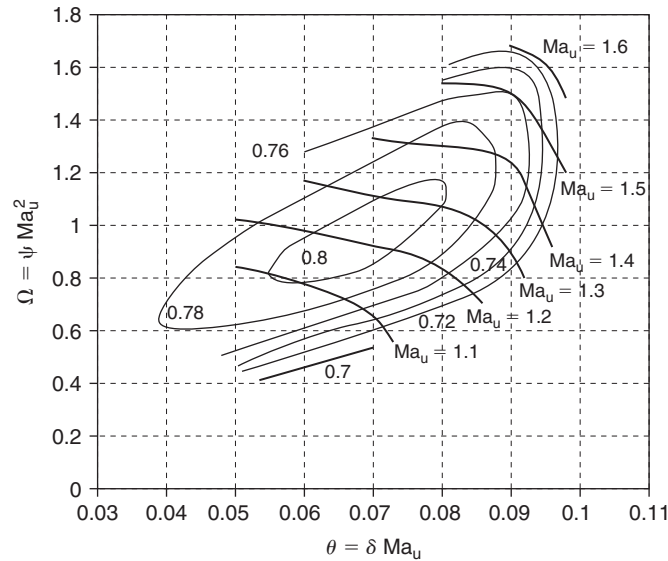
As it is not always possible to meet this constraint, it is often necessary to provide check valves at the outlet of the machine, or more complex devices when it is not enough. Instrumentation and modern control provide opportunities to detect the onset of surge, which is accompanied by changes in pressure and flow as well as in suction temperature for axial compressors. The anti-surge control must be able to react very quickly given the phenomenon speed, increasing the flow through the opening of a bypass valve.

7.3.4 Practical calculation of dynamic compressors

To be able to size their compressors quickly with sufficient accuracy, manufacturers take full advantage of the similarity rules. The main difficulty, however, is that the situation is not as simple as in the case of positive displacement compressors.

In the latter case, in fact, an entire range of machines can be represented with sufficient accuracy by the same set of charts giving the volumetric efficiency and the compression ratio as a function of compression ratio.

In the case of turbomachinery, this is approximately true, and manufacturers prefer to use a characteristic per wheel, if they want good accuracy, because the shapes of efficiency islands may vary significantly from one machine to another, even for a given range. However they use similarity rules for the flow, and, very often, performance maps are plotted in a particular system of axes, combining the enthalpy and flow factors (or Rateau coefficients) and the wheel Mach number.


FIGURE 7.3.11

Centrifugal compressor performance map

We find generally a head coefficient in the ordinate and a flow coefficient in the abscissa. York in France, a leading manufacturer of compressors for industrial refrigeration, uses as ordinate the Ω factor introduced earlier, and as abscissa a factor θ product of δ and $(M_a)_u$ and therefore proportional to $(M_a)_c$

$$\Omega = \frac{\Delta h_s}{C_s^2} = \mu (M_a)_u^2$$

$$\theta = \frac{\dot{V}}{C_s D^2} = \delta (M_a)_u$$

$C_s = \sqrt{\gamma r T_a}$ being the speed of sound at inlet and μ and δ the Rateau coefficients.

The characteristic obtained has the form given figure 7.3.11.

The practical calculation of a compressor runs as follows.

We are given the volume flow at the inlet and the desired compression ratio, as well as the suction conditions, which enables us to calculate the speed of sound C_s .

On a thermodynamic chart, using either tables or equations of state or ThermoOptim, we determine the isentropic compression work τ_s , which gives the value of Ω .

We choose *a priori* a machine i.e. a wheel diameter, which determines the value of θ .

On the performance map, it is then possible to check if the wheel chosen is well suited, that is to say if the operation point is at the right of the efficiency maximum to avoid any risk of surge.

Knowledge of the wheel coefficient μ allows us to determine the Mach number and hence the tangential velocity U .

Since $U = \pi DN/60$, the rotation speed can be deduced.

It is then possible to study the behavior at variable flow and constant speed ($(M_a)_u = \text{Const.}$), and the possible operation at part load and variable speed, to determine if the proposed operating ranges are compatible with the possibilities of the machine.

7.3.5 Pumps and fans

The mechanical and thermodynamic study of flows in pumps and fans is to a very large extent similar to that of dynamic compressors, but with an important simplification: for them it is quite legitimate to assume that the **fluid is incompressible**.

The expression for the isentropic work is considerably simplified, since $\Delta h_s = v\Delta P$ or $\Delta h_s = \Delta P/\rho$. For a pump, the data provided is generally the pressure head H , and g being the acceleration due to gravity, $\Delta h_s = gH$.

Under these conditions, a pump or fan will be represented in Thermoptim by the same component as a compressor. The steam power plant cycle model presented in section 9.1 specifically calls for such a component to represent the plant feedwater pump whose role is to compress at high pressure the cycle water condensed at low pressure.

We will not detail here the various technological solutions that exist for pumps or fans.

Note however that a critical phenomenon can occur at the pump inlet: cavitation, which occurs when the suction pressure falls below the saturated vapor pressure of the fluid at the temperature considered. No precaution is taken in Thermoptim to ensure that cavitation in a pump is prevented.

Let us recall that the conditions of non-cavitation are given by the manufacturers as a hydraulic minimum load that must exist at the pump inlet. Called the NPSHR (Net Positive Suction Head Required), it is determined experimentally and depends on the wheel rotation speed. The NPSHR equals the net positive suction height available (NPSHA) minus the absolute saturation vapor pressure of the fluid. It is expressed in meters.

The NPSHA, i.e. that which exists at the pump inlet, must exceed the NPSHR, whose value is generally determined as the threshold below which cavitation appears in the pump and degrades its efficiency by 3%.

To avoid cavitation in a pump, reduce the pressure drop in suction to prevent the tank pressure becoming too low and, in the case of a suction pump, prevent the suction height being too great.

7.4 COMPARISON OF THE VARIOUS TYPES OF COMPRESSORS

7.4.1 Comparison of dynamic and displacement compressors

Before we compare the axial and centrifugal compressors, it is interesting to situate them in relation to displacement compressors. As already mentioned, the fundamental difference between these two types of machines is that dynamic compressors operate with a constant pressure head, while displacement compressors have a constant volume ratio.

Generally speaking, dynamic compressors are well suited for compressing large fluid flows. For small flows, they must rotate at very high speeds to maintain reasonable efficiencies, which requires fragile and expensive multiplying gear. Displacement compressors are then preferable, as such problems do not arise.

A simple calculation can give an idea on the speeds required in turbomachinery.

In order for the flow to remain close to adiabatic, it is necessary that the speeds of the machines are large enough. The previous examples have shown that the magnitude of wheel Mach numbers are routinely about 1.5.

Equation (7.3.16) gives:

$$ND = \frac{1.5}{\pi} \sqrt{\gamma r T}$$

Moreover (7.3.18) provides another relationship between N and D :

$$ND^3 = \frac{4\dot{V}}{\varphi\pi^2}$$

We deduce:

$$D = 0.922 (\gamma r T)^{-0.25} \sqrt{\frac{\dot{V}}{\varphi}} \quad (7.4.1)$$

$$N = 0.518 (\gamma r T)^{0.75} \sqrt{\frac{\varphi}{\dot{V}}} \quad (7.4.2)$$

In general:

$$0.518(\gamma r T)^{0.75} \sqrt{\frac{\varphi_{\min}}{\dot{V}}} < N < 0.518(\gamma r T)^{0.75} \sqrt{\frac{\varphi_{\max}}{\dot{V}}} \quad (7.4.3)$$

For air at 300 K, and expressing N in rpm, we get:

$$20,000 \sqrt{\frac{\varphi_{\min}}{\dot{V}}} < N < 200,000 \sqrt{\frac{\varphi_{\max}}{\dot{V}}}$$

φ is between 0.01 and 0.6 for centrifugal compressors, and 0.3 and 1 for axial compressors.

For centrifugal compressors we obtain:

$$20,000 \sqrt{\frac{1}{\dot{V}}} < N < 155,000 \sqrt{\frac{1}{\dot{V}}}$$

and for axial compressors:

$$110,000 \sqrt{\frac{1}{\dot{V}}} < N < 200,000 \sqrt{\frac{1}{\dot{V}}}$$

For flow $\dot{V} = 10 \text{ l/s} = 0.01 \text{ m}^3/\text{s}$ (already a significant value), the speed should exceed 200,000 rpm with a centrifugal compressor, and 1.1 million rpm for an axial compressor, that is to say be 140 to 750 times greater than that of a piston compressor (1,500 rpm). It is clear that such speeds are totally unrealistic, which is why dynamic compressors are not used for small flow rates.

Dynamic compressors are well suited for compressing large fluid flow-rates, but only under relatively low pressure ratios.

For very large capacities (beyond a few MW on the shaft), dynamic compressors have however virtually no competitors, although the screw machines allow us to reach increasingly high capacities.

The absence of valves and many other moving parts is an important advantage for dynamic compressors which, when well balanced, are easier to maintain than displacement compressors.

7.4.2 Comparison between dynamic compressors

Centrifugal compressors are characterized by an enthalpy factor higher than axial machines, and a lower flow factor.

- at a given pressure, the flow is lower in a centrifugal compressor than in an axial compressor;
- the design of centrifugal compressor cells allows intermediate cooling between each compression stage, whereas this is impossible in the axial dynamic compressors. This significantly reduces the compression work, as has been shown before;

- for the same value of the peripheral velocity U , the axial compressors require a larger number of stages (in a ratio of 3 to 4), given the lower values of the power factor μ ;
- for this reason, axial compressors are preferred when the pressure ratio is low. However, to increase the power factor, manufacturers select higher peripheral speeds for axial machines;
- axial compressors have a performance map flatter and therefore less stable than centrifugal ones.

Centrifugal compressors can maintain a stable operation over a flow range much wider than axial machines, which justifies the latter being mainly used at constant flow and speed.

7.5 EXPANSION

Nowadays, most expanders are turbines.

The theory of turbines is very close to that of dynamic compressors, the thermodynamics of expansion being distinct from that of compression essentially by some definition changes.

7.5.1 Thermodynamics of expansion

In the preceding pages we explained the laws of compression, indicating that those of expansion differ only by a different definition of isentropic efficiency. This short section provides relations for expansion.

The isentropic work is still given by (7.1.5) or (7.1.6).

7.5.1.1 Irreversible expansion

In an irreversible expansion, shaft work is less than the isentropic work, because the irreversibilities have the effect of increasing the entropy of the fluid and its temperature, and are therefore reflected by a shift (a-r) to the right of the isentropic (a-s) (Figure 7.5.1).

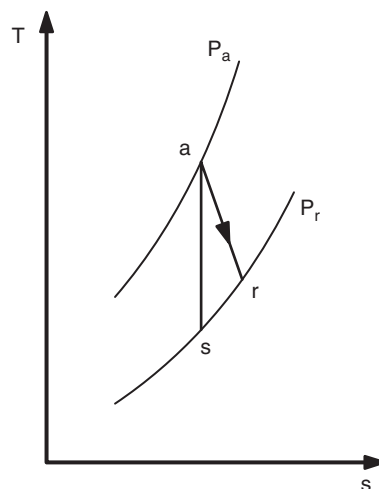


FIGURE 7.5.1

Real expansion process

We define in this case the isentropic efficiency by:

$$\eta_s = \frac{\tau}{\tau_s} = \frac{h_r - h_a}{h_s - h_a} \quad (7.5.1)$$

This definition, the reverse of that of the isentropic compression efficiency, leads to a value $\eta_s < 1$.

Again, it must be stressed that given the current state of our knowledge, we are not able to assess *a priori* the value of the expansion isentropic efficiency, which is measured experimentally.

7.5.1.2 Polytropic expansion

Similarly to what we did for compression, we define a polytropic expansion as a process in which, for any infinitely small stage, the isentropic efficiency remains constant and equal to the polytropic efficiency η_p .

$$\eta_p = \frac{vdP + Tds}{vdP} = \frac{dh}{dh - Tds} \quad \delta\tau_s = \frac{1}{\eta_p} dh$$

Posing:

$$\frac{k-1}{k} = \eta_p \frac{\gamma-1}{\gamma} \quad (7.5.2)$$

We find the polytropic law (7.1.9): $Pv^k = \text{Const.}$

With this convention, the shaft work in a polytropic expansion can also be written according to equation (7.1.6):

$$\tau = \frac{\gamma}{\gamma-1} P_a v_a \left[\left(\frac{P_r}{P_a} \right)^{(k-1)/k} - 1 \right]$$

The difference in entropy is independent of c_p and T for a polytropic expansion and can be expressed as:

$$\begin{aligned} \Delta s &= (1 - \eta_p) R \ln \left(\frac{P_a}{P_r} \right) \quad (\text{open systems}) \quad \text{or} \\ \Delta s &= (1 - \eta_p) R \ln \frac{v_r}{v_a} \quad (\text{closed systems}) \end{aligned}$$

7.5.1.3 Calculation of a heated polytropic for an open system

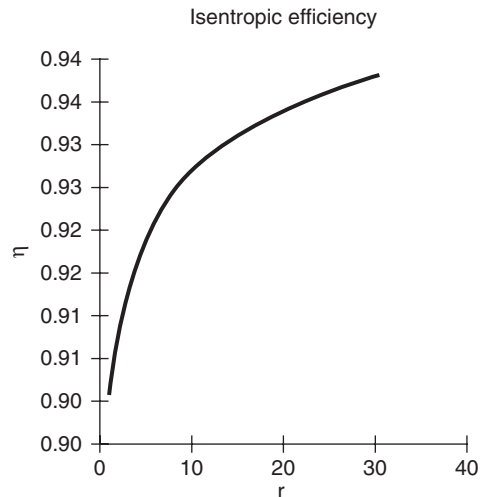
If you know the polytropic coefficient k of the process, T_r is calculated by:

$$T_r = T_a \left(\frac{P_r}{P_a} \right)^{(k-1)/k}$$

If one assumes that the reversible polytropic reference passes through the inlet and outlet points, we must first identify the polytropic efficiency η_{pref} by applying between these two points $\Delta s = (1 - \eta_p) R \ln(P_r/P_a)$.

The shaft work for the reversible polytropic is then:

$$\tau_{\text{ref}} = \frac{1}{\eta_p} (h_r - h_a)$$

**FIGURE 7.5.2**

Isentropic efficiency function of expansion ratio

Knowing the process efficiency η (isentropic or polytropic), we can deduce the actual work of expansion:

$$\tau = \frac{\eta}{\eta_{\text{pref}}} (h_r - h_a)$$

The heat to provide is then:

$$Q = h_r - h_a - \tau = \left(1 - \frac{\eta}{\eta_{\text{pref}}}\right) (h_r - h_a) \quad (7.5.3)$$

While a polytropic compression leads to $k > \gamma$, we obtain in the case of a polytropic expansion: $k < \gamma$.

Unlike what happens in a compressor, given a constant polytropic efficiency (0.9 in Figure 7.5.2), the expansion isentropic efficiency increases when the expansion ratio increases.

This arises because the irreversibilities taking place at high temperature (and pressure) are partially recovered in the subsequent expansion stages, as they have the effect of warming the fluid.

7.5.2 Calculation of an expansion in ThermoOptim

In ThermoOptim the calculation of expansions is done in a manner analogous to that of compression, with the same screen. You should therefore refer to what was presented in section 7.1.5.

7.5.3 Turbines

Geometrical arrangement

The general layout of a turbine is given Figure 7.5.3. The stator is made of guide nozzles which accelerate the fluid, while the wheel (rotor) converts into mechanical energy at least part of the enthalpy available.

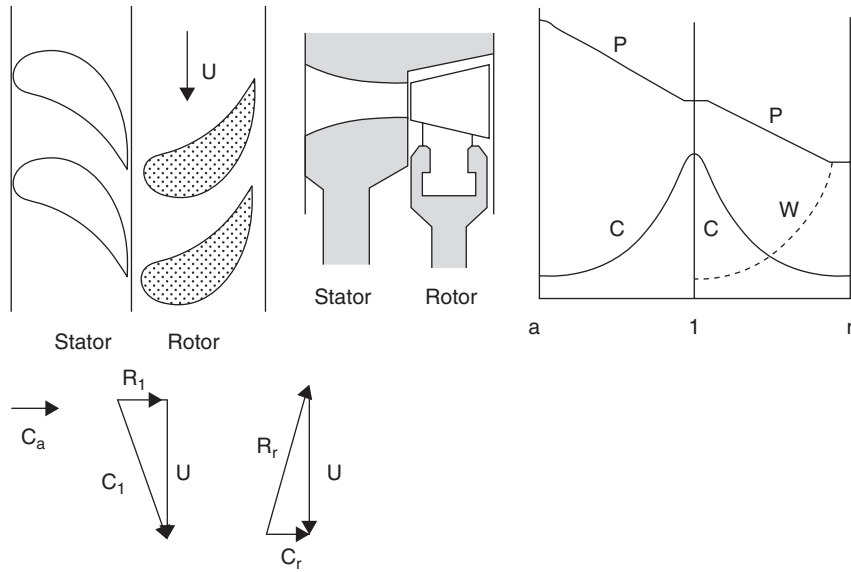


FIGURE 7.5.3
Velocity and pressure profile in an axial turbine stage

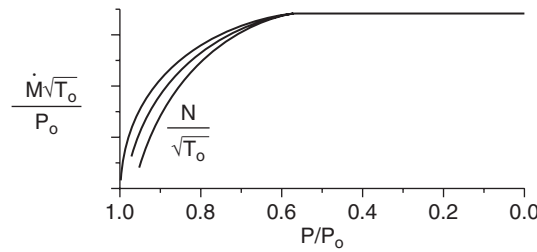


FIGURE 7.5.4
Turbine performance map

Changes in pressure and fluid velocity in a turbine

In a turbine, the evolution of the fluid is an expansion. The compressible flow equations indicate that for a subsonic regime, the section of the vein should decrease, and the velocity increase. This evolution takes place in two steps (Figure 7.5.3): in the stator, the absolute velocity increases, while in the impeller the relative velocity increases, and the absolute velocity decreases.

7.5.4 Turbine performance maps

Just as we did section 7.3.3.1, we will only present in this section some general results concerning performance maps of turbines, which will be completed in Chapters 15 of Part 3 and 37 of Part 5 dealing with the off-design behavior of machines.

In the case of a turbine (Figure 7.5.4) it is conventionally the pressure ratio which is used as abscissa. As ordinate, we find the corrected mass flow or isentropic efficiency of the machine. The curve parameter is still the corrected rotation speed, which plays a secondary role.

We can see the flexibility of turbines to adapt to various operating conditions: efficiency tends to deteriorate only when we dramatically reduce the pressure ratio or the speed. This flexibility is

particularly due to the flow stability in the blades due to the gradient of pressure therein. But what is most remarkable is the stability of the flow for the high pressure ratios, which comes from the supersonic regime, which takes place in at least part of the machine (the flow is choked at the place where the speed of sound is reached).

The limiting value reached by the flow, when the pressure ratio exceeds the critical ratio is called critical flow. It is proportional to the throat section, which is obviously independent of the rotation speed, which explains the weak influence of this parameter.

In a supersonic nozzle the corrected mass flow is proportional to the throat section and independent of inlet conditions. When the nozzle is caused to operate outside the rated conditions, the fluid flow somehow adapts to the shape of the duct. The decrease in efficiency resulting from this adaptation is especially important when one wants to exceed the design pressure ratio.

As the expansion ratio remains above its critical value, the flow stays below the critical flow. When its value decreases beyond this value, the flow maintains a constant value.

If you want to go beyond the critical expansion ratio in a converging – diverging nozzle, the flow cannot increase sufficiently, and the expansion continues beyond the exit section with large oscillations at the outlet of the nozzle.

Indeed, if the flow is supersonic and the pressure in the outlet chamber does not match that used for the design, the following phenomenon takes place: if the outlet chamber pressure is greater than the nominal pressure, there is hyper-expansion in the nozzle, and thus sharp contraction at the outlet, otherwise, there is hypo-expansion in the nozzle, and thus sudden expansion at the exit.

The explanation for this phenomenon is clear: beyond the contracted section, the fluid velocity exceeds the speed of sound. Consequently, the conditions set on the outlet vein of this section may no longer influence the flow at the inlet of the throat. It continues downwards to the throat as if the final pressure was the rated outlet pressure, and if the actual pressure is different, a discontinuity is inevitable.

7.5.5 Degree of reaction of a stage

The study of the energy balance of a stage showed that the enthalpy change takes place partly in the rotor, and partly in the diffuser. We call the degree of reaction ε the fraction of the enthalpy change that takes place in the rotor. With the notation of Figure 7.3.3, we have:

$$\varepsilon = \frac{h_1 - h_a}{h_r - h_a} = \frac{h_1 - h_a}{\Delta h} \quad (7.5.4)$$

By definition, ε is between 0 and 1.

In a dynamic compressor stage $0.5 \leq \varepsilon \leq 1$, is commonly obtained. The lower limit ($\varepsilon = 0.5$) is approximated in the axial dynamic compressors. As for the upper limit (pure reaction: $\varepsilon = 1$), it is reached in the case of a single stage machine whose diffuser is nonexistent or of negligible effectiveness.

In a turbine stage, pure reaction is impossible. Two limiting cases frequently arise:

- **impulse turbines**, in which $\varepsilon = 0$: any expansion of the fluid is then carried out in fixed blades or nozzles, at the inlet of the wheel, and the inlet and outlet pressures of the rotor are equal;
- **reaction turbines**, where $\varepsilon = 0.5$: the expansion is then evenly distributed between the nozzle and the wheel.

Each of these two types of turbine has advantages and disadvantages of its own. As we have said, it is not our intention to develop here in detail the theory of turbines. Simply note that the impulse

turbines are generally used for head stages of multistage sections or for small capacity units, while reaction turbines are proving well suited for the low-pressure sections.

Indeed, a first advantage of using **impulse turbines** in the high pressure sections is that the entire expansion being made in the stator, the rotor is not subjected to a high pressure difference, which limits the mechanical constraints. A second advantage is that the flow in these turbines can be reduced by using partial injection, which is to only supply a fraction of fluid in the stator vanes. This type of operation is made possible in this case because the pressure is the same on both sides of the rotor, and no parasitic flow is expected in the non-injected parts.

However, the efficiencies of these turbines are slightly (2–3%) worse than those of **reaction turbines**, which are subjected to significant axial thrust, and do not use partial injection.

Because irreversibilities taking place in the top stages are partially recovered in subsequent stages, we can tolerate that their efficiency is slightly lower, which allows us to use impulse turbines in this case.

7.6 COMBUSTION

Combustion phenomena are of particular importance in the study of energy technologies, because they are the source of most heat and power production in the world: more than 90% of global consumption of primary commercial energy comes from burning coal, oil or natural gas.

The study of combustion is to determine the state and composition of combustion products, and consequently, their thermochemical properties including the amount of energy that is involved in the reactions. Moreover, the combustion conditions largely determine the quantities of pollutants emitted by energy technologies.

The purpose of this section is to determine as closely as possible the combustion characteristics that are important in terms of energy: the thermodynamic properties of the products (c_p , M , h , s), the energy released by combustion (ΔH_r), the concentration of unburned hydrocarbons (UHCs) and pollutants.

From these elements, it becomes possible to optimize the combustion, i.e. to obtain the best combustion efficiency by adjusting the air/fuel ratio or the excess air, which sets out the flame temperatures and losses by the fumes.

To achieve this goal it is necessary to know how to characterize fuels and write the complete reactions, stoichiometric and with excess or lack of air, taking into account the dissociation where it exists, which requires knowledge of general principles that govern equilibrium reactions (law of mass action), and finally calculate the energies released.

In the remainder of this book, we will always assume that the combustion reaction involves gaseous species, and that the various components are treated as ideal gases. Dalton's law then allows us to consider that the combustion products follow the ideal gas law.

The fundamentals you should make sure to understand are the following: air factor λ (7.6.2.4), adiabatic combustion temperature (7.6.4.6), CO_2 dissociation (7.6.3.2), quenching temperature (7.6.1.6) and heating value (7.6.4.5).

7.6.1 Combustion phenomena, basic mechanisms

Combustion reactions are rather unusual chemical reactions, typically brutal, where the non-equilibrium is the rule, equilibrium the exception. In these circumstances, it is still impossible to determine exactly during the reaction the evolution of thermodynamic functions characterizing the systems involved. They can only be calculated assuming that equilibrium conditions are met before and after the time of combustion.

7.6.1.1 Complete reactions, dissociation

Generally, a chemical reaction involving two reactants and two products can be written as:



Experience shows that the unfolding of a combustion reaction is highly dependent on temperature.

At low temperature, the reactants generally do not react spontaneously. For the reaction to start, it is necessary to bring an activation energy, usually in the form of an electric spark. They say that the mixture is in false equilibrium. If the reaction is triggered artificially, it is brutal, and total if the temperature remains low enough. The combustion is said to be complete, or without dissociation.

At high temperature, reaction is usually incomplete. The composition of the reaction medium depends on the degree of progress of this reaction, the ratio between the number of moles of reactants that have been converted and the total number of moles of reactants. This degree of progress depends on the kinetics and the law of mass action at equilibrium. The reactants are not completely oxidized, and we talk of dissociation. If, starting from such a situation, we gradually decrease the temperature of reactants, the composition stabilizes and remains unchanged only above a certain threshold. It is said there is quenching of the reaction.

In the energy systems that we study, combustion will be either complete or incomplete, depending on cases. We show in this section how it can be calculated with some simplifying assumptions.

The general thermodynamic study of combustion reactions is part of the thermodynamics of chemical processes. In this chapter, we limit ourselves to only those aspects necessary for our purposes, i.e. mainly the study of variations of the thermodynamic functions of the reactive mixture (internal energy, enthalpy, entropy) caused by variations in chemical composition.

The study of the mechanism of the reaction kinetics (limit of false equilibria, means of triggering the reaction mixture in a false equilibrium, methods of propagation of the reaction, kinetics etc.) is much more complex. We will discuss it here only very briefly and qualitatively.

In what follows, as has been said in the introduction, we limit ourselves mainly to the study of combustion reactions in the gaseous phase. Even when fuel is introduced as a liquid (oil, diesel), the products are then present in gaseous form.

7.6.1.2 Combustion of gaseous fuel mixtures

A gaseous fuel mixture, in practice generally composed of air and fuel gas, is defined by its molar or mass composition.

It is customary to relate the composition of any mixture to that of the stoichiometric mixture, i.e. with exactly the amount of oxygen required for complete combustion. The richness R is defined as the ratio of the number of moles (or mass) of fuel in a predetermined amount of mixture, to the number of moles (or mass) of fuel in the stoichiometric mixture.

$R = 1$ corresponds to stoichiometric mixture, $R < 1$ to excess air, and $R > 1$ to excess fuel (lack of air). In subsection 7.6.2.4 we will introduce two more quantities directly related to richness, which are also widely used for the study of non-stoichiometric combustion: air factor λ and excess air e .

Conditions of self-ignition and propagation of combustion

We have seen that a fuel mixture based on a given fuel is generally stable at room temperature. By heating, it is possible to trigger the combustion reaction from a certain temperature, called self-ignition. The H_2 mixtures burn spontaneously at 550°C , those based on CO and CH_4 around 650°C . It sometimes happens that a self-ignition delay appears, which can reach 200 K for CH_4 .

The auto-ignition temperature depends of course on the fuel and the composition of the mixture, but it is also a decreasing function of pressure, with some peculiarities (cool flames, long self-ignition delays), for which we refer to the literature.

The value of self-ignition temperature is that it defines an upper limit which must not be reached, whether for reasons of safety when handling fuel, or for more specific applications, such as burning in gasoline engines.

When a fuel mixture is heated to a temperature above its self-ignition temperature, the reaction is triggered after some delay, the said auto-ignition delay, which becomes shorter at higher temperatures. This delay is related to basic mechanisms of combustion presented in paragraph 10.6.1.5.

Moreover, in a given mixture of air and fuel, combustion, initiated locally by a spark, can only spread if the richness is between two limits said lower inflammable R_i and higher inflammable R_s . If the richness is outside of this interval, the mixture is either too lean or too rich, and combustion cannot be maintained. These limits depend on the temperature and fuel type. At room temperature, limits R_i and R_s for most hydrocarbons are respectively close to 0.5 and 4. They diverge as the temperature increases.

Flame propagation

To avoid self-ignition of gaseous fuels, it is necessary that the mixture is ignited locally before reaching the self-ignition temperature one way or another. In practice, an electric spark is generally used for this purpose.

Once the mixture is ignited, combustion spreads from the ignition point, in a reaction zone called the flame front, corresponding to the surface which separates the burned gases from the mixture still intact. The case where the fuel and oxidizer form a homogeneous mixture before the start of the reaction is referred to as premixed flame. Experience shows that the propagation can take place in two very different modes: **deflagration** and **detonation**. The difference between them is the relative speed at which the flame front moves in the mixture.

In the deflagration, this speed is low, the order of several cm/s to a few m/s, whereas in the detonation, it far exceeds the speed of sound in the mixture (several thousands of m/s).

In the deflagration, the combustion is mainly propagated by conduction: the layer of combustion gas heats the next layer of still intact mixture. When it is in turn brought to the auto-ignition temperature, it ignites, and so on. The gases being poor conductors, the propagation speed is low.

In detonation, the combustion is propagated by a shockwave that moves at a speed exceeding the speed of sound in the mixture, causing an almost instantaneous reaction at its passage, with sudden changes in velocity, pressure and temperature. Given this shockwave, detonation is a very dangerous combustion mode, which causes engines to deteriorate rapidly. Very abrupt changes in pressure induce, in any parts submitted to the thrust of the gases, very destructive steep front elastic waves. The joints are subjected to shocks, valves and seats leak, deformed by the wave. When it occurs in an engine, it is usually called **knocking combustion mode**. In addition, when the fuel is a hydrocarbon, the detonating combustion is always initiated by a decomposition of the molecule, releasing black smoke and the engine gets dirty. We will study in detail in Chapter 13 of Part 3 what solutions are adopted to prevent detonation in internal combustion reciprocating engines.

Study of the deflagration

A mixture whose richness is between the flammability limits burns with a certain deflagration speed. This speed, often called laminar velocity, is the velocity of the flame relative to the reaction mixture that feeds it, in a laminar flow. Its value, which also depends strongly on the nature of the fuel, is a function of richness, temperature and pressure.

In general, for a given temperature, the maximum speed of deflagration corresponds to a richness slightly above 1, often around 1.2. Deflagration speeds are also low, a few cm/s to a few m/s. For a given richness, they are an increasing function of temperature and a decreasing function of pressure.

Turbulence exerts a complex effect on the deflagration speed: it increases it significantly if it is already noticeable at rest; it decreases it near the flammability limit otherwise, and under these

conditions can prevent the spread of combustion (blowing on a fire stirs it up if it is intense, blows it out otherwise).

7.6.1.3 Combustion of liquid fuels

The phenomena described above for gaseous fuels are similar in the case of liquid fuels, with some differences.

A droplet of a liquid fuel that is injected into a mass of air, ignites spontaneously when the temperature exceeds a certain value, called fuel self-ignition temperature T_{ai} . This temperature depends mainly on the fuel, and incidentally on air pressure, diameter and drop speed.

The self-ignition temperatures thus measured range from 350°C to 500°C depending on the fuel. Note that they are relatively low, much lower than those of gaseous fuel mixtures.

Ignition and combustion delays

Experience shows that, when injecting a droplet of liquid fuel into an air mass whose temperature T exceeds the self-ignition temperature T_{ai} , it does not catch fire instantly, but after some delay, the said inflammation delay, which depends mainly on the difference $(T - T_{ai})$ and the type of fuel, secondarily on the diameter and drop velocity. The mechanisms involved are complex, part of the liquid fuel generally evaporating to form, mixing with the oxidant, the reactive medium that self-ignites depending on its composition and pressure and temperature conditions.

In addition, complete combustion requires an additional delay, the said combustion, which, apart from the difference $(T - T_{ai})$, depends essentially on the diameter and drop velocity as well as air turbulence.

When T exceeds T_{ai} , the ignition delay is never very large, but it rarely falls below 2 milliseconds. The combustion delay is similar, provided that the fuel is finely pulverized (an average diameter of drops of a few microns) and injected at high speed, at a pressure exceeding 100 bar. Nevertheless, the overall ignition and combustion delay is of the order of several milliseconds.

Diffusion flames

Unlike premixed flames, where the fuel and oxidizer are mixed before the start of the reaction, the combustion of fuel introduced in the liquid state in the oxidizer is governed by the speed at which reactive chemical species inter-diffuse. This is called the diffusion flame. The reaction zone of such a flame is thicker than that of a premixed flame. Richness varies from infinite value in the fuel to zero in the oxidizer. There are laminar diffusion flames (candles, oil lamps) and turbulent confined diffusion flames whose applications are numerous, either in industry or in conventional diesel engines.

PRACTICAL APPLICATION

Main Difference between Diesel and Gasoline Engines

An important difference between a gasoline engine and a diesel engine is not in the mode of introducing fuel, which in modern gasoline engines is also injected, but when the fuel is introduced, which determines the nature of gas when the reaction starts and the type of combustion which takes place inside the engine, as will be explained in detail in Chapter 13 of Part 3.

In the gasoline engine, fuel is introduced well in advance so that the cylinder is full, when ignition occurs, of a substantially homogeneous gaseous mixture. In the diesel engine, fuel is injected at the last moment and burned as fine liquid droplets as and when it is introduced (diffusion flame).

7.6.1.4 Thermodynamics of combustion at equilibrium

The law of mass action is fundamental to studying the incomplete combustion reactions at equilibrium. It can be easily derived from the second law of thermodynamics. Let us first express the Gibbs energy of the gas put into play.

Expressions (5.6.6) and (5.6.7) allow us to calculate the molar Gibbs energy of an ideal gas, from $G = H - TS$:

$$H - H_0 = \int_{T_0}^T C_p(t) dt \quad S = S_0 + \int_{T_0}^T \frac{C_p(t)}{t} dt - R \ln \frac{P}{P_0}$$

If the index 0 values represent the reference state, the value of the Gibbs energy at temperature T and any pressure is given by:

$$G = H - TS = G_0^*(T) + RT \ln \frac{P}{P_0}$$

$G_0^*(T)$ representing the term independent of P in the Gibbs energy.

Note that $G_0^*(T)$ **is not** the reference state Gibbs energy G_0 . This way of decomposing G has the sole purpose of separating variables P and T .

If, as is customary, $P_0 = 1$ bar, we get:

$$G - G_0^* = RT \ln P \quad (7.6.2)$$

Let us consider combustion equation 7.6.1. We will investigate how one writes the equilibrium condition (5.4.22). By definition, the degree of reaction is the ratio ϵ of the number of moles of a reactant (usually the first of the equation) that reacted, to the total number of moles of this reactant capable of reacting.

At equilibrium, $dT = 0$, $dP = 0$, and equation (5.4.22) ($\sum \mu_i dn_i$)_{T,P} = 0 becomes:

$$(-\mu_1 \nu_1 - \mu_2 \nu_2 + \mu_3 \nu_3 + \mu_4 \nu_4) d\epsilon = 0$$

This equation must be verified regardless of the value of ϵ . We have:

$$-\mu_1 \nu_1 - \mu_2 \nu_2 + \mu_3 \nu_3 + \mu_4 \nu_4 = 0$$

However, for an ideal mixture, the chemical potential is equal to the partial Gibbs energy (5.4.23):

$$\mu_i = G(T, P_i)$$

Using equation (7.6.2) and separating variables, we find:

$$-rT(-\nu_1 \ln P_1 - \nu_2 \ln P_2 + \nu_3 \ln P_3 + \nu_4 \ln P_4) = -\nu_1 G_{01}^* - \nu_2 G_{02}^* + \nu_3 G_{03}^* + \nu_4 G_{04}^*$$

The second part of the equation represents the difference between the terms independent of the pressure of products and reactants free energies, and is sometimes called the free enthalpy change of reaction, denoted ΔG_0 , expressed in molar variables.

ΔG_0 is defined, recall, for a given reference state, that we choose here the temperature of the mixture and $P_0 = 1$ bar: $\Delta G_0 = f(T, P_0)$. Logarithmic terms can be grouped in the form:

$$\Delta G_0 = -RT \ln \frac{P_3^{\nu_3} P_4^{\nu_4}}{P_1^{\nu_1} P_2^{\nu_2}}$$

ΔG_0 being a function only of temperature, the term under the logarithm is itself a function of temperature only, and is independent of the system pressure (but of course depends on the reference pressure P_0).

K_p is defined as the equilibrium constant, with:

$$k_p = \frac{P_3^{\nu_3} P_4^{\nu_4}}{P_1^{\nu_1} P_2^{\nu_2}} \quad \text{and} \quad \Delta G_0 = -RT \ln K_p$$

At equilibrium, the partial pressures of the components are proportional to their mole fractions: $P_i = x_i P$. Therefore:

$$K_p = \frac{x_3^{\nu_3} x_4^{\nu_4}}{x_1^{\nu_1} x_2^{\nu_2}} P^{\nu_3 + \nu_4 - \nu_1 - \nu_2} \quad (7.6.3)$$

P is the pressure of the system, ν_i are the stoichiometric coefficients of the combustion reaction, and x_i the mole fractions of various constituents in products.

Equation (7.6.3) is called the **law of mass action**. Combined with the balance equations of chemical species involved, it allows us, if we know the variation of K_p with temperature, to determine the equilibrium concentrations of the components for a given reaction.

The presence of non-reactant gases does not question the law of mass action. However, it can strongly influence the progress of the reaction, since the partial pressures are changed, because of the increased total number of moles in the mixture.

When several reactions can take place in the same mixture, the laws of mass action for the different reactions must be checked simultaneously, knowing they are coupled together because, of course, the calculation of the partial pressures cannot be done independently.

Table 7.6.1 gives the values of the equilibrium constants for the main reactions that may occur in combustion. It shows that for all these reactions, K_p is an increasing function of temperature, which means that the degree of reaction increases with temperature. Note that, for this set of values, the pressure must be expressed in bar, and the coefficients used in the equations are the stoichiometric coefficients.

One can obtain an estimate of K_p from the approximate formula valid in limited temperature ranges:

$$\ln(K_p) = A - \frac{B}{T}$$

For the reaction known as water gas $O_2 + H_2 \leftrightarrow CO + H_2O$, in the range 1000 to 2200 K, covering much of the usual combustions, we take as values $A = 3.387$ and $B = 3753$, P being expressed in bar and T in Kelvin.

7.6.1.5 Elements of chemical kinetics

In many cases, and as soon as we are to take into account emissions of pollutants, the assumptions of complete combustion are too restrictive. It is then necessary to refine the calculations to determine as precisely as possible the degree of reaction. This is possible by using thermodynamics, if time is sufficient for equilibrium to be reached, and otherwise by using chemical kinetics. In this section we give some elements to address this particularly difficult issue.

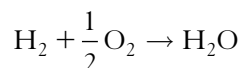
As indicated above, a fuel mixture is generally stable at room temperature. Statistical thermodynamics can explain this: the reaction depends on the number of shocks that may arise between the various reactants, and hence temperature.

Specifically, chemical kinetics reveals that the actual mechanism of combustion can be decomposed into a series of simple reactions, called basic steps, which involve reactive species called free radicals (atoms or groups of atoms with one or more unpaired electrons).

TABLE 7.6.1Values of the equilibrium constant K_p

T (K)	500	1000	1500	2,000	2,500
$H_2 \leftrightarrow 2H$	$5 \cdot 10^{-41}$	$5 \cdot 10^{-18}$	$3 \cdot 10^{-10}$	$3 \cdot 10^{-6}$	0.0006
$O_2 \leftrightarrow 2O$	$1 \cdot 10^{-46}$	$2 \cdot 10^{-20}$	$2 \cdot 10^{-11}$	$4 \cdot 10^{-7}$	0.0002
$N_2 \leftrightarrow 2N$	$2 \cdot 10^{-96}$	$9 \cdot 10^{-44}$	$4 \cdot 10^{-27}$	$8 \cdot 10^{-19}$	$9 \cdot 10^{-14}$
$H_2O \leftrightarrow H_2 + 1/2O_2$	$1 \cdot 10^{-23}$	$9 \cdot 10^{-11}$	$2 \cdot 10^{-6}$	0.0003	0.006
$H_2O \leftrightarrow OH + 1/2H_2$	$7 \cdot 10^{-27}$	$5 \cdot 10^{-12}$	$5 \cdot 10^{-7}$	0.0002	0.0054
$CO_2 \leftrightarrow CO + 1/2O_2$	$9 \cdot 10^{-26}$	$6 \cdot 10^{-11}$	$5 \cdot 10^{-6}$	0.0013	0.0363
$1/2O_2 + 1/2N_2 \leftrightarrow NO$	$2 \cdot 10^{-9}$	$9 \cdot 10^{-5}$	0.0033	0.02	0.0593
$CO_2 + H_2 \leftrightarrow CO + H_2O$	0.0073	0.6934	2.5645	4.529	6.0814
T (K)	3,000	3,500	4,000	4,500	5,000
$H_2 \leftrightarrow 2H$	0.0248	0.3451	2.5119	11.858	40.926
$O_2 \leftrightarrow 2O$	0.0126	0.2399	2.1878	12.19	48.529
$N_2 \leftrightarrow 2N$	$2 \cdot 10^{-10}$	$5 \cdot 10^{-8}$	$3 \cdot 10^{-6}$	$8 \cdot 10^{-5}$	0.0011
$H_2O \leftrightarrow H_2 + 1/2O_2$	0.0454	0.1941	0.5781	1.3583	2.6915
$H_2O \leftrightarrow OH + 1/2H_2$	0.0543	0.2838	0.975	2.5586	5.5081
$CO_2 \leftrightarrow CO + 1/2O_2$	0.3273	1.5488	4.9204	11.995	24.322
$1/2O_2 + 1/2N_2 \leftrightarrow NO$	0.1222	0.2042	0.2992	0.4009	0.5058
$CO_2 + H_2 \leftrightarrow CO + H_2O$	7.2111	7.9799	8.5114	8.8308	9.0365

For example, the following reaction as such has a negligible probability of occurring:



For it to take place, where M is a partner of any collision (O_2 , H_2 , N_2 , ...), a chain like this must be put into place:

- initiation $O_2 + M \rightarrow 2 O \cdot + M$
- branching $O \cdot + H_2 \rightarrow OH + H \cdot$
- branching $O_2 + H \rightarrow O \cdot H + O \cdot$
- propagation $O \cdot H + H_2 \rightarrow H_2O + H \cdot$

The initiation reaction produces the first free radicals. In a reaction involving a hydrocarbon, it usually corresponds to a thermal decomposition of the molecule, releasing a $H \cdot$. The branching is an essential step that multiplies the number of available radicals in the reaction, while the propagation preserves their number, while participating in the production of intermediate or final products. Breaking reactions can finally complete the chain by transforming a free radical into a stable chemical species, either in homogeneous phase or in contact with walls.

The reaction path can be explained in the light of what was just seen: when the temperature is low (less than the self-ignition temperature), the number of free radicals is very low, and the breaking reactions consume them all, so that combustion cannot take place. Above a certain temperature, this situation is reversed, and the number of free radicals increases. The conditions are then ripe for burning to develop.

All these phenomena explain why a combustion reaction actually has a very high degree of complexity. If you want to be precise, it is necessary to follow in detail the various chemical species that may appear, and consider all relevant equations.

For example, for methane, you can find in the literature mechanisms that consider 46 species reacting as a function of 234 elementary coupled equations: 129 decomposition reactions of CH_4 , 21 reactions of hydrogen (H , H_2) and oxygen (O , O_2), and 84 reactions characteristic of the formation of nitrogen oxides NO during combustion.

It is certainly possible to build simplified models of the overall reaction, according to various methods. To understand the main kinetic phenomena, experience proves that it is necessary to distinguish at least three phases in the combustion of a hydrocarbon:

1. decomposition of fuel molecules by pyrolysis, producing olefins C_nH_2 , also called intermediate hydrocarbons and free radicals H , O and OH ;
2. oxidation of hydrocarbon radicals and intermediates to CO and H_2 ;
3. oxidation of CO and H_2 to give the final products of combustion CO_2 and H_2O .

7.6.1.6 Quenching temperature

Thermodynamics of combustion at equilibrium allows one, from the law of mass action, to determine the degree of progress of reactions depending on the temperature and pressure. For this law to be applicable it is necessary first that the reaction speeds are larger than the residence time of reactants in the combustion chamber, and second that cooling conditions for the fumes are known.

For most combustion reactions, the assumption of a medium at equilibrium can be chosen without introducing too much error. An exception should however be made as we will see in section 7.6.5 for the oxidation reaction of nitrogen, which leads to the formation of NO_x . This reaction has a very slow kinetics, so that the degree of reaction is generally much less advanced than at equilibrium.

The study of combustion kinetics is also necessary if one wants to explain the quenching phenomena that appear when dissociation takes place (at temperatures above 1800 K), followed by a sudden cooling of the fumes.

Due to dissociation, some combustion reactions are not complete. The speed of slow reactions may then not be sufficient in the case of rapid decrease in temperature, so that molecular recombinations that would have taken place normally (that is to say at equilibrium, the reactions being reversible) cannot be attained.

In these conditions unburned hydrocarbons may remain. It is said that there is quenching of the reaction. This explains the presence of CO in the flue gas, even with excess oxygen and for a homogeneous mixture. We call the quenching temperature the temperature to be used in the law of mass action to get the actual exhaust gas composition.

You should refer to specialized literature for further developments on this subject. In what follows, unless otherwise stated, we always assume that chemical reactions could develop and achieve equilibrium without kinetic considerations affecting these phenomena.

7.6.2 Study of complete combustion

In this section we will deal with complete combustion, that is to say, such that all possible oxidations are carried out. After presenting the different ways of representing the oxidizer (usually air) and fuel, we will study successively the non-stoichiometric and stoichiometric combustion. In the next section, we will see how to take into account the existence of unburned hydrocarbons.

7.6.2.1 Air composition

A combustion reaction involves the oxidation of a fuel with oxygen or a substance containing oxygen, such as air. In most cases in practice, it is air, and it is accepted as a first approximation that all components other than oxygen are inert during the reaction.

TABLE 7.6.2
COMPOSITION OF NORMAL AIR

Component	Molar fraction %	Molar mass kg/kmol	Mass fraction %
N ₂	0.781	28	0.756
Ar + CO ₂	0.009	(40)	0.012
O ₂	0.21	32	0.232
N ₂ atmosph.	0.79	(28.15)	0.768

The composition of normal air is given in Table 7.6.2. To simplify the study of combustion reactions, other inert gases are combined with nitrogen, by defining an atmospheric nitrogen which allows us to consider the dry air as a mixture of two ideal gases, whose composition is indicated below. From these values, it follows that the ratio (atmospheric nitrogen)/oxygen is **3.76 in volume**, and 3.31 in mass.

In ThermoOptim, calculations are made with greater precision, the number of components being up to the user. Among the protected ideal gases, i.e. whose composition cannot be changed by the user, we find the above defined atmospheric air.

7.6.2.2 Fuel composition

To study the quality of combustion, it is convenient to represent the fuel by a standardized formula reflecting its actual composition. For an ash-free fuel, the chemical elements to be retained are: carbon, hydrogen, oxygen, nitrogen and sulfur.

The fuel can therefore be described by the formula: C H_y O_x N_z S_u

The stoichiometric coefficients y, x, z and u can be easily determined:

- * from mass fractions (C), (H), (O), (N) and (S), which gives:

$$y = \frac{12.01 (H)}{1.008 (C)}, \quad x = \frac{12.01 (O)}{16 (C)}, \quad z = \frac{12.01 (N)}{14.008 (C)}, \quad u = \frac{12.01 (S)}{32.07 (C)} \quad (7.6.4)$$

- * from the exact formula if it is a pure substance or a mixture of pure chemically defined substances, relating the chemical formula to the unit of carbon. For compound C_nH_mO_p we get :

$$y = \frac{m}{n}, \quad x = \frac{p}{n} \quad (7.6.5)$$

- * from volume or mole fractions if it is a gaseous fuel.

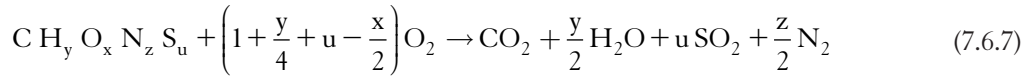
For a mixture of fractions [H₂], [CO], Σ [C_nH_m], [CO₂], [N₂], [H₂S], [SO₂], we get:

$$\begin{aligned} y &= \frac{2[H_2] + \Sigma m[C_n H_m] + 2[H_2S]}{[CO] + \Sigma n[C_n H_m] + [CO_2]} & x &= \frac{[CO] + 2[CO_2] + 2[SO_2]}{[CO] + \Sigma n[C_n H_m] + [CO_2]} \\ z &= \frac{2[N_2]}{[CO] + \Sigma n[C_n H_m] + [CO_2]} & u &= \frac{[H_2S] + [SO_2]}{[CO] + \Sigma n[C_n H_m] + [CO_2]} \end{aligned} \quad (7.6.6)$$

7.6.2.3 Stoichiometric combustion

We call a stoichiometric combustion a combustion without excess or lack of air, where all available oxygen is completely consumed.

Assuming that nitrogen reacts only in negligible proportions and is found after combustion in molecular form, the general equation of a stoichiometric combustion is:

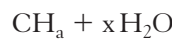


Depending on circumstances, coefficient $(1 + (y/4) + u - (x/2))$ may be greater or less than unity, depending on the existing availability of oxygen in the fuel. In most cases $x \leq y/2 + 2u$, but for some lean gases, the reverse situation may exist

For most conventional fuels, the values of z and u are very low and often negligible, while the condition $x \leq y/2$ is always verified. We can then simplify the symbolic formulation above by writing:

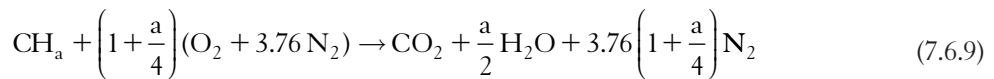
$$1 + \frac{y}{4} - \frac{x}{2} = 1 + \frac{a}{4} \quad (7.6.8)$$

which leads to the conclusion that formula $C H_y O_x$ becomes:



a represents what is called hydrogen available for combustion referred to the complete oxidation of a carbon unit, and $a = y - 2x$.

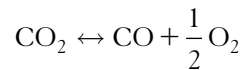
With these conventions, the complete oxidation of fuels of formula $(CH_a + xH_2O)$ can be described by the equation:



while there is conservation of the constitutive water $x H_2O$.

This reaction is the fuel combustion without excess or lack of air.

If there is lack of air, some of the carbon is oxidized into carbon monoxide CO. To fully determine the reaction we have seen above that it is necessary to study the conditions of chemical equilibrium of the dissociation reaction of carbon dioxide, which depend primarily on temperature and correspond to the equation:



Combustion quality

The combustion quality is primarily determined by two factors:

- the combustion efficiency, which characterizes the degree of fulfillment of the chemical reaction, or if one prefers, the absence of unburned hydrocarbons or incompletely oxidized compounds;
- the level reached by the combustion temperature, determined by the ratio of the amount of heat released by burning to the amount of reactants and products.

In practice, we can optimize combustion by playing on an excess of air. A large excess air ensures that at any point, enough oxygen is available for combustion and therefore reduces the risk of unburned hydrocarbons. However, it dilutes the fumes, whose temperature drops.

7.6.2.4 Non stoichiometric combustion

When the combustion is not stoichiometric, it can be defined in several ways, usually by its excess air e , or its lack of air $(-e)$, or the richness R already introduced in section 7.6.1.2, or its inverse the air factor λ . The formulations vary according to existing professional practice. For example, it is

customary to speak of richness for gasoline engines, or excess air for boilers. In ThermoOptim, we have selected the air factor, very useful in practice.

Excess air is the percentage of air not consumed by the stoichiometric reaction.

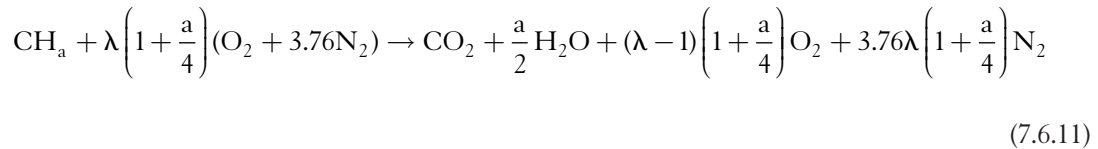
Richness R is defined as the ratio of the number of fuel moles in a given quantity of mixture, to the number of fuel moles in the stoichiometric mixture.

From these definitions, it follows the equivalence:

$$R = \frac{1}{1+e} \quad \text{and} \quad \lambda = 1+e = \frac{1}{R} \quad (7.6.10)$$

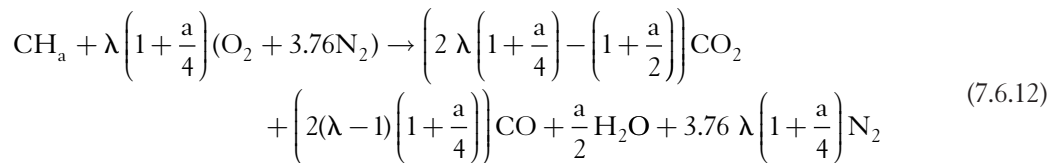
Let us consider how a non-stoichiometric reaction is written as a function of air factor λ :

In case of excess air, λ is greater than 1, and there is too much oxygen. The reaction writes:



In case of lack of air, λ is less than 1, and while there is enough oxygen to oxidize all the carbon in carbon monoxide, and a fraction in carbon dioxide, the reaction becomes:

$$1 > \lambda > \frac{\left(1 + \frac{a}{2}\right)}{2\left(1 + \frac{a}{4}\right)} \quad (\text{neglecting dissociation of CO}_2 \text{ in H}_2\text{O})$$



If the lack of air is more important, there is not even enough oxygen to form all the carbon monoxide.

7.6.3 Study of incomplete combustion

In most cases, the combustion is not complete: for many reasons, various products including unwanted pollutants exist in the flue gas. Efforts are generally made to minimize this phenomenon penalizing both energy production and the environment, but it cannot be completely avoided.

In this chapter we explain the principle of calculations that can be performed to characterize the incomplete combustion reactions. The results we obtain are the basis of combustion characterization methods from the flue gas analysis, which are of great practical importance. Note that the analysis of gases can be made before or after condensation of water they contain. In principle, of course, one passes from one to another without difficulty, provided the humidity of the air before combustion is known.

If these data are missing (which is most common), it is best to proceed on the basis of dry gas, that is to say after they have been sufficiently cooled so that the water they contain is condensed and is eliminated.

7.6.3.1 Mechanisms of formation of unburned hydrocarbons

The formation of unburned hydrocarbons can come from two main causes: either from lack of oxygen, related to poor homogeneity of the mixture of oxidizer/fuel or from a lack of reactivity of combustion, particularly due to too low a temperature.

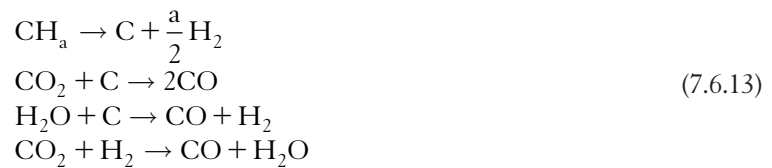
The mechanisms involved are very complex and cannot be described exhaustively in the context of this book. However, we can consider three limiting cases corresponding to the previous causes.

In the first case, fuel CH_a can be locally heated at high temperature in a CO_2 and H_2O environment, complete combustion products having not diffused to make room for oxygen. The fuel may then, due to the high temperature, be decomposed into carbon and hydrogen, strongly reducing, which will separate the molecules of CO_2 and H_2O .

This type of situation occurs very frequently: in the boilers or combustion chambers of gas turbines, where the fuel is fed into a burner, then mixed with the oxidizer, and burned. Whatever the nature of the fuel (gas, liquid or solid) and burner technology, a homogeneous mixture is not immediately realized, so that local areas may exist lacking air, even in the presence of overall excess air.

A chain of reactions between these components is then established, as determined in first approximation by the law of mass action, and therefore the conditions of pressure and ambient temperature.

The global chemical equations involved are as follows with of course many more basic steps (see 7.6.1.5):



In the second case, the fuel is decomposed in a more complex manner, the most volatile parts being easily vaporized in the gas phase and oxidized, while the heavier undergo cracking which enriches them in carbon. The phenomenon leads to the formation of dry or oily soot depending on whether or not hydrogen is completely released. Tar or heavily polluting smoke can also be formed. This situation exists in some boilers in the presence of significant excess air and can occur in diesel engines incorrectly set.

In the third case, the reaction is locally quenched on the walls of the combustion chamber, due to a double phenomenon: on the one hand, the surface temperature is lower than the flame and secondly the wall inhibits the branching and propagation of free radical reactions, which reduces dramatically the combustion kinetics.

This occurs especially in reciprocating internal combustion engines. In gasoline engines, there is a deposition on different surfaces (cylinder head, cylinder, piston, valves) of a layer of partially processed fuel mixture. The result is the presence in the exhaust of unburned hydrocarbons (often referred to as UHCs), which can to some extent be equated to a methane CH_4 equivalent.

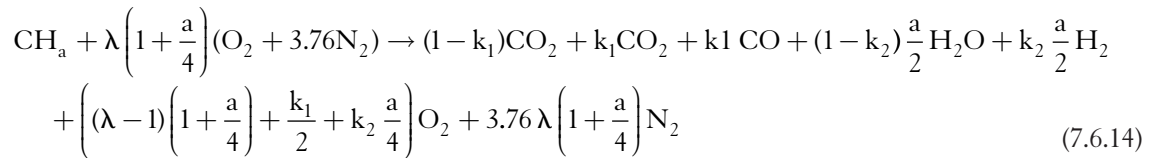
In diesel engines, the phenomenon is due to the strong heterogeneity of combustion: liquid fuel is injected into a mixture of hot air and combustion products, which burns by self-ignition, and whose nature changes during the combustion between pure air and exhaust gases. At the center of the jet, richness is infinite, whereas it is null in some areas. There can thus be simultaneously excess air in a zone of the chamber, and lack of air in another. Thus, a wrongly set diesel engine can simultaneously produce soot, unburned hydrocarbons of the CH_4 type and CO .

In what follows, we will show how the calculations can be conducted to characterize the combustion of three main categories of incomplete reactions. It is possible to study the combustion phenomena in a finer way, but at the cost of significant complication of the calculations, which must then

be made with heavy computer calculation programs, which bring into play simultaneously up to several hundreds of dissociation equations.

7.6.3.2 Composition of fumes without soot or unburned hydrocarbons

In the first case where the only unburned hydrocarbons are CO and H₂, we can write the combustion equation as follows:



The equilibrium between species giving unburned hydrocarbons is governed by the equation:



As can be seen, because the reaction involves a constant number of moles, this equilibrium is independent of pressure, and is a function of temperature alone. According to the law of mass action, we have here:

$$K_p = \frac{[\text{CO}][\text{H}_2\text{O}]}{[\text{CO}_2][\text{H}_2]} = \frac{k_1(1 - k_2)\frac{a}{2}}{(1 - k_1)k_2\frac{a}{2}} = \frac{k_1(1 - k_2)}{(1 - k_1)k_2} \quad (7.6.16)$$

We get thus: $k_2(1 - k_1)K_p = k_1(1 - k_2)$

$$k_2 = \frac{k_1}{k_1 + K_p(1 - k_1)} \quad (7.6.17)$$

Let $k = k_1$, to simplify the notations.

For a given fuel, the combustion can then be described by only three parameters: λ , air factor, k , CO₂ rate of dissociation and K_p .

The analysis of dry flue gas (after condensation and removal of H₂O) then provides the volume or partial molar fractions. Letting Σ be the sum of fractions of various constituents, we get:

$$\Sigma = 4.76\lambda \left(1 + \frac{a}{4} \right) + \frac{a}{2} + \frac{k}{2} - \frac{3K_p(1 - k)}{k + K_p(1 - k)} \frac{a}{4} \quad (7.6.18)$$

Let

$$g(k) = - \frac{K_p(1 - k)}{k + K_p(1 - k)} \frac{a}{4} \quad (7.6.19)$$

we get:

$$(1) \quad [\text{CO}_2] = \frac{1 - k}{\Sigma}$$

$$(2) \quad [\text{CO}] = \frac{k}{\Sigma}$$

$$(3) \quad [\text{N}_2] = \frac{3.76\lambda \left(1 + \frac{a}{4}\right)}{\Sigma}$$

$$(4) \quad [\text{O}_2] = \frac{\lambda \left(1 + \frac{a}{4}\right) + \frac{k}{2} - 1 + g(k)}{\Sigma}$$

$$(5) \quad [\text{H}_2] = \frac{ka}{2(k + K_p(1 - k))\Sigma}$$

$$(6) \quad \Sigma = 4.76\lambda \left(1 + \frac{a}{4}\right) + \frac{a}{2} + \frac{k}{2} + 3g(k)$$

These volume fractions depend only on four parameters: λ , k and K_p , characterizing combustion, and a characterizing the fuel.

Suppose that we know $[\text{CO}]$ and $[\text{CO}_2]$ (we shall see later that their determination is relatively easy).

(1) and (2) can be combined to give k , by:

$$(7) \quad k = \frac{[\text{CO}]}{[\text{CO}] + [\text{CO}_2]}$$

and recombining with (2) :

$$(8) \quad \Sigma = \frac{1}{[\text{CO}] + [\text{CO}_2]}$$

If a and K_p are known (which implies that the quenching temperature of the reaction is known), $g(k)$ can be calculated, and λ is provided by (6). Then (3), (4) and (5) allow one to fully characterize the reaction.

$$\lambda = \frac{[\text{N}_2]}{3.76 \left(1 + \frac{a}{4}\right) ([\text{CO}] + [\text{CO}_2])} \quad (7.6.20)$$

If K_p is not known, the value of $[\text{O}_2]$ allows us to eliminate $g(k)$ between (3) and (6), and thus determine λ .

In the case where in addition the value of a is uncertain, knowledge of $[\text{H}_2]$ allows us, as we can ascertain, to solve the problem.

PRACTICAL APPLICATION

Practical Calculation of Combustions

The developments presented in this section are of paramount importance in practice:

- When analysis of dry flue gas is available, they allow one to fully characterize the combustion by determining the value of the CO_2 dissociation rate and the quenching temperature;
- When the value of the CO_2 dissociation rate and the quenching temperature are known or estimated, they allow us to fully calculate the combustion, as for example in the gas turbine model presented section 9.3 of this Part.

They have been implemented in Thermoptim and constitute the basis for the practical calculation of all combustions taking place in internal combustion engines or boilers which are presented in this book, namely in Chapters 12, 13 and 16 of Part 3.

Establishment of the Biard chart

Now let us suppose the fuel is known, and therefore the value of a . The determination of λ and k can be done by choosing two independent relations among the five previous equations, since we set the value of K_p by studying the reaction at a given temperature T .

Note that $[\text{CO}]$ and $[\text{H}_2]$ are proportional, so we can often only consider their sum.

Some devices directly determine the amount of unburned hydrocarbons by measuring the heat from the catalytic oxidation of $\text{CO} + \text{H}_2$, whose heating values are close enough to be assimilated.

The detection of $[\text{CO}_2]$ and $[\text{O}_2]$ being relatively easy, it is usually from their equations that λ and k are determined.

The system:

$$[\text{CO}_2] = \frac{1-k}{\Sigma}$$

$$[\text{O}_2] = \frac{\lambda \left(1 + \frac{a}{4}\right) + \frac{k}{2} - 1 + g(k)}{\Sigma}$$

can be rewritten as:

$$\Sigma = 4.76\lambda \left(1 + \frac{a}{4}\right) + \frac{a}{2} + \frac{k}{2} + 3g(k)$$

$$\Sigma [\text{CO}_2] = 1 - k$$

$$\Sigma [\text{O}_2] = \lambda \left(1 + \frac{a}{4}\right) + \frac{k}{2} - 1 + g(k)$$

By expanding, we get:

$$\left[4.76 \left(1 + \frac{a}{4}\right) + \frac{a}{2} + \frac{k}{2} + 3g(k)\right] [\text{CO}_2] = 1 - k$$

$$\lambda = \frac{1 - k - \left(\frac{a}{2} + \frac{k}{2} + 3g(k)\right) [\text{CO}_2]}{4.76 \left(1 + \frac{a}{4}\right) [\text{CO}_2]} \quad (7.6.21)$$

Replacing λ in the $[\text{O}_2]$ equation we get:

$$(1 - k) (4.76[\text{O}_2] - 1) + \left(\frac{a}{2} + 4.76 - 3.76 \frac{k}{2} + 1.76g(k)\right) [\text{CO}_2] = 0 \quad (7.6.22)$$

For $k = \text{Const.}$, this relationship defines in the plane ($[\text{O}_2]$, $[\text{CO}_2]$) a bundle of straight lines which all pass through point O of coordinates (0.21, 0) (Figure 7.6.1).

They cut the y-axis at coordinates:

$$\left[0; \frac{1 - k}{\frac{a}{2} + 4.76 - 3.76 \frac{k}{2} + 1.76g(k)}\right]$$

For $k = 0$, maximum point P has coordinates:

$$\left[0; \frac{1}{4.76 + 3.76 \frac{a}{4}} \right]$$

Note that line $k = 0$ corresponds to perfect combustion, without unburned hydrocarbons. Point P represents then the neutral or stoichiometric combustion.

$$\text{Elsewhere } [\text{CO}] = \frac{k}{\Sigma} \quad \text{and} \quad [\text{H}_2] = \frac{ka}{2(k + K_p(1-k))\Sigma}$$

We have:

$$\frac{[\text{CO}]}{[\text{CO}_2]} = \frac{k}{1-k}$$

$$\frac{[\text{H}_2]}{[\text{CO}_2]} = \frac{ka}{2(k + K_p(1-k))(1-k)}$$

Both expressions depend only on k , not λ , $[\text{O}_2]$ or $[\text{CO}_2]$.

We can therefore directly graduate lines $k = \text{const.}$ in $([\text{CO}]/[\text{CO}_2])$ or $([\text{H}_2]/[\text{CO}_2])$.

For $\lambda = \text{Const.}$, the curve linking $[\text{CO}_2]$ and $[\text{O}_2]$ is given by parametric equations based on k :

$$[\text{CO}_2] = \frac{1-k}{\Sigma} \tag{7.6.23}$$

$$[\text{O}_2] = \frac{\lambda \left(1 + \frac{a}{4} \right) + \frac{k}{2} - 1 + g(k)}{\Sigma}$$

In the general case they are decreasing curves concave upwards.

All these curves can be represented in the Biard chart, established for a given quenching temperature, an example of which is given Figure 7.6.1.

Establishment of the Ostwald chart

In some cases it is possible to simplify the above expressions by a number of additional approximations.

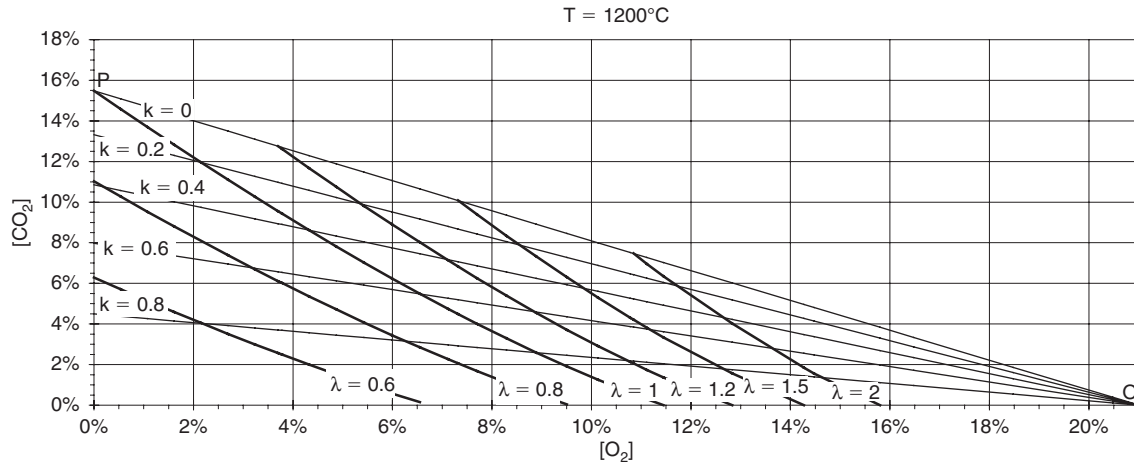
In the temperature range of normal combustion in the presence of excess air (1000–1500 K), we have seen that constant K_p of the law of mass action can be approximated by the equation:

$$K_p = \exp(3.387 - (3753/T)), \text{ which varies here between 0.7 and 2.6.}$$

Assuming that in the expression of K_p , k_1 and k_2 are very small compared to 1, we obtain:

$$K_p = \frac{k_1}{k_2}$$

Experience shows that we can consider that the equilibrium is frozen when the fume temperature drops below a certain limit. We assume in what follows that it can be characterized by a K_p value close to 2.


FIGURE 7.6.1

 Biard chart for light fuel oil ($T_{\text{quench}} = 1200^{\circ}\text{C}$)

Combustion can then be described by two parameters only:

λ , or e , characterizing the excess air, and $k = k_1 = 2k_2$.

The above equations are simplified, since function $g(k)$ becomes linear and we can eliminate k in the relationship between $[\text{CO}_2]$ and $[\text{O}_2]$. All curves $\lambda = \text{Const}$ define in this case a second straight line bundle.

This double bundle has the following interesting features:

- line $k = 0$ passes through point O, of coordinates:

$$[\text{CO}_2]_{\text{O}} = 0$$

$[\text{O}_2]_{\text{O}} = 1/4.76 = 0.21$ which corresponds to $\lambda = \infty$
and through point P of coordinates

$$[\text{CO}_2]_{\text{P}} = \frac{1}{4.76 + 3.76 \frac{a}{4}}$$

$[\text{O}_2]_{\text{P}} = 0$ which corresponds to $\lambda = 1$

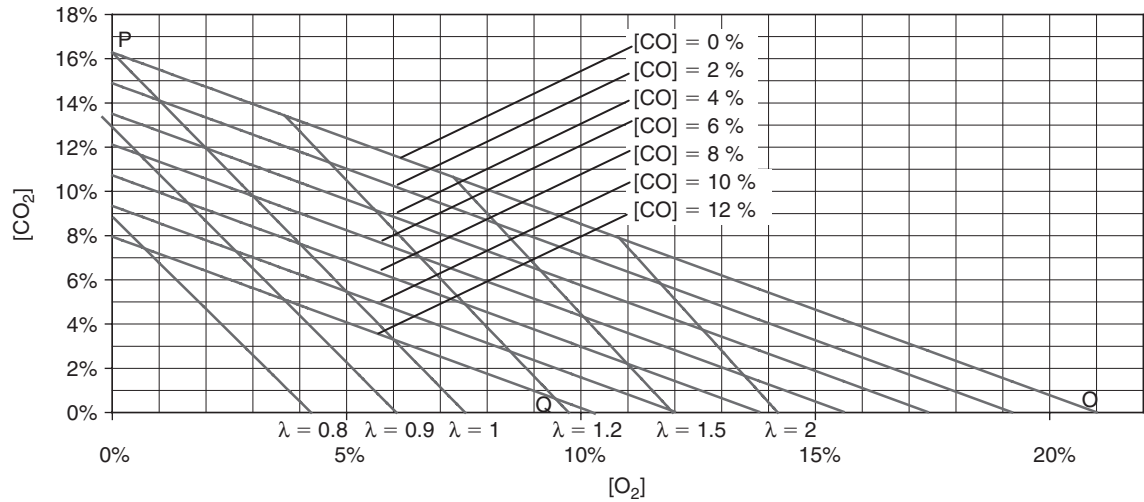
The slope of this line is equal to $-4.76/(4.76 + 3.76(a/4))$

- O is the point common to all the straight lines $k = \text{const}$, since it is determined by the air composition;
- line $k = 1$ is the x-axis of equation $[\text{CO}_2] = 0$;
- line $\lambda = 1$ passes through point P above, and meets the x-axis ($k = 1$) in Q, with coordinates:

$$[\text{CO}_2]_{\text{Q}} = 0 \quad [\text{O}_2]_{\text{Q}} = \frac{1}{2 \left(4.76 + \frac{1}{4} \right)} = 0.095$$

and whose position is independent of a . This line has slope:

$$\frac{-8.52}{4.76 + 3.76 \frac{a}{4}}$$

**FIGURE 7.6.2**

Ostwald chart for heavy fuel

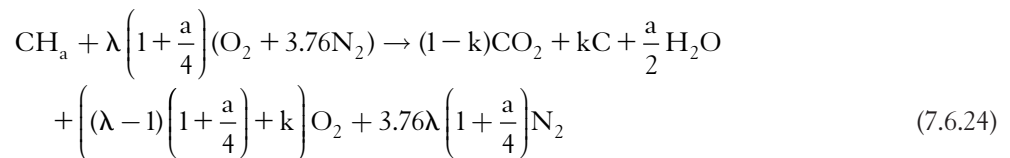
Any normal combustion must have a composition ($[CO_2]$, $[O_2]$) located in the triangle OPQ, the closest to P.

This is called an Ostwald chart. It has the appearance of Figure 7.6.2.

The assumption of linearity of the iso-air ratio curves is better verified in the case of heavy fuel oil than for natural gas.

7.6.3.3 Composition of fumes with soot and without CO or HC

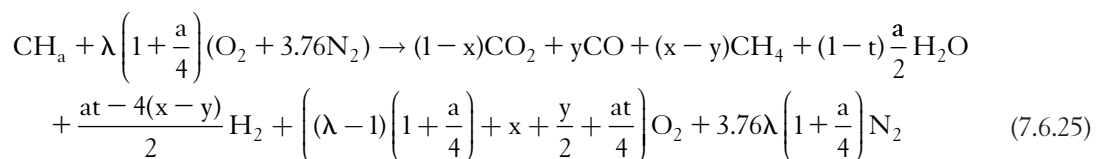
If one accepts that in case of low activation of the reaction, there is essentially dry soot composed of carbon, the combustion equation becomes:



An analysis similar to the previous would allow one to determine the concentrations of the different species.

7.6.3.4 Composition of fumes without soot and with CO and HC

In the third case, when the unburned hydrocarbons are of type CO, HC(CH₄) and H₂, we can write the combustion equation as follows:



The law of mass action gives here:

$$K_p = \frac{[\text{CO}][\text{H}_2\text{O}]}{[\text{CO}_2][\text{H}_2]} = \frac{y(1-t)^{\frac{a}{2}}}{(1-x)^{\frac{at-4(x-y)}{2}}} \quad (7.6.26)$$

Here also calculations could be carried out as in 7.6.3.2.

7.6.3.5 Analysis of fumes

The above paragraphs show the relevance of knowing the composition of the fumes. It allows us to fully characterize the combustion reaction, and therefore to get access to all the thermodynamic properties and energy products. To analyze the smoke, two broad categories of methods exist: discontinuous and continuous analyzers.

With the exception of high precision but heavy and expensive devices, such as chromatographs and spectrometers, discontinuous analyzers are generally relatively imprecise. They are based either on selective chemical absorption of fume components (Orsat analyzers), or on the measure of their thermal conductivity (catharometers), or on calorimetric methods (measurement of unburned hydrocarbons by combustion on catalytic hot wire).

The continuous monitors are now much used, as pretty accurate (about 1% of full scale), and very practical for use because they operate continuously. There are four main categories:

- infrared analyzers selective type NDIR (Non Dispersive Infra Red) are used to measure concentrations of CO₂, CO or unburned hydrocarbons (UHCs). Their principle is to compare the IR absorption bands of these gases with those of standard gases;
- flame ionization detectors (FID) type analyzers provide a much better accuracy than previous analyzers to measure the concentration of unburned hydrocarbons (UHCs). Their principle is to measure the electrical conductivity of smoke, which is directly proportional to the concentration of charged particles, i.e. for hydrocarbon molecules, the number of carbon atoms C;
- the chemiluminescence analyzers are used to detect nitrogen oxides NO_x. Their principle is to measure the infrared radiation emitted during the oxidation of NO to NO₂ by ozone O₃;
- pneumo-paramagnetic analyzers determine the oxygen concentration O₂ in the fumes. Their principle is to measure the magnetic susceptibility¹ of smoke, which is almost equal to that of oxygen, other gases having magnetic susceptibilities from 100 to 200 times lower, with the exception of nitrogen oxides present in very small quantities.

Table 7.6.3 summarizes the various types of analyzers used.

For most energy applications, knowledge of the first three gas concentrations is generally considered sufficient, data on NO_x only being required for pollution controls, and concentrations of other gases being calculated from relationships of the type we have established in the preceding pages. As we have indicated, we generally consider that the unburned hydrocarbons UHCs are in the form of a methane equivalent CH₄.

¹ the magnetic susceptibility H of a substance is equal to its permeability μ minus one unit, μ being the ratio of the magnetic flux density in the substance to the magnetic flux density in the vacuum. Among all gases present in the fumes, O₂, NO and NO₂ are the only paramagnetic ($H > 0$), the others being diamagnetic ($H < 0$).

TABLE 7.6.3
VARIOUS TYPES OF ANALYZERS

	principle	scale
CO ₂	selective infrared analyzers (NDIR)	0–5 %
		0–20 %
CO	selective infrared analyzers (NDIR)	0–2.5 %
		0–25 %
HC	selective infrared analyzers (NDIR)	0–10 %
		flame ionization detector (FID)
		0–100 %
		0–10 ppm
		0–100 ppm
		0–1000 ppm
		0–10000 ppm
O ₂	paramagnetism	0–21 %
NO _x	chemiluminescence (CL)	

7.6.4 Energy properties of combustion reactions

7.6.4.1 Thermodynamic properties of species in reaction

One of the main objectives of combustion studies is the determination of energy exchanges that occur when chemical reactions take place.

For this, it suffices to know the internal energies or enthalpies of reactants and products, because the energy exchange at stake does not depend on intermediate reactions, but only on initial and final states of chemical species in reaction.

We define the combustion **heat of reaction** as the change in internal energy or enthalpy of the mixture, depending on whether the reaction takes place at constant volume or constant pressure.

For a reaction at constant volume, we have:

$$Q_v = (\Delta U_r)_v = (U_p - U_r)_v$$

At constant pressure:

$$Q_p = (\Delta H_r)_p = (H_p - H_r)_p \quad (7.6.27)$$

Evidently, the calculation of heats of reaction implies knowledge of the internal energies U_r and U_p or enthalpies H_r and H_p of reactants and products. As mentioned previously, the principle of their calculation is based on the assumption that the different constituents are reacting in the gaseous state, and each of them is comparable to an ideal gas. Their mixture under these conditions is itself an ideal gas.

If we note x_i the molar concentrations and y_i the mass concentrations of the various constituents, we have, let us recall:

$$P_i = x_i P$$

$$M = \sum x_i M_i$$

In mass units

$$h = \sum y_i h_i$$

$$s = \sum y_i s_i(T, P_i) = \sum \left(y_i \int \frac{c_{pi}(t)}{t} dt - r y_i \ln P_i \right)$$

In molar units

$$H = \sum x_i H_i$$

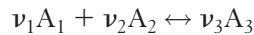
$$S = \sum x_i S_i (T, P_i) = \sum \left(x_i \int \frac{C_{pi}(t)}{t} dt - R x_i \ln P_i \right)$$

Note that in an equilibrium reaction, the x_i and y_i depend on temperature, because of the law of mass action. The evaluation of h_i and s_i is based on a reference common to all substances, at a temperature of 25°C and a pressure of 1 bar. The internal energy and enthalpy of different substances, known as heats of formation u_f or h_f are determined in this reference state by methods that are outside the scope of this book; they are available in tables (e.g. JANAF Tables, Chase et al. 1985).

7.6.4.2 Enthalpies of formation

For all elements, or simple substances, the value of enthalpy of formation h_f is chosen equal to 0 in the reference state. For compound substances, it is not zero, but its value is the enthalpy consumed or released during the chemical reaction that leads to the development of the compound.

If we have:



with A_1 and A_2 simple substances of enthalpies of formation equal to 0,

$$h_B = (H_p - H_r)_p = H_p$$

The determination of thermodynamic functions, temperature and pressure of the reaction is then done using formulas (5.6.5) (5.6.6) and (5.6.7) for ideal gases.

$$h(T) = h_f + \int_{298.15}^T c_p(t) dt \quad (7.6.28)$$

7.6.4.3 Entropies of reference

Similarly, we can tabulate the values of entropy of different substances in this reference state. For this purpose, reasoning is based on a principle, derived on experimental observations, sometimes called the third law of thermodynamics, which states that when the temperature approaches absolute zero, the entropy of pure substances approaches zero.

Reference entropies can thus be determined by integration between 0 and 298.15 K of equation:

$$ds = \frac{dh}{T} - v \frac{dP}{T}$$

For an ideal gas, for $P_0 = 1$ bar,

$$s_0 = \int_0^{298.15} \frac{c_p(t)}{t} dt$$

s_0 is usually read directly from tables, and calculating the entropy of an ideal gas at temperature T and pressure P is done by applying equation (5.6.7):

$$s = s_0 + \int_{298.15}^T \frac{c_p(t)}{t} dt - r \ln(P) \quad (7.6.29)$$

TABLE 7.6.4
ENTHALPIES AND ENTROPIES OF FORMATION

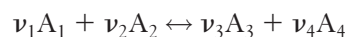
		M kg/kmol	h₀ kJ/kmol	s₀ kJ/kmol/K
Carbon monoxide	CO	28.01	-110,530	197.56
Carbon dioxide	CO ₂	44.01	-393,520	213.64
Water (vapor)	H ₂ O	18.02	-241,820	188.72
Water (liquid)	H ₂ O	18.02	-285,830	69.92
Methane	CH ₄	16.04	-74,850	186.16
Ethylene	C ₂ H ₄	28.05	52,280	219.83
Ethane	C ₂ H ₆	30.07	-84,680	229.49
Ammonia	NH ₃	17.04	-46,190	192.33
Acetylene	C ₂ H ₂	26.04	226,730	200.85
Propane	C ₃ H ₈	44.09	-103,850	269.91
n-Butane	C ₄ H ₁₀	58.12	-126,150	310.12
n-Pentane	C ₅ H ₁₂	72.15	-146,440	348.69
n-Hexane	C ₆ H ₁₄	86.17	-167,200	388.40
n-Heptane	C ₇ H ₁₆	100.20	-187,820	427.77
n-Octane	C ₈ H ₁₈	114.22	-208,450	466.73
Benzene	C ₆ H ₆	78.11	82,930	269.20
Methyl alcohol	CH ₃ OH	32.05	-200,670	239.70
Ethyl alcohol	C ₂ H ₅ OH	46.07	-235,310	282.59

Table 7.6.4, extracted from (Holman, 1988), gives the enthalpies and entropies of formation of some common substances.

7.6.4.4 Heats of reaction

Once the enthalpies of formation of various chemical species are known, the calculation of heat of reaction is simple.

Let us use general equation 7.6.1 considered at the beginning of the chapter:



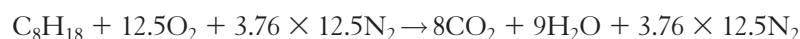
Let us note h_{fi} the enthalpies of formation of the A_i .

We obtain the heat of reaction by writing:

$$-\Delta H_r = \nu_1 h_{f1} + \nu_2 h_{f2} - \nu_3 h_{f3} - \nu_4 h_{f4} \quad (7.6.30)$$

In an equilibrium reaction, the heat of reaction ΔH_r is a function of ν_i and thus x_i . Therefore, when the reaction is not complete or there is dissociation, the heat of reaction is different from that obtained under stoichiometric conditions, as shown in the following example.

Let us calculate for example the heat of reaction of octane for a stoichiometric reaction:



$$-\Delta H_r = h_{fC_8H_{18}} + 12.5h_{fO_2} - 8h_{fCO_2} - 9h_{fH_2O}$$

$$-\Delta H_r = -208450 + 0 - 8(-393520) - 9(-285830) = 5,512,180 \text{ kJ/kmol}$$

The molar mass of octane being 114.22 kg/kmol, its heat of reaction mass is equal to:

$$-Q_p = 48,259 \text{ kJ/kg}$$

If the reaction is not stoichiometric, but occurs in the absence of air, the formation of carbon monoxide decreases the heat of reaction.

For richness equal to 1.25, for example, the reaction becomes:



$$-\Delta H_r = \Delta h_{f\text{C}_8\text{H}_{18}} + 10\Delta h_{f\text{O}_2} - 3\Delta h_{f\text{CO}_2} - 5\Delta h_{f\text{CO}} - 9\Delta h_{f\text{H}_2\text{O}}$$

$$-\Delta H_r = -208450 + 0 - 3(-393520) - 5(-110530) - 9(-285830) = 4,097,230 \text{ kJ/kmol}$$

i.e. a decrease of 25.7% over the stoichiometric reaction.

7.6.4.5 Higher and lower heating value

In most cases, the reaction products are found in the gaseous state at the end of combustion, but it is possible at low temperature, that some of them are liquid or even solidify, releasing a heat of condensation or solidification.

The problem arises especially during the combustion of hydrocarbons, water appearing among the products. The maximum energy release is obtained when the water contained in the fume is liquefied. The complete value of the heat of reaction is named Higher Heating Value or HHV. Where all the water produced remains in the vapor state, it is given the name of Lower Heating Value or LHV. If only a fraction of the water condenses, the heat of reaction is an intermediate value between the HHV and LHV.

Based on the above definitions, we identify four heating values which are particularly interesting: at constant pressure or volume, and lower or higher.

In fact, heating values at constant pressure and volume are substantially equal. However, enthalpies of vaporization are far from negligible (for water, it is approximately 45 MJ/kmol at 0°C). So there are significant differences between the values of fuel HHV and LHV, and it is important to specify which one is used.

In conclusion, therefore, to determine the energies involved in a complete combustion reaction, you should use the fuel heating value, specifying whether it is the higher heating value (HHV) or the lower heating value (LHV).

The heating values of specific fuels commonly used in internal combustion engines are fairly close to each other. One can indeed show that hydrocarbon LHV range is from 44 MJ/kg to 40 MJ/kg when we consider products of distillation of increasing molar weight.

For gaseous fuels, heating values are generally expressed in kJ/m^3_{N} . They are obtained by dividing the heat of reaction in kJ/kmol by the volume occupied by a normal kilomol (0°C, 1 bar), i.e. 22.414 m^3 .

In ThermoOptim, the LHV values of gases are displayed in the compound gas editor screen.

7.6.4.6 Adiabatic flame temperature

If we assume that the reaction takes place without heat exchange with the outside, that is to say adiabatically, it is possible to calculate the temperature reached by the mixture.

To do this, simply write that the enthalpy of the products is equal to that of the reactants in the initial state.

Temperature T_{ad} is thus given by:

$$H_p = H_{p0} + \int_{T_0}^{T_{\text{ad}}} C_{p,p}(t) dt = H_r \quad (7.6.31)$$

with

$$H_r = H_{r0} + \int_{T_0}^{T_r} C_{p_r}(t) dt$$

Values with index 0 are relative to the reference state (298.15 K, 1 bar), and T_r is the temperature of the reactants when the combustion has been initiated.

We therefore should resolve:

$$\int_{T_0}^{T_{ad}} C_{p_p}(t) dt = H_{r0} - H_{p0} + \int_{T_0}^{T_r} C_{p_r}(t) dt$$

Since by definition $(-\Delta H_r) = H_{r0} - H_{p0}$

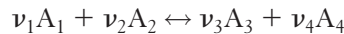
$$\int_{T_0}^{T_{ad}} C_{p_p}(t) dt = (-\Delta H_r) + \int_{T_0}^{T_r} C_{p_r}(t) dt \quad (7.6.32)$$

In the general case of an equilibrium reaction in the presence of dissociation, this equation can be very complex, since ΔH_r depends on T_{ad} by the law of mass action.

In the case where the reaction is complete, (7.6.32) corresponds to solving a polynomial with real coefficients in T_{ad} , which can be done iteratively, for example.

In practice, the calculation of adiabatic temperature T_{ad} has a number of pitfalls. It is particularly important to take into account the variation in the number of moles during the reaction. For this, the best way is probably to think in molar units and to use the coefficients of the chemical reaction.

With the general equation considered earlier in this chapter:



We have seen that the calculation of the heat of reaction is very simple by writing:

$$-\Delta H_r = \nu_1 \Delta h_{01} + \nu_2 \Delta h_{02} - \nu_3 \Delta h_{03} - \nu_4 \Delta h_{04}$$

For this reaction, the general equation (7.6.32) becomes:

$$(\nu_3 + \nu_4) \int_{T_0}^{T_{ad}} C_{p_p}(t) dt = (-\Delta H_r) + (\nu_1 + \nu_2) \int_{T_0}^{T_r} C_{p_r}(t) dt$$

Where C_p represents the molar heat capacity.

It is also possible to take into account incomplete reactions (non-stoichiometric conditions, dissociation), provided the value of equilibrium constants K_p are set, iterating once the temperature T_{ad} is known.

7.6.4.7 Combustion in boilers

To design and conduct boilers, the assumption is often made that the combustions are complete, to avoid too complex calculations. Moreover, volume flows involved are of importance, because of their influence on losses from fume and combustion efficiency. The practice has led to them being characterized by notions of airflow required and smoke developed.

7.6.4.7.1 Airflow required and smoke developed

Assuming complete combustion, the energy released is characterized by its heating value, higher or lower. To qualify the gas volumes involved, airflow required and smoke developed are introduced,

whose main value is to firstly determine the losses through the smoke, and secondly to design the air and exhaust fumes supply arrangements.

We define the **airflow required** V_{an} (or neutral air volume) as the amount of air necessary and sufficient to ensure complete combustion of the unit quantity of fuel (or neutral stoichiometric combustion) and **smoke developed** V_{fn} (or neutral volume of smoke) as the amount of gas produced by combustion of the theoretical unit of fuel. In the latter case, you must specify whether you are interested in dry gas (V_{fns}), that is to say sufficiently cooled so that water vapor is totally condensed or in moist fumes (V_{fnh}). By default, the smoke developed relates to dry gas (V_{fns}).

Reaction in the presence of excess air is in turn characterized by the actual volume of air V_{ar} and the real volume of smoke (dry V_{frs} or moist V_{frh}).

Given the definition of air factor:

$$V_{ar} = \lambda V_{an}$$

Moreover, the volume of smoke in the presence of excess air is equal to the smoke developed, plus the excess air, which did not participate in the combustion reaction:

$$V_{frs} = V_{fns} + (\lambda - 1)V_{an}$$

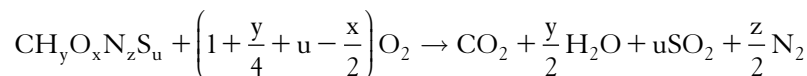
$$V_{frh} = V_{fnh} + (\lambda - 1)V_{an}$$

Let us recall that these relationships are valid if the reaction is complete, i.e. if there are no unburned hydrocarbons or formation of nitrogen oxides NO_x , otherwise the oxygen balance is no longer verified. If the fuel is gaseous, the unit used to quantify is the normal cubic meter, or if liquid or solid, the kilogram. Airflow required, smoke developed and air or smoke volumes are expressed in m^3/m^3 or m^3/kg .

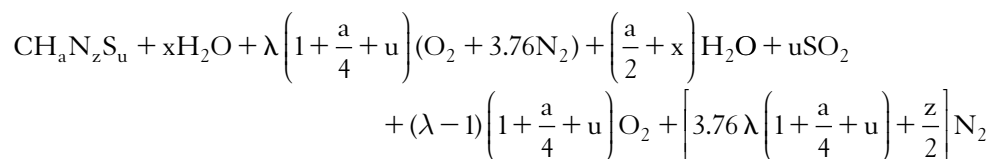
7.6.4.7.2 Relationships with excess air and flue gas composition

It is possible to generalize the developments presented in paragraph 7.6.3, to investigate the relationship between excess air, flue gas composition and airflow required and smoke developed. In what follows, we refer to dry gas. The reasoning can be easily transposed to moist smoke.

The stoichiometric equation for the complete combustion of any fuel has been established above (7.6.7):



In the presence of excess air, and introducing hydrogen available for combustion we obtain:



In what follows, the concentrations of species may be referred to either dry or moist smoke. What matters is that the calculations are done consistently.

$$[CO_2] = \frac{1}{V_{fr}}$$

$$[\text{O}_2] = \frac{(\lambda - 1) \left(1 + \frac{a}{4} + u \right)}{V_{\text{fr}}} = \frac{(\lambda - 1) \frac{V_{\text{an}}}{4.76}}{V_{\text{fr}}}$$

$$\frac{[\text{O}_2]}{0.21} = \frac{(\lambda - 1) V_{\text{an}}}{V_{\text{fr}}} = \frac{(\lambda - 1) V_{\text{an}}}{V_{\text{fn}} + (\lambda - 1) V_{\text{an}}} = 1 - \frac{V_{\text{fn}}}{V_{\text{fn}} + (\lambda - 1) V_{\text{an}}}$$

Let us call $[\text{CO}_2]_0$ the CO_2 concentration of flue gases (dry or moist, as the case may be) obtained for a stoichiometric combustion.

$$[\text{CO}_2]_0 = \frac{1}{V_{\text{fn}}} \quad \frac{[\text{O}_2]}{0.21} = 1 - \frac{[\text{CO}_2]}{[\text{CO}_2]_0}$$

$$\frac{[\text{CO}_2]}{[\text{CO}_2]_0} + \frac{[\text{O}_2]}{0.21} = 1 \quad (7.6.33)$$

Here we find a generalization of Equation 7.6.22 presented above. In taking average values for $[\text{CO}_2]_0$, we obtain the following relations:

natural gas:

$$[\text{CO}_2] = 0.12 \left(1 - \frac{[\text{O}_2]}{0.21} \right)$$

LPG:

$$[\text{CO}_2] = 0.14 \left(1 - \frac{[\text{O}_2]}{0.21} \right)$$

heating oil:

$$[\text{CO}_2] = 0.15 \left(1 - \frac{[\text{O}_2]}{0.21} \right)$$

heavy fuel:

$$[\text{CO}_2] = 0.16 \left(1 - \frac{[\text{O}_2]}{0.21} \right)$$

coal:

$$[\text{CO}_2] = 0.18 \left(1 - \frac{[\text{O}_2]}{0.21} \right) \text{ to } 0.2 \left(1 - \frac{[\text{O}_2]}{0.21} \right)$$

Moreover, as:

$$[\text{O}_2] = \frac{(\lambda - 1) \frac{V_{\text{an}}}{4.76}}{V_{\text{fr}}}$$

$$[\text{O}_2] = \frac{(\lambda - 1) V_{\text{an}}}{4.76(V_{\text{fn}} + (\lambda - 1) V_{\text{an}})} \quad (7.6.34)$$

$$[\text{O}_2] = \frac{V_{\text{ar}} (\lambda - 1)}{V_{\text{fr}} 4.76 \lambda}$$

$$\lambda = 1 + e = \frac{1}{1 - \frac{[\text{O}_2]}{0.21} \frac{V_{\text{fr}}}{V_{\text{ar}}}} \quad (7.6.35)$$

$$e = \lambda - 1 = \frac{V_{\text{fr}}}{V_{\text{an}}} \frac{1}{\frac{0.21}{[\text{O}_2]} - 1} \quad (7.6.36)$$

These last three expressions can often be simplified by considering only a first approximation for most fuels, $V_{\text{ar}} \approx V_{\text{fr}}$. They allow, knowing the oxygen concentration of the smoke, the excess air to be directly determined. The latter is widely used because it helps to know the excess air from the airflow required and smoke developed, which depend only on the fuel, and the value of the oxygen concentration of fumes.

7.6.4.7.3 Summary combustion tables

When the fuel is characterized by its weight formula, the determination of combustion is as follows. For each component, we calculate:

- the number of moles per kg of fuel ($nm = 1000 \times \% \text{mass}/M$);
- the number of moles of oxygen reacting (nm for C or S, $nm/2$ for H_2);
- the associated nitrogen (3.76 times the number of moles of oxygen) (the airflow required (mol/kg) is deduced by summing);
- the number of moles of CO_2 , SO_2 , N_2 , H_2O in the products; the smoke developed (mol/kg) is deduced by summing.

Values in $\text{m}^3\text{N}/\text{kg}$ are obtained by multiplying previous values by 0.02214.

Table 7.6.5 provides the calculations for stoichiometric combustion of methane, with determination of airflow required and smoke developed.

Based on the theoretical analysis presented above, we can see that one of the main characteristics of fuels is the ratio a of the number of hydrogen atoms to that of carbon. Sometimes it is rather its reverse, $C/H = 1/a$ which is used.

A classification of fuels most often used in boilers can be found in Table 7.6.6.

7.6.4.8 Combustion efficiency

In a boiler or a heat engine, the total energy released by combustion is not always used: a part is carried away by the fumes, another corresponds to losses through the walls etc.

To characterize these losses, we introduce the concept of combustion efficiency, one difficulty being that definitions vary according to the authors and the types of use.

When it is possible to isolate the combustion from other phenomena, it is quite natural to call combustion efficiency the ratio of useful energy at the output of the combustion chamber to the energy theoretically available to the burner. The losses in the combustion chamber in this case essentially correspond to losses through the walls and loss by incomplete combustion, which can be characterized by the concept of LHV (or possibly HHV) efficiency, the ratio of energy available in the burner to the heating value of the fuel.

$$\eta_c = \frac{\text{useful energy}}{\text{LHV}}$$

$$\eta_c = \frac{\text{LHV} - \text{losses by walls} - \text{losses by incomplete combustion}}{\text{LHV}}$$

TABLE 7.6.5
METHANE COMBUSTION

	Fuel			Neutral air		Flue gas			
	% mass	M	comp.	O ₂	N ₂	CO ₂	SO ₂	N ₂	H ₂ O
C	75	12.01	62.44	62.44	234.78	62.44		234.78	
H ₂	25	2.02	124.01	62.44	233.13			233.13	124.01
total	100	9.51	186.45	124.45	467.92	62.44	0.00	467.92	124.01
				Neutral air	592.37	Dry neutral flue gas			530.36
						Moist neutral flue gas			654.37
Neutral air volume					13.271	m ³ n/kg			
Dry neutral flue gas volume					11.872	m ³ n/kg			
Water vapor volume					2.625	m ³ n/kg			
Moist neutral flue gas volume					14.497	m ³ n/kg			
V _{fns} /V _{an}				89.46%					
CO ₂ volume					1.390	m ³ n/kg			
N ₂ volume					10.482	m ³ n/kg			
CO _{2n}				11.71%					
HHV					12.28	kWh/kg			
LHV					10.78	kWh/kg			
C/H		0.25							

TABLE 7.6.6
CLASSIFICATION OF FUELS

Fuel	C/H	HHV	LHV	V _{fns} /V _{an}	V _{fnh}	CO _{2n}
<i>gaseous</i>		kWh/m ³	kWh/m ³			
		<i>gaz</i>	<i>gaz</i>		<i>m³n</i>	<i>%</i>
natural gas	0.269	12.28	11.15	0.908	11.72	12.06
Com. propane	0.41	27.4	24.7	0.917	25.4	14.1
Com. butane	0.42	35.5	32	0.926	33.1	14.3
<i>liquid/solid</i>		kWh/kg	kWh/kg		<i>m³n</i>	<i>%</i>
light fuel oil	0.54	12.7	11.9	0.937	12.02	15.28
heavy fuel oil	0.68	11.52	10.89	0.947	11.12	16.06
coal	0.88		7.3 à 9	0.962		18 à 20
dry wood	0.66	5.4–5.8	5.1–5.4	0.99	5.1–5.3	20
garbage			2	0.977	2.78	

$$\eta_{LHV} = \frac{\text{LHV} - \text{losses by incomplete combustion}}{\text{LHV}}$$

η_{LHV} is the combustion efficiency as calculated in Thermoptim.

When the combustion cannot be isolated from other phenomena, things become more difficult. For example, in an automobile engine cylinder, the combustion starts at the end of the compression phase and continues during the early phase of expansion. The precise definition of combustion efficiency becomes very complex.

In boilers, combustion takes place simultaneously with the exchange of heat by convection and radiation between the combustion products and the heated fluid. The losses in this case include

three terms: the incomplete combustion losses, losses through the walls, and losses by the fumes, usually predominant, corresponding to the enthalpy of the still hot gases released into the air.

We then often define the combustion efficiency as the ratio of useful energy actually transferred to the fluid to the energy theoretically available to the burner. As the first two types of losses are generally lower than the loss by the fumes, they are frequently neglected. The combustion efficiency is then:

$$\eta_c = \frac{\text{useful energy}}{\text{LHV}} = \frac{\text{LHV} - \text{loss by the fumes}}{\text{LHV}} = 1 - \frac{\text{loss by the fumes}}{\text{LHV}}$$

The combustion efficiency in this case depends crucially on the temperature of the fumes, the smoke losses being directly proportional. We understand why it is desirable to cool the smoke as much as possible when it is possible to do so.

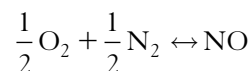
7.6.5 Emissions of gaseous pollutants

The major gaseous pollutants are sulfur, nitrogen and carbon oxides. In addition, emissions of CO₂, a fatal combustion product, are now increasingly regarded as pollutants because of their impact on the greenhouse effect.

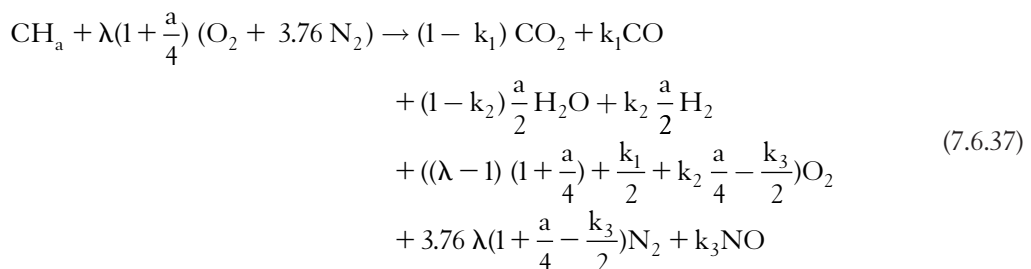
SO₂ (sulfur dioxide) and SO₃ (sulfur trioxide) emissions depend only on the sulfur content of fuels, the formation of SO₃ resulting from complete oxidation of sulfur. At low temperature, SO₃ combines with flue gas condensation to form highly corrosive sulfuric acid H₂SO₄. The reaction beginning at temperatures below 180°C, it is imperative that the fumes are discharged above this limit in cases where the fuel is heavy fuel oil (3.5% S). Finally, the stack height is determined by the minimum levels of ground-level concentration of SO₂.

NO_x nitrogen oxides come in the forms of NO (nitric oxide) and NO₂ (nitrogen dioxide). They come either from the presence of nitrogen in the fuel or from an unwanted oxidation of the air nitrogen. It was shown that the rate of formation of nitrogen oxides from fuel impurities is much higher than that from the air nitrogen, since the binding energy of the nitrogen molecule is much greater than that which connects the nitrogen atoms to carbon atoms or hydrogen.

To limit the emission of nitrogen oxides from the combustion air, several possibilities exist: to lower the excess air (though this increases the temperature), making a staged combustion, or flue gas recirculation, thereby lowering flame temperatures without increasing the excess oxygen. One can indeed show that the excess oxygen (and air) promotes the onset of nitrogen oxides, by studying the reaction:



If we complete equation (7.6.14) of unburned hydrocarbons formation to reflect the dissociation of nitrogen, we can write:



The constant K_p of the law of mass action for the dissociation reaction of nitrogen is very low (between 10^{-5} and $3 \cdot 10^{-2}$ for temperatures between 1,000 and 2,200 K).

Under these conditions, k_3 is very small, and $k_3/2$ can be neglected before the number of moles of oxygen, of nitrogen and total.

Therefore, at equilibrium:

$$[\text{NO}] = K_p[\text{O}_2]^{0.5}[\text{N}_2]^{0.5} \quad (7.6.38)$$

Since $[\text{N}_2]$ is almost constant and close to 78%, we get:

$$[\text{NO}] = 0.88K_p[\text{O}_2]^{0.5}$$

$[\text{O}_2]$ being an increasing function of excess air, $[\text{NO}]$ is too.

This equilibrium value, however, is rarely reached, because the kinetics of NO formation is much slower than that of combustion. The concentration limit is thus lower than that which would suggest the maximum temperatures were reached, but instead the reaction freezes very early, so it is difficult to limit emissions of nitrogen oxides.

Carbon monoxide CO is a product of incomplete combustion, which indicates a malfunction of the boiler.

Global CO₂ emissions

To estimate CO₂ emissions, at a country or global level, from the combustion of fossil fuels or biomass, there are a number of methodological problems, briefly discussed below.

Firstly, the amounts of primary fuels recorded include non-energy uses that do not result in CO₂ emissions (such as use of oil as feedstock for petrochemicals, and bitumen). It follows that, strictly speaking, you must deduct non-energy uses from the primary balance.

Secondly, the amount of CO₂ emitted depends on the fuels burned, whose diversity disappears from primary balances, where you only find three categories: coal, oil and natural gas. Equivalence ratios, often varying from one country to another, are used for conversions, and as we have only aggregated values, we can only adopt an average estimation method. This can be even more delicate when all primary energy is usually expressed in a common unit, usually a ton of oil equivalent.

Finally, in practice, many reactions are incomplete, due to the onset of dissociation at high temperature. In this case, the energies involved may differ significantly from theoretical values corresponding to complete reactions.

7.6.6 Calculation of combustion in Thermoptim

The combustion screen (Figure 7.6.3) is the most complex of those of processes, given the number of existing options. You should refer to the beginning of section 7.1.5 for an overview of the process screens.

7.6.6.1 Declaration of fuel

In case of excess air, non-stoichiometric complete combustion of fuel CH_a with atmospheric air is given by equation (7.6.11). Thermoptim uses a generalized equation of this type, where the oxidizer can be any compound gas including oxygen, and fuel is either given as CH_a , or declared as a pure or compound gas. The definition of fuel is in the upper right of the screen (Figure 7.6.4).

If the fuel is a pure or compound gas, it may contain one or more of the following reactants: CO, H₂S, C_nH_mS_pO_q, n, m, p and q being decimal numbers less than 100. Inert gases taken into account are: Ar, CO₂, H₂O, N₂, SO₂. Note that the fuel is always assumed to be gaseous, which may cause a slight error if it is in the liquid state.

The fuel and oxidizer can both contain reactive oxygen and inert gases, even if it is normal that the fuel contains no oxygen, nor the oxidizer fuel. It is thus possible to calculate complex combustion,

FIGURE 7.6.3

Combustion screen in ThermoOptim

FIGURE 7.6.4

Fuel process link

such as that of a fuel mixture made before introduction into the combustion chamber (fresh charge of a gasoline engine).

The reaction products are CO_2 , H_2O , SO_2 as well as CO and H_2 if there is dissociation, and fuel if the reaction is not complete.

The software analyzes the chemical formulas of the fuel and oxidizer components, and deduces the reaction that takes place. Calculations can then be executed. Chemical formulas are obtained by decoding the names of the substances.

When the fuel is a gas, the name that appears on the screen (here “fuel”) should be that of a process (e.g. a process-point) to determine its flow rate. The process itself is connected to a point to specify the substance name and state.

The example below is taken from the Getting Started example n° 2² « gas turbine ». It relates to the natural gas available at the LNG terminal of Gaz de France at Montoir de Bretagne (France) and illustrates how to declare a fuel whose composition is given Figure 7.6.5.

² <http://www.thermoOptim.org/sections/logiciels/thermoOptim/documentation/guide-prise-en-mains/switchLanguage/en>

component name	molar fraction	mass fraction
CH4 `methane	0.871	0.758966
C2H6 `ethane	0.088	0.1437279
C3H8 `propane	0.025	0.05987759
C4H10 `n-butane	0.008	0.02525591
N2	0.008	0.01217253

FIGURE 7.6.5

Fuel composition

Each constituent, except for nitrogen, is a fuel, whose chemical formula appears in the first part of the name that sometimes is followed by a comment, separated from the formula by the character « ` ». By analyzing the chemical formula of each constituent and its molar fraction, ThermoOptim completely characterizes the fuel.

This substance is associated to a point, allowing specification of its temperature, which is taken into account for the calculation of the outlet gas temperature. The flow rate is associated with a process-point, whose name serves as parameter for the combustion.

To find the oxidizer flow rate, the software searches if there is a process whose outlet point is the inlet point of the combustion process, or if it is connected to a node. Messages inform the user if a problem occurs, either because there are several processes that lead to the inlet point, or because no process or node is connected to it.

When the fuel is given in the form CH_a (“ CH_a type” must be selected), it is necessary to enter the values of a , and of its enthalpy of formation h_{f0} (relative to the formulation CH_2). It is then impossible to specify the flow rate.

7.6.6.2 Open systems and closed systems

It is necessary to specify if the combustion takes place in an open or closed system.

For open systems, the pressure must be set to a certain value. It can be done either «by the user», which means that this value will be that of the outlet, or «by the inlet point», which corresponds to a combustion at constant pressure equal to that of the upstream oxidizer.

For closed systems, one can choose between three possibilities: set volume, set pressure, or constant temperature combustion. For the two first cases, two different modes of setting the volume or the pressure exist: «by the user» or «by the inlet point». In the third case, the combustion temperature is constant and equal to that of the upstream oxidizer.

In the two last cases (set pressure and constant temperature), the volume varies with combustion, so that a part of the energy liberated by the combustion transforms directly into mechanical energy due to the expansion of the volume.

The first law of thermodynamics indicates indeed that internal energy variation (ΔU) is the algebraic sum of the heat ($(-\Delta H_r \eta_{LHV} \eta_{th})$) and the work ($W = -\int P dv$) received by the system.

ThermoOptim calculates the value W and displays it just below the value of the energy liberated in the combustion. This value is subsequently taken into account as useful energy when the cycle balance is calculated. One can refer, for more understanding of this subject, to examples on diesel³ and spark ignition⁴ engines presented in the portal.

7.6.6.3 Characteristics of combustion

The dissociation of CO_2 to CO can be taken into account by checking the appropriate option. In the case of atmospheric air the combustion reaction is given by equations (7.6.14) and (7.6.15).

³ <http://www.thermoOptim.org/sections/enseignement/cours-en-ligne/seances-diapason/session-s38en-exercice>

⁴ <http://www.thermoOptim.org/sections/enseignement/cours-en-ligne/seances-diapason/session-s39en-exercice>

This equilibrium is independent of pressure, and is a function of temperature. With the assumption that the kinetics of combustion is sufficiently fast for the equilibrium to be reached, the law of mass action can be written:

$$K_p = \frac{[\text{CO}][\text{H}_2\text{O}]}{[\text{CO}_2][\text{H}_2]} = \frac{k_1(1 - k_2)}{(1 - k_1)k_2} = f(T_f)$$

ThermoOptim uses an approach of this type, but generalized.

If one chooses to take dissociation into account, a frame is displayed in which must be entered k_1 , dissociation rate of CO_2 , and T_f quenching temperature which is used for calculating the constant K_p .

To account for any heat loss from the combustion chamber, not necessarily adiabatic, we introduce a thermal efficiency η_{th} , initialized to 1 by default (right at the center of the screen). This efficiency differs from the combustion efficiency η_{LHV} , calculated by the software based on the dissociation rate and the quenching temperature (see 10.6.4.8).

In the bottom left of the screen are located two fields, one corresponding to the air factor λ , and the other to the temperature T_c at the end of combustion. It is possible to set either of these values, and calculate the other, or to calculate both from the fuel and oxidizer flows. The air ratio may be higher or lower than 1. If it is below 1, the software considers this a lack of combustion air leading to the formation of carbon monoxide CO . If the air ratio is too low for all available carbon to be oxidized to CO , a message warns the user.

7.6.6.4 Calculation options

The option «Calculate T» determines the outlet gas temperature T_c , from the value set for λ . If the fuel is a gas, the mass flow rate of the « fuel » process is adjusted in order that the relationship between the volume flow rates of oxidizer and fuel is equal to the air factor.

The mass flow rate of the combustion process is set equal to the sum of fuel and oxidizer flow rates, which means that the combustion process behaves, at the hydraulic level, as a flow rate mixer.

The option «Calculate lambda» determines λ , from the value of T_c set. Flow rate calculation rules are analogous to those of the preceding option. If the enthalpy released by the stoichiometric combustion does not allow it to reach the desired temperature, a message warns the user.

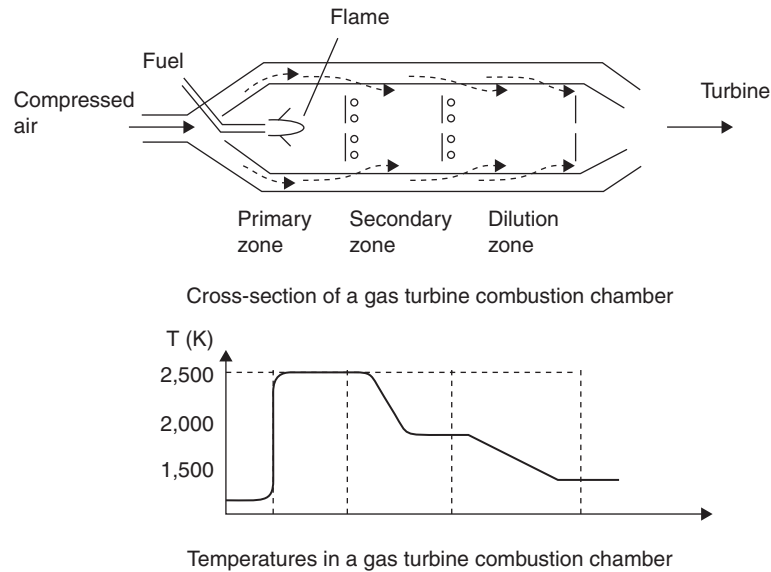
The option “Set the fuel flow rate” determines λ and T_c from the characteristics of the oxidizer and the fuel, which must be a gas. The mass flow of the combustion process becomes equal to the sum of the flows of fuel and oxidizer. If the fuel is type CH_a , nothing is done.

When combustion is calculated, the value of combustion efficiency η_{LHV} is determined. An example is given in Chapter 9.3.

7.6.6.5 Special case of pre-mixed reactants

As indicated above, it is possible to burn a reactant mix that is prepared before it is introduced to the combustion chamber (for example a fuel-air mixture prepared in a carburetor, which can be easily modeled in ThermoOptim by a mixer node). In this case, there is no longer a need to specify a fuel that is already present in the oxidizer. In order that the software knows that this is the case, it is necessary to choose option « CH_a type», and set the values of a and h_{f0} to zero, or select option “pre-mixed” (versions 1.4 and above).

As it is clear in this case that the notion of air factor λ loses its meaning, this parameter is used to represent the burnt fraction of the reactants ξ . If $\xi < 1$, we assume that only a fraction ξ of the mix has reacted, and that $(1 - \xi)$ has not reacted. Combustion gases are then considered as a dual gas mixture: first the reaction products, including inert gases, and second the fraction of the initial mix that has not reacted. This allows one to start from a given mix, and to separate its combustion in several phases, for example constant volume, then constant pressure, then constant temperature.

**FIGURE 7.6.6**

Sketch of a combustion chamber

One can refer, for more understanding of this subject, to the example on spark ignition engines cited above.

7.6.7 Technological aspects

Technologically, energy production combustions take place in two general classes of devices: combustion chambers (reciprocating or continuous flow), and boilers. The first are used to produce high pressure and temperature combustion gases that are then expanded, e.g. in a turbine. The latter realize simultaneously in the same chamber combustion and transfer to a fluid of the heat available in exhaust gases. We limit ourselves in what follows to a brief overview of these technologies, which will be discussed in more detail in Part 3.

7.6.7.1 Combustion chambers

For example, the combustion chamber of a gas turbine must satisfy severe constraints: ensure complete combustion of fuel, minimize the pressure drop (which represents an increase in compression), ensure good temperature stability at the turbine inlet, and occupy a volume as small as possible while allowing proper cooling of the walls.

The chart in Figure 7.6.6 is a section of a flame tube type combustion chamber, very commonly encountered in practice.

The compressed air exiting the compressor enters on the left side. It splits into two streams, one that provides wall cooling, the other entering directly into the combustion chamber, where it serves as oxidizer for the fuel injected into the central part. Given the low excess air locally, the flame reaches a high temperature (up to 2500 K) in the primary zone. Through holes at the periphery of the flame tube, the outside air mixes with exhaust gases in the transitional zone, where the temperature drops to around 2000 K, and in the dilution zone, where one seeks to achieve a gas flow temperature as stable as possible to avoid the risk of local or momentary overheating.

In flame tube cylinder chambers, six to twelve tubes of this type are mounted in parallel around the axis of the gas turbine. They are interconnected in order to balance the pressures and enable propagation of the ignition.

These flame tubes are very compact, their dimensions amounting to several tens of centimeters at most. Subjected to intense and high temperature heat fluxes, the materials they contain are resistant steel sheet potentially coated with ceramic.

7.6.7.2 Boilers

Boilers are much larger than combustion chambers, because of the need to transfer fume heat to another fluid, which requires large exchange surfaces. In many applications, this fluid is pressurized water, which vaporizes inside the boiler, which then behaves like a triple heat exchanger as the water passes from liquid form (economizer), vaporizes (vaporizer), and becomes steam (superheater).

There are two main types of boilers, known from the fluid that circulates inside the tubes: fire tube boilers, and water tube boilers.

In the first, the flame develops in a corrugated tube, then the flue gases pass inside tubes, in one or more passes, water being at the outside.

Within the second type, water circulates by natural or forced convection between two drums placed one above the other, through a network of tubes. The flame develops in a furnace lined with tubes that absorb the radiation. A second tube bundle receives heat by convection from the flue gases. The water rises in the tubes subjected to radiation, and falls by the convection assembly.

The fire tube boilers can achieve flue gas temperatures lower (220 to 250°C) than water-tube boilers (300°C) without an economizer, which gives them a slightly better efficiency.

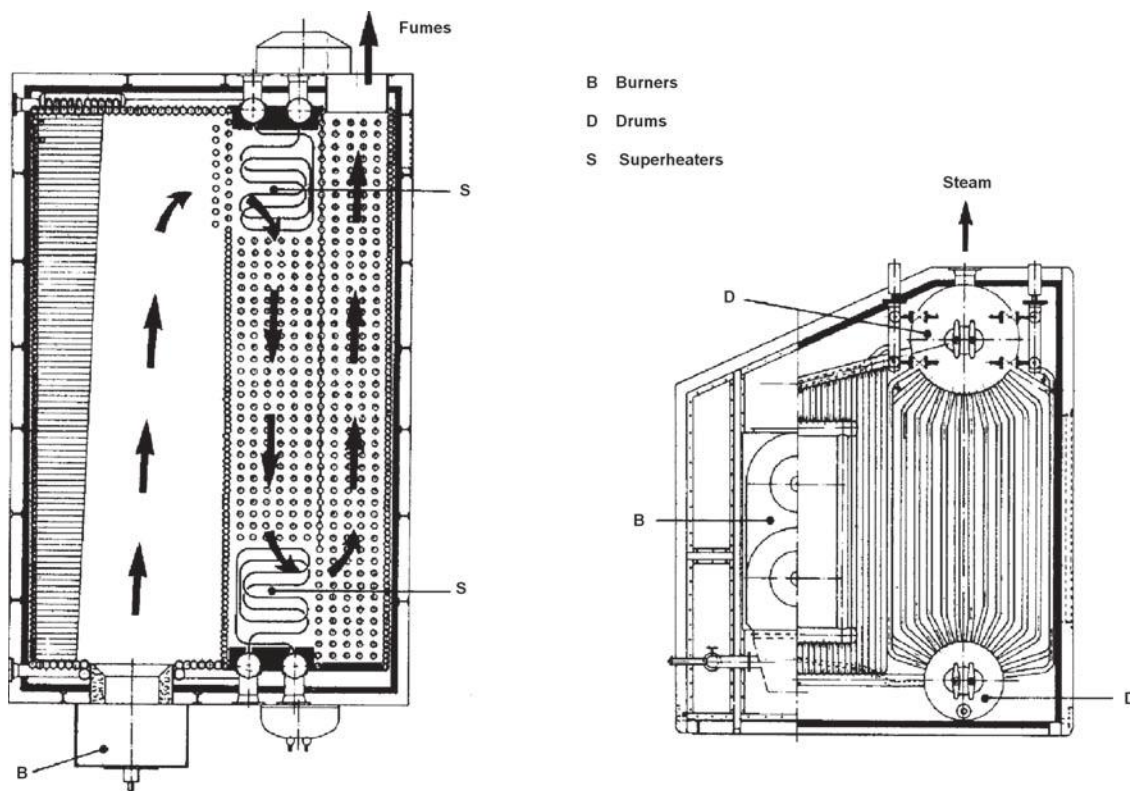


FIGURE 7.6.7
Industrial boiler (courtesy Techniques de l'Ingénieur — Génie énergétique)

However, the former are limited to capacities lower than the latter, for reasons of mechanical strength and safety (with a very large volume of water under pressure). Their main area of use is the supply of saturated steam under low pressure (<15 bar), and represent over 60% of the French stock of boilers, against 20–25% for water tube boilers, which are well suited for the supply of superheated steam at medium and high pressure.

A water tube boiler consists of a furnace where the combustion takes place leading to flame temperatures from 1200 to 1500°C, and whose walls are lined with smooth or finned steel pipes, which contain the pressurized water (50 to 180 bar). Heat is transferred primarily by radiation and by convection. For heat to be transferred, it is necessary that the total tube area is very large, which prohibits the use of high-grade steels: their surface temperature is limited to about 650°C.

Figure 7.6.7 shows two sectional views of a Carosso water tube steam boiler. The circulation of water between the two large drums D is provided by thermosiphon, vaporization taking place in the tube bundle that connects them.

7.7 THROTTLING OR FLASH

We call throttling the adiabatic expansion of a fluid in a fixed wall device such as a filter, a valve, or a refrigerator expansion valve. The process being adiabatic $Q = 0$. Since the walls are fixed, $\tau = 0$.

If the kinetic energies are negligible, which is usually the case, the first law is then written $\Delta h = \tau + Q = 0$. Throttling is an isenthalpic process.

In Thermoptim, the throttling process screen (Figure 7.7.1) is one of the simplest, as only one action can be performed. You should refer to the beginning of section 7.1.5 for an overview of the process screens. The calculation of the process is to determine the temperature and entropy of the outlet point knowing its pressure and enthalpy. An example is given in section 9.2. This process can also model a flash expansion.

The screenshot shows the 'Throttling' process screen in Thermoptim. The process is named 'throttling' and is of type 'throttling'. The energy type is set to 'other'. The inlet point is 3, and the flow rate is 1. The system is set to 'open system'. The calculated outlet point properties are as follows:

Property	Inlet Point 3	Outlet Point 4
T (°C)	41.33	-26.37
P (bar)	12	1
h (kJ/kg)	258.39	258.39
quality	0	0.42817

FIGURE 7.7.1

Throttling process screen in Thermoptim

7.8 WATER VAPOR/GAS MIXTURES PROCESSES

In section 5.6.7 we presented the definitions and conventions for moist mixtures, i.e. in practice mixtures of a compound gas and water whose composition may vary due to condensation or vaporization of this water. In this same section, we outlined the principles governing the calculation of these mixtures. The main practical application of these studies is air conditioning to control temperature and humidity in indoor environments, but the problem is more general.

In this section we present the basic treatments that undergo moist mixtures, and we illustrate each with examples pertaining to air. Air processing cycles involve different processes discussed below (Wang et al., 2000).

To represent these processes, professional practice has established the use of Carrier or psychrometric charts, or Mollier charts for moist mixtures (see Figure 5.6.20 to 5.6.22) of the kind that are built into ThermoOptim.

The main processes that can undergo moist mixtures are: mixture, heating, cooling, with or without water condensation, humidification, by water or steam, dehumidification, and finally, for air conditioning applications, it is often useful to determine the supply conditions for obtaining desired comfort.

In what follows, we present these basic operations and associated technologies, recall the equations that come into play, and how they can be determined with ThermoOptim and represented in moist mixture charts.

7.8.1 Moist process screens

To study changes that may undergo a moist mix, a “moist” process has been introduced. In fact, it corresponds to six different processes, which are distinguished by their category. The screen looks like the one given in Figure 7.8.1, but it varies slightly depending on the category. You should refer to the beginning of section 7.1.5 for an overview of process screens.

This is a “supply” moist process, to calculate the supply conditions for maintaining desired comfort, given water and thermal loads.

Before detailing how to use this screen, which will be done in section 7.8.7, let us point out some points valid for all moist processes.

First, ThermoOptim calculates moist mixture processes to the extent that they are represented by their dry gas and specific or relative humidity. The reason is simple: this mode of representation eliminates the need to introduce a new substance for each value of relative humidity.

It should be noted that this way of working is quite exceptional in ThermoOptim: for all other processes, the calculations are made from the exact composition of the substance considered. If then the coupling must be made between moist processes and other processes, care should be taken to link them with moist mixtures of appropriate composition.

In addition, the quantities being preferentially expressed in specific units, flows that appear on the moist processes are dry gas flows.

The concept of effectiveness is often used to describe the actual processes versus theoretical or ideal processes. In practice, these generally correspond to changes whose final state is saturated (full humidification, cooling to saturation).

The upper right corner of the screen recalls the general characteristics of the process, while the left shows the inlet and outlet points, indicating their temperature, pressure, enthalpy and specific humidity.

The settings of the various categories of moist processes and calculation methods are located in the central and lower right parts.

process type

energy type set flow closed system observed

dry gas mass flow rate open system

inlet point $m \Delta O'$

T (°C)
P (bar)
h (kJ/kg)
w (kg/kg)

type

sensible total heat ratio
water load
thermal load

outlet point

T (°C)
P (bar)
h (kJ/kg)
w (kg/kg)

Calculate the supply conditions, the dry gas flow rate being known
 Calculate the supply conditions, the supply temperature being known

FIGURE 7.8.1

Supply process in Thermoptim

7.8.2 Moist mixers

7.8.2.1 Principle and equations

A moist mixer is used to determine the particular properties of mixture of several moist gases. This operation takes for example place when two pipes containing mixtures of different humidities come together to form a single vein. In practice, it is most often air mixtures in air conditioning systems, for example a mixture of outdoor air and recycled inside air (see Example 9.4).

The operation being adiabatic, the total enthalpy and the total mass flow rate are always conserved. For two branches, one obtains:

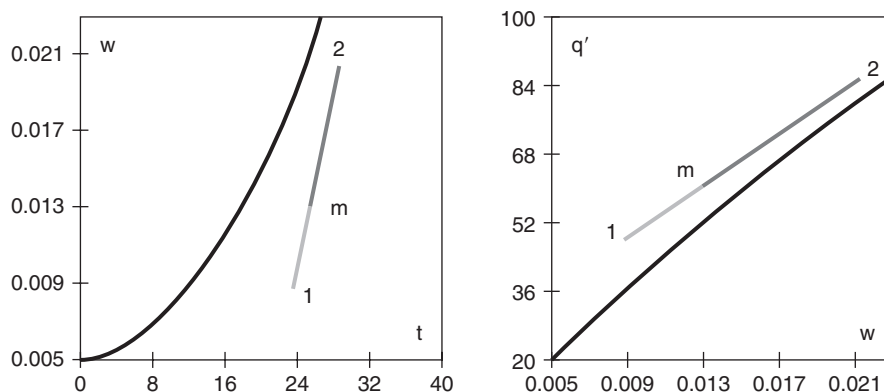
$$\begin{aligned}\dot{m} q'_{\text{mix}} &= \dot{m}_1 q'_1 + \dot{m}_2 q'_2 \\ \dot{m} &= \dot{m}_1 + \dot{m}_2\end{aligned}$$

There is usually conservation of the total specific humidity:

$$\dot{m} w_{\text{tot}} = \dot{m}_1 w_1 + \dot{m}_2 w_2 \quad (7.8.1)$$

except where there is supersaturation, in which case a portion of the water is condensed. In this case, the liquid water must be subtracted from the specific humidity.

The three previous equations show that in a (w, q') coordinate system, and when there is no supersaturation, the point representative of the mixture is the barycenter of the two points representing the moist mixtures, the coefficients being equal to their mass flow rates. It follows that the three points are aligned, and that the determination of the mixture can be done simply graphically in a moist mixture chart using this system of axes. In the Carrier (w, t) chart, this is only true in first approximation.


FIGURE 7.8.2

Moist mixture in Carrier and Mollier charts

node	<input type="text" value="mixer"/>	type	<input type="text" value="moist gas mixer"/>	<input type="button" value="<"/>	<input type="button" value=">"/>
main process	<input type="button" value="display"/>	m global	<input type="text" value="1"/>	<input type="button" value="Duplicate"/>	<input type="button" value="Save"/>
cooling	<input type="text"/>	h global	<input type="text" value="0.952"/>	<input type="button" value="Suppress"/>	<input type="button" value="Close"/>
water involved	<input type="text"/>	T global	<input type="text" value="25.8"/>	<input type="button" value="Calculate"/>	

process name	m abs	T (°C)	H
indoor flow	0.7	24	-0.852
outdoor flow	0.3	30	5.16

FIGURE 7.8.3

Moist gas mixer

The representation of the mixture of two moist air flows 1 and 2 in the chart is given in Figure 7.8.2. The mixture *m* is located at the junction of the two light and dark aligned segments.

The enthalpy being conserved, we begin by looking at the saturation conditions q'_{mix} . If the saturated specific humidity w_{sat} exceeds w_{tot} , $w_{\text{mix}} = w_{\text{tot}}$. Otherwise, $w_{\text{mix}} = w_{\text{sat}}$.

The dry temperature is in the first case that corresponding to q'_{mix} and w_{mix} , and in the second that of saturation.

7.8.2.2 Calculation of a mixture in ThermoOptim

The moist mixer node can determine the properties of a moist mixture of several dry or moist gases.

A moist mixer (Figure 7.8.3) differs from a simple mixer as follows:

- firstly, it accepts as branches moist as well as non-moist processes. Since the flow of moist processes is referred to the dry gas, the moist mixer makes the necessary corrections;
- second, its main vein must be a moist process. If this is not the case, a message warns the user, and the calculations are done as if it were a simple mixer.

In general, the outlet point is located on the mixing line. In case of supersaturation, a message informs the user and ThermoOptim searches the mixing point on the saturation curve, ensuring conservation of enthalpy. Excess water is then displayed in the upper right.

The values that are displayed are not expressed relative to dry gas.

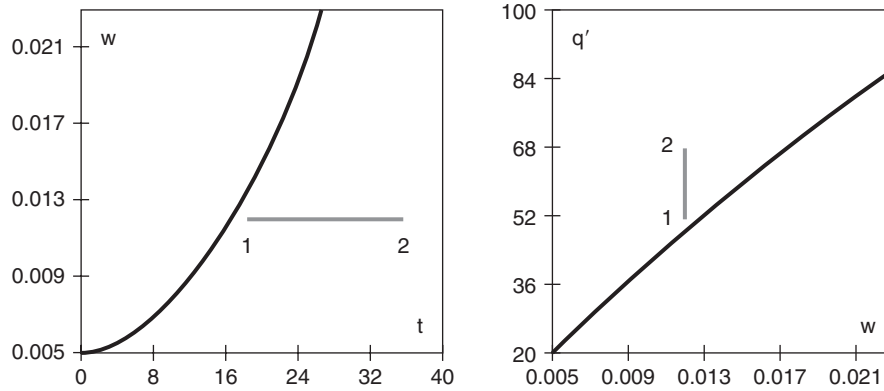


FIGURE 7.8.4

Moist heating in Carrier and Mollier charts

7.8.3 Heating a moist mixture

7.8.3.1 Principle and equations

The heating of a moist mixture is a constant moisture operation. In the Carrier chart, it is represented by a horizontal segment oriented to the left, in the Mollier chart by a vertical segment oriented upwards (Figure 7.8.4).

The heating is generally carried out in heating coils that can be of several types:

- air coils traversed by hot water supplied by boilers;
- air coils forming the condenser of a refrigerating machine (see Figure 7.8.6);
- electric battery heated by the Joule effect.

The equation is:

$$\Delta Q' = m_{\text{air}} (q'_2 - q'_1) \quad (7.8.2)$$

After processing, it reduces to:

$$\Delta Q' = m_{\text{air}} (1 + w) (h_{\text{mm}2} - h_{\text{mm}1}) \quad (7.8.3)$$

h_{mm} being the enthalpy of the moist mixture .

If $\Delta Q'$ is known, we reverse the equation, which gives t_2 .

7.8.3.2 Calculation of heating in Thermoptim

This process (Figure 7.8.5) can perform various calculations of evolution of a moist mixture. Depending on circumstances, the water content of the inlet and outlet points can be the same or different.

Two actions are possible here:

- * calculate the process, assuming the inlet and outlet points are known, in which case $\Delta Q'$ and the water involved are determined;
- * determine the state of the outlet point, the enthalpy change and the water involved being known.

7.8.4 Cooling of moist mix

7.8.4.1 Principle and equations

To cool a moist mixture, it is passed through a special heat exchanger called a cooling coil, which can be cooled by ice water or by direct evaporation of a refrigerant (Figure 7.8.6). The mixture

process: heating type: water vapor/gas mixtures

energy type: other set flow

dry gas mass flow rate: 11.98322

inlet point: cooled air display m ΔQ' 27.67 Calculate

T (°C): 11.73 type: heating

P (bar): 1.0133

h (kJ/kg): -13.15

w (kg/kg): 0.00790082

sensible/total heat ratio: 1

water involved: 0

outlet point: supply display

T (°C): 14

P (bar): 1.0133

h (kJ/kg): -10.87

w (kg/kg): 0.00790082

Calculate the process, the outlet point being known

Calculate the outlet point, m ΔH and the water involved being known

FIGURE 7.8.5
Moist heating process

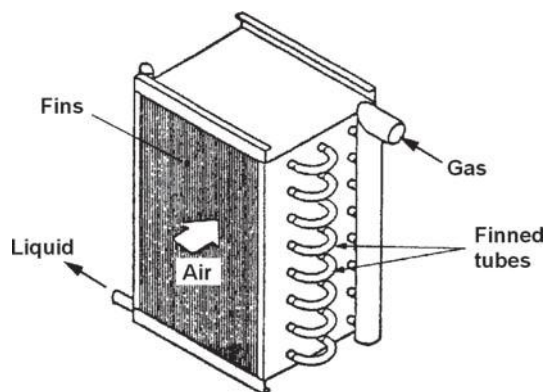


FIGURE 7.8.6
Cooling coil (courtesy Techniques de l'Ingénieur — Génie énergétique)

being in contact with the cold surfaces sees its temperature decrease. Depending on circumstances, there may be condensation or not. If there is no condensation, specific humidity remains constant and cooling can be represented by a horizontal segment oriented to the left in the Carrier chart, and vertically oriented downwards in the Mollier chart. If condensation occurs, which is very often the case, the segment is oriented to the bottom left in both charts (Figure 7.8.7).

Theoretical perfect cooling in a cooling coil of infinite size would cool the moist mixture at the coil saturation temperature. It is customary to characterize a real process in taking this cooling as theoretical reference, introducing effectiveness ϵ of the cooling coil and its average surface temperature t_s .

In the U.S. another approach is generally retained: the bypass factor method is based on the assumption that a part of the total flow which goes through the coil is never in contact with the cold

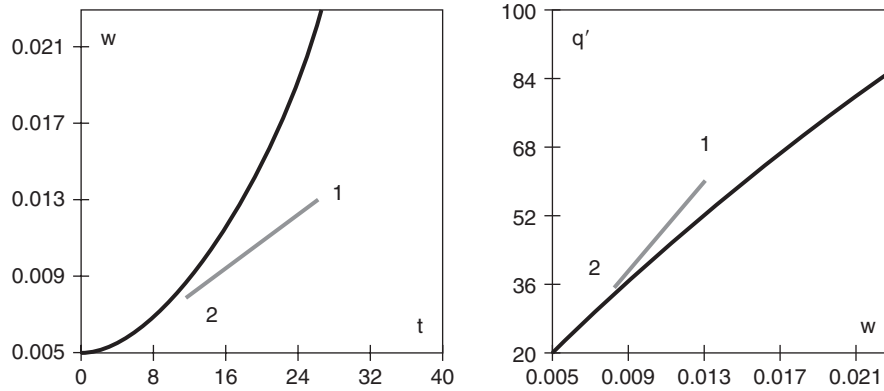


FIGURE 7.8.7

Moist cooling in Carrier and Mollier charts

surface: it bypasses it. Thus the final state of the air exiting the cooling coil corresponds to the mix between both streams. Calling b the bypass factor, we could easily show that $\varepsilon = 1 - b$.

The advantage of both methods is that values of ε and b of a given coil are coil characteristics largely independent of conditions of use.

To calculate point 2, we first search the saturation conditions $w_{\text{sat}}(t_s)$:

$$w_{\text{sat}}(t_s) = \frac{M_{\text{H}_2\text{O}}}{M_{\text{dg}}} \frac{P_{\text{sv}}}{P - P_{\text{sv}}} \quad \text{and} \quad q'(t_s, w_{\text{sat}})$$

We calculate the end moist properties in view of effectiveness:

$$\varepsilon = \frac{w_2 - w_1}{w_{\text{sat}} - w_1}$$

which gives:

$$w_2 = \varepsilon w_{\text{sat}} + (1 - \varepsilon)w_1 \quad (7.8.4)$$

$$q'_2 = \varepsilon q'(t_s, w_{\text{sat}}) + (1 - \varepsilon)q'_1$$

We then search t_2 such that $q'_2 = q'(t_2, w_2)$.

A problem may arise when, in the psychrometric chart, the line from point 1 intersects the saturation curve at two points. Indeed, in this case the point calculated from effectiveness may be in the saturated zone. This is called early condensation. Two possibilities exist: if one sets the outlet point specific humidity w_2 , the end point lies on the saturation curve for $w_{\text{sat}} = w_2$; if we set the effectiveness, it is on the saturation curve for $q'_{\text{sat}} = q'_2$. We must therefore ensure that the point is not found in the saturated zone.

7.8.4.2 Calculation of cooling in Thermoptim

This process (Figure 7.8.8) allows one to study the cooling of a moist mixture on a cooling coil, with or without condensation.

The cooling conditions are specified on the right of the screen: surface temperature and effectiveness of the cooling coil, if both are known. If the effectiveness is not known, the outlet point humidity must be given to calculate the process.

The screenshot shows a software interface for a moist cooling process simulation. The interface is organized into several sections:

- Process Settings:** process: cooling, type: water vapor/gas mixtures, energy type: other, set flow.
- Flow and System Settings:** dry gas mass flow rate: 0.987165, closed system, open system, observed.
- Inlet Point:** mixed air, display button, $m \Delta Q'$: -26.96, Calculate button.
- Inlet Properties:** T (°C): 25.8, P (bar): 1.0133, h (kJ/kg): 0.952, w (kg/kg): 0.01300203.
- Outlet Point:** cooled air, display button.
- Outlet Properties:** T (°C): 11.73, P (bar): 1.0133, h (kJ/kg): -13.15, w (kg/kg): 0.007900819.
- Process Parameters:** type: cooling, sensible/total heat ratio: 0.532909, water involved: -0.005035735, effectiveness: 0.750889197, surface temperature °C: 7.
- Calculation Options:**
 - Calculate the process, the cooling coil efficiency being known
 - Calculate the process, the outlet point's humidity being known

FIGURE 7.8.8

Moist cooling process

Two actions are possible here:

- the effectiveness being set, calculate the outlet point moisture. If early condensation occurs (see above), the outlet point is sought on the saturation curve, the enthalpy being calculated from the effectiveness of the battery;
- the humidity of the outlet point being set, calculate its temperature and the coil effectiveness. In case of early condensation (see above), the outlet point is searched on the saturation curve for the specific humidity desired.

7.8.5 Humidification of a gas

7.8.5.1 Principle and equations

To humidify a gas, we can proceed in two ways:

- injecting steam into the gas, usually slightly superheated, or spraying water in very fine droplets with a diameter of 5 to 20 μm by ultrasound or compressed air, making sure to avoid condensation on the walls (Figure 7.8.9);
- spraying water to form rain that wets the gas (Figure 7.8.10), the contact surface between gas and water being very important and the gas being far from the saturated state, the water vaporizes and the gas humidity increases. In this case, the vaporization of water requires heat input, which can be supplied by both water and gas, or gas alone, in which case it is called adiabatic humidification. With this type of device there is however a risk of bacterial growth and it is therefore less used.

Humidification is mainly used in air conditioning, for example to humidify in winter a very dry outside air before blowing it in a warm interior, or in summer to provide passive cooling.

As has been presented for the cooling of a moist mixture, the reference being the theoretical wetting leading the gas to saturation, the real humidification is characterized by the previously defined effectiveness ϵ .

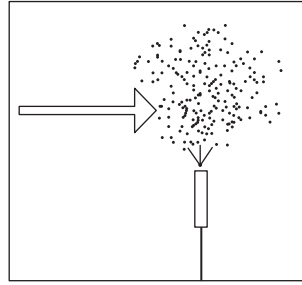


FIGURE 7.8.9
Steam humidification

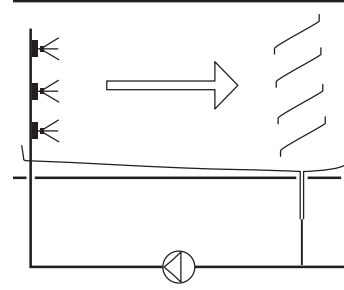


FIGURE 7.8.10
Humidification by water spray

Cases of non-adiabatic humidification (vapor or liquid water)

If we know the humidification effectiveness ε , we first find the boundary saturation conditions w_{sat} :
Such as

$$w_{\text{sat}} = w_1 + \frac{m_{\text{water}}}{m_{\text{air}}}$$

and

$$q'(t, w_{\text{sat}}) = q'_1 + (w_{\text{sat}} - w_1) h_{\text{H}_2\text{O}} \quad (7.8.5)$$

with

$$w_{\text{sat}} = \frac{M_{\text{H}_2\text{O}}}{M_{\text{dg}}} \frac{P_{\text{sv}}(t)}{P - P_{\text{sv}}(t)}$$

We then calculate the final moist conditions in view of effectiveness:

$$w_2 = \varepsilon w_{\text{sat}} + (1 - \varepsilon) w_1$$

$$q'_2 = \varepsilon q'(t, w_{\text{sat}}) + (1 - \varepsilon) q'_1 \quad (7.8.6)$$

We then seek t_2 such that $q'_2 = q'(t_2, w_2)$.

If we know the water absorbed by the fluid m_{water} , w_2 is directly calculated:

$$w_2 = w_1 + \frac{m_{\text{water}}}{m_{\text{air}}}$$

We then seek t_2 such as $q'(t_2, w_2) = q'_1 + (w_2 - w_1) h_{\text{water}}$.

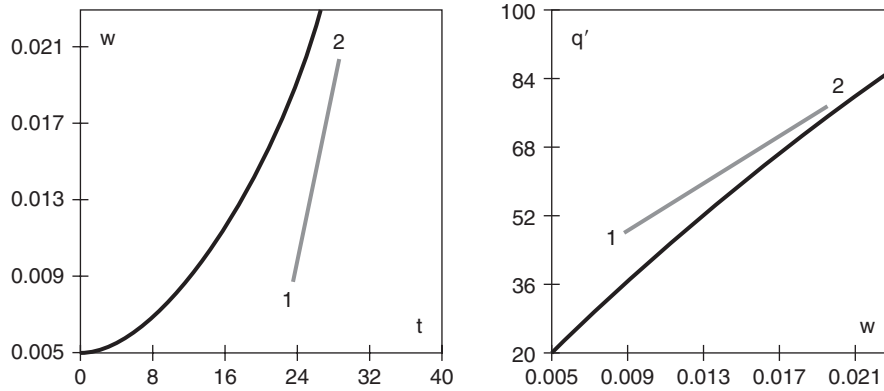
If we seek the boundary saturation conditions, we deduce the effectiveness ε .

Humidification by water or steam spraying is reflected in the Carrier chart by a line segment tilted to the right or left according to the enthalpy of the fluid injected, and in the Mollier chart by a segment inclined towards the right. Figure 7.8.11 shows a humidification with steam superheated at 115°C.

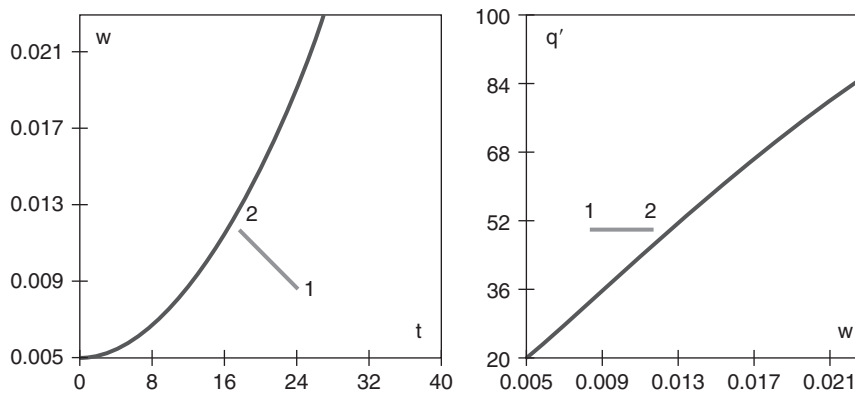
Case of adiabatic humidification

We begin by looking at the saturation conditions at the wet-bulb temperature $w_{\text{sat}}(t')$:

$$w_{\text{sat}}(t') = \frac{M_{\text{H}_2\text{O}}}{M_{\text{dg}}} \frac{P_{\text{sv}}(t')}{P - P_{\text{sv}}(t')} \quad \text{and} \quad q'(t', w_{\text{sat}})$$


FIGURE 7.8.11

Spray humidification in Carrier and Mollier charts


FIGURE 7.8.12

Adiabatic humidification in Carrier and Mollier charts

We calculate the final moist conditions in view of effectiveness:

$$w_2 = \varepsilon w_{\text{sat}} + (1 - \varepsilon)w_1 \quad (7.8.7)$$

$$q'_2 = \varepsilon q'(t_s, w_{\text{sat}}) + (1 - \varepsilon)q'_1$$

We then seek t_2 such that $q'_2 = q'(t_2, w_2)$

Adiabatic humidification is reflected in the Carrier chart by a line segment tilted to the left corresponding to $t' = \text{Const.}$, and in the Mollier chart by a nearly horizontal segment, q' being approximately constant (Figure 7.8.12).

7.8.5.2 Calculation of humidification in Thermooptim

Two distinct but similar types of processes are used to study either water or steam humidification, or adiabatic humidification (Figure 7.8.13).

The humidification conditions are specified on the right of the screen: water or steam temperature and pressure, and humidifier effectiveness, if known. If effectiveness is not known, the outlet point humidity must be given to calculate the process.

Two actions are possible here:

- the effectiveness being set, calculate the outlet point moisture. If condensation occurs early (when the line connecting the inlet point at the point of the saturation curve at the surface

FIGURE 7.8.13

Adiabatic humidificator screen

temperature intersects the saturation curve at two points), the outlet point is sought on the saturation curve, the enthalpy being calculated from the humidifier effectiveness;

- calculate the outlet point to get the desired humidity. When there is early condensation (see above), the outlet point is searched on the saturation curve for the specific humidity desired. The effectiveness of the humidifier is then calculated.

7.8.6 Dehumidification of a mix by desiccation

7.8.6.1 Principle and equations

In order to dehumidify a moist mixture by desiccation it passes over a bed of solid hygrophilic adsorbent, which extracts moisture from the gas by exothermic physical (adsorption), or physico-chemical (chemisorption) effect. The regeneration of the desiccant is made by the opposite effect, warming. Among the systems that accomplish desiccation, one of the most used takes the form of a rotary regenerative heat exchanger which simultaneously dehumidifies an air stream and regenerates part of the desiccant (Figure 7.8.14).

The same equations govern the two effects.

The equation of adsorptive dehumidification or desiccant regeneration is provided by the enthalpy balance, which is written here, L_s being the heat of sorption:

$$(1 + w_2)(h_{mm}(t_2) - h_{mm}(0^\circ\text{C})) - (1 + w_1)(h_{mm}(t_1) - h_{mm}(0^\circ\text{C})) + L_s(w_2 - w_1) = 0 \quad (7.8.8)$$

Knowing w_2 , simply invert this expression in t_2 , taking care that the composition of the moist mixture varies between points 1 and 2.

Knowing t_2 , w_2 is obtained by expressing the above equation as a function of dry gas, which leads to a simple first order polynomial equation in w_2 .

Dehumidification by adsorption results on the Carrier chart in a line segment tilted to the right, and on the Mollier chart in a segment close to the horizontal, q' increasing slightly (Figure 7.8.15).

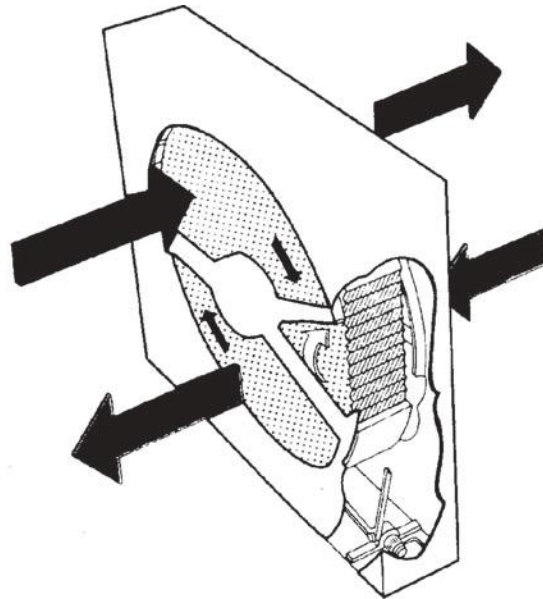


FIGURE 7.8.14

Rotary regenerative heat exchanger (courtesy Techniques de l'Ingénieur — Génie énergétique)

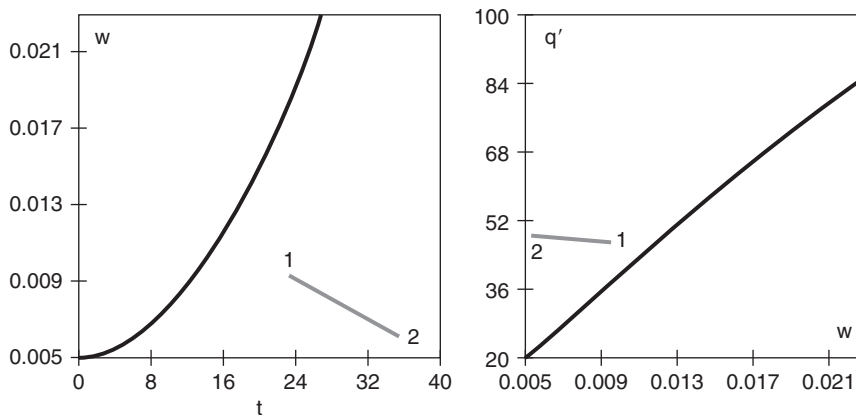


FIGURE 7.8.15

Desiccation process in Carrier and Mollier charts

That the operation is carried out at substantially constant enthalpy does not mean it is free in terms of energy, since the desiccant must be regenerated.

7.8.6.2 Calculation of a desiccation in Thermoptim

This process (Figure 7.8.16) allows the study of dehumidification by desiccation or regeneration of the desiccant. Different types of desiccant materials are proposed, their name and their heat of sorption being displayed in the right of the screen in kJ/kg. If the user wishes he can change the latter.

Two actions are possible here:

- the outlet point temperature being known, calculate its moisture;
- calculate the outlet point temperature to obtain the desired humidity.

Note that the same process calculates both desiccation and the desiccant regeneration, according to the relative values of the inlet point and outlet point. For regeneration, the software does not check, however, if the temperature is sufficient.

The screenshot shows a software interface for a desiccation process simulation. The process is set to 'desiccation' with a type of 'water vapor/gas mixtures'. The energy type is 'other'. The inlet point is 'supply' and the outlet point is 'indoor air'. The dry gas mass flow rate is set to 1. The calculated values are: inlet temperature 14°C, pressure 1.0133 bar, enthalpy -10.87 kJ/kg, and humidity 0.007900819 kg/kg. The outlet temperature is 24°C, pressure 1.0133 bar, enthalpy -0.852 kJ/kg, and humidity 0.009291657 kg/kg. The sensible total heat ratio is 7.27722. The substance used is 'microporous silicagel', with a sorbed water value of -0.003452848 and a sorption heat of 2,900. The interface also includes buttons for 'Save', 'Close', 'Suppress', 'Calculate', and 'display'.

FIGURE 7.8.16

Desiccation process

7.8.7 Determination of supply conditions

7.8.7.1 Principle and equations

In air conditioning a space, we often experience the following problem: we want to maintain the atmosphere inside a building at a given dry bulb temperature and relative humidity. External climatic conditions are known: dry bulb temperature and relative humidity. We must evacuate the internal and external thermal loads of known magnitude, and a quantity of water corresponding to the internal gains. Depending on countries, calculations are slightly differently expressed: in the U.S. for example, sensible \dot{Q}_s and latent \dot{Q}_l loads are considered (T. Agami Reddy, 2001) while in France we talk of enthalpy \dot{Q}_s and water \dot{m}_{eau} loads (AICVF, 1999). This simply means that in the first case, water to be extracted is directly converted in energy terms (BTU/hr or kW), while in the second it is expressed in kg/s.

L_{water} being the latent heat of evaporation at indoor air temperature, we have:

$$\dot{Q}_l = \dot{m}_{\text{eau}} L_{\text{water}}$$

In addition, for reasons of hygiene and comfort, the supply temperature should generally not be less than a given value, and the proportion of recirculated air should not exceed a limit. You have then to determine the supply conditions, that is to say the flow rate \dot{m}_{air} and state of the air blown, so that the atmosphere obtained is the desired one.

1) if the air flow is known, equations are:

balance on water:

$$w_{\text{su}} = w_1 + \frac{\dot{m}_{\text{water}}}{\dot{m}_{\text{air}}} \quad (7.8.9)$$

enthalpy balance:

$$q'(t_{su}, w_{su}) = q'_1 + \frac{\dot{Q}_s + \dot{m}_{water} h_{water}(t_1)}{\dot{m}_{air}} \quad (7.8.10)$$

$h_{water}(t_1)$ being the enthalpy of water at temperature t_1 .
or (U.S. notations)

$$q'(t_{su}, w_{su}) = q'_1 + \frac{\dot{Q}_s + \dot{Q}_l}{\dot{m}_{air}}$$

You therefore determine w_{su} , then seek t_{su} such that $q' = q'(t_{su}, w_{su})$.

2) if the supply temperature is known, the method is as follows:

balance on water:

$$\dot{m}_{air} = \frac{w_{su} - w_1}{\dot{m}_{water}} \quad (7.8.11)$$

enthalpy balance:

$$q'(t_{su}, w_{su}) = q'_1 + \frac{\dot{Q}_s + \dot{m}_{water} h_{water}(t_1)}{\dot{m}_{air}} (w_{su} - w_1) \quad (7.8.12)$$

t_{su} being known, w_{su} can be calculated by:

$$q'(t_{su}, w_{su}) = h_{dg}(t_{su}) - h_{dg}(0^\circ\text{C}) + w_{su}(h_{H_2O}(t_{su}) - h_{H_2O}(0^\circ\text{C})) + w_{su}L_{0water}$$

$$w_{su} = \frac{q'_1 - w_1 \left(\frac{\dot{Q}_s}{\dot{m}_{water}} - h_{lwater} \right) - h_{dg}(t) + h_{dg}(0^\circ\text{C})}{h_{H_2O}(t_{su}) - h_{H_2O}(0^\circ\text{C}) + L_{0water} - \frac{\dot{Q}_s}{\dot{m}_{water}} - h_{lwater}(t_1)} \quad (7.8.13)$$

Note that eliminating \dot{m}_{air} from equations (7.8.9) and (7.8.10) yields:

$$\theta = \frac{q'_1 - q'_1}{w_{su} - w_1} = \frac{\dot{Q}_s + \dot{m}_{water} h_{water}(t_1)}{\dot{m}_{water}}$$

θ is called the enthalpy-moisture ratio. It expresses that variations of specific enthalpy and humidity are proportional whatever the air flow rate value \dot{m}_{air} : all points lying on a straight line called the condition line or load line satisfy the sensible and latent loads, i.e. are solutions of equations (7.8.9) and (7.8.10).

The position of point “su” on the line determines the value of \dot{m}_{air} . It depends on various factors, such as the maximum allowable temperature difference to avoid any inconvenience (usually 6 to 12°C according to the technique used).

7.8.7.2 Calculation of supply conditions in Thermoptim

This process connects the point describing the known indoor conditions (inlet point) to the point corresponding to the supply conditions sought (outlet point). Its screen is given at the beginning of this section (Figure 7.8.1).

Let us point out that the determination of supply conditions does not really correspond to what we called a Thermoptim process until now: this is strictly speaking a misnomer. The problem is

finding the thermodynamic state of air to be blown into the space to be cooled in order to compensate for thermal and water loads.

There are two possible options in this case:

- determine the temperature and the specific humidity of the supply point when the dry gas flow rate is known;
- set the supply temperature, so that Thermoptim determines the specific humidity of the supply point, as well as the dry gas flow rate required.

Fields in the right of the screen allow you to enter the water (rate of moisture gain) and thermal (sensible rate of heat gain) loads to be removed, respectively in kg/s and kW, which defines the supply line. It is assumed that the water load must be dissipated at the inside point temperature. Note that units here are not exactly those generally used in the US where the water load is usually directly expressed in kW.

Thermoptim then calculates the value of the sensible/total heat ratio (also known as sensible heat factor SHF or sensible heat ratio SHR) which is the ratio of the rate of sensible heat gain \dot{Q}_s (in kW) for the space to the rate of total energy gain for the space $\dot{Q}_s + \dot{Q}_l$ (in kW). As this ratio is proportional to the slope of the supply or condition line, the ASHRAE psychrometric chart includes a protractor which facilitates drawing the condition line.

In France the SHR is replaced by the ratio, directly expressed in the psychrometric chart units, between changes in enthalpy and specific humidity. Known as the “slope ratio γ ”, it is equal to the enthalpy-moisture ratio θ .

$$\frac{\Delta h_s}{\Delta h_{\text{tot}}} = \frac{Q}{Q + m_{\text{eau}} h_{\text{leau}}}$$

7.8.8 Air conditioning processes in a psychrometric chart

Figure 7.8.17 summarizes how the different air conditioning processes can be represented in a psychrometric chart.

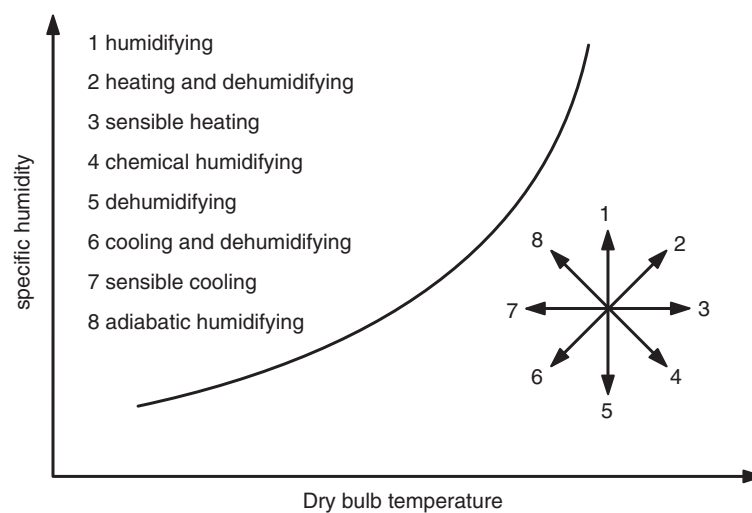


FIGURE 7.8.17

Air conditioning processes in a psychrometric chart

PRACTICAL APPLICATION**Summer and Winter Air Conditioning Cycles**

Air conditioning has progressively developed in recent decades, leading to continued progress in the various disciplines that make up what is known as HVAC (Heating, Ventilation, and Air Conditioning).

The various processes which have been studied in this section are put in practice in Chapter 21 of Part 3, where two examples show how basic treatments can be combined to form a proper air conditioning unit, combining mixture of outdoor air and indoor air, cooling, heating. . .



[CRC_pa_2]

7.9 EXAMPLES OF COMPONENTS REPRESENTED BY EXTERNAL CLASSES

In section 6.4 we introduced the ThermoOptim extension mechanism which allows us to add to the software components not existing in the core.

In this section we give three examples of such components: nozzles, diffusers and ejectors, limiting ourselves to the presentation of models and interface components. Examples of external class Java code will be given in Chapter 23 of Part 4.

7.9.1 Nozzles

An adiabatic nozzle is a fixed component that allows one to convert in kinetic energy the pressure of a gas. When the flow is subsonic, the section of the nozzle decreases, and when it becomes supersonic, it increases, giving the device the shape of Figure 7.9.1, called Laval (see section 7.3.2.3), the flow in the throat being at sonic speed.

In this section, we present a model for representing an adiabatic nozzle. After a brief reminder of the thermodynamics of the nozzle, we will present the screen of the external component defined in class `Nozzle.java`⁵.

7.9.1.1 Thermodynamics of an adiabatic nozzle

We assume in what follows that the fluid passing through the nozzle at least locally can be considered as a perfect gas, taking a well-chosen value of its specific heat capacity c_p . The notations are those of section 7.3.2.

The nozzle being adiabatic, we can easily show that the fluid stagnation temperature is equal to the isentropic stagnation temperature, even in the presence of irreversibilities:

$$T_{is} = T_a + \frac{C^2}{2c_p} \quad (7.3.8)$$

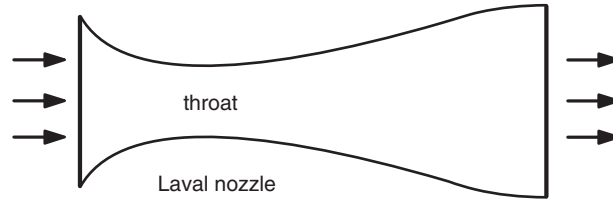
By introducing the Mach number of flow:

$$Ma = \frac{C}{\sqrt{\gamma r T}}$$



[CRC_In_7]

⁵<http://www.thermoOptim.org/sections/logiciels/thermoOptim/modelotheque/modele-tuyere>

**FIGURE 7.9.1**

Sketch of a nozzle

and noticing that:

$$c_p = \frac{\gamma r}{\gamma - 1}$$

It comes:

$$\Delta T = T_{is} - T_a = \frac{C^2}{2c_p} = \frac{\gamma - 1}{2} Ma^2$$

Equation (5.6.8) gives the isentropic stagnation pressure:

$$PT^{\gamma/(\gamma-1)} = \text{Const.} \quad \text{or} \quad P_{is} = P_a \left(\frac{T_{is}}{T_a} \right)^{\gamma/(\gamma-1)}$$

We find:

$$P_{is} = P \left(1 + \frac{\gamma - 1}{2} Ma^2 \right)^{\gamma/(\gamma-1)} \quad (7.3.9)$$

Both relations (7.3.8) and (7.3.9) can be interpreted as follows: in any isentropic flow of a perfect gas in a tube with fixed walls, the stagnation temperature and pressure are conserved.

If the flow is adiabatic, but not reversible, its law is no longer an isentropic, but a polytropic. With the usual assumptions, the above relations are transformed as shown below.

Firstly, the first law can also be written as before $\Delta h = C^2/2$

The gas being assumed perfect: $\Delta h = c_p \Delta T$

The total enthalpy being conserved, the stagnation polytropic and isentropic temperatures are equal:

$$T_p = T_a + \frac{C^2}{2c_p} = T_{is} \quad (7.3.8)$$

The polytropic equation gives the stagnation pressure:

$$PT^{k/(k-1)} = \text{Const} \quad \text{or} \quad P_p = P_a \left(\frac{T_p}{T_a} \right)^{k/(k-1)}$$

We find:

$$P_p = P_a \left(1 + \frac{\gamma - 1}{2} Ma^2 \right)^{k/(k-1)} \quad (7.9.1)$$

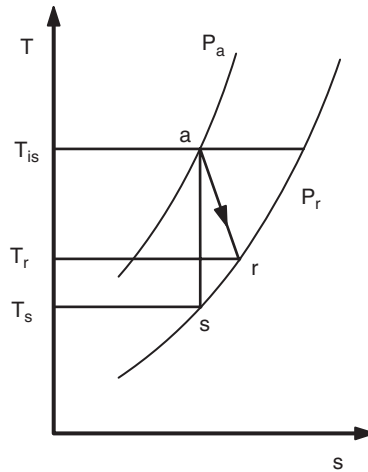


FIGURE 7.9.2

Nozzle process in a (T, s) chart

The polytropic stagnation pressure is not equal to the isentropic stagnation pressure, the irreversibilities resulting in losses.

In a nozzle, we know the initial and final pressures, and we can consider as a first approximation that the initial velocity is negligible.

Reasoning on the conversion of the pressure energy in velocity, the difference in inlet and outlet pressures ($P_a - P_r$) could theoretically provide a difference in enthalpy $\Delta h_s = h_A - h_S$ corresponding to a kinetic energy $C^2_{0a}/2$ (Figure 7.9.2). Because of irreversibilities, the exit point is R and not S, determinable if one knows the isentropic efficiency η_s :

$$\eta_s = \frac{h_A - h_R}{\Delta h_s} \quad (7.9.2)$$

We deduce the output velocity, which gives:

$$C = \sqrt{2\eta_s |\Delta h_s|}$$

With the assumption that the gas is perfect, we can also write (7.9.2) as:

$$\eta_s = \frac{T_A - T_R}{T_A - T_S} \quad (7.9.3)$$

Which leads to

$$C = \sqrt{2\eta_s c_p T_a \left[1 - \left(\frac{P_r}{P_a} \right)^{(\gamma-1)/\gamma} \right]} \quad (7.9.4)$$

These relationships allow us to fully characterize the process.

In the model, we have generalized the above expressions to take into account the gas velocity existing at the inlet.

7.9.1.2 Calculation of the nozzle sections

A well-known result of fluid mechanics is that a sonic nozzle should be formed by a convergent, whose section reduces until sonic conditions are established at the throat, followed by a diverging cross-section increasing downstream of the throat. We call a Laval nozzle such convergent-divergent configuration. Since the velocity of the gas nozzle exit is supersonic, we must identify the sections at the throat and at the outlet of the nozzle.

Section S_c of the throat is given by equation (7.9.5):

$$\frac{\dot{m}\sqrt{T_a}}{P_a} = \sqrt{\frac{\gamma}{r}} S_c \left[\frac{2}{\gamma+1} \right]^{(\gamma+1)/2(\gamma-1)} \quad (7.9.5)$$

The output section is calculated just knowing the speed and condition of the gas nozzle exit.

7.9.1.3 Design of the external component

General

Two calculation methods are possible: to determine the output pressure knowing the output velocity, or to determine the output velocity knowing the output pressure.

Model parameters are:

- the gas inlet velocity (m/s);
- the isentropic efficiency of the process;
- either the gas output velocity (m/s), or the gas pressure at the exit of the nozzle, depending on the calculation option chosen.

Model input data are as follows (provided by the inlet component):

- the gas temperature T_a (°C or K) at the nozzle inlet;
- the gas pressure P_a (bar) at the nozzle inlet;
- the gas flow rate \dot{m} (kg/s).

The outputs are:

- either the gas pressure at the exit of the nozzle, or the gas outlet velocity (m/s), depending on the calculation option chosen;
- the gas temperature at the nozzle exit.

Graphical interface

A graphical interface for the component can be deduced (Figure 7.9.3). You have to build the bottom left of the screen, the rest being defined as a Thermoptim standard.

The input data are supplied by the inlet process of the system in which the component is inserted: gas flow and inlet point state.

Sequence of calculations

The sequence of calculations is as follows:

- update of the component before calculation with the values of the inlet process and point;
- update with the settings of the external component screen;
- calculation of the output pressure or velocity and of the outlet point state;
- update of the external component screen.

The problems encountered in practice at each of these steps are quite similar to those presented in the documentation provided in Volume 3 of Thermoptim reference manual. You should refer to it for further explanations.

The screenshot shows the ThermoOptim software interface for a nozzle component. The 'process' is set to 'nozzle' and 'type' is 'external'. The 'energy type' is 'other'. The 'inlet point' is '4 ter' and the 'outlet point' is '5'. The 'nozzle' section includes the following parameters:

Parameter	Value
inlet velocity (m/s)	0
isentropic efficiency	0.9500
Mach number	2.316
outlet pressure (bar)	0.30700
outlet velocity (m/s)	1153.96
outlet section	0.3455
minimum section	0.1494

The 'Calculate' button is highlighted, and the 'Calculate outlet velocity' radio button is selected.

FIGURE 7.9.3

Nozzle screen

We show in section 12.2 of Part 3 how this component can be used to model a turbojet in ThermoOptim.

7.9.2 Diffusers

An adiabatic diffuser is a fixed component that serves to convert into pressure a portion of the kinetic energy available in a gas. When the flow velocity is subsonic, the section of the diffuser increases (see section 7.3.2.3). The initial relative velocity of the outside air can thus achieve a dynamic compression in the inlet diffuser of a jet engine: the kinetic energy of intake air is converted into pressure.

In this section, we present a model for representing an adiabatic diffuser. After a brief reminder of the thermodynamics of the diffuser, we present the screen of the external component defined in class Diffuser.java⁶.

7.9.2.1 Thermodynamics of adiabatic diffuser

We assume in what follows that the fluid passing through the diffuser can at least locally be considered as a perfect gas, taking a well-chosen value of its specific heat capacity c_p . The notations are those in section 7.3.2.

The diffuser being adiabatic the stagnation temperature of the fluid is given by (7.3.8).

$$T_i = T + \frac{C^2}{2c_p} \quad (7.3.8)$$

⁶<http://www.thermoOptim.org/sections/logiciels/thermoOptim/modelotheque/modele-diffuseur>

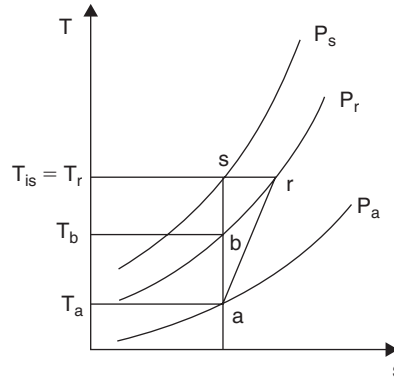


FIGURE 7.9.4
Diffuser in a (T, s) chart

By introducing the flow Mach number:
It comes

$$\Delta T = T_{is} - T_a = \frac{C^2}{2c_p} = \frac{\gamma - 1}{2} Ma^2$$

The isentropic stagnation pressure is given by (7.3.9).

$$P_{is} = P \left(1 + \frac{\gamma - 1}{2} Ma^2 \right)^{\gamma/(\gamma - 1)} \quad (7.3.9)$$

Both relations (7.3.8) and (7.3.9) can be interpreted as follows: in any isentropic flow of a perfect gas in a tube with fixed walls, the stagnation temperature and pressure are conserved.

If the flow is adiabatic, but not reversible, its law is no longer an isentropic, but a polytropic.

With the usual assumptions, the above relations become, as established for the nozzle:

$$P_p = P_a \left(1 + \frac{\gamma - 1}{2} Ma^2 \right)^{k/(k - 1)} \quad (7.9.1)$$

The dynamic pressure due to the initial kinetic energy would compress the gas to pressure P_s if there were no irreversibility (Figure 7.9.4), and lead to point S at temperature $T_s = T_{is}$ and entropy $s_S = s_A$. Because of irreversibilities, the exit point is R, at the same isentropic stagnation temperature, but at pressure P_r lower than P_s . R can be determined if one knows the isentropic efficiency η_s of the diffuser, B being the corresponding point of the isentropic compression from P_a to P_r :

$$\eta_s = \frac{h_B - h_A}{h_R - h_A}$$

The gas being assumed perfect,

$$h_R - h_A = h_S - h_A = c_p \frac{\gamma - 1}{2} Ma^2$$

Which gives *in fine*:

$$P_r = P_a \left(1 + \eta_s \frac{\gamma - 1}{2} \text{Ma}^2 \right)^{\gamma/(\gamma-1)} \quad (7.9.6)$$

These relationships allow to fully characterize the process: (7.9.6) provides the stagnation pressure, and therefore the static pressure if we know the residual velocity (generally low and therefore negligible). The temperature of point B can be deduced, its entropy being known. If the isentropic efficiency is given, you can determine point R.

In the model, we have generalized the above expressions to take into account the gas velocity existing at the outlet.

7.9.2.2 Ratio of stagnation pressures

Let us call ε_p the ratio of the real stagnation pressure to the isentropic stagnation pressure. $\varepsilon_p \leq 1$, called the stagnation pressure ratio, is very commonly used to characterize diffusers, for which the assumption of adiabaticity can often be accepted, but not that of a reversible flow.

If η_p is the polytropic efficiency, equations (7.3.9) and (7.9.1) provide:

$$\varepsilon_p = \left(\frac{P_p}{P_{is}} \right) = \left(1 + \frac{\gamma - 1}{2} \text{Ma}^2 \right)^{(\eta_p - 1) \gamma / (\gamma - 1)} \quad (7.9.7)$$

The isentropic efficiency η_s can also be expressed as a function of ε_p :

$$\eta = \frac{\left(\frac{P_r}{P_a} \right)^{(\gamma-1)/\gamma} - 1}{\left(\frac{P_r}{P_a} \right)^{(k-1)/k} - 1}$$

All calculations done, we find:

$$\eta_s = \frac{\left(1 + \frac{\gamma - 1}{2} \text{Ma}^2 \right) \varepsilon_p^{(\gamma-1)/\gamma} - 1}{\frac{\gamma - 1}{2} \text{Ma}^2} \quad (7.9.8)$$

Knowing ε_p , we can find the corresponding isentropic efficiency and thus the stagnation pressure.

7.9.2.3 Design of the external component

General

Two calculation methods are possible: to determine the output pressure knowing the output velocity, or to determine the output velocity knowing the output pressure.

Model parameters are:

- the gas inlet velocity (m/s);
- the isentropic efficiency of the process;
- either the gas output velocity (m/s), or the gas pressure at the exit of the diffuser, depending on the calculation option chosen.

FIGURE 7.9.5

Diffuser screen

Model input data are as follows (provided by the inlet component):

- the gas temperature T_a (°C or K) at the diffuser inlet;
- the gas pressure P_a (bar) at the diffuser inlet;
- the gas flow rate \dot{m} (kg/s).

The outputs are:

- either the gas pressure at the exit of the diffuser, or the gas outlet velocity (m/s), depending on the calculation option chosen;
- the gas temperature at the diffuser exit.

Graphical interface

A graphical interface for the component can be deduced (Figure 7.9.5). You have to build the bottom left of the screen, the rest being defined as a Thermoptim standard.

The input data are supplied by the inlet process of the system in which the component is inserted: gas flow and inlet point state.

Sequence of calculations

The sequence of calculations is as follows:

- update of the component before calculation with the values of the inlet process and point;
- update with the settings of the external component screen;
- calculation of the output pressure or velocity and of the outlet point state;
- update of the external component screen.

The problems encountered in practice at each of these steps are quite similar to those presented in the documentation provided in Volume 3 of Thermoptim reference manual. You should refer to it for further explanations.

PRACTICAL APPLICATION

Determination of the Thrust of a Turbojet

A turbojet engine used in aviation is a simple modification of a gas turbine open cycle: the turbine and the compressor form a gas generator whose sole purpose is to generate hot gas at high pressure. The energy available in the gas is converted into kinetic energy in a nozzle. The thrust results from the difference of momentum between intake and exhaust gases.

The turbojet also includes an inlet diffuser, which is used to create a static precompression at the compressor inlet when the airplane is in flight, and thus reduce compression work.

Both nozzle and diffuser model presented in this section may be used for building models of turbojets as explained in sections 12.2.1.9 to 12.2.11 of Part 3.

7.9.3 Ejectors

An ejector or injector (Figure 7.9.6) receives as input two fluids normally gaseous but which may also be liquid or two-phase (Chunnanond, 2004):

- the high pressure fluid called primary fluid or motive;
- the low pressure fluid, called secondary fluid or aspirated.

The primary fluid is accelerated in a converging-diverging nozzle, creating a pressure drop in the mixing chamber, which has the effect of drawing the secondary fluid. The two fluids are then mixed and a shock wave may take place in the following zone (throat in Figure 7.9.6). This results in an increase in pressure of the mixture and reduction of its velocity which becomes subsonic. The diffuser then converts the residual velocity into increased pressure.

The ejector thus achieves a compression of the secondary fluid at the expense of a decrease in enthalpy of the primary fluid.

The three most important parameters to characterize the overall efficiency of an ejector are:

- the **entrainment ratio** w , ratio of the secondary to primary mass flow-rates;
- the **pressure lift ratio**, the ratio of the static pressure at the outlet of the diffuser to the static pressure of the secondary fluid;
- a **section ratio** (minimal on maximum or primary flow on entrained flow etc.), which determines its geometry.

Note here that one of the practical problems encountered in the use of an ejector in a cycle is that its efficiency depends on many of its operating conditions: the compression ratio obtained is obviously a function of the entrainment ratio but a variation of the latter induces a change in the optimum geometry of the ejector, which is obviously impossible to achieve.

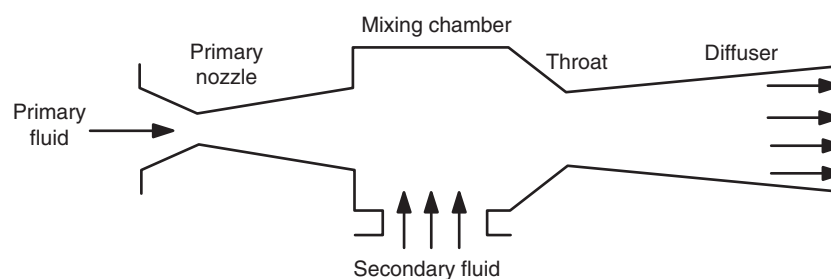


FIGURE 7.9.6

Cross section of an ejector

It follows that an ejector is poorly adapted to operation outside of design conditions.

7.9.3.1 Thermodynamics of an ejector

Ejector modeling is mostly based on the assumption that primary and secondary fluids can be treated as ideal gases in the mixing chamber, which is roughly justified given the low pressure therein. However, there are also cases where one of these fluids is liquid or two-phase, so that the mixture can be biphasic, and several hypotheses can be selected: either carry out calculations with the properties of a real fluid while using the hypothesis of a single-phase flow, or neglect the liquid phase when computing velocities, or consider an equivalent fluid.

PRACTICAL APPLICATION

Ejector Refrigeration Cycles

The value of introducing an ejector in a refrigeration cycle is mainly to reduce, or even eliminate, the compression work, relatively large as the fluid is compressed in the gaseous state.

Several refrigeration cycles using ejectors are currently being investigated. Some of them are presented in section 19.6.3 of Part 3:

- cycles without compressor, whose advantage is to replace the compressor work by a much smaller work consumed by the pump and by heat supplied by a generator at medium or high temperature;
- cycles with compressor, where the ejector is simply used to reduce the throttling irreversibility of a conventional refrigeration cycle, creating a slight pressurization before compression.



[CRC_pa_3]

The calculation of the ejector (one-dimensional model) is based on the following assumptions:

- the expansion of the primary and secondary fluids in the inlet nozzle is assumed to be adiabatic, taking into account the irreversibilities by an isentropic efficiency;
- the pressure remains constant in the mixing chamber (there are constant mixing section ejectors, but they are less efficient than others and we do not consider them here);
- when the mixed flow is supersonic, a normal shock can take place in the mixing chamber, which slows down the fluid and creates an overpressure;
- compression in the diffuser is assumed to be adiabatic, taking into account the irreversibilities by an isentropic efficiency;
- fluid properties are uniform in any section.

The model we used is that proposed by Li and Groll (2005), which presents the advantage of being formulated in a manner independent of fluid properties. We have slightly reformulated and expanded it to take account of any shock, these authors implicitly limiting themselves to cases where the mixed flow is subsonic.

In this model, we simplify the calculations assuming *a priori* that we know the pressure drop between the secondary flow suction pressure P_e and that at the inlet of the mixing zone P_b . We will consider that it is proportional to P_e . It is clear that in practice, we do not know the value of this factor, which is not directly measurable. If we want to set a value of the output pressure ejector P_d or pressure lift ratio P_d/P_e , we must then iterate on the value of this factor, which is easy to do once the model is set and validated.

The model assumes that the ejector is comprised of 4 main areas:

- the motive flow expansion area;
- the entrained flow expansion area;

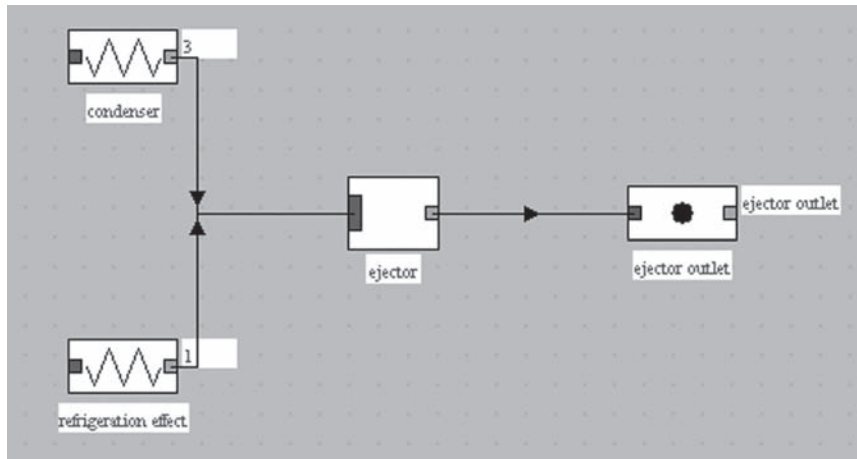
**FIGURE 7.9.7**

Diagram of the ejector component

- the mixing zone, with possible shock;
- the diffuser.

7.9.3.2 Setting equations

m_{mi} and m_{si} being the mass-flows of motive and secondary streams, the entrainment ratio is:

$$w = \frac{m_{si}}{m_{mi} + m_{si}} \quad (7.9.9)$$

Motive flow expansion area

We will use the index mb to characterize the outlet state of the fluid, which expands adiabatically:

$$\begin{aligned} s_{mb,is} &= s_{mi} \\ h_{mb,is} &= f(s_{mi}, P_b) \\ h_{mb} &= h_{mi} - \eta_s(h_{mi} - h_{mb,is}) \end{aligned} \quad (7.9.10)$$

The fluid velocity at the inlet being negligible, its output value is:

$$C_{mb} = \sqrt{2(h_{mi} - h_{mb})}$$

The specific volume v_{mb} allows you to know the flow area per unit of total mass flow rate:

$$a_{mb} = \frac{v_{mb}}{C_{mb}(1+w)} \quad (7.9.11)$$

Entrained flow expansion area

We will use index sb to characterize the outlet state of the fluid, which expands adiabatically:

$$\begin{aligned} s_{sb,is} &= s_{si} \\ h_{sb,is} &= f(s_{si}, P_b) \\ h_{sb} &= h_{si} - \eta_s(h_{si} - h_{sb,is}) \end{aligned} \quad (7.9.12)$$

The fluid velocity at the inlet being negligible, its output value is:

$$C_{sb} = \sqrt{2(h_{si} - h_{sb})}$$

The specific volume v_{sb} allows you to know the flow area per unit of total mass flow rate:

$$a_{sb} = \frac{v_{sb}}{C_{sb}} \frac{w}{(1+w)} \quad (7.9.13)$$

Mixing zone

We will use index mix to characterize the mix output state, which can only be determined iteratively by solving simultaneously in pressure the conservation equations of mass flow, momentum and enthalpy.

Solving these equations shows that there may be one or two mixing pressure(s). The physical explanation is as follows: if the mixed flow is supersonic, a recompression with “normal” shock wave takes place because the outlet pressure is greater than that of the flow. The two mathematical solutions correspond to pressures before and after the shock.

The conservation of momentum reads:

$$P_b(a_{mb} + a_{sb}) + \frac{C_{mb}}{(1+w)} + \frac{wC_{sb}}{(1+w)} = P_{mix}(a_{mb} + a_{sb}) + C_{mix} \quad (7.9.14)$$

The enthalpy equation writes:

$$h_{mi} + wh_{si} = (1+w) \left(h_{mix} + \frac{C_{mix}^2}{2} \right) \quad (7.9.15)$$

The conservation of the mass flow writes:

$$v_{mix} = (a_{mb} + a_{sb})C_{mix} \quad (7.9.16)$$

We will retain as a solution, if there are two, the highest pressure, which is equivalent to taking the lowest, and solve the equations of the shock wave below. This way is more precise, the following equations being strictly speaking valid only for perfect gases.

Shock wave

If there is a shock wave, the equations are as follows, x being the inlet (supersonic), and y the outlet (subsonic):

$$M_y^2 = \frac{M_x^2 + \frac{2}{\gamma-1}}{\frac{2\gamma}{\gamma-1} M_x^2 - 1} \quad (7.9.17)$$

$$\frac{P_y}{P_x} = \frac{1 + \gamma M_x^2}{1 + \gamma M_y^2} \quad (7.9.18)$$

$$\frac{T_y}{T_x} = \left(\frac{P_y}{P_x} \right)^2 \left(\frac{M_x}{M_y} \right)^2 \quad (7.9.19)$$

node type

main process m global

h global

T global

process name	m abs	T (°C)	H
refrigeration effect	0.8	-21.37	386.7
condensor	1.3503	41.33	258.39

FluidEjector

Pout: 1.247 Tout: -21.443 Pmi/Pout: 9.624 Pout/Psi: 1.247 xout: 0.628 D P: 0.02000 Pmel: 1.203

Amb (mm2): 696.435 Asb (mm2): 5965.349

Pe/Pb factor

nozzle isentropic efficiency

diffuser isentropic efficiency

Friction factor

FIGURE 7.9.8

Screen of the ejector component

We show in section 19.6.3 of Part 3 how this component can be used in ThermoOptim to model ejector refrigeration cycles.

REFERENCES

- T. Agami Reddy, *Psychrometrics and comfort*, Handbook of Heating, Ventilation, and Air Conditioning, (Edited by J.F. Kreider), CRC Press, 2001, ISBN 0-8493-9584-4
- AICVF *Conception des installations de climatisation, et de conditionnement de l'air*, Collection des guides de l'AICVF, PYC Edition, Paris, octobre 1999.
- R. F. Boehm, *Pumps and fans*, *The CRC handbook of thermal engineering*, (Edited by F. Kreith), CRC Press, Boca Raton, 2000, ISBN 0-8493-9581-X.
- Chase et al. *Janaf thermochemical tables*, J. Phys. Chem. Ref. Data, Vol 14 Suppl. 1, 1985
- K. Chunnanond, S. Aphornratana, *Ejectors: applications in refrigeration technology*, Renewable and Sustainable Energy Reviews 8 (2004) 129–155.
- R. Cohen, E. Groll, W. H. Harden, K. E. Hickman, D. K. Mistry, E. Muir, *Compressors*, *The CRC handbook of thermal engineering*, (Edited by F. Kreith), CRC Press, Boca Raton, 2000, ISBN 0-8493-9581-X.
- T. Giampaolo, *Compressor handbook, Principles and practice*, The Fairmont Press, Lilburn, CRC Press, Boca Raton, 2010, ISBN 0-88173-615-5
- J.P. Holman, *Thermodynamics*, 4th Edition, Mc Graw-Hill, 1988.
- D. Li, A. Groll, *Transcritical CO2 refrigeration cycle with ejector-expansion device*, International Journal of Refrigeration 28 (2005) 766–773
- S. K. Wang, Z. Lavan P. Norton, *Air Conditioning and Refrigeration Engineering*, CRC Press, Boca Raton, 2000, ISBN 0-8493-0057-6.

FURTHER READING

- J.G. Conan, *Réfrigération industrielle*, Eyrolles, Paris, 1988.
- B. Crétinon, B. Blanquart, *Air humide, Notions de base et mesures*, Techniques de l'Ingénieur, Traité Génie énergétique, BE 8 025.
- R. Dehausse, *Mécanique des fluides III*, Polycopiés de l'Ecole des Mines de Paris.
- T. Destoop, *Compresseurs volumétriques*, Techniques de l'Ingénieur, Traité Mécanique et chaleur, B 4 220.
- E. Esposito, *Température et composition des gaz brûlés*, Techniques de l'Ingénieur, Traité Généralités, A 1 610, A 1 611.
- E. Esposito, *Cinétique chimique*, Techniques de l'Ingénieur, Traité Généralités, A 1 620.
- E. Esposito, *Inflammation spontanée*, Techniques de l'Ingénieur, Traité Généralités, A 1 625.
- M. Feidt, *Energétique Thermodynamique – Concepts et Applications*, Dunod, 2006, ISBN 9782100490660.
- Gaz de France, *Combustibles gazeux et principes de la combustion*, BT 104, Paris, 1992.
- I. Glassman, *Combustion*, 3rd Edition, Academic Press, Inc, Dec 1996.
- E. M. Goodger, *Combustion calculations, theory, worked examples and problems*, The MacMillan Press, London, 1977.
- J. C. Guibet, *Les carburants et la combustion*, Techniques de l'Ingénieur, Traité Mécanique et chaleur, B 2 520, B 2 521.
- K.K. Kuo, *Principles of combustion*, John Wiley & Sons, Oct. 2000.
- A. Lallemand, *Compression et détente des gaz ou des vapeurs*, Techniques de l'Ingénieur, Traité Génie énergétique, BE 8 013.
- G. Manfrida, S. Stecco, *Le turbomachine*, Pitagora Editrice, Bologne, 1990.
- M. Pluviose, *Turbomachines hydrauliques et thermiques – Exercices commentés*, Eyrolles, Paris, 1988.
- M. Pluviose, Ch. Périlhon, *Turbomachines: Description. Principes de base*, Techniques de l'Ingénieur, Génie mécanique, BM 4 280
- B. Raynal, *Les techniques d'analyse des gaz de combustion et leurs applications dans le domaine des moteurs thermiques*, Revue Générale de Thermique, n° 162–163 juin–juillet 1975, Paris.
- P. Reboux, Polycopiés de l'Ecole des Mines de Paris, *mécanique des fluides I, II*. Polycopiés du Centre de Formation aux Techniques Gazières, *principes de fonctionnement des turbocompresseurs centrifuges*.
- G. Riollet, *Théorie des turbines à vapeur et à fluide compressible*, Techniques de l'Ingénieur, Traité Mécanique et chaleur, B 330-2.
- G. de Soete, A. Feugier, *Aspects physiques et chimiques de la combustion*, Editions Technip, Paris, 1976.
- D. Spalding, *Combustion and mass transfer*, Pergamon Press, Oxford, 1979.
- G. Vrinat, *Production du froid, Technologie des machines industrielles*, Techniques de l'Ingénieur, Traité Mécanique et chaleur, B 2 365.
- L. Vivier, *Turbines à vapeur et à gaz*, Ed. Albin Michel, Paris, 1965.
- M. de Vlaminck, P. Wauters, *Thermodynamique et turbines*, Ed. Ciaco, Paris, 1988.
- F.A. Williams, *Combustion theory*, 2nd Edition, Addison Wesley Publishing Company, Dec. 1985.

This page intentionally left blank

Heat Exchangers

Abstract: Heat exchangers are devices for transferring heat between two fluids at different temperatures. In most cases, the two fluids are not in contact, and the transfer is through an exchange area. Within the dividing wall, the heat transfer mechanism is conduction, and on each of both surfaces in contact with fluids, convection almost always predominates. In many cases, fluids are single phase, whether gas or liquid. However, there are three main types of heat exchangers in which phase changes occur: the vaporizer or evaporator where it vaporizes a liquid, the condenser where steam is liquefied and evaporative condensers where both fluids change phase.

In practice, heat exchangers are of great importance in many energy systems in which heat is transferred, especially when attempting to recover thermal energy. They can play a critical role in the performance of energy systems involving internal heat exchange, such as regeneration or combined cycles, whose optimization requires one to minimize the internal irreversibilities related to internal temperature differences.

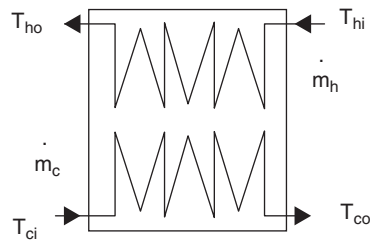
The concepts you should make sure you understand are the principles (8.1), effectiveness ϵ , number of transfer units NTU (8.2.1) and pinch (8.2.4).

Keywords: heat exchanger, heat transfer coefficient, thermal resistance, NTU, LMTD, pinch, shell and tube, air coils, plate, thermocoupler.

8.1 PRINCIPLES OF OPERATION OF A HEAT EXCHANGER

The study of heat exchangers in an energy system can be done at very different levels of difficulty depending on the objectives that we pursue:

- the most basic approach, very simple to implement, is to balance the heat exchanger in terms of enthalpy by determining for example the outlet temperature of a fluid when the inlet temperatures and flow rates of the two fluids are known, as well as an outlet temperature;
- the problem can be posed in reverse, if the two outlet temperatures are known and only one inlet. The approach remains simple. One can indeed show that a heat exchanger has five degrees of freedom and once five are set among the input and output temperatures and flow-rates, the sixth is directly deduced;
- it is also customary to characterize a heat exchanger by either an effectiveness or a minimum temperature difference between the two fluids (called pinch). Solving this problem is also fairly simple if four quantities are known. Note that, very often in the study of energy systems, heat

**FIGURE 8.1.1**

Heat exchanger sketch

exchanger calculations are not explored further. They indeed already provide sufficient information to conduct preliminary analysis of many cycles, especially at the functional level, apart from specific technological considerations. The theory shows, as we see in this chapter, that this approach allows us to characterize an exchanger by what we call the UA , the product of the internal heat exchange coefficient between the two fluids U by its exchange area A ;

- to go further and determine the exchange surface required, calculations are much more complicated, requiring a thorough knowledge of the inner operation of heat exchangers, in order to estimate as precisely as possible the value of U . There is actually a very important qualitative leap between the basic arithmetic of balancing the heat exchanger and what we call its technological design, which will be discussed Chapter 35 of Part 5.

In a heat exchanger, the fluid flows can be performed in multiple arrangements.

One can easily show that thermodynamically, the most efficient heat exchanger is the counter-flow heat exchanger (Figure 8.1.1), but other concerns than the thermodynamic effectiveness are taken into account when designing a heat exchanger: the maximum permissible temperatures in one fluid, or more often considerations of size, weight or cost.

It follows that the configurations of exchangers that are encountered in practice are relatively numerous.

However, we can gather these configurations in three main geometries:

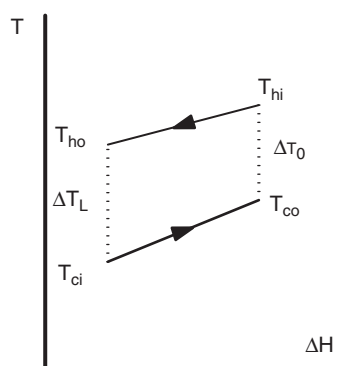
- counter-flow, in which fluids flow in parallel and in opposite directions;
- parallel-flow, in which fluids flow in parallel and in the same direction;
- cross-flow, in which fluids flow in perpendicular directions.

We will denote the hot fluid by index h , and the cold fluid by index c . Besides the geometric configuration, exchanger sizing or performance depends on many parameters and variables:

- mass flows \dot{m}_h and \dot{m}_c passing through them;
- inlet temperatures T_{hi} and T_{ci} and outlet temperatures T_{ho} and T_{co} of both fluids;
- heat exchange coefficients U_h and U_c of each fluid;
- thermal resistance of the wall e/λ ;
- the surface A of the exchanger;
- the pressures of both fluids, almost constant;
- the thermophysical properties of fluids, which are used to determine coefficients U_h and U_c . It is essentially the heat capacity c_p , the density ρ , thermal conductivity λ , and viscosity μ .

In what follows, we will assume that the heat exchange coefficients U_h and U_c and thermophysical properties of fluids maintain a constant value at any time in the entire heat exchanger.

If this assumption is not verified, then in order to study the performance of the exchanger, it is necessary to divide it into small volume elements, in which these properties can be considered constant. The calculations are then much more cumbersome.

**FIGURE 8.1.2**

LMTD notations

Finally, we always assume that the heat exchanger is globally adiabatic, that is to say there is no heat exchange with the surroundings.

8.1.1 Heat flux exchanged

It can be shown, where fluid flow is pure (parallel or counter-flow), that the heat flux exchanged between the two fluids is given by the formula:

$$\phi = UA\Delta T_{ml} \quad (8.1.1)$$

$$\text{with } \Delta T_{ml} = \frac{\Delta T_0 - \Delta T_L}{\ln \frac{\Delta T_0}{\Delta T_L}} \quad (8.1.2)$$

A being the exchange surface, U the overall heat exchange coefficient (see next section), ΔT_{ml} the logarithmic mean temperature difference, and ΔT_0 and ΔT_L the differences in fluid temperatures respectively at one end and at the other end of the exchanger, with the convention: $\Delta T_0 > \Delta T_L$.

Care must be taken that we speak of temperature differences between the two fluids at the entrance and exit of the exchanger (dimensions 0 and L), and not differences of inlet temperatures ($T_{hi} - T_{ci}$) and output temperatures ($T_{ho} - T_{co}$) of the fluids.

In the example in Figure 8.1.2, we have:

$$\Delta T_0 = T_{hi} - T_{co} \quad (8.1.3)$$

$$\Delta T_L = T_{ci} - T_{ho}$$

When the flow configuration is more complex, we introduce a correction factor F (less than 1), which is given by charts calculated or determined experimentally, most often provided by manufacturers.

Equation (8.1.1) becomes:

$$\phi = UAF\Delta T_{ml} \quad (8.1.4)$$

This formula shows that to transfer a given flux ϕ , if we wish to reduce the irreversibilities and therefore ΔT_{ml} , we need the product UA to be the largest possible, which can be done either by increasing the surface, but this directly affects the cost, or by increasing the U value, which is an aim sought by all heat exchanger designers.

In this chapter, the design of the heat exchanger will be limited to determining the product UA of the exchanger surface A by the overall heat transfer coefficient U , the accurate estimation of the latter depending on the internal constructive details of the exchanger.

In general, the design of heat exchangers is a compromise between conflicting objectives, whose two main ones are:

- a large exchange area is desirable to increase the effectiveness of heat exchangers, but it results in high costs;
- small fluid flow sections increase the values of the heat exchange coefficients U_h and U_c defined in the next section, and thus reduce the area, but they also increase pressure drops.

8.1.2 Heat exchange coefficient U

We only deal in Chapter 35 of Part 5 of the precise determination of U and the study of pressure drops in heat exchangers, not that these difficult issues lack interest, quite the contrary, but because, as for other components, we are not currently looking to complete their detailed internal design: we limit ourselves to dealing with their integration into systems that are energy technologies. We will only present here the principles governing the calculation of U .

Thermal science teaches us that for a flat plate heat exchanger, the overall heat transfer coefficient U is such that its inverse, called thermal resistance, is the sum of thermal resistances between the two fluids:

$$\frac{1}{U} = \frac{1}{h_h} + \frac{e}{\lambda} + \frac{1}{h_c} \quad (8.1.5)$$

h_h being the heat transfer coefficient between the hot fluid and the wall, h_c the heat transfer coefficient between the cold fluid and the wall, e the wall thickness and λ the thermal conductivity of this wall.

If the wall is composed of several layers of different materials, or if other deposits have covered the wall, this formula becomes:

$$\frac{1}{U} = \frac{1}{h_h} + \sum_{k=1}^n \frac{e_k}{\lambda_k} + \frac{1}{h_c} \quad (8.1.6)$$

The overall thermal resistance is the sum of $(n + 2)$ thermal resistances, the largest of them being the one that slows down the more heat that is exchanged.

For example, in the case of a gas/liquid heat exchanger, the convection coefficient can be 10 to 100 times lower on the gaseous side than on the liquid side. The thermal resistance of the wall and the liquid side are generally negligible, and U is approximately equal to h gas side.

In this case, we seek to increase the gas side exchange surface by using fins. The previous formulas are complicated, and as the surfaces of cold and hot sides are not the same, we introduce a warm side global exchange coefficient U_h , such that its inverse is:

$$\frac{1}{U_h} = \frac{1}{\eta_{0,h} h_h} + \frac{e}{\frac{A_w}{A_h} \lambda} + \frac{1}{\frac{A_c}{A_h} \eta_{0,c} h_c} \quad (8.1.7)$$

with A_h and A_c total exchange areas warm and cold sides, A_w exchanger wall surface, and $\eta_{0,h}$ and $\eta_{0,c}$ overall fin effectiveness on warm and cold sides (see section 8.1.3).

There is also a cold side global exchange coefficient U_c , with of course:

$$U_c A_c = U_h A_h$$

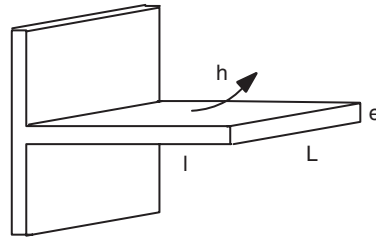


FIGURE 8.1.3
Rectangular fin

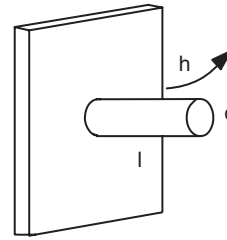


FIGURE 8.1.4
Needle fin

8.1.3 Fin effectiveness

For a thin rectangular fin ($e \ll 1$, Figure 8.1.3), we can show that the fin effectiveness, defined as the ratio of heat actually exchanged to the heat that would be exchanged if the fin was at the temperature of the base, is:

$$\eta_a = \frac{\tanh(ml)}{ml}$$

$$\text{with } m = \sqrt{\frac{2h}{\lambda e}} \quad (8.1.8)$$

For fins of different shapes, the value of m changes. For example, for circular needle fins (Figure 8.1.4):

$$m = \sqrt{\frac{4h}{\lambda d}} \quad (8.1.9)$$

For other geometries, we refer to the literature (Incropera, Dewitt, 1996).

The total flux exchanged is equal to the sum of the fluxes exchanged on the one hand by the fins (area A_a) and on the other hand by the wall between the fins (area $A - A_a$). This defines an overall effectiveness η_0 equal to the ratio of the flux actually exchanged to the flux that would be exchanged if the entire surface was at the temperature of the base:

$$\eta_0 = \frac{hA_a\eta_a + h(A - A_a)}{hA} = 1 - \frac{A_a}{A}(1 - \eta_a) \quad (8.1.10)$$

8.1.4 Values of convection coefficients h

The values of convection coefficients h_h and h_c depend on fluid thermophysical properties and exchange configurations. Further explanations will be given in Chapter 35 of Part 5 on technological design.

These coefficients can be estimated from correlations giving the value of Nusselt number $Nu = hd_h/\lambda$, as a function of Reynolds $Re = \rho V d_h/\mu$ and Prandtl $Pr = \mu c_p/\lambda$ numbers.

The hydraulic diameter d_h is equal to the ratio of four times the flow area S to the wetted perimeter p : $d_h = 4S/p$ (if there are isolated walls, the perimeter of heat exchange must be considered).

Inside tubes, the formula most used is that of Mac Adams:

$$Nu = 0.023 Re^{0.8} Pr^{0.4} \quad (8.1.11)$$

For flow perpendicular to tubes, several options exist, such as Colburn:

$$\text{Nu} = 0.33 \text{Re}^{0.6} \text{Pr}^{0.33} \quad (8.1.12)$$

In general, the exponent of the Reynolds number is between 0.5 and 0.8, and that of the Prandtl number between 0.33 and 0.4. Bontemps et al. (1998) give values of correlations for very special finned geometries.

For gases, Pr varies little with temperature and remains between 0.7 and 0.75. It can therefore be considered constant without committing an error.

For liquids, it is imperative to consider the temperature in the computation of Pr. Knowing the values c_{p0} , λ_0 and μ_0 for T_0 , and development of the first order of the heat capacity:

$$c_p = c_{p0} + c_{pb}(T - T_0)$$

We obtain, for most liquids (water excluded), a good approximation of the variation of Pr with temperature by formula:

$$\text{Pr} = \frac{c_{p0} + c_{pb}(T - T_0)}{[\lambda_0 - 2 \cdot 10^{-4}(T - T_0)] \left[\frac{T - T_0}{233} + \mu_0^{-0.266} \right]^{3.758}} \quad (8.1.13)$$

8.2 PHENOMENOLOGICAL MODELS FOR THE CALCULATION OF HEAT EXCHANGERS

To size a heat exchanger, it is possible to use relations (8.1.1) or (8.1.4), but they assume the logarithmic mean temperature difference is known, which is rarely the case.

8.2.1 Number of transfer units method

A method simpler to use, and especially for more general use, is the NTU, or number of transfer units, method developed by Kays and London (1984). This method has the advantage of requiring the knowledge of fluid inlet temperatures, and not those of those at the outlet.

By definition, NTU is defined as the ratio of the product UA of the heat exchanger to the minimum heat capacity rate.

$$\text{NTU} = \frac{UA}{(\dot{m} \cdot c_p)_{\min}} \quad (8.2.1)$$

We call R the ratio (less than 1) of the heat capacity rates:

$$R = \frac{(\dot{m}c_p)_{\min}}{(\dot{m}c_p)_{\max}} \leq 1 \quad (8.2.2)$$

and ε the effectiveness of the exchanger, defined as the ratio between the heat flux actually transferred and the maximum possible flux:

$$\varepsilon = \frac{\phi}{\phi_{\max}} \quad (8.2.3)$$

We can show that ϕ_{\max} , that would be obtained for a counter-flow heat exchanger of infinite length, is:

$$\phi_{\max} = (\dot{m}c_p)_{\min} \Delta T_i$$

ΔT_i is the difference between inlet temperatures of both fluids. Figure 8.2.1 gives the appearance of the temperature profile in a heat exchanger. Note that here the abscissa used is the enthalpy exchanged, not the length of the exchanger, which explains, with the assumption that the heat capacities are constant, that this rate is linear, not exponential.

Note also that ΔT_{\max} and ΔT_{\min} are the temperature differences within each of the two fluids and not between them as in figure 8.1.2.

$$\text{As } \phi = (\dot{m}c_p)_{\min} \Delta T_{\max} = (\dot{m}c_p)_{\max} \Delta T_{\min} \quad (8.2.4)$$

$$\text{we have: } \varepsilon = \frac{\Delta T_{\max}}{\Delta T_i} \quad (8.2.5)$$

$$\text{Since } \phi = UA\Delta T_{\text{ml}} = (\dot{m}c_p)_{\min} \Delta T_{\max} = (\dot{m}c_p)_{\max} \Delta T_{\min}$$

$$NTU = \frac{UA}{\dot{m}c_{p\min}} = \frac{\Delta T_{\max}}{\Delta T_{\text{ml}}}$$

NTU measures the ability of the exchanger for changing the temperature of the fluid whose capacity rate is lower.

This is indeed an indicator of the quality of the equipment: the more efficient the heat exchanger, the more it allows for heating or cooling a fluid with a low temperature difference compared with the other.

When U varies along the surface of the exchanger,

$$NTU = \frac{1}{\dot{m}c_{p\min}} \int_0^A U \, dA$$

For example, in the example of Figure 8.2.1, where $(\dot{m}c_p)_h < (\dot{m}c_p)_c$ we have:

$$(\dot{m}c_p)_{\min} = (\dot{m}c_p)_h$$

$$\Delta T_i = T_{hi} - T_{ci}$$

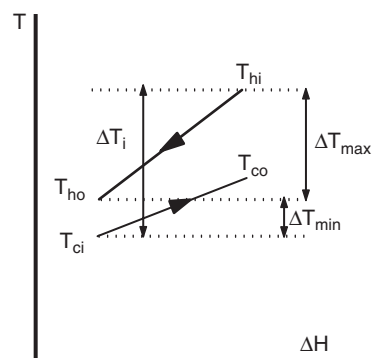


FIGURE 8.2.1

Effectiveness notations

$$\Delta T_{\max} = T_{hi} - T_{ho} \quad \text{and}$$

$$\varepsilon = \frac{T_{hi} - T_{ho}}{T_{hi} - T_{ci}} \quad (8.2.6)$$

With these definitions, it is possible to show that there is a general relation of type:

$$\varepsilon = f(\text{NTU}, R, \text{flow pattern}) \quad (8.2.7)$$

In practice, it suffices to have a set of relationships corresponding to flow patterns representative of exchangers studied, and the design of a heat exchanger is made on the basis on the one hand of the balance equations (8.2.4) and on the other hand of the internal equation (8.2.7).

If we know the flow-rates of both fluids, their inlet temperatures and the heat flux transferred, the procedure is as follows:

- we start by determining the outlet temperatures of fluids from equation (8.2.4);
- we deduce the fluid heat capacity rates $\dot{m}c_p$ and their ratio R ;
- the effectiveness ε is calculated from equation (8.2.5);
- the value of NTU is determined from the appropriate (NTU, ε) relationship;
- UA is calculated from equation (8.2.1).

If you know UA, (8.2.1) gives the value of NTU, and you can determine ε from the appropriate (NTU, ε) relationship. Equation (8.2.5) allows you to calculate the heat transferred.

In both cases, the enthalpy balance provides the outlet temperatures. This method therefore connects the UA product to the exchanger performance, and the surface is deduced from an estimate of the value of the exchange coefficient U .

As shown in (8.2.6), ε measures the “temperature” effectiveness of the exchanger, i.e. the fraction of the maximum difference in temperature between the fluids which is communicated to that with the lower heat capacity rate.

The value of the method proposed by Kays and London is its generality because of the formal appearance of $(\dot{m}c_p)_{\min}$ and $(\dot{m}c_p)_{\max}$.

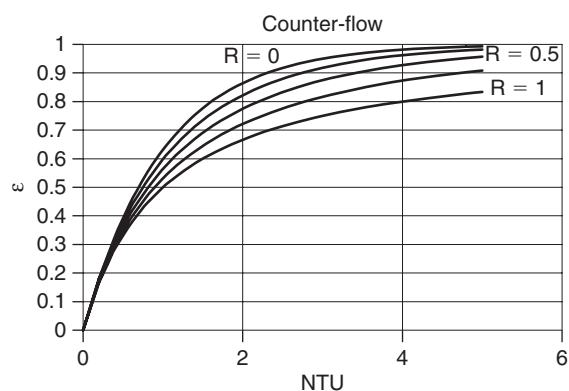
Phenomenological (ε , NTU) models provide only the exchanger UA product. As we have seen in section 8.1.2, the calculation of U depends on many factors they do not take into account. We will show in Chapter 35 of Part 5 the types of technological design models which can be built to assess U .

Given its advantages, this method has been very successful and is now widely used. As we shall see, it is often even generalized to size heat exchangers other than those we have considered here, where it will be recalled we assumed that heat exchange coefficients U_h and U_c and fluid thermo-physical properties keep a constant value.

Experience shows that, on a thermodynamic level, (ε , NTU) models generally represent well the behavior of many types of exchangers, even more complex than those we have studied so far. It is especially what we have done in Thermoptim for thermocouplers, whose mechanism is complementary to the heat exchangers allowing components other than “exchange” processes to connect to one or more “exchange” processes to represent thermal couplings (see section 8.3.7).

8.2.2 Relationship between NTU and ε

In the pages that follow, we give relations between ε and NTU function of R , and their inverses which can be expressed simply, as well as the corresponding graphs in which curves represent ε function of NTU, for R varying from 0 to 1, top to bottom, by steps of 0.25.

**FIGURE 8.2.2**

Counter-flow heat exchanger chart

8.2.2.1 Counter-flow heat exchangersFor a counter-flow heat exchanger, analytical expressions are, for $R \neq 1$:

$$NTU = \frac{1}{1-R} \ln \frac{1-\varepsilon R}{1-\varepsilon} \quad (8.2.8)$$

$$\varepsilon = \frac{1 - \exp(-NTU(1-R))}{1 - R \exp(-NTU(1-R))}$$

For $R = 1$

$$\varepsilon = \frac{NTU}{1 + NTU}$$

The corresponding chart is given Figure 8.2.2.

8.2.2.2 Parallel-flow heat exchangers

For a parallel-flow heat exchanger:

$$NTU = -\frac{1}{1+R} \ln(1 - \varepsilon(1+R)) \quad (8.2.9)$$

$$\varepsilon = \frac{1 - \exp(-NTU(1+R))}{1+R}$$

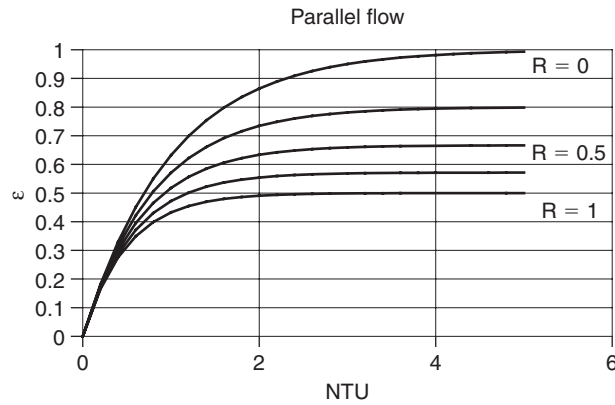
The corresponding chart is given Figure 8.2.3.

8.2.2.3 Cross-flow heat exchangersFor a $((\dot{m}c_p)_{\min})$ mixed fluid cross-flow heat exchanger:

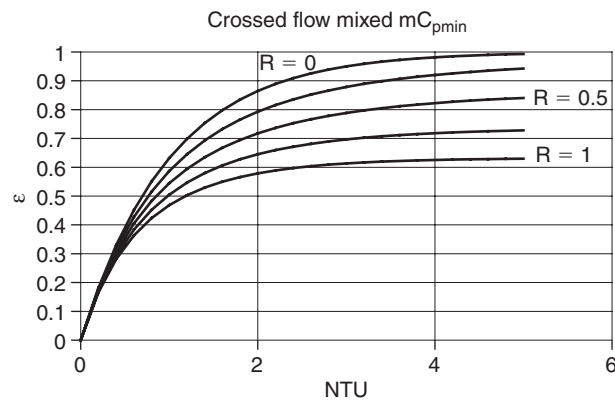
$$NTU = -\frac{1}{R} \ln[1 + R \ln(1 - \varepsilon)] \quad (8.2.10)$$

$$\varepsilon = 1 - \exp\left(\frac{-\Gamma}{R}\right) \quad \text{with} \quad \Gamma = 1 - \exp(-RNTU)$$

The corresponding chart is given Figure 8.2.4.


FIGURE 8.2.3

Parallel-flow heat exchanger chart


FIGURE 8.2.4

 Cross-flow heat exchanger chart (mC_{pmin})

 For a ($(\dot{m}c_p)_{max}$) mixed fluid cross-flow heat exchanger:

$$NTU = -\ln \left[1 + \frac{1}{R} \ln(1 - \epsilon R) \right] \quad (8.2.11)$$

$$\epsilon = \frac{1}{R} [1 - \exp(-\Gamma R)] \quad \text{with} \quad \Gamma = 1 - \exp(-NTU)$$

The corresponding chart is given Figure 8.2.5.

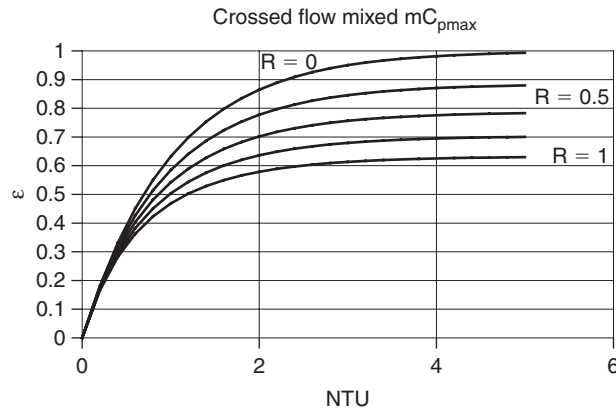
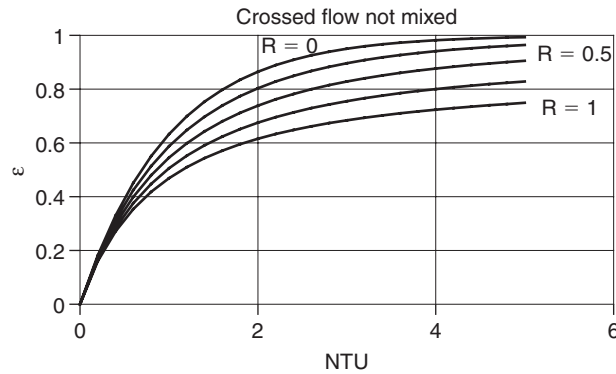
For a non-mixed fluid cross-flow heat exchanger (Holman, 1989), the corresponding chart is given Figure 8.2.6.

$$\epsilon = \left[1 - \exp \left(\frac{-\Gamma NTU^{0.22}}{R} \right) \right] \quad \text{with} \quad \Gamma = 1 - \exp(-R NTU^{0.78}) \quad (8.2.12)$$

8.2.2.4 Shell and tube heat exchangers

For a tube and shell heat exchanger (see 8.4.1.1), the following relationships are valid for one pass, regardless of the number of passes of tubes in the shell:

$$NTU = \frac{1}{\sqrt{1+R^2}} \ln \left[\frac{2 - \epsilon(1+R + \sqrt{1+R^2})}{2 - \epsilon(1+R - \sqrt{1+R^2})} \right] \quad (8.2.13)$$

**FIGURE 8.2.5**Cross-flow heat exchanger chart (mC_{pmax})**FIGURE 8.2.6**

Cross-flow heat exchanger chart (not mixed)

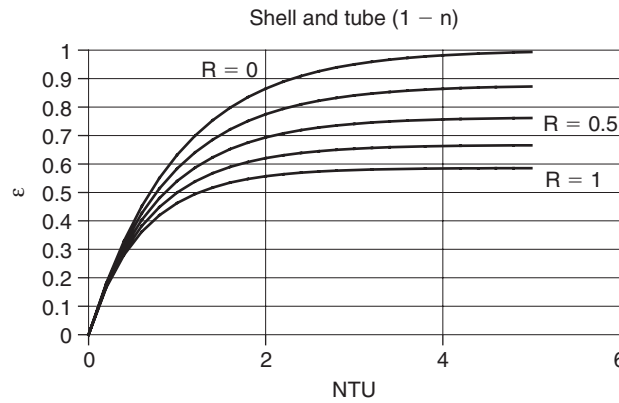
$$\text{Posing } \Gamma = \sqrt{1 + R^2}$$

$$\varepsilon = \frac{2}{1 + R + \Gamma \frac{1 + \exp(-NTU\Gamma)}{1 - \exp(-NTU\Gamma)}}$$

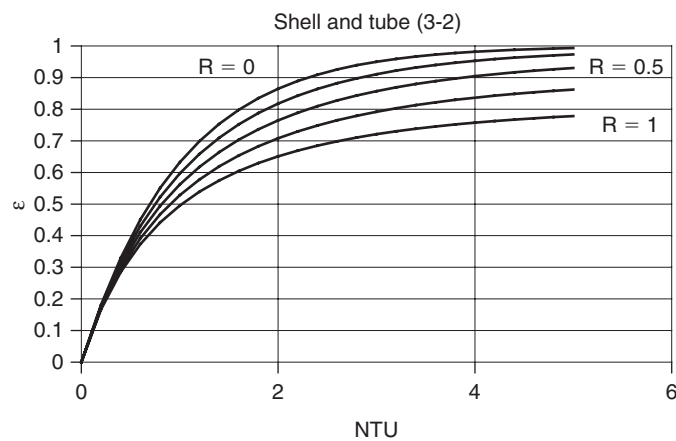
The corresponding chart is given Figure 8.2.7.

For a multiple pass exchanger, with the assumption that the fluid is stirred between passes and the NTU is distributed evenly between the channels of identical configurations placed in global counter-flow arrangement, we will establish relationship (8.2.26) (section 8.2.4.1) which is simplified here to give, p being the number of passes and ε_p the effectiveness of each pass, depending on NTU_p :

$$NTU = pNTU_p \quad \varepsilon = \frac{1 - \left[\frac{1 - R\varepsilon_p}{1 - \varepsilon_p} \right]^p}{R - \left[\frac{1 - R\varepsilon_p}{1 - \varepsilon_p} \right]^p} \quad (8.2.14)$$


FIGURE 8.2.7

Shell and tube heat exchanger chart (1-n)


FIGURE 8.2.8

Shell and tube heat exchanger chart (3-2)

For example, for a shell and tube heat exchanger with three double passes, we get the chart given in Figure 8.2.8.

If we seek an overall effectiveness ϵ , calling $A = (1 - R\epsilon_p)/(1 - \epsilon_p)$, then:

$$A = \left[\frac{1 - R\epsilon}{1 - \epsilon} \right]^{1/P} \quad \epsilon_p = \frac{\left[\frac{1 - R\epsilon}{1 - \epsilon} \right]^{1/P} - 1}{\left[\frac{1 - R\epsilon}{1 - \epsilon} \right]^{1/P} - R} \quad (8.2.15)$$

NTU_p is deduced, then NTU .

If we seek a NTU value, we deduce NTU_p , then ϵ_p , and finally ϵ .

8.2.3 Matrix formulation

In the case where $(\dot{m}c_p)_h < (\dot{m}c_p)_c$, (8.2.6) can be rewritten as:

$$T_{ho} = (1 - \epsilon)T_{hi} + \epsilon T_{ci} \quad (8.2.16)$$

Moreover, (8.2.4) gives: $\Phi = (\dot{m}c_p)_{\min}(T_{hi} - T_{ho}) = (\dot{m}c_p)_{\max}(T_{co} - T_{ci})$

Given (8.2.2):

$$\begin{aligned} T_{co} - T_{ci} &= R(T_{hi} - T_{ho}) = R(T_{hi} - (1 - \epsilon)T_{hi} - \epsilon T_{ci}) \\ T_{co} &= R\epsilon T_{hi} + (1 - R\epsilon)T_{ci} \end{aligned} \quad (8.2.17)$$

(8.2.16) and (8.2.17) can also be expressed in matrix form:

$$\begin{pmatrix} T_{ho} \\ T_{co} \end{pmatrix} = \begin{pmatrix} 1 - \epsilon & \epsilon \\ R\epsilon & 1 - R\epsilon \end{pmatrix} \begin{pmatrix} T_{hi} \\ T_{ci} \end{pmatrix} \quad (8.2.18)$$

If we had considered a system where $(\dot{m}c_p)_h > (\dot{m}c_p)_c$, the matrix system would have been:

$$\begin{pmatrix} T_{ho} \\ T_{co} \end{pmatrix} = \begin{pmatrix} 1 - R\epsilon & R\epsilon \\ \epsilon & 1 - R \end{pmatrix} \begin{pmatrix} T_{hi} \\ T_{ci} \end{pmatrix} \quad (8.2.19)$$

With $R = (\dot{m}c_p)_c / (\dot{m}c_p)_h$

If so we note:

$$\epsilon_h = \inf \left(\epsilon, \frac{(\dot{m}c_p)_c}{(\dot{m}c_p)_h} \epsilon \right) \quad \text{and} \quad \epsilon_c = \inf \left(\epsilon, \frac{(\dot{m}c_p)_h}{(\dot{m}c_p)_c} \epsilon \right)$$

we obtain a generalized matrix formulation which remains always valid:

$$\begin{aligned} \begin{pmatrix} T_{ho} \\ T_{co} \end{pmatrix} &= \begin{pmatrix} 1 - \epsilon_h & \epsilon_h \\ \epsilon_c & 1 - \epsilon_c \end{pmatrix} \begin{pmatrix} T_{hi} \\ T_{ci} \end{pmatrix} \\ \begin{pmatrix} T_{ho} \\ T_{co} \end{pmatrix} &= A \begin{pmatrix} T_{hi} \\ T_{ci} \end{pmatrix} \end{aligned} \quad (8.2.20)$$

This relationship can be altered to express not the outlet temperatures as a function of inlet temperatures, but temperatures from one end of the exchanger in relation to those from the other. We can readily obtain:

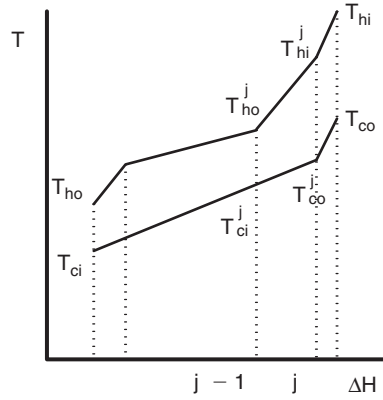
$$\begin{pmatrix} T_{hi} \\ T_{co} \end{pmatrix} = \begin{pmatrix} \frac{1}{1 - \epsilon_h} & -\frac{\epsilon_h}{1 - \epsilon_h} \\ \frac{\epsilon_c}{1 - \epsilon_h} & 1 - \frac{\epsilon_c}{1 - \epsilon_h} \end{pmatrix} \begin{pmatrix} T_{ho} \\ T_{ci} \end{pmatrix} = B \begin{pmatrix} T_{ho} \\ T_{ci} \end{pmatrix} \quad (8.2.21)$$

A third formulation is used to express the temperatures of the hot fluid in terms of those of the cold fluid:

$$\begin{pmatrix} T_{ho} \\ T_{hi} \end{pmatrix} = \begin{pmatrix} \frac{1 - \epsilon_h}{\epsilon_c} & 1 - \frac{1 - \epsilon_h}{\epsilon_c} \\ \frac{1}{\epsilon_c} & 1 - \frac{1}{\epsilon_c} \end{pmatrix} \begin{pmatrix} T_{co} \\ T_{ci} \end{pmatrix} = C \begin{pmatrix} T_{co} \\ T_{ci} \end{pmatrix} \quad (8.2.22)$$

8.2.4 Heat exchanger assemblies

When we cannot achieve in a single exchanger the desired heat transfer, it is possible to combine various heat exchangers, either in series or in series-parallel.


FIGURE 8.2.9

Assembly in series

8.2.4.1 Assembly in series

Given their poor performance, parallel-flow type heat exchangers are not put in series. Consider an assembly of heat exchangers in series.

Let us call T_{hi}^j and T_{ho}^j the inlet and outlet temperatures of the hot fluid in exchanger j , T_{ci}^j and T_{co}^j those of the cold fluid. Given the serial arrangement, we have:

$$T_{co}^j = T_{ci}^{j+1} \quad \text{and} \quad T_{hi}^j = T_{ho}^{j+1}$$

Let us before:

$$\varepsilon_h^j = \inf \left(\varepsilon^j; \frac{(\dot{m}c_p)_{ci}}{(\dot{m}c_p)_{hi}} \varepsilon^j \right)$$

$$\varepsilon_c^j = \inf \left(\varepsilon^j; \frac{(\dot{m}c_p)_{hi}}{(\dot{m}c_p)_{ci}} \varepsilon^j \right)$$

We have, using formulation (8.2.21):

$$\begin{pmatrix} T_{hi}^j \\ T_{co}^j \end{pmatrix} = \begin{pmatrix} \frac{1}{1-\varepsilon_h^j} & -\frac{\varepsilon_h^j}{1-\varepsilon_h^j} \\ \frac{\varepsilon_c^j}{1-\varepsilon_h^j} & 1-\frac{\varepsilon_c^j}{1-\varepsilon_h^j} \end{pmatrix} \begin{pmatrix} T_{ho}^j \\ T_{ci}^j \end{pmatrix} = \mathbf{B}_j \begin{pmatrix} T_{ho}^j \\ T_{ci}^j \end{pmatrix} \quad (8.2.23)$$

$$\begin{pmatrix} T_{ho}^{j+1} \\ T_{ci}^{j+1} \end{pmatrix} = \mathbf{B}_j \begin{pmatrix} T_{ho}^j \\ T_{ci}^j \end{pmatrix} \quad \text{if } i < n$$

$$\begin{pmatrix} T_{hi} \\ T_{co} \end{pmatrix} = \mathbf{B}_n \begin{pmatrix} T_{ho}^n \\ T_{ci}^n \end{pmatrix} \quad \text{if } j = n$$

$$\begin{pmatrix} T_{hi} \\ T_{co} \end{pmatrix} = \mathbf{B}_n \begin{pmatrix} T_{ho}^n \\ T_{ci}^n \end{pmatrix} = \mathbf{B}_n \mathbf{B}_{n-1} \begin{pmatrix} T_{ho}^{n-1} \\ T_{ci}^{n-1} \end{pmatrix}$$

$$\begin{pmatrix} T_{hi} \\ T_{co} \end{pmatrix} = \prod_{i=n}^{i=1} \mathbf{B}_i \begin{pmatrix} T_{ho} \\ T_{ci} \end{pmatrix} \quad (8.2.24)$$

Knowing the hot and cold inlet temperatures in the system, this formula gives directly the corresponding outlet temperatures.

The inverse of the matrix \mathbf{B}_j is equal to:

$$\mathbf{B}_j^{-1} = \begin{pmatrix} 1 - \frac{\varepsilon_h^j}{1 - \varepsilon_c^j} & \frac{\varepsilon_h^j}{1 - \varepsilon_c^j} \\ -\frac{\varepsilon_c^j}{1 - \varepsilon_c^j} & \frac{1}{1 - \varepsilon_c^j} \end{pmatrix}$$

$$\det(\mathbf{B}_j) = \frac{1 - \varepsilon_c^j}{1 - \varepsilon_h^j}$$

Product $\mathbf{B}_j \mathbf{B}_k = \mathbf{B}_{jk}$, which represents the heat exchanger obtained by serializing exchangers j and k , in that order, is such that:

$$\varepsilon_h^{jk} = 1 - \frac{(1 - \varepsilon_h^j)(1 - \varepsilon_h^k)}{1 - \varepsilon_h^j \varepsilon_c^k}$$

$$\varepsilon_c^{jk} = 1 - \frac{(1 - \varepsilon_c^j)(1 - \varepsilon_c^k)}{1 - \varepsilon_h^j \varepsilon_c^k}$$

It is clear that $\mathbf{B}_j \mathbf{B}_k \neq \mathbf{B}_k \mathbf{B}_j$

Moreover, if we subtract the second line of (8.2.23) from the first, we get:

$$T_{ho}^{j+1} - T_{ci}^{j+1} = \frac{1 - \varepsilon_c^j}{1 - \varepsilon_h^j} (T_{ho}^j - T_{ci}^j) \quad (8.2.25)$$

$$T_{ho}^{n+1} - T_{ci}^{n+1} = \prod \frac{1 - \varepsilon_c^j}{1 - \varepsilon_h^j} (T_{ho}^1 - T_{ci}^0)$$

This relationship can also be written in terms of minimum pinch (see 8.2.6), giving a constraint to meet for off-design operation, considering as separated heat exchangers the endothermic and exothermic areas (see section 22.2 of Part 3).

For a counter-flow arrangement of n exchangers containing fluids with identical and constant thermophysical characteristics, whose intermediate effectiveness is ε_i , we deduce that the overall effectiveness ε can be expressed as:

$$\varepsilon = \frac{1 - \prod_{i=1}^{i=n} \frac{1 - R\varepsilon_i}{1 - \varepsilon_i}}{R - \prod_{i=1}^{i=n} \frac{1 - R\varepsilon_i}{1 - \varepsilon_i}} \quad (8.2.26)$$

If $R = 1$, this expression becomes:

$$\varepsilon = \frac{\sum_{i=1}^{i=n} \frac{\varepsilon_i}{1 - \varepsilon_i}}{1 - \sum_{i=1}^{i=n} \frac{\varepsilon_i}{1 - \varepsilon_i}} \quad (8.2.27)$$

These relationships lead to the following addition rule: the global NTU corresponding to overall effectiveness ε is equal to the sum of NTU_i of each module corresponding to its partial efficacy ε_i .

8.2.4.2 Assembly in series-parallel

With the same assumptions as above regarding the constancy of the fluid thermophysical characteristics, two cases may arise, whether the fluid that passes through heat exchangers in series is the hot or cold fluid.

Let us suppose here that the cold fluid passes horizontally in series in all exchangers while the hot fluid is divided into n parallel branches.

Relation (8.2.20) gives here:

$$\begin{pmatrix} T_{ho}^j \\ T_{co}^j \end{pmatrix} = A_j \begin{pmatrix} T_{hi}^j \\ T_{ci}^j \end{pmatrix} \quad \text{with } T_{ci}^j = T_{co}^{j-1}$$

We can get a recurring matrix relation as follows:

$$\begin{pmatrix} T_{ho}^j \\ T_{hi}^j \\ T_{co}^j \end{pmatrix} = \begin{pmatrix} 0 & 1 - \varepsilon_h^j & \varepsilon_h^j \\ 0 & 1 & 0 \\ 0 & \varepsilon_c^j & 1 - \varepsilon_c^j \end{pmatrix} \begin{pmatrix} T_{ho}^{j-1} \\ T_{hi}^{j-1} \\ T_{co}^{j-1} \end{pmatrix}$$

$$\begin{pmatrix} T_{ho}^j \\ T_{hi}^j \\ T_{co}^j \end{pmatrix} = \mathbf{D}_j \begin{pmatrix} T_{ho}^{j-1} \\ T_{hi}^{j-1} \\ T_{co}^{j-1} \end{pmatrix}$$

$$\mathbf{D}_j \mathbf{D}_k = \mathbf{D}_{jk} = \begin{pmatrix} 0 & 1 - \varepsilon_h^j + \varepsilon_c^k \varepsilon_h^j & \varepsilon_h^j (1 - \varepsilon_c^k) \\ 0 & 1 & 0 \\ 0 & \varepsilon_c^j + \varepsilon_c^k (1 - \varepsilon_c^j) & (1 - \varepsilon_c^j)(1 - \varepsilon_c^k) \end{pmatrix}$$

$$1 - \varepsilon_c^{jk} = (1 - \varepsilon_c^j)(1 - \varepsilon_c^k)$$

$$\varepsilon_h^{jk} = \varepsilon_h^j (1 - \varepsilon_c^k) = \frac{\varepsilon_h^j}{(1 - \varepsilon_c^j)} (1 - \varepsilon_c^j) (1 - \varepsilon_c^k) = \frac{\varepsilon_h^j}{(1 - \varepsilon_c^j)} (1 - \varepsilon_c^{jk})$$

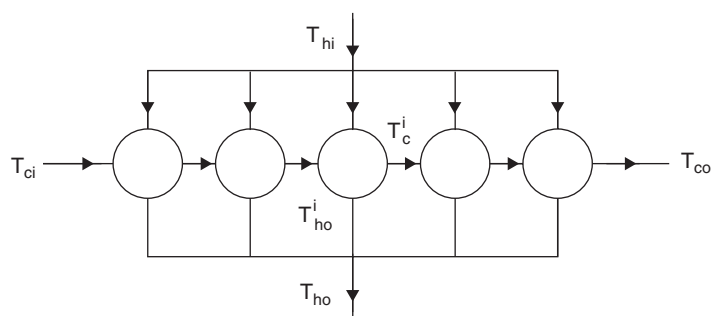
The hot fluid outlet temperature T_{ho} is obviously the barycentric average of the T_{ho}^j , weighted by the heat capacity rates in each branch.

The relationship providing the overall effectiveness is here:

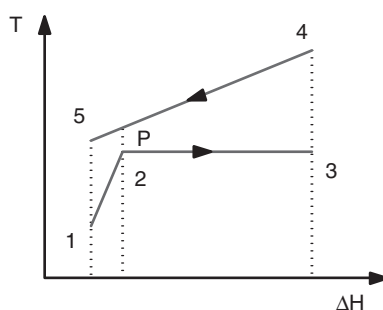
$$1 - \varepsilon = \prod_{i=1}^{i=n} (1 - \varepsilon_i) \quad (8.2.28)$$

knowing that ε should always be calculated for the fluid passing through heat exchangers in series. This relationship can be transformed by noting that $\text{NTU} = -\ln(1 - \varepsilon)$ for $R = 0$, and leads to the following addition rule: the overall NTU of a set of exchangers in series-parallel is obtained by summing the NTU_i related to the fluid flowing through them in series, calculated for a heat capacity rate ratio $R = 0$.

$$\text{NTU}(\varepsilon, R = 0) = \sum_{i=1}^{i=n} \text{NTU}_i(\varepsilon, R = 0)$$

**FIGURE 8.2.10**

Assembly in series-parallel

**FIGURE 8.2.11**

Pinch point

8.2.5 Relationship with the LMTD method

The log-mean temperature difference method (LMTD) starts from equation (8.1.4):

$$\phi = UAF\Delta T_{ml}$$

It is possible to switch from a calculation method to another using relationship:

$$\Delta T_{ml} = \frac{\varepsilon \Delta T_i}{NTU}$$

8.2.6 Heat exchanger pinch

A heat exchanger pinch is defined as the minimum temperature difference between both fluids. For a simple exchanger without phase change, it is:

$$\begin{aligned} (T_{ho} - T_{ci}) & \quad \text{if } (\dot{m}c_p)_h \leq (\dot{m}c_p)_c \\ (T_{hi} - T_{co}) & \quad \text{if } (\dot{m}c_p)_h \geq (\dot{m}c_p)_c \end{aligned}$$

Consider the graphical representation of a double exchanger consisting of an economizer followed by an evaporator, in the $(T, \Delta H)$ graph where the temperature is the ordinate and enthalpies involved the abscissa (Figure 8.2.11).

The fluid which evaporates is represented by the lower curve (1-2-3), which presents an angular point 2 corresponding to the beginning of the boiling. The hot fluid cools from 4 to 5, by decreasing its sensible heat.

On segments (1–2) and (4–5) we have $\Delta H = \dot{m}c_p \Delta T$, and thus $\Delta T = 1/\dot{m}c_p \Delta H$.

The slopes of segments (1–2) and (4–5) are equal to the inverse of the heat capacity rates of the corresponding fluids. For segment (2–3), we obviously have $\Delta T = 0$, vaporization taking place at constant temperature for a pure component or azeotrope.

At point 2 on the diagram P is the minimum temperature difference between the two fluids, called pinch. This point plays a fundamental role in the design of heat exchangers, as it represents the smallest difference in temperature in the device, and thus corresponds to the most constrained area of the system.

The importance of the pinch is most evident in problems of complex heat exchanger network design, to the point that powerful optimization methods based on this concept have been developed. We present in Chapter 22 of Part 3 the ThermoOptim method derived from the pinch method, which aims to find the best integration of the whole network.

The exchanger, sized according to the pinch, operates outside this point with temperature differences greater than the minimum pinch between the two fluids. The irreversibilities depend directly on the gap ΔT between the hot and cold fluids. They are even lower than the slopes of hot and cold fluids are close to one another, that is to say that the R ratio of their heat capacity rates is close to unity. The heat exchanger which has the least irreversibility is the one whose heat capacity rates are equal and whose temperature difference is equal to the minimum allowable pinch.

8.3 CALCULATION OF HEAT EXCHANGERS IN THERMOPTIM

In ThermoOptim, a heat exchanger is not represented by a particular component, but by a connection established between two “exchange” processes representing the hot and the cold fluids. This way of working has many advantages. In particular, it is possible to design fluid networks at the hydraulic level, to calculate their thermodynamic state, and to thermally connect them only at a later time. For example, when attempting to optimize the design of a network of heat exchangers, it is not necessary to define *a priori* fluid pairings. In addition, it is clear that a heat exchanger aims precisely at linking changes in two fluids, which is consistent with the mode of representation adopted in the package.

We begin by presenting the “exchange” processes, then we show how they can be connected to form a heat exchanger.

8.3.1 “Exchange” processes

An “exchange” process is used to calculate the heating or cooling of a fluid between two states represented by upstream and downstream points.

Its screen (Figure 8.3.1) is similar to that of the compression process, with fewer options. You should refer to the beginning of section 7.1.5 for an overview of the process screens.

The middle-right part displays the following:

- a field that sets the minimum accepted pinch for this fluid. This parameter can be used in sizing heat exchangers;
- an option “pinch fluid method” used to indicate that the process must be taken into account in optimization calculations by thermal integration (see Volume 2 of the reference manual of the software).

Two complementary calculation methods can be chosen according to the option chosen in the bottom right of the screen:

process: type:

energy type: set flow

flow rate (t/s): closed system open system observed

inlet point: m Δh (MW):

T (°C):
P (bar):
h (kJ/kg):
quality:

set volume flow inlet volume flow:
 set molar flow molar flow:
 pinch method fluid minimum pinch:

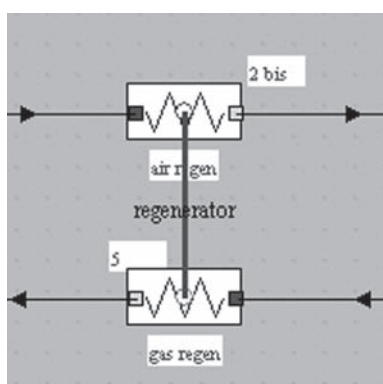
outlet point:

T (°C):
P (bar):
h (kJ/kg):
quality:

Calculate m Δh, the outlet point being known
 Set m Δh and modify the outlet point

FIGURE 8.3.1

Exchange process

**FIGURE 8.3.2**

Exchanger link

- “Calculate $m\Delta H$, the outlet point being known” assesses the enthalpy $m\Delta h$ involved in the process;
- “Calculate $m\Delta H$ and modify the outlet point” recalculates downstream point temperature to ensure that the enthalpy $m\Delta h$ involved in the process is equal to the value entered in the field $m\Delta H$.

8.3.2 Creation of a heat exchanger in the diagram editor

To represent the heat exchanger in the diagram editor, we use non-oriented links connecting two components of type “exchange”.

An “exchange” component has in its center a small maskable exchanger connection port (Figure 8.3.2), which appears (as a small blue or red circle) only when the mouse is located above it, or when it is connected with another such component to represent a heat exchanger.

hot fluid		cold fluid	
name	regenerator	type	unmixed crossflow
fluid	regen gas	fluid	regen air
Thi (°C)	531.75722656	Tci (°C)	375.53164063
Tho (°C)	421.66582795	Tco (°C)	492.70083008
mh	1.01666177	mc	1
Cph	1.12877479	Cpc	1.07826066
m ΔHh	-126.33892703	m ΔHc	126.33892703
constraints	<input type="radio"/> unconstrained <input type="radio"/> minimum pinch <input checked="" type="radio"/> set effectiveness	DTmin: 0 epsilon: 0.75	UA: 4.61443984 R: 0.939593413 NTU: 4.27952167 LMTD: 42.49710486
calculation method	<input checked="" type="radio"/> design <input type="radio"/> off-design		

FIGURE 8.3.3

Heat exchanger screen

To make the connection, click on this port of one component and drag the mouse to the same port of another component and then release the button. During the connection the name of the exchanger is asked for. Once the heat exchanger settings are entered, the port is blue for the cold fluid, and red for the hot one.

A heat exchanger is created in the simulator when an exchanger link exists in the diagram and the two “exchange” components that it connects correspond to two “exchange” processes in the simulator which are sufficiently well defined (it is particularly necessary that their inlet and outlet temperatures are different, that they have been calculated so that the value of Delta H is not zero, and that one is warming while the other cools). By default, the exchanger is initialized with a “counter-flow” type.

8.3.3 Heat exchanger screen

The connection is done in two stages, one for the hot part, and one for the cold part.

The screen (Figure 8.3.3) contains information about the hot fluid in the middle left part, while that for the cold fluid is in the right part. To connect a fluid, if not done in the diagram editor, you must double-click the name field, then choose the process from the list. Besides the values of temperatures, flow rates, heat capacities and enthalpies involved, constraints exist on the temperatures and flow rates used to manage the heat exchanger calculations, allowing one to distinguish between the variables of the problem, those set and those to be calculated.

Possible types of exchangers are: counter-flow, parallel, cross-flow, mixed or not, and multi-pass shell and tube (p-n) (see 8.4.1.1).

In the bottom left, there are three buttons to optionally specify the absence or presence of implicit constraints on temperatures (see below). In the lower right are placed options for defining the calculation method (“design” or “off-design”).

8.3.4 Simple heat exchanger design

A heat exchanger connects two «exchange» processes. One of them is a hot fluid which corresponds to a substance that gets colder, while the other is a cold fluid that gets hotter. Once the

coupling of the processes is made, the design problem is the following: it is necessary on the one hand to conserve enthalpy in the heat exchanger, and on the other hand to respect some temperatures constraints.

Given that there are four temperatures (two for each fluid) and two flow rates, the problem has five degrees of freedom once the enthalpy is conserved. One can furthermore show that at least one of the two flow rates has to be set, otherwise the problem is indeterminable.

For temperatures, one can either set explicit constraints (for example the fluid inlet temperatures), or implicit constraints (the value of the heat exchanger effectiveness, or the pinch minimal value). To set an effectiveness value, enter it in the ϵ field, and click on button «set effectiveness». To set a «minimal pinch», click on the corresponding button. The minimal pinch value is initialized, when the heat exchanger is created, or when one double-clicks in this field, with a value equal to the half sum of the minimum pinches defined in both hot and cold processes (see section 8.3.1).

For the problem to have a solution, it is necessary to set a total of five constraints, among which there is a flow rate. If one of them is implicit (effectiveness or minimal pinch), four have to be explicit (3 temperatures and 1 flow rate, or 2 temperatures and 2 flow rates), or otherwise all five have to be explicit (a single flow rate or a single temperature is free). These conditions are necessary, but not sufficient. This is why the software analyzes all the constraints proposed. If there is a solution, it is found. Otherwise, a message tells the user that the calculation is impossible.

PRACTICAL APPLICATION

Practical design of a heat exchanger

Several examples of practical design of heat exchangers are given in the book or in the portal, showing how this section can be put in practice:

- The condenser of the steam power plant Thermoptim modeling example is designed in two alternative ways, by setting either a minimum pinch or a given effectiveness (section 9.1.7 of this Part);
- The internal exchanger of a regenerative gas turbine is sized in Diapason session S23En;
- The design of the three part heat exchanger coupling a gas turbine to a steam cycle to form a single pressure combined cycle is explained in Diapason session S41En;
- The detailed technological design of a tube and fin heat exchanger used to cool compressed air before storing it is presented in section 38.2.1 of Part 5.



[CRC_pa_4]

One can note that the design of heat exchangers is always made with the implicit hypothesis that thermophysical properties of the fluids remain constant in the heat exchanger, but this hypothesis is not made during the calculation of the processes. Therefore, when one recalculates a temperature on the basis of heat exchanger equations, slight differences may exist between the values displayed on the heat exchanger screen and that of the corresponding processes, or between the values of the enthalpies involved in both hot and cold fluids. If a high accuracy is required, one may have to make first a heat exchanger design calculation, then iterate. Convergence is obtained quickly. Also note that if one of the two flow rates is not set in the exchanger, it is recalculated, even if the corresponding process is “set flow”.

When a heat exchanger is designed, one of the flow rates being calculated, that of the exchange process is recalculated, as well as those of the processes located upstream as long as they are directly connected. The propagation stops when a node or a combustion process is encountered.

8.3.5 Generic liquid

Let us recall that a particular substance called «generic liquid» exists in the database. It is a liquid at atmospheric pressure, whose specific heat is equal to 1 kJ/kg/K. It can be used to simulate any liquid not included in ThermoOptim that one wants to use in a heat exchanger.

Indeed, in the energy equations used for calculating heat exchangers, the flow rate \dot{m} and the specific heat c_p always appear by their product $\dot{m}c_p$, called the heat capacity rate. Therefore, if c_p is set equal to 1, the value which is displayed in the flow rate field of the heat exchanger screen is that of the product $\dot{m}c_p$.

Instead of entering in the database a large number of different liquids, it is thus possible to make use of a single one: the generic liquid.

Suppose that you want to study a liquid whose specific heat is $c_{p\text{liq}}$. If the liquid flow rate is set to \dot{m}_{liq} , enter in the exchange process flow rate field the value ($\dot{m}_{\text{liq}} \cdot c_{p\text{liq}}$). Set the other constraints and calculate the heat exchanger.

If the liquid flow rate is to be calculated, set the other constraints and calculate the heat exchanger. The value of the liquid flow rate will be equal to the value returned by ThermoOptim in the flow rate field, divided by $c_{p\text{liq}}$.

The introduction of external substances limits, however, the interest in using the generic liquid. Indeed, it is relatively easy to model the thermodynamic behavior of a liquid (see Chapter 23 of Part 4), so that adding a new liquid can be done relatively simply, and allows one then to study with more precision and increased ease of interpretation the cycles which it is put in.

8.3.6 Off-design calculation of heat exchangers

A behavioral model of a heat exchanger must answer the following question: how does the exchanger adapt when its input variables are changed? These are its inlet temperatures T_{hi} and T_{ci} and mass flows \dot{m}_h and \dot{m}_c passing through. A behavior model should determine outlet temperatures T_{ho} and T_{co} of both fluids based on these four input variables. There are two more unknowns than for the sizing problem, but the heat exchanger being selected, we know its area A .

Chapter 35 of Part 5 specifically addresses this issue. In this section we content ourselves with some elementary remarks.

To have a behavior model, we must give a law $U = U(T_{hi}, T_{ci}, \dot{m}_h, \dot{m}_c)$.

With equation (8.1.5) and analysis of section 8.1.4 we can write:

$$\frac{1}{U} = \frac{1}{h_h} + \frac{e}{\lambda} + \frac{1}{h_c}$$

$Nu = k Re^a Pr^b$ with $Nu = h d_h/\lambda$, $Re = \dot{m}/\mu$, $Pr = \mu C_p/\lambda$

To take into account changes in exchange coefficients h in off-design operation, we can make a number of assumptions:

- neglect the resistance by conduction through the wall;
- when the fluids are of the same type (gas, liquid or biphasic), either equally distribute the resistances between the hot and cold sides, or ask the user to provide a method for allocating them;
- neglect the liquid or two-phase side resistance in the presence of a gas;
- neglect the two-phase side resistance in the presence of liquid.

In relating the current values to design values, marked by index d , each h value is expressed in the general case, in the form:

$$\frac{h}{h_d} = \left(\frac{\lambda}{\lambda_d} \right)^{1-b} \left(\frac{\dot{m}}{\dot{m}_d} \right)^a \left(\frac{\mu}{\mu_d} \right)^{b-a} \left(\frac{C_p}{C_{p_d}} \right)^b \quad (8.3.1)$$

For gases, Pr is approximately constant, and this expression simplifies:

$$\frac{h}{h_d} = \left(\frac{\lambda}{\lambda_d} \right) \left(\frac{\dot{m}}{\dot{m}_d} \right)^a \left(\frac{\mu}{\mu_d} \right)^{-a} \quad (8.3.2)$$

Recall that, typically, we have: $0.5 \leq a \leq 0.8$ and $0.33 \leq b \leq 0.4$ and also that polynomial expressions of λ , μ and C_p as a function of temperature can be found in the literature.

It is generally verified and assumed that the thermal resistance of the wall of the exchanger e/λ can be neglected. Then equations (8.1.5) and (8.3.1) or (8.3.2) combine to form, exponent' corresponding to the correlation for the cold fluid:

$$\frac{1}{U} h_{hd} \left(\frac{\lambda_h}{\lambda_{hd}} \right)^{b-1} \left(\frac{\dot{m}_h}{\dot{m}_{hd}} \right)^{-a} \left(\frac{\mu_h}{\mu_{hd}} \right)^{a-b} \left(\frac{C_{p_h}}{C_{p_{hd}}} \right)^{-b} + h_{cd} \left(\frac{\lambda_c}{\lambda_{cd}} \right)^{b'-1} \left(\frac{\dot{m}_c}{\dot{m}_{cd}} \right)^{-a'} \left(\frac{\mu_c}{\mu_{cd}} \right)^{a'-b'} \left(\frac{C_{p_c}}{C_{p_{cd}}} \right)^{-b'} \quad (8.3.3)$$

As can be seen, U depends in a fairly complex way on the exchanger input variables, including flow rates.

If, for simplicity, we neglect the influence of temperature, it becomes:

$$\begin{aligned} \frac{1}{U} &= h_{hd} \left(\frac{\dot{m}_h}{\dot{m}_{hd}} \right)^{-a} + h_{cd} \left(\frac{\dot{m}_c}{\dot{m}_{cd}} \right)^{-a'} \\ U &= \frac{h_{hd} \left(\frac{\dot{m}_h}{\dot{m}_{hd}} \right)^{-a} h_{cd} \left(\frac{\dot{m}_c}{\dot{m}_{cd}} \right)^{-a'}}{h_{hd} \left(\frac{\dot{m}_h}{\dot{m}_{hd}} \right)^{-a} + h_{cd} \left(\frac{\dot{m}_c}{\dot{m}_{cd}} \right)^{-a'}} \end{aligned} \quad (8.3.4)$$

However, in the literature, laws generally used are much simpler, probably because the identification of the parameters of equation (8.3.4) cannot be made by linear regression. These laws ignore the influence of temperature and consider only that of the flow:

$$U \approx C[\dot{m}_h]^n [\dot{m}_c]^m \quad (8.3.5)$$

Given the differences in form between these two equations, we recommend great caution when using the second.

(ϵ , NTU) models can thus be used as global models: for a given heat exchanger, if one knows the NTU (or UA) evolution law based on flow rates of the two fluids passing through the exchanger, a (ϵ , NTU) model determines the evolution of ϵ when the operating conditions of the heat exchanger vary.

In ThermoOptim the “off-design” calculation mode allows one to calculate in a simplified manner off-design operation of the heat exchanger by the NTU method. In this case, the software considers that the four input variables of the exchanger are set. No correction is made on the exchange

coefficients, but it is possible to modify by hand the UA value in the exchanger screen, if we assume a law of evolution such as equation (8.3.4) or (8.3.5).

All off-design operation procedures apply to the study of a **pre-designed heat exchanger**. Let us also recall that, to use the NTU method, we implicitly make the hypothesis that the thermophysical properties of the fluids remain constant in the heat exchanger.

The procedure updates the component inlet links, starting from the exchange processes, then calculates the outlet temperatures, and balances the heat exchanger at the enthalpy level. Points and processes associated with the component are updated as a function of the results.

8.3.7 Thermocouplers

Thermocouplers complete heat exchangers by allowing components other than exchange processes to connect to one or more exchange processes to represent a thermal coupling. This mechanism does not encompass the exchanger mechanism: two exchange processes cannot be connected by a thermocoupler.

This mechanism has a number of benefits, because it can be used to represent many thermal couplings that do not constitute a heat exchange in the traditional sense, like for example cooling the walls of the combustion chamber of a reciprocating engine, cooled compression, and above all supply or removal of heat from multi-functional external components.

Figure 8.3.4 is an illustration of this: an absorption refrigeration cycle, whose absorption-desorption system is defined and integrated in an external process, is fed with steam that exits the evaporator then enters the condenser. This cycle involves the mixture LiBr-H₂O, whose properties are modeled either directly in the external process, or in an external substance, and requires high temperature heat supply to the desorber and medium temperature heat removal from the absorber. The representation of these heat exchanges is possible thanks to the thermocoupler mechanism: the external process calculates the thermal energies that must be exchanged, and the thermocoupler recalculates the corresponding “exchange” process, which updates its downstream point.

process: absorber-generator type: external

energy type: other set flow

inlet point: 1 flow rate: 0.93

m Δh: 74.74

closed system open system observed

outlet point: 2

LiBr absorption

absorber temperature (°C)	39.000
desorber temperature (°C)	102.646
solution exch. efficiency	0.654
absorber load	-2995.417
desorber load	3069.364
Rich solution fraction	0.404
Poor solution fraction	0.354
Rich solution flow	12.002
Poor solution flow	11.072
reference	

absorber desorber

FIGURE 8.3.4

Absorber-generator screen

The types of thermocouplers used by an external component appear in the lower right hand corner of the screen. Double click on one of the types to open the screen of the corresponding thermocoupler.

Given that thermocouplers are a type of heat exchanger, it is valuable as stated in section 8.3.1 to define them by values such as effectiveness ε , UA, NTU or LMTD, that can be calculated using similar equations. The component sends to each of its thermocouplers the equivalent values for flow rates, inlet and outlet temperatures and thermal energy transferred, which they must take into account in their calculations. Specific methods are provided in the external class code and are not user-modifiable.

However, there are limits to the similarities with exchangers: for example, temperature cross-overs unacceptable in an exchanger may occur in a thermocoupler, leading to absurd values.

So it is best to transmit values that are unlikely to lead to this type of situation. One possible solution is to assume that the thermocoupler is isothermal for calculations of characteristics that are similar to exchanger characteristics. For example, a combustion chamber may be assumed to be at mean temperature between its upstream and downstream points when calculating the cooling. This assumption is not absurd and may prevent a temperature crossover between the cooling fluid and the gases that cross the component.

In the case of the absorption machine presented above, we assumed that the absorber and desorber were isothermal.

The absorber thermocoupler screen is given Figure 8.3.5. If we had not taken the temperature of the absorber as a reference for the exchange calculations, keeping the temperatures of the steam entering and exiting the external process, we would have ended up with a temperature crossover.

For external processes that accept several thermocouplers and for external nodes, the potential complexity of the calculations prevents the exchange process from driving the thermocoupler. Its thermal load is always set by the external component. This is why there are fewer options for calculating a thermocoupler than for a heat exchanger: the user can only choose between calculating the outlet temperature of the exchange process (at a given flow rate) and the flow rate, when the temperature is known.

FIGURE 8.3.5

Thermocoupler screen

Note that on the thermocoupler screen, the external component fluid can be selected as a pinch fluid and a minimum pinch value can be entered (see optimization method, Chapter 22 of Part 3).

Finally, note that the off-design calculation method is not available for thermocouplers, as their behavior can deviate significantly from that of a conventional heat exchanger.

8.4 TECHNOLOGICAL ASPECTS

There are a wide variety of heat exchangers developed to solve different problems. Capacities range from a few watts (electronics) to several hundred megawatts (condensing power plants). Uses relate as well to industry as to the residential and tertiary sectors, agriculture and transport. The temperature range varies from a few Kelvin for cryogenic applications to over 1000°C for some applications. The materials are usually metal, but also plastic or ceramic. Among the common configurations the following can be distinguished.

8.4.1 Tube exchangers

These are cheaper and thus more widespread. Among them, two categories are particularly used for energy applications: the shell and tube exchangers, and air coils.

8.4.1.1 Shell and tube exchangers

Very robust and economical, they are particularly used for liquid-liquid or liquid-vapor exchange (Figure 8.4.1). In the energy field, applications of this type of exchanger are numerous (hot gas heat recovery, evaporator and condenser of refrigeration machines etc.) A bundle of parallel tubes is welded or bolted at both ends to thick perforated plates and traversed by one of the two fluids, while the other flows outside the tubes, in different modes depending on the type of exchanger. At both ends, boxes distribute or collect the fluid that passes inside the tubes while a shell, usually cylindrical, ensures the confinement of the other fluid. The tubes may be arranged in a triangular or square pitch, the second being more compact and better in terms of heat exchange, but more

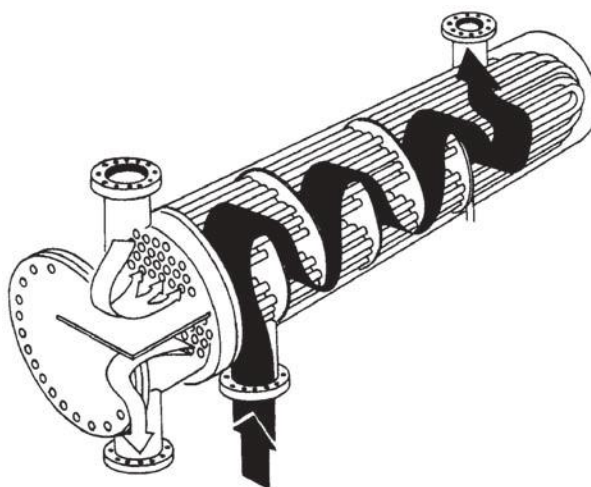


FIGURE 8.4.1

Shell and tube heat exchanger (courtesy Techniques de l'Ingénieur — Génie énergétique)

difficult to clean. These exchangers are called (p, n), figure p representing the number of passes of the fluid outside the tubes, and figure n the number of passes of the fluid inside the tubes.

Technologically, the disadvantages of these exchangers are first that they represent a non-evolutive geometry, second that they can be difficult to clean, and finally that they are unsuitable if the temperature difference between the two fluids exceeds 50 K, due to differential expansion induced.

8.4.1.2 Air coils

Finned heat exchangers, called air coils, or just coils, are used when a fluid is a gas and the other a liquid or a fluid being vaporized or condensed. An example of a cooling coil is given in Figure 7.8.6. In these exchangers, the gas side convective coefficients are much smaller than others, and the addition of fins increases the exchange surface and thus thermally balances the heat exchanger (Figure 8.4.2).

8.4.2 Plate heat exchangers

They are composed of embossed plates of various profiles, in which the two fluids exchanging heat pass alternately. They have a variable but highly developed exchange surface, which enables a very compact design (Figure 8.4.3).

More expensive than tubular heat exchangers, they offer better exchange coefficients and can (for those which are not welded but gasketed) be modified by changing the number of plates, making them scalable.

Plate-fin heat exchangers (Figure 8.4.4) are a variant with extended surfaces primarily used for gas-gas heat transfer. Corrugated fins are placed between plates in order to enhance heat transfer and give stiffness.

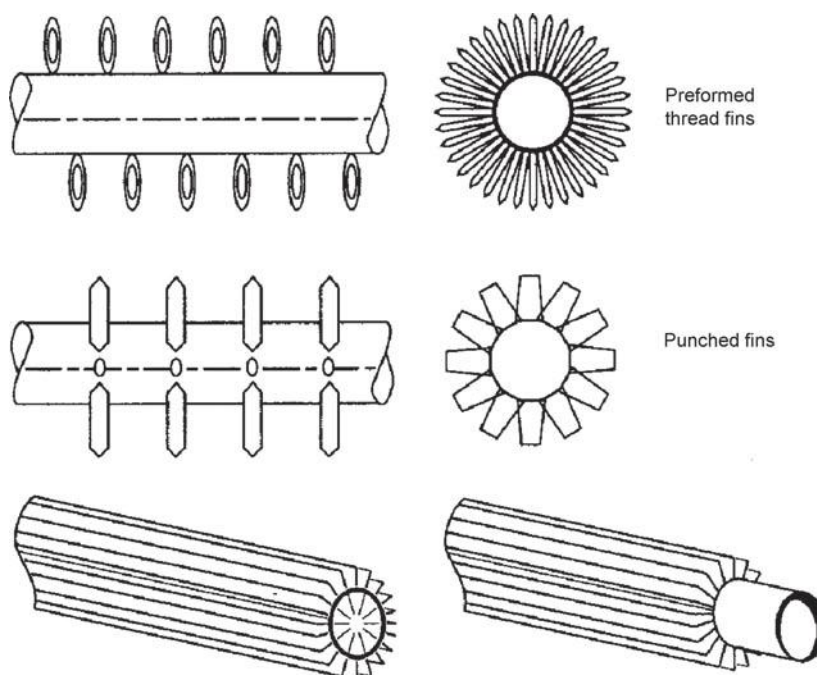


FIGURE 8.4.2

Examples of fins (courtesy Techniques de l'Ingénieur — Génie énergétique)

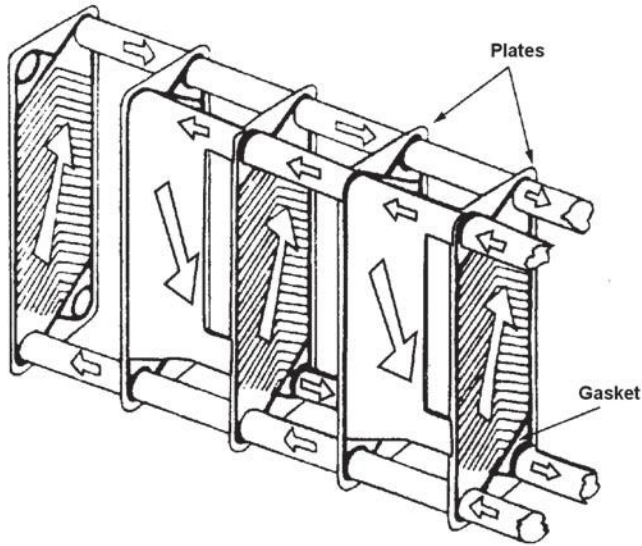


FIGURE 8.4.3
Plate heat exchanger (courtesy Techniques de l'Ingénieur — Génie énergétique)

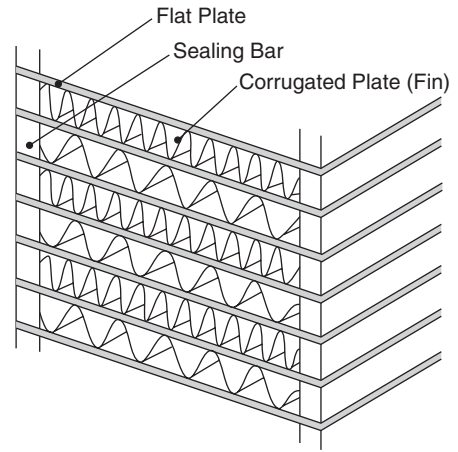


FIGURE 8.4.4
Plate-fin heat exchanger, Extract from (Kakac & Liu, 2002), with permission

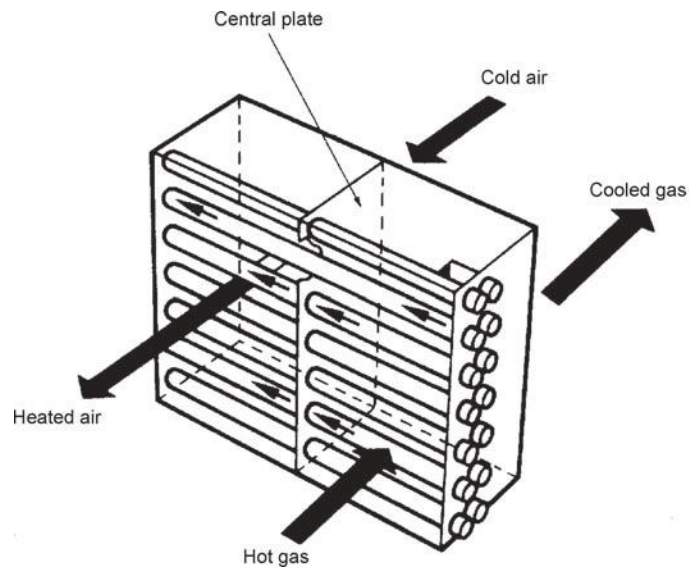


FIGURE 8.4.5
Heat pipe (courtesy Techniques de l'Ingénieur — Génie énergétique)

8.4.3 Other types of heat exchangers

There are many other types of heat exchangers, but they are little used for energy conversion, so we will not detail them. Let us include as a reminder heat pipe exchangers (Swanson, 2000), (Figure 8.4.5), often used between two gas flows but also very expensive, or regenerator rotary or static exchangers (Figure 7.8.9), where the two fluids exchange heat through a solid matrix.

8.5 SUMMARY

A heat exchanger can be modeled by the number of transfer units NTU method. While it is perfectly appropriate for studying the insertion of a heat exchanger in a thermodynamic cycle, such a phenomenological model, however, only gives access to the heat exchanger UA product, while the assessment of U can be particularly complex, as explained Chapter 35 of Part 5. The success of this model is such that it is often used as a behavior model for a particular heat exchanger by adding a UA evolution law, function for example of fluid flows through the exchanger.

REFERENCES

- Bontemps et al, *Technologie des échangeurs thermiques*, Techniques de l'Ingénieur, GRETh, ISBN 2-85059-003-07, Paris, 1998.
- F. P. Incropera, D. P. Dewitt, *Fundamentals of heat and mass transfer*, 4th Edition, John Wiley and Sons, 1996.
- S. Kakac, H. Liu, *Heat exchangers, Selection, rating, and thermal design*, 2nd edition, CRC Press, Boca Raton, 2002, ISBN 0-8493-0902-6.
- W. M. Kays, A. L. London, *Compact Heat Exchangers*, Mac Graw Hill, 1984.
- R. K. Shah, K. J. Bell, *Heat exchangers, The CRC handbook of thermal engineering*, (Edited by F. Kreith), CRC Press, Boca Raton, 2000, ISBN 0-8493-9581-X.
- L. W. Swanson, *Heat pipes, The CRC handbook of thermal engineering*, (Edited by F. KREITH), CRC Press, Boca Raton, 2000, ISBN 0-8493-9581-X.

FURTHER READING

- B. Pierre, *Dimensionnement des échangeurs de chaleur*, Revue Générale de Thermique, Paris, n° 260–261 Août-septembre 1983.
- E. M. Smith, *Thermal design of heat exchangers, a numerical approach*, Wiley, Chichester, 1997.

This page intentionally left blank

Examples of Applications

Abstract: In previous chapters, we explained how operate the various components involved in energy technologies, we established key relationships that allow one to calculate their performance and we presented the corresponding Thermoptim screens.

We now have all the elements to start studying complete systems, considered as assemblies of these components. Without wishing to spoil the contents of Part 3 that will be devoted to a detailed study of thermal plants and machinery (engines, refrigeration machines, air conditioning), we will show in this chapter how to implement the results we obtained.

Therefore, in this section, we present some simple examples of how energy technologies can be described and calculated in Thermoptim.

We will consider:

- a steam power plant cycle, simple at first, then with some improvements;
- a single-stage refrigeration cycle;
- the cycle of a gas turbine similar to that presented in the introduction;
- an air conditioning installation.

The three former have been qualitatively analyzed in Chapters 2 and 3 of Part 1, to which you may refer. Plots of these cycles in the $(h, \ln(P))$ and (T, s) entropy charts are discussed in particular.

Before you start entering models in Thermoptim, we recommend you to study Diapason initiation session S07En_init¹ which introduces all the software concepts needed.

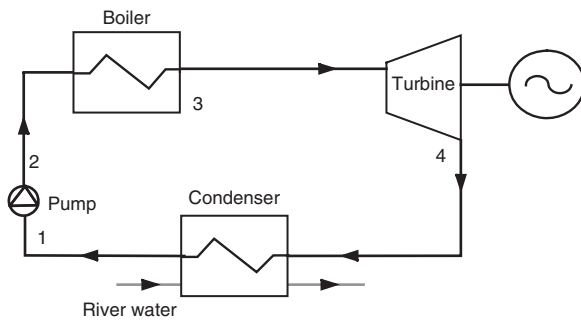
Keywords: steam power plant, refrigeration, gas turbine, air conditioning, HVAC.

9.1 STEAM POWER PLANT CYCLE

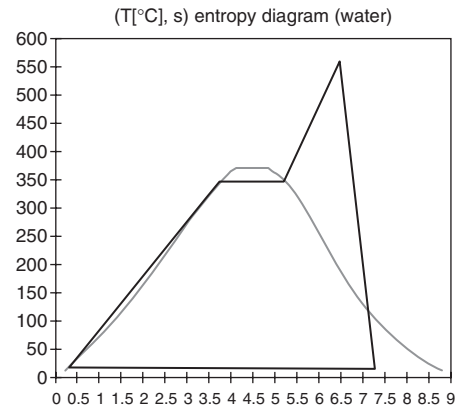
9.1.1 Principle of the machine and problem data

Let us recall (section 2.1.1 of Part 1) that the basic cycle of a steam power plant is essentially a boiler where the fuel (solid, liquid or gas) is burned for generating steam (usually superheated) which is then expanded in a steam turbine whose shaft provides the motor work (Figures 9.1.1 and 9.1.2).

¹http://www.thermoptim.org/sections/enseignement/cours-en-ligne/seances-diapason/session-s07en_init-first

**FIGURE 9.1.1**

Sketch of a steam power plant

**FIGURE 9.1.2**

Steam power plant cycle in an entropy chart

The steam leaving the turbine is completely liquefied to water in a condenser before a pump restores the boiler pressure. Since water is compressed in the liquid state, the compression work is almost negligible compared to the work recovered on the turbine shaft.

This is an external combustion cycle, allowing use of a variety of fuels (including uranium). In most countries, over 90% of the stock of thermal power plants was until recently composed of this type.

In this example the flow rate of liquid water is 1 kg/s. Point 1 state is: temperature of approximately 20°C and low pressure (0.023 bar). A pump, whose isentropic efficiency is assumed equal to 1, pressurizes water at 195 bar (point 2).

The pressurized water is then heated (at constant pressure) in a flame boiler (fuel-oil, coal, natural gas). The heating is comprised of three steps:





- heating of the liquid water in the economizer from 20°C to approximately 355°C, boiling point temperature at 195 bar: process (2-3a) on the entropy chart;
- vaporization at constant temperature 355°C in the vaporizer: process (3a-3b);
- superheating from 355°C to 590°C in the superheater: process (3b-3).

The vapor is then expanded in a turbine whose isentropic efficiency is equal to 0.85 until the pressure of 0.023 bar is reached: process (3-4). The liquid-vapor mix is finally condensed in liquid water in a condenser. The cycle is thus closed.

9.1.2 Creation of the diagram

Run ThermoOptim. The Diagram Editor screen is displayed (Figure 9.1.3).

It has a palette with the various components available (heat exchanges, compressors, turbines, combustion chambers, mixers, dividers, external components etc.), and a working panel where these components are placed and interconnected by links.

The diagram of the steam plant unambiguously indicates which components should be selected: the pump, which is a type of compressor , the boiler, which is actually represented here by three processes of the exchange type , to distinguish the different heating phases of water (in the economizer, the vaporizer and the superheater), the turbine, which is an expansion device  and the condenser, which is of exchange type .

To represent the feedwater pump, select a compressor component on the palette and place it on the editor by clicking the crosshair cursor at the appropriate location. A property editor is opened (Figure 9.1.4). Name the compressor “pump”.

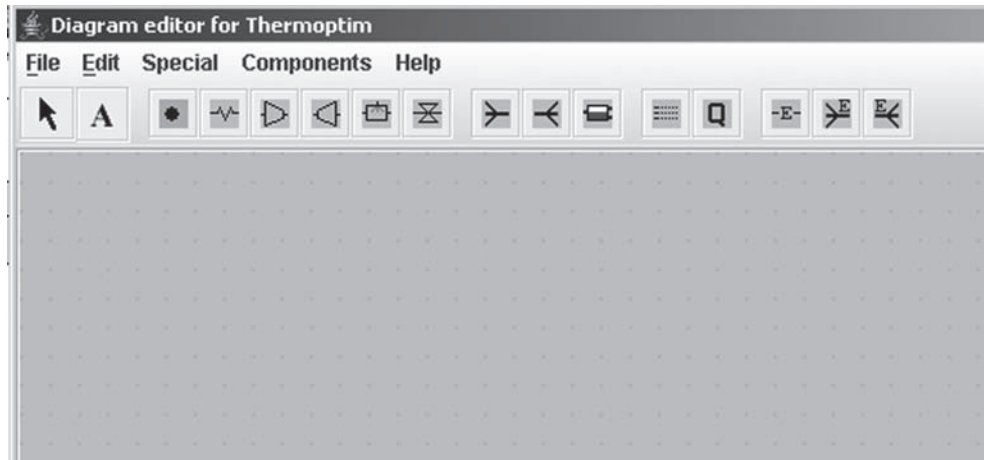
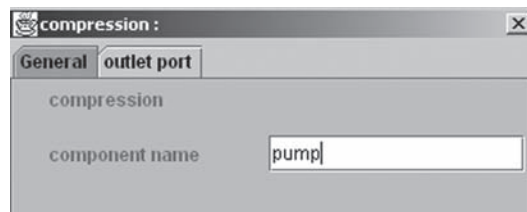
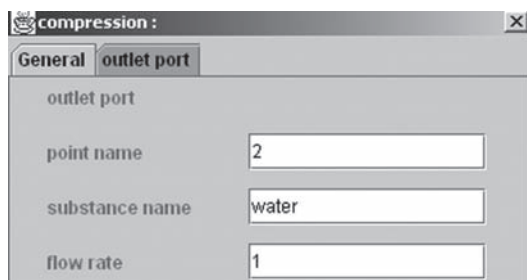
**FIGURE 9.1.3**

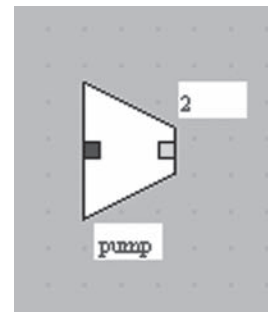
Diagram editor

**FIGURE 9.1.4**

Property editor

**FIGURE 9.1.5**

Outlet port settings

**FIGURE 9.1.6**

Pump

Then click on the “outlet port” tab (Figure 9.1.5). Name the point “2” and enter the substance name “water”. By default, the flow rate is set to 1 which is appropriate here. Then click the button “Apply” to validate the two tabs. The component appears on the screen (Figure 9.1.6).

Similarly create three exchange components corresponding to the economizer (outlet point 3a), the evaporator (outlet point 3b), and the superheater (outlet point 3), one expansion component corresponding to the turbine (outlet point 4), and one exchange component corresponding to the condenser (outlet point 1). In all cases, the substance is water. You get for example the result in Figure 9.1.7.

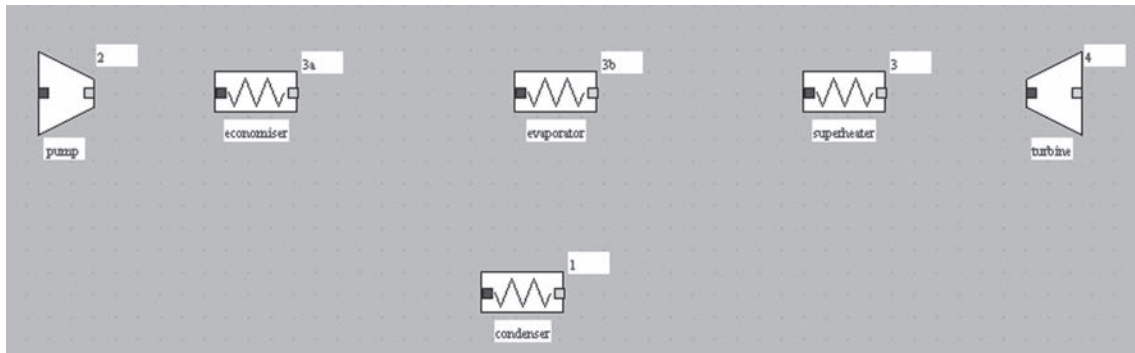


FIGURE 9.1.7

Diagram without links

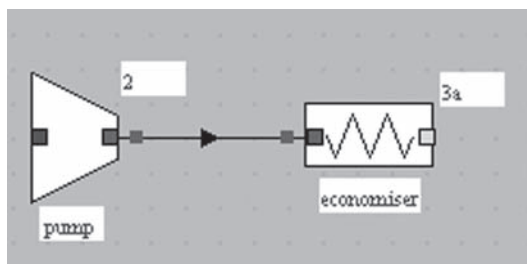


FIGURE 9.1.8

Connected components

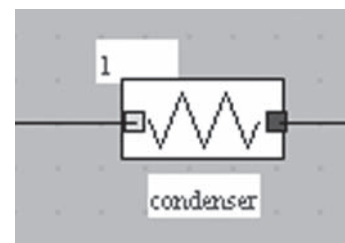


FIGURE 9.1.10

Component oriented to the left

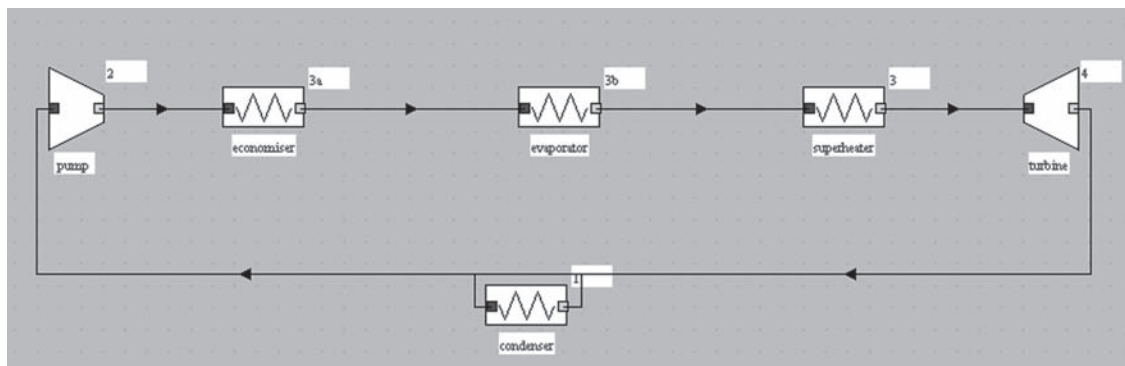


FIGURE 9.1.9

Diagram with links

To connect the components, click on the green outlet port of one of them (e.g. the pump). The cursor becomes a crosshair and a line extends from the port if you drag the mouse. Drag the cursor to the blue inlet port of the destination component (e.g. the economizer) while keeping the mouse clicked, and release the mouse. A link is established (Figure 9.1.8). Proceed similarly for all components. You obtain the result of Figure 9.1.9.

By default, all components are oriented from the left to the right. When a loop appears in a diagram, it is convenient to orient some components from the right to the left. Here, you can change the condenser orientation by selecting it and clicking the item “flip vertical” on the Edit menu or by typing F1. You obtain the diagram of Figure 9.1.10.

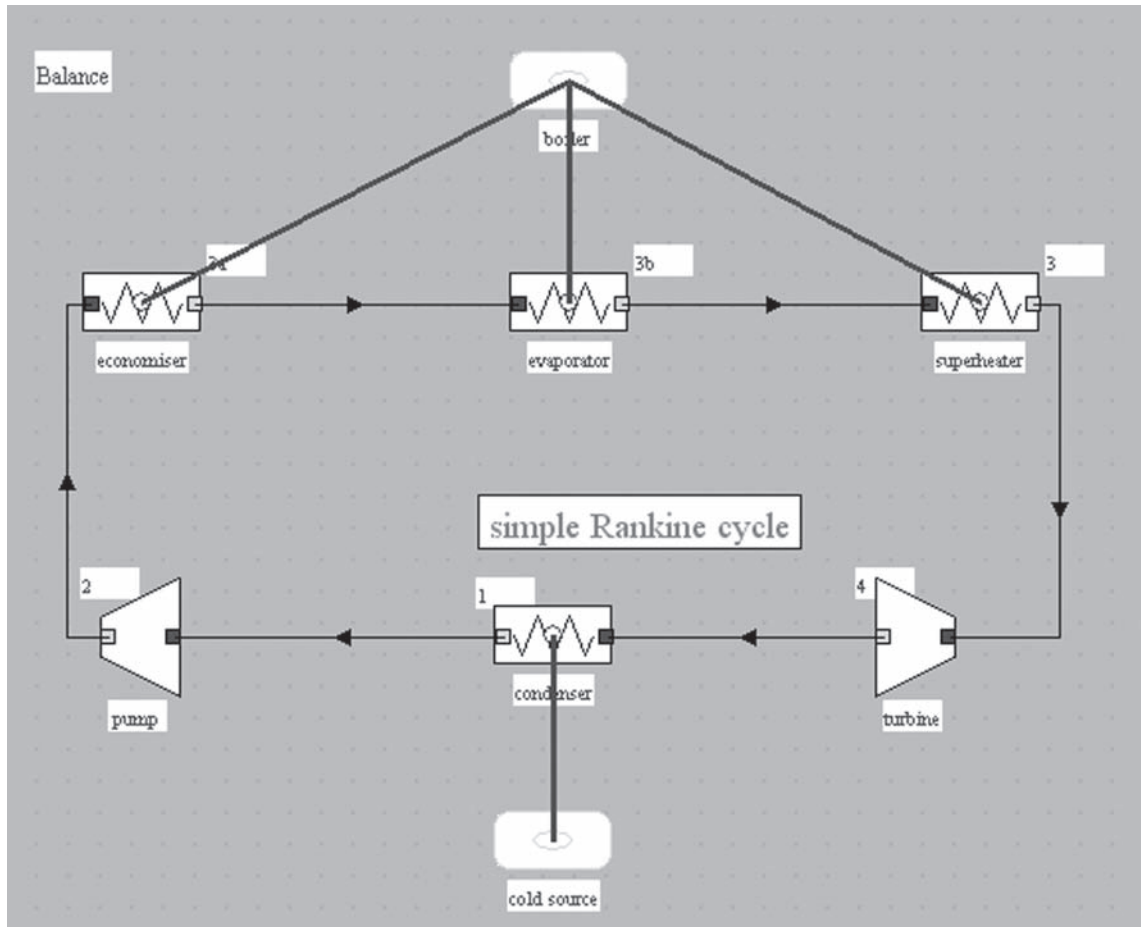



FIGURE 9.1.11

Final layout of the cycle

name	<input type="text" value="steam cycle"/>
Description	<input type="text" value="basic steam cycle for getting started with Thermoptim"/>

FIGURE 9.1.12

Diagram description frame

In order to improve the diagram appearance, you can add a text, two “external source” type components , one for the boiler, and the other one for the cold source, as well as a “Balance” type component which allows you to display the balance values. Thus, the enthalpies exchanged with the external sources can be shown. The result is given in Figure 9.1.11 (a title has been added to the diagram).

At this stage, the qualitative description of the cycle is complete. To facilitate archiving of your diagrams, you can associate a name and description, by selecting the line “Description” of menu File (Figure 9.1.12).

Then save your diagram by giving it a name with the extension .dia: “steam1.dia” for example.

By connecting the components, you spread some information from upstream to downstream, so that all names and substances of the input ports are automatically initialized as you can verify by selecting a component and displaying its properties (F4 or Edit menu).

The spread of substance names and flow rates is automatic when connecting components representing simple processes. It is thus not necessary to enter them during the initial definition of components that are subsequently connected downstream of another process.

Note that, to enter the substance name, you may either type it if you know it, or get it from the list of substances available in the database which can be displayed by double-clicking in the substance name field and expanding the list, in which case you choose the one you want.

9.1.3 Creation of simulator elements

To create the elements of the simulator, the easiest and most secure way is to use the diagram/simulator interface that can be opened from the Special menu. Then click the button “Update the element table.” The screen is shown in Figure 9.1.13.

The list of transferable elements is displayed in a table, and the user can select those he wishes to create or update. In front of each, an “X” marks the box “Diagram”, while the box “simulator” is empty. The right column shows which components are selected, that is to say which should be taken into account during operations conducted from the interface. By default, all components are selected, but a button allows you to deselect them all if you wish. Otherwise, by double-clicking a row in the table, you select it or not.

To transfer all the simulator components, click the button “Update the simulator from the diagram”. You are requested to name the project. Enter e.g. “steam cycle”. Once the transfer is complete, the project screen (Figure 9.1.14) appears.

Six processes and six points have been created with a default setting (1 bar and 300K). To finish creating the model, you must now open each screen of points and processes created, and set them. You can do that either from the simulator project screen, or from the diagram editor by double-clicking on components to access the processes, and on links to access points (you can also open them from the process screens).

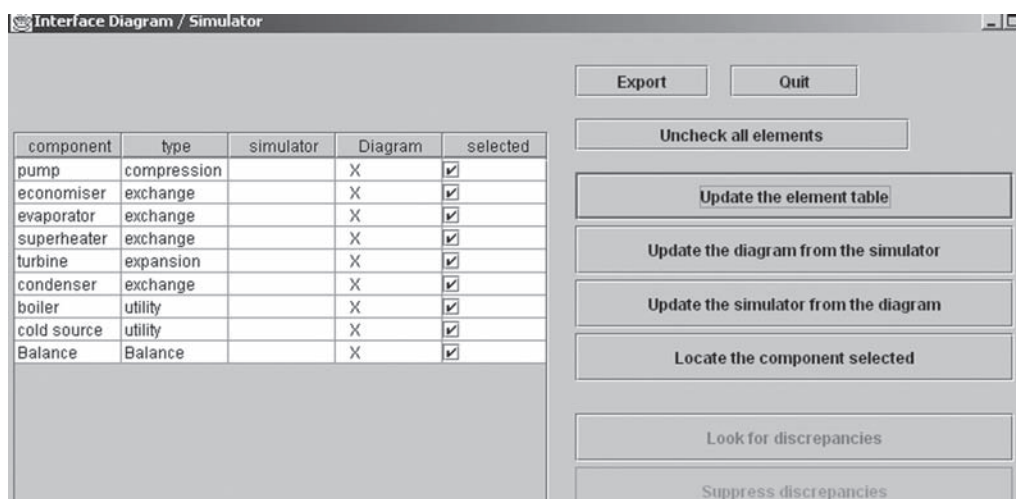


FIGURE 9.1.13

Diagram – simulator interface

9.1.4 Setting points

Enter the point 1 substance state (Figure 9.1.15). Its pressure is known (0.023 bar), and it is in the liquid state at the saturation temperature. To find its temperature, click on “set the saturation temperature”. The other intensive variables can then be calculated by clicking the button “Calculate” (by default, the quality is set to 0, which corresponds to the liquid state).

Point 1 is now set.

For point 2, indicate the only information known about it, its pressure $P = 195$ bar. Currently both its temperature and its enthalpy are not known.

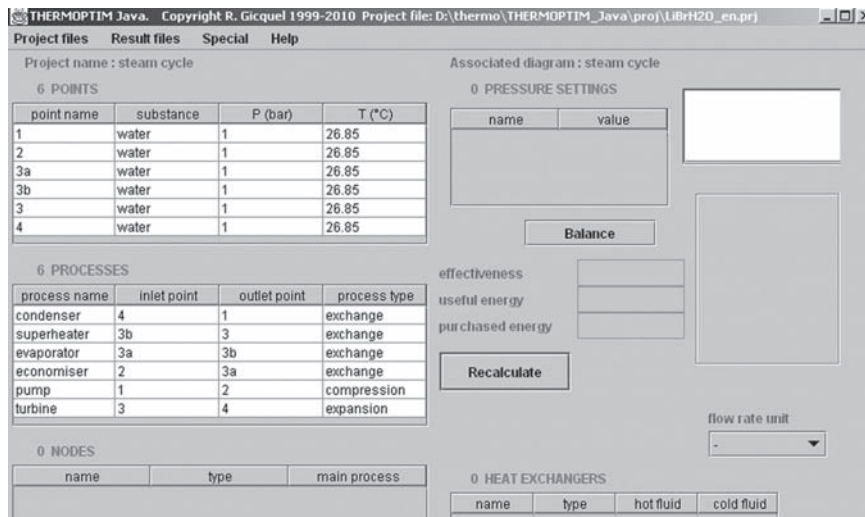


FIGURE 9.1.14

Simulator screen

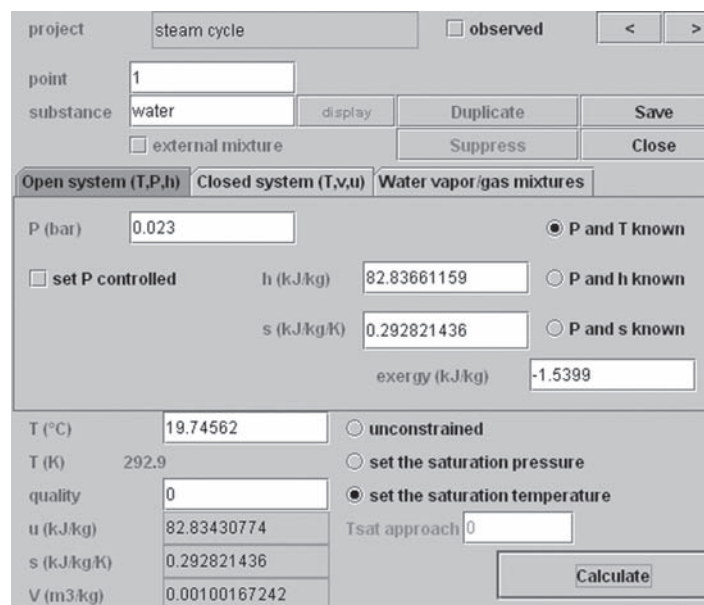


FIGURE 9.1.15

Point screen

process: pump type: compression

energy type: useful set flow

flow rate: 1 closed system open system observed

inlet point: 1 m Δh: 16.46

T (°C): 19.74562 Q: 0

P (bar): 0.023 adiabatic non adiabatic

h (kJ/kg): 82.84 isentropic reference polytropic reference

quality: 0

isentropic eff.: 1

outlet point: 2 polytropic exponent: 1,214.28069

T (°C): 20

P (bar): 165 compression ratio (>= 1): 7,173.91 calculated set

h (kJ/kg): 99.3

quality: 0

Set the efficiency and calculate the process
 Calculate the efficiency, the outlet point being known

FIGURE 9.1.16

Pump screen

For point 3a enter 195 bar corresponding to the beginning of vaporization. To do that, enter the pressure, and set the saturation temperature and the quality equal to 0. As the point 3a state is totally defined, the other variables can be calculated.

Similarly, point 3b can be defined as being at pressure 195 bar, at the saturation temperature and its quality is equal to 1. Point 3 is at 833.15 K (590°C) and 195 bar. It can also be calculated.

The last point to define is point 4. Only its pressure is known: 0.023 bar.

9.1.5 Setting of processes

Start for example with liquid compression between points 1 and 2 (Figure 9.1.16).

You have the choice between four modes of compression: adiabatic or polytropic, for open systems or for closed systems. For the first ones, the compression ratio is that of pressures, for second ones, that of volumes. It can be either calculated, as it is the case here, where the outlet pressure is known, or set, in which case the latter is calculated from the inlet pressure.

You can select two calculation modes. In the first case (“Set the efficiency and calculate the process”), the outlet point state is calculated from that of the inlet point and the efficiency value. For the second one (“Calculate the efficiency, the outlet point being known”), the efficiency value is calculated on the basis of both inlet and outlet points considered as set. Choose here the first case, which is selected by default.

Make your selection by clicking on the appropriate options, and enter the efficiency value (isentropic or polytropic) for compression. In the present case, the inlet point is liquid, and only ideal compressions are modeled for liquids, except for water. Choose here: isentropic, isentropic efficiency equal to 1, and open systems.

Point 2 state is calculated with the corresponding enthalpy change. The value of the compression ratio is shown (about 7174).

For the economizer (3-3a), the vaporizer (3a-3b), and the superheater (3b-3), the upstream and downstream point states are known and the calculation is very simple. Just make sure that the method of calculation (bottom right corner) is “Calculate m ΔH, the outlet point being known” and click “Calculate”. Moreover, since the boiler is the energy injected into the cycle, choose “purchased” for the type of energy at the top left of the screen (the default value is “other”).

FIGURE 9.1.17

Turbine screen

Balance	
effectiveness	0.3897
useful energy	1,310
purchased energy	3,360

FIGURE 9.1.18

Balance

You can now set the expansion (3-4). The screen that is presented (Figure 9.1.17) is like the one for compression. Choose the type of expansion (here adiabatic of isentropic efficiency 0.85), and calculate the process. The exact state of point 4 and the enthalpy of expansion are then determined.

Calculate the condenser, as you did for the other “exchange” processes.

At this stage, the cycle is totally defined, and you can calculate the balance by clicking the “Recalculate” button in the simulator screen (Figure 9.1.18).

The energy purchased, useful energy, and the cycle efficiency are then determined. Save it in a file with extension .prj, e.g. “steam1.prj”. Save also the diagram file as “steam1.dia” by selecting item “Save As” of menu File of the diagram editor.

You can directly view the point state values on the diagram, by selecting item “Show values” in the Special menu or by typing F3 (Figure 9.1.19).

9.1.6 Plotting the cycle on thermodynamic chart

Plotting the cycle on thermodynamic charts can be carried out as follows: the charts are accessible through the line “Interactive charts” on the “Special” simulator menu, which opens an interface similar to that which connects the simulator and the diagram editor. Double-click in the upper left field and select “Vapors” from among the proposed list and choose water as substance (“Substance” menu).

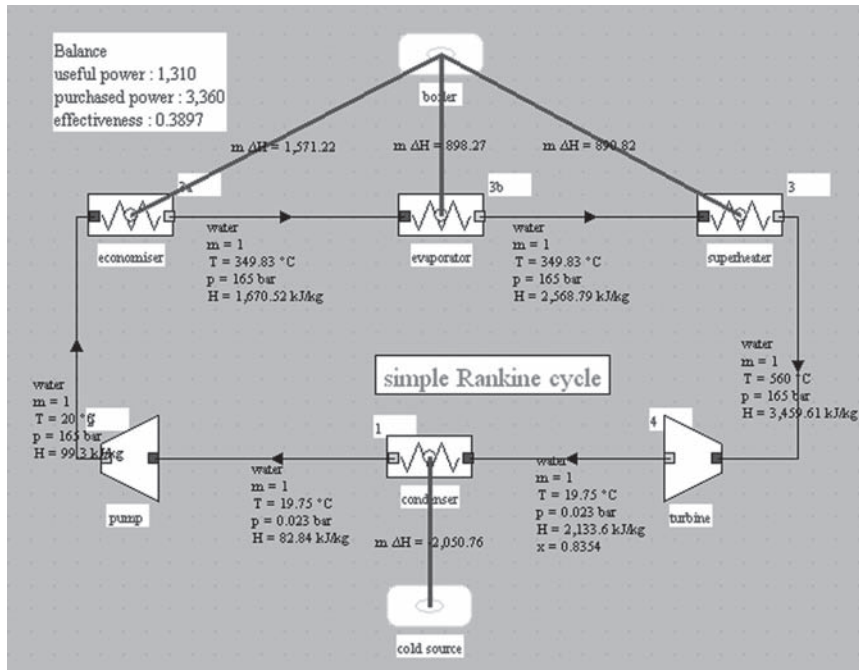


FIGURE 9.1.19
Diagram with values displayed

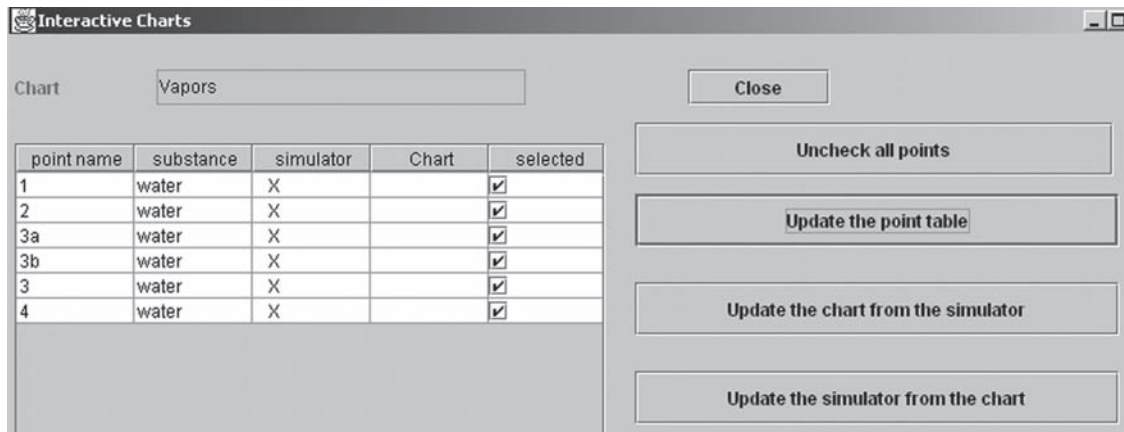


FIGURE 9.1.20
Simulator-chart interface

The “Chart” menu allows you to select the type of chart on which the cycle will be plotted. Select here line (h, p).

Then go back to the “Interactive Chart” frame, and click on “Update the point table” which gives Figure 9.1.20.

The interface between the simulator and the interactive charts includes several fields and buttons, and a table showing the various points which exist in the project or were defined as cycle points in the chart (there are none here).

The two first columns show the names and the substances of the points. When a point is part of the simulator project, an “X” appears in the third column, and when it is part of the chart cycle points, an “X” appears in the fourth one. Here, there are only simulator points.

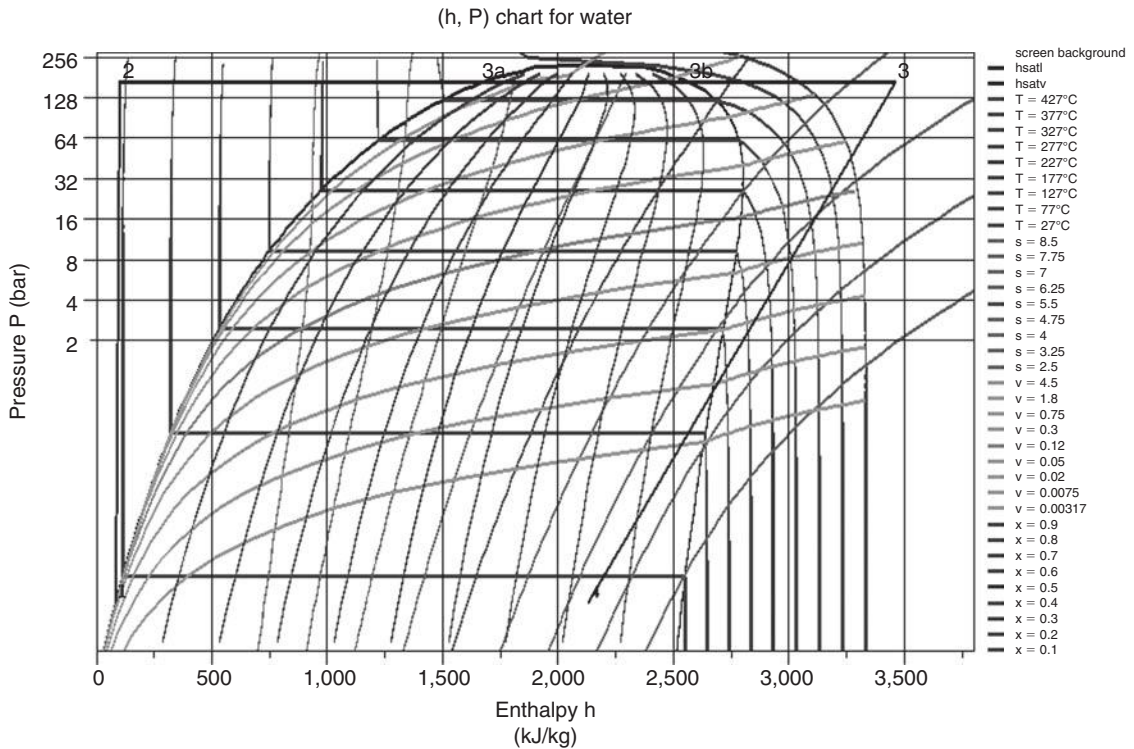


FIGURE 9.1.21

Plot in the (h, ln(P)) chart

The last table column titled “selected” shows the point status: only the selected points are being taken into account in the transfers between the simulator and the charts. To change a point status, double-click on the corresponding line. Here we want to plot all points, so we keep them all selected.

Now, click on “Update the chart from the simulator” to have the points transferred to the chart, and select “Connected Points” in menu Cycle. If necessary, change the axis layout in the “Chart” menu. You get the result shown Figure 9.1.21.

As indicated at the beginning of this chapter, more explanations on the plot of cycles in thermodynamic charts are given in Chapters 2 and 3 of Part 1.

THERMPT
[CRC_In_10]

9.1.7 Design of the condenser

For designing the condenser, it is necessary to introduce a cooling fluid, e.g. a river water, with a fluid inlet (“river inlet” at 10°C and 1 bar) and a fluid outlet (“river outlet” at 1 bar and a provisional value $T = 15^\circ\text{C}$), which can be represented by new process-points on the working panel. Also enter a new exchange process (“river”) to be placed between them. For the time being, its flow rate is set to 120 kg/s.

Place these components on the working panel as before, after removing the external heat sink, and then create the corresponding simulator types by entering for pinch minimum, a value of 8 K for the river process (heat exchange between liquids), and 9 K for the condenser. The diagram becomes as shown Figure 9.1.22.

Now calculate the “river” process as the heat exchanger construction can only be done if the enthalpy in this process is not equal to zero.

To create the heat exchanger, place the mouse on either the condenser or the “river” process. In the middle of the component appears a small blue circle which is a heat exchanger connection

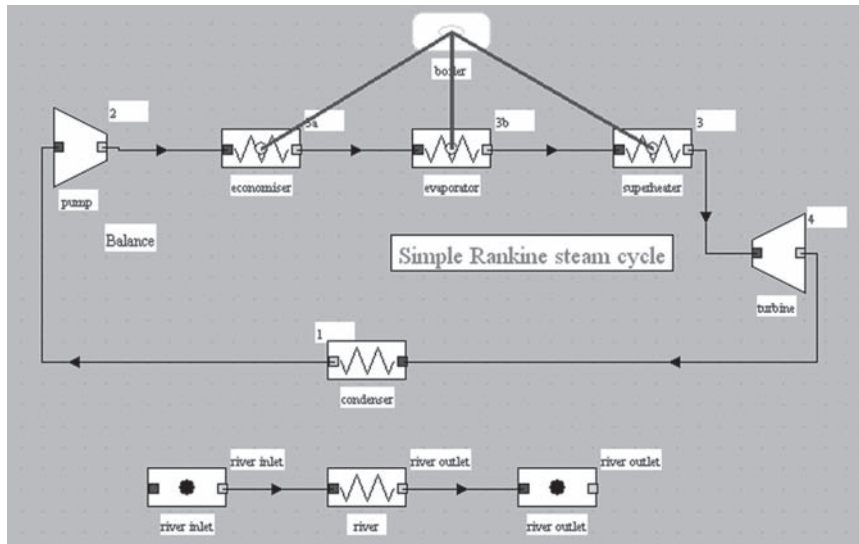


FIGURE 9.1.22
Initial presentation of the condenser

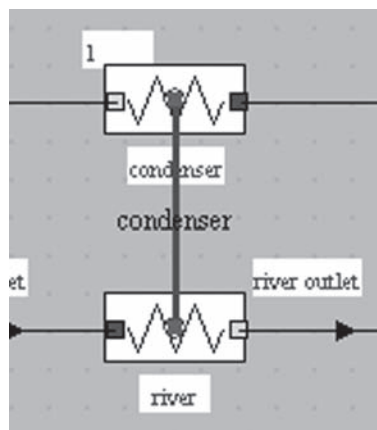


FIGURE 9.1.23
Condenser in the diagram editor

port. Click on it and drag the mouse above the corresponding port of the other component (the “river” process or the condenser).

The name of the heat exchanger (“condenser”) is asked for. Once you have entered it, the exchanger is symbolized by a link between the two processes (Figure 9.1.23).

Note that the heat exchanger cannot be created if the two processes it matches have not been previously calculated in the simulator. Based on the enthalpy changes of the fluids in these processes, the software indeed determines firstly which warms up and which cools, and secondly the value of heat capacity rates brought into play.

To create the heat exchanger in the simulator environment, double-click twice on the link. The screen of Figure 9.1.24 appears.

By default, it is of the counter-flow type. Temperatures and flow rate values are updated from the processes, and average specific heats in the heat exchanger are evaluated.

When, as for this condenser, the outlet temperature of one of the fluids is equal to its inlet temperature, a difference of 0.1 K is set.

The screenshot shows a software interface for configuring a condenser. At the top, there are fields for 'name' (set to 'condenser') and 'type' (set to 'counterflow'). Below these are buttons for '<', '>', 'Save', 'Suppress', and 'Close'. The interface is divided into 'hot fluid' and 'cold fluid' sections. The 'hot fluid' section has a 'display' button and fields for Thi (19.74562), Tho (19.64562), mh (1), and Cph (20,507.6). The 'cold fluid' section has a 'display' button and fields for Tci (10), Tco (12.74562077), mc (178.25493962), and Cpc (4.19018032). There are also fields for m ΔHh and m ΔHc. At the bottom, there are radio buttons for 'unconstrained' (selected), 'minimum pinch', and 'set effectiveness'. There are also fields for DTmin and epsilon. On the right, there are fields for UA, R, NTU, and LMTD, and radio buttons for 'design' (selected) and 'off-design'. A 'Calculate' button is located in the top right of the main area.

FIGURE 9.1.24

Condenser screen before settings

In order to design the heat exchanger, it is now necessary on the one hand to enter its type, and on the other hand to specify which temperatures and flow rates have to be calculated, the others ones being set.

We have shown (see section 8.3.4) that the problem has five degrees of freedom and that at least one of the two flow rates has to be set.

For temperatures, one can define explicit constraints (set values) or implicit constraints: one sets a value for the heat exchanger effectiveness, or the pinch is set equal to a minimal value.

To set an effectiveness value, it is necessary to enter it in the “epsilon” field and to select the “set effectiveness” option. To set a “minimal pinch”, select the corresponding option; in this case, the software calculates the minimal pinch as being equal to the half-sum of the minimal pinches set in each of the processes that the heat exchanger matches, but it can be subsequently modified.

For example, suppose we set the minimum pinch (here 7 K), as well as steam temperatures and flow, and inlet temperature of the river water.

To size the heat exchanger, select calculation mode “design” and click “Calculate”. Let us recall that the design of heat exchangers is always made with the implicit assumption that the thermo-physical properties of the fluid remain constant throughout the exchanger, while this assumption is not made in the calculation of processes. It follows that when the temperature is recalculated based on the equations of heat exchangers, slight differences may exist between the value of the heat exchanger and that of the corresponding process.

For a very good accuracy, one must iterate several times. After two or three calculations, you get the result in Figure 9.1.25.

The effectiveness is $\varepsilon = 0.28$, the number of transfer units is $NTU = 0.33$, the heat capacity ratio is $R = 0.0394$, and the product of the exchange surface by the exchange coefficient is $UA = 248.5 \text{ kW/K}$. The river flow rate is equal to 178.25 kg/s . The log-mean temperature difference LMTD is 8.25 K .

The enthalpy exchanged is equal to $2\,051 \text{ kW}$, and the outlet river temperature, that was initialized at 15°C , is equal to 12.7°C , the minimal pinch being equal to 9 K for the water that condenses, and 8 K for the river, which leads to a value of $(9 + 8)/2 = 7 \text{ K}$ for the heat exchanger.

If we set the effectiveness to 0.5 instead of the minimum pinch, the result is given in Figure 9.1.26.

FIGURE 9.1.25
Condenser screen

FIGURE 9.1.26
Condenser screen 0.5 effectiveness

The effectiveness is $\varepsilon = 0.5$, the number of transfer units is $NTU = 0.997$, the heat capacity ratio is $R = 0.0205$, and the product of the exchange surface by the exchange coefficient is $UA = 293.4 \text{ kW/K}$. The river flow rate is equal to 100 kg/s . The log-mean temperature difference LMTD is 7 K .

The outlet water temperature of the river is now equal to 14.87°C . Note that the pinch ($T_{hi} - T_{co}$) is less than the minimum specified in the processes. ThermoOptim accepts this result: it is up to the user to ensure that the data entered is consistent. By requesting a higher effectiveness than that obtained for the minimum pinch conditions, the user decides not to respect this constraint.

By varying the different parameters, it is possible to test various sizings of the condenser.

Save the diagram and project files, for instance respectively as `steam_cond.dia` and `steam_cond.prj`.

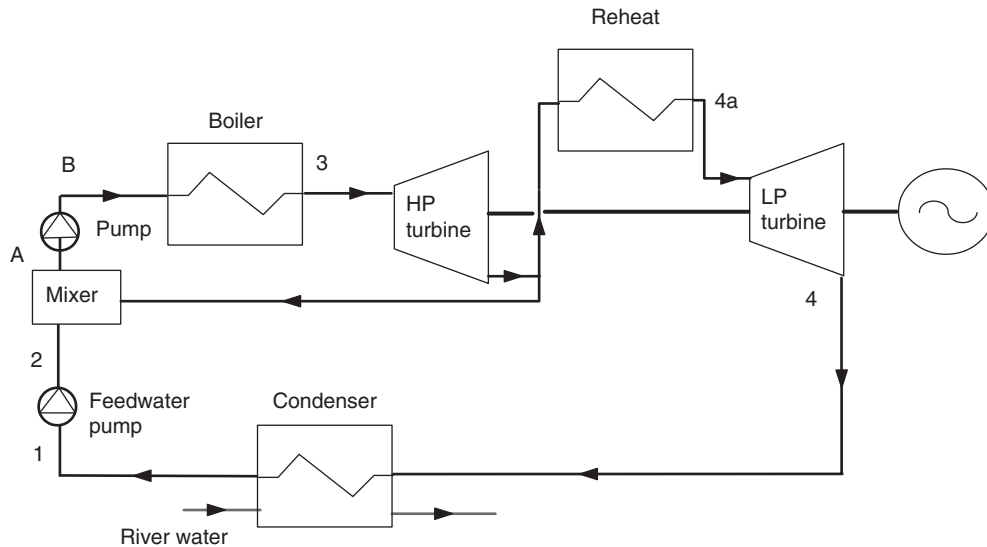


FIGURE 9.1.27
Reheat and extraction steam cycle

9.1.8 Cycle improvements

In this section, we just present shortly the reheat and extraction cycle which is detailed in section 16.1.5 of Part 3.

9.1.8.1 Cycle with reheat

To improve the Rankine cycle, one can approximate the Carnot cycle with reheat cycles. In this case, one begins by partially expanding the steam, which is then redirected to the boiler, where it is reheated at the new pressure, until it reaches the maximal temperature of the cycle. If need be, this operation can be repeated several times, which allows one to approach a para-isothermal process, and therefore increases the average level of the cycle temperature heat source side.

This leads to efficiency gains of a few percent, and especially an increase of the quality of the vapor at the turbine outlet. It is always favorable to extend the life duration of the turbine blades, because liquid droplets are quite abrasive. The price to pay is however a higher complexity, but this improvement has no major technological impact on the plant, as in any case the expansion has to be fractioned.

9.1.8.2 Cycle with extraction

Another way to improve the cycle is to undertake partial regeneration by using part of the heat rejected during the expansion for preheating the pressurized liquid water before it enters the boiler.

With the enthalpy of the steam being largely greater than that of the liquid, it is possible to pre-heat the liquid by a small extraction of steam during expansion.

It should be noted that due to extraction, the mass flow rate of the fluid that evolves is not the same in the different parts of the machine. If ϵ is the steam extracted, and fluid flow between points 4a, 3c, 4, 1 and A is $(1 - \epsilon)$ kg/s, then the flow rate that evolves between points A, 3a, 3b, 3 and 4a is equal to 1.

Of course, for the operation to be possible, it is necessary that the steam extracted at point P is at higher temperature than that of the liquid. In practice, reheat is thus limited. Furthermore, one can combine reheat and extraction by extracting the vapor just before the reheat (Figure 9.1.27).

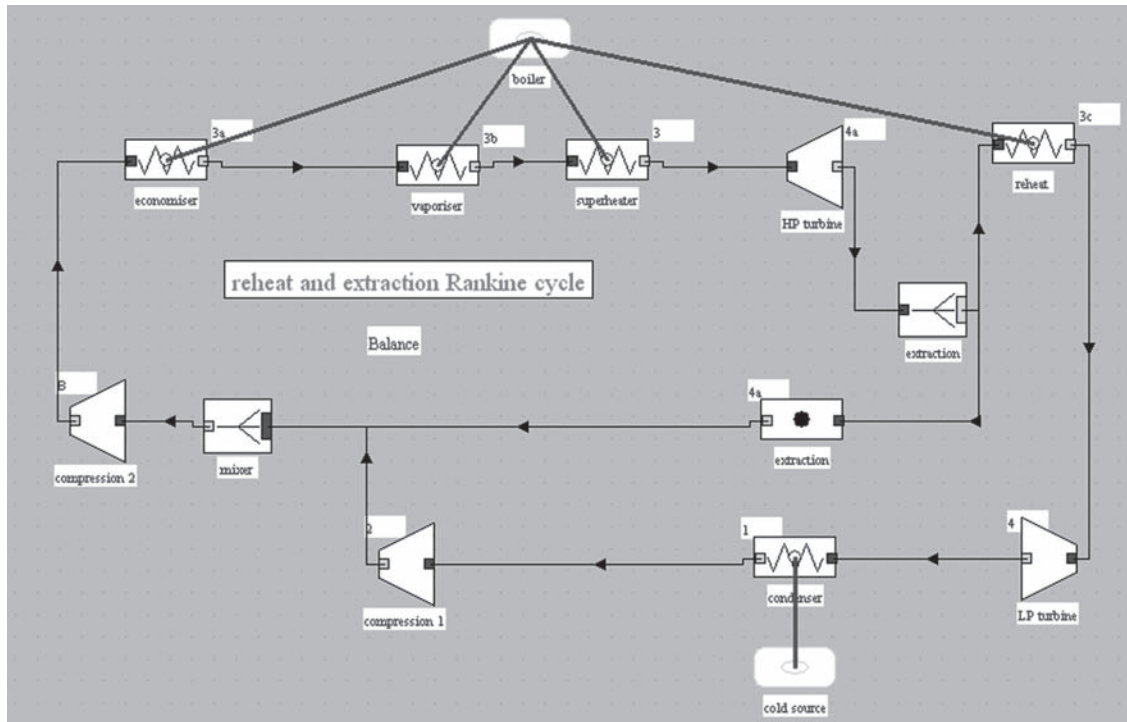


FIGURE 9.1.28

Reheat and extraction steam cycle in the diagram editor

Let us now introduce in the cycle studied previously a reheat at 30 bar and a 15% extraction, in order to see the impact that these modifications have on the cycle efficiency.

9.1.9 Modification of the model

To introduce the reheat, you have to create two new points, 4a at the outlet of the first expansion at 30 bar, and 3c, at 30 bar and 833.15 K. Create as well two new processes, to represent the reheat (4a-3c) (purchased energy) and the second expansion (3c-4) (useful energy).

In addition, you must modify the first expansion, that takes place between points 3 and 4a (no more 3 and 4). To avoid all confusion between the two expansions, you will also rename the first one, which becomes HP turbine, and name the second LP turbine.

To introduce the extraction, it is necessary that you create a divider, representing the split of the main vein at the outlet of the first expansion, and a mixer.

To make things simple, we will suppose that the extracted steam and the water at the outlet of the condenser are mixed (usually they are connected by a heat exchanger). Furthermore, it is necessary to introduce a second pump for fractioning the pressurization of the liquid water with an intermediate step at 30 bar ("compression 1" between point 1 at 0.023 bar and point 2 at 30 bar, and "compression 2" between point A at 30 bar and point B at 195 bar). You will for instance take an extraction of 15%.

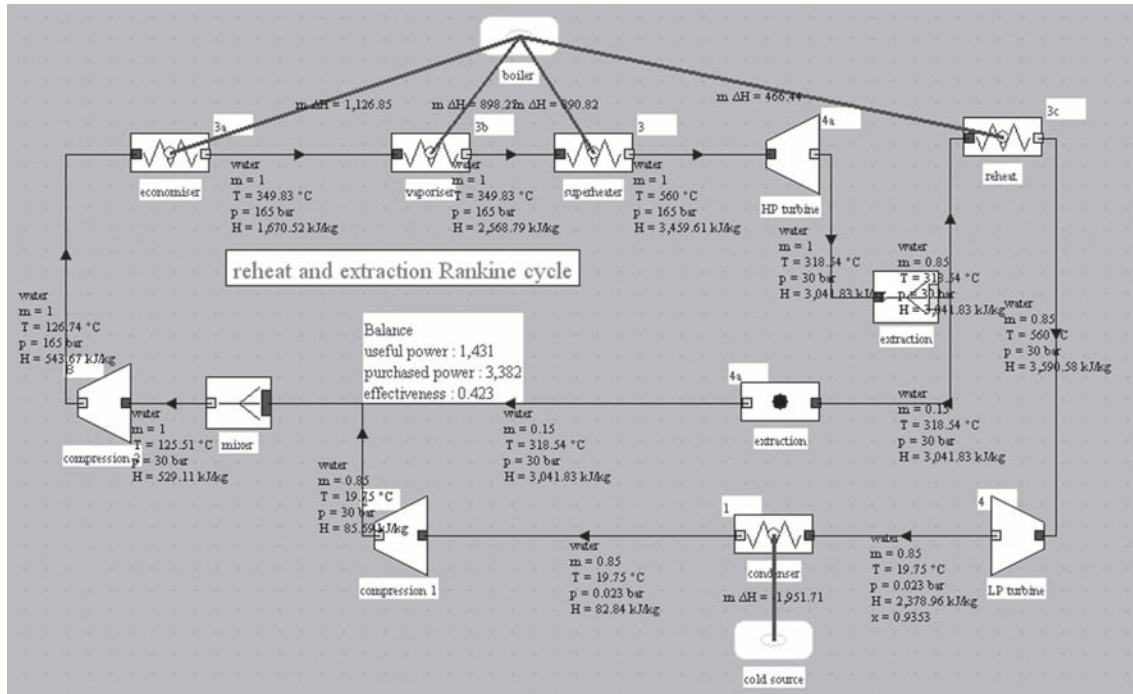
When you have added these new components and made the appropriate connections (disconnecting the links which are no more valid such as that between the HP turbine and the condenser), you obtain a new diagram similar to the one presented in Figure 9.1.28.

Watch out: make sure that the inlet point ("A") of the process downstream of the mixer (here "compression 2") is entered in its inlet port tab as this is not done automatically when you connect

Balance	
effectiveness	0.423
useful energy	1,431
purchased energy	3,382

FIGURE 9.1.29

Balance

**FIGURE 9.1.30**

Synoptic view of the reheat and extraction steam cycle

the mixer to it. Also, both inlet points of the divider branches (process-point “extraction” and process “reheat”) should be the same (“4a”) as the outlet one of its main vein, as their state is the same.

To create the corresponding simulator elements, use the Diagram/Simulator interface, and set their parameters. The LP isentropic efficiency is the same as that of the HP turbine (0.85). Once the components are transferred to the calculator, you can enter these settings.

The mixer is calculated automatically, but not the divider. In the divider, the setting of the flow factors determines how the main vein is split between the two branches. As you want a 15% extraction, enter 0.85 for the “reheat” branch flow factor, and 0.15 for the “extraction” one, as ThermoOptim will compute the flow distribution proportionally to these values. Calculate the divider, and save it. You can also set the flow-rate in the “extraction” process to 0.15 kg/s. The divider will automatically calculate the other flow-rate.

All types thus being defined, you obtain the balance of the cycle by clicking the “Recalculate” button, which gives Figure 9.1.29.

The useful power is now 1,430 kJ/kg (it has declined given that 15% of the flow rate does not pass through the second turbine), but the efficiency of the cycle has increased to 42.3% (Figure 9.1.30).

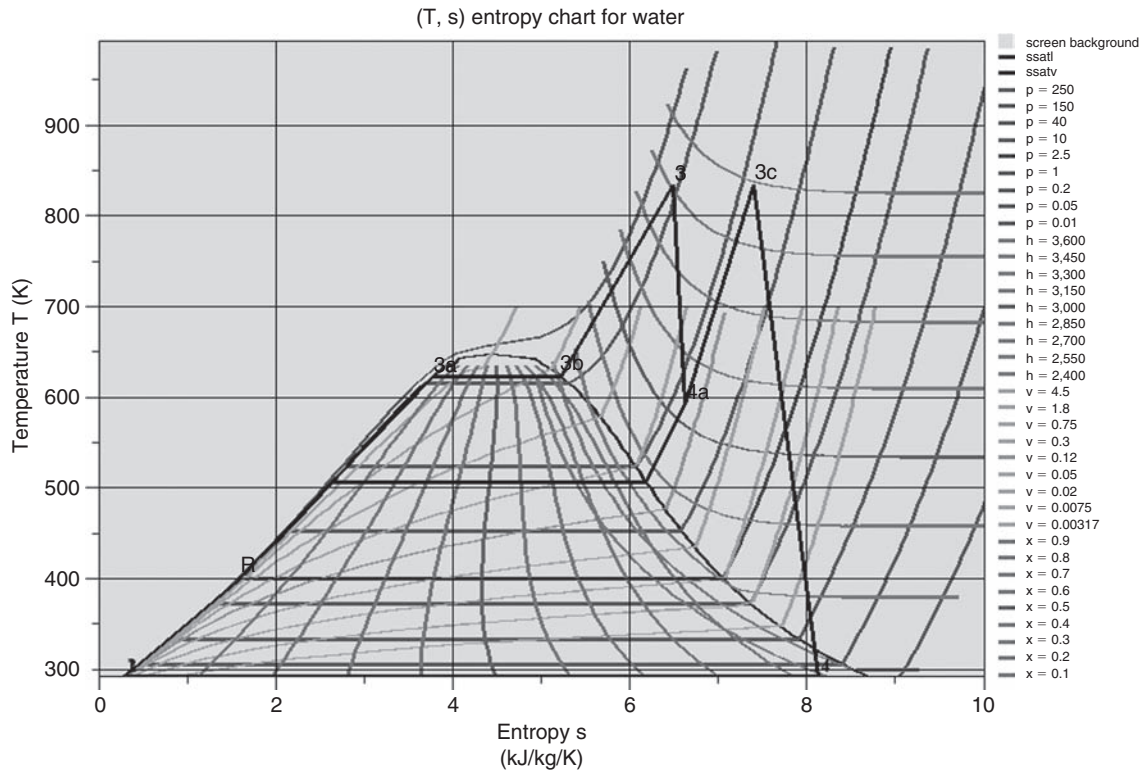


FIGURE 9.1.31

Plot of the reheat and extraction steam cycle

Save the diagram and project files, for instance respectively as steam3.prj for the project and steam3.dia for the diagram.

To plot the cycle on the entropy diagram, choose (T, s) in the “Chart” menu. With some modifications to display the extraction, it is shown in Figure 9.1.31.

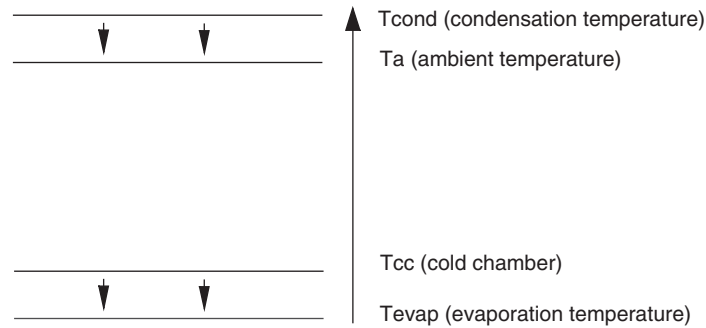
All explanations on how to improve the cycle plot are given in the ThermoOptim Interactive vapor chart manual², available in the software documentation.

9.2 SINGLE STAGE COMPRESSION REFRIGERATION CYCLE

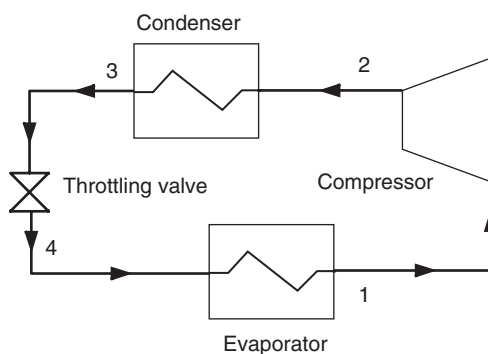
9.2.1 Principle of the machine and problem data

Let us recall (section 2.1.2 of Part 1) that, in a refrigeration system, one seeks to maintain a cold chamber at a temperature below ambient. The idea is to evaporate a refrigerant at low pressure (and therefore low temperature) in a heat exchanger in contact with the cold chamber. For this, we need the refrigerant temperature T_{evap} to be lower than that of the cold chamber T_{cf} . The fluid is then compressed at a pressure such that its condensation temperature T_{cond} is greater than the ambient temperature T_{a} . It is then possible to cool the fluid by heat exchange with ambient air until it becomes liquid. The liquid is then expanded by isenthalpic throttling at low pressure and directed into the evaporator. The cycle is thus closed.

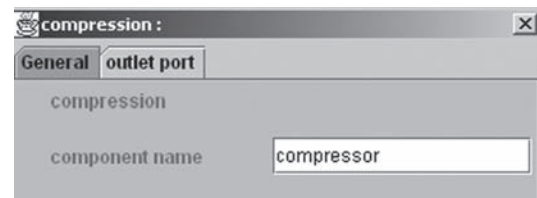
²<http://www.thermoOptim.org/sections/logiciels/thermoOptim/documentation/manuel-reference>

**FIGURE 9.2.1**

Heat fluxes in a refrigeration cycle

**FIGURE 9.2.2**

Compression refrigeration cycle

**FIGURE 9.2.3**

Property editor

Figure 9.2.1 illustrates the enthalpy transfers that take place in the cycle. Small arrows pointing downwards represent the heat transfers, which, as seen, comply with the second law of thermodynamics, heat flowing from warm to cold temperatures. The long upwards arrow represents the enthalpy contribution of the compressor, which allows the fluid temperature to be raised (the heat quantities are not proportional to the length of arrows).


In our example, the problem data are: a R134a compression refrigeration cycle operates between a suction pressure of 1 bar and a condenser pressure of 12 bar (Figure 9.2.2).

Before entering the compressor, the gas is superheated by 5 K above the saturation temperature, and before entering the expansion valve, the liquid is sub-cooled by 5 K. The compressor isentropic efficiency is 0.75. Model the refrigeration cycle and calculate its performance.

9.2.2 Creation of the diagram

Run ThermoOptim. The diagram editor screen is displayed (Figure 9.1.3).

It has a palette with the various components available (heat exchanges, compressors, turbines, combustion chambers, mixers, dividers, external components etc.), and a working panel where these components are placed and interconnected by links.

The sketch of the refrigeration cycle unambiguously indicates which components should be selected: the compressor , the condenser, which is actually represented here by two processes of

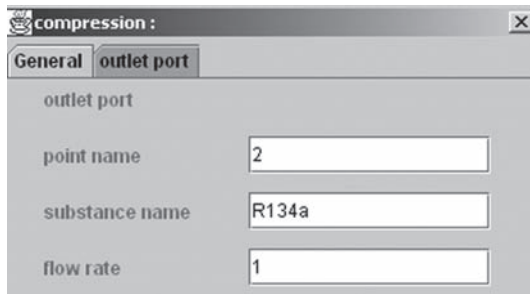


FIGURE 9.2.4
Outlet port settings

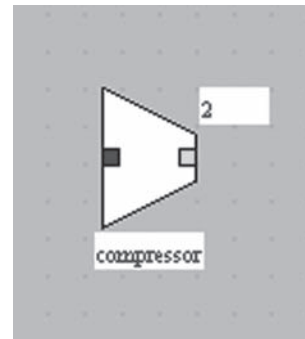


FIGURE 9.2.5
Compressor

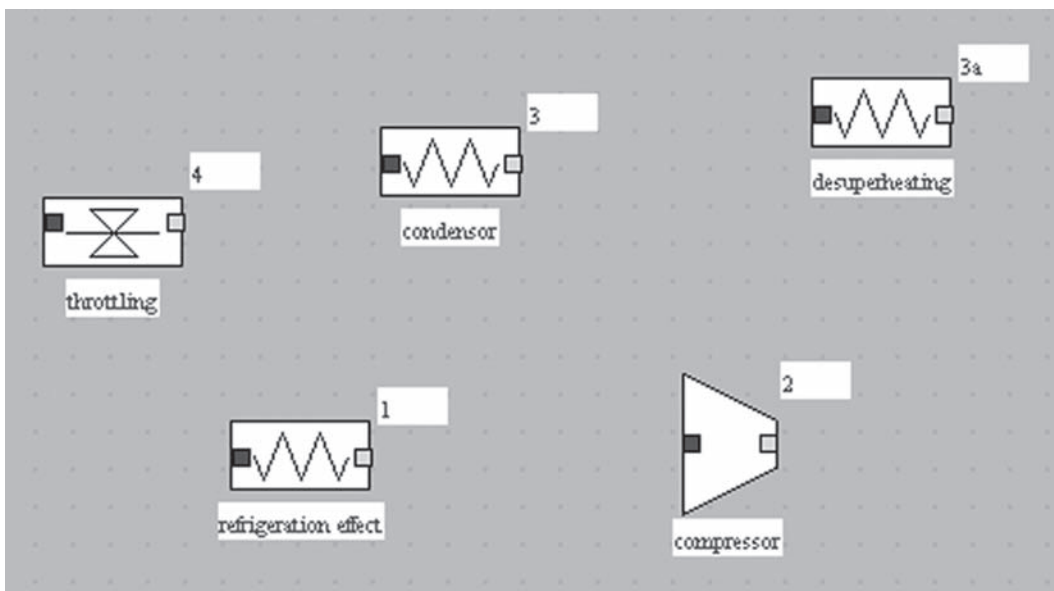





FIGURE 9.2.6
Diagram without links

the exchange type , to distinguish the different cooling phases of R134a (gaseous in the desuperheater, condensing in the condenser), the expansion valve, which is a throttling  and the evaporator providing the refrigeration effect, which is of exchange type .

To represent the compressor, select a compressor component on the palette and place it on the editor by clicking the crosshair cursor at the appropriate location. A property editor is opened. Name the component “compressor” (Figure 9.2.3), then click on the “outlet port” tab (Figure 9.2.4).

Name the point 2, enter the substance name “R134a”. By default, the flow rate is set to 1 which is appropriate here. Then click the button “Apply” to validate the two tabs. The component appears on the screen (Figure 9.2.5).

Similarly create two exchange components corresponding to the desuperheater (outlet point 3a), the condenser (outlet point 3), a throttling component for the expansion valve (outlet point 4), and one exchange component corresponding to the evaporator (outlet point 1). In all cases, the substance is R134a. You get for example the result in Figure 9.2.6.

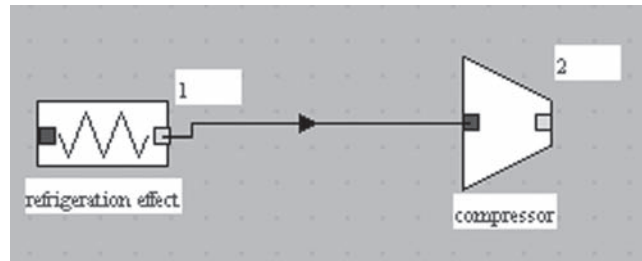


FIGURE 9.2.7
Connected components

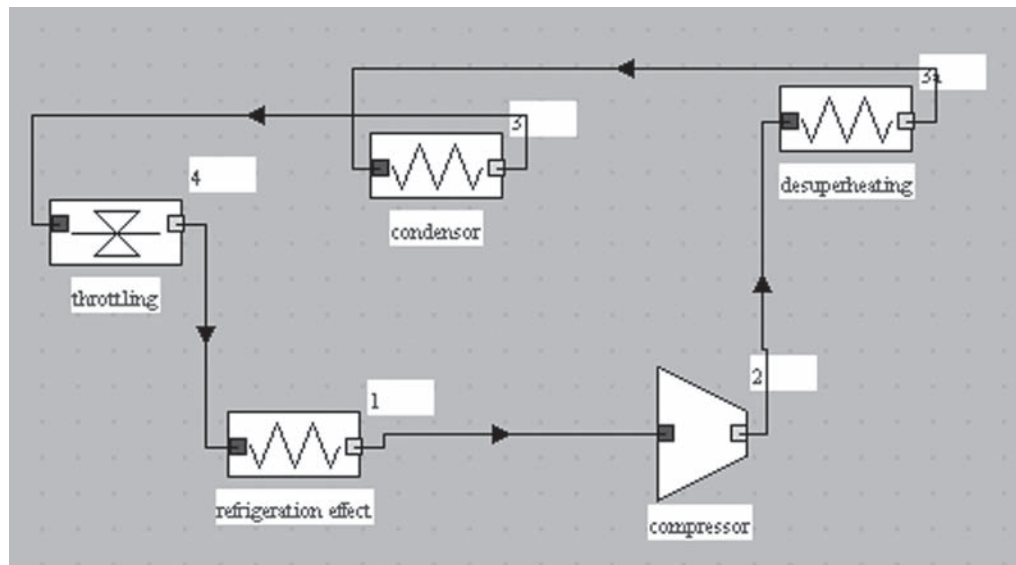



FIGURE 9.2.8
Diagram with links

To connect the components, click on the green outlet port of one of them (e.g. the refrigeration effect). The cursor becomes a crosshair and a line extends from the port if you drag the mouse. Drag the cursor to the blue inlet port of the destination component (e.g. the compressor) while keeping the mouse clicked, and release the mouse. A link is established (Figure 9.2.7). Proceed similarly for all components. You obtain the result of Figure 9.2.8.

By default, all components are oriented from the left to the right. When a loop appears in a diagram, it is convenient to orient some components from the right to the left. Here, you can change the desuperheater, condenser and expansion valve orientation by selecting them and clicking item “flip vertical” of menu Edition or typing F1. The diagram is given Figure 9.2.9.

In order to improve the diagram appearance, you can add a text, two “external source” type components , one for the condenser, and the other one for the cold source, as well as a “Balance” type component which allows you to display the balance values. Thus, the enthalpies exchanged with the external sources can be shown. The result is given in Figure 9.2.10 (a title has been added to the diagram).

At this stage, the qualitative description of the cycle is complete. To facilitate archiving of your diagrams, you can associate a name and description, by selecting the line “Description” on the File menu (Figure 9.2.11).

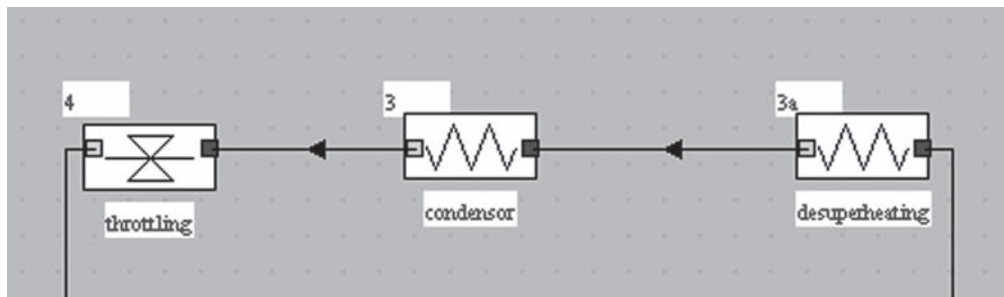


FIGURE 9.2.9
Components oriented to the left

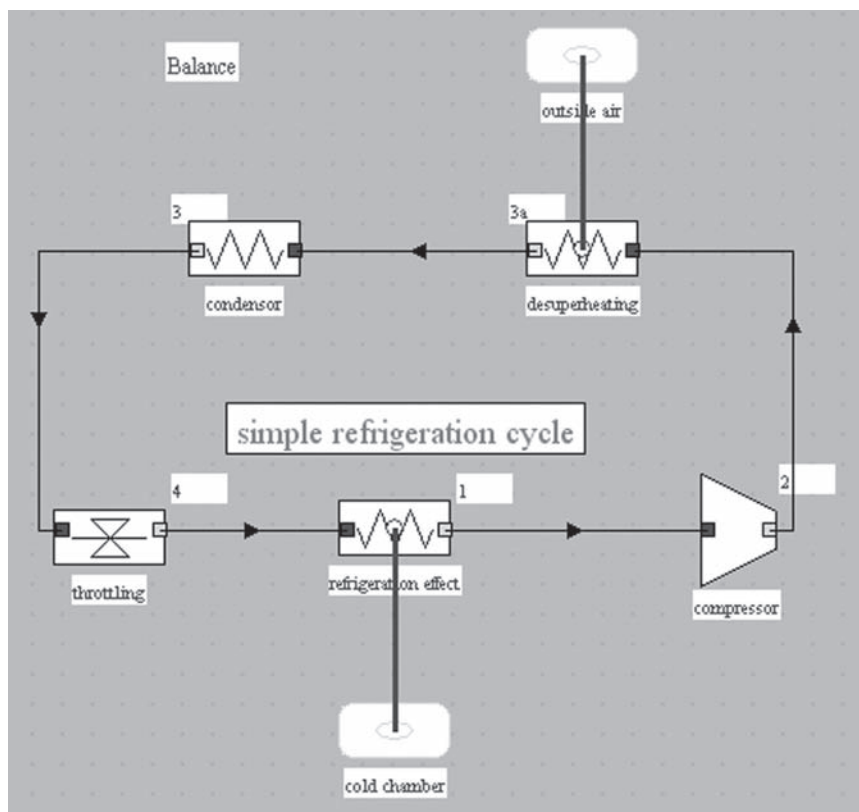


FIGURE 9.2.10
Final layout of the cycle

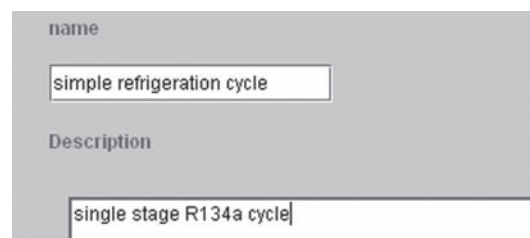


FIGURE 9.2.11
Diagram description frame

Then save your diagram by giving it a name with the extension .dia: “refrig1.dia” for example.

By connecting the components, you spread some information from upstream to downstream, so that all names and substances of the input ports are automatically initialized, as you can verify by selecting a component and displaying its properties (F4 or Edit menu).

The spread of substance names and flow rates is automatic when connecting components representing simple processes. It is thus not necessary to enter them during the initial definition of components that are subsequently connected downstream of another process.

Note that, to enter the substance name, you may either type it if you know it, or get it from the list of substances available in the database which can be displayed by double-clicking in the substance name field and expanding the list, in which case you choose the one you want.

9.2.3 Creation of simulator elements

To create the elements of the simulator, the easiest and most secure way is to use the diagram/simulator interface that can be opened from the Special menu. Then click the button “Update the element table.” The screen is shown in Figure 9.2.12.

The list of transferable elements is displayed in a table, and the user can select those he wishes to create or update. In front of each, an “X” marks the box “Diagram”, while the box “simulator” is empty. The right column shows which components are selected, that is to say which should be taken into account during operations conducted from the interface. By default, all components are selected, but a button allows you to deselect them all if you wish. Otherwise, by double-clicking a row in the table, you select it or not.

To transfer all the simulator components, click the button “Update the simulator from the diagram”. You are requested to name the project. Enter e.g. “simple refrigeration cycle”. Once the transfer is complete, the project screen (Figure 9.2.13) appears.

Five points and five processes have been created with a default setting (1 bar and 300K). To finish creating the model, you must now open each screen of points and processes created, and set them.

You can do that either from the simulator project screen, or from the diagram editor by double-clicking on components to access the processes, and on links to access points (you can also open them from the process screens).

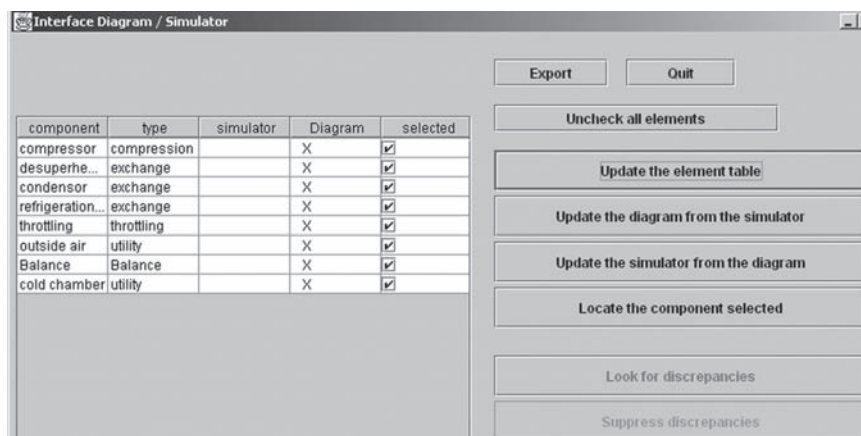


FIGURE 9.2.12

Diagram – simulator interface

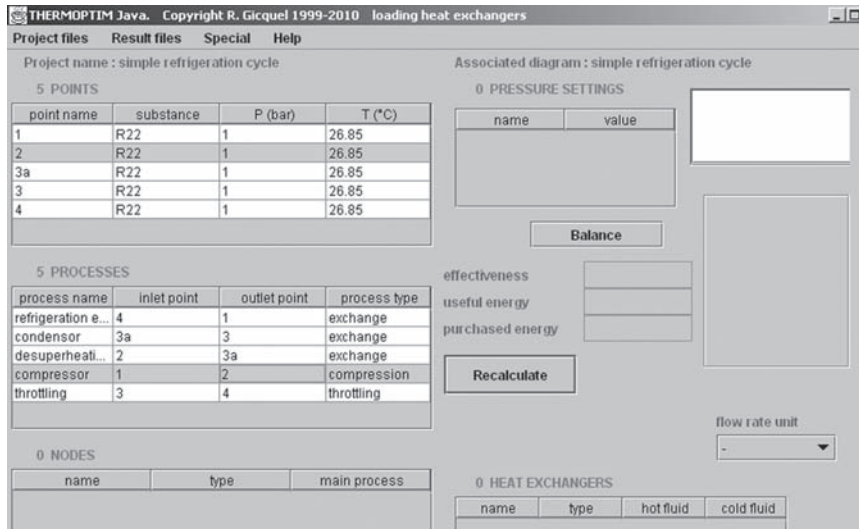


FIGURE 9.2.13
Simulator screen

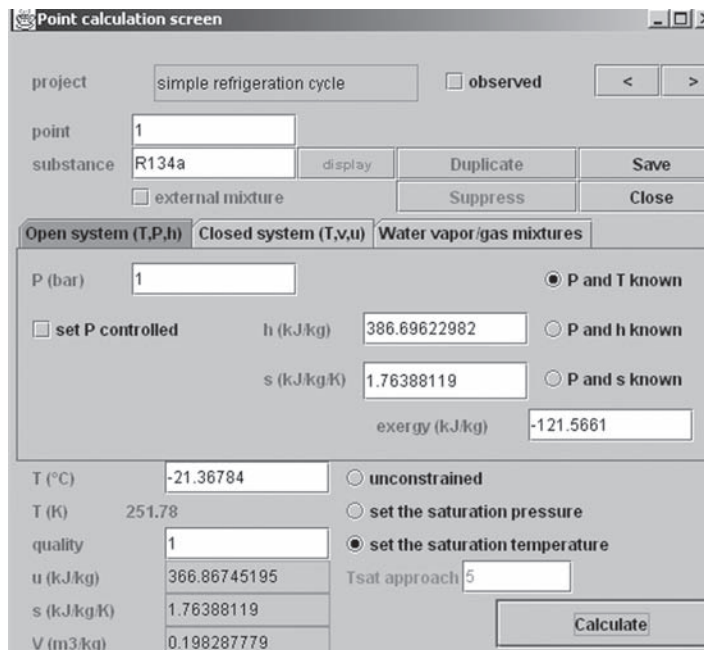


FIGURE 9.2.14
Point screen

9.2.4 Setting points

Begin by setting point 1 representing the compressor inlet gas (Figure 9.2.14).

The point is calculated in open system, the pressure is 1 bar, and the saturation temperature set, with a T_{sat} approach equal to 5 K.

For compressor outlet point 2, indicate the only information known about it, the pressure (12 bar). Currently both its temperature and its enthalpy are not known.

Point 3a at the desuperheater outlet is at 12 bar and on the saturation curve, its quality being set to 1.

FIGURE 9.2.15

Compressor screen

Point 3 at the condenser outlet is at 12 bar, subcooled by 5 K ($T_{\text{sat approach}} = -5\text{K}$). It can also be calculated. The last point to define is point 4. Its pressure is 1 bar, and it is set to saturation temperature, its quality being not known.

9.2.5 Setting of processes

You have the choice between different modes of compression: adiabatic or not, with an isentropic or polytropic reference. For open systems, the compression ratio is that of pressures, for closed systems, that of volumes. It can be either calculated, as is the case here, where the outlet pressure is known, or set, in which case the latter is calculated from the inlet pressure.

To calculate point 2, open the “compressor” process and select “adiabatic”, “isentropic reference”, efficiency equal to 0.75, choose “Set the efficiency and calculate the process” as calculation mode then click “Calculate”. Finally, choose energy type “purchased” because the compression work is to be supplied to the cycle, while the default compression type processes are created with the “useful” energy type. You get the result given Figure 9.2.15.

For the desuperheater (2-3a), and condenser (3a-3), the inlet and outlet points are known and the calculation is very simple. Just make sure that the calculation method (bottom right corner) is “Calculate $m \Delta H$, the outlet point being known” and click “Calculate”.

The calculation of the expansion valve is also very simple as it is an isenthalpic throttling, there is no particular setting: the quality of point 4 is set so that its enthalpy is equal to that of point 3.

The calculation of the cooling effect (4-1) is not a problem once point 4 determined. Simply because it is this effect which is the cycle useful energy, specify that type double-clicking in the “energy type” at the top left of the screen (Figure 9.2.16).

The refrigeration cycle is thus fully described and its balance can be calculated (Figure 9.2.17).

The mechanical compression work is equal to 71 kW, the cooling effect being 128 kW, which corresponds to a coefficient of performance COP equal to 1.8.

You can view the results by clicking “Show values” in the Special menu of the diagram editor or by typing F3 (Figure 9.2.18).

Finally, save the project file, for instance as `refrig1.prj`.

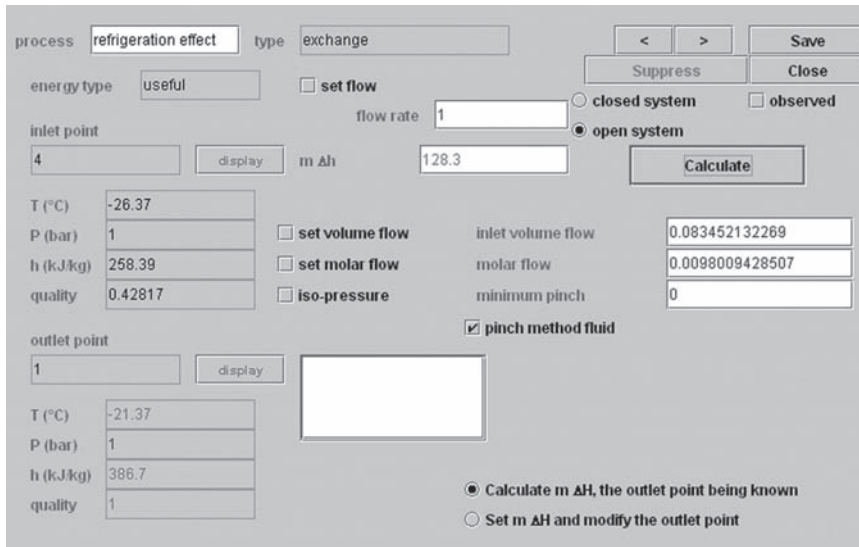


FIGURE 9.2.16
Evaporator screen

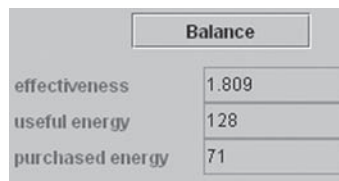


FIGURE 9.2.17
Balance

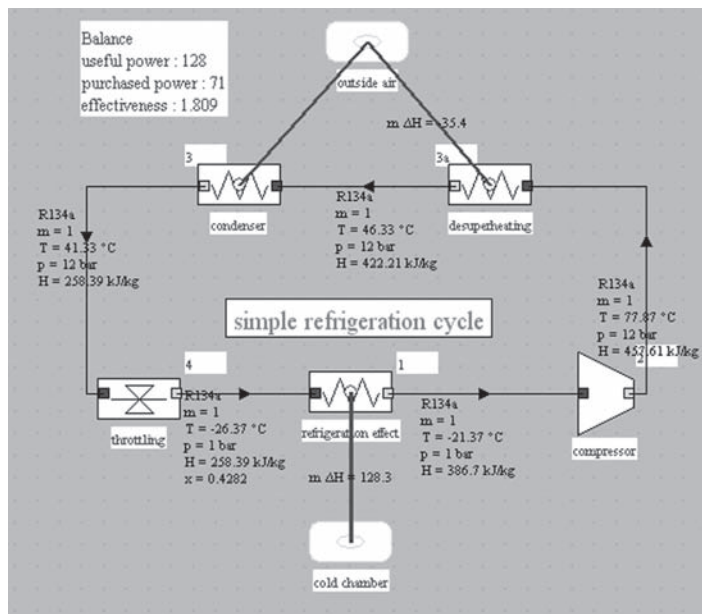


FIGURE 9.2.18
Diagram with values displayed

Like that which has been presented in the steam cycle example, it would be very easy to represent this cycle on one of the thermodynamic charts for R134a. We leave the reader to do so, or to refer to the Part 1 as indicated before.

Note that, in order not to burden this diagram, we have not included all the elements of a real refrigeration system: it lacks the coolant and the cooled chamber.

9.3 GAS TURBINE CYCLE

9.3.1 Principle of the machine and problem data

The operating principle of the gas turbine has already been presented in section 2.1.1 of Part 1. This machine is composed of three elements (Figure 9.3.1), a compressor, a combustion chamber and a turbine.




In this example, a gas turbine burning natural gas without dissociation sucks 1 t/s of air at 15°C and 1 bar and compresses it at 19 bar in a 0.85 polytropic efficiency compressor, and expands the burnt gases in a 0.85 polytropic efficiency turbine. The temperature of the gases at the turbine inlet is 1150°C.


The objective is to model the gas turbine and calculate its efficiency.

9.3.2 Creation of the diagram

Run Thermoptim. The diagram editor screen is displayed (Figure 9.1.3).

It has a palette with the various components available (heat exchanges, compressors, turbines, combustion chambers, mixers, dividers, external components etc.), and a working panel where these components are placed and interconnected by links.

The sketch of the gas turbine unambiguously indicates which components should be selected: the compressor , the combustion chamber , and the turbine, which is an expanding device .

In addition, we will add a fuel inlet, an air inlet and a gas outlet, all three represented by processes-points . The last two are not absolutely necessary, but they allow better cycle display, as we shall see later. A process-point mainly allows one to associate a flow-rate to a point.

Begin by selecting a compression component on the palette and place it on the editor by clicking the crosshair cursor at the appropriate location. The property editor is opened (Figure 9.3.2).

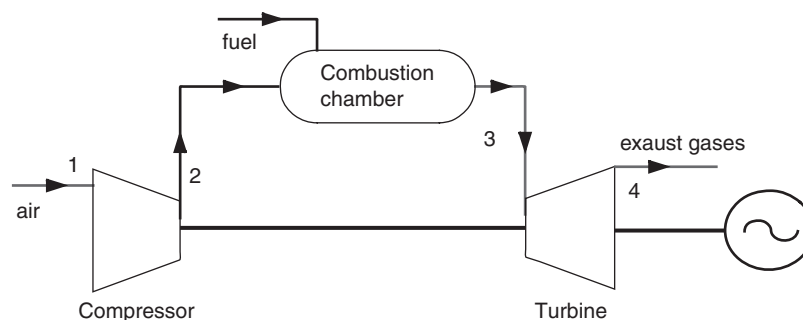
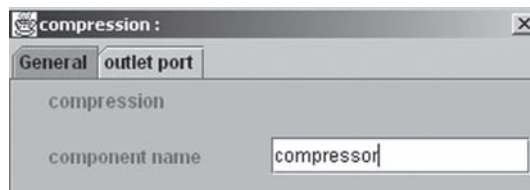
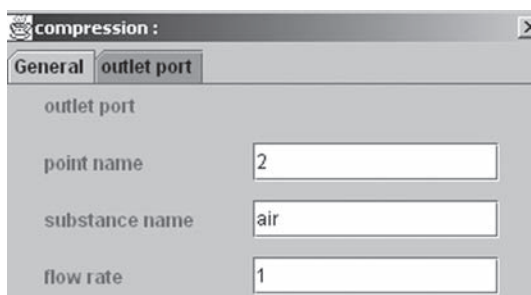


FIGURE 9.3.1

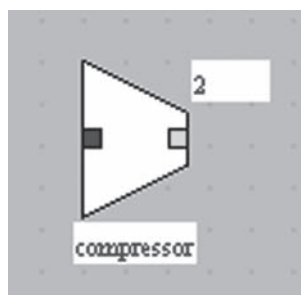
Sketch of a gas turbine

**FIGURE 9.3.2**

Property editor

**FIGURE 9.3.3**

Outlet port settings

**FIGURE 9.3.4**

Compressor

Click on the outlet port tab (Figure 9.3.3), and enter the name of the point (2), the name of the substance (air) and flow (1 t/s). Then click the “Apply” button to validate the two tabs. The component appears on the screen (Figure 9.3.4).

For process-points, it is particularly simple (Figure 9.3.5), as the component name is the same as those of the inlet and outlet points (if you wish you may however choose different names for the point and for the component). Enter its name (air inlet), then that of the substance (air), and the flow rate (1 t/s).

You can now create the other elements of the cycle, namely two process-points corresponding to the fuel and the gas outlet, one combustion chamber (outlet point 3, substance burnt gases), and one expansion component corresponding to the turbine (outlet point 4). It is not necessary to select the turbine substance, as that of the combustion chamber outlet will be automatically propagated when the components are connected.

Note that, to enter the substance name, you may either type it if you know it, or get it from the list of substances available in the database which can be displayed by double-clicking in the substance name field and expanding the list, in which case you choose the one you want.

In our case, the fuel is natural gas, which is defined in the ThermoOptim database, called “Montoir natural gas” (Figure 9.3.6).

The burnt gas substance can be either chosen from among the non-protected gases or created as a new gas (you just indicate the name you wish and ThermoOptim automatically creates it).

You end up with a diagram such as Figure 9.3.7.

To connect the components, click on the green outlet port of one of them (e.g. the air inlet). The cursor becomes a crosshair and a line extends from the port if you drag the mouse. Drag the cursor to the blue inlet port of the destination component (e.g. the compressor) while keeping the mouse clicked, and release the mouse. A link is built (Figure 9.3.8). Proceed similarly for all components. You obtain the result of Figure 9.3.9.

At this stage, the qualitative description of the cycle is complete. To facilitate archiving of your diagrams, you can associate a name and description, by selecting the line “Description” of menu File (Figure 9.2.11).

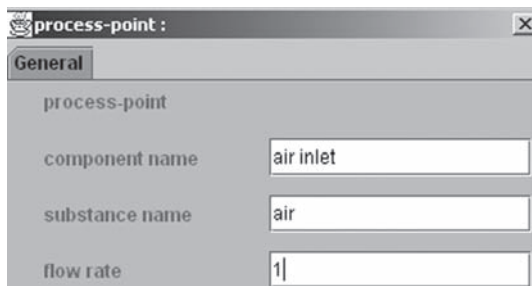


FIGURE 9.3.5
Process-point

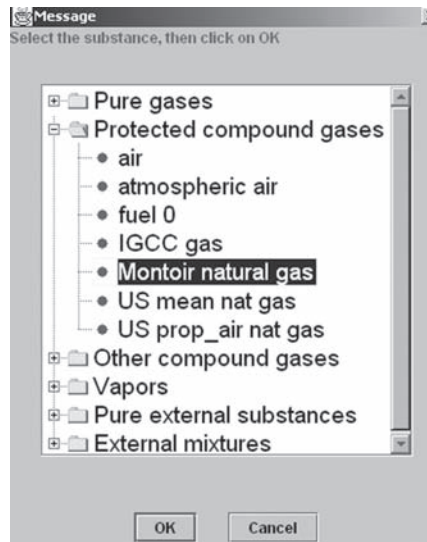


FIGURE 9.3.6
Substance list

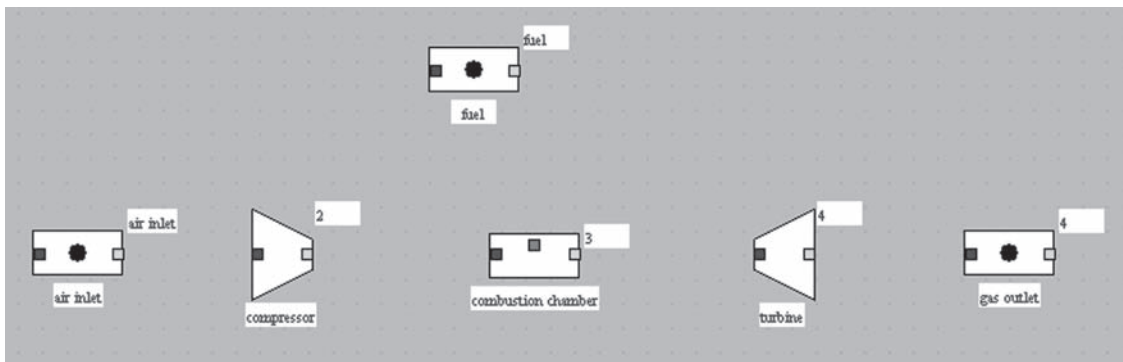


FIGURE 9.3.7
Diagram without links

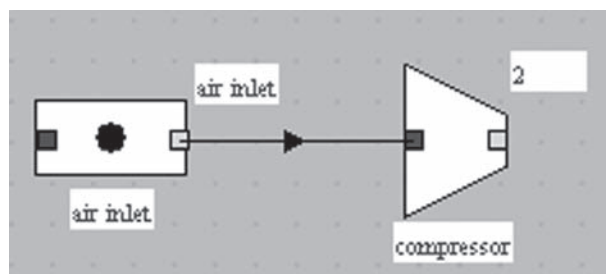


FIGURE 9.3.8
Connected components

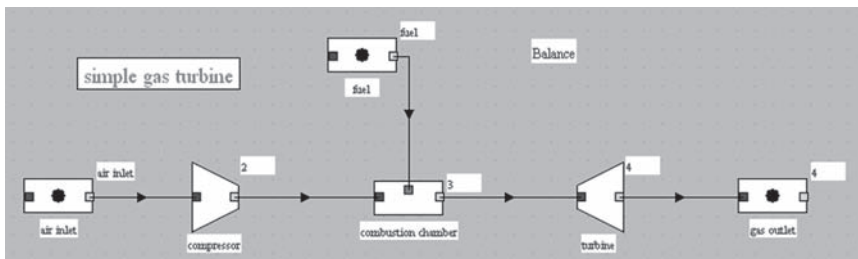


FIGURE 9.3.9
Diagram with links

name

gas turbine

Description

simple gas turbine

FIGURE 9.3.10
Diagram description frame

Interface Diagram / Simulator

Export Quit

Uncheck all elements

Update the element table

Update the diagram from the simulator

Update the simulator from the diagram

Locate the component selected

Look for discrepancies

Suppress discrepancies

component	type	simulator	Diagram	selected
gas outlet	process-pol...		X	<input checked="" type="checkbox"/>
fuel	process-pol...		X	<input checked="" type="checkbox"/>
air inlet	process-pol...		X	<input checked="" type="checkbox"/>
compressor	compression		X	<input checked="" type="checkbox"/>
turbine	expansion		X	<input checked="" type="checkbox"/>
Balance	Balance		X	<input checked="" type="checkbox"/>
combustion...	combustion		X	<input checked="" type="checkbox"/>

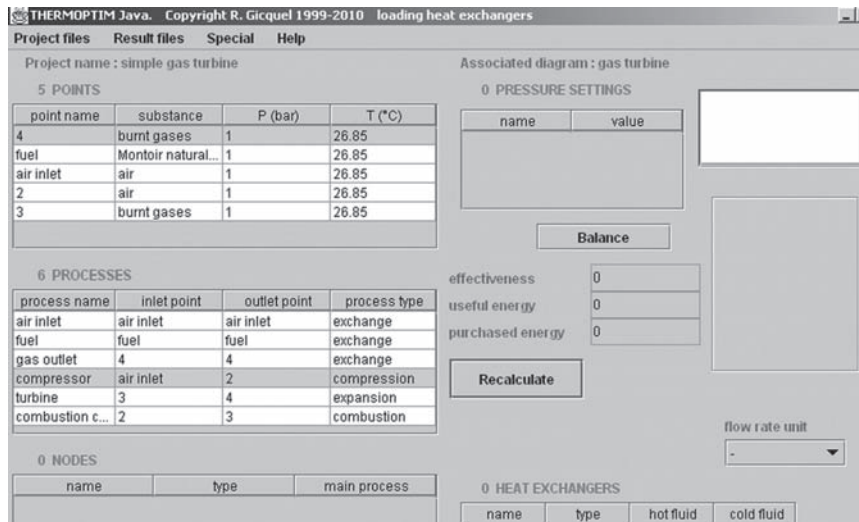
FIGURE 9.3.11
Diagram – simulator interface

Then save your diagram by giving it a name with the extension .dia: “GT.dia” for example.

By connecting the components, you spread some information from upstream to downstream, so that all names and substances of the input ports are automatically initialized, as you can verify by selecting a component and displaying its properties (F4 or Edit menu).

9.3.3 Creation of simulator elements

To create the elements of the simulator, the easiest and most secure way is to use the diagram/simulator interface that can be opened from the Special menu. Then click the button “Update the element table.” The screen is shown in Figure 9.3.11.

**FIGURE 9.3.12**

Simulator screen

The list of transferable elements is displayed in a table, and the user can select those he wishes to create or update. In front of each, an “X” marks the box “Diagram”, while the box “simulator” is empty. The right column shows which components are selected, that is to say which should be taken into account during operations conducted from the interface. By default, all components are selected, but a button allows you to deselect them all if you wish. Otherwise, by double-clicking a row in the table, you select it or not.

To transfer all the simulator components, click the button “Update the simulator from the diagram”. You are requested to name the project. Enter e.g. “gas turbine”. Once the transfer is complete, the project screen (Figure 9.3.12) appears.

Six processes and five points have been created with a default setting (1 bar and 300 K). To finish creating the model, you must now open each screen of points and processes created, and set them. You can do that either from the simulator project screen, or from the diagram editor by double-clicking on components to access the processes, and on links to access points (you can of course also open them from the process screens).

9.3.4 Setting points

Enter the state of point “air inlet” substance. We know its pressure (1 bar) and temperature (15°C). It can be calculated (Figure 9.3.13).

For point 2, the only information known about it is its pressure $P = 19$ bar. For the time being we ignore its temperature or enthalpy. Point 3 is at 19 bar and 1150°C, combustion end temperature. These values can be entered. However, the composition of the burnt gases is not known. It must be calculated by the “combustion chamber” process.

The fuel can be defined as being at pressure 20 bar and temperature 15°C. It can be calculated.

The last point to define is point 4. Only its pressure is known: 1 bar.

9.3.5 Setting of processes

Start with the compression between points “air inlet” and 2 (Figure 9.3.14). You have the choice between different modes of compression: adiabatic or not, with an isentropic or polytropic

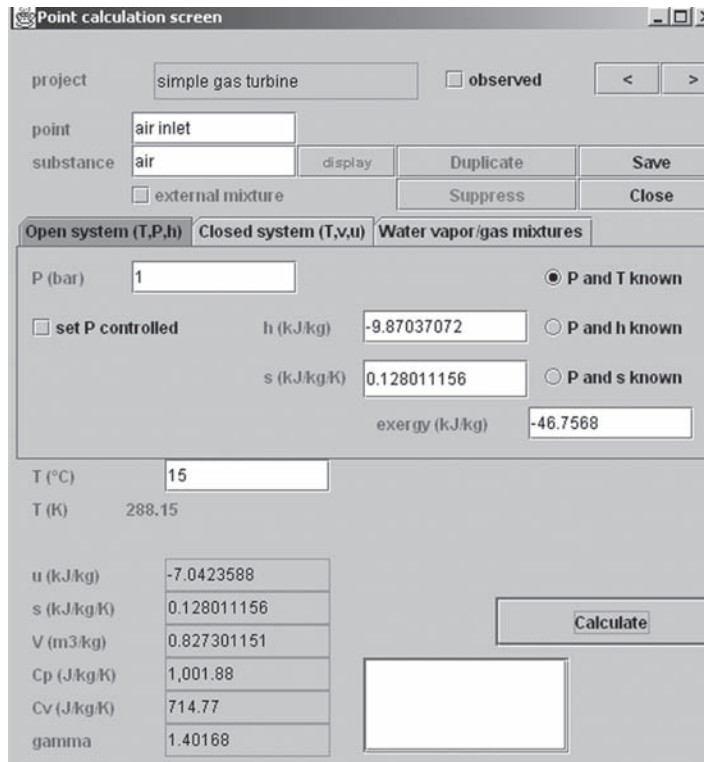


FIGURE 9.3.13
Point screen

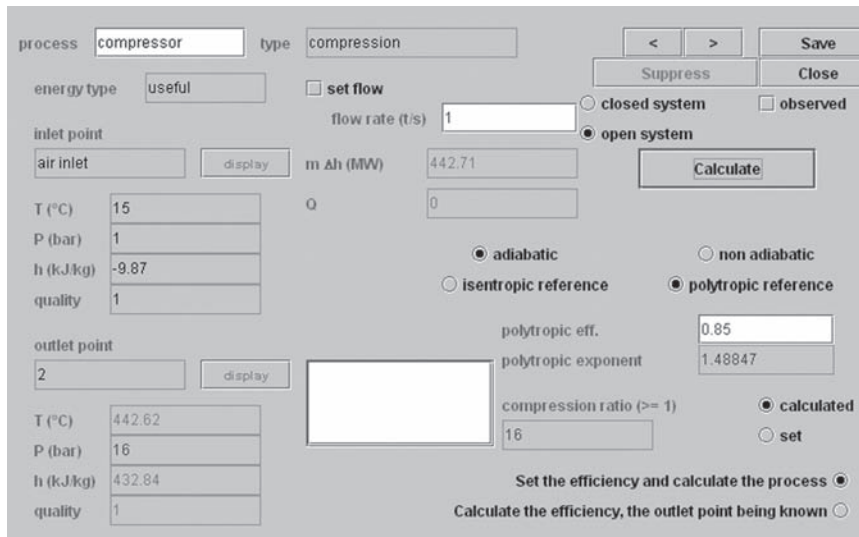


FIGURE 9.3.14
Compressor screen

reference. For open systems, the compression ratio is that of pressures, for closed systems, that of volumes. It can be either calculated, as is the case here, where the outlet pressure is known, or set, in which case the latter is calculated from the inlet pressure.

Choose here: adiabatic, polytropic efficiency equal to 0.85, and open system.

FIGURE 9.3.15

Combustion chamber screen

Select calculation method “Set the efficiency and calculate the process”, then click “Calculate”. Point state 2 is calculated as well as the corresponding enthalpy change. The value of the compression ratio is shown (here 16).

The combustion calculation is more complex: the combustion temperature is set to 1150°C. Enter this value in the lower right field and select “Calculate lambda” (Figure 9.3.15). As the dissociation is not taken into account, there is no need to define its rate or to enter the quenching temperature. In addition, as we neglect the thermal losses of the chamber, its efficiency is set to 1.

The process can be calculated by clicking “Calculate”. The air factor lambda is calculated, as well as the fuel flow rate, automatically updated in its process-point, and the chamber flow rate is displayed.

The burnt gas composition is determined. It can be displayed by clicking the red button “display” located to the right of the substance name in point 3 screen (Figure 9.3.16).

The expansion process can now be calculated (Figure 9.3.17). Its polytropic efficiency is 0.85. The exact state of point 4 and the enthalpy of expansion are then determined.

At this stage, the cycle is totally defined, and you can calculate the balance by clicking “Recalculate” in the simulator screen.

The energy purchased, useful energy, and the efficiency of the cycle are then determined (Figure 9.3.18).

The state of the various cycle points can also be directly displayed on the diagram as in Figure 9.3.19 (item Show values of menu Special or F3).

This is why we introduced the two process-points “air inlet” and “gas outlet”: they allow us to show the state of the corresponding points.

Finally, save the project file, for instance as GT.prj.

The representation of this cycle on a thermodynamic chart poses problem indeed, owing to the fact that it is not the same fluid which flows through the whole machine: the change of composition in the combustion chamber prohibits in theory plotting the cycle in only one chart. Strictly speaking, such a plot makes no sense. You may refer to section 3.7.2 of Part 1 for further discussion on this issue.

Gas composition burnt gases

The first figure column from the left selects the input values from among molar and mass fractions

component name	molar fraction	mass fraction
CO2	0.03215996	0.04949052
H2O	0.05980526	0.03767364
O2	0.141611	0.1584484
N2	0.7576949	0.7421938
Ar	0.00872887	0.0121936

Line edition PCI = 0 (kJ/kg)

File Save Save as ... Export... Create a humid gas Print Cancel

FIGURE 9.3.16
Flue gas composition

process type

energy type set flow

inlet point flow rate (t/s) closed system observed

open system

$m \Delta h$ (MW)

Q

adiabatic non adiabatic

isentropic reference polytropic reference

polytropic eff.

polytropic exponent

expansion ratio (≥ 1) calculated set

outlet point

T (°C)

P (bar)

h (kJ/kg)

quality

Set the efficiency and calculate the process

Calculate the efficiency, the outlet point being known

mechanically balanced with

FIGURE 9.3.17
Turbine screen

Balance	
effectiveness	<input type="text" value="0.3577"/>
useful energy	<input type="text" value="318"/>
purchased energy	<input type="text" value="890"/>

FIGURE 9.3.18
Balance

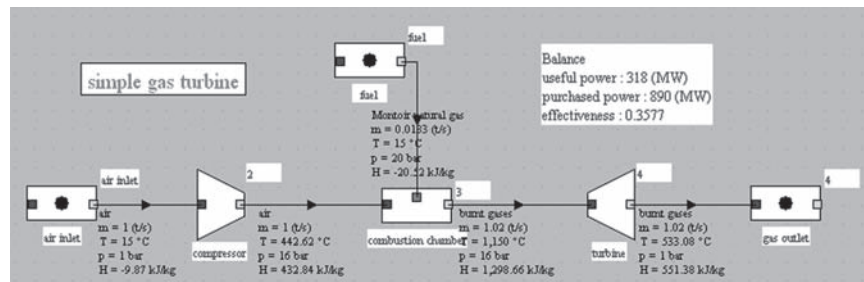
**FIGURE 9.3.19**

Diagram with values displayed

9.4 AIR CONDITIONING INSTALLATION

9.4.1 Principle of installation and problem data

The facility that we are going to study corresponds to a large building like an airport located in a hot and humid climate, which is to be cooled. For this, we have a ventilation system that allows air to blow in different parts of the building. For reasons of hygiene it is necessary to renew the air, but some can be recycled, however, which reduces air conditioning needs.

So some of the indoor air is recycled and mixed with outside air. This mixture must be treated before being injected into the ventilation system so that its state corresponds to the supply conditions. These are calculated so that the internal and external heat and moisture loads corresponding to internal gains are removed. In addition, for reasons of hygiene and comfort, air generally should not be blown below a certain temperature value.

A possible treatment of the mixed air is to cool it, condensing excess water to obtain a specific humidity corresponding to the supply conditions, then warming it at the supply temperature. There are others, but we will present this one here.

The problem data are as follows: we seek to maintain the internal ambience of the building at a temperature of 24°C (297.15 K) and a relative humidity equal to 50%. External climatic conditions are the following: temperature to equal 30°C (303.15 K), and relative humidity of 80%.

It is necessary to remove external and internal thermal loads of 192.9 kW , as well as a quantity of water equal to 90 kg/h , that is 0.01997 kg/s .

Knowing that, for sanitary and comfort reasons, the supply temperature must not be less than 14°C (287.15 K), and that the recycled air proportion must not exceed 70%, the purpose of the exercise is to determine:

- the supply conditions;
- a way of processing of the outdoor air/recycled air mix.

In this example, we cannot use the diagram editor, since moist processes are not yet represented there. The modeling must thus be done directly in the simulator environment.

When you start Thermoptim, the screen in Figure 9.4.1 is displayed.

Begin by creating a new project, named “air conditioning”. To do this, type Ctrl N or select line “New Project” of File menu, then enter the name.

In this exercise, all points will be of the same dry gas, air, and constant pressure, 1 atm (1.01325 bar).

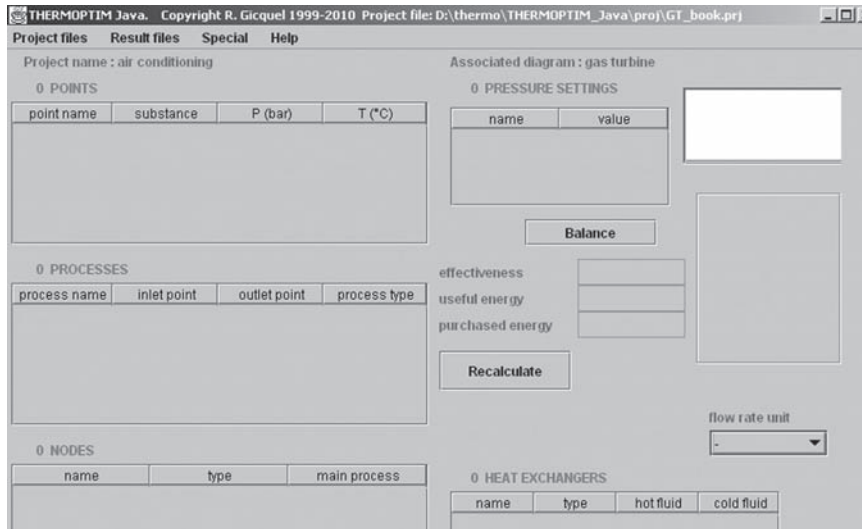


FIGURE 9.4.1
Simulator screen

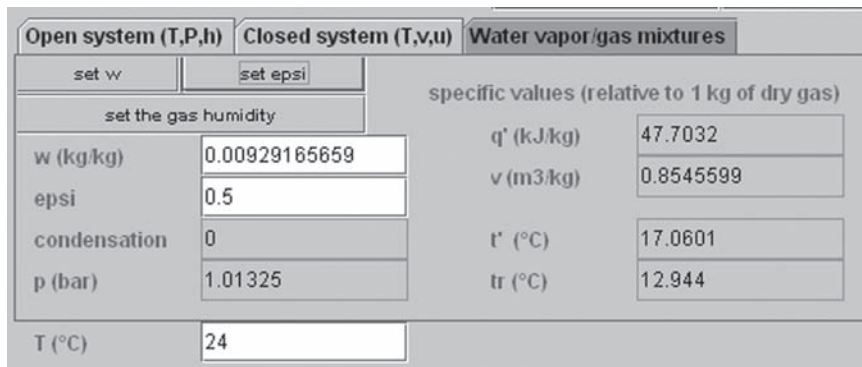


FIGURE 9.4.2
Water vapor/gas mixture point

9.4.2 Supply conditions

Begin by creating two points named “indoor air” and “outdoor air”, and setting their respective temperatures and relative humidities, as well as a third point, named “supply”, with a temperature of 14°C.

To do this, double-click in the header of the points table, enter the names of the point and the substance. For the latter, you can either select from the list of the substances of the data base, which appears if you double-click in the name field, or enter it directly. In the latter case, you need to type a line feed after entering the name, so that ThermoOptim know that the typing is over.

Enter the values of temperature and pressure, and calculate the point, then select the “Water vapor/gas mixtures” tab, and enter either the specific humidity w if known, or more simply the relative humidity since ϵ is given. As appropriate, then click on “set w ” or “set ϵ ”, so that the moist properties of the point are determined.

For the indoor air point, for example, you obtain the result of Figure 9.4.2.

Then, create a supply water vapor/gas mixture process, connecting the points “indoor air” and “supply” (Figure 9.4.3). To do this, double-click in the header of the process table, select “water

process: type:

energy type: set flow

dry gas mass flow rate: closed system open system

inlet point: m ΔO':

T (°C): type:

P (bar): sensible/total heat ratio:

h (kJ/kg): water load:

w (kg/kg): thermal load:

outlet point:

T (°C):

P (bar):

h (kJ/kg):

w (kg/kg):

Calculate the supply conditions, the dry gas flow rate being known

Calculate the supply conditions, the supply temperature being known

FIGURE 9.4.3

Supply process

Open system (T,P,h) Closed system (T,v,u) Water vapor/gas mixtures

set the gas humidity

w (kg/kg): specific values (relative to 1 kg of dry gas)

epsi: q' (kJ/kg):

condensation: v (m3/kg):

p (bar): t' (°C):

T (°C): tr (°C):

FIGURE 9.4.4

Moist gas setting results

vapor/gas mixtures” and “supply”. To connect points, double-click in the fields below “inlet point” and “outlet point”, and select each time the name of the desired point in the list.

Enter the values of the thermal and water loads in the appropriate field with a negative sign because they are to be removed, and choose option “Calculate the supply conditions, the supply temperature being known”, then click “Calculate”.

The flow rate is determined, as well as the “supply” point moisture (Figure 9.4.4).

9.4.3 Properties of the mix (outdoor air/recycled air)

The first step of the air treatment is to calculate the properties of the mix (outdoor air/recycled air), which is then cooled. Mix calculation is done in a particular node, called the moist gas mixer. Like all nodes, its definition has two parts: the main vein and branches.

Start by creating the cooling type moist process main vein. To do this create two new points, called “mixed air” and “cooled air”, and connect them by a moist gas process of the cooling type

process name	m abs	T (°C)	H
indoor flow	0.7	24	-0.852
outdoor flow	0.3	30	5.16

FIGURE 9.4.5

Moist mixer

Open system (T,P,h)		Closed system (T,v,u)		Water vapor/gas mixtures	
set w		set epsi		specific values (relative to 1 kg of dry gas)	
set the gas humidity				q' (kJ/kg)	58.998
w (kg/kg)	0.0130016927	v (m3/kg)	0.864746	t' (°C)	20.5464
epsi	0.624768512	tr (°C)	18.092		
condensation	0				
p (bar)	1.0133				
T (°C)	25.80019531				

FIGURE 9.4.6

Moist mixer outlet poin

named “cooling” (“mixed air” at the inlet and “cooled air” at the outlet). Then build two processes—points associated with points “outside air” (flow rate 0.3) and “indoor air” (flow 0.7), and connect them as branches of the mixer.

To create the mixer, double-click in the header of the node table and choose “moist gas mixer”. To select the main vein, double-click in the corresponding field and choose “cooling” in the list. To declare each of the two branches, click on “add a branch” and then choose the correct process in the proposed list.

Once the mixer is built, you can calculate it (Figure 9.4.5).

The state of the mixer output point you get is given in Figure 9.4.6.

9.4.4 Air treatment

The problem now is how to treat the mixed air (25.8°C, $w = 0.013$) to get the supply conditions (14°C, $w = 0.00792$). One solution is to cool it at specific humidity equal to that of the supply air, then reheat to the desired temperature.

To calculate the cooling process, choose a realistic cooling coil surface temperature (for example 7°C), check the “Calculate the process, the outlet point’s humidity being known” option, and set the outlet point (“cooled air”) humidity to that of the supply point ($w = 0.0079$ kg/kg). Then click “Calculate”, so that ThermoOptim researches the required coil effectiveness.

You obtain the following results: the temperature of the cooled air is equal to 11.78°C, and the cooling coil effectiveness is 75%.

The screenshot shows a software interface for a moist cooling process simulation. The process is named "cooling" and is of type "water vapor/gas mixtures". The energy type is "other" and "set flow" is checked. The dry gas mass flow rate is 0.9871652. The inlet point is "mixed air" with a temperature of 25.8°C, pressure of 1.0133 bar, enthalpy of 0.952 kJ/kg, and humidity of 0.01300169 kg/kg. The outlet point is "cooled air" with a temperature of 11.73°C, pressure of 1.0133 bar, enthalpy of -13.15 kJ/kg, and humidity of 0.00790082 kg/kg. The process type is "cooling" and the sensible/total heat ratio is 1.0. The water involved is -0.06112488 kg/kg, and the effectiveness is 0.750876702. The surface temperature is 7°C. The interface includes buttons for "Save", "Suppress", "Close", "Calculate", and "display". At the bottom, there are two radio buttons: "Calculate the process, the cooling coil efficiency being known" (unselected) and "Calculate the process, the outlet point's humidity being known" (selected).

FIGURE 9.4.7

Moist cooling process

The screenshot shows a software interface for a moist heating process simulation. The process is named "heating" and is of type "water vapor/gas mixtures". The energy type is "other" and "set flow" is checked. The dry gas mass flow rate is 11.98322. The inlet point is "cooled air" with a temperature of 11.73°C, pressure of 1.0133 bar, enthalpy of -13.15 kJ/kg, and humidity of 0.00790082 kg/kg. The outlet point is "supply" with a temperature of 14°C, pressure of 1.0133 bar, enthalpy of -10.87 kJ/kg, and humidity of 0.007900821 kg/kg. The process type is "heating" and the sensible/total heat ratio is 1.0. The water involved is 0 kg/kg. The interface includes buttons for "Save", "Suppress", "Close", "Calculate", and "display". At the bottom, there are two radio buttons: "Calculate the process, the outlet point being known" (selected) and "Calculate the outlet point, m ΔH and the water involved being known" (unselected).

FIGURE 9.4.8

Moist heating process

To determine the required Delta Q, you must connect points “cooled air” and “supply” by a heating moist process of the same flow-rate as the “supply” process (Figure 9.4.8).

9.4.5 Plot on the psychrometric chart

Return to the simulator screen and open the psychrometric chart through the Chart/Simulator interface (Figure 9.4.9). Double-click in the box at the top left to select the desired chart type (here “Psychrometric”). Then come back to the interface and click “Update the point table”, which gives you the result displayed in Figure 9.4.9. The interface between the simulator and interactive charts

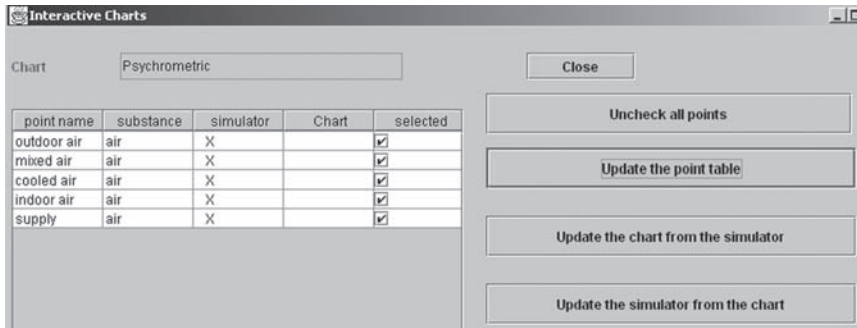


FIGURE 9.4.9
Simulator-chart interface

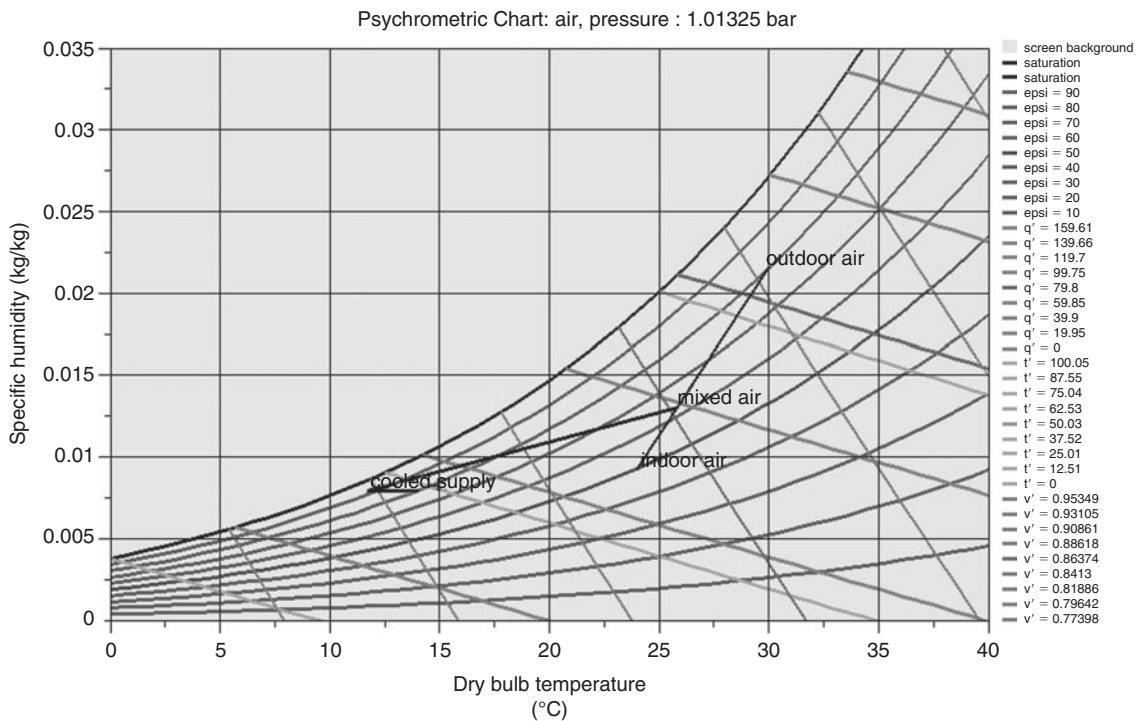


FIGURE 9.4.10
Cycle on the psychrometric chart

includes several fields and buttons, and a table showing the various points which exist in the project or which have been defined as points in the chart cycle editor (there are none here).

The first two columns show the name and substance of points. If a point is defined in the simulator, an “X” appears in the third column, if it belongs to a chart cycle, an “X” is displayed in the fourth.

Click “Update the chart from the simulator” to transfer the values of selected points from the simulator to the chart. Points are transferred by trying to put them as far as possible in the right order, but it may be necessary to reorder them correctly to get a nice plot. The cycle point editor is used to do this if necessary (refer to the chart reference manual if you need guidance). Finally, select “Connected points” in the “Cycle” menu. You get the result in Figure 9.4.10.

The air treatment cycle is shown in the chart, the air mixture being as it should be on the mix line that connects the indoor and outdoor air points.

General Issues on Cycles, Energy and Exergy Balances

Abstract: This chapter is composed of three main sections. The first discusses issues related to cycle analyses, and in particular what is meant by the notion of efficiency or effectiveness.

The second one explains how to establish enthalpy and exergy balances.

We will show in the third section that it is possible to automate the preparation of exergy balances, even for complex systems, by introducing a new type of diagram called by A. Valero (2000) a productive structure. This is a graph allowing us to represent the product or consumption of exergy of the various components in an energy system.

Note that all of section 10.3, devoted to productive structures, is intended for readers experienced in thermodynamics, and that therefore some of the examples that are presented correspond to cycles that will be dealt with in Part 3. We advise the reader not familiar with these cycles to refer to this third Part or to read section 10.3 only in a second reading of the text.

Keywords: Efficiency, effectiveness, enthalpy and exergy balances, productive structures.

10.1 GENERAL ISSUES ON CYCLES, NOTATIONS

As shown by the examples of Chapter 9, in many practical applications, such as in steam power plants, the fluid undergoes a series of processes that lead it to return in its original condition. This is called a cycle.

In some cases (internal combustion engines) exhaust gases are released into the atmosphere, so it is inappropriate to speak of a cycle. However, in a simplified approach to these processes, we can assume that the thermodynamic properties of the discharging fluid are the same as those of the incoming fluid, so that we can consider that the fluid flows through a partial cycle, the said open-cycle, which could be closed by a complementary dummy process, which then allows one to compare it to other closed cycles. By extension, we are used to talking of a cycle to describe the representation of the succession of changes undergone by thermodynamic fluids being involved in energy technologies.

10.1.1 Motor cycles

On Earth, the mechanical energy comes in two main forms:

- potential energy, mainly from the attraction of gravity, is that of a substance at rest in altitude: e.g. energy contained in water from a dam;
- kinetic energy is possessed by a moving substance: energy from wind, rivers etc.

Under these two forms available mechanical energy is far below the numerous needs of today's human societies, which correspond to transport (23% of the French energy balance), generation of electricity or farm machinery and industrial drives etc.

Only since the mid-eighteenth century did man become capable, thanks to the discoveries of Watt and Papin, of transforming heat into mechanical energy. Since then, considerable progress has been made in the development of engines, and technological developments continue apace, because of scientific advances and environmental constraints that continue to become stricter.

To convert heat into mechanical energy, in almost all cycles used, the working fluid is successively compressed and heated, and finally expanded. If the cycle is open, the fluid is then discharged in the surroundings, if it is closed, it is cooled and then compressed again. The various engines that are used differ by:

- the type of thermodynamic cycle used;
- the nature of the working fluid flowing through them;
- the types of hot source and compression and expansion devices used.

Different typologies can thus be established. Generally, there are:

- compressible fluid engines, where the fluid remains in the state of gas or steam throughout the cycle. In this case, a compressor is of course necessary. Depending on circumstances, the heat source used is the boiler or combustion chamber of an open cycle if the technical fluid contains oxygen (usually air);
- condensable fluid engines, in which the fluid changes state: at the condenser outlet, it is a liquid which is compressed by a pump, then heated and converted into steam in a boiler, steam which is then expanded in a turbine or piston engine. The compression work, proportional to the fluid specific volume, is much lower in these engines than in previous ones.

A distinction is also commonly made between:

- internal combustion engines, operating in an open cycle, where the heat source is a combustion chamber;
- external combustion engines, operating in a closed cycle, where the heat source is a boiler.

It is clear that these different categories overlap. For our part, we chose to present in Part 3 first the internal combustion engines: gas turbines and derivative engines (Chapter 12), gasoline engines and diesel engines (Chapter 13), then the external combustion engines: the Stirling engine (Chapter 14) and steam power plants (Chapters 16 and 17).

10.1.2 Refrigeration cycles

In a motor cycle, heat is provided to produce mechanical energy. A refrigeration cycle operates in reverse: it receives mechanical energy which is used to raise the temperature level of the heat.

Three types of refrigeration cycles are commonly used:

- refrigeration cycles (Chapter 19 of Part 3);
- heat pump cycles (Chapter 19 of Part 3);
- mechanical vapor compression cycles (Chapter 25 of Part 4).

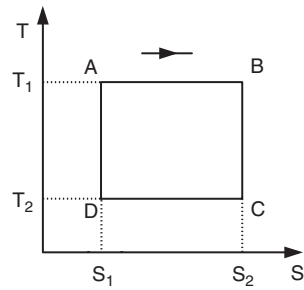


FIGURE 10.1.1
Carnot cycle

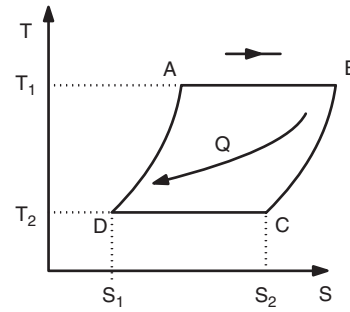


FIGURE 10.1.2
Regenerative cycle

The first two differ only by the levels of operating temperature and the desired effect. In refrigeration cycles, we try to cool a cold chamber, while a heat pump is used for heating.

10.1.3 Carnot cycle

Readers interested in a more detailed presentation of the Carnot cycle can refer to section 5.4.3 of this Part. It is known that the effectiveness of such a cycle is equal to $\eta = 1 - T_2/T_1$, if T_1 and T_2 are the temperatures of hot and cold sources (Figure 10.1.1).

This value corresponds to the maximum efficiency for a two-source machine, but the realization of a Carnot cycle presents many difficulties:

- firstly because in practice there must be some difference in temperature between the machine and the hot and cold sources during processes AB and CD;
- secondly because the realization of isothermal compression CD or isothermal expansion AB poses many technological problems.

We have indeed seen (section 5.3.6 of this Part) that for various reasons one is generally led to use stationary devices to exchange heat, and adiabatic machines to achieve compression or expansion.

The actual motor cycles thus significantly differ from the Carnot cycle, isotherms AB and CD being most often replaced by isobars or isovolumes. However, attempts of course are made for expansion BC and compression AD to approach isentropic.

10.1.4 Regeneration cycles

We can imagine cycles where the isentropic compression AD and expansion BC are replaced by other processes, each of them being deduced from the other by a translation in the entropy diagram (Figure 10.1.2). This is called regeneration.

In these circumstances, it is theoretically possible to make all the internal and external heat exchanges at constant temperature, and the ideal cycle with regeneration reaches the same efficiency as that of the Carnot.

In practice, the internal heat exchange is of course not at constant temperature, and we introduce the notion of regenerator effectiveness to characterize performance.

PRACTICAL APPLICATION

Improvement of a gas turbine performance thanks to regeneration

If its compression ratio is moderate, it is possible to increase the performance of a gas turbine by using a regenerator. An example is given in section 12.1.5.1 of Part 3. In this example, the main improvement is in efficiency (increase of about 70% with a regenerator of effectiveness equal to 0.83). A variant using a staged compression with intercooler would allow the capacity to be also improved.

Other examples of regenerative motor cycles are given in Part 3 (Stirling cycle Chapter 14, extraction and reheat steam cycle section 16.1.2).

10.1.5 Theoretical and real cycles

What essentially distinguishes cycles, are firstly the states (gaseous or liquid) in which the working fluid is likely to be, and secondly the nature of the changes it undergoes.

The study of heat engines allows, from the theoretical thermodynamic cycle analysis, to include all the constraints that one faces when trying to convert heat into mechanical or electric power, or vice versa mechanical energy in heating or cooling.

In practice, as we shall see, many technological difficulties arise, and real cycles often deviate significantly from the theoretical cycles we can calculate. The study of a particular machine thus depends heavily on the technical devices, especially mechanical and thermal, which are involved, and we will try in what follows to take into account these peculiarities as far as possible.

The presentation of theoretical cycles still is of great interest because they represent the thermodynamic reference, and determine the limits it is possible to achieve in terms of efficiency, for example. The study of cycles can thus effectively guide the engineer in his approach to improving engines.

10.1.6 Notions of efficiency and effectiveness

It may be helpful at this stage to specify what is meant by the notion of efficiency or effectiveness, although we have already used it several times.

In the general case, it is quite intuitive: for a heat engine aiming at converting heat into mechanical power, it is the ratio of the power output to the heat supplied to the machine: $\eta = \tau/Q_1$.

Difficulties arise because the terms “power output” or “heat supplied to the machine” may not have a single meaning.

Heat supplied

The hot source provides some heat energy Q_0 , determined by fuel flow rate and combustion conditions. We have seen that, even assuming complete combustion, the heat received depends on the enthalpy of condensation of water recovered. Generally, Q_0 is calculated relative to the lower heating value (LHV) of the fuel, which amounts to slightly underestimating its potential. When combustion is incomplete, things can get considerably complicated, as we showed in section 7.6.

Now suppose Q_0 is determined. In general, some of that heat escapes from the hot source, and is not transferred to the working fluid. These are losses by convection, conduction and radiation from the boiler or the combustion chamber, potential losses from flue gases etc. These losses can be characterized by a boiler efficiency η_{bo} equal to the ratio of heat supplied Q_1 to Q_0 .

Power output

The net power τ produced by the machine is by definition equal to the difference between the power delivered τ_d , and the internal power consumption τ_c , with agreement to positively express their values. If they are calculated algebraically it is equal to their sum.

τ_d is equal to the sum of the powers provided by the different shafts of the expansion devices, and τ_c to the total power consumed in the shafts of compression devices.

We call thermodynamic efficiency, or internal efficiency η_i , the ratio of power produced τ to Q_1 .

Power τ does not correspond entirely to that which is delivered by the engine because auxiliary equipment is necessary so that the whole system can work. Their role is to supply fuel to the engine, to provide lubrication and cooling etc.

In addition, a number of internal frictions must be overcome. One generally groups together as mechanical losses of all these levies on the available power, which drops accordingly. They may be represented by a mechanical efficiency η_m , the total efficiency being equal to the product of the latter by the internal efficiency defined above: $\eta = \eta_i \cdot \eta_m$.

In more general terms, when dealing with relatively complex cycles, one is led to adopt a broader definition of efficiency or effectiveness: it is the ratio of the useful energy effect to the purchased energy put in.

$$\eta = \frac{\text{useful energy effect}}{\text{purchased energy}}$$

This way of working is similar to that used in Thermoptim (section 6.3.1). It has the advantage of remaining valid in all cases for both motor cycles and refrigeration cycles. In the latter case, we no longer talk of efficiency but rather of COP coefficient of performance (see sections 19.3 and 20.1 of Part 3).

Note that some purists prefer to reserve the term efficiency for the Carnot efficiency, and recommend the use of effectiveness in other cases. We have not, however, given the wide use of the efficiency word in industry.

10.2 ENERGY AND EXERGY BALANCE

The performance analysis of various technologies discussed in this book leads in a conventional way to calculate their energy balances. We will also show the additional interest that building exergy balances may have, which poses no particular problem but needs to be done very carefully as otherwise errors can be committed.

In the sections dealing with the various applications, we will see how in practice the energy and exergy balances can be established, and how they differ. We limit ourselves here to present the principles, suggesting the reader wishing to deeper explore the question to refer to the literature, relatively abundant today, including the books of L. Borel and M. Moran cited in reference (Borel & Favrat, 1987, Moran, 1989).

This section being of general application for all cycles, we place it at the end of Part 2, before the various case studies to be presented in Parts 3, 4 and 5. Some cycles used to illustrate particular exergy balances will therefore be explained in other sections, to which the reader unfamiliar with them may refer. Note also that the introduction of exergy balance is a relatively difficult exercise which is available only to experienced energy engineers and scientists.

10.2.1 Energy balances

The general method described in section 5.3.5 of this Part shows how to establish an enthalpy balance. For a system in steady state (in which case we will restrict ourselves), it is simply to

recognize rates of heat flux, useful work and enthalpy at boundaries, and possibly in special cases like a combustion reaction (although this is in contradiction with the first law) to reintroduce a term of power generation in the volume. Thus, the general equation of balance for a control volume becomes:

$$\left\{ \begin{array}{l} \text{inward} \\ \text{transport by} \\ \text{the surface} \end{array} \right\} - \left\{ \begin{array}{l} \text{outward} \\ \text{transport by} \\ \text{the surface} \end{array} \right\} + \left\{ \begin{array}{l} \text{transfer} \\ \text{through} \\ \text{the surface} \end{array} \right\} + \left\{ \begin{array}{l} \text{generation} \\ \text{in the} \\ \text{volume} \end{array} \right\} = 0 \quad (10.2.1)$$

Building an energy balance does not generally pose a particular difficulty.

These balances are very useful and widely used, particularly in engineering and design departments. However, they have an important limitation: derived from the first law, they do not take into account the quality of energy, so that one kWh of electricity has the same value as one kWh of heat, and this irrespective of temperature level. To reflect this quality, we must add the state function introduced by the second law, entropy.

The theory of exergy, succinctly presented in section 5.5, provides a quite rigorous framework to quantify the thermodynamic quality of any system, open or closed, in steady-state or not. It is increasingly accepted as the preferred tool to compare and optimize thermodynamic cycles, thanks to exergy balances.

10.2.2 Exergy balances

Exergy depends on both the system state and the chemical composition of its elements. It differs from energy in that the latter is preserved while exergy is destroyed whenever irreversibilities exist. Since it is not a conservative quantity, equation (10.2.1) cannot be applied and a specific approach should be used.

Let us recall some results established in section 5.5. For an open multitherm system in steady-state traversed by a constant flow of fluid, which exchanges work and heat with n external sources at constant temperatures T_k , and the environment at temperature T_0 , the exergy equation (5.5.3) can be rewritten as:

$$\Delta x_{hi} = \tau - \Delta x_h + \sum_{k=1}^n x_{qk} \quad (10.2.2)$$

Δx_{hi} represents the exergy dissipation resulting from irreversibilities, τ the work received by the system, Δx_h the exergy variation of the fluid passing through it, $x_{qk} = \theta_k Q_k$ the heat-exergy or useful heat received from source at temperature T_k , $\theta_k = 1 - T_0/T_k$ being called the Carnot factor.

Equation (10.2.2) shows that the maximum work that an open system can provide is equal to the sum of heat-exergies of sources with which it exchanges heat, minus the change in exergy of the fluid passing through it and the exergy destroyed due to irreversibilities.

When the heat sources are no longer at constant temperature, when several shaft systems must be considered and the system is crossed by several fluids, equation (10.2.2) must be replaced by a more complicated one.

To calculate irreversibilities of each component j , it becomes (10.2.3):

$$\Delta x_{hij} = \sum_{k=1}^n x_{qjk} - m_j \Delta x_{hj} + \tau_j \quad (10.2.3)$$

If the heat exchange takes place at variable temperature:

$$x_{qk} = \int_{T_a}^{T_b} \left(1 - \frac{T_0}{T_k}\right) \delta Q_k \quad (10.2.4)$$

Assuming a linear variation of heat exchange function of T:

$$x_{qk} = \left(1 - \frac{T_0}{T_b - T_a} \ln \left(\frac{T_b}{T_a}\right)\right) Q_k$$

To calculate irreversibilities in a heat exchanger, simply add member by member (10.2.3) equations related to each fluid flowing through it. If it is adiabatic (no heat losses with the surroundings) heat-exergies are zero. As the useful work is zero, the irreversibility is equal to the sum of exergy variations of both fluids.

In section 5.5.5 we introduced the exergy efficiency of a system, always between 0 and 1, and higher than the irreversibilities are low. It is defined as the ratio of exergy uses to exergy resources. Exergy resources are the sum of all exergies that we had to provide to the cycle from outside. Exergy uses represents the net balance of the cycle, i.e. the algebraic sum of exergies produced and consumed within it.

If the system consists of components satisfying equation (10.2.3), this general definition is mathematically translated by equation (10.2.5):

$$\eta_x = 1 - \frac{\sum(\Delta x_{hij})}{\sum(\Delta x_{qj}^+) + \sum(\tau_j^+)} \quad (10.2.5)$$

The denominator represents the exergy provided, i.e. the sum of positive heat-exergies and useful work provided to the cycle. The numerator is the sum of the cycle irreversibilities.

10.2.3 Practical implementation in a spreadsheet

PRACTICAL APPLICATION

Exergy balance spreadsheet

For simple cycles, establishing an exergy balance poses no particular difficulty but needs to be done very carefully otherwise errors can be committed.

To facilitate this task, a spreadsheet, named ExerBalanceThopt.xls has been prepared for you. Downloadable from the Thermoptim-UNIT portal, it gathers a number of worksheets related to the examples illustrating Thermoptim use. It is complemented by a detailed methodological note which explains how to reuse Thermoptim result files.

In addition, the Diapason e-learning module S06En, which deals specifically with exergy balances, will guide you through your first steps, and modules S23En, S28En and S32En will help you build the exergy balance of a gas turbine, a steam plant or a vapor compression refrigeration machine.

In practical terms, and although the procedure is not yet automated within the package, the exergy balance of a cycle can be established in the following manner when it is modeled in Thermoptim:

- once the model is properly set and calculated the results file can be exported (line “Export exergy calculations” menu “Result files”). This is a text file that can easily be read in a spreadsheet, and in which different values are calculated for a number of point state functions (intensive variables) and the energy and exergy involved in processes;

- the first lines of this file can be copied into a spreadsheet prepared before. You should take care that the spreadsheet does not always recognize the thousands separator, and it may be necessary to make a global suppression of that separator (for this, copy the separator, select “Delete” from the menu “Edit” of the spreadsheet, paste the separator in the search field without putting anything in the replacement field, and then click” Replace All”);
- you must then carefully correct by hand the part of the worksheet that makes the exergy balance, as the lines for the different processes should be constructed differently (see below equations 10.2.6 and 10.2.7) depending on whether they relate to adiabatic expansion or compression or heat exchanges with the outside. For the latter, you must also specify the value of the source temperature.

Finally, you should take into account in $\Sigma(\tau_j^+)$ the powers supplied to the system from outside;

- if you only have the demo version of ThermoOptim you must slightly modify the spreadsheet to recalculate the exergies brought into play in the processes from the values calculated in the points screens and from the flow-rates involved, which must be copied one by one.

For simple processes, through which flows a fluid flow-rate m , equation (10.2.2) is rewritten as appropriate:

- for adiabatic processes ($Q = 0, \tau = m\Delta h$)

$$\Delta x_{hi} = m\Delta h - m\Delta x_h \quad (10.2.6)$$

- for processes without work and with heat exchange with a source at temperature T ($\tau = 0, Q = m\Delta h$)

$$\Delta x_{hi} = m\Delta x_h + \left(1 - \frac{T_0}{T}\right)m\Delta h \quad (10.2.7)$$

On the worksheet in Figure 10.2.1, the ThermoOptim result file appears in the upper part, and in the bottom the lines that need to be corrected. The connection between the lower and upper is made by the cell formulas, those in red should not be modified, except in special cases discussed below, while those in blue correspond to the mechanical power put into play, and those in black to heat exchange with outside sources. The important thing to check is first that each line applies to a suitable component (the order of processes in ThermoOptim file is unpredictable because it depends on that of their creation), and second the temperatures T_k are entered correctly. You should correct line by line the balance calculation by copying and pasting. Note in the example of Figure 10.2.1 that appears a process-point (“extraction”) that obviously does not participate in the exergy balance. We can remove it if desired, first from the lower and then from the upper part to avoid losing references and formulas.

In addition to this formatting of the bottom of the spreadsheet, it may be necessary to perform a number of changes, depending on the case treated. They are listed below.

First, mixers not being processes in ThermoOptim, they are not automatically included in the exergy balance of this worksheet. It is therefore necessary to add them by hand, equation (10.2.3) including only the variation of exergy within the component, since the mixer is adiabatic and without work.

For the combustion chambers, heat-exergy is replaced by the fuel exergy input. According to the authors, the literature indicates that the exergy of a fuel is close to its LHV or its HHV. These two values differing little, and given the fact that we seek to establish an approximate balance, we will follow those who equate it with its LHV available in ThermoOptim.

Another special case is non-closed cycles, in which the exergy entering the cycle and leaving it must be taken into account. The calculation of Δx_h must then be amended.

The example of the simple gas turbine given Figure 10.2.2 illustrates these two points. Here, the exergy entering and leaving the cycle is taken into account thanks to an extra line called “intake/

PROCESSES								
name	inlet poi	outlet poi	type	Delta_H	Delta_Xh	type_ener	flow rate	
compression 2	A	B	compressio	14.295664	14.31288	useful	1	
compression 1	1	2	compressio	2.5500864	2.5505656	useful	0.85	
HP turbine	3	4a	expansion	-417.4732	-454.2578	useful	1	
IP turbine	3c	4	expansion	-1029.872	-1208.666	useful	0.85	
condenser	4	1	exchange	-1951.709	-31.65426	other	0.85	
economiser	B	3a	exchange	1127.1161	494.9766	purchased	1	
extraction	4a	4a	exchange	0	0	other	0.15	
reheat	4a	3c	exchange	466.43689	275.51642	purchased	0.85	
superheater	3b	3	exchange	890.82009	523.33668	purchased	1	
vaporiser	3a	3b	exchange	898.27444	482.72377	purchased	1	
enthalpy balance				exergy balance				
component	dh	τ	Q	Tk	dxq	dxh	dxhi	% overall losses
compression 2	14	14				14	0	0%
compression 1	3	3				3	0	0%
HP turbine	-417	-417				-454	37	3%
IP turbine	-1030	-1030				-1209	179	13%
condenser	-1952		-1952	288.15	0	-32	32	2%
economiser	1127		1127	1600	924	495	429	32%
extraction	0		0			0	0	0%
reheat	466		466	1600	382	276	107	8%
superheater	891		891	1600	730	523	207	15%
vaporiser	898		898	1600	737	483	254	19%
mixer						-99	99	7%
cycle								100%
				sigma(xq+)			2773	
				sigma(tau+)			0.00	
energy efficiency		42.29%		exergy efficiency		52%		

FIGURE 10.2.1

Exergy balance of a reheat and extraction steam cycle

enthalpy balance				exergy balance				
component	dh	τ	Q	Tk	dxq	dxh	dxhi	% overall losses
compressor	443	443				402	40	7%
turbine	-761	-761				-796	35	6%
combustion chamber	890		890		890	619	270	47%
intake / exhaust						-225	225	39%
cycle								100%
				sigma(xq+)			890	
				sigma(tau+)			0.00	
energy efficiency		35.77%		exergy efficiency		36%		

FIGURE 10.2.2

Exergy balance of a simple gas turbine

exhaust”. It represents a very significant part of losses. When there is internal heat exchange, as is the case in combined cycles, the calculation of the exergy loss also needs to be amended as discussed above: it is equal in absolute value to the algebraic sum of the changes of exergy of the two fluids which exchange heat. Since there is internal exchange, it is obviously useless to calculate the related heat-exergy.

If you want to know the details of losses in the different internal exchangers, it is necessary to change the Δx_{hi} formula for fluids brought into play, by coupling the corresponding lines. If we simply make an overall balance, just sum up the overall exergy variation of all fluids.

For example, for the single pressure combined cycle of Figure 10.2.3, the following lines must be matched: lines HRSG 3 and below corresponding to the economizer, HRSG 2 and below to the vaporizer and HRSG 1 and below to the superheater. For clarity, it is of course possible to change the order of lines in the lower and higher parts of the worksheet so that the fluids matched are displayed together as shown in this figure.

component	enthalpy balance			exergy balance			% overall losses	
	dh	τ	Q	Tk	dxq	dxh		dxhi
HRS3 3	-101		-101			-50	15	5,96%
economizer	101		101			35		0,00%
HRS3 2	-91		-91			-57	10	3,80%
vaporizer	91		91			47		0,00%
HRS3 1	-52		-52			-37	8	2,93%
superheater	52		52			29		0,00%
feedwater pump	1	1				1	0	0,00%
turbine	-91	-91				-107	16	6,09%
condenser	-154		-154	288,15		-5	5	1,83%
air compressor	243	243				221	22	8,66%
gas turbine	-376	-376				-394	19	7,36%
combustion chamber	466		466		466	323	143	55,75%
intake / exhaust						-20	20	7,63%
						26		
cycle	90	-223	312			12	257	100%
				$\sigma(xq+)$		466		
				$\sigma(\tau+)$		0,00		
energy efficiency		47,76%	exergy efficiency		45%			

FIGURE 10.2.3

Exergy balance of a single pressure combined cycle

10.2.4 Exergy balances of complex cycles

Even using the spreadsheet above, building the exergy balance of a somewhat complicated system can be difficult in practice, and this for two main reasons:

- first, as many changes must be made to the spreadsheet, even though each is relatively simple, their number increases the risk of error;
- second, exergy balances being not conservative, there is no simple way to check the consistency of the result.

It turns out that it is possible to automate the preparation of exergy balances, even for complex systems, by introducing a new type of diagram called by Valero a productive structure. This is a graph allowing us to represent the product or consumption of exergy of the various components in an energy system.

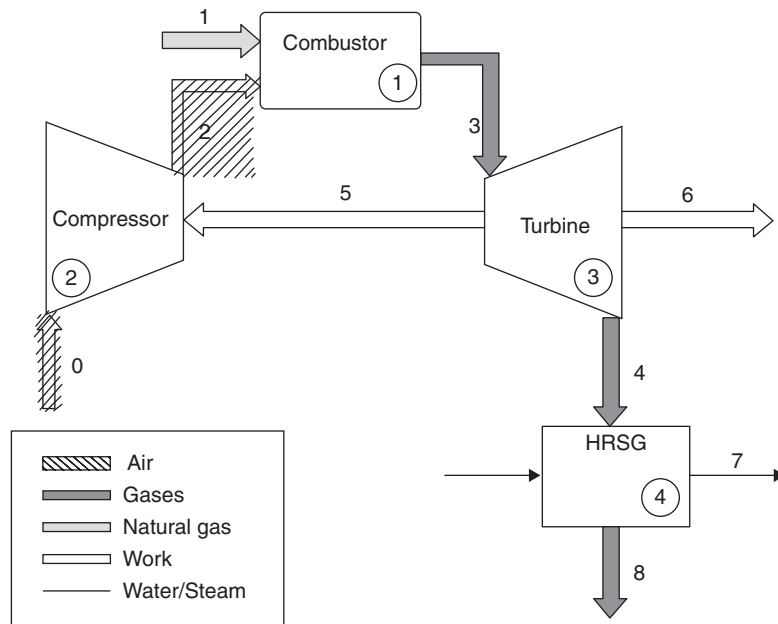
To avoid any misunderstanding, let us specify that it is of course quite possible to do without productive structures when building up exergy balances. However, as soon as the system studied becomes a bit complex, this is, as we have seen, a path strewn with obstacles, difficult to verify because these balances are non-conservative. The method we present, based on productive structures, proves a useful guide, which secures and simplifies the work to a very large extent. Indeed, productive structures:

- enable a very eloquent graphical representation of exergy flows in energy systems;
- can be largely automatically generated when one has a ThermoOptim diagram and its thermodynamic settings;
- facilitate and secure building up exergy balances;
- in addition lead to thermo-economic analyses for those who wish to perform.

10.3 PRODUCTIVE STRUCTURES

10.3.1 Establishment of a productive structure

For Valero, a productive structure is comprised of productive and dissipative units (PDU), junctions and branches. Each flow of different nature or cost is represented by a link at the location where it is distributed.

**FIGURE 10.3.1**

Physical sketch

Each PDU is characterized by its own product flow, but can also have other outlet flows or sub-products. To produce them, it consumes external resources or products provided by other units. At each junction, a product flow is obtained by summing up inlets of the same nature but from different origins.

10.3.2 Relationship between the diagram and the productive structure

The following example, presented in (Valero et al., 2000), shows how a productive structure is related to the physical sketch. It deals with a gas turbine used in a cogeneration plant (production of superheated steam at 20 bar), the cogeneration heat exchanger (HRSG) being modeled in a simplified way (Figure 10.3.1). The B_i are the exergy flows of the various streams (except for B_5 , which represents the mechanical power consumed by the compressor), the F_i are the exergy resources (fuels), and the P_i are the exergy products.

In this example, the heat exchanger is modeled globally. If it is represented as the coupling between two processes exchanging heat, we can consider that F corresponds to the exergy variation of the hot fluid, and P the exergy variation of the cold fluid. The heat exchanger balance stems from that.

The derivation of the productive structure from the physical diagram can be explained as follows: each PDU allows one to calculate the exergy balance of a component, following usual rules for exergy calculations: each unit gets “fuels” F_i which can be of three types (heat-exergy or chemical exergy, work, or exergy transfer from fluids which flow through it). One or several “products” P_i come out of it. These P_i are of two types (exergy variation of fluids which flow through it or work).

In a productive structure (Figure 10.3.2), the PDU are represented by rectangles, whereas lines which connect them correspond to the exergy flows which are exchanged: “fuels” at the inlet and “products” at the outlet. As an exergy flow can be distributed between several PDUs, it is necessary to introduce what we shall name pseudo-nodes to represent the exergy mixers and dividers. In the productive structure, the mixers (or junctions) are depicted as rhombs, and the dividers (branches) as circles.

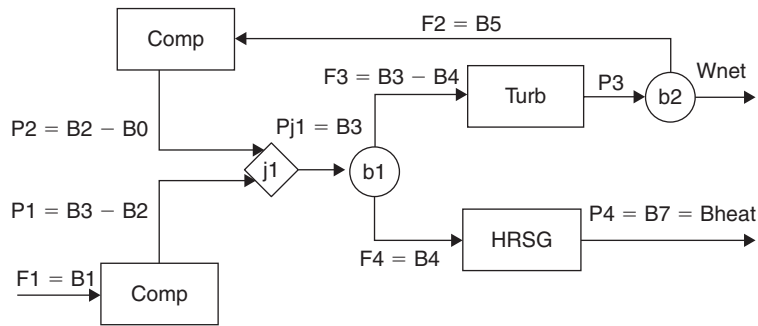


FIGURE 10.3.2
Productive structure

No.	Subsystem	Fuel	Product	Technical production coefficients
1	Combustor	$F_1 = B_1$	$P_1 = B_3 - B_2$	$k_{cp} = F_1/P_1$
2	Compressor	$F_2 = B_5 = W_{cp}$	$P_2 = B_2 - B_0$	$k_{cp} = F_2/P_2$
3	Turbine	$F_3 = B_3 - B_4$	$P_3 = B_5 + B_6 = W_{cp} + W_{net}$	$k_{gt} = F_3/P_3$
4	HRSG	$F_4 = B_4$	$P_4 = B_7 = B_{HEAT}$	$k_{HRSG} = F_5/P_5$
5	Junction	$P_1 = B_3 - B_2$ $P_2 = B_2 - B_0$	$P_{j1} = B_3$	$r_1 = P_1/P_{j1}$ $r_2 = P_2/P_{j1}$
6	Branching 1	$P_{j1} = B_3$	$F_3 = B_3 - B_4$ $F_4 = B_4$	
7	Branching 2	$P_3 = B_5 + B_6 = W_{cp} + W_{net}$	$F_2 = B_5 = W_{cp}$ $B_6 + W_{net}$	

FIGURE 10.3.3
Fuels and products

TABLE 10.3.1

	F		P				
	x_q^+	τ^+	Δx_h^+	Δx_h	τ	η_{exer}	Δx_{hi}
Compressor		B5		B2-B0		$(B_2 - B_0)/B_5$	$B_5 - (B_2 - B_0)$
Combustion	B1			B3-B2		$(B_3 - B_2)/B_1$	$B_1 - (B_3 - B_2)$
Turbine			B3-B4		$B_5 + \tau_{net}$	$(B_5 + \tau_{net})/(B_3 - B_4)$	$B_3 - B_4 - (B_5 + \tau_{net})$
HRSG			B4	B7		B_7/B_4	$B_4 - B_7$

At this stage, we should highlight that there is some subjectivity in the definition of the resources and products. This issue is debated in the exergy community, and we shall rely on Valero et al. (2000) and Kotas (1995), who explicitly say that every component is designed with a precise objective, which allows us to dismiss uncertainties (Valero speaks of “productive purpose” and Kotas of “desired output”). Once this objective is made explicit, we shall consider with Kotas that the exergy resources are the “necessary inputs” to provide the desired output. The exergy efficiency of the components is then what he calls the rational efficiency ψ , defined as the ratio of the exergies coming out of the system to the exergies entering it F_i , or as 1 minus the ratio between the irreversibilities and the F_i .

With these conventions, the expressions of the F_i and the P_i are given in Figure 10.3.3, and the exergy balances of the various PDUs in Table 10.3.1.

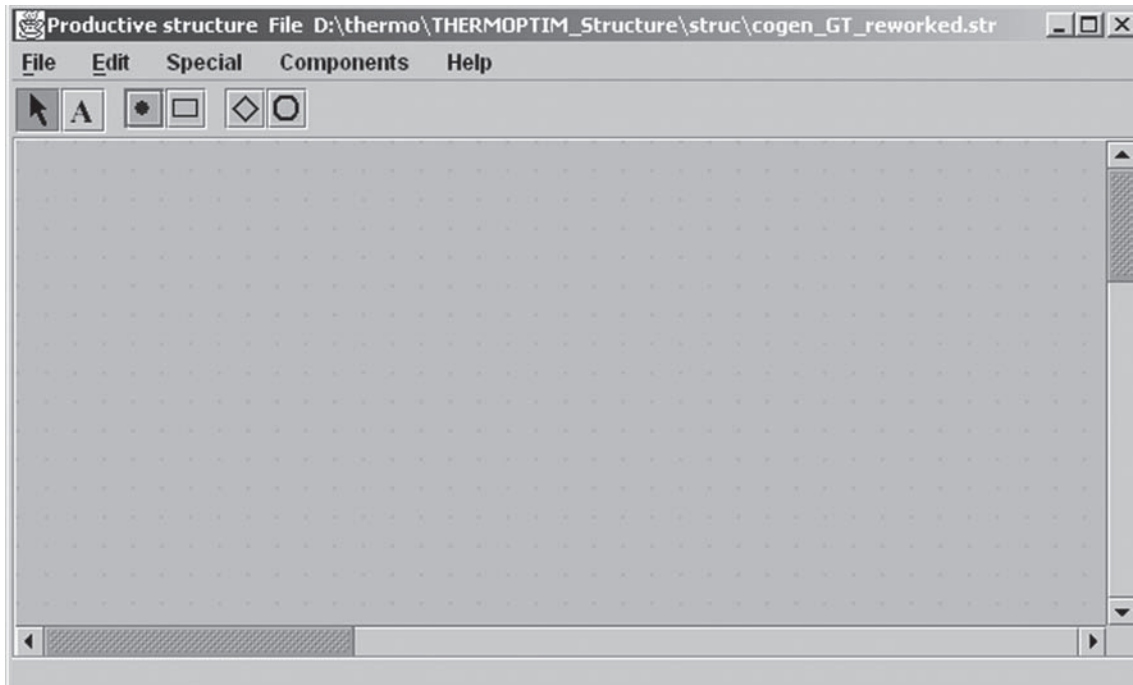


FIGURE 10.3.4
Productive structure editor





One should also note that purely dissipative units provide no product, so that their exergy efficiency is equal to 0.

According to Valero, the main limitation of the initial exergy cost theory was to define the productive structure from the same flows and components as those of the physical structure. This creates difficulties for the treatment of dissipative units and plant residues. Another challenge is to identify useful products as co-products or by-products.

Once the productive structure is known, the F_i can be expressed as a function of the P_i , as shown in Table 10.3.1: $F_i = k_i P_i$, k_i being the reciprocal of the component exergy efficiency. The thermoeconomic model is derived from that.

10.3.3 Implementation in ThermoOptim

A new editor with the various components used in the production structures has been developed¹ (Figure 10.3.4).

It is available from the Special menu screen of the simulator (Ctrl B). You find on the palette icons for processes-points  to represent the input and output flows, for productive or dissipative units , and for junctions  and branches .

You construct a productive structure either manually by selecting the icons on the palette, placing them on the work plan, and connecting them with links, analogous to the way a diagram is built, or by automatically generating the productive structure from the simulator and the physical diagram.

¹This version, still being developed, is available only on request.

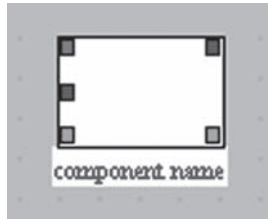


FIGURE 10.3.5
Productive unit

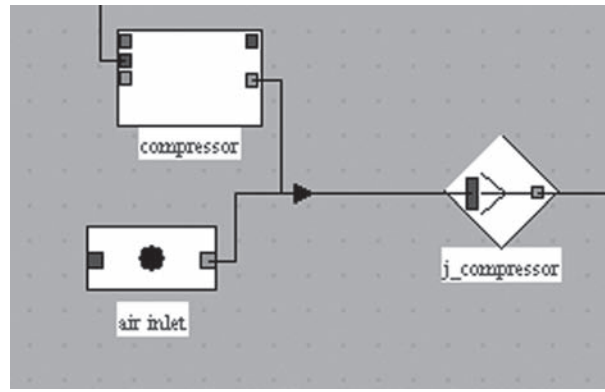


FIGURE 10.3.6
Provider component

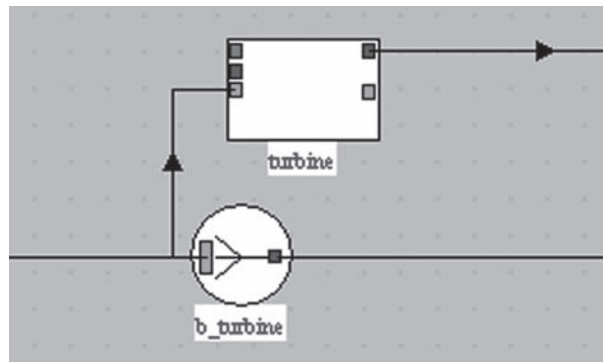


FIGURE 10.3.7
Receiver component

The exergy resources being of three possible types, and the products of two, a productive unit is represented by a rectangle with three inlet ports and two outlet ones (Figure 10.3.5), whose colors are differentiated in order to distinguish the various types of exergy flows and to allow to graphically separate resources and products.

The inlet port colors are the following: red for fuel, blue for mechanical power, and green for fluid exergy variation; the outlet port colors: blue for mechanical power, and green for fluid exergy variation.

The exergy flow values can be displayed on the links, which are colored similarly.

The exergy of a fluid going through a component can increase or decrease. If it increases, we say that the component is an exergy provider, if it decreases that it is an exergy receiver.

A provider is represented by a productive unit with an output junction, with two incoming links: the one going out of the green port of the productive unit (outlet exergy flow), and the one corresponding to the inlet exergy flow (Figure 10.3.6).

In this figure, the total exergy available at the outlet of pseudo-node “j_compressor” is the sum of two values: first the exergy flow at the inlet of the component, represented by process-point “air inlet”, and second the exergy variation of the fluid in the compressor, which receives it under a mechanical form. The pseudo-mixer or junction “j_compressor” is used to model this addition.

An exergy receiver is represented by a productive unit with a branch at the inlet, with two outgoing links: the one arriving at the green port of the PDU (inlet exergy flow), and the one corresponding to the outlet exergy flow (Figure 10.3.7).

On this figure, the total exergy available upstream of the turbine separates in two parts: first the one which is the turbine “fuel” and is converted under a mechanical form, and second the one which remains available at the turbine outlet. The pseudo-divider or branch “b_turbine” is used to model this division.

It should be noted that, for provider components (those for which $\Delta x_h > 0$), $P_i = \Delta x_h$. For turbines (for which $\Delta x_h < 0$) $P_i = \tau$. Throttlings being purely dissipative, $P_i = 0$.

10.3.4 AUTOMATION OF THE CREATION OF THE PRODUCTIVE STRUCTURE

It is possible to construct by hand with Thermoptim the productive structure of an energy system, but this is not the best way to operate if one knows the physical sketch, as is usually the case.

The productive structure can very well be inferred from the physical sketch (Thermoptim diagram) and thermodynamic parameters (Thermoptim project). Provided that the environment temperature T_0 is properly initialized, it serves to distinguish exergy provider and receiver components, and calculate the exergy balances of UPDs.

10.3.4.1 Creating the diagram

In a first step, we create all productive or dissipative units within the rules of correspondence mentioned above. Since it usually takes two icons for each component (the productive unit and the node), the diagram is expanded by multiplying the point coordinates by a certain factor, then the two icons are slightly offset so that they do not overlap, and finally all input and output exergy flows are connected. The names of pseudo-nodes are obtained by preceding those of the PDU by “j_” for joints, and “b_” for branches.

It should be noted that this way of working may result in the introduction of junctions in series and/or of branches in series, which may be grouped in order to simplify the productive structure. This happens when several providers or several receivers appear sequentially in the physical diagram. This is for instance the case when a phase change heat exchanger such as a steam generator is represented by three exchangers in series. Examples below illustrate this point.

Therefore, in a second step, pseudo-nodes in series are identified and can be grouped. In order to avoid errors, real nodes appearing in the physical structure are not automatically suppressed. This can be done by hand if it is deemed preferable.

Do not forget to connect to another node links from a divider removed or leading to a deleted mixer. It is also possible that the surplus PDUs may be removed from the productive structure. This is particularly the case of process-points connecting two nodes in the physical diagram, which are present only because nodes cannot be directly connected in Thermoptim, and have no reason to appear in the productive structure. If they have the same name as one of the two nodes, they are not linked. Otherwise, they must be removed by hand.

In a third step, we end up entering productive structure data, setting exergy balance screens presented below. For example, the blue exergy inputs (mechanical power) are not connected at this stage, as temperatures of outside sources with which heat-exergy is exchanged are not defined.

In Thermoptim the logical connection between the productive structure and the simulator is the component name. You should therefore give the PDU the same name as the corresponding simulator element.

10.3.4.2 Setting PDUs

Each productive unit allows one to open a component exergy balance screen, in which can be entered the settings which are required for calculating the exergy resources and products, as well as the component irreversibility and exergy efficiency (Figures 10.3.8 and 10.3.9).

FIGURE 10.3.8

Exergy balance of a turbine

FIGURE 10.3.9

Exergy balance of a exchange process with internal exchange

Once these settings are entered the component exergy balance can be calculated.

Double clicking the productive unit opens a screen which allows some settings in order to calculate component exergy resources and products, as well as irreversibilities and exergy efficiency, which, by shortcut, we denote by establishing the exergy balance of the component.

Figure 10.3.8 shows the screen of a turbine PDU whose exergy balance can be determined without specific settings: the exergy resource is provided by the fluid exergy variation (ΔXh^+), the product is the mechanical power (τ), and the exergy efficiency and irreversibilities are also determined.

When the component is of the exchange type (Figure 10.3.9), different possibilities exist.

- If it is a **fluid inlet or outlet**, which corresponds to a process-point connected only upstream or downstream, its total exergy (physical and chemical) must be taken into account. Note that this may influence the overall balance because the methods of calculating various exergy properties are not the same;

- If it is a **fluid outlet** rejected in the environment, the exergy is lost, which corresponds to an irreversibility. If on the contrary this exergy has an external value, it is an exergy product without irreversibility. The exergy calculation screen is provided with an option to specify this (Valuable exergy);
- When internal heat exchanges occur, as for instance in combined cycles, the exergy loss calculation must also be modified: it is equal, in absolute terms, to the algebraic sum of the exergy variations of both fluids exchanging heat. The component exergy balance screen has an option (Internal exchange) for this setting (Figure 10.3.8). We shall see later that, in the overall exergy balance, the exergy variations of both fluids are displayed between brackets, the two exchange processes being grouped next to one another for clarity (Figure 10.3.26);
- Lastly, when heat exchange takes place with an external energy source, the heat-exergy involved must be assessed, which requires knowledge of the source temperature. This information may be entered in the exergy balance screen. The exergy calculation screen is provided with an option to specify this situation (External Source), and a field for entering the source temperature.

For throttlings, the input exergy is the inlet relative exergy, and the output exergy the outlet relative exergy. The irreversibility is equal to their difference.

As exergy providers are represented by PDUs coupled to mixers, it is necessary to clearly distinguish these pseudo-mixers from the real ones which appear in the physical system, as the irreversibility in a real mixer may stem from different sources:

- reduction of a fluid pressure (pressure drop);
- mixing with composition change.

A table showing how the different ThermoOptim core components should be represented as PDUs can be found on the ThermoOptim UNIT portal.

External components can also be represented in a productive structure. You should refer to Volume 3 of the software reference manual for details on that.

Once a productive structure is built, the exergy balances of the various components may be calculated either one by one in their respective screens, or by opening, from the editor Special menu, a screen allowing to do it globally for the entire project, building a table whose rows correspond to each component, plus one for the whole system.

The latter gives as resource the sum of positive heat-exergies and useful work provided $\sum(\Delta x_{qj}^+) + \sum(\tau_j^+)$, as product the sum of the exergies leaving the system, the system exergy efficiency, and the sum of irreversibilities. Examples are given next section.

If the rules for building the exergy-balance adopted in ThermoOptim do not give satisfaction, the user can export it in order to modify it in a spreadsheet.

10.3.5 Examples

10.3.5.1 Steam cycle example

The diagram of the facility has been presented section 9.1, and the value of key parameters are given in Figure 9.1.19. To create the productive structure, open the editor screen (Special menu of the simulator), then select the line “Diagram transfer” of the Special menu of the editor. The productive structure you get is given Figure 10.3.10.

Two dividers and three mixers are in series. Select the line “Suppress nodes in excess” and select, for dividers and mixers, the option “OK (except the physical model)”. The productive structure becomes that of Figure 10.3.11.

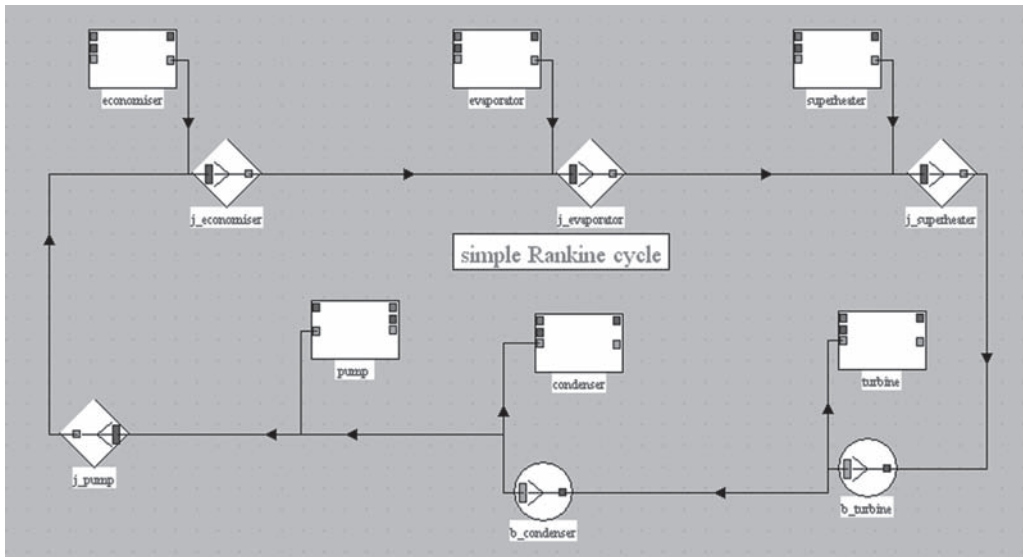


FIGURE 10.3.10
Automatically generated productive structure of a steam cycle

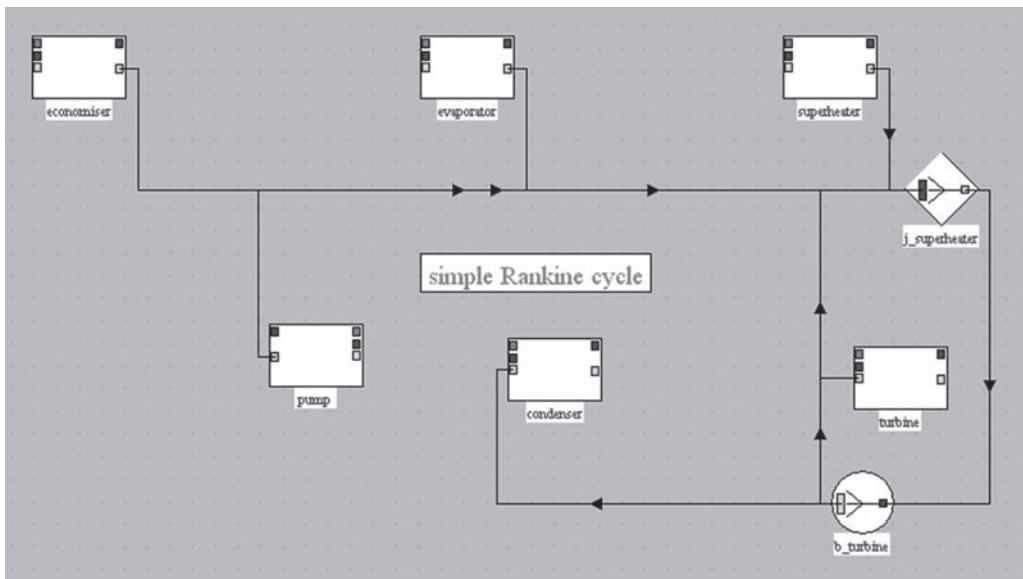


FIGURE 10.3.11
Productive structure of the steam cycle, excess nodes removed

Rework the structure for better readability, by shifting components from left to right or right to left. Result you get is close to that of Figure 10.3.12.

This diagram is not yet completely set. If we try to build the full project exergy balance, we obtain the result in Figure 10.3.13.

The last column, titled “settings”, gives some summary information on the settings considered: the pump is an external exergy input, because it is not connected to the turbine and the condenser and the boiler are considered to be exchanging heat-exergy with a source at 0°C, which is obviously absurd.

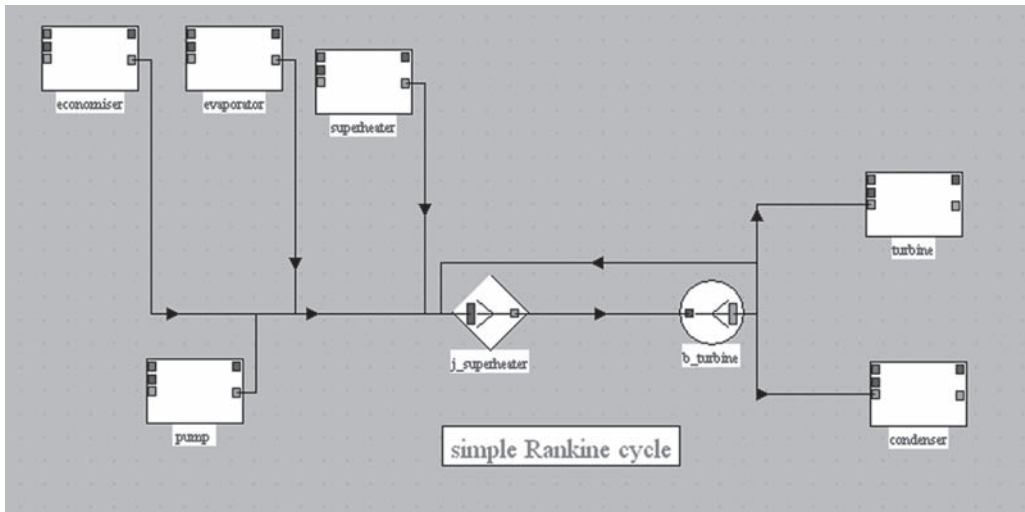


FIGURE 10.3.12
Productive structure of steam cycle, slightly reworked

component	Resource	Product	Exergy efficiency	Irreversibilities	% total	settings
turbine	1,556.221	1,326.014	0.852073	230.207	-0.1667	
pump	16.797	16.47	0.980537	0.3269	-0.0002367	compr
economiser	0	566.951	0	-653.216	0.473	Tk = 0 °C
evaporator	0	482.724	0	-532.052	0.3852	Tk = 0 °C
superheater	0	523.337	0	-572.256	0.4143	Tk = 0 °C
condenser	33.261	-112.617	-3.38589	145.878	-0.1056	Tk = 0 °C
global	16.797	2,786.409	83.224	-1,381.112	1	

FIGURE 10.3.13
Exergy balance before setting

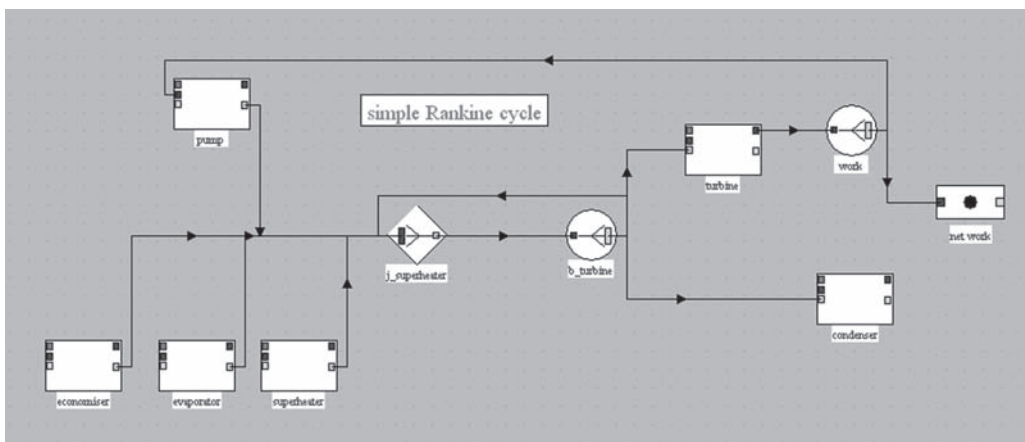


FIGURE 10.3.14
Productive structure of steam cycle with mechanical coupling

In the productive structure, the mechanical coupling between the turbine and the pump is missing. We represent it by a divider at the turbine outlet, with two branches, one representative of this coupling, and the other of the net power available (Figure 10.3.14).

This productive structure is interpreted as follows: the steam power plant is a machine which receives an external exergy input in the boiler, and by internal recycling, exergy is provided to the pump, which are the two production units in the left of the screen.

component	Resource	Product	Exergy efficiency	Irreversibilities	% total	settings
pump	16.797	16.47	0.980537	0.3269	0.0002261	
turbine	1,556.221	1,326.014	0.852073	230.207	0.1592	
economiser	1,287.979	566.951	0.440186	721.028	0.4988	Tk = 1,326.85 °C
evaporator	736.501	482.724	0.655429	253.777	0.1755	Tk = 1,326.85 °C
superheater	730.389	523.337	0.716518	207.052	0.1432	Tk = 1,326.85 °C
condenser	33.261	0	0	33.261	0.02301	Tk = 15.00 °C
global	2,754.869	1,309.217	0.4752	1,445.652	1	

FIGURE 10.3.15

Exergy balance of the full project

enthalpy balance				exergy balance				
component	dh	τ	Q	Tk	dxq	dxh	dxhi	% overall losses
condenser	-2051		-2051	288.15	0	-33	33	2%
superheater	891		891	1600	730	523	207	14%
evaporator	898		898	1600	737	483	254	18%
economiser	1571		1571	1600	1288	567	721	50%
pump	17	17				16	0	0%
turbine	-1326	-1326				-1556	230	16%
cycle	0	-1309	1309			0	1446	100%
				sigma(xq+)		2755		
				sigma(tau+)		0.00		
energy efficiency		38.97%	exergy efficiency		48%			

FIGURE 10.3.16

Exergy balance of the steam cycle calculated with the spreadsheet

This exergy is partly converted into mechanical form in the turbine and partly dissipated in the condenser. The net work is the fraction of mechanical power not recycled.

To end up building the productive structure, we still have to set the temperature of outside sources with which heat-exergy is exchanged, i.e. the boiler and condenser. We will respectively choose 1600 K (1326.85°C) and 288.15 K (15°C).

To enter these values, double-click the PDU concerned or their line in the overall exergy balance screen, and enter them into the field “Source T (°C)”. Then save the productive structure.

The exergy balance of the full project is given in Figure 10.3.15, the environment temperature T_0 being recalled in the top right (it is editable in the Global Settings screen of the simulator).

With some minor differences related to how the exergy of the fluids are calculated, it leads to the same values as calculated by the spreadsheet (Figure 10.3.16).

10.3.5.2 Example of a refrigeration cycle

The diagram of the facility has been presented section 9.2, and the value of key parameters are given in Figure 10.3.17. To create the productive structure, open the editor screen (Special menu of the simulator), then select the line “Diagram transfer” of the Special menu of the editor. The productive structure you get is given Figure 10.3.18.

Four dividers are in series. Select the line “Suppress nodes in excess” and select option “OK (except the physical model)”. The production structure becomes that of Figure 10.3.19.

Rework the structure for better readability, by shifting components from left to right or right to left. The result you get is close to that of Figure 10.3.20.

This productive structure is interpreted very simply: the refrigerating machine receives an external exergy input in the compressor. This exergy is partly converted into the evaporator (refrigeration effect), the rest being dissipated in the condenser and the expansion valve (throttling).

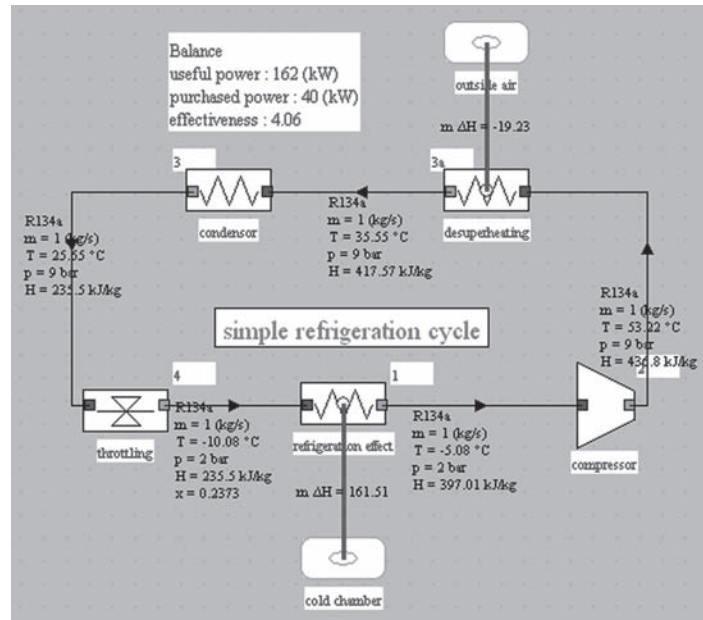


FIGURE 10.3.17
Physical diagram of refrigeration cycle

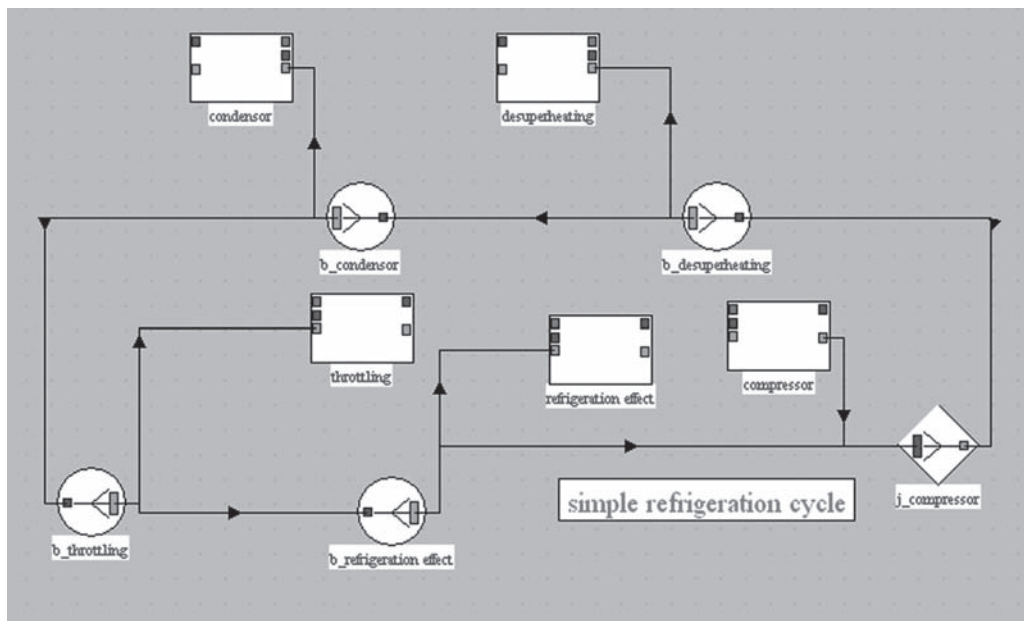


FIGURE 10.3.18
Automatically generated productive structure of a refrigeration cycle

This diagram is not yet completely set. If one tries to build the full project exergy balance, we obtain the result in Figure 10.3.21.

The last column, titled “settings”, gives some summary information on the settings considered: the compressor is an external exergy input, and the condenser and evaporator are considered to be exchanging heat-exergy with a source at 0°C, which is obviously absurd.

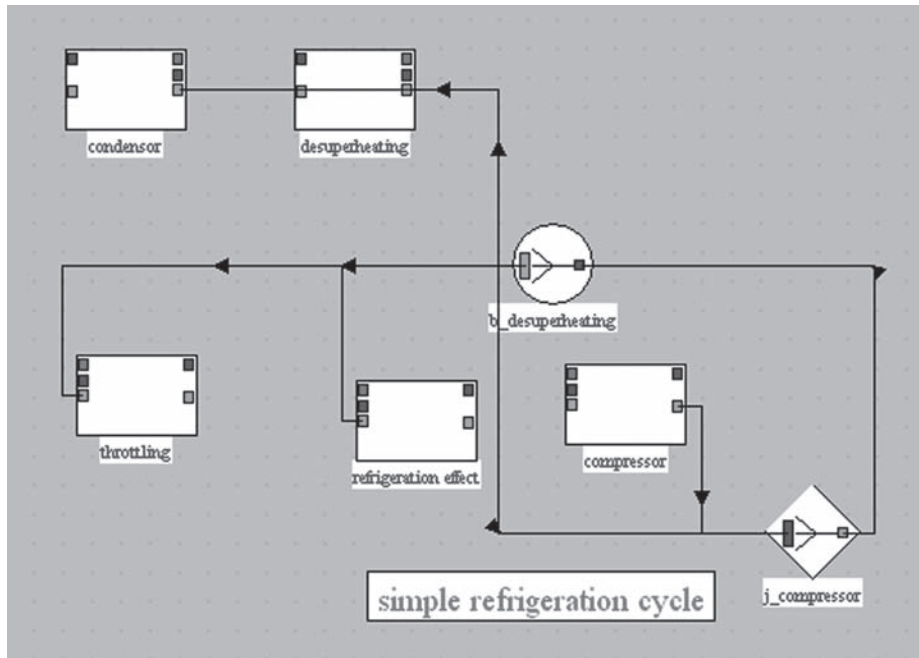


FIGURE 10.3.19
Productive structure of the refrigeration cycle, excess nodes removed

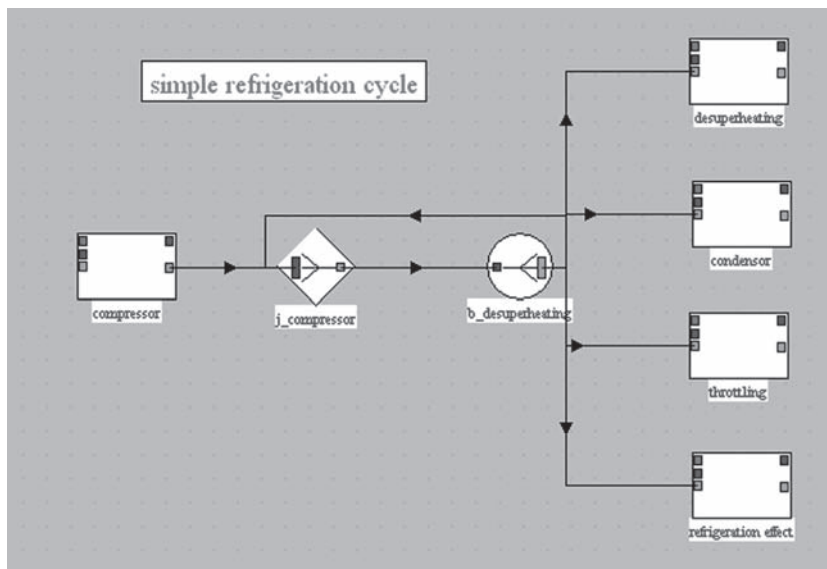


FIGURE 10.3.20
Productive structure of refrigeration cycle, slightly reworked

To end up building the productive structure, we still have to set the temperature of outside sources with which heat-exergy is exchanged, i.e. the evaporator and condenser. We will respectively choose 270.15 K (-3°C) and 288.15 K (15°C).

To enter these values, double-click the PDUs concerned or their line in the overall exergy balance screen, and enter them into field “Source T ($^{\circ}\text{C}$)”. Then save the productive structure.

component	Resource	Product	Exergy efficiency	Irreversibilities	% total	settings
throttling	4.024	0	0	4.024	0.1992	
compressor	39.797	32.845	0.825308	6.952	0.3441	compr
desuperheating	1.681	-1.056	-0.628162	2.738	0.1355	Tk = 0 °C
refrigeration eff...	15.358	8.869	0.577504	6.489	0.3212	Tk = 0 °C
global	39.797	7.813	0.4923	20.203	1	

FIGURE 10.3.21

Exergy balance before settings

component	Resource	Product	Exergy efficiency	Irreversibilities	% total	settings
throttling	4.024	0	0	4.024	0.1386	
compressor	39.797	32.845	0.825308	6.952	0.2394	compr
desuperheating	1.681	0	0	1.681	0.05789	Tk = 15.00 °C
condensor	11.782	0	0	11.782	0.4058	Tk = 15.00 °C
refrigeration eff...	15.358	10.761	0.700701	4.597	0.1583	Tk = -3.00 °C
global	39.797	10.761	0.2704	29.036	1	

FIGURE 10.3.22

Exergy balance of the full project

component	enthalpy balance				exergy balance				% overall losses
	dh	$\dot{\tau}$	Q	Tk	dxq	dxh	dxhi		
refrigeration effect	162		162	270.15	-11	-15	5	16%	
condensor	-182		-182	288.15	0	-12	12	41%	
desuperheating	-19		-19	288.15	0	-2	2	6%	
compressor	40	40				33	7	24%	
throttling	0	0				-4	4	14%	
cycle	-162	40	-201			0	29	84%	
				sigma(xq+)		0			
				sigma(tau+)		39.80			
energy efficiency		4.06	exergy efficiency		27%				

FIGURE 10.3.23

Exergy balance of the refrigeration cycle calculated with the spreadsheet

The exergy balance of the full project is given in Figure 10.3.22, the environment temperature T_0 being recalled in the top right (it is editable in the Global Settings screen of the simulator).

It leads to the same values as calculated by the spreadsheet (Figure 10.3.23).

These two examples are relatively simple: their main interest is to illustrate the procedure for establishing productive structures and exergy balances associated.

10.3.5.3 Example of the cogeneration gas turbine

We have modeled in Thermoptim the example proposed by Valero, and we set it the best possible given the values that we could estimate. The diagram and parameter values are given in Figure 10.3.24.

The production structure that we built is given in Figure 10.3.25. It corresponds to the diagram provided by Valero, with the proviso that we represented the air inlet and detail of the cogeneration exchanger.

This production structure is interpreted as follows: the gas turbine receives a chemical exergy supply from the fuel, and by internal recycling, exergy is provided to the compressor. This exergy is converted partly into mechanical form in the turbine and partly into heat in the recovery steam generator HRSG, the remainder being dissipated by discharge into the atmosphere. The net work is the fraction of mechanical power not recycled.

The exergy balance of the full project is given Figure 10.3.26.

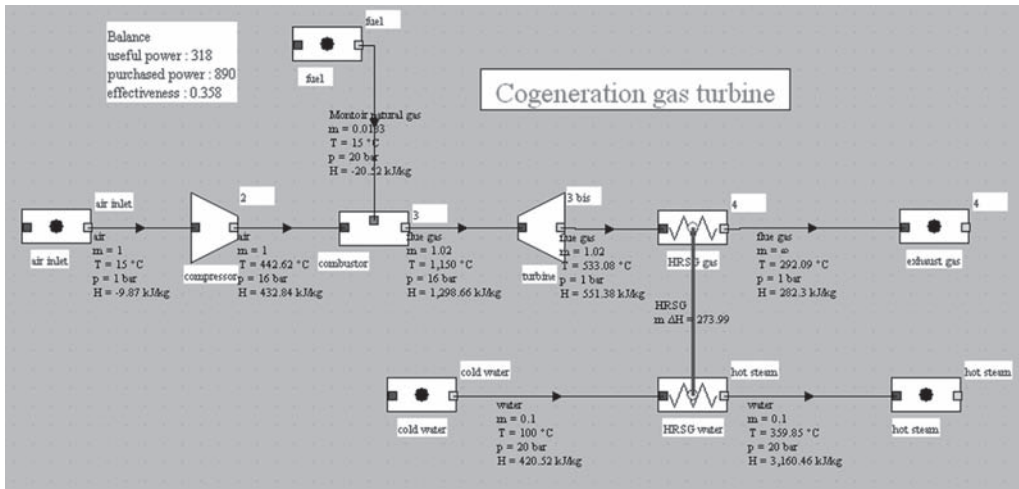


FIGURE 10.3.24
Physical diagram of the cogeneration gas turbine

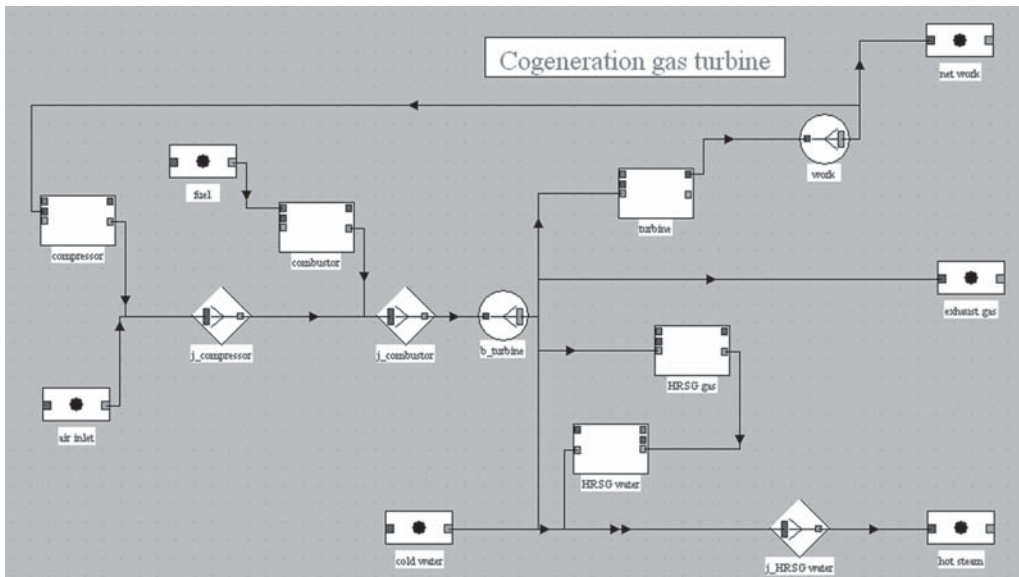


FIGURE 10.3.25
Productive structure in Thermoptim

component	Resource	Product	Exergy efficiency	Irreversibilities	% total	settings
fuel	897.041	0	0	0	0	
compressor	442.713	402.238	0.908574	40.476	0.08269	
turbine	796.411	760.935	0.955456	35.475	0.07248	
combustor	0	613.556	0.683978	275.989	0.5639	
cold water	4.593	0	0	0	0	
hot steam	114.66	114.66	0	0	0	
HRSG gas	157.841	0	0	(157.841)	(0.3225)	HRSG
HRSG water	0	110.067	0	(-110.067)	(-0.2249)	HRSG
exhaust gas	0	0	0	89.749	0.1834	loss
global	901.634	432.882	0.4571	489.463	1	

FIGURE 10.3.26
Exergy balance of the full project

10.3.6 CONCLUSION

The great advantage of this approach is that the exergy balances are automatically built, while the spreadsheet calculations are asking us each time to take great care if we are to avoid mistakes.

Indications in the last column of the full exergy balance allow one to easily verify the setting of the productive structure, and thus reduce the risk of error.

Note that once the exergy balances of the various components are evaluated, it is possible to display the values of exergy flows on the productive structure.

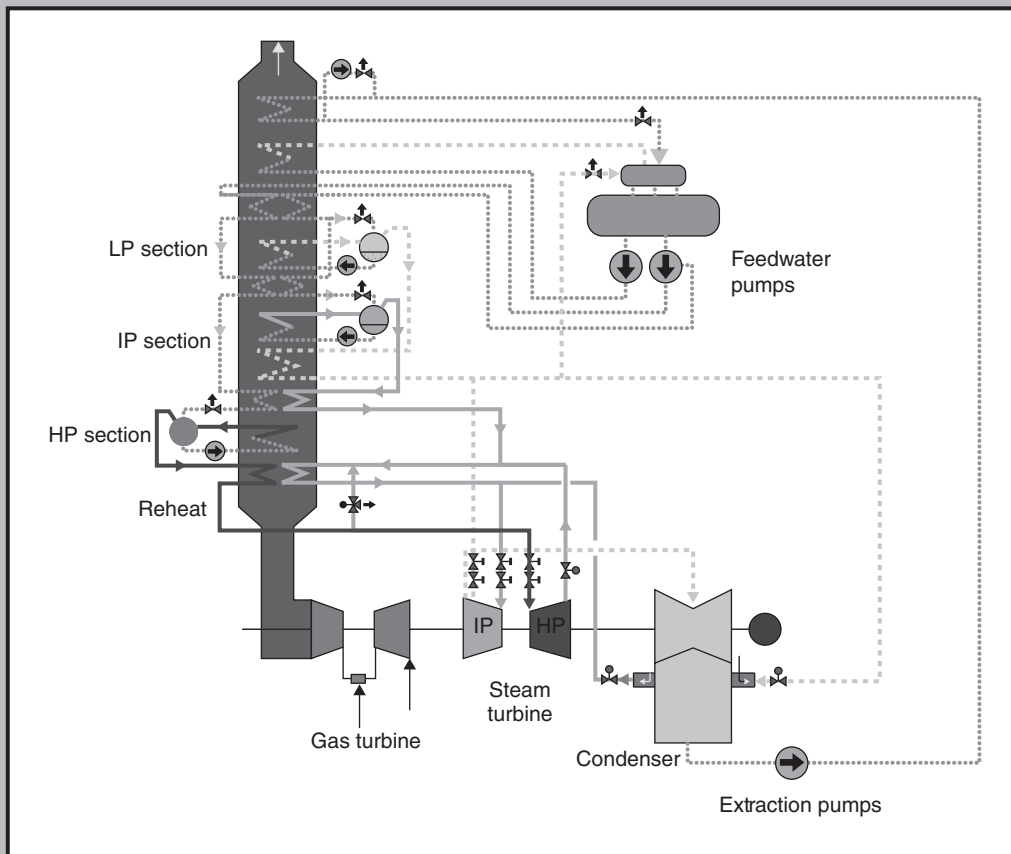
REFERENCES

- A. Bejan, G. Tsatsaronis, M. Moran. *Thermal design and optimization*, Wiley publishers, 1996.
- L. Borel. *Introduction aux nouveaux bilans énergétiques*, Entropie n° 153, 154, Paris, 1990.
- L. Borel, D. Favrat. *Thermodynamique et énergétique*, Presses Polytechniques Romandes, Lausanne, Vol. 1 (De l'énergie à l'exergie), 2005, Vol. 2 (Exercices corrigés), 1987.
- T.J. Kotas. *The Exergy Method of Thermal Plant Analysis*, 2nd edition, Krieger Publishing Company, USA, 1995.
- A. Lallemand. *Thermodynamique appliquée: Bilans entropiques et exergétiques*, Techniques de l'Ingénieur, Traité Génie énergétique, BE 8 008.
- M. Moran. *Availability analysis: a guide to efficient energy use*, Prentice Hall, New York, 1989.
- A. Valero, L. Serra, J. Uche. *Fundamentals of thermoeconomics*, Lectures 1–3, Euro summer course on sustainable assessment of clean air technologies, 3–8 April 2000. Lisbon. Centro Superior Tecnico, available from CIRCE, Research Center for Energy Resources and Consumption: [http://teide.cps.unizar.es:8080/pub/publicir.nsf/codigos/0153/\\$FILE/cp0153](http://teide.cps.unizar.es:8080/pub/publicir.nsf/codigos/0153/$FILE/cp0153).

This page intentionally left blank

3

Main Conventional Cycles



Part 3 discusses how the foundations laid in the first two Parts can be applied to main conventional cycles

This page intentionally left blank



Introduction: Changing Technologies

Abstract: The energy sector is generally considered technologically mature and not prone to experience severe and rapid technological developments, because on the one hand the rigidity of its sectors and secondly the long lifetime of the equipment used. One might therefore conclude that technological innovation can play only a secondary role in the global energy problem. The analysis of changes over last 30 years shows that this is not true and on the contrary that technological innovation could be the key to our energy future. During this period, many limits thought impassable were exceeded, and many records established.

Advances in exploration and oil production have led to exploitation of new deposits in countries outside OPEC. The new oil supplies and reductions in consumption due to various substitutions and savings made have played a decisive role in turning the oil market as experienced in 1986.

The development of combined cycles allows countries to produce electricity with an efficiency approaching 60% today, while 40% seemed economically unattainable before, and through energy efficiency, energy intensity, which represents the energy needed to produce one unit of GDP, fell by 30% in 20 years in France and in many OECD countries.

Meanwhile, the unit quantities of pollutants from energy processing and use equipment fell sharply, and this trend should continue in the future. Even when international energy prices were relatively low, the development of new energies such as controlled fusion, fuel cells, solar technologies etc. continued around the world.

Keywords: technological innovation, reserves, resources, exploration, production, environment, ozone layer, greenhouse effect.

From the control of fire to that of the atom, the development of human societies has been largely based on the conquest of power. In all countries, energy has gradually become one of the essential factors of economic and social development, as well as capital, labor and natural resources, and which no one can now do without.

After decades during which cheap energy was flowing smoothly, forty years ago we entered a period where crises have become the rule. This change in the energy landscape is particularly worrying because the impact of energy crises on human societies is now considerable: economic recession, rising unemployment due to oil price shocks, shortages of traditional fuels due to fuelwood crisis, rupture of the ozone layer, increasing greenhouse effect and acid rain due to energy releases.

While one might have thought that the energy sector would know only limited and slow technological developments, dramatic changes have occurred in recent decades, the movement being far from over. In this chapter we will try to highlight the reasons behind this apparent paradox by considering briefly the overall context in which energy technologies are inserted, which is marked by a number of characteristics:

- Many technology solutions are in strong competition for engines, used in particular for propulsion and power generation. The choice depends on several criteria, as of course the specific type of use, energy sources available and their cost, emission regulations etc. The main problems concern the availability of fuel, ECT efficiencies and control of combustion conditions, which determine the emission of pollutants. The growth of electricity remaining very important in the world (often much higher than that of Gross Domestic Product (GDP)), the needs are considerable, both for centralized and decentralized units;
- for refrigeration cycles, two technologies compete: mechanical vapor compression and liquid absorption. The second remaining still quite marginal, it will be reviewed here only briefly. The main problem encountered for vapor compression cycles is that the vast majority of them used until recently refrigerants that destroy the ozone layer, now banned by international agreements;
- Energy being ubiquitous in modern societies, the financial stakes are considerable. The competition is very open as many technological solutions exist to satisfy a given final energy need.

Even if it is sometimes eclipsed for the general public by other topics, energy plays such an important role in today's society that it will remain a key concern in terms of strategy, economy and environmental protection, in both industrialized and developing countries.

First, the geopolitical context of energy and especially oil is such that chronic tension risks will persist much longer in terms of supply, as shown by the Gulf crisis in 1990 and the recent oil shock.

Furthermore, in terms of overall energy use, the various scenarios all agree to predict a sharp increase in energy demand, except in case of very rapid diffusion of best technologies (this hypothesis remains somewhat unlikely due to existing fleets and barriers to technology transfer).

Finally, and even in the absence of any threat to supplies, the deepening and especially the globalization of environmental damage caused by fossil fuels (greenhouse effect, acid rain, depletion of the ozone layer), could undermine the foundations of the global energy system (90% of global energy contributes to CO₂ emissions).

So energy supplies remain in a constant vulnerable situation, which justifies further action to increase the supply (fossil fuels, nuclear, renewable energies). But it is equally essential to intensify efforts to control demand and to enter now the transition to a redeployment of the energy mix that will prevail during this century.

The real solution can only come from the development of first technologies allowing to reduce the ECT consumption and hence the level of pollution by source, and secondly, at least in the medium term, of clean renewable energies competitive with fossil fuels.

If you look at what were the main drivers of technological changes in recent decades, three points should be developed specifically.

1.1.1 LIMITATION OF FOSSIL RESOURCES AND GEOPOLITICAL CONSTRAINTS

The first driver (at least chronologically) was the limited fossil fuel resources and their uneven distribution in the world, that make their availability random and thus justify the search for alternatives.

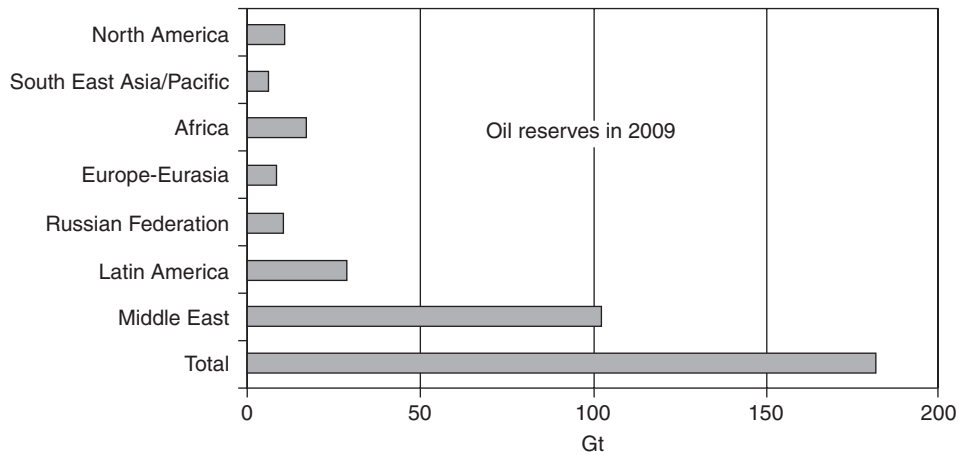


FIGURE 11.1.1

Proved oil reserves

The analysis of **energy reserves and resources** allows us to estimate how long fossil fuels will be used globally or by region. It is however important to bear in mind that the concept of reserves is essentially dynamic: they vary over time depending on the one hand on economic conditions, and secondly on exploration and production activity. The notion of resource is more blurred, as it may include not only future production, but also past production (ultimate resources).

The proven **oil** reserves were estimated late 2009 (Figure 11.1.1) at about 180 billion tons, nearly 42 years of production (R/P). It is important to note that today the recovery rates hardly exceed 34% on average and it is believed that technical progress leading to an improvement of 1 point of this factor would result in extra reserves of 5.5 Gt, i.e. nearly two years of current world consumption.

Given the strategic importance for the medium and long term of synthetic hydrocarbons production, it is important to estimate the reserves corresponding to non-conventional oil. We include in the latter heavy and extra heavy oils (API density below 20° and 10°), tar sands and oil shale. According to some experts, the reserves for these energy sources are the same as those of conventional oil.

Proven reserves of natural gas were estimated 185,000 billion m³ at the end of 2009, or about 170 billion toe (tons oil equivalent), that is to say slightly less than oil reserves, with a R/P ratio of about 60 years.

The **proven coal reserves** are estimated at slightly less than 850 Gt, or about 530 Gtoe, with a R/P ratio of 133 years. Perhaps more than any other form of fossil energy, recoverable reserves of coal will depend on **technological progress**. The long-term issues of coal liquefaction and gasification are such that we can expect significant breakthroughs in the years to come.

Uranium reserves are very difficult to estimate both given the differences in conversion efficiency by technology, and lack of reliable data in some areas. We can consider that, with the current nuclear reactors, they correspond to about 35 Gtoe, or just under a quarter of proven reserves of oil or natural gas, or almost 60 years of electricity production.

Figure 11.1.2 summarizes the current non-renewable energy reserves.

On the basis of these figures, it is possible to show that for several decades or even over a century we have enough fossil fuel to meet worldwide demand. There is no problem in the immediate global availability, but the uneven geographical distribution of reserves is likely to lead any time to pressure on supplies. In addition, of course, qualities and costs of these energies are highly variable depending on the case.

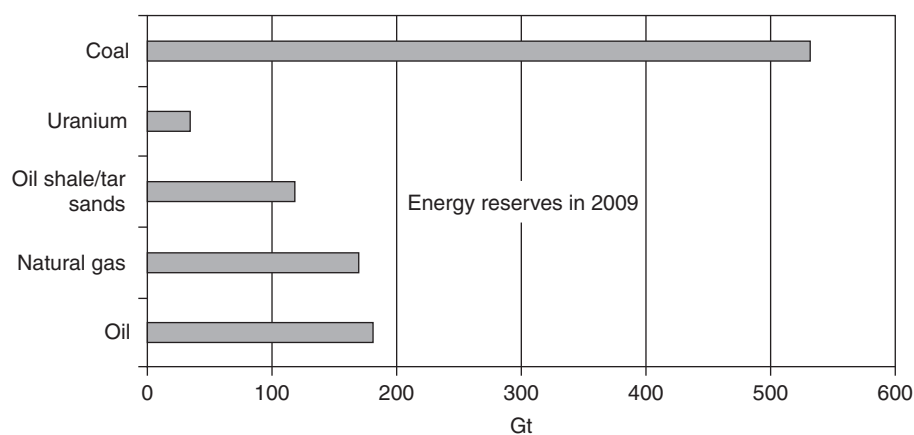


FIGURE 11.1.2

World energy resources

Exploration and production in the oil sector

After the first oil shock, oil companies have invested heavily (increased budgets for R&D by factors of up to 4) in programs to diversify oil supplies in a timely manner, which enabled them to discover new fields outside OPEC and develop quite remarkable new technologies, as for example in off-shore fields.

In 1986, as prices have fallen, oil companies have had to face another challenge: the additional costs acceptable before were no longer. However, as the effectiveness of technological innovation had been demonstrated, the R&D programs have generally not been questioned: they have been redirected to the new goal that was the reduction of costs to maintain and renew oil production outside OPEC. The new oil shock of course puts in question the agenda of all the technological advances in the oil and gas sectors.

In exploration-production, this resulted in the development of the most promising technologies among those which had previously been developed, such as:

- **3D seismic** enabling:
 - First in exploration, with a much better representation of the ground, to reveal new structures and to drill with success rates well above the standards before;
 - secondly in development, a better appreciation of the flow physical properties and the nature of the fluids contained in reservoirs;
 - finally in production, to better follow the evolution of the field and guide the drilling of complex track and large deflection wells, leading to a sharp increase in the recovery rate.
- **drilling tools and techniques**, that have evolved in recent years, with:
 - Reduced costs (small diameter drilling *slim hole*, *coiled tubing* technology);
 - deviated drilling allowing to develop well architectures increasingly complex and better drainage of reserves. Offsets greater than 8,000 m drilled for a total length of 8,700 m have already been made, and this limit will soon exceed 10,000 m.
- **multiphase pumping** should be a great progress in the deep offshore production (especially beyond 1000 m of water).

All these technological advances have yielded very significant results:

- a very strong reduction of technical cost in the oil industry, which is expected to continue in the future;
- a very large increase in the rate of oil recovery, which can reach 60% in some fields, while it was limited to 40% 25 years ago. The global average recovery rate has increased from 25–30% in 1985 to 30–35% today;

- a reassessment of world oil reserves (between 1982 and 1992, additional oil reserves corresponded to 4.4 Gt for new fields, and 4 times more or 19 Gt for revisions and extensions of fields already known);
- the discovery and introduction of new oil basins in different regions (South America, Africa, Asia-Pacific, Western Europe, CIS).

11.2 LOCAL AND GLOBAL ENVIRONMENTAL IMPACT OF ENERGY

The second driver of technological change in chronological order, but today the first in importance is the environmental impact of energy technologies. Indeed, even if non-renewable energy were available without restriction, the total volume of energy technology pollutant emissions has become so important that current consumption patterns should be questioned.

Since the early 1970s, environmental problems have seriously begun to educate the public. Neglected for a moment, especially at the height of the oil shocks, they have since returned to the agenda.

The relationship of energy to the environment is complex and takes many forms, from extraction of primary energy to final use. Its aspects can be local, international or even global. Pollution is a major problem in industrialized countries, but also in developing countries where, in addition, the extensive use of firewood can lead to uncontrollable acceleration of deforestation, and thus desertification.

Recently, energy has been found to be directly involved in major issues such as the accumulation of CO₂, the breakdown of the ozone layer, acid rain and urban pollution, as well as risks of nuclear accidents (Chernobyl, Fukushima). Given the objective of this book, we only deal with issues related to gaseous emissions, which have a direct impact on regulations concerning energy technologies.

11.2.1 Increase in global greenhouse effect

Similar to the mechanism used in a greenhouse or in a thermal solar collector we call **greenhouse warming** the influence of the atmosphere on the radiative balance of the earth through the absorption of infrared radiation emitted from earth to space.

The greenhouse effect is due to gases in the atmosphere, which absorb a portion of the incident radiation. The gases have absorption rays corresponding to different wavelengths. The diagram in Figure 11.1.3 gives a schematic indication of the effect of absorption by CO₂ of the radiative flux of long wavelength emitted by the earth, and shows absorption by two rays, centered on wavelengths $\lambda_1 = 4.5 \mu\text{m}$ and $\lambda_2 = 14.5 \mu\text{m}$. The incident solar radiation of short wavelength (visible from 0.4 to 0.8 μm) is almost fully transmitted by the atmosphere and absorbed at the surface of the earth, which heats and re-emits into space at 4 K radiation of long wavelength (infrared from 0.8 to 100 μm), a more and more important part of which is absorbed by greenhouse gas emissions. Their concentration having increased in recent decades, a gradual warming of the planet has been observed and could lead to significant changes in climate.

Greenhouse gases are emitted by many human activities (transport, heating, cooling, industry, livestock, waste etc.), including the burning of fossil fuels (coal, oil and gas) that produces CO₂, remaining on average more than a century in the atmosphere before being recycled into “carbon sinks” such as vegetation. The main absorbing gases in the infrared are water vapor H₂O, carbon dioxide CO₂, methane CH₄, nitrous oxide N₂O, chlorofluorocarbons (CFCs R11 and R12 in particular) and some noble gases. Their contributions to the increase of greenhouse gases are highly variable (50% for CO₂, 15% for CH₄, 9% for N₂O), and depend on their concentration, a saturation

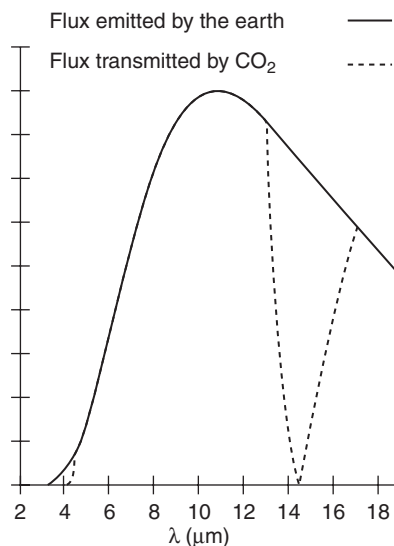


FIGURE 11.1.3

Greenhouse effect

phenomenon occurring beyond a certain threshold, which explains why the variations of concentration of water vapor has no significant impact on the greenhouse effect, although this is the most absorbing gas vis-à-vis the radiation.

All models predict that emissions of greenhouse gases will continue to rise strongly in the near future, as they did in recent decades, and their atmospheric concentrations will increase. The concentration of CO_2 in the atmosphere has indeed increased from 280 ppm to 360 ppm in a century, while it remained within a range of 170 ppm to 280 ppm during the 200,000 previous years.

The international community has responded by creating in 1988 the Intergovernmental Panel on Climate Change (IPCC), under the United Nations Environment Programme (UNEP) and World Meteorological Organization (WMO). The IPCC is charged with evaluating the scientific evidence on climate change, to assess the ecological and socio-economic impact, and propose strategies for prevention and adaptation.

IPCC reports confirm the climatic influence of greenhouse gas emissions, already demonstrated by many recent statistical anomalies, like the phenomenon of El Niño, which caused unusual droughts and floods in Latin America. Scientists have found that greenhouse gases are responsible for a 0.6 to 0.9°C increase of average temperature at the surface of the earth since the preindustrial era, which was partially obscured by the thermal inertia of the oceans and the increasing presence of aerosols in the atmosphere. It is estimated that the average temperature at the surface of the earth could rise another 1.8 to 4°C by 2100, resulting in a rise of 18 to 60 cm of sea level.

Although we do not know very well what will be the local climatic consequences of the increase in the greenhouse effect, IPCC experts believe that major disruptions are inevitable, with increased frequency and intensity of natural disasters (droughts, floods, storms, cyclones).

The United Nations Framework Convention on Climate Change was ratified in 1992 following the Rio de Janeiro Summit. Under this agreement, effective March 21, 1994, the OECD countries, Ukraine and Russia have pledged to stabilize their emissions of greenhouse gases by the year 2000 at the same level as in 1990. In December 1997, at the Kyoto Summit, which led to the Kyoto Protocol entered into force in February 2005, these commitments have been extended for the period 2008–2012: the industrialized countries pledged to reduce by an average of 5.2% their emissions of greenhouse gases over the period 2008–2012 as compared to 1990, the European Union for its part

undertaking to reduce its emissions by 8%. As part of an agreement within the European Union, France must stabilize its emissions (target 0%).

Despite all the work done over the past twenty years to better understand the mechanisms of the greenhouse effect, many unknowns still exist, because of:

- interactions between clouds, oceans, and polar ice caps;
- size and nature of sources and sinks of CO₂.

In contrast, the share in the global warming of the various gases caused by humans, sometimes called the “radiative forcing” is better known. To evaluate the toxicity of a gas in terms of greenhouse effect, an index is used known as Global Warming Potential (GWP). It represents the relative ability of a greenhouse gas to participate in radiative forcing, and is 1 for CO₂.

The contribution of a gas to the greenhouse effect depends on the one hand on the amount of emissions, and on the other hand on two factors taken into account in the calculation of GWP: its absorption properties in the infrared and its residence time in the atmosphere. This last factor being very variable from one gas to another (several hundred years for CO₂, between 10 and 15 years for CH₄), it is necessary to agree on an appropriate integration time horizon (ITH). The GWP can then be determined by calculating the cumulative radiative forcing on the ITH chosen. The IPCC has conducted assessments of GWP on ITH of 20, 100 and 500 years. As the figures presented in the literature generally represent an ITH of a century, we will retain that value in this book.

Improved efficiencies

Stabilize the concentration of CO₂ in the atmosphere will require considerable effort, because of the inertia of the phenomena involved and the residence time of gases in the atmosphere.

While following the 1986 oil counter-shock there had been a noticeable reduction in the search of better efficiencies for energy technologies, improved performance of all engines once again became a primary goal of manufacturers, the aim being this time to reduce the mass of CO₂ emitted per kWh. We will return to this question in almost all chapters of this Part.

CO₂ capture and sequestration

Nearly 90% of global energy supplies being provided by fossil fuels, the emission of carbon dioxide appears as a secondary product for which there is currently no alternative, nor to increase CO₂ earth capture capacity, large scale reforestation projects colliding many technical and socio-cultural constraints.

Sequestering CO₂ is therefore increasingly seriously considered, at least in high capacity and stationary plants, and then storing it in caverns or in deep oceans. This point is precisely the subject of Chapter 28 of Part 4.

11.2.2 Reduction of the ozone layer

Since the undoubtedly experimental demonstration by English and Japanese researchers in 1985, of a hole in the ozone layer over Antarctica during the austral spring (decrease by half to two thirds of the normal thickness), the international community was particularly active. The breaking of the ozone layer is due to many gases, including those containing chlorine, and whose use was then about 60% directly related to energy applications: production of thermal insulating foam and use as refrigerants in air conditioning and refrigeration.

Aware of the negative environmental impact of chlorofluorocarbons (CFCs), industrial producers have conducted major research programs to develop substitutes. Two broad classes of products have mainly been studied: hydrochlorofluorocarbons (HCFCs) and hydrofluorocarbons (HFCs). HCFCs are similar to CFC molecules some chlorine bonds being replaced by hydrogen bonds, while HFCs

have no more chlorine atoms. The stability of HCFC molecules being much less than that of CFCs, they are largely destroyed in the lower atmospheric layers, and only a small fraction of the chlorine atoms they contain can be found in the stratosphere, making these molecules much less harmful to the ozone layer.

However, reducing their potential for ozone destruction is accompanied by a modification of their technical characteristics, which leads to the questioning of many previous technological solutions, and presents many challenges to the refrigeration and air conditioning industry.

The first international agreement concluded in this respect is the Montreal Protocol, which took effect in early 1989, and decided to freeze CFC consumption at 1986 levels, followed by a reduction of 20% in 1993, and a second reduction of 30% in 1999. The movement then continued, and in 1990 in London, there was agreement on an amendment resulting in an acceleration of the process, with the goal of banning outright from 2000, all CFCs and halons, and a questioning of HCFCs, because they still contain chlorine.

Regulation of the European Commission in March 1991 provided for the cessation of production and consumption of CFCs by 1 June 1997. In November 1992, in Copenhagen, a new amendment was still moving this date to 1 January 1996.

As is done for greenhouse gas emissions, assessing the harmfulness of a gas in terms of destruction of the ozone layer is performed using an index known as Ozone Depletion Potential (ODP). This index is 1 for CFC 11.

This issue mainly concerning the refrigeration industry, it is developed in Chapter 19.

11.2.3 Urban pollution and acid rain

Acid rain is a phenomenon that leads to the degeneration of forests, especially in Central and Northern Europe. The share attributable to energy is far from being clearly established, but it seems obvious that it plays an important role, because of emissions of sulfur and nitrogen oxides that occur during combustion of coal or oil. Uses under investigation are first electricity generation and transport, and to a lesser extent space heating. The fight against acid rain in Europe has thus resulted in the decision to equip motor vehicles with catalytic converters.

In large cities, exceeding the threshold concentrations of certain pollutants during peak pollution has alerted the public. It therefore appears increasingly necessary to reduce pollutant emissions in vehicles and energy production facilities.

Regarding transport, electronic control injection systems helped to make significant gains in reducing pollutants (decreased 50-fold in 30 years and 10 over the last twenty years) but they are insufficient to meet the new requirements imposed by international regulations (see Chapter 19).

After consultation with manufacturers, the European Union has enacted two directives laying down a number of objectives.

Combustion optimization

Aware of the growing challenges associated with reducing sulfur and nitrogen oxides, energy technology manufacturers invest more in search of a better control of combustion conditions, particularly for engines and electricity power generation etc. We will make numerous references to this in Chapters 12, 13 and 16, where we examine the technological solutions proposed. Let us simply indicate at this stage that the problems are very different in conventional thermal power plants, where the combustion chambers are large, the pressure being close to atmospheric, and in internal combustion engines, where combustion takes place in much more compact volumes, with increasingly brief residence times and under high pressure.

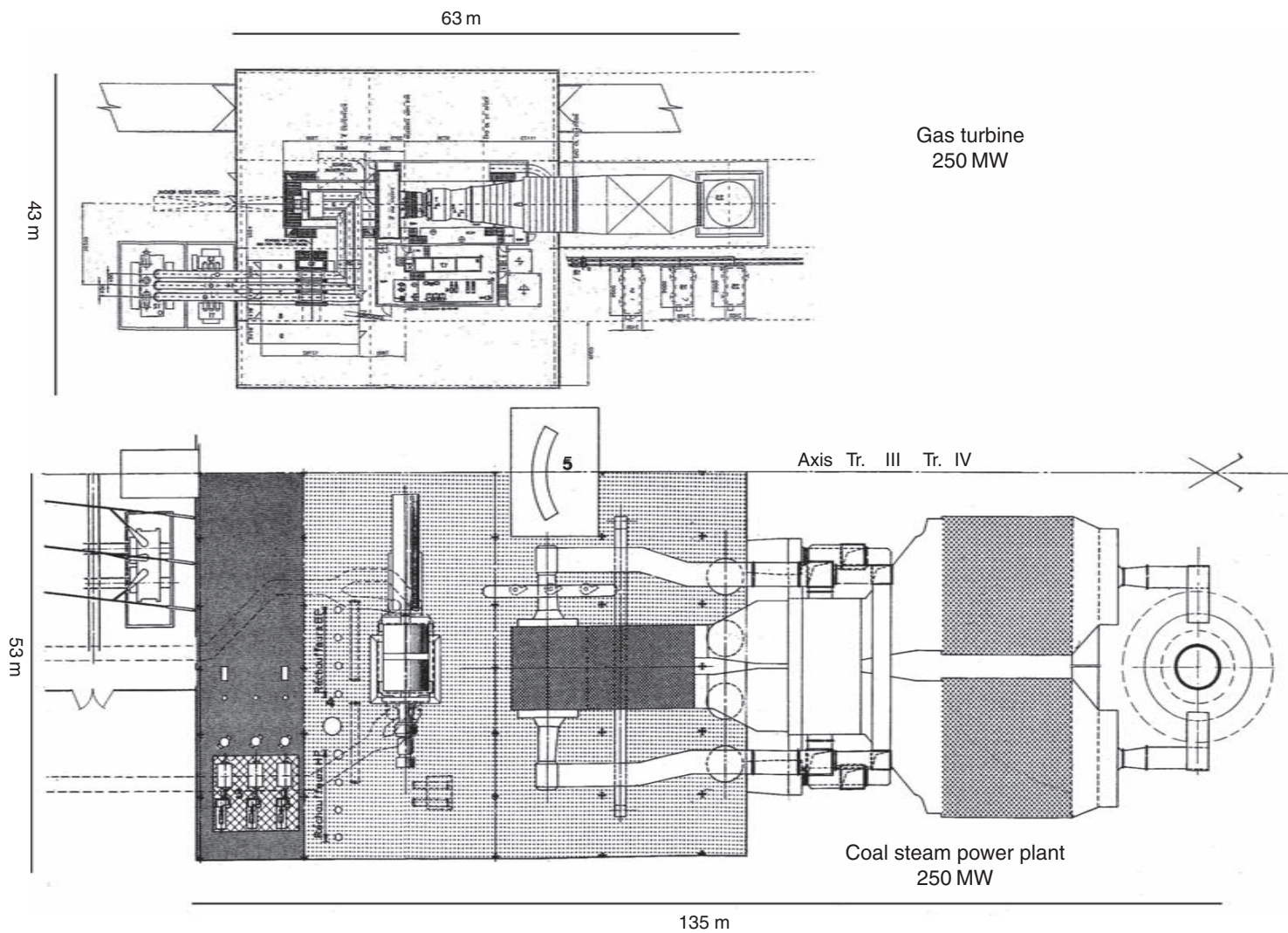


FIGURE 11.1.4

Comparison of a coal plant and a gas turbine, Documentation Alstom Power

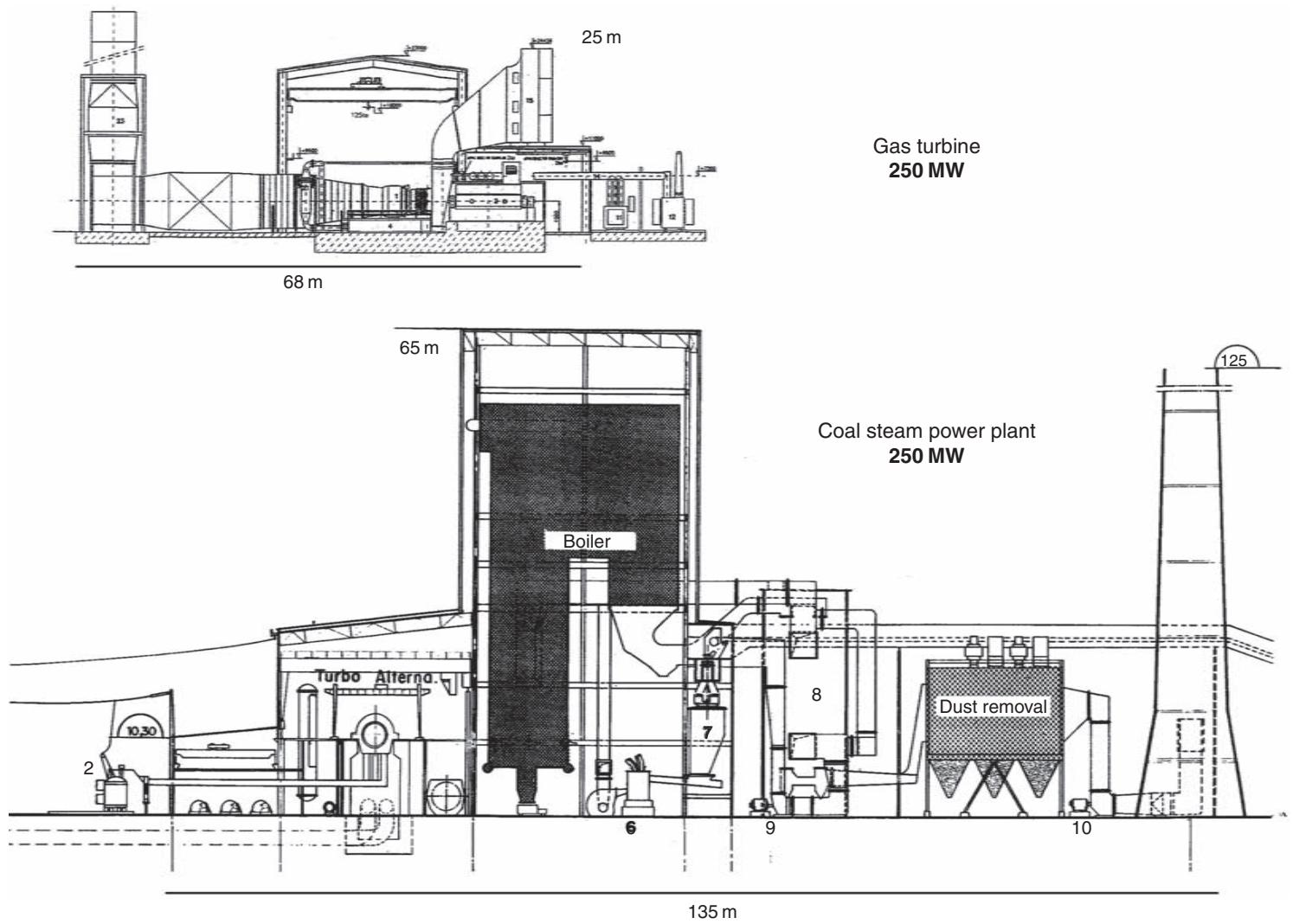


FIGURE 11.1.5
Documentation Alstom Power

By way of illustration, Figures 11.1.4 and 11.1.5 are used to compare the size of two typical 250 MWe power plants, one using a steam cycle with conventional pulverized coal boiler, the other a modern gas turbine:

- the burner of the coal boiler typically has a single ground base of $11\text{ m} \times 11\text{ m}$ and a height of 27 m, a volume of 3200 m^3 , its net efficiency is around 39%, which corresponds to a thermal power of $250/0.39 = 641\text{ MW}$;
- the gas turbine (GT 26 ALSTOM, Figure 12.1.4) has a capacity of 260 MWe and an efficiency of 36% for a combustion chamber volume of only 4 m^3 , which corresponds to a thermal power of $260/0.36 = 722\text{ MW}$.

The thermal power released per m^3 of combustion chamber is about 200 kW/m^3 for the coal plant, while the gas turbine is 180 MW/m^3 , i.e. is 900 times larger. This very important difference comes from the fact that in the case of boilers, there is a barrier (mechanical and thermal) between the fumes and the working fluid, which limits the heat transfer, whereas in the gas turbine, energy is released directly into the working fluid. We shall see in Chapter 12 that this induces severe constraints especially at the combustion chamber and the first expansion stages of the turbine.

11.3 TECHNOLOGY TRANSFER FROM OTHER SECTORS

The third driver of technological change is consistent with progress in other fields which have a direct impact on the energy sector.

Three of them are worth mentioning here, the first two being related to Information and Communication Technology:

- Theoretical and numerical modeling and computerized codes have played and will continue to play a fundamental role in technological change. Progress in software and increased computing power of today's computers make possible once unthinkable modeling and optimizations that improve the performance of many energy technologies;
- in a related field, progress in electronics and real time control allows us to pilot facilities according to protocols much more accurate than some years ago and to improve their reliability;
- progress on materials also have a direct impact on energy technologies, whether the protection of gas turbine blades, catalysts for exhaust converters etc.

Electricity generation from natural gas

Recent developments in gas turbines and combined cycles offer a striking example of results quickly brought by technological innovation in the energy sector. These technologies, until recently still regarded as relatively marginal, are poised to play a leading role in the structure of power plant fleets. They are much less sensitive to scale effects than conventional power plants, for which the increase in size was a competitiveness factor. Factory-made, they come in modular form and are assembled on site within a much shorter time. The benefits are numerous:

- it is possible to stagger investments, thereby reducing financial costs;
- The footprint is smaller than that of conventional power plants;
- A large power unit is composed of several modules in parallel, thereby facilitating maintenance;
- the difference between centralized and decentralized production is reduced, which helps diversify the production sites and thus reduces network vulnerability.

Recent progress on ground machines is largely the result of a technology transfer from the aviation world. In fact, most jet engines used in aviation today are variations of the open cycle gas turbine. For 50 years, the tremendous growth experienced by the aviation market has helped fund major technology development programs on these engines, which led to the development of highly efficient and competitive gas turbines.

11.4 TECHNOLOGICAL INNOVATION KEY TO ENERGY FUTURE

As we have seen, the energy sector is currently facing many technological developments, which follow on from research undertaken for nearly 25 years in response to the first oil crisis and environmental constraints. These changes, which affect both energy production and use, are partly the result of progress in related areas, such as materials, automation, fluid mechanics and others, partly the result of the discovery and implementation of more efficient thermodynamic cycles, particularly with regard to combustion.

Given the strategic nature of the energy sector, deeply intertwined with the entire world economy, states have quickly realized that they could not let the market act as sole regulator. Therefore it is completed in most countries by a national energy policy, which generally retains two main objectives: to increase supply (by the investment in production and diversification of supply sources) and to decrease demand (through greater energy efficiency and behavior modification).

Technological innovation is an essential component of energy policy. Like prices, the performance improvements which it leads to also have the effect of increasing supply and decreasing demand. It therefore constitutes a direct alternative to price adjustments.

We know that the technological cost structure of oil is such that its price may be set roughly equally between a floor value, which in fact corresponds substantially to the cost of production in the Middle East (a few dollars per barrel), and a cap value, determined by the cost of other competing energy sources. The difference between these values has been and remains very high (above 15 dollars per barrel of oil equivalent), which explains the high magnitude of past oil shocks. To reduce this differential, there is no alternative but to lower the cost of other energy sources.

This is precisely what technological innovation can lead to. It allows the conversion of current production and energy use sectors and the emergence of new sectors, such as synthetic hydrocarbons, solar energy, nuclear fusion, enhanced oil recovery, or reduction of energy consumption of use equipment etc.

In addition to its direct impact on the evolution of energy intensity, technological innovation has other advantages, among which are two major ones: Firstly, it is a very interesting alternative to the classical price adjustment, which potentially eventually allows us to limit the adverse effects of oil shocks, in addition, it is the only way to reduce the negative impact of energy consumption on the environment.

Schematically, we can say that when prices rise, energy supply is growing, given that alternative sources previously uneconomic become competitive, while demand decreases, users reducing their consumption when they can. The market is thus the main classical mechanism of adjustment between supply and demand. It must however be noted that this mechanism works imperfectly when price changes are brutal, as demonstrated by the past oil shocks, with adverse effects that we know about on most economies (deterioration of the terms of trade, recession, unemployment).

Conversely, the technology mechanism of adjustment generally has a positive impact on the economy as a whole, because it results in job creation to produce new technologies, increased productivity and therefore competitiveness, industrial development of high added value products etc.

Technological innovation appears as the only way to help develop energy systems that have both the characteristics of durability, reasonable cost, low environmental damage and adaptation to an increased demand for goods and services, that is to say technology able to meet the long term challenges avoiding if possible the cyclical short term crises. Faced with uncertainties about the energy future of the planet, it is a major key to long-term energy transition.

Already, as we have shown, significant R&D projects in the energy sector have begun to bear fruit, and new developments will emerge in the coming years. For example, the most ambitious energy program, the Program Vision 21 of the U.S. Department of Energy shows very high goals for 2015: 60% efficiency on HHV (higher heating value) in power generation from coal, and over 75% LHV (lower heating value) from natural gas, simultaneous production of electricity, heat (85–90% efficiency in cogeneration), and synfuels or hydrogen, modularity and flexibility etc.

For this, the program identifies as one of its five priorities the development of advanced systems integration and systems analysis (see Chapter 22). Another area focuses on the key technologies to develop, many of which relate directly to gas turbines: separation membranes for oxygen and hydrogen, high temperature heat exchangers, flexible gasification, gas purification, advanced combustion systems, multi-fuel gas turbines, fuel cells, advanced development of fuels and chemicals, high temperature materials resistant to corrosive atmospheres, virtual demonstration and numerical modeling, advanced control and measuring progress, particularly in the environmental field, and advanced modularization and manufacturing.

Other changes in our energy landscape may emerge soon, such as the development of electric vehicles, fuel cells or solar energy.

To prepare for these changes, we must maintain a very open technology watch, and avoid locking ourselves into single sector approaches: the emergence of a new energy system is likely, as a result of possible energy substitutions, to concern many other sectors that appear yet well established. Thus, technological advances must be measured not only in terms of technical performance (efficiency, power, cost), but also increasingly taking into account the various external effects on which policy makers rely to make their decisions.

REFERENCES

GIEC, <http://www.unfccc.de/resource/convkp.html>

Intergovernmental Panel on Climate Change, *Impacts, adaptation, and mitigation of climate change: scientific-technical analyses*, Cambridge University Press, New York, 1996.

Intergovernmental Panel on Climate Change, *Summary for Policymakers*, IPCC WGI Third Assessment Report, Geneva, 2001.

John W. Mitchell, *Energy engineering*, J. Wiley, New York, 1983, ISBN 10 0471087726.

FURTHER READING

J. C. Balaceanu. *Développement Technologique et Prospective Energétique: les scénarios technologiques*, Annales des Mines, Paris, janvier 1990.

S. Boussena. *Prix du pétrole et stratégies de l'OPEP*, Revue de l'Energie, Paris, n° 456, février 1994.

CPDP. *Bulletins du Comité Professionnel Du Pétrole*, Paris.

X. Boy de la Tour. *Technologies pétrolières: les nouvelles frontières*, Revue de l'Energie, Paris, n° 456, février 1994.

R. Gicquel. *Introduction aux Problèmes Energétiques Globaux*, Economica, Paris, 1992.

R. Gicquel. *Transition énergétique et innovation technologique: quelques développements récents concernant la production d'électricité à partir de gaz naturel*, Colloque International "Les Energies du 21ème siècle", UNESCO, Paris, 7–8 décembre 1995.

A. Giraud. *Géopolitique de l'énergie dans un monde en transition*, Revue de l'Energie, Paris, n° 456, février 1994.

M. Hafner. *Gaz Naturel et Electricité, Analyse technologique et économique de la génération d'électricité et du transport de gaz pour les pays du bassin méditerranéen*, Thèse de Doctorat, Ecole des Mines de Paris, 1994.

IFP. *dossier Panorama 96*, Pavillon Gabriel, Paris, 25 janvier 1996.

Ph. Jaud. *Faut-il piéger le gaz carbonique émis par les centrales thermiques?*, Revue Epures, DRD EDF 1999, Paris.

B. Leide. *De la Réactivité Résiduelle des Gaz Brûlés dans la Turbine de Détente des Futures Turbines à Gaz*, Thèse de Doctorat, Ecole des Mines de Paris, 1994.

Mission interministérielle pour l'effet de serre: <http://www.effet-de-serre.gouv.fr/index.cfm>.

This page intentionally left blank

Internal Combustion Turbomotors

Abstract: Today, gas turbines are experiencing a very strong development in many applications: air transport, power generation, cogeneration, driving machines (compressors and pumps). Among the arguments in their favor include their small size, excellent power to weight ratio, their quick start, good performance and low emissions of pollutants.

Two broad categories of gas turbines are generally distinguished: industrial gas turbines, heavy and robust, and aeroderivative gas turbines, much lighter and efficient but also more expensive.

Indeed turbojets used in aviation today are in fact variations of the gas turbine open cycle. The aviation market has helped fund major technology development programs on these engines, which led to the development of highly efficient gas turbines.

This chapter is mainly devoted to the analysis of gas turbine and turbojet component technologies and basic cycles. Advanced cycles based on gas turbines (combined cycles, cogeneration plants, oxycombustion cycles, etc.) are presented in Chapters 17 and 18 of Part 3 and 24 and 28 of Part 4.

Keywords: compression, expansion, combustion, regeneration, gas turbine, shaft, nozzle, diffuser; ramjet, rocket engine.

12.1 GAS TURBINES

12.1.1 Operating principles

In its simplest and most common form (Figure 12.1.1), a gas turbine (GT), also called combustion turbine, is composed of three elements:

- a compressor, usually centrifugal or axial, which is used to compress the ambient air at a pressure between 10 and 30 bar in modern machines;
- a combustion chamber in which fuel is injected under pressure, combusted with air previously compressed (the latter in large excess in order to limit the exhaust gases temperature at the turbine inlet);

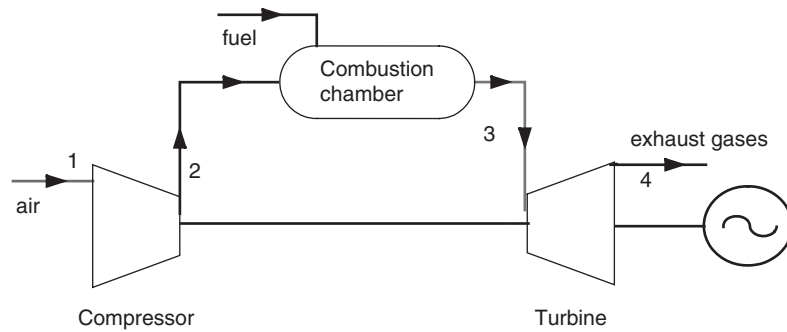


FIGURE 12.1.1

Sketch of a gas turbine

- a turbine, usually axial, in which are expanded the high temperature gases exiting the combustion chamber. A significant proportion (60–70%) of the work recovered on the shaft of the turbine is used to drive the compressor.

In this form the gas turbine engine is a continuous stream internal combustion engine. Note that the gas turbine term comes from the working fluid state, which remains gaseous, and not the fuel used, which can be both gaseous and liquid (gas turbines typically use natural gas or light petroleum distillates). There are also closed cycle gas turbines, used for special applications, including nuclear, as we shall see below and in Chapter 29 of Part 4. Of course, then it is an external combustion engine.

To achieve compression ratios r of 20 or 30, the **compressor** is multistage, with sometimes intermediate cooling to reduce the work consumed. Axial rotors are made of a stack of discs, either mounted on a central shaft, or drum assembled on their periphery. The materials used are aluminum or titanium alloys for the first stages and steel alloys and refractory alloys for last stages that can withstand temperatures up to 500°C.

The **combustion chamber** is normally constructed of refractory alloy. Various types will be presented later.

In open cycle gas turbines, the main technological constraints are at the first stages of the **expansion turbine**, through which flow the exhaust gas at high temperature.

The parts most at risk are especially rotor blades, which are very difficult to cool and in addition particularly sensitive to abrasion. It is therefore important to use a very clean fuel (no particles and chemicals that may form acids), and limit the temperature depending on the mechanical characteristics of the blades.

The materials used for turbine blades are refractory alloys based on nickel or cobalt, and manufacturers intend to make use of ceramics in the future.

As the cycle efficiency is itself an increasing function of temperature, major technological developments have been devoted to the fabrication, first of efficient cooling systems of the blades, and second of materials resistant at high temperatures. For half a century, there has been a gradual increase (about 20°C per year) of the turbine inlet temperature, now reaching 1300 to 1500°C.

Two broad categories of gas turbines are generally distinguished: industrial gas turbines, heavy and robust, but of average performance (efficiency η between 28 and 38%), and gas turbines derived from aviation or “aeroderivative” much more efficient and light (η between 35 and 42%), but also more expensive. The capacities of the first range from tens of kW (microturbines) to several hundreds of MW, while those of aeroderivative machines are generally between a few hundred kW to tens of MW, corresponding to those of aircraft engines. We shall indeed see in section 12.2.2 that most jet engines used in aviation today are in fact variations of the gas turbine open cycle. The aviation market has helped fund major technological development programs on these engines, which led to the development of highly efficient gas turbines, which could supplant industrial gas turbines,

or allow hybrid turbine design of enhanced efficiencies and low cost, including components of existing jet engines for high pressure compressor and turbine sections, and industrial parts for low-pressure sections.

Early gas turbines were manufactured at the beginning of the twentieth century, in France by the Société Anonyme des Turbomoteurs in Paris and in Switzerland by the Brown Boveri company in Neuchatel. The net work produced by these machines is equal to the difference between the useful work done by the turbine and the work required to compress the air. In the early achievements, it was very low, and it was not until the 1930s that industrial applications have really started to grow, thanks to the improved performance of compressors and turbines, mainly due to advances in the understanding of gas flows, which continue today with 3D modeling.

For thirty five years, gas turbines have been experiencing a very strong development in many applications: air transport, power generation, cogeneration, driving machines (compressors and pumps), marine propulsion, where they make a growing breakthrough. Arguments in their favor include their small size, excellent power to weight ratio, good performance and low emissions of pollutants.

Among other advantages of gas turbines, we can mention:

- their startup is very fast: while it takes 24 hours to start up some steam plants, a gas turbine reaches its rated speed in 15 to 20 minutes, and capacity can be modulated very rapidly between the full load and 20 to 30% of this value;
- auxiliary equipment is small and cheap, and there is no need of water for cooling the cycle, since the exhaust gases are released into the atmosphere. In addition, the construction time on site is reduced, because the machine is assembled in factory.

Investment costs range from 350 Euros/kW for machines between 1 and 10 MW to approximately 180 Euros/kW for units larger than 50 MW. The price per kW installed, however, is higher because of auxiliary equipment and infrastructure. For electricity generation, it varies between 300 and 450 Euros/kW.

Their main drawback is the use of clean fuels, which is therefore generally expensive. Also note that their performance depends significantly on site conditions, and degrades when the outside temperature rises or when the pressure drops.

12.1.2 Examples of gas turbines

12.1.2.1 Industrial gas turbines

Siemens gas turbine of Figure 12.1.2 is characterized by silo combustion chambers (multi-fuel, emission control, radiative protection of turbine blades).

12.1.2.2 Aero-derivative gas turbines

Rolls Royce SM1C two shaft turbine (Figure 12.1.3) (marine propulsion) has a capacity of 20 MW, a compression ratio $r = 22$ (5 + 11 stages of compression, 2 + 2 expansion). Its turbine inlet temperature is 740°C.

The Alstom Power GT24/26 gas turbine of Figure 12.1.4 is a new generation of aero-derivative turbine, in the sense that, although developed using aviation techniques, there is no equivalent turbojet, given its high capacity (180/260 MW) and its combustion mode (sequential). Its characteristics are as follows: $r = 30$ (22 stages of compression, 1 + 4 expansion), turbine inlet temperature 1255°C; $\eta = 37.5\%$. The GT 24 has a rotation speed of 3,600 rpm to provide electricity at 60 Hz, while the GT 26 rotates at 3,000 rpm (50 Hz). Designed with equivalent mechanical stress in the blades, their capacities are respectively 180 and 260 MW, and their masses (with their bases) approximately 225 and 370 tons.

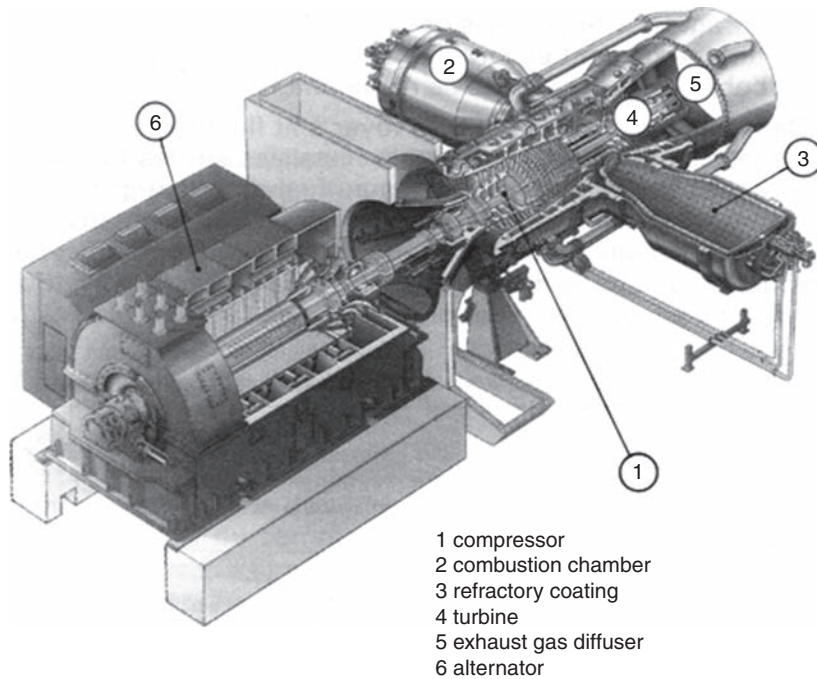


FIGURE 12.1.2

Siemens gas turbine, Extract from *Techniques de l'Ingénieur, Génie Energétique*

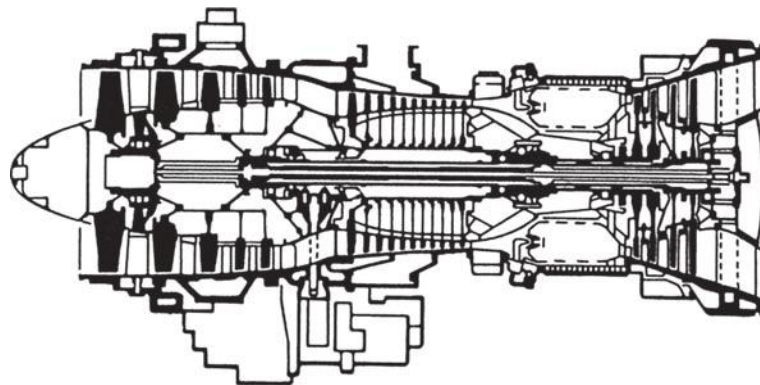


FIGURE 12.1.3

Rolls Royce SMIC, Reproduced courtesy of Rolls-Royce plc

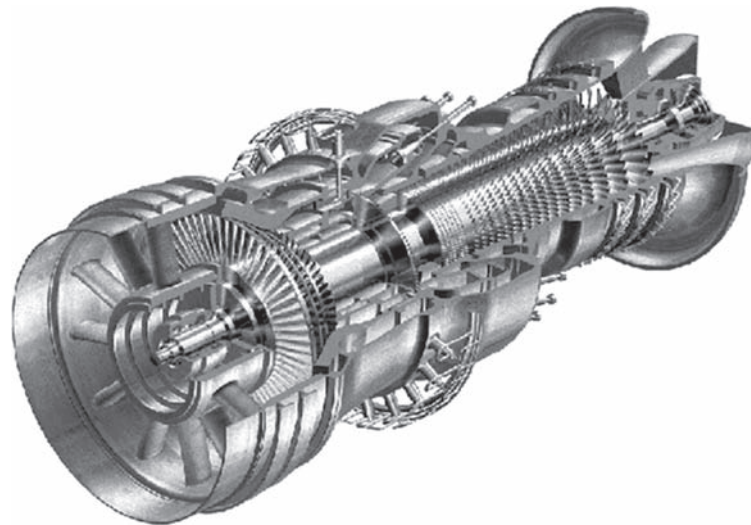
Figures 11.1.4 and 11.1.5 presented in Chapter 11 give an idea of the approximate size of a power plant based on this gas turbine: a base of 50 m by 70 m and a height of 25m.

12.1.3 Major technological constraints

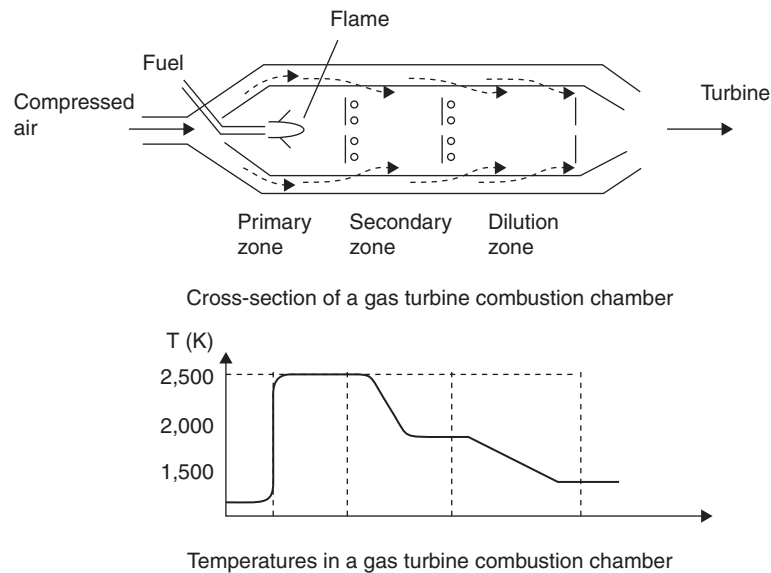
12.1.3.1 Combustion chamber

The combustion chamber of a gas turbine, especially those derived from aviation, must satisfy severe constraints:

- ensure complete combustion of fuel;
- reduce emissions of pollutants;

**FIGURE 12.1.4**

Alstom Power GT24/26, Documentation Alstom Power

**FIGURE 12.1.5**

Temperatures in a combustion chamber

- minimize pressure drop (which represents an increase in compression work);
- ensure good stability of the turbine inlet temperature;
- occupy as small a volume as possible while allowing proper cooling of the walls.

The diagram in Figure 12.1.5 shows a section of a flame tube combustion chamber, very commonly encountered in practice.

The compressed air exiting the compressor enters on the left side. It splits into two streams, one that provides wall cooling, the other entering directly into the combustion chamber, where it serves as oxidizer to the fuel injected in the central part. Given the low excess air locally, the flame reaches a high temperature (up to 2,500 K) in the primary zone. Through holes at the periphery of the flame tube, the outside air is mixed with exhaust gases in the transitional zone, where temperature drops

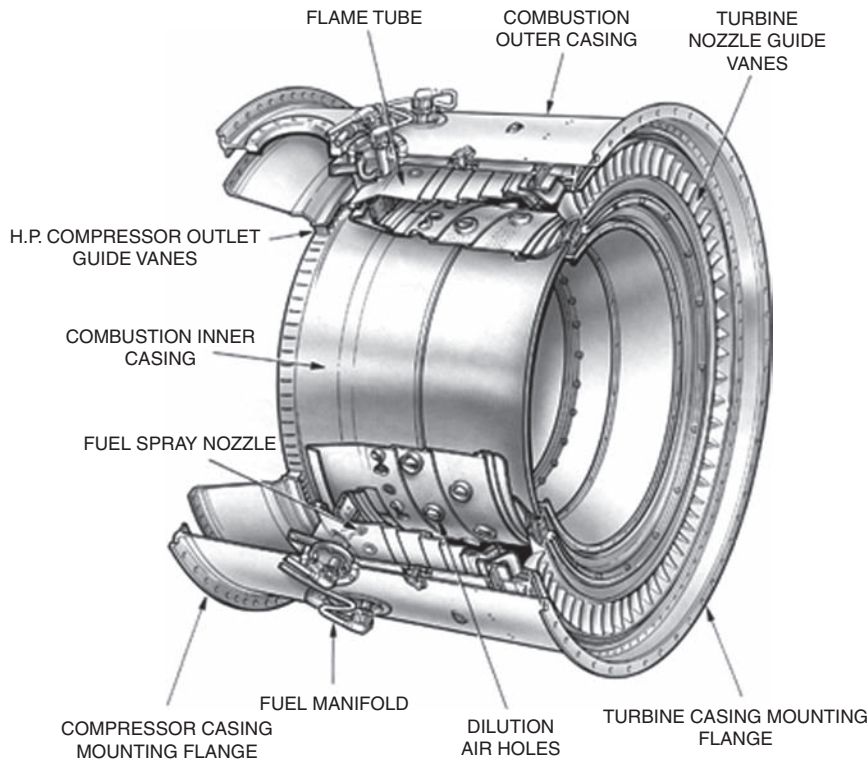


FIGURE 12.1.6

Annular combustion chamber, Reproduced courtesy of Rolls-Royce plc

around 2,000 K, and in the dilution zone, where one seeks to achieve a gas flow temperature as stable as possible to avoid the risk of local or momentary overheating.

In cylinder flame tube chambers, six to twelve tubes of this type are mounted in parallel around the axis of the gas turbine. They are interconnected in order to balance the pressures and enable propagation of the ignition.

Two other types of chambers are available:

- silo chambers (see industrial turbine of Figure 12.1.2): in this case, chambers, separated from the axis, are much larger, allowing better control of combustion, including emission of pollutants (NO_x);
- annular chambers (see Figures 12.1.4 and 12.1.6): the chamber has a single volume, annular, fuel being injected in several points. This arrangement yields a shorter flame and better combustion efficiency.

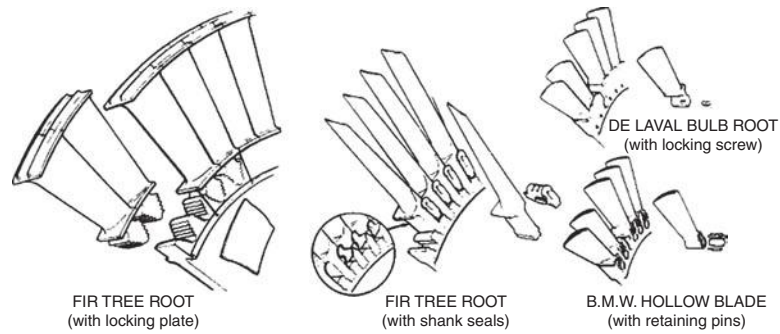
The efforts of manufacturers now focus on reducing emissions of pollutants, particularly nitrogen oxides.

12.1.3.2 First expansion stages

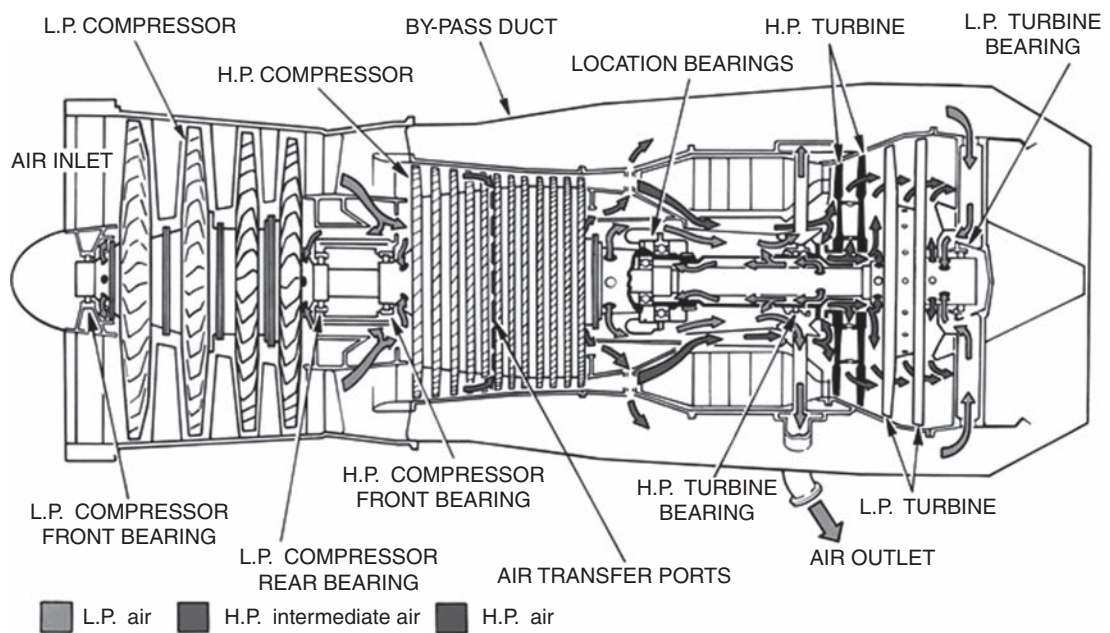
In open cycle gas turbines, the major technological constraint is the maximum temperature that can withstand both the elements of the combustion chamber and the first turbine stages, which are subject to the flow of exhaust gases. The parts most at risk are especially rotor blades (Figure 12.1.7), which are very difficult to cool and particularly sensitive to abrasion.

The problem is even more difficult to resolve due to the fact that the shapes of the fixed nozzles and mobile blades of the turbines are very complex, especially in small units derived from aviation.

To make the cooling, air is taken at different levels of the compressor, depending on the desired pressure for reinjection into the turbine (Figures 12.1.8 and 12.1.9).

**FIGURE 12.1.7**

Various methods of attaching blades to turbine discs, Reproduced courtesy of Rolls-Royce plc

**FIGURE 12.1.8**

Blade cooling in a turbojet, Reproduced courtesy of Rolls-Royce plc

This air passes inside the blades, through a carefully designed set of baffles, and then is evacuated with the exhaust gases, either at the trailing edge, or by allowing some porosity through the wall. Figure 12.1.10 shows three types of configurations selected to enhance the cooling: cavity (1) and channel (2) blades, forced convection, porous and transpiration cooled blades (3).

Figures 12.1.11 and 12.1.12 show another technique, using a more complex network of channels, the multiperforated blades. In aero-derivative gas turbines of the most powerful last generation, cooling of the blades is no more carried out by air circulation, but by water vaporization, which can benefit from the high heat transfer coefficients in a two-phase system.

The analytical and numerical models that will be presented later in this chapter do not specifically take into account the cooling of the blades in the calculations of gas turbines. The interested reader will find explanations on how to do it in the thesis of H. Abdullah (1988) referenced at the end of the chapter.

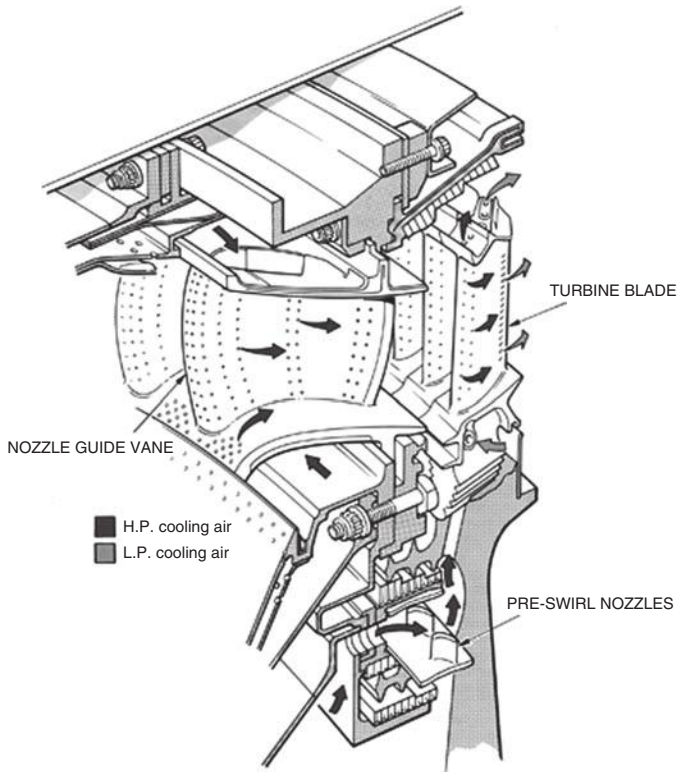


FIGURE 12.1.9
Detail of turbine cooling, Reproduced courtesy of Rolls-Royce plc

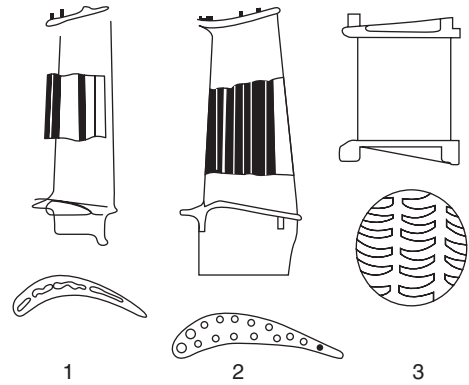


FIGURE 12.1.10
Detail of blade cooling, Documentation Snecma

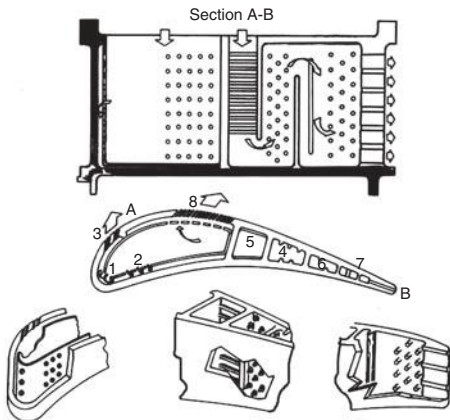


FIGURE 12.1.11
Detail of blade cooling, Documentation Snecma

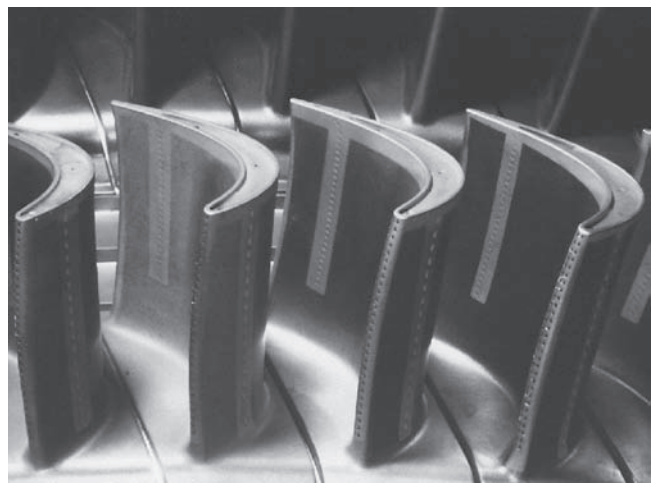


FIGURE 12.1.12
Blade assembly, Documentation Alstom Power

12.1.4 Basic cycles

As we have seen (see Figure 12.1.1), a gas turbine consists of three components: a compressor, a combustion chamber and a turbine.

For the reasons stated in section 5.3.6 of Part 2, the compressor and turbine can be assumed to be adiabatic. As to the combustion chamber, at first approximation we can make the assumption that it is isobaric.

Let us call τ_c the compressor work, τ_t the work done by the turbine, \dot{m}_c , \dot{m}_t the flow-rates passing through them, \dot{m}_f that of fuel and Q_{cc} the heat generated by combustion.

The enthalpy balances of the three components give here:

$$\begin{aligned}\tau_c &= \dot{m}_c(h_2 - h_1) > 0 \\ \tau_t &= \dot{m}_t(h_4 - h_3) < 0 \\ Q_{cc} &= \dot{m}_t h_3 - \dot{m}_c h_2 = \dot{m}_f \text{LHV} > 0\end{aligned}$$

The cycle efficiency is written:

$$\eta = \frac{|\tau_t| - |\tau_c|}{\dot{m}_f \text{LHV}}$$

This model based on the component enthalpy balances is very general and rigorous, but incomplete as models of fluids have not been selected. In what follows, we will show the very sensitive differences in results which are obtained depending on the assumptions made at that level.

12.1.4.1 Perfect gas cycle without irreversibilities

The basic thermodynamic cycle used in gas turbines is the Brayton cycle. It is assumed that the air passing through the gas turbine is perfect and there is no irreversibility. Its plot in an entropy chart is given in Figure 12.1.13. Note that this representation has meaning because it is assumed here that the working fluid remains the same throughout the cycle. In a real gas turbine, the change in gas composition strictly prohibits plotting it on a single chart, although this is frequently done.

In the open cycle, the compressor sucks air into the atmosphere and pressurizes it. At high pressure, heat is supplied by burning a fuel with air. The products of combustion at high temperature and high pressure are then expanded in a turbine to produce mechanical energy. A portion (approximately 60 to 70%) of the output is used to drive the compressor, usually mounted directly on the turbine shaft. The difference between the expansion work and compression work is equal to the useful work of the machine, which corresponds to about one third of the work done by the turbine.

In the standard air Brayton cycle, we assume as a first approximation that the working fluid in the turbine is air, as in the compressor. In fact, this is not quite rigorous, first because the mass

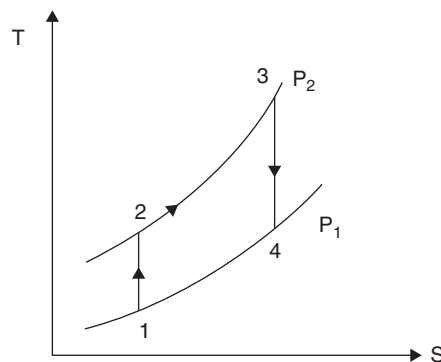
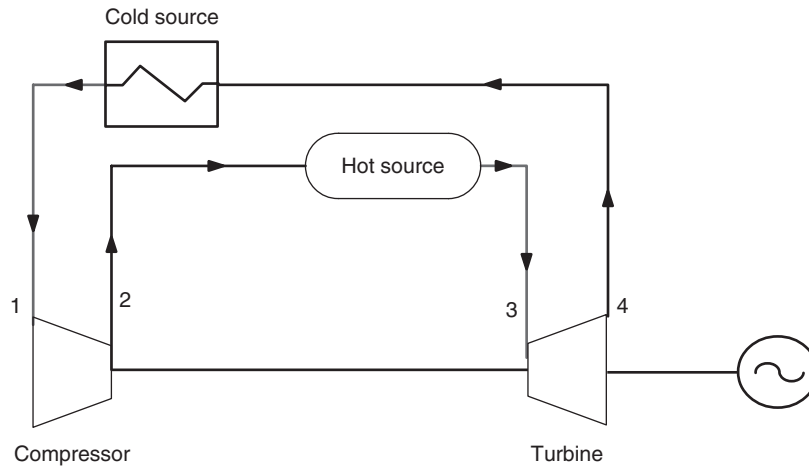


FIGURE 12.1.13

Theoretical open Brayton cycle

**FIGURE 12.1.14**

Sketch of a closed cycle gas turbine

flow into the turbine is a little higher because of the mass-rate of fuel, and secondly because the thermodynamic properties of combustion products differ from those of air. But we can neglect this point as there is usually a large excess of air during combustion.

In a closed cycle, the gas turbine exhausts are cooled at low temperature in a heat exchanger, before being recirculated to the compressor, whose output is then supplied to the high temperature heat exchanger, as direct combustion of the working fluid is no longer possible. The introduction of these two exchangers has the effect of increasing costs and lowering heat exchange effectiveness. However, it allows the average pressure of the cycle to be significantly increased, and thus its specific power. All things considered, it is justified only in special cases.

Such a cycle is shown in the diagram in Figure 12.1.14.

With the assumption of a constant flow-rate in the machine, the cycle efficiency is:

$$\eta = \frac{(h_3 - h_4) - (h_2 - h_1)}{h_3 - h_2}$$

Air being assumed perfect, we have: $h = c_p T + \text{Const.}$, or $\Delta h = c_p \Delta T$.

Moreover, on isentropes 1–2 and 3–4 of Figure 12.1.13, we have (equation (5.6.8) of Part 2):

$$\frac{P_2}{P_1} = \frac{P_3}{P_4} = \left(\frac{T_2}{T_1} \right)^{\gamma/(\gamma-1)} = \left(\frac{T_3}{T_4} \right)^{\gamma/(\gamma-1)}$$

$$\eta = 1 - \frac{T_1 - T_4}{T_2 - T_3}$$

$$\eta = 1 - \left(\frac{P_2}{P_1} \right)^{(1-\gamma)/\gamma} \quad (12.1.1)$$

We see that, assuming first that the fluid follows the perfect gas law, and secondly there is no irreversibility, the efficiency is an increasing function of the compression ratio.

12.1.4.2 Perfect gas cycle with irreversibilities

In reality, we know that the compression and expansion do not follow an isentrope but are irreversible adiabatic (Figure 12.1.15).

Even if we keep the assumption of perfect air, it is desirable to refine the model by taking into account irreversibilities.

Isentropic formulation

Taking into account the isentropic efficiencies of the compressor η_c (between 0.88 and 0.92), and of the turbine η_t (near 0.86), the cycle efficiency is given by equation 12.1.2.

$$\eta = \frac{\eta_t(h_3 - h_4) - (h_2 - h_1)}{h_3 - h_2'} \quad (12.1.2)$$

Introducing ratios:

$$\theta = \frac{T_3}{T_1}, \quad \beta = \frac{\gamma - 1}{\gamma}, \quad \text{and} \quad r = \frac{P_2}{P_1},$$

we get

$$\begin{aligned} h_2 - h_1 &= c_p T_1 (r^\beta - 1) \\ h_3 - h_4 &= c_p T_3 (1 - r^{-\beta}) \\ h_3 - h_4 &= c_p T_1 \theta (1 - r^{-\beta}) \\ h_3 - h_2' &= c_p (T_3 - T_2') \\ h_3 - h_2' &= c_p T_1 \left(\theta - 1 - \frac{r^\beta - 1}{\eta_c} \right) \end{aligned}$$

All calculations done, we get:

$$\eta = \frac{(r^\beta - 1)(\eta_c \eta_t \theta - r^\beta)}{r^\beta (\eta_c (\theta - 1) + 1 - r^\beta)} \quad (12.1.3)$$

The graph in Figure 12.1.16 shows that the efficiency drops significantly as compared to the theoretical cycle, and there is an optimum compression ratio, which is an increasing function of the ratio θ of the inlet temperatures in the turbine and the compressor, and depends on the isentropic efficiencies of these devices and γ , ratio of heat capacities of the working fluid.

Polytropic formulation

This way of working is however not the most relevant, especially if one looks at the influence of compression ratio r on the performance of the machine, as isentropic compression and expansion efficiencies η_c and η_t are then a function of r . As has been shown in section 7.1.3.2 of Part 2, it is preferable to use a polytropic formulation, and this is all the more justified that compressors and turbines are most often multistage axial machines, whose polytropic efficiency is then substantially equal to the isentropic efficiency of a stage.

Introducing ratios β_c for the compressor and β_t for the turbine:

$$\begin{aligned} \beta_c &= \frac{k_c - 1}{k_c} = \frac{1}{\eta_{pc}} \cdot \frac{\gamma - 1}{\gamma} \\ \beta_t &= \frac{k_t - 1}{k_t} = \eta_{pt} \frac{\gamma - 1}{\gamma} \end{aligned}$$

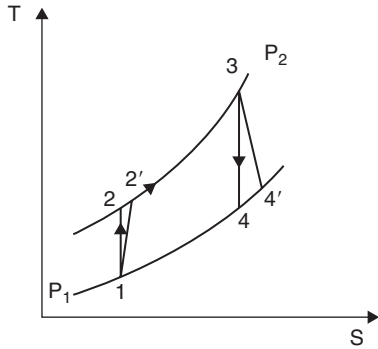


FIGURE 12.1.15
Actual open Brayton cycle

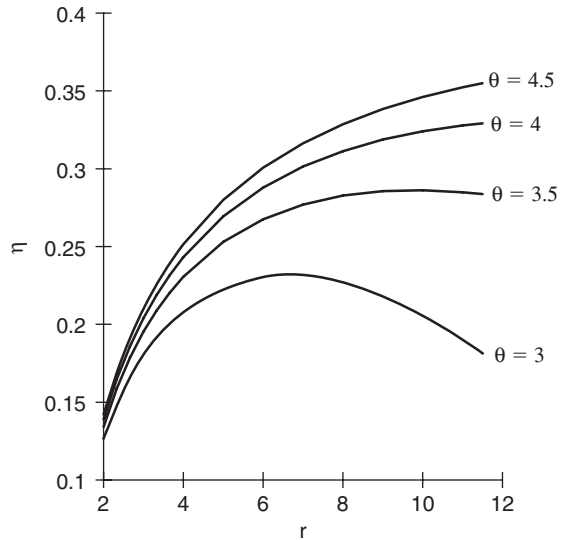


FIGURE 12.1.16
Efficiency of the open Brayton cycle

We get:

$$T_{2'} = T_1 \left(\frac{P_2}{P_1} \right)^{\beta_c} = T_1 r^{\beta_c}$$

$$T_{4'} = T_3 \left(\frac{P_1}{P_2} \right)^{\beta_t} = T_1 \theta r^{-\beta_t}$$

The efficiency of the Brayton cycle with irreversibilities is equal to:

$$\eta = \frac{(T_3 - T_{4'}) - (T_{2'} - T_1)}{T_3 - T_{2'}} \tag{12.1.4}$$

$$\eta = \frac{\theta(1 - r^{-\beta_t}) + 1 - r^{\beta_c}}{\theta - r^{\beta_c}}$$

The output power can be expressed in dimensionless form by dividing its value by the product $c_p(T_3 - T_1) = c_p T_1(\theta - 1)$.

We get:

$$W_0 = \frac{\theta(1 - r^{-\beta_t}) + 1 - r^{\beta_c}}{\theta - 1} \tag{12.1.5}$$

From these two expressions it is possible to plot the chart of Figure 12.1.17, which shows for various values of θ and r , curves binding η and W_0 . This chart shows that the compression ratio value leading to the maximum power output is not that which leads to the best efficiency.

The maximum efficiency is obtained for compression ratios greater than those which result in maximum power, because for a given turbine inlet temperature, the temperature of exhaust gases is even lower than the compression ratio is high.

As the upper curves are relatively flat, manufacturers generally prefer to optimize their engines for maximum power, even if the efficiency slightly drops.

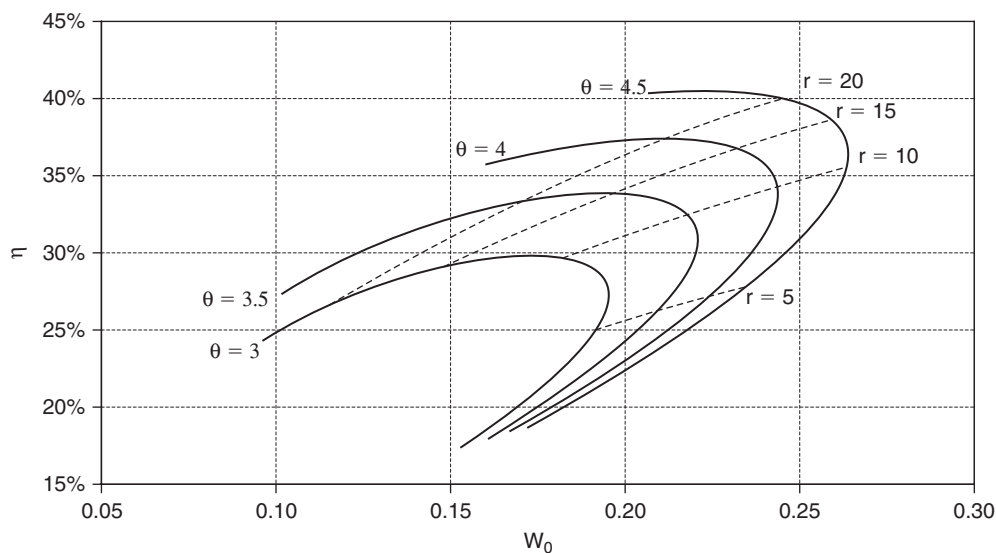


FIGURE 12.1.17

Efficiency and reduced power of a gas turbine

These curves also show that the maximum efficiency is an increasing function of θ . To obtain high efficiencies, it is thus necessary to increase as much as possible the turbine inlet temperature. Today, efficiencies above 40% are obtained with compression ratios equal to 30, and an installed capacity exceeding 220 MW. These values are increasingly getting closer to steam plant limits.

12.1.4.3 Modeling with ThermoOptim

In the analytical developments above, we have assumed that the machine was traversed by a constant flow of perfect air, when in reality the mass flow and gas composition vary, and their heat capacities depend on temperature.

If we want to eliminate this assumption, the analytical calculations quickly become intractable. However, it is quite possible to model with good accuracy various gas turbine cycles with ThermoOptim as discussed in the following sections. It is in this sense that the method proposed in this book complements the classical approach to obtain results much more accurate and believable.

The interested reader can in particular study the sensitivity of flue gas composition to settings he chooses for the combustion chamber. In particular if he takes into account the dissociation of CO_2 , unburned gases (CO , H_2) will appear in the fumes.

The simple cycle is the subject of the third example given at the end of Part 2 (section 9.3). If he wants to know how to build step by step such a ThermoOptim model, the reader may refer to this example or to the corresponding Getting Started guide downloadable from the portal¹. Figure 12.1.18 shows the result of such modeling.

This gas turbine has been designed with a compression ratio equal to 16 and a turbine inlet temperature equal to $1,150^\circ\text{C}$. By varying the pressure of the cycle, we get the chart in Figure 12.1.19 which gives the evolution of efficiency in terms of useful work. The maximum efficiency is obtained for a compression ratio of 27, and the maximum power for 11.

It is also possible to model a closed cycle gas turbine. If the gas is perfect, the results provided by the software match those obtained analytically: the calculated efficiency is the same as that given by equation (12.1.4). The reader can verify that this is the case for a helium gas turbine operating between 2 and 18 bar (Figure 12.1.20).

¹ <http://www.thermoOptim.org/sections/logiciels/thermoOptim/documentation/exemples/turbine-gaz-simple>

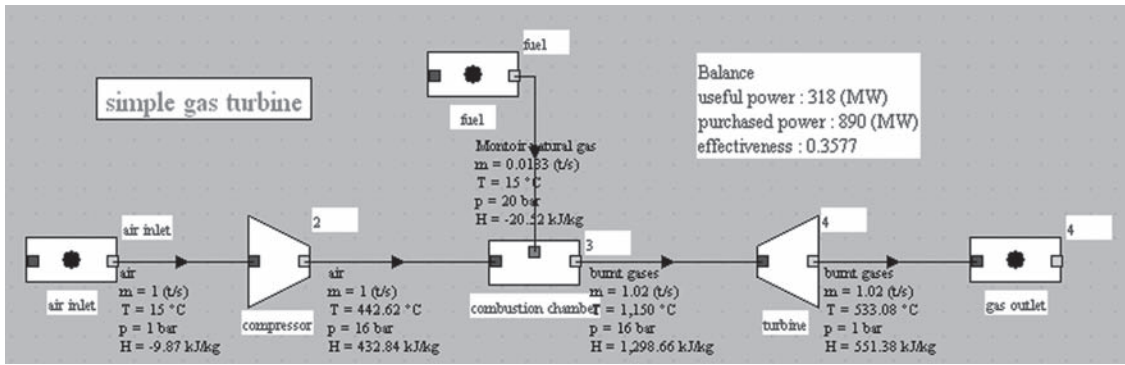


FIGURE 12.1.18

Synoptic view of an open cycle gas turbine

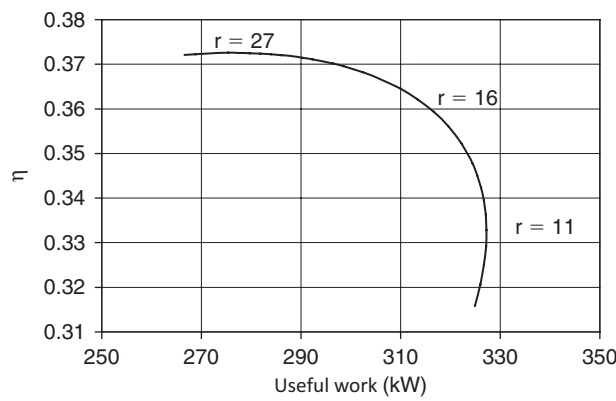


FIGURE 12.1.19

Efficiency and power of a gas turbine

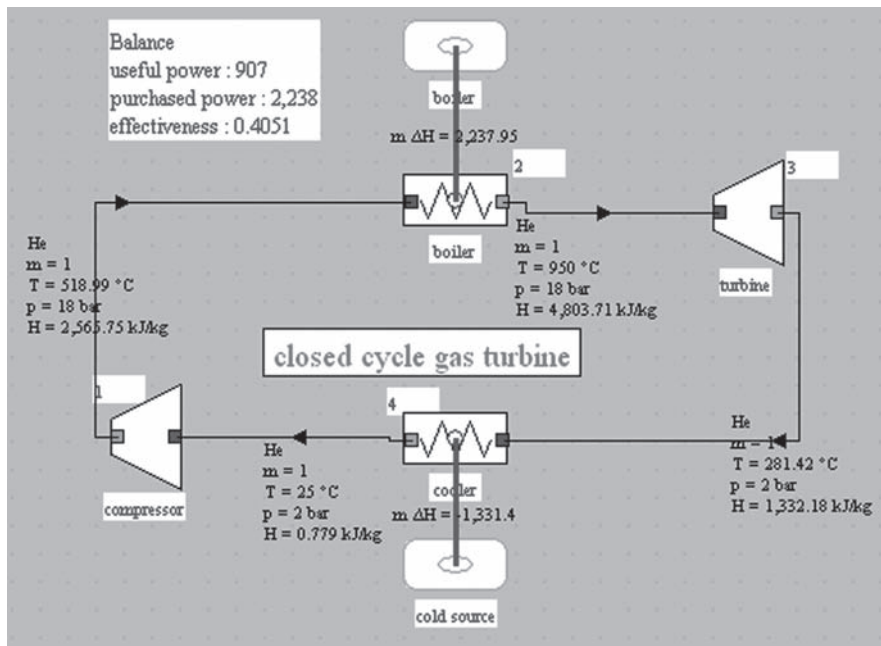


FIGURE 12.1.20

Synoptic view of a closed cycle gas turbine

12.1.4.4 Energy and exergy balances

From the open-cycle GT model developed with ThermoOptim, it is easy to build the energy balance of the cycle by completing a table of type 12.1.1.

The efficiency here is the ratio of the work provided by the cycle to the heat generated by combustion.

To build up the exergy balance, we must begin by setting a temperature and pressure reference. We take here $T_0 = 288.15\text{ K}$ (15°C) and $P_0 = 1\text{ bar}$, corresponding to the gas turbine air suction conditions. Table 12.1.2 can then be built up step by step, following the guidance of section 10.2.3 of Part 2 which is summarized below.

TABLE 12.1.1
GAS TURBINE ENTHALPY BALANCE

Point	flow-rate (kg/s)	h (kJ/kg)	
fuel	0.0183	-21	
air inlet	1	-10	
2	1	433	
3	1.0183	1,299	
4	1.0183	551	
Process	τ (kW)	Q (kW)	Δh (kW)
compression	443	0	443
combustion		890	890
expansion	-761	0	-761
cycle	-318	890	571
energy efficiency		35.77%	

TABLE 12.1.2
GAS TURBINE EXERGY BALANCE

Point	Flow-rate (kg/s)	h (kJ/kg)	s (kJ/kg/K)	xh (kJ/kg)				
fuel	0.0183	-21	-1.2	324				
air inlet	1	-10	0.13	-47	Δx_{h_comb}	614		
2	1	433	0.26	355	comb_eff	69%		
3	1.01827	1,299	1.18	957				
4	1.01827	551	1.3	175				
Exergy balance								
$T_0 = 288.15\text{ K} = 15^\circ\text{C}$								
Process	τ (kW)	Q (kW)	$m\Delta h$ (kW)	$m\Delta s$ (kW/K)	Δx_q (kW)	$m\Delta x_h$ (kW)	Δx_{h_i} (kW)	% loss
compression	443		443	0.14		402	40	7%
combustion		890	890	0.94	890	614	276	47.8%
expansion	-761		-761	0.12		-796	35	6.1%
exhaust						-226	226	39.1%
cycle	-318	890	571	1		-7	578	100.0%
sigma(x_q+))		890						
sigma(tau+))		0.00						
Exergy efficiency								35%

For each component, Equation 10.2.3 is written:

$$\Delta x_{hij} = \sum_{k=1}^n x_{qjk} - m_j \Delta x_{hj} + \tau_j$$

It can be simplified here because heat-exergies are all zero. On the other hand there is the problem of its extension to the case of the combustion chamber, which is resolved simply by replacing the heat-exergy by the fuel input exergy. The exergy literature indicates, according to authors, that the exergy of a fuel is close to its LHV or its HHV.

These two values differ little eventually, and given the fact that we seek to establish an approximate balance, we will follow those who equate it with its LHV available in Thermoptim.

The exergy balance of the combustion chamber is then easily built: per kg of air, the fuel releases an exergy equal to 890 kJ. The exergy change of the fluids in the chamber being equal to 614 kJ, the irreversibilities are equal to 276 kJ. The exergy efficiency of the chamber is equal to 69%, while its energy efficiency is 100% because it is adiabatic. If we took into account the pressure drop, the efficiency would be somewhat lower.

In Table 12.2, losses are given as percentage of total irreversibilities. It shows that they are mainly concentrated in the combustion chamber and exhaust, and they are substantially equal in compressor and turbine (their polytropic efficiencies being equal).

Finally, the cycle being not closed, equation 10.2.5 should be amended to reflect the exhaust gas residual exergy, which adds to irreversible losses. The reference conditions for the calculation of enthalpies and entropies differing from that chosen for the environment, it is important to make the corresponding correction.

Ways to improve gas turbine performance can be deduced from the exergy balance:

- increase the cycle temperature to increase the combustion efficiency. We have already discussed the technological limitations that are encountered at this level;
- recover the exergy available in the exhaust. We will now discuss possible solutions.

12.1.5 Cycle improvements

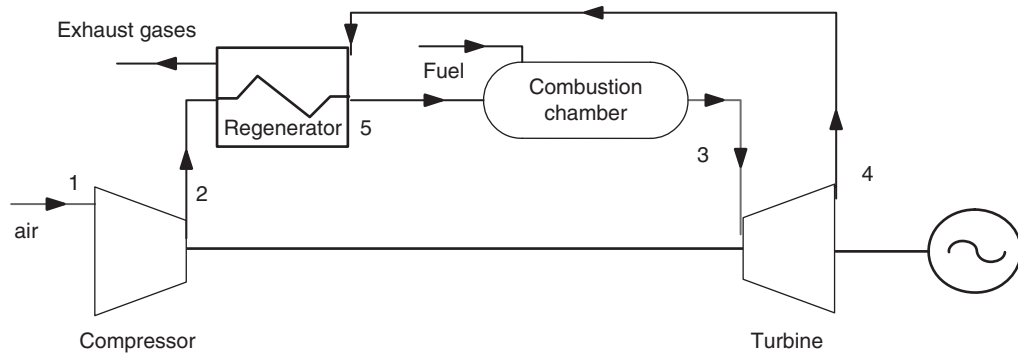
12.1.5.1 Cycle with regeneration

Most gas turbines work in open cycle and discharge gases at high temperature (500–600°C) in the atmosphere. For taking advantage of their value, it is sometimes possible to use them to preheat the air leaving the compressor. As shown in Figures 12.1.21 and 12.1.22, we can recover at least part ($h_5 - h_{2'}$) of the maximum available enthalpy ($h_{5'} - h_{2'}$). This is called **regeneration**. Microturbines, with a capacity of several tens of kW, generally use this cycle.

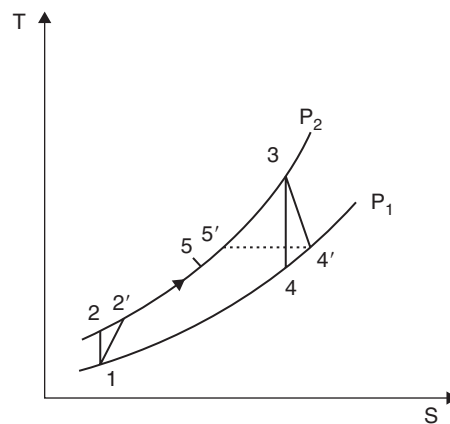
We call regenerator effectiveness the ratio $\varepsilon = (h_5 - h_{2'}) / (h_{5'} - h_{2'})$, which characterizes the fraction of the available enthalpy actually recoverable.

The heat to be provided to the cycle is reduced in this case to $(h_3 - h_5)$. With assumptions and notations of section 12.1.4.2, we get:

$$\begin{aligned} h_3 - h_5 &= c_p(T_3 - T_5) \\ T_{2'} &= T_1 r^{\beta_c} & T_3 &= \theta T_1 \\ T_{4'} &= T_1 \theta r^{-\beta_t} \\ T_5 &= T_{2'} + \varepsilon(T_{4'} - T_{2'}) = [r^{\beta_c} + \varepsilon(\theta r^{-\beta_t} - r^{\beta_c})]T_1 \\ h_3 - h_5 &= c_p T_1 [\theta(1 - \varepsilon r^{-\beta_t}) + (\varepsilon - 1)r^{\beta_c}] \end{aligned}$$

**FIGURE 12.1.21**

Sketch of a regenerative gas turbine

**FIGURE 12.1.22**

Regenerative Brayton cycle in the entropy chart

$$\eta = \frac{\theta(1 - r^{-\beta_c}) + 1 - r^{\beta_c}}{\theta(1 - \varepsilon r^{-\beta_c}) + (\varepsilon - 1)r^{\beta_c}} \quad (12.1.6)$$

For example, let us study the performance of a gas turbine sucking air at 1 bar and 21°C and compressing it to 4 bar; at the exit of the combustion chamber, its temperature is equal to 816°C, the isentropic efficiencies of compressor and turbine being respectively equal to 85% and 90%. For this cycle, the overall efficiency without regeneration is equal to 24.2%. With a regenerator of effectiveness 0.83, it reaches 40.9%.

The addition of the regenerator thus increases by almost 70% the cycle efficiency. Note that, under such conditions, gas turbine performance is quite correct.

Figure 12.1.23 shows the shape of the efficiency of the regenerative gas turbine given by equation (12.1.6) for two values of effectiveness: 0.85 and 0.5. The four curves in each family correspond to different values of θ : 3, 3.5, 4 and 4.5.

We note that the interest of the regenerator is even better when the compression ratio is low. Indeed, beyond a certain limit, itself a function of θ , the fluid heating in the compressor is such that temperature $T_{2'}$ at the output of the compressor becomes higher than temperature $T_{4'}$ at the end of expansion. The regenerator can no longer function and becomes useless.

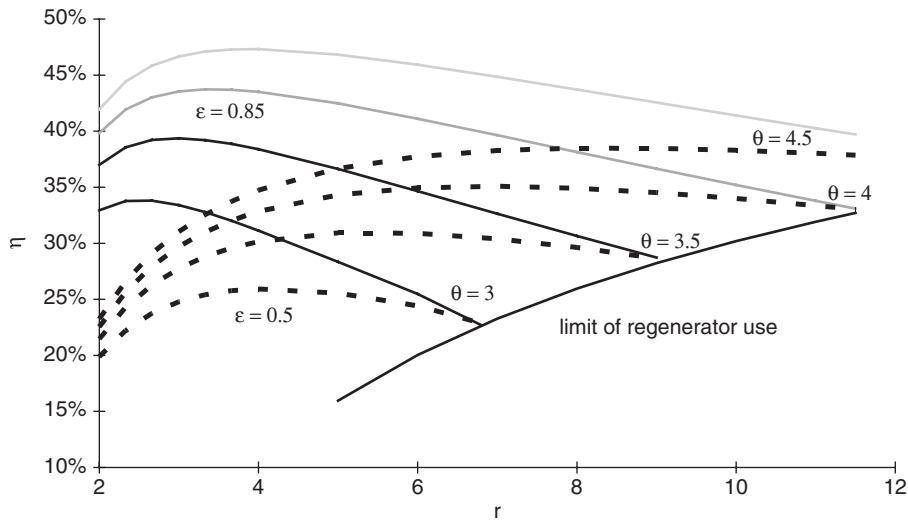


FIGURE 12.1.23
Limits of the regenerative Brayton cycle

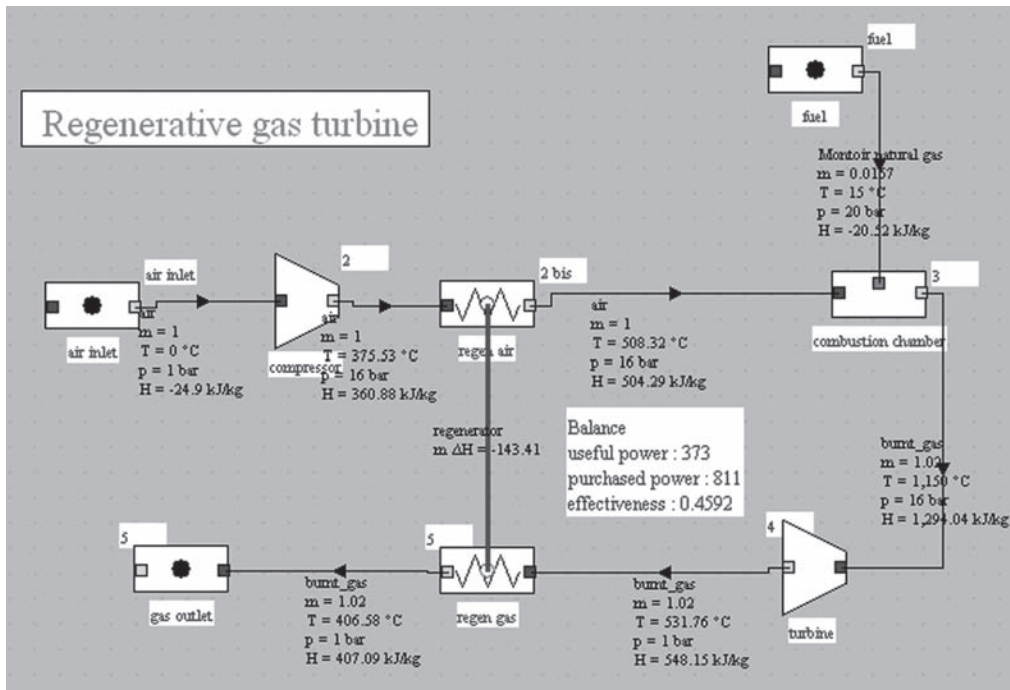


FIGURE 12.1.24
Synoptic view of a regenerative gas turbine

This condition, independent of ϵ , is given by:

$$T_{2'} \leq T_{4'} \quad r^{\beta_c} \leq \theta r^{-\beta_t} \quad \text{or} \quad r \leq \theta^{1/(\beta_c + \beta_t)}$$

As shown in the graph of Figure 12.1.23, all curves corresponding to the same θ and different values of ϵ intersect at the point where $T_{2'} = T_{4'}$.

The analytical results above are of course no more valid when we no longer assume that the working fluid is unique and perfect.

Building a model with Thermoptim poses no particular problem. In the example shown in Figure 12.1.24, we started from the gas turbine studied in Figure 12.1.18 and we added a regenerator of effectiveness $\varepsilon = 0.85$.

A parametric study varying the compression ratio allows the chart in Figure 12.1.25 to be plotted. Maximum power is obtained for $r = 16$, and maximum efficiency for $r = 6$. The influence of the compression ratio is the inverse of that observed for the simple gas turbine.

Given that the current trend, as noted above, consists in increasing the compression ratio, regeneration is poorly suited for modern machinery using advanced technologies, except sequential combustion turbines (see section 12.1.5.3). Instead, it is almost always used for small turbines (25–500 kW), called micro-turbines. We shall see in Chapter 17 that combined cycles can valorize the residual enthalpy available in the exhaust gases when regeneration cannot be used.

The exergy balance of a regenerative gas turbine can be built similarly to that of the simple gas turbine. The only precaution is to calculate the irreversibilities in the regenerator as shown in section 10.2.2 of Part 2. Table 12.1.3 can thus be built step by step.

The exergy efficiency rises from 35% to 46% thanks to the regenerator, but there are still significant losses in the exhaust.

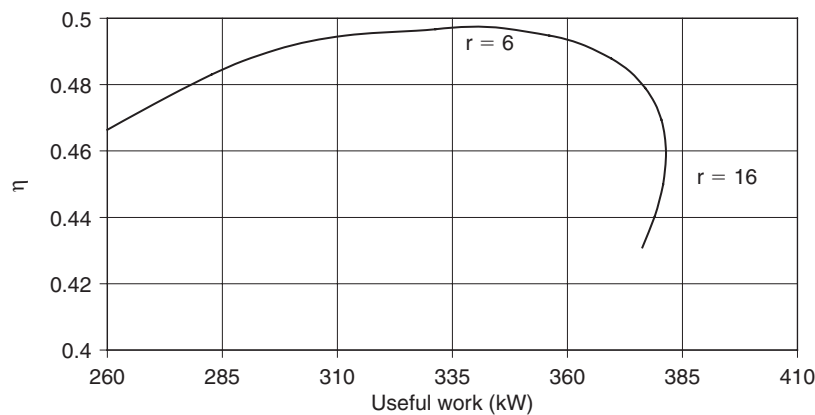


FIGURE 12.1.25

Efficiency and power of a regenerative gas turbine

TABLE 12.1.3

REGENERATIVE GAS TURBINE EXERGY BALANCE

Exergy balance process	$T_0 = 288.15\text{ K} = 15^\circ\text{C}$							
	τ (kW)	Q (kW)	$m\Delta h$ (kW)	$m\Delta s$ (kW/K)	Δx_q (kW)	$m\Delta x_h$ (kW)	Δx_i (kW)	% loss
air compr.	392	0	392	0.09		367	26	5.77%
comb. ch.			830	0.86	830	583	247	54.89%
turbine	-774	0	-774	0.13		-810	36	8.04%
regen. gaz		-146	-146	-0.20		-89	2	0.49%
regen. air		146	146	0.20		87		0.00%
exhaust						-138	138	30.81%
cycle	-381	0	449			-	449	100.00%
$\sigma(x_q+)$		830						
$\sigma(\tau+)$		0,00						
Exergy efficiency								46%

In this model, the exchanger losses remain small because it is a counter-flow unit working with a relatively low log-mean temperature difference (approximately 27K), and especially because we have neglected pressure drops, which would increase the compression work and reduce the expansion work.

12.1.5.2 Cycle with intercooler

We know that we can reduce the compression work by conducting a staged compression with intermediate cooling (see section 7.1.4 of Part 2).

Figure 12.1.26 shows the result of a simulation obtained for the gas turbine of Figure 12.1.18, by providing an intermediate pressure equal to 4 bar and a compressed air cooling at 20°C (we shall show an example where further cooling is provided by an exchanger with ambient air of effectiveness equal to 0.8).

The gain in efficiency is low, but the capacity is however greatly increased.

The graph in Figure 12.1.27 shows that for this type of machine, the efficiency and capacity are both increasing functions of the compression ratio, to the extent that sufficient intermediate cooling is provided. The difficulty is that the morphology of aeroderivative machines that lead to the best performance, is generally not well suited to intermediate cooling, so that this solution is rarely used.

12.1.5.3 Sequential combustion cycle

However, it is often easier to insert a sequential combustion than an intercooling, as the combustion chamber is much smaller than a cooling exchanger.

The Alstom Power GT24/26 gas turbine presented in Figure 12.1.4 is an example of this type of machine, where, after a first expansion at an intermediate pressure, the gases are redirected into a second combustion chamber before being expanded in a LP turbine.

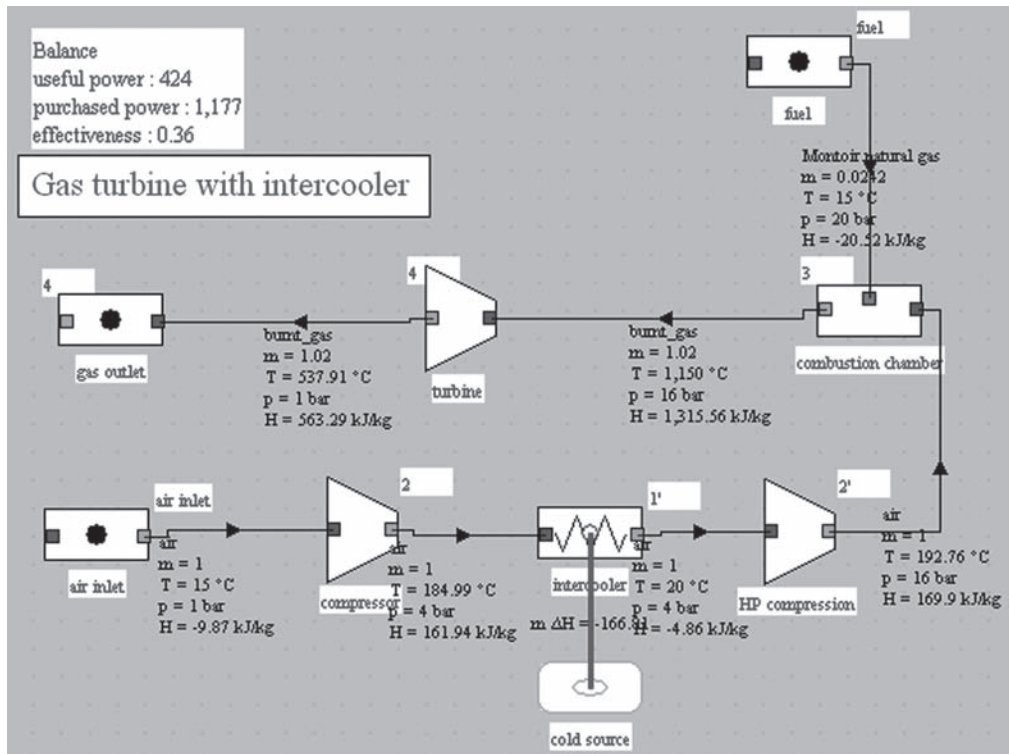
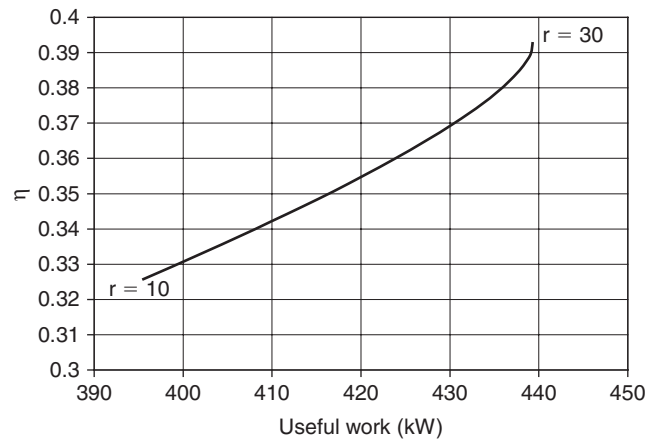
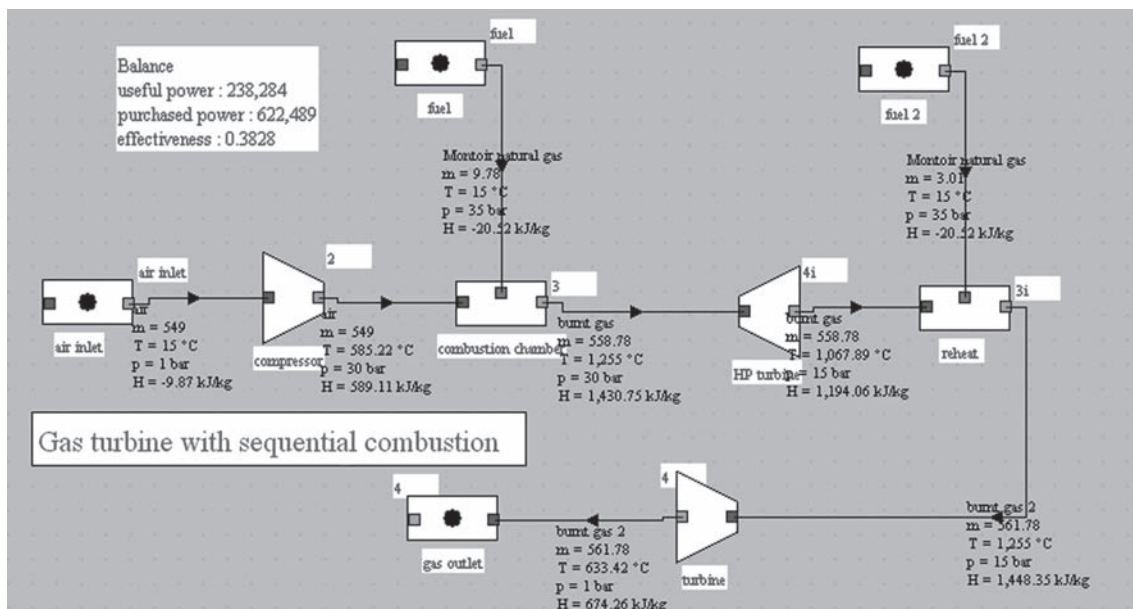


FIGURE 12.1.26

Synoptic view of a gas turbine with intercooler

**FIGURE 12.1.27**

Efficiency and power of a gas turbine with intercooler

**FIGURE 12.1.28**

Synoptic view of a gas turbine with sequential combustion

Figure 12.1.28 shows a model of the GT 24/26, with values close to those given by the manufacturer. By varying the intermediate pressure, we obtain the chart of Figure 12.1.29 which gives the efficiency as a function of power output.

Since the inlet temperature in the LP turbine is constant (1,255°C) the higher the intermediate pressure, the lower the expansion outlet temperature, and thus the lower the losses in the exhaust, which explains that the best efficiency is obtained for $P_{4i} = 18$.

12.1.5.4 Cycle with intercooling, sequential combustion and regeneration

Another cycle improvement involves combining the above changes by performing a two-stage compression with intermediate cooling and expansion with multi-stage sequential combustion, and a regenerator which can then be used without temperature crossover (Figure 12.1.30).

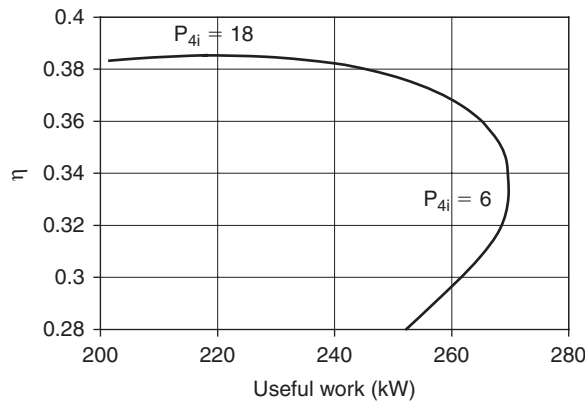


FIGURE 12.1.29
Efficiency and power of a gas turbine with sequential combustion

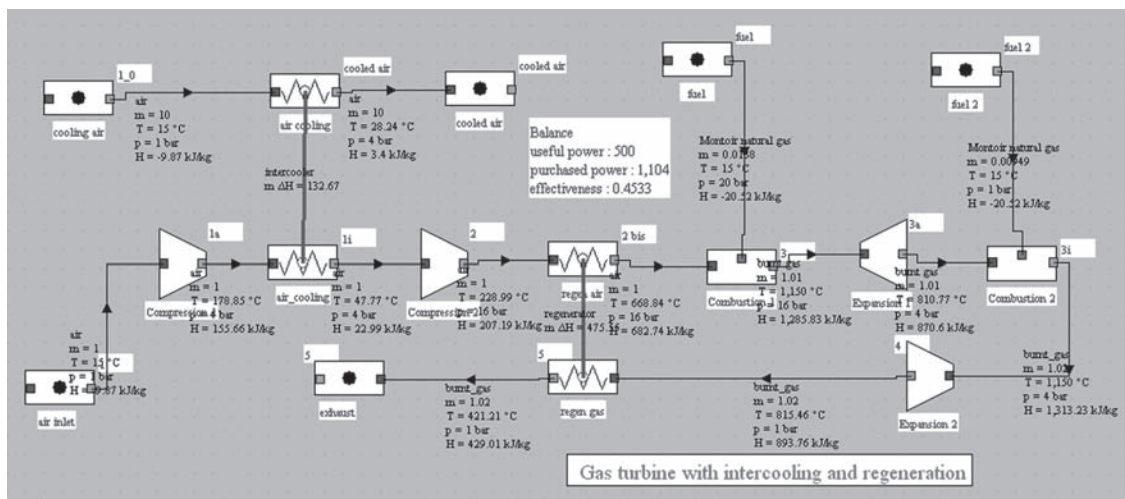


FIGURE 12.1.30
Synoptic view of a gas turbine with intercooling, sequential combustion and regeneration

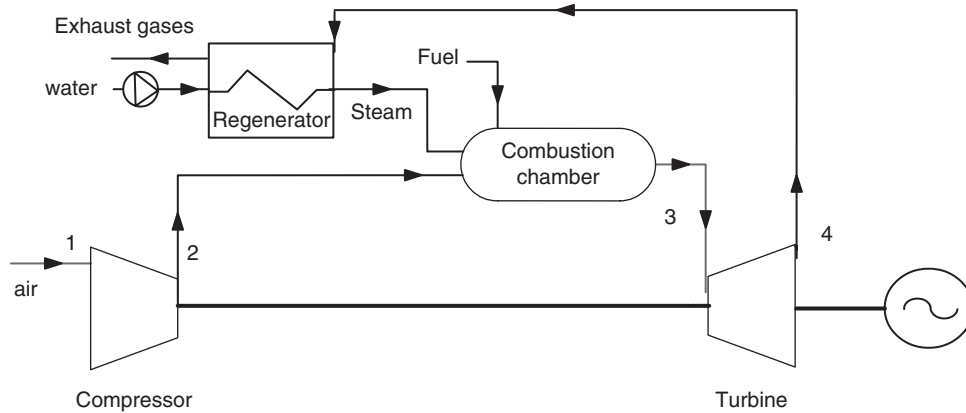
It is thus possible to perform para-isothermal compression and expansion, so that the global cycle is similar to a regenerative cycle with two isotherms and two isobars whose performance is equal to the Carnot cycle.

The efficiency thus increases accordingly, but at the cost of increased complexity and higher cost. It thus departs significantly from the initial simplicity of the gas turbine.

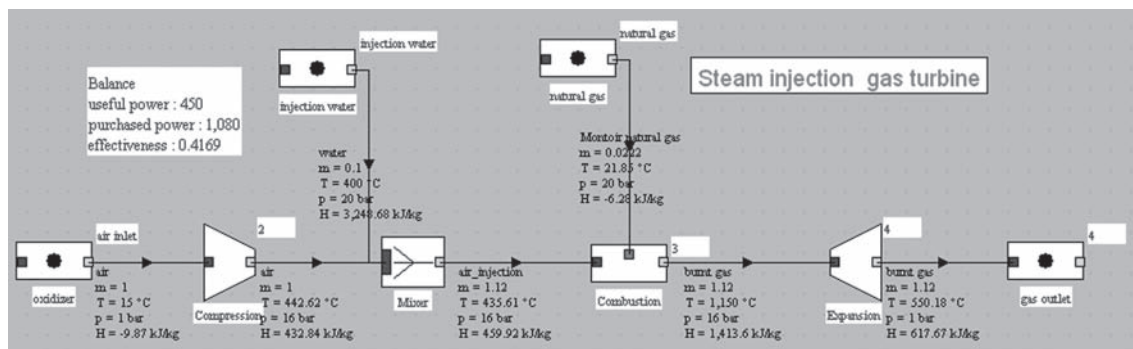
12.1.5.5 Steam injection cycle

Another way to improve the cycle efficiency, and above all the power available on the turbine shaft, is to inject steam into the combustion chamber (Figure 12.1.31). It is thus possible to recover part of the enthalpy of the exhaust gases, and increase the mass flow through the turbine. Moreover, this mode of operation reduces emissions of nitrogen oxides NOx. This type of cycle can achieve efficiencies near 45% in practice, but has the disadvantage of requiring water.

The thermodynamic analytical study of these cycles is more complex than that of the regenerative cycle previously studied, and will not be treated here. Their modeling in Thermoptim poses no particular problem (Figure 12.1.32), at least insofar as there is no need to detail the operation of the heat recovery steam generator (HRSG), which will be discussed in Chapter 17.

**FIGURE 12.1.31**

Steam injection gas turbine

**FIGURE 12.1.32**

Synoptic view of a steam injection gas turbine

12.1.5.6 Cooled gas turbine

The performance of gas turbines being very sensitive to the intake air temperature (see section 12.1.6.1), it may be advantageous to cool the air in an artificial way, using a compression refrigeration cycle. This is particularly the case in hot countries where power needs are time varying, and where the peak call is often due to air conditioning needs during the hottest hours. In such circumstances it may be economically attractive to produce ice during off-peak hours and use this ice as a cold source to cool the intake air during peak hours. The machine efficiency is slightly improved, but especially its capacity is substantially increased.

Figure 12.1.33 corresponds to a gas turbine where the ambient air at 30°C is cooled at 1°C. The gain in efficiency is 1 point, but power is increased by 12.5%. Explanations on the refrigeration cycle are given in section 19.3.

12.1.6 Mechanical configurations

Until now, we basically thought in terms of machine design, whereas the precise calculation of the components is up to manufacturers, who alone have the appropriate tools.

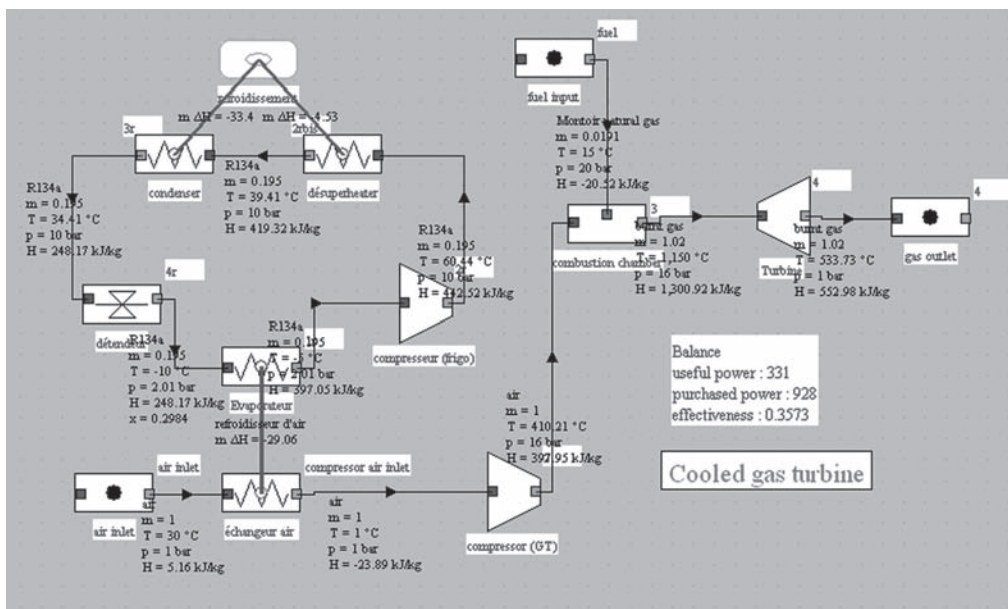


FIGURE 12.1.33
Synoptic view of a cooled gas turbine

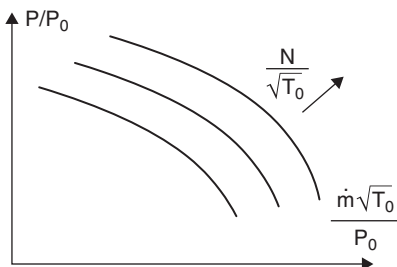


FIGURE 12.1.34
Compressor characteristics

In this section we shall look at part load operation of gas turbines, which involves using models capable of representing at least approximately their adaptation to operating conditions. The characteristics of compressors and turbines has been established on the basis of similarity relations in the chapter on turbomachinery (section 7.3.3.1 of Part 2), and we limit ourselves here to some essential qualitative indications.

Let us recall that the characteristics of a machine are a chart allowing its operating points to be defined for different values of its tuning parameters. To plot that of a GT, it is necessary to superimpose the compressor and turbine characteristics, which requires, for the operation to be possible, to choose consistent coordinate systems.

The characteristics of a compressor have the appearance of Figure 12.1.34. For different reduced rotation speeds the pressure ratio drops when the corrected flow increases.

In Figure 12.1.35 turbine characteristics are presented as for the compressor with the corrected flow-rate in abscissa, not ordinate (Figure 7.5.4 of Part 2) as it is usually done. Although the theoretical characteristics do not depend on the rotation speed, this is in reality not entirely true, because shocks occur in the rotor outside the rated conditions, but the characteristics dispersion is very low.

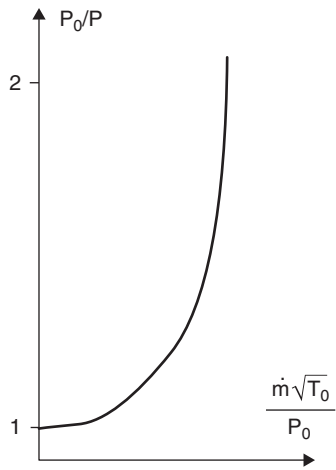


FIGURE 12.1.35
Turbine characteristics

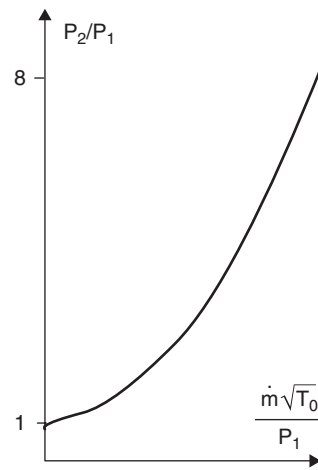


FIGURE 12.1.36
Turbine characteristics relative to compressor inlet conditions

This characteristic is plotted for a reduced flow-rate relative to admission conditions in the turbine (T_3 , P_2). For the gas turbine study, we must relate them to admission conditions in the compressor (T_1 , P_1).

Beyond the critical expansion ratio, the turbine corrected flow-rate remains constant:

$$\frac{\dot{m}\sqrt{T_3}}{P_2} = K$$

Replacing T_3 by θT_1 , and P_2 by $P_1 (P_2/P_1)$, we get:

$$\frac{\dot{m}\sqrt{T_1}}{P_1} = K \frac{P_2}{P_1} \frac{1}{\sqrt{\theta}}$$

Relative to admission conditions in the compressor, the performance map of the turbine thus takes the shape of Figure 12.1.36, for a given value of θ .

12.1.6.1 Single shaft turbine

The simplest gas turbine is, as we noted above, a machine where the compressor and turbine are coupled on the same shaft, which directly drives the recipient machine.

By neglecting the influence of the fuel mass flow-rate, it follows that the mass flow through the compressor and turbine have the same value and that, neglecting the pressure drop in the combustion chamber, the inlet pressure in the turbine is equal to the pressure at the compressor outlet.

To obtain the characteristics of the complete gas turbine, it is in this case possible to superimpose those of the compressor and turbine, resulting in the graph in Figure 12.1.37.

Knowing θ and N , we determine point of operation M , which allows the pressure P_2 and the flow-rate to be deduced as well as isentropic compression and expansion efficiencies, when the characteristics of the compressor and turbine are equipped with them.

The values of compression and expansion work can be estimated from the approximate analytic expressions (12.1.7) and (12.1.8).

$$W_c = \dot{m}\tau_c = \dot{m} \frac{\tau_{cs}}{\eta_c} = \frac{\dot{m}}{\eta_c} c_p T_1 (r^\beta - 1) \quad (12.1.7)$$

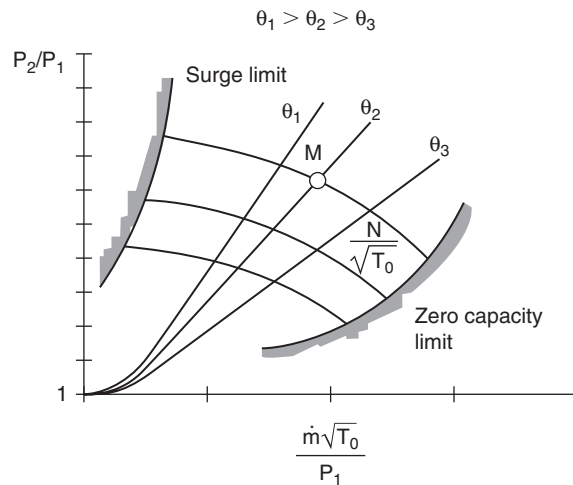


FIGURE 12.1.37

Single shaft gas turbine characteristics

$$W_t = \dot{m}\tau_t = \dot{m}\eta_t\tau_{ts} = \dot{m}\eta_{tc_p}\theta T_1(1 - r^{-\beta}) \quad (12.1.8)$$

The useful range of the graph is limited in its upper left by the surge line or a curve θ_{\max} , and on the bottom right by a curve corresponding to a zero value of the available power, corresponding to $W_c = W_t$.

From the foregoing it is clear that the effective power of a gas turbine is a highly complex function of both the geometric characteristics of the machine and its operating conditions.

For this type of engine, it is thus not possible in the general case to determine a characteristic graph which should directly show the power output or torque depending for example on the rotation speed. To do so, we must at least specify the admission conditions in the machine and the value of θ chosen for the machine.

Indeed, a parameter such as outside temperature evolving between winter and summer from about -15°C to 25°C , the capacity of the machine varies over plus or minus 20% around its average value obtained for approximately 5°C , and the efficiency of plus or minus 10%, the maximum performance being achieved during winter.

The diagram in Figure 12.1.38 illustrates this, showing how the nominal operating point, changes from A in winter to B in summer.

At **partial load**, to adjust the power supplied by the gas turbine to that requested by the user machine, the operator has in principle several possibilities:

- **reduce the flow-rate** (Figure 12.1.39), for example by creating an artificial pressure drop through control valves located between the compressor and turbine;

Indeed, if the rotation speed N remains fixed and the flow rate decreases, the operating point must pass from M to M' , the increased pressure ratio leading to overheating.

If it is desired that the θ value does not vary (adjusting combustion at constant temperature T_3), the operating point has to go down to M'' , which requires creating an artificial pressure drop. The pressure ratio drops significantly, as do the efficiency and power of the machine.

As this type of setting (partial injection) is furthermore complex in mechanical terms, it is almost never adopted in practice because of these two reasons.

- **Reduce the temperature** (Figure 12.1.40), by decreasing the amount of fuel injected. If the speed remains constant, the operating point switches to P , which significantly deteriorates the cycle, given the shape of the efficiency islands (see section 7.3.3 of Part 2);

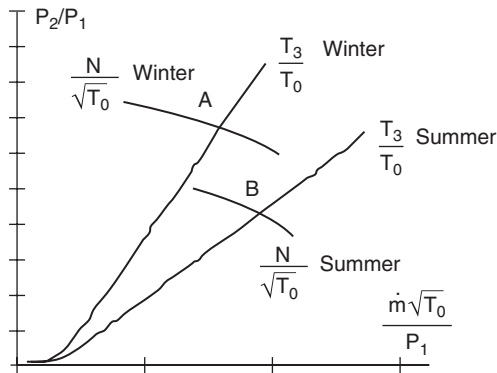


FIGURE 12.1.38
Summer-winter adaptation of a single shaft gas turbine

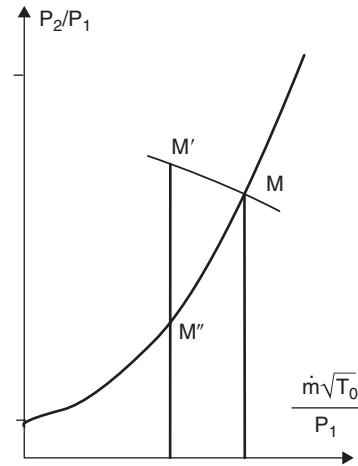


FIGURE 12.1.39
Flow-rate control

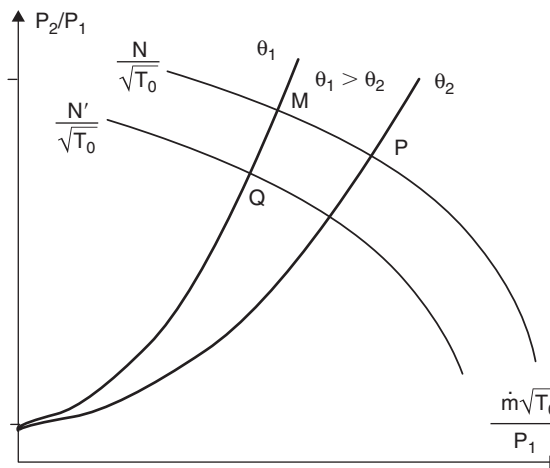


FIGURE 12.1.40
Temperature or speed control

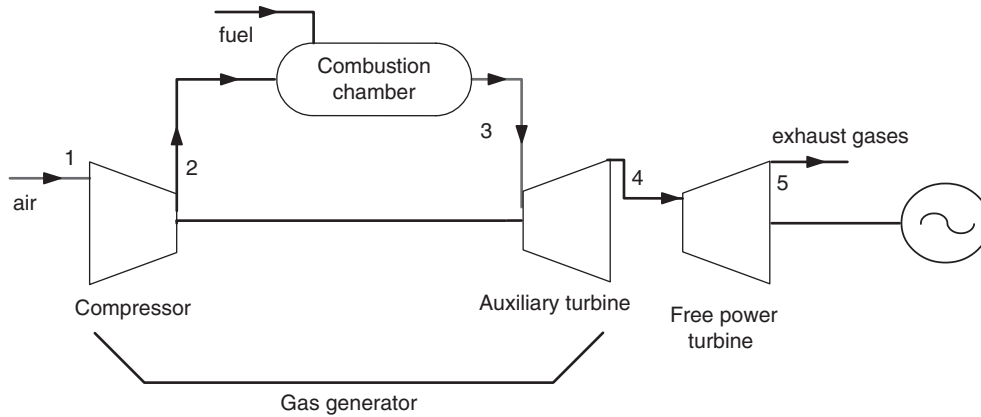
- **reduce the speed** (Figure 12.1.40), which sets the machine to point Q. The pressure ratio and flow rate dropping, the performance deteriorates significantly, too.

It is possible, however, playing simultaneously on the speed and θ , if θ_{\max} is not reached, to arrange for the turbine adaptation curve to differ little from a iso-efficiency line, and thus limit the efficiency losses due to system operating at partial load. Of course the control must be capable of taking into account very precisely the characteristics of the machine.

In these circumstances, we find that a single shaft turbine is poorly suited for operation at partial load, especially if the speed is set (as in electricity generation for example). However, in case of sudden discharge of the receiving machine, the runaway speed of the gas turbine will be low, the compressor absorbing, as we have seen, almost two thirds of the power supplied by the turbine.

12.1.6.2 Twin shaft turbine

The limits of adaptation of the single shaft turbine lead to the idea of separating it into two parts according to their respective functions: first the auxiliary turbine, usually located upstream, whose

**FIGURE 12.1.41**

Two shaft gas turbine

role is solely to drive the compressor, and second the useful power turbine, driving the receiver machine (Figure 12.1.41). We can distinguish the gas generator, upstream, and the mechanical energy generator, downstream.

The gas generator being mechanically independent of the receiver machine, its speed can vary without constraint.

Representing the characteristics of such a machine is no longer possible on a single map, even if the mass flow rate remains constant at first approximation through the assembly, because the pressure that develops between the two turbines varies so that the matching conditions of the gas generator (equal power consumed by the compressor and supplied by the auxiliary turbine) can be met.

Part load operation is obtained by simultaneously playing on the fuel injection and the rotation speed, as indicated above, which reduces the gas generator flow rate. The power output can be adjusted by maintaining acceptable efficiency in a much wider range than with a single shaft turbine (80% of nominal output at 60% load, 60% at 30% load). However, the nominal efficiency is slightly lower than that of the single shaft gas turbine, due to increased friction losses, and the installation cost is slightly higher.

Twin shaft facilities are mainly used when seeking a good performance over a wide range of power variation of the receiving machine. This is particularly the case in transport, in particular aeronautical propulsion, which we will study further.

An additional advantage of two shaft gas turbines is that it is possible to run the gas generator at high speed (between 20,000 and 30,000 rpm), which allows for very compact structures. In particular, manufacturers of aircraft engines have developed very powerful techniques, using hollow shafts to reduce congestion caused by the presence of two shafts.

Finally, startup problems are greatly simplified since we can start the gas generator at its rated speed before coupling the useful turbine to the receiving machine. This provides a reserve power to overcome the starting torque of the latter, which is not the case in single shaft systems.

Some manufacturers even offer three shaft machines, such as Rolls Royce with its Trent industrial turbine, of 50–60 MW capacity, which reaches an efficiency of 42.5% with a compression ratio equal to 35. The mass of the Trent being equal to about 29 t, this machine has one of the largest specific capacities of the market (1.8 kW/kg). Its design has benefited from the experience gained on the RB211, built in nearly 300 units over the past thirty years. Figure 12.1.42 shows the gas generator of the RB211, which, coupled with a Cooper-Bessemer power turbine, delivers about 26 MW for a compression ratio equal to 20, with an efficiency of 38%.

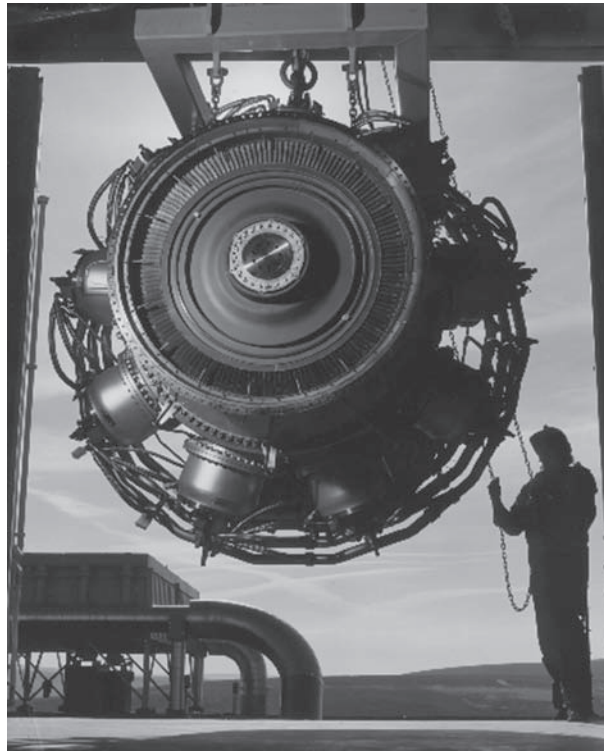


FIGURE 12.1.42

RB211 gas generator, Reproduced courtesy of Rolls-Royce plc

12.1.7 Emissions of pollutants

As is the case for other types of engines, combustion in gas turbines discharges pollutants, which are mainly carbon monoxide, unburned hydrocarbons and nitrogen oxides NO_x. Due to the large excess of air that still exists, it is mostly the latter which is difficult to limit.

However, very significant progress has been made in the development of low emission combustion chambers, called low NO_x chambers. Rejection rates of NO_x below 10 ppm are common today, which ranks the gas turbine among the cleanest engines, well ahead compared to reciprocating engines.

However, emission standards becoming stricter in some countries it may be necessary to go further. If you want to eliminate these discharges, it is possible to use catalytic purification of gases, which can be achieved either by injecting into the flue gas downstream of the machine a reducing gas such as ammonia (Selective Catalytic Reduction or SCR), thereby dividing by about 5 the concentration of NO_x, or by using the SCONO_x technology, which uses a catalyst to reduce CO and NO_x while destroying volatile organic compounds (VOCs) other than methane. This system, which operates at temperatures between 150 and 370°C fits well into heat recovery steam generators (HRSG) of combined cycle or cogeneration facilities discussed in Chapters 17 and 18, and has various advantages over the SCR catalyst purification, especially neither to form sulfates nor particulates smaller than 2.5 μm.

12.1.8 Outlook for gas turbines

The performance of gas turbines are expected to rise further in coming years because of technology transfer from aerospace and major R&D programs underway in the area, in particular in the United States.

With the ambition to revolutionize the future of military aerospace propulsion systems, the U.S. (Department of Defense, Defense Advanced Research Projects Agency, and all major U.S. manufacturers of aviation turbines) have launched in 1988 the IHPTET program (Integrated High Performance Turbine Engine Technology). Specifically, the program aimed to:

- double the “thrust/weight” propulsion capacity by the year 2005 to double the aircraft range and load;
- reduce the specific consumption by 30–50% with improved components, new materials, and a turbine inlet temperature above 1,950°C;
- use components in non-metallic materials and metal matrix in order to simplify design, reduce the number of parts needed, improve lifetime and reduce costs.

The program, which ended in 2005, has made significant progress and is succeeded by the Affordable Advanced Turbine Engines (AATE) program. As compared to year 2000 fielded engine levels, its objectives can be summarized as follows: reduce specific fuel consumption by 25%, improve shaft horsepower to weight ratio by 65%, improve design life by 20%, reduce production and maintenance cost by 35%, and reduce development cost by 15%.

Outlet temperatures of gas turbine combustion chambers should continue to grow in the future, despite the already high levels achieved. Refer to section 12.2.1.8 for further discussion of this issue.

Moreover, manufacturers will continue their efforts to increase the compactness of their machines, leading to stronger and stronger constraints on the design of certain components such as combustion chambers. Already we have seen in the introductory chapter that their compactness is several hundred times greater in gas turbines than in conventional coal plants (Figures 11.1.4 and 11.1.5). The movement should be continued: for example, an increase of 60% capacity (at equivalent size) was obtained between two generations of two Alstom Power gas turbines of the same size. Figure 12.1.43 presents a superposition of these machines: GT13E2, 165 MW in the lower part, and the GT 26, 265 MW in the upper part. A human figure is used to display the size of the machines (to fix ideas, the thermal block of the latter has a mass of about 350 t). The size reduction of the combustion chamber is particularly telling.

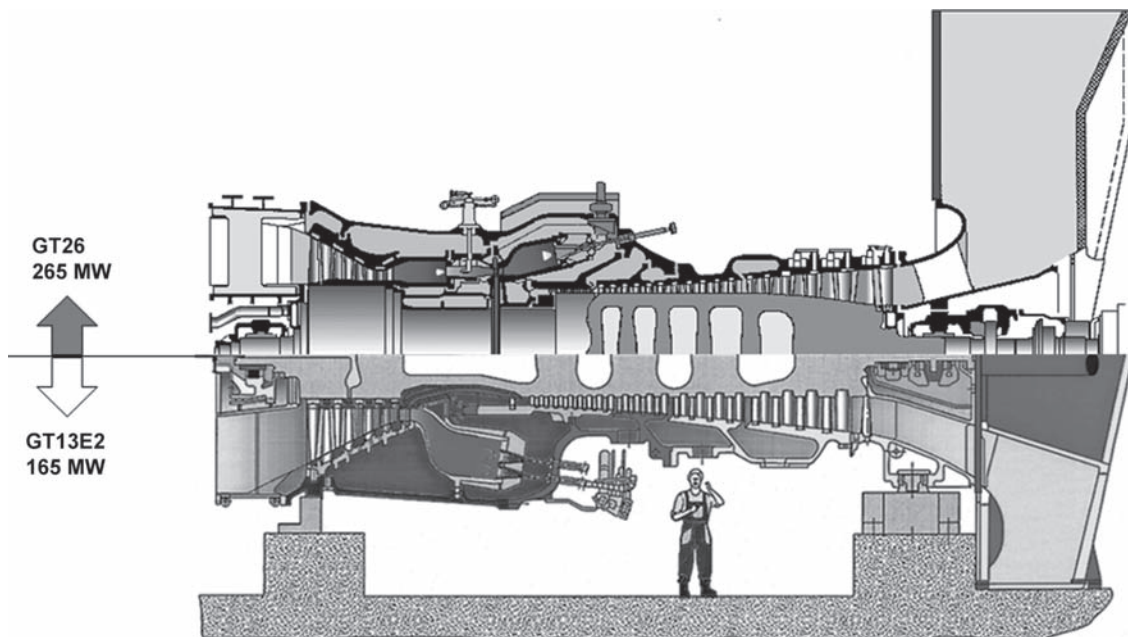


FIGURE 12.1.43

Comparison of two generations of Alstom Power gas turbines, Documentation Alstom Power

12.2 AIRCRAFT ENGINES

For years, airplanes have been propelled by propellers driven by gasoline engines. Even today, this is the best solution for small airplanes. When, for larger aircraft, the propeller is kept in view of its excellent performance, it is often driven by a turboprop engine using an open cycle gas turbine. However, turbojet engines have replaced the propeller for the propulsion of many aircraft, including most long-haul airliners. It is also the only engine that is suitable for supersonic flight, and it thus equips most military aircraft. At very high speeds, and for the propulsion of long range missiles, the jet engine reaches its limits, and the ramjet is used because it provides very good efficiency. However, it cannot operate autonomously at take-off, which must then be provided by a turbojet or rocket engine.

In this chapter we will examine in turn the principles of operation of the turbojet, the turboprop engine, the ramjet and the rocket engine. We refer the reader interested in detailed analyzes of these engines to the authoritative book by A. F. El-Sayed (2008), *Aircraft propulsion and gas turbine engines*.

12.2.1 Turbojet and turboprop engines

12.2.1.1 Principles of operation

A jet engine of the type that is commonly used in aviation is a simple modification of a gas turbine open cycle studied previously: the turbine is sized to only drive the compressor (Figures 12.2.1 to 12.2.3). At the turbine outlet, the excess energy available in the gas at high pressure and temperature

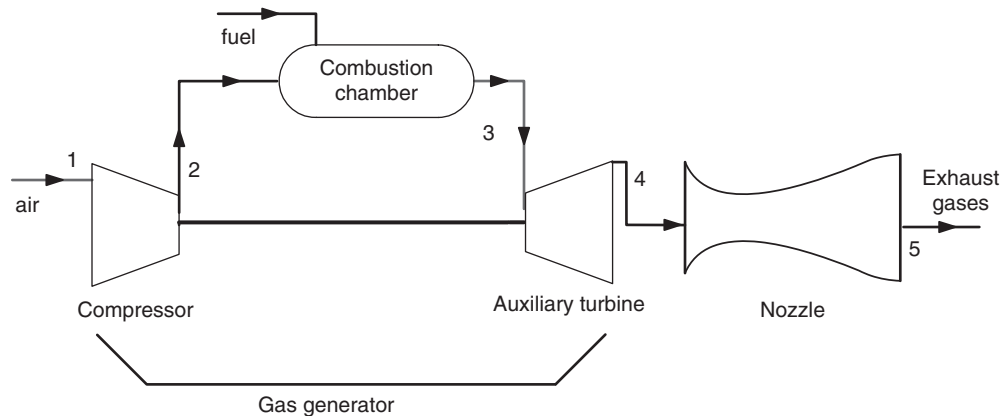


FIGURE 12.2.1

Sketch of a turbojet

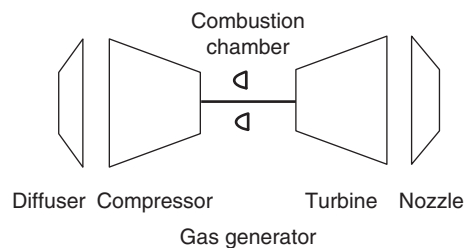
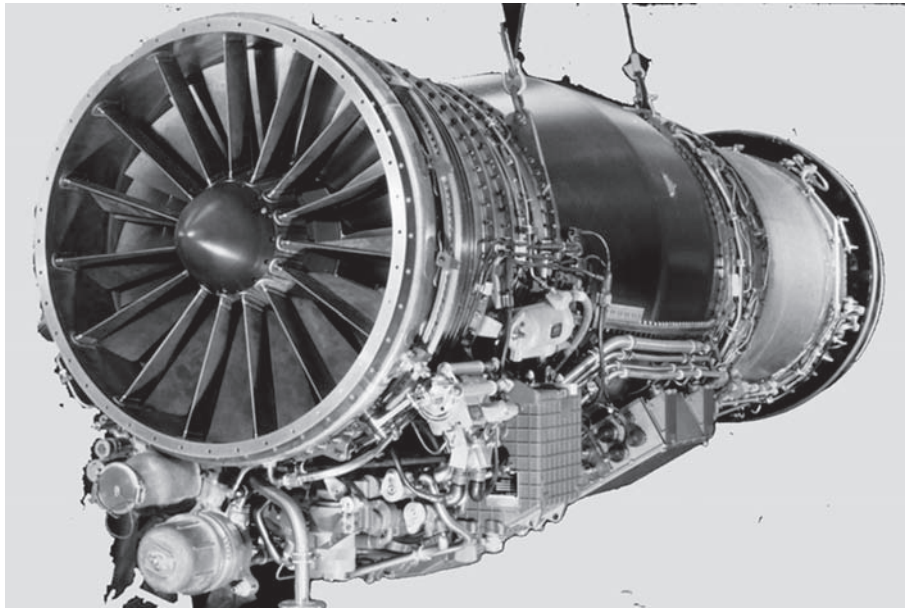


FIGURE 12.2.2

Turbojet

**FIGURE 12.2.3**

M88-2 engine (© Snecma Moteurs)

is converted into kinetic energy in a nozzle. The thrust results from the difference of momentum between intake and exhaust gases.

It also includes an inlet diffuser, which is used to create a static precompression at the compressor inlet (Figure 12.2.2).

A turbojet is therefore the combination of a diffuser, a gas generator and a nozzle. The study of the functioning of the gas generator made above remains entirely valid. Note, however, that one of the characteristics of turbojet engines is that they operate in highly variable conditions of pressure and temperature: at sea level, take off and landing, the pressure is close to 1 bar and the temperature may reach 40°C. In flight, pressure drops due to the altitude and reaches a few tenths of a bar, while the temperature drops below -40°C. Under these conditions, the jet engine is required to operate with widely varying values of the reduced flow. This leads to problems of adaptation of the turbine and nozzle.

Figure 12.2.3 shows a M88-2 Snecma turbojet equipping the French Rafale fighter. This engine has a turbine inlet temperature of 1,577°C, a mass of 897 kg, a length of 3.54 m and an inlet diameter of 0.7 m. Its maximum thrust is 50 kN (about 5 t) without afterburners, and 75 kN with (see section 12.1.1.5). The high temperature level reached in this engine requires specific blade protection devices that will be discussed in section 12.2.1.8.

By definition, the thrust is equal to:

$$F = \dot{m}(C_1 - C_5) \quad (12.2.1)$$

C_1 being the speed of the aircraft, and C_5 that of the gas at the nozzle exit.

Propulsion power is therefore:

$$W_p = FC_1 = \dot{m}C_1(C_1 - C_5)$$

W_p must be compared to the kinetic power available at the reactor outlet:

$$W_c = \dot{m} \left(\frac{C_1^2}{2} - \frac{C_5^2}{2} \right)$$

We can thus define the propulsive efficiency: $\eta_p = \frac{W_p}{W_c} = \frac{C_1(C_1 - C_5)}{\frac{C_1^2}{2} - \frac{C_5^2}{2}}$

$$\eta_p = \frac{2}{1 + \frac{C_5}{C_1}} \quad (12.2.2)$$

The higher the velocity C_1 , the better the propulsive efficiency.

$$\eta_p = \frac{1}{1 + \frac{C_5 - C_1}{2C_1}} \quad (12.2.3)$$

Expression (12.2.3) also shows that for a given velocity C_1 , the propulsive efficiency is even better than the exhaust gas relative velocity ($C_5 - C_1$) is low.

The **thermal efficiency** η_{th} is in turn defined as the ratio of kinetic power to heat Q .

We have:

$$\eta_{th} = \frac{C_5^2 - C_1^2}{2Q} \quad (12.2.4)$$

Assuming that $C_1 \approx C_4$, which is perfectly legitimate given the other assumptions made, we have:

$$h_5 + \frac{C_5^2}{2} = h_4 + \frac{C_4^2}{2}$$

It is customary to analyze the operation of the engine at both the fixed point, that is to say on the ground, and in flight. The first analysis being simpler and very close to that of the gas turbine, we will begin with it.

For all these calculations, we will retain modeling assumptions similar to those chosen for the study of the gas turbine. However, the temperatures reached being higher than in terrestrial machines, we will consider the change in gas heat capacity by introducing two values of c_p , one at low temperature for the air compression phase, noted as previously c_p , and the other at high temperature for the entire flue gas expansion, denoted c_{pg} .

12.2.1.2 Operation at fixed point

As before, we retain the polytropic formulation, with, in addition to ratios β_c for the compressor and β_t for the turbine, a ratio β_p for the propulsion nozzle:

$$\beta_c = \frac{k_c - 1}{k_c} = \frac{1}{\eta_{pc}} \frac{\gamma - 1}{\gamma}$$

$$\beta_t = \frac{k_t - 1}{k_t} = \eta_{pt} \frac{\gamma_g - 1}{\gamma_g}$$

$$\beta_p = \frac{k_p - 1}{k_p} = \eta_{pp} \frac{\gamma_g - 1}{\gamma_g}$$

β_t and β_p are calculated from γ_g , ratio of specific heat capacities at constant pressure and volume for hot gas and not air.

It comes, r being the compression ratio, and r_t the expansion ratio in the turbine:

$$T_2 = T_1 \left(\frac{P_2}{P_1} \right)^{\beta_c} = T_1 r^{\beta_c} \quad (12.2.5)$$

$$T_4 = T_3 \left(\frac{P_4}{P_2} \right)^{\beta_t} = T_1 \theta r_t^{-\beta_t} \quad (12.2.6)$$

The mechanical equilibrium condition of the compressor and turbine allows the intermediate pressure P_4 to be determined:

$$c_p(T_2 - T_1) = c_{pg}(T_3 - T_4) \quad (12.2.7)$$

The temperature of gases leaving the propulsion nozzle is given by:

$$T_5 = T_4 \left(\frac{P_1}{P_4} \right)^{\beta_p} \quad (12.2.8)$$

The heat supplied to the cycle in the combustion chamber is:

$$Q = c_{pg}T_3 - c_pT_2 \quad (12.2.9)$$

and

$$\eta_{th} = \frac{c_{pg}(T_4 - T_5)}{c_{pg}T_3 - c_pT_2}$$

Figure 12.2.5 gives the appearance of the thermal efficiency of the cycle. Its evolution is similar to that of Figure 12.1.16 established for the gas turbine, which is quite normal, since the only difference in assumptions is the inclusion of a thermal capacity of gases other than that of air at low temperature.

12.2.1.3 Flight operation

Compared to the fixed point, the main differences in the flight operation come from the speed of the aircraft which is no longer zero, and pressure and temperature of intake air, which are much lower (typically $P = 0.01$ bar and $T = -50^\circ\text{C} = 223$ K at altitude 10,000 m).

The major effect is the speed that creates a dynamic compression in the inlet diffuser of the jet engine: the kinetic energy of intake air is converted into pressure energy in the diffuser (evolution (0–1) on the cycle shown in Figure 12.2.6). For a given state 4, the compression and consequently the expansion work is thus reduced.

Air being assumed to be perfect, equations (7.3.8) and (7.3.9) of Part 2 govern this slowdown assuming isentropic evolution. If we consider it polytropic, equation (7.3.8) remains valid, and the calculation of the final pressure must be slightly modified. By introducing for consistency ratio β_d for the inlet diffuser, and noting T_0 and P_0 the suction temperature and pressure, we get:

$$T_1 = T_0 \left(\frac{P_1}{P_0} \right)^{\beta_d} = T_0 r^{\beta_d} \quad (12.2.10)$$

As:

$$T_1 = T_0 + \frac{C_1^2}{2c_p} \quad (12.2.11)$$

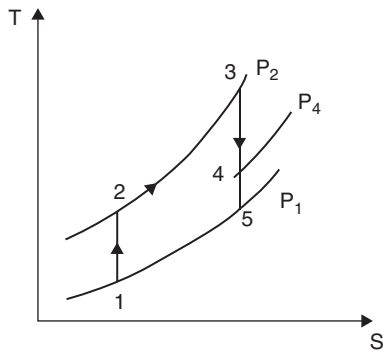


FIGURE 12.2.4
Theoretical turbojet cycle in an entropy chart

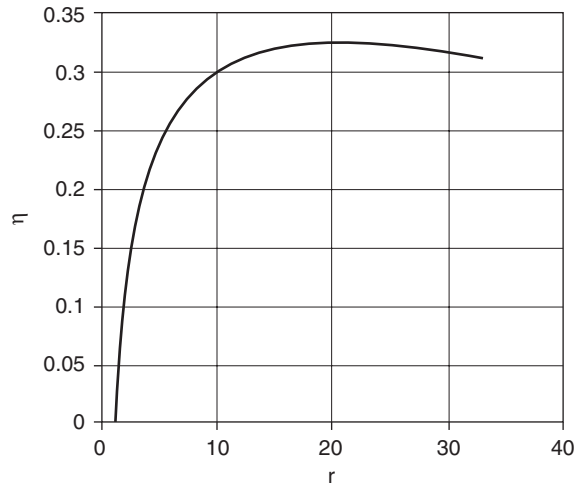


FIGURE 12.2.5
Efficiency function of compression ratio

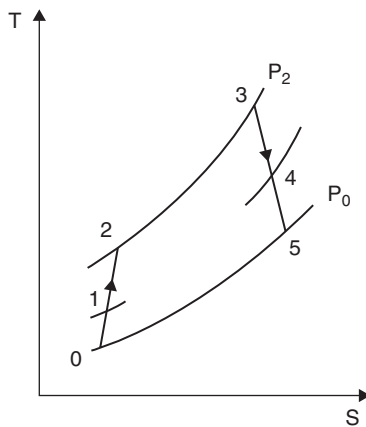


FIGURE 12.2.6
Actual turbojet cycle in an entropy chart

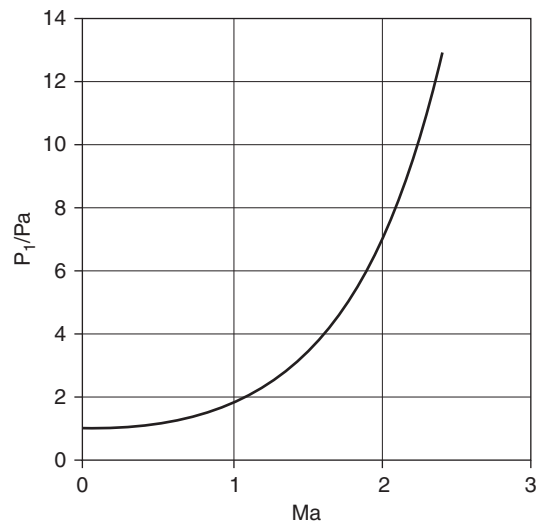


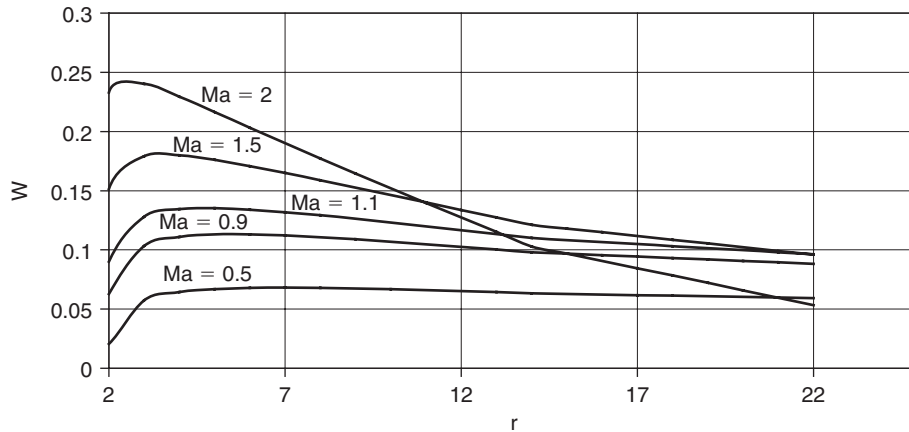
FIGURE 12.2.7
Dynamic compression function of Mach number

The inlet pressure in the compressor can be calculated. As function of the Mach number, we get:

$$P_1 = P_0 \left(1 + \frac{\gamma - 1}{2} \text{Ma}^2 \right)^{1/\beta_d} \quad (12.2.12)$$

The dynamic pressure depends on the speed of the aircraft, and leads to compression ratios close to those in Figure 12.2.7. For low speeds, its influence is relatively small, but then it grows very fast.

As the compressor continues to compress the air by providing its own compression ratio, the overall ratio quickly becomes very high. At Mach 2, for example, the dynamic compression ratio is about 7. If the compressor has a compression ratio equal to 10, the overall ratio is 70, which is considerable. The rest of the cycle is determined relatively easily. We shall just give relations for calculating the points, without writing the final analytical expressions which we get, as they present only a limited interest.

**FIGURE 12.2.8**

Propulsion power function of compression ratio

Let us assume that the turbine inlet temperature T_3 is given: it is, as we have seen, determined by the mechanical resistance of the first expansion blades.

The compression outlet temperature T_2 is given by (12.2.5), the expansion outlet temperature T_4 by (12.2.6). Equation (12.2.7) still expresses the equality of work done by the turbine and consumed by the compressor, and determines the intermediate pressure P_4 .

The velocity of gases leaving the nozzle is given by (12.2.13):

$$C_5 = \sqrt{2c_p(T_4 - T_5) + C_1^2} \quad (12.2.13)$$

Thrust (direction opposite to velocity) is:

$$F = \dot{m}(C_1 - C_5)$$

The power output is equal to the thrust multiplied by the velocity of the aircraft:

$$W_p = FC_1 \quad (12.2.14)$$

As for the gas turbine, we can define a dimensionless power by dividing W_p by the enthalpy Δh which should be provided to heat air from T_0 to T_3 :

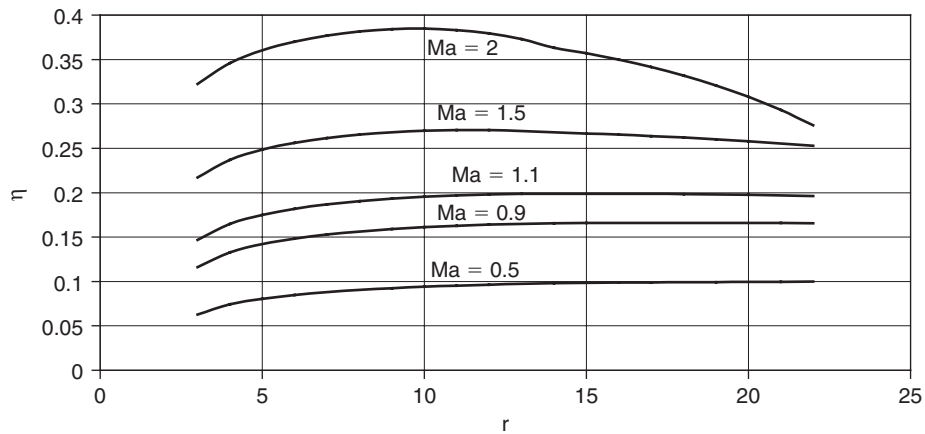
$$\Delta h = c_{pg}T_3 - c_pT_0$$

It is thus possible to plot graphs showing the evolution of reduced power and efficiency in terms of compression ratio for various values of Mach number, that is to say aircraft speed.

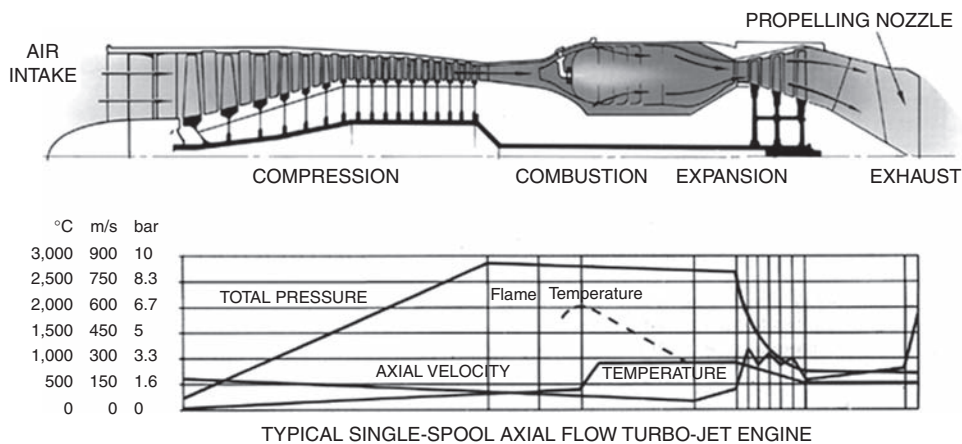
Figure 12.2.8 shows that the power output increases with the Mach number (which is clearly explained as dynamic compression depends directly on it), while the compression ratio decreases with this value. This is explained because, to offset the compression work, we must expand the hot gases in the turbine. The turbine inlet temperature being set, the greater the compression ratio, the more the turbine outlet temperature decreases, and therefore the more the enthalpy available in the nozzle is reduced.

We deduce therefore that supersonic aircraft jet engines require compression ratios even lower than the flight speed is high. We shall see section 12.2.2.1 that the limiting case is that of the ramjet, in which the compressor and the turbine become unnecessary in view of the importance of dynamic compression.

However, turbojets for subsonic planes require high compression ratios. The need for power at both fixed point for takeoff and flight at low speed leads to the adoption of two-stage configurations of compressors with compression ratios between 10 and 30 depending on the machines.

**FIGURE 12.2.9**

Efficiency function of compression ratio

**FIGURE 12.2.10**

Flow in a turbojet, Reproduced courtesy of Rolls-Royce plc

Figure 12.2.9 also shows that, as we have seen while studying gas turbines, the compression ratio leading to the maximum thermal efficiency is still higher than that which leads to the maximum power.

The **overall efficiency** is equal to the product of the propulsive efficiency by the thermal efficiency, changes in thermal and propulsive efficiencies as a function of compression ratio being opposite.

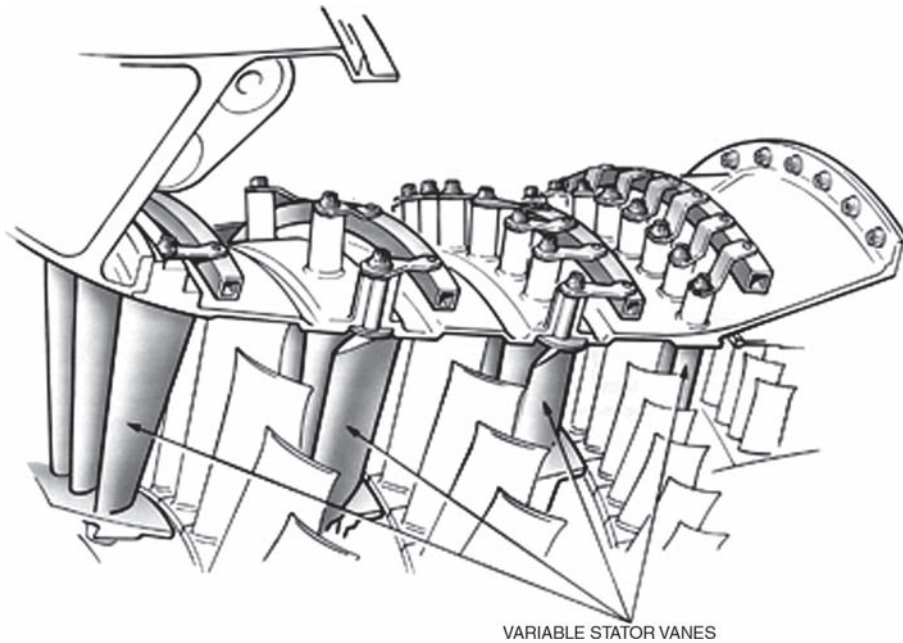
$$\eta_g = \eta_p \eta_{th}$$

Figure 12.2.10, which shows schematically the evolution of temperature, velocity and pressure in a jet engine, lets you view the changes of the working fluid in the various components of the machine.

Moreover, operating at highly variable conditions can lead to incorporate variable stator vanes in high compression ratio compressors, as shown in Figure 12.2.11. They act as control devices of the flow sucked .

Example of turbojet

Consider a jet engine sucking air at $T_1 = -40^\circ\text{C}$ and a pressure $P_1 = 0.35$ bar. The plane speed is $C_1 = 100$ m/s. At the outlet of the combustion chamber we assume that the gas temperature is

**FIGURE 12.2.11**

Variable inlet vanes, Reproduced courtesy of Rolls-Royce plc

$T_3 = 1,100^\circ\text{C}$, and its pressure 3.5 bar. We seek to calculate the thrust for a mass flow equal to 1 kg/s, and propulsion, thermal and overall efficiencies, assuming air and hot gases to be perfect gases and the processes to be also perfect, and neglecting dynamic compression ($Ma = 0.33$).

With the previous notations, we get:

$$T_1 = -40^\circ\text{C} = 233 \text{ K} \quad T_3 = 1,100^\circ\text{C} = 1,373 \text{ K}$$

$$T_2 = 233 \cdot 10^{0.286} = 450 \text{ K} \quad T_4 = 1,373 + 233 - 450 = 1,156 \text{ K}$$

$$T_5 = 1373 \cdot 0.1^{0.286} = 711 \text{ K}$$

$$C_5 = \sqrt{2c_p(T_4 - T_5) + C_1^2}$$

In this case:

$$C_5 = \sqrt{2,000(1,156 - 711) + 10,000} = 948 \text{ m/s}$$

The thrust is then:

$$F = \dot{m}(C_1 - C_5) \quad F = 1(100 - 948) = -848 \text{ N}$$

The power output is equal to the thrust multiplied by the aircraft velocity:

$$W_p = FC_1 = 84.8 \text{ kW}$$

The propulsive efficiency is $\eta_p = \frac{2}{1 + \frac{948}{100}} = 19.1\%$

The thermal efficiency is $\eta_{th} = 1 - 0.1^{0.86} = 48.2\%$

The **overall efficiency** is very low: 9.2%

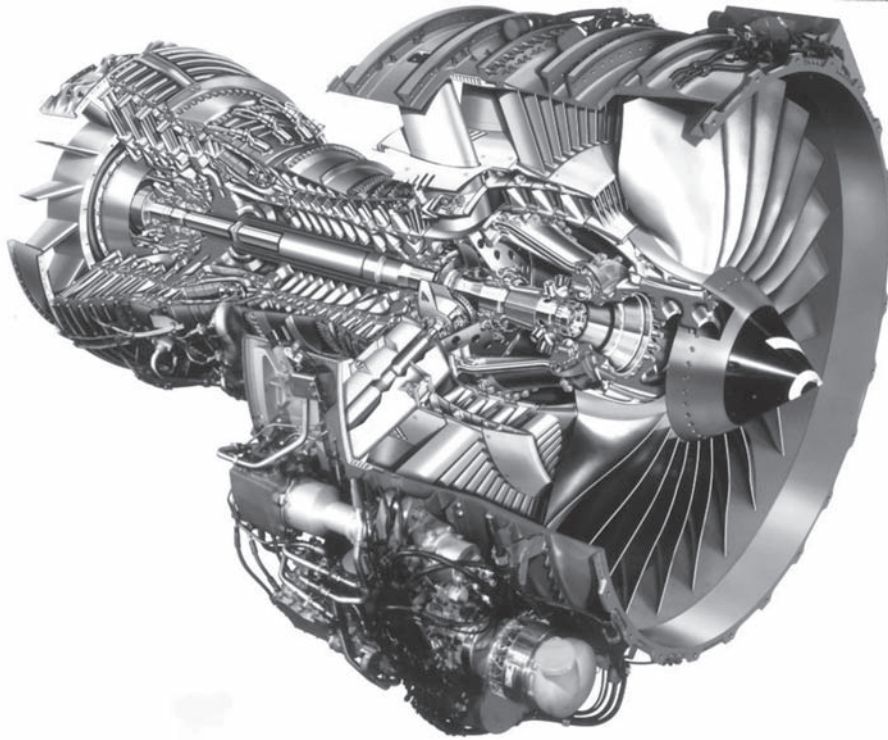


FIGURE 12.2.12

Cutaway of the CFM56-7 engine (© Snecma Moteurs)

12.2.1.4 Turbofans

The example we just discussed showed that overall efficiency remains low because there is a tradeoff between a good thermal efficiency, which involves providing gases with a high kinetic energy in the nozzle, and a good propulsive efficiency, which requires a low relative gas velocity at the nozzle exit.

In the case of the turbojet we just studied, where the flow through the gas generator is the same as that which passes through the nozzle, this problem has no satisfactory solution. In contrast, the turbofan engine (Figure 12.2.12) reconciles these two apparently contradictory requirements by accelerating to a speed barely higher than that of the plane an air flow (called secondary flow) complementary to that which flows through the gas generator. This operation is made possible thanks to an additional low pressure compressor, called a fan, also driven by the turbine.

The dilution ratio is the ratio of secondary flow to primary flow. It can reach 10 for some jet engines. Propulsion is then ensured by a large air flow at low speed and a small flow of exhaust gases from the primary classical cycle. The need to withdraw from the turbine power consumed by the fan alters however the thermal efficiency by reducing the available enthalpy at the turbine outlet.

Overall, however, the operation appears to be very interesting, with consumption reductions around 40%.

Figure 12.2.12 shows a CFM56-7B CFMI turbojet used on Boeing 737 Next Generation. This engine has a dilution ratio close to 5.3, a compression ratio of 32.7, a length of 2.63 m and a fan diameter of 1.55 m for a mass of about 2 t. Its maximum thrust is equal to 121 kN, about 12 t. Between 1996 and late 1999, nearly 400 aircraft were equipped with 1,000 of these engines.

12.2.1.5 Afterburner

Another way to increase the thrust is to raise the temperature of the turbine outlet gases to give them a higher enthalpy, and thus a higher speed at the nozzle exit. In order to limit the inlet

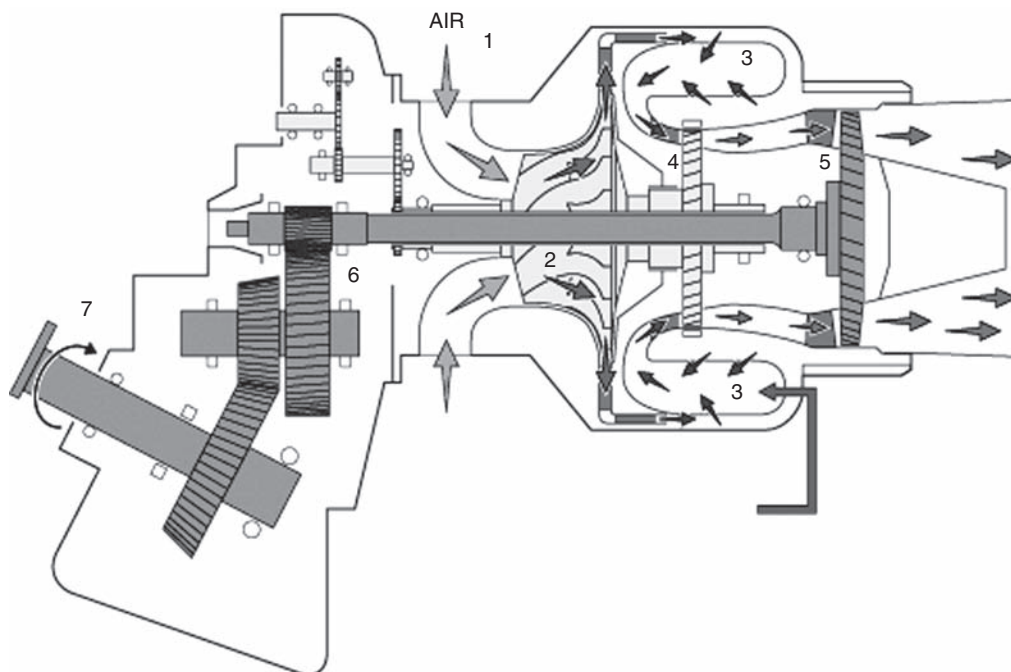


FIGURE 12.2.13

Schematic of Arrius engine, © Turbomeca

temperature in the turbine, the initial combustion takes place with high excess air, so a large amount of oxygen is available. As the nozzle can also withstand high temperatures, it is possible to reach temperatures near 2,000 K. We can get an extra push by nearly 50%, but this requires a significant additional fuel consumption. The M88 jet engine of Figure 12.2.3 is equipped with an afterburner.

12.2.1.6 Performance of turbojets

The efficiency of a jet engine varies greatly with the speed of the aircraft. Beyond 800 km/h, it begins to supplant the propeller, whose efficiency declines, because of flow problems encountered when approaching supersonic speeds. The increase in speed associated with the development of air transport has been made possible by the development of jet engines, whose use became widespread over the last 45 years.

Today we achieve overall efficiencies of about 25% for single flow turbojets, 30% in turbofan flying subsonic around 800 km/h and above 45% at Mach 2.

12.2.1.7 Turboprops

Another variant of the gas turbine used for propulsion is the aircraft turboprop, single gas turbine directly coupled to the propeller of an airplane or helicopter. Depending on circumstances, there may be one or two shafts (Figure 12.2.13), in which case the free turbine is coupled to the propeller. Note that the turboprop is a kind of limiting case of a turbofan engine where the fan is replaced by the propeller, and where the nozzle becomes useless.

Figures 12.2.13 and 12.2.14 show a Turbomeca Arrius 2B2 turboprop equipping Eurocopter type EC 135 T1 helicopters, which can carry a pilot and six passengers.

About 1,000 such 600 kW engines were built since 1983. Its dimensions are: length 0.95 m, height 0.7 m and width 0.4 m, for a mass, including equipment, of 107 kg.

On the schematic section of Figure 12.2.13, the air is sucked in 1, then passes through the impeller 2, where it is compressed before being routed to the combustion chamber 3. The exhaust gases

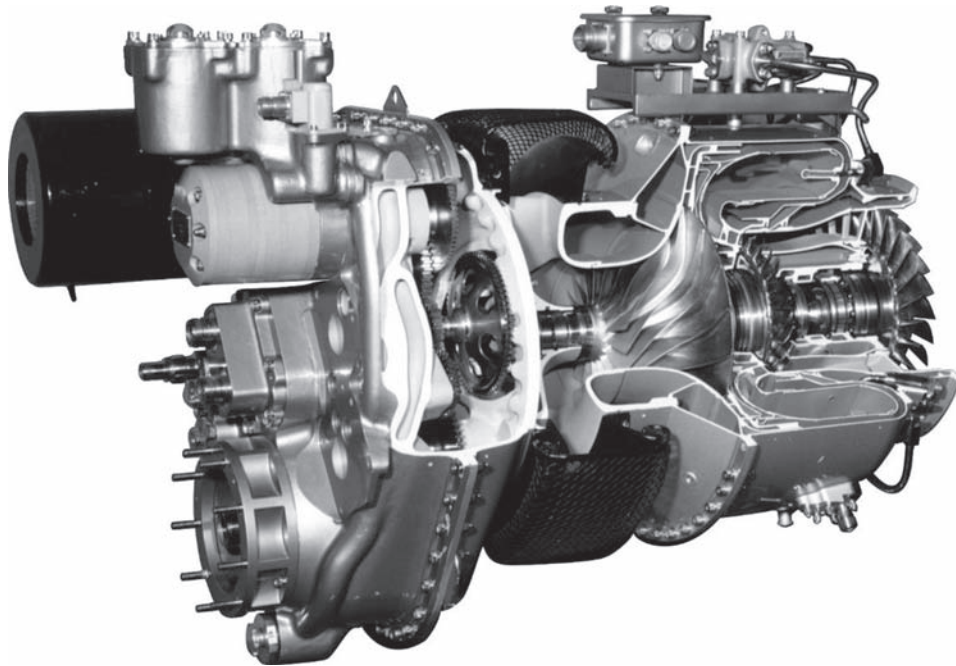


FIGURE 12.2.14

Cutaway of the Arrius engine, © Turbomeca

are then expanded in turbines 4 and 5, mechanically coupled to compressor 2 and, through gear 6, to drive shaft 7. Figure 12.2.14, which represents a cutaway, shows how the various engine components are assembled.

Figure 12.2.15 provides details of the centrifugal impeller during machining.

12.2.1.8 Protection of blades

In section 12.1.3.2 we showed the main provisions used to cool the expansion turbine blades. However, as the turbine inlet temperature increases, these devices are no longer sufficient to protect the blades, subjected to both creep and severe cyclical thermomechanical fatigue.

In the most advanced engines, the materials used in their manufacture are nickel based monocrystalline superalloys obtained by unidirectional solidification, far superior to polycrystalline due to the absence of grain boundaries. This solution has limits however, because the starting melting temperature of the best alloys is about 1,300°C, and their mechanical durability requires temperatures not to exceed 1,000°C on the metal. In addition, hot gases containing oxygen, an anti-oxidant treatment of the blade surface is necessary.

These alloys must be protected either by chemical vapor deposition, or increasingly by ceramic thermal barriers, the only way to achieve combustion chamber exit temperatures above 1,500°C. These multilayer coatings with a thickness of 80 to 150 μm allow reduction by 0.8 to 1.5°C of the alloy temperature for a 1 μm ceramic thickness, depending on the type of cooling and the nature of the thermal barrier. Their development is very difficult given the many technological problems that arise: hanging on the alloy, flaking, cracking, etc.

Some solutions for jet engines are being transferred to land-based gas turbines, taking into account the specifications and different economic conditions (fewer mass constraints, reduced low-cycle fatigue, but tenfold lifetime, fuels of lesser quality, etc.).

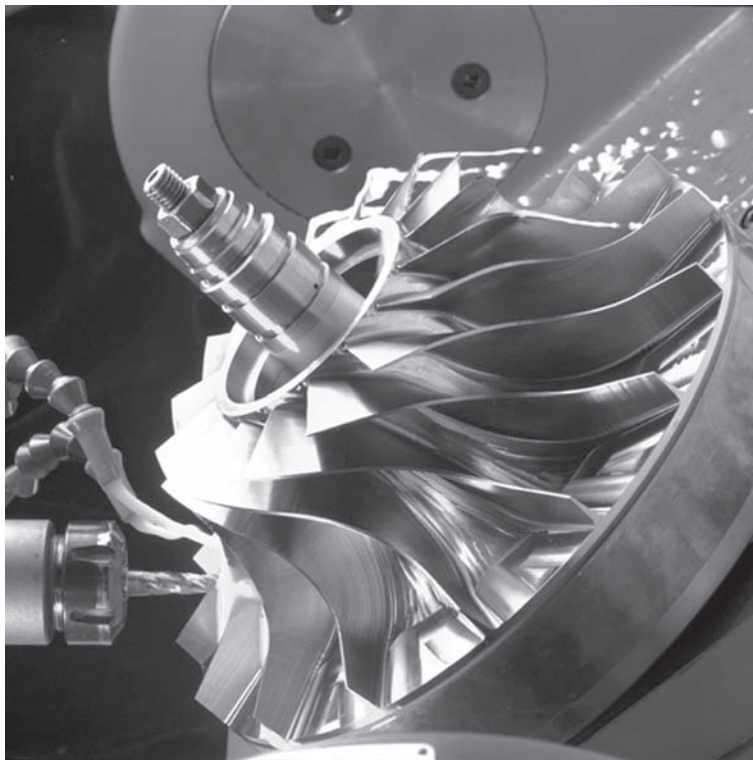


FIGURE 12.2.15

Centrifugal impeller during machining, Photo A. Gonin

12.2.1.9 Modeling a single flow jet engine with Thermoptim

In the analytical developments above, we have assumed that the machine was traversed by a constant flow of perfect air, when in reality the mass flow and gas composition vary, and their heat capacities depend on temperature.

If we want to eliminate this assumption, the analytical calculations quickly become intractable. Nevertheless, it is quite possible to model with good accuracy various turbojet cycles with Thermoptim.

However, Thermoptim core components are not sufficient to build such models: to represent the inlet diffuser and the exit nozzle, it is here necessary to use two external classes introduced in Part 2, sections 7.9.2 and 7.9.1. The physical models chosen are presented there.

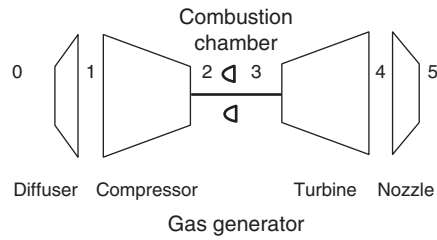
We show in this section how to model a single flow jet engine whose sketch is given in figure 12.2.16, and its Thermoptim diagram in Figure 12.2.17.

Diffuser component

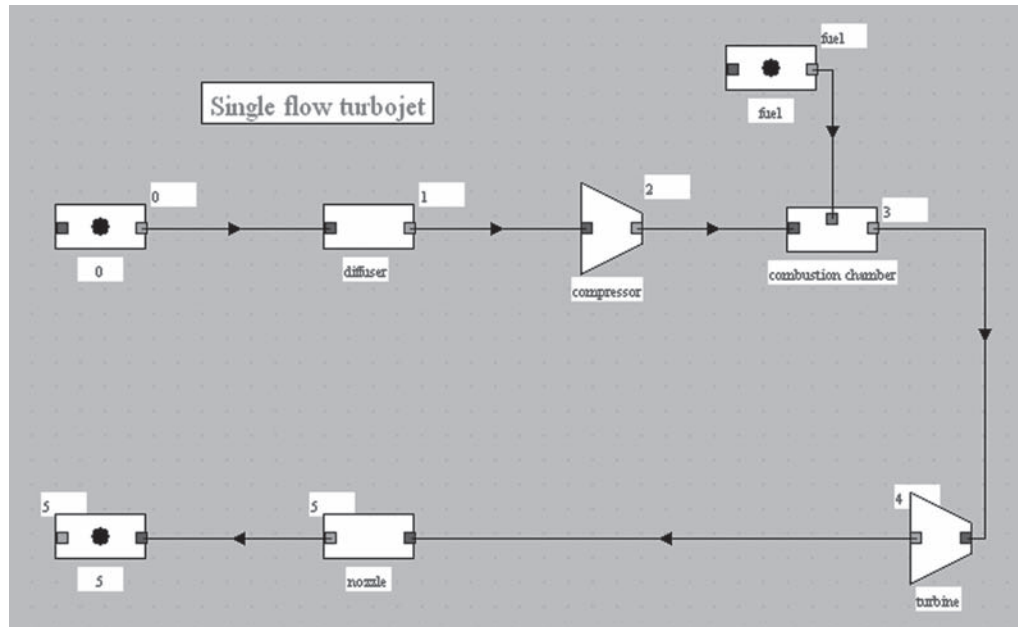
For the diffuser, two calculation methods are possible: to determine the output pressure knowing the output velocity, or to determine the output velocity knowing the output pressure. Assuming that the output velocity is negligible, the first mode is to be selected.

Model parameters are:

- the gas inlet velocity (m/s);
- the isentropic efficiency of the process (0.9);
- either the gas output velocity (m/s), or the gas pressure at the exit of the diffuser, depending on the calculation option chosen.

**FIGURE 12.2.16**

Single-flow turbojet

**FIGURE 12.2.17**

Thermoptim diagram of a single flow turbojet

Model input data are as follows (provided by the inlet component):

- the gas temperature at the inlet of the diffuser T_a ($^{\circ}\text{C}$ or K);
- the gas pressure at the inlet of the diffuser P_a (bar);
- the gas flow rate \dot{m} (kg/s).

The outputs are:

- either the gas pressure at the exit of the diffuser, or the gas outlet velocity (m/s), depending on the calculation option chosen;
- the gas temperature at the diffuser exit.

Figure 12.2.18 shows an example of settings for a flight speed of 224 m/s (Mach 0.75) and an altitude of 10 km (pressure of 0.285 bar). With a diffuser isentropic efficiency of 0.9, the dynamic pressure is equal to 0.105 bar.

Nozzle component

For the nozzle, two calculation methods are possible: to determine the output pressure knowing the output velocity, or to determine the output velocity knowing the output pressure, which is generally the case.

FIGURE 12.2.18

Diffuser screen

Model parameters are:

- the gas inlet velocity (m/s), generally low;
- the isentropic efficiency of the process (0.95);
- either the gas output velocity (m/s), or the gas pressure at the exit of the nozzle, depending on the calculation option chosen.

Model input data are as follows (provided by the inlet component):

- the gas temperature at the inlet of the nozzle T_a (°C or K);
- the gas pressure at the inlet of the nozzle P_a (bar);
- the gas flow rate \dot{m} (kg/s).

The outputs are:

- either the gas pressure at the exit of the nozzle, or the gas outlet velocity (m/s), depending on the calculation option chosen;
- the gas temperature at the nozzle exit.

Other settings

We may at first be satisfied with a simple model where we assume that we know the compression ratio and the flow passing through the machine, and polytropic or isentropic compressor and turbine efficiencies. The calculation model then poses no particular problem.

Once the model is built, it becomes possible to calculate the engine performance. The specific thrust, and the ratios of power and consumption to thrust are among magnitudes most commonly used for this.

The expression of the thrust is here, taking into account the variation of the flow-rate through the engine due to fuel injection:

$$F = \dot{m}_0 C_0 - \dot{m}_5 C_5$$

process type

energy type set flow

inlet point flow rate closed system observed

open system

T (°C)	<input type="text" value="864.57"/>
P (bar)	<input type="text" value="2.1552"/>
h (kJ/kg)	<input type="text" value="936.88"/>
quality	<input type="text" value="1"/>

outlet point

T (°C)	<input type="text" value="403.29"/>
P (bar)	<input type="text" value="0.265"/>
h (kJ/kg)	<input type="text" value="401.28"/>
quality	<input type="text" value="1"/>

nozzle

inlet velocity (m/s)

isentropic efficiency

Mach number

outlet pressure (bar)

outlet velocity (m/s)

outlet section

minimum section

Calculate outlet pressure

Calculate outlet velocity

FIGURE 12.2.19

Nozzle screen

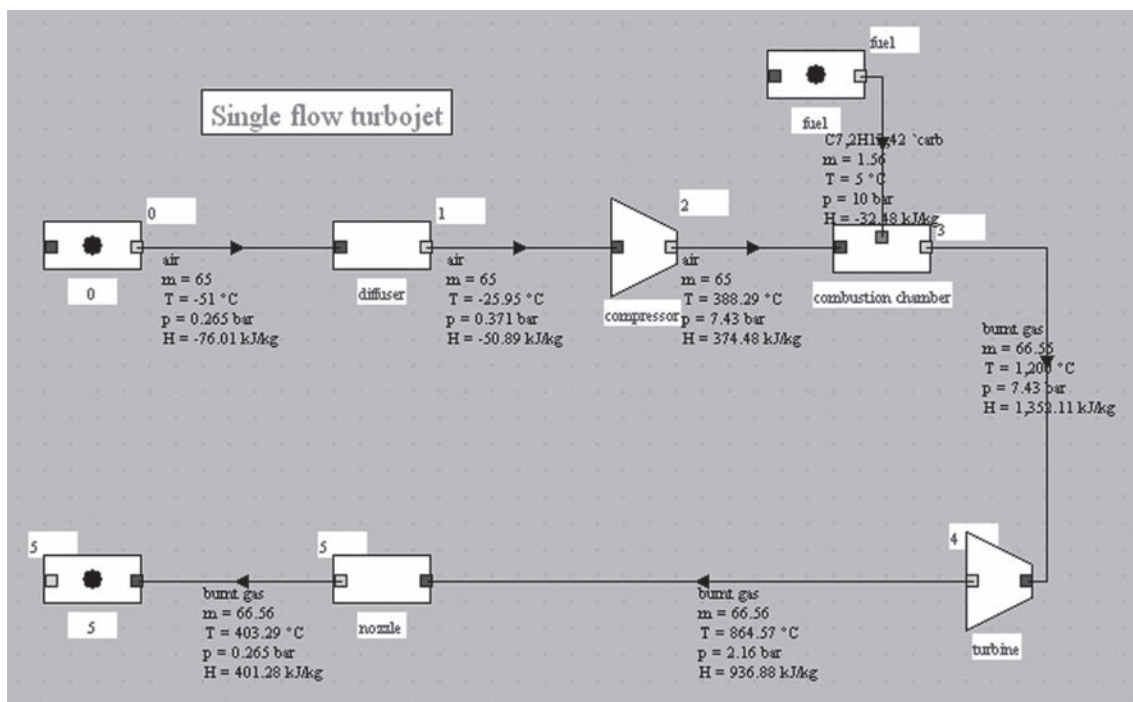


FIGURE 12.2.20

Synoptic view of single-flow jet engine

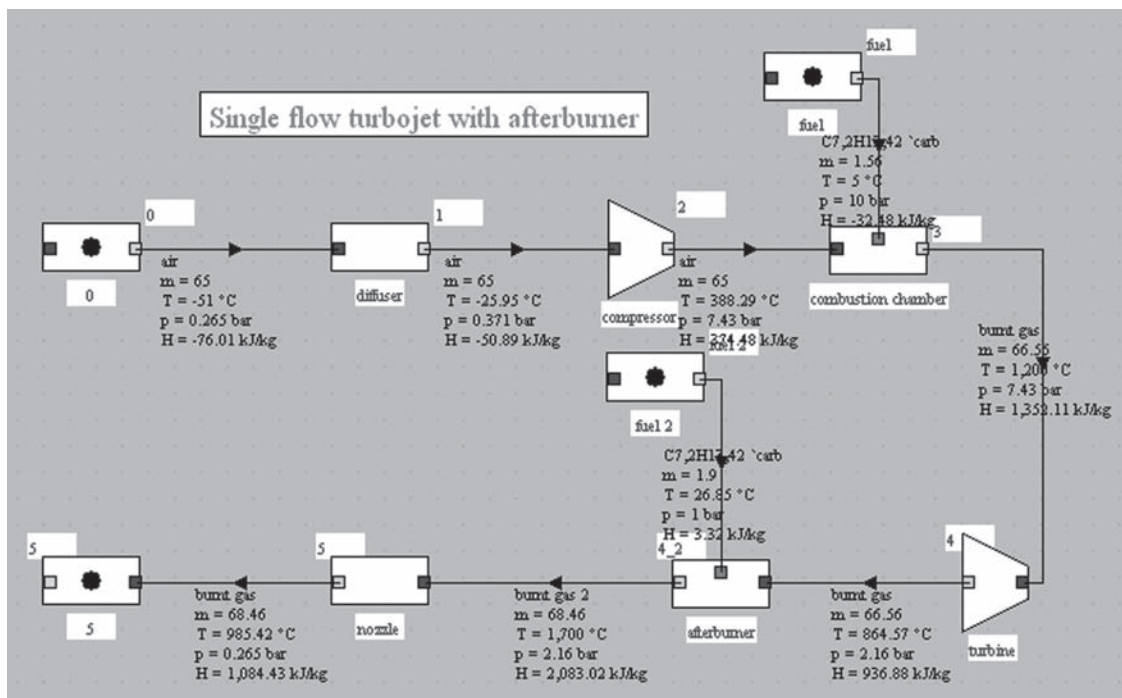


FIGURE 12.2.21
Synoptic view of a turbojet with afterburner

The power W is the product of thrust by the aircraft speed:

$$W = FC_0$$

The mass flow-rate of fuel is:

$$\dot{m}_c = \dot{m}_5 - \dot{m}_0$$

We get:

$$F = 54.73 \text{ kN}, \quad W = 12.3 \text{ MW}, \quad \text{and} \quad \dot{m}_c = 1.61 \text{ kg/s}.$$

These quantities are often expressed as reduced, thrust F being given referred to the intake air flow and fuel flow to the thrust, respectively, giving values of $0.842 \text{ kN s kg}^{-1}$ and $0.0294 \text{ kg kN}^{-1} \text{ s}^{-1}$.

An afterburning can also be taken into account by adding a second combustion chamber after the turbine outlet (Figure 12.2.21).

If you want to pursue this model, see the guidance pages² on turbojets available in the ThermoOptim-UNIT portal.

12.2.1.10 Establishment of an external class for “driving” calculations

Simple driver

The model we have developed is well suited to the achievement of an external driver to guide the calculations.

A driver can coordinate recalculations of a ThermoOptim project under specific rules. For our model, it can coordinate updates of the diffuser, the nozzle and the compression ratio in the whole

²<http://www.thermooptim.org/sections/enseignement/cours-en-ligne/fiches-guides-td-projets/fiche-sujet-fg2>

Exterior conditions

plane mach number

ambient pressure (bar)

ambient temperature (K)

Single compression ratio calculation

compression ratio

specific thrust

specific fuel consumption

Various compression ratios simulation

initial compression ratio

final compression ratio

FIGURE 12.2.22

Driver for turbojet

project, calculate the quantities sought, even if they are not directly accessible, possibly save a file, and thus greatly facilitate sensitivity studies.

A driver is in the form of a particular ThermoOptim external class, as shown in section 23.7 of Part 4.

Figure 12.2.22 shows a possible screen for the driver, with above the definition of the conditions outside the aircraft, in the middle the compression ratio value to be entered to perform a single calculation, and at bottom entry of the compression ratio limits to make several calculations (10 in this case) and save the results. The values of specific thrust and specific fuel consumption calculated by the driver are the same as those given above. The code for this driver is included with the guidance pages.

Driver taking into account the characteristics of turbomachinery

Using a driver also allows much more complicated modeling to be performed than that which we did as a first step, where we assumed the compression ratio and the flow through the machine, and the compressor and turbine isentropic efficiencies were all known. Such a model will be presented in section 38.5 of Part 5. Figure 12.2.23 shows the results from such a model when varying the turbine inlet temperature.

12.2.1.11 Modeling a turbofan engine with ThermoOptim

It is also possible to similarly model a turbofan, with high or low bypass ratio.

We must split the airflow entering the engine at the outlet of the diffuser. One part is directed towards the combustion chamber and then to two turbines in cascade, one being balanced with the engine compressor, and the other with that of the fan, as shown in the diagram of Figure 12.2.24. Two nozzles are then used to calculate the velocity of ejected gases, and therefore the engine thrust.

Note that two specialized simulators for modeling jet engines are available on the Internet: GasTurb, created by J. Kurzke (www.gasturb.de) and GSP (Gas turbine Simulation Program) by National Aerospace Laboratory of the Netherlands (www.gspteam.com).

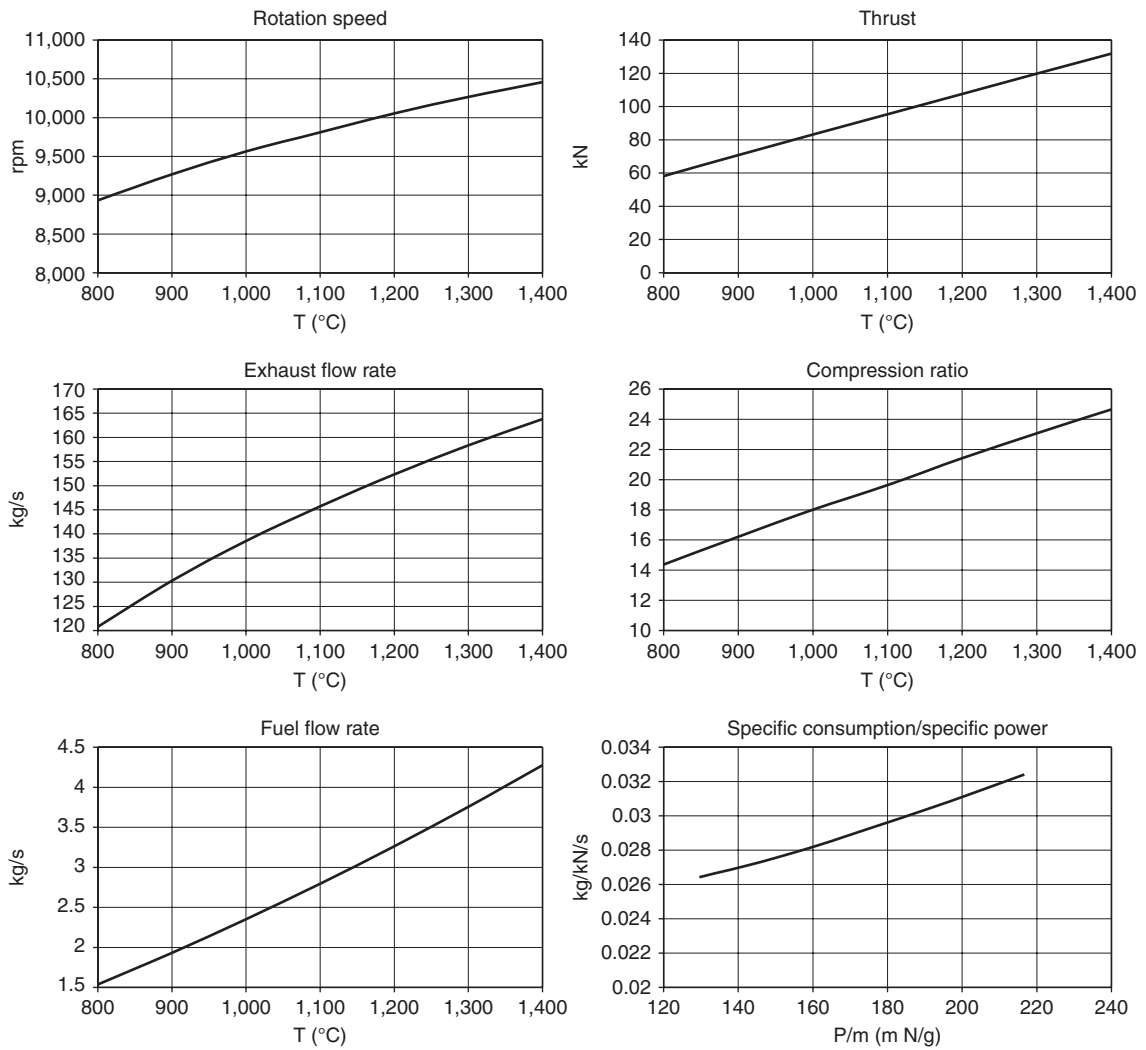


FIGURE 12.2.23
Simulation results (flight Mach = 0.9, altitude 10,000 m)

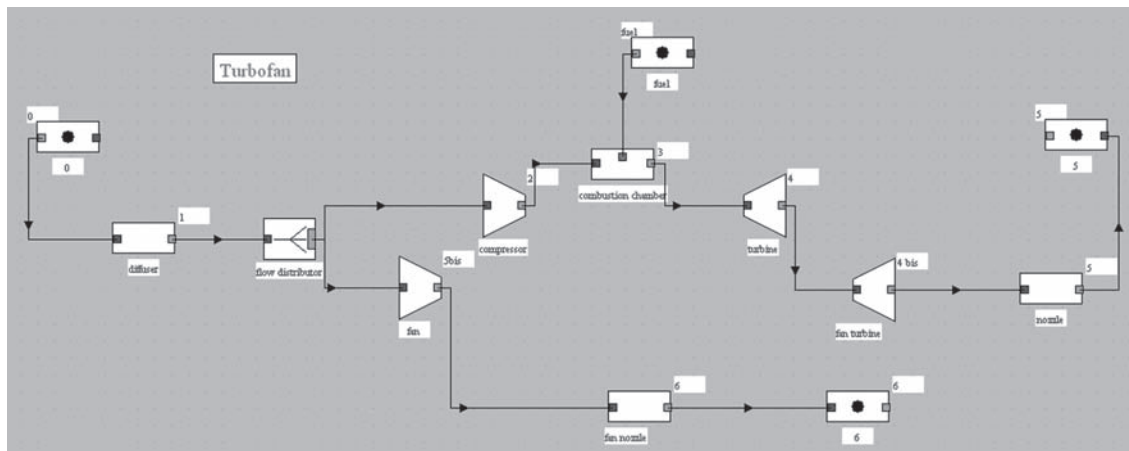
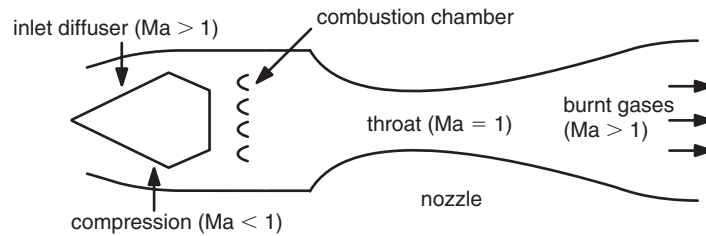
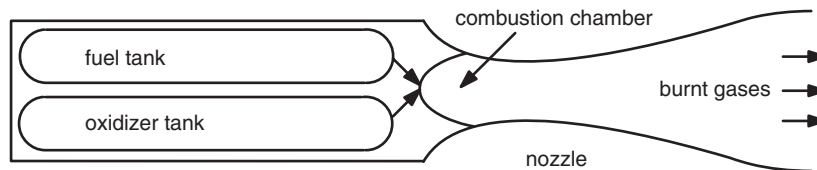


FIGURE 12.2.24
Diagram of a turbofan

**FIGURE 12.2.25**

Sketch of a ramjet

**FIGURE 12.2.26**

Sketch of a rocket engine

12.2.2 Reaction engines without rotating machine

12.2.2.1 Ramjet

Figure 12.2.8 has shown us that as the speed increases, the required compression ratio decreases. At very high speeds, it becomes possible to waive the compressor off if the stagnation pressure is sufficient to provide alone a compression ratio high enough for propulsion. As the turbine is only there to drive the compressor, it also becomes unnecessary. This is why the ramjet engine is very simple with no moving parts. A ramjet operates on a principle similar to the turbojet, with the difference that it has no rotating machine (Figure 12.2.25). In its simplest form, it consists of a diffuser, a combustion chamber and a nozzle.

In the diffuser, the incoming air is slowed down and compressed, then it burns at constant pressure in the combustion chamber and is finally expanded at high speed in the nozzle. The thrust equation is the same as that of the jet engine (12.2.1).

The ramjet can only operate at very high speeds, otherwise it is impossible to achieve in the diffuser sufficient compression to compensate for friction losses and irreversibilities in the engine.

At very high flight speeds (Mach > 3), ramjet engines are the most successful, reaching overall efficiencies of about 50%. The intercontinental rocket-propelled ramjets have a range of over 8,000 km at 15,000 m altitude. Their start is provided by a liquid or powder rocket. This type of engine has the added advantage of costing far less than jet engines because of its simplicity, which is sought for devices such as missiles, which are used only once.

12.2.2.2 Rockets

A rocket is a jet engine carrying its fuel and oxidant, and which thus may operate outside the atmosphere (Figure 12.2.26). Combustion takes place at constant pressure in a chamber in communication with a nozzle from which the gases escape at high temperature and speed.

The thrust here is expressed as:

$$F = -C_5 \dot{m} - S_s (P_s - P_a) \quad (12.2.15)$$

S_s being the output section of the nozzle, P_s and P_a the outlet and atmospheric pressures.



FIGURE 12.2.27

Nozzle of Ariane 5 solid booster MPS (© Snecma/Studio Pons)

If $P_s = P_a$, or outside the atmosphere, the thrust is reduced to $F = -C_s \dot{m}$.

One of the great interests of the rocket, in addition of course of its ability to operate outside the atmosphere, is that its thrust is independent of its own speed. It develops a major power at startup, unlike the ramjet.

Rocket engine applications are propelling missiles or launchers used to orbit space vehicles.

We call propellants or propergols the liquid or solid substances burned in a rocket engine. We characterize the performance of a propellant by its specific impulse I_s , which is the time during which a mass of 1 kg produces a thrust of 9.81 N.

Solid propellants, (usually powders) are oxidizer/fuel mix previously metered, which burn very rapidly on their surface. Once the burning is started, it cannot be stopped.

For example, the solid rocket motor (MPS from the French Moteurs à Propergol Solide) equips the Ariane 5 two-stage solid boosters (SRBs or EAPs from the French Étages d'Accélération à Poudre) located on either side of the cryogenic main stage (EPC from the French Étage Principal Cryotechnique), which ensure the launcher takeoff during the first two minutes, up to an altitude of 56 km (Mach 6.5), with a gas flow of 2 t/s at 3,000 K. The propellant is a composite based on ammonium perchlorate and polybutadiene loaded with aluminum. Its specific impulse I_s is 270 s. The MPS has a total mass of 268 t, including 238 t of fuel. Its maximum thrust in vacuum is 6,700 kN.

Figure 12.2.28 provides an overview of the Ariane 5 launcher. On this figure, we recognize in 1 the Vulcain engine, which will be discussed further, in 2 the MPS nozzle, which is also seen in the inverted position Figure 12.2.27. 3, 4 and 5 are the three segments of the EAP, 5 containing the igniter. 6 is the payload (here two satellites within bunk beds), 7 and 8 liquid oxygen and hydrogen tanks. The nozzle is adjustable and the MPS can direct the thrust up to 6° .

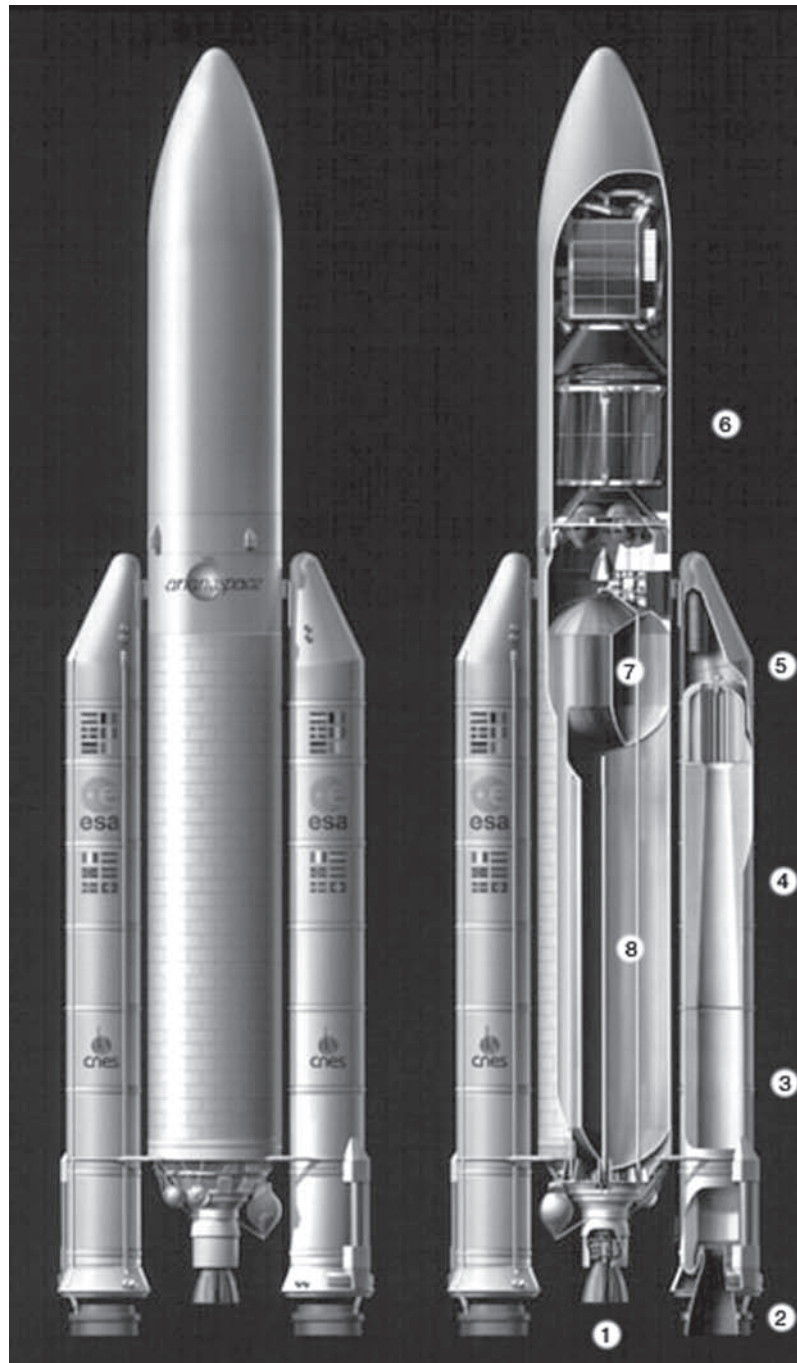


FIGURE 12.2.28

Cutaway of Ariane 5, photo D. Ducros, © Arianespace

The liquid propellants are known as storable if they can be stored at room temperature and cryogenic if they must be kept at very low temperatures. They are called hypergolic if they ignite by simple contact of the oxidizer and fuel. Different pairs of propellants are used for launch vehicle propulsion:

- kerosene-oxygen ($I_s = 375$ s);
- hydrazine (N_2H_4) – nitric acid (HNO_3) (hypergolic, $I_s = 300$ s);

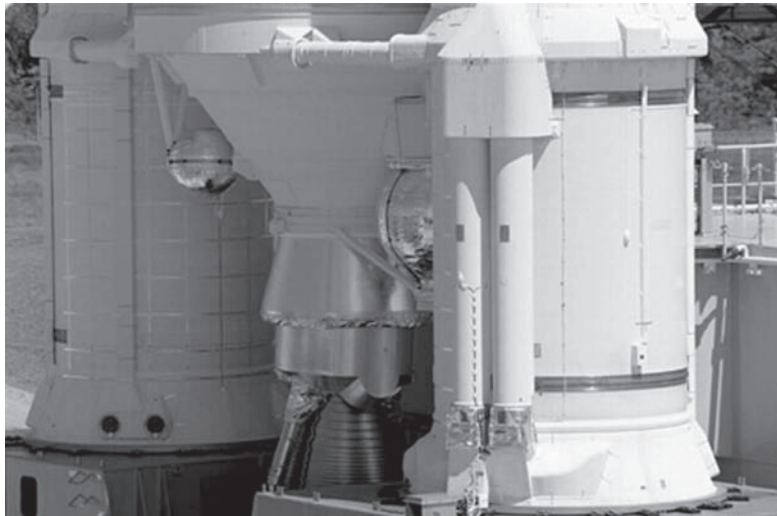


FIGURE 12.2.29

Ariane 5 on table, photo D. Corvaja, © ESA/Arianespace

- UDMH ($\text{N}_2\text{H}_2(\text{CH}_3)_2$) – nitrogen tetroxide (N_2O_4), UDMH being safer to handle than hydrazine;
- hydrogen – oxygen ($I_s = 470$ s).

This pair, which provides the best specific impulse, is used both for the U.S. space shuttle and for the Ariane 5 EPC. It has the disadvantage of being cryogenic and dangerous to handle.

To transfer the propellants from their storage tanks into the combustion chamber, two solutions are possible:

- either pressurize the tank by injecting a gas (usually helium). The structure of the reservoir should be capable of withstanding a pressure higher than that of the combustion chamber;
- or use a turbopump driven by a flow of gas drawn one way or another by the combustion gases. The system is more complex but achieves higher supply pressures and the weight of tanks is reduced.

The Vulcain engine of Ariane 5 provides the relay of the MPS described above. Figure 12.2.29 shows the bottom of the launcher on its table, in Kourou. The engine appears positioned between the two EAP solid boosters (3 m in diameter and 27 m in height), and under the EPC (5.4 m in diameter and 30 m in height). Two large tanks of liquid hydrogen and oxygen (8 and 7 in Figure 12.2.28), respectively maintained at 20 K and 90 K contain 25 t and 130 t of propellant. The ratio of their molar masses explains that the volume occupied by oxygen is about a quarter of that required for hydrogen.

For a 1,700 kg mass, a 3 m height and a 1.76 m nozzle exit diameter, the Vulcain engine develops a thrust of 1140 kN, with the ejection of a 260 kg/s stream of flue gas at 110 bar and 3,500 K. The speed of the gas flow is 4,000 m/s. Its thermal power is 3,800 MW, the equivalent of a very large nuclear power plant (three units).

The motor is fed with propellant by two turbopumps driven by the auxiliary combustion in a gas generator of 3% of the propellants:

- the hydrogen turbopump rotates at 33,000 rpm and has a power of 12 MW, the equivalent of two high speed locomotives, for a mass of 240 kg;
- the 3.7 MW oxygen turbopump is running at 13,000 rpm.

In such an engine, technological constraints are extremely severe:

- temperature gradients are very high, the tanks being at cryogenic temperatures while other parts are in contact with the combustion gases;



FIGURE 12.2.30

Ariane 5 launch, photo P.F. Benaiteau, © ESA/CNES/Arianespace

- pure oxygen is an oxidant that could damage some mechanical parts in a few milliseconds and must be fully enclosed;
- the gas generator works with a large excess of hydrogen to reduce thermal stresses in the supply circuit;
- excess hydrogen makes the gas exiting the gas generator highly combustible. Sealing of the oxygen turbopump must thus be ensured by a flow of helium;
- the 1.76 m exit diameter nozzle must be cooled by an extraction of liquid hydrogen discharged without combustion.

Applying formula 12.2.15 provides for the Vulcain engine:

- in the vacuum, thrust is equal to $F = 4,000 \times 260 = 1,040 \text{ kN}$;
- on earth $F = 4,000 \times 260 - 2.43 (0 - 105) \approx 800 \text{ kN}$, considering that the pressure of the gas flow is negligible compared to atmospheric pressure.



FIGURE 12.2.31

Vulcain 2 engine (© Snecma/Studio Pons)

Figure 12.2.30 shows the Ariane launch (Flight 119-AR504). It clearly shows both MPS developing their full power, and the Vulcain engine ready to take over from them.

Figure 12.2.31 presents the Vulcain 2 engine which followed from 2002 Vulcain in the Ariane 5 Evolution program. This figure shows the main engine parts, including one of the two turbopump ejection nozzles and modified divergent cooled by turbine exhaust gas.

Its main features are: height 3.60 m diameter nozzle exit 2.15 m, total mass 2,040 kg, thrust 1,350 kN propellant mass increased by 10% and specific impulse 434 s.

REFERENCES

H. Abdallah, *Analyse énergétique, exergetique et économique des cycles de turbine à combustion*, Thèse de Doctorat, Université de Nantes, 27 novembre 1998.

A. F. El-Sayed, *Aircraft propulsion and gas turbine engines*, CRC Press, Boca Raton, 2008, ISBN 978-0-8493-9196-5.

- M. Giraud, J. Silet, *Turbines à gaz aéronautiques et terrestres*, Techniques de l'Ingénieur, Traité Mécanique et chaleur, B 4 410.
- IHPTEET, *Air dominance through propulsion superiority*, site Web: <http://www.pr.afrl.af.mil/divisions/prt/ihptet/brochure/Intro.htm>.
- L. Vivier, *Turbines à vapeur et à gaz*, Ed. Albin Michel, Paris, 1965.

FURTHER READING

- R. Bidard, J. Bonnin, *Energétique et turbomachines*, Collection de la DER d'EDF, Eyrolles, Paris, 1979.
- G. Bidini, S. Stecco, *Motori a combustione interna*, Pitagora Editrice, Bologna, 1993.
- Instantanes Techniques, *Le lanceur Ariane 5: des innovations tous azimuts*, Instantanés Techniques, Paris, automne 1995, pp. 27–47.
- C. Kempf, *Les centrales électriques à cycle combiné*, Revue de la Société des Electriciens et des Electroniciens, décembre 1999, Paris.
- L. S. Langston, *Introduction to gas turbines for non engineers*, Global gas turbine news, volume 37, 1997, n° 2.
- F. Ribes, J. L. Meyer, *Microturbines pour la production décentralisée*, Revue de la Société des Electriciens et des Electroniciens, décembre 1999, Paris.
- Rolls Royce, *The jet engine*, 5th edition, 1996, ISBN 0 902 121 2 35, Derby.
- P. Stouffs, S. Harvey, *Energétique avancée des cycles à turbomachines*, Cours de DEA Thermique, Energétique et Génie des Procédés, septembre 1996, Nantes.
- K. Tasadduq, A. Lasalmonie, *Les matériaux structuraux chauds pour turbomachines*, Annales des mines, Paris, février 1995.
- Vision 21 Program Plan, *Clean Energy Plants for the 21st Century*, Federal Energy Technology Center, Office of Fossil Energy, US Department of Energy.

This page intentionally left blank

Reciprocating Internal Combustion Engines

Abstract: In this chapter, we will first present the operating principles of reciprocating internal combustion engines (ICE). After discussing briefly the analysis of their cycles and then their overall performance, we will study in more detail the consequences of combustion chemical kinetics on the operation and design of these engines. A brief discussion on turbochargers will follow, then we will examine how emissions of pollutants can be controlled.

Reciprocating engine capacity ranges for usual application from less than 1 kW to about 1 MW. The crowning achievement use of these machines is the propulsion of road vehicles.

There are two main types of reciprocating internal combustion engines:

- spark ignition engines, whose principle was established by the French Beau de Rochas in 1860, and the first project carried out by the German Otto in 1876. Although some of these engines burn gaseous fuels, we will qualify them in the following of gasoline engines;
- compression ignition engines, called Diesel, by the name of their German inventor who patented them in 1892.

Keywords: spark ignition, diesel, combustion, reciprocating, 4 stroke, 2 stroke, carburetor, injection, supercharging, pollution.

Piston machines occupy a prominent place among internal combustion engines. This situation stems from two causes:

1. By their periodical operation, these machines are particularly suitable for processes where the temperature reaches high values. Being in contact with the fluid at various stages of process, the walls of the machine are subject to an average temperature well below the maximum temperature, whereas in a continuous flow machine such as gas turbine, some parts are constantly subjected to this temperature. In addition, the velocities being much lower in piston machines, the fluid/wall exchange coefficients are smaller. Finally, the average heat flux received by the walls is low enough that, with adequate cooling, we can keep them in good working condition while producing inside the cylinder combustion at more than 2500 K, which as we have seen in section 12.1.3, would be quite impossible in a continuous flow machine.
2. Internal combustion engines are widely used for propulsion of vehicles of small and medium capacity. Indeed the piston engine adapts much better to this use than the turbine engine, which is feasible only with very high characteristic speed, and therefore must rotate at considerable speed when power is moderate, with interposition of fragile and expensive reducing gear.

It is customary to distinguish the modes of operation of spark ignition and diesel engines by characterizing each by a different cycle, the Beau de Rochas cycle (or Otto depending on the authors) is characterized by a constant volume combustion and the diesel cycle by combustion at constant pressure. In fact, especially in fast engines, we will see later that the combustion delays are such that more complex cycles must be considered if one wishes to be precise. In these circumstances, what distinguishes the two types of engines is not so much the theoretical cycle than combustion characteristics, including kinetics, studied in section 7.6.1 of Part 2, which follow very different laws depending on whether the fuel is volatile or not. So we understand that the complexity of the physicochemical phenomena taking place during combustion in an engine piston is such that the basic ideal cycles just allow approaching reality in a relatively simplified way.

13.1 GENERAL OPERATION MODE

Animations illustrating the operation of these engines were made by the French Navy and soundtracks added in Diapason sessions S35En_PBV and S35En_4t2t to which we recommend you refer¹ to supplement the explanations in this section.

All reciprocating internal combustion engines operate on the same general process described schematically Figure 13.1.1. A variable volume is defined by a cylinder, one of the bases of which is fixed, called head, and the other is a movable piston in the cylinder bore, driven by a connecting rod system. In a four-stroke engine, the organs that control the inlet or exhaust valves are actuated by push buttons coupled to the drive shaft by a camshaft.

In various ways, depending on whether the engine is two or four stroke (see section 13.1.1), fresh gas is introduced into the cylinder at atmospheric pressure during the intake phase (fuel mixture formed in advance in conventional gasoline engines, clean air in diesel engines).

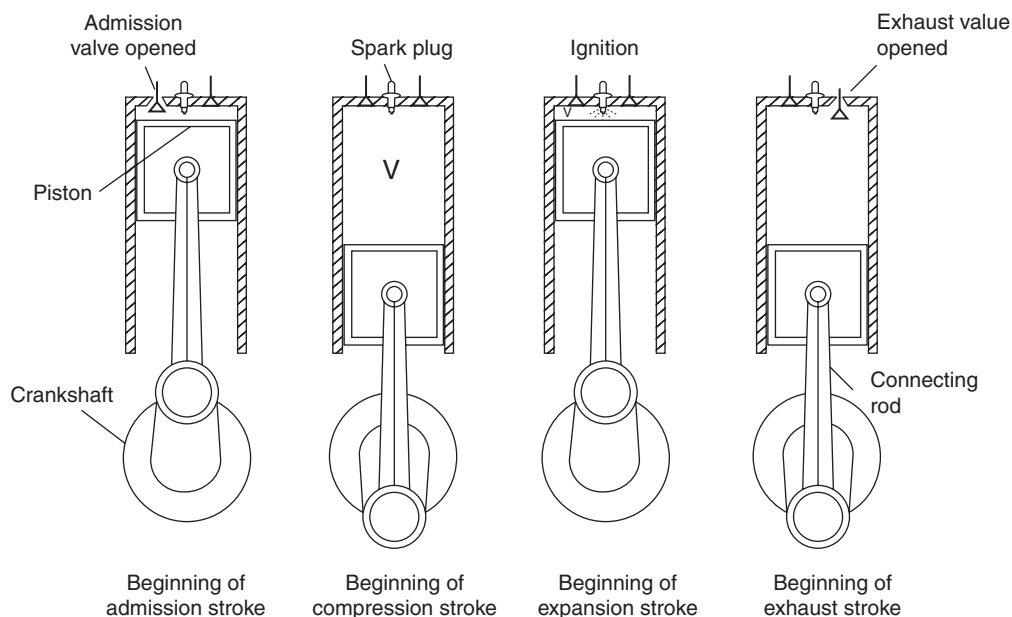


FIGURE 13.1.1

Four-stroke operation mode

¹ http://www.thermoptim.org/sections/enseignement/cours-en-ligne/seances-diapason/session-s35en_4t2t-4-and

The piston being at a distance from the bottom of the cylinder, the intake port is closed, the volume V between the piston and the bottom being occupied by a certain charge of fresh gas.

Approaching the bottom of the cylinder, the piston compresses the charge in the volume v of the combustion chamber, that is to say the remaining space when the piston reaches the end of his stroke, called top dead center or TDC. This compression is substantially adiabatic and occurs without appreciable internal friction. The operating key factor is the volumetric compression ratio $\rho = V/v$, a geometric characteristic of the cylinder.

The combustion reaction is then triggered, either by local ignition of the mixture in gasoline engines or by injecting fuel into the compressed air in diesel engines. The combustion occurs during a relatively short time, while the piston continues its stroke. In practice, it occurs in a mode intermediate between the constant volume combustion and combustion at constant pressure. The piston continuing to move away from the bottom of the cylinder, the burned gases expand until the end of the stroke (bottom dead center or BDC), then are evacuated and replaced by a new charge of fresh gas.

Figure 13.1.2 shows the general configuration of a Pielstick PC2-6B high capacity diesel engine (up to 18 cylinders of 630 kW, 400 mm bore, 500 mm stroke). An 18 cylinder engine running at 530 rpm developing 11.34 MW has a mass of 130 t. It measures 10.24 m long, 3.6 m wide and 3.8 m

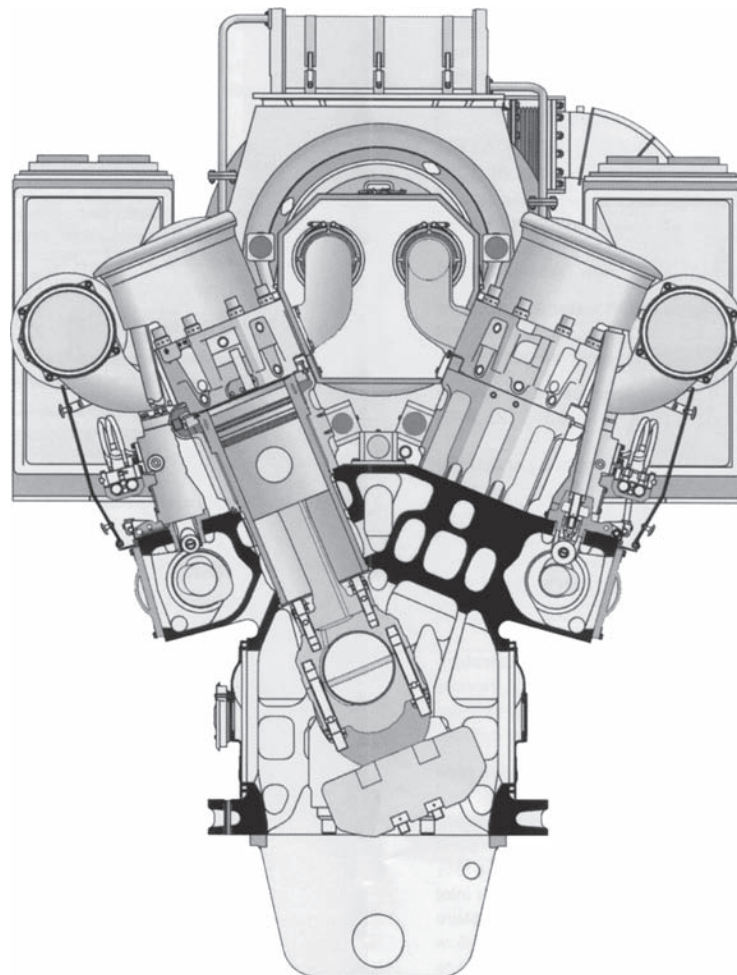
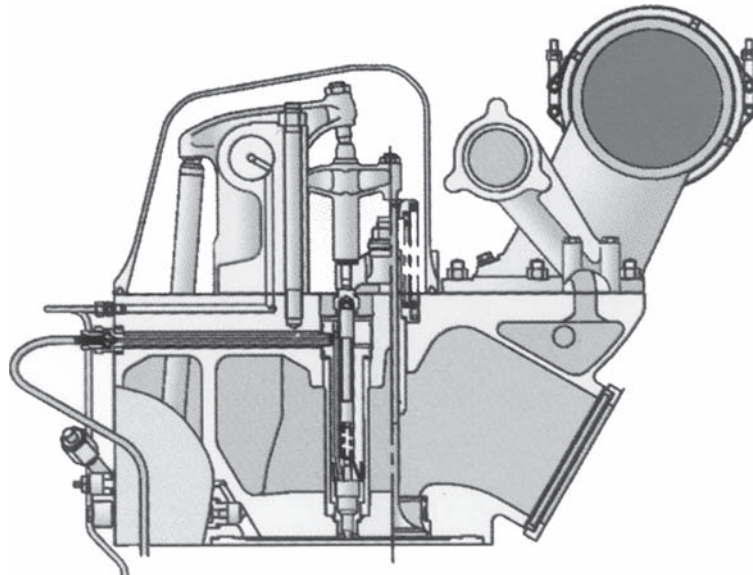


FIGURE 13.1.2

Cross section of a SEMT Pielstick PC2-6B engine

**FIGURE 13.1.3**

Pielstick engine crankshaft

**FIGURE 13.1.4**

Pielstick engine valve block

in height. Figures 13.1.3 to 13.1.5 show details of a crankshaft, the top of a head with the opening control valve (rocker and rocker arm), and a connecting rod.

An important difference between a gasoline engine and a diesel engine is not in the mode of introducing fuel, which in some gasoline engines is also injected, but when the fuel is introduced, which determines the nature of gas when the reaction starts.

In the gasoline engine, fuel is introduced well in advance so that the cylinder is full, when ignition occurs, of a substantially homogeneous mixture. In the diesel engine, fuel is injected at the last moment and burned as and when it is introduced.

For this reason, in general, gasoline engines burn gas or volatile liquid fuels, and diesel non volatile liquid fuels, but one may also burn in gasoline engines liquid fuels with low volatility sprayed very finely, and in diesel pressurized gaseous fuel or volatile liquid fuels.

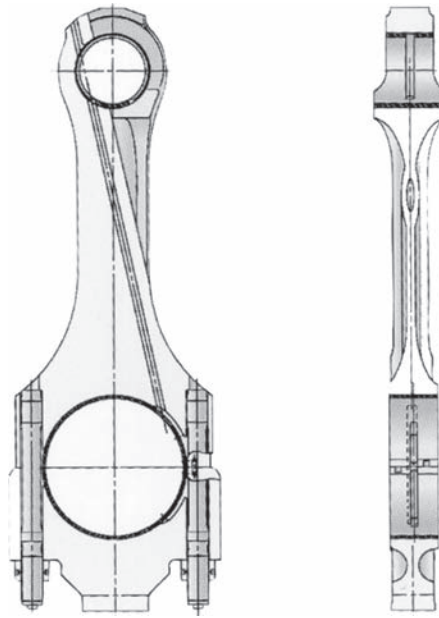


FIGURE 13.1.5
Pielstick engine rod

13.1.1 Four- and two-stroke cycles

According to the method used to evacuate gases and replace them with a fresh charge, there are two operation modes known as four-stroke and two-stroke.

In **four-stroke** cycles, the most common, the head of the cylinder is pierced by two holes, controlled by valves, which put it in communication with the intake and exhaust manifolds (Figure 13.1.6). Note the difference with reciprocating compressors, where valves are not controlled, but opened by differences in pressure between the cylinder and these manifolds.

The evolution of gas pressure and specific volume in the cylinder is often represented in the Watt diagram (Figure 13.1.7). At the end of expansion in 3, the exhaust valve opens, pressure drops to atmospheric pressure and the piston performs a full stroke to the head thus driving gases out. When it reaches the TDC in 5, the exhaust valve closes and the inlet opens. Moving away, the piston draws a fresh charge of gas. In 4, the BDC, the intake valve closes and compression 4-1 begins followed by combustion 1-2 and expansion. It is therefore a simple cycle in four strokes, hence the name four-stroke engine.

In **two-stroke** engines (Figure 13.1.8), exhaust occurs at the end of the expansion stroke through holes made in the side wall at such a level that they are unmasked by the piston at BDC. At the same time or shortly after, intake ports are opened which connect the cylinder with a manifold filled with fresh gas at a pressure slightly higher than that prevailing in the exhaust manifold.

The opening of the exhaust ports in 3 drops the pressure at the exhaust manifold (Figure 13.1.9), then the opening of the exhaust port produces a sudden burst of fresh gas, which drives flue gases to the exhaust manifold. The discharge gases and their replacement with fresh gas (**scavenging**) are carried out during a short time at the end of the expansion stroke and the beginning of the next one. The exhaust ports are closed, and then come compression 4-1, combustion 1-2 and expansion. The entire operation takes place in two simple strokes, hence the name two-stroke cycle.

This mode is used primarily for diesel engines, because to be effective, the scavenging must be done by excess, a certain amount of fresh gas flowing directly from the inlet to the exhaust.



FIGURE 13.1.6
Four-stroke engine, © French Navy

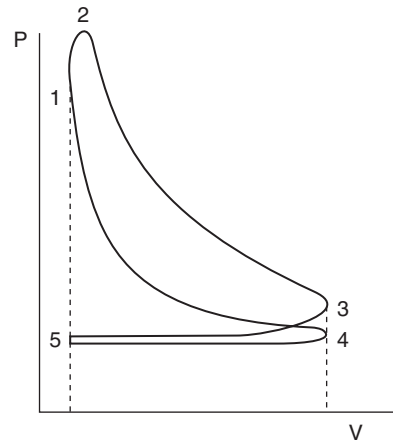


FIGURE 13.1.7
Four-stroke cycle

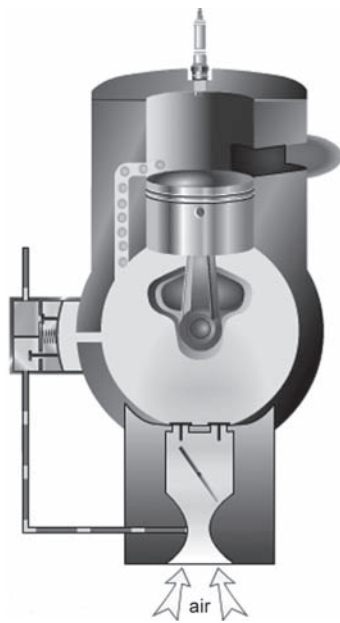


FIGURE 13.1.8
Two-stroke engine © French Navy

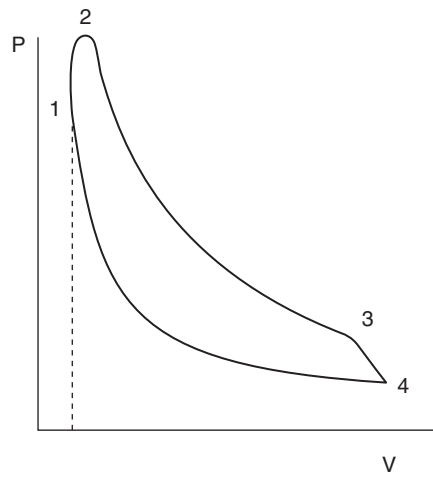
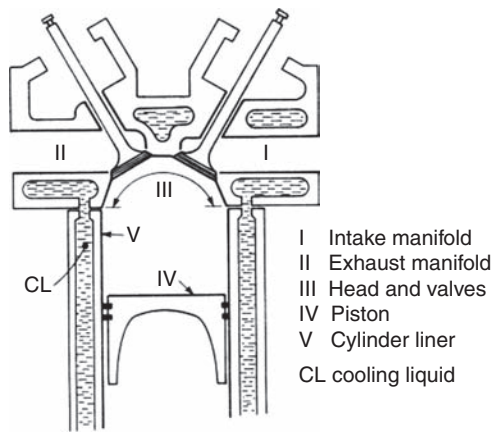
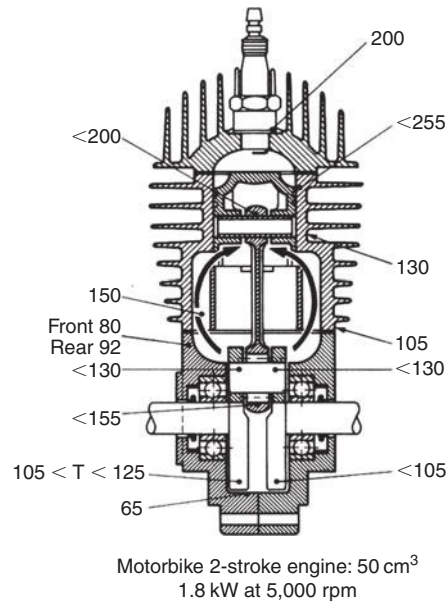


FIGURE 13.1.9
Two-stroke cycle

**FIGURE 13.1.10**

Cylinder water cooling, Extract from *Techniques de l'Ingénieur, Génie Mécanique*

**FIGURE 13.1.11**

Cylinder air cooling, Extract from *Techniques de l'Ingénieur, Génie Mécanique*

As fresh gas is typically a fuel mixture in gasoline engines, it is important not to lose any this way. There are however two-stroke gasoline engines in which either the fuel is injected directly into the cylinder, or the scavenging is done systematically by default (motorcycles, Fig. 13.1.11).

In general, fast engines are four-stroke, which seems *a priori* paradoxical, since a two-stroke operation can double the power for a given speed and thus appears more suitable for high capacity motors.

But it turns out that achieving efficient scavenging raises enormous difficulties in fast engines due to the extremely short time allowed for discharge. Moreover, in the two-stroke cycle, the average temperature is much higher in the cylinder, and in fast engines, where the friction of rings on the cylinder releases intense heat, it becomes impossible to maintain the piston temperature at an acceptable level.

13.1.2 Methods of cooling

The cylinder sidewalls and bottom of gasoline engines are always strongly cooled, usually by circulating water in holes in the walls (Figure 13.1.10), and sometimes in small-capacity motors with highly developed outer fins subject to a violent air current (Figure 13.1.11 shows the temperatures reached at different points in a two-stroke engine of small displacement).

With regard to pistons, we must distinguish two different cooling methods:

- in small and medium capacity engines, of reduced bore, the slider-type piston (rod hinged directly on the piston), almost always in a good conductor alloy, is not cooled directly, but only by ring contact with the cylinder walls;
- in industrial engines of large bore, the hollow piston is traversed by a flow of water brought by clips or articulated pipes.

The non-cooled piston construction mode is permissible only up to an upper bore, as long as the temperature at the center of the piston does not exceed a certain value, which depends also on the operation mode, being lower for diesel than for gasoline engines and for two-stroke engines than for four-stroke.

13.2 ANALYSIS OF THEORETICAL CYCLES OF RECIPROCATING ENGINES

In its classic form, the elementary study of cycles is based on rather crude approximations: the working fluid is equated with air, and itself equated to a perfect gas, and processes are considered perfect. To be more precise, we must consider:

- the mass and the actual chemical composition of the working fluid, which varies according to the phases of the cycle, due to the introduction of fuel and combustion;
- variations of the specific heat with temperature;
- molecular dissociation at high temperature;
- losses related to the renewal of the charge;
- combustion kinetics;
- heat exchanges between the working fluid and the engine walls;
- mechanical friction and auxiliary consumption.

We begin by studying ideal cycles that lend themselves to easy thermodynamic analysis, and then we give guidance on how to take into account main non-idealities.

Although highly simplified, these cycles allow us indeed to draw some important conclusions that are not challenged by further analysis, such as those relating to the influence on engine performance of volumetric compression ratio, combustion conditions (constant volume, constant pressure), or the initial pressure in the cylinder etc.

13.2.1 Beau de Rochas ideal cycle

Analyses of ideal cycles exclude intake and exhaust phases of two or four stroke real cycles. As a first approximation, the operation of gasoline engines can be represented by a cycle called Beau de Rochas or Otto, which is reduced, as indicated below, to four simple processes shown in Figure 13.2.1 in a Watt diagram and entropy chart:

- constant volume combustion 1-2;

Triggered at the end of compression, when the piston speed is zero, the combustion is supposed to be fast enough to be considered instantaneous, and therefore at constant volume, which is especially warranted in the slow engines:

$$v_2 = v_1 \quad Q_{12} = c_v (T_2 - T_1) > 0 \quad W_{12} = 0$$

- isentropic expansion 2-3

Here we find the conventional assumption in expansion:

$$s_3 = s_2 \Rightarrow T_3 (v_3)^{\gamma-1} = T_2 (v_2)^{\gamma-1} \quad W_{23} = c_v (T_3 - T_2) < 0 \quad Q_{23} = 0$$

- cooling at constant volume 3-4

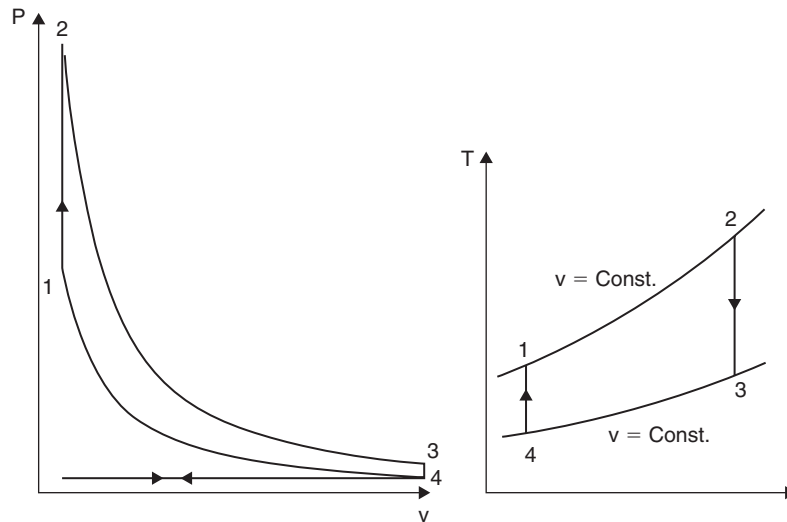
By the end of expansion, opening the exhaust valve makes the pressure in the cylinder suddenly drop. It is assumed here that the discharge is instantaneous:

$$v_4 = v_3 \quad Q_{34} = c_v (T_4 - T_3) < 0 \quad W_{34} = 0$$

- isentropic compression 4-1

Here we find the conventional assumption in compression:

$$s_1 = s_4 \Rightarrow T_1 (v_1)^{\gamma-1} = T_4 (v_4)^{\gamma-1} \quad W_{41} = c_v (T_1 - T_4) > 0 \quad Q_{41} = 0$$

**FIGURE 13.2.1**

Beau de Rochas theoretical cycle

The net internal work is:

$W = W_{23} + W_{41} = -(Q_{12} + Q_{34})$, and the cycle efficiency is:

$$\eta_{\text{th}} = \frac{|W|}{Q_{12}} = 1 + \frac{Q_{34}}{Q_{12}}$$

$$\eta_{\text{th}} = 1 - \frac{T_3 - T_4}{T_2 - T_1} = 1 - \frac{T_2 \left(\frac{v_2}{v_3} \right)^{\gamma-1} - T_4}{T_2 - T_4 \left(\frac{v_4}{v_1} \right)^{\gamma-1}}$$

$$\text{However, } \frac{v_3}{v_2} = \frac{v_4}{v_1} = \rho$$

We have thus:

$$\eta_{\text{th}} = 1 - \frac{1}{\rho^{\gamma-1}} = 1 - \frac{T_4}{T_1} \quad (13.2.1)$$

We see here the interest to increase as much as possible the compression ratio. As will be shown in section 13.4.1, it is limited in practice by the conditions of non-knocking in the cylinder.

It is surprising to see that but a single parameter is involved in the expression of efficiency. The reason is that the Beau de Rochas cycle has the same efficiency as a Carnot cycle operating between temperatures T_4 and T_1 . In fact, it is as if the pressure and the temperature rise resulting from combustion at constant volume had no influence on overall performance.

The efficiency of Beau de Rochas cycle depends only on the geometric design of the engine, without the initial conditions intervening. In contrast, the value of γ plays decisive influence, as shown by curves of Figure 13.2.2.

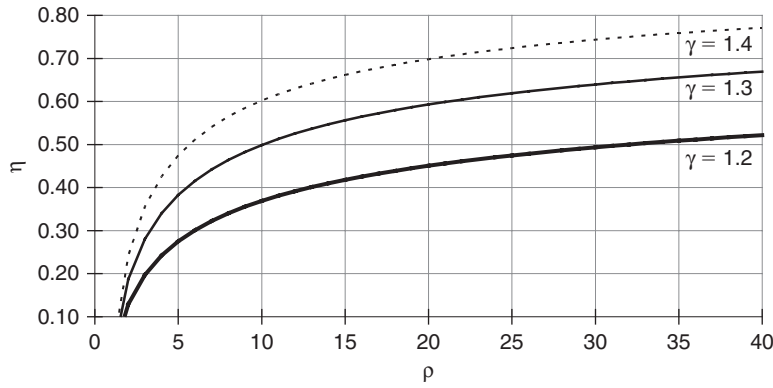


FIGURE 13.2.2
Beau de Rochas theoretical efficiency

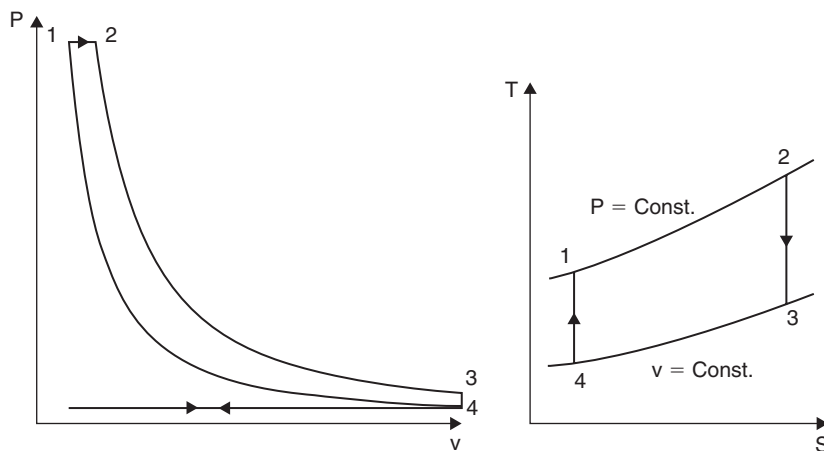


FIGURE 13.2.3
Diesel theoretical cycle

Given the overwhelming influence of γ it is much more realistic, if we keep the assumption of perfect working fluid, to calculate γ at an average temperature, much higher than the intake temperature T_4 .

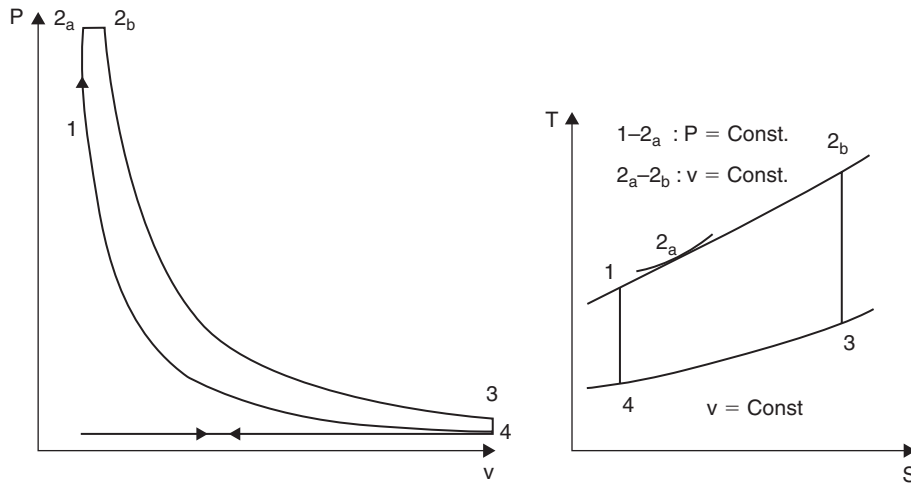
13.2.2 Diesel cycle

The general assumptions that were made during the analysis of Beau de Rochas cycle are made here again, and will not be repeated.

The fundamental difference between the diesel cycle and the Beau de Rochas cycle is the replacement of the constant volume combustion by combustion at constant pressure, as shown by Watt and entropy diagrams of Figure 13.2.3. It is assumed here the hypothesis still mostly valid for slow engines, that the expansion of gases due to combustion exactly compensates, in terms of pressure, the expansion due to the stroke.

Introducing the ratio ϵ of volumes at the beginning and end of combustion (cutoff ratio), we can simply express the cycle efficiency.

$$\eta_{th} = \frac{Q_{12} - Q_{34}}{Q_{12}} = \frac{c_p(T_2 - T_1) - c_v(T_3 - T_4)}{c_p(T_2 - T_1)}$$

**FIGURE 13.2.4**

Mixed cycle

All calculations done, we obtain:

$$\eta_{th} = 1 - \frac{1}{\gamma} \frac{1}{\rho^{\gamma-1}} \frac{\varepsilon^\gamma - 1}{\varepsilon - 1} \quad (13.2.2)$$

The diesel cycle efficiency depends on the volumetric compression ratio and heat provided, which sets the value of expansion during combustion, that is to say ε .

13.2.3 Mixed cycle

In fact, as we have seen, the combustion is neither at constant volume nor constant pressure, and a better approximation can be obtained by considering that it starts at constant volume and ends at constant pressure, as shown in diagrams of Figure 13.2.4.

Such a cycle, known as dual combustion or mixed, or Sabathé, can be expressed using three parameters:

- ρ volumetric compression ratio;
- $\lambda = P_{2a}/P_1$ ratio of the combustion pressure to the compression pressure;
- $\varepsilon = V_{2b}/V_{2a}$ initial expansion ratio.

Heat quantities supplied and discharged become:

$$Q_{12a} = c_v (T_{2a} - T_1) \quad Q_{2a2b} = c_p (T_{2b} - T_{2a}) \quad Q_{34} = c_v (T_4 - T_3)$$

The efficiency is equal to:

$$\eta_{th} = 1 + \frac{Q_{34}}{Q_{12a} + Q_{2a2b}}$$

By expressing temperature in terms of the parameters defined above, we get:

$$T_1 = T_4 \left(\frac{v_4}{v_1} \right)^{\gamma-1} = T_4 \rho^{\gamma-1}$$

$$\begin{aligned}
T_{2a} &= T_1 \frac{P_{2a}}{P_1} = \lambda T_1 = T_4 \lambda \rho^{\gamma-1} \\
T_{2b} &= T_{2a} \frac{v_{2b}}{v_{2a}} = \varepsilon T_{2a} = T_4 \varepsilon \lambda \rho^{\gamma-1} \\
T_3 &= T_{2b} \left(\frac{v_{2b}}{v_3} \right)^{\gamma-1} = T_{2b} \rho^{1-\gamma} \left(\frac{v_{2b}}{v_{2a}} \right)^{\gamma-1} = T_4 \varepsilon \lambda \rho^{\gamma-1} \rho^{1-\gamma} \varepsilon^{\gamma-1} = T_4 \varepsilon^\gamma \lambda
\end{aligned}$$

The efficiency becomes:

$$\begin{aligned}
\eta_{th} &= 1 - \frac{c_v(T_3 - T_4)}{c_v(T_{2a} - T_1) + c_p(T_{2b} - T_{2a})} \\
\eta_{th} &= 1 - \frac{c_v(\varepsilon^\gamma \lambda - 1)}{c_v(\lambda \rho^{\gamma-1} - \rho^{\gamma-1}) + c_p(\varepsilon \lambda \rho^{\gamma-1} - \lambda \rho^{\gamma-1})} \\
\eta_{th} &= 1 - \frac{\lambda \varepsilon^\gamma - 1}{\rho^{\gamma-1}(\lambda - 1 + \gamma \lambda(\varepsilon - 1))} \tag{13.2.3}
\end{aligned}$$

Obviously, we get the Beau de Rochas cycle by making $\varepsilon = 1$ in this expression:

$$\eta_{th} = 1 - \frac{\lambda - 1}{\rho^{\gamma-1}(\lambda - 1)} = 1 - \frac{1}{\rho^{\gamma-1}}$$

and the diesel cycle by making $\lambda = 1$:

$$\eta_{th} = 1 - \frac{1}{\gamma} \frac{1}{\rho^{\gamma-1}} \frac{\varepsilon^\gamma - 1}{\varepsilon - 1}$$

The graph in Figure 13.2.5 compares the efficiencies of the three diesel, mixed and Beau de Rochas cycles.

In light of the curves, one would think that the Beau de Rochas cycle efficiency is better. In practice, the opposite is true, firstly because the compression ratios of diesel engines are much larger than those of gasoline engines, and partly because actual cycles are more like the mixed cycle.

Mixed cycle maximum pressure

From the expression of the mixed cycle efficiency, we can establish a relationship between the total heat supplied Q and the cycle maximum pressure P_{max} .

$$\begin{aligned}
Q &= Q_{12a} + Q_{2a2b} = c_v(T_{2a} - T_1) + c_p(T_{2b} - T_{2a}) \\
\lambda &= \frac{P_{2a}}{P_1} = \frac{T_{2a}}{T_1} \quad \varepsilon = \frac{v_{2b}}{v_{2a}} = \frac{T_{2b}}{T_{2a}} \\
Q &= c_v T_1((\lambda - 1) + \lambda \gamma(\varepsilon - 1)) \\
Q &= c_v T_4 \rho^{\gamma-1}(\lambda - 1 + \gamma \lambda(\varepsilon - 1)) \\
P_{max} &= \lambda P_1 = \lambda \rho^\gamma P_a = \frac{P_a \rho^\gamma}{1 + \gamma(\varepsilon - 1)} \left(\frac{Q}{c_v T_4 \rho^{\gamma-1}} + 1 \right) \tag{13.2.4}
\end{aligned}$$

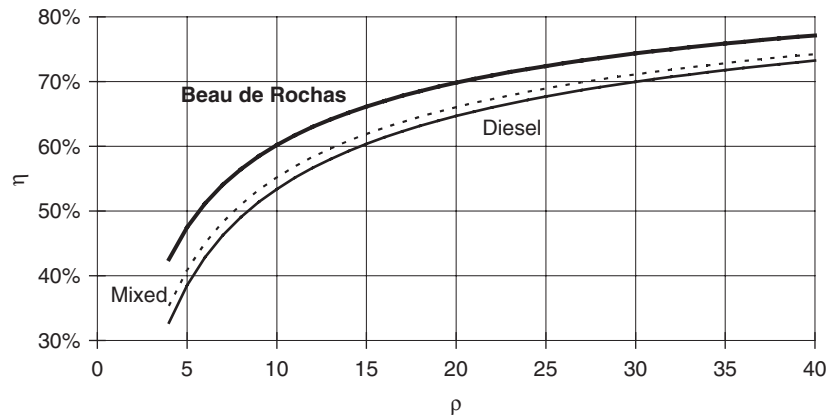


FIGURE 13.2.5

Comparison of the three cycles

However, these cycles still lack realism, and deviate quite significantly from real cycles. Their relevance can be characterized by a quantity called shape efficiency, which is equal to the ratio of actual cycle work measured on the bench to the calculated work.

To fix ideas, the magnitudes of shape efficiency values obtained with the above assumptions are:

- 50 to 65% for the Beau de Rochas cycle;
- 60 to 70% for the diesel cycle;
- slightly better for the mixed cycle, but still low.

13.2.4 Theoretical associated cycles

For more realism, it is imperative to take into account on the one hand heat carried away by cooling water, on the other hand mass (diesel) and composition (diesel, gasoline engine) variations of the working fluid during combustion, and finally the influence of temperature on gas heat capacities.

M. Thelliez (1989) proposes a theoretical cycle associated with the real cycle, shown Figure 13.2.6, where ρ is the compression ratio, ρ_p the relative isobaric combustion stroke, and ρ_T the relative isothermal combustion. This cycle involves a non-adiabatic combustion in three stages: constant volume, constant pressure, constant temperature, which leads to much better shape efficiency. The complexity of the calculations is significantly higher but the shape efficiencies then exceed 90%, so that the ventilation of shape losses (10%) between the walls and the exhaust pipe lead to an error of about 1–2 points (out of 100) on this share, which corresponds to an accuracy far greater than that obtained by the usual balances, given convection and radiation losses from the engine and its accessories, which may represent more than 10% of the initial energy. Readers interested in further developments can refer to (Thelliez, 1989).

Such a theoretical associated cycle considers the main cycle (closed phases) and the pumping loop. The calculations are carried out with the following simplifying assumptions:

- constant combustion efficiency along the cycle (quenched dissociation, equal to that obtained at the exhaust); this assumption overestimates the efficiency at the beginning of combustion and underestimates it at the end of combustion;
- mixture of ideal gases;
- wall losses “marrying” the combustion law: this assumption overestimates the wall losses at the beginning of combustion and underestimates them at the end of combustion, so there is some compensation for apparent heat which is taken into account in the cycle calculation;
- in the case of a diesel engine we take into account the change in mass and specific ideal gas constant according to the excess air at the point considered, as well as the variation of specific internal

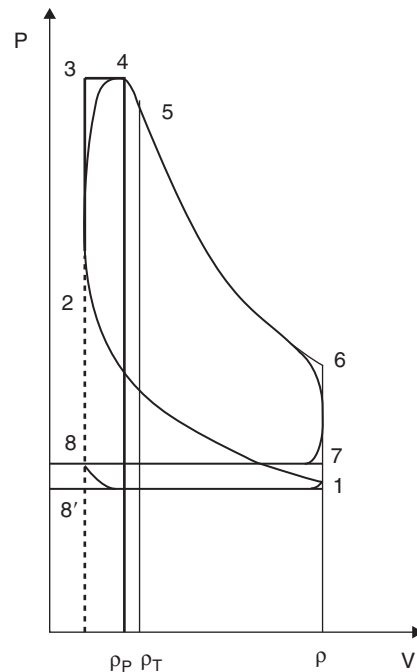


FIGURE 13.2.6

Theoretical associated cycle

energy depending on temperature and air factor λ (given assumptions 1 and 2), namely: $m(\lambda)$, $r(\lambda)$, $u(T, \lambda)$, $h(T, \lambda)$. It follows similar expressions for $c_p(T, \lambda)$, $c_v(T, \lambda)$, and $\gamma(T, \lambda)$;

- in the case of a gasoline engine we take also into account change in above quantities (except the mass remains constant) with temperature and composition, the latter being characterized by the mass fraction of fuel burned ζ : $r(\zeta)$, $u(T, \zeta)$, $h(T, \zeta)$, $c_p(T, \zeta)$, $c_v(T, \zeta)$, and $\gamma(T, \zeta)$.

The identification of the theoretical associated cycle is then done with the following steps:

- gas analysis;
- pumping loop;
- phase without combustion;
- combustion phase.

Although more complex, calculations can still be done on a spreadsheet, and are quite accessible. Note, however, that taking into account the variation of specific heat of gases with temperature introduces implicit equations in T to be solved by iterations.

Such modeling can also be done by Thermoptim as we shall see later sections 13.4.4.1 and 13.5.7.

Although very simplified compared to reality, these theoretical cycles highlight the importance of certain factors such as the compression ratio or combustion type, showing the value for better efficiency of operating at constant volume rather than constant pressure. We will now study how the piston engine characteristic curves are conventionally presented, which will in particular allow us to take into account a crucial variable that we have not yet considered: the rotation speed.

13.3 CHARACTERISTIC CURVES OF PISTON ENGINES

The characteristic curves of a piston engine are very different from those of turbomachinery, as the principles of operation are quite different here.

The main quantities used are the mean effective pressure (or the power factor), the engine torque, rotation speed and specific fuel consumption, whose presentations vary from country to country. However, even if the quantities used vary according to the authors, the transition from one mode of representation to another is usually quite easy, as we will see.

13.3.1 Effective performance, MEP and power factor

The work produced by a displacement machine in a reversible cycle can be calculated from expression: $W = -\int P dV$

The calculation of the integral giving the cycle work is complex and relies on detailed dimensional quantities, difficult to compare from one engine to another. Therefore, to facilitate comparisons, we introduce more accessible quantities: the displacement V_s and the mean pressure MP.

For all displacement machines, the concept of swept volume or displacement is indeed important because it represents a fundamental geometric characteristic of the machine. The ratio of the cycle work W to engine displacement has the dimension of a pressure. It is called mean pressure MP, or sometimes equivalent mean pressure difference ΔP_e .

$$MP = \Delta P_e = \frac{\int P dV}{V_s} \quad (13.3.1)$$

It represents the pressure that should be applied to the piston to produce the same work as that provided by the engine. This definition clearly shows the proportional relationship between pressure and the average work done by the engine.

We can also use a dimensionless power factor W_0 , ratio of the MP to the engine inlet pressure P_1 :

$$W_0 = \frac{MP}{P_1}$$

We get this way a simple expression of the work done by the machine:

$$W = W_0 P_1 V_s$$

In practice, one must take into account cycle irreversibilities, which leads as we shall see later to identify two mean pressures: the indicated mean effective pressure IMEP, and the mean effective pressure MEP.

13.3.2 Influence of the rotation speed

Let us call P_e the output power, ω the rotation speed, W_c the work produced by a cylinder during a cycle, n the number of cylinders, and i the intermittency factor, number of cycles per revolution, i.e. 0.5 for a 4-stroke engine, and 1 for a 2-stroke.

With these notations, we have:

$$P_e = \frac{\omega}{2\pi} W_c \cdot i \cdot n_c \quad (13.3.2)$$

As $\omega = 2\pi N/60$, we get, K being a constant:

$$P_e = KN$$

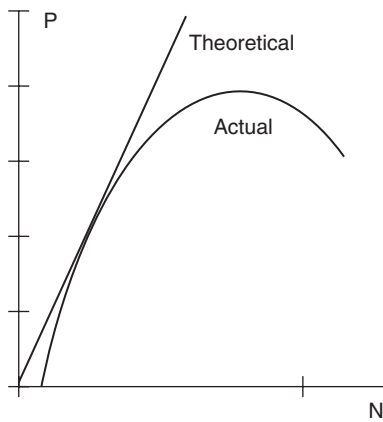


FIGURE 13.3.1
Power function of speed

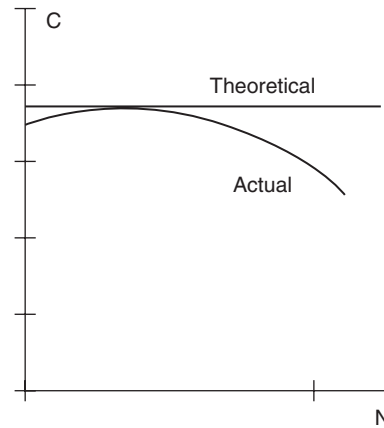


FIGURE 13.3.2
Torque function of speed

The motor torque is in turn given by equation:

$$C = \frac{P}{\omega} = \frac{W_c}{2\pi} \cdot i \cdot n_c = K' \quad (13.3.3)$$

In a cyclic displacement machine, the output power should be at first approximation proportional to the rotation speed, while the torque and efficiency of the machine should not depend on it. In practice, however, things are not so simple, because of interference phenomena that occur, particularly at very low and very high speeds.

At low speeds, heat losses within the machine (wall effect, conduction losses etc.) and leak losses take values disproportionate with the useful power. Therefore, the efficiency, the work provided and the torque all fall.

At high speeds, another category of losses sees its influence grow: mainly internal losses and admission and discharge losses. These losses are substantially proportional to the square of the fluid velocity, which explains why they become dominant.

Under these conditions, the laws of evolution of the engine power and torque relative to the rotation speed take the general appearance of Figures 13.3.1 and 13.3.2.

As a first approximation, and in most speeds encountered, we can consider that the relationship between power and speed is almost proportional. As power is also proportional to the MEP and the power factor, we can in practice use interchangeably as abscissa of the characteristic curves one of the four magnitudes P, MEP, W_0 or N, which explains that presentations may differ from one country to another.

Moreover, these curves are only valid at full load. Part-load operation results in significant differences depending on whether it is a gasoline or a diesel engine. In the first case, we shall see that it is impossible to reduce richness below a lower limit R_i , which necessitates adjusting the engine by varying the pressure drop at the admission, by means of a valve which just strangles the gas stream admitted. It is customary in this case to give the “torque-speed” curves for different values of throttle opening, the corresponding pressure drop playing a major role.

For diesel engines, this type of problem does not arise, and we can control the power by varying the amount of fuel injected. It is not necessary to introduce an additional pressure drop, and torque characteristics are much less steep than in the previous case, as shown in Figures 13.3.3 and 13.3.4.

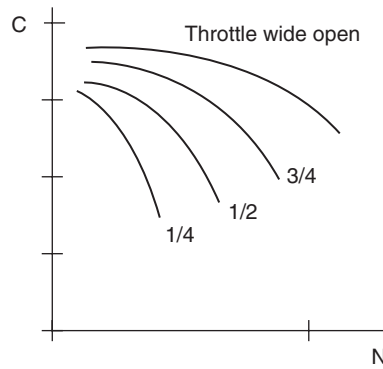


FIGURE 13.3.3
Gasoline part-load torque

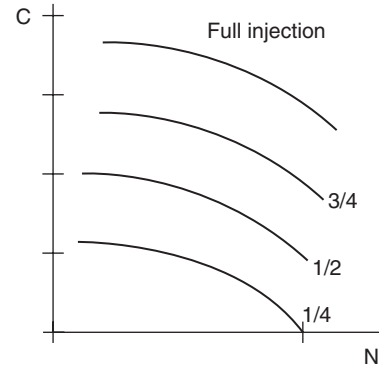


FIGURE 13.3.4
Diesel part-load torque

13.3.3 Indicated performance, IMEP

We have so far neglected losses of mechanical origin, that are often taken into account, as shown in section 10.1.6 of Part 2, by means of a mechanical efficiency η_m . In section 13.3.4 we will show that to be accurate, it is preferable to operate differently.

We can therefore consider that the effective power P_e is the product of the internal or indicated power P_i by the mechanical efficiency η_m :

$$P_e = \eta_m P_i$$

We adopt thus the convention to identify the thermodynamic proper performance by index i , and the overall performance by index e .

Under these conditions, we define the indicated mean effective pressure IMEP:

$$\text{IMEP} = \frac{W_{ci}}{V_s} = \frac{\text{MEP}}{\eta_m} \quad (13.3.4)$$

13.3.3.1 Volumetric efficiency

A number of factors are reducing the mass of fresh gas entering the cylinder during the intake phase: the residual presence of smoke, the high temperature of the walls, which has the effect of dilating the fresh gas, admission losses, which cause the pressure in the cylinder to be slightly less than atmospheric pressure, and finally the exhaust counter-pressure. Moreover, acoustic phenomena related to the charge pulsating flow may, depending on the case, either decrease it (known as filling holes), or instead increase it (this is called natural supercharging). This pulsating flow naturally stems from the reciprocation of the piston and the opening and closing of valves.

To characterize these losses, we define a volumetric efficiency C_r , such that the mass of the fresh gas charge admitted by cycle is equal to:

$$m_a = C_r \rho_a V_s = C_r V_s \frac{P_a}{r T_a} \quad (13.3.5)$$

We can show that, in the absence of acoustic phenomena that we have just mentioned, if f is the residual gas rate, ρ the volumetric compression ratio, and if admission conditions are identified by index 1 , the volumetric efficiency is given by:

$$C_r = (1 - f) \frac{\rho}{\rho - 1} \frac{r_a}{r_1} \frac{T_a}{T_1} \frac{P_1}{P_a} \quad (13.3.6)$$

In practice, C_r is about 0.80 to 0.85 for a gasoline engine, and around 0.9 for a diesel engine.

13.3.3.2 Determination of the indicated mean effective pressure

Moreover, introducing richness R and the air fuel ratio AFR for stoichiometric combustion, we can write: $m_c = m_a R/AFR$, and the amount of heat released by combustion is equal to:

$$Q_c = m_c LHV = R/AFR LHV m_a$$

In practice, for conventional fuels, we have, both for gasoline and diesel:

$$\frac{LHV}{AFR} \approx \frac{42}{14} = 3 \text{ MJ/kg.}$$

The indicated efficiency η_i is equal to the ratio of indicated work per cycle W_{ci} to Q_c :

$$\eta_i = \frac{AFR W_{ci}}{LHVR m_a} \quad (13.3.7)$$

By replacing m_a by its value, we obtain for W_{ci} :

$$W_{ci} = \eta_i C_r V_s \frac{LHV}{AFR} R \frac{P_a}{r T_a} \quad (13.3.8)$$

By definition of IMEP, we get: $IMEP = W_{ci}/V_s$

$$IMEP = \eta_i C_r \frac{LHV}{AFR} R \frac{P_a}{r T_a} \quad (13.3.9)$$

13.3.3.3 Experimental determination of the indicated efficiency

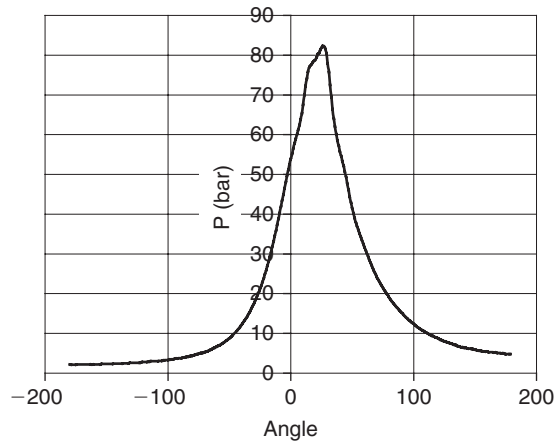
As noted above, the gap between real and theoretical cycles does not allow precise determination of the indicated efficiency. To know this, it is necessary to carry out bench tests. A record is made of the pressure versus the crank angle (Figure 13.3.5). Knowing the geometric characteristics of the engine, we can easily relate pressure to the stroke: we can thus introduce the equations of the kinematic system piston-connecting rod-crankshaft, such as those proposed by Clos in Treaty B 2800 "Technologie des moteurs alternatifs à combustion interne" of Techniques de l'Ingénieur:

$$x = r \left[\lambda - \frac{1}{4\lambda} - \frac{3}{64\lambda^3} + \cos \theta + \left(\frac{1}{4\lambda} + \frac{1}{16\lambda^3} \right) \cos 2\theta - \frac{\cos 4\theta}{64\lambda^3} \right]$$

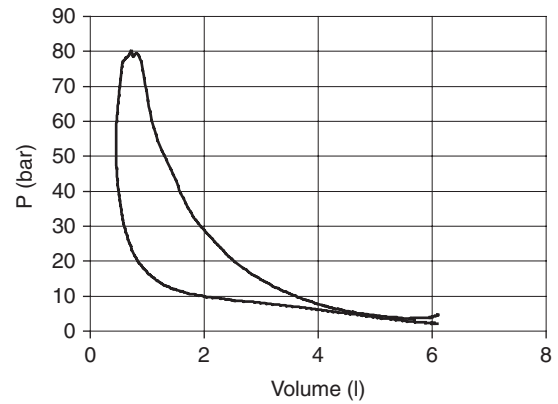
- θ is the crankshaft angle;
- r is the half-stroke (the distance between the pin and the shackle axis);
- λ is the ratio L/r of the connecting rod centerline and the half-stroke;
- x is the position of the piston axis on the rod.

We can thus get the real cycle in a (P, v) diagram (Figure 13.3.6). The indicated work is deduced by simple integration.

Figures 13.3.5 and 13.3.6 are from tests conducted on a supercharged diesel engine, which were courteously provided by Prof. M. Tazerout, of École des Mines de Nantes.

**FIGURE 13.3.5**

Bench pressure curve

**FIGURE 13.3.6**

Diesel Watt diagram

13.3.3.4 Shape efficiency

To characterize the gap between real and theoretical cycle we introduced, as indicated in paragraph 13.2.3, the shape efficiency η_f , defined as the ratio of actual efficiency to theoretical efficiency.

As a first approximation, we obtain an order of magnitude of current indicated efficiencies of automotive engines by writing $\eta_i = \eta_f \cdot \eta_{th}$, η_{th} being the theoretical Beau de Rochas or Diesel cycle efficiency.

For gasoline engines, we have:

$$\eta_i = 0.65 \left(1 - \frac{1}{\rho^{\gamma-1}} \right) \quad (13.3.10)$$

For diesel engines:

$$\eta_i = 0.7 \left(1 - \frac{1}{\gamma} \frac{1}{\rho^{\gamma-1}} \frac{\varepsilon^\gamma - 1}{\varepsilon - 1} \right) \quad (13.3.11)$$

With these assumptions, we obtain as an order of magnitude for IMEP values:

- for a gasoline engine ($\rho = 7$, $R = 1$, $C_r = 0.85$) IMEP = 10.4 bar;
- for a diesel engine ($\rho = 15$, $\varepsilon = 1.5$, $R = 0.65$, $C_r = 0.9$) IMEP = 9 bar.

These values are only very approximate, actual processes being much more complex.

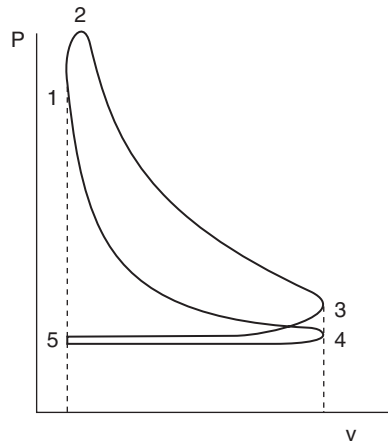
13.3.4 Effective performance, MEP

Indicated performance is representative of the motor internal thermodynamic behavior, but does not take into account certain losses, such as pumping losses for the renewal of the charge or mechanical losses due to friction and auxiliaries.

13.3.4.1 Pumping losses

In a four-stroke engine, useful work during one cycle is equal to the algebraic sum of the motive power corresponding to the (4-1-2-3) process and the power spent for charge renewal (3-5-4), called pumping work (Figure 13.3.7).

It is customary to characterize the pumping work by a mean pumping pressure MPP.

**FIGURE 13.3.7**

Watt diagram

The value of MPP is directly related to admission pressure drops, which, as noted, are proportional to the square of the rotation speed. Specifically, they decompose into three categories:

- pressure drop in valves;
- pressure drop in the intake and exhaust manifolds;
- inertial effects of gas flow in intake pipes.

Overall, they result in a parabolic law of type:

$$\text{MPP} = KN^2$$

13.3.4.2 Friction losses

Friction losses are of dissipative type, and hence related to the piston velocity. To characterize them, we introduce the mean friction pressure MFP, which can be considered in first approximation as a linear function of the engine rotation speed.

For a series gasoline engine, it is about:

$$\text{MFP} = 0.7 + 1.75 \cdot 10^{-4}(N - 1000)$$

For a diesel engine, it is slightly higher:

$$\text{MFP} = 0.8 + 6 \cdot 10^{-4}(N - 1000)$$

N is expressed in revolutions per minute, and MFP in bar.

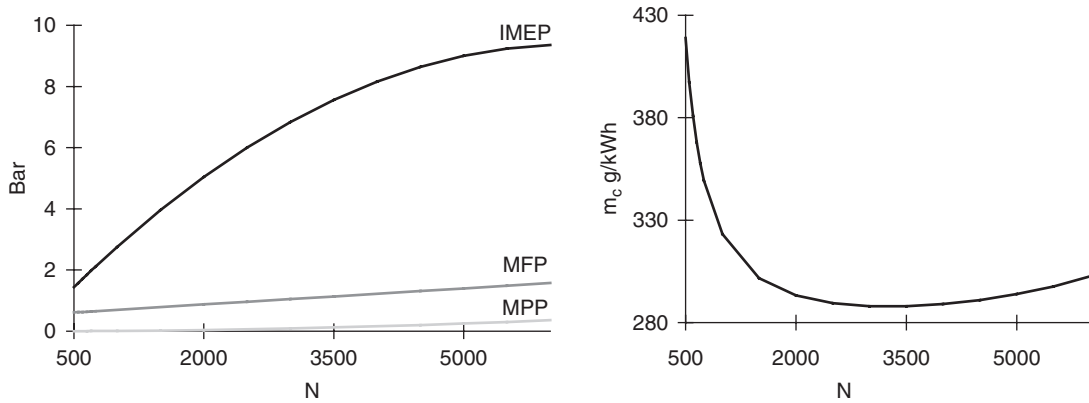
Overall, therefore, the engine performance is given by:

$$\text{MEP} = \text{IMEP} - \text{MFP} - \text{MPP}$$

The magnitudes of MFP are, as shown by the above formulas, around 1 bar, whereas MPP varies between 0.1 and 0.4 bar approximately, depending on engine speed. The above analysis thus shows that the mechanical efficiency η_m is far from constant.

13.3.5 Specific consumption of an engine

To characterize the performance of an engine, the concept of specific consumption is often used. The specific consumption m_c is usually expressed in g/kWh. It represents the amount of fuel which must be burned to produce one kWh of mechanical power.

**FIGURE 13.3.8**

Effective performance of a reciprocating engine

η being the overall efficiency of the engine, it comes:

$$m_c = \frac{1}{\eta(\text{LHV})} \quad (13.3.12)$$

For example, in the case of octane (LHV = 48,000 kJ/kg = 13.33 kWh/kg), and with an efficiency equal to 0.3, we have:

$$m_c = \frac{1}{0.3 \cdot 13.33} = 250 \text{ g/kWh}$$

Like other characteristics, m_c depends on the rotation speed.

Indeed, one can put
$$m_c = \frac{m_{ci}}{\eta_m}$$

with $m_{ci} = 1/\eta_i(\text{LHV})$ internal or indicated specific consumption.

η_i is the internal thermodynamic efficiency independent of the rotation speed N , m_{ci} is constant, and we get:

$$m_c = \frac{K}{\eta_m} = K \frac{\text{IMEP}}{\text{MEP}} = K \frac{1}{1 - \frac{\text{MFP} + \text{MPP}}{\text{IMEP}}} \quad (13.3.13)$$

Knowing the evolution laws of IMEP, MPP and MFP as a function of the rotation speed, it is possible to plot the evolution of the specific consumption (Figure 13.3.8).

We see that there is a speed at which the specific fuel consumption is minimal.

At constant speed, if we assume that the friction and pumping losses vary little with load, the specific consumption as a function of MEP looks like a hyperbola (Figure 13.3.9).

We see that the specific consumption tends to infinity as $\text{MEP} = \text{MFP} + \text{MPP}$, that is to say when the engine is idling. When the mean pressure becomes very low and negative, that is to say when the engine is used as a brake, specific fuel consumption tends to be closer to 0. This is strictly true for diesel cycle where you cut the fuel injection, and approximately true for Beau de Rochas cycle, where the power is strangled at its maximum by the throttle.

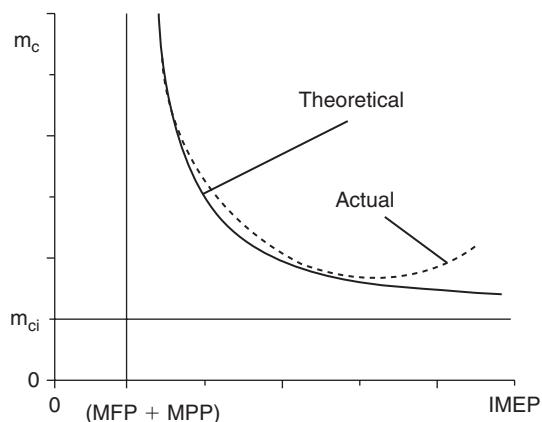


FIGURE 13.3.9
Engine specific consumption

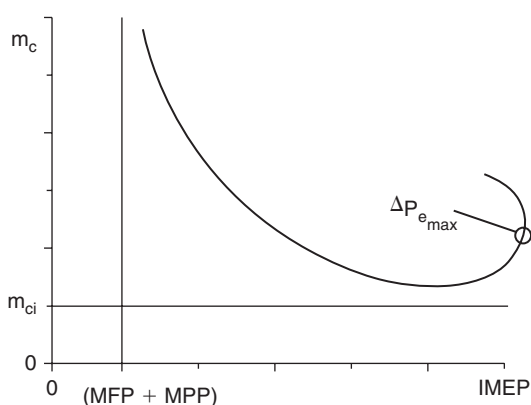


FIGURE 13.3.10
Gasoline engine specific consumption

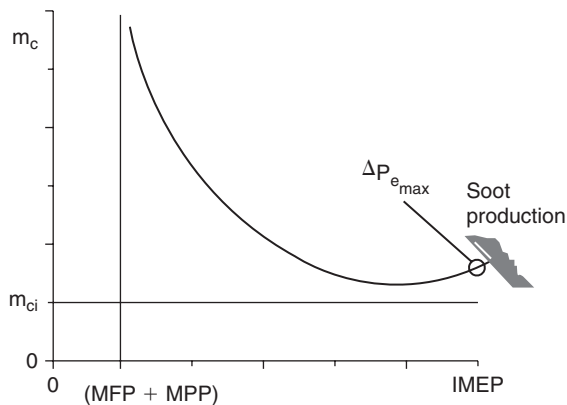


FIGURE 13.3.11
Diesel engine specific consumption

The specific consumption tends asymptotically to its internal value m_{ci} with increasing MEP. Indeed, the relative magnitude of losses decreases more and more.

This $m_c = f(\text{MEP})$ characteristics is approximately consistent with reality, as shown in Figures 13.3.10 and 13.3.11 representing the characteristics of gasoline and diesel engines: at nearly full load, we must consider a significant increase in specific fuel consumption, particularly in the case of gasoline engines for the reasons mentioned above.

The shape of characteristics presented above are only valid at constant speed, the latter affecting the internal efficiency and friction.

The specific consumption varies with speed, according to characteristics that depend on usage. If, for example, we talk of land traction, several curves $\text{MEP} = f(N)$ are shown depending on the land slope. The gearbox is specifically responsible for maintaining as much as possible the system operating point in the most favorable area.

The analysis of theoretical cycles and overall performance of piston engines have allowed us to identify the main parameters on which it is possible to play to optimize and control their operation. Once the compression ratio and fuel (and therefore its LHV) selected, the variables that can be used to control the engine are essentially the heat provided (fuel flow) and the intake pressure. We have already said that a key difference between gasoline and diesel is precisely at this level.

To go further it is necessary to separate the study of gasoline and diesel engines, to reflect the influence of combustion chemical kinetics on the operation and design of these different engine

types (see sections 13.4 for gasoline engines and 13.5 for diesel engines). We refer the reader to section 7.6 of Part 2 for a presentation of the basic mechanisms governing combustion phenomena.

13.4 GASOLINE ENGINE

In a conventional gasoline engine, when the reaction starts, the combustion chamber is filled with an almost homogeneous combustible mixture. The basis for the study of combustion in these engines is the chemical kinetics of fuel gas mixtures, the main problem encountered in gasoline engines being the control of combustion conditions to prevent knocking.

13.4.1 Limits of knocking and octane number

The simplest solution is to set an upper limit to the compression ratio $\rho = V/v$. The experience shows that a given engine running at specified speed and burning a particular fuel, begins to detonate when ρ exceeds a certain value, which depends mainly on the fuel.

It is therefore necessary to classify fuels according to their ability to detonate. For this, we proceed as follows in order to get rid of the type of engine used for testing: we test at given speed in an experimental engine with adjustable head, a continuous series of fuels obtained by mixing in variable proportions a highly explosive fuel, normal heptane C_7H_{16} and a low explosive fuel, iso-octane C_8H_{18} .

We thus get the law of variation $V/v = f(x)$, of the limit compression ratio as a function of the iso-octane content x of the mixture. To classify any fuel F , we test the same engine at the same speed and determine the limit volumetric ratio ρ_c for which knocking occurs (measured by an electro-mechanical system recording pressure changes in the cylinder). Expressed as a percentage, value x_c such as $\rho_c = f(x_c)$ is called **octane number** i of the fuel. This characteristic presents the advantage of being independent of the engine used. ρ values range from 4 (for $i = 0$) to 12 (for $i = 100$) for standard test motor (CFR engine of the Cooperative Fuel Research Committee). Note that the value of i may exceed 100 for some fuels such as ethanol or benzene, less explosive than the iso-octane.

We are in practice led to define two octane numbers: the Research Octane Number or RON, characteristic of the behavior in mild operating conditions (low load, urban) and the Motor Octane Number or MON, characteristic of the behavior in severe operating conditions (high loads, high speed traffic on highway etc.).

For conventional fuels, the MON is 10 to 12 points less than the RON, the values of the latter being between 97 and 99 for premium fuels, and between 89 and 92 for regular gasoline.

In order of increasing octane number, fuels usually rank as follows: acetylene, normal saturated hydrocarbons (alkanes), branched chain hydrocarbons, alcohols, ethers, carbon monoxide. In a series of hydrocarbons, octane number decreases when the number of carbon atoms increases.

We can considerably increase the octane number of gasoline by incorporating:

- either significant proportions (5–20%) of low explosive fuels, such as alcohols (methanol CH_3OH or ethanol C_2H_5OH) or methyl ether (MTBE methyltertiobutylether $C_4H_9-O-CH_3$ and TAME tertioamylmethylether $C_5H_{11}-O-CH_3$);
- or very low quantities (parts per thousand) of an organometallic compound, tetraethyl lead, $Pb(C_2H_5)_4$, which presumably acts as a catalyst inhibiting the production of volatile compounds. However, the dosage of these additions must be limited to prevent corrosion of exhaust valves by lead. In addition, these additives are incompatible with catalytic converters that are spreading increasingly to limit emissions of nitrogen oxides NO_x . We will discuss these issues in section 13.8 on prevention of air pollution from combustion.

For a given octane number, the limit value of V/v depends on the motor and its regime. It increases when the speed increases, and is strongly influenced by the design of the combustion chamber. It can be raised substantially by increasing the turbulence of the mixture when it burns.

In slow industrial reduced turbulence motors, the V/v limit can reach 10 when the fuel is produced by a gas furnace or dry coke gasifier containing only carbon monoxide. In modern, high speed and enhanced turbulence traction motors, it reaches 6.5 for a fuel of octane number 80, 8 with alcohol premium grade fuels, and can exceed 10 when the fuel is pure alcohol.

In any event, whatever the progress made, the compression ratio of a gasoline engine is limited, because of the non-knocking condition, well below the values achievable in a diesel engine. As the internal efficiency η_i is a function of that ratio, the efficiency of gasoline engines is significantly lower than that of diesel engines. This condition has also limited the possibilities for use in gasoline engines of various provisions allowing the performance of internal combustion engines (supercharging, insulation of cylinder and piston walls etc.) to be improved.

13.4.2 Strengthening of turbulence

We have seen in section 7.6.1.2 of Part 2 that in the absence of significant turbulence, the deflagration speeds V_d are low, a few cm/s to few m/s. Given these values, one of the hardest problems in the development of fast gasoline engines, after ruling out the knocking, is to accelerate deflagration so that the combustion process takes place in a timely manner. It seems very difficult to solve if we compare the time required to travel the distance between the spark plug and the farthest point of the combustion chamber (at speed V_d), with the combustion duration time.

To fix ideas, consider an engine of 100 mm bore, running at 3,000 rpm. The flame has to travel a hundred millimeters to sweep the combustion chamber. With $V_d = 5$ m/s, very high value if the fluid is at rest, this corresponds to a lag of one-fiftieth of a second. However, at 3,000 rpm, it is precisely the duration of a complete revolution, and that corresponding to a 30° crank rotation (to which it would be desirable to limit the combustion duration) is twelve times lower.

To limit the ignition delay, a first arrangement, still used, is to practice some ignition advance, characterized by the angle A between the axis of the crank and that of the cylinder before TDC, when the spark occurs.

But the advance A should not exceed a certain value, beyond which the combustion becomes explosive (due to the expansion of gases already burned, the early combustion significantly increases the temperature of the unburned gas at the end of the compression phase, so as to exceed the autoignition limit). In addition, the spark advance has the serious defect to create a variable delay in inverse proportion of the engine speed, so that a given value of A is too large at low speed (engine knocks), and inadequate at high speed. We will deepen the study of the ignition advance in a later section (13.8.2) on combustion control.

In reality, it is by communicating high turbulence to the mix during combustion that we get to accelerate the deflagration speed in high speed motors. This is achieved by an appropriate arrangement of outlets of the intake valves in the chamber, so that gases enter the engine at high speed which is preserved during compression. The design of the combustion chamber is generally made so that the piston movement may generate the sought turbulence.

Note, however:

- that the turbulence has the defect of substantially increasing heat exchange coefficients and harmful wall actions, first heating during admission, which reduces the charge and the mean pressure, and also increasing heat losses during combustion and expansion;
- that it does not raise the lower richness limit (beyond which the combustion becomes impossible), quite the contrary;

- however, the variation of turbulence with speed plays in the desired direction and therefore has a self-regulating effect because it increases with speed, which automatically decreases the combustion duration.

We have seen that a second serious defect specific to gasoline engines is that it is impossible to control power, as would be most rational, by decreasing the amount of fuel. To reduce it, we use more or less defective means, e.g. in traction motors, creating a throttling at admission (by closing the throttle) which lowers the efficiency a lot.

Overall, the efficiency of gasoline engines drops thus quickly when the load decreases and the idling consumption is high. This point was developed in section 13.3.2.

13.4.3 Formation of fuel mix, fuel injection electronic systems

In a spark-ignition engine, the fuel mixture formation can take various forms depending on the fuel and the technique used.

When the fuel is gaseous mixture, formation presents no difficulty. The mixer must simply be located at a sufficient distance from the intake valves, and adjusting richness can be easily carried out by a valve controlling the gas flow.

It is much more difficult to obtain a homogeneous mixture in gasoline engines burning a volatile liquid fuel. The conventional method for forming the mixture is to use a carburetor consisting essentially of a float chamber feeding a jet, which injects the fuel sprayed into the admitted air stream in a throttling of the vein (Figure 13.4.1).

In modern gasoline engines, however, electronic fuel injection is increasingly used, this mainly to better regulate the combustion by controlling very precisely the amount of fuel injected. This carburization mode is particularly imperative when using catalytic converters, which require that richness be held in a very narrow range around stoichiometry. This is discussed in section 13.8.

13.4.3.1 Carburetors

The sketch of a conventional carburetor is given in Figure 13.4.1. Calling ρ_a the density of air, ρ_c that of fuel (gasoline), s the section of the jet, S that of the diffuser throat, P the pressure at the throat of the diffuser, P_a the atmospheric pressure (at which is the float chamber), h the height

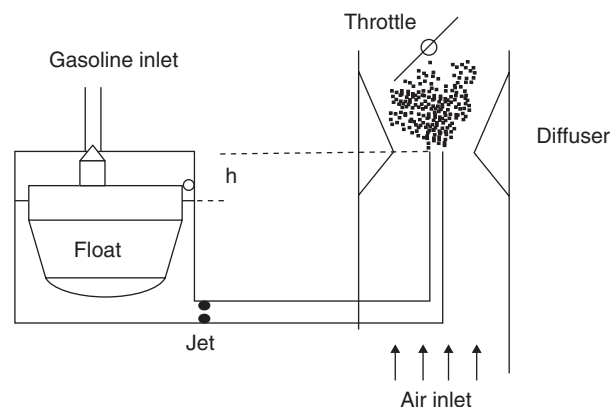
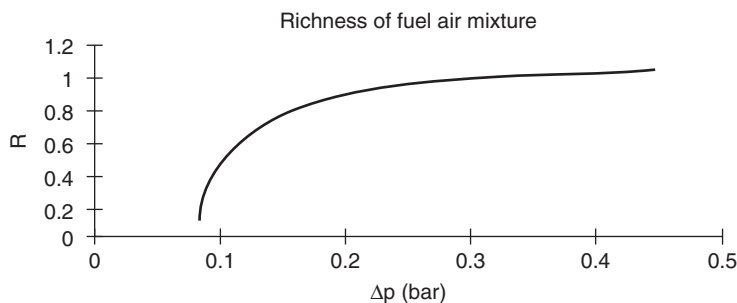


FIGURE 13.4.1

Sketch of a carburetor

**FIGURE 13.4.2**

Richness of fuel air mixture

difference between the jet throat and the constant level tank, we can calculate the velocity at the diffuser throat for air and gasoline:

$$C_a = k \sqrt{\frac{P_a - P}{\rho_a}} \quad \text{for air} \quad C_c = k' \sqrt{\frac{P_a - P - h\rho_c}{\rho_c}} \quad \text{for gasoline}$$

The ratio $SC_c\rho_c/SC_a\rho_a$ of the mass flow of gasoline to that of air, equal to the ratio R/AFR , air fuel ratio, is proportional to richness R . We have thus:

$$R = K \frac{s}{S} \sqrt{\frac{\rho_c}{\rho_a}} \sqrt{1 - \frac{h\rho_c}{P_a - P}} \quad (13.4.1)$$

This relationship does not include viscosity terms. It shows that the fuel mixture richness has the appearance of Figure 13.4.2.

It reveals two improvements to be made to the carburetor considered:

- for richness not to fall below a minimum value R_0 , there must be a special jet, called idling, which goes into action as soon as $\Delta P = P_a - P$ falls below a limit value;
- the richness law shows the impossibility of having R constant when $(P_a - P)$ varies. It is therefore necessary to correct it by introducing an “automaticity jet”, to modulate the amount of air injected as a function of depression.

Moreover, carburetors have a cold starting device (choke) and an accelerator pump, designed to respond quickly to sudden power demand by mechanically injecting a greater amount of gasoline.

Finally, it is only possible to obtain a homogeneous mixture if air is warm enough, and fuel volatile enough for it to be fully and rapidly vaporized at the outlet of the carburetor, at the expense of air sensible heat. The prerequisite for this is very easily found, if we assume that Dalton’s law applies to the mixture of air and fuel vapor, which is almost always the case given the low partial pressure of fuel vapor in the mixture.

Let x be the number of moles of fuel per air mole, C_{pm} and C_{lm} the respective molar heats of air and liquid, $L_m(T)$ and $P_s(T)$ the fuel molar latent heat of vaporization and saturation pressure.

For the fuel to be completely vaporized in the air, without heat addition, it is necessary that the partial pressure of fuel vapor $P_c = x \cdot P_a$ is below the saturation pressure at the final temperature of the mixture T_{fm} . Ultimately, the minimum final temperature is given by $P_c = P_s(T_{fm})$. The correspondent minimum air initial temperature T_{im} is obtained by writing the first law as follows: the enthalpy of one mole of air at T_{im} and x moles of liquid at T_0 is equal to the enthalpy of the mixture at T_{fm} . Dalton’s law being valid, the change in enthalpy of the mixture (equal to zero, the process being adiabatic and the walls fixed) is equal to the sum of changes in enthalpies of the constituents, the liquid being vaporized at T_{fm} .

These variations are equal to:

- for air $C_{pm}(T_{fm} - T_{im})$
- for the fuel $x(L_m(T_{fm}) + C_{lm}(T_{fm} - T_0))$

We thus get:

$$T_{im} = T_{fm} + \frac{x}{C_{pm}}(L_m(T_{fm}) + C_{lm}(T_{fm} - T_0)) \quad (13.4.2)$$

For richness equal to 1, assuming $T_0 = 15^\circ\text{C}$, we find $T_{im} = 7^\circ\text{C}$ for hexane, 48°C for octane, and 122°C for ethyl alcohol. As a result, already in the case of octane, T_{im} is far beyond ambient temperature.

It is possible to preheat the air upstream of the carburetor, making it flow in a channel heated by exhaust gases. The method is used, but sparingly, as excessive heating is dangerous, and especially reduces the admitted charge (the volumetric efficiency decreases) and mean pressure.

Ultimately, in engines burning regular gasoline and *a fortiori* premium gasoline, the condition of adiabatic vaporization is not fully satisfied. But even when this condition is met, vaporization is far from immediate. Both due to the carburetor imperfections, which does not regularly distribute fuel into the air, and due to the vaporization delay, the pipe out of the carburetor includes liquid droplets in a more or less long distance. The liquid proportion increases rapidly when the air temperature drops below T_{im} .

13.4.3.2 Electronic fuel injection

The development of electronics and smart sensors capable of providing to a microprocessor real-time information on the instantaneous state of the engine made possible the realization of extremely sophisticated carburetion and ignition engine management systems, capable, for an acceptable cost, of controlling the engine operation and in particular to sharply reduce emissions of pollutants.

These systems have gradually replaced carburetors by fuel injection electronics, enabling more specific dosing than the former. Figure 13.4.3 shows an electric throttle device, and Figure 13.4.4 a cutaway of a high-pressure-injection arrangement, with the gasoline injector at the top of the cylinder head. We present these systems in more detail in section 13.8, after dealing with emissions of different pollutants.

Among the various advantages of injection near or into the cylinder, let us say by the way that it solves the problem of fuel vaporization, if properly adjusted to evenly distribute the liquid in the intake air. It can thus improve the homogeneity of the mixture and make it unnecessary to preheat the air, which increases the maximum charge and average pressure.

13.4.4 Real cycles of gasoline engines

13.4.4.1 Differences between theoretical and real cycles

Real cycles deviate significantly from theoretical cycles presented in section 13.2, for several reasons:

- the working fluid is not a perfect gas. In reality, there are two fluids of different chemical compositions (Figure 13.4.5): the air/fuel mix during the compression phase, and the mixture of combustion products during the expansion phase. To increase the accuracy of calculations, we should at least adopt the assumption of ideal gas behavior and calculate the thermodynamic properties of working fluid based on Dalton's law taking account of specific heat changes with temperature;
- at the very high temperatures reached in the Beau de Rochas cycle, molecular dissociation plays a role. Under these conditions, state 2 can be rigorously determined only by combined iterations on the temperature and composition of combustion products.



FIGURE 13.4.3
Electric throttle device, Photo: Bosch.



FIGURE 13.4.4
High-pressure-injection arrangement, Photo: Bosch.

Figure 13.4.6 shows that the effect of molecular dissociation is to significantly lower peak pressure reached in the theoretical cycle, and in turn increase the pressure at point 3 because of molecular recombinations that occur during expansion.

Molecular dissociation has also the effect of slightly lowering the internal efficiency of the cycle, with a particularly noticeable effect when the combustion temperature is very high, i.e. for a richness close to 1, or an excess air close to 0.

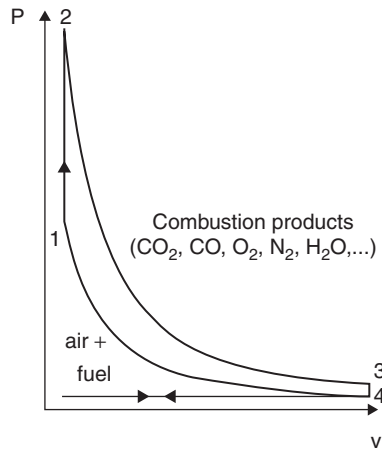


FIGURE 13.4.5
Beau de Rochas cycle

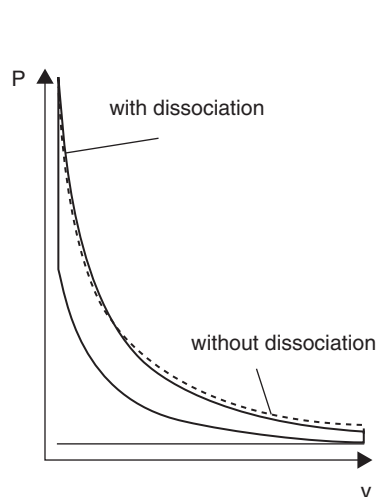


FIGURE 13.4.6
Influence of dissociation

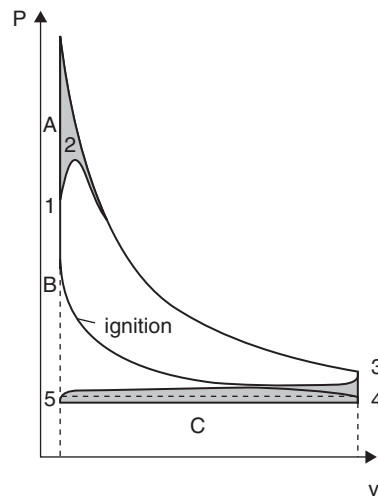


FIGURE 13.4.7
Theoretical and real cycle

Among other causes of cycle deformation, we can mention:

- pumping power, or fraction of the power consumed internally to ensure the renewal of the charge (pressure drop at fresh gas admission and burned gas exhaust);
- the $P(v)$ law during combustion, which is not strictly comparable to a isochoric followed by isobaric, as assumed in the mixed cycle;
- wall actions that make compression and expansion not strictly follow the isentropic law.

These three causes make that the indicator diagram of an engine on a bench take the form shown in Figure 13.4.7.

In gasoline engines, since combustion is not instantaneous, it is necessary to trigger the ignition before the piston reaches TDC. This is called ignition advance, which we seek to optimize so that the decrease of the diagram area be as small as possible (areas A and B in gray in Figure 13.4.7).

The pressure drop across the inlet and outlet valves induces a pumping power corresponding to a negative area in the diagram (shaded area C). To minimize the drawbacks of these losses, valves

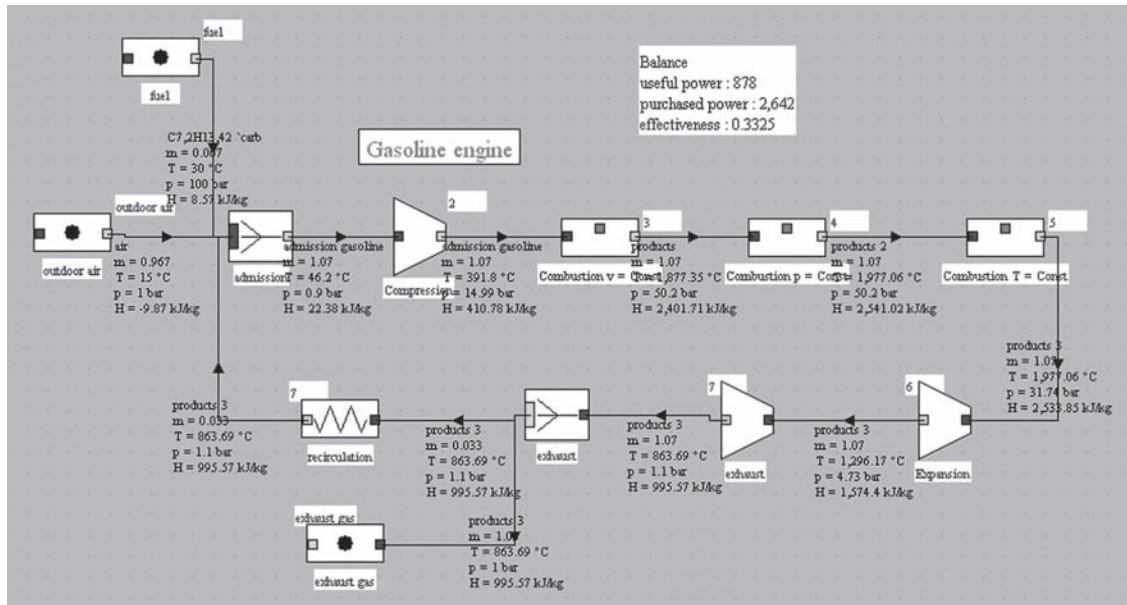


FIGURE 13.4.8

Synoptic view of a gasoline engine

slightly overlap, that is to say exhaust valves are opened before the piston reaches the BDC, and admission valves closed after it has crossed the BDC.

Finally, the cylinder walls play a thermal shunt role between the upper and lower parts of the diagram, and distort isentropes (2-3) and (4-1), reducing the effective area of the diagram.

Moreover, the overall efficiency drops due to the partial filling of the cylinder during the intake phase, and this because of three main reasons: the residual presence of smoke, the warming of the charge in contact with hot surfaces, and admission pressure drop.

In practice, unless one uses very sophisticated two- or three-dimensional models, which require in particular to provide combustion laws taking into account the flame propagation and walls losses, one can hardly make calculations beyond the consideration of changes in the chemical composition of the working fluid and dissociation as suggested in (Thelliez, 1989) (see section 13.2.4). To go from internal theoretical efficiency thus defined to the actual cycle efficiency, we must introduce an empirical correction, the shape efficiency, the ratio of the actual efficiency to the cycle theoretical efficiency.

Figure 13.4.8 shows the results provided by a gasoline engine Thermoptim model with a theoretical associated cycle of the type introduced in section 13.2.4. This model, presented in detail in the Diapason session S39En², is far from precise, but it takes realistically into account the combustion of the fuel mixture, as well as changes in the specific heat capacity depending on the composition of the working fluid and temperature. It calls for a few comments:

- the fuel mixture is prepared here once and for all in the “admission” mixer, whose upstream branches are ambient air, fuel and a fraction of recirculated gas coming from the dead space that still exists in the cylinder (3.3% by mass);
- the fuel mixture combustion is calculated by checking the option “pre-mixed” in combustion Thermoptim screens (Figure 13.4.9);
- it occurs in three phases, as proposed by M. Thelliez (1989) (section 13.2.4), gas composition in the cylinder varying accordingly;
- expansion occurs in two steps: in closed system between points 5 and 6, then open system from 6 to 7 in valves and exhaust pipes.

² <http://www.thermoptim.org/sections/enseignement/cours-en-ligne/seances-diapason/session-s39en-exercice>

fuel

pre-mixed

dissociation

dissociation degree: 0.07

quenching temp. (°C): 1,500

combustion eff.: 0.97434

chamber efficiency: 0.81

ksi: 0.742

T (°C): 1,877.3491065711

Calculate T

set pressure

set volume

set temperature

by the inlet point

by the user

FIGURE 13.4.9

Combustion settings

13.4.4.2 Abnormal combustion

Combustion in engines may have various abnormalities, such as knocking, pre-ignition and re-ignition.

Knocking is caused by an explosion that causes a sudden pressure increase in the cylinders. At low speed, it appears that knocking is related to the RON, and at high-speed to the MON supplemented by a term characteristic of the olefin content and cracking mode used for refining.

Pre-ignition is self-ignition caused by a hot spot in the cylinder, which can be formed by the electrodes of the spark plug if they are too insulated. Hot spots, however, generally result from deposits formed on the cylinder head or piston during combustion. When these deposits stem from the ashes of the engine oil (low fuse barium and calcium salts), they can cause more than 1,000°C hot spots and degenerate into a knock of catastrophic consequences for the engine (piston melting).

Re-ignition is characterized by an ability of the engine to run when the ignition is off. It is a low temperature self-ignition mainly due to the RON.

13.4.4.3 Performance of gasoline engines

The effective thermal efficiency of gasoline engines is lowered relative to the theoretical efficiency by two main causes:

- First, waste heat, as a result of incomplete combustion as well as wall losses, reduces the power output;
- Secondly, mechanical losses absorb a fraction of the work which is variable but never less than 12% and much higher in small capacity engines.

Efficiency losses vary widely from one engine to another. Loss by incomplete combustion is much more important in liquid fuel engines than in those that use a gaseous fuel, due to incomplete vaporization problems mentioned above. Losses ranging between 5 to 20% may exist, according to operating conditions.

Wall losses are even higher than the dimensions and the piston reduced linear velocity are small. As a guide, the cooling water discharges generally between 25 and 33% of the heating value of fuel.

Under these conditions, the actual efficiency of gasoline engines never exceeds 32%, falling to about 25% in average capacity traction gasoline motors.

13.5 DIESEL ENGINES

In a diesel engine, liquid fuel is injected at the end of compression in a combustion chamber filled with clean air, and should immediately burn afterwards. This characteristic has two important consequences:

- the absolute necessity of self-ignition: indeed, a spark would likely be ineffective in bursting in air, and, moreover, the mixture in the chamber being not homogeneous, the conditions of combustion propagation would be very bad;
- the need for high excess air, due to the heterogeneity of the mixture: introduced at the last moment, and therefore poorly distributed, the fuel must have enough oxidizer.

13.5.1 Compression ignition conditions

In a diesel engine, air temperature at the time of injection, i.e. at the end of compression, depends essentially on the compression ratio $\rho = V/v$ and incidentally on air temperature T_0 and wall actions, these consisting of heating during the admission and start of compression and cooling at the end of compression. These effects roughly offset each other in a cooled wall chamber and air temperature at the time of injection differs little from what would give an isentropic compression.

As this temperature is an increasing function of V/v , the need for self-ignition has the effect of setting a lower compression ratio limit, the opposite of what happens in gasoline engines, where the non-knocking condition sets an upper limit to this ratio.

As to the practical limit of V/v for a particular fuel for proper combustion in all cases, care must be taken that an adequate margin of safety exists, as self-ignition must occur under the worst conditions, i.e. as low as the outside temperature at start might be (the walls being cold), and secondly be frank enough to allow combustion even at maximum speed. The lower limits of V/v are thus dependent on engine speed, and are significantly higher in high-speed motors than in slow engines. In the latter, the limit V/v can be lowered to 13 for fuels easy to ignite (light distillates), reaches 14 for medium fuel oil, and up to 15 and even 16 for very heavy and slightly hydrogenated oils.

Note that these values significantly exceed those of most gasoline engines, even burning low explosive fuels. Similarly, pressure at the end of compression is much higher in diesel engines: it can exceed 50 bar. Under these conditions, to avoid overloading the joints, one tries to minimize the pressure at the end of combustion by strictly controlling it. The question presents itself very differently in slow and fast engines.

13.5.2 Ignition and combustion delays

We saw in section 7.6.3.1 of Part 2 that the overall ignition and combustion delay is the order of several milliseconds. In slow diesel engines (marine engines running between 80 and 250 rpm), it is very small compared to the cycle duration, and in this case, there is no particular difficulty in controlling the combustion: injection can be adjusted so that the pressure does not exceed 10–20% of P_2 , and we are very close to a constant pressure combustion.

The situation is quite different in high speed diesel engines, where speeds exceed 3,000 rpm. The duration of one revolution is then less than 20 milliseconds, and that corresponding to a rotation of 30° , in which it would be desirable to confine the combustion is less than 1.7 milliseconds. Without special precautions, it becomes much less than the overall ignition and combustion delay. It becomes very difficult to produce combustion on time while controlling the pressure. If, for compensating ignition delay, injection is triggered too early before TDC, there is a serious risk: the fuel vaporizing

partially in the air before catching fire, forms a combustible gas mixture that can detonate when combustion starts. Combustion is extremely brutal, engine joints deteriorate rapidly, and furthermore, the decomposition of explosive molecules of fuel produces black smoke that fouls the engine.

It is therefore essential in high speed diesel engines to reduce to an absolute minimum the ignition delay. A first step in this direction is to burn in these engines only fuel with self-ignition temperature and ignition delay as small as possible.

From this point of view fuels are classified by testing them in an experimental engine operating with a given V/v , at a given speed. The ignition delay is measured on a pressure-time diagram. The point where injection starts is known from the timing of the fuel pump and the point where combustion starts is characterized by a very definite change of slope on the curve. We can thus establish an intrinsic characterization of fuels following the cetane number (cetane number of diesel fuel is the cetane (a highly flammable hydrocarbon) fraction of a mixture of cetane and mesitylene (a low flammable hydrocarbon), which has the same ignition delay as the fuel processed).

In practice, high speed diesel engines burn almost exclusively light distillates, which is, in the range of products of petroleum distillation, the easiest fraction to ignite and burn in diesel. However, the specification of the cetane number for diesel is much less common than that of octane for gasoline, because, ultimately, the ignition delay depends mainly on structural arrangements adopted to accelerate ignition and combustion.

These provisions are very varied.

First, one generally takes for high speed diesel a V/v well above the limit: the latter is close to 13 in slow engines and, in high speed diesel, it commonly reaches 16 and sometimes 18 or even 20.

A second method, widely used, is to produce injection, or derive a fraction of it, in a part of the combustion chamber called the auxiliary chamber, whose walls are systematically poorly cooled. This is called a divided chamber. The auxiliary chamber is connected to the rest of the combustion chamber through a narrow opening. The air that is expelled during compression is heated by the action of the walls and throttled through the orifice, and is thus heated to a higher temperature than the rest of the chamber. In addition a high turbulence reigns, and, conversely, the expulsion of burnt gases from the auxiliary chamber during combustion and the beginning of expansion creates a significant turbulence in the rest of the combustion chamber. These progressive combustion conditions have another interest: that of reducing the combustion noise, which can be quite high in a direct injection chamber, as ignition occurs abruptly when the self-ignition conditions (temperature and delay) are met.

The method has two variants:

- in **prechamber engines** (Figure 13.5.1), the injector opens directly into the prechamber. The fuel burns very quickly and undergoes incomplete combustion, and then under the effect of pressure, incompletely burned gases are expelled at high speed into the main chamber, where combustion ends. An obstacle is placed in the path of the fuel jet to help divide and mix it with air. This type of chamber is quieter, but its efficiency is lower than others. Until recently, it was the type of configuration chosen for passenger cars for which comfort is an important criterion;
- in **swirl chamber engines** (Figure 13.5.2), geometry is optimized to minimize pressure drops (larger discharge section, tangential outlet in the main chamber), which improves efficiency, but at the price of a slightly higher combustion noise.

All these provisions are more or less in default at startup, the action of cold walls lowering the temperature. This is why some engines are equipped with electric heaters that heat up before starting (glow plugs) either a specific area of the chamber, or the air stream admitted.

It is obviously impossible to accurately analyze the effect of provisions as complex as those mentioned, and the development of high speed engines is the result of empirical trial and error. Nevertheless, despite the reduction in ignition delay, combustion is less well controlled in these engines than in slow engines. The pressure is much higher, so that maximum pressures of 70 and even 80 bar are reached.

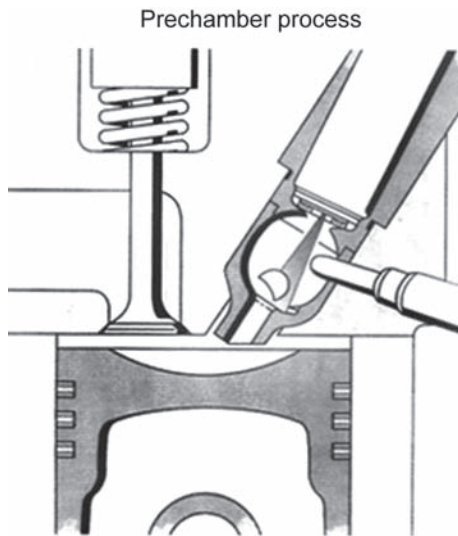


FIGURE 13.5.1
Prechamber, Extract from Bosch Technical Papers

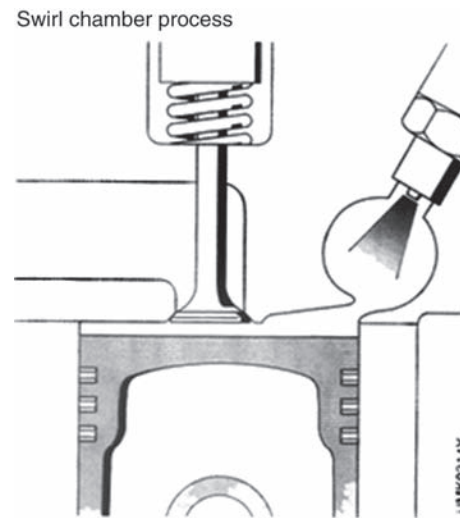


FIGURE 13.5.2
Auxiliary chamber, Extract from Bosch Technical Papers

In high-speed direct injection diesel engines, the piston and the chamber are simply designed so that a high turbulence is maintained during injection. Fuel must be mixed as homogeneously as possible without recourse to a prechamber, which induces particularly severe production constraints (Figure 13.5.3). The piston geometry is optimized to increase turbulence, and the injector is multi-hole. The efficiency of this type of engine is 20% higher than prechamber engines, but its noise is much higher because the combustion pressure is more difficult to control.

Due to the development of “Common Rail” injection systems allowing achievement of very fine control of the injection, and therefore better management of these pressures, direct injection is spreading today in many diesel engines, even small displacement ones. You should refer to section 13.9.1.2 for further developments on this subject.

13.5.3 Air utilization factor

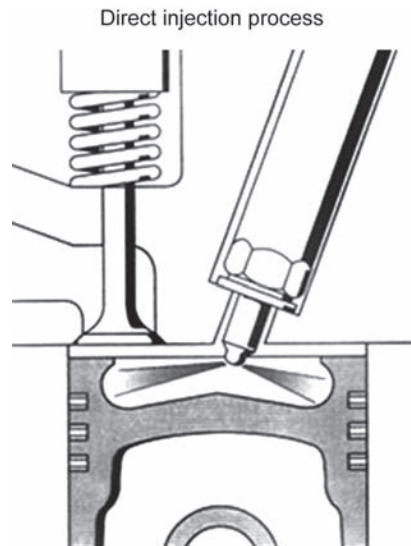
The injection of fuel at the last moment does not, as we have seen, allow it to spread evenly in the chamber, so as to fully utilize the air, and when the mass m of fuel exceeds a certain value m_m always substantially less than the mass m_{max} that could burn the air admitted, the combustion is incomplete, and the engine produces black smoke and fouls.

A key objective of diesel, whether slow or high speed, is to raise as much as possible the ratio m_m/m_{max} , or maximum air utilization factor (note that this rate is equivalent to richness, but the term richness is for homogeneous mixtures). This is achieved by giving the jets the greatest possible penetration and increasing turbulence during combustion.

Currently, the air utilization factor drops to 40% in slow imperfect scavenging two-stroke engines, with opposite blowdown holes, rarely exceeds 60% in slow four-stroke engines without significant turbulence, and can reach 75 or even 80% in divided chamber engines.

If the air utilization factor cannot exceed a certain value, it can be as small as desired. In contrast to what happens in a gasoline engine the mass of fuel injected can be reduced near zero in a diesel, and the operation remains perfectly regular. The adjustment of diesel is thus always done by varying m , and is much more economical than that of gasoline engines.

The result is that diesel is better suited than gasoline engine for operation at reduced load, and its average efficiency is closer to maximum efficiency.

**FIGURE 13.5.3**

Direct injection, Extract from Bosch Technical Papers

13.5.4 Thermal and mechanical fatigue

If the theoretical thermal efficiency of diesel is much better than that of a gasoline engine, this advantage has a counterpart: the diesel organs are subjected to exceptionally high thermal and mechanical fatigue, which complicates the construction and increases the costs.

With regard to mechanical fatigue, the normal maximum pressures are much higher in the case of diesel, but also the joints and the cylinder must be designed to withstand much higher occasional accidental pressures. Three phenomena may indeed generate significant overpressure:

- first, the excess air would burn a much more significant quantity of fuel;
- secondly, the peak pressure is limited, even in high speed motors, at a fraction of that produced by combustion at constant volume;
- finally, there may be unintended presence of an excess of fuel, resulting in a much more intense combustion which can lead, at constant volume, to a pressure three times the rated pressure.

It is almost impossible to prevent abnormal combustion from occurring accidentally, in the case of leakage of fuel during compression or massive movement of oil. The excess fuel introduced into the air vaporizes prematurely, and combustion is at constant volume, thus explosive. It is imperative that such events, so exceptional be they, do not lead to the engine destruction. Ultimately, the components of a diesel engine should be calculated with a wide safety margin, much higher than that required in a gasoline engine.

Thermal fatigue is also higher in diesel, in contrast to what the theory may indicate. Indeed, the theoretical calculation assumes the fuel is evenly distributed in excess air, and it leads to moderate combustion temperatures, substantially lower than those achieved in the gasoline engine. In reality, the fuel is concentrated in a fraction of the air where combustion takes place without appreciable excess air, and, in the flame jet coming out of the injector, the temperature is extremely high. As pressure and speed are also very high, the exchange coefficients are significant, thus subjecting the parts in contact with the jet to heat flux well above that given to the walls of a gasoline engine.

Finally, the proper functioning of a diesel engine requires very good maintenance, as an efficient self-ignition is compromised by a minimal sealing defect type roundness of the cylinder or ring rupture, which does not significantly disturb the operation of a gasoline engine.

For all these reasons, for a given speed and capacity, a diesel engine is much heavier and expensive than a gasoline engine and its maintenance costs are also higher. The increase in depreciation expense and maintenance offsets to some extent the reduction of fuel expenses.

13.5.5 Cooling of walls

There is an important difference between the cooling conditions of gasoline and diesel engines: whereas in the former case, all internal walls, as well as the cylinder of the combustion chamber, must be maintained at a moderate temperature to avoid self-ignition of the mixture by a hot spot, in diesel, only the side walls exposed to ring friction must be cooled.

The walls of the combustion chamber, the bottom of the piston and the cylinder head may be covered with a heat-resistant alloy and insulated from cooled parts. This method reduces wall losses and improves combustion. However, it increases the heating of the intake air.

13.5.6 Fuels burnt in diesel engines

Slow motors can burn the less volatile liquid fuels, heavy fuel oil, oil shale and tar, with the sole condition that these liquids are refined, that is to say are the result of distillation. The experience shows that a diesel powered by crude liquid fuel fouls faster or slower, because of tarry deposits erasing rings and requiring frequent complete revisions.

Attempts to burn in diesel pulverized solid fuel (lignite, coal) have been unsuccessful so far due to rather fast fouling of the engine, especially from abrasion caused by mineral ashes which mix with the lubricating oil.

You can burn in a diesel gaseous fuel compressed in advance at a pressure sufficient for injection, provided there is an auxiliary injection of liquid fuel to start the combustion (dual-fuel engines, cf. section 13.4.5.2).

Finally, we have seen that high speed diesels burn almost exclusively light distillates.

13.5.7 Real cycles of diesel engines

The origin of the differences between real cycle and theoretical cycle is almost the same for diesel as for gasoline engines. However, the effect of dissociation is less sensitive because of the presence of large excess air. Under these conditions, it can legitimately be neglected in almost all cases.

Figure 13.5.4 shows the results provided by a Thermoptim model of a diesel engine with an associated theoretical cycle of the type presented in section 13.2.4.

This model, presented in detail in the Diapason session S38En³, calls for some comments:

- The intake charge includes ambient air and a fraction of recirculated gas coming from the dead space that still exists in the cylinder (3.3% by mass). Its composition is determined in the “inlet” mixer;
- combustion takes place in three phases, as proposed by M. Thelliez (1989), the fuel being injected three times (section 13.2.4);
- expansion occurs in two steps: in closed system between points 5 and 6, then in open system from 6 to 7 in valves and exhaust pipes.

³ <http://www.thermoptim.org/sections/enseignement/cours-en-ligne/seances-diapason/session-s38en-exercice>

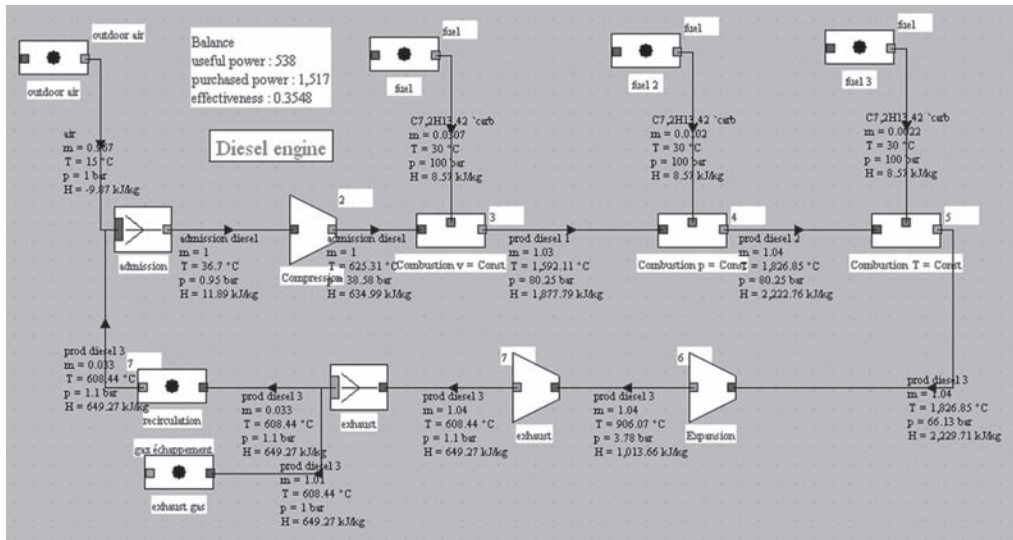


FIGURE 13.5.4

Synoptic view of a diesel engine

Design settings			
Max pressure	<input type="text" value="80.0000"/>	Compression ratio	<input type="text" value="14.0000"/>
Max temperature (°C)	<input type="text" value="1827.0000"/>	Capacity (l)	<input type="text" value="9.2000"/>
EGR ratio (%)	<input type="text" value="3.4000"/>	Rotation speed (rpm)	<input type="text" value="1500.0000"/>
Thermal losses (%)	<input type="text" value="19.0000"/>	Suralimentation ratio	<input type="text" value="1.0000"/>
lambda T Cste	<input type="text" value="12.0000"/>	Cooling flow rate	<input type="text" value="2.0000"/>

FIGURE 13.5.5

Diesel driver settings

WORKED EXAMPLE

Modeling of a Diesel engine cycle

This example shows how a Diesel engine cycle can realistically be modeled with Thermoptim. It is presented in the portal guidance pages (<http://www.thermoptim.org/sections/enseignement/cours-en-ligne/fiches-guides-td-projets/fiche-guide-fg20>).

Such a model is a little difficult to set, given its complexity. Once it is built, it is possible to develop an external driver class of the kind to be presented in section 23.7 of Part 4.

It is possible to define a driver for entering the main parameters characterizing the motor (Figure 13.5.5), such as peak pressure and temperature of the cycle, capacity and rotation speed, fraction of heat transferred to coolant, engine compression ratio, air/fuel ratio or supercharging.

The engine modeled above was characterized by a maximum pressure of 80 bar, a maximum temperature of $1,827^\circ\text{C}$, a gas recirculation rate of $0.033/0.967 = 3.4\%$, 19% losses, a compression ratio of 14, non-supercharged (see section 13.7), and we had set the flow of cooling water to 2 kg/s.

Simulation results		Calculate	
efficiency	0.38384	Intake flow rate	0.97928
useful energy	362.92412	combustion flow	0.02176
torque	2.31045	total flow	1.05609
purchased energy	945.52832	exhaust losses	351.31348
cooling energy	89.82519	pumping losses	6.40698
exhaust temperature	635.46817	Air/fuel ratio	22.50460

FIGURE 13.5.6

Diesel driver results

Its displacement was not specified, nor the rotation speed. Taking 1,500 rpm for the latter value, the displacement is about 9.2 l.

Once these values entered, the model is fully reparameterized and the corresponding solution can be sought, which leads to the results presented in Figure 13.5.6, where the values of flow rates and powers were divided by 2 to account for a number of thermodynamic cycles of a cylinder per unit time of 0.5, the engine being assumed to be 4-stroke.

The causes of efficiency reduction in diesel engines are similar to those outlined for gasoline engines: heat waste and mechanical losses.

However, the actual thermal efficiencies are well above those of gasoline engines. For non-turbocharged engines, they can reach 40% in good conditions, and they usually exceed 32% in the most adverse conditions (low-capacity engines, two-stroke engines with imperfect scavenging).

These results can be improved by supercharging, studied in section 13.7.

13.6 DESIGN OF RECIPROCATING ENGINES

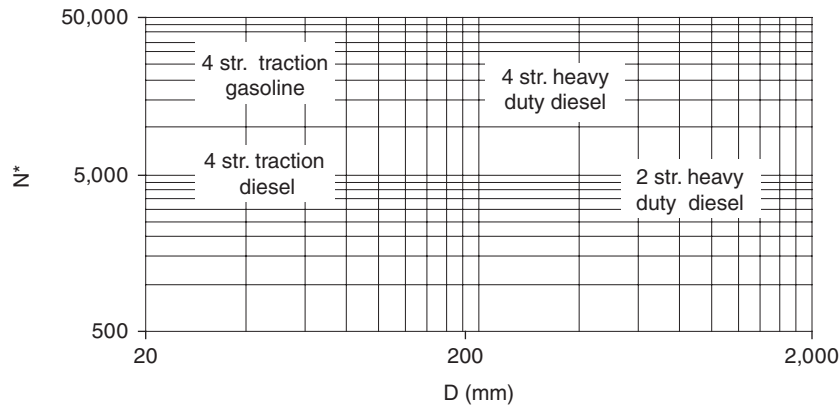
In section 13.3 we saw that the power provided by a given engine and the IMEP can be defined by relations (13.3.2) and (13.3.9), which are rewritten, showing the MEP:

$$P_e = \text{MEP} V_s \frac{N}{60} n_c i \quad (13.6.1)$$

$$\text{MEP} = \eta_m \eta_i C_r \frac{\text{LHV}}{\text{AFR}} R \frac{1}{v_a} \quad (13.6.2)$$

with the previous notations:

- η_i internal efficiency;
- η_m mechanical efficiency;
- C_r volumetric efficiency ;
- v_a specific volume of intake air;
- AFR stoichiometric air fuel ratio;
- R richness;
- (LHV) fuel heating value;

**FIGURE 13.6.1**

Reciprocating engine design chart

TABLE 13.6.1

Engine type	rated MEP (bar)	C _m (m/s)	L/D
Little traction engine	6–12	8–17	1–1.2
Heavy duty 4stroke	5.5–7	6–7	1–1
Same with supercharger	9–20	5–10	1–1
Heavy duty 2stroke	9–11	5–10	1.5–2

- n_c number of cylinders;
- N rotation speed;
- i number of cycles per revolution: 0.5 for a 4 stroke, 1 for a 2-stroke.

Moreover, $V_s = \frac{\pi D^2}{4} L$

D being the inside diameter of the cylinder (bore), L is the piston stroke.

If we introduce in (13.6.1) the elongation of the cylinder L/D and the average speed of the pistons $C_m = 2LN/60$, we get:

$$V_s = \frac{\pi}{4} \left(\frac{D}{L} \right)^2 60^3 \frac{C_m^3}{8N^3} \quad \text{and} \quad \frac{P_e}{n_c} = \frac{\pi}{32} \text{MEP} \left(\frac{L}{D} \right)^{-2} 60^2 \frac{C_m^3}{N^2} i \quad (13.6.3)$$

C_m and L/D are fundamental technology quantities in the design of an engine: C_m must not exceed a certain value (10 to 20 m/s) to minimize the inertial effects due to reciprocation of the piston and to reduce wear at the contact between the rings and the cylinder liner, while L/D must remain close to unity so that the shape of the chamber enhances combustion.

We thus arrive at a similarity law applicable to a wide range of designs:

$$N^* = \left(\frac{\pi}{32} \right)^{0.5} (\text{MEP})^{0.5} \left(\frac{L}{D} \right)^{-1} C_m^{1.5} i^{0.5} \quad (13.6.4)$$

with $N^* = (N/60) (P_e/n_c)^{0.5}$ standard speed cylinder, that is to say, related to the power unit in a cylinder.

Figure 13.6.1 gives an overview of the $N^* = f(D)$ range generally covered in various types of engines.

For an approximate design, we can use magnitudes given in Table 13.6.1.

13.7 SUPERCHARGING

13.7.1 General

Supercharging is to feed an engine at a pressure greater than atmospheric pressure, using an auxiliary compressor. Its main purpose is to increase the indicated mean effective pressure IMEP and thus reduce the overall size and weight of the engine.

Indeed, the engine capacity is roughly proportional to the mass flow of working fluid passing through it. In a piston engine, for a given speed of rotation, the volume flow is defined by geometry. To increase capacity, it is sufficient to reduce the specific volume of the working fluid, which is precisely what supercharging does.

In other words, to refer to the previous analysis, supercharging can increase the volumetric efficiency C_r to values greater than unity, when it is naturally limited to values between 0.8 and 0.9 (see section 13.3.3.1).

Originally, superchargers have been developed for aviation, to compensate the power loss in altitude due to the low air pressure. Since then supercharging has become very widespread, particularly in diesel engines, where it is often provided by a self-powered turbocharger driven by exhaust gases, such as those presented in Figures 13.7.1 and 13.7.2.

This supercharging mode has indeed many advantages: a turbine/compressor assembly is mounted between the intake and exhaust engine manifolds. The turbine (2 in Figure 13.7.1) and compressor (1) are coupled and form a completely independent system, mechanically unconnected with either the main engine, or with any receiver, so that on the one hand the turbine shaft work automatically balances the compressor work, and secondly the speed of the unit can be adjusted at will, independently of that of the engine.

13.7.2 Basic principles

In the final expansion phase, the exhaust valves are opened earlier than in a normally aspirated engine, and used to drive a turbine directly coupled to a, usually centrifugal, compressor placed

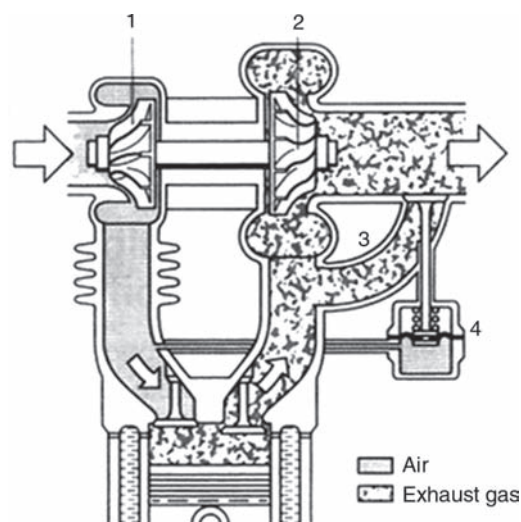


FIGURE 13.7.1

Turbocharger, Extract from Bosch Technical Papers

between the air filter and the intake manifold. An intercooler helps prevent potential gains due to the pressure rise are lost due to the increase of temperature.

The cycle is modified as shown in Figure 13.7.3. The engine work, equal to the net work, since the group is mechanically independent, is thus increased by work $(P_s - P_e)(v_s - v_1)$ produced during the intake and expansion strokes and the mean pressure is increased by $(P_s - P_e)$.

We call volumetric efficiency coefficient s the ratio of the specific volume of air at standard conditions (P_a, T_a) , to that of the air in the intake manifold v_s .

$$s = \frac{v_a}{v_s} = \frac{P_s T_a}{P_a T_s}$$

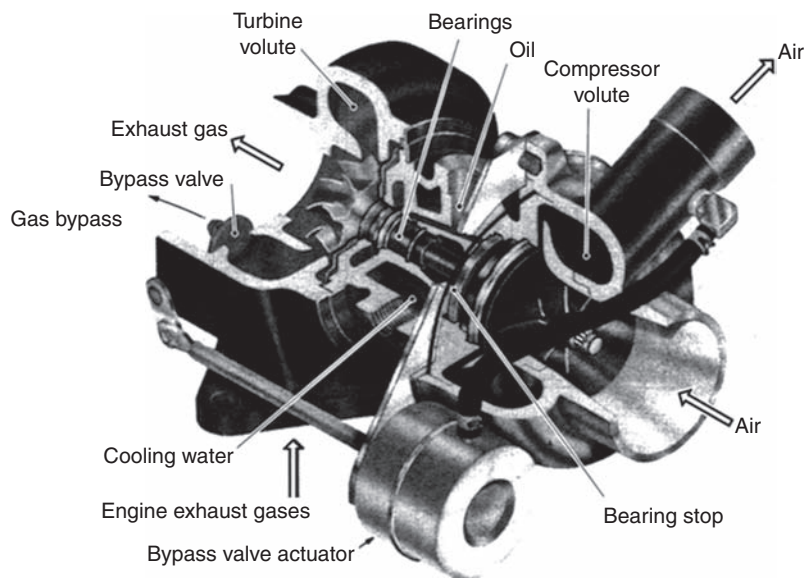


FIGURE 13.7.2

Cutaway of a turbocharger, Extract from *Techniques de l'Ingénieur, Génie Mécanique*

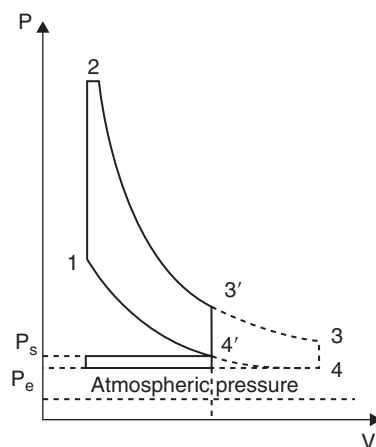


FIGURE 13.7.3

Supercharged cycle

If we assign an index 0 to the magnitudes relative to aspirated (not supercharged) engine, we obtain for the supercharged engine:

$$C_r = s C_{r0} \quad \text{IMEP} = s \text{IMEP}_0$$

The volumetric efficiency coefficient s is naturally less than the compression ratio achieved by the supercharger, especially if it does not include an intercooler.

For gasoline and diesel car engines, volumetric efficiency coefficients take values between 1.2 and 1.8 approximately. They exceed 2 for diesel truck engines and can reach up to 4 for heavy duty diesel engines greatly supercharged.

13.7.3 Conditions of autonomy of a turbocharger

For the turbocharger to run, it is obviously necessary that the power consumed by the compressor τ_c be equal to that delivered by the turbine τ_t . With assumptions and notations of section 12.1.4.2, we get:

$$\begin{aligned} \tau_c &= \frac{1}{\eta_c} \dot{m}_c c_{pa} T_a \left(\left(\frac{P_s}{P_a} \right)^{(\gamma_a - 1)/\gamma_a} - 1 \right) \\ \tau_t &= \eta_t \dot{m}_t c_{pg} T_g \left(1 - \left(\frac{P_a}{P_{et}} \right)^{(\gamma_g - 1)/\gamma_g} \right) \\ \tau_t &= \tau_c \\ \left(\frac{P_s}{P_a} \right)^{(\gamma_a - 1)/\gamma_a} - 1 &= \eta_c \eta_t \frac{\dot{m}_t c_{pg}}{\dot{m}_c c_{pa}} \theta \left(1 - \left(\frac{P_a}{P_{et}} \right)^{(\gamma_g - 1)/\gamma_g} \right) \end{aligned} \quad (13.7.1)$$

$\eta_c \eta_t$ is the overall efficiency of the turbocharger, generally about 0.4 to 0.5.

θ is the absolute temperature ratio between the turbine inlet and the compressor inlet.

Relationship (13.7.1) allows us to study the influence of the compressor inlet conditions and turbine outlet conditions on overall performance. For example, if the temperature of exhaust gas is 500°C, it is necessary to obtain a compression ratio close to 2.

In practice, we must also take into account interference phenomena that were not included in this succinct analysis, including:

- intake pressure drop (filter, tubing), about 0.15 bar;
- exhaust pressure drop (classic exhaust tubing \approx 0.3 bar, catalytic converter \approx 0.6 bar);
- pulsed flows in the intake manifolds and exhaust ports, linked to the valve opening frequency;
- inertial effects due to changes in engine speed.

13.7.4 Adaptation of the turbocharger

As the turbine/compressor assembly is totally independent of the engine, you can opt for machines running at high speed and therefore high efficiency. In addition, installation is very flexible and the compression ratio can be regulated in a wide range, as explained below.

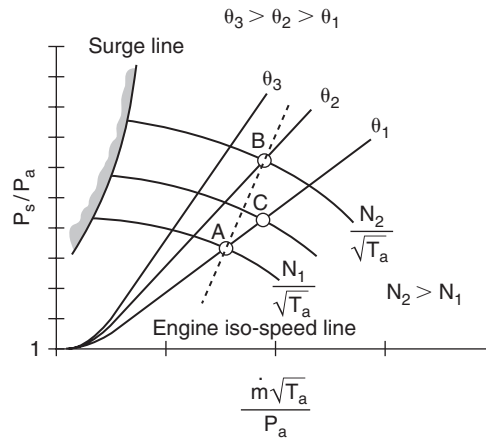


FIGURE 13.7.4

Characteristics of a turbocharger

The turbocharger looks like a gas generator of the type we studied section 12.1.6.2, where the combustion chamber is replaced by the engine. The study of the off-design operating regime, can, to a considerable extent, be based on analysis made in paragraph 12.1.6.1 for the single shaft gas turbine.

It is thus possible to obtain the complete characteristics of the turbocharger by superimposing those of the compressor and turbine (Figure 13.7.4).

At constant motor speed and variable load:

An increase in load results in increased fuel consumption and, correspondingly, of exhaust temperature T_{et} and intake air flow (at constant richness).

This results in an increase in θ and $\dot{m}_c \sqrt{T}/P_a$.

The operating point thus goes from A to B (dashed line on the graph in Figure 13.7.4), which results in an acceleration of the turbocharger rotation speed.

Under these conditions, the compression ratio increases, and thus the volumetric efficiency coefficient s . The turbocharger adapts naturally to the engine load, which is a very significant advantage and one of the major advantages of this device.

At variable motor speed, and constant load:

At constant load, we can consider as a first approximation that the exhaust gas temperature T_{et} remains constant. An increase in the rotation speed simply means an increase in the intake air flow-rate. θ remains constant, while $\dot{m}_c \sqrt{T}/P_a$ increases. The operating point moves from A to C along the turbine characteristic $\theta = \theta_1$.

Again, the compression ratio increases, and thus boosts the volumetric efficiency coefficient s , which has the effect of increasing the torque. At high speeds, therefore, the torque tends to increase, when it drops in a normally aspirated engine.

However, these considerations do not solve all the problems of turbocharger adaptation to changes in speed and engine load. Indeed, the contribution of the supercharger is so useful that the user wishes to dispose of it at low rpm ($N \approx 2,000$ rpm) so that the torque is more important, i.e. for a relatively low gas flow. Sized to function properly under these conditions, the turbocharger is too small for the gas flow at high speed. It is therefore necessary to provide either a bypass that diverts part of the exhaust gas flow, as shown in Figure 13.7.1 (3 and 4) or adjustable turbine blades (wastegate, blow-off valves).

13.7.5 Conclusions on supercharging

Supercharging significantly reduces specific losses of the main engine in relative value, so that the effective efficiency can be increased by almost 10%. Indeed, heat loss decreases, because the exchange coefficients grow more slowly than the density and mechanical losses are also lowered due to the reduction of the swept volume.

However, the main interest of supercharging often resides in reducing the cost associated with the increase of the mean pressure.

It is important to note that the benefits are lower for supercharged gasoline engines than for diesel engines, except particular application such as aviation or competition. Indeed, we saw that one of the most limiting constraints for these engines is the non-knocking condition, which sets an upper limit to the volumetric compression ratio. This condition is necessary in the supercharged gasoline engines, whose compression ratio must usually be reduced, which has the effect of lowering the internal efficiency of the engine. Supercharging can be justified only if power gain is imperative, for a given weight and size.

13.8 ENGINE AND POLLUTANT EMISSION CONTROL

13.8.1 Emissions of pollutants: Mechanisms involved

Pollution from automobile engines stems from incomplete burning. Indeed, if combustion was perfect, the exhaust would only include water vapor, carbon dioxide and nitrogen gas, completely innocuous vis-à-vis air pollution and health, except as regards the greenhouse effect. In this section we are mainly interested in gasoline engines, and we then give some indication on diesel engines.

Main gasoline engine pollutants are:

- carbon monoxide CO (1%);
- unburned hydrocarbons UHC (0.1 to 0.3%);
- nitrogen oxides NO_x (0.1 to 0.3%).

These three pollutants are harmful to health, and the last two are involved in the phenomena of acid rain. The accurate determination of emissions of pollutants can be approached only by the application of the law of mass action studied in section 7.6.1.4 of Part 2, taking into account the kinetics of combustion, but accurate calculations are limited because these assumptions are only very roughly verified in an engine cylinder. Studies show, however, that richness and its reverse air factor λ have a significant impact on emissions of various pollutants, as shown in Figure 13.8.1.

Emissions of carbon monoxide increase with richness, especially when its value exceeds 0.93, which also corresponds to the maximum emission of nitrogen oxides. The content of unburned hydrocarbons in turn passes through a minimum for a rather lean mixture ($R = 0.8$) and is growing quite substantially with richness when it exceeds 1.

Depending on the air factor, these evolutions obviously follow inverse laws.

To reduce emissions, you can:

- **limit the formation of pollution** during combustion. This solution had been retained until recently by European manufacturers, who had adopted it since the early 1970s, reducing about 60% the volume of specific emissions, achieving energy conservation and optimizing combustion. This solution has its limits, because it is impossible, due to dissociation, to achieve a perfect combustion;
- **destroy the pollution** caused by combustion before discharging the exhaust gases into the atmosphere. This is the route chosen first in the U.S. and Japan, and subsequently in Europe. This is

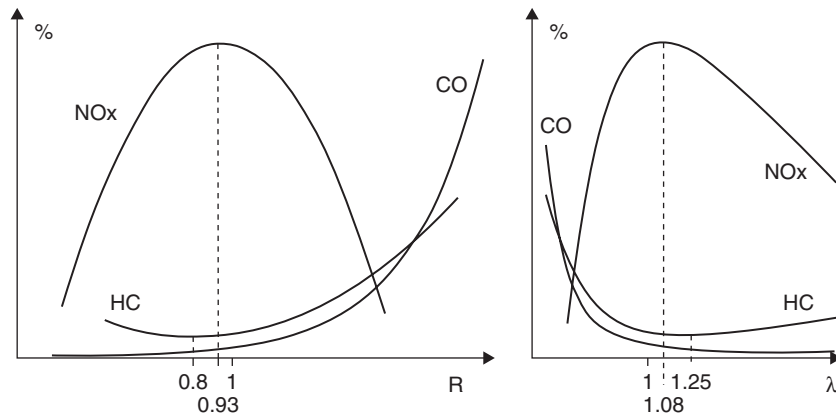


FIGURE 13.8.1

Gasoline engine pollutant emissions

done using a catalytic converter, i.e. a treatment system catalyzed by precious metals (platinum, palladium, rhodium) which is placed on the exhaust line, in order to destroy almost all pollutants. Today this is the most efficient way, but it is expensive and tends to increase by a few per cent (2–5) the engine consumption.

In addition, to be effective, catalytic converters forbid the use of leaded fuels. Catalysts are indeed “poisoned” by lead (as well as phosphorus). As lead is also in itself a pollutant with harmful effects on health, refiners have sought to develop lead-free fuels. Since this element had been introduced to increase the gasoline octane number, it was necessary to compensate the decrease of octane due to abandoned lead by additives and other treatments. To do this, refiners have had to step up new refinery processes, as addition of oxygenated organics (e.g. ethanol) is limited because of the need to vaporize the fuel (see section 13.4.3.1). The solution therefore requires a further refining of gasoline, which is an additional manufacturing cost varying from a few cents per liter for unleaded gasoline (MON 85/RON 95) to about 10 cents per liter for unleaded high octane number premium (MON 88/RON 98).

13.8.2 Combustion optimization

In order to reduce pollutant emissions and maximize fuel use, it is necessary to control combustion in the best possible way. This is achieved firstly by optimizing the engine design, partly by improving carburetion systems, and finally mastering ignition conditions at best.

13.8.2.1 Optimization of engine design

The engine design has a significant influence on its performance and the emission of pollutants: efficiency is an increasing function of the volumetric compression ratio, but it is the same for NOx emissions, since they depend directly on temperature in the combustion chamber. The geometry of the latter strongly influences the formation of unburned hydrocarbons, so manufacturers are moving to small compact surface chambers. The position and number of spark plugs or valves play a significant role on the quality of the ignition as well as pressure drop and turbulence in the chamber. Intake pipes, well sized, may allow a natural boost favorable for performance.

13.8.2.2 Changes in fuel systems

Tests on gasoline engines have shown they can develop a maximum power for a slight lack of air ($R \approx 1.15$ or $\lambda \approx 0.85$), and their maximum efficiency is obtained with a slight excess air ($R \approx 0.8$

or $\lambda \approx 1.2$). Moreover, the best idle is obtained for stoichiometric conditions ($R = \lambda = 1$), and a lack of air of 15 to 25% ($R \approx 1,25$ or $\lambda \approx 0.8$) is favorable for good acceleration.

It follows that there is no optimal value of richness or air factor that allows all user requirements to be met. In practice, values between 0.9 and 1.1 are generally accepted. To keep richness in a narrow range, it is necessary to determine with reasonable accuracy the amount of air sucked in, and mix the corresponding amount of fuel. Manufacturers have therefore initially focused their efforts on improving fuel systems depending on the engine load.

Until recently, the most popular fuel systems were carburetors. However there is now a clear trend in favor of fuel injection systems in the intake manifolds, a development that reflects the following reasons:

- injection allows very precise metering of fuel depending on load condition and engine speed, and therefore allows better control emissions of pollutants;
- injection can be performed in the immediate vicinity of valves, thus limiting the risk of fuel condensation on the intake manifolds. Moreover, if we use one injector per cylinder, we are certain to get a good distribution of the mixture;
- removing the carburetor, we can optimize air flow in the intake manifolds, which allows a better volumetric efficiency, and therefore improves the engine performance;
- finally, we solve with the required accuracy the various difficulties we have raised during the study on carburetors in section 13.4.3.1: providing fuel for acceleration, cold start, idling.

We will see later that the most efficient pollution control systems (multifunctional “three ways” catalytic converters) require that the air ratio be maintained within a very narrow range around 1, which only injection systems are capable of achieving.

13.8.2.3 Adaptation of the ignition

However, the best fuel system is not sufficient to ensure perfect combustion: it is also necessary to best fit the ignition point depending on the engine load and speed.

In section 13.4.2 we saw that, given combustion propagation delays in the chamber, it is necessary both to create turbulence, and secondly to cause the ignition before the piston reaches the top dead center TDC.

It is indeed fundamental that ignition is performed at a particular time (point Z_a , curve 1 in Figure 13.8.2), which varies with load and engine speed. If a spark is created too early (point Z_b , curve 2), there is a risk of knocking, the temperature at the end of compression being too high. If it

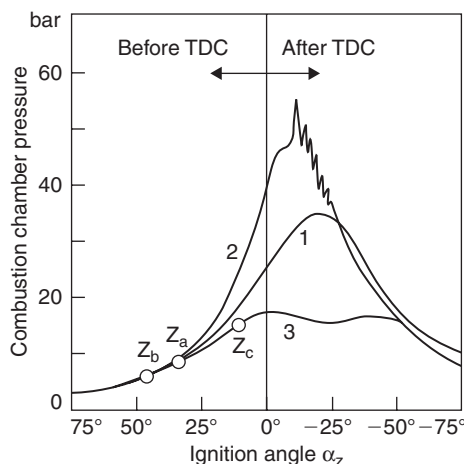


FIGURE 13.8.2

Pressure inside cylinder function of advance ignition, Extract from Bosch Technical Papers

is delayed (point Z_c , curve 3), the combustion begins only when the piston descends, and the cycle is highly truncated. In both cases, efficiency and engine power drop, and many disorders may appear, among which, in case of premature ignition, knocking, rapidly fatal to the engine. We characterize the ignition advance by the angle of the crankshaft from its position at TDC.

In a first approximation we can consider that the combustion delay varies little with load and engine speed for a given mixture richness. In fact, if the chamber design effectively promotes turbulence, these delays decrease as speed increases, but this variation is small compared to the crankshaft rotation speed.

It is therefore necessary to constantly adjust the ignition advance based on load and engine speed.

13.8.2.4 Engine control

Until recent years, the mechanical and vacuum advancement of the timing was the only way to modulate advance according to engine conditions. These mechanical systems used weights progressively deviating from the igniter rod under the action of centrifugal force, depending on engine speed. A further correction was made by a suction capsule connected to the intake manifold and controlled by pressure extraction on both sides of the throttle.

Although already very efficient, these mechanical devices could only generate advance correction curves of simple shape, like the one shown on the right side of the illustration in Figure 13.8.4. They were therefore unable to take into account finer ignition adjustments, in particular to reduce emissions of pollutants.

Indeed, the composition of exhaust gases, in particular the concentration of NO_x and unburned hydrocarbons, can be significantly influenced by the ignition advance angle, as shown by the curves of Figure 13.8.3.

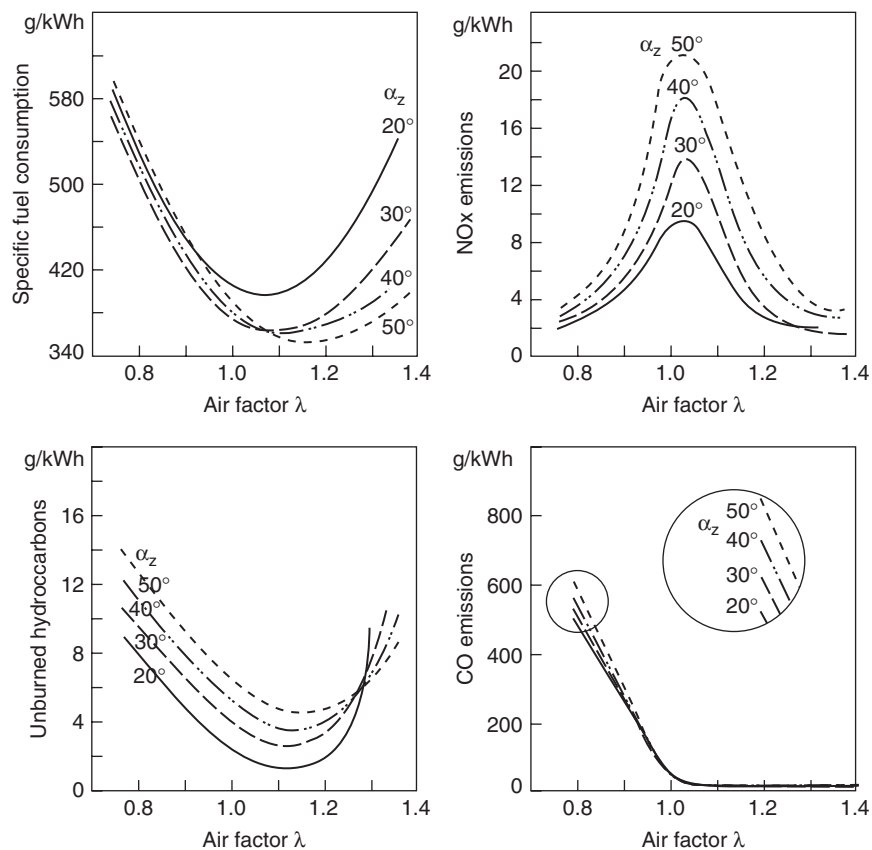


FIGURE 13.8.3

Influence of air factor and ignition angle α_z on emissions and specific consumption, Extract from Bosch Technical Papers

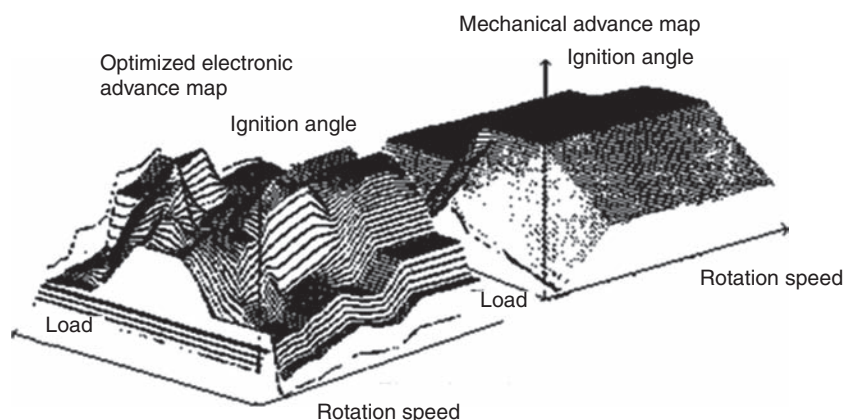


FIGURE 13.8.4

Mechanical and electronic combustion maps, Extract from Bosch Technical Papers

This shows that the optimum advance angle increases with air factor λ , due to the increased ignition delay due to fuel dilution. The NO_x concentration increases, as shown in equation (7.6.38) of Part 2, when $[\text{O}_2]$ increases and the temperature is high, then drops for high λ when the temperature decreases.

These curves also show the need to find a compromise between environmental constraints, which lead to choose low ignition advances, and specific fuel consumption, for which values a little higher are preferable.

To optimally control combustion, it is necessary to regulate the ignition advance by taking into account not only the load (the more it increases, the more the temperature of the exhaust gas rises, which allows afterburning in expansion and expulsion phases, with reduction of CO and unburned hydrocarbons but increased NO_x) and the engine speed (when the engine speed increases, friction increases, as well as pollutants) but also the temperatures of intake air, coolant and exhaust gas, as well as throttle position.

It is now possible to do this by using electronic ignition control, which uses a network of characteristics called ignition map, determined on a test bench and implemented on a microprocessor.

Figure 13.8.4 compares the fine mapping obtained with an electronic control compared to that provided by a mechanical drive.

13.8.3 Catalytic purification converters

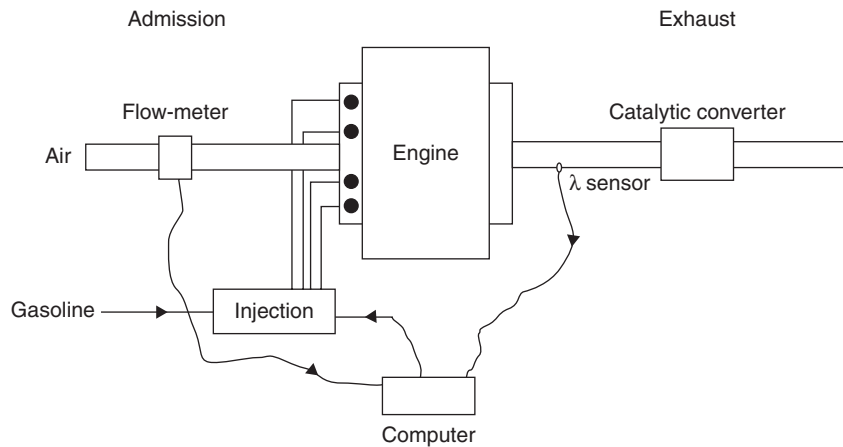
A catalytic converter comprises:

- the catalytic converter itself;
- auxiliary devices which should be added to a conventional engine to ensure proper operation of the process (e.g. electronic fuel injection for three-way converters, or injection of additional air for one way catalysis).

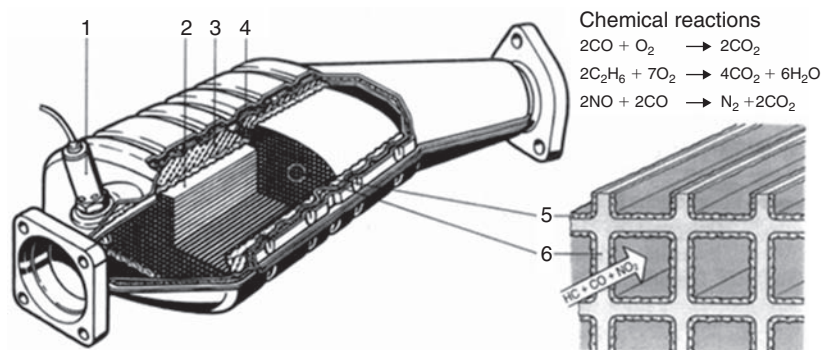
We distinguish now two techniques:

- simple oxidation catalysis (one way catalysis) that can act on CO and HC;
- multi-functional catalysis, more commonly known as three-way, that allows to act on CO, HC and NO_x by simultaneous chemical reactions of oxidation and reduction (Figures 13.8.5 and 13.8.6).

The catalytic converter, of size similar to that of a conventional exhaust line, is placed on the pipe near the engine in order to process hot exhaust gases.

**FIGURE 13.8.5**

Three-way catalytic conversion

**FIGURE 13.8.6**

Three-way catalytic converter, Extract from Bosch Technical Papers

It contains a catalyst which is in the form of a deposit of precious metals (1 to 3 g per converter) on a porous monolithic ceramic honeycomb, to develop a large surface area.

Catalytic converters are a very effective technique of remediation: over 90% of conversion in new condition when the engine and catalyst are warm.

The one-way catalysts require oxygen in the exhaust gases, which can be achieved by an air pump fitted to the vehicle. However, this technique does not require sophisticated carburetion or injection device. Being without action on the nitrogen oxides, the oxidation catalyst must be coupled to a device for reducing such pollution. This is achieved by recycling a fraction of exhaust gases to the admission.

With three-way catalyst converters, a perfectly balanced and uniform air fuel mixture must be ensured, which can now be performed by controlled electronic fuel injection. In fact, for achieving simultaneous removal of the three pollutants, the composition of exhaust gases should remain within a very narrow range.

Figure 13.8.6 shows the cutaway of a catalytic converter, with the oxygen sensor (1), the ceramic monolith (2), a flexible metallic grid (3), a jacketed heat insulation (4), a platinumium coating (5), and a ceramic or metal support (6).

This is only possible by controlling fuel injection by a sensor (the said Lambda sensor by reference to air ratio) that continuously doses the oxygen content of exhaust gases.

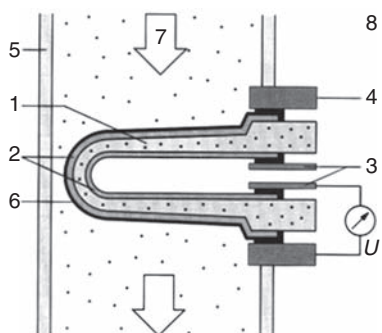


FIGURE 13.8.7
 Lambda sensor in exhaust line, Extract from Bosch Technical Papers

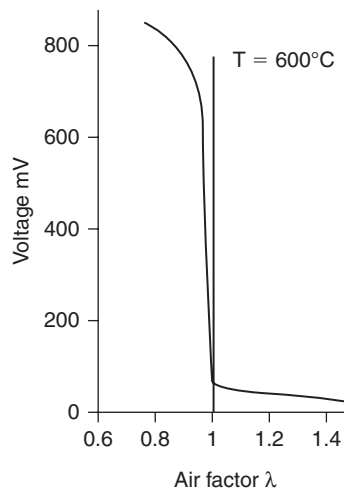


FIGURE 13.8.8
 Lambda sensor characteristic curve

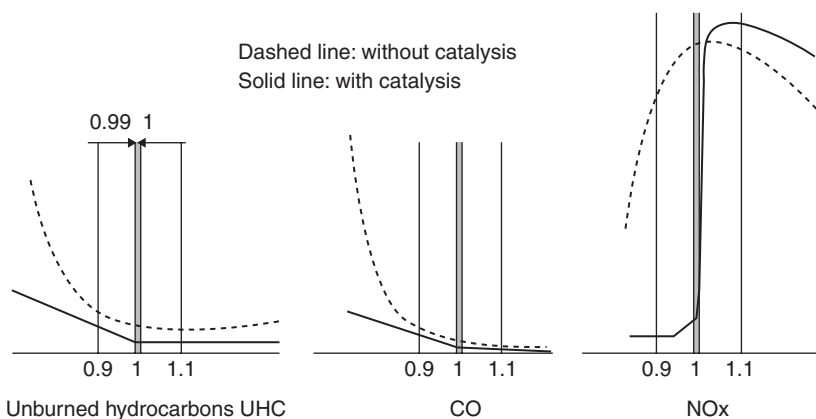


FIGURE 13.8.9
 Catalytic conversion effectiveness

This sensor consists of a body in solid electrolytic ZrO_2 material (porous ceramic, allowing diffusion of oxygen). As shown in Figure 13.8.8, the 2-point lambda sensor has a very steep voltage characteristic, to detect the value 1 of the air factor λ .

Figure 13.8.7 shows the configuration of tube-type lambda oxygen sensor in the exhaust pipe, with the special ceramic (1), the electrodes (2), the contact (3), the exhaust pipe (5), the porous protective layer ceramic (6), the exhaust gases (7) and air (8).

Several types of sensors are available: two-point sensors, possibly heated to better control their operating temperature and better reduce emissions, planar sensors, obtained by screen printing, which, using a special processing circuit, deliver a continuous measure of the air factor between 0.7 and 4, which allows for even finer control.

The effectiveness of catalysis is highlighted by the curves of Figure 13.8.9, which show, according to the air factor, the reductions in emissions of the various pollutants: it shows that if we want both to reduce NO_x emissions and HC and CO emissions, it is imperative that the value of λ stays within a very narrow band (between 0.99 and 1 for a conversion of 90% of pollutants).

This means a slight loss of engine efficiency relative to the optimum (obtained, as we have seen, for $\lambda \approx 1.2$).

This comes from the fact that we are pursuing two seemingly contradictory goals: on the one hand to reduce nitrogen oxides, which imposes work in the absence of oxygen, and also to further oxidize CO_2 and H_2O as well as the unburned hydrocarbons and carbon monoxide, which requires oxygen.

With the catalysts, it is possible to combine these different operations, but with the imperative of fully controlling the oxygen dosage, which can be done thanks to the Lambda sensor because of its very steep voltage characteristic for $\lambda = 1$.

If the value of λ falls below 0.99 or exceeds 1, the efficiency of catalytic converters falls rapidly: 65% for $\lambda = 0.98$ or 1.01, 40% for $\lambda = 0.97$ or 1.02.

It is for this reason that the use of a “three ways” catalytic converter can only be justified with a very precise control of fuel and combustion, that is to say with injection and electronic ignition control devices of the type we presented above.

Lambda control completes the control by ignition mapping, associating it with a closed loop on the oxygen content of exhaust gases. It is thus possible to further refine the settings for the engine by maintaining λ in the desired [0.99 – 1] band. However, the Lambda sensor gives a reliable signal only above a temperature of about 350°C. At startup, therefore, the lambda control is inoperative and the controller must operate in open loop.

The cost of the sole catalytic converter is about 400 Euros, which represents roughly half the total cost of a complete system including the adaptation of the motor supply (injection, λ probe).

13.8.4 Case of diesel engines

In a diesel engine pollution problems occur slightly differently. Indeed, because of the large excess air, complete combustion is more easily achieved, provided that the conditions of penetration of the fuel jet do not favor the formation of CO and soot, as a result of local oxygen deficit (the presence of inert gases – or excess air – reduces the partial pressures of the constituents, and therefore increases the degree of reaction).

In principle, CO and soot are normally oxidized during the main phase of combustion and even during expansion. However, sometimes adverse conditions prevent this combustion from taking place, leading to pollution of exhaust gases by the excess soot, which then forms an opaque cloud characteristic of diesel engines incorrectly set: one speaks of particulate emissions.

13.8.4.1 Emissions of gaseous pollutants

For the rest, the gas pollution problems occur similarly in diesel and gasoline engines. However, due to excess air, emissions of carbon monoxide and unburned hydrocarbons are reduced, and the lower combustion temperature limits those of nitrogen oxides. Without after-treatment, these emissions are somewhat lower than in a gasoline engine.

The essential problem is that the three-way catalytic converters cannot be used because of the value of lambda. There is also the specific problem of sulfur dioxide, which must be removed at the refinery.

A compromise must again be made between performance and emissions of pollutants. This is particularly the case when one seeks to limit nitrogen oxides, whose formation is favored (compared to gasoline engines) by the presence of excess air. Maximum power and efficiency are obtained by using injection advance, that is to say, by injecting the fuel before the piston reaches the TDC, to account for the ignition delay (of the order of 2 milliseconds) and ensure that the combustion actually starts at about the end of compression.

By renouncing this injection advance, we greatly limit the levels of pressure and temperature in the cylinder during combustion, thereby significantly reducing the formation of nitrogen oxides, but at the cost of a deterioration of efficiency and power.

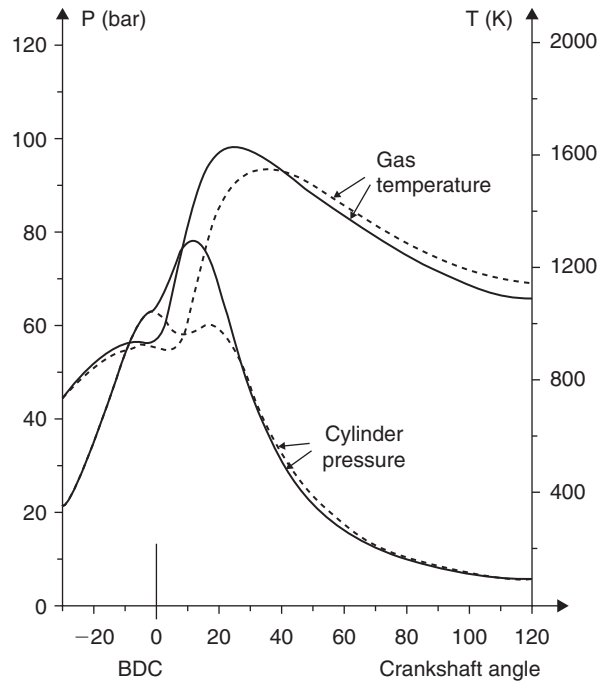


FIGURE 13.8.10

Pressure in diesel cylinder, Extract from *Techniques de l'Ingénieur, Traité Mécanique et chaleur*

Figure 13.8.10 shows the shape of changes in temperatures and pressures for a heavy-duty engine set:

- in the first case (solid lines) with a slight injection advance, which leads to a MEP of 9.5 bar, a specific consumption of 220 g/kWh and a NO_x concentration of 1,000 ppm;
- in the second case (dashed curves) without injection advance (MEP of 8.9 bar, specific consumption of 235 g/kWh, NO_x concentration of 600 ppm).

NO_x emissions reduction is remarkable (40%), but it comes at the cost of almost 7% over-consumption.

13.8.4.2 Particulate emissions

The particles emitted by diesel engines are mainly soot (carbon), and to a lesser extent, hydrocarbons and aerosols from fuel, lubricant or sulfates.

Chemically, they are often unpleasant odorous aldehydes that could harm human health due to the presence of aromatic compounds. Their small size (diameter of one micron) allows them to remain suspended in the atmosphere, generating white, blue or black smoke characteristic of the exhaust gas of a diesel engine incorrectly set.

To convert these particles, the most effective solution today is to use a particulate filter that ensures separation of exhaust gases and their subsequent removal. It is possible, due to excess air in the gas, to further oxidize CO, HC and particulates, but NO_x treatment involves the use of a specific device. One can for example use the SCR process (Selective Catalytic Reduction), where an aqueous solution of urea is sprayed on the gas, which is transformed into ammonia by hydrolysis, and subsequently reduces nitrogen oxides.

Particulate filters are generally made of extruded ceramics shaped as honeycomb, filled alternately with plugs, to force gas through the material. Self-cleaning filter is provided by the combustion of soot, which takes place if temperature exceeds 550°C. To avoid clogging, additives allow this limit to be lowered to 200–250°C.

13.9 TECHNOLOGICAL PROSPECTS

For the future, two trends may be identified: firstly the further improvement of performance of each type of engines we have considered, with particular emphasis on the limitation of their environmental impact, and secondly their integration in more integrated complex systems, such as combined cycle or cogeneration units.

13.9.1 Traction engines

Progress in traction engines will be fostered by standards set by national regulations concerning maximum limits of pollutant discharges for vehicles. This is a set of more and more stringent standards which apply to new vehicles. In Europe, stages currently considered for light passenger and commercial vehicles are Euro 5 (2008) and Euro 6 (2014).

13.9.1.1 Direct gasoline injection

Similar to developments made for diesel, direct injection is being developed for gasoline engines, two technologies being in competition: lean-burn and stratified charge, such as those developed in Japan since 1997 by Mitsubishi and Toyota, and high stoichiometric exhaust gas recirculation (EGR, Figure 13.9.1), which correspond to the choice made by Renault, the first models equipping the Mégane since 1999.

The goal here is not only to optimize the nominal performance of the engine, but also to reduce losses at low speed due to pumping and arising from the impossibility, in a conventional gasoline engine, to ensure complete stable combustion below the flammability threshold of the fuel mixture (air/fuel ratio close to 22/1, while the stoichiometry is achieved for 14.6/1). The idea is to circumvent this difficulty by achieving, thanks to the injector, a heterogeneous mixture in the chamber, but of suitable composition near the spark plug, so that combustion may then spread to the rest of the chamber.

Undoubtedly, the Japanese technology leads to the most important efficiency gains: 30–40% reduction in consumption at low speed, 25% on Japanese test cycles, whereas the stoichiometric direct injection does not exceed 15–20% decrease in consumption. In both cases, pumping losses are greatly reduced thanks to high exhaust gas recirculation (EGR), which, while reducing NO_x emissions, reduces depression caused by the throttle placed in the intake pipes (Figure 13.9.1). In both cases also, the compression ratio can be substantially increased without risk of knocking (12.5 in lean, 11.5 in stoichiometric mix, against 10.5 in a multipoint injection engine).

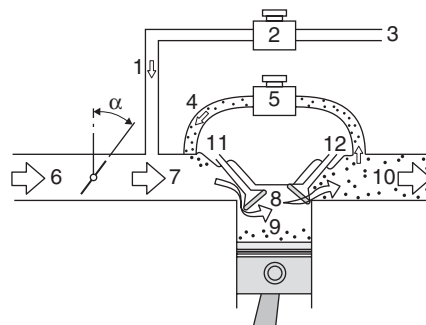


FIGURE 13.9.1

Cylinder charge in a gasoline engine, Extract from Bosch Technical Papers

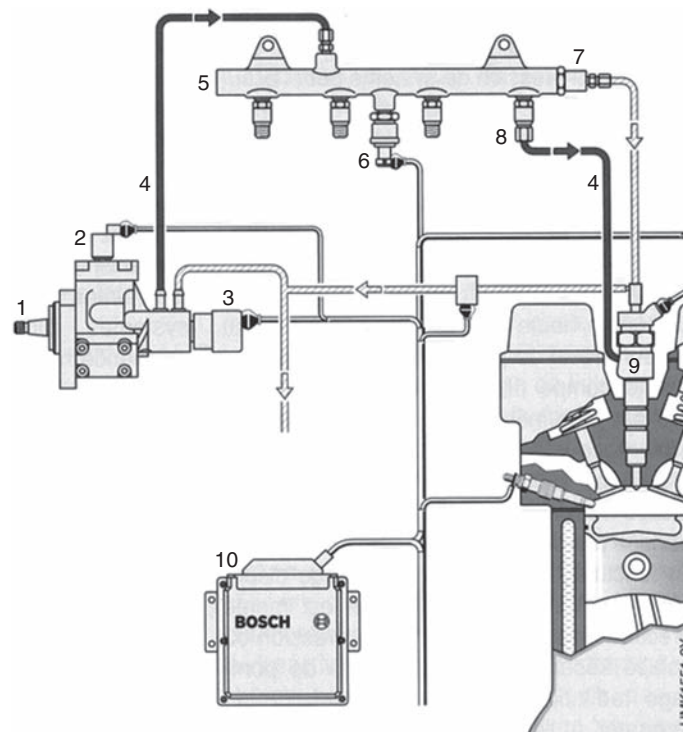


FIGURE 13.9.2

Common Rail HP circuit, Extract from Bosch Technical Papers

However, the Japanese technology has the disadvantage of being incompatible with three-way catalyst converters currently available. Under these conditions, even if emissions of pollutants are much reduced compared to a gasoline engine without gas after-treatment, they are much higher than European standards. This explains why Renault has opted for the other technology, reserving the possibility of implementing lean-burn engines when the corresponding deNO_x catalysts will be available.

Figure 13.9.1 shows main factors on which depends the cylinder charge in a gasoline engine, with the air and fuel vapor (1), the purge valve with variable aperture (2), the link to the evaporative emission control system (3), the EGR (4), the EGR valve with variable aperture (5), the air flow-rate (6 and 7), the fresh charge (8), the residual gas charge (9), the exhaust gas (10), the intake and exhaust valves (11 and 12), α being the throttle valve angle. Obviously, pressures in 6, 7, 8 and 10 strongly influence the volumetric efficiency C_v .

13.9.1.2 Direct injection diesel

Direct injection is not a new concept, far from it. Most semi fast or slow diesels use it. In the fast engines, it was not used until recently because it had several drawbacks (particulate emissions due to the heterogeneity of fuel distribution, engine noise etc.) and did not accelerate enough combustion. The solution adopted was to use pre-chambers, which increased the losses through the walls and throttling.

The work on direct injection has initially focused on diesel, the aim being to avoid the problems that previously existed when used in fast engines. The obvious solution today is the Common Rail technology which appears the best compromise on the technical-economic level. On Figure 13.9.2, appear the following components: the high pressure pump (1), element deactivation valve (2), pressure regulator (3), high pressure fuel pipes (4), common rail (5), rail pressure sensor (6), pressure limiter (7), flow rate limiter (8), injector (9), electronic computer (10).

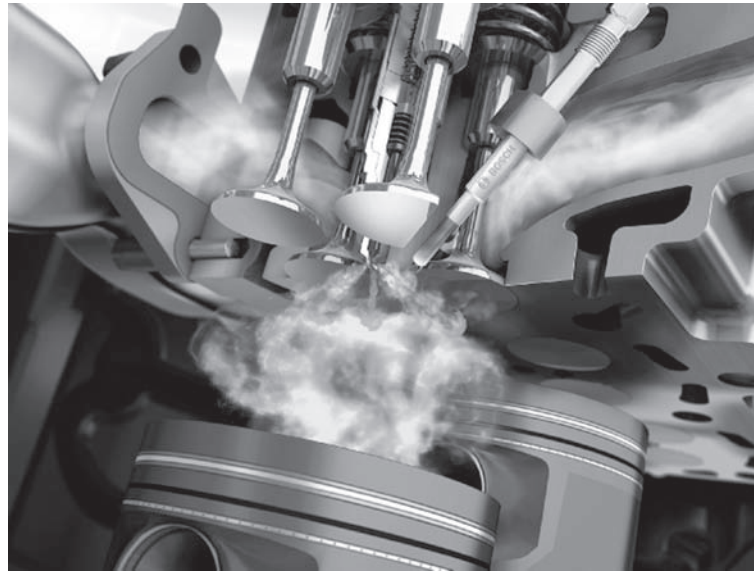


FIGURE 13.9.3

Common Rail high-pressure direct injection system, Photo: Bosch.

Broadly, it is to distribute the fuel through a pipe common to all the injectors, and to steer them through electromagnetic devices. The very high “rail” pressure (1,300–1,500 bar), and the very small diameter holes of the injectors (less than 200 microns) allow extremely fine fuel atomization to be achieved, which vaporizes immediately and burns in air much better than was possible with conventional systems.

Figure 13.9.3 shows the fuel jet coming out of the injector in four directions. In the foreground on the right appears the glow plug which allows to heat fresh air when the engine is cold.

The conventional injection pumps only realizing a main injection of triangular profile, the pressure and flow vary substantially proportionally during the injection, when it would be desirable to drive them separately. Common Rail allows for a sequential injection in three phases to optimize the combustion

- a pre-injection called pilot injection of 1 to 2 mm³ of fuel in a few microseconds with an angle advance of about 20°, allowing a gradual rise in temperature before the main injection, to obtain a more silent combustion;
- the main injection;
- and a post-injection at approximately 200° angle to improve deNO_x catalysis when installed.

The use of Common Rail is now leading to greatly improved performance for diesel.

The introduction of particulate filters (micro-carbon spherules with a diameter close to 0.05 microns) should allow in the coming years reduction of particulate emissions at the limit of what is measurable. It is in this technology that PSA has invested the most in recent years, the new HDi engine already equipping some of its cars like the 607, and new engines being built for both its own needs and as part of its agreement with Ford. The performance of this engine is much improved compared to those of indirect injection engines of the previous generation:

- 20% reduction in consumption (and thus CO₂ emissions);
- a decrease of 40% of CO, 50% of unburned hydrocarbons and 60% of particulates at a constant level of NO_x;
- gains in driveability (over 50% increase in torque at low rpm), reduced noise and vibration.

This progress is attributable partly to direct injection, and partly to the engine downsizing (12%) and the reduction of internal friction (reduced consumption of 1.5 to 2% at low and medium speed).

13.9.1.3 Developments in common

Generally, all manufacturers seek to reduce pumping losses and increase cylinder filling, the finding being that, given the way cars are used in practice, engines run only very rarely at full capacity, which leads to very low real efficiencies, especially for gasoline engines.

Besides the work on direct injection which was presented earlier, many manufacturers seek to have greater flexibility in the engine geometry. Two main developments are under consideration:

- variation of compression ratio (VCR) by changing the volume of the cylinder. The objective here is to be able to vary at will the compression ratio, if possible cylinder by cylinder, typically within a range between 7 and 17. Several techniques are under study. Saab has developed an engine that has an articulated head that allows the compression ratio of all cylinders to simultaneously be changed, while Peugeot and Nissan are working on concepts of cylinder by cylinder control by means of linkage mechanisms in several parties and while the MCE-5 consortium is to develop a new promising technology (www.mce-5.com);
- decoupling the control of valve openings from the crankshaft rotation, either through mechanical devices or through electromagnetic systems (called Camless). Although it is unlikely that this solution emerges before the adoption of 24 or 48 V voltage for DC electrical system, it is particularly attractive because it would manage the openings of the valves according to protocols currently unfeasible, such as to bypass certain cylinders at low revs. This could lead to variable displacement engines inconceivable today;
- the combination of a VCR with Camless can devise very interesting strategies allowing the adaptation of the engine at varying operating conditions, with change of reference cycle (adoption of the Atkinson or Miller cycle to remove the throttle with adjustment of the fresh gas admitted thanks to the intake valves and prolonged expansion to recover increased mechanical power: the compression ratio can then be much lower than that of expansion).

Some manufacturers like Renault are working on **downsizing**, which seeks an engine of geometric dimensions reduced by 30 to 50%, improved performance by reducing pumping losses, heat and friction, or even the number of cylinders.

To reduce emissions of pollutants, some manufacturers like Peugeot are planning to use a very important **exhaust gas recirculation** (EGR). In order not to lower the volumetric efficiency, it is then necessary to cool the gas before reinjection into the cylinder.

Further research is being performed in parallel on replacing the **starter and alternator** by systems allowing improved power management (Integrated Starter Alternator Flywheel (ISAF), Stop and Go), improved turbochargers etc.

Hybrid vehicles combining a combustion engine and electric propulsion are also on the agenda. Several systems are being considered, the engine may be a diesel engine or a gas turbine. The engine is then coupled with a starter generator and produces electricity that is either directly consumed in electric motors for propulsion, or stored in lithium batteries. The advantage of such a device is that production of electricity and demand are to a large extent decoupled. It is thus possible on the one hand to operate the engine in much better conditions than if it has to adapt to real-time needs of the vehicle, and secondly to stop it at certain times (urban), the vehicle running then only on batteries, which turns it into zero-emission vehicle.

Toyota has been selling for some years the Prius, whose engine is a gas turbine, and Peugeot has tested a diesel hybrid powertrain with an average consumption of 80 g/kWh as against 140 for a conventional vehicle.

13.9.1.4 Fuel economy foreseen

Figures 13.9.4 and 13.9.5 illustrate fuel economies that are foreseen for both gasoline and diesel engines in the following years.

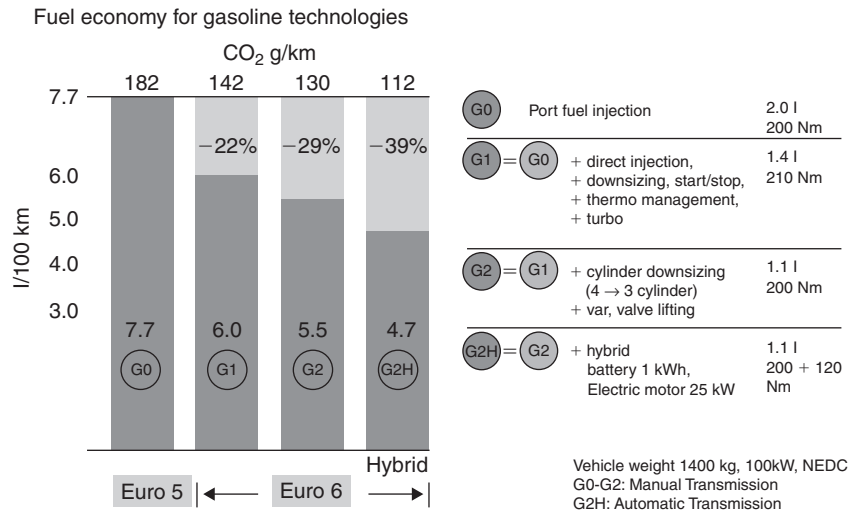


FIGURE 13.9.4
 Comparison of drive concepts for gasoline engines, Photo: Bosch.

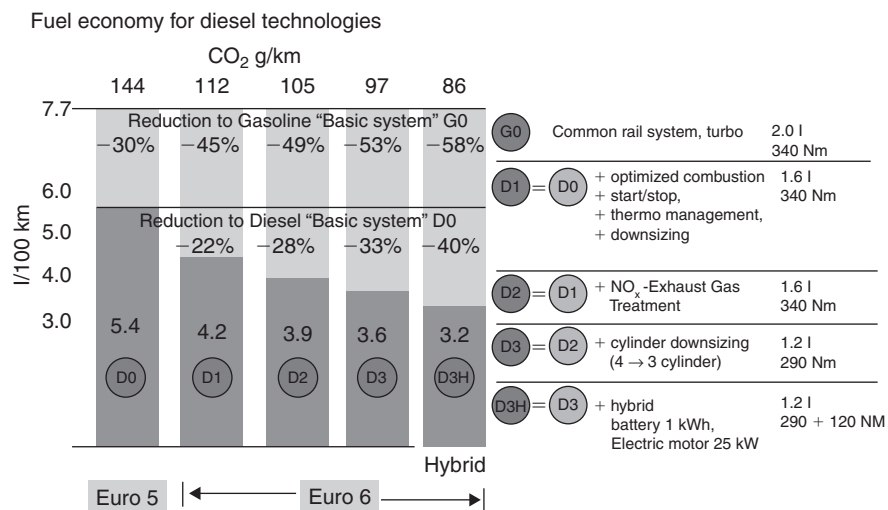


FIGURE 13.9.5
 Comparison of drive concepts for diesel engines, Photo: Bosch.

Thanks to progressive innovation, fuel consumption and CO₂ emissions of diesel and gasoline engines are expected to reduce by about 30 percent by 2015.

13.9.2 Large gas and diesel engines

On large reciprocating engines, technological developments are continuing in two directions.

13.9.2.1 Gas engines

For several years gas diesel engines of increased capacity have been developed. The range of diesel gas is a few hundred kW to medium-speed machines with a capacity of 6MW and should

be increased to 10 MW soon. The ignition can be controlled either by spark plug as in a gasoline engine, or by injection of pilot fuel.

Spark-ignition engines used in cogeneration plants generally use lean mixture, like that which is being sought in Japanese gasoline direct injection engines. For energy production, combustion of a stoichiometric mixture leads to a lower power density and more abundant emissions requiring three-way catalysis.

Ignition is provided by spark plugs placed directly into the combustion chamber for small engines up to 1 MW, and for more powerful engines, in a pre-chamber, the design of which determines the level of emissions and the temperature of which limits the power reached given the risk of knocking in the main chamber.

For higher capacity gas engines, ignition is achieved by pilot injection of fuel in quantities less than 1% of the total gas consumption. The diesel fuel is ignited by diesel effect and releases enough energy to ignite lean gas/air mixtures.

Finally, significant progress has been made in the engine control in order to take into account the gas composition and heating value, which are not constant.

13.9.2.2 Heavy duty diesel engines

Since the early 70s, the consumption of heavy duty diesel engines has been reduced by 15% and capacity increased by 35%. Moreover, to develop diesel combined cycle technology (see section 17.4), manufacturers have sought to increase the operating temperature of diesel engines. As the attempts to introduce ceramics have proved unsuccessful, they turned to new alloys, new designs and new manufacturing methods, such as the use of laser surface treatment. Hence a profound change of the cylinder: new uncooled piston crown, anti-polishing ring insulation, much more resistant valves and valve seats, composite structure of the head etc. The interested reader can find a good summary of these developments in (Neef et al, 1999). Installation costs of heavy diesel engines range between 300 and 350 Euros/kW.

REFERENCES

- Bosch, *Commandes pour moteurs à essence*, Cahiers Techniques, Stuttgart, 1999.
- Bosch, *Commandes pour moteurs diesel*, Cahiers Techniques, Stuttgart, 2000.
- Ch. Clos, *Technologie des moteurs alternatifs à combustion interne*, Techniques de l'Ingénieur, Traité Mécanique et chaleur, B 2800.
- M. Gratadour, *Application de la suralimentation aux moteurs*, Techniques de l'Ingénieur, Traité Mécanique et chaleur, B 2 630.
- A. Parois, *Suralimentation par turbocompresseur*, Techniques de l'Ingénieur, Traité Génie Mécanique, BM 2 631.
- M. Thelliez, *Analyse énergétique des cycles des moteurs à combustion interne au moyen d'un cycle théorique associé*, Entropie, 1989, n° 148, pp. 41–49.

FURTHER READING

- J. Andrzejewsky, M. Thelliez, *Coefficient de remplissage et taux de gaz résiduels*, Entropie, 1987, n° 134, pp. 95–100.
- R. Carreras, M. Quera, A. Comas, A. Calvo, *Maquinas térmicas*, LMTA, ETS d'Enginyeria Industrial, Universitat Politècnica de Catalunya, Terrassa, 2001
- B. Geoffroy, *Distribution à soupapes*, Techniques de l'Ingénieur, Traité Mécanique et chaleur, B 2805.

- J.C. Guibet, *Carburants et moteurs*, Publications de l'IFP, Editions Technip, Paris, 1987.
- A. Haupais, *Combustion dans les moteurs diesel*, Techniques de l'Ingénieur, Traité Mécanique et chaleur, B 2700.
- J. P. Moranne, *Refroidissement des moteurs à combustion interne*, Techniques de l'Ingénieur, Traité Mécanique et chaleur, B 2830.
- T. de Neef, B. Mouille, P.A. Destailleur, *La production d'énergie au moyen de systèmes diesel modernes*, Revue de la Société des Electriciens et des Electroniciens, décembre 1999, Paris.
- J. Rauch, *Insonorisation et remplissage des moteurs à piston*, Techniques de l'Ingénieur, Traité Mécanique et chaleur, B 369,9.
- B. Raynal, *Moteurs thermiques et pollution atmosphérique, origine et réduction des polluants*, Techniques de l'Ingénieur, Traité Mécanique et chaleur, B 378,1.
- F. Roux, *Graissage des moteurs thermiques alternatifs*, Techniques de l'Ingénieur, Traité Mécanique et chaleur, B 2750.
- M. Thelliez, *Analyse des produits de combustion d'un moteur à combustion interne*, VIIe Congreso de Ingeniera Mecanica. Valencia, décembre 1988.
- J. Trapy, *Moteur à allumage commandé*, Techniques de l'Ingénieur, Traité Génie Mécanique, BM 2540.

This page intentionally left blank

Stirling Engines

Abstract: The Stirling engine is an external combustion reciprocating gas engine which operates under the closed regenerative cycle shown on the entropy diagram in Figure 14.1.1. As we shall see later, its theoretical efficiency is equal to that of Carnot, which explains the fascination it exerts on many researchers.

The first patent for this engine type was introduced in 1816 by Scotsman Robert Stirling who sought to develop a device safer than steam engines. As its technical fluid was air in the nineteenth century, it is known as hot-air engine which quickly became a huge success. Its applications are numerous, such as industrial water pumping as well as domestic or space ventilation. Since the early twentieth century, internal combustion reciprocating engines and the development of electric motors gradually dethroned Stirling engines, which are now much less used.

Keywords: compression, expansion, combustion, Stirling, displacer, regenerator, para-isothermal cycle.

By the mid-30s, the Dutch company Philips invested heavily in this technology, in order to have small generators for autonomous power supply for isolated radio stations or relays, with the aim of developing a silent motor, operating with a minimum maintenance, and good efficiency.

The Philips work yielded many significant breakthroughs, and has enabled the power density to increase by 50, completely renewing the development prospects of the Stirling engine. In 1957

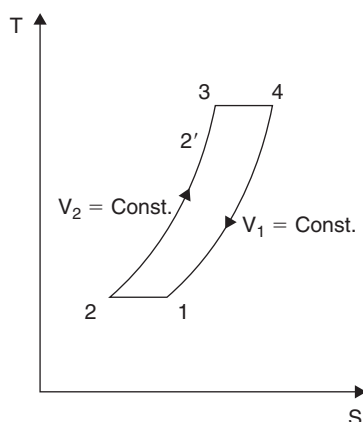


FIGURE 14.1.1

Stirling cycle

General Motors teamed up with Philips to develop a motor for traction, but in spite of technical successes, the partnership was not renewed 10 years later.

Today, many experts agree in considering that the Stirling engine could experience a significant rise in the future considering first its benefits, including protection of the environment, and secondly the many hot sources that could be used. It has particular strengths for uses such as marine propulsion, especially submarines, for small power electricity generation in isolated areas from different energy sources (solar, biomass, fossil fuels) and for small cogeneration. The interested reader can refer to (Stouffs, 1999) for a description of the state of the art in Stirling engines.

4.1 PRINCIPLE OF OPERATION

The basic principle of a Stirling engine is very simple: a gas enclosed in a cylinder closed with a piston is successively heated and then cooled. The pressure difference which is established in the enclosure can be transformed into motor work. The difficulty is that it is virtually impossible, given the thermal inertia of the cylinder, to heat and cool it quickly enough so that the system operates under optimum conditions. Robert Stirling's idea was to put the gas in motion by introducing a special device whose operation we will analyze, the **displacer**. The engine structure is shown in Figure 14.1.2.

In a main vessel can move on the one hand a working piston and on the other hand a displacer, whose role is to transfer the working fluid from the compression volume to the expansion volume, and *vice versa*.

During displacement the fluid passes successively in one direction or another, in the boiler at temperature T_3 , the regenerator, and the cooler at temperature T_1 .

The cycle includes four phases illustrated by the diagrams of Figures 14.1.3 to 14.1.6 and the entropy diagram of Figure 14.1.1.

During the compression phase (Figure 14.1.3), the displacer is in high position, and the fluid confined in the cold zone is compressed by the working piston in its upward stroke, which requires the provision of work W_{12} .

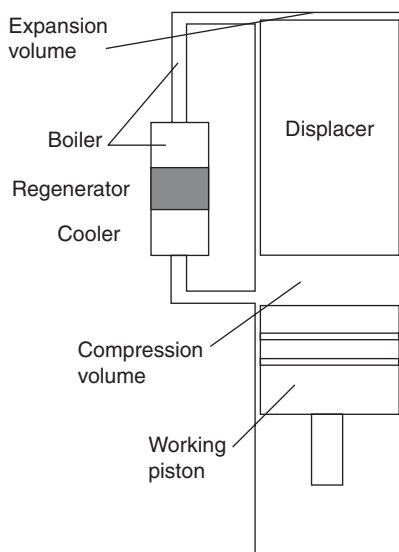


FIGURE 14.1.2

Sketch of a Stirling cycle

At point 2, the piston is at top dead center and the displacer is moved in the low position, which has the effect of transferring the compressed fluid, which passes (Figure 14.1.4) from the cold zone to the hot zone, starting with warming up in the regenerator, then receiving heat from the boiler. This process takes place at constant volume, the pressure increasing in the ratio of temperatures T_3 and T_1 .

During expansion phase (Figure 14.1.5), the fluid expands into the expansion volume, where it continues to be heated by the boiler tubes. This expansion has the effect of pushing the working piston down, and provides useful work W_{34} . During this phase, the displacer and the piston move together.

During the last phase (Figure 14.1.6), after the working piston reaches bottom dead center, the displacer is moved in the upper position, which has the effect of transferring the fluid from the hot

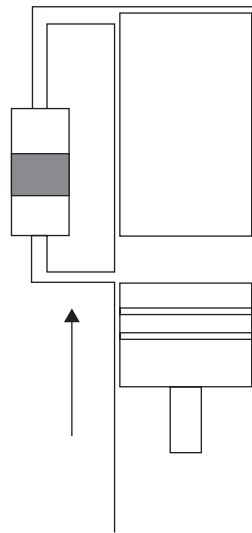


FIGURE 14.1.3
Compression phase

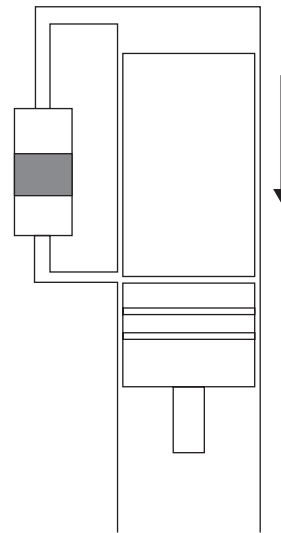


FIGURE 14.1.4
Constant volume heating

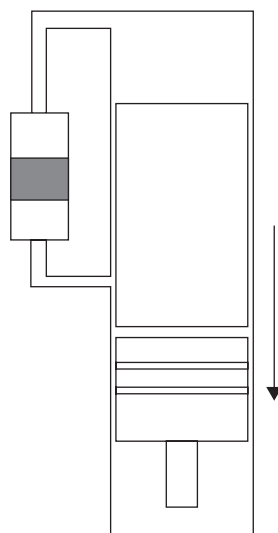


FIGURE 14.1.5
Expansion phase

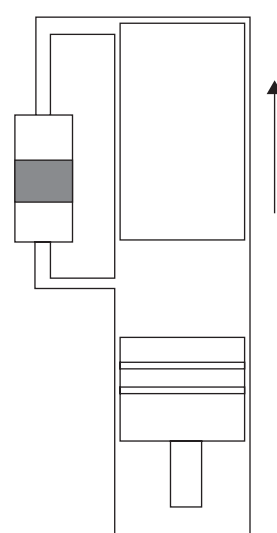


FIGURE 14.1.6
Constant volume cooling

zone (expansion volume) to the cold zone (compression volume). During the transfer at constant volume, the fluid begins to yield its heat to the regenerator, before being cooled by the cooler.

Note that the displacer does not produce work. Pressure on its two opposite faces is always the same, if we neglect the pressure drop in the three heat exchangers (heater, regenerator and cooler).

In practice, the relative movements of the displacer and piston are obtained in various ways, especially by mechanical devices made from rods and crankshafts. Movement, which was described above as being discontinuous, is in reality very nearly sinusoidal, and a phase shift of about 90° between the displacer and working piston is generally accepted.

14.2 PISTON DRIVE

The main considerations that guide the choice of a coupling mechanism between the movements of the two pistons are:

- Systems should be simple and therefore inexpensive to manufacture and maintain;
- Dynamic aspects are essential, both in terms of stress repartition and vibration;
- The Stirling engine is a closed cycle engine, quiet by nature, and this quality should not be affected by the drive mechanisms;
- Finally, we search systems as tight as possible because, as discussed below, one of the Stirling engine characteristics is to operate at relatively high pressures.

The most used mechanisms are connecting rods, rhombic drive (Figure 14.2.1), cylinder rods and gliding rods. The interested reader will find illustrations in (Walker, 1973) and (Reader, 1983).

Several geometric configurations have been proposed for producing Stirling engines. The procedure we presented is that of single-acting piston, where piston and displacer are two separate bodies.

There is another category of engines, known as double-acting piston, in which the working piston also plays the role of displacer. This is made possible by coupling together a number of cylinders (between 3 and 6), and adjusting the relative movements of the pistons in the cylinders so that the

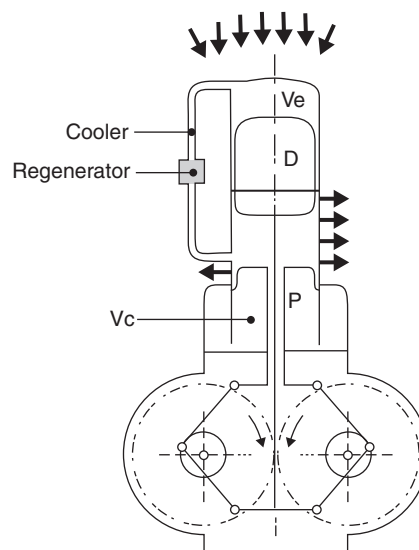


FIGURE 14.2.1

Rhombic drive, Extract from *Techniques de l'Ingénieur, Génie Mécanique*

expansion phase of one of them corresponds to the displacement phase of another. The fluid is thus transferred successively between two cylinders. By placing the cylinders around an axis, it is possible to produce compact engines that share the same boiler burner and have a very efficient drive system.

Free-piston Stirling engines have also been made, in which the working piston and displacer are not coupled mechanically, but through the working fluid. This type of arrangement makes it possible assembling a linear alternator around the working piston, to realize hermetic motors, and thus solve sealing problems mentioned above.

14.3 THERMODYNAMIC ANALYSIS OF STIRLING ENGINES

In what follows, having quickly established the theoretical cycle efficiency, we consider two cycles representative of Stirling engines: the ideal cycle with imperfect regenerator and the para-isothermal Stirling cycle, in which isotherms are replaced by an adiabatic followed by an isovolume.

14.3.1 Theoretical cycle

The theoretical Stirling cycle (Figure 14.1.1) decomposes as shown below.

Between points 1 and 2, the fluid is compressed at constant temperature. We must provide work W_{12} given by equation (7.1.2) of Part 2:

$$W_{12} = r T_1 \ln(\rho),$$

ρ being the volumetric compression ratio v_1/v_2

As on an isotherm, $du = \delta W + \delta Q = c_v dT = 0$, it is necessary to extract heat $Q_{12} = -W_{12}$.

Between points 2 and 3, heat Q_{23} is supplied to the fluid at constant volume.

Between points 3 and 4, the fluid is expanded at constant temperature, and provides work W_{34} :

$$W_{34} = -r T_3 \ln(\rho)$$

We should also provide the fluid with heat $Q_{34} = -W_{34}$.

Between points 4 and 1, heat Q_{41} is extracted from fluid at constant volume. As the heat transfers (2-3) and (4-1) take place at the same temperature levels, and as the fluid is assumed to be perfect, both isovolumes can be deduced by translation and it is possible, assuming the existence of a perfect regenerator, to ensure that:

$$Q_{23} + Q_{41} = 0$$

The amount of heat to provide to the cycle is then Q_{34} , and the useful work ($-W_{12} - W_{34}$).

The cycle efficiency is:

$$\eta = \frac{-W_{12} - W_{34}}{Q_{34}} = \frac{r \ln(\rho)(T_3 - T_1)}{r T_3 \ln(\rho)} = 1 - \frac{T_1}{T_3} \quad (14.3.1)$$

The efficiency of the theoretical Stirling cycle is equal to that of Carnot.

This result largely explains the interest in the Stirling engine: its theoretical cycle has the best efficiency that allows the second law of thermodynamics. However it is extremely difficult to make isotherm compressions or expansions (see section 5.3.6 of Part 2), as the compression or expansion machines are compact machines rotating at high speed. Furthermore, achieving heat exchange close to isothermal would require a large exchange surface and low transfer rates.

In practice, Stirling engines deviate significantly from the theoretical cycle consisting of two isotherms and two isovolumes, and their efficiency is far below the Carnot efficiency. There are several other reasons:

- first, the regenerator is not perfect, and only a fraction of the available energy is actually recovered between phases (2-3) and (4-1);
- second, heating and cooling do not occur only during the expansion and compression phases. These are not perfect isotherms, and in some cases, may be close to adiabatic, or, more generally, heated or cooled polytropics.

As we will show, it is possible to somehow refine Stirling engine models by considering more complex cycles, but the exercise has its limits because the continuous movement of the piston and displacer creates losses of aerodynamic nature (pressure drops, establishment of pressure waves caused by the pulsating flow) that are extremely difficult to model, especially analytically. The interested reader will find in (Walker, 1973) an analysis proposed by Schmidt in 1861, taking into account a harmonic motion of the moving parts, or may refer to the literature for more advanced developments. However, even today, the modeling of Stirling engines is still unsatisfactory, particularly as regards the simulation of instantaneous temperature and pressure fields prevailing in the various heat exchangers that make up these engines (Stouffs, 1999).

In this book, we limit ourselves to two simple models: the ideal cycle and the para-isothermal cycle. We present only one model made with Thermoptim, noting that its use does not really go beyond the limits of these theoretical models, especially when the working fluid is helium, which can legitimately be regarded as perfect. Some basic assumptions of the software (steady-state components in particular) are not met here.

14.3.2 Ideal Stirling cycle

In the ideal cycle (see Figure 14.1.1), the fluid still follows two isotherms and two isovolumes but effectiveness ε of the regenerator is less than 1.

$$\varepsilon = \frac{T_{2'} - T_1}{T_3 - T_1}$$

In addition to heat Q_{34} , we must therefore provide the cycle with heat $Q_{2'3}$.

$$\eta = \frac{-W_{12} - W_{34}}{Q_{34} + Q_{2'3}}$$

$$\eta = \frac{r \ln(\rho)(T_3 - T_1)}{r \ln(\rho)T_3 + Q_{2'3}}$$

Introducing the ratio $\zeta = T_1/T_3$ we get:

$$Q_{2'3} = c_v(T_3 - T_{2'}) = c_v(T_3 - T_1 - \varepsilon(T_3 - T_1)) = c_v T_3(1 - \zeta)(1 - \varepsilon)$$

$$Q_{2'3} = \frac{r}{\gamma - 1} T_3(1 - \zeta)(1 - \varepsilon)$$

$$\eta = \frac{r \ln(\rho)(T_3 - T_1)}{r \ln(\rho) T_3 + \frac{r}{\gamma - 1} T_3(1 - \zeta)(1 - \varepsilon)}$$

$$\eta = \frac{\ln(\rho)(1-\zeta)}{\ln(\rho) + \frac{(1-\zeta)}{\gamma-1}(1-\varepsilon)} \quad (14.3.2)$$

$$\eta = \frac{(\gamma-1)(1-\zeta)\ln(\rho)}{(\gamma-1)\ln(\rho) + (1-\zeta)(1-\varepsilon)}$$

The curve in Figure 14.3.1 gives the appearance of efficiency depending on volume ratio ρ for $\xi = 0.3$ and $\varepsilon = 0.75$.

The importance of the γ value can be seen on this graph. It seems preferable to use monatomic or diatomic gases. In practice, fluids used until now were air, hydrogen or helium.

Moreover, the efficiency of this cycle increases with the volumetric compression ratio.

We can also calculate a dimensionless work W_0 , ratio of useful work to the product of pressure P_1 by the swept volume ($V_1 - V_2$):

$$W_0 = \frac{-W_{12} - W_{34}}{P_1(V_1 - V_2)}$$

The swept volume is:

$$V_1 - V_2 = V_1 \frac{(\rho - 1)}{\rho}$$

$$W_0 = \frac{r \rho \ln(\rho)(T_3 - T_1)}{P_1 V_1 (\rho - 1)} = \frac{r \rho T_3 \ln(\rho)(1 - \zeta)}{P_1 V_1 (\rho - 1)}$$

$$W_0 = \frac{T_3 \rho \ln(\rho)(1 - \zeta)}{T_1 (\rho - 1)}$$

$$W_0 = \frac{\rho \ln(\rho)(1 - \zeta)}{\zeta(\rho - 1)} \quad (14.3.3)$$

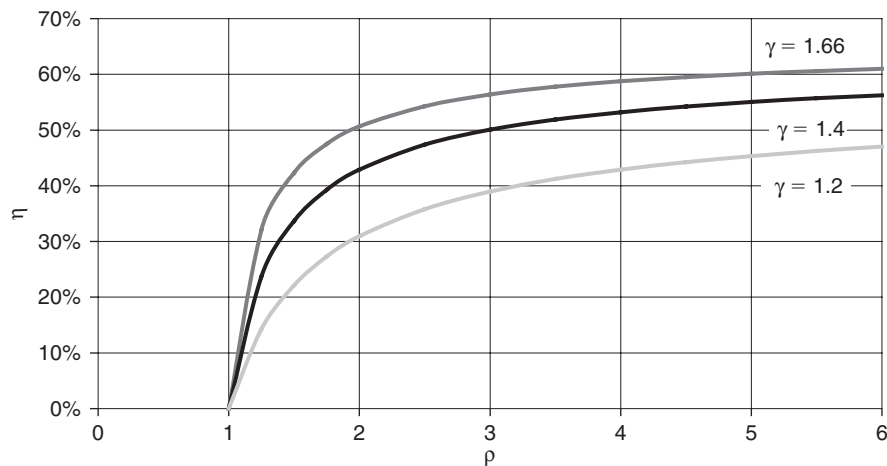
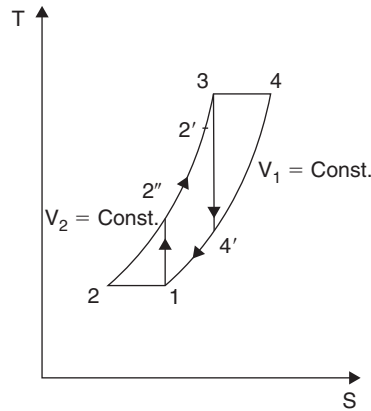


FIGURE 14.3.1

Stirling engine efficiency

**FIGURE 14.3.2**

Para-isothermal cycle

The ideal Stirling cycle is not fully satisfactory because the expressions of efficiency it provides are in contradiction with an experimental fact: there is an optimum volumetric ratio (a value between 2 and 3) for which efficiency is maximum.

14.3.3 Paraisothermal stirling cycle

The para-isothermal Stirling cycle seeks to remedy the inadequacies of the ideal cycle, better approaching real processes undergone by the fluid. If one refers to the principle of operation outlined in section 14.1, we note that a significant portion of heat exchange between the fluid and the outside takes place not during the phases of compression and expansion, but during the transfer of fluid, when it goes into the cooler or boiler.

In the para-isothermal cycle (Figure 14.3.2), it is assumed that isotherm (1-2) is replaced by adiabatic compression (1-2), followed by cooling (2''-2), and that isotherm (3-4) is replaced by adiabatic expansion (3-4'), followed by heating (4'-4).

Under these conditions the heat to provide to the cycle becomes:

$$Q = Q_{2'3} + Q_{4'4}$$

and expression of the compression and expansion work is no longer that of the isotherm (equation (7.1.3) of Part 2) but that of the adiabatic (calculated in closed system).

$$\eta = \frac{-W_{12''} - W_{34'}}{Q_{2'3} + Q_{4'4}}$$

$$W_{12''} = \frac{P_1 v_1}{\gamma - 1} (\rho^{\gamma-1} - 1) = \frac{\zeta P_3 v_3}{\gamma - 1} (\rho^{\gamma-1} - 1)$$

$$W_{34'} = \frac{P_3 v_3}{\gamma - 1} (\rho^{1-\gamma} - 1)$$

$$Q_{2'3} = \frac{r}{\gamma - 1} T_3 (1 - \zeta)(1 - \varepsilon)$$

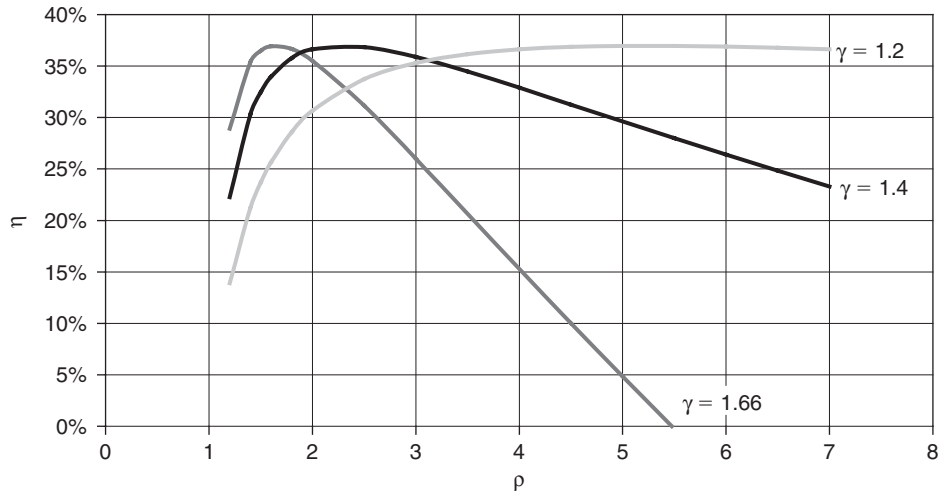


FIGURE 14.3.3
Stirling engine efficiency

$$Q_{44} = c_v(T_4 - T_{4'}) = c_v(T_4 - T_3\rho^{1-\gamma}) = \frac{r}{\gamma-1} T_3(1 - \rho^{1-\gamma})$$

$$\eta = \frac{-\frac{\zeta P_3 v_3}{\gamma-1}(\rho^{\gamma-1} - 1) - \frac{P_3 v_3}{\gamma-1}(\rho^{1-\gamma} - 1)}{\frac{r}{\gamma-1} T_3(1 - \zeta)(1 - \varepsilon) + \frac{r}{\gamma-1} T_3(1 - \rho^{1-\gamma})}$$

$$\eta = \frac{(1 - \rho^{1-\gamma}) - \zeta(\rho^{\gamma-1} - 1)}{(1 - \zeta)(1 - \varepsilon) + (1 - \rho^{1-\gamma})} \quad (14.3.4)$$

The shape of the efficiency function of the volumetric ratio is given in Figure 14.3.3. It shows a maximum, which is between 1.8 and 5 depending on the fluid used. These results are much closer to experimental reality of engines built to date.

If we show θ , reverse of ζ , representative of the heating, the efficiency becomes (Figure 14.3.4):

$$\eta = \frac{\theta(1 - \rho^{1-\gamma}) - (\rho^{\gamma-1} - 1)}{(\theta - 1)(1 - \varepsilon) + \theta(1 - \rho^{1-\gamma})} \quad (14.3.5)$$

The power factor W_0 can also be determined analytically:

$$W_0 = \frac{-W_{12''} - W_{34'}}{P_1(V_1 - V_2)} = \frac{\rho}{(\rho - 1)} \frac{-W_{12''} - W_{34'}}{\rho_1 V_1}$$

$$W_0 = \rho \frac{-\frac{\zeta P_3 v_3}{\gamma-1}(\rho^{\gamma-1} - 1) - \frac{P_3 v_3}{\gamma-1}(\rho^{1-\gamma} - 1)}{r T_3 \zeta (\rho - 1)}$$

$$W_0 = \rho \frac{(1 - \rho^{1-\gamma}) - \zeta(\rho^{\gamma-1} - 1)}{\zeta(\rho - 1)(\gamma - 1)}$$

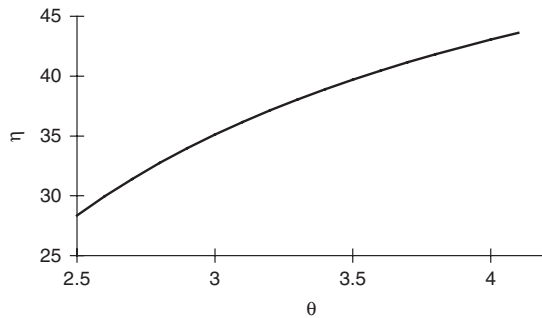


FIGURE 14.3.4
Stirling engine efficiency function of θ

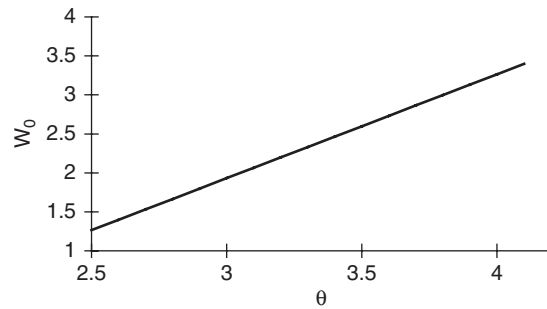


FIGURE 14.3.5
Stirling engine power factor function of θ

$$W_0 = \frac{\rho(1 - \rho^{1-\gamma})(1 - \zeta\rho^{\gamma-1})}{\zeta(\rho - 1)(\gamma - 1)} \quad (14.3.6)$$

W_0 is a linear function of θ (Figure 14.3.6)

$$W_0 = \frac{\rho(1 - \rho^{1-\gamma})}{(\rho - 1)(\gamma - 1)} (\theta - \rho^{\gamma-1}) \quad (14.3.7)$$

To fix ideas, cooling is often provided with water at about 40°C, 313 K, and the maximum temperature is around 750°C, 1023 K, which gives a value of θ around 3.3. The curves of Figures 14.3.4 and 14.3.5 give the look of efficiency and power factor as a function of θ around this value.

14.4 INFLUENCE OF THE PRESSURE

By definition of W_0 , the work W that may be provided by an engine of displacement V_s is equal to $W = W_0 P_1 V_s$.

In the case of the Stirling engine, theory suggests therefore, which is verified by experience, that the power is roughly proportional to the fluid pressure: for a given capacity, it is possible to have a machine either compact (small V_s) and under high pressure, or larger with lower working pressure.

One generally seeks to use very high pressures (about 100 to 200 bar), and the limit is determined by the particular sealing problems at the joints between the piston and the casing of the machine. The difficulties encountered at this level partly explain why in the past, the Stirling engine development has been slower than that of its competitors.

Experience also shows that the efficiency itself is an increasing function of pressure, probably because of improved heat transfer within the machine.

Finally, the almost proportional relationship existing between the work done by the engine and the pressure therein allows control of the machine by varying the pressure, which is generally done.

In all cases, the risks of leakage are important and there should be a mechanism for resetting the pressure of the working fluid, especially when it is a light gas, like hydrogen.

14.5 CHOICE OF THE WORKING FLUID

The study of the para-isothermal cycle suggests that the same maximum efficiency can be obtained with different values of γ , but for different volumetric ratios, and experience does not invalidate this conclusion.

TABLE 14.6.1

Heat rejection per kW of useful power

	Cooling water	Flue gas
Gasoline engine	1.00	1.33
Diesel engine	0.56	1.22
Stirling engine	1.39	0.39

The choice of the fluid depends more on thermal and fluid mechanics considerations than thermodynamics. From this point of view, hydrogen is very attractive, with a heat capacity 14 times greater than air and nearly three times larger than that of helium. However, it poses specific containment problems.

Ultimately, the choice of the working fluid is strongly dependent on the type of engine and its operating conditions. A careful optimization study must be done.

14.6 HEAT EXCHANGERS

The various heat exchangers that appear in a Stirling engine are the cooler, the regenerator and the boiler. We have already seen how heavily the engine efficiency depends on the effectiveness of these very specific exchangers.

14.6.1 Cooler

The design of the cooler is less problematic than the other two heat exchangers, insofar as the cold source is most often water. This is a relatively conventional exchanger.

Note however that in a Stirling engine, the heat removed by cooling water is a much larger percentage of the heat of combustion than in a reciprocating internal combustion engine.

Table 14.6.1 gives an indication of the amount of heat removed by cooling water and exhaust for different types of engines.

14.6.2 Regenerator

The regenerator is a key component of the Stirling engine. It generally consists of a porous material of high heat capacity, to ensure the best heat exchange with the fluid. Ideally, its axial conductivity should be as low as possible so that it retains a good stratification, but its radial conductivity should be high so that its temperature is uniform.

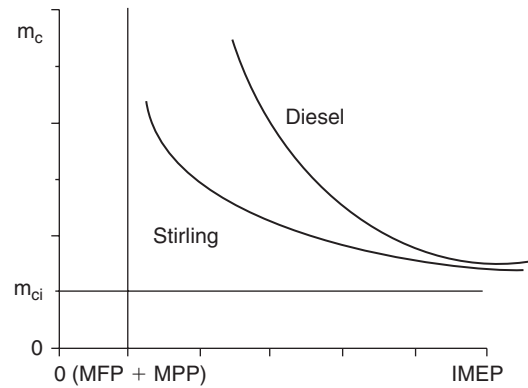
As in the case of the boiler, there is a contradiction between seeking a reduction in pressure drop and an increase in heat transfer between the fluid and the regenerator.

The regenerator is by far the exchanger which transfers most energy in the Stirling engine: its capacity should generally be between 5 and 10 times that of the engine, or even more.

Despite all these difficulties, we are now able to make very efficient regenerators, of effectiveness about 0.9.

14.6.3 Boiler

The boiler is used to transfer heat from the heat source to the working fluid in the hot zone. As the Stirling engine follows a closed cycle, it is possible to use a wide variety of hot sources, classically as burners, or even more particular as heat pipes or the furnace of a solar concentrator.

**FIGURE 14.7.1**

Specific consumption

In the classic case of a burner, the boiler is subjected on one side (outside the tubes) to the action of combustion gases, possibly corrosive, but at low pressure, and on the other side (inner tubes) to the internal pressure of the engine (above 100 bar). Once the steady state reached, variations in temperature are of relatively low amplitude, but at startup, the boiler is subject to strong dilatation. These operating conditions generate high stresses, and only very strong materials can be used.

In addition, we seek to optimize the design of the boiler so that pressure drops will be as low as possible, which requires large diameters, but also so that the dead volume is reduced and the heat exchange coefficients are high, which requires small diameters. A compromise must therefore be found between all these requirements, which requires careful analysis.

14.7 CHARACTERISTICS OF A STIRLING ENGINE

The shape of the specific consumption curve of a Stirling engine is much flatter than that of a reciprocating internal combustion engine (Figure 14.7.1). Indeed, one can consider that the work required to run the motor with no load is substantially proportional to the compression work with no load, itself proportional to $(\rho^{\gamma-1} - 1)$. The compression ratio being much lower in a Stirling engine, the no-load losses are lower too, and experience confirms this analysis, as shown by the curve in Figure 14.7.1.

We have already indicated that it is possible to modify the work provided by a Stirling engine by acting on the working fluid pressure. It is this way that we can at best regulate the engine. In fact, acting on the amount of heat injected into the boiler induces too high delays, and carries the risk of overheating which can weaken the tube mechanical strength, already strained because of the pressure difference that exists between inside and outside.

The control principle is therefore, firstly to vary the average pressure of the working fluid depending on the desired capacity, using a compressor and an annex fluid reserve, which are needed to compensate for leaks, and secondly, to pilot the amount of fuel injected into the combustion chamber through a temperature control of tubes at a value possibly modified by the user. In addition, a Stirling engine runs much quieter than diesel or gasoline because the combustion is continuous, and torque is more regular.

Figures 14.7.2 to 14.7.4 show various views of a 750 We and 5 kW thermal power WhisperGen cogeneration module of New Zealand society Whispartech. Its Stirling engine is four-piston double-acting kinematic type. Its dimensions are: width 450 mm, depth 500 mm, height 750 mm, and its mass is 90 kg. In Figure 14.7.2, the combustion chamber is situated in the upper part, the heating

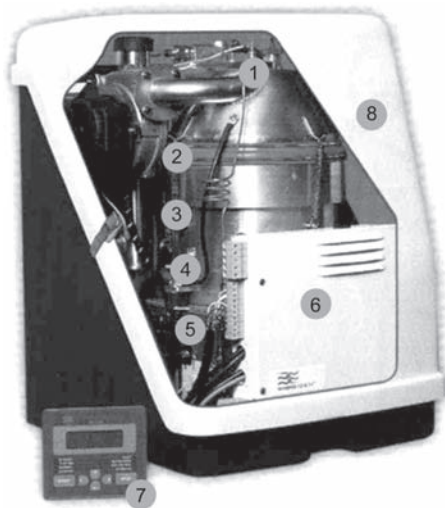


FIGURE 14.7.2
WhisperGen module, Documentation WhisperTech

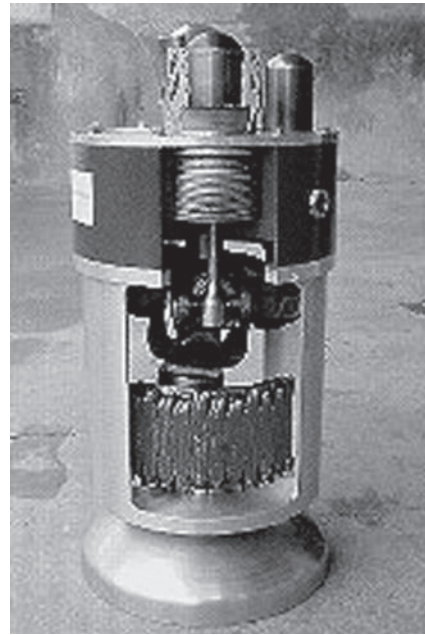
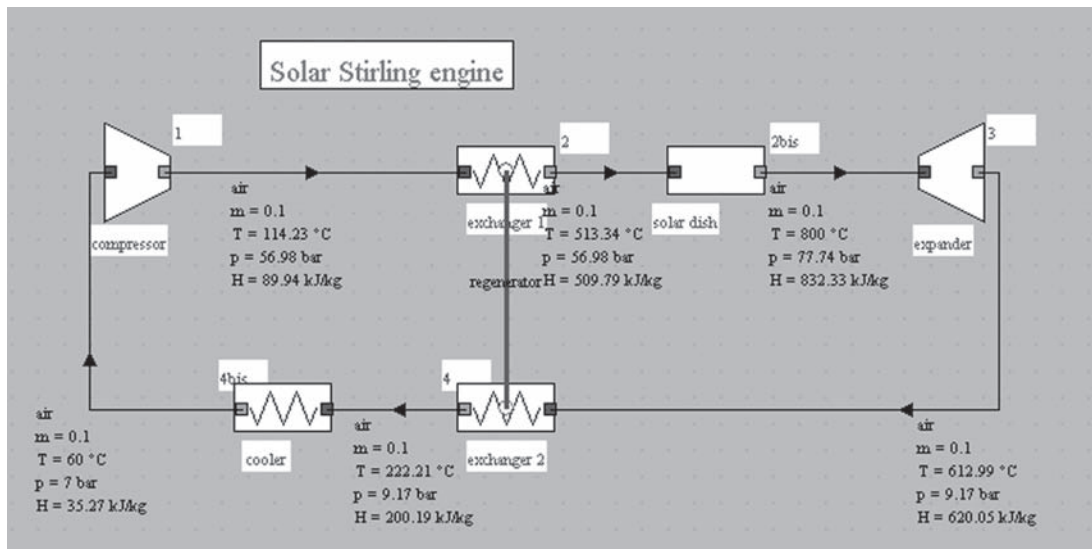


FIGURE 14.7.3
Cutaway of the WhisperGen module, Documentation
WhisperTech



FIGURE 14.7.4
WhisperGen module in test, Documentation DR-GDF

**FIGURE 14.8.1**

Synoptic view of a solar Stirling engine

and cooling heat exchangers, respectively in 2 and 3, the drive mechanism in 4, the alternator in 5, and the microprocessor control and the control box in 6 and 7. These features can be found on the cutaway of Figure 14.7.3.

14.8 SIMPLIFIED STIRLING ENGINE THERMOPTIM MODEL

The ThermoOptim model that we present corresponds to a Stirling engine placed in the focal region of a solar dish such as that presented in section 30.4 of Part 4. Although rather simple, this model allows us, however, to illustrate how to operate. It could be improved by developing well-designed external classes, especially to represent the regenerator.

This model implements six components:

1. a compressor operating in closed system, set compression ratio (here taken equal to 7);
2. an exchange process representing the hot part of the regenerator;
3. an external process corresponding to the solar concentrator. The latter is a variant of class SolarConcentrator.java that performs calculations in a closed system;
4. an expansion process operating in a closed system of set expansion ratio (here taken equal to 7);
5. an exchange process representing the cold part of the regenerator, and coupled by a heat exchanger representing the hot part;
6. an exchange process to model heat transferred to the cold source.

We retained as hypothesis on the one hand that compression is partially cooled and expansion partially heated, their polytropic efficiencies being equal to 0.9, and secondly that the effectiveness of the regenerator is equal to 0.8.

The results provided by the model are summarized in Figure 14.8.2, which shows the screen of the external driver developed to build up its energy balance. Its code is presented in section 23.7 of Part 4.

The power output is 26.8 kW, and the efficiency 41%.

solar Stirling energy balance			
	power	heat	
compression	22.320	-18.410	Calculate
expansion	-49.140	33.280	
solar collector		32.250	
external cooling		-20.300	
net power	-26.820		
			efficiency
total heat supply		65.530	0.410

FIGURE 14.8.2

Stirling engine driver screen

This model is not entirely satisfactory, since the regenerator model is made using components operating in an open system, like that of the external cooling. The mix of components operating in a closed system and others in open system also has the effect that the overall balance is not entirely satisfactory.

REFERENCES

G.T. Reader, C. Hooper. *Stirling engines*, Spon Editors, London 1983.

P. Stouffs. *Machines thermiques non conventionnelles, état de l'art, applications, problèmes à résoudre*, Société Française des Thermiciens, Thermodynamique des machines thermiques non conventionnelles, Comptes rendus de la journée du 14 octobre 1999.

G. Walker. *Stirling-cycle machines*, Clarendon press, Oxford 1973.

FURTHER READING

G. Descombes, J. L. Magnat. *Moteurs non conventionnels*, Techniques de l'Ingénieur, Traité Génie Mécanique, BM 2593.

W. B. Stine. *A compendium of solar dish/Stirling technology*, Sandia national laboratories, SAND93-7026 UC-236, 1994.

This page intentionally left blank

Steam Facilities (General)

Abstract: Steam is widely used in energy conversion systems, because it has many assets. This chapter deals with steam networks and thermodynamic optimization of their design.

The main components which compose these networks are presented and major problems related to their use are discussed: deaerators, water treatment, blowdown, boilers, steam generators, impulse and reaction turbines, extraction and back-pressure turbines, condensers and cooling towers.

Technologically, we will discuss only those aspects that affect energy balance of facilities. Therefore, despite their fundamental importance in practice, we will not discuss security issues related to pressure, or those relating to differential dilatation of facilities, or the layout of the piping system.

Keywords: water, steam, deaerator, water treatment, boiler, feedwater, blowdown, economizer, vaporizer, superheater, impulse turbines, reaction turbines, extraction, back-pressure, cooling tower.

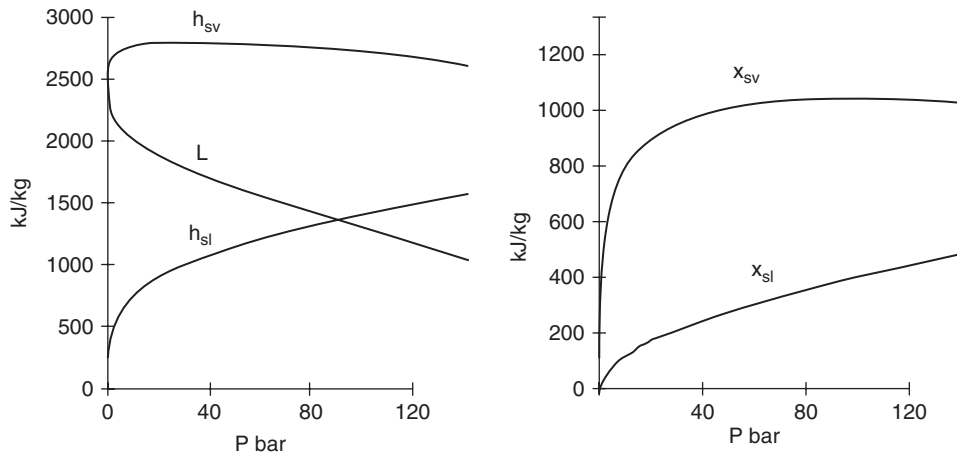
15.1 INTRODUCTION

Water vapor (steam) is a fluid that has many advantages, which explains why its use is so widespread:

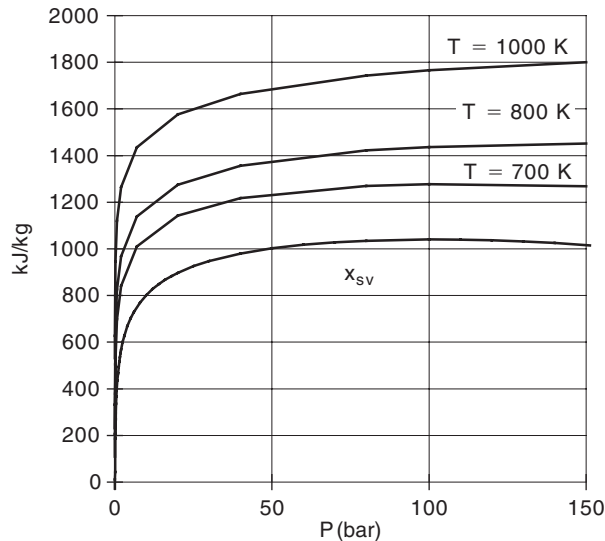
- Firstly, it is natural, inexpensive, available almost everywhere, non-polluting, and poses no fire hazard;
- its thermodynamic characteristics are very attractive, especially its very high latent heat of vaporization. The temperature and pressure levels to which it can be used do not pose particular technological problems, as long as certain precautions are taken;
- it has many uses, especially the possibility of generating driving force by expansion, and of course to transfer heat as a single phase (liquid or vapor) as well as a two-phase fluid;
- Finally, it can be produced in boilers burning many fuels including heavy oil, coal, garbage etc.

15.2 STEAM ENTHALPY AND EXERGY

As shown in graphs of Figure 15.2.1, the specific enthalpy of saturated steam h_{sv} remains almost constant between 10 and 70 bar, the decrease of the latent heat of vaporization L being offset by the growth of the liquid saturation enthalpy h_{sl} .

**FIGURE 15.2.1**

Enthalpy and exergy of steam

**FIGURE 15.2.2**

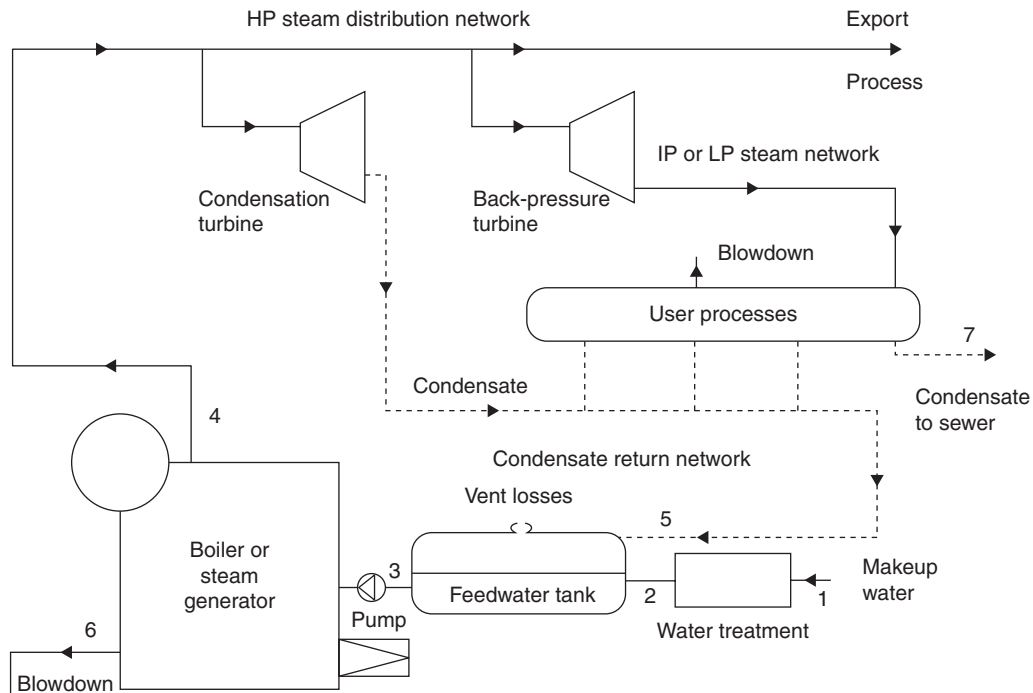
Steam exergy

Similarly, the saturated steam exergy (calculated for $T_0 = 300$ K) increases very rapidly up to about 40 bar, and then remains relatively stable.

The graph in Figure 15.2.2 shows that, at given superheating temperature T , steam exergy increases sharply from 0 to 50 bar, and then varies relatively little with pressure. For $T = 700$ K (427°C) it reaches a maximum for $P = 100$ bar.

The exergy charts of Figures 5.6.13 and 5.6.14 of Part 2, set for $T_0 = 288.15$ K, confirm these findings and directly provide exergy available in a greater range of pressures and temperatures.

Given that increased pressure induces increasingly expensive mechanical stresses, there is usually an economic optimum at pressure level between 30 and 80 bar, except for special facilities such as steam power plants of very high capacity.

**FIGURE 15.3.1**

Steam system

15.3 GENERAL CONFIGURATION OF STEAM FACILITIES

The diagram in Figure 15.3.1 shows the different components of a steam network:

- water supply: raw water comes in 1, bottom right. This water must be treated to prevent network fouling and corrosion. In 2, the treated water is introduced into the feedwater tank, where it mixes with the condensate returning from the network, after use by the various processes or heating or production of power equipment;
- water deaeration: the feedwater tank shown also plays a fundamental role: to deaerate the water. Deaeration eliminates gases dissolved in water, especially carbon dioxide and oxygen, very corrosive for the boiler and the return piping. Moreover, the presence of air or non-condensable gases has the effect of limiting the exchange coefficients by forming a film that opposes heat transfer, increasing the gap between the condensation and coolant temperatures;
- steam generator: at the deaerator output, water is pressurized by a feedwater pump, then headed to the steam generator, where it is heated as a liquid in the economizer, vaporized in the vaporizer, and then superheated. Separators provide dry vapor to prevent liquid water from being carried in the steam system. This drive phenomenon called priming can sometimes occur despite precautions taken. The causes may be either a bad water treatment, which leads to too high a salt concentration, a sudden call of steam or a boiler design error. Although the words boiler and steam generator can be considered synonymous, we reserve the second to describe devices without combustion;
- blowdown: without it, as salts dissolved in water do not vaporize, their concentration in the boiler increases beyond acceptable values (corrosion) due to the introduction of additional water in 1;
- steam utilization stations: superheated steam in 4 exits the boiler and is routed to utilization stations. As indicated, it is common for steam systems to consist of several sub-networks,

high pressure HP (>40 bar), intermediate pressure IP (≈ 20 bar) and low pressure LP (4 bar), depending on user needs. Part of the steam can also be exported to another part of the plant or external customers. A turbine and various processes are shown in the diagram;

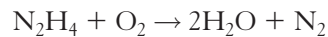
- condensate return: after use, steam is expanded, typically at atmospheric pressure, and condensate are redirected to the feedwater tank (5), if they are clean enough, discharged to the sewer (7) otherwise. Moreover, condensate discharges are performed for various reasons in utilization stations, thanks to steam traps. All these losses account for the need to provide extra water.

15.4 WATER DEAERATION

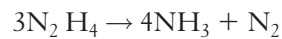
Deaeration can be achieved by chemical or thermal processes.

15.4.1 Chemical deaeration

The reactant used to extract oxygen is hydrazine (N_2H_4):



The excess hydrazine decomposes in the boiler in nitrogen and ammonia:



Ammonia taken away by steam helps to raise the condensate pH, and combines with carbon dioxide to produce ammonia bicarbonate. In case of chemical deaeration, the use of copper in the condensate return system should be prohibited.

The use of chemical deaeration is limited to small installations, or as an adjunct to thermal deaeration.

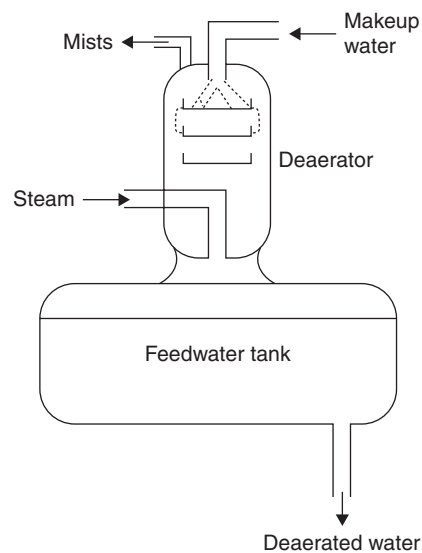


FIGURE 15.4.1

Sketch of a deaerator

15.4.2 Thermal deaeration

According to Henry's Law, the solubility of a gas is proportional to its partial pressure in the gas phase, the proportionality coefficient ϕ being function of temperature. In the case of oxygen, ϕ passes through a minimum around 100°C and varies little between 75 and 125°C.

Deaeration is ensured by boiling the feedwater, which reduces the partial pressure of O₂ and CO₂ (Figure 15.4.1). Gases released are then discharged into the atmosphere either through a vent if the pressure of the deaerator is greater than atmospheric pressure, or by extraction through a vacuum pump if it is lower.

The main drawback of vacuum deaeration is that in case of leakage, there is air intake, which is exactly counter-productive. Therefore deaerators typically operate at a slight overpressure, at temperatures around 110 to 120°C and up to 150°C. Condensate return temperature being between 50 and 80°C, it is necessary to provide additional heat to the feedwater tank. At the deaerator output, the oxygen content of the feedwater is between 0.007 and 0.02 mg/l.

15.5 BLOWDOWN

To maintain the concentration of salts in the boiler within limits recommended by manufacturers, it is necessary to practice condensate discharges, continuous or intermittent, which are based on the one hand on the quality of makeup water, and on the other hand on the proportion of condensate return. They are called blowdown.

They are characterized by the blowdown rate D/V, ratio of blowdown to steam produced. Sc being the limit boiler concentration, and Sb the average concentration in the feedwater tank, a mass balance on salt entering and exiting the boiler ($DSc - SbV = 0$ at equilibrium) easily shows that D/V is given by formula: $D/V = Sb/Sc$

Depending on circumstances, Sb and Sc are expressed in mg/l or °f (French degree).

For different salt classes, values of D/V to be met are successively calculated, and the highest is selected.

Without going into details of water treatment, it is important to know that the main existing salts are the following:

- incrustant salts (calcium, magnesium) characterized by total hardness TH, which measures the "hardness" of water (°f);
- alkaline salts (potassium hydroxide), characterized by the simple total alkali RT, and total alkali TAC (°f), the difference between the two values being linked to the presence of bicarbonates;
- chlorides, silicates, phosphates and sulfites, which are measured in mg/l. The measurement of chloride is often performed because it gives an indication of the total salt content, to which it is roughly proportional for a given facility.

As shown in Table 15.5.1, water characteristics recommended by manufacturers are the more stringent at high pressure.

The blowdown rate D/V can sometimes reach high values, especially in high pressure boilers, where concentrations limits Sc are low. This can result in significant energy loss if the residual enthalpy of the condensate discharges is not recovered, for example to provide the energy necessary for the proper functioning of the deaerator. For this it is possible to expand the steam discharges in a drum and send the flash steam in the feedwater tank or deaerator. The sensible heat of liquid expanded condensate discharges can also optionally be recovered in an economizer.

For example, if one has a feedwater of total alkali strength equal to 4, blowdown rate is equal to 3.3% at a pressure below 15 bar, 8% at a pressure between 25 and 35 bar, and 20% between 45 and 55 bar.

TABLE 15.5.1

Vapor pressure (bar)	< 15	25–35	45–55
Feedwater			
pH (cold)	8.5	8.5	8.5
TH maxi (°f)	0.3	0.15	0.05
Max oxygen (mg/l)	0.1	0.03	0.01
Boiler water			
Mini pH measured at 25°C	11.5	11.2	10.5
TAC maxi (°f)	120	50	20
TAC mini (°f)	25	15	5
Total salinity (mg/l)	2 500	1 500	1 000
Phosphates (mg/l PO ₄)	>30	>30	>30
Max silicate (mg/l SiO ₂)	150	40	15
Max SiO ₂ /TAC	1.5	1	1

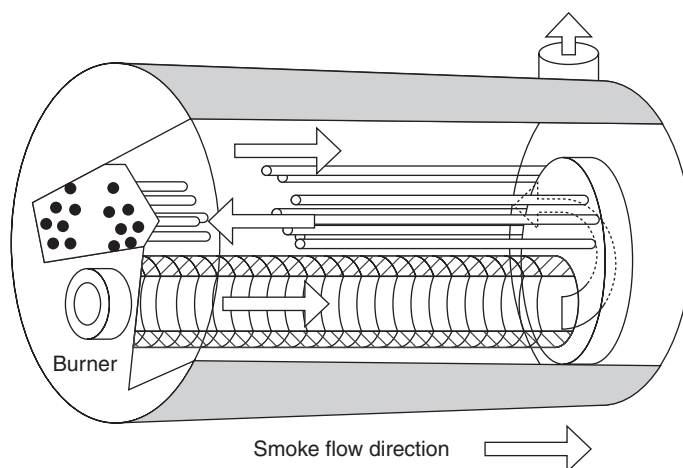


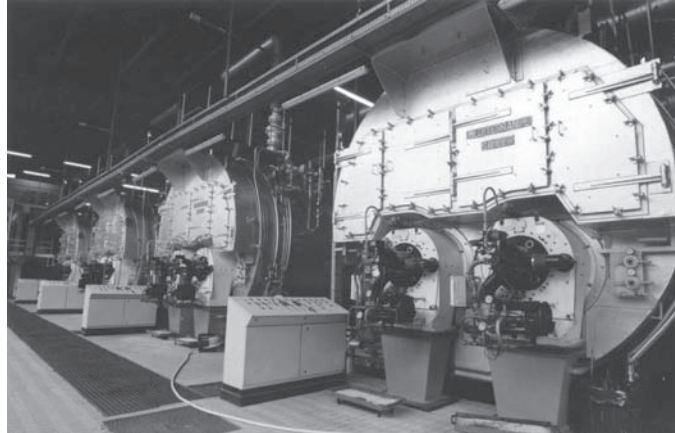
FIGURE 15.6.1
Fire tube boiler

15.6 BOILER AND STEAM GENERATORS

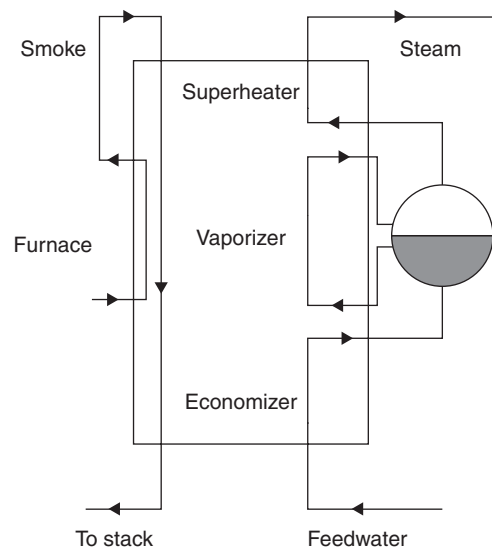
15.6.1 Boilers

There are two main types of boilers, known from the fluid that circulates inside the tubes: fire tube boilers, and water tube boilers.

- * in the first (Figures 15.6.1 and 15.6.2), the flame develops in a corrugated tube, then flue gases pass inside tubes, in one or more passes, water being on the outside;
- * within the second type (Figure 7.6.7 of Part 2), water circulates by natural or forced convection between two drums placed one above the other, through a network of tubes (except in supercritical boilers which will be studied in section 16.1.6). The flame develops in a furnace lined with tubes that absorb the radiation. A second tube bundle receives its heat from the flue gases by convection. The water rises in the tubes subjected to radiation, and falls by the convection assembly.

**FIGURE 15.6.2**

Industrial boilers, Documentation SECC

**FIGURE 15.6.3**

Boiler exchange configuration

Fire tube boilers can achieve flue gas temperatures lower (220 to 250°C) than water-tube boilers (300°C) without an economizer, which gives them a slightly better efficiency.

However, the former are limited to capacities lower than the latter, for reasons of mechanical strength and safety (very large volume of water under pressure).

Their main domain of use is the supply of saturated steam at low pressure (<15 bar), which represents over 60% of the French fleet of boilers, against 20–25% for water tube boilers, which are well suited for the supply of superheated steam at medium and high pressure.

A boiler has three successive functions:

- heat pressurized feedwater (in the economizer) to the vaporization temperature corresponding to the pressure;
- vaporize steam;
- and finally superheat steam at the desired temperature.

It behaves like a triple heat exchanger, and may be represented in terms of heat exchange by the diagram in Figure 15.6.3.

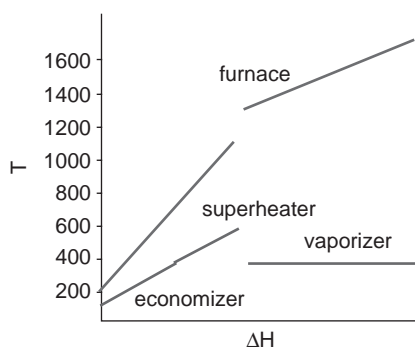


FIGURE 15.6.4
Temperatures in a boiler

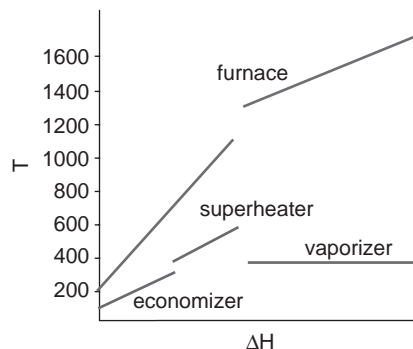


FIGURE 15.6.5
Temperatures in a boiler with vaporizer approach

In a conventional high temperature boiler, flame temperature reaches very high values (1400 to 1500°C). Heat is transmitted to steam mainly in form of radiation, with very high flux densities (100–200 kW/m²). Steel tubes are, for economic reasons, limited to temperature of 650°C maximum, which requires them to be very well cooled from the inside. Given the low gas exchange coefficients, this is only possible if the fluid that passes through the tubes is liquid, or better still, two-phase.

For this reason, the first exchanger is the furnace-vaporizer. Upon exiting the furnace, gas temperature has dropped significantly (800–900°C) and convection takes over from radiation. The second series of gas-gas exchangers corresponds to superheaters. At the output, fumes are cooled at around 600°C, and residual enthalpy is then used in economizers, gas-liquid heat exchangers which ensure the heating of water at its boiling temperature at the pressure considered. Where appropriate, a heater can then be used (in large boilers) to preheat combustion air.

The exhaust temperature of flue gases in the atmosphere should be as low as possible to maximize the efficiency of the boiler. The need to avoid condensation of smoke prevents however cooling as much as desirable, as it contains sulfur oxides which can form corrosive acids.

The graph in Figure 15.6.4 illustrates in an enthalpy diagram heat exchange in a classic steam plant boiler. The upper curves correspond to furnace and smoke cooling, the lower ones to the evolution followed by water. The discontinuity between the two segments of the upper curve is due to the furnace radiative contribution.

As shown, heat exchange is done with very large temperature differences, always greater than 180 K. At the end of the economizer, they are above 250 K. If the boiler control is not perfect, there are in these conditions significant risks that the vaporization starts in economizer, which is not designed for that. To prevent this malfunction, liquid heating is stopped before reaching the boiling point, maintaining an approach temperature difference of the order of a few tens of degrees. The missing enthalpy is then supplied by the vaporizer. The graph in Figure 15.6.4 is amended as shown in Figure 15.6.5.

15.6.2 Steam generators

According to what has been stated above, we call steam generators (SG) devices where heat is not provided by combustion. Among them, we will focus here particularly on devices for recovering heat in thermal effluents, including gas (the heat recovery steam generators (HRSG) are sometimes called recovery boilers). Nuclear power plant steam generators are presented in section 16.4.

Most HRSGs are variations of water tube boilers. The main differences come from the fact on the one hand that the temperature levels of effluents are much lower than those achieved in a boiler,

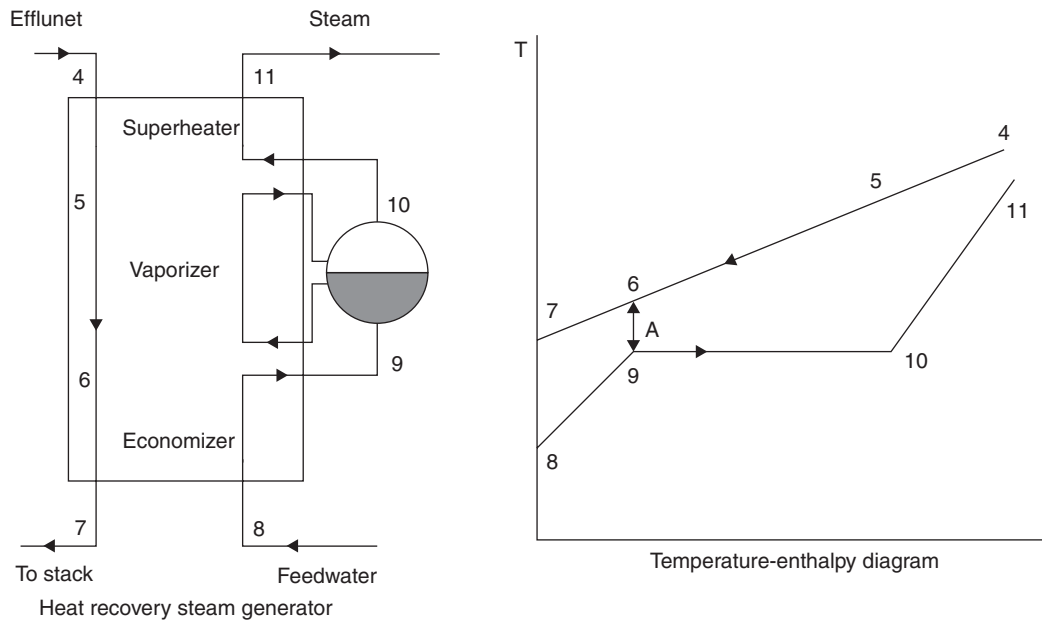


FIGURE 15.6.6

Steam generator exchange configuration

and on the other hand that heat exchange takes place only by convection. Nothing in these conditions prevents the superheater from being positioned upstream of the vaporizer, and the HRSG operating sketch and enthalpy diagram become as shown in Figure 15.6.6.

At point 6 on the diagram, you can see a minimum A in the temperature difference between the two fluids, called the pinch (see section 8.2.6 of Part 2). This point plays a fundamental role in the design of HRSGs, as it represents the smallest difference in temperature in the facility. To reduce the cost of equipment, it is preferable that the pinch is not too low. However, the thermodynamic optimization of the complete system requires it to be as small as possible.

Particular attention should be paid to the HRSG design at this pinch, which must exceed a minimum value of about $10\text{--}15^\circ\text{C}$, otherwise vaporization cannot be done at the desired temperature.

Moreover, exhaust gas temperature T_7 (stack temperature) must be high enough to avoid condensation of sulfur oxides that may be present. This temperature differs depending on the fuel used. The lowest values ($<90^\circ\text{C}$) are obtained with natural gas. With light oil T_7 is recommended to be greater than $120\text{--}130^\circ\text{C}$ and $150\text{--}170^\circ\text{C}$ with heavy oil.

But a second requirement must be met: one must avoid, at the beginning of the economizer, any condensation on heat exchanger tubes at a temperature just above T_8 , steam cycle condensation temperature. For this, it is sometimes necessary to provide a partial economizer recirculation.

In the same manner as in classic steam plant boilers it may be necessary to restrict liquid reheat to avoid boiling in the economizer. The differences in temperature between the water system and the effluent being much smaller than in a boiler, the temperature difference may be lower.

15.6.3 Boiler operation

The vaporizer consists of two drums superimposed and connected by two bundles of tubes called hot leg and cold leg (Figure 15.6.7). In the upper tank, the emulsion produced by the vaporization in the hot leg crosses water separators and steam dryers. Separated water goes back down through the cold leg, and mixes with water from the feedwater tank.

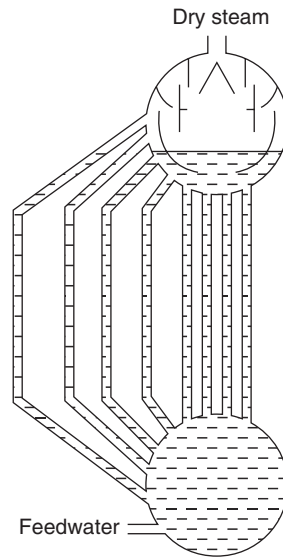


FIGURE 15.6.7

Water tube drums

In the vaporizer passes a total flow greater than that of steam produced. We call recirculation rate τ the ratio:

$$\tau = \frac{\text{total flow rate}}{\text{steam flow rate}}$$

The recirculation flow is obviously equal to $(\tau - 1)$ times the steam flow.

According to boilers, water flows either naturally or through a pump. The current values of τ are around 8 to 10.

15.6.4 Optimization of pressure level

In the case of a boiler, due to the very high temperatures that are reached in the furnace, as shown in Figure 15.6.5, there is no pinch: the boiler efficiency is independent of the steam system pressure level, which can be chosen solely based on use constraints.

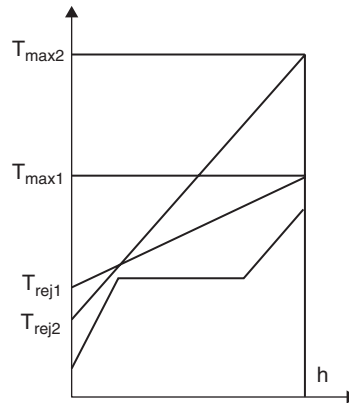
In the case of energy recovery from effluents, this is not necessarily the case: the recovery efficiency depends on both the effluent temperature and the pressure level of the steam system.

As shown in the graph in Figure 15.6.8, for a given steam pressure (and hence a given pinch), and for a fixed maximum enthalpy, we find that, when T_{\max} varies, it is as if the effluent line pivoted around the pinch.

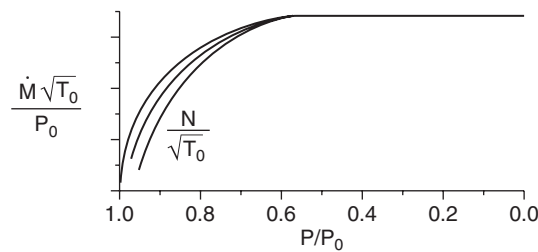
Because the effluent cools from T_{\max} , maximum temperature to T_{rej} , the exhaust temperature, T_{rej} should be as low as possible so that energy recovery is maximized.

Calling T_{rejlim} the limit exhaust temperature compatible with the corrosive condensation constraints, we can qualify the maximum energy recovery by an effectiveness which depends only on the nature of the effluent:

$$\varepsilon_{\text{ef}} = \frac{T_{\max} - T_{\text{rej}}}{T_{\max} - T_{\text{rejlim}}}$$

**FIGURE 15.6.8**

Effluent line

**FIGURE 15.7.1**

Characteristics of a turbine

As shown in Figure 15.6.8, at given T_{\max} , T_{rej} increases (and therefore ε_{cf} decreases) when the network pressure level increases. Optimization of steam system can no longer be done independently of the HRSG. We shall see in Chapter 17 the implications this has for the design of combined cycles.

15.7 STEAM TURBINES

For a given rotation speed N , the performance map of a turbine has the appearance of Figure 15.7.1.

As can be seen, there is a flow rate limit corresponding to the establishment of a sonic flow at the nozzle throat: the flow is said to be choked.

The graphs in Figure 15.7.2 provide the look of the characteristics of the turbine (inlet pressure function of the mass flow when the outlet pressure is set, and outlet pressure function of the mass flow when the inlet pressure is set).

15.7.1 Different types of steam turbines

Depending on their use, there are four broad categories of turbines (Figure 15.7.3):

- condensing turbines, where steam is completely expanded at a pressure of about 0.02 to 0.04 bar, and then liquefied in a condenser cooled by ambient air or by water. This type of turbine is mainly used in the power production facilities;

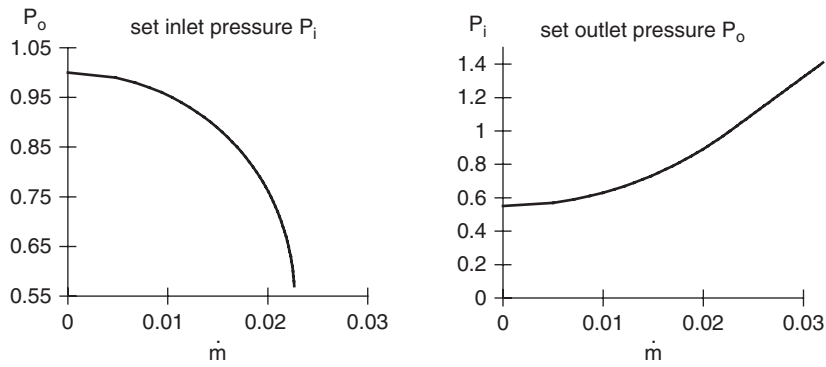


FIGURE 15.7.2

Turbine characteristics

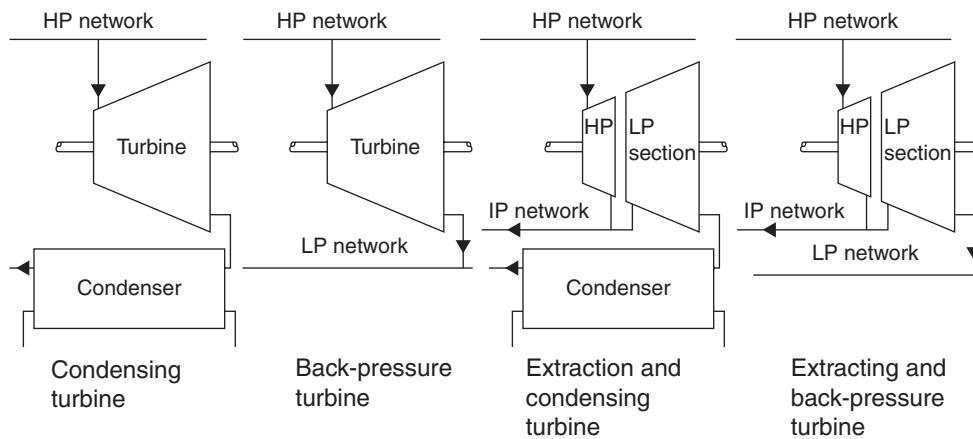


FIGURE 15.7.3

Different types of steam turbines

- back-pressure turbines, in which vapor pressure is expanded from HP pressure (>40 bar) at low pressure (about 4 bar). This type of turbine allows production of mechanical power or electricity thanks to the high temperature and pressure that can be obtained in a boiler, while using the residual enthalpy for various processes;
- extracting and condensing turbines, in which vapor undergoes partial expansion at an intermediate pressure (about 20 bar) in a high pressure section. One part is directed to a user network, while the rest of the steam is expanded in a low-pressure section, as in a condensing turbine. This type of turbine finds an important field of application in cogeneration plants whose requirements for heat are likely to vary considerably over time;
- extracting and back-pressure turbines, in which steam escapes at low pressure in a LP network instead of being condensed.

Most steam turbines are multistage axial turbines, which can be grouped into two broad classes, depending on how expansion is divided between the stator and rotor (let us recall, cf. section 7.5.5 of Part 2 that the degree of reaction ε of a stage is the fraction of the enthalpy change that takes place in the rotor):

- **impulse turbines**, in which the degree of reaction ε is 0: any expansion of the fluid is then carried out in fixed blades or nozzles, upstream of the wheel, and pressures upstream and downstream of the rotor are equal;
- **reaction turbines**, where $\varepsilon = 0.5$: expansion is then evenly distributed between the nozzle and the wheel.

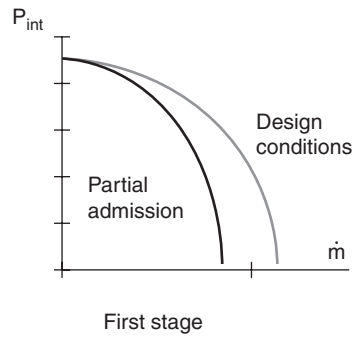


FIGURE 15.7.4
First stage partial admission

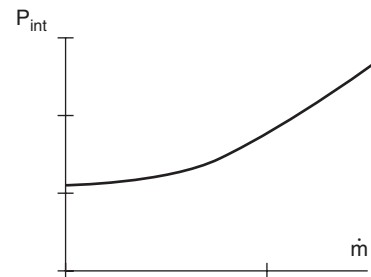


FIGURE 15.7.5
Behaviour of downstream stages

Each of these two turbine types has advantages and disadvantages of its own: the impulse turbines are generally used for multistage turbine head stages or for small capacity units, while reaction turbines turn out to be well adapted for low-pressure turbines.

15.7.2 Behavior in off-design mode

The characteristics presented above allow us to give some indication on the part-load operation of a steam turbine. We assume in what follows that the rotation speed of the turbine does not vary, which is usually the case. However, as the characteristics of the turbines are relatively insensitive to the rotation speed, the reasoning presented retains its full generality.

Remember however that a more comprehensive study of the off-design behavior of turbines will be conducted in Chapter 37 of Part 5. The following considerations are limited to steam turbines.

The change in work τ_r supplied by a turbine, for a fixed inlet temperature T_a , which is usually the case in a boiler, can be obtained either by changing the flow-rate \dot{m} or by acting on the expansion ratio P_r/P_a .

In practice, two methods of power control are used in turbines:

- fixed pressure control, where flow is modulated by action on control valves;
- sliding pressure control, where pressure in the boiler changes.

15.7.2.1 Fixed pressure control

This adjustment method, the most common and simplest, can be used if the turbine topping stages are of the impulse type. To achieve this, we proceed in two complementary ways.

Firstly, we feed the first stage only partially, by blocking some of the distributors. In these circumstances, the passage section devoted to the steam is reduced in proportion to the number of valves closed. The characteristic of the first turbine stage is modified as shown in the diagram in Figure 15.7.4 (P_{int} is the pressure at the outlet of this stage).

In the rest of the turbine, the flow area of the steam has not been amended, and the characteristics remain unchanged. Assuming that the output pressure P_r does not vary (case of a condenser for example), the operating point moves on the characteristics to adapt to new conditions (reduced flow). This results in a decrease of P_{int} , inlet pressure in these stages and at the outlet of the first stage (Figure 15.7.5).

The pressure difference in the first stage therefore increases accordingly, which on the one hand is partially offsetting the decline in flow due to the closure of valves, and also operates the first stage with an inappropriate pressure ratio. So its isentropic efficiency drops.

The graph of Figure 15.7.6 shows the evolution of the turbine operating point, which passes from A to B, while the flow-rate decreases.

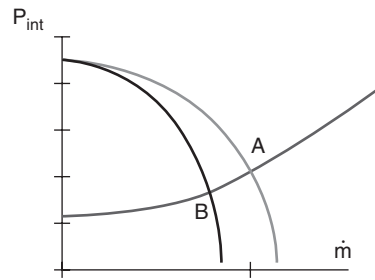


FIGURE 15.7.6
Fixed pressure control

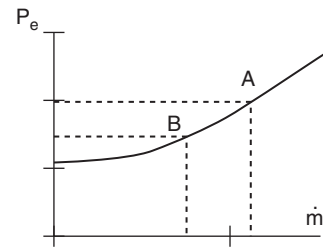


FIGURE 15.7.7
Sliding pressure control

All these effects are reflected both in lower flow-rate and lower specific work supplied by the turbine, which reduces the work done τ_t . Then, since the valve closure is done continuously, we use a steam partial throttling before it enters the turbine first stage. Under these conditions, the drop in enthalpy in the turbine is reduced by irreversibilities due to throttling, which further reduces their work.

15.7.2.2 Sliding pressure control

This control method, which has been used only for the last seventy years, is to feed the turbine at substantially constant temperature by varying the pressure in the boiler. Under these conditions, the characteristics of the entire turbine according to the inlet pressure look as shown in Figure 15.7.7. A decrease of P_a induces well in a decrease in flow, the operating point moving from A to B. It is of course possible to remove valves of the adjustment wheel. However, they are usually kept in order to use if appropriate control by partial admission or throttling if necessary.

The sliding pressure control presents a number of advantages over fixed pressure control:

- it reduces the compression work of the feed pump, which, although small, is not always negligible;
- working at sliding pressure, the inlet temperature in the topping stage remains constant, which helps limit the transient thermal stresses in this device;
- the expansion efficiency is not as affected by the part-load as it is in the alternative control because of the many irreversibilities that arise. However, this gain may be offset by any loss of efficiency on the full cycle, due to the lower steam pressure.

In contrast, the sliding pressure adjustment also has some drawbacks:

- the steam generator must be able to adapt to the change in pressure, which means that its inertia is small. This adjustment method is therefore excluded for boilers with fire tubes. Obviously, it is therefore the boiler that has to operate at variable temperatures;
- when several turbines are connected in parallel, each must be powered by a separate boiler in order to adjust them independently in this way.

The examples presented above are based on the so-called “cone” rule, experimentally highlighted by Stodola in 1922. This rule, described in detail in section 37.4.3 of Part 5, states that the function $f(\dot{m}, P_a, P_r) = 0$ relating mass flow, inlet pressure and outlet pressure of the turbine operating in variable conditions is a conical surface.

15.7.3 Degradation of expansion efficiency function of steam quality

When the expansion of a fluid (usually steam) extends beyond the dew point curve, vapor begins to condense and droplets appear. The phenomenon is not immediate, because the equilibrium

conditions are not met, but it occurs gradually, more and more as the steam quality increases. The presence of these droplets leads to:

- mechanical damage of the front edges of turbine blades;
- reduction of the expansion isentropic efficiency.

For these two reasons, the permissible quality limit at the end of expansion should not be below about 0.8. To account for expansion isentropic efficiency degradation, we can use relation (15.7.1), α being the Baumann coefficient, close to 1, η_{hum} and η_{dry} being respectively the isentropic efficiencies for the humid zone and dry steam.

$$\frac{\eta_{\text{hum}}}{\eta_{\text{dry}}} = 1 - \alpha(1 - x) \quad (15.7.1)$$

This relationship shows that an increase of 1 point of the quality reduces the isentropic efficiency by about 1 point. It is not currently taken into account in the wet expansion calculated by Thermoptim. The reader can refer to the book by MM. de Vlaminck and Wauters (1988) for detailed explanations on this subject.

15.7.4 Temperature control by desuperheating

As we shall see, the optimization of a cycle generally leads to work with superheating temperatures technologically as high as possible. To regulate the temperature around this value, it is common to use steam desuperheating, an operation which involves injecting into superheated steam pressurized cold water from the feedwater tank. The injection, which is usually done between two elements of the superheater, is controlled by a control valve that adjusts the flow injected according to the superheater outlet temperature.

The industrial cogeneration facility studied in section 18.5.2 specifically implements such a desuperheating.

Note that this setting mode introduces a thermodynamic irreversibility because it mixes two flows at very different temperatures. In cycles where the conventional heat source temperature was very high, this irreversibility did not affect the overall efficiency, but this is no longer necessarily the case when the source is average temperature hot effluent, as in a cogeneration facility or combined cycle.

15.8 CONDENSERS, COOLING TOWERS

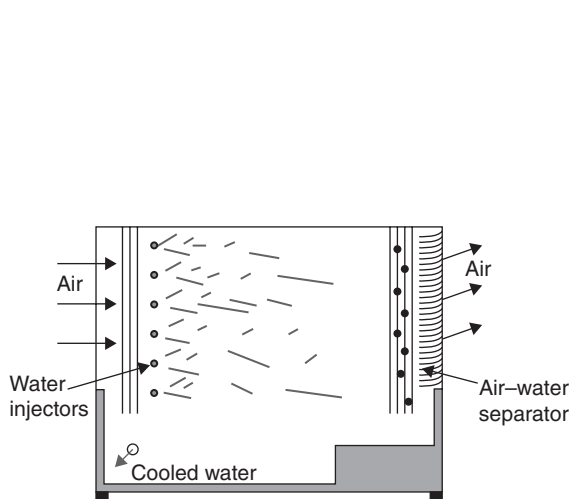
The performance of steam systems operating in closed circuit are very sensitive to conditions in which steam may be condensed. Indeed, a condenser is a heat exchanger of a particular type, phase change, whose thermal equilibrium determines the condensation temperature of steam, and thus its condensation pressure.

The cycle low pressure, which directly determines the power that the turbine can produce, is thus determined by the condenser.

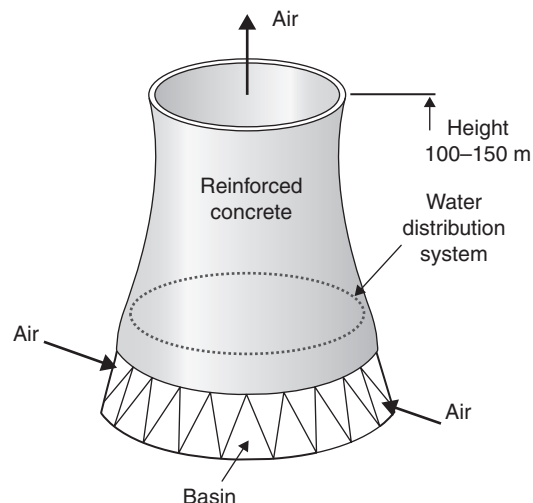
Heat power transferred to the condenser is typically removed by cooling water flowing inside the tubes, which must be renewed (open-loop cooling) or cooled by contact with ambient air (air cooling).

For systems that operate in open loop, cooling water is drawn and released directly in the sea or a river, after passing through the condenser, while in others, condenser cooling water circulates in closed circuit cooled with air, usually in a cooling tower.

In both cases, the amount of water required is very important, which is a burden, especially in the context of global warming and depletion of water resources. Section 16.1.7 introduces innovative cycles today proposed to reduce this constraint.

**FIGURE 15.8.1**

Direct contact cooling tower (Extract from *Techniques de l'Ingénieur – Génie énergétique*)

**FIGURE 15.8.2**

High-capacity power plant cooling tower (Extract from *Techniques de l'Ingénieur – Génie énergétique*)

As heat exchangers have been studied in Chapter 34 of Part 2, we will not develop more water-cooled condensers. In this section, we present cooling towers, previously not addressed.

15.8.1 Principle of operation of cooling towers

A cooling tower is a heat exchanger of a particular type that discharges heat in the surrounding air in the form of both sensible heat and latent heat due to the increase of its moisture. By working this way, it is possible to cool a fluid at a temperature a few degrees above the ambient air wet bulb temperature (and possibly below its dry bulb temperature), at the cost of a water consumption of about 5% of that which water cooling would require. Both economically and environmentally, cooling towers are very interesting systems, in particular in hot and dry climates.

There are two main types of cooling towers, called direct contact or open-cycle, and indirect contact or closed-cycle.

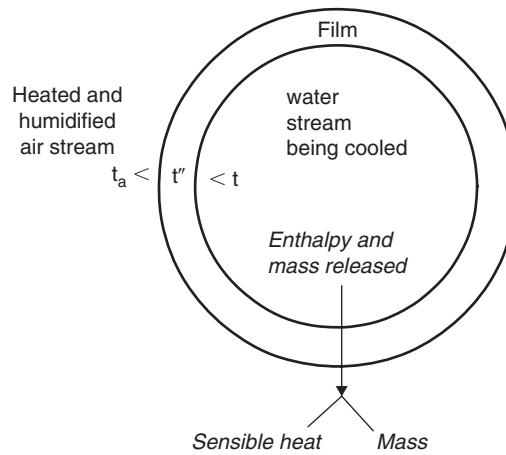
In a direct contact tower (Figures 15.8.1 and 15.8.2), hot water is cooled in contact with ambient air either by spraying fine droplets, or by runoff along flow surfaces. Both fluids being in contact, heat is exchanged by convection, and part of the water vaporizes, thereby increasing the humidity. If it is not saturated, it starts to cool in an almost adiabatic process, before warming up along the saturation curve. Therefore water may come out at a temperature lower than ambient air.

An indirect contact tower involves two circuits known as external and internal. In the latter, the cooling fluid, which can be arbitrary, remains confined in a tube bundle around which the external cooling circuit water runs. It warms on contact, then is cooled by exchange with ambient air by the same mechanism as in a direct contact tower.

15.8.2 Phenomenological model

The theoretical modeling of cooling towers is quite complex given the multiplicity of transfers that take place. The 2000 ASHRAE Handbook (Chapter 36) presents the theory proposed in 1961 by Baker and Shyrock, which considers (Figure 15.8.3) three media exchanging mass and energy:

- the flow of water that cools;
- the air flow which is heated and whose moisture increases;
- an interstitial film.

**FIGURE 15.8.3**

Sketch of transfers

The assumptions are:

- air leaving the tower is nearly saturated;
- the interstitial film is air saturated with moisture, at the water temperature;
- the Lewis number is equal to 1;
- thermal resistance on the liquid side is negligible compared to that on the air side (for indirect contact towers, it is assumed that the air-liquid film temperature gradient is equal to that of air-water cooling).

The water balance of a small tower element of surface ΔA , writes with our usual notations:

$$\Delta Q_{\text{water}} = \dot{m} C_{p_{\text{water}}} \Delta T_{\text{water}}$$

This energy is used firstly to heat air (ΔQ_s), and secondly to evaporate water absorbed by air (ΔQ_L).

$$\Delta Q_s = k_s \Delta A (t'' - t_a)$$

k_s being the heat exchange coefficient in the presence of mass transfer, t'' being the film temperature (assumed equal to that of water) and t_a that of air.

$$\Delta Q_L = k' \Delta A L_{\text{water}} (w''_{\text{sat}} - w_{\text{asat}})$$

k' being the conductance referred to mass transfer, w''_{sat} the film saturation moisture and w_{asat} that of air.

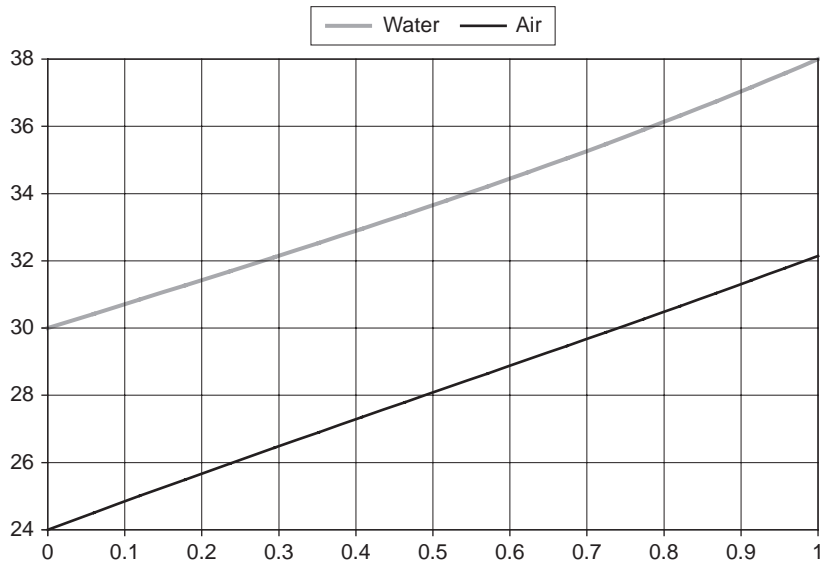
We have thus:

$$\Delta Q_{\text{water}} = \dot{m} C_{p_{\text{water}}} \Delta T_{\text{water}}$$

$$\Delta Q_{\text{water}} = k_s \Delta A (t'' - t_a) + k' \Delta A L_{\text{water}} (w''_{\text{sat}} - w_{\text{asat}})$$

In turbulent regime, Sc and Pr being the Schmidt and Prandtl numbers and Le the Lewis number, it can be shown that k and k' are related by the following equation:

$$\frac{k_s}{k' C_{p_{\text{air}}}} = \left[\frac{Sc}{Pr} \right]^{2/3} = Le^{2/3} \quad (15.8.1)$$

**FIGURE 15.8.4**

Profile of temperature in a direct contact cooling tower

It turns out that for water-air mixture, $Le \approx 1$ as long as $t_{\text{water}} < 50^\circ\text{C}$, as shown by Merkel in 1921 when he proposed to consider that for cooling towers $Le = 1$.

With this assumption, the above equation is simplified, showing the specific enthalpy q' :

$$\Delta Q_{\text{water}} = \dot{m} C_{p_{\text{water}}} \Delta T_{\text{water}} = k' \Delta A [C_{p_{\text{air}}} (t'' - t_a) + L_{\text{water}} (w''_{\text{sat}} - w_{\text{asat}})]$$

$$\Delta Q_{\text{water}} = k' \Delta A [q'_{\text{sat}}(t'') - q'_{\text{sat}}(t_a)] \quad (15.8.2)$$

This equation can be modified and allows us to write, per unit of water mass flow:

$$\frac{k' \Delta A}{\dot{m}_{\text{water}}} = \frac{C_{p_{\text{water}}} \Delta T_{\text{water}}}{q'_{\text{sat}}(t'') - q'_{\text{sat}}(t_a)} \quad (15.8.3)$$

This equation can be numerically integrated along the cooling tower, leading to results in Figure 15.8.4, which shows the evolution of temperatures in the tower as a function of reduced distance between its input and output.

This gives a performance indicator of the cooling tower, which appears in good agreement with experimental data.

Let us now recall a characteristic of heat exchangers, the number of transfer units NTU introduced Chapter 8 of Part 2.

Equation 8.2.1 of Part 2 gives the value of NTU:

$$NTU = \frac{UA}{(\dot{m} \cdot c_p)_{\min}} = \frac{\Delta T_{\max}}{\Delta T_{\text{ml}}} \frac{UA}{(\dot{m} \cdot c_p)_{\min}} \frac{\Delta T_{\text{ml}}}{\Delta T_{\max}}$$

As the heat fluxes exchanged are equal, $UA \Delta T_{\text{ml}} = (\dot{m} C_p)_{\min} \Delta T_{\max}$, and:

$$NTU = \frac{\Delta T_{\max}}{\Delta T_{\text{ml}}}$$

NTU can be physically interpreted as the ratio of the maximum variation in temperature in one of the fluids to the log-mean temperature difference between them. This is indeed an indicator of the quality of the device: the more efficient the heat exchanger, the more it allows for heating or cooling a fluid with a low temperature difference with the other.

The concept of NTU can be generalized by considering not the ratio of the temperature variations, but that of the enthalpy differences. One may in particular put in the denominator the average logarithmic difference of specific enthalpy of saturated air taken at the temperatures of the two fluids, and in the numerator the variation of enthalpy Δh of one the two fluids, the two being equal.

$$\text{NTU} = \frac{\Delta h}{\Delta h_{\text{ml}}} \text{ or } \text{NTU} = \frac{\Delta h}{\Delta q'_{\text{sat ml}}}$$

In these conditions, equation (15.8.3) of the tower elementary heat balance that we integrated is like an elementary NTU and integration provides the NTU of the tower. To differentiate it from normal NTU in exchangers, we will note it with index m (Merkel).

$$\Delta \text{NTU}_m = \frac{k' \Delta A}{\dot{m}_{\text{water}}} = \frac{C_{\text{Pwater}} \Delta T_{\text{water}}}{q'_{\text{sat}}(t'') - q'_{\text{sat}}(t_a)} \quad \text{NTU}_m = \int \frac{C_{\text{Pwater}} \Delta T_{\text{water}}}{(q'_{\text{sat}}(t'') - q'_{\text{sat}}(t_a))}$$

It is indeed an indicator of how difficult it is to realize the heat transfer in the cooling tower. Incorporating complex coupled phenomena of energy and mass exchange and dependent on technology implementation, it is not possible to give a simple expression.

We call the “approach” the pinch of the tower, i.e. the difference between the outlet temperature of the water and the wet bulb temperature of ambient air (4 K in the example in Figure 15.8.4) and the “range” the value of ΔT_{water} (8 K in this example).

NTU_m is usually given as a function of four variables: $\dot{m}_{\text{water}}/\dot{m}_{\text{air}}$ and T'_{ai} , the wet bulb air inlet temperature, as well as either the two water temperatures T_{wi} (inlet) and T_{wo} (outlet), or the values of range ($T_{\text{wi}} - T_{\text{wo}}$) and approach ($T_{\text{wo}} - T'_{\text{ai}}$).

If they operate in the same environment with the same water inlet temperature and fluid mass flow of same ratio, two different cooling towers will cool more or less water depending on the quality of their design: the better resulting in the lowest value of T_{wo} , and thus having a greater NTU_m .

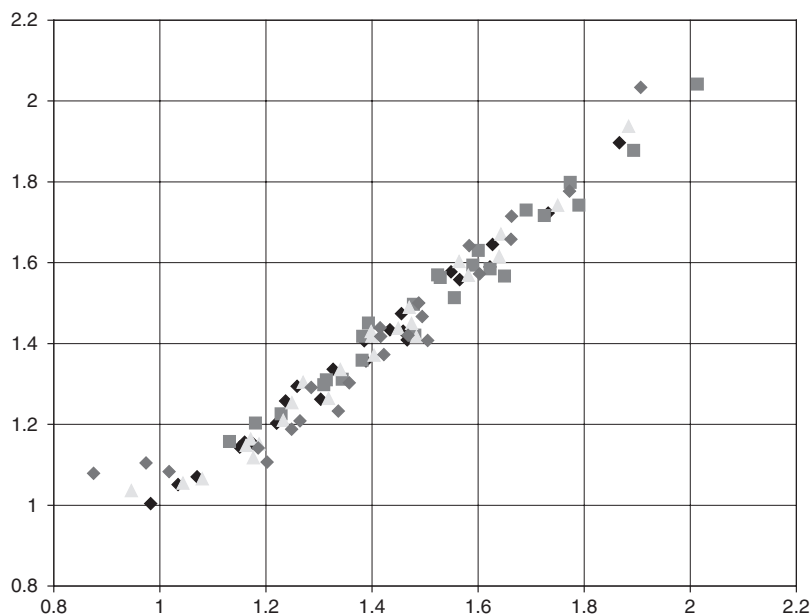
15.8.3 Behaviour models

Many authors have investigated the modeling of cooling towers, and sought expressions of NTU_m that are both easy to calculate and in agreement with experimental results. Since this is primarily an indicator of performance, it is not in itself unacceptable that there is a degree of arbitrariness in its definition, to the extent however that conventions are well specified.

15.8.3.1 Merkel model

Experience shows that when we modify the four input variables of a given cooling tower, NTU_m takes different values, which follow a behavior similar to the following, n and m being with negative values between -1.1 and -0.35 , and C being between about 1 and 2.5. C, m and n are called the tower coefficients.

$$\text{NTU}_m = C \left[\frac{\dot{m}_{\text{water}}}{\dot{m}_{\text{air}}} \right]^n \quad (15.8.4)$$

**FIGURE 15.8.5**Mapping of manufacturer data and NTU_m correlation**TABLE 15.8.1**

	F1221 40 hp	F1221 50 hp	F1221 60 hp	F1221 70 hp
C	2.19	1.87	1.93	2.06
n Merkel	-0.860	-0.968	-1.009	-1.171
r^2	0.970	0.982	0.963	0.853

or

$$NTU_m = C[\dot{m}_{\text{water}}]^n[\dot{m}_{\text{air}}]^{-m} \quad (15.8.5)$$

Note that one of the difficulties encountered when attempting to identify parameters C , n and m , is that available data are often incomplete. Manufacturers provide the values of inlet air wet bulb temperature, range and approach, as well as water flow, but not the value of the air inlet humidity. They are often content to give the power consumed by the air fan, or at best its volume flow, so that identification of the thermodynamic state of air in the tower is inaccurate. When conducting tests, it is also often very difficult to measure the actual airflow that passes through the machine.

Figure 15.8.5 shows very good correspondence between the values of NTU_m calculated for the same model of cooling tower (Marley F1221) with four different fan engines (40, 50, 60 and 70 hp). This figure was obtained from values provided in the manufacturer's catalog and volume flow rates communicated to us. A linear regression allows us to identify, for correlation (15.8.4), the values of the coefficients given in Table 15.8.1, with correlation coefficients r^2 .

Relation (15.8.4) also shows that for a given water flow, the larger the air flow, the smaller the tower can be. However, pressure drop and thus fan consumption are increasing functions of the air-flow (air velocities are generally between 1.5 and 4 m/s).

For indirect contact towers, the fact that the fluid to be cooled is contained within the internal circuitry increases thermal resistance. We obtained good correlations by increasing slightly the approach, by values between 0.7 and 1.6 K. This is easily explained when one considers that this device leads to lower NTU_m value, which is consistent with what should happen physically.

15.8.3.2 Cooling technology institute calculator

The Cooling Technology Institute has developed a tool called Toolkit, whose demo version is freely downloadable (<http://www.cti.org/>), which integrates the differential equation (15.8.3) giving NTU_m . A comparison with our results yields a very small difference, less than 2%, presumably due to a difference in fluid property modeling.

The mass flow of water being noted L and that of air G , the expression of NTU_m in American literature is generally:

$$NTU_m = \frac{K_a V}{L} = \int \frac{C_{p_{\text{water}}} \Delta T_{\text{water}}}{(q'_{\text{sat}}(t'') - q'_{\text{sat}}(t_a))}$$

In English units, $C_{p_{\text{water}}}$ being equal to 1, may disappear from the expression.

The cooling tower characteristics obtained have the appearance given in Fig 15.8.6, in bi-logarithmic coordinates. Abscissa is the ratio of the mass flow of water to that of air $L/G = \dot{m}_{\text{water}}/\dot{m}_{\text{air}}$ and ordinate is NTU_m . The design value is displayed in orange, as well as a curve representing the behavior model law (15.8.4). Yellow curves are iso-approach lines. By selecting a rectangle on the chart, zoom is shown (double-click restores the original scale).

This chart can be used to characterize a given tower:

- the value of NTU_m for design conditions is calculated;
- the line of slope n and constant C is plotted and adjusted on the design point;

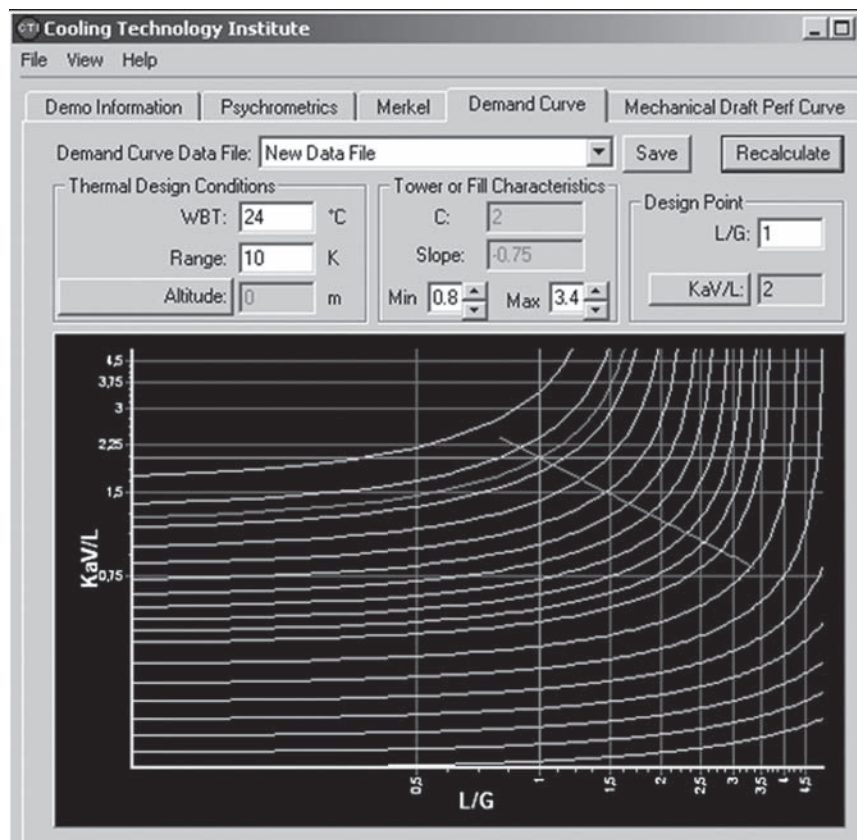


FIGURE 15.8.6

Cooling tower characteristics

- for other operating conditions, determined by the fluid flows, the abacus allows us to find, at abscissa L/G and on the tower characteristic line, the new values of NTU_m and approach, which determines the outlet water temperature and therefore the capacity. The air outlet temperature is deduced. For another cooling or other air wet bulb temperature, it is possible to recalculate another abacus. Knowing the values of variables (NTU_m , L/G) from the original chart, we get the new approach.

For example, the design conditions of Figure 15.8.6 correspond to an approach of 3.55 K (obtained by right-clicking the point in question).

15.8.3.3 Analogies with heat exchangers

Since it is the change in enthalpy of saturated moist air which best characterizes the air thermodynamic behavior, a number of authors consider that it is as if water did exchange with a fictitious fluid whose specific heat at constant pressure is equal to the average heat capacity of moist saturated air C_{pa}^{sat} , but it is also possible to express it in terms of specific heat of dry air.

We must therefore beware of the conventions used to avoid mistakes in calculations. The key is to be perfectly uniform throughout the approach: we must ensure that conventions used for identifying the values of C and n from experimental values are the same as those used to calculate ϵ and NTU .

The interested reader should refer to the referenced documents for more details.

One can for example calculate as average heat capacity that of moist saturated air between the extremes of water:

$$\bar{c}_{pa}^{sat} = \frac{h_a^{sat}(T_a^{min}) - h_a^{sat}(T_a^{max})}{T_a^{min} - T_a^{max}} \quad (15.8.6)$$

The flux transmitted to the air can be written $\phi = \epsilon \dot{m}_{da}(q'_{sat}(T_{wi}) - q'(T_a))$

It is ϵ times the maximum flux, equal to the product of the mass flow of dry air (index da) by the difference between the specific enthalpy of the air at water inlet temperature and its specific enthalpy at the entrance the tower. Furthermore:

$$R = \frac{C_{p_{water}}}{C_{p_a}^{sat}}, \quad \text{and} \quad NTU = C \left[\frac{\dot{m}_{water}}{\dot{m}_{air}} \right]^n$$

The values of C and n are identified from experimental data and the appropriate (ϵ , NTU) relation (see section 8.2.2 of Part 2). Values of these parameters are proposed in the literature (Kreith, 1999).

15.8.3.4 Recknagel method

In this model, effectiveness is only defined by temperatures:

$$\eta = \frac{T_{wo} - T_{wi}}{T_{wo} - T_{ai}^{sat}}$$

The model assumes that this effectiveness is given by equation: $\eta = C_t (1 - e^{-\lambda})$

With:

C_t constant called "tower characteristic"

$\lambda = I_0/I_{min}$ ratio of relative airflows I_0 and I_{min}

In an ideal cooling tower $I_{min} = \dot{m}_{air_min}/\dot{m}_{water}$ is the minimum airflow required for cooling a certain water flow-rate \dot{m}_{water} from T_{wi} to T_{wo} . This flow is obtained by reading a chart with T_{ai}^{sat} and T_{wi} as inputs (Figure 15.8.7).

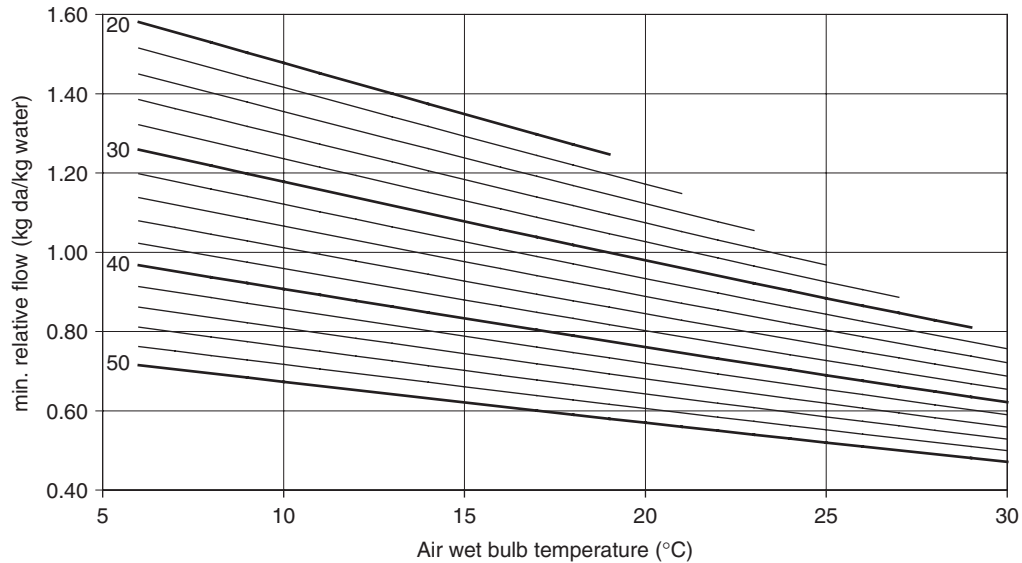
**FIGURE 15.8.7**

Chart for determining the minimum relative airflow I_{\min}

I_0 is the relative airflow actually necessary, i.e. the ratio between the airflow and the flow of water through the tower $I_0 = \dot{m}_{\text{air}} / \dot{m}_{\text{water}}$ (with the U.S. notations $I_0 = G/L$).

Finally, the tower characteristic C_t must be determined for each type of cooling tower, experimentally or through manufacturer curves.

The chart for determining the relative flow I_0 of minimum air is based on the equation linking the change in enthalpy of air to that of water, after simplification by the assumptions of the Merkel analysis mentioned above.

energy conservation

$$dT_{\text{water}} = \frac{\dot{m}_{\text{air}}}{(\dot{m}_{\text{water}} - d\dot{m}_{\text{water}})} \left[\frac{dh_{\text{air}}}{C_{p_{\text{water}}}} - dw_{\text{air}} T_{\text{wi}} \right]$$

mass conservation: $\dot{m}_{\text{air}} dw_{\text{air}} = d\dot{m}_{\text{water}}$

We deduce therefore that

$$dT_{\text{water}} = \frac{\dot{m}_{\text{air}} dh_{\text{air}}}{\dot{m}_{\text{water}} C_{p_{\text{water}}}}$$

Thus after integration

$$I_0 = \frac{\dot{m}_{\text{air}}}{\dot{m}_{\text{water}}} = C_{p_{\text{water}}} \frac{T_{\text{wi}} - T_{\text{wo}}}{h_{\text{ao}} - h_{\text{ai}}}$$

I_{\min} is defined as the minimum relative airflow, that is to say, in the ideal case (tower effectiveness equal to 1) where water is cooled at moist air temperature $T_{\text{ai}}^{\text{sat}}$ and air heats up at T_{wi} . Furthermore, not knowing air relative humidity, we have made the same assumption as for the calculation of I_0 : we assume that air is saturated.

All calculations done, we obtain:

$$I_{\min} = \frac{\dot{m}_{\text{air}_{\min}}}{\dot{m}_{\text{water}}} = C_{p_{\text{water}}} \frac{T_{\text{wi}} - T_{\text{ai}}^{\text{sat}}}{h_{\text{a}}(T_{\text{wi}}^{\text{sat}}) - h_{\text{a}}(T_{\text{ai}}^{\text{sat}})} \quad (15.8.7)$$

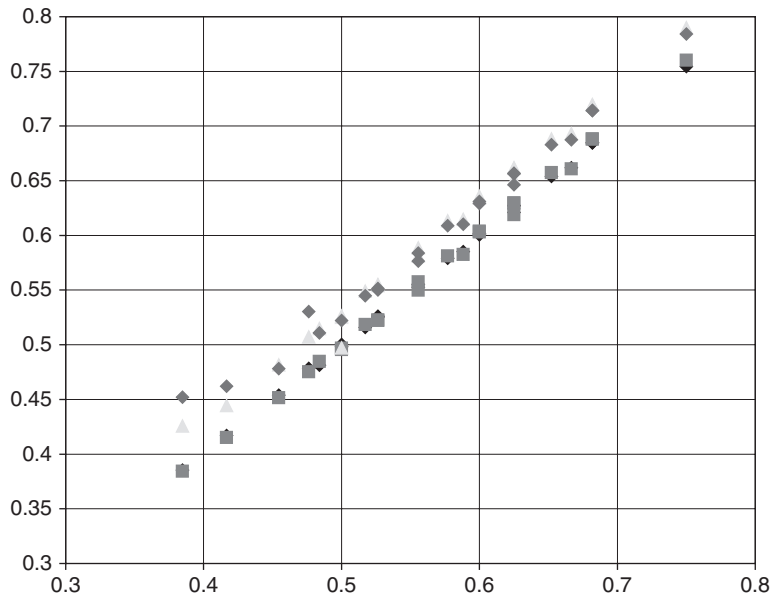


FIGURE 15.8.8
Mapping of manufacturer data and correlation η

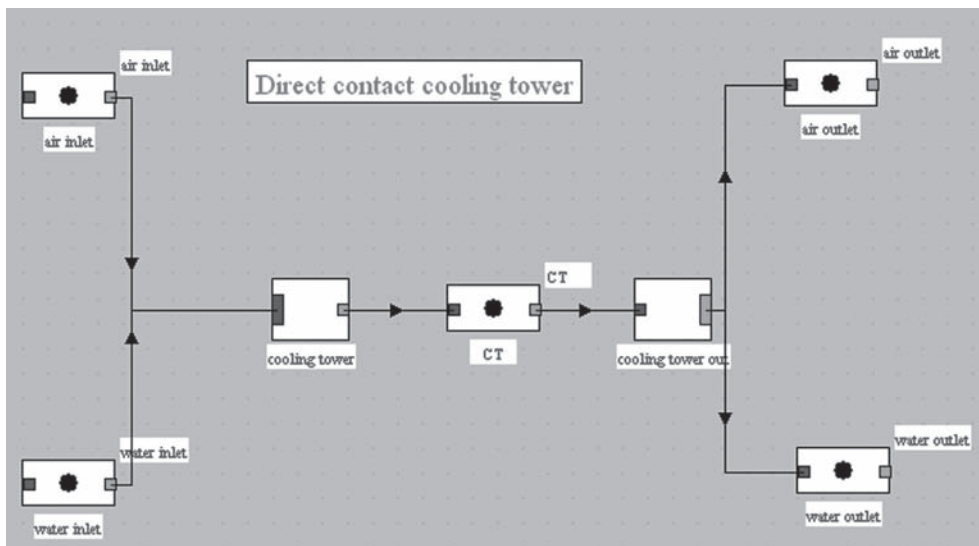


FIGURE 15.8.9
Diagram of the direct contact cooling tower component

Plotting this equation in a reference [wet bulb temperature/relative minimum air flow], for a given water inlet temperature, we obtain the abacus of Figure 15.8.7.

The great advantage of this Recknagel model is that it is very easy to implement, calculating I_0 and I_{min} being quite simple. Our own comparisons of this approach on data available to us on the one hand has shown that it is very reliable, and also lead us to propose a slight modification: the tower characteristic C_t , constant in the original method may be replaced by a linear function of the approach: $C_t = C - a(T_{wi} - T'_{ai})$.

Figure 15.8.8 shows, for the same tower type as in Figure 15.8.5, the correspondence between the values of η calculated from the manufacturer data and using the correlation changed to reflect the

TABLE 15.8.2

	F1221 40 hp	F1221 50 hp	F1221 60 hp	F1221 70 hp
C	1.08	1.03	1.04	1.07
a	-0.010	-0.013	-0.014	-0.019
r ²	0.83	0.97	0.92	0.732

influence of approach. The values of C and a are given in Table 15.8.2. The dispersion is slightly larger than with the Merkel model, but it remains very low.

15.8.4 Modeling a direct contact cooling tower in ThermoOptim

A direct contact cooling tower is crossed by two separate streams: air and water, which exchange matter and energy through an interface. It behaves like a quadrupole receiving two fluid inputs, and whose two others come out.

This poses a slight difficulty in building a ThermoOptim model, since the only components available are either processes or nodes. The solution is to form the quadrupole by combining an input mixer and an output divider, the two being connected by a process-point playing a passive role.

For the model to be coherent the calculations made by both nodes are synchronized. More precisely, the outlet divider takes control of the mixer, whose role is limited to perform an update of the coupling variables associated with the input streams. The model structure is given Figure 15.8.9. Its code will be presented in section 23.6 of Part 4.

WORKED EXAMPLE

Refrigeration machine condenser with cooling tower

This example corresponds to a R134a refrigeration machine ensuring the production of 200 kW of cooling at -12°C , whose condenser is cooled by air at 25°C .

The objective is to compare the performance of the machine depending on whether one uses an air exchanger with a pinch of 16K or a cooling tower, the minimum pinch between water and the refrigerant being below 12K. The result is an increase of the COP of about 19% when the cooling tower is used.

It is presented in the portal guidance pages (<http://www.thermoOptim.org/sections/enseignement/cours-en-ligne/fiches-guides-td-projets/fiche-sujet-fg6>), but requires the knowledge of refrigeration cycles presented Chapter 19.



[CRC_we_5]

REFERENCES

- D.R. Baker, H.A. Shryock, *A comprehensive approach to the analysis of cooling tower performance*, ASME Transactions, Journal of Heat Transfer, 339, 1961.
- J.E. Braun, S.A. Klein, J.W. Mitchell, *Effectiveness Models for Cooling Towers and Cooling Coils*, ASHRAE Transactions, Vol. 92, Part 2, p. 164–174, 1989, ASHRAE Handbook 2000, “Cooling Towers”, chapter 36
- G. Riollet, *Théorie des turbines à vapeur et à fluide compressible*, Techniques de l’Ingénieur, Traité Mécanique et chaleur, B 330-2.
- M. De Vlamincq, P. Wauters, *Thermodynamique et Turbines*, CIACO, Louvain-la-Neuve, 1988.
- L. Vivier, *Turbines à vapeur et à gaz*, Ed. Albin Michel, Paris, 1965.

FURTHER READING

- A. Bricard, L. Tadrist, *Echangeurs de chaleur à contact direct*, Techniques de l'Ingénieur, Traité Génie énergétique, BE 9 565.
- P. Lemoine, *Refroidissement des eaux*, Techniques de l'Ingénieur, Traité Génie énergétique, BE 2 480.
- P. Lemoine, *Réfrigérants atmosphériques*, Techniques de l'Ingénieur, Traité Génie énergétique, BE 2 481.
- B. Manas, *Aéroréfrigérants secs*, Techniques de l'Ingénieur, Traité Génie énergétique, BE 2 482.
- G. Manfrida, S. Stecco, *Le Turbomacchine*, Pitagora Editrice, Bologna, 1990.
- A. F. Mills, *Cooling towers*, *The CRC handbook of thermal engineering*, (Edited by F. Kreith), CRC Press, Boca Raton, 2000, ISBN 0-8493-9581-X.
- M. Pluviose, *Turbomachines hydrauliques et thermiques*, Exercices commentés, Eyrolles, Paris, 1988.

Classical Steam Power Cycles

Abstract: We present in this chapter steam power plants cycles, which are used today mainly for centralized electricity generation: the Hirn (or Rankine with superheating) cycle and variants that are made to optimize efficiency.

Most steam power plants using these cycles are either conventional, i.e. boiler flame burning mainly coal or oil, or nuclear. However, other hot sources are also used, although on a much smaller scale: solar energy in solar power plants (see Chapter 30 of Part 4), geothermal energy (see Chapter 31 of Part 4), gas or liquid waste of any kind, provided that their temperature level is sufficient. Given its current economic importance, Chapter 17 is devoted to the particular case of combined cycles where the waste gas is a gas turbine exhaust gas.

Keywords: Steam power plant, extraction, reheat, feedwater heater, supercritical, binary water/ammonia cycles, expansion, combustion, supercritical, flame power plants, Hirn, Rankine, denitrification, fluidized bed, pressurized, IGCC, nuclear, pressurizer, moisture separator reheater, PWR, EPR.

16.1 CONVENTIONAL FLAME POWER CYCLES

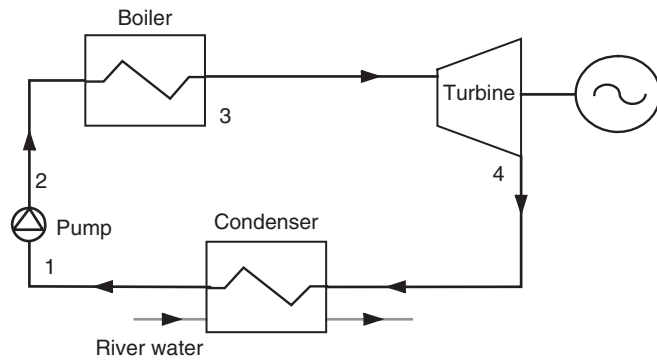
16.1.1 Basic Hirn or Rankine cycle with superheating

Hirn (or Rankine with superheating) cycle uses a condensable fluid, which is cooled at a temperature and pressure sufficient for it to be fully liquefied before compression. Under these conditions, the compression work is almost negligible compared to the expansion work (although it represents about 60% in a gas turbine). The compressed liquid is vaporized and superheated in the boiler by heat exchange with the hot source, then expanded and condensed. Fluid two-phase state during condensation and vaporization phases is very favorable for heat transfer.

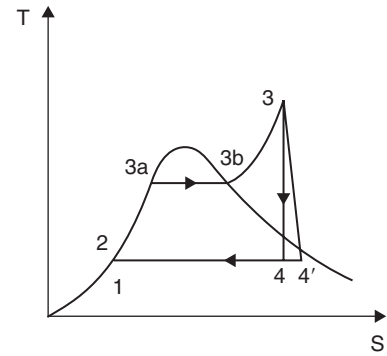
The block diagram of a steam power plant operating on the ideal Hirn cycle is given in figure 16.1.1 (we return to the cycle studied as an example in section 9.1 of Part 2). The numerical values chosen here correspond to a conventional fossil-fired plant cycle, whose technologies will be discussed in section 16.2.

Such a plant includes four basic components: a pump, a boiler, a turbine and a condenser, through which passes the same water flow-rate.

For reasons stated in section 5.3.6 of Part 2, the pump and the turbine can be assumed adiabatic. As for the boiler and condenser, at first approximation we can make the assumption that they are isobaric.

**FIGURE 16.1.1**

Sketch of a steam power plant

**FIGURE 16.1.2**

Steam cycle in an entropy chart

16.1.1.1 Cycle description

At point 1, water is liquid, at a temperature of approximately 20°C and at low pressure (0.023 bar). A pump pressurizes it to 165 bar (point 2), which represents a significant compression ratio (around 7,000).

Compression (1-2) of the liquid can be legitimately considered isentropic and temperature T remains approximately constant. As the liquid isobars are virtually merged with the beginning of the vaporization curve (see section 5.6.6.1 of Part 2), point 2 is virtually identical with point 1 on the entropy diagram of Figure 16.1.2.

Pressurized water is then heated at high temperature in the boiler, heating comprising the following three steps, clearly visible in Figure 16.1.2:

- liquid water heating in the economizer from 20°C to approximately 355°C , dew point temperature at 165 bar: process (2-3a) in the entropic chart. Point 3a is on the vaporization curve at ordinate 355°C on the same isobar as point 2;
- vaporization at constant temperature 355°C in the vaporizer: process (3a-3b). Vaporization being carried out at constant pressure and temperature, it results in the chart in a horizontal segment 3a-3b. Point 3b is therefore on the descending branch of the vaporization curve, or dew point curve, at its intersection with the horizontal line of temperature 355°C , still at the 165 bar pressure P_2 ;
- superheating from 355°C to 560°C in the superheater: process (3b-3). Point 3 is still assumed to be at the same pressure, but at temperature $T_3 = 560^{\circ}\text{C}$. It is thus at the intersection of isobar $P = 165$ bar and the horizontal of ordinate $T = 560^{\circ}\text{C}$.

Process (3-4) is an adiabatic expansion from 165 bar to 0.023 bar. In the ideal cycle, obtained without irreversibility and hence constant entropy, point 4 is at the intersection of the vertical passing through point 3 and isobar 0.023 bar. The point being in the mixed zone, the latter is confused with the horizontal $T \approx 20^{\circ}\text{C}$. The quality here is $x = 0.74$. The real point 4' is at the same pressure as point 4, but its entropy is different because of irreversibilities (larger by the second law). Its enthalpy can be determined if one knows the turbine isentropic efficiency. Two cases may arise:

- either point 4' is in the mixed zone, and it is also on isotherm $T \approx 20^{\circ}\text{C}$, closer to the dew point curve;
- or it is in the vapor zone, on isobar $P = 0.023$ bar, at $T > 20^{\circ}\text{C}$.

For example, with an isentropic efficiency of 0.85, the point at the end of expansion is 4', at the right of 4, and quality reaches the value of 0.84.

The liquid-vapor mixture is then condensed to liquid state in a condenser, heat exchanger between the cycle and the cold source, e.g. by water from a river. The cycle is thus closed.

Property	Value
M (kg/kmol)	18.015
Pc (bar)	221.2
Tc (°C)	374.15
Vc (m3/kg)	0.00317
quality x	0
T (°C)	19.746
h (kJ/kg)	82.837
u (kJ/kg)	82.834
s (kJ/kg/K)	0.29282
v (m3/kg)	0.00100167

FIGURE 16.1.3

Calculator inverter

16.1.1.2 Cycle modeling

The technical fluid (water) condensing, it is of course impossible to model it with the approximation of perfect or ideal gas, and thus to obtain simple analytical performance expressions for this plant.

To determine the water state at the cycle different points, it is necessary to use a table or chart, or to have a property calculator of the type of the applet that we presented in Chapter 6 of Part 2. Moreover, the fluid flow-rate being constant throughout the cycle, we will reason on a 1 kg/s flow for simplicity.

The calculation of points where pressure and temperature are known is simple (points 1 and 3, not considering intermediate points 3a and 3b): to obtain their state simply enter these values in the applet specifying as appropriate if the saturation temperature is set, and providing in this case the value of x , then click “Calculate”, the calculation mode being “P,T,x” (Figure 16.1.3 shows the calculation of point 1). This gives us:

$$\begin{aligned} h_1 &= 82.84 \text{ (kJ/kg)} \text{ (the exact value of } T_1 \text{ is provided: } 19.75^\circ\text{C)} \\ h_3 &= 3459.6 \text{ (kJ/kg)} \\ s_3 &= 6.5 \text{ (kJ/kg/K)} \end{aligned}$$

The state of point 4 is calculated in “P, s” mode entering s_3 and P_4 :

$$h_4 = 1899.6 \text{ (kJ/kg)} \quad (\text{the quality is } 0.74)$$

The work done by the turbine is deduced immediately for the ideal cycle:

$$-\tau_t = h_3 - h_4 = 1560 \text{ kJ/kg}$$

The compression work in the pump can be calculated in two ways:

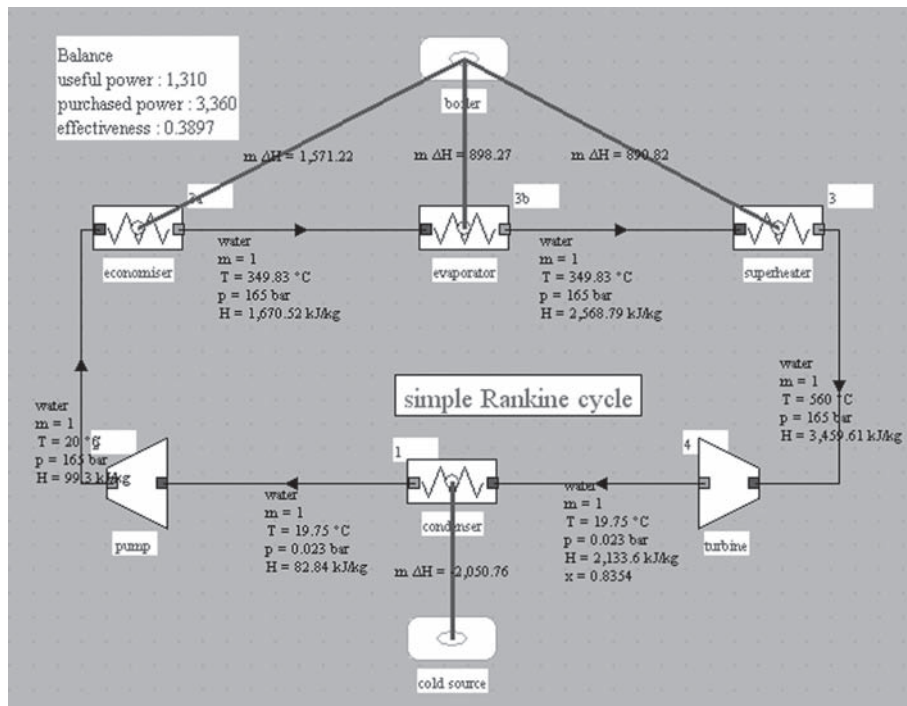
- either by approximating the constant liquid mass volume equal to $10^{-3} \text{ m}^3/\text{kg}$ (P must be expressed in Pa and not in bar);

$$\tau_p = v\Delta P = 10^{-3} 165 10^5 = 16.5 \text{ kJ/kg} \quad (\text{or about one hundredth of } |\tau_t|)$$

- or by operating as for the turbine, point 2 being determined by $s_2 = s_1$.

$$\tau_t = h_2 - h_1 = 99.29 - 82.84 = 16.45 \text{ kJ/kg.}$$

As can be seen, the difference is negligible.

**FIGURE 16.1.4**

Synoptic view of a Hirm cycle

Heat from boiler is:

$$Q_{ch} = h_3 - h_2 \quad (\text{here } 3360 \text{ kJ/kg})$$

Heat rejected by the condenser is:

$$Q_c = h_4 - h_1 \quad (\text{here } 1816 \text{ kJ/kg})$$

The cycle efficiency is, neglecting the compression work:

$$\eta = \frac{h_3 - h_4}{h_3 - h_2} = 46\%$$

Taking into account an expansion isentropic efficiency $\eta_t = 0.85$, the calculations are a little more complex (see section 7.5 of Part 2). By definition of isentropic efficiency, point 4' enthalpy, at the end of compression is:

$$h_{4'} = h_3 + \eta_t(h_4 - h_3) = 2133.6 \text{ (kJ/kg)}$$

Its quality may be calculated by the applet in “P, h” mode. It is 0.84.

The overall efficiency is equal to 39% or 60% of that of a Carnot cycle operating between 20°C and 560°C .

As discussed below, it is possible to improve this cycle by various methods, including by reheat and extraction. Note that the cycle maximum temperature and pressure, set here at 560°C and 165 bar, are limited by durability of the materials that make up the boiler, usually made of steel for cost reasons.

We have calculated the cycle step by step in order to show the sequence of operations. It is also very easy to model it directly in Thermoptim, as explained in Example 9.1 of Part 2 or one of the Getting Started guides. The diagram of Figure 16.1.4 shows the result we obtain. To detail the three

TABLE 16.1.1
ENTHALPY BALANCE OF SIMPLE STEAM CYCLE

Point	Flow-rate (kg/s)	h (kJ/kg)	
1	1	83	
2	1	99	
3a	1	1671	
3b	1	2569	
3	1	3460	
4'	1	2134	
Process	τ (kW)	Q (kW)	Δh (kW)
(1-2)	16		16
(2-3a)		1571	1571
(3a-3b)		898	898
(3b-3)		891	891
(3-4')	-1326		-1326
(4'-1)		-2051	-2051
cycle	-1310	1310	
energy efficiency		38.97%	

stages of water heating, the boiler has been represented here with three exchange processes in series: the economizer, the evaporator and superheater.

16.1.2 Energy and exergy balance

From the model developed with ThermoOptim, it is easy to draw the energy balance of the cycle by completing a table of type 16.1.1.

The efficiency here is the ratio of the work provided by the cycle to the heat generated by the boiler.

To build up the exergy balance, we must begin by giving a reference temperature and pressure. We take here $T_0 = 288.15 \text{ K}$ (15°C) and $P_0 = 1 \text{ bar}$, corresponding to conditions of mid-season in France. Table 16.1.2 can then be built step by step, following the guidance of section 10.2.3 of Part 2 which is summarized below. We also assume that the boiler is a monothermal hot source at 1600 K . To embed in this balance the boiler exergy losses, we should model the combustion and represent the boiler as a series of three heat exchangers. For simplicity, we will not do it here. The exergy efficiency obtained may if desired be multiplied by an estimate of that of the boiler, close to 70%.

For each component, Equation (10.2.3) of Part 2 is written:

$$\Delta x_{hij} = \sum_{k=1}^n x_{qjk} - m_j \Delta x_{hj} + \tau_j$$

In Table 16.1.2, losses are given as percentage of total irreversibilities. They show that they are mainly concentrated in the boiler and the turbine, and in contrast they are negligible in the condenser, while the energy balance would suggest that this component transfers most energy, since it discharges almost 60% of the heat cycle to the outside.

Specifically, the economizer (2-3a) alone accounts for nearly 50% of the exergy losses, other losses being distributed nearly equally between the vaporizer, the superheater and the turbine.

TABLE 16.1.2

EXERGY BALANCE OF THE SIMPLE STEAM CYCLE

Point	Flow rate	h (kJ/kg)	s (kJ/kg/K)	xh (kJ/kg)
1	1	83	0.29	-2
2	1	99	0.29	15
3a	1	1671	3.78	582
3b	1	2569	5.22	1065
3	1	3460	6.50	1588
4'	1	2134	7.29	32

Exergy balance $T_0 = 288.15\text{ K} = 15^\circ\text{C}$

Process	τ (kW)	Q (kW)	$m\Delta h$ (kW)	$m\Delta s$ (kW/K)	T_k (K)	Δxq (kW)	$m\Delta xh$ (kW)	Δxhi (kW)	loss
(1-2)	16		16		288		16		
(2-3a)		1571	1571	3.49	1600	1288	567	721	49.9%
(3a-3b)	898	898	1.44	1600	737	483	254	17.6%	
(3b-3)		891	891	1.28	1600	730	523	207	14.3%
(3-4')	-1326		-1326	0.80	1600		-1556	230	15.9%
(4'-1)		-2051	-2051	-7.00	288		-33	33	2.3%
cycle	-1310	1310						1446	100.0%
sigma(x_q +)		2755							
sigma(tau +)		0.00							
exergy efficiency		47.6%							

Figure 16.1.5 shows a plot of this cycle in an exergy entropy (s , x_h) chart. Point 3 representing the end of the isobaric superheating is situated at the maximum of the isotherm $T = 560^\circ\text{C}$, which immediately shows that the pressure and temperature were carefully chosen to maximize the steam exergy.

Ways of improving the steam cycle can be deduced from the exergy balance:

- increase the average temperature of the cycle by resorting to reheats;
- reduce the exergy losses in the economizer by making extractions.

We will now examine how these operations are realized in practice.

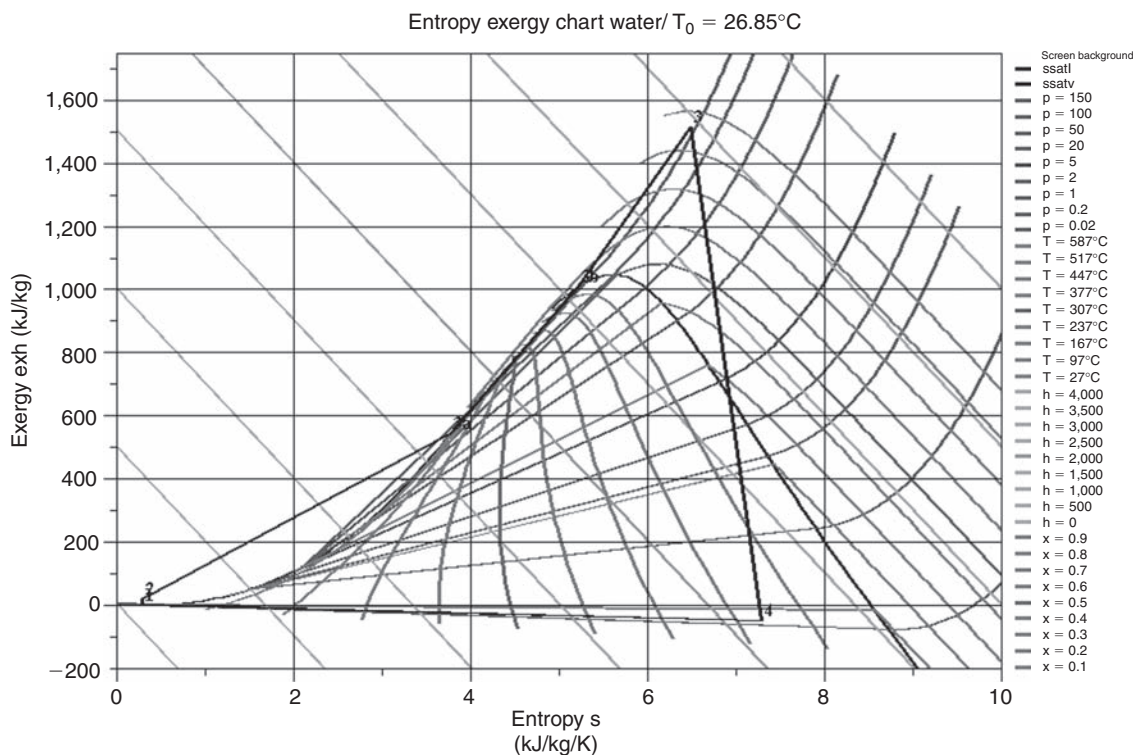
16.1.3 Thermodynamic limits of simple Hirn cycle

The relatively low Hirn cycle efficiency compared to that of the Carnot cycle is due to its shape in an entropy chart, which differs significantly from a rectangle.

In the chart of Figure 16.1.6, we see that it is *a priori* possible to approach the Carnot cycle by changing the Hirn cycle in several ways. In practice, all these ideas are however faced with various impossibilities.

Cycles (1-a-d-e) or (1-b-3-4) are impossible because the compression (1-a) or (1-b) in the liquid would require enormous pressures.

Cycle (f-c-d-e) would presuppose that one is able to achieve isentropic compression and expansion in the two-phase zone, which is now technologically impossible.

**FIGURE 16.1.5**Simple steam cycle in (s, ex_h) chart

To improve the performance of the cycle, we first select a fluid having a sharply ascending saturation curve, and we seek to increase the average temperature at which heat is provided, as discussed below.

Water appears to be an excellent working fluid for the Hirn cycle, with its critical temperature of 374°C and its high latent heat of vaporization at ambient pressure and temperature. Its low viscosity helps limit consumption of auxiliaries, and its low cost and its non-toxicity put it in a very good position relative to its competitors. However, for some applications, other fluids can sometimes be more appropriate.

Water does not, however, have only benefits: the condensation at 20°C implies that we maintain a somewhat low vacuum in the condenser (0.023 bar), which requires a complex device for extracting air, given inevitable leaks, especially since it is necessary to use huge low-pressure turbines considering its very low specific volume at 20°C , which induces very large volume flows, and thus very large flow sections and high velocities. This may lead to residual velocity losses at the turbine outlet if all the kinetic energy available is not converted into work.

Thus, in the example discussed above, the specific volume of steam at the end of expansion, in point 4', is equal to about $40\text{ m}^3/\text{kg}$, when at point 3, it is $0.02\text{ m}^3/\text{kg}$.

The volume expansion ratio is considerable: it is close to 2,000.

The great variation in volume flow during the expansion represents a major technological constraint of steam plants.

16.1.4 Cycle with reheat

A first idea to improve the Hirn cycle is to approach the Carnot cycle by conducting reheats. In this case, we begin by partially expanding the fluid, then it passes again into the boiler, where it is

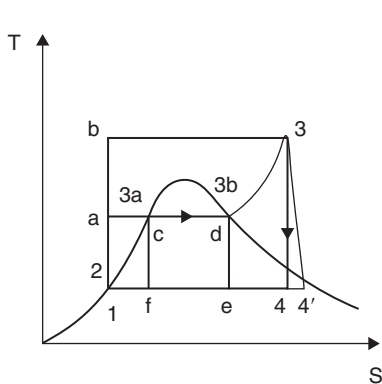


FIGURE 16.1.6
Impossible Carnot cycles

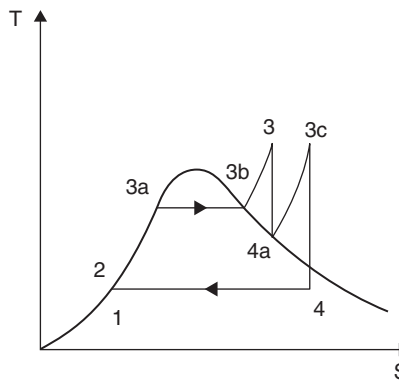


FIGURE 16.1.7
Reheat Hirn cycle

heated, at the new pressure, at the maximum cycle temperature (Figure 16.1.7). This operation can optionally be repeated several times, generating what is called a para-isothermal cycle.

This results in efficiency gains of a few percent, and most importantly, as shown in the chart, increased quality at the end of expansion, which is always valuable to extend the life of turbine blades, for which liquid droplets are abrasive.

The price however is a higher complexity, but as the expansion must be staged anyway, this improvement has no major technological impact on the power plant.

16.1.5 Cycle with extraction

Another way to improve the cycle is to undertake partial regeneration by using part of the heat rejected during expansion for preheating the pressurized liquid water before it enters the boiler. Exergy analysis has indeed shown that the major irreversibilities of the cycle take place in the economizer (2-3a). This is because this process is the one in which the temperature difference with the hot source is maximum: heat at high temperature is used to warm water below 100°C.

Complete regeneration cannot of course be done, because changes (2-3a) and (3-4) cannot be deduced from each other by translation. However, it is possible to take advantage of regeneration to quite significantly improve the Hirn cycle.

As the steam enthalpy is largely greater than that of the liquid, it is possible to preheat the liquid by a small steam extraction during expansion.

Of course, for the operation to be possible, it is necessary that the steam extracted at point P is at higher temperature than that of the liquid. In practice, reheat is thus limited to point A (Figure 16.1.8).

It is of course possible, if the economic study validates, to combine reheat and extraction by extracting steam just before the reheat (Figures 16.1.9 and 16.1.10).

It should be noted that due to extraction, the mass flow rate of the fluid that evolves is not the same in the different parts of the machine. If ϵ is the steam extracted, the fluid flow between points 4a, 3c, 4, 1 and A is $(1 - \epsilon)$ kg/s, and the flow-rate that evolves between points A, 3a, 3b, 3 and 4a is equal to 1.

The balance of the feedwater heater can be set as follows: it receives $(1 - \epsilon)$ kg/s of liquid in state 2 and ϵ kg/s of steam in state 4a. 1 kg/s of liquid at state A comes out of it.

We therefore have:

$$(1 - \epsilon)h_2 + \epsilon h_{4a} = h_A$$

We can thus determine ϵ .

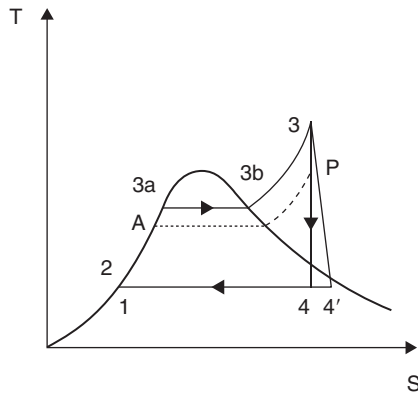


FIGURE 16.1.8
Extraction Hirn cycle

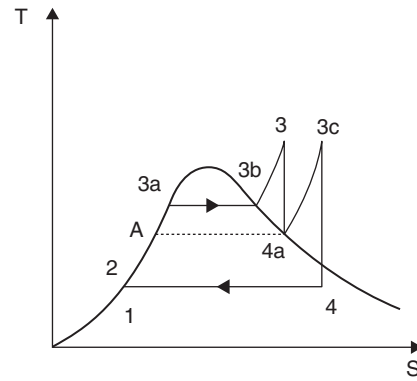


FIGURE 16.1.9
Extraction and reheat Hirn cycle in the entropy chart

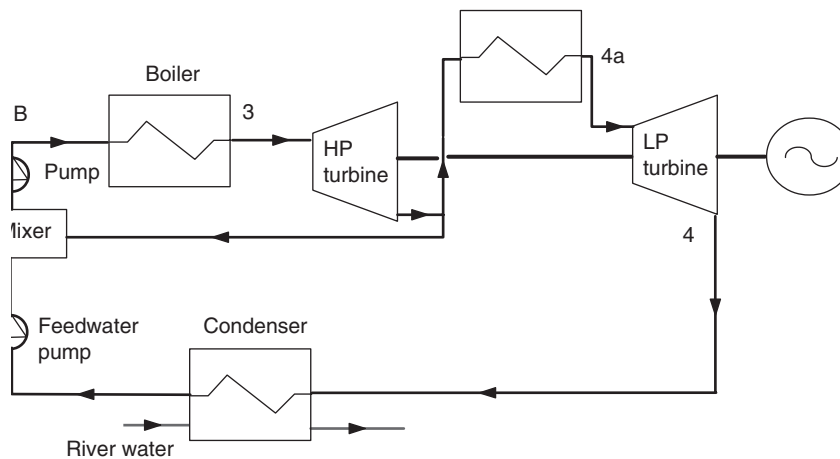


FIGURE 16.1.10
Extraction and reheat Hirn cycle

In practice, in high-capacity power plants used in electricity generation, several extractions are used (from 6 to 9), the various feedwater heaters operating at temperatures ranging from 30 to 50 K. The calculation of extractions is then done step by step, using the following recurrence formula:

$$\varepsilon_i = \left(1 - \sum_{k=1}^{i-1} \varepsilon_k \right) \frac{h_{Ai} - h_{Ai+1}}{h_{4ai} - h_{Ai+1}}$$

Technologically, feedwater heaters can be of various types.

A first embodiment is to mix the two fluids, since they differ only by their state and not by their nature. The best heat exchange is thus obtained. However, it is necessary to equalize pressures in each mixer, which requires a cascading compression of liquid. This solution, although attractive in thermal terms, was abandoned in favor of conventional tubular shell and tube heat exchangers, steam condensing outside the tubes.

At the condenser exit, an extraction pump compresses the liquid at a pressure at least equal to the saturation pressure at point A, to avoid partial evaporation in tubes. Various provisions of heat exchangers and recovery pumps can then be used. At the end of heating, the liquid is compressed to the desired pressure by a feedwater pump.

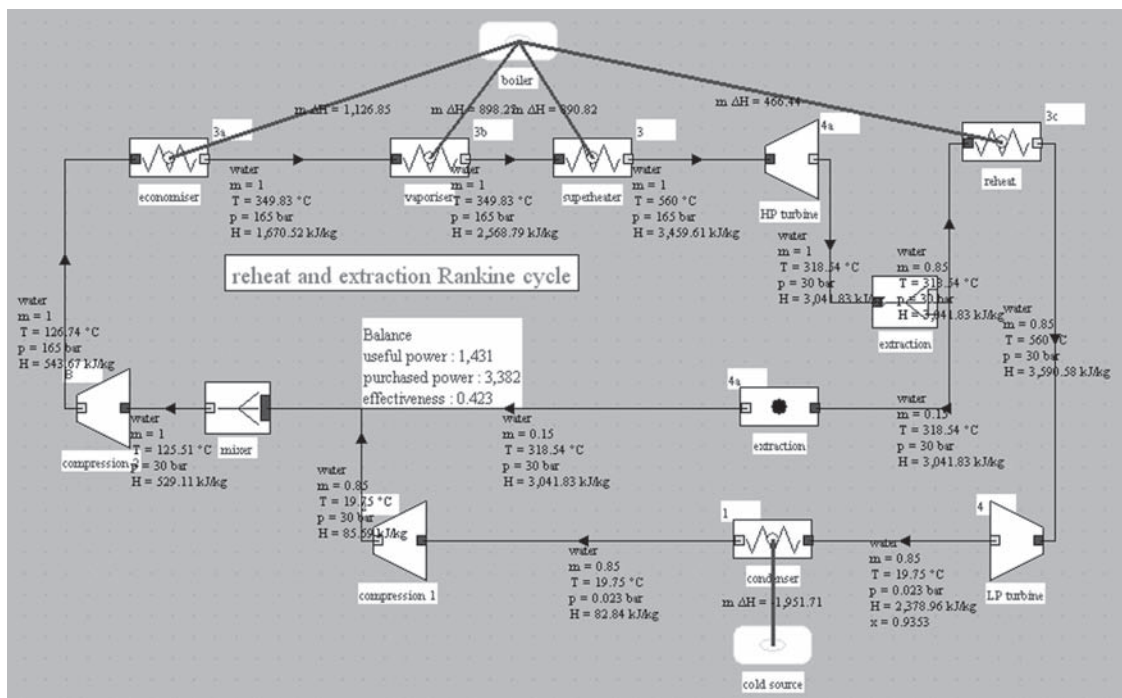


FIGURE 16.1.11

Synoptic view of a reheat and extraction cycle

Because of extractions, the mass flow passing through the turbine stages is gradually reduced until about one third in conventional thermal power plants, and 45% in pressurized water nuclear power plants. The result is a lessening of the previously mentioned strong constraint of having to convey increasingly important flow volumes during expansion. Extractions thus have an additional advantage.

Overall, extractions may contribute to an improvement of almost five points of the internal efficiency of the Hirn cycle. Combined with reheat, the gain is about 7 percentage points, a 20% higher efficiency than the basic cycle.

The synoptic view of a reheat and extraction cycle modeled in ThermoOptim is given in Figure 16.1.11. Its plot in a (h, s) Mollier chart is given in Figure 16.1.12 (isovolumes have not been plotted to improve chart readability).

16.1.6 Supercritical cycles

As we shall see in the next section, the optimum technical and economic capacity of flame Hirn cycles until recent years matched with boiler conditions of about 560°C and 165 bar, leading, with a reheat and without extraction, to a thermodynamic efficiency close to 40%. To significantly increase the efficiency, it is possible to use so-called supercritical cycles in which water pressure exceeds the critical pressure of 221.2 bar.

The result is obviously much higher stress for boiler tubes. Progress on the creep tube resistance can provide technological solutions unthinkable a short time ago. For example, the pipe thickness needed to withstand a pressure of 225 bar and a temperature of 600°C changed from 250 mm with steel P22 at 2.25% Cr, to 93 mm with P91 steel with 9% Cr, and 68 mm with steel HCM12A at 12% Cr (Jayet-Gendrot et al, 1999).

Another constraint faced by supercritical boilers is the following: due to the absence of vaporizer, you cannot cool the furnace by pipe screens traversed by boiling water with very high heat transfer coefficients. This is why a different technology is used, without drum separator, in so-called

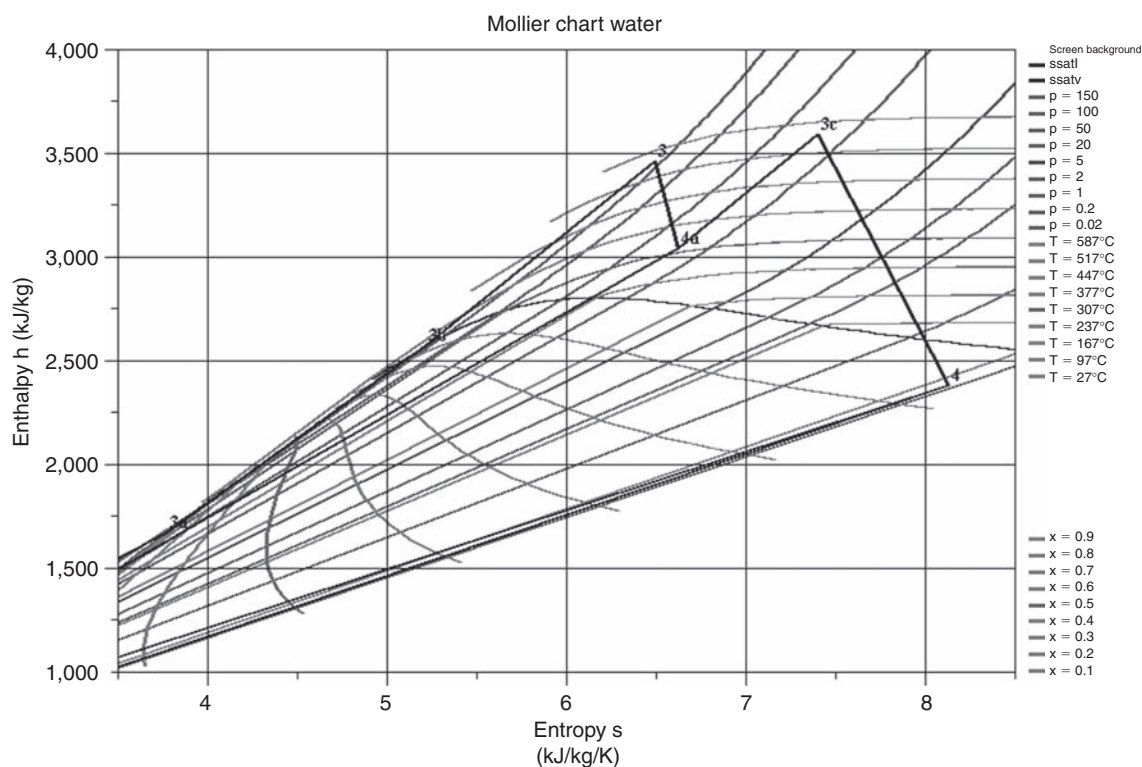


FIGURE 16.1.12

Cycle with reheat and extraction in the Mollier chart

mono-tubular boilers (improperly because in reality the layers of tubes are arranged in parallel), or in English “once-through” to indicate the absence of recirculation. These tubes are fluted with internal and external fins, mounted in spiral bundles.

Supercritical cycles are not new (40% of former Soviet Union plants are supercritical, as well as more than 150 plants in the U.S.). The recent trend is to seek out increasingly high boiler conditions, and two reheats. To fix ideas, we modeled in Thermoptim such an advanced supercritical steam cycle. The efficiency reaches 47.7% (against 40% for a conventional subcritical cycle). Figures 16.1.13 and 16.1.14 show the cycle synoptic view, and its plot in a (s, x_h) exergy chart.

In this example, we have simplified things by keeping an expansion isentropic efficiency of 0.85 for the different turbines. As the expansion takes entirely place in the dry zone, higher values could have legitimately been taken (see section 15.7.4).

Thus, this technology provides efficiency gains between 6 and 10% depending on the steam pressure and temperature conditions, for a cost increased by 3 – 5%. As the addition of supercritical boilers offers more flexibility at the operational level than conventional drum boilers, their use is spreading more and more. Project Thermie 700 involving many EU manufacturers and utilities aims to achieve LHV efficiencies of 50%.

16.1.7 Binary cycles

We pointed out in section 16.1.3 that one of the drawbacks of steam is the great value of its specific volume at low temperature, which results in:

- first, low pressure stages have large exhaust sections and huge fins that work at the strength limit of the material;

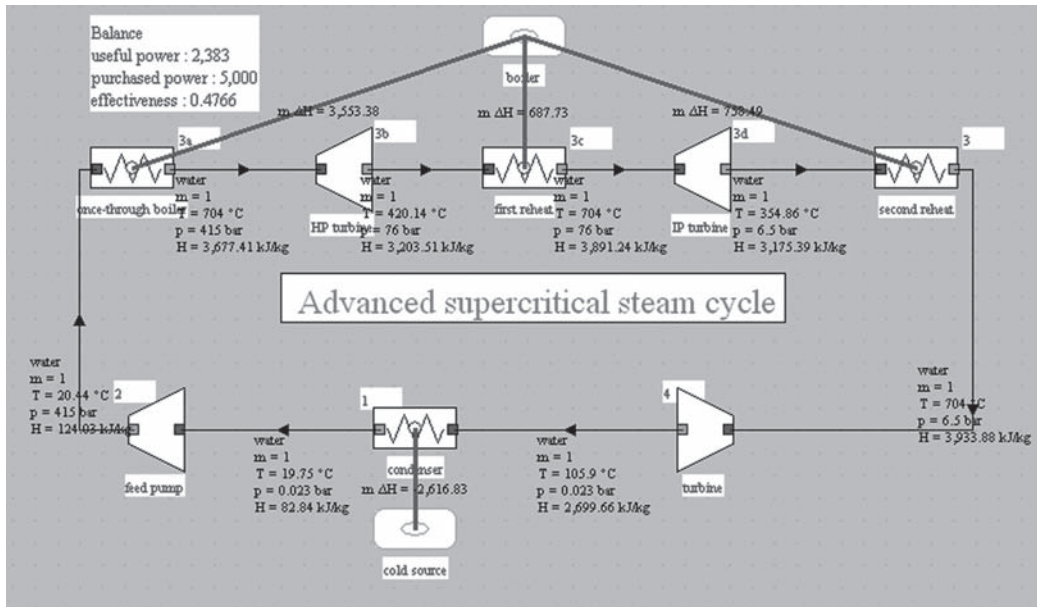


FIGURE 16.1.13
Synoptic view of a supercritical steam cycle

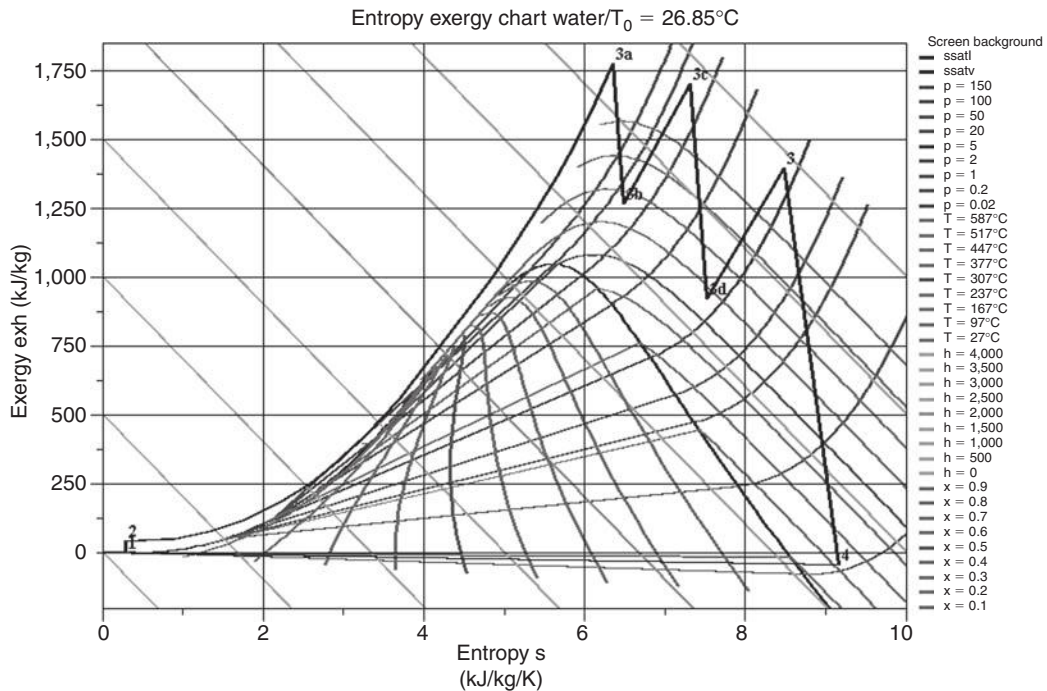


FIGURE 16.1.14
Supercritical steam cycle in the entropy-exergy chart

- second, losses by residual velocity may exist when the condensing temperature is very low (see section 37.4.4 of Part 5).

To overcome these drawbacks, we consider the use of binary water/ammonia cycles in which steam is replaced, in the terminal portion of the low-pressure expansion (when its specific volume is very

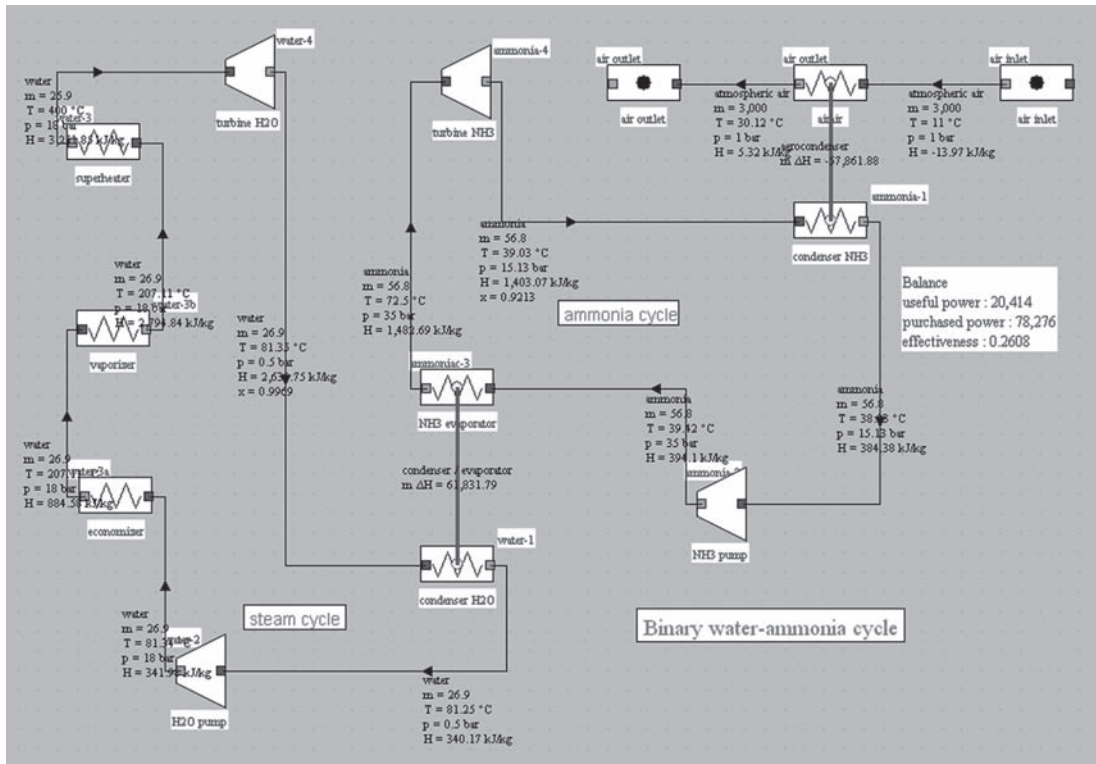


FIGURE 16.1.15

Synoptic view of a binary water-ammonia cycle

high), by ammonia which, under the same conditions of temperature, would be about 120 times more dense. Thermoptim model of such a cycle is given in Figure 16.1.15.

In this cycle, ammonia plays a dual role:

- it transfers heat between the LP steam turbine outlet and the cold source i.e. ambient air;
- it serves as working fluid expanding in a second turbine that replaces the low-pressure steam turbine stages.

Steam is condensed in a condenser/boiler consisting of bundles of tubes on which occur steam condensation and ammonia vaporization, the temperature difference between the two fluids being close to 7°C. Ammonia vapor is then expanded to produce work in an ammonia turbine driving an alternator.

After expansion, the vapor condenses in contact with the cold source. Heat transfer between the condensing ammonia vapor and air takes place in an air condenser made up of finned tubes. After condensation, ammonia is pressurized, the bottom cycle being thus closed.

If the use of wet cooling towers is called into question because of the growing environmental constraints (scarcity of water resources and global warming), the use of binary cycles of this type could become widespread. Recent summer heat waves have shown that the solutions currently being implemented will not continue to be used in the future if temperature continues to rise. Other fluids than ammonia may also be considered.

16.2 TECHNOLOGY OF FLAME PLANTS

According to statistics from the International Energy Agency, the main fuel burned in flame power plants in 1998 was coal (38.4% of world total), followed by power plants based on gas turbines

(16.1%) that are the subject of Chapters 12 and 17, oil representing less than 9% of the total. The reason is that the world coal reserves are among the largest fossil energy sources, far ahead of oil or natural gas, especially in countries like China.

Coal accounts for about 60% of global electricity production from fossil fuels and its share will likely increase in the long term, even though natural gas has recently gained significant market share.

Traditional coal plants being highly polluting technologies because of their emissions of many gases (SO_x, NO_x) and dust, they no longer meet current emission standards. Various solutions have been developed to replace them. We present below their main characteristics, after some indication on technological constraints common to flame power plants.

16.2.1 General technological constraints

One of the major technological limitations of flame cycles is the strength of steel boiler tubes, subjected to both high pressure and high temperature. We have already presented in section 15.6.1 the general implications of this constraint on the configuration of heat exchangers in boilers.

Water or steam flows through these tubes at pressures up to 150 or 300 bar. On the exterior, they are in direct contact with hot combustion gases at a pressure close to atmospheric or a few tens of bars at most in some cases. They are therefore subject to both a high pressure difference, and high convective and radiative flux. Unless we use very expensive special steels, the levels of pressure and temperature must be limited.

It was demonstrated a few years ago that the technological limit of conventional pulverized coal or oil plants is supercritical steam generators at 240 bar and a capacity of 1300 MW. However, economically, the installed capacity in existing fleets is generally between 500 and 900 MW, turbine inlet conditions being close to 165 bar and 560°C. Without desulfurization, the efficiency reaches 40% in these conditions. On average, however, the efficiency of national plant fleets is closer to 34%.

Other technological constraints of all steam plants are the following:

- first, steam quality at the end of expansion should not be too low otherwise too large liquid droplets form, which constitute a dangerous abrasive for mechanical blades. 0.7 is considered a lower limit that it is important not to reach, and generally one seeks not to exceed 0.85 (see section 15.7.3);
- secondly, as we have already said, the steam specific volume at the low pressure turbine outlet is extremely high, which induces very high volume flow rates, i.e. huge flow sections, high flow velocity and gigantic wheel diameters, especially in nuclear power plants (see section 16.3.3);
- finally, the condenser pressure is very low, so that air leakage is inevitable. We must therefore always extract air from the condenser, which results in significant energy consumption (up to 0.5% of the plant capacity), especially since, for reasons of simplicity, low efficiency steam ejectors are generally used.

WORKED EXAMPLE

Extraction of noncondensable gases from a condenser

This example analyses the use of ejectors to remove the noncondensable gases from the condenser of a steam propulsion engine of the Merchant Marine, to understand the mechanisms that come into play and to estimate its impact on the energy balance of the ship.

It is presented in the portal guidance pages (<http://www.thermoptim.org/sections/enseignement/cours-en-ligne/fiches-guides-td-projets/fiche-guide-fg21>).



16.2.2 Main coal power plants

16.2.2.1 Pulverized oil or coal plants (PO or PC)

Traditional oil and coal plants use a Hirn cycle with reheat and several extractions, like those discussed above, operating at about 160 bar and 560°C.

They differ primarily by the boiler, more voluminous in the case of coal. To ensure proper combustion, the fuel must indeed be divided as finely as possible to guarantee a large contact area with the oxidant (usually air). Coal is thus pulverized in very large mills, and then blown into the boiler where it ignites, the boot being provided by an auxiliary oil input.

This very old technology is perfectly controlled, but, despite progress in recent decades, particularly in low-NO_x burners, it does not meet the standards for present emissions of pollutants. It is therefore necessary to add generally quite expensive fume treatment devices for desulfurization (flue gas desulfurization FGD), denitrification (and dust removal in the case of coal).

Figures 11.1.4 and 11.1.5 presented in Chapter 11 give an idea of the size of a coal power plant of 250 MW: a base of 50 m by 135 m and a boiler height of 65 m.

As we have seen in section 16.1.5, another line of development of this technology is supercritical plants where steam pressure exceeds 300 bar. Superheating temperature today reaches 600°C, and 700 °C is expected in the next few years, with the goal of exceeding 50% LHV efficiency, if technical and economic viability can be obtained.

Figure 16.2.1 shows the engine room of a 620 MW coal plant.

16.2.2.2 Circulating fluidized bed plants (CFB)

Since the 1970s, we looked for combustion processes which can significantly reduce pollutant emissions during low quality fuel combustion, such as pitches or petroleum cokes, coals with high ash and sulfur etc.

Fluidized bed technology involves blowing a gas vertically beneath a layer of solid particles of suitable size. At a certain gas velocity, the particles are raised and the layer swells, creating a suspended medium whose behavior is similar to a fluid: the bed is said to be fluidized. If the gas velocity increases, the particles are mixed and transported: the bed becomes turbulent.

In a fluidized bed boiler, high sulfur fuels and lime are mixed, and air is blown, producing calcium sulfate, environmentally neutral, dismissed with ashes. The fuel desulfurization rate is

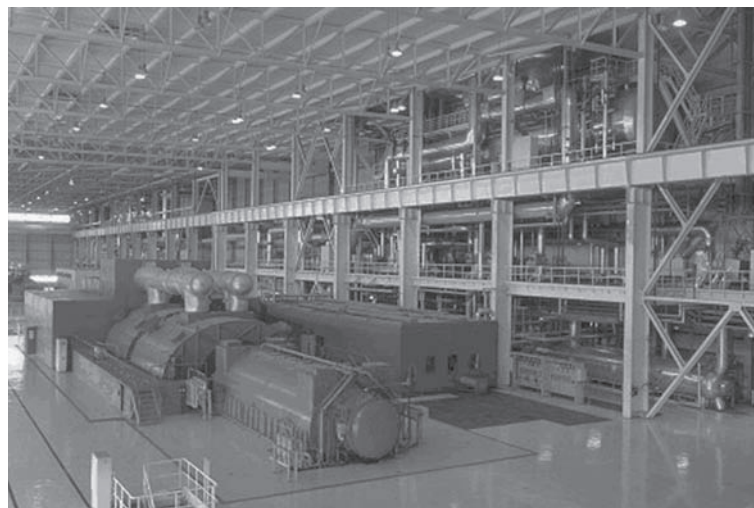


FIGURE 16.2.1

620 MW coal plant engine room, Documentation Alstom Power

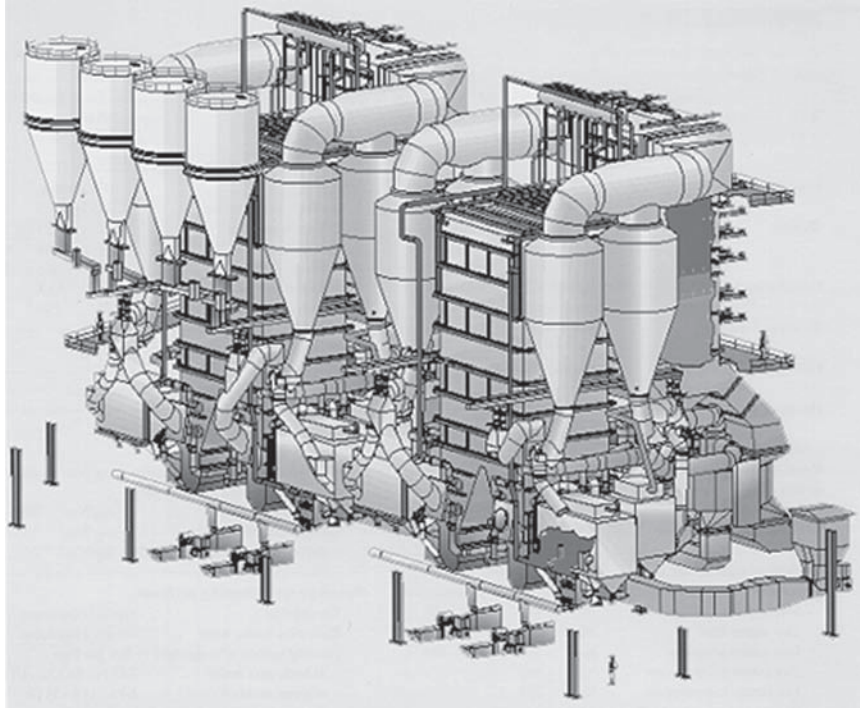


FIGURE 16.2.2

Red Hills circulating fluidized bed plant, Documentation Alstom Power

above 90%, and may even reach 97 or 98% in some facilities. This very simple desulfurization system is 15% cheaper than flue gas desulfurization processes of the type that we are now obliged to implement in boilers with PO or PC to meet regulations.

In a circulating fluidized bed boiler, particles are separated from flue gas in cyclones and then re-injected at the bottom of the boiler. It is thus possible to increase their residence time in the boiler and to obtain more complete chemical reactions, allowing fluidized bed boilers to operate at a lower temperature of about 850°C for example instead of 1300°C in a conventional pulverized coal boiler. The formation of nitrogen oxides can be reduced.

The current success of this technology is related to its relatively low capital cost (compared to a technique with PO or PC smoke treatment), and its ability to burn low quality fuels.

With about 240 units in operation throughout the world, CFB plants are perfectly ripe technology up to capacities of 250 MWe (Gardanne plant). 600 MW units are under consideration. Figure 16.2.2 shows the configuration of the Red Hills plant of 2×250 MW, cyclones being clearly visible. The transition to supercritical cycle is facilitated by the favorable combustion conditions (heat fluxes and temperatures lower than in a conventional PO or PC plant).

16.2.2.3 Pressurized fluidized bed plants (PFBC)

A variant of air circulating fluidized bed plants consists of burning coal at a pressure of 15 to 20 bar and still at a temperature of 850–900°C in the presence of limestone, then remove dust from fumes at the furnace outlet and expand them in a gas turbine, which typically produces 20% of the cycle total capacity and drives the air compressor. The fluidized bed is cooled in parallel by a conventional steam cycle, and the whole can achieve efficiencies of 42%.

The advantage of this recent technique is to use a more compact boiler because of the pressure, and increase the overall efficiency due to the presence of the gas turbine. It is therefore particularly well suited for the rehabilitation of existing units in areas where space is limited. The main constraint

is the technological success of the hot dust removal, which is necessary so that gases can be expanded in the turbine without undue risk of corrosion (special turbines specifically designed for this purpose are being used).

In existing plants, the fluidized bed is not recirculated, the related technological problems being not yet fully mastered.

16.2.2.4 Integrated coal gasification combined cycle plants (IGCC)

Integrated coal gasification combined cycle (IGCC) plants are highly complex, involving a large number of heat exchangers, and may operate with different fuels at different times of their operation. They typically include (Figure 16.3.6 of Part 4) units for:

- Producing a low heating value synthesis gas within a gasifier using solid fuels such as coal, petroleum coke, etc.;
- Cooling the synthesis gas through a cold gas recirculation (quench);
- raw gas washing (dust removal and sulfur treatment);
- Partial recovery of the syngas sensible heat in the recovery steam generator HRSG;
- clean gas combustion with compressed air into the combustion chamber of a gas turbine which generates electricity and hot gas flow;
- Producing steam at high, medium and low pressures (respectively denoted HP, IP and LP) by exchange with hot gases in the HRSG;
- expansion of the steam generated through turbines connected to a generator.

The integration of such a system is particularly complex and must take into account design (technical and economic) as well as exploitation constraints. The Thermoptim optimization method presented in chapter 22 has been used successfully to model the Puertollano IGCC plant (Gicquel et al, 2001).

The great advantage of this technology is to reduce emissions of gaseous pollutants far beyond current standards and strongly reduce solid waste, while resulting in excellent efficiency (45%).

Its main drawback is its capital and operating costs, which are today estimated to be 25% higher than that of a PO or PC plant with fume treatment.

16.2.3 Emissions of pollutants

The very large coal reserves in the world and their geographical spread are very strong arguments for the use of this fuel in power plants. Comprehensive efforts are made to develop combustion technologies as clean as possible, as we have seen in previous sections, in particular to reduce the production of nitrogen oxides NO_x. Beyond these developments already mentioned, research focuses on reducing emissions of heavy metals like mercury, trapping particulates or capture and sequestration of CO₂.

More and more, we must thus expect an increasing integration of chemical processes upstream and downstream of power plants, the case of IGCC being a prime example. Despite all the interest and timeliness of this work, they are outside the field we have set ourselves in this book and we shall not present them in detail, merely referring the interested reader to the literature.

16.3 NUCLEAR POWER PLANT CYCLES

In nuclear power plants using steam cycles, heat can be provided either directly in the reactor (Boiling Water Reactor (BWR) or by an intermediate heat transfer fluid which transfers heat from the nuclear reactor core (Pressurized Water Reactor (PWR)). As briefly mentioned in Chapter 12, some nuclear reactors are coupled to closed Brayton cycles.

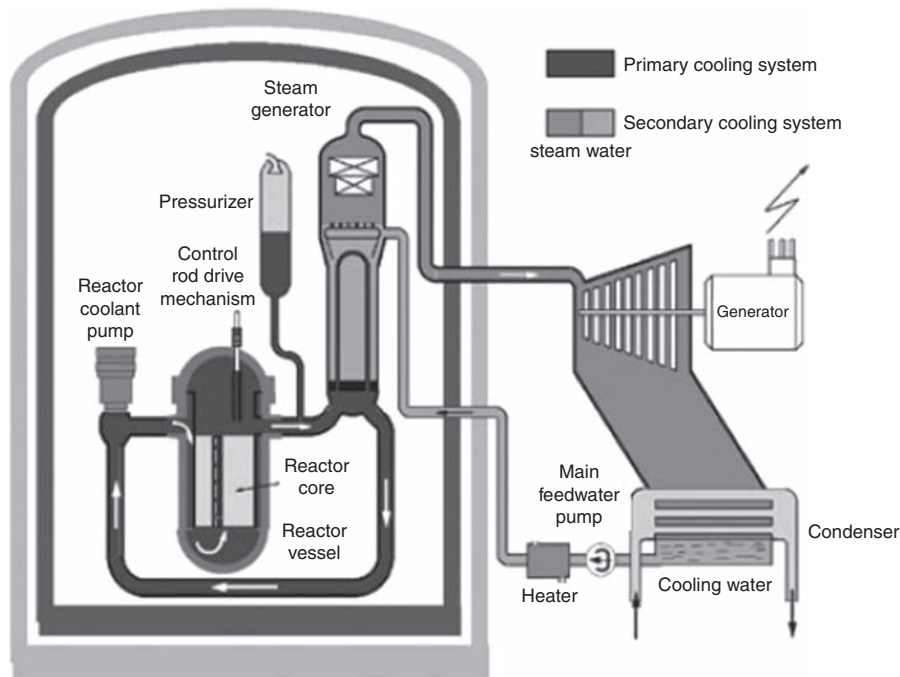


FIGURE 16.3.1

Sketch of a Pressurized Water Reactor, Documentation Areva

In this section we look more specifically at the PWR, the most industrially developed. In Chapter 29 of Part 4 we will expand our analysis by presenting the main types of cycles that are considered to be used in future nuclear reactors.

In a Pressurized Water Reactor, for safety reasons, the maximum steam cycle temperature and pressure are limited at levels well below those used in flame plants. In current PWR plants (unit said N4), pressure in the generator is about 60 bar and the steam temperature rarely exceeds 275°C.

The block diagram of a PWR is given in Figure 16.3.1. On the left side of the diagram appears the containment structure comprising three main organs:

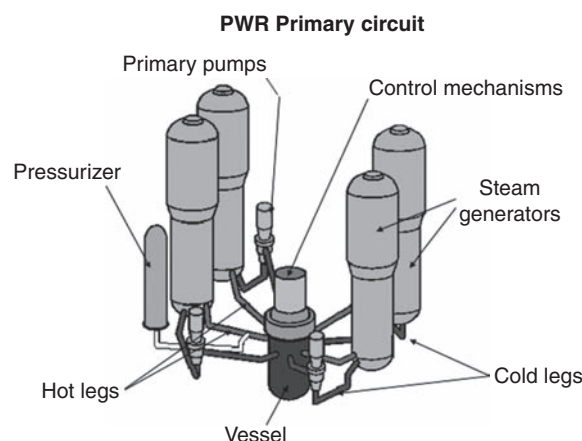
- the reactor with its control system (control rod drive mechanism);
- the steam generator;
- the pressurizer.

These three devices are connected by the primary circuit, including connecting pipes, and reactor coolant pumps, which circulate the coolant in the direction of the arrows.

The steam generator is connected to the secondary circuit located outside the containment structure, which corresponds to the thermodynamic cycle followed by steam, symbolized in the diagram by a turbine, condenser, feedwater pump and a heater.

16.3.1 Primary circuit

In a PWR, extraction of heat from the nuclear core involves two circuits for safety reasons, the cooling fluid (water under pressure) in contact with the reactor core being radioactive, due to fission products migrating through the cladding, and products dissolved in water (mainly due to corrosion), which capture neutrons. To prevent contaminated water from being in contact with the outside and passing through electricity production cycle components, the working fluid is separate from the coolant.

**FIGURE 16.3.2**

Nuclear boiler, Documentation Areva

The choice of this fluid is based on the qualities of water as a coolant (high heat capacity), environmentally and for use (stability, safety, availability). However, it imposes a strong constraint: the need to ensure that water remains in liquid state in the reactor vessel, to avoid local superheating of the nuclear fuel due to the presence of steam inducing low heat exchange coefficients.

For this, water must be maintained at a pressure higher than the saturation pressure at its maximum temperature in the reactor core. The whole primary circuit needs to withstand this maximum pressure, which results in severe mechanical stresses. The whole of this circuit is sized accordingly, and the system pressure is regulated with great precision to avoid either an overpressure that could cause circuit leakage or rupture, or a pressure decrease, given the risk of boiling in the core and fusion of the fuel. The pressurizer role is precisely to ensure this function.

A compromise must be found between safety constraints, thermodynamic cycle efficiency and installation costs. In existing plants, the maximum temperature of the thermodynamic cycle is set at about 280°C and the primary circuit at about 330°C. Specifically, the temperature of the primary circuit changes from about 290°C (zero power) to 325°C (maximum power).

To ensure non-boiling primary water, the coolant system pressure is set at 155 bar, corresponding to a saturation temperature of 345°C, which provides a small safety margin. Such pressure is already high and imposes severe technological constraints at all levels.

To accurately control the primary circuit pressure, the pressurizer is a reservoir containing water in two-phase state, pressure and temperature being linked by the saturated pressure law (paragraph 5.6.5.1 of Part 2).

To control the pressure, one simply regulates the temperature, which is done by heating or cooling (by spray) water in the pressurizer. It is in communication with the entire primary system, and sets its pressure (Figures 16.3.1 and 16.3.2).

The rest of the primary circuit (Figure 16.3.2) consists of three pump unit/steam generator sets. Pumps have just the role of ensuring that the primary water circulates throughout the reactor, and simply offset the pressure drops (about 8 bar).

16.3.2 Steam generator

The steam generator (SG) is able to transfer the total power of the reactor to the secondary circuit, with a very low temperature difference, as the performance of the thermodynamic cycle increases as its temperature does.

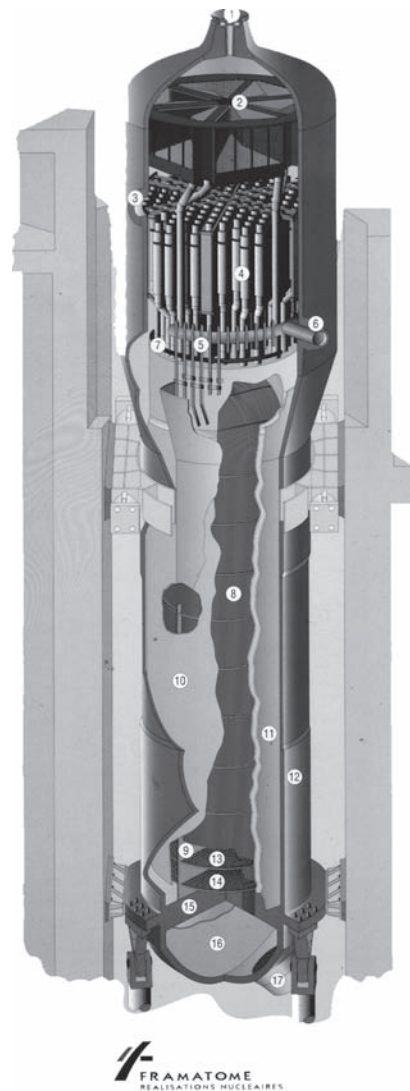


FIGURE 16.3.3

Nuclear steam generator, Documentation Framatome

We have seen that the primary water temperature varies between 290 and 325°C. The presence of feedwater heaters in the secondary circuit (see below), makes the secondary water enter the generator at a temperature of about 220°C.

The current performance of the SGs used in PWRs (Figure 16.3.3) lead to a maximum output temperature of about 275°C.

Given the low temperature differences between primary and secondary circuits, the need to transfer significant power forbids in practice achieving any superheating in the SG, because the exchange coefficients between the primary liquid and superheated steam would be too small.

Therefore, the type of steam generators used by virtually all manufacturers of nuclear boilers corresponds to Figure 16.3.3.

Primary water enters the SG in the lower part of the unit via a pipe hidden in the figure, and symmetric of port 17, from which it exits cooled. This water passes, from the bottom up in the back of the figure, and down in its front, inside perforated plates designed to distribute the flow between the inverted U-shaped tubes (bundle 8).

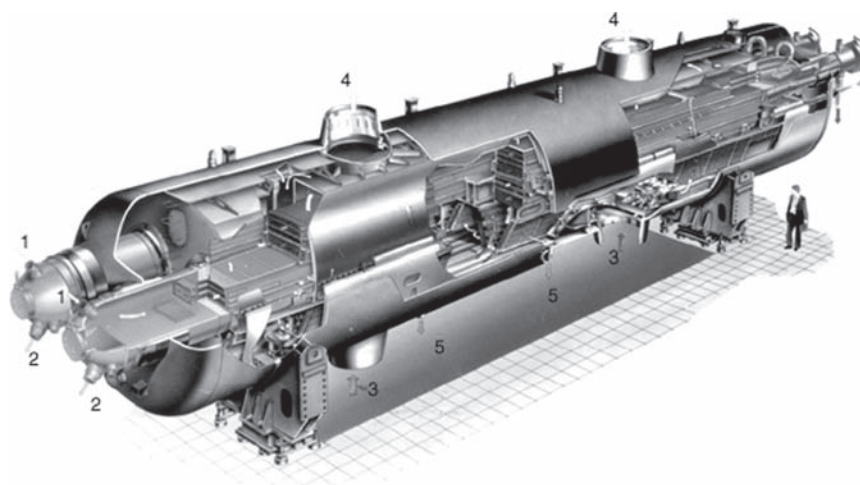


FIGURE 16.3.4

Moisture separator reheater (Documentation Alstom Power)

Water from the secondary circuit enters in pipe 6 in the liquid state at a temperature of about 220°C and a pressure of about 70 bar. It is distributed in the periphery of the SG by torus 5, provided with tubes that allow it to flow into jacket 11 located between the outer wall 12 and the bundle 10, which acts as economizer. It then follows an upward flow around the bundle, inside envelope 10, and partially vaporizes with a steam quality between 0.2 and 0.4, in a regime of nucleate boiling leading to very high heat exchange coefficients.

The two-phase emulsion then passes through cyclone separators 4 and then dryers 2. The liquid fraction falls to the bottom of the SG and is recirculated with the feedwater (the recirculation rate is between 2 and 4.5). The vapor fraction reaches a quality above 0.997, and exits through top port 1, to be directed towards the turbine high-pressure section.

16.3.3 Secondary circuit

A peculiarity of PWR nuclear power plant SGs is, as we have seen, that there is no initial superheat. Complete expansion of steam from this state would lead to too low a steam quality, which would be both disadvantageous in terms of performance, and fatal to the mechanical strength of turbine blades. The solution adopted consists in using a special organ called the moisture separator reheater (MSR), to split the expansion by providing a reheat at a pressure of about 11 bar, which can increase efficiency and meet the quality constraint at the end of expansion.

A moisture separator reheater (Figure 16.3.4) receives steam partially expanded with a quality close to 0.87, the liquid phase of which is separated and directed to feedwater heaters, while the steam passes through a heat exchanger traversed internally by a low flow of saturated steam at high pressure (and therefore higher temperature), which condenses. On the cutaway of Figure 16.3.4, live steam enters in 1 and leaves condensed in 2, while the steam to be superheated enters in 3 and exits in 4, condensate discharges being done in 5. For a 1,500 MW unit, two moisture separator reheaters of 370 tons each are needed. 24.8 m long, their height is 6 m and their width 5.3 m.

Figure 16.3.5 shows a synoptic view of a N4 PWR (excluding extractions) modeled in ThermoOptim. The model of the moisture separator reheater is given in the upper right of the figure. It includes a separator (named dryer on the diagram) and a heat exchanger between average pressure steam and the extraction of saturated steam at high pressure (called superheater in the diagram).

At the steam generator outlet, a fraction of the flow is diverted to the superheater, while the main stream is expanded at 11 bar. A separator recovers the vapor which is superheated by exchange

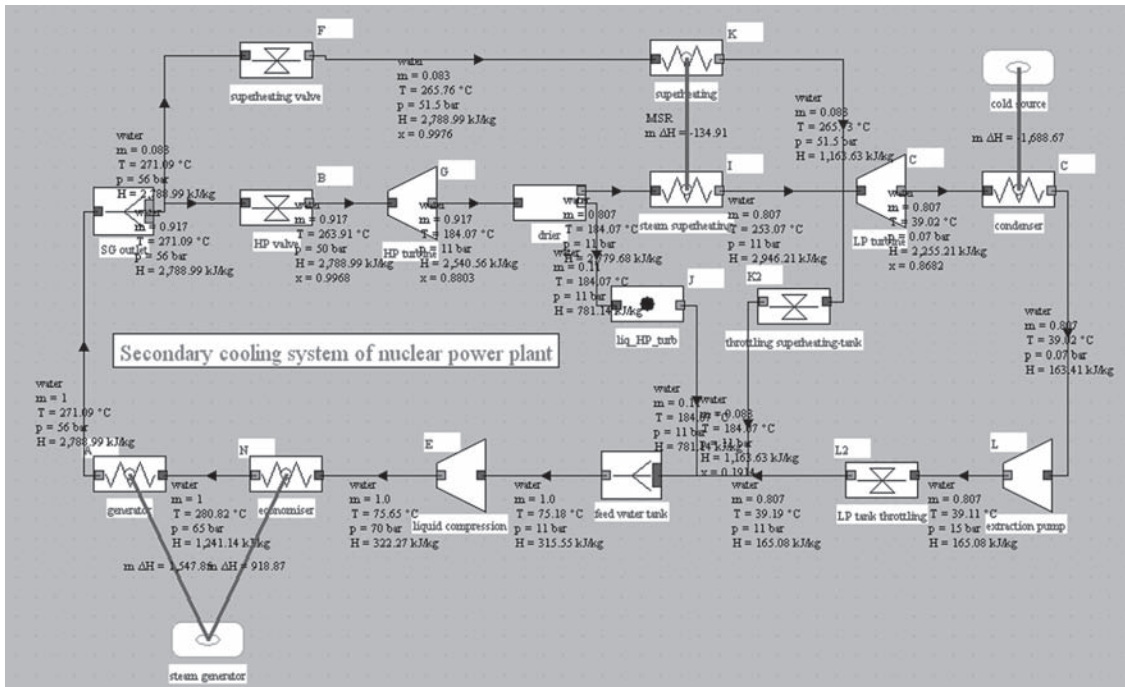


FIGURE 16.3.5
Synoptic view of a N4 PWR cycle

with the fraction of flow which was discussed above. Superheated steam is then condensed and expanded, and headed towards the feedwater tank where the other streams flow. Water is then delivered under pressure to feed the steam generator.

The cycle efficiency is equal to 31.4%. The extractions that actually take place allow it to reach about 33.5%. The cycle plot on a water entropy chart is given in Figure 16.3.6.

Among other nuclear plant cycle features, we must mention the large value of flow rates. In fact, on the one hand the useful work per unit of flow rate is about 60% lower than in conventional coal or oil plants, on the other hand their optimum technical and economic unit capacities are much larger (900 or 1300 MWe against approximately 600 in the others). Mass and volumes flow rates are very high. At turbine low-pressure section exit, velocities must be limited to increase efficiency and protect the condenser, which leads to design giant turbines (diameter up to 7 m) with very large sections of passage. The only solution to meet the mechanical constraints at the end of the blades is therefore for these important capacities, to halve the rotation speed of the turbine, which is then 1500 rpm.

Figure 16.3.7 shows the engine room of a nuclear power plant of 1000 MW. One can clearly see the shaft with the generator coupled to the different turbines and moisture separator reheaters on the sides.

WORKED EXAMPLE Modeling of a N4 PWR cycle

This example shows how a N4 PWR cycle with moisture separator reheater (MSR) can realistically be modeled with ThermoOptim. It is presented in the portal guidance pages (<http://www.thermooptim.org/sections/enseignement/cours-en-ligne/fiches-guides-td-projets/fiche-guide-fg15>).

This model is rather simple insofar as no extraction or reheat is taken into account, except for the moisture separator reheater.

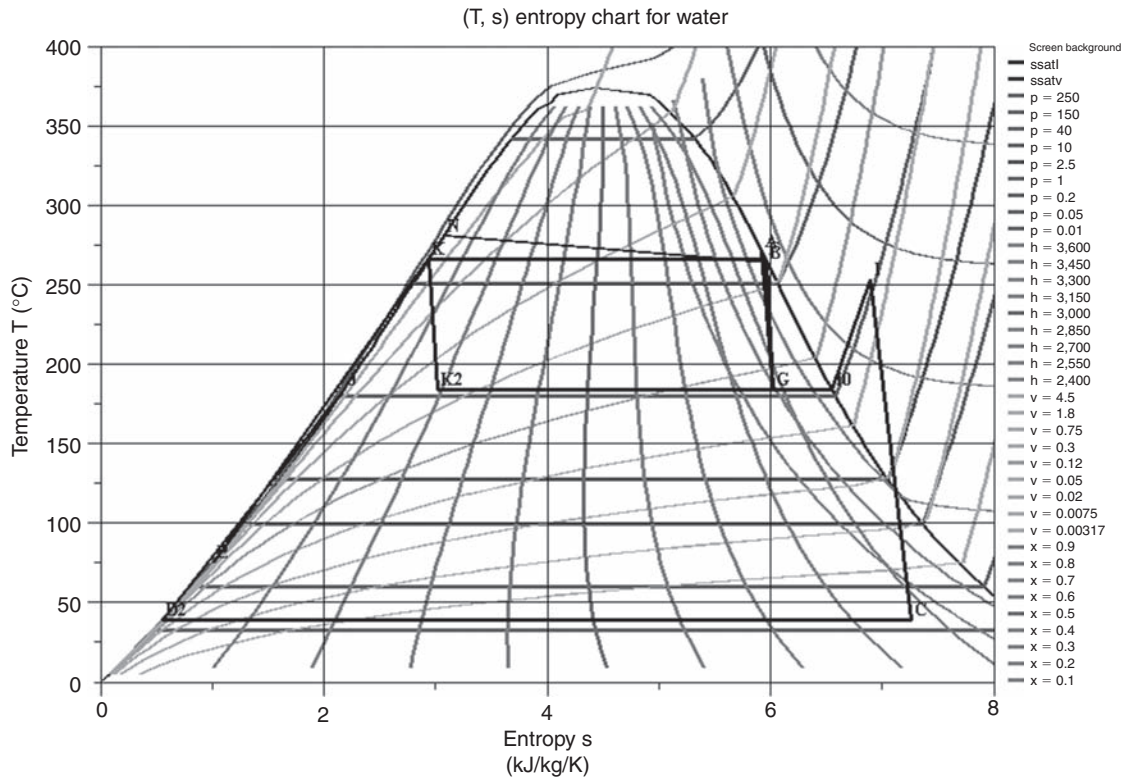


FIGURE 16.3.6
N4 PWR cycle in the entropy chart

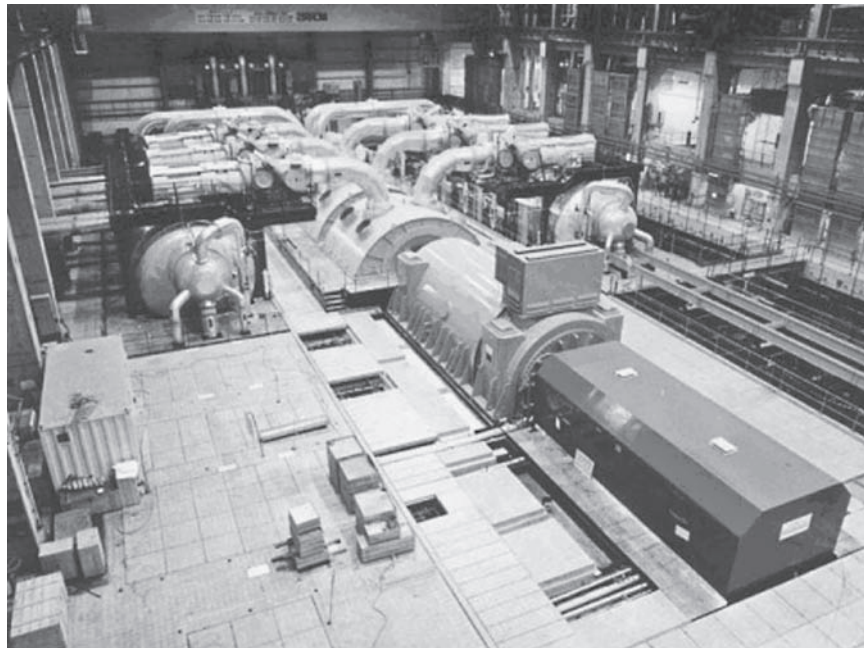


FIGURE 16.3.7
PWR engine room, Documentation Alstom Power

TABLE 16.3.1
PWR THERMODYNAMIC CHARACTERISTICS

Type	Q (MW)	τ (MWe)	HP (bar)	T (°C)	η
CP0	2785	921	52.2	267	33.1%
CP1	2785	921	52.2	267	33.1%
CP2	2785	881	49.3	263	31.6%
P4	3817	1289	66.7	283	33.8%
N4	4270	1457	67.4	283	34.1%
EPR	4500	1600	78.0	293	35.6%

16.3.4 Industrial PWR evolution

PWR has had the greatest development on an industrial scale. In France, the Messmer Plan adopted in 1973 led to the construction of a sixty plants of this type. The technology has evolved over the years, with as main models (known as units):

- 900 MWe: 34 units of type CP0 (Bugey), CP1 (Tricastin) and CP2 (Saint Laurent);
- 1300 MWe: 20 units of type P4 (Paluel);
- 1450 MWe: 4 units of type N4 (Chooz B);
- EPR, European Pressurized Reactor of 1600 MWe, whose construction is scheduled in Flamanville.

Existing plants, called second generation (see Chapter 29 of Part 4), were developed under American Westinghouse license. With an average age of about 25 years, their life, initially scheduled for 30 years, could be extended to 40 or even 50 years if the reliability of their materials is sufficient.

The EPR, which belongs to the third generation, is the result of a partnership dating from the early 1990s between Areva and Siemens. It is an evolution of French N4 and German Konvoi units leveraging the experience and intended to further increase the reliability of PWR plants and reduce costs.

This type of plant should replace those of the existing type if it is confirmed that the nuclear option should be retained, whether for economic, environmental (CO₂) and security of supply reasons. Indeed, Generation IV plants under development will not be commercially available before 2030.

Table 16.3.1 presents a summary of the main thermodynamic parameters of PWR technology: thermal power Q, net electrical power τ , inlet and pressure temperature, net efficiency.

It shows that the main quantitative leaps have been made between CP2 and P4 and between N4 and EPR.

REFERENCE

S. Jayet-Gendrot, F. Arnoldi, P. Billard, C. Dorier, Y. Dutheillet, L. Lelait, D. Renaud, *Des matériaux innovants pour un sujet brûlant*, Revue Epures, DRD EDF 1999, Paris.

FURTHER READING

A. Bernard, *Production électrique avec gazéification intégrée*, Revue de la Société des Electriciens et des Electroniciens, décembre 1999, Paris.

R. Gicquel, M. Williams, K. Aubert, *Optimisation du cycle eau-vapeur d'une centrale IGCC*, Conférence HPC'01, Paris, septembre 2001.

- Ph. Jaud, *Quels moyens de production pour le siècle prochain, l'avenir du thermique à flamme*, Revue Epures, DRD EDF 1999, Paris.
- M. Klaeylé, F. Nandjee, *Technologie de gazéification intégrée à un cycle combiné*, Techniques de l'Ingénieur, Traité Génie énergétique, BE 8 920.
- G. Labat, *La chaudière à lit fluidisé circulant: mariage de l'écologie et de l'économie*, Revue de la Société des Electriciens et des Electroniciens, décembre 1999, Paris.
- A. Lallemand, *Production d'énergie électrique par centrales thermiques*, Techniques de l'Ingénieur, Traité Génie électrique, D 4 002.
- O. Marquette, R. Bussac, S. Dal Secco, F. Marchand, S. Ignaccolo *Les chaudières à charbon pulvérisé: une technologie éprouvée à fort potentiel d'évolution*, Revue Epures, DRD EDF 1999, Paris.
- J.-M. Monteil *Centrale à cycle combiné, Théorie, performances, modularité*, Techniques de l'Ingénieur, Traité Génie énergétique, BE 8 905.
- J.-M. Monteil, *Centrale à cycle combiné, Composants potentiels*, Techniques de l'Ingénieur, Traité Génie énergétique, BE 8 906.
- J.-M. Monteil, *Centrale à cycle combiné, Fonctionnement, exploitation, exemple*, Techniques de l'Ingénieur, Traité Génie énergétique, BE 8 907.
- R. Serres, *Nucléaire, l'outil compétitif d'EDF*, Revue de la Société des Electriciens et des Electroniciens, décembre 1999, Paris.
- L. Tua, *Centrales à lit fluidisé sous pression*, Techniques de l'Ingénieur, Traité Génie énergétique, B 8925.

This page intentionally left blank

Combined Cycle Power Plants

Abstract: The excellent efficiencies reached today by combined cycle power plants (above 60% LHV), are the result of integration into a single production unit of two complementary technologies in terms of temperature levels: gas turbines, which operate at high temperature (in an aero-derivative turbine gases typically enter at 1300°C in the expansion turbine, and come out at around 500°C), and steam plants, which operate at lower temperatures (between 450°C and 30°C in this case).

In section 12.1.5.1 we saw that regeneration can significantly increase the performance of the Brayton cycle, but the percentage of energy recovered is even lower than the temperature and pressure levels of this cycle are higher. In modern gas turbines, regeneration is rarely possible or economically worthwhile. Another way to enhance the residual enthalpy of the exhaust gases is to use them as a heat source for a second cycle of production of mechanical energy. **Combined cycles** correspond to this new generation of thermal power plants.

Keywords: compression, expansion, combustion, combined cycle, HRSG, afterburner:

The principle of a combined cycle is to operate in cascade one or more gas turbines, followed by a steam power plant whose heat source is the cold source of gas turbines (Figure 17.1.1). Under these conditions, the gas turbine exhaust gas is recovered in a recovery boiler that produces steam that is then expanded in a condensing turbine. The combined cycle thus obtained is a particularly successful marriage in the search for improved thermal performance: with currently available machines,

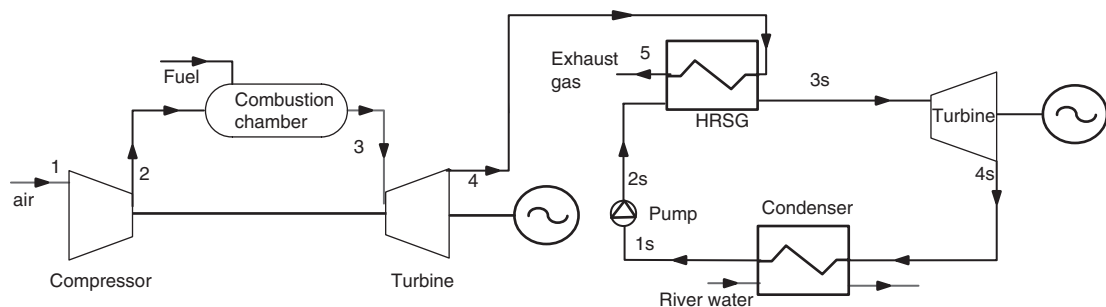


FIGURE 17.1.1

Sketch of a combined cycle

efficiencies exceed 55% and are higher than those we can hope, even in the medium term, of the most advanced future steam plants.

As we shall see next section, in a simple combined cycle of the type described below, the gas turbine provides two-thirds of the total capacity. The steam turbine, fueled by superheated steam conditions of 85 to 100 bar and 510–540°C, provides the remaining third.

17.1 COMBINED CYCLE WITHOUT AFTERBURNER

The simplest combined cycle (that is to say, without afterburner) is shown in Figure 17.1.1: as the temperature of the gas turbine exhaust gas can exceed 550°C, the maximum temperature level reached in a steam cycle, it is quite possible to recover the enthalpy available at the output of a gas turbine to heat a steam cycle.

With some simplifying assumptions, it is possible to construct an entropy chart allowing, for a set of suitable scales, to superimpose the two thermodynamic cycles (Figure 17.1.2). In this diagram, where the work done is proportional to the area of the cycle, the gas turbine provides more power than the steam engine (two-thirds of the total in practice).

We can sometimes improve the cycle efficiency by using the various changes discussed during the presentation of the steam cycle: reheat and extractions.

However, as discussed below, the problem of steam cycle optimization differs substantially from that of large steam power plants, due to the pinch that appears in the heat recovery steam generator (HRSG).

17.1.1 Overall performance

The enthalpy exchange in a combined cycle can be summarized by the diagram in Figure 17.1.3.

- the gas turbine receives heat \dot{Q}_g from the hot source. It provides on the one hand a useful work τ_g , and secondly a heat ($Q_v + Q_p$). The first term is the heat supplied to the steam cycle, the second losses;
- the steam cycle produces useful work τ_v , and the condenser rejects heat Q_c .

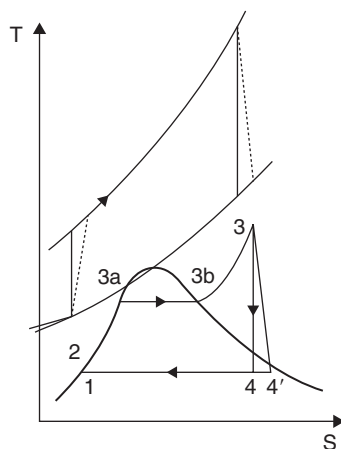


FIGURE 17.1.2
Combined cycle in the entropy chart

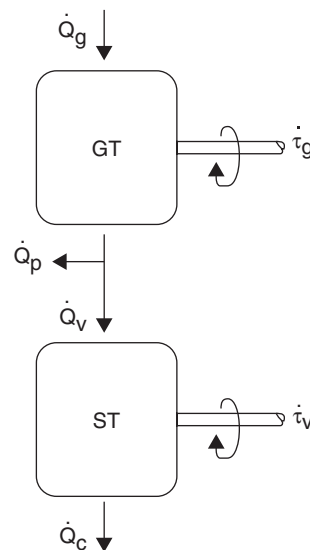


FIGURE 17.1.3
Block diagram of a combined cycle

Let us call η_g the gas turbine efficiency, η_v that of the steam cycle, η_{cc} that of the combined cycle, and ε the HRSG effectiveness, that is to say the ratio of Q_v to $Q_p + Q_v$:

$$\varepsilon = \frac{Q_v}{Q_p + Q_v} = \frac{Q_g}{Q_p + Q_v} \frac{Q_v}{Q_g} = \frac{1}{1 - \eta_g} \frac{Q_v}{Q_g}$$

$$\eta_{cc} = \frac{\tau_g + \tau_v}{Q_g} = \eta_g + \eta_v \frac{Q_v}{Q_g} = \eta_g + \varepsilon(1 - \eta_g)\eta_v$$

$$\eta_{cc} = \eta_g + \varepsilon(1 - \eta_g)\eta_v \quad (17.1.1)$$

The combined cycle efficiency is equal to the sum of that of the gas turbine and the product of its complement to 1 by the HRSG effectiveness and the steam cycle efficiency.

For example, with $\eta_g = 0.29$, $\eta_v = 0.32$, $\varepsilon = 0.83$, we obtain $\eta_{cc} = 0.48$.

17.1.2 Reduced efficiency and power

The reduced power introduced section 12.1.4.2 can also be expressed here as:

$$W_0 = \eta_{cc} \frac{\theta - r^{\beta_c}}{\theta - 1} \quad (17.1.2)$$

Assuming at first approximation that the steam cycle efficiency varies linearly with gas turbine exhaust temperature, we obtain in terms of overall efficiency and power the abacus shown in Figure 17.1.4. We can recognize the lower left part corresponding to the gas turbine alone (Figure 12.1.17). The contribution of the steam cycle is particularly significant: 50 to 60% more capacity and efficiency gains of 30–50% depending on temperature and compression ratio.

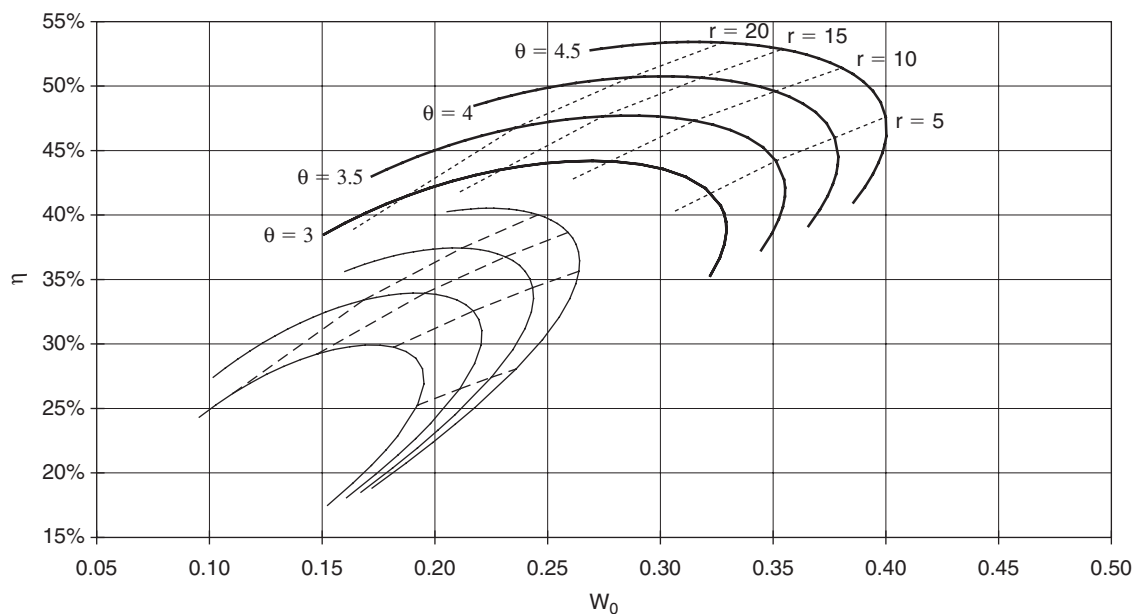


FIGURE 17.1.4

Efficiency and useful work of a combined cycle

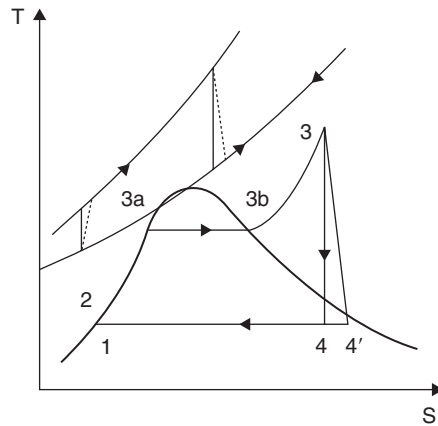


FIGURE 17.2.1

Combined cycle with afterburner

17.2 COMBINED CYCLE WITH AFTERBURNER

It is also possible to perform an afterburning of gas turbine exhaust, to have more power in the steam cycle, and especially to better control the combined cycle. This is called combined cycle with afterburner (Figure 17.2.1). The efficiency drops slightly because of course the heat generated by the afterburner is not valued in the GT. In this case, the total power is divided about equally between each machine.

This type of cycle is mainly appropriate when converting conventional steam plants in combined cycle plants, by adding a topping gas cycle. The conventional plant having its boiler, afterburning can be achieved without needing large investment.

17.3 COMBINED CYCLE OPTIMIZATION

Thermodynamic analysis of combined cycle without afterburner showed that overall performance is given by equation (17.1.1): $\eta_{cc} = \eta_g + \varepsilon(1 - \eta_g)\eta_v$

This expression shows that it is as important to optimize the steam cycle as the recovery steam generator, and thus its effectiveness ε . Difficulties arise because the problem is highly constrained and there may be conflicts between these two objectives.

We have already given some indication in section 15.6.2 on the problem of optimizing the HRSG. In particular, we saw that the gas discharge temperature in the atmosphere must be high enough to avoid condensation. But as we also seek to reduce them as much as possible to recover the enthalpy available, we see that in general it is unnecessary to perform high extraction on this type of steam plant, gains remaining low.

The optimization of such a combined cycle is based on the reduction of its internal irreversibilities, which can be grouped into three broad categories: mechanical irreversibilities, that take place in the compressor and turbines, combustion irreversibilities, and purely thermal irreversibilities, related to temperature differences in the heat exchangers.

Much has already been done to limit the mechanical irreversibilities, and reducing combustion irreversibility is directly related to the maximum temperature of the fumes, which itself depends on the strength of the combustion chamber materials and above all of the initial expansion stages in the gas turbine (stator and rotor).

So we focus in what follows only on the reduction of thermal irreversibilities, i.e. on the optimization of plants whose turbine outlet temperature is fixed. These irreversibilities result from differences in temperature between the hot and cold parts of the cycle.

In cogeneration plants (CHP) studied in Chapter 18, problems arise in a similar manner, especially if steam needs at medium and high pressure are important.

In a combined cycle plant, the vein of hot gases exiting the gas turbine must be cooled by water of the steam recovery cycle. In a single pressure cycle, water enters the heat exchanger in the liquid state at about 30°C after being compressed by the feedwater pumps downstream of the condenser. It is heated at the boiling temperature corresponding to its pressure (economizer), then vaporized at constant temperature and superheated before being expanded in the steam turbine. The diagram in Figure 15.6.7 shows the heat transfer within the heat exchanger between hot gases and water. The associated enthalpy diagram shows that if we set for technical reasons a pinch minimum value (temperature difference between both fluids) between points 6 and 9 on the one hand, and between points 4 and 11 on the other hand, heat exchanges take actually place with much larger differences in nearly all of the heat exchanger. This stems from the need to vaporize water, which induces a very important “plateau” at a constant temperature.

The example in Figure 17.3.1 corresponds to such a combined cycle. Hot gases exit the gas turbine at 559°C and maximum pressure of the steam cycle is equal to 120 bar. In these circumstances it is impossible to cool gases below 169°C, which represents a significant loss.

WORKED EXAMPLE

Modeling of a combined cycle in ThermoOptim

This example shows how to model with ThermoOptim a combined cycle and fit the steam cycle flow rate knowing the one which flows through the gas turbine. It is presented in the Diapason session S41En (<http://www.thermooptim.org/sections/enseignement/cours-en-ligne/seances-diapason/session-s41en-single>).



[CRC_pa_4]

The combined cycle exergy balance can be built as explained in section 10.2.3 of Part 2, resulting in Table 17.3.1.

The exergy efficiency reaches 45%, the main irreversibilities being still located in the combustion chamber (56%). Other losses are spread fairly evenly among the various components and exhaust. In descending order, they take place in the air compressor, gas turbine, steam turbine, economizer, evaporator, superheater, exhaust and condenser.

Irreversibilities in turbomachines represent 22% of the total. Manufacturers continue in their efforts to reduce them, and very significant progress has already been made in recent decades. Therefore opportunities for improvement are becoming fewer.

Losses in the HRSG and those in the exhaust are linked, as we have already seen. They represent 12.7% and 29% of losses outside the combustion chamber. Their reduction is therefore an important issue. The ideal heat exchange corresponds to the case where the curve of gas cooling and that water of heating would be parallel. The heat exchanger would then operate in counter-flow and irreversibility would be minimal. This is not feasible with water, and the single pressure cycle has strong internal irreversibilities.

To improve the cycle performance, we use multiple steam cycles at different pressure levels (two, three or even four). Figure 17.3.2 shows the value of using multi-level pressure: with some simplifying assumptions and a choice of scales, we can superimpose on an entropy chart gas turbine and steam power plant cycles. In all three cases, the grey surface represents work provided for the same heat input in the gas turbine. The rectangle in the dashed line is the Carnot cycle.

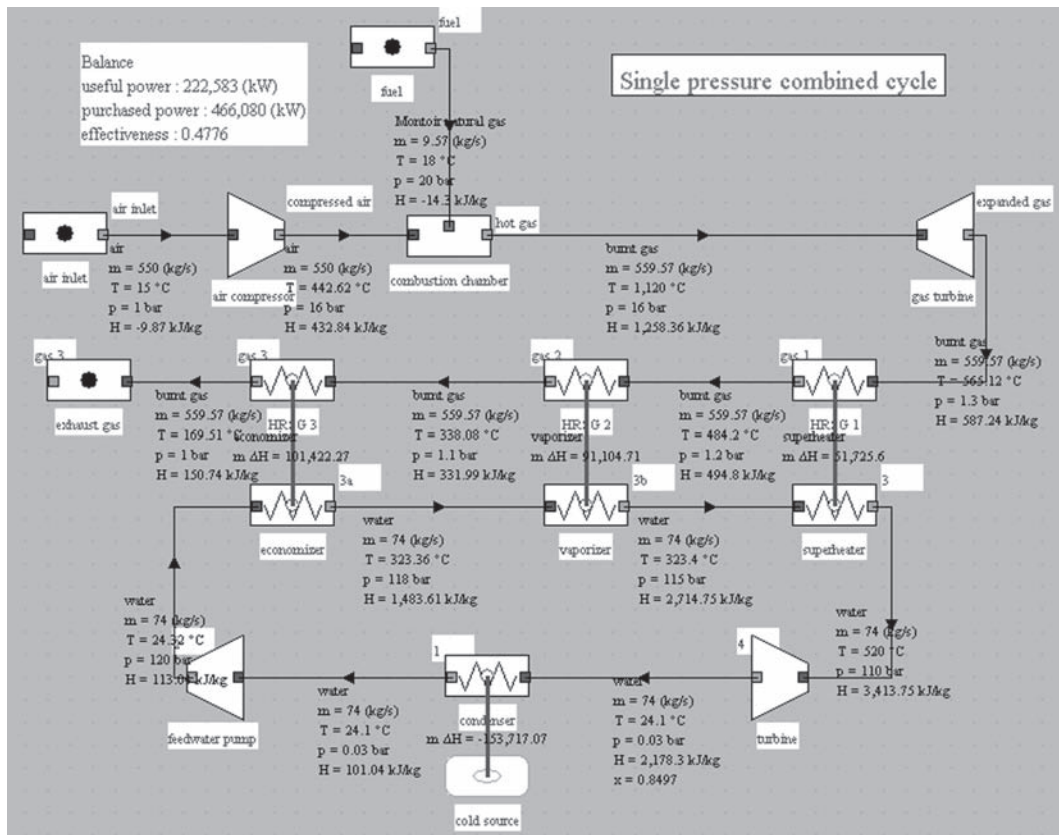


FIGURE 17.3.1
Synoptic view of a single pressure combined cycle

TABLE 17.3.1
EXERGY BALANCE OF SINGLE PRESSURE COMBINED CYCLE

Exergy balance process	$T_0 = 288.15\text{ K} = 15^\circ\text{C}$							
	τ (MW)	Q (MW)	$m\Delta h$ (MW)	T_k (K)	Δx_q (MW)	$m\Delta x_h$ (MW)	Δx_{hi} (MW)	% loss
HRSG 3		-101	-101			-50	15	5.96%
Economizer			101	101			35	
HRSG 2		-91	-91			-57	10	3.80%
Vaporizer			91	91			47	
HRSG 1		-52	-52			-37	8	2.93%
Superheater			52	52			29	
Feedw. pump	1		1				1	
Steam turbine	-91		-91			-107	16	6.09%
Condenser		-154	-154	288	0	-5	5	1.83%
Air compr.	243		243				221	8.66%
Gas turb.	-376		-376			-394	19	7.36%
Comb. ch.			466		466	323	143	55.75%
Asp/exhaust						-20	20	7.63%
Cycle	-223	312	90			-12	257	100.0%
Sigma(x_q+)			466					
Sigma($\tau+$)			0.00					
Exergy efficiency			45%					

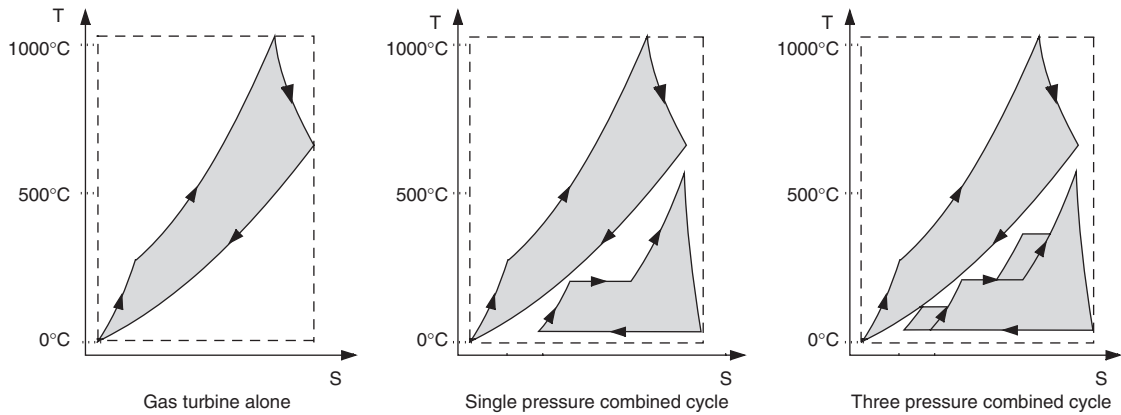


FIGURE 17.3.2

Comparison of work provided by a gas turbine and combined cycles

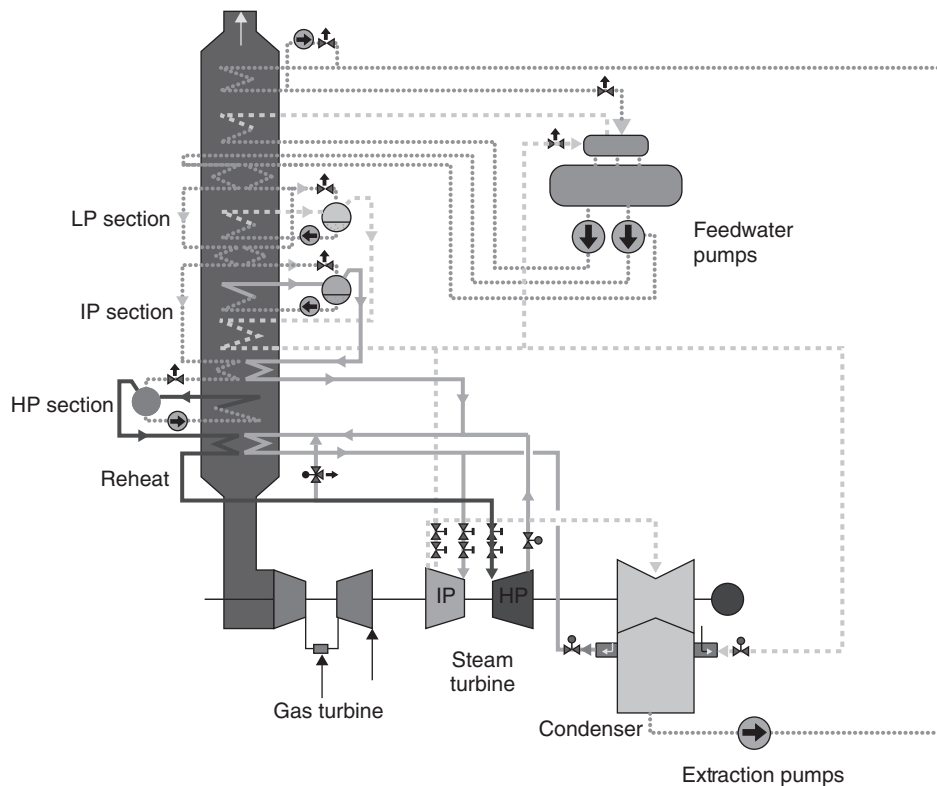


FIGURE 17.3.3

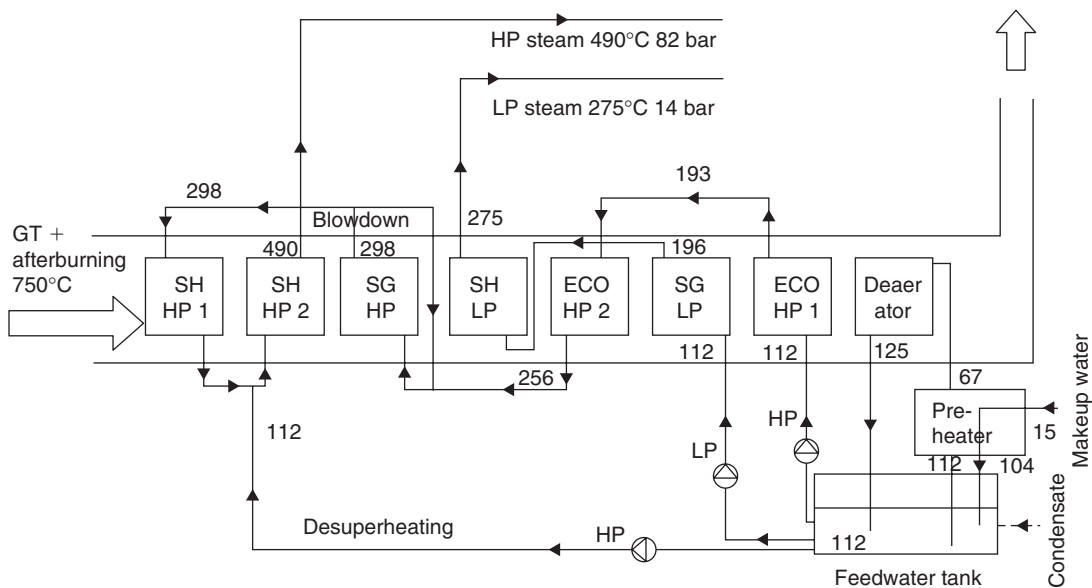
Three pressure HRSG, Documentation Alstom Power

The left figure corresponds to a single gas turbine, the middle to a single pressure combined cycle, and the right to a three pressure combined cycle. The gain provided by the increased number of pressure levels is very clear, but designing the HRSG is a complex optimization problem and quite new, which does not arise in conventional boilers.

The optimization of such cycles is a complex problem, because to get the better cooling of the hot gas stream, there are many degrees of freedom on the pressure levels, on the corresponding flow rates, and on placement of heat exchangers (in series or in parallel). Figure 17.3.3 gives an example

**FIGURE 17.3.4**

Supercritical mono-tubular HRSG, Documentation Alstom Power

**FIGURE 17.3.5**

Exchanger arrangement of a dual pressure HRSG

of an industrial three pressure HRSG, with the whole combined cycle. Figure 17.3.4 shows the look of a supercritical mono-tubular HRSG and Figure 17.3.5 shows the exchanger arrangement of a dual pressure HRSG for a non-optimized cogeneration unit.

This optimization problem is quite new. It did not arise in old power plants, in which very large irreversibilities occurred for technical and economic reasons related to the thermal resistance of steel boilers and sulfur content of fumes. There is no proven method to solve it.

The optimization method presented in Chapter 22, known as Systems Integration, is the extension to the case of power generation or cogeneration plants, of the pinch method developed in the context of chemical engineering to optimize the configuration of very large exchanger networks (such as those of a refinery).

The example presented section 12.6 shows in particular how this method can be implemented to size a dual pressure combined cycle.

17.4 GAS TURBINE AND COMBINED CYCLES VARIATIONS

Other cycles, more complex to study, have been proposed and are the subject of various studies and experiments. They will be presented in Chapter 24 of Part 4. Two of them are particularly interesting and can yield high efficiencies, because the heat exchange with the exhaust gases is made with very low irreversibility: the humid air cycle and the Kalina cycle.

In the humid air cycle, the air leaving the compressor is humidified in a saturator with water heated by exhaust gases. It leaves the saturator cooled and is then preheated in a regenerator before being directed to the combustion chamber and then into the turbine. This cycle looks a little like a steam injection cycle, but its performance is much better.

The Kalina cycle is a combined cycle variation where water is replaced by a water-ammonia mix which vaporizes and condenses with a temperature glide.

Furthermore, many variations are possible in combined cycles: for example it is possible in the gas turbine, to make an intermediate cooling during compression, or a reheat. More complex cycles are under investigation. Their detailed presentation is beyond the scope of this book: we limit ourselves to some thermodynamic considerations on a key combined cycle component: the recovery steam generator. For other developments, the reader may refer to the thesis of H. Abdullah (1988) referenced at the end of Chapter 12.

Finally, we will study in the next chapter cogeneration plants, for simultaneous production of mechanical power and heat, among which will appear some variants of the combined cycles considered above.

17.5 DIESEL COMBINED CYCLE

We discussed in section 13.9.2.1 the rise of temperatures in diesel engines. This has achieved the following gains, particularly suitable for use in combined cycle:

- mechanical efficiency increased from 45% to 47%;
- enthalpy of exhaust gas increased from 27% to 32%;
- cooling losses reduced from 24% to 16%.

Today, a less than 100 MW diesel combined cycle based on medium-speed diesel engine reaches an overall efficiency of 55%, which makes it competitive with gas turbines in this capacity range.

17.6 CONCLUSIONS AND OUTLOOK

The very high efficiencies provided by combined cycles explain the enthusiasm for these plants, and the rapid development of their market: one of the largest such plant in operation, Futtsu in Japan, has an installed capacity of 2,000 MW.

Among the many benefits of combined cycles, we can mention:

- as for gas turbines, combined cycles are normally designed standardized and modular, so that different components are factory built and assembled quickly on site, while a steam power plant must be calculated and built case by case;
- thus, combined cycles have almost no effect of scale. It is not necessary to construct a single unit of large capacity: we can start with small units, and add others as demand grows;

- due to the excellent efficiencies that are achieved and also the use of fuels with low sulfur and nitrogen, the environmental impact of these technologies is much lower than that of their competitors: CO₂ emissions are only equal to 40% of those of coal steam plants, and they require three times less water cooling;
- in the same way, the combined cycle footprint is close to 80 m²/MW, against about 200 m²/MW for a steam power plant. It is therefore easier to locate them close to consumption areas.

One major limitation is that gas turbines require the use of clean fuel (expensive), such as natural gas or light distillates, which excludes the use of heavy fuel oil or coal, traditional basic fuels for power plants. However, development of coal gasification would allow this energy source to fuel these efficient combined cycles.

In the coming years, efficiencies should rise from 50 to 60%, and prices fall further, thereby increasing the economic competitiveness of these machines.

REFERENCES

- R. I. Crane, *Thermodynamics of combined cycle plant*, Von Karman Institute for Fluid Dynamics, Lecture Series 1993, Combined Cycles for Power Plants.
- J. H. Horlock, *Combined Power plants, past, present and future*, CogenTurboConference, Portland, 1994.
- C. Kempf, *Les centrales électriques à cycle combiné*, Revue de la Société des Electriciens et des Electroniciens, décembre 1999, Paris.

FURTHER READING

- P. Stouffs, S. Harvey, *Energétique avancée des cycles à turbomachines*, Cours de DEA Thermique, Energétique et Génie des Procédés, septembre 1996, Nantes.

Cogeneration and Trigeneration

Abstract: We call **cogeneration** the combined production of thermal energy and mechanical energy or electricity (CHP for Combined Heat and Power), and **trigeneration**, or combined cooling, heating, and power generation (CCHP), the simultaneous production of mechanical energy, heating and cooling. Since electricity is often the form in which high value energy is produced, sometimes we will for brevity omit in the following to refer to mechanical energy.

The basic idea of cogeneration is that combustion takes place at very high temperatures (above 1,000°C), while the need for heat in industry or for heating occurs at lower temperatures, generally between 80°C and 300°C. In these circumstances it is quite possible, when using combustion to meet heating needs, to take advantage of this temperature difference to generate electricity through an engine cycle. The heat source of the engine cycle is the boiler or the combustion chamber, and the cold source corresponds to the heat needs.

It is also theoretically possible to produce heat at high temperature on the premises producing electricity, but this generally proves bad as heat is much less easy to transport than electricity.

Keywords: cogeneration, trigeneration, CHP, CCHP, gas turbine, heat and power, total energy, heat-power ratio, back-pressure, extracting and condensing turbines, Stirling, micro-turbine, diesel, gas engine, district heating.

The main advantage of cogeneration cycles is that they are among the most efficient in terms of energy and exergy. However, their economic interest should be assessed in each situation, particularly in a country like France where electricity prices are very attractive to industry.

Generally, the objectives pursued by CHP are twofold: firstly to achieve economies of operation, and secondly to ensure security of electricity supply at least for part of the units. Given their purposes, cogeneration plants can be grouped into three classes:

- “heat and power” installations where heat is the commodity, electricity being a byproduct allowing to give a better value to the fuel. This is the case of large plants using heat or district heating or garbage incineration facilities. Priority is given to the provision of heat, electricity, easily transportable, being valued by selling power surpluses to utilities. In the event of mains utility failure, the plant operates in island mode;
- “total energy” systems seeking to ensure electrical autonomy, heat being the byproduct. They are generally off-grid plants and ships;

- not autonomous facilities, undersized for economic reasons, for which a supplement is provided by utilities for electricity and by a conventional boiler for heat. The installation works only when electricity prices are high and heat needs high. This type of installation is quite common, and is often the one that leads to the best financial results for the company.

Technically, it is customary to classify CHP into two families, depending on the engine cycle used:

- boiler and steam turbine systems, which are widespread, as the benefits of this configuration has been known for over a century. They can use a wide variety of fuels, including coal or waste;
- internal combustion engine systems, which use either gas turbines or reciprocating engines (especially diesel and gas engines). Heat is recovered from exhaust gases as well as coolants and lubricants. Only liquid and gaseous fuels can be used in these engines.

This classification does however not cover all the scenarios. As we have shown in section 14.7, there are units such as Stirling engine cogeneration, which is an external combustion engine. Finally, when the plant produces at the same time heat, motive power and cooling, it is called trigeneration or combined cooling, heating, and power generation (CCHP).

18.1 PERFORMANCE INDICATORS

A cogeneration plant produces both heat and electricity. To describe its performance in both regulatory and technical terms, we introduce a number of indicators, defined below.

Let us call Q_c the heat supplied to the cogeneration machine, that is to say, released by the combustion reaction, Q_u the useful heat, τ the mechanical energy or electricity produced. In what follows, these different energies are expressed in the same units, usually kWh or MJ.

Let us call:

- mechanical efficiency the ratio $\eta_m = |\tau|/Q_c$;
It characterizes the performance of the facility as a generator of electricity. The best mechanical efficiencies are obtained in conventional power plants where $Q_u = 0$.
- overall efficiency the ratio $\eta_g = |\tau + Q_u|/Q_c$;
It characterizes, in terms of energy, the overall efficiency of the facility.
- exergy efficiency the ratio $\eta_x = |\tau + (1 - T_0/T)Q_u|/Q_c$;
 T_0 is the temperature of the environment and T is the temperature at which heat is provided. It allows, through the introduction of the Carnot factor, to characterize the temperature level at which heat is provided.
- heat-power ratio the ratio $CF = Q_u/|\tau|$;
It is representative of the distribution of energy between heat and electricity.
- specific equivalent consumption the ratio $C_E = (Q_c - |Q_u|/\eta_c)/|\tau|$.

η_c being an average conventional boiler effectiveness, usually taken equal to 0.9.

It represents the primary energy consumption leading to the production of one kWh of electricity. In fact, this is not quite the case, because heat provided Q_c is final energy and not primary energy, which induces a slight bias. The indicative value of C_E for a conventional power plant is greater than 2.5, when it is only 1.7 for a combined cycle plant of 60% efficiency.

These indicators, as defined above for a given operating point, are likely to vary depending on operating conditions, including the environment temperature. To estimate their average values over a long period, such as the heating season or a year, they are calculated from the cumulative values of variables considered.

The regulator has used some of them to determine if an energy facility may or may not be considered as a cogeneration unit, which determines its ability to sell electricity to utilities. Although it is not our intention in this book to deal with regulatory issues, we note that criteria at the end of 2000 were in France:

- the average annual total efficiency must exceed 65%;
- the average annual heat – power ratio must be above 50%.

18.2 BOILERS AND STEAM TURBINES

In a boiler and steam turbine cogeneration plant there is, depending on the case, a single turbine called back-pressure, or two turbines called extracting and condensing (see Figures 18.2.1 and 15.7.3).

In back-pressure turbines, well adapted as heat needs change little, steam produced in the boiler at an initial pressure generally between 30 and 50 bar, is expanded at a pressure (called back-pressure) of about 2–6 bar and temperatures of 130 to 160°C. This steam is then used directly in processes or district heating.

In extracting and condensing turbines all the steam passes through the high pressure section, which behaves like a back-pressure turbine. A fraction is then extracted to feed processes or district heating, while the remainder is expanded in a low-pressure section and finally condensed either by air (Figure 18.2.1) or by water cooling.

This type of turbine can largely decouple the production of electricity from that of heat, and is therefore very well suited for cogeneration facilities used for space heating. In summer, extraction is minimal and electricity production maximal, in winter it is the opposite.

The overall plant efficiency of back-pressure facilities, however, is slightly higher than that of extracting and condensing units, because in the latter, part of the heat is discharged to the condenser. These configurations are widely used for applications where heat needs are important, as in garbage incinerators (Municipal solid waste incineration or MSWI), central heating networks, heavy industries.

We may to some extent modulate the fraction of the load which is taken to supply the district heating network, and, where appropriate, by-pass the turbine low-pressure section or heating network. Only a detailed study of the off-design behavior of the various components of the system, taking into account the respective rates of sale of heat and electricity, can determine the economic optimum.

Under these conditions, the heat-power ratio CF can vary from one plant to another or during operation. For smaller units (a few hundred kilowatts), values of 8 to 15 are customary. For larger installations, this ratio drops to values between 3 and 5. Overall efficiency is generally excellent, above 80% even for large values of heat-power ratio. Mechanical efficiency is quite low, between 6 and 22%, and specific equivalent consumption C_E varies from 1.6 to about 3.

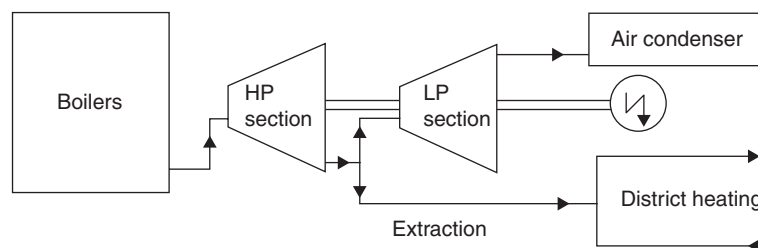


FIGURE 18.2.1

Boiler and steam turbine cogeneration unit

18.3 INTERNAL COMBUSTION ENGINES

Efficiencies of internal combustion engines are quite variable depending on type and size: 15 to 22% for small gas turbines (micro-GT), 35–40% for large modern gas turbines, 25 to 30% for small gas engines, and 35–45% for large diesel and gas engines. Moreover, the efficiency of reciprocating engines varies little with the rotation speed, while that of gas turbines, which operate at nearly constant air flow depends strongly on the load.

Heat is rejected either in exhaust gases or by cooling water, according to a distribution that varies widely depending on the engine type, as shown in Tables 14.1.1 and 18.3.1 (you should refer to Chapters 12 and 13 for more details on the operation of internal combustion engines).

Moreover, the strong excess air (400%) used in gas turbines means that their exhaust gases contain a lot of oxygen (16 to 18% O₂). It is therefore possible to exploit these gases (usually very clean, especially if the fuel used is natural gas), continuing the combustion processes in furnaces or boilers, or even using them directly as drying fluid.

Given these characteristics, it is obvious that possible configurations are very diverse in terms of internal combustion engine cogeneration.

18.3.1 Reciprocating engines

The simplest and most common solution is the production of either hot water at a temperature of 100°C, or superheated steam at 110–120°C, as auxiliary to a classical boiler (Figure 18.3.1). Depending on its purity, water can be directly heated in the engine, or must pass through a low temperature heat exchanger. It then recovers the exhaust gas heat in a heat exchanger placed in series. Hundreds of such units of all capacities (a few kW to several MW) are installed worldwide.

TABLE 18.3.1
POWER DISCHARGED BY kW OF USEFUL POWER

	Cooling water ($T \approx 80-100^{\circ}\text{C}$)	Exhaust ($T \approx 400-500^{\circ}\text{C}$)
Small gas engine	1.00	1.33
Diesel	0.56	1.22
Gas turbine		1.8–3.5

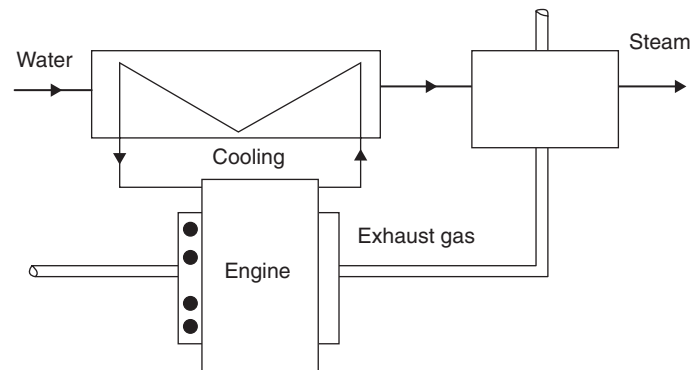


FIGURE 18.3.1

Internal combustion engine cogeneration unit

A second solution is to cool the engine by an air flow which, in series, provides a convective cooling, and then passes through a recovery heat exchanger on oil, the supercharger intercooler if it exists, the classic radiator cooling system, and finally an air/flue gas exhaust. Hot air is then used for drying, its enthalpy being, if necessary, raised by a supplementary burner.

The engine can also be used for air conditioning, driving a compressor directly connected on the shaft, to obtain industrial cooling or chilled water, heat recovered being used for purposes of either heating or cooling in an absorption machine. An alternator can at times be coupled to the engine instead of the compressor, which allows, according to the tariffs of electricity and refrigeration needs, to modulate the production.

The reciprocating engine may finally directly drive a heat pump compressor. The overall efficiency of the system can be very high, given the coefficients of performance of heat pumps.

The heat-power ratio CF is quite low, between 0.5 and 1.5. Overall efficiency is generally very good, above 70%. Mechanical efficiency is usually very high, between 30 and 35% for small gas engines, and up to 45% for large diesel and gas engines. Specific equivalent consumption C_E is of the order of 1.6 to 2.

18.3.2 Gas turbines

In gas turbines, the total residual heat is found in the exhaust. The performance of the cogeneration system is directly related to the recovery of these gases.

One solution is to cool exhaust gases in an air-fumes heat exchanger which can heat the air which is then used for many applications. If the turbine is stopped, an auxiliary boiler ensures the supply of heat to meet the plant needs. One generally uses several cascading recovery exchangers on the exhaust, so it can be cooled as much as possible and air is available at different temperatures for various uses.

Another solution, widely used today, especially to replace an existing boiler, is to install a heat recovery steam generator (HRSG) at the output of the gas turbine. The problem of optimizing the recovery exchangers is very similar to the one we have discussed in section 17.3: the best configuration must indeed both cool at best the GT exhaust and provide heat at the highest temperature level possible as needed.

Figures 18.3.2 and 18.3.3 show the two main components of a cogeneration plant for district heating network of this kind built by the Société d'Exploitation des Centrales de Chauffage (SECC). The turbine is a Solar Mars 1000, 10.4 MWe, 15 m long, 3 m high and 3 m wide. Its total mass (turbine,

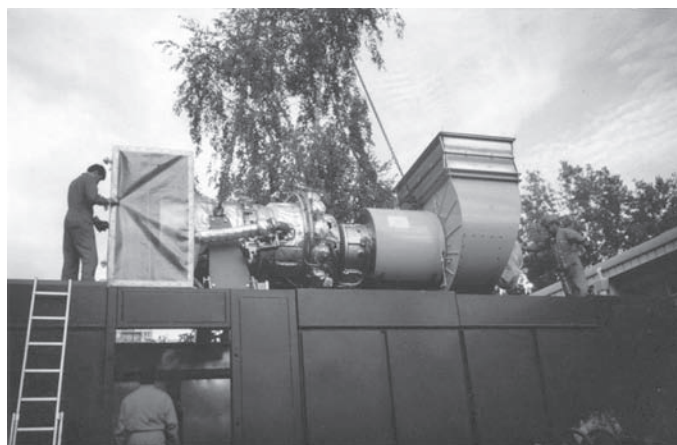


FIGURE 18.3.2

Cogeneration gas turbine, Documentation SECC



FIGURE 18.3.3

Cogeneration HRSG, Documentation SECC

gearbox, alternator) is about 100 t. The 14.5 MW water tube and single pressure level recovery boiler, brand Bono, has a height of 6.5 m and a width of 5.5 m, a mass of 45 t. In the foreground, the photo shows the bypass chimney that allows for a bypass of the boiler. The vaporization drums are also clearly visible.

As we have seen, we can also use an afterburner, which can raise the enthalpy of fumes in pursuing the combustion of residual oxygen in a boiler or furnace. This method avoids the investment of various smoke-air exchangers needed in the previous case. The boiler and burner are of a somewhat unusual type given the level of exhaust gas temperature and composition. It can however be used only if the fuel is desulfurized. Given the cost of light distillates and kerosene, it is generally adapted to natural gas.

The afterburner may also be used in combination with a recovery exchanger, and thus allows better control of the thermal power depending on the needs. The gas turbine flow is nearly constant so that its efficiency is the best possible (cf. example in section 18.5.2).

When the gas turbine used is a micro-turbine rated less than 100 kW, it is enough to heat water, either upstream of an existing boiler, or for hot water uses. The recovery exchanger is then simpler and less expensive than a HRSG. Example presented in section 18.5.1 corresponds to this configuration.

Another very efficient scheme is to directly use the exhaust gases as hot fluid in a dryer. As in the case of the reciprocating engine, the turbine itself is placed in the airflow, so that all losses can be recovered, leading to an overall efficiency close to 1. In addition, the output pressure of the exhaust gas is sufficient to avoid any fan. The hot gas temperatures (400–500°C) being compatible with many industrial requirements, applications of this method are numerous.

If necessary, the two principles above can be combined. Finally, the gas turbine can, like the reciprocating engine, be used to directly drive a compressor or heat pump.

In many cases it may be advantageous to choose a configuration combining a gas turbine and one or more steam turbines to convert into electricity a portion of the heat recovered from the GT exhaust. It is thus possible to design cogeneration combined-cycles, with many variations possible, for example using a back-pressure steam turbine. The performance of these facilities is generally excellent, and they lend themselves well to the rehabilitation of existing cogeneration units, the GT replacing the old boiler (see Example in section 18.5.2).

Heat-power ratio CF is slightly higher than for reciprocating engines, between 0.8 and 1.8. Overall performance is generally very good, above 80%. Mechanical efficiency varies with the size of the gas turbine between 25 and 30% for small units and up to 40% for very large ones. Specific equivalent consumption C_E is between 1.4 and 1.7.

TABLE 18.4.1
COMPARISON OF DIFFERENT TECHNOLOGIES

	Capacity	η_g	η_m	CF	C_E
Stirling	0.5–100kW	>70%	15 to 30%	1.2 to 7	1.8 to 2.6
Micro-GT	25–75kW	>80%	25 to 32%	1.5 to 2.2	1.5 to 1.7
Engines	0.05–50MW	>70%	25–45%	0.5 to 1.8	1.6 to 2
GT	5–200MW	>80%	35–40%	0.8 to 1.3	1.4 to 1.6
ST	0.5–200MW	>80%	6 to 22%	3 to 12	1.6 to 3
GT + ST	20–200MW	>80%	>40%	0.8 to 1.2	1 to 1.4

18.4 CRITERIA FOR SELECTION

In general, CHP leads to a better use of primary energy than is allowed for separate production of heat and mechanical power. However, the decision-maker rarely views the problem in terms of primary energy saving: he must justify his choices based on the micro-economic context in which they operate.

Before deciding to use a cogeneration facility, it is necessary to make an extensive study of energy and thermal needs and their evolution over time. Indeed, the corresponding investments are generally high, and, to amortize them, the facility must operate at its optimum economic point as long as possible when the energy price is justified, and if possible at about 80–90% of the maximum engine capacity, range leading to the best technical performance.

The profitability calculation depends fundamentally on operating conditions and their evolution over time, each facility representing a special case that requires detailed study. It is particularly important to properly ensure that the statutory criteria authorizing the resale of electricity to utilities will be respected.

If security considerations require the use of an independent mechanical power production unit, it is almost certain that its use in cogeneration will be profitable, the overhead being limited to expenses for heat recovery, often well below those corresponding to the engine and alternator.

Moreover, the technical solution choice depends on many factors. For purposes of comparison, Table 18.4.1 provides approximate values of the different performance indicators for key possible technologies. The first two rows correspond to what is now called micro-cogeneration, based on Stirling engines or small capacity micro turbines. The configuration GT + ST is representative of hybrid solutions between cogeneration and combined cycle, an example of which is given below (18.5.2).

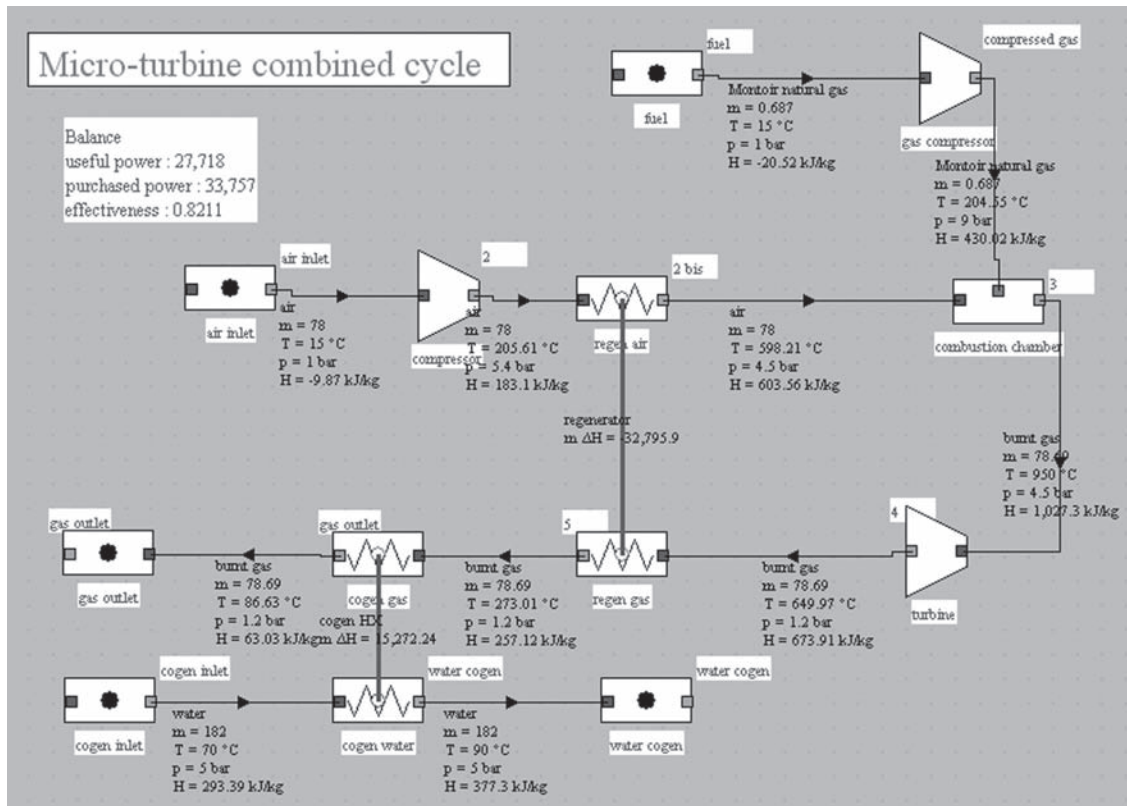
18.5 EXAMPLES OF INDUSTRIAL PLANTS

We give below two examples of industrial facilities involving gas turbines. The first is relatively simple: a micro-turbine is used to generate electricity and to preheat water in liquid form in an economizer while the second, more complex, uses an aero-derivative gas turbine of average capacity, with or without afterburner, a steam cycle and a boiler. The system configuration changes depending on the heating requirements (which vary with outside temperature).

The two cases presented correspond to actual installations in operation. Their name is omitted at the request of manufacturers who exploit them.

18.5.1 Micro-gas turbine cogeneration

A micro-gas turbine is a gas turbine of small capacity (several tens of kW), typically operating with a low compression ratio and with a regenerator to improve performance (see section 12.1.5.1).

**FIGURE 18.5.1**

Synoptic view of a micro-gas turbine cogeneration plant

In the plant we are interested in, a micro-turbine of 100 kW is used to warm 1.82 kg/s of water from 70 to 90°C. The turbine sucks 0.78 kg/s of air that is compressed at 5 bar, then passes through a regenerator before being heated to 950°C in the combustion chamber burning natural gas. Gases are expanded at a temperature of 650°C and then pass successively through the regenerator and the cogeneration exchanger (Figure 18.5.1). A gas compressor is required to raise the pressure of natural gas from the distribution network.

Modeling such a facility in ThermoOptim poses no particular problem, and leads to the diagram of Figure 18.5.1. Here useful energy includes not only compression and expansion work, but also thermal energy supplied to the water circuit, which leads, for the use conditions adopted, to an overall efficiency of nearly 82%: about 125 kW of electrical power and 153 kW of heat for a fuel consumption of 340 kW. Mechanical efficiency is 36.7% and heat-power ratio is 1.23.

The exergy balance of the cycle can be built and yields Table 18.4.2

The exergy efficiency is only 41%, that is to say half the overall cogeneration efficiency. This is partly explained by strong irreversibilities in heat exchangers, working with important log-mean temperature difference (LMTD, cf. section 8.1.1 of Part 2) (60 K for the regenerator, and 73 K for the CHP exchanger).

Exergy balance properly highlights the distribution of irreversibilities: more than half in the combustion chamber, and about 15% in each of the two heat exchangers, which, as we have seen, are not optimized. Exhaust gas losses are however almost negligible.

18.5.2 Industrial gas turbine cogeneration

The second cogeneration plant that we present is much more complex, and of a higher capacity.

TABLE 18.4.2

MICRO-GT COGENERATION EXERGY BALANCE

Exergy balance		$T_0 = 288.15\text{ K} = 15^\circ\text{C}$						
process	τ (kW)	Q (kW)	$m\Delta h$ (kW)	$m\Delta s$ (kW/K)	Δx_q (kW)	$m\Delta x_h$ (kW)	Δx_{hi} (kW)	loss
Air compr.	151		151	0.04		139	12	5.8%
Gas compr.	3		3	0.00		3		0.2%
Comb. ch.			340	0.37	340	233	107	53.6%
Turbine	-278		-278	0.06		-297	18	9.2%
Regen. gas		-327	-327	-0.41		-208	31	15.8%
Regen. air		327	327	0.52		177		
Cogen. gas		-153	-153	-0.34		-55	27	13.4%
Cogen. water		153	153	0.43		28		
Exhaust						-4	4	2.0%
Cycle	-125		215	1		20	199	100.0%
Sigma(x_q+)		340						
Sigma(τ+) 		0.00						
Exergy efficiency				41%				

WORKED EXAMPLE**Cogeneration plant producing electricity and providing heat to a district heating**

This example which corresponds to a real-world case, has been modeled in detail by S. Candelier and is presented in the Diapason session S47En (<http://www.thermooptim.org/sections/enseignement/cours-en-ligne/seances-diapason/session-s47en-district>).

This cogeneration plant produces electricity and provides heat to the district heating network of a town of 30,000 inhabitants. This is a “heat-power” type installation, where the heat is the commodity, electricity being a byproduct sold to the utility to valorize the fuel.

We only give in this section some extracts from this work and present the main results.

HDPT

[CRC_we_8]

The heating system is a circuit of pressurized water whose temperature is between about 90°C and 130°C. The circuit exits the facility at its maximum temperature, then passes through the city exchange sub-stations ensuring the heating and/or domestic water heating of homes, buildings, hospitals, school groups etc. Finally it returns to the plant at its minimum temperature to be heated again.

City heat requirements vary throughout the year depending on climatic conditions. The plant must adapt to these needs and adjust the thermal power it provides to the network.

18.5.2.1 Facility description

The facility has three independent circuits which exchange only heat (Figure 18.5.2):

- a **gas turbine (GT)**, connected to a generator, provides about 80% of site electricity production. Gases exiting the GT at about 450°C are burned again with a small amount of fuel. Flue gases, whose temperature is about 600°C, warm steam circuit water in a recovery boiler, then the water of the urban network. Finally they are released into the atmosphere at about 150°C, through the chimney;
- a **steam circuit** provides the remaining 20% of electricity production. Water is heated into steam and then superheated in the recovery boiler by exhaust fumes from the GT. A desuperheating is

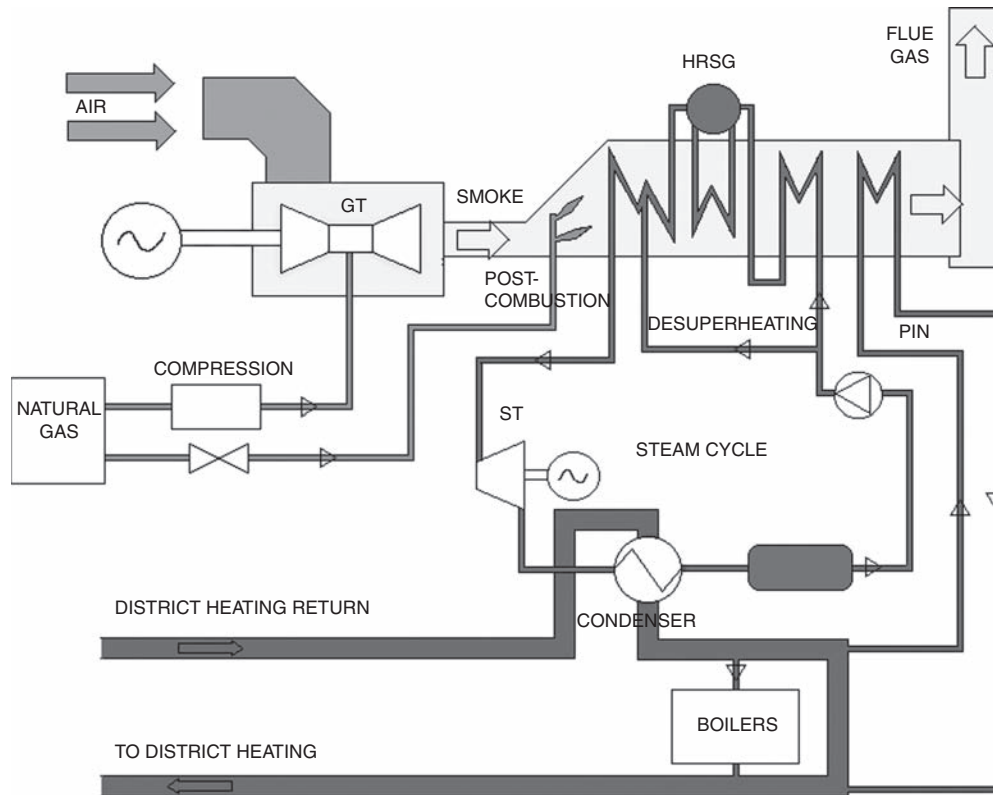


FIGURE 18.5.2

Schematic overview of the cogeneration plant

performed in the middle of the boiler to regulate the steam turbine inlet temperature. It is then expanded in a steam turbine (ST) connected to a generator. In the condenser, in which pass both the steam circuit and the urban network, steam is condensed. Finally, liquid water is directed to the feedwater tank and pumped into the recovery boiler;

- the **urban network** is traversed by hot liquid water under pressure. The latter returns at minimum temperature. It is then reheated in the condenser, where it acts as a heat sink. Part of this water is heated in the recovery boiler in a heat exchanger called “pin”. The flow in the pin is limited. If the thermal contributions from the condenser and the pin do not meet the network needs, the remainder is provided by boilers in derivation.

In this example, we modeled all three circuits and their interactions by heat exchangers, and then determined the energy balance of the plant, and different efficiencies of the cogeneration plant: mechanical (or electric), heat, global, and heat-power ratio in different operating cases.

18.5.2.2 Operating cases

The plant must adapt to the needs of the district heating system providing the hot water circuit with a thermal power which depends on climatic conditions and, in average, on outdoor temperature (from 38 MW, 1,130 t/h of water between 90 and 120°C at 5°C to 64 MW, 1,370 t/h of water between 90 and 130°C at -5°C).

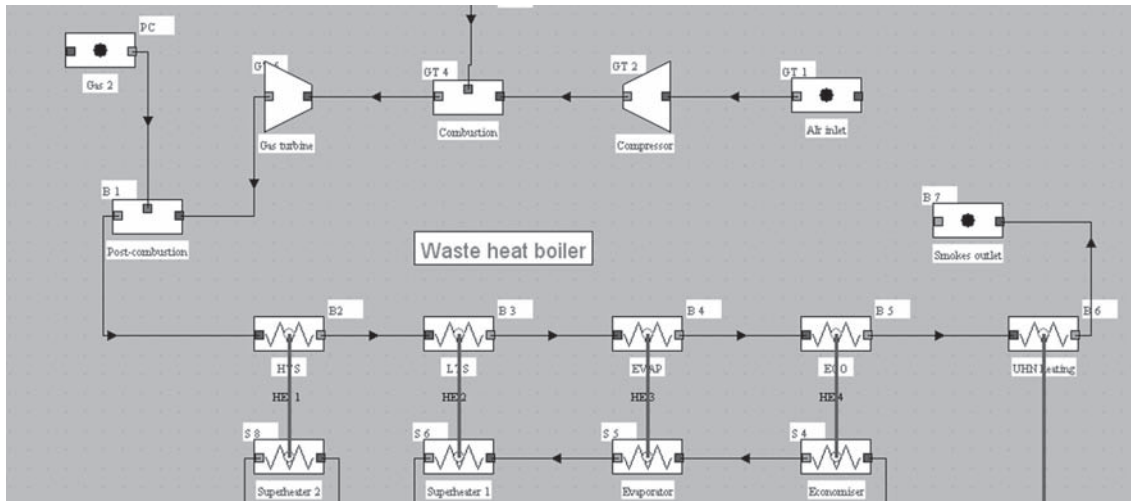


FIGURE 18.5.3

Recovery steam generator

The plant can supply heat to the hot water circuit in three ways: through the steam circuit condenser, the pin, and the by-pass boilers. The maximum flow in the steam circuit is 70 t/h. For low heat requirements, boilers are not used and a lower steam flow rate is circulated. It therefore requires less heat input at the recovery boiler (the steam turbine inlet temperature must always be the same: 485°C). For this, the temperature of the smoke is controlled by adjusting the fuel flow in the afterburner (the GT still operating at substantially the same regime, we may alter neither the exhaust gas flow nor its temperature). Direct heating of water from district circuit in the pin then decreases. The more the heat needs are important, the greater the steam circuit flow, and the fuel flow in the afterburner to achieve the maximum steam throughput of 70 t/h in the circuit. When the thermal needs of the urban system can no longer be provided by the condenser and the pin, the boilers are put in operation.

Two operating cases and their limiting cases may be distinguished:

- **very important heat demand** $T_{\text{out}} < T_{\text{lim}}$: the flow in the steam circuit is maximum, i.e. 70 t/h. The afterburner is at maximum. The thermal energy provided in the condenser and the pin is at maximum. The boilers are in operation and provide the necessary input;
- **smaller heat demand** $T_{\text{out}} > T_{\text{lim}}$: boilers are off. The thermal energy provided by the condenser and the pin is not at maximum. The flow in the steam circuit is less than 70 t/h, the afterburner is not at maximum;
- **the limiting case** corresponds to maximum afterburning and steam output of 70 t/h. Thermal power is then in the condenser 43.9 MW and 7.4 MW in the pin. The total power recovered by the hot water circuit is 51.3 MW. This roughly corresponds to $T_{\text{out}} = T_{\text{lim}} = 0^\circ\text{C}$.

18.5.2.3 Modeling in Thermoptim

The model can be decomposed into four interconnected modules: the gas turbine and steam circuit are simple variants (due to the afterburner and desuperheating vein) of examples presented in sections 12.1.4.3 and 16.1.1; the recovery boiler which connects them (Figure 18.5.3), and the district heating network (Figure 18.5.4) are the other two sub-modules.

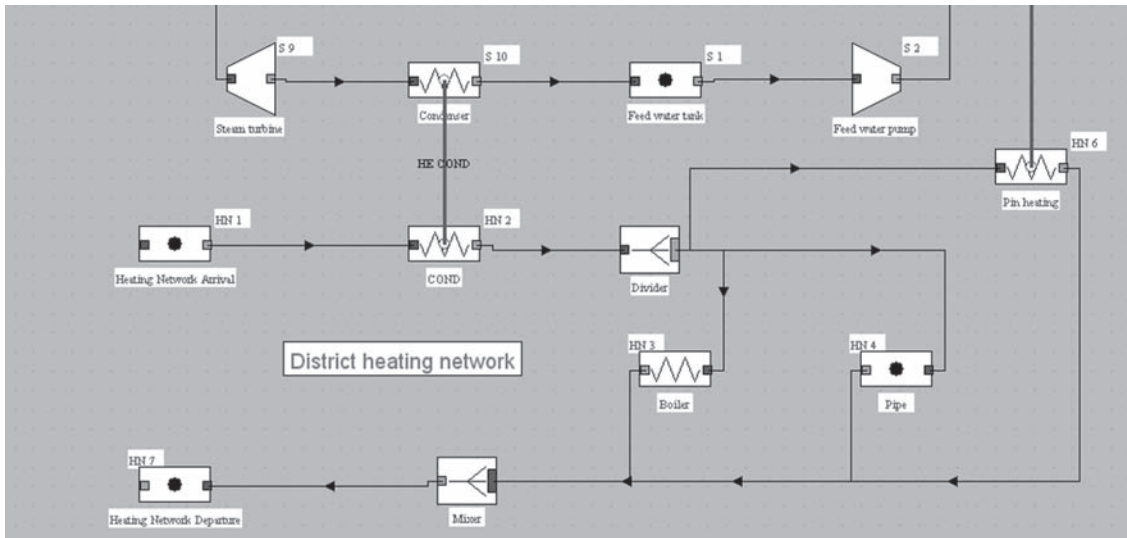


FIGURE 18.5.4
District heating network

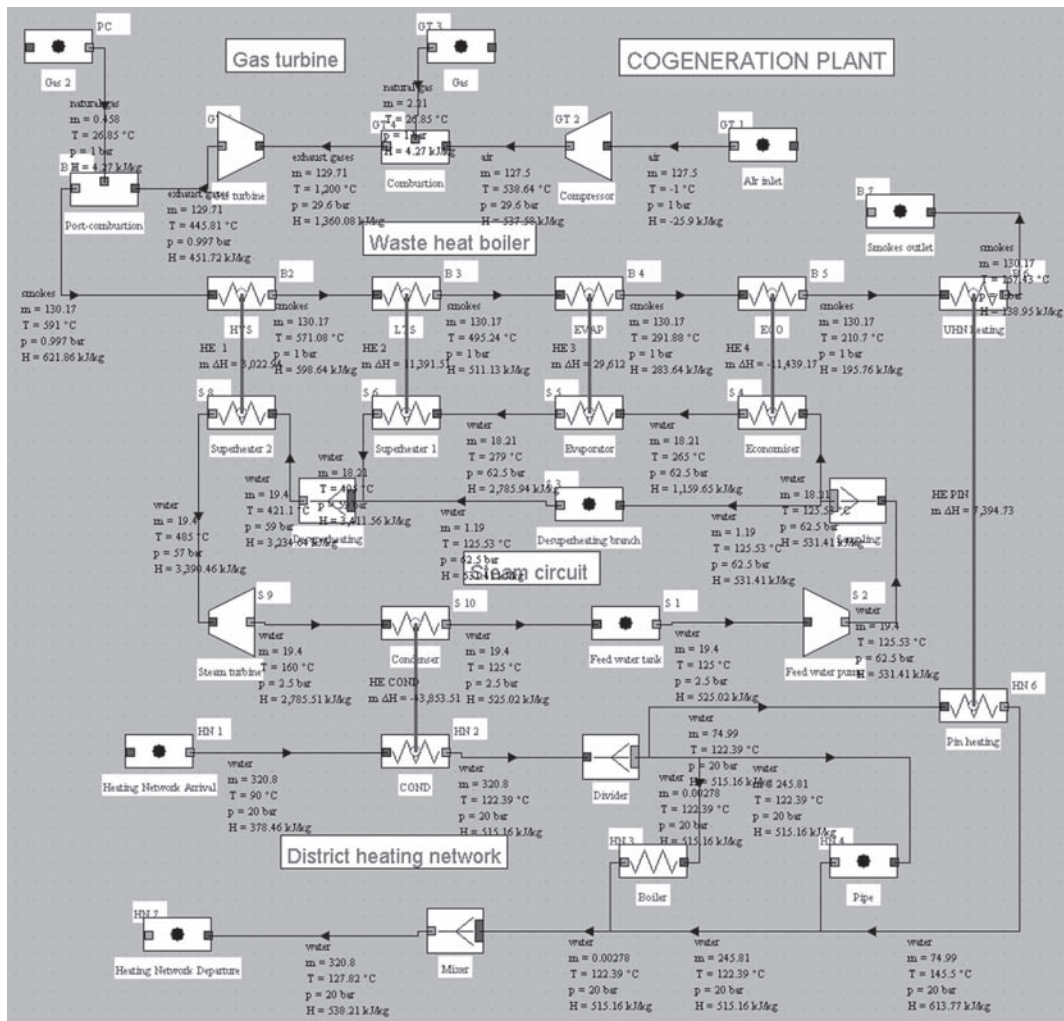


FIGURE 18.5.5
Industrial cogeneration plant

TABLE 18.5.1
COGENERATION ENERGY BALANCE

Outside temperature	−5°C Power (MW)	−1°C Power (MW)	2°C Power (MW)
GT combustion	107.9	107.9	107.9
Afterburner	22.4	22.4	14.3
Boilers	11.5		
TOTAL purchased power	141.7	130.2	122.2
GT Turbine	117.8	117.8	117.8
GT compressor	71.8	71.8	71.8
Net GT power	46.0	46.0	46.0
ST power	11.7	11.7	9.8
TOTAL Mechanical power	57.7	57.7	55.8
Condenser	43.9	43.9	36.7
Pin heating	7.4	7.4	7.5
Boilers	11.5		
TOTAL useful thermal power	62.7	51.2	44.2
TOTAL useful power	120.5	109.0	100.0
Mechanical efficiency	40.7%	44.3%	45.7%
Overall efficiency	85.0%	83.7%	81.8%
Heat-power ratio	1.09	0.89	0.79

The whole model leads to results shown in Figure 18.5.5 for an outside temperature of -1°C . Table 18.5.1 shows the influence of this parameter on the main global indicators used in cogeneration.

18.6 TRIGENERATION

We talk of trigeneration to describe methods for simultaneous production of mechanical power (usually electricity), heat and cooling. Trigeneration is thus somehow a generalization of the CHP.

So that we can use trigeneration, it is imperative that on the one hand we may need in one place heat and cooling, which is quite rare, and that on the other hand we have an electricity production system.

We speak here of two types of trigeneration plants:

- plants for producing cooling and heating for supermarkets;
- absorption installations powered by a micro-gas turbine and also producing hot water.

18.6.1 Production of central heating and cooling for a supermarket

In supermarkets, it is common, at least in winter, to have simultaneously needs to heat the store and cool rooms and refrigerated display cases, at temperatures either positive or negative.

It may be economically feasible, especially if the supermarket has its own emergency generator, to use trigeneration. Most of the time, related facilities are diesel or gas engines, whose cooling heat is used for heating, and whose shafts drive vapor compression refrigeration machines.

18.6.2 Trigeneration by micro turbine and absorption cycle

As we have seen, a micro-gas turbine is a gas turbine of small capacity (several tens of kW), typically operating with a low compression ratio and with a regenerator to improve performance.

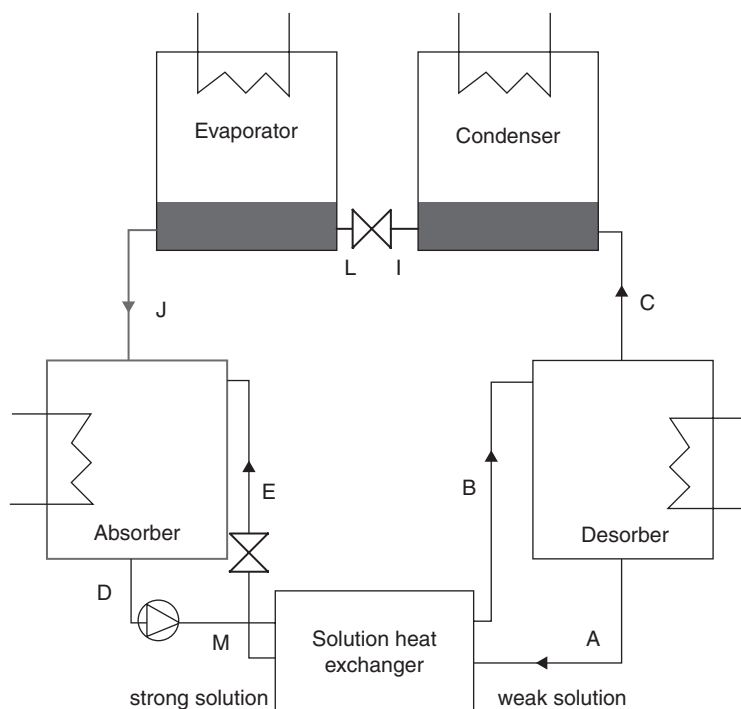


FIGURE 18.6.1

Sketch of the absorption cycle

We are interested here in a trigeneration plant where gases coming out of a 125 kWe micro-turbine are used both to provide the necessary heat to the desorber of a LiBr-H₂O absorption machine (Figure 18.6.1) and secondly to produce 0.5 kg/s of hot water at about 80°C. The turbine sucks 0.78 kg/s of air that is compressed at 5 bar, then passes through a regenerator before being heated to 950°C in the combustion chamber burning natural gas. Gases are expanded at 650°C and then pass successively through the regenerator, the desorber and the cogeneration heat exchanger. A gas compressor is required to raise the pressure of natural gas from the distribution network. This is a variant of CHP example presented section 18.5.1.

The modeling of this facility uses thirty components, representing several hundred coupled equations. All these components are available in Thermoptim core, with the exception of sub-system (absorber-solution exchanger-desorber) of the absorption refrigeration cycle (the three lower elements of the sketch in Figure 18.6.1), which replaces the compressor of a vapor compression cycle. We thus understand the interest of the external class mechanism in a case like this: by adding a specialized component to represent the missing module, the work involved is much smaller than if we had to write a program to model the whole cycle.

So we just have to create an external component to represent the module which does not exist, which firstly involves the LiBr-H₂O pair, whose properties can be modeled either directly in the external component or as a particular external substance. Furthermore this module requires both a heat supply at high temperature in the desorber, and heat extraction at medium temperature in the absorber. Representation of thermal coupling is possible using two thermocouplers, called “absorber” and “desorber” on the diagram in Figure 18.6.2: the external component “generator-absorber” calculates the thermal energy to be exchanged, and each thermocoupler recalculates the “exchange” process to which it is connected. Thermocouplers are presented in section 8.3.7 of Part 2.

In this section, we explain how in practice to create this component, after giving results of the entire system simulation. To be easily comprehensible, the model presented here is relatively

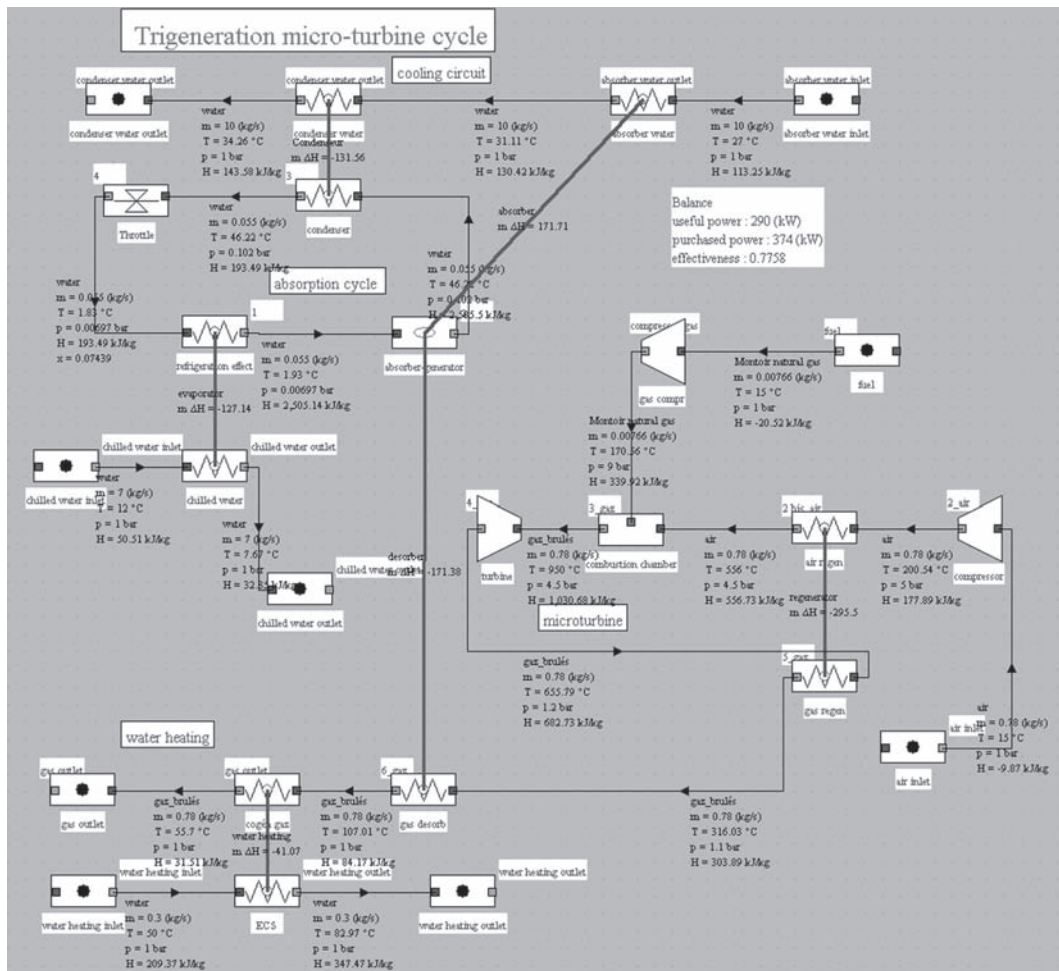


FIGURE 18.6.2

Synoptic view of the trigeneration plant

simple thermodynamically, easily calculable with the assumptions made. It thus presents several limitations: in particular, as it is implemented, it allows a direct calculation of the component knowing the temperature of the absorber and the desorber and the solution exchanger effectiveness, but not an inverse calculation where we seek to determine, for given operating conditions, one of these quantities. However, it has the great advantage of being already sufficiently complicated to show clearly problems that arise during the creation of an external component, and solutions that help solve them.

18.6.2.1 Model results

Once the missing component is created, modeling the trigeneration plant poses no particular problem, and leads to the diagram in Figure 18.6.2, in which we recognize in the top left the refrigeration cycle with its cooling circuit, in the middle-right the micro-turbine, and in the lower left the hot water production exchanger.

The setting of the micro-turbine is that of an existing industrial machine, but the trigeneration plant itself is fictitious: we have simply sought to recover the available enthalpy in the gas turbine exhaust to produce cooling and heat hot water.

In the synoptic view of Figure 18.6.2, useful energy includes not only the compression and expansion work, but also the cooling energy and thermal energy supplied to the water system,

which leads, for these conditions, to an overall efficiency of about 78% which corresponds to approximately 125 kW of electrical power, 176 kW of heat input to the desorber, providing 127 kilowatts of cooling power, and 40 kW of hot water heat, for a fuel consumption of 375 kW. Mechanical efficiency is 32.7%, and heat-power ratio 1.76. The COP of the single-effect absorption cycle is equal to 0.72.

18.6.2.2 Design of the external component

The missing component is the external subsystem (absorber-solution exchanger-desorber) of the absorption cycle using the pair LiBr-H₂O (Figure 18.6.1). The model used is that of a simple effect machine with the following assumptions (note that in what follows, for reasons of consistency of notations, strength or weakness of the solution is expressed relative to the refrigerant (water) and not to the solvent (lithium bromide), unlike the usual convention in the U.S., which is that adopted by ASHRAE):

- the desorber and condenser are at the same pressure;
- the absorber and evaporator are at the same pressure;
- the refrigerant vapor leaving the evaporator is saturated;
- the liquid refrigerant leaving the condenser is saturated;
- the refrigerant vapor leaving the desorber is saturated at the equilibrium temperature of the solution weak in refrigerant at desorber pressure;
- the weak solution is boiling at the exit of the desorber, assumed isothermal;
- the strong solution leaves saturated the absorber, assumed isothermal.

Model parameters are:

- the absorber and desorber temperatures;
- the heat exchanger solution effectiveness.

The input data of the model are as follows (provided by other system components):

- the absorber and desorber pressures;
- the refrigerant flow-rate.

The outputs are:

- the absorber and desorber thermal loads;
- the weak and strong solution concentrations;
- the weak and strong solution flow-rates.

A component graphical interface can be deduced (Figure 18.6.3). The bottom third of the screen has to be created, the rest being defined as Thermoptim standard.

Parameters correspond to the first three lines added, the results of calculations to others. Below are listed the two types of thermocouples that the component defines and sets.

The input data are provided by other components of the global model: the refrigerant flow set by the upstream “cooling effect” process is here 0.055 kg/s, the absorber pressure (point 1) is equal to 0.00697 bar, corresponding to an evaporation temperature of 1.93°C and desorber pressure (point 2) is equal to 0.102 bar, corresponding to a condensing temperature of 46.22°C.

A peculiarity of this component is that it does not change its downstream point 2, whose state is considered given. It would of course be possible to approach the problem from another angle, but as we said earlier, we do not want to overcomplicate things in this example.

The screenshot shows a software interface for configuring an external component. The process is named 'absorber-generator' and is of type 'external'. The energy type is set to 'other'. The flow rate is 0.055. The inlet point is 1, and the outlet point is 2. The inlet properties are: T (°C) = 1.93, P (bar) = 0.00697, h (kJ/kg) = 2,505.14, and quality = 1. The outlet properties are: T (°C) = 46.22, P (bar) = 0.102, h (kJ/kg) = 2,585.5, and quality = 1. The m Δh value is 4.42. The system is configured as an 'open system'. The LiBr absorption parameters are: absorber temperature (°C) = 40.000, desorber temperature (°C) = 100.000, solution exch. efficiency = 0.800, absorber load = -171.707, desorber load = 176.037, Rich solution fraction = 0.399, Poor solution fraction = 0.364, Rich solution flow = 1.006, and Poor solution flow = 0.951. The reference is set to 'simple effect cycle'. Buttons for 'Save', 'Close', 'Suppress', 'Calculate', and 'display' are visible.

FIGURE 18.6.3

GUI of the external component

18.6.2.3 Thermodynamic model

The model equations are obtained as follows.

LiBr-H₂O mixture

The LiBr-H₂O mixture is modeled using the equations proposed by ASHRAE, provided in section 5.6.8.4 of Part 2.

Absorber

The weak refrigerant solution is sprayed into rain and washes the refrigerant vapor at low pressure, which is absorbed, releasing its heat of condensation and heat of dilution.

This heat Q_{abs} is extracted by cooling water which then cools the condenser.

With the assumption that the absorber is at a constant temperature T_{abs} and the strong solution is saturated, the absorber equations are the following:

The equation of solution saturated vapor pressure $P_{\text{abs}} = P(x_{\text{sr}}, T_{\text{abs}})$ provides the concentration of the strong saturated solution and therefore its enthalpy $h_{\text{srD}} = h(x_{\text{sr}}, T_{\text{abs}})$.

Known data: $m_r, h_{r1}, T_{\text{abs}}, P_{\text{abs}}$

Unknown: $m_{\text{sr}}, m_{\text{sp}}, x_{\text{sp}}, h_{\text{spE}}$

Conservation of mass: $m_r + m_{\text{sp}} = m_{\text{sr}}$

Conservation of mass of solution: $(1 - x_{\text{sp}}) m_{\text{sp}} = (1 - x_{\text{sr}}) m_{\text{sr}}$

These two equations provide m_{sp} and m_{sr} if x_{sr} , x_{sp} and m_r are known:

$$m_{sr} = m_r \frac{1 - x_p}{x_r - x_p}$$

$$m_{sp} = m_f \frac{1 - x_r}{x_r - x_p}$$

Conservation of enthalpy: $m_r h_{r1} + m_{sp} h_{spE} = m_{sr} h_{srD} + Q_{abs}$
There are 8 variables, 4 known and 3 equations.

Generator/desorber

The solution strong in refrigerant is introduced at high pressure in the high-temperature generator where it boils by contact with tubes heated either directly by a fuel or by steam. Steam produced is almost pure refrigerant, due to the saturation pressure difference between the two fluids. It is then directed to the condenser. The depleted solution is extracted to be recycled.

With the assumption that the generator is at a constant temperature T_{gen} and the weak solution is saturated, the equations are:

The inversion of the equation of the solution saturated vapor pressure $P_{gen} = P(x_{sp}, T_{gen})$ provides concentration x_{sp} , and enthalpy h_{spA}

New data: h_{r2} , T_{gen} , P_{gen}

New unknowns: h_{srB} , h_{spA}

Conservation of enthalpy: $m_r h_{r2} + m_{sp} h_{spA} = m_{sr} h_{srB} + Q_{gen}$

There are 5 variables, 3 data and 1 equation.

Solution exchanger

At this stage, two equations are missing to solve the model. They correspond to the solution heat exchanger:

$$\varepsilon = f(T_A, T_B, T_D, T_E)$$

$$m_{sp} (h_{spA} - h_{spE}) = m_{sr} (h_{srB} - h_{srD})$$

Sequence of calculations

Specifically, the sequence of calculations is as follows:

1. update the component before calculation by loading the values of m_r , h_{r1} and P_{abs} from the upstream point;
2. reading T_{abs} , T_{gen} and ε on the external component screen;
3. inversion of $P_{abs} = P(x_{sr}, T_{abs})$ for x_{sr} then h_{srD} ;
4. loading values h_{r2} and P_{gen} from the downstream point;
5. reverse $P_{gen} = P(x_{sp}, T_{gen})$ for x_{sp} and then h_{spA} ;
6. computing of m_{sp} and m_{sr} ;
7. calculation of T_B and T_E thanks to solution exchanger equations;
8. calculation of h_{srB} and h_{spE} assuming that these points are in equilibrium at their respective temperature and concentration;
9. calculation of thermal loads Q_{abs} and Q_{gen} ;
10. update of the external component display;
11. update and calculation of the associated thermocouples.

WORKED EXAMPLE**Modeling of a Trigeneration Plant**

The modeling of a micro-turbine LiBr-H₂O trigeneration plant is presented in a guidance page of the Thermoptim-UNIT portal (<http://www.thermoptim.org/sections/enseignement/cours-en-ligne/fiches-guides-td-projets/fiche-guide-td-fg12-sur>).

The resolution of the thermodynamic model presented in this section is explained, with its implementation in the external class LiBrAbsorption.



[CRC_we_9]

REFERENCES

- Ashrae, *Fundamentals Handbook (SI), Thermodynamics and Refrigeration Cycles*, 2001.
 S. Candelier, *Modélisation d'une installation de cogénération industrielle avec Thermoptim*, École des Mines de Paris, juillet 2001, Paris.

FURTHER READING

- P. Barroyer, *La cogénération pour la production décentralisée d'énergie*, Revue de la Société des Electriciens et des Electroniciens, décembre 1999, Paris.
 P. Daverat, *Moteurs à gaz et cogénération*, Revue Générale de Thermique, n° 383, novembre 1983, n° spécial Cogénération, Etat de l'art, applications, Paris.
 R. Gicquel, M. Williams, K. Aubert, *Optimisation du cycle eau-vapeur d'une centrale IGCC*, HPC'01, Paris, septembre 2001.
 C. Levy, *Cogénération en génie climatique*, Techniques de l'Ingénieur, Traité Mécanique et chaleur, BE 9 340.

This page intentionally left blank

Compression Refrigeration Cycles, Heat Pumps

Abstract: In a motor cycle, heat is provided to produce mechanical energy. A refrigeration cycle operates in reverse: it receives mechanical energy which is used to raise the temperature level of the heat.

Three types of refrigeration cycles are commonly used:

- refrigeration cycles;
- heat pump cycles;
- mechanical vapor compression cycles (Chapter 25 of Part 4).

The first two, which will be presented in this chapter, differ only by the levels of operating temperature and the desired effect. In refrigeration cycles, we try to cool a cold chamber; while a heat pump is used for heating. They put into play refrigeration fluids of various compositions, which allow one to transfer heat at low temperature to a medium at high temperature.

In this chapter, after having presented the principle of operation of these cycles, we discuss a major environmental issue: the impact of these fluids on global warming. Then we analyze the main thermodynamic cycles which are generally used. Finally we present the different technologies of refrigeration components, in particular compressors.

Keywords: compression, expansion, combustion, throttling, nozzle, ejector, refrigerant, substitution fluids, blends, CFC, HCFC, HFC, piston, scroll, screw, hermetic, expansion valve.

19.1 PRINCIPLES OF OPERATION

In a refrigeration plant, we try to maintain a cold chamber at a temperature below ambient. The principle (Figure 9.2.2 of Part 2) is to evaporate a refrigerant at low pressure (and therefore low temperature) in a heat exchanger in contact with the cold chamber. For this, we need temperature T_{evap} of the refrigerant to be lower than that of the cold chamber T_{cf} . The fluid is then compressed at a pressure such that its condensation temperature T_{cond} is greater than the ambient temperature T_{a} . It is then possible to cool the fluid by heat exchange with ambient air until it becomes liquid. The liquid is then expanded at low pressure by isenthalpic throttling, and directed into the evaporator. The cycle is thus closed.

Figure 9.2.1 of Part 2 illustrates the enthalpy transfers that take place in the facility.

The effectiveness of such a cycle is defined as the ratio of useful energy to purchased energy. Thus it is the ratio of heat extracted from evaporator to compressor work. Because its value is generally greater than 1, we prefer to speak of Coefficient of Performance or COP.

19.2 CURRENT ISSUES

The first refrigeration cycles that were made around 1875 used fluids such as ammonia, sulfur dioxide or carbon dioxide. Subsequently, in the first half of the twentieth century emerged new fluids derived from methane and ethane (chlorofluorocarbons CFCs) and hydrochlorofluorocarbons (HCFCs). For many reasons, both technical (thermodynamic performance, compatibility with oils, seals, metals, acceptable pressures etc.) and social acceptability (low flammability and toxicity etc.), these fluids have gradually taken the place of the old, in the exception of ammonia, still used in industrial facilities, including food. In particular, a CFC and an HCFC, R12 (CCl_2F_2) and R22 (CHClCF_2), have come to be used in 75% of the French fleet of refrigeration (1998), while all of these fluids represented over 90% of the total.

The commercial name of CFCs uses the following convention: it is a two or three digit number XYZ. The leftmost digit X, if any, equals the number of carbon atoms minus one. The Y equals the number of hydrogen atoms plus one, and Z equals the number of fluorine atoms. The rest of the molecule consists of atoms of chlorine, unless it contains bromine, in which case the number is followed by the letter B and the number of bromine atoms: for example, the R125 has the chemical formula C_2HF_5 , and R114B2 has the chemical formula $\text{C}_2\text{F}_4\text{Br}_2$. Inorganic refrigerants are designated by 700, plus their molecular weight.

19.2.1 Stopping CFC production

Two environmental concerns came abruptly to question the widespread use of CFCs: the breakdown of the ozone layer and the increasing greenhouse effect. As explained section 11.2.2, it was very quickly decided to stop production of CFCs and halons, and to challenge that of HCFCs, as they still contain chlorine. All these measures led to the industrial refrigeration major technological revolution that began in 1994 and is not complete.

Problems occur differently in the case of designing a new installation or changing the fluid in an existing one. In the latter case, it is necessary that the thermodynamic properties of the replacement fluid are similar to those of the original, whereas in the first case the change can sometimes lead to improved performance of the facility. In any case, many technological problems must be studied, such as compatibility with lubricants, choice of the dehydrator, adjusting the expansion valve etc.

To complicate things, regulations differ between countries, depending on commitments they have taken under international agreements. A final element to consider is that large uncertainties remain for the future, especially as regards the fate of high GWP HFCs.

In this book, it is impossible to review all options and constraints on the issue of replacement refrigerants. So we will just make a fairly general presentation, referring to the literature the reader interested in further developments.

Let us recall that the evaluation of the harmfulness of a gas to the global environment can be estimated as follows:

- in terms of destruction of the ozone layer, especially through an index known by its English name of Ozone Depletion Potential (ODP), whose value is equal to 1 for R11;
- in terms of greenhouse gases by using an index called the Global Warming Potential (GWP), which is 1 for CO_2 , and the calculation of which involves choosing an integration time horizon (ITH), usually chosen equal to 100 years.

For complex technologies like those used for refrigeration, the latter index is not sufficient, because firstly the refrigerants are normally not directly released into the atmosphere, and secondly there is an indirect effect that is due to CO₂ emissions corresponding to the energy consumed by the plant during its lifetime, which itself depends on the structure of the national electricity generation fleet. We therefore define another index, known as Total Equivalent Warming Impact (TEWI).

The TEWI takes into account according to equation (19.1.1) the direct impact based on refrigerant charge m , gas leakage during the lifetime n (annual percentage f) and at the machine end of life (recycling factor α), and indirect impact due to energy consumption E .

$$\text{TEWI} = \text{GWP} \cdot f \cdot m \cdot n + \text{GWP} \cdot m (1 - \alpha) + n \cdot E \cdot \beta \quad (19.1.1)$$

To fix ideas, $f \approx 5$ to 10%, $\alpha \approx 0.5$, $n \approx 15$, $\beta \approx 0.1$ kg/kWh for France, and $\beta \approx 0.55$ kg/kWh for Europe, the difference reflecting the capacity of the French nuclear power plants.

The calculation of equation (19.1.1) may seem a bit complex, but it allows one to compare very different technologies and to account for both direct and indirect effects. As shown in this formula, the value of TEWI can be decreased by reducing the refrigerant charge of facilities (m) and increasing their containment (f), which justifies the efforts being made in this direction by manufacturers.

19.2.2 Substitution of fluids

CFC replacement fluids can be grouped in three broad categories: transition fluids, zero ODP fluids, and zero ODP and low GWP fluids.

19.2.2.1 Halogenated transition fluids

The most immediate solution to look for CFC replacement fluids has been working on hydrochlorofluorocarbons (HCFCs), a priori relatively close on the chemical level and less harmful to the ozone layer. However, these fluids are non-zero ODP that either are already banned or soon will be by the signatory countries of the Montreal Protocol and the agreements that followed, so they are only a short term solution, hence the name transition fluids. The fluids of this family are R22, R123, R124 and R142b for pure substances, as well as blends, mainly based on R22.

19.2.2.2 Halogenated zero-ODP fluids

In the longer term, the only acceptable halogenated fluids vis-à-vis the ozone layer are hydrofluorocarbons (HFCs), which do not contain chlorine atoms and have a zero ODP. The fluids of this family are R134a, R125, R32 and R143a for pure substances and blends thereof.

R134a in particular has successfully established itself in recent years as an alternative to a fairly large number of installations. Its thermodynamic properties are very close to those of R12, which it can replace in many applications, but it also reveals an appropriate alternative for various uses previously allocated to R22, provided, however, that a number of technological changes are made (including a larger compressor displacement).

The main drawback presented by these fluids is that if their ODP is zero, their GWP is very high (1,300 for R134a, 3,200 for R125, 580 to R32, 4,400 for R143a), and their molecules, very stable, have atmospheric lifetimes of several tens or even hundreds of years. Their contribution to the greenhouse effect is potentially important, and their production is as such likely to be questioned sooner or later.

19.2.2.3 Zero ODP and low GWP fluids

The only alternative fluids not harmful to the ozone layer and greenhouse effect are non-halogenated fluids such as ammonia (R717), propane (R290), isobutane (R600a), carbon dioxide (R744) and water (R718).

The first three have flammability constraints (as well as toxicity and compatibility with certain metals such as copper for the first) that limit their use. The latter cannot be used for negative temperatures, and R744 cycles today have efficiencies significantly lower than the others.

Ammonia, butane and propane having very good thermodynamic characteristics, they represent serious alternatives, and their use has grown significantly in recent years. 30% of European new domestic refrigerators now use butane, particularly in northern Europe.

Despite its relatively low performance and high pressures that it requires, carbon dioxide is considered as a fluid for vehicle air conditioning systems, where the risk of leakage is high and challenges the use of high GWP R134a.

19.2.2.4 Blends

In the preceding paragraphs, we have repeatedly mentioned the possible use of blends as replacement fluids. Manufacturers of refrigerants in fact consider that with the exception of R134a, it is now unlikely to find pure fluids that have thermodynamic properties allowing them to be perfect substitutes to the old ones. However, mixing pure fluids in proportions well chosen, it is possible to obtain more suitable features, which explains the interest in the blends.

As explained section 5.6.8 of Part 2, the liquid-vapor equilibrium behavior of blends, however, is generally different from that of pure substances, the quality of each component moving between limits that depend on pressure and temperature, due to the distillation that takes place. In section 19.6.2 we examine the implications of these phenomena for refrigeration cycles.

Table 19.2.1 gives the properties of a number of refrigerant blends (ODP, GWP for 100 years, glide temperature, molar mass, boiling temperature T_b at atmospheric pressure, temperature and critical pressure T_c and P_c).

19.2.2.5 Substitutions considered

We have seen that fluids being challenged by the Montreal Protocol and its amendments represented 90% of applications: essentially two CFCs, R11 and R12, banned from 1994 and two HCFCs, R22 and R502 (a blend), banned from 2014.

Their main applications are as follows:

- R11: water chillers;
- R12: domestic refrigeration, automobile air conditioning;
- R22 (the most sold): food and industrial cooling, transport refrigeration;
- R502 (48.8% R22, 51.2% R115, blend used as substitute of R22 for high compression ratios): supermarket refrigeration, refrigerated transport.

TABLE 19.2.1
PROPERTIES OF SOME REFRIGERANT BLENDS

Name	ODP	GWP	ΔT_g °C	M kg/kmol	T_b °C	T_c °C	P_c bar
R 502	0.4	5490	0	111.6	-46	82	40.2
R 404A	0	3260	0.7	97.6	-47	73	37.4
R 407C	0	1530	7.4	86.2	-44	87	46.3
R 410A	0	1730	<0.2	72.6	-51	72	49.5

Today, possible replacement fluids are as follows:

- R134a (HFC) for R12 (domestic and commercial cooling);
- R404A (HFC 44% R143a, 52% R125, 4% R134a blend) for R22 (commercial refrigeration, refrigerated transport);
- R407C (HFC 23% R32, 25% R125, 52% R134a blend) for R22 (small and medium capacity air conditioning);
- R410A (HFC 50% R32, 50% R125 blend) a possible candidate to replace R22 (air-conditioning, transport refrigeration).

19.3 BASIC REFRIGERATION CYCLE

19.3.1 Principle of operation

Let us begin by studying the following problem, which is similar (except for numerical values) to the example discussed in section 9.2 of Part 2: a R134a compression refrigeration cycle operates between evaporating pressure of 2 bar and condenser pressure of 9 bar (Figure 9.2.2 of Part 2).

Such a machine consists of four components: a compressor, a condenser, an expansion valve (or throttling valve) and an evaporator, through which passes the same fluid flow-rate.

For reasons stated in section 5.3.6 of Part 2, the compressor can be assumed adiabatic and the expansion valve isenthalpic. As for the condenser and evaporator we can at first approximation assume that they are isobaric.

19.3.1.1 Description of the cycle

The cycle is as follows:

- at point 1 (e.g. $P_1 = 2$ bar, $T_1 = -10^\circ\text{C}$ for R134a), the fluid is compressed at pressure $P_2 = 9$ bar. If the compression is reversible, it is isentropic, and leads to point 2 ($T_2 = 41^\circ\text{C}$), otherwise, taking into account compression isentropic efficiency $\eta = 0.8$, it leads to point 2' ($T_{2'} = 48.5^\circ\text{C}$);
- the fluid is then cooled in a double heat exchanger: desuperheating process (2-3a), and condenser itself where it is liquefied at temperature T_3 corresponding to the saturation pressure P_2 (35.5°C here), process (3a-3);
- when it is fully liquefied, it is expanded by isenthalpic throttling at pressure P_1 , corresponding to temperature T_1 : process (3-4), its quality defining its composition ($x = 0.31$ here);
- it is then vaporized in an evaporator, the heat of vaporization being provided by the chamber to be cooled: process (4-1).

The basic refrigeration cycle just described is shown schematically in Figure 19.3.1 on the $(h, \ln(P))$ chart, generally used for their study, and Figure 19.3.2 on the entropy chart.

As we can see, this cycle differs from the reverse Hirn cycle by two main aspects:

- point 1 is located on the vaporization curve, rather than in the mixed zone. This stems from the inability to compress the liquid. We therefore wish to ensure that the fluid is entirely in the vapor phase before it enters the compressor. In practice, it is even slightly superheated;
- throttling (3-4) replaces two Hirn cycle processes: liquid compression and liquid heating. It is surprising that no attempt is made to recover the expansion enthalpy theoretically available at point 3. In fact, isentropes are almost vertical at this location in the $(h, \ln(P))$ chart, so that the enthalpy change is very small and practically non-recoverable in most cases. It is much easier and cheaper to settle for throttling through a valve, which is sometimes a simple capillary tube.

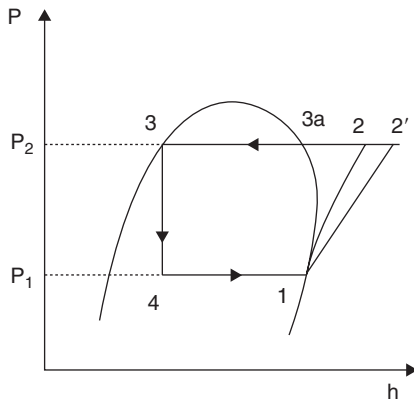


FIGURE 19.3.1
Refrigeration cycle in the $(h, \ln(P))$ chart

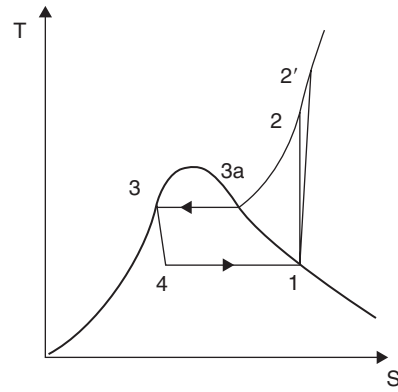


FIGURE 19.3.2
Refrigeration cycle in the entropy chart

19.3.1.2 Cycle modeling

The technical fluid (R134a) condensing, it is of course impossible to model it with the approximation of perfect or ideal gas, and thus to obtain simple analytical expressions of this machine performance.

To determine the fluid state at the different points in the cycle, it is necessary to use a table or chart, or to have a property calculator of the type of the applet that we presented in Chapter 6 of Part 2. Moreover, the fluid flow being constant throughout the cycle, we will reason on a 1 kg/s flow for simplicity.

Calculation of points where pressure and temperature are known is simple (points 1 and 3, not considering intermediate point 3a): to obtain their state simply enter these values in the corresponding applet specifying as appropriate if the saturation temperature is set, and providing in this case the value of x , then click “Calculate”, the calculation mode being “P, T, x ” (Figure 19.3.3 shows the calculation of point 1). This gives us:

$$h_1 = 392.45 \text{ kJ/kg (the exact value of } T_1 \text{ is provided: } -10.1^\circ\text{C)}$$

$$h_3 = 249.78 \text{ kJ/kg}$$

The state of point 2 is calculated in “P, s ” mode entering s_1 and P_2 :

$$h_2 = 423.92 \text{ kJ/kg (} T_2 = 41.2^\circ\text{C)}$$

The compression work can be immediately deduced for the ideal cycle:

$$\tau_c = h_2 - h_1 = 31.5 \text{ kJ/kg (for isentrope)}$$

The state of point 4 is calculated in “P, h ” mode entering h_3 and P_4 . Its quality is equal to 0.31.

The heat rejected to the condenser is:

$$-Q_c = h_2 - h_3 = 184 \text{ kJ/kg}$$

The heat removed from the evaporator:

$$Q_f = h_1 - h_4 = 143 \text{ kJ/kg}$$

Vapors

1,1,1,2-tetrafluoroethane C2H2F4

water
ammonia
butane
methane
propane
R11
R12
R13
R134a

p (bar) 2

T (°C) -10.079

quality x 1

saturation temperature set

Calculate info

M (kg/kmol)	102.031	T (°C)	-10.079
Pc (bar)	40.593	h (kJ/kg)	392.449
Tc (°C)	101.06	u (kJ/kg)	372.305
Vc (m3/kg)	0.00195351	s (kJ/kg/K)	1.7327
quality x	1	v (m3/kg)	0.100721

FIGURE 19.3.3

Calculator inverter

In the case of refrigeration we define the cooling coefficient of performance COP_c :

$$COP_c = \frac{Q_f}{\tau_c} = \frac{h_1 - h_4}{h_2 - h_1} = 4.5$$

For the perfect cycle, at the temperature specified above, one kWh of compression mechanical energy allows to extract 4.5 kWh of cooling at the evaporator.

Taking into account a compression isentropic efficiency η_t equal to 0.8, the calculations are a little more complex (see section 7.2 of Part 2). By definition of isentropic efficiency, enthalpy of point 2' at the end of compression is:

$$h_{2'} = h_1 + (h_2 - h_1)/\eta_c = 431.78 \text{ kJ/kg} \quad (\text{i.e. } T_{2'} = 48.5^\circ\text{C})$$

For the real cycle, irreversibility in the compressor reduces the COP_f which is only 3.6 here.

We calculated the cycle step by step in order to show the sequence of operations. It is also very easy to model it directly in Thermoptim, as explained in Example 9.2 of Part 2 or one of the getting started guides. The synoptic view in Figure 19.3.4 shows the result obtained for the compression cycle with irreversibilities.

Note that an actual refrigeration system comprises, besides the elements shown in Figure 9.2.2 of Part 2, various elements such as filters, a liquid reservoir, an oil separator, non-return valves and pressure regulators.

19.3.2 Energy and exergy balances

From the model developed with Thermoptim, it is easy to build the energy balance of the cycle by filling a table of type 19.3.1.

To build the exergy balance, we must begin by giving a reference temperature and pressure. We take here $T_0 = 288.15 \text{ K}$ (15°C) and $P_0 = 1 \text{ bar}$, corresponding to conditions of mid-season in

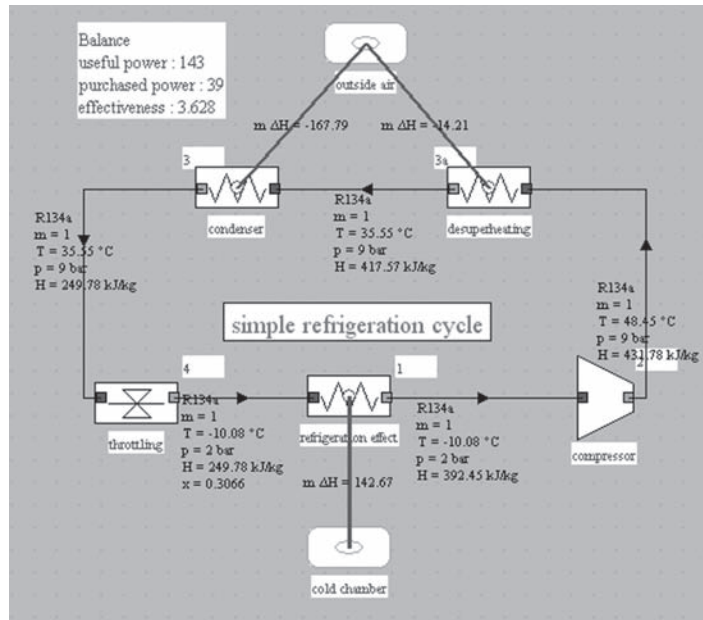


FIGURE 19.3.4
Synoptic view of a simple refrigeration cycle

TABLE 19.3.1
SIMPLE REFRIGERATION CYCLE ENTHALPY BALANCE

Point	Flow rate (kg/s)	h (kJ/kg)	
1	1.00	392.45	
2	1.00	431.78	
3a	1.00	417.57	
3	1.00	249.78	
4	1.00	249.78	
Process	τ (kW)	Q (kW)	Δh (kW)
(1-2')	39.33		39.33
(2-3a)		-14.21	-14.21
(3a-3)		-167.79	-167.79
(3-4)			
(4-1)		142.67	142.67
cycle	39.33	-39.33	
Coefficient of Performance			362%

France. Table 19.3.2 can then be built step by step, following the guidance of section 10.2.3 of Part 2. For each component, Equation (10.2.3) of Part 2 is written:

$$\Delta x_{hij} = \sum_{k=1}^n x_{qjk} - m_j \Delta x_{hj} + \tau_j$$

For most components, with the exception of the evaporator, which is assumed in contact with a cold chamber at 270 K, it simplifies because heat-exergy is zero.

TABLE 19.3.2
SIMPLE REFRIGERATION CYCLE EXERGY BALANCE

Point	Flow rate (kg/s)	h (kJ/kg)	s (kJ/kg/K)	xh (kJ/kg)
1	1.00	392.45	1.73	-106.84
2	1.00	431.78	1.76	-74.91
3a	1.00	417.57	1.71	-76.07
3	1.00	249.78	1.17	-87.24
4	1.00	249.78	1.19	-93.24

Exergy balance		$T_0 = 288.15\text{ K} = 15^\circ\text{C}$							
Process	τ (kW)	Q (kW)	$m\Delta h$ (kW)	$m\Delta s$ (kW/K)	Tk (K)	Δxq (kW)	$m\Delta xh$ (kW)	Δxhi (kW)	loss
(1-2')	39.33		39.33	0.03			31.92	7.41	24.9%
(2-3a)		-14.21	-14.21	-0.05	288.15		-1.15	1.15	3.9%
(3a-3)		-167.79	-167.79	-0.54	288.15		-11.17	11.17	37.5%
(3-4)				0.02	288.15		-6.00	6.00	20.2%
(4-1)		142.67	142.67	0.54	270	-9.59	-13.60	4.01	13.5%
cycle	39.33	-39.33				-9.59		29.74	100%
sigma(x_q+) 				0					
sigma(tau+) 				39.33					
Exergy efficiency									24.4 %

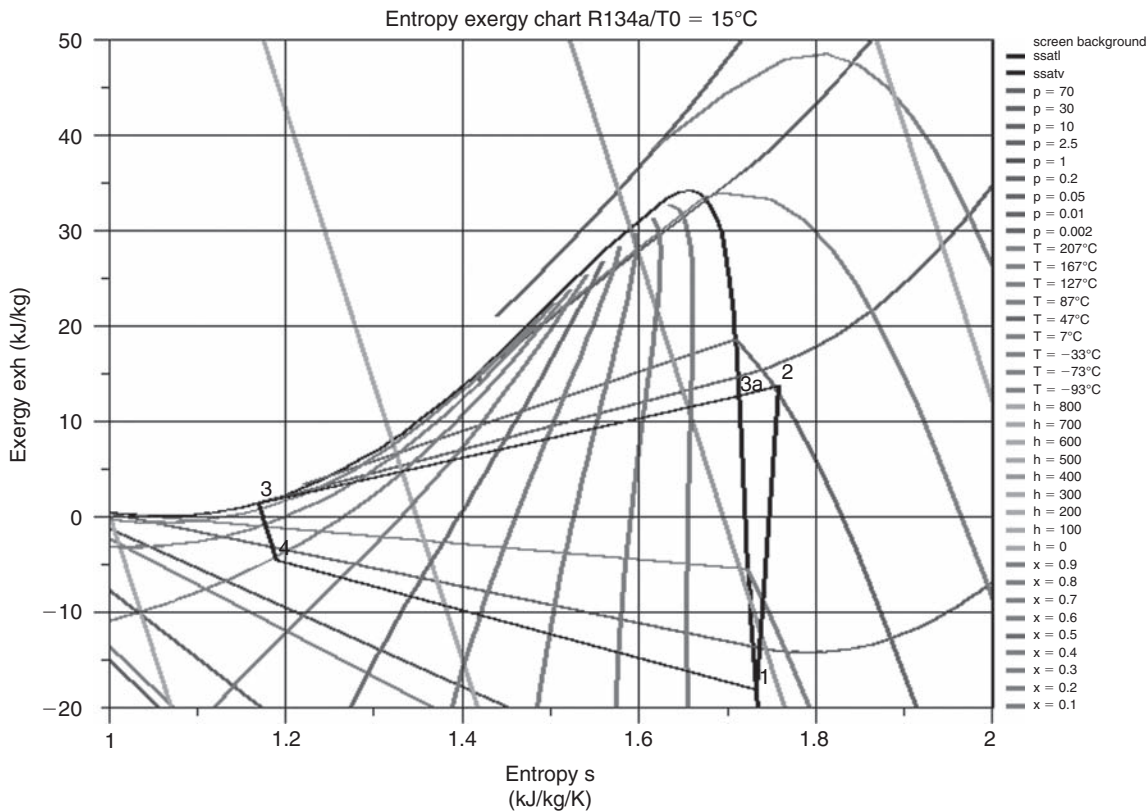


FIGURE 19.3.5
Refrigeration cycle on (s, ex_h) chart

In Table 19.3.2, the losses are given as percentages of total irreversibilities. They are almost evenly divided between the compressor (25%), the condenser (37.5%), the expansion valve (20%) and the evaporator (13.5%).

The main difference with the energy balance, which showed a COP of 3.6 is that the cycle efficiency is actually very low: three quarters of the exergy provided by the compressor to the fluid is dissipated in losses.

On the exergy entropy diagram of Figure 19.3.5, it is clear that the R134a exergy decreases in both the condenser and the evaporator. In the first, heat-exergy is negative because the fluid temperature is higher than that of the environment (positive Carnot factor) and heat is provided by the system (and therefore negative).

In the second, the fluid temperature is lower than that of the environment (negative Carnot factor) and heat is received by the system (and therefore positive). Isenthalpic expansion also induces an exergy drop.

Both exchangers and the expansion valve are components where the fluid exergy decreases. To close the cycle, it is necessary to provide the fluid with exergy corresponding to that lost. This is the role of the compressor, and exergy charts allow us to understand the need for this exergy input.

19.4 SUPERHEATED AND SUB-COOLED CYCLE

19.4.1 Single-stage cycle without heat exchanger

It is possible to improve the performance of this cycle by making minor modifications:

- firstly, for technological reasons, it is preferable to provide a slight superheating in 1 (3 to 5 K) to prevent liquid droplets from being sucked into the compressor;
- similarly, it is better to ensure that the expansion valve is fed with pure liquid, leading to sub-cool the liquid in point 3 (8 to 10K). In addition, this process reduces the vapor quality at the end of throttling, and thus increases the cooling effect at constant compression work.

Consider the performance of the cycle as amended: compression work increases slightly (from 39.3 to 39.8 kJ/kg), energy extracted in the evaporator increases (from 143 to 161.5 kJ/kg) and COP_c is greater than 4 (Figure 10.3.17 of Part 2).

To achieve the superheating, one usually just slightly oversizes the evaporator, or leaves uninsulated a length of tube at the evaporator outlet.

For subcooling, through which performance improvement is achieved, it depends on the temperature of the hot source with which the high pressure part of the cycle exchanges heat. If the temperature is low enough for the sub-cooling to be achieved, one just slightly oversizes the condenser. If it is too high, two possibilities exist for fluid sub-cooling: by exchange either with another outside source if exists, or with the fluid leaving the evaporator, by performing an internal exchange providing both subcooling and superheating.

19.4.2 Single-stage cycle with exchanger

The synoptic view of such a cycle modeled in ThermoOptim is given in Figure 19.4.1.

The calculation shows that the performance of this cycle is slightly lower than that of the previous (compression work does not vary much (from 39.8 to 39.5 kJ/kg), but energy extracted in the evaporator decreases (from 161.5 to 152.8 kJ/kg), and COP_c falls to 3.86). This is because the

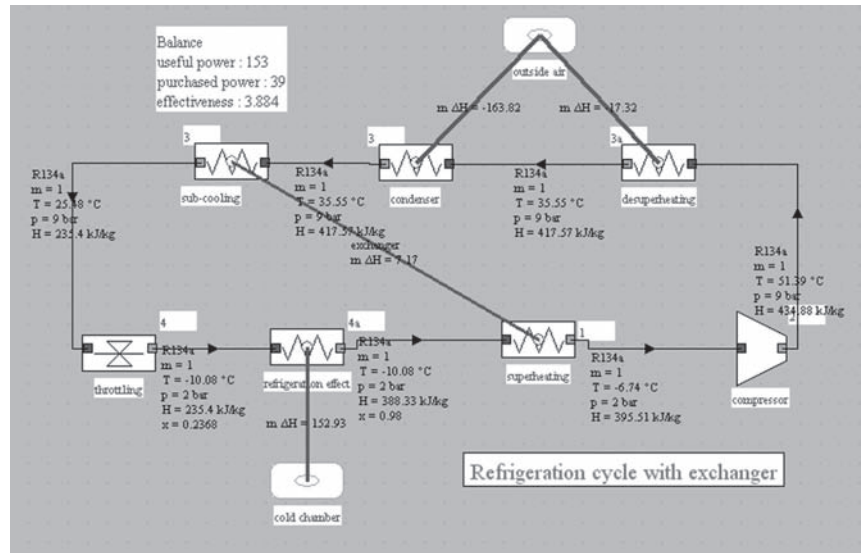


FIGURE 19.4.I

Cycle with heat exchanger

subcooling of 10 K can be assured only slightly reducing the refrigeration effect. Performance is better than that of the cycle without subcooling, but worse than that of the cycle where the subcooling is provided by heat exchange with the outside.

19.5 TWO-STAGE CYCLES

Performance of cycles that we studied so far deteriorates when the temperature difference ($T_1 - T_2$) increases. Indeed, the ideal refrigeration cycle, which is the reverse of the Carnot cycle, would have as COP_c:

$$\text{COP}_c = \frac{T_2}{T_1 - T_2}$$

It is clear that the value of COP_c is even larger than the difference ($T_1 - T_2$) is low. When it increases, the compression ratio increases accordingly, which has the effect of:

- bringing down isentropic and volumetric efficiencies. Since a split compression reduces the compression work with intermediate cooling, these three factors combine to justify the complication of the cycle;
- increasing the compressor discharge temperature up to very high values, with the risk of oil breakdown.

When the compression ratio exceeds 6, the single-stage cycle reaches its limits and must be replaced by multi-stage cycles. In practice, most refrigeration systems of this type are two-stage.

19.5.1 Two-stage compression cycle with intermediate cooling

We have shown in section 7.1.4 of Part 2 that, whenever it is necessary to split compression, it may be advantageous to cool the fluid between two stages. When the refrigeration cycle must operate with a high compression ratio, a variant of the basic cycle precisely does that.

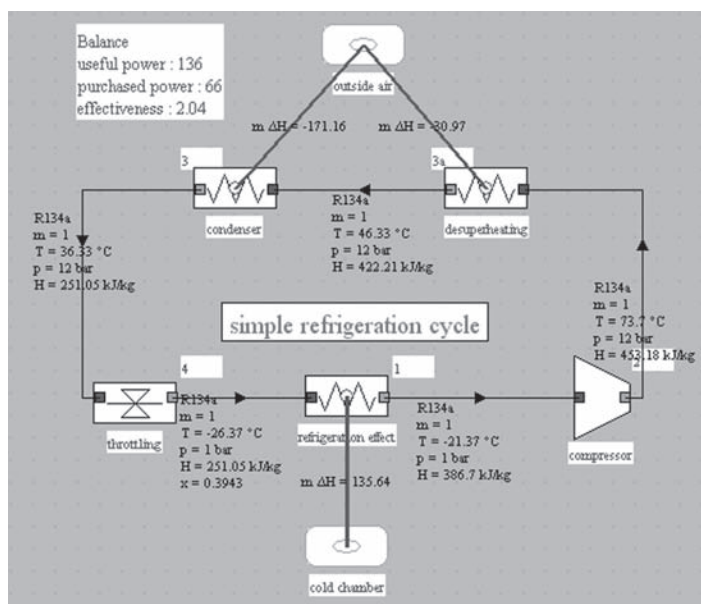


FIGURE 19.5.1
High pressure ratio simple cycle

Cooling can be ensured by the condenser external heat source, or another cooler if exists.

Consider the cycle studied in 19.4.1, i.e. with subcooling of 10 K and 5 K superheating, but without heat exchanger, and this time working between 1 and 12 bar (Figures 19.5.1 and 19.5.2). Its COP is equal to 2, the refrigeration effect being 135.6 kJ/kg, and the compression work 66.5 kJ/kg.

Consider what can be done by splitting the compression. The single stage compression ratio being equal to 12, the intermediate pressure can be chosen equal to 3.5 bar at first approximation.

Maintaining an isentropic efficiency equal to 0.8, the compression end temperature is equal to 23.6°C, that is to say less than that of condenser cooling air (assumed to be at 25°C).

With intermediate cooling from 24°C to 10°C, the COP is slightly improved and passes to 2.1 (Figures 19.5.3 and 19.5.4). The gain is low, and this cycle will not work without an additional heat sink.

19.5.2 Compression and expansion multistage cycles

To ensure both the internal cooling of the vapors exiting the low pressure compressor, and also increase in the vaporization plateau, it is interesting to split the expansion. The simplest and most effective cycle is called a total injection cycle.

In this cycle, vapor exiting the LP compressor and two-phase fluid leaving the HP expansion valve are mixed in a bottle which acts like a capacitor and a separator, the vapor being sucked into the HP compressor, while the liquid phase passes through the LP expansion valve (Figures 19.5.5 to 19.5.8).

This results in a significant improvement of the refrigeration cycle, whose COP reaches 2.34, which is 17% better than that of the single-stage cycle.

The refrigeration effect is 180 kJ/kg, and the compression work 76.8 kJ/kg. The compression work is more important than in the basic cycle, because of the circulation, in the HP cycle, of a mass flow rate (1.4 kg/s) greater than in the LP cycle (1 kg/s).

Other variants of this cycle can be used: partial injection cycle, medium pressure evaporator cycle etc.

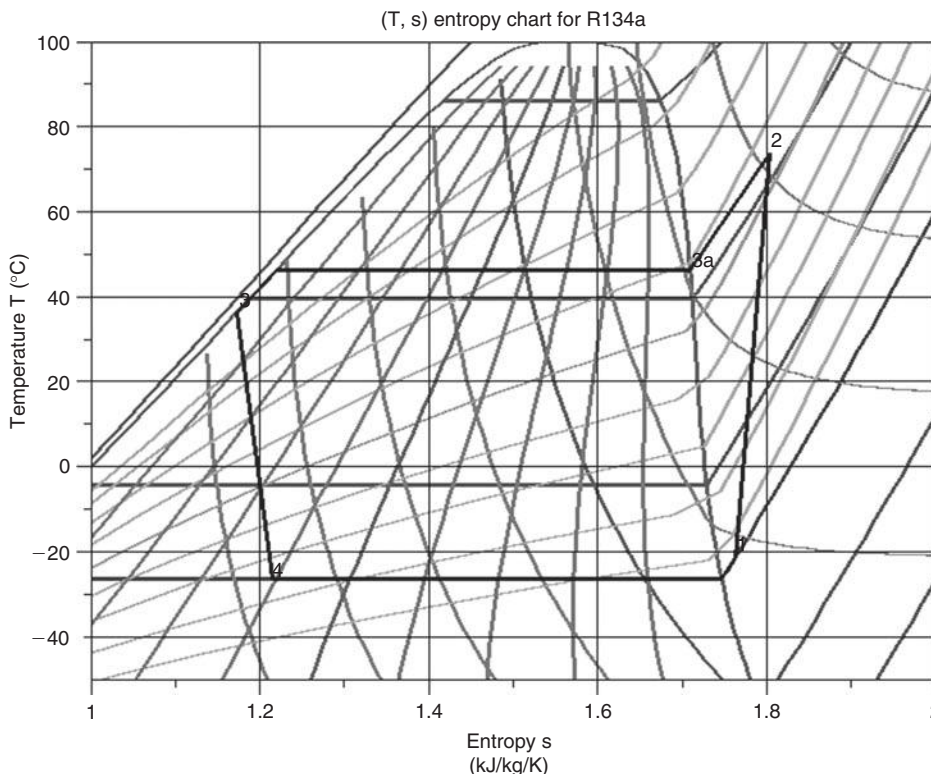


FIGURE 19.5.2
High pressure ratio simple cycle in the entropy chart

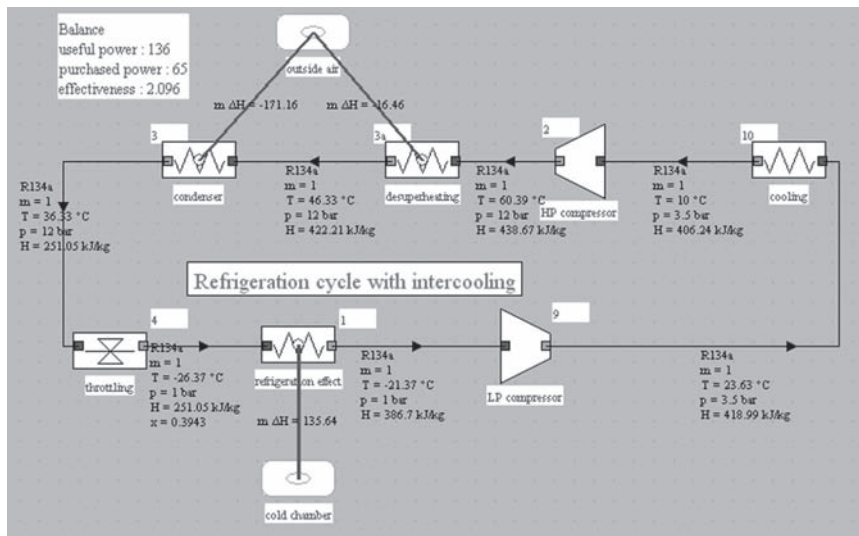


FIGURE 19.5.3
Two-stage compression cycle with intermediate cooling

In the partial injection cycle, only the vapor phase after the high pressure expansion valve is mixed with the vapor exiting the low pressure compressor (Figure 19.5.9).

The performance of this cycle is slightly worse than that of the previous (COP equal to 2.33) because the compression work is slightly higher, the IP vapor being less cooled before recompression.

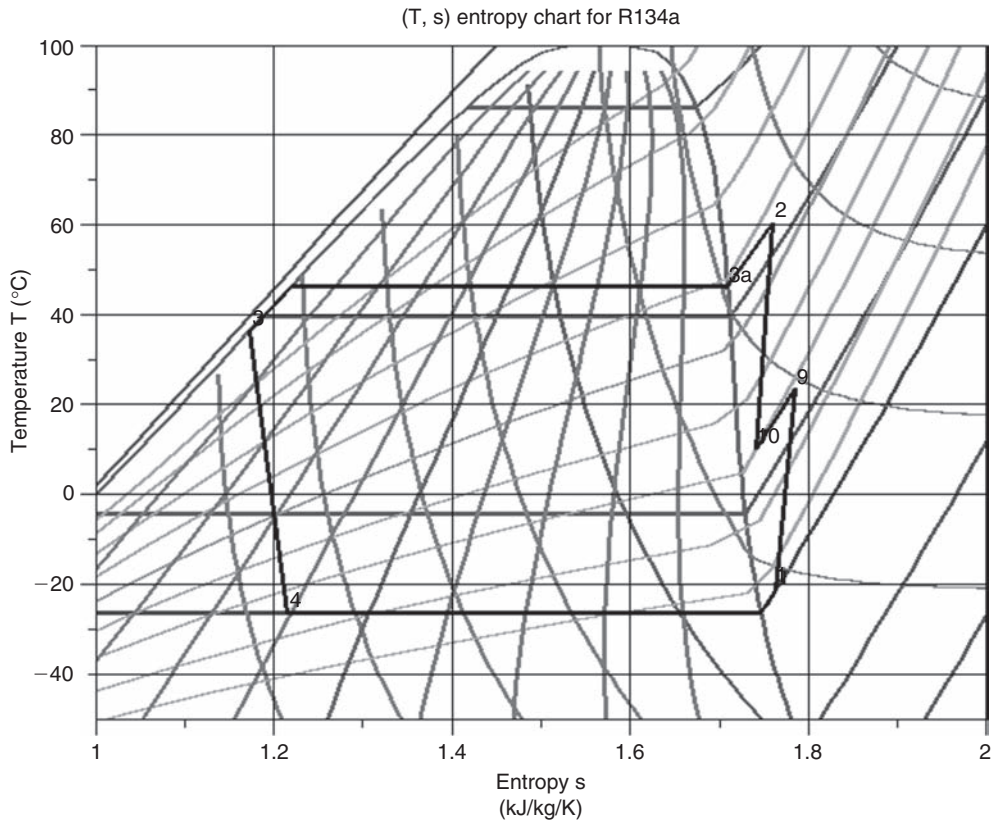


FIGURE 19.5.4

Two-stage compression cycle with intermediate cooling in the entropy chart

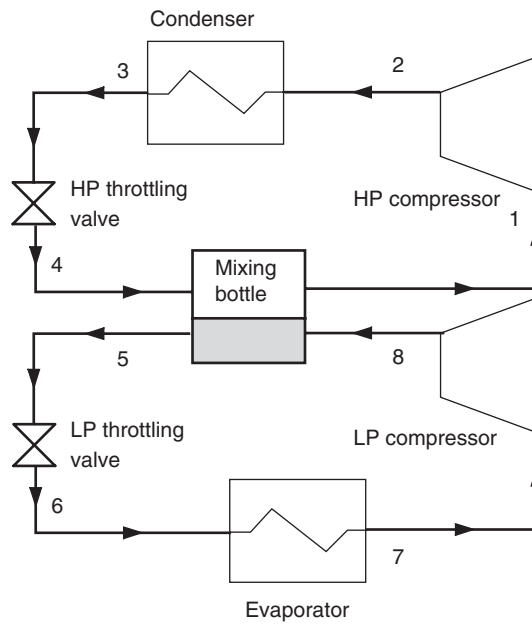


FIGURE 19.5.5

Sketch of a total injection two-stage compression cycle

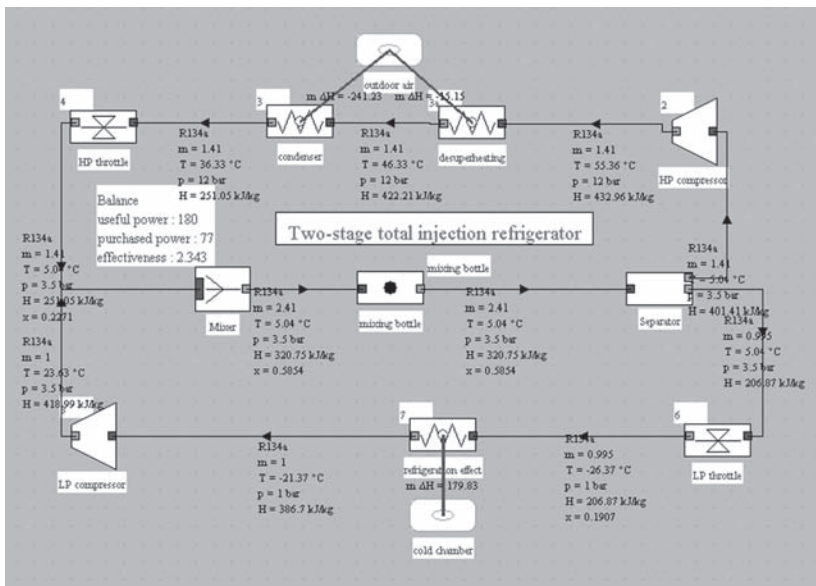


FIGURE 19.5.6
 Synoptic view of a total injection two-stage compression cycle

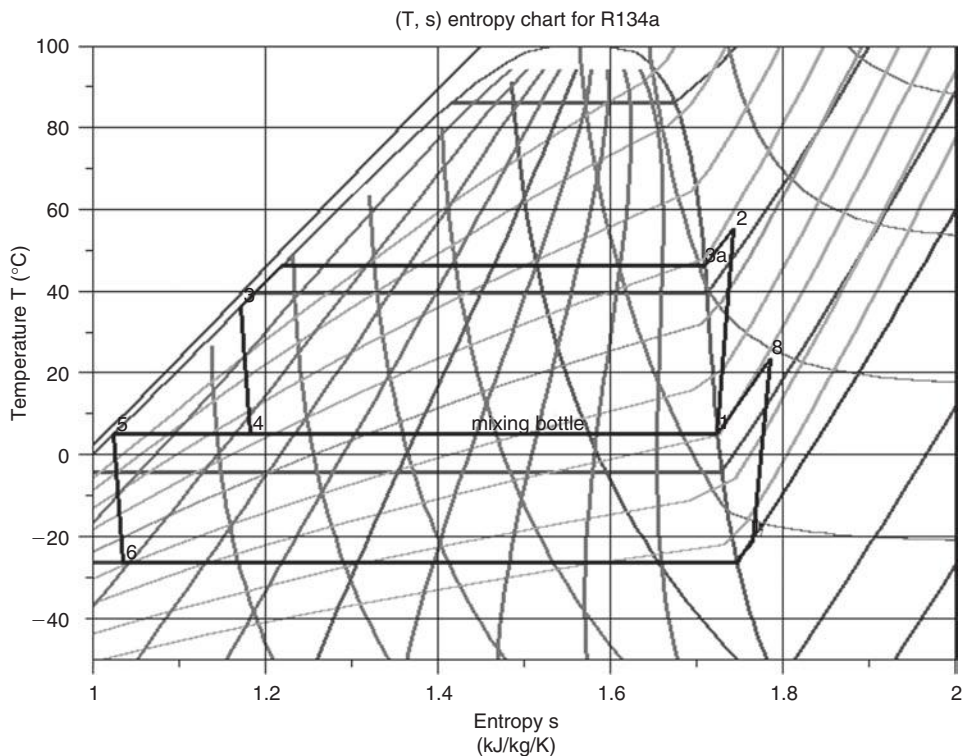


FIGURE 19.5.7
 Total injection two-stage compression cycle in the entropy chart

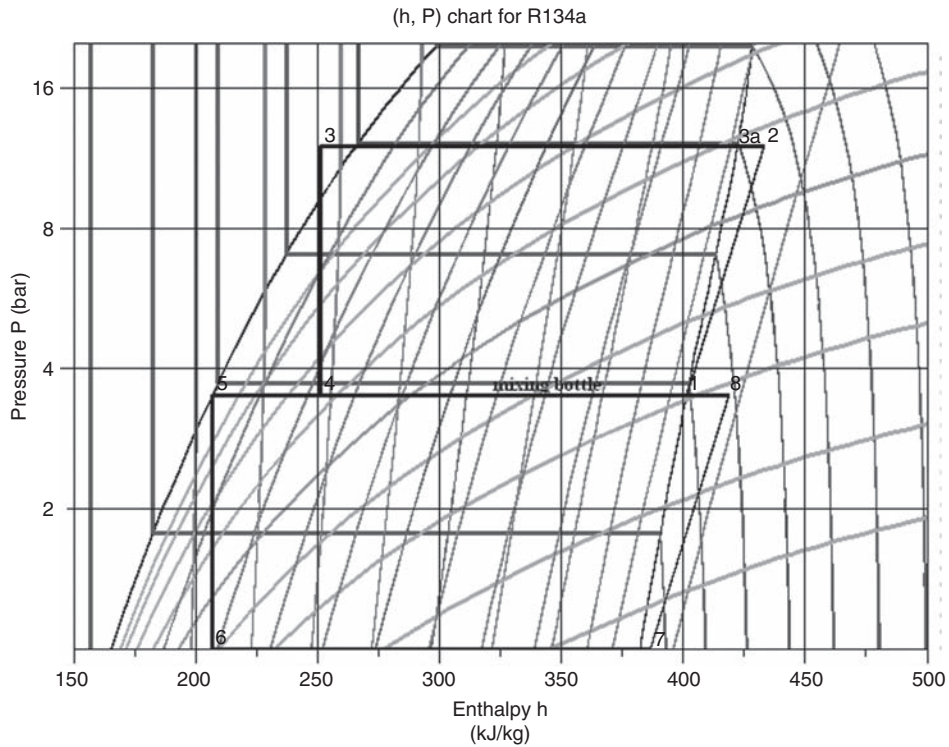


FIGURE 19.5.8
Total injection two-stage compression cycle in the (h, ln(P)) chart

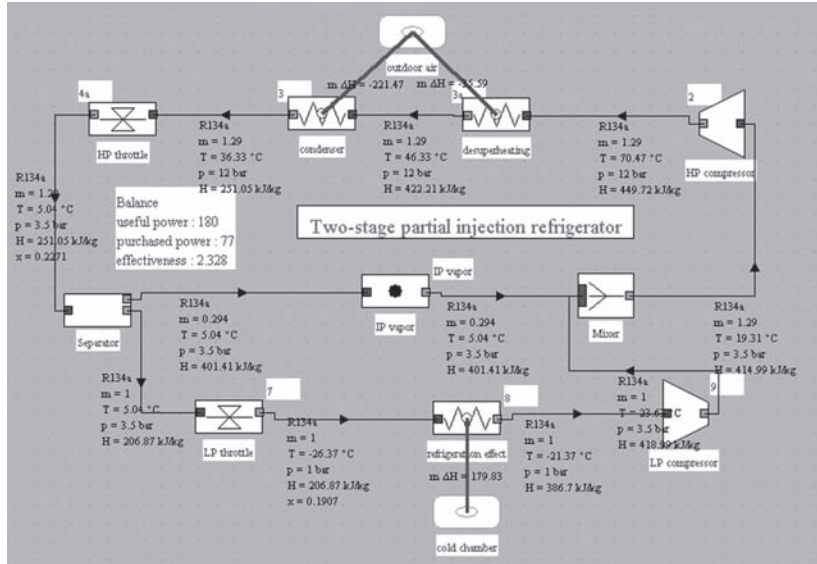


FIGURE 19.5.9
Synoptic view of a partial injection two-stage compression cycle

In the medium pressure evaporator cycle, some of the liquid leaving the IP separator is directed to a second evaporator allowing cooling at a temperature corresponding to the intermediate pressure IP (Figure 19.5.10). It is thus possible to cool two media at two different temperatures.

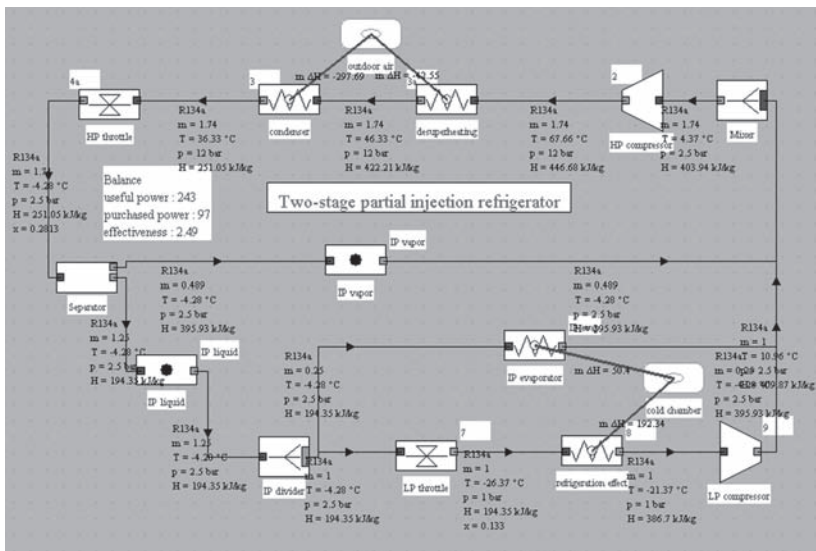


FIGURE 19.5.10
Synoptic view of a medium pressure evaporator cycle

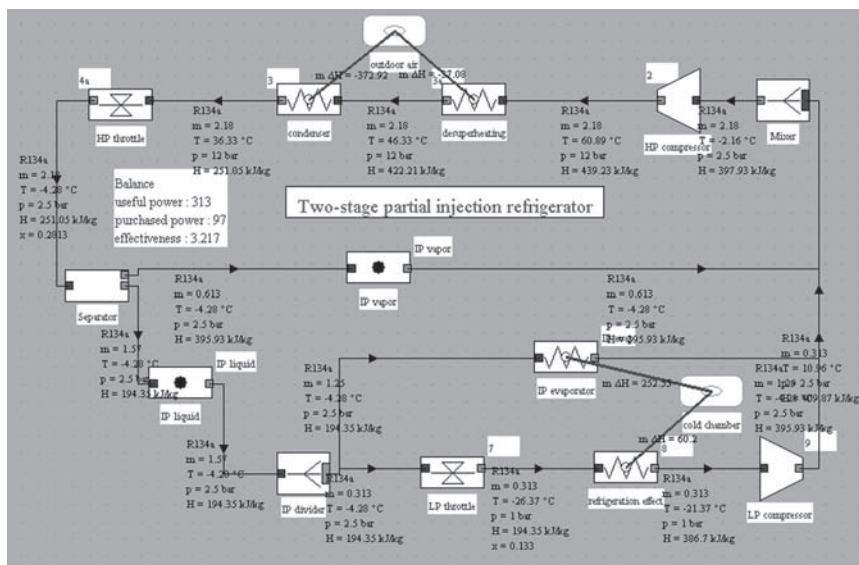


FIGURE 19.5.11
Synoptic view of a medium pressure evaporator cycle

The average COP is increased, since a fraction of the cooling effect takes place at the intermediate temperature. It is 2.49 when 1/5 of total liquid flow expansion valve output is directed to HP through the evaporator, but it would be 3.22 if the ratio was reversed, as in Figure 19.5.11.

By changing the mass flow-rate value passing through the IP evaporator relative to the total mass flow in the IP divider, the balance of the load between the two heat exchangers varies, allowing the machine to adapt to the demand. Note that, when the ratio of these two flow rates varies from 0 to 1, we switch from the two-stage cycle configuration between 1 and 12 bar to a single-stage cycle configuration between 3.5 and 12 bar.

19.6 SPECIAL CYCLES

19.6.1 Cascade cycles

When the temperature difference ($T_1 - T_2$) exceeds 80 to 100K, it is not possible to cool with a single fluid. Indeed, there is no fluid that is well adapted to such different temperature levels, and it is preferable to use two-cycle cascade, the evaporator of one of them serving as the condenser of another. The two cooling circuits are then independent from the hydraulic, but thermally coupled with the evaporative condenser.

The optimization of the global cycle is a complex problem, the temperature choice in the evaporative condenser being an important parameter. We give here an example corresponding to a milk sterilization cascade, a system used to simultaneously sterilize milk at 72°C and cool it at 5°C.

The system involves a cascade of two cycles, one at high temperature using R245ca, and one at low temperature using ammonia.

Milk comes from a tank at 5°C. It begins by being preheated at 66°C in a heat exchanger and is then pasteurized at 72°C in the condenser (90°C) of the topping cycle. At the outlet of the sterilizer, it is pre-cooled at 11°C by exchange with the incoming milk, then cooled at 5°C in the evaporator of the bottoming cycle.

Figure 19.6.2 shows the synoptic view of such a facility, the topping cycle being two-stage total injection.

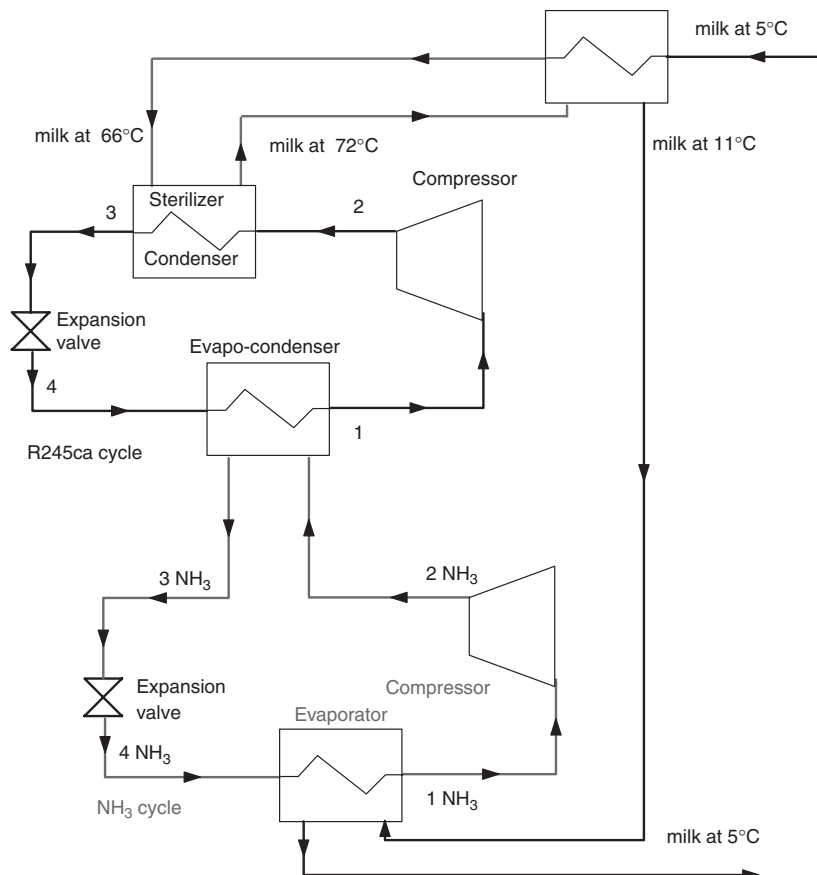


FIGURE 19.6.1

Sketch of the milk sterilization cascade

19.6.2 Cycles using blends

As mentioned above, blends have a behavior that deviates quite substantially from that of pure substances in the liquid-vapor equilibrium zone, because of the appearance of a fractional distillation.

In section 19.3.2, we considered a simple R134a compression refrigeration cycle operating between an evaporation pressure of 2 bar and a condensation pressure of 9 bar, and we presented the look of this cycle in different pure substance charts. Let us now consider a R407C cycle, with an evaporation temperature of 0°C ($P = 5$ bar) and a condensation pressure of 18 bar, used in air conditioning. The isentropic efficiency of the compressor is equal to 0.8.

At point 1, before entering the compressor, the gas is superheated by 5 K above the dew point temperature equal to 2.47°C.

It therefore enters the compressor at 7.47°C and leaves it at 75.15°C. It is then desuperheated at 46.05°C, dew point at 18 bar, and then condensed at 41.29°C, bubble temperature at this pressure and subcooled by 5 K in liquid state before entering the expansion valve. Its quality at the end of throttling is equal to 0.276.

Cycle modeling with Thermoptim leads to the results presented in Figure 19.6.3.

On the entropy diagram (Figure 19.6.4), to increase readability, we have not shown iso-quality curves. Point 1 slightly overheated compared to the saturated vapor is placed on isobar 5 bar. Irreversible compression results in an increase of entropy. Cooling with outside air has three stages: de-superheating (2-3a) in the vapor zone, condensation on line segment (3a-3b) inclined because of temperature glide, and a slight sub-cooling (3b-3) which almost coincides with the liquid saturation curve.

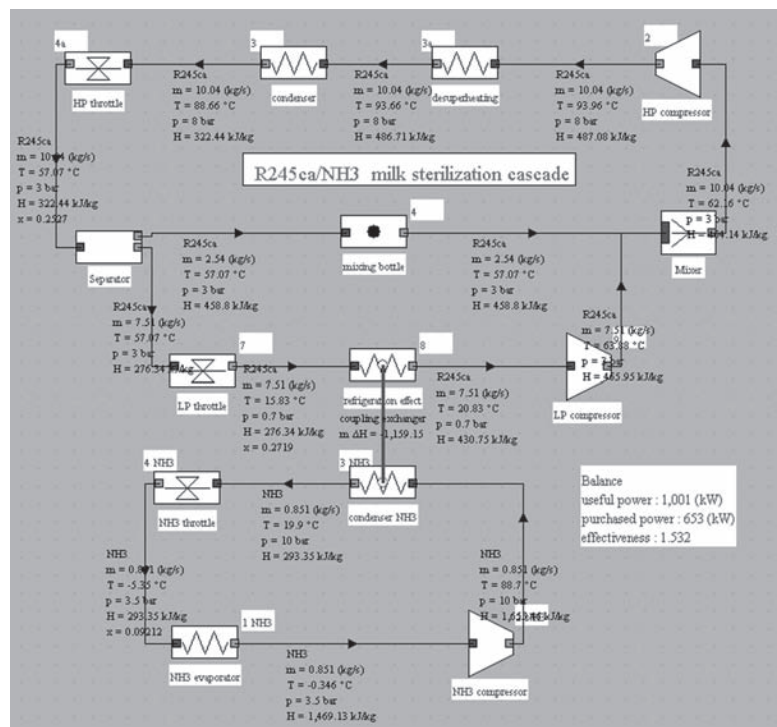


FIGURE 19.6.2

Synoptic view of the milk sterilization cascade

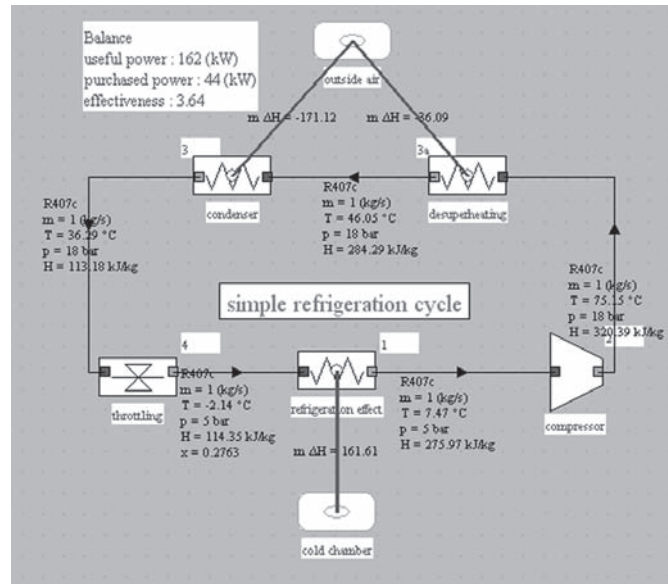


FIGURE 19.6.3

Synoptic view of a R407c refrigeration cycle

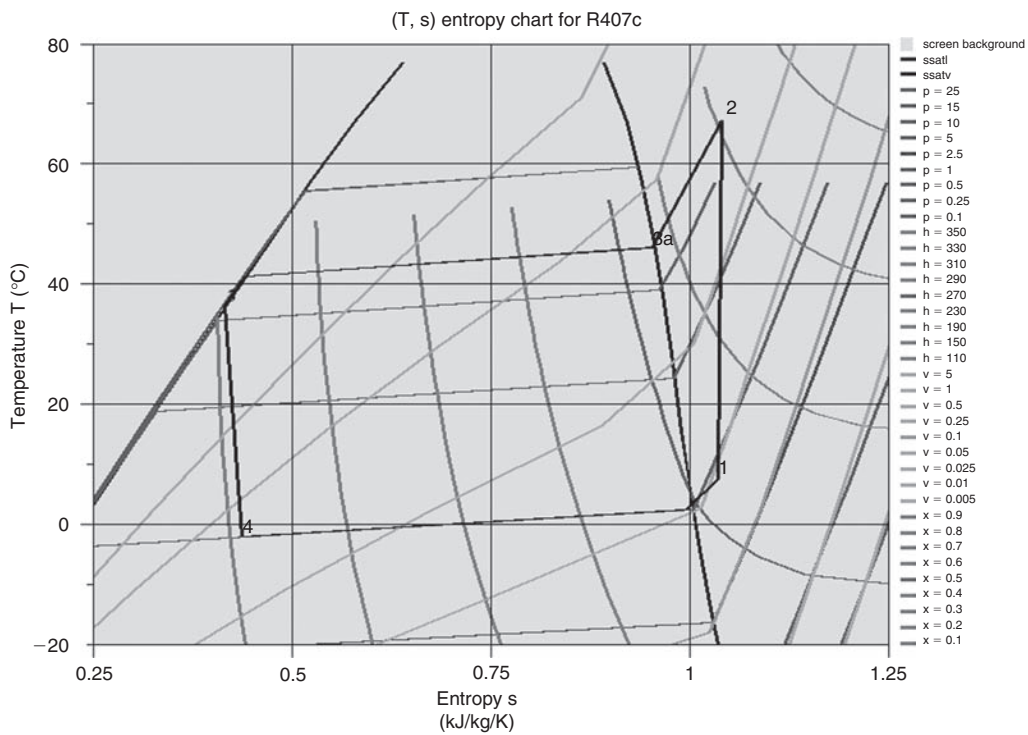


FIGURE 19.6.4

R407c refrigeration cycle in (T,s) chart

Isenthalpic throttling (3-4) leading to an increase of entropy, point 4 is located within the zone of vapor-liquid equilibrium (quality equal to 0.27).

On the (h, ln(P)) chart (Figure 19.6.5), to increase readability, we have not shown iso-quality curves. Irreversible compression results in an increase of entropy.

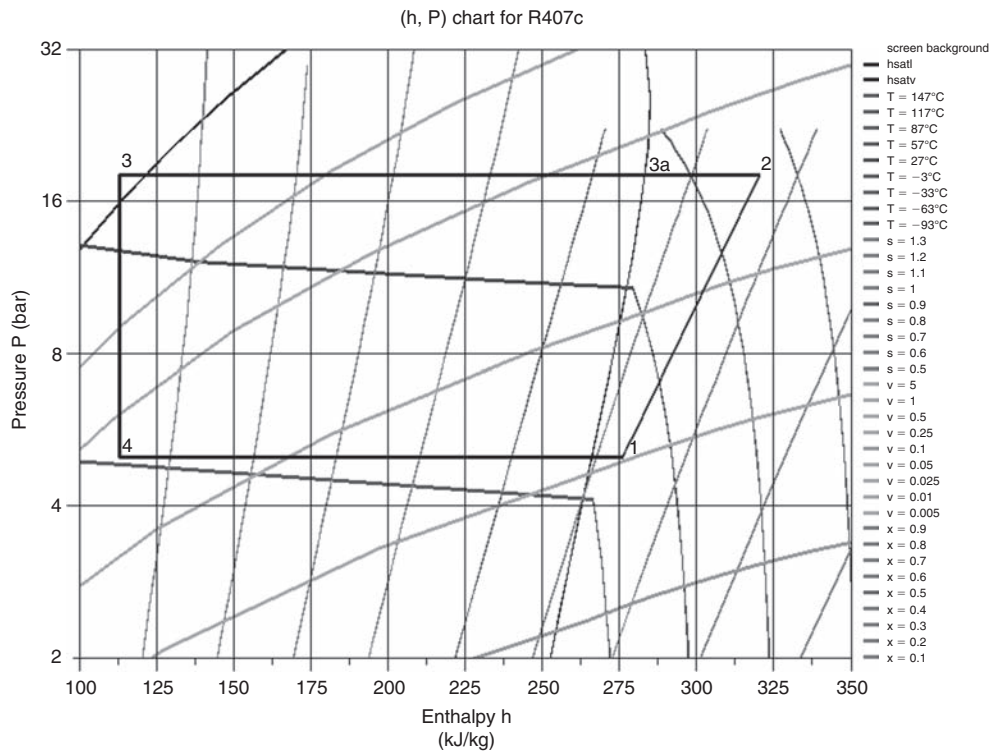


FIGURE 19.6.5

R407c refrigeration cycle in (h, log P) chart

If we neglect the pressure drop in the condenser, the whole cooling is still here in the horizontal (2-3), the three parts representing desuperheating, condensation itself and subcooling appearing distinctly. The only difference with the pure substance chart is that in the area of liquid-vapor equilibrium, isotherms are inclined rather than horizontal segments.

19.6.3 Cycles using ejectors

An ejector or injector (Figure 19.6.6) receives as input two fluids normally gaseous but which may also be liquid or two-phase (Chunnanond, 2004):

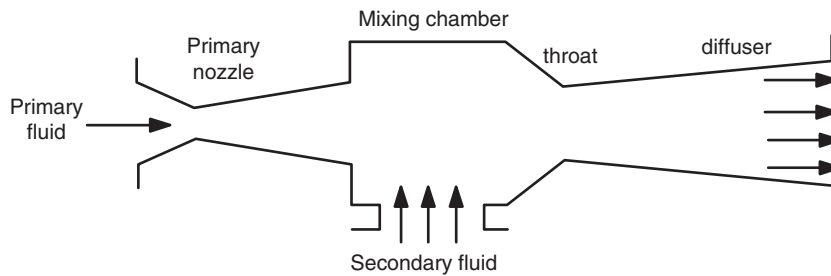
- the high pressure fluid called primary or motive;
- the low pressure fluid, called secondary fluid or aspirated.

The primary fluid is accelerated in a converging-diverging nozzle, creating a pressure drop in the mixing chamber, which has the effect of drawing the secondary fluid. The two fluids are then mixed and a shock wave may take place in the following zone (throat in Figure 19.6.6). This results in an increase in pressure of the mixture and reduction of its velocity which becomes subsonic. The diffuser then converts the residual velocity in increased pressure.

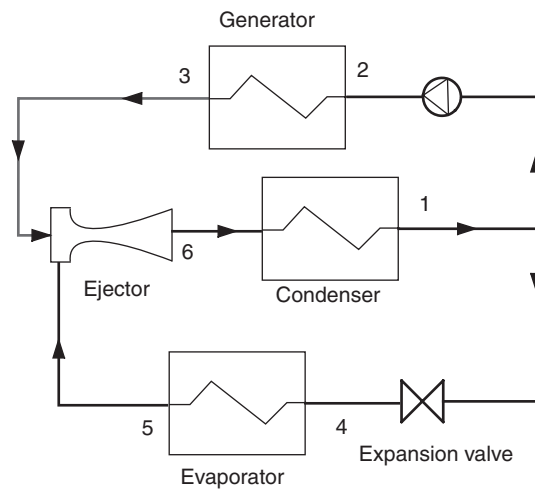
The ejector thus achieves a compression of the secondary fluid at the expense of a decrease in enthalpy of the primary fluid.

We established in section 7.9.3 of Part 2 an ejector model that has been implemented in a Thermoptim external class for simulating cycles, including refrigeration, involving this component.

The value of introducing an ejector in a refrigeration cycle is mainly to reduce, or even eliminate, the compression work, relatively large as the fluid is compressed in the gaseous state.

**FIGURE 19.6.6**

Cross section of an ejector

**FIGURE 19.6.7**

Ejector refrigeration cycle

19.6.3.1 Cycles without compressor

An ejector refrigeration cycle without compressor (Figure 19.6.7) is as follows:

- at the condenser outlet, part of the flow is directed to a pump that compresses the liquid, at the price of a very low work;
- the liquid under pressure is vaporized in a generator at a relatively high temperature (about 100°C), and possibly superheated, the temperature depending on fluid thermodynamic properties. Heat supplied to the generator is a purchased energy;
- this superheated vapor is then used in the ejector as motive fluid;
- the part of the liquid that was not taken up by the pump is expanded in the evaporator, then headed to the ejector as secondary fluid;
- the mixture leaving the ejector is condensed in the condenser and the cycle is complete.

The advantage of this cycle is to replace compressor work by a much smaller work consumed by the pump and by heat supplied by a generator at medium or high temperature, which can be done using thermal effluents or solar collectors.

In Figure 19.6.8, we have plotted in a $(h, \ln(P))$ chart an example of R123 cycle suggested by Sun and Eames (1996). The plant diagram and the ejector screen are given in Figures 19.6.9 and 19.6.10. Thermoptim model results seem quite close to those (fairly synthetic) provided by the authors.

The efficiency remains very low as compared to that of an absorption cycle, even single-effect (see section 18.6.2), but the system is very simple technologically.

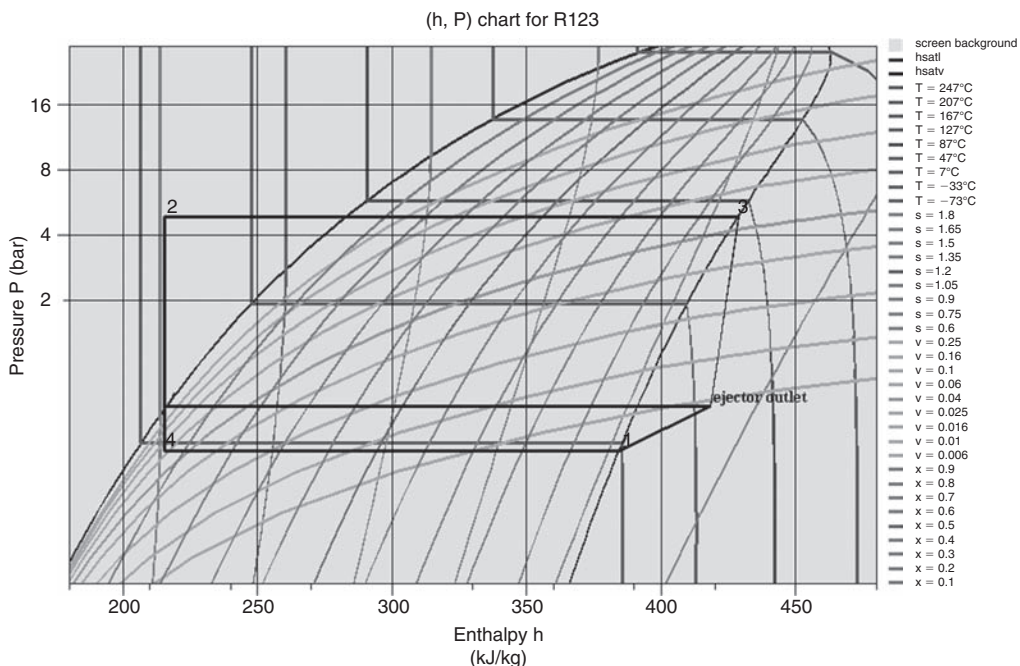


FIGURE 19.6.8
Ejector refrigeration cycle in a (h, ln(P)) chart

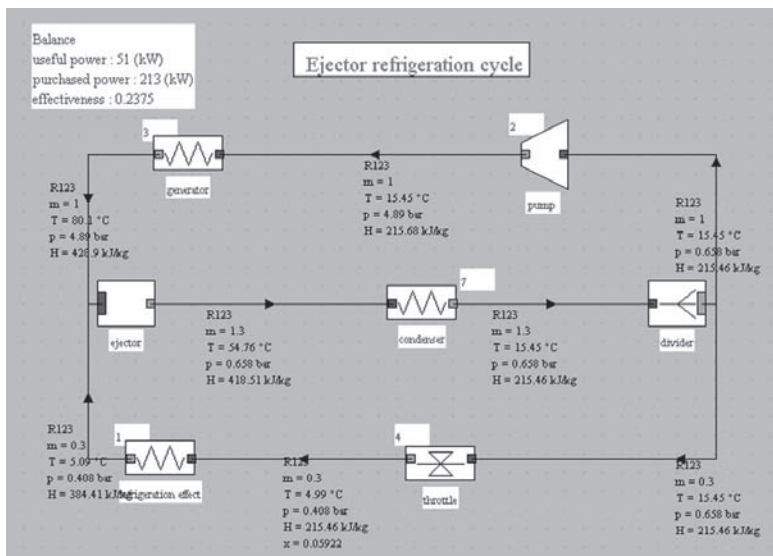


FIGURE 19.6.9
Synoptic view of an ejector cycle

However, one point to consider is that an ejector only works in good conditions if the ratio of internal sections is adapted to boundary conditions it faces. If the ratio of primary to secondary pressures departs from the rated values, there is an important risk that it is not well adapted, the performance of the cycle dropping then.

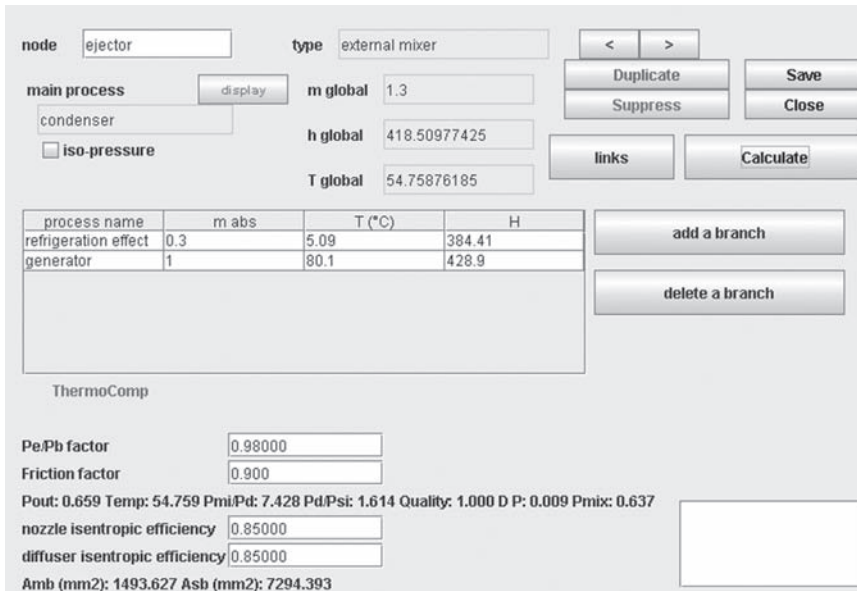


FIGURE 19.6.10

Ejector screen

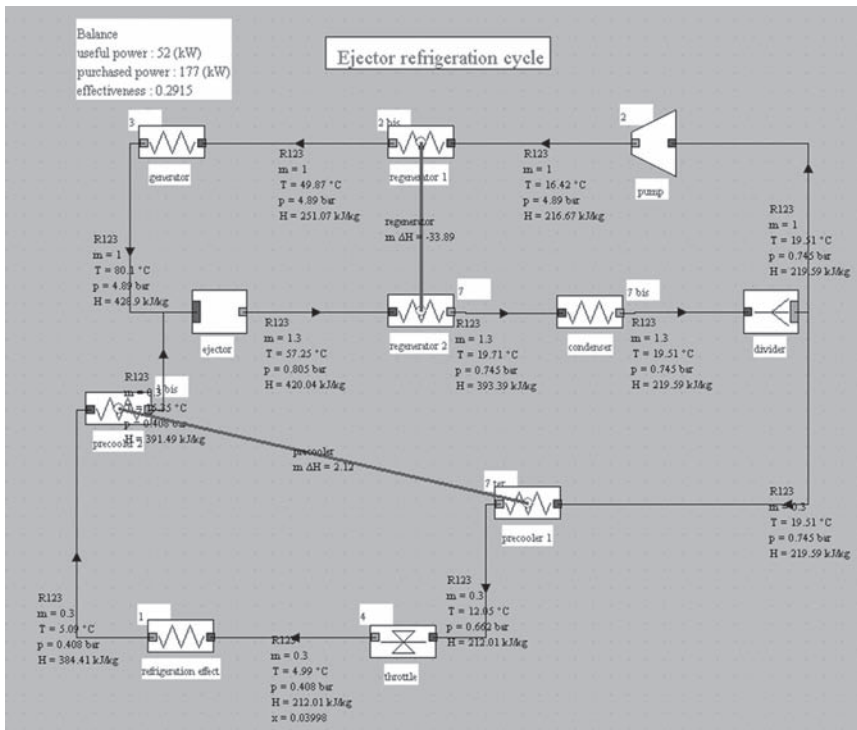
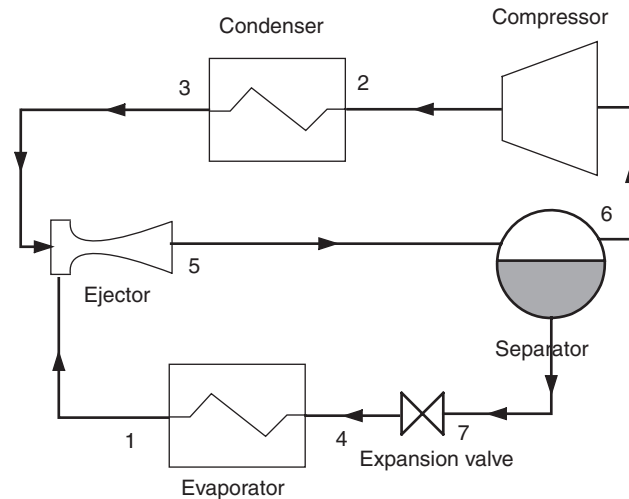


FIGURE 19.6.11

Synoptic view of the improved ejector cycle

This cycle can be slightly improved by the incorporation of a precoolers, which especially allows an increase in the cooling effect, and a regenerator, which reduces heat to provide to the generator (Figure 19.6.11).

**FIGURE 19.6.12**

Cycle with compressor

19.6.3.2 Cycles with compressor

The ejector may also simply be used to reduce the throttling irreversibility of a conventional refrigeration cycle, creating a slight pressurization before compression (Figure 19.6.12), as proposed by Kornhauser (1990). In this case, the motive fluid is a liquid that expands and becomes diphasic, carrying over and compressing the aspirated fluid. The compression ratio achieved by the ejector is then much lower than in the previous case.

Consider as an example, the single stage R134a cycle studied in section 19.5.1, working between 1 and 12 bar, whose COP was 2. The insertion of an ejector allows, as shown in Figure 19.6.13, to obtain an increase in COP of about 20%, similar to the benefit of a two-stage cycle.

Note that the reduced flow of refrigerant in the evaporator is offset by the decrease in quality at the expansion valve output, leading to a cooling capacity almost constant while the compression work drops.

A variant of this cycle is obtained using as primary fluid, not the liquid under pressure, but a supercritical fluid, especially CO_2 (Li and Groll, 2005). The principle remains the same, but the pressure obtained is higher than in the case of liquid. In this case also, adapting the operation of the ejector to a variation of its use conditions may be problematic.

This cycle with compressor and ejector however presents a major constraint: the flow distribution between the branches at high and low pressure must always be consistent with the quality of the refrigerant at the outlet of the ejector, which requires the implementation of special controls. For this reason the diagram shows a divider and a mixer at the separator output in Figure 19.6.14.

We consider that at point 3 flows 1 kg/s of supercritical CO_2 at 40°C and 100 bar, and that at point 1, at the evaporator outlet, CO_2 vapor is at 40 bar and 10°C, which represents superheating of about 5°C.

Supercritical CO_2 is expanded in the ejector, which allows it to entrain the vapor, and recompress it slightly.

The two-phase mixture at the ejector outlet is separated, the complement to 1 kg/s vapor flow being remixed with the liquid stream before entering the expansion valve then the evaporator. The main flow of vapor is compressed at 100 bar and then condensed at 40°C.

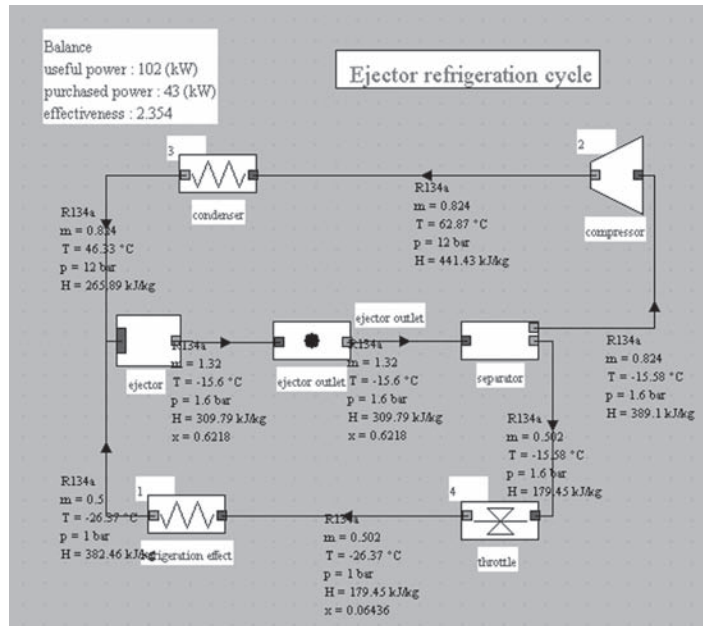


FIGURE 19.6.13
 Synoptic view of a cycle with ejector and compressor

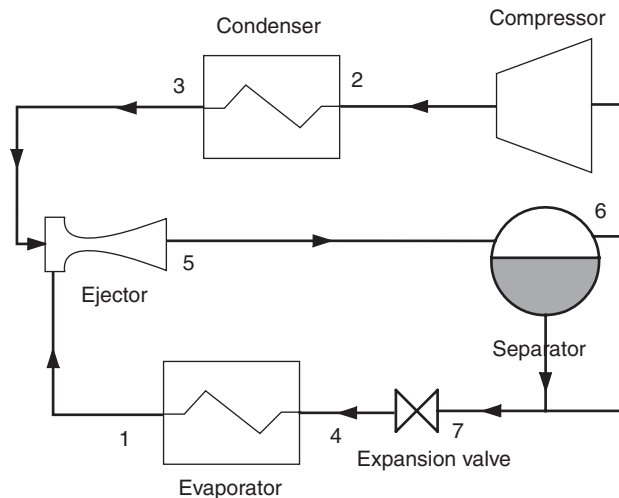


FIGURE 19.6.14
 Cycle with ejector and compressor

The ThermoOptim synoptic view of the facility is given in figure 19.6.15, and, for comparison, the diagram of a cycle without ejector is given in figure 6.9.16. The gain on the COP is clear.

19.6.4 Reverse Brayton cycles

As its name implies, a reverse Brayton cycle achieves a cooling effect by reversing the gas turbine Brayton cycle studied in Chapter 12, i.e. that of the gas turbine studied in section 12.1: a gas is compressed, cooled, and then expanded (Figure 19.6.17). The end of expansion temperature being low, this gas can be used to cool an enclosure, either by direct contact, especially if it is air, or through a heat exchanger.

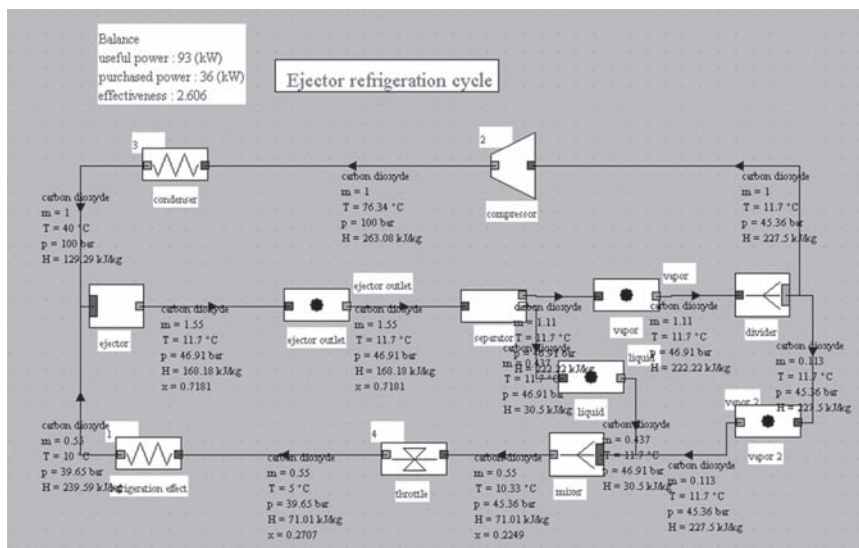


FIGURE 19.6.15
Synoptic view of the cycle with supercritical CO₂ ejector

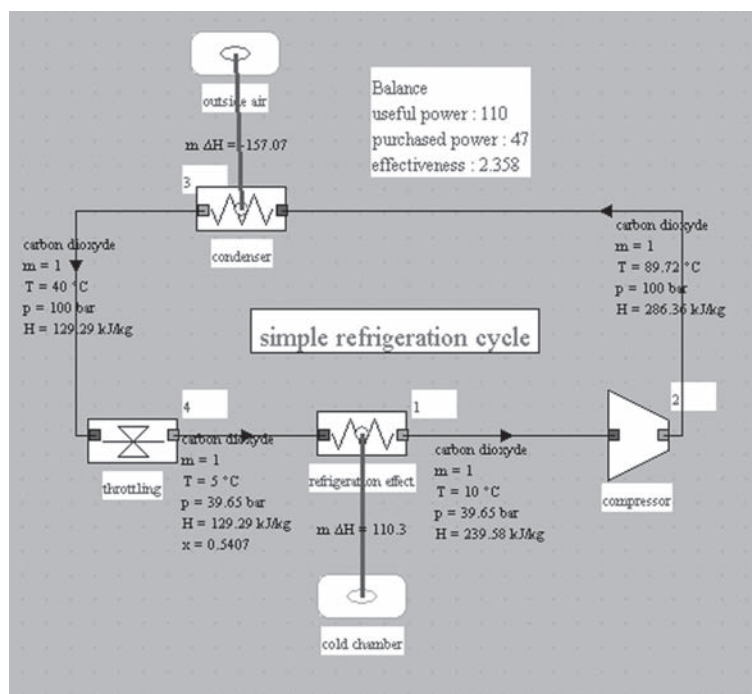


FIGURE 19.6.16
Classical cycle without ejector

Consider for example an open reverse Brayton cycle used to cool the passenger compartment of an automobile to reduce CO₂ emissions.

The working fluid is air which undergoes the following processes:

- 1–2 adiabatic compression at 2.5 bar in a compressor of polytropic efficiency 0.875;
- 2–3 isobaric cooling of the compressed air with outside air in a heat exchanger;
- 3–4 adiabatic expansion in a turbine of polytropic efficiency 0.875.

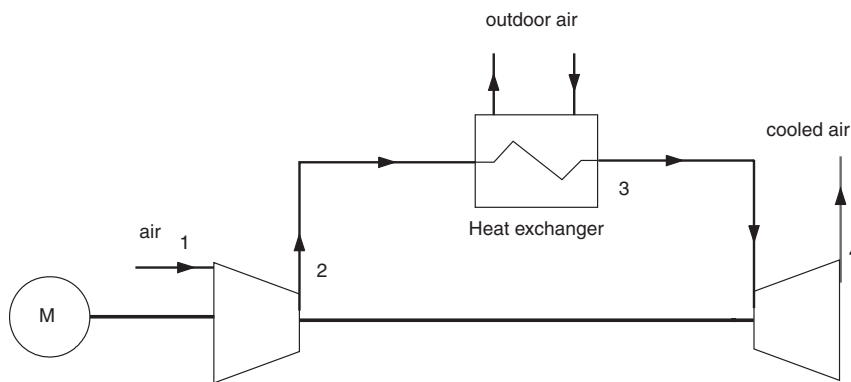


FIGURE 19.6.17
Sketch of an open reverse Brayton cycle

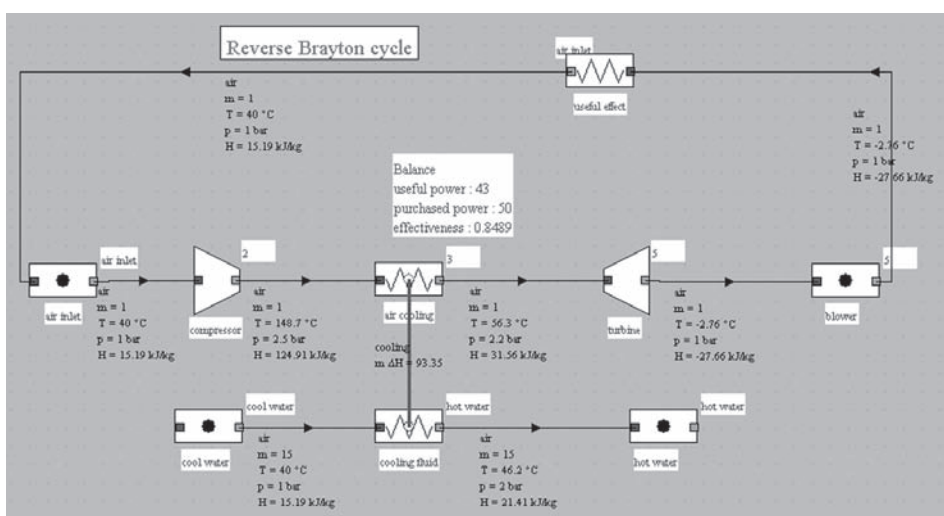


FIGURE 19.6.18
Synoptic view of an open reverse Brayton cycle

The ThermoOptim synoptic view of such a cycle is given in Figure 19.6.18.

The interior of the vehicle is represented by process “useful effect”. Air at 40°C is sucked by the compressor and exits at about 150°C. External cooling via a water heat exchanger allows the air flow to be cooled at 56°C. It is then expanded in the turbine and exits at -3°C. This cold air is then blown into the cabin.

As can be seen, the cycle efficiency is not very high (0.85), but the system is relatively simple, and has moreover the advantage of not releasing any greenhouse gases in the event of accidental break-age of pipes.

Air reverse Brayton cycle was until recently widely used in aircraft for in flight cabin air conditioning.

19.7 HEAT PUMPS

In refrigeration cycles that we studied so far, the practical effect is the extraction of heat by the evaporator. We can also design a machine whose useful effect is heating by waste heat available in the condenser. We call such a machine a heat pump, whose cycle is very similar to that used in refrigeration. It differs only by temperature levels, and therefore the working fluid.

For a heat pump, we define a heating COefficient of Performance COP_h :

$$COP_h = \frac{-Q_c}{\tau_c} = \frac{h_2 - h_3}{h_2 - h_1} = 1 + COP_c \quad (19.7.1)$$

Indeed, the first law states that all the energies involved are discharged at the condenser, that is to say, the heat energy taken from the cold source plus the mechanical energy of compression.

Heat pumps can raise the level of temperature of a cold source with excellent efficiency, as long as the temperature difference is not too important.

This heating method is very attractive if one has a source of free heat at a sufficient temperature. For space heating, it has one drawback: the COP_h decreases gradually as the heating needs are increasing, as the temperature difference between the cold source and heating system increases simultaneously.

Heat pump applications in industry are as follows, T_e and T_c being respectively the temperatures of evaporation and condensation:

- $T_e < 20^\circ\text{C}$, $T_c < 80^\circ\text{C}$: standard conventional heat pumps, marketed and available in a catalog;
- $20^\circ\text{C} < T_e < 80^\circ\text{C}$, $T_c < 130^\circ\text{C}$: specific heat pumps, though derived from refrigeration equipment, but adapted to higher operating temperatures;
- for higher temperatures, such material is no longer appropriate. Mechanical vapor compression studied in section 25.2 of Part 4 may be a solution, if the cold source is in the form of vapor.

Compressors used in practice are of three types: reciprocating ($P < 200\text{ kW}$), screw ($100\text{ kW} < P < 1\text{ MW}$), or centrifugal ($P > 800\text{ kW}$).

Currently, the main markets for heat pumps in industry concern drying of temperature sensitive products or slow migration of moisture and energy recovery in plants where there are simultaneous and comparable requirements of heat and cooling.

Since the cycle of a heat pump is similar to that of an air conditioner, it is possible to design reversible machines that can provide these two functions. Thus, in the residential and tertiary sector, the main market for heat pumps is the case where they can be used for winter heating, and summer air conditioning. In Japan, for example, where climatic conditions are particularly suited, millions of heat pumps are used. They are equipped with a reversing valve which allows one to shift from summer to winter use and vice-versa.

The whole problem of using a heat pump is to have a cold source for free at a suitable temperature and with sufficient heat available. For space heating, various solutions are possible:

- a river, lake or sea;
- the ground around a house, in which case the evaporator is buried;
- a pair of wells to power a geothermal heating system, such as for heating the Maison de la Radio in Paris;
- gas or liquid waste in residential buildings or factories;
- outdoor air, but evaporator frosting problems exist when air temperature is between 0°C and 5°C .

Defrosting can take various forms:

- hot air blowing;
- heating resistors;
- circulation of hot gas by-passing gas leaving the compressor;
- reversing the cycle by inverting the roles of the condenser and evaporator.

19.7.1 Basic cycle

The Thermoptim synoptic view of a heat pump is given in Figure 19.7.1, and its cycle is shown in Figure 19.7.2 on the entropy chart.

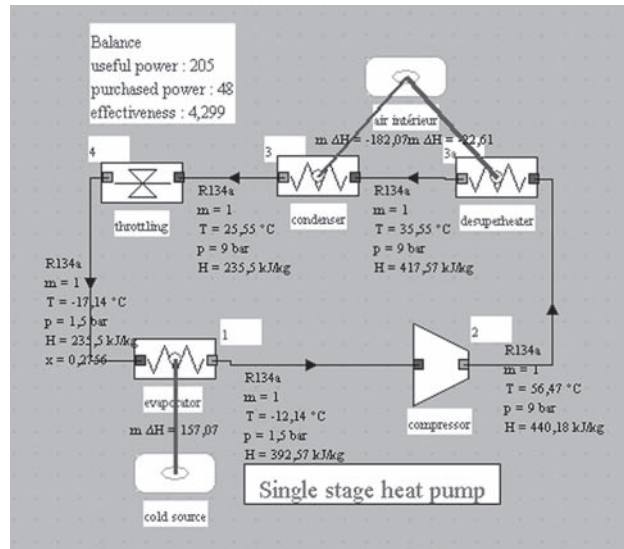


FIGURE 19.7.1
Synoptic view of a heat pump

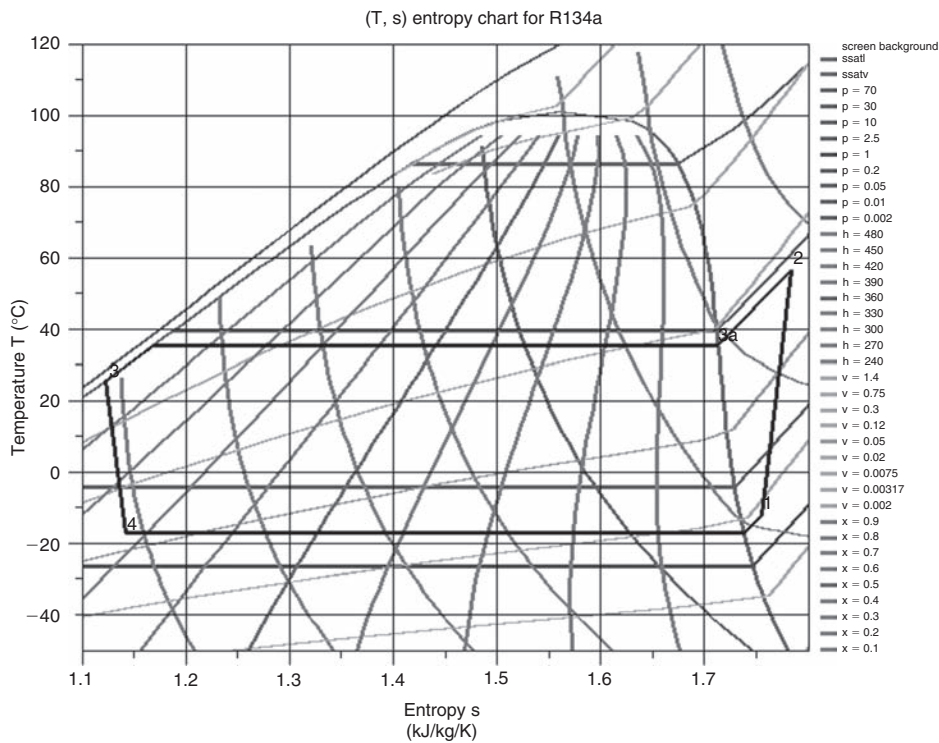


FIGURE 19.7.2
Heat pump cycle in the entropy chart

19.7.2 Exergy balance

To build the exergy balance of a heat pump, we must begin by giving a reference temperature and pressure. We take here $T_0 = 273.15 \text{ K}$ (0°C) and $P_0 = 1 \text{ bar}$, corresponding to winter conditions in France. Table 19.7.1 can then be built, the losses being given as percentage of total irreversibilities.

TABLE 19.7.1
HEAT PUMP EXERGY BALANCE

Exergy balance		$T_0 = 273.15\text{K} = 0^\circ\text{C}$						
Process	τ (kW)	Q (kW)	$m\Delta h$ (kW)	T_k (K)	Δxq (kW)	$m\Delta xh$ (kW)	Δxhi (kW)	loss
Compressor	48		48			40	8	25.7%
Desuperheater		-23	-23	288.15	-1.18	-3	2	6.3%
Condenser		-182	-182	288.15	-9.48	-21	11	36.0%
Expansion valve						-5	5	17.3%
Evaporator		157	157	263.15	-5.97	-10	5	14.6%
Cycle	48	-48			-17		31	100.0%
Sigma(x_i +)								
Sigma(tau +)		48						
Exergy efficiency			35%					

TABLE 19.7.2
CLASSICAL BOILER EXERGY BALANCE

Exergy balance		$T_0 = 273.15\text{K} = 0^\circ\text{C}$			
Process	τ (kW)	Q (kW)	$m\Delta h$ (kW)	$m\Delta xh$ (kW)	Δxhi (kW)
Heating circuit		205	205	26	117
Boiler		-205	-205	-143	
Cycle				-117	117
Exergy efficiency			18%		

They are almost evenly divided between the compressor (25%), the condenser (37.5%), the expansion valve (20%) and the evaporator (13.5%).

Again, the big difference with the energy balance, which showed a COP_h of 4.3 is that the cycle efficiency is actually very low: two-thirds of the exergy provided by the compressor to the fluid are dissipated in losses.

Now consider what would be the exergy balance of a conventional heating boiler providing the same power of 205 kW. Consider for this a boiler which would cool the smoke from 1,500°C to 80°C, to heat water for a heating circuit from 30°C to 50°C.

This is a kind of heat exchanger whose exergy balance is shown in Table 19.7.2. Exergy efficiency is equal to 18%, about half that of the heat pump.

If the heating was done by Joule effect in an electric boiler for example, the exergy efficiency of the cycle would be even lower, equal to the ratio of the exergy gained by the heating circuit (26 kW) to the exergy consumption (205 kW), i.e. 12.7%.

These figures illustrate the value of the heat pump, much more efficient than electric heating or combustion, since, for space cooling, it is unnecessary to provide heat at high temperature.

19.8 TECHNOLOGICAL ASPECTS

19.8.1 Desirable properties for fluids

The main desirable properties of refrigerants are:

- high latent heat of vaporization, since heat transfer takes place mainly in two-phase mode in the evaporator and condenser;

TABLE 19.8.1

PROPERTIES OF SOME PURE REFRIGERANTS

Name	Formula	ODP	GWP	M kg/kmol	T _b °C	T _c °C	P _c bar	γ
R 11	CFCl ₃	1	4,000	137.4	23.8	198	44.1	1.13
R 12	CF ₂ Cl ₂	1	8,500	120.9	-29.8	111.8	41.1	1.14
R 13	CClF ₃	1	11,700	104.5	-81.4	28.8	38.7	1.17
R 22	CF ₂ HCl	0.055	1,700	86.5	-40.8	96.2	49.9	1.18
R 123	CHCl ₂ CF ₃	0.02	93	152.9	27.9	183.7	36.7	1.08
R 32	CH ₂ F ₂	0	580	52	-51.7	78.2	58	1.24
R 125	CF ₃ CHF ₂	0	3,200	120	-48.1	66.3	36.3	1.1
R 134a	CF ₃ CH ₂ F	0	1,300	102	-26.1	101.1	40.6	1.1
R 717	NH ₃	0	0	17	-33.3	133	114.2	1.31
R 290	CH ₃ CH ₂ CH ₃	0	3	44.1	-42.1	96.8	42.5	1.14
R 600a	CH(CH ₃) ₃	0	3	58.1	-11.7	135	36.5	1.11
R 744	CO ₂	0	1	44	78.4	31.1	73.7	1.3
R 718	H ₂ O	0	0	18	100	374.2	221	1.33

- a saturation vapor pressure at the same time not too small at low temperature and not too large at high temperature, to limit the compression ratio and avoid technological problems induced by high pressures;
- low vapor specific volume, to limit the size of the different compression devices;
- high critical temperature for the shape of the cycle to be as close as possible to that of Carnot;
- specific heat capacity at constant pressure c_p large enough to avoid too high a compressor outlet temperature;
- high chemical stability and good compatibility with the lubricant;
- the fluid should be nonflammable and nontoxic;
- and as environmentally friendly as possible.

Unfortunately, no currently known fluid possesses all these properties, and manufacturers are doubtful, at least in the near future, of finding new ones which do.

The choice of a fluid is the result of a compromise between its different qualities and the constraints of the installation in question. By the importance given to each of the above properties, fluid rankings may be slightly different, which explains why different solutions are adopted by refrigeration equipment manufacturers.

As mentioned in section 19.2.1, chlorofluorocarbons were the best fluids until their action on the ozone layer would lead to their withdrawal. Table 19.8.1 gives the properties of a number of pure refrigerants (chemical formula, ODP, GWP for 100 years, molar mass, boiling temperature at atmospheric pressure T_b , temperature and critical pressure T_c and P_c , ratio γ of heat capacities at constant pressure and volume).

Table 19.8.2 gives the properties of a number of refrigerant blends (ODP, GWP for 100 years, temperature glide, molar mass, boiling temperature at atmospheric pressure T_b , temperature and critical pressure T_c and P_c).

19.8.2 Refrigeration compressors

In refrigeration systems, displacement or dynamic compressors are used depending on the case, sections 7.2 and 7.3 of Part 2 being respectively dedicated to them; readers interested in further developments on this matter should refer to them. We just give here some details on specific refrigeration features.

TABLE 19.8.2

PROPERTIES OF SOME REFRIGERANT BLENDS

nom	ODP	GWP	ΔT_g °C	M kg/kmol	T_b °C	T_c	P_c bar
R 502	0.4	5490	0	111.6	-46	82	40.2
R 404A	0	3260	0.7	97.6	-47	73	37.4
R 407C	0	1530	7.4	86.2	-44	87	46.3
R 410A	0	1730	<0.2	72.6	-51	72	49.5

**FIGURE 19.8.1**

Scroll spiral, Documentation Maneurop

In addition to piston, screw and centrifugal compressors, there is a fourth type of compressor that is widespread in refrigeration: spiral or scroll compressors (Figures 19.8.1 to 19.8.3) whose operating characteristics are close to screw machines (existence of a constructive V_i and losses by over- or under-compression if the compression ratio deviates from the actual constructive value, cf. section 7.2.2 of Part 2).

In this type of compressor, two cylindrical spirals, one fixed and one mobile (Figure 19.8.2) identically shaped, roll by sliding one on another, locking gas pockets of variable volume, which provides compression. The gas is sucked at the circumference and discharged in the center.

The advantages of this device are the lack of valves, the simple mechanism and hence its low cost and its silence, low mechanical losses, the possibility to rotate at high speeds, lack of vibration, light weight, reliability and low torque.

Technological problems are mainly in the machining of spirals and the seal between each spiral and the bottom of its conjugate. These compressors can operate without oil.

We can classify refrigeration compressors in three broad categories:

- open compressors (Figure 19.8.4) are manufactured in a frame independent of the motor, which is therefore outside. This provision, usually reserved for high-capacity machines, facilitates the maintenance of the compressor or the engine, but requires a good seal at the shaft that connects them, otherwise air inlets or refrigerant leakage can be expected;
- in hermetic compressors instead (Figures 19.8.3 and 19.8.7), the motor and compressor both bathe in the fluid vapor. It is then possible to enclose everything in a single housing, thereby ensuring a perfect seal. The disadvantage is that the whole is not removable and that on-site

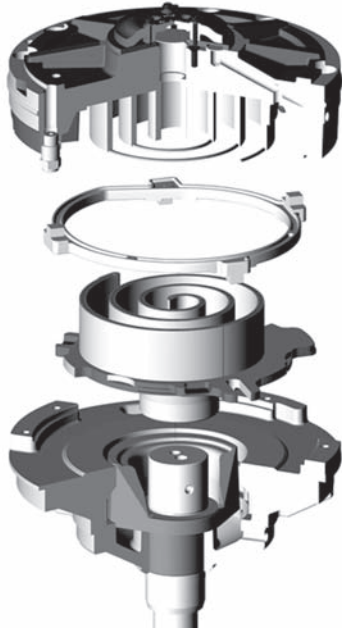


FIGURE 19.8.2
Cutaway of a scroll compressor, Documentation Maneurop

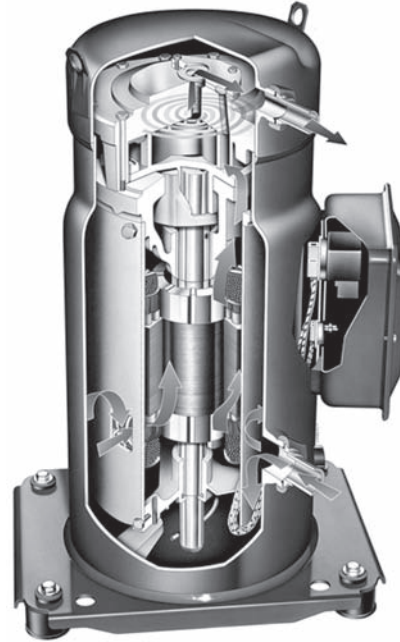


FIGURE 19.8.3
Scroll compressor cutaway, Documentation Maneurop

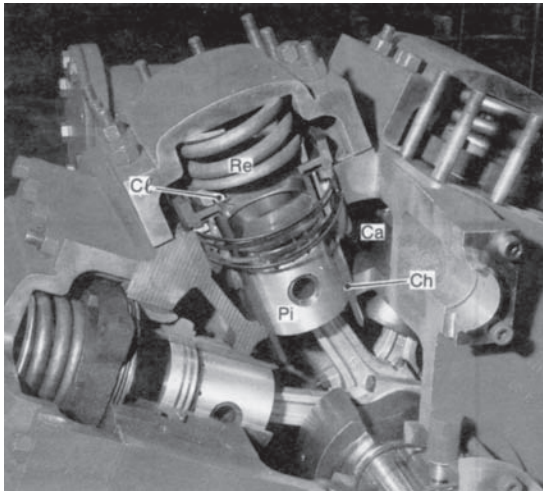


FIGURE 19.8.4
Cutaway of a piston compressor, Extract from Techniques de l'Ingénieur, Génie Energétique

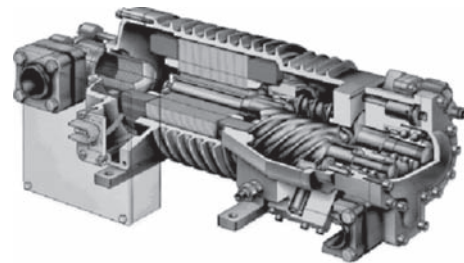


FIGURE 19.8.5
Accessible hermetic screw compressor, Documentation Bitzer

maintenance is impossible. The electric motor is typically an induction one and the fluid must be an electrical insulator. This type of configuration is restricted to low capacities (75–500 W), the compressor being as appropriate piston or rotary;

- accessible hermetic compressors (Figure 19.8.5) have the same advantages in terms of hermetic sealing, but with the added opportunity to intervene on site. They are reserved for intermediate capacity ranges (500 W – 500 kW).



FIGURE 19.8.6

Tandem compressors, Documentation Maneurop

Note finally that it is better (and regulatory beyond a certain capacity) to provide a protective device for reciprocating compressors in case of liquid suction, which may take place if superheating at the evaporator outlet is incorrectly set (this is called a liquid stroke). The solution generally adopted is to provide a bolt, pressed against the cylinder by a spring of high stiffness (such as that noted Re in Figure 19.8.4).

In normal operation, the set remains closed, and in case of liquid stroke, the head is raised and the cylinder is placed in communication with the discharge.

Compressors are often mounted in tandem, either to achieve high compression ratios, or to allow a better adaptation to a load variable over time (Figure 19.8.6).

As a guide, here are some dimensional values of industrial chillers: a 100 kW ammonia open piston compressor machine has a length of 3.7 m, a width of 1.75 m, a height of 1.7 m and a mass of 4.3 tons empty, and a 300 kW ammonia screw compressor machine is 3.9 m long, 1.7 m wide, 2.3 m high, its mass being 9 t (York Corporation).

19.8.3 Expansion valves

Valves used in refrigeration machines can be simple capillary tubes of diameter 0.6 to 2.8 mm, or thermal expansion valves (Figure 19.8.8) whose opening is controlled by the fluid temperature at the evaporator exit.

Two control modes are used: internal pressure equalization, which optimizes the filling of the evaporator, and external pressure equalization thanks to a pressure sensor downstream of the evaporator, which compensates for its pressure drop.

19.8.4 Heat exchangers

Chapter 8 of Part 2 being devoted to heat exchangers, the reader interested in further developments on this matter may refer to it.

The most simple heat exchangers used in refrigeration are twin-tube exchangers (Figure 19.8.9) running counter-flow, generally helically wound to reduce their size.

Plate heat exchangers are also used, but the most widespread are finned tube air coils for evaporators and condensers, inside which flows the refrigerant, air being outside.

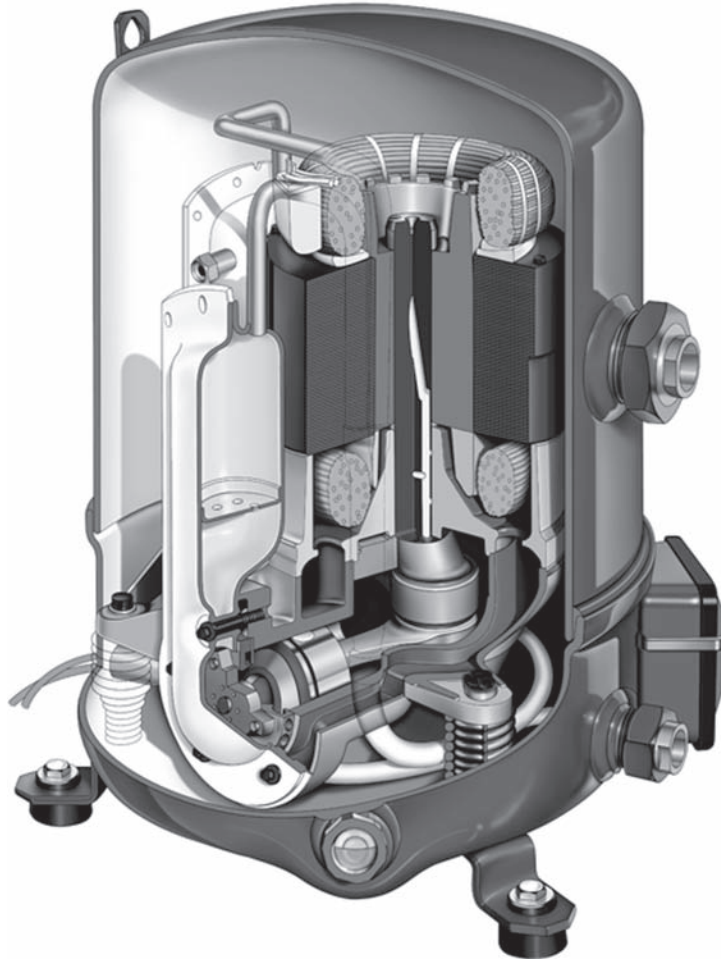


FIGURE 19.8.7
Hermetic piston compressor cutaway, Documentation Maneurop

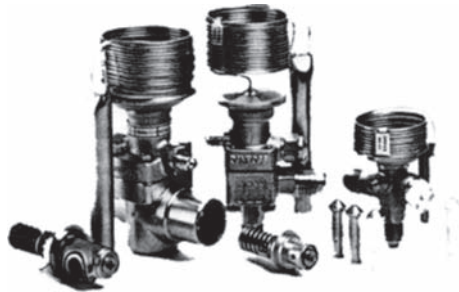


FIGURE 19.8.8
Thermal expansion valves, Extract from Techniques de l'Ingénieur, Génie Energétique



FIGURE 19.8.9
Twin-tube heat exchanger

19.8.5 Auxiliary devices

To function properly, refrigeration systems include a number of auxiliary devices:

- oil separators whose function is to rid the vapor leaving the compressor from oil that could mix with the fluid, in order first to redirect it towards the motor housing, and secondly to avoid the properties of refrigerant being altered (including reduction of heat exchange coefficients);
- dehydrators for removing any water from the circuit;
- variety of pressure switches, whose role is to prevent the system pressure to exceed certain limits.

19.8.6 Variable speed

Refrigeration plant motors generally do not operate continuously: they are regulated by a control device that stops them when the temperature of the chamber is cooled within a range of a few degrees or tenths of degrees around a set point. The result is that they work intermittently, and often far from the design conditions that would achieve the best efficiencies. With a variable speed drive, it becomes possible to achieve significant energy gains, for pumps, condenser and evaporator fans as well as for compressors.

Since the cost of variable speed drive motors has greatly declined in recent years because of advances in power electronics, a major effort is made by manufacturers so that their equipment can operate at variable speed.

A number of issues must however be resolved:

- lubrication of reciprocating compressors usually requires operation at a speed greater than 50% of the rated speed;
- volumetric efficiency λ drops, as the relative importance of HP/LP leakage increases;
- the tightness of screw and scroll compressors is more difficult to achieve;
- the balance of evaporators and condensers must be reconsidered.

REFERENCES

- M. Duminil, *Machines thermofrigorifiques*, Techniques de l'Ingénieur, Génie énergétique, BE 9. 730–9736
- Ashrae, *Fundamentals Handbook* (SI), Thermophysical properties of refrigerants, 2001.
- K. Chunnanond, S. Aphornratana, Ejectors: applications in refrigeration technology, *Renewable and Sustainable Energy Reviews* 8 (2004) 129–155.
- D. Clodic, Y. S. Chang, *Nouveaux fluides frigorigènes, caractéristiques et performances*, MAD l'outil froid, n° 16, novembre 1999.
- J.G. Conan, *Réfrigération industrielle*, Eyrolles, Paris, 1988.
- D.W. Sun, I.W. Eames, *Performance characteristics of HCFC-123 ejector refrigeration cycle*, *Int. J. Energy Res.* 20 (1996) 871–885.
- A.A. Kornhauser, *The use of an ejector as a refrigerant expander*. Proceedings of the 1990 USNC/IIR—Purdue refrigeration conference, Purdue University, West Lafayette, IN, USA, 1990, p. 10–19.
- D. Li, A. Groll, *Transcritical CO₂ refrigeration cycle with ejector-expansion device*, *International Journal of Refrigeration* 28 (2005) 766–773.

FURTHER READING

- T. Destoop, *Compresseurs volumétriques*, Techniques de l'Ingénieur, Traité Mécanique et chaleur, B 4 220.
- A. Gac, *Conduite automatique des installations frigorifiques*, Techniques de l'Ingénieur, Traité Mécanique et chaleur, B 9 765.
- G. Vrinat, *Production du froid, Technologie des machines industrielles*, Techniques de l'Ingénieur, Traité Mécanique et chaleur, B 2 365.
- S. K. Wang, Z. Lavan, P. Norton, *Air Conditioning and Refrigeration Engineering*, CRC Press, Boca Raton, 2000, ISBN 0-8493-0057-6.

Liquid Absorption Refrigeration Cycles

Abstract: The main interest of the liquid absorption refrigeration cycles is that they require only low power compared to their counterparts in mechanical vapor compression (less than 1%). Using a three-temperature thermodynamic cycle, they allow direct use of medium or high temperature heat to produce cooling, requiring little or zero mechanical energy input. As such, their theoretically total efficiency in terms of primary energy is greater than that of vapor compression cycles.

Moreover, they involve fluids whose impact on the ozone layer and the greenhouse effect is zero: ODP = GWP = 0. However, they require an input of heat at intermediate or high temperature, so that their indirect impact is not necessarily zero: it depends on the energy source used.

Another advantage of liquid absorption cycles is that they can be used in integrated energy facilities producing both mechanical power, heat at intermediate temperature and cooling. This is known as trigeneration, and total efficiencies obtained are extremely high (see section 18.6.2).

You should refer to section 5.6.8.4 of Part 2 for a presentation of Oldham and Merkel charts which are used for the study of absorption cycles, as well as of the LiBr-H₂O couple equations.

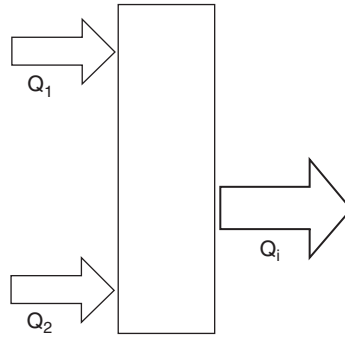
Keywords: absorption, absorber, desorber, rectifier, solution exchanger, trigeneration.

20.1 INTRODUCTION

An absorption machine exchanges heat with at least three heat sources at three different temperature levels. Let us mark by index 1 the hot source, 2 the cold one and *i* the intermediate temperature source, and call *W* the work put into play in the machine and ΔS the entropy generation. Writing the two laws of thermodynamics leads to equations 20.1.1 and 20.1.2.

$$W + Q_1 + Q_i + Q_2 = 0 \quad (20.1.1)$$

$$\frac{Q_1}{T_1} + \frac{Q_i}{T_i} + \frac{Q_2}{T_2} = \Delta S \quad (20.1.2)$$

**FIGURE 20.1.1**

Absorption machine principle

Two cases can be distinguished according to whether the temperature of the environment is or is not above the temperature of the cold source.

In the first case, which corresponds to the refrigeration cycle, the machine cools an enclosure at low temperature and rejects heat into the environment, T_i being greater than or equal to T_0 .

In the second case, which corresponds to the heat pump cycle, the machine extracts heat from the cold source (which may be the environment) and uses it to heat a chamber at intermediate temperature T_i .

Let us consider the first case, and assume that the intermediate temperature source is the environment, T_i being equal to T_0 .

Combining equations 20.1.1 and 20.1.2, we get:

$$W = -Q_c \left(1 - \frac{T_0}{T_c} \right) - Q_f \left(1 - \frac{T_0}{T_f} \right) + T_0 \Delta S \quad (20.1.3)$$

The first and the third term being negative and the second positive, this equation shows that work W may be zero, that is to say that it is possible to design a three-temperature machine for producing refrigeration cooling without consuming work. In practice however, many absorption chillers include circulating pumps.

20.2 STUDY OF A $\text{NH}_3\text{-H}_2\text{O}$ ABSORPTION CYCLE

An ammonia absorption cycle machine has eight main components (Figure 20.2.1):

- a desorber-rectifier, which receives heat flux from the heat source, and wherein enters the strong solution at high pressure, preheated in solution exchanger (B). The exiting fluids are on the one hand, the almost pure refrigerant vapor (NH_3) (C), and secondly the depleted solution (A);
- the condenser, from which exits the vapor condensed and possibly sub-cooled (I), the heat removed being rejected in the surroundings;
- a refrigerant expansion valve, which reduces the pressure of the refrigerant, exiting in the two-phase state at low temperature (L);
- an evaporator where the refrigerant at low temperature and pressure is vaporized and possibly slightly superheated (J), extracting useful heat (refrigeration effect) from the cold source;
- an absorber, in which enters the vaporized refrigerant and the weak solution preheated in solution exchanger, and out of which flows the strong solution (D), the heat removed being rejected in the surroundings;

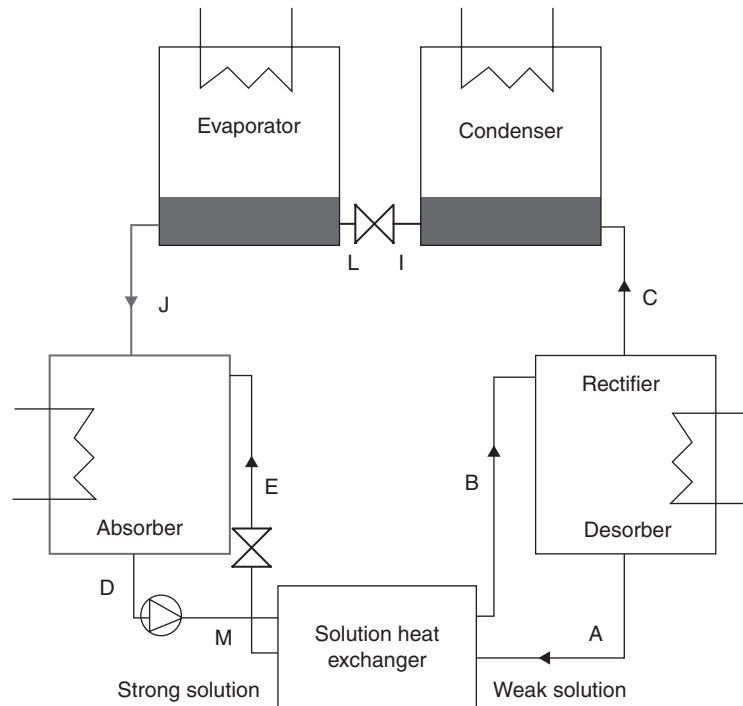


FIGURE 20.2.1

Sketch of a $\text{NH}_3\text{-H}_2\text{O}$ absorption cycle

- a solution heat exchanger, which allows for internal regeneration between the strong solution and the weak solution;
- a pump which is needed to pressurize the strong solution before it enters the heat exchanger;
- an expansion valve at the outlet of the heat exchanger which reduces the weak solution pressure to that of the absorber.

Note that the condenser, the refrigerant expansion valve and the evaporator work the same way as in a vapor compression refrigeration cycle.

We discuss below such a cycle and represent it both in isobaric equilibrium lenses and in the Merkel chart, then we plot it in Oldham chart. The numerical values for constructing these charts were obtained from a software package developed by the Centre for Energy Studies of Mines ParisTech (École des Mines de Paris) from equations proposed by Ziegler and Trepp (1984). This software has also been coupled to Thermoptim.

The purpose of this section being simply to illustrate the use of thermodynamic charts, the cycle used is a theoretical cycle, in which some real cycle irreversibilities are neglected. Readers interested in a very detailed study of these cycles may refer to Techniques de l'Ingénieur articles No. BE 9735 and BE 9736 by Maxime Duminil. They will find there detailed explanations on how to calculate a rectification.

In the desorber, which receives a heat supply, the strong solution is partially vaporized (B-C) at 120°C , and partially depleted and heated (B-A) at 140°C . B-C is a horizontal segment on the isobaric equilibrium lens of Figure 20.2.2, and an oblique segment on the Merkel chart of Figure 20.2.3, which is easily constructed using auxiliary curves. B-A follows in both cases the saturated isobaric line. Point A determination assumes that we are given an assumption about the operation of the desorber: either the temperature T_A , or the liquid mass fraction of weak solution x_p , or the

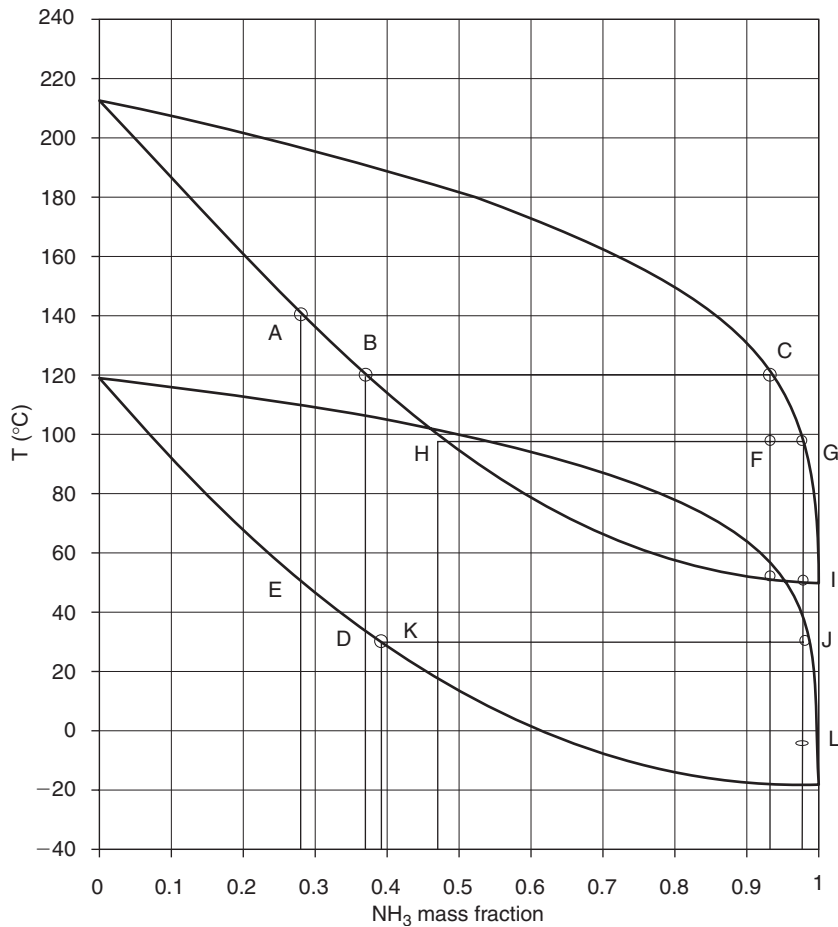


FIGURE 20.2.2

Isobaric equilibrium lenses at 2 and 20 bar

heat. Note that the depletion of the solution is made possible by a special arrangement of the apparatus, e.g. counter-flow, otherwise $T_A = T_C$. It is important to emphasize this point because very often in literature the implicit or explicit assumption is made that the desorber is isothermal, while presenting points A, B and C positioned in the Merkel chart as in our example, which is physically impossible.

A: $T = 140^\circ\text{C}$, $P = 20$ bar, $x = 0.28$ weak liquid exiting counter-flow desorber

B: $T = 120^\circ\text{C}$, $P = 20$ bar, $x = 0.37$ strong liquid beginning vaporization

C: $T = 120^\circ\text{C}$, $P = 20$ bar, $y = 0.93$ vapor stemming from the strong liquid

The vapor exiting the desorber in C is then rectified, that is to say slightly cooled (here at 97°C) because its quality in refrigerant is insufficient. This operation (not described here because it is outside the scope of this book) results in almost pure vapor in G ($y = 0.995$). Determining point G (on the dew point curve) assumes that its temperature or vapor quality is given. A very small amount of liquid (H) also leaves the rectifier. It generally falls into the absorber where it is mixed with the weak liquid. Point H is deduced simply from G on both charts: it is on the bubble curve at the temperature and pressure of G.

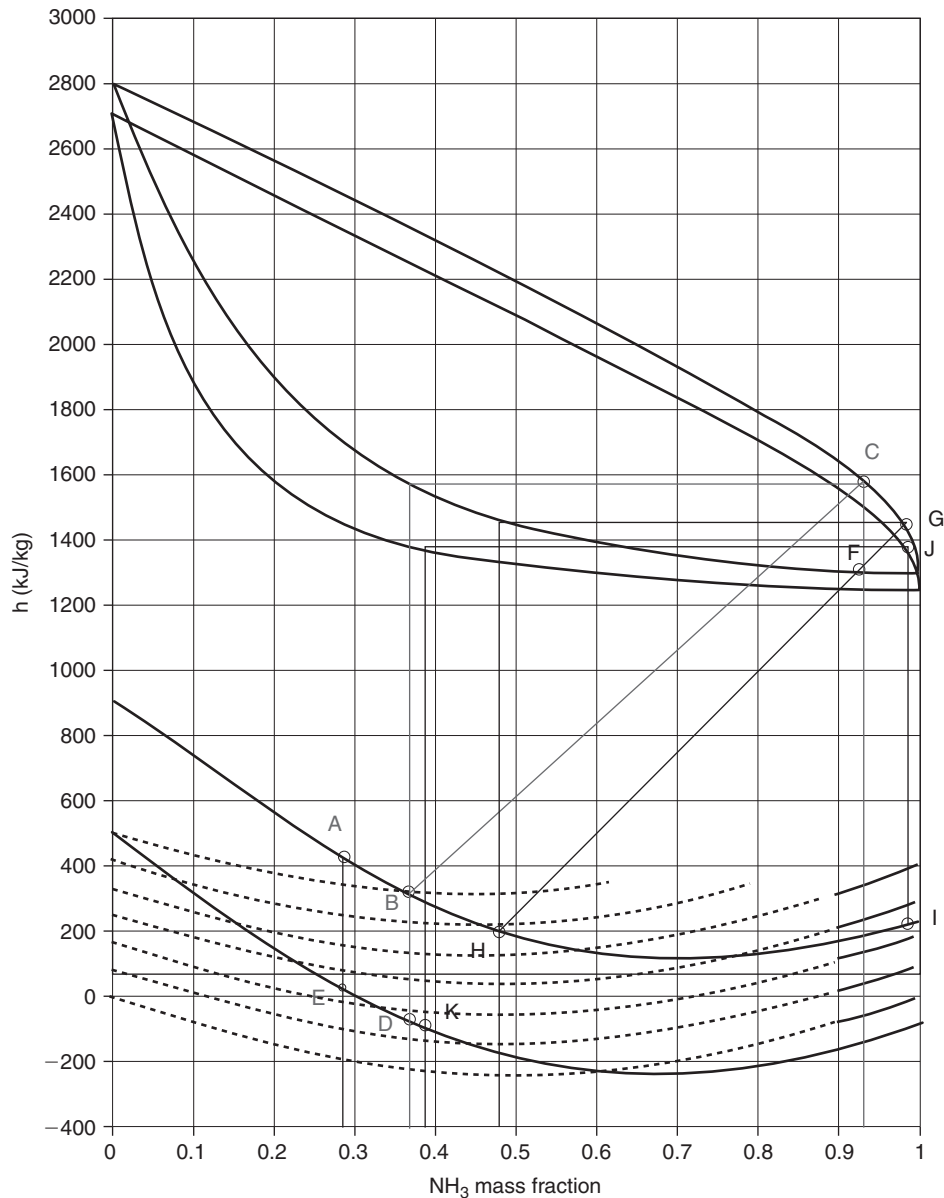


FIGURE 20.2.3

Merkel chart

G: $T = 97^{\circ}\text{C}$, $P = 20$ bar, $y = 0.995$ vapor rectifier output

H: $T = 97^{\circ}\text{C}$, $P = 20$ bar, $x = 0.47$ liquid rectifier output

F: $T = 97^{\circ}\text{C}$, $P = 20$ bar, $z = 0.93$ average rectifier state

The refrigerant vapor is directed to the condenser, which it exits in I, at high pressure and 54°C . It is then expanded isenthalpically (point L in two-phase zone at low pressure). The refrigerant is then vaporized in the evaporator at point J. To determine points I and L, we generally assume that the refrigerant is pure, and we use the ammonia (h, P) or (T, s) chart.

I: $T = 54^\circ\text{C}$, $P = 20$ bar, $y = 0.995$ condensed liquid condenser outlet

L: $T = -15^\circ\text{C}$, $P = 2$ bar, $z = 0.995$ two-phase throttling output, evaporator inlet

The weak solution heats the strong solution in a liquid-liquid regenerator heat exchanger. Mass fractions x_r and x_p of both solutions being constant, these two processes are substantially vertical segments (AE) and (DB) in both charts that we consider. Note in the Merkel chart that enthalpies involved are comparable and temperature levels consistent. As the flow-rates of the two solutions are slightly different, heat exchange can take place. Strictly speaking, points E and B are not located exactly on the bubble curves corresponding to their pressure: their exact state depends on the characteristics of the solution heat exchanger. For simplicity of analysis, we will not consider this discrepancy in what follows: we simply estimate *a posteriori* the effect of this assumption.

D: $T = 30^\circ\text{C}$, $P = 2$ bar, $z = 0.37$ strong liquid absorber exit

E: $T = 55^\circ\text{C}$, $P = 2$ bar, $z = 0.28$ weak liquid solution heat exchanger exit

In the absorber, the vapor (assumed pure) coming out of J is condensed in K, then mixed with weak liquid to give the strong solution that exits in D, the operation involving heat extraction. The determination of point D assumes that we are given an additional assumption on the operation of the absorber: either the value of the quality of the strong solution or its temperature, or heat extracted. As mentioned above, point B is obtained from D, knowing its pressure and x_r .

J: $T = 45^\circ\text{C}$, $P = 2$ bar, $y = 0.995$ vapor evaporator outlet

K: $T = 45^\circ\text{C}$, $P = 2$ bar, $x = 0.395$ vapor condensed in the absorber

To be precise, we should represent point M at the output of the strong solution pump. However, as the compression in the liquid state is almost isothermal, and involves a small amount of work, M is almost coincident with D, knowing that it is not in the liquid-vapor equilibrium state, but in the liquid sub-cooled state.

M: $T = 30^\circ\text{C}$, $P = 20$ bar, $z = 0.37$ strong solution pump output

Calling \dot{m} the refrigerant flow, \dot{m}_p the weak solution flow, \dot{m}_r the strong solution flow, the desorber material balance (total mass flow rate and mass flow of refrigerant) provides:

$$\dot{m}_r = \dot{m} + \dot{m}_p \quad (20.1.4)$$

$$\dot{m}_r(1 - x_r) = \dot{m} + \dot{m}_p(1 - x_p) \quad (20.1.5)$$

This system of equations allows to express \dot{m}_r and \dot{m}_p in terms of \dot{m} , x_p and x_r :

$$\dot{m}_r = \dot{m} \frac{1 - x_p}{x_r - x_p} \quad (20.1.6)$$

$$\dot{m}_p = \dot{m} \frac{1 - x_r}{x_r - x_p} \quad (20.1.7)$$

Enthalpies involved in the processes are (under the simplifying assumptions that we used, including assuming points B and E on their respective bubble curves):

$$\text{Condenser: } Q_{\text{cond}} = \dot{m}(h_I - h_G)$$

$$\text{Evaporator: } Q_{\text{evap}} = \dot{m}(h_J - h_I)$$

TABLE 20.2.1

STATE OF ABSORPTION CYCLE POINTS

T (°C)	P (bar)	z	x	y	h (kJ/kg)	m (kg/s)
A	140	20		0.28		450
B	120	20		0.37		325
C	120	20			0.93	1575
D	30	2	0.37			-65
E	55	2		0.28		50
F	97	20	0.93			1300
G	97	20	0.995			1440
H	97	20				200
I	54	20			0.995	232
J	45	2			0.995	1375
K	45	2		0.395		-60
L	-15	2	0.995			232
M	45	20				-60

$$\text{Desorber: } Q_{\text{des}} = \dot{m}h_C + \dot{m}_p h_A - \dot{m}_r h_B$$

$$\text{Absorber: } Q_{\text{abs}} = -\dot{m}h_J - \dot{m}_p h_E + \dot{m}_r h_D$$

$$\text{Solution heat exchanger: } Q_{\text{sol}} = \dot{m}_r (h_B - h_D) = \dot{m}_p (h_A - h_E)$$

Work of the strong solution pump: $W = \dot{m}_r (h_M - h_D) \neq 0$, which we can estimate equal to $v\Delta P$.

The COP is defined as the ratio of useful energy Q_{evap} to purchased energy ($Q_{\text{des}} + W$).

By neglecting work W , we get:

$$\text{COP} = \frac{\dot{m}(h_J - h_I)}{\dot{m}h_C + \dot{m}_p h_A - \dot{m}_r h_B} \quad (20.1.8)$$

$$\text{COP} = \frac{(h_J - h_I)}{h_C + \frac{1-x_r}{x_r-x_p} h_A - \frac{1-x_p}{x_r-x_p} h_B} \quad (20.1.9)$$

This way of working includes the implicit assumption that the solution exchanger is balanced, which is not totally verified as shown in Tables 20.2.1 and 20.2.2, valid for a cycle without subcooling at the condenser outlet.

However, the lowest temperature in the absorber being equal to 30°C we can easily use the cold source to sub-cool the liquid refrigerant at that temperature, which lowers the enthalpy of points I and L, and thus the vapor quality after expansion. The enthalpy change in the evaporator increases, and the COP increases slightly (about 10%, from 0.4 to 0.44).

It is possible to represent the points of this cycle at the vapor-liquid equilibrium in the Oldham chart (Figure 20.2.4). We call this representation the solution cycle. It has the characteristic shape of a diamond that we have discussed section 5.6.8.4 of Part 2. Note that the analyses that this type of chart allows are much more cursory than those provided by the Merkel chart: the only information available are the pressures, temperatures and mass fractions of the solution.

TABLE 20.2.2
PERFORMANCE OF THE ABSORPTION CYCLE

Condenser	-1208
Evaporator	1143
Desorber	2900
Absorber	-2230
Strong solution exchanger	2730
Weak solution exchanger	3200
Pump work	5 (estimate)
COP	0.394

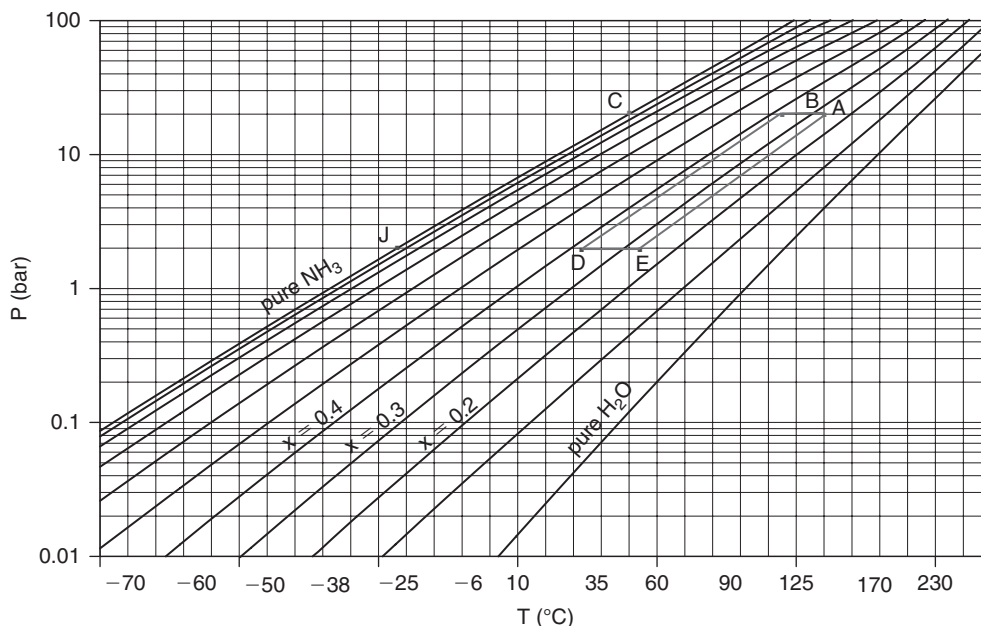


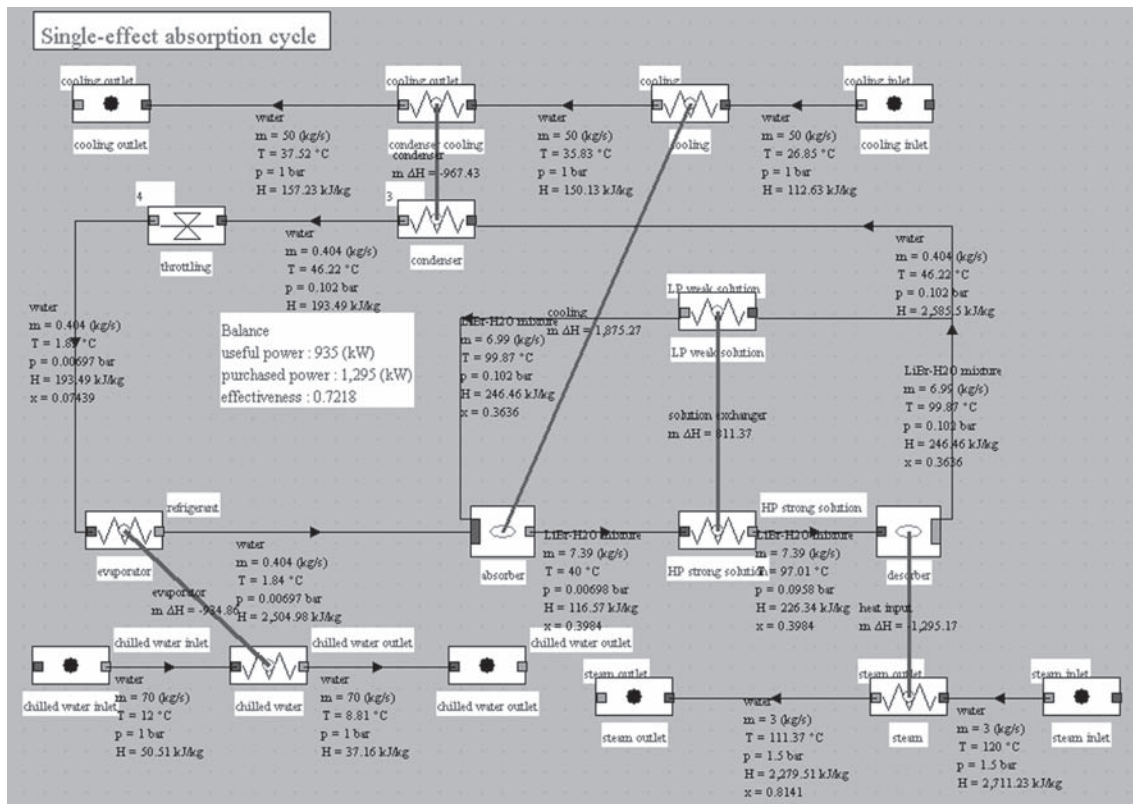
FIGURE 20.2.4
Representation in the NH₃-H₂O Oldham chart

The absorption cycle that we have presented operates through a process called single-effect, leading to relatively limited performance. If you have a heat source hot enough, you can use more efficient cycles, known as multiple effect or cascade. The interested reader can refer to the literature.

20.3 MODELING LiBr-H₂O ABSORPTION CYCLE IN THERMOPTIM

Modeling a cycle using the pair LiBr-H₂O is easier than what we have just seen since we can consider that water vapor in the desorber outlet is almost pure, so that the rectifier of Figure 20.2.1 becomes useless. The diagram of the machine is a little simplified. As also the properties of the pair can be easily modeled using equations (5.6.51 to 53) of Part 2, the cycle can be modeled with Thermoptim without too much difficulty, using three external classes¹ to represent the mixture

¹ These classes are available in Thermoptim model library: <http://www.thermoptim.org/sections/logiciels/thermoptim/modelotheque>

**FIGURE 20.2.5**

Synoptic view of a single-effect absorption cycle

properties, the absorber and the desorber, since, as we said above, condenser, refrigerant expansion valve and evaporator operate the same way as in a vapor compression refrigeration cycle.

The absorber and desorber are modeled by two external nodes which exchange heat with the outside, as a high temperature input in the desorber, and an intermediate temperature cooling in the absorber.

Representation of thermal coupling is possible using two thermocouples, called “heat input” and “cooling” on the synoptic view in Figure 20.2.5: Each node calculates the external heat energy that must be exchanged, and each thermocouple recalculates the “exchange” process to which it is connected.

On this synoptic view, we recognize in the central part the absorption machine, with the three sources with which it exchanges heat: above the cooling at medium temperature, in the lower left part chilled water, and at the bottom right high temperature steam.

Cooling energy is considered here as useful energy and thermal energy supplied to desorber as purchased energy, which leads to a single effect absorption cycle COP equal to 0.72.

REFERENCES

- M. Duminil, *Machines thermofrigorifiques*, Techniques de l'Ingénieur, Génie énergétique, BE 9. 730 à 9 736.
- B. Ziegler Ch. Trepp, *Equation of state for ammonia-water mixtures*, Revue Internationale du Froid, Vol. 7, Number 2, Butterworth, march 1984.

This page intentionally left blank

Air Conditioning

Abstract: Rising living standards in industrialized countries has been accompanied by increasingly large demands in terms of thermal comfort conditions in residential and commercial buildings. Air conditioning has progressively developed in recent decades, leading to continued progress in the various disciplines that make up what is known as HVAC (Heating, Ventilation, and Air Conditioning).

To size an air conditioning system we must first be able to evaluate the thermal and water loads to import or evacuate. These loads depend on the climate and conditions of occupancy. They vary throughout the year and the design of an air conditioning system can only be made by taking into account these factors.

In this chapter, we will only deal superficially with these issues. The interested reader should refer to the literature listed in the bibliography, including ASHRAE publications.

Keywords: air conditioning, HVAC, chiller, humidifier, dehumidifier, moist mixture processes nozzle, condition line.

21.1 BASICS OF AN AIR CONDITIONING SYSTEM

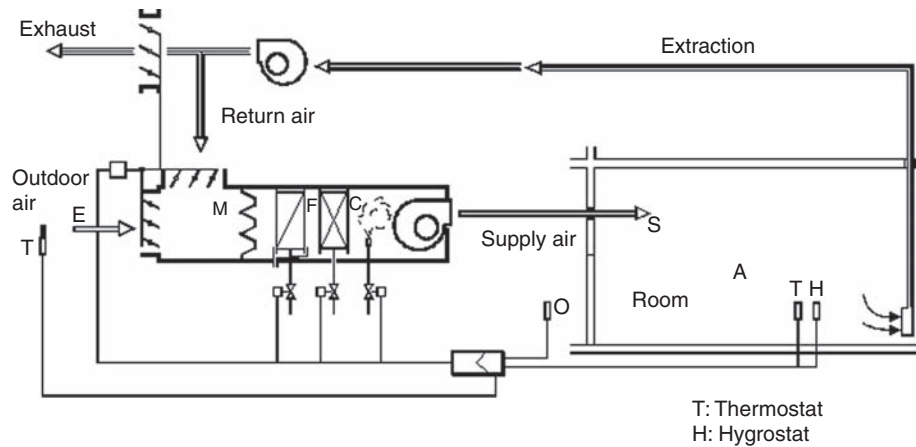
An air conditioning system involves basic devices that have been studied in section 7.8 of Part 2, to which we refer the reader for further developments:

- mixers;
- heaters;
- chillers, with or without water condensation;
- humidifiers, by water or steam;
- dehumidifiers.

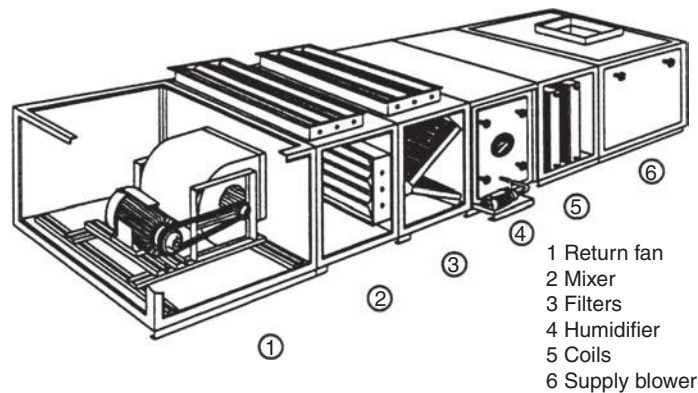
Figure 21.1.1 shows how looks like an air conditioning system and how it fits into a building.

The room is represented in the lower right. It has two sets of airflow veins, one for extraction and one for blowing. To cool the room, a certain air flow is “supplied” through vents. As this blown air mixes with room air, heat and water balance is achieved. Supply conditions are determined so that this equilibrium corresponds to the desired comfort conditions (see section 7.8.7 of Part 2).

Air extracted is partly discharged outside, and partly recycled, the recirculation rate depending on hygiene standards in force. Return air is mixed with fresh air, optionally preheated, the mixture being then “processed” so that its state corresponds to the supply conditions desired.

**FIGURE 21.1.1**

Air conditioning system, Documentation R. Casari

**FIGURE 21.1.2**

Cutaway of an air treatment vein, Documentation R. Casari

Figure 21.1.2 shows the cutaway of an air treatment vein set showing various boxes including a return fan, mixer, filters, humidifier, coils and a supply blower.

The design of an air conditioning system comprises a series of distinct steps:

- climatic conditions of reference that will be used to calculate the enthalpy and water loads must be first determined. In practice, it is based on climatic data published by national meteorological services, which are eventually corrected as indicated below. The values to take into account are not the extreme conditions but those likely to be reached or exceeded a few days per year on average. For winter, corrections must be made to temperatures at high altitude sites (-1°C every 200m) and cities ($+1$ to 2°C depending on the size of the metropolitan area), and an estimate of relative humidities can be obtained simply (100% along the coast or a lake, 90% elsewhere);
- environmental conditions must then be defined (T. Agami Reddy, 2001). For specific industrial applications, refer to the information of AICVF Guides in France or ASHRAE in the U.S. For comfort cooling, it should be noted that most healthy people do not feel any noticeable difference as long as the relative humidity is between 30 and 60% and the temperature is below 25°C . As a first approximation we can therefore choose for summer a temperature of 25°C and a relative humidity of 60%, and for winter temperatures of 19 or 20°C and a relative humidity of 30%;

- once these values are chosen, it becomes possible to calculate loads. Depending on countries, calculations are slightly differently expressed: in the U.S. for example, sensible and latent loads are considered while in France we talk of enthalpy and water loads (AICVF, 1999). This simply means that in the first case, water to be extracted is directly converted in energy terms, while in the second it is expressed in kg/s. Detailed calculation of heat loss from a building are outside the scope of this book: you should refer to the AICVF Guides (1999) or methods proposed by CSTB or ASHRAE (A. Rabl, P. Curtiss, 2001). Sensible (or enthalpy) load Q_s is given by equation (21.1.1), in which φ_p represents losses through the walls, φ_i losses by air infiltration (which should certainly not be confused with those due to air renewal that are implicitly taken into account by the calculation method), φ_s solar gains and P the set of internal gains due to occupants, lighting, appliances, machinery, office equipment etc.

$$Q_s = \varphi_p + \varphi_i + \varphi_s + P \quad (21.1.1)$$

- the supply or **condition line** can then be determined as explained in section 7.8.7.1 of Part 2:

With French notations:

$$\gamma = \frac{\Delta q'}{\Delta w} = \frac{\dot{Q}_s + \dot{m}_{\text{water}} h_{\text{water}}(t_1)}{\dot{m}_{\text{water}}} \quad (21.1.2)$$

With US notations:

$$\text{SHR} = \frac{\dot{Q}_s}{\dot{Q}_s + \dot{Q}_l}$$

In the psychrometric chart, the condition line is the line of slope SHR or γ passing through the point representing the desired comfort conditions. Each point of this line corresponds to a different supply flow-rate.

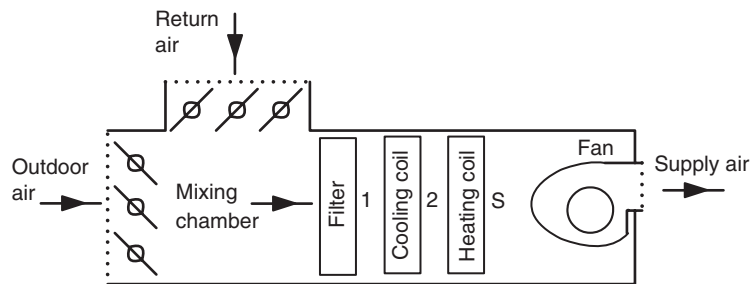
The actual flow-rate value depends on various factors, such as the maximum allowable temperature difference to avoid any inconvenience (usually 6 to 12°C according to the technique used), or the rate of mixing required (generally between 3 and 20 volumes/hour) to ensure good uniformity without drafts;

- Once the supply point is determined, it remains to choose an air treatment for bringing a mixture of outdoor air and indoor air in this state. The recirculation rate depends on hygiene constraints. The more important it is, the higher the energy expenditure will be. The following examples show how basic treatments can be combined to form a proper air conditioning unit. Note that in first approximation the fan heats pumped air by about 1°C. In winter this means less heating need, and in summer greater cooling need.

21.2 EXAMPLES OF CYCLES

There are many possible air conditioning cycles, and their presentation is beyond the scope of this book (Mitchell & Braun, 2012). We will, therefore, present only two examples of typical installations of summer cooling and winter heating.

The equations governing moist air processes were established in section 7.8 of Part 2. Thermoptim has screens available to address them. Note however that the diagram editor does not yet have components representing moist processes. Modeling cannot be done graphically (guidance on how to describe a project are given in the Getting Started guide on air conditioning and in section 9.4 of Part 2).

**FIGURE 21.2.1**

Summer air conditioning cycle

21.2.1 Summer air conditioning

The facility that we are going to study corresponds to the cooling of a large building like an airport located in a hot and humid climate. As this example has been treated in detail in section 9.4 of Part 2, we simply will summarize here the main results.

The problem data are as follows: we seek to maintain the internal ambience of the building at a temperature of 24°C (297.15 K) and a relative humidity equal to 50%. External climatic conditions are: temperature equal to 30°C (303.15 K), and relative humidity of 80%. It is necessary to remove external and internal thermal loads of 162.6 kW , as well as a quantity of water equal to 60 kg/h , i.e. 0.01667 kg/s .

Knowing that, for sanitary and comfort reasons, the supply temperature must not be less than 14°C (287.15 K), and that the recycled air proportion must not exceed 70%, the purpose of the exercise is to determine:

- supply conditions;
- a way of processing of the outdoor air/recycled air mix.

A possible treatment of the mixed air is to cool it, condensing water in excess to obtain specific humidity corresponding to the supply conditions, then warm it to supply temperature. There are others, but we will present this one here.

The first step is to determine the supply conditions, by solving equation (7.8.13) of Part 2, which Thermoptim can do. The calculation leads to the following: a flow rate of 12 kg/s , specific humidity $w = 0.0079$, and temperature $t = 14^{\circ}\text{C}$.

The second step calculates the state of the mixed air (section 7.8.2 of Part 2). This yields specific humidity $w = 0.013$, and temperature $t = 25.8^{\circ}\text{C}$ (point 1).

The air conditioning unit chosen requires cooling mixed air in the dehumidifier to $w = 0.0079$, then reheat it at $t = 14^{\circ}\text{C}$.

The cooling coil chosen has a surface temperature of 7°C . A perfect theoretical cooling in an infinite surface coil would lead to cool the wet mixture at the temperature of the coil in the saturated state (we have added a fictitious point 0 to represent it). As indicated in section 7.8.4.1 a real process is characterized taking as reference the theoretical cooling to point 0 and introducing either the cooling coil effectiveness ϵ (here 75%) or its bypass factor b such as $b = 1 - \epsilon$ (here 25%). Its calculation (section 7.8.4 of Part 2) shows that the mixture is then cooled at 11.7°C (point 2).

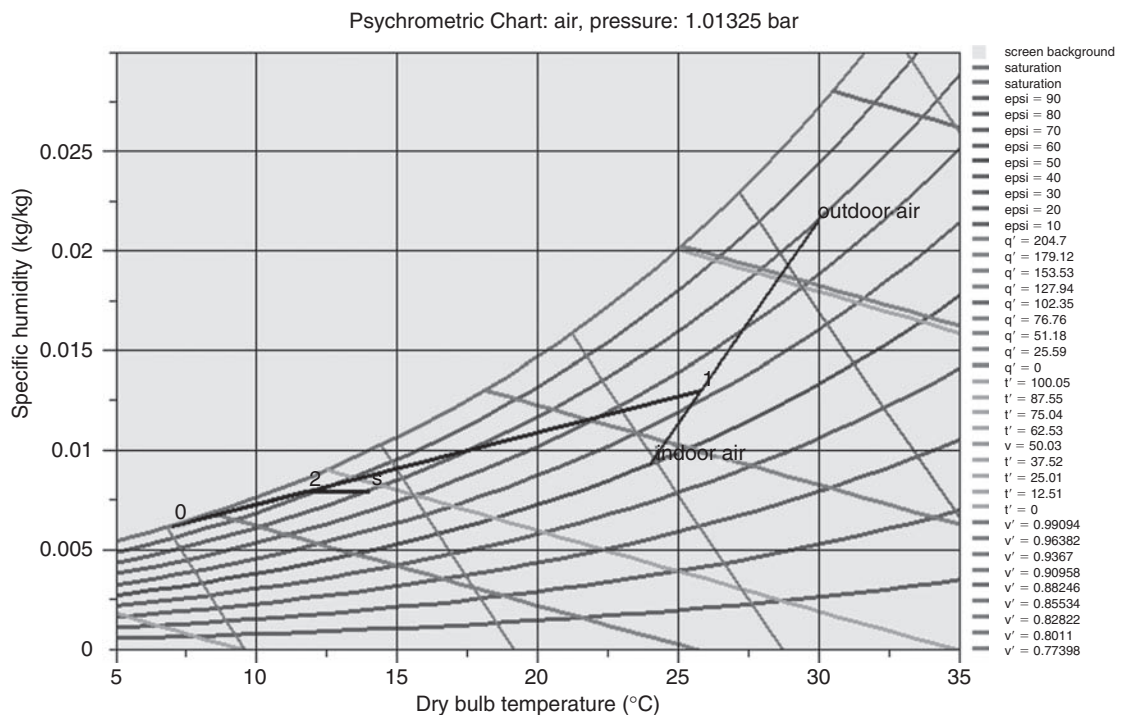
The heater allows it to be brought to the desired supply temperature (point S). Table 21.2.1 gives the properties of the various points of interest.

The plot of the cycle on the psychrometric charts is given in Figures 21.2.2 and 21.2.3.

TABLE 21.2.1

SUMMER AIR CONDITIONING POINT PROPERTIES

Point name	Dry bulb temp. (°C)	Specific humidity (kg/kg)	Relative humid. (RH)	Spec. enth. (kJ/kg)	Wet bulb temp. (°C)	Spec. volume (m ³ /kg)
Outdoor air	30	0.02155	0.8	85.1836	27.09	0.8887
Indoor air	24	0.00929	0.5	47.7032	17.06	0.8546
Mixed air (1)	25.8	0.01300	0.6248	58.998	20.55	0.8648
0	7	0.00621	1	22.623	7	0.8017
Cooled air (2)	11.7	0.00790	0.923	31.6851	11.04	0.8175
Supply (S)	14.0	0.00790	0.7956	33.9941	12.0	0.824

**FIGURE 21.2.2**

Summer air conditioning in the Carrier psychrometric chart

21.2.2 Winter air conditioning

The facility that we will study corresponds to the heating of a large building like a bank, located in a cool, moist climate. For this, we have a ventilation system that allows air to blow in different parts of the building. For reasons of hygiene it is necessary to renew the air, but some can be recycled, however, which reduces heating needs.

So we recycle some of the indoor air that is mixed with outside air, previously preheated to prevent condensation on the ducts or jamming of registers. This mixture must be treated before being injected into the ventilation system so that its state corresponds to the supply conditions. These are calculated so that the external thermal loads are compensated by taking into account internal inputs. It is assumed that the water load is zero and air temperature is 27°C.

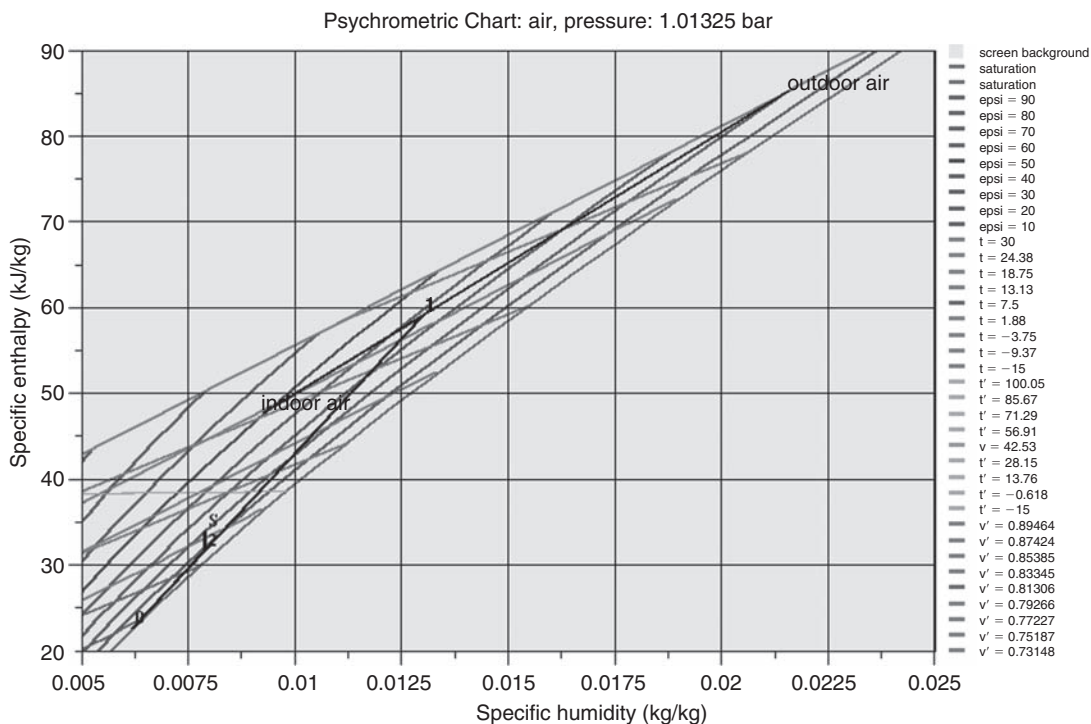


FIGURE 21.2.3

Summer air conditioning in the Mollier psychrometric chart

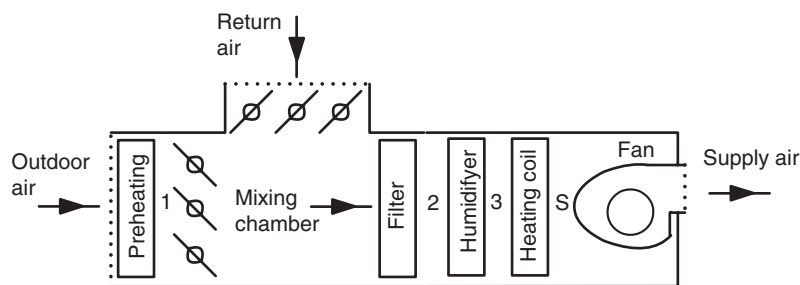


FIGURE 21.2.4

Winter air conditioning cycle

A possible treatment of the mixed air is to humidify it adiabatically until its specific humidity corresponds to the desired supply conditions and then to warm it up at the desired air temperature (Figure 21.2.4). There are others, but this will be presented here.

The problem data are as follows: we seek to maintain the atmosphere inside the building at a temperature of 20°C and a relative humidity of 30%. External climatic conditions are: temperature equal to -10°C and relative humidity of 90%. We must provide a heat input of 100 kW off ventilation, but no water. To avoid parasite condensation, fresh air is preheated at 14°C (point 1).

Knowing that, for reasons of hygiene and comfort, the proportion of return air should not exceed 70%, the purpose of the exercise is to determine:

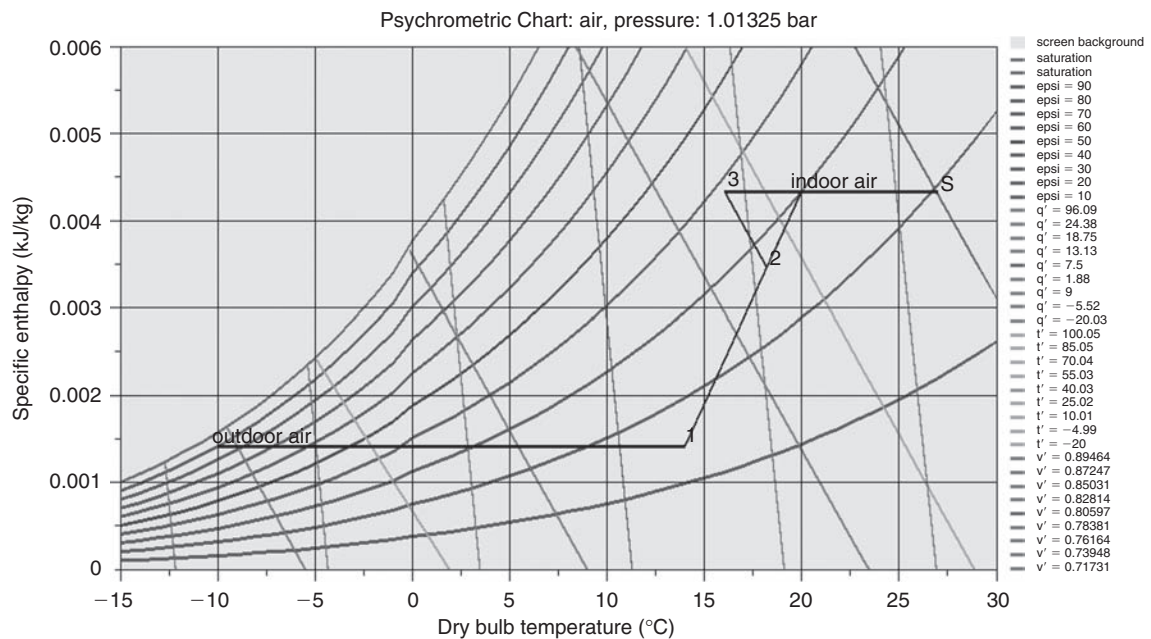
- supply conditions;
- a way of processing of the outdoor air/recycled air mix.

We have neglected here the blowing fan air warming (about 1°C).

TABLE 21.2.2

WINTER AIR CONDITIONING POINT PROPERTIES

Point name	Dry bulb temp. (°C)	Specific humidity (kg/kg)	Relative humid. (RH)	Spec. enth. (kJ/kg)	Wet bulb temp. (°C)	Spec. volume (m ³ /kg)
Outdoor air	-10	0.001415	0.9	-6.50	-10.32	0.7473
Preheat air (1)	14	0.001415	0.144	17.6	4.509	0.8155
Indoor air	20	0.004334	0.3	31.04	10.84	0.8364
Mixed air (2)	18.2	0.003461	0.268	27.0	9.034	0.830
Humid. air (3)	16.0	0.004334	0.385	27.0	9.08	0.8250
Supply (S)	27	0.004334	0.197	38.1	13.71	0.8564

**FIGURE 21.2.5**

Winter air conditioning in the Carrier psychrometric chart

The first two steps are similar to those of the previous example. The calculation of supply conditions leads to the following: a flow-rate of 14.1 kg/s, specific humidity $w = 0.0433$, and temperature $t = 27^\circ\text{C}$.

The specific humidity of outside air is $w = 0.0014$. It is preheated at 14°C (point 1). For indoor recycled air $w = 0.0043$. Given the rate of recirculation, humidity is here $w = 0.0346$, and temperature 18.2°C (point 2).

It is therefore necessary to moisten the mixture at the supply humidity, for example in an adiabatic humidifier. Its effectiveness is calculated: 23.7%, the temperature of the moist mixture being 16.2°C (point 3). Recall that an adiabatic humidification is achieved by spraying water to form a rain sprinkling the air, the heat needed to vaporize the water being supplied by air. As is done to cool a moist mixture, the reference is a theoretical humidifying leading the air to saturation, the real wetting being characterized by its effectiveness ϵ .

A heat addition for heating the mixture at 27°C is necessary (see section 7.8.3 of Part 2) (point S). Table 21.2.2 gives the properties of the various points of interest.

The plot of the cycle on the psychrometric charts is given in Figures 21.2.5 and 21.2.6.

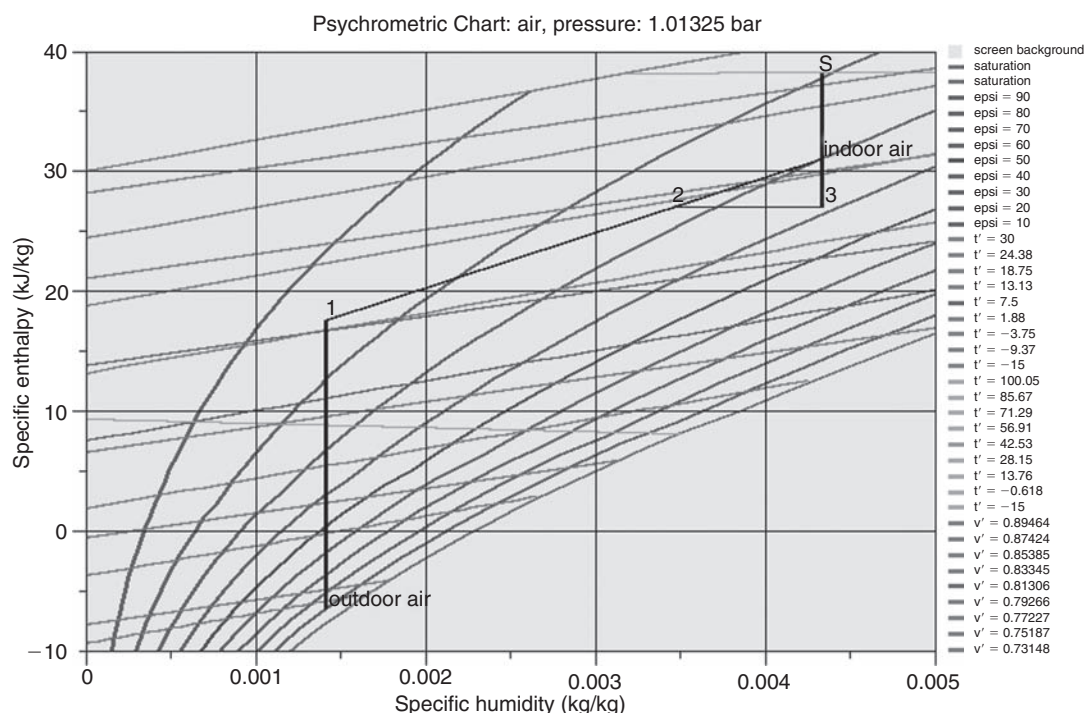


FIGURE 21.2.6

Winter air conditioning in the Mollier psychrometric chart

REFERENCES

- Mitchell J. W. & Braun J. E., *Principles of HVAC in Buildings*, John Wiley and Sons, Inc, January 2012.
- A. Bensafi, *Air humide: Traitement et conditionnement de l'air*, Techniques de l'Ingénieur, Traité Génie énergétique, BE 8 026.
- M. Duminil, *Air Humide*, Techniques de l'Ingénieur, Traité Mécanique et chaleur, B 2 220.
- AICVF, *Conception des installations de climatisation, et de conditionnement de l'air*, Collection des guides de l'AICVF, PYC Edition, Paris, octobre 1999.
- R. Casari, *Cahier Technique, données théoriques et technologiques, conduite de projets, mallette pédagogique Conditionnement d'air*, septembre 1992, Paris, Documentation interne, École des Mines de Paris.
- T. Agami Reddy, *Psychrometrics and comfort, Handbook of Heating, Ventilation, and Air Conditioning*, (Edited by J.F. Kreider), CRC Press, Boca Raton, 2001, ISBN 0-8493-9584-4
- A. Rabl, P. Curtiss, *Energy calculations – Building loads, Handbook of Heating, Ventilation, and Air Conditioning*, (Edited by J.F. Kreider), CRC Press, Boca Raton, 2001, ISBN 0-8493-9584-4.

FURTHER READING

- M. Raoult, Coord., *La vapeur d'eau, mode d'emploi*, PYC Edition, Paris, Janvier 2000.
- S. K. Wang, Z. Lavan, P. Norton, *Air Conditioning and Refrigeration Engineering*, CRC Press, Boca Raton, 2000, ISBN 0-8493-0057-6.

Optimization by Systems Integration

Abstract: The global optimization of thermal systems has been the subject of a number of studies in recent years. We refer the reader to the publications of Grossmann and Sargent (1978) and Floudas and Grossmann (1986) cited in the bibliography. These studies typically rely on applied mathematics sophisticated methods, which are cumbersome and hermetic for physicists or engineers, leaving little room for intuition or physical sense. As a result, they do not allow them to take full advantage of their experience, and prove ultimately to be medium quality design tools.

It therefore seems appropriate to set up hybrid methods, allowing at best exploitation of the physical properties of the systems considered. In this spirit, systems integration is a particularly powerful and interesting tool that we develop in this chapter, after presenting pinch method fundamentals, its applications to heat exchanger network design and the pinch minimization algorithm. We then show how systems integration is implemented in Thermoptim, and conclude by giving a concrete example (optimization of a dual pressure combined cycle). It should be noted now that the demo, education and standard versions of Thermoptim do not provide access to these tools.

Keywords: systems integration, optimization, pinch method, heat exchanger network, composite curve, carnot factor difference curve.

Traditional approaches in thermodynamic systems optimization, valid for maximizing one by one the various components of a facility, remain insufficient to guide the designer in choosing the best configuration of the entire system.

As shown by the heat recovery steam generators (HRSG) used in the combined cycle example (sections 15.6.2 and 17.3), specific irreversibilities appear in addition to those of each element, since the various components are assembled together. These irreversibilities can be described as systemic because they depend mainly on relative positioning of components. Reducing these irreversibilities allows an increase in the effectiveness of the systems considered, including through better internal regeneration.

Thermal integration, or pinch method is a relatively recent method (dating back to the eighties) for designing the most efficient heat exchanger and utility networks in an energy facility or a process plant.

It is based on thermodynamic laws and the study of heat exchanged between streams to be cooled (availabilities) and warmed (needs). It allows minimization of the exchanger network internal irreversibilities, and thus improvement in its performance.

The main interests of this method are:

- It is a visual and graphic method, which allows the engineer to keep a physical approach of the phenomena, while very often optimization methods are purely numerical;
- But most importantly, optimization is performed without any *a priori* assumptions about the heat exchanger network configuration, which is defined only at a later time;
- It has become widespread over the past twenty years because it proved it could reduce **both capital costs and operating expenses**, which is generally not the case.

22.1 BASIC PRINCIPLES

Consider a system in which matter is transformed by various processes, some exothermic, other endothermic. Each of these processes receives or provides heat. If you want to optimize the overall energy expenditure, to reduce external inputs, you must make the best of all heat internally available. Thermal or heat integration provides a rigorous method for this, to optimize the overall configuration of the facility, and ensure greater consistency between needs and energy availability.

For simplicity, we first present the basic principles of heat integration without using exergy analysis, then we shall generalize our approach.

22.1.1 Pinch point

The basic principle of heat integration is to classify all heat needs depending on temperature levels to which they relate, in order to find the best match of hot and cold streams. For this we use for example the graph already introduced in section 8.2.6 of Part 2, where temperature is in ordinate and enthalpies involved in abscissa (enthalpy diagram of Figure 22.1.1). Note that for purely thermal exchanges, enthalpies are equal to heat exchanged. In this diagram, an assembly economizer-vaporizer without superheating appears as in Figure 22.1.1. The fluid which evaporates corresponds to the lower curve (1-2-3), which presents an angular point 2 corresponding to the beginning of the boiling. The hot fluid is cooled from 4 to 5, by decreasing its sensible heat.

On segments (1-2) and (4-5) we have $\Delta H = \dot{m}c_p \Delta T$, and thus $\Delta T = 1/\dot{m}c_p \Delta H$.

The slopes of segments (1-2) and (4-5) are equal to the inverse of the heat capacity rates of the corresponding fluids. On segment (2-3) we have obviously $\Delta T = 0$, the vaporization taking place at constant temperature for a pure component or azeotrope.

We see at point 2 a minimum temperature difference P between both fluids, called pinch. This point plays a fundamental role in the design of heat exchanger networks, as it represents the smallest difference in temperature in the facility.

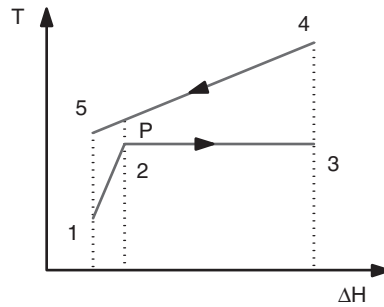
To reduce the cost of equipment, it is preferable that the pinch is not too low. However, the thermodynamic optimization of the complete system often requires it to be as small as possible. In general, the pinch point is the most constraint zone in the thermal system.

On this graph it is clear that below the pinch, the slope of the segment representing the cold fluid is greater than that corresponding to the hot fluid:

$$\frac{1}{\dot{m}c_{pc}} > \frac{1}{\dot{m}c_{ph}} \quad \dot{m}c_{ph} > \dot{m}c_{pc}$$

Above the pinch, the reverse is true: $\dot{m}c_{ph} < \dot{m}c_{pc}$

The heat exchanger, sized according to the pinch, works outside this point with larger temperature differences between the two fluids, which indicates an increase in irreversibility, without any

**FIGURE 22.1.1**

Pinch point

compensation, which is therefore not desirable. However, given the peculiarity of the exchanger considered here (it is an evaporator which therefore has a vaporization plateau), it is not possible to reduce these irreversibilities except by using a condensable vapor as hot fluid (note (see section 25.2 of Part 4) that it is precisely what brings mechanical vapor compression when possible).

As discussed below, the pinch point is a break in the thermal system and leads to an independent study of each zone. In most cases, facilities are designed so that such points are located between the various elements.

For a more complex system, heat integration leads one to rank needs and energy availability as a function of temperature, then plot them on a (T, h) diagram.

22.1.2 Integration of complex heat system

We begin by illustrating thermal integration on a relatively simple case, from an article by Gourlia (1989), to which the reader may refer for details.

Consider a plant with the following energy availability, for example related to exothermic processes:

Stream 1	220 – 40°C	1,800 kW
Stream 2	320 – 200°C	2,400 kW
Stream 3	140 – 40°C	800 kW
Stream 4	100°C	1,200 kW
Boiler	600°C	1,900 kW

and where the needs are:

Stream 5	40 – 320°C	6,000 kW
Stream 6	220°C	600 kW

In this factory, enthalpies available in streams 1 to 4 correspond to releases, and so are somehow “free” calories whose value we seek to maximize, while the 1,900 kW provided by the boiler at 600°C is of another kind: it is purchased energy, provided by a “hot utility”, that we generally seek to minimize. The value of 1,900 kW was determined in a conventional manner by an engineering and design department.

Thermal integration will allow, as we shall see below, first to determine the minimum amount of heat required by utilities and their temperature levels, and secondly to define a suitable exchanger network for the plant to operate. Before explaining the methods that lead to these results, we first generalize the presentation that was made of the enthalpy diagrams.

22.1.2.1 Plot of the composite curve

The temperature level at which heat may be exchanged being a major constraint in the design of a heat exchanger network, we begin by sorting heat brought into play depending on this parameter.

For this, we usually assume a linear variation of enthalpy which can be transferred by sensible heat (assumption of constant heat capacities of streams that come into play). We perform a combination of availability and needs for the different temperature intervals of the system, whose bounds are determined by the original specifications, as summarized previously.

In order of increasing temperatures, this combination is as follows, needs and availability being assumed to be at first approximation linear functions of temperature between the different bounds:

Availability:

< 40°C	0	
< 100°C	$1800(100 - 40)/(220 - 40) + 800(100 - 40)/(140 - 40) = 1,080 \text{ kW}$	streams 1 and 3
$\leq 100^\circ\text{C}$	$1080 + 1200 = 2,280 \text{ kW}$	streams 1, 3 and 4
< 140°C	$2280 + 1800(140 - 100)/(220 - 40) + 800(140 - 100)/(140 - 40) = 3,000 \text{ kW}$	streams 1 and 3
< 200°C	$3000 + 1800(200 - 140)/(220 - 40) = 3,600 \text{ kW}$	stream 1
< 220°C	$3600 + 2400(220 - 200)/(320 - 200) + 1800(220 - 200)/(220 - 40) = 4,200 \text{ kW}$	streams 1 and 2
< 320°C	6,200 kW	stream 2
$\leq 600^\circ\text{C}$	8,100 kW	boiler

Needs:

< 40°C	0	
< 220°C	$6000(220 - 40)/(320 - 40) = 3,857 \text{ kW}$	stream 5
$\leq 220^\circ\text{C}$	$3857 + 600 = 4,457 \text{ kW}$	streams 5 and 6
< 320°C	6,600 kW	stream 5

We can plot these energies in a (T, h) diagram seeking to maximize the value of enthalpies according to their respective temperature levels. We overlap the needs and availability curves shifting them so that the first one is below the second.

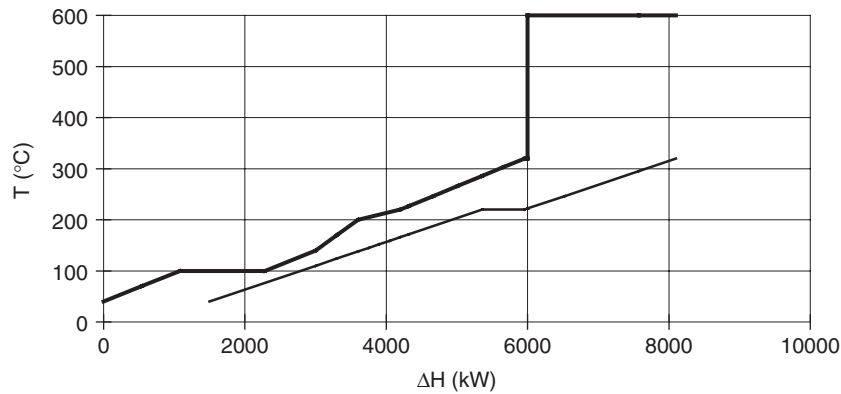
This gives the diagram in Figure 22.1.2, the so-called composite curve (CC). The bold line represents the cumulative availability depending on the temperature, the fine line, that of requirements. In the example shown, the temperature levels of availability are sufficient to ensure the provision of needs, and there remains a surplus of 1,500 kW between 40 and 100°C, which must be removed by cold utilities, for example by a cooling tower exchanging with ambient air.

The diagram shows the existence of a pinch at 100°C, 2,280 kW, which corresponds to about 24 K difference between the two curves. It also allows the temperature differences in each area to be known, and therefore the exact size of heat exchangers. It is unnecessary to size them too tight if they operate with large temperature differences. Note that nothing prevents that there are several pinches, the extreme case being that of a counter-flow heat exchanger between two fluids of the same heat capacity rate, in which case the temperature difference between them remains constant, which corresponds an infinite number of pinches.

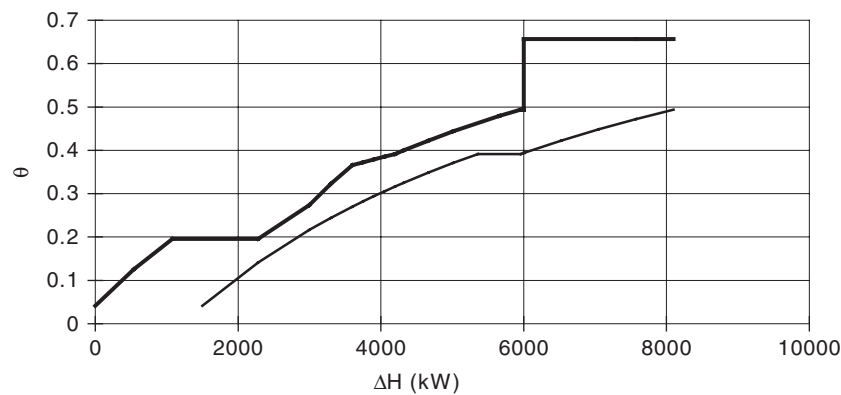
In the example shown, curves do not intersect on the chart. In other cases, they can do, which means we must provide more energy. Heat integration allows the best location for it to then be chosen.

22.1.2.2 Exergy representation of the composite curve

So far, we reasoned, for simplicity, in a (T, h) diagram, whose physical meaning is quite telling. A more general reasoning way, though less directly accessible, is to use as ordinate, not temperature, but the Carnot factor $\theta = 1 - T_0/T$.

**FIGURE 22.1.2**

Composite Curves

**FIGURE 22.1.3**

Exergy Composite Curve

Such a representation has a double interest:

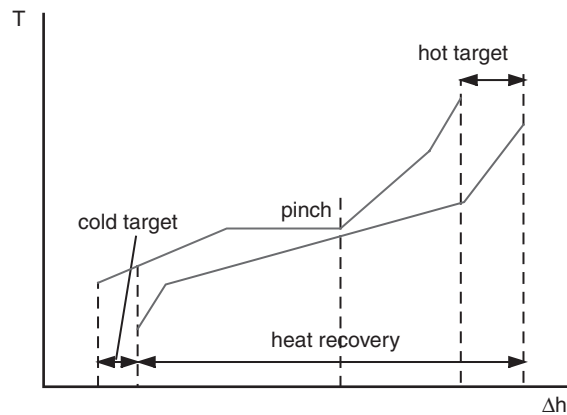
- first, the area between the two curves corresponds, for purely thermal systems¹, to the exergy destroyed, that is to say to irreversibilities;
- second it is well suited for comparison between thermal and noble energies (mechanical or chemical).

The diagram in Figure 22.1.3 relates to the thermal system studied. We see here that the irreversibilities are almost evenly distributed between 2,500 and 5,500 kW, but they are more important at low and high temperatures.

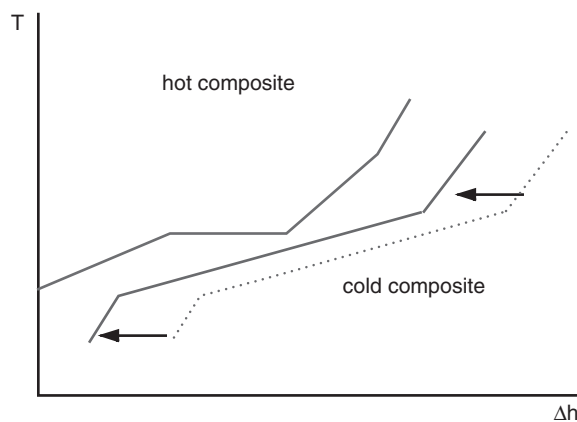
Although thermodynamically more instructive, the exergy approach is seldom used consistently in thermal integration studies. Two main reasons can explain this phenomenon:

- first, exergy reasoning is less generalized in engineering departments than energy reasoning, its implementation being a bit trickier, with greater risks of error for the uninitiated;
- secondly, we have already noted that thermal integration methods allow the user to reason physically, that is to say essentially qualitatively, as we shall see later. An energy approach of the type that we will now expose reveals itself usually sufficient.

¹These are systems receiving no work from external forces, where streams exchanging sensible heat are assumed incompressible, whether gas or liquid, and where the flows are without pressure drop. In this case, $ds = c_p dT/T$, and $dx_{hi} = c_p T_0 (1/T - 1/(T + \Delta T))dT$, which corresponds to the area between the Carnot factors of both streams exchanging heat with a temperature difference ΔT .

**FIGURE 22.2.1**

Endothermic and exothermic zones

**FIGURE 22.2.2**

Shifting composite curves

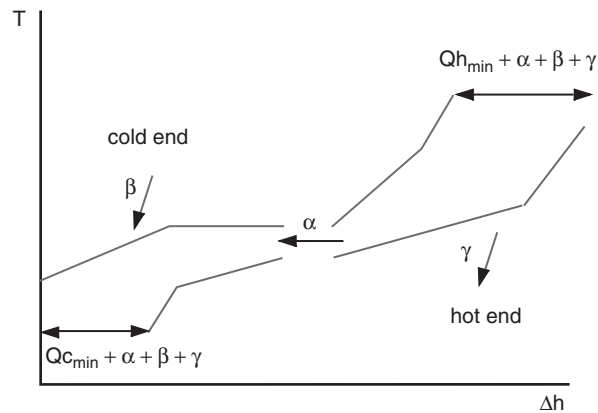
22.2 DESIGN OF EXCHANGER NETWORKS

This brief overview has shown the usefulness of thermal integration to view irreversibilities in a complex system. It allowed us to highlight temperature differences within heat exchangers, but not to define the overall architecture of the network. That is what we shall see in this section. We content ourselves, for reasons that have just been explained, with a classical enthalpy approach.

On the composite curve (Figure 22.2.1), the pinch distinguishes two zones:

- the lower zone, where “cold” streams (needs) are unable to absorb all the available heat in “hot” streams (availability), a surplus having to be discharged through a complementary coolant. This area, excess heat, generally behaves as a heat source, and is called exothermic zone or cold-end;
- the upper zone, where the situation is dual to the previous one: the need for heat of “cold” streams is above the enthalpy available in “hot” streams, and additional heating is necessary. This area, lacking heat, behaves as a heat sink area and is called endothermic or hot-end.

As shown in Figure 22.2.2, dragging the cold composite from right to left, we vary the gap with the hot composite, gap representative of thermal irreversibilities. When the pinch value is zero, no heat transfer exists between these two zones: the pinch separates the system in two thermally independent parts. This is obviously a borderline case. It corresponds to the case where the heat absorbed by the endothermic zone and the one rejected by the exothermic zone are minimal.

**FIGURE 22.2.3**

Plus-Minus principle

When the pinch value is not zero (Figure 22.2.3), heat absorbed at high temperature and released at low temperature are both increased by the same amount α , which corresponds to heat passing through the pinch between both zones (it is called cross-pinch heat transfer). Similarly, heat provided in the exothermic zone (β), or a cooling in the endothermic zone (γ) increases the need for hot and cold utilities. So we see an additional advantage of thermal integration: highlighting the pinch point, it reduces α to minimum economic size and therefore allows design of the best heat exchanger networks in upper and lower areas. Indeed, an exchanger design error in one of the areas, resulting in an increase of the enthalpy exchanged, leads inevitably to an oversizing of the other zone.

The method presented in section 22.3.4 allows for determining an exchange configuration of the network minimizing heat gain by utilities in the hot endothermic zone, and extraction of heat from cold utilities in the exothermic area. This configuration, optimal at least according to this criterion, may often reflect a greater number of heat exchangers than other arrangements. It may therefore be necessary to consider other alternatives, which is done by relaxing the criteria above.

22.3 MINIMIZING THE PINCH

As searching the pinch by dragging one from the other composite curves is neither very easy nor very precise, Professor B. Linnhoff proposed a method whose main lines we give here. It is to work directly on the enthalpy balances by temperature levels, while when building the CC, we dissociated the curve of the availability from that of needs.

The pinch minimization algorithm is used to determine the minimum energy consumption corresponding to the minimum pinch, called the **hot target**. The original Linnhoff algorithm, of which it is derived, is known as the Problem Table Algorithm PTA.

The algorithm can be decomposed into four steps:

- shift all minimum and maximum temperatures by $\Delta T_{pinch}/2$, subtracting it for hot streams, and adding it for cold streams (by doing this, it is certain that heat exchange between streams at the same shifted temperature can take place);
- determining the problem temperature intervals by sorting the upper and lower temperature limits;
- building enthalpy balances (by temperature interval) of hot and cold composites and their difference;
- building the overall summary table and determination of the minimum hot utility value (the hot target).

TABLE 22.3.1

Stream	$\dot{m} c_p$ (kW/K)	T_s (°C)	T_t (°C)	ΔH (kW)
1	10	40	220	1800
2	20	200	320	2400
3	8	40	140	800
4	1200	100	101	1200
5	21	40	320	6000
6	600	220	221	600

TABLE 22.3.2

DATA WITH SHIFTED TEMPERATURES

Stream	$\dot{m} c_p$ (kW/K)	type	T_{inf} (°C)	T_{sup} (°C)	ΔH (kW)
1	10	hot	35	215	1800
2	20	hot	195	315	2400
3	8	hot	35	135	800
4	1200	hot	95	96	1200
5	21	cold	45	325	6000
6	600	cold	225	226	600

22.3.1 Implementation of the algorithm

22.3.1.1 Shifting temperatures

To be certain that the hot and cold streams may exchange heat when grouped in an appropriate temperature interval, we must make sure that a temperature difference ΔT_{pinch} always exists between them. To do so, simply we slightly modify their temperature levels:

- for hot streams, reducing them by $\Delta T_{pinch}/2$;
- for cold streams, increasing them by $\Delta T_{pinch}/2$.

The value of ΔT_{pinch} is arbitrary: it depends on the problem considered. We generally retain about 16 to 20 K for an exchange between gas and 8–10 K for liquids. For two-phase exchange, these values may be reduced.

It is also possible, when studying a complex system, to retain minimum pinch values differing according to the streams considered. It is in that the algorithm chosen in ThermoOptim differs from Linnhoff's. However, in the example that follows, we will consider for simplicity a single value.

For example, let us come back to the problem studied above, but without showing the enthalpy supplied by hot utilities (boiler at 600°C) or extracted by cold utilities (cooling tower).

By setting an artificial $\Delta T = 1$ K for evaporation-condensation, to avoid having segments of zero slope, the specifications can be summarized in Table 22.3.1.

Taking into account ΔT_{pinch} (10 K here), we obtain Table 22.3.2 giving shifted temperature intervals. Obviously, the enthalpies that are involved are not affected by this shift.

22.3.1.2 Search of temperature intervals

The second step determines the problem temperature intervals by sorting the bounds of the stream upper and lower temperatures.

TABLE 22.3.3
CLASSIFICATION BY TEMPERATURE INTERVAL

Interval	T_i (°C)	T_{i+1} (°C)	Streams	$T_i - T_{i+1}$ (K)	$\Sigma(\dot{m} c_p)$ (kW/K)	ΔH_{bd} (kW)
1	325	315	*5*	10	21.43	214
2	315	226	*5,2*	89	1.43	121
3	226	225	*5,2,6*	1	601.43	601
4	225	215	*5,2*	10	1.43	14
5	215	195	*5,2,1*	20	-8.57	-171
6	195	135	*5,1*	60	11.43	686
7	135	96	*5,1,3*	39	3.43	134
8	96	95	*5,1,3,4*	1	-1196.60	-1197
9	95	45	*5,1,3*	50	3.43	171
10	45	35	*1,3*	10	-18.00	-180

We sort all bound temperatures T_{inf} and T_{sup} in order of decreasing values, which in this case leads to the ten temperature intervals of Table 22.3.3.

22.3.1.3 Establishment of enthalpy balances

We then build up the enthalpy balances (by temperature interval) of hot and cold composites and their difference.

For each temperature interval, we identify the streams flowing through it (fourth column of Table 22.3.3). The streams being so classified, we can group them by type, and calculate enthalpy balances of each interval, using formulas (22.3.1 to 22.3.3), index b referring to needs, d to availability of, and bd being the difference between them:

$$\Delta H_b = (T_i - T_{i+1}) \Sigma \dot{m} c_{pb} \quad (22.3.1)$$

$$\Delta H_d = (T_i - T_{i+1}) \Sigma \dot{m} c_{pd} \quad (22.3.2)$$

$$\Delta H_{bd} = \Delta H_b - \Delta H_d = (T_i - T_{i+1}) (\Sigma \dot{m} c_{pb} - \Sigma \dot{m} c_{pd}) \quad (22.3.3)$$

ΔH_b and ΔH_d represent the enthalpy changes of needs and availability in interval i. They thus correspond to hot and cold composite segments.

ΔH_{bd} is positive if the heat requirements exceed the availability, and negative otherwise. It represents the net enthalpy balance of the interval, and is used on the one hand to determine the minimum pinch, and secondly to draw the Grand Composite Curve GCC (Figure 22.3.1). This gives Table 22.3.4.

22.3.1.4 Determination of the minimum target

Finally, we establish the overall summary Table 22.3.3, which determines the minimum target.

Note that enthalpies available in an interval (negative by construction) are at a sufficient temperature to be used in all intervals of higher order: if for example, in interval i, we have a surplus of energy, it can be used to heat a stream in interval i + 1.

It is thus possible to identify a cascade of temperatures and corresponding enthalpy balances, obtained by subtracting the values of ΔH_{bd} calculated (Table 22.3.4).

Table 22.3.4 shows that the maximum enthalpy deficit is equal to 1,605 kW, in the absence of the boiler. It takes place between intervals 7 and 8, at 95°C (the value of 96°C is artificial, because it comes from the 1 K temperature difference introduced to avoid a zero slope vaporization segment).

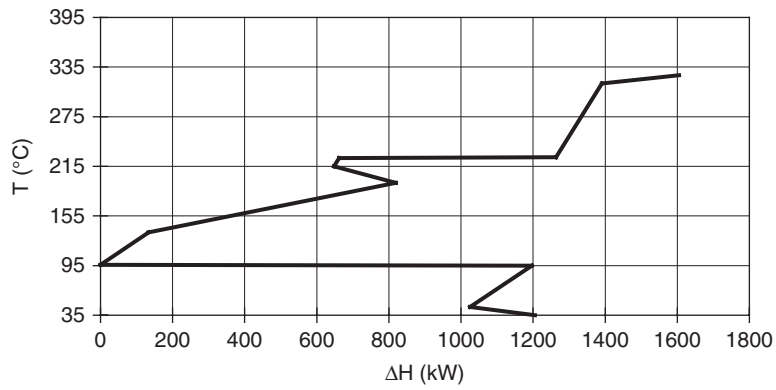


FIGURE 22.3.1
Shifted Grand Composite Curve

TABLE 22.3.4

Interval	T_i (°C)	T_{i+1} (°C)	ΔH_{bd} (kW)	sum (kW)
1	325	315	214	-214
2	315	226	127	-341
3	226	225	601	-943
4	225	215	14	-957
5	215	195	-171	-786
6	195	135	686	-1471
7	135	96	134	-1605
8	96	95	-1197	-409
9	95	45	171	-580
10	45	35	-180	-400

TABLE 22.3.5

Interval	T_i (°C)	T_{i+1} (°C)	ΔH_{net} (kW)	(kW) 1605
1	325	315	214	1391
2	315	226	127	1264
3	226	225	601	662
4	225	215	14	648
5	215	195	-171	819
6	195	135	686	134
7	135	96	134	0
8	96	95	-1197	1196
9	95	45	171	1025
10	45	35	-180	1205

The system pinch is located there. Given the value of ΔT_{pinch} chosen, this corresponds to 100°C for hot streams and 90°C for cold streams. The deficit must be offset by a $\Delta H_{min} = 1,605$ kW input. Its value is 295 kW lower than that retained by the engineering and design department (1,900 kW). If we provide the missing 1,605 kilowatts at high temperature, we obtain Table 22.3.5.

Endothermic and exothermic zones are evident, the first comprising intervals 1–7 and the second 8–12. At the pinch, the enthalpy flow that passes from one interval to another is zero by construction.

As can be seen, the great interest of the pinch minimization algorithm is to allow one to relatively simply determine the minimum value of the heat input to be provided to the system.

If we plot the curve on a graph whose abscissa is the fifth column of Table 22.3.5 and ordinate the third (with one additional point which has coordinates $(\Delta H_{\min}, T_1)$) we obtain the shifted temperature Grand Composite Curve, which gives, for each temperature, the cumulative net enthalpy balance (Figure 22.3.1).

22.3.2 Establishment of actual composite curves

Once the target known (here $\Delta H_{\min} = 1605 \text{ kW}$), we can return to the actual temperatures, and recalculate the actual needs and availability composite curves, reusing part of the pinch minimization algorithm:

- determining the problem actual temperature intervals by sorting the actual upper and lower temperature bounds. The procedure is the same as before, but we start from Table 22.3.1 instead of Table 22.3.2;
- building hot and cold composite enthalpy balances (by temperature interval). The procedure is also similar, but there is no need to calculate ΔH_{bd} , unless you want to draw the actual Grand Composite Curve. Then you obtain the values of ΔH_{b} and ΔH_{d} for each actual temperature interval;
- composite curve plot. The plot of the hot composite curve poses no problem: we know its origin, which corresponds to the lowest hot stream temperatures and a zero enthalpy. Interval by interval, by combining H_{d} values, it is constructed without difficulty.

Moreover, the maximum enthalpy of the cold composite curve is equal to the sum of the maximum enthalpy of the hot composite and the minimum target ΔH_{\min} . Its maximum temperature is the highest temperature of cold streams. Interval by interval, by deducting values of ΔH_{b} from this maximum, the cold composite is built. Its minimum corresponds to the enthalpy value to evacuate by external cooling (the cold target). The actual composite curves are shown in Figure 22.3.2.

22.3.3 Plot of the Carnot factor difference curve (CFDC)

The construction of exergy composite curves (Figure 22.3.3) is no problem, since it is a simple change of ordinate axis: $\theta = 1 - T_0/T$.

To plot the CFDC, things are somewhat more complex because you must reverse the two composites. Since they are composed of a series of segments, the procedure is as follows:

- search all the values of enthalpies of the two composite interval bounds;
- identify by linear interpolation for each enthalpy bound of the cold composite, the corresponding value of the temperature of the hot composite;
- identify by linear interpolation for each enthalpy bound of the hot composite, the corresponding value of the cold composite temperature.

This gives a table showing, for all values of the enthalpies corresponding to slope changes of one or the other composites, the temperature values of the hot or cold composites. The curve is inverted, and the CFDC deduced by simple difference and change of ordinate (Figure 22.3.4).

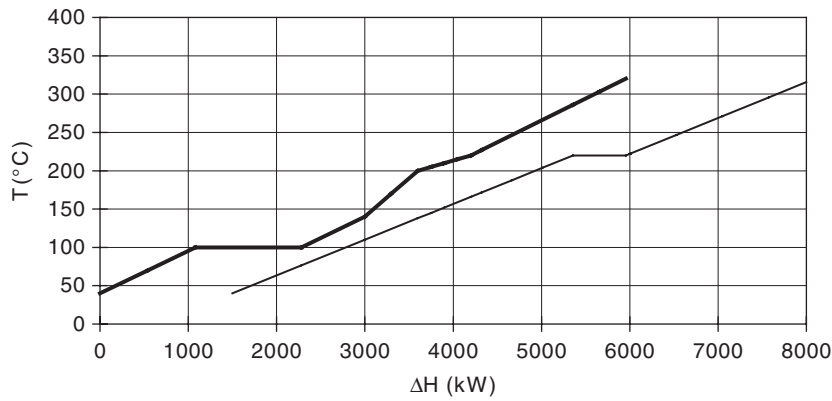


FIGURE 22.3.2
Actual Composite Curves

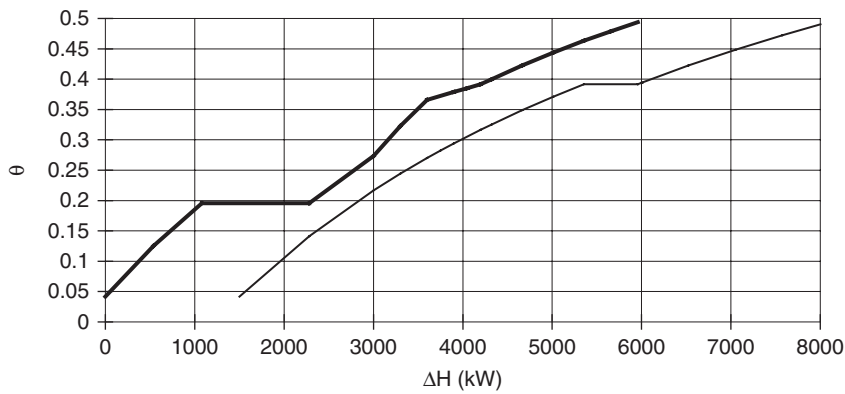


FIGURE 22.3.3
Exergy composite curves

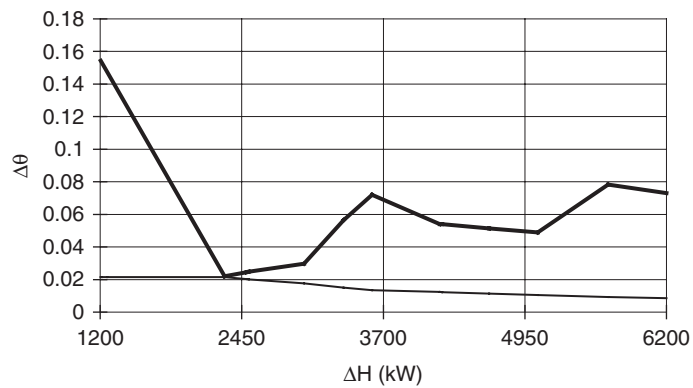
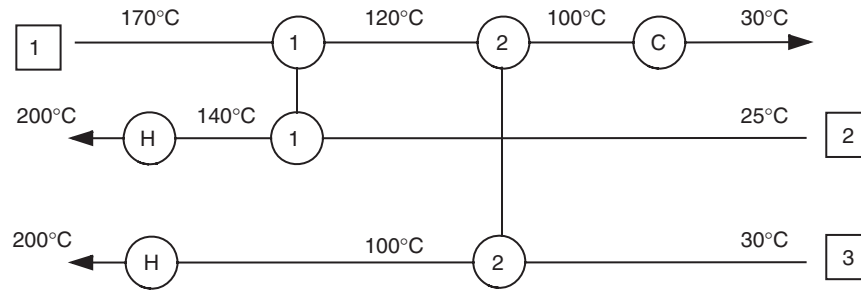


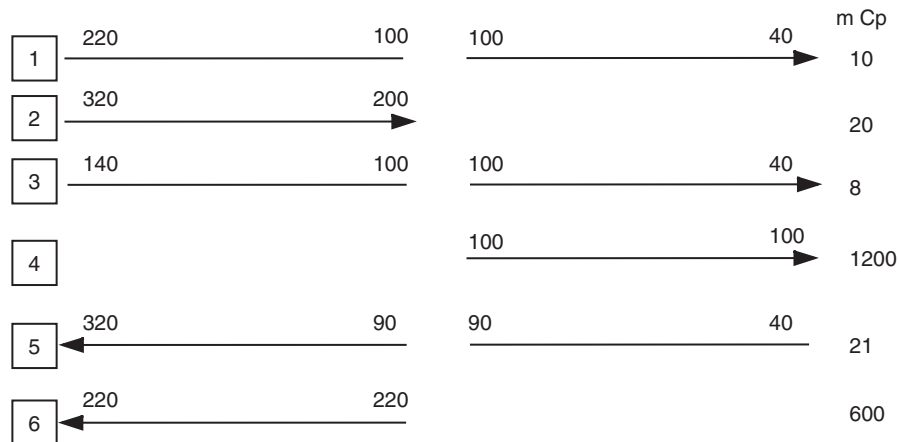
FIGURE 22.3.4
Carnot factor difference curve

Of course, if you do not know the temperature levels of the hot target and external cooling, you can only plot the CFDC on the part of the abscissa common to the two composites. Pinch being minimal, it is located on the Locus of Minimal Pinches LMP (see 22.4.1), here with $\Delta T_{\text{pinch}} = 10 \text{ K}$.

The power supplied by hot utilities equals 1,605 kW, when it was 1,900 kW in the original system, which represents a saving of 15.6%. In addition, energy discharge is reduced from 1,500 to

**FIGURE 22.3.5**

Grid Diagram

**FIGURE 22.3.6**

Initial grid diagram

1,205 kW, which represents a reduction of almost 20%. These savings are accompanied by a reduction in capital expenditure since the endothermic and exothermic zone exchange surfaces are also reduced accordingly. Thermal integration allows in cases like this, quite common in practice, achievement of both investment and operation savings, although frequently you can only obtain one at the expense of the other.

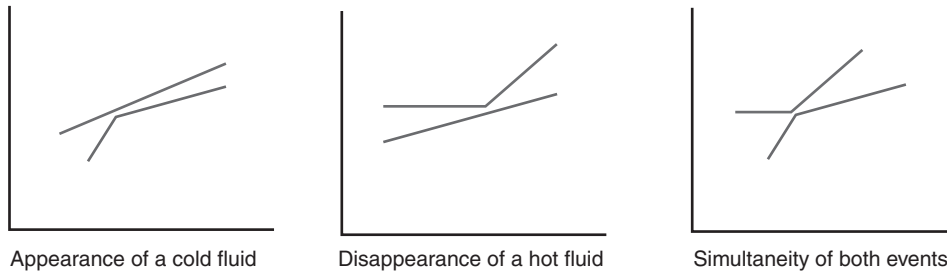
22.3.4 Matching exchange streams

22.3.4.1 General procedure

Heat integration is a valuable guide to design the overall architecture of the exchanger network by choosing the best pairs of streams exchanging heat. For this, we should first represent the system in a grid diagram of the type presented in Figure 22.3.5. Streams are represented by oriented horizontal segments, and heat exchangers by vertical links connecting the pairs of streams matched, identified by a number. Utilities are represented by a circle marked H if they are hot, and C if they are cold.

In this example, a hot stream is cooled from 170 to 120°C in a first heat exchanger, while stream 2 is heated from 25 to 140°C. Stream 1 is then cooled at 100°C in heat exchanger 2, while stream 3 is heated from 30 to 100°C. Finally, a cold utility cools stream 1 to 30°C while streams 2 and 3 are heated by two hot utilities at the final temperature of 200°C.

Let us now study the previous energy system. It involves six streams, as shown in Figure 22.3.6. Pinch is located in the central division, the actual stream temperatures (that is, not shifted by ΔT_{pinch})

**FIGURE 22.3.7**

Different types of pinches

being shown. Note that streams 2 and 6 are present only in the endothermic zone, and stream 4 in the exothermic area.

The problem now is to choose the best pairing of streams.

Note first that for a pinch to exist, if we accept the assumption of constant heat capacity rate, there must be, as shown in Figure 22.3.7:

- either appearance of a new cold stream (need);
- or disappearance of a hot stream (availability);
- or simultaneity of both events: onset of a cold stream and disappearance of a hot stream.

This is because, at the pinch, heat flow constraints are automatically satisfied:

- exothermic zone $\sum \dot{m} c_{ph} \geq \sum \dot{m} c_{pc}$;
- endothermic zone $\sum \dot{m} c_{ph} \leq \sum \dot{m} c_{pc}$.

The procedure is as follows:

- separately study endo- and exothermic zones;
- begin the design at the pinch and depart gradually from it, to deal first with the most constrained problem;
- import energy in the endothermic zone, export only from the exothermic zone;
- maximize the load of heat exchangers (to minimize their number).

In practical terms, the problem does not usually have a single solution, and a number of difficulties can arise. To find an acceptable solution, a number of constraints must first be met, as indicated below.

For the heat transfer to be done, it is obviously necessary that the heat capacity rate constraint is met in each heat exchanger, without infringing the second law of thermodynamics. If this rule is broken, it may be necessary to split some streams, as we shall see later.

Moreover, as we must not cool by utilities in the endothermic zone, this implies that at the interval level located just above the pinch, all hot streams must be cooled by cold streams, i.e. that the number of cold streams must be greater than or equal to that of hot streams. Again, if this rule is not respected, one or more cold streams must be split.

Dual manner, the number of hot streams in the interval located just below the pinch must be greater than or equal to that of cold streams.

In our case, at the pinch, streams selected are given in table 22.3.6 for the first interval of the endothermic zone. This corresponds to hot stream 4 disappearance.

22.3.4.2 Analysis of the endothermic zone

As shown in Table 22.3.6, the only cold stream in the first interval is 5, while there are two hot streams. We must then split this stream in two.

To find how, look at what happens in the interval above (No. 6). Streams selected are given in Table 22.3.7.

TABLE 22.3.6

Number	$\dot{m} c_p$ (kW/K)	ΔH (kW)
1	-10	-390
3	-8	-312
5	21.4	835.7

TABLE 22.3.7

Number	$\dot{m} c_p$ (kW/K)	ΔH (kW)
1	-10	-600
5	21.4	1285.7

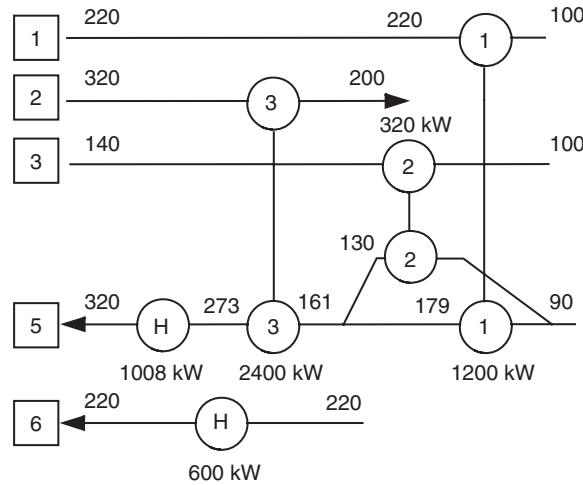


FIGURE 22.3.8

Endothermic zone grid diagram

Stream 3 disappears. Therefore the corresponding load must be supplied to stream 5, which gives: $\dot{m} c_{p52} = \dot{m} c_{p3} = 8$.

We deduce $\dot{m} c_{p51} = 13.4$, which, to exhaust stream 1 with a total of 1,200 kW, leads to an exit temperature of heat exchanger 1 equal to 179°C.

Streams 1 and 3 being exhausted, only 2 still contains availability (2,400 kW), which must be shared between the divided stream 5 and stream 6.

Several possibilities exist, one being to transfer the entire load in 6 (600 kW), and part of the residual load on the first branch of 5 (1,800 kW on 1,888 required). However, this scenario leads to a failure in terms of temperature.

It is better to remix both stream 5 branches at the outlet of heat exchangers 1 and 2:

The temperature of the mixture is given by:

$$179 \dot{m} c_{p51} + 130 \dot{m} c_{p52} = T \dot{m} c_{p5} \quad T = 160.9^\circ\text{C}$$

A single exchanger then allows to exhaust stream 2. Its balance is given by:

$$2400 = (T - 160.9) \dot{m} c_{p5}$$

We find a stream 5 outlet temperature equal to 273°C.

The grid diagram is given in Figure 22.3.8.

Note that the heat input to be provided by utilities is equal to 1,608 kW, i.e. slightly more than 1,605 kW demonstrated previously. This is because the 10 K pinch was located around 95°C, not 96°C, as the study of the energy cascade had indicated.

As shown by the analysis of the GCC, other possibilities exist if one wants utilities to be used at least in part at lower temperature. Indeed, in our mode of reasoning, we start from the pinch and we depart gradually, allowing utilities to match the load in the zone bounds.

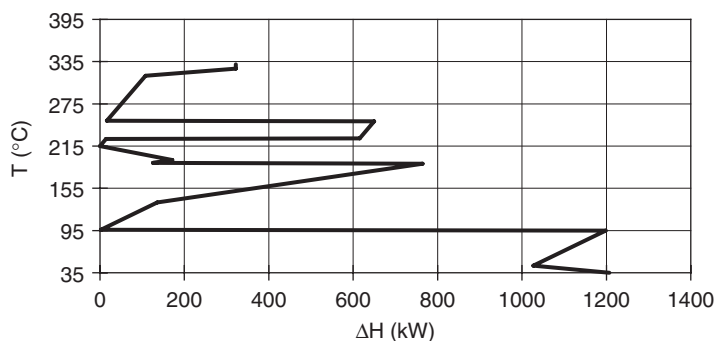


FIGURE 22.3.9

GCC with utility pinches

If we wish to incorporate them minimizing their irreversibility, we must consider them as additional streams to be integrated into the heat cascade, which complicates things a bit and usually results, as we shall see, in an increased number of heat exchangers, and therefore in a higher total installation cost.

The new GCC which is obtained in that case is given in Figure 22.3.9.

It shows three new pinches, at 250, 225 and 215°C, which are different from the first: they are utility pinches, introduced arbitrarily to optimize their thermal levels. As the latter two are very close, they can be initially aggregated.

The heat exchanger network design can be made using the procedure given above, starting from each successive pinch. To avoid problems, you should first deal with the most constrained pinch, if any. In this case, the problem being relatively simple, just treat them by decreasing temperature level.

Above the 250°C pinch, the constraint on the maximum heat is met with streams 2 and 5. We can further maximize the load on 2, which allows exchange of 1,300 kW in exchanger 1 and to heat 5 from 245 to 305°C. Heat exchanger 2 can then provide from H_1 the 320 kW missing for 5 to reach 320°C.

Below this pinch, the constraint on the heat capacity rates is met between 5 and H_2 . It is not possible to maximize the load on 5 because, slightly above the 215°C pinch, we have seen there exists a fourth 225°C pinch due to stream 6, where it is imperative to pair H_2 and 6. H_2 and 6 being both evaporation/condensation heat exchangers, it may be advantageous to maximize the load on this fourth exchanger, which leaves only 35 kW available on No. 3, in which the inlet temperature of 5 is equal to 243°C.

Two streams are then to be matched, 2 and 5, for a 700 kW load. We can check the accuracy of calculations by the consistent level of inlet and outlet temperatures of heat exchanger No. 5.

Below the 215°C pinch, we can begin by matching 5 and 2, to deplete the 400 kW available in stream 2, which determines the inlet temperature of 5 in heat exchanger 6: 191°C. Given the levels of stream temperatures, it is then necessary for heat exchanger No. 7 to provide the coupling between 5 and H_3 , which leads to an inlet temperature of 5 in this exchanger equal to 161°C.

Among the streams remaining, only 1 can exchange heat with 5 at this temperature level. If the load on heat exchanger 8 (1,200 kW) is maximized, the inlet temperature of 5 in this exchanger becomes equal to 106°C, which is borderline, the pinch being normally 10°C. To do so would require stream 3 to take over from 1 at a higher temperature, but it would add a heat exchanger, so we accept this additional constraint.

Finally, the remaining 320 kW can be exchanged between 3 and 5 in a heat exchanger No. 9. As before, a verification of the correctness of calculations can be performed at this level.

We obtain ultimately the result of Figure 22.3.10.

The total number of heat exchangers, utilities included, is now 9 instead of 5, an increase of over 50%, which is quite large, and, except in special cases, not generally justified. We note however that the proposed method can handle in a relatively simple manner even complex situations.

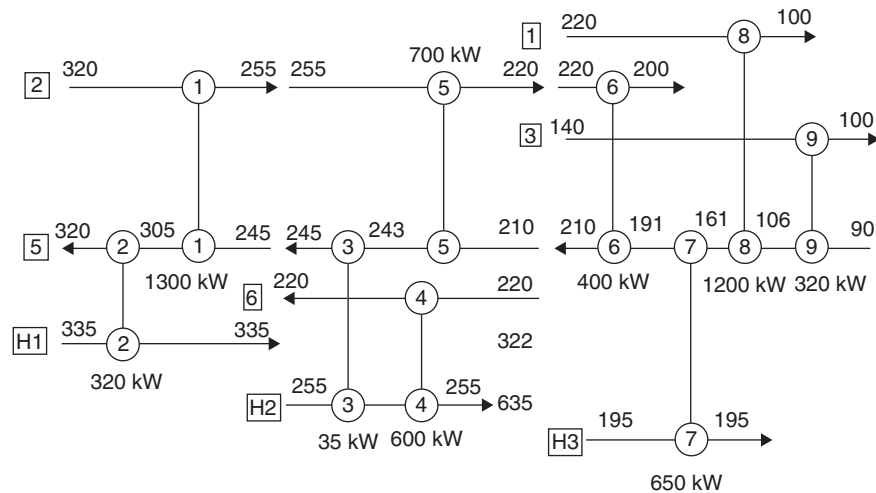


FIGURE 22.3.10

Endothermic zone grid diagram with utilities

TABLE 22.3.8

Number	$\dot{m}c_p$ (kW/K)	ΔH (kW)
1	-10	-600
3	-8	-480
4	-1200	-1200
5	21.4286	1071

22.3.4.3 Analysis of the exothermic zone

Streams selected at the first interval are given in Table 22.3.8.

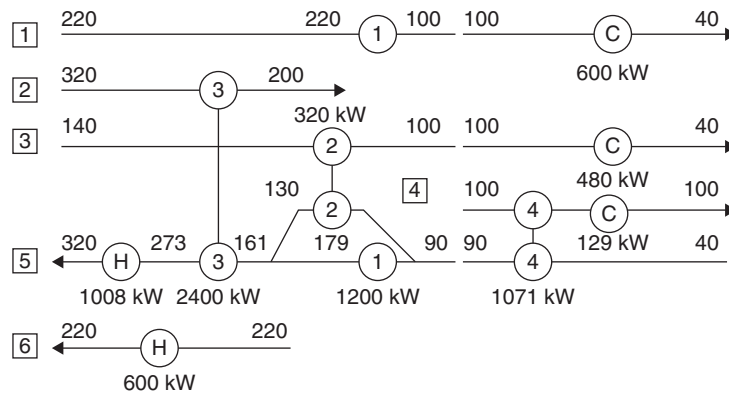
Throughout the exothermic zone, the only cold stream is 5 and, at the pinch, the constraint $\dot{m}c_{pc} \geq \dot{m}c_{pf}$ cannot be verified unless it is matched to stream 4. By maximizing the load of this exchanger (5), and knowing that the inlet temperature of 5 is 40°C, we obtain $h_5 = \dot{m}c_{p5} (90 - 40) = 1,071$ kW.

Stream 5 being completely warmed by that heat addition, it cannot provide cooling for the entire 4 nor for 1 and 3, which must be performed by cold utilities, for a total of 1,209 kW.

Coming back to the first analysis of the endothermic zone, we end up with the grid in Figure 22.3.11.

As demonstrated by studying the endothermic zone variant where utilities were placed so as to reduce irreversibilities, a number of difficulties can arise when determining the architecture of the exchanger network. In our case, we chose on the one hand to finally operate with a 6 K pinch to avoid being forced to introduce an additional heat exchanger, and secondly we took as main constraint the 225°C pinch, given the existence of the vaporization-condensation for streams 6 and H₂. Very frequently in practice, we are confronted with problems of this kind or other, leading to amend the procedure described above.

Various advanced methods are used to pursue further optimization of the network, depending on the configurations identified and prosecuted criteria (economic in most cases, including research of the minimum number of heat exchangers). You will find in the literature, and especially in the book by Linnhoff (1982), developments relating to these methods (Trivedi, 2000).

**FIGURE 22.3.11**

Grid diagram of the whole heat exchanger network, hot-end left, cold-end right

22.3.5 Thermal machines and heat integration

Thermal integration allows one to highlight the pinches, which determines an exchanger design constraint: a pinch occurs when the average slope of needs is higher on the left, and lower on the right than that of availability. Once these values known, it is possible to make a technical and economic optimization calculation of the exchange process by a sensitivity analysis on cost variations around these points.

The pinch being created by changes in slope, we must, as far as possible:

- pair streams of similar slopes;
- carefully consider the position of latent heat exchangers;
- not hesitate to export excess heat from the exothermic zone, if they can find a use elsewhere;
- not hesitate to import heat in the endothermic zone if any are missing.

Thermal integration also provides as we will see useful insights on the placement of heat engines.

22.3.5.1 Placement of heat pumps

You should refer to Chapter 19 for a detailed presentation of heat pumps. The opportunity to use a heat pump can be analyzed from the composite curves or GCC: this requires the existence of two zones with similar needs and availability, availability temperature being slightly insufficient. The heat pump then raises the temperature level of availability, which is valued at the sole price of the energy consumed by the compressor. Thus, if conditions are met, this transfer can greatly reduce the need for both hot and cold utilities. This means that the heat pump evaporator is situated in the exothermic zone and the condenser in the endothermic area. If this rule is not satisfied, the heat pump acts as a simple heat exchanger, its overall coefficient of performance (COP) being limited to 1 and, more often, its inclusion in the system has no interest at the economical level.

22.3.5.2 Placement of heat engines, cogeneration

Similarly, one can use these curves to assess interest to include in the system internal combustion engines to make CHP (see Chapter 18). It can be shown that only two configurations may in practice be retained: the engine must be placed either in the endothermic zone or in the exothermic area, but never in between. In the first case, we produce mechanical energy using exergy available from a hot source at high temperature (e.g. a boiler) and process requirements at a lower temperature, while in the second, process thermal effluents are given higher value, providing engine work between them and the environment. The latter case is economically feasible only if the discharge temperature is sufficiently higher than that of the environment.

22.4 OPTIMIZATION BY IRREVERSIBILITY ANALYSIS

22.4.1 Component irreversibility and systemic irreversibility

We have previously shown that the existence of a minimum pinch introduces a change in the nature of the optimization problem: the global optimum does not necessarily correspond to that of components. This finding leads us to distinguish two types of irreversibilities: component irreversibilities (CI), and systemic irreversibilities (SI).

To clarify this distinction, let us come back to the HRSG case of section 15.6.2, used in energy recovery on an effluent. Its CFDC is shown in Figure 22.4.1. The total irreversibility (area between the two exergy composites CC, corresponding to the area subtended by the CFDC) cannot be reduced without changing the minimum difference in temperature that has been set.

If the pinch value is ΔT_{pinch} , the minimum Carnot Factor Difference Curve is:

$$\frac{T_0 \Delta T_{\text{pinch}}}{T(T + \Delta T_{\text{pinch}})} \approx \frac{T_0 \Delta T_{\text{pinch}}}{T^2}.$$

We can make the locus of minimum pinches (LMP) appear on the CFDC, resulting in a thin line, monotonically decreasing curve in Figure 22.4.1.

Irreversibilities that lie below this curve depend only on the value adopted for ΔT_{pinch} , and therefore on the minimum temperature differences within heat exchangers. Taking place inside components, they can be described as component irreversibilities (CI).

Those located above the LMP come from the system configuration. They can therefore be called systemic irreversibilities (SI).

On the graph in Figure 22.4.2, CIs are shown in dark grey, and SIs in light grey.

More generally, we call component irreversibility an irreversibility related to the internal functioning of a single component independently of the rest of the system under consideration, and systemic irreversibility an irreversibility which can be modified only by changing the system configuration.

The case of a single heat exchanger is worth discussing in more detail. In such a heat exchanger (e.g. the economizer corresponding to the left part of Figure 22.4.2), the boundary conditions (temperatures and flow rates) are set by the rest of the system. The irreversibilities in the heat exchanger consist on the one hand of the pinch value (CI dark grey in Figure 22.4.2), and secondly the significant difference between the water and gas heat capacity rates (SI light grey in Figure 22.4.2). As long as we do not change heat capacity rates, we can change the overall irreversibilities only by playing on the CIs, that is to say on the pinch value.

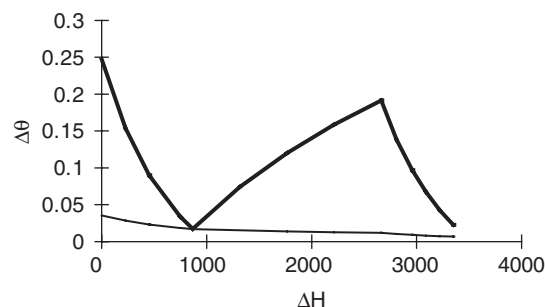
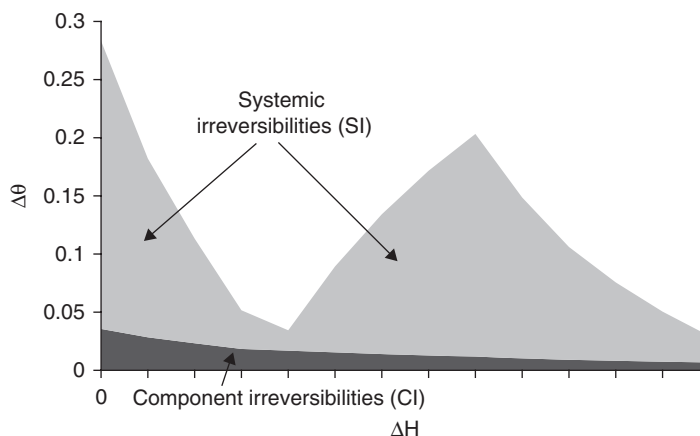
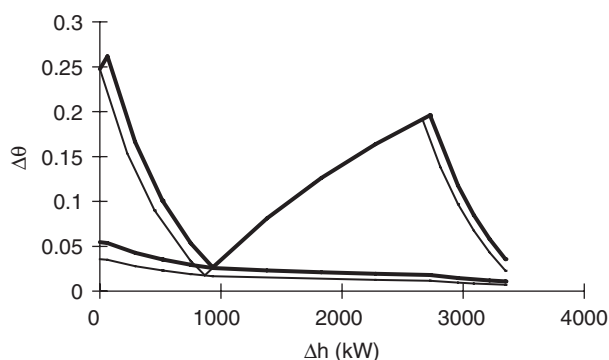


FIGURE 22.4.1

CFDC of a single pressure HRSG

**FIGURE 22.4.2**

Component and system irreversibilities

**FIGURE 22.4.3**

Impact of a pinch value change

If we now consider an existing counter-flow heat exchanger, it is easy to show that minimum irreversibility is obtained when heat capacity rates are equal. In this case, the temperature difference between the fluids is constant and equal to the minimum pinch. The overall irreversibility is equal to the CI. For cross-flow heat exchangers, things are more complex, but the minimum irreversibility is also obtained for a capacity rate ratio close to 1.

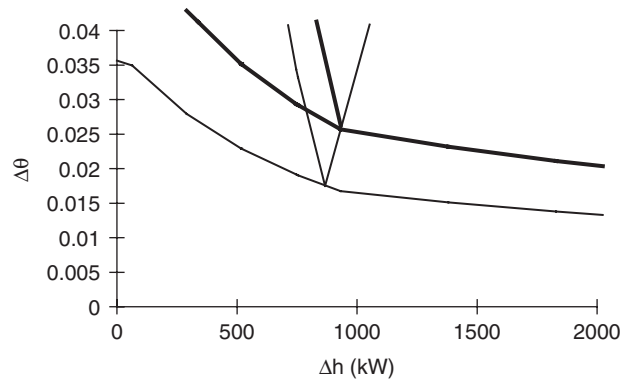
If we consider the previous case, and set a larger minimum pinch, the CFDC and the LMP are moved upwards. The CIs increase, while the SIs remain unchanged, as shown in Figures 22.4.3 and 22.4.4.

The CFDC (equipped with LMP) allows the main constraints of the problem to be viewed in a very summarized way: all pinches are highlighted, as well as the CIs and SIs. As we shall see later, we know immediately where to focus our efforts when attempting to optimize the system.

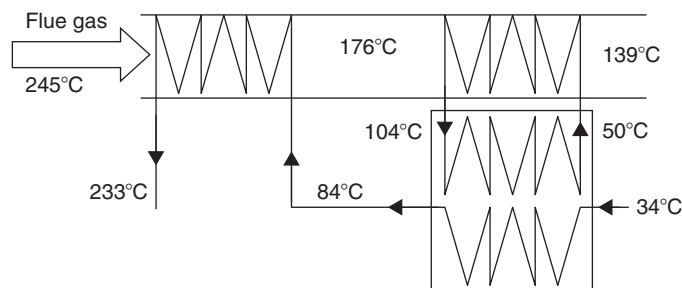
Considering the limiting case where the pinches and sub-cooling approach are assumed to be zero (which requires infinite exchange surfaces), the needs (steam) and availability (effluent) curves touch at pinch points (here, 9 and 11 in Figure 15.6.7). The CI being zero, the only remaining irreversibilities are then SIs.

But the problem can also be viewed from another perspective: consider for this a component in a zone with important SIs. Clearly it is unnecessary to minimize the CIs beyond the value of SIs, since they cannot be deleted. Under these conditions, the SIs represents a potential of CIs which may be used to improve the component functioning.

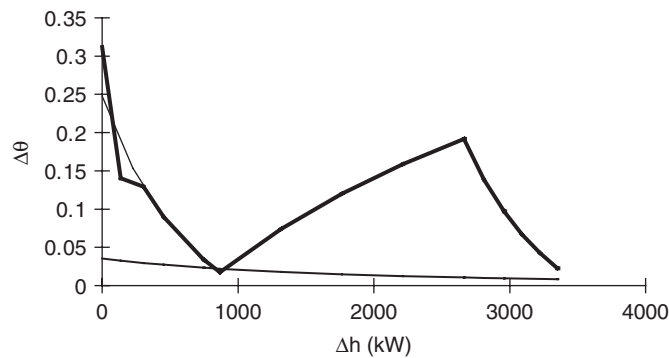
Two examples illustrate this. The first relates to recovering heat from flue gas through a stream at a temperature below dew point (for example water at a condenser outlet). Even if the release

**FIGURE 22.4.4**

Impact of a pinch value change (enlarged)

**FIGURE 22.4.5**

Anti-condensation intercooler

**FIGURE 22.4.6**

CFDF with the anti-condensation intercooler

average temperature is above $T_{rejl\lim}$ (see section 15.6.4), there is the risk of local condensation against the wall of the cold heat exchanger.

The condensation of water vapor, in the presence of gaseous sulfur or nitrogen oxides, leads to the formation of corrosive acids, which requires the use of expensive heat exchangers, glass or stainless steel. If heat exchange takes place at a location where there are large enough SIs, another way to do this is to add a double anti-condensation intercooler with a coolant flow between on the one hand smoke, and on the other hand the condenser outlet water (Figure 22.4.5). The result is obviously additional CIs, but it introduces no penalty as long as it remains below the local SIs.

(Component) irreversibilities introduced by the intercooler come in deduction of SIs existing in the left part of the CFDC. Thus, they introduce no additional penalty (Figure 22.4.6).

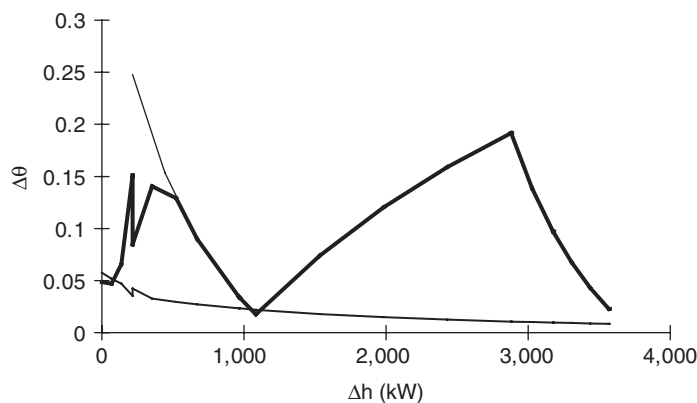


FIGURE 22.4.7

CFDF with the anti-condensation intercooler and the new streams

Here we must mention a small problem: some caution is necessary when using enthalpy diagrams or their exergy equivalents such as CFDC, because the x-axis, which represents the cumulative enthalpies, is likely to vary when changing the system.

For simplicity, we presented Figure 22.4.6 the CFDC corresponding to the energy recovery system on the effluent, but not including the bottom of the intercooler ensuring the exchange between liquid water and the stream coolant. Strictly speaking, it would have been necessary to introduce two new streams, one representing availability (the stream that cools), and other needs (the stream which is heated). The cumulative curves of requirements and availability are then both shifted, and comparison of charts is somewhat complicated. This is shown by the CFDC in Figure 22.4.7, where we have drawn in thin lines the initial curve being shifted by enthalpy exchanged in the intercooler. In this graph, the final SI is even lower, due to the inclusion of CI on both sides of the double intercooler.

More generally, for more complex systems, it will be observed on the curves obtained by thermal integration slight differences from one configuration to another. These differences are not surprising, and are of no importance in practice, the proposed method using essentially the qualitative nature of these curves.

The second example concerns flame boilers. In a conventional combustion boiler (Figure 15.6.3), protection of tubes irradiated by flames requires that the first heat exchanger is the furnace-vaporizer. The flow of water first in liquid form then as steam is not counter-flow of the smoke (Figure 15.6.4).

However, the resulting CIs have no influence on the boiler efficiency, since the temperature difference between the two streams is in any way such that there are larger SIs.

In both cases, we use the potential of CI corresponding to the SI to circumvent a technological constraint of non-thermodynamic nature, without any detriment to system performance. Long time indeed, thermal engineers have known how to use the irremediable SI when available. In the design of heat exchangers for example, they allow to obtain important LMTD, and thus reduce exchange surfaces. The contribution of the proposed method is to distinguish them easily from component irreversibility, in order to use them at best.

22.4.2 Optimization method

The optimization method we recommend is very simple and can be summarized by three main rules:

- highlight pinches by heat integration, and seek to minimize irreversibilities that exist at each pinch or cross them;

- highlight systemic irreversibilities (SI), and then try to reduce them if possible by modifying the system configuration and wisely using the potential of “free” component irreversibility (CI) to which they correspond;
- once the minimum energy target obtained by applying the first two rules, use all degrees of freedom of the system to place exchangers in the most relevant manner at the technological and economic levels.

Rule 1

The basic idea here is that to optimize a thermal system, we must always begin with looking at what happens at its most constrained zones: pinches. So we must begin by highlighting pinches, using thermal integration, then we should focus on the study of components existing at their level. If they are not optimized, reducing their irreversibilities will always prove beneficial.

Care will be taken there on a certain type of irreversibility, sometimes masked (not taken into account in the CFDC) but actual: those from the connection that may exist, including by mixing, between streams located on both sides of a pinch (desuperheating presented section 15.7.4 may be an example). That’s what we called irreversibilities crossing the pinch.

Rule 2

If we use heat integration, we can draw the CFDC, and therefore view system irreversibilities. By adding the LMP, we very clearly identify the systemic irreversibilities.

Note that the potential of CIs can only be exploited to the extent that the component in question is not itself located at a pinch (“pinched” component). Indeed, if the component is pinched, any increase in its irreversibility is reflected by an increase in overall irreversibilities. However, any component not pinched has the potential of CIs.

When this potential is fully exploited, a new pinch appears at this level. There is thus a close connection between pinches and component irreversibility: given our definitions, pinches are the places where the potential of CIs is zero. Any improvement in this area comes either from a change in system configuration or a reduction of local component irreversibility.

Moreover, in order for rule 2 to be put into practice, the SI should be effectively transformable into CI potential, which is not always the case. For example, in heat exchangers, SI which comes from differences in heat capacity rates cannot be transformed into CI potential internally recoverable.

The SI being irretrievably lost, we must employ them at best, even to the emergence of new pinches. If they cannot be used to reduce the need for energy input, they can be valorized in the heat exchanger design, allowing sizing the best exchange surfaces given the temperature difference.

Finally, recall that we have assumed, at the beginning of the analysis, that heat capacity of streams are constant. Having highlighted the pinches, and therefore the corresponding temperature threshold values, it may be necessary in a second phase to refine the calculations taking into account their variation with temperature.

Rule 3

The above rules allow minimization of the energy consumption of the system, but by ignoring certain technological and economic considerations that may prove decisive in practice. The algorithms determine a solution compatible with the first two laws of thermodynamics, but it can be either too expensive or inappropriate for off-design operation of the facility.

In this sense, the result in terms of energy consumption must be considered more as an objective value than as the best solution (this is why it is called a target). The idea here is that we should start from this extreme case and use it as a guide to match the different streams by creating an exchanger network suited to the problem, considering all the existing degrees of freedom. For this, we use on the one hand the teachings of heat integration on exchanger network design, and secondly

the experience of practitioners of engineering companies accustomed to complex energy system engineering.

The proposed method is thus a complementary tool in the service of design engineers, whose originality and power can shed systemic light on the plant they are studying.

All thermal integration methods we have presented so far are only applicable for systems with free configuration, that is to say where the placement of some heat exchangers is not *a priori* imposed.

The Thermoptim systemic integration method is however much more general in scope, and can be used for systems with partially frozen configuration, with only slight modifications of thermal integration algorithms. However, to avoid making the presentation, we will not study them here, leaving the reader to refer to the article (Gicquel, 1996).

22.5 IMPLEMENTATION IN THERMOPTIM

22.5.1 Principle

If you disregard the relatively complex theory that this method is based on which has been exposed in previous sections, the Thermoptim optimization method is relatively easy to present and use.

In order to be able to vary the system parameters easily, Thermoptim provides a modeling environment in which simulation functions and optimization method are closely interconnected.

Practically speaking, the method can be broken down into two main phases:

- The first phase consists of describing the system without making any assumptions about how the exchangers are matched (this is called a non-constrained system), and seeking to optimize the energy or exergy recovered (electric power produced, power cogenerated, etc.) using thermal integration algorithms to make sure there are no temperature incompatibilities. The iterative procedure consists of simulating changes in the key system parameters (flow rates, temperatures, pressure levels) and optimizing the performance, while using the pinch method to make sure that you are not introducing any additional high temperature heat needs and that you are minimizing low temperature discharges. The distinction between component irreversibilities (specific to their own operation) and system irreversibilities (related to the system architecture) tells you how much freedom you have in terms of design. At this point in the method, the people in charge of optimization and the process designers will exchange information back and forth. One of the advantages of this method is that you can get an idea of the optimization possibilities at any time. All the usual thermal integration graphics tools are accessible, as well as the Carnot Factor Difference Curve, which is well suited to the problem at hand;
- The second phase, once the system is optimized, consists of designing a compatible heat exchanger network (the use of the optimization method ensures that a compatible configuration does exist), by matching and splitting streams as necessary (in series or parallel). Thermoptim proposes exchange blocks so you can define the system progressively in phases, by matching streams starting at the most restricted areas, namely the pinches. If there are technological or financial issues that make it necessary to choose an exchanger configuration other than the one that gives the best performance, it will become apparent during this phase.

Up to now we assumed that the exchanger system was not known. If it is known, you can obviously use Thermoptim to model and test it. You can compare the initial configuration with the configuration that a non-constrained optimization would have given. It is also possible to preset just some of the heat exchangers and optimize the rest of the system. Thermoptim will combine the constrained exchangers and the free exchangers, which facilitates the global optimization of the system.

Let us summarize the main features of ThermoOptim optimization method:

- it is a variant of the pinch method focusing on the analysis of the Carnot Factor Difference Curve (CFDC), which is obtained by subtracting the cold composite from the hot composite, thus highlighting the system irreversibilities;
- more precisely, the minimization of the pinch (obtaining the minimum energy target) is made by a variant of Linnhoff's algorithm. One difference is that several values of the minimum pinch can be used, depending on the type of stream: for example, values of ΔT_{pinch} can be taken equal to 16 K for gases, 8 K for liquids and 6 K for boiling or condensation exchanges. A second difference is that temperatures are shifted by $\Delta T_{\text{pinch}}/2$ only for calculating the minimum energy target. Subsequently, only the actual temperatures are used, so as not to distort the irreversibility calculation;
- the CFDC allows thermodynamic losses of two kinds to be visually distinguished: the first, called component irreversibilities CIs, are characteristic of component operation, while the second, called system irreversibilities SIs, are specific to the system architecture;
- highlighting pinches, this method visualizes in a very physically speaking way areas of the system whose design must be done with special care. It is a valuable guide where previously were employed heuristics methods requiring sometimes many iterations;
- determining exactly the maximum achievable gains, it defines a target which is then used to precisely quantify the gap between the theoretical optimum and the best solution on the technical and economic terms;
- distinguishing between component irreversibilities and system irreversibilities, it shows where the degrees of freedom of systemic origin are that can be used to circumvent, without any penalty in terms of energy, singular technological constraints. Once the target is determined, exchange blocks can help match the streams.

PRACTICAL APPLICATION

Thermal integration of the Gourlia example with ThermoOptim

This example shows how to model with ThermoOptim the thermal integration problem presented in sections 22.1 to 22.3, and proposed by Gourlia in his 1989 paper. It explains how to use the pinch method tools available in the software.

It is presented in the Diapason session IT2En (<http://www.thermoOptim.org/sections/enseignement/cours-en-ligne/seances-diapason/session-it2en>). Diapason session IT1En may help you getting started with the pinch method (<http://www.thermoOptim.org/sections/enseignement/cours-en-ligne/seances-diapason/session-it1en>).



[CRC_pa_6]

22.5.2 Optimization frame

All the functions specific to optimization are accessible from the optimization frame (Figure 22.5.1). They work in close coordination with the simulator, so you can easily modify the system parameters but are separated, however, mainly to simplify ThermoOptim use for those who do not need them.

To get access to the optimization screen, type Ctrl M or select “Optimization tools” in the “Special” menu of ThermoOptim professional version.

It is comprised of three main tables:

- the fluid table contains all the exchange streams in which the “pinch method fluid” option is selected. These are fluids which are processed by the variant of the Problem Table Algorithm implemented in ThermoOptim;
- the interval table contains the list of intervals which are built by the PTA variant;
- the heat exchanger block table contains the exchange blocks which can be defined in order to facilitate stream matching in heat exchangers.

8 fluids			Export	
name	Tinf (°C)	Tsup (°C)		
GT exhaust	78.26892	508.75918		
ECOHP1 vap	24.40876	128.35		
ECOHP2 vap	128.35	310.9608		
ECOLP	24.11282	147.09025		
EVHP vap	310.9608	311.0608		
EVLP vap	147.09025	147.19025		
SHHP1 vap	310.9608	450		

14 intervals					Export	
interval n*	Tinf (°C)	Tsup (°C)	Nb of fluids	m Δh		
1	458	500.76	1	-4,763.8		
2	318.96	458	2	-9,660.81		
3	314.96	318.96	1	-445.64		
4	314.06	314.96	2	-52.26		
5	313.96	314.06	3	14,906.67		
6	283	313.96	2	-1,797.72		
7	155.09	283	3	-6,351.9		

Display observed types			
name	type	flow rate / P (bar)	m Δh / T (°C)
HP pump	compression	11.3	118.96
LP pump	compression	3.94	1.82

0 Heat exchanger blocks			Export	
name	type	main process		

DT MPL	11
T hot utilities (°C)	726.85
T cold utilities (°C)	26.85
T0 exergy (°C)	0
total needs	46,870.21
heat input	0
heat extraction	1,090.67
<input type="button" value="Iterate"/> <input type="button" value="Stop"/>	
max. number of recalculations	30
test value	0.01
iterations : 2 / test : 0.001	
effectiveness	0.5985
useful energy	59,136
purchased energy	98,803
<input type="button" value="Close"/>	

FIGURE 22.5.1

Optimization screen

In the right part of the screen appear several fields, five of which are editable:

- $DT\ LMP$ is the minimum pinch value used for plotting the locus of minimum pinches. By default it is set to 11 K;
- $T\ hot\ utilities$ is the temperature used to plot the hot utility target (heat input requirements). By default it is set to 1,000 K;
- $T\ cold\ utilities$ is the temperature used to plot the cold utility target (heat extraction requirements). By default it is set to 300 K;
- $T_0\ exergy$ is the value used for environment temperature reference in exergy calculations. By default it is initialized to the value set in ThermoOptim global settings. If it is changed in the optimization screen, this does not affect other exergy calculations performed by the simulator;
- $total\ needs$ represents the sum of all the enthalpies of the cold streams;
- $heat\ input$ is the value of the additional heat which may have to be provided to the hot streams if the total needs exceed the heat available when pinches are taken into account. This value is also often referred to as the “energy target”;
- $heat\ extraction$ represents the value of the heat which must be extracted from the system by cold utilities. It should be noted that the existence of pinches explains that, as shown above, there may be at the same time a need for a heat input (at high temperature) and for a heat extraction (at low temperature).

22.5.2.1 Fluid table

When you double-click on one of the fluids listed in the fluid table, a frame appears such as in Figure 22.5.2.

It summarizes the data which is processed by the PTA and cannot be directly modified by the user, as it is built from the corresponding process which can be shown by clicking on the “display” button.

FIGURE 22.5.2

Fluid frame

process name	mCp	
GT exhaust	-111.409908...	
ECOHP2 vap	53.3455304...	
EVHP vap	149124.8	

FIGURE 22.5.3

Interval frame

22.5.2.2 Intervals

Interval analysis plays an important role in pinch methods, as they allow understanding of how the different streams are distributed. In particular the analysis of the intervals around the pinch is of basic importance for efficiently matching streams in heat exchangers.

The intervals can be displayed either from the optimization frame, or from the composite charts, by double-clicking on the diagram: the corresponding temperature is calculated, and the interval in which it is contained is displayed.

When you double-click on one of the lines of the interval table, the screen of Figure 22.5.3 appears.

In the upper left zone are shown the number of the interval, its temperature bounds T_{sup} and T_{inf} and the algebraic sum of the heat capacity rates $\dot{m} c_p$ of the different streams contained in the interval.

On the right are indicated the sum of the enthalpy needs and availabilities in the interval and the corresponding enthalpy balance.

The list of the streams which are located in or cross the interval is displayed in the table with the value of their heat capacity rate $\dot{m} c_p$. If you double-click on one of them, the corresponding process frame is shown.

22.5.2.3 Heat exchanger blocks

Heat exchanger blocks have been introduced in order to facilitate heat exchanger matching when a main process exchanges heat with several processes as for instance when one seeks to recover heat from gas turbine flue gases. In such a case the main hot stream has to be split (in series and/or in parallel) in several sub-processes to be matched with the different cold streams. The role of heat exchanger blocks is to provide assistance for dividing the main exchange process: one begins by grouping fluids to be matched in blocks which are balanced at the enthalpy level; in a second step, the choice is made between series or parallel matching, and lastly the main vein can be further divided.

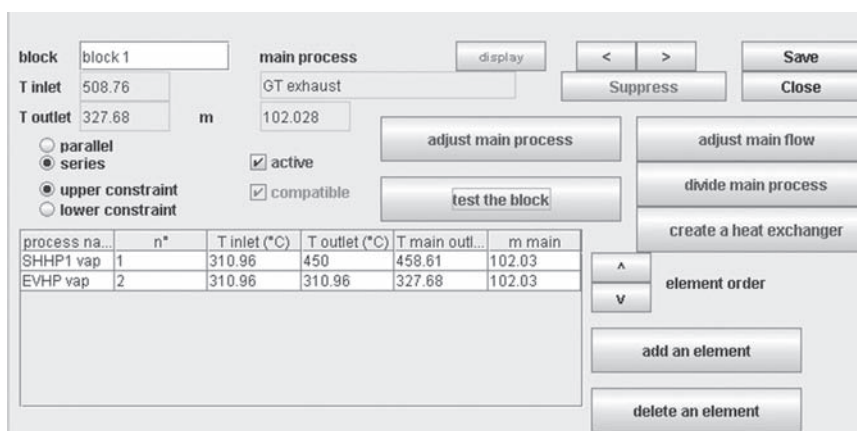


FIGURE 22.5.4
Heat exchanger block screen

Heat exchanger blocks are only used as part of the optimization method. They differ from the classical heat exchangers which are accessible from the main simulator screen. When heat exchanger blocks have been defined, it is possible to divide the main process in as many sub-processes as required. Once this division is made, classical heat exchangers can be easily built from the block frame (Figure 22.5.4).

The name of the block appears in the upper left zone. On its right is the double-clickable field defining the main process (here “GT exhaust”), which may be displayed by clicking on the red button “display”.

Below the block and main process names are located options which allow one to characterize the block: its elements may be matched in series or in parallel, and the block may be “upper” or “lower constraint” as explained below. The block may be “active” or not: only those blocks which are active are taken into account in the optimization method for the mixed problem when some heat exchangers are set. If the block is balanced at the enthalpy level and the temperatures of the different fluids comply with the pinch constraints, the block is “compatible”.

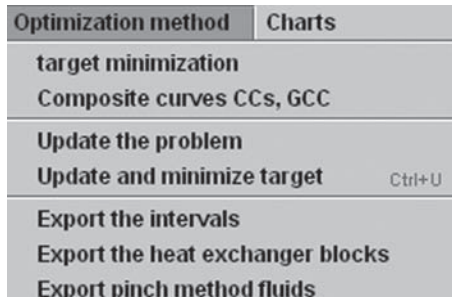
On the lower left part of the frame is a table where are listed the different streams which are to be matched with the main process. They can be added either by double-clicking in the table headband or by clicking the button “add an element”. They can be removed by clicking the button “suppress an element”. The stream order may be modified by selecting one of them and shifting it using the two arrows on the right of the table. If you double-click the table, the process corresponding to the fluid is shown.

Four blue buttons allow one to use the block:

- “adjust main process” button allows you to adjust the block enthalpy balance by modifying the inlet or outlet temperature of the main process. Thermoptim calculates the total enthalpy corresponding to the different elements which have been selected and sets that of the main vein to that value. If the “upper constraint” is selected, the minimum temperature of the vein is modified (the outlet one for a hot stream, and the inlet one for a cold fluid). If the “lower constraint” is selected, this is done conversely;
- “test the block” button allows you to check the block consistency. Before activating it, it is necessary that the main process be adjusted by clicking the previous button. Thermoptim checks the temperature compatibility between the main vein and the different block elements;
- once a block is valid, it is possible to divide it into smaller blocks matching a part of the main vein and one of each of the block elements. If the “series” checkbox is selected, the main vein is divided in series into as many parts as there are block elements, of the same flow rate as the main vein, the intermediate temperatures being calculated. If the “parallel” checkbox is selected,

**FIGURE 22.5.5**

Message prompted in case of block division

**FIGURE 22.5.6**

Optimization menu lines

**FIGURE 22.5.7**

Chart menu lines

the main vein is divided in parallel into as many branches as there are block elements, of the same temperatures as the main vein, their flow rate being calculated proportionally to the enthalpy of the divided block. Furthermore, you can ask Thermoptim to automatically build the divider and the mixer which connect the main vein divided branches. Thermoptim automatically names the new types which it creates, adding *_0*, *_1*... to the existing names, except for the mixer (*MIX_xxx*) and the divider (*DIV_xxx*). If a type of that name already exists, it is modified. Warning: the corresponding components of the diagram editor are not automatically created. You can do it from the Diagram / Simulator interface;

- the fourth button named “create a heat exchanger” allows you to automatically start building the classical heat exchanger corresponding to a block comprised of a single element. If the two fluids of the block are already connected in an existing heat exchanger, a message warns you. In any case, the heat exchanger screen is shown. If it is just created, you have to finish setting it, by selecting the constraints and the type of calculation, before calculating it. By default, the heat exchanger type is created of the counter-flow type, but you can change it if you wish to do so.

22.5.2.4 Optimization menus

- *target minimization* corresponds to the shifted temperature PTA;
- *Composite curves CCs, GCC* builds up the composite curves;
- *Update the problem* updates the optimization elements from the process table;
- *Update and minimize target* combines the third and first items;
- *Export the intervals* creates a text file named “interv.txt” in subdirectory “pinch” containing all the information on intervals;
- *Export the heat exchanger blocks* creates a text file named “HXblock.txt” in subdirectory “pinch” containing all the information on the heat exchanger blocks, as well as preliminary computations of the exchanger characteristics (effectiveness, NTU, LMTD, UA value);
- *Export the pinch method fluids* creates a text file in subdirectory “pinch” containing all the information on the problem data;
- *Plot the Carnot Factor curves* plots the exergy composite curves;

- *Plot the mixed HX-TI Curves* plots the composite curves obtained when part of the heat exchanger network is set;
- *Plot the CFDC* plots only the Carnot Factor Difference Curve;
- *Plot composite curves* plots all these curves.

The two latter menu items are enabled only when either the Carnot Factor or the mixed HX-TI curves have been calculated.

22.6 EXAMPLE

Typically, a heat recovery steam generator (HRSG) such as those used to generate steam in combined cycles is a good example of a complex system which can be optimized thanks to ThermoOptim optimization method. You should refer to chapters 15 and 17 for a detailed presentation of the peculiarities of such heat exchangers. In a HRSG, steam is produced at 2 to 4 pressure levels, which can be freely chosen within certain limits.

WORKED EXAMPLE

Thermal integration of a dual pressure combined cycle with ThermoOptim

This example explains how to solve with ThermoOptim the thermal integration problem of a dual pressure combined cycle. It shows how to use the pinch method tools available in the software.

It is presented in the portal guidance pages (<http://www.thermoOptim.org/sections/enseignement/cours-en-ligne/fiches-guides-td-projets/fiche-guide-td-fgl1-sur>).



[CRC_we_10]

In this example, we only make use of part of the method, our main goal being to illustrate the use of the different ThermoOptim screens which are related to optimization: for example we will not need to distinguish systemic and component irreversibilities.

The problem is defined as follows: a gas turbine whose compressor and turbine polytropic efficiencies are equal to 0.9, whose compression ratio is 20 and whose turbine inlet temperature is equal to 1,220°C sucks 100 kg/s of air at 10°C. We wish to design a dual pressure HRSG capable of powering a cycle with two steam turbines whose isentropic efficiencies are equal to 0.85. The pressure and condensing temperature are respectively 0.03 bar and 24.1°C. The cycle maximum temperature and pressure are set at 450°C and 100 bar. Pump isentropic efficiencies are equal to 0.95, and the low pressure superheating temperature is set to 548.15 K (275°C). In this study, the cycle will be a simple reheat Rankine cycle, but the method can be used with much more complex ones. The minimum flue gas stack temperature is set to 75°C.

A model of the GT of the type described in section 12.1.4.3 (Figure 12.1.18) may be easily constructed. The net power produced is 43,690 kW; the efficiency is 44.2% and about 102 kg/s of exhaust gas exit at 509°C. Their composition is given in Figure 22.6.1.

The criterion is the pinch method minimum target: for a given cycle pressure value, one seeks the maximum flow rate which does not require an additional heat input.

In practice, the procedure is the following:

- set the flue gas stack temperature to 75°C;
- set up two simple steam cycles with HP and LP pressure settings;

component name	molar fraction	mass fraction
CO2	0.03558442	0.05483373
H2O	0.06617345	0.04174105
O2	0.1343288	0.1505017
N2	0.7552133	0.7407539
Ar	0.008699999	0.01216955

FIGURE 22.6.1

Flue gas composition

- select all exchange fluids (the gas turbine flue gas, the economizers, the vaporizers and the superheaters) as pinch fluids with the appropriate minimum pinches (16 K for gases, 8 K for liquids, 6 K for the evaporator);
- select the autoflow checkbox if necessary;
- set the HP and LP pump flow rates; as the other cycle processes are located downstream from them, their flow rates will automatically be updated;
- select the “observed” checkbox in the HP and LP pump processes; they will thus directly appear in the Optimization screen.

22.6.1 Determination of HP and LP flow rates

In practice, we first seek the highest possible flow rate for the HP cycle, which amounts to considering initially a single pressure level or to set the flow in the LP line to zero. Pressure of 100 bar is about the maximum exergy for 450°C superheating (Figure 5.6.13 of Part 2).

This requires starting by setting a value of HP pump flow-rate, then using the recalculation engine for propagating changes to the whole cycle (by iterating until the values stabilize the enthalpy balance).

Open the Optimization frame (Figure 22.5.1) by pressing Ctrl M or selecting the appropriate menu item.

In the optimization frame, select the menu item “Update and minimize target” or type Ctrl U. If the flow rate is lower than the maximum limit, the tables are updated and no message appears. If the flow rate is too large there is a need for a heat input and a message informs you. In the first case, you may increase the flow rate. In the second case you must decrease it.

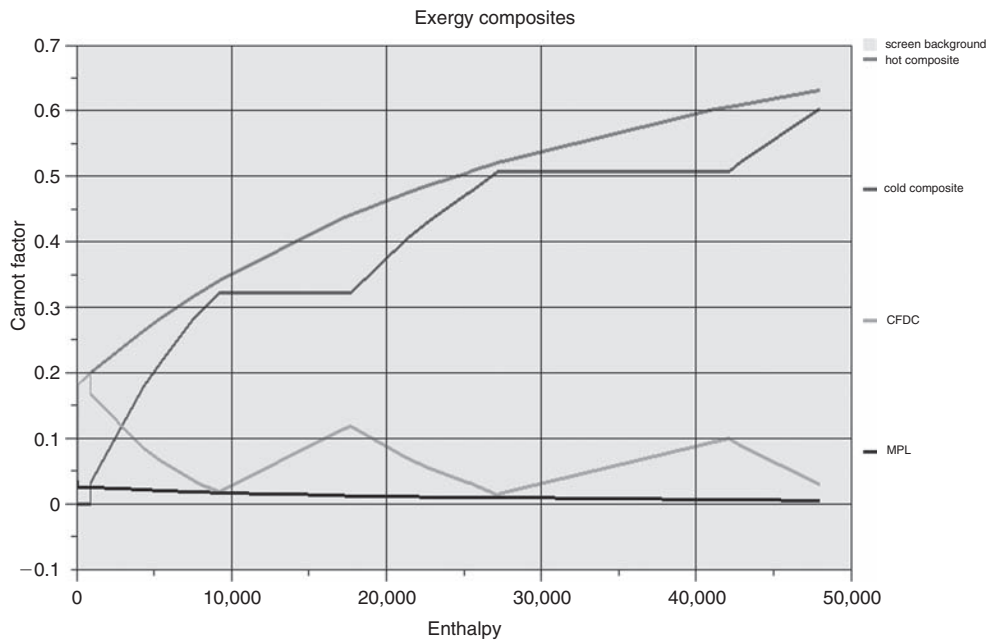
To do this double-click the “HP pump” line in the bottom left table of the Optimization screen (figure 22.5.1), modify the flow in the process screen, and recalculate the process and then the project. Then make a new update of the optimization problem, and iterate until you find the maximum flow rate that does not require an energy input. After some testing, you find the HP flow leading to the lowest pinch (11.3 kg/s).

The net power produced is 56,424 kW, which corresponds to over 29% increase compared to the GT alone. The efficiency is 57.1%.

It then remains to find the LP pressure and flow-rate leading to better recovery. After some tests, a pressure of 4.4 bar and a flow rate of 3.94 kg/s are used to cool gases at about 88°C. The net power output is 59.136 kW, which corresponds to almost 5% increase compared to single pressure HRSG.

You can have a graphical display of the exergy composite curves by selecting menu item “Plot the Carnot Factor curves” of menu “Charts” (Figure 22.6.2).

At this point we have exhausted the available enthalpy in exhaust gases, and therefore optimized the enthalpy recoverable, but not the exergy available. If we slightly increase the LP pressure and recalculate the maximum rate without heat input, we find that the net power is growing although the exhaust gases are not completely cooled.

**FIGURE 22.6.2**

Composites and CFDC of the optimized HRSG

Two pinches are visible, one around 310°C, and the second around 150°C. As we see, to completely cool the exhaust gases, there should be a third pressure level.

22.6.2 Matching fluids in heat exchangers

In ThermoOptim, intervals are displayed in shifted temperatures after pinch minimization has been performed, and actual temperatures after the plot of the composite curves. We will consider the latter case.

As the most constrained zone for fluid matching in heat exchangers is located at pinches, one must analyze intervals at their level, knowing that the heat capacity rates of the fluids matched in each exchanger must comply with the following inequalities (in absolute values):

- just above the pinch: $\dot{m}c_{ph} < \dot{m}c_{pc}$;
- just below the pinch: $\dot{m}c_{ph} > \dot{m}c_{pc}$.

The upper pinch (interval 4), is created by the appearance of the HP vaporizer. At that level existing fluids are given Figure 22.6.3:

- just above, the constraints are met if the HP vaporizer is matched with the flue gas (the constraint writes $111.4 < 14,981$), the superheater being moved upstream (for the latter, the constraint writes $0 < 41.93$);
- just below (Figure 22.6.4), the constraint is also verified ($111.4 > 53.26$).

However a third fluid appears in the following interval: the LP superheater. We shall see later that, even if the pinch constraint is verified below the HP evaporator, it will be necessary to parallelize the LP superheater and the HP economizer.

Obviously the flue gas has to be divided into two parts, one above and one below the pinch. This will also be true for the lower pinch (interval 8), which is created by the appearance of the LP vaporizer.

process name	mCp	
GT exhaust	-111.409908...	
ECOHP2 vap	53.2586586...	
EVHP vap	14981.6061...	

FIGURE 22.6.3

Interval 4 streams

process name	mCp	
GT exhaust	-111.409908...	
ECOHP2 vap	53.2586586...	

FIGURE 22.6.4

Interval 5 streams

process name	mCp	
GT exhaust	-111.409908...	
ECOHP2 vap	53.2586586...	
ECOLP	16.5955313...	
EVLP vap	8378.74591...	

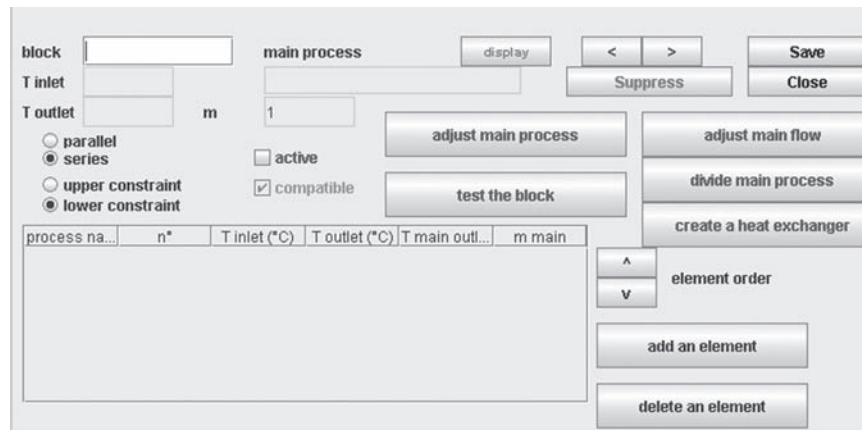
FIGURE 22.6.5

Interval 8 streams

process name	mCp	
GT exhaust	-111.409908...	
ECOHP2 vap	53.2586586...	
ECOLP	16.5955313...	

FIGURE 22.6.6

Interval 9 streams

**FIGURE 22.6.7**

Default heat exchanger block

Above the pinch the streams of Figure 22.6.5 exist.

As previously, the constraints can be met by matching the LP evaporator with the flue gas at that level ($111.4 < 8,378$) and moving the other exchangers upstream ($0 < 53.83$, and $0 < 8.36$).

Below the pinch, the situation is that of Figure 22.6.6. The LP vaporizer and superheater have disappeared, replaced by the LP economizer. Here heat capacity rate constraints can only be met if the flue gas vein is split into two parts, as there is only one hot stream and the constraints are that each cold stream capacity flow rate must be lower than that of a hot stream: the HP and LP economizers have to be parallelized.

Furthermore, the HP economizer crosses the pinch zone and must therefore be cut into two parts, which we will name ECOHP vap 1 and ECOHP vap 2.

You can see that this information has been directly obtained by analyzing the stream distribution at pinch level. Knowing that, it becomes possible to start matching the streams in heat exchangers. Using the heat exchanger blocks enables to do that progressively, without having to decide on the detailed placement of the heat exchangers in a first step.

We have seen that the need for parallelization occurs only below the lower pinch, and that other heat exchangers can be put in series. We will then divide the HRSG in two main blocks. To do that, begin by creating two intermediate points, one inside the HP economizer and one inside the flue gas vein, and split these two units into two streams. For the time being it is not necessary to know the exact temperatures of these points.

Go to the optimization screen and double-click in the headband of the heat exchanger blocks zone located at the upper right of the screen. The screen of Figure 22.6.7 appears.

block 1

T inlet 508.76

T outlet 327.06

main process GT exhaust

102.028

parallel

series

upper constraint

lower constraint

active

compatible

adjust main process

test the block

process na...	n*	T inlet (°C)	T outlet (°C)	T main outl...	m main
SHHP1 vap	1	310.96	450	458.61	102.03
EVHP vap	2	309.96	310.96	327.06	102.03

adjust main flow

divide main process

create a heat exchanger

element order

FIGURE 22.6.8

Heat exchanger block with settings

block 2

T inlet 327.06

T outlet 230.18

main process GT ex2

102.028

parallel

series

upper constraint

lower constraint

active

compatible

adjust main process

test the block

process na...	n*	T inlet (°C)	T outlet (°C)	T main outl...	m main
ECOHP2 vap	1	128.35	309.96	230.18	91.82
SHLP vap	2	147.09	275	230.18	10.21

adjust main flow

divide main process

create a heat exchanger

element order

FIGURE 22.6.9

Block 2 screen

block 3

T inlet 230.18

T outlet 153.16

main process GT ex3

102.028

parallel

series

upper constraint

lower constraint

active

compatible

adjust main process

test the block

process na...	n*	T inlet (°C)	T outlet (°C)	T main outl...	m main
EVLP vap	1	146.09	147.09	153.16	102.03

adjust main flow

divide main process

create a heat exchanger

element order

FIGURE 22.6.10

Block 3 screen

It is similar to a node, the controls being of course different. Name it (for instance “block 1”) and select the main vein by double clicking in the corresponding field. Choose “GT exhaust” from among the list of exchange processes proposed. Its inlet and outlet temperatures are displayed. Select then the different elements which have to be matched with the main vein, either by double-clicking in the headband of the table, or by clicking on the button named “add an element”. Start by the HP superheater, and the HP vaporizer. Set then the checkboxes located in the upper left part of the screen: “series”, “upper constraint” as the upper temperature of the main vein is set (here the inlet one), and “active” to indicate that the block is selected.

Now that the different streams are selected, you can adjust the block enthalpy balance by clicking the button named “adjust main process”. Thermoptim calculates the total enthalpy corresponding to the different elements which have been selected and sets that of the main vein to that value. If “upper constraint” is selected, the minimum temperature of the vein is modified. If “lower constraint” is selected, this is done conversely. Then click “test the block” to verify that the block can be built. You get the result in Figure 22.6.8.

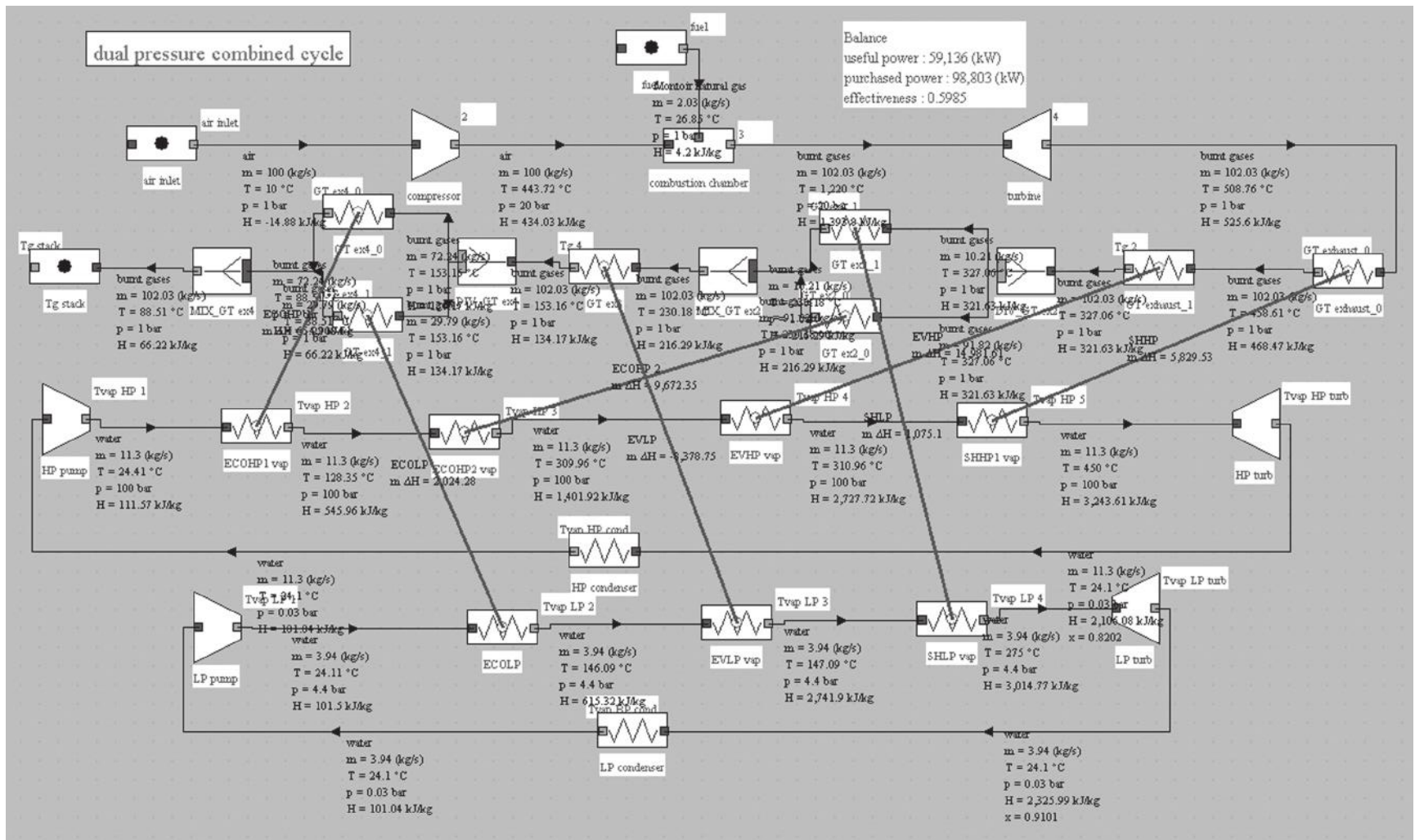
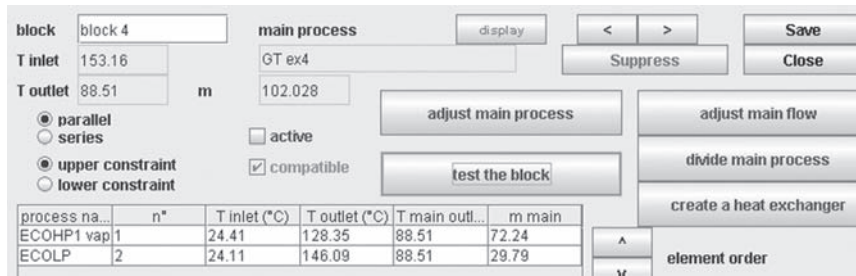


FIGURE 22.6.11
 Synoptic view of the combined cycle

**FIGURE 22.6.12**

Block 4 screen

Intermediate temperatures of the main vein are then calculated: 458.61°C at the superheater outlet, and 327.06°C at the vaporizer outlet.

Create a new exchange process (GT ex2) to represent the cooling of the burnt gas downstream the GT exhaust process whose outlet temperature has been modified.

The block above the upper pinch being built, you can operate in a similar manner to build the block between the two pinches. In this case a problem arises when you adjust the block, the LP superheater temperature being too high for it to be placed downstream of the HP economizer. It is therefore necessary to parallelize this block. However, a temperature constraint appears if you try to parallelize the three streams.

Ultimately, the only possible solution is to start by parallelizing the LP superheater and HP economizer (Figure 22.6.9), and put the LP vaporizer downstream of this block (Figure 22.6.10).

Create a new exchange process (GT ex3) to represent the cooling of the burnt gas downstream the GT ex2 process whose outlet temperature has been modified.

As the block is in parallel, the main vein is parallelized in as many branches as there are elements, each having the same temperature, their flow-rates being calculated in proportion to the enthalpy of the divided block. We obtain here 91.82 kg/s of gas for HP economizer, and 10.21 kg/s for LP economizer.

Finally, the last block parallelized below the lower pinch can also be constructed (Figure 22.6.12).

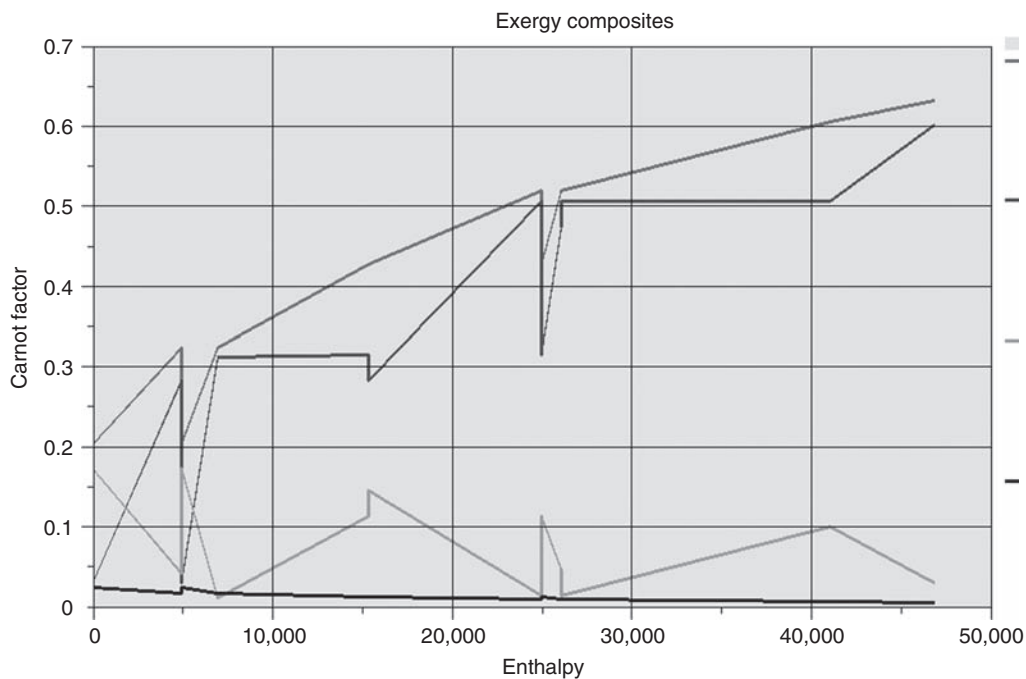
Create a new exchange process (GT ex4) to represent the cooling of the burnt gas downstream the GT ex3 process whose outlet temperature has been modified.

Once this matching is done, the main structure of the heat exchanger network is determined. It becomes possible to go into more details using the button named “divide main process” which builds up the various heat exchangers which appear in the block, either in series or in parallel, depending on the case.

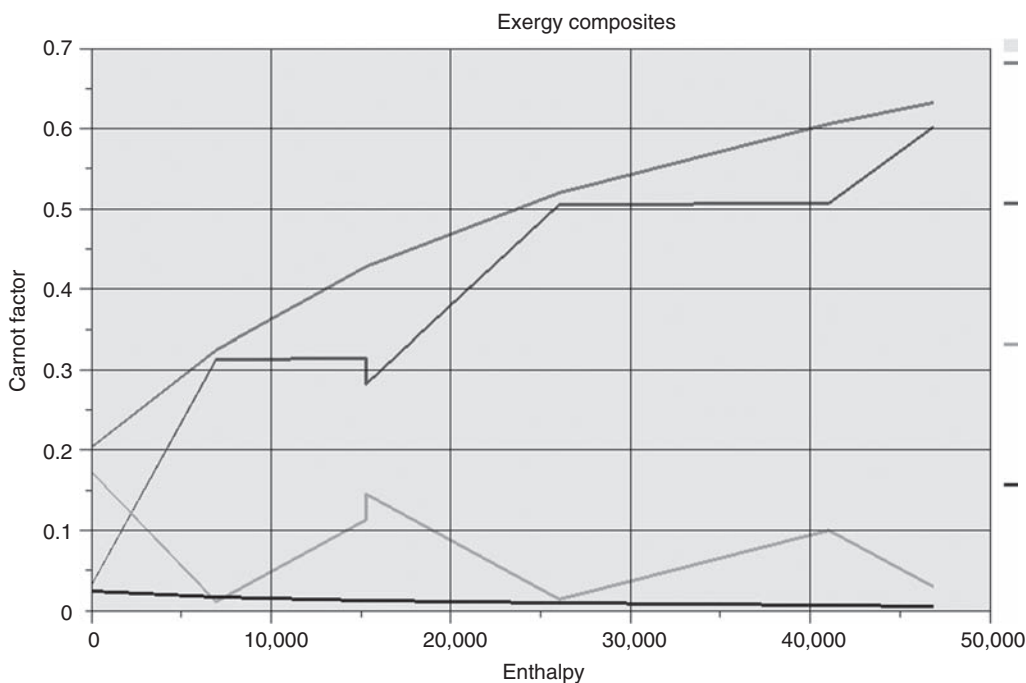
As stated in section 22.5.2.3, new points and processes are created. Once these sub-blocks built, they can be converted in heat exchangers by the button “create a heat exchanger”, then set. In a case like this, the stream inlet temperatures and flow rates are known, and the outlet temperature of the steam-side stream. The calculation option is unconstrained. Gradually, we can define the whole heat exchanger network.

When we divide fluids and repeat the pinch minimization operation, we see that there is a slight deviation from the results given in the previous phase. This is because thermal integration algorithms operate under the assumption that the specific heat of gas is constant throughout the cooling, and equal to the average value obtained by dividing the total enthalpy by the mass flow. Thus when the stream is divided, the midpoint has a heat capacity slightly different from that which had been considered initially, and a small adjustment is needed. In this example, we can ultimately choose the mass flow rates equal to 11.5 kg/s for the HP line, and 3.72 kg/s for the LP line. The total power produced is slightly increased (59,261 kW), and the cycle efficiency reaches 60%.

Figure 22.6.11 shows the synoptic view of the combined cycle obtained.

**FIGURE 22.6.13**

Mixed problem composites and CFDC

**FIGURE 22.6.14**

Mixed problem composites and CFDC (smoothed curves)

It is also possible to resume systemic optimization by imposing only part of the exchangers, those which have been declared active. In this case, this is not, however, of particular interest.

The menu line “Plot the mixed HX-TI curves” allows representation of the composite curves including on the one hand the selected exchangers, and on the other hand streams not selected

which are taken into account by the optimization method (for details, you should refer to article (Gicquel, 1996)). Figures 22.6.13 and 22.6.14 show what one gets for the case we just discussed if all blocks are selected. In the first, heat exchangers in parallel are not smoothed, in the other they are.

REFERENCES

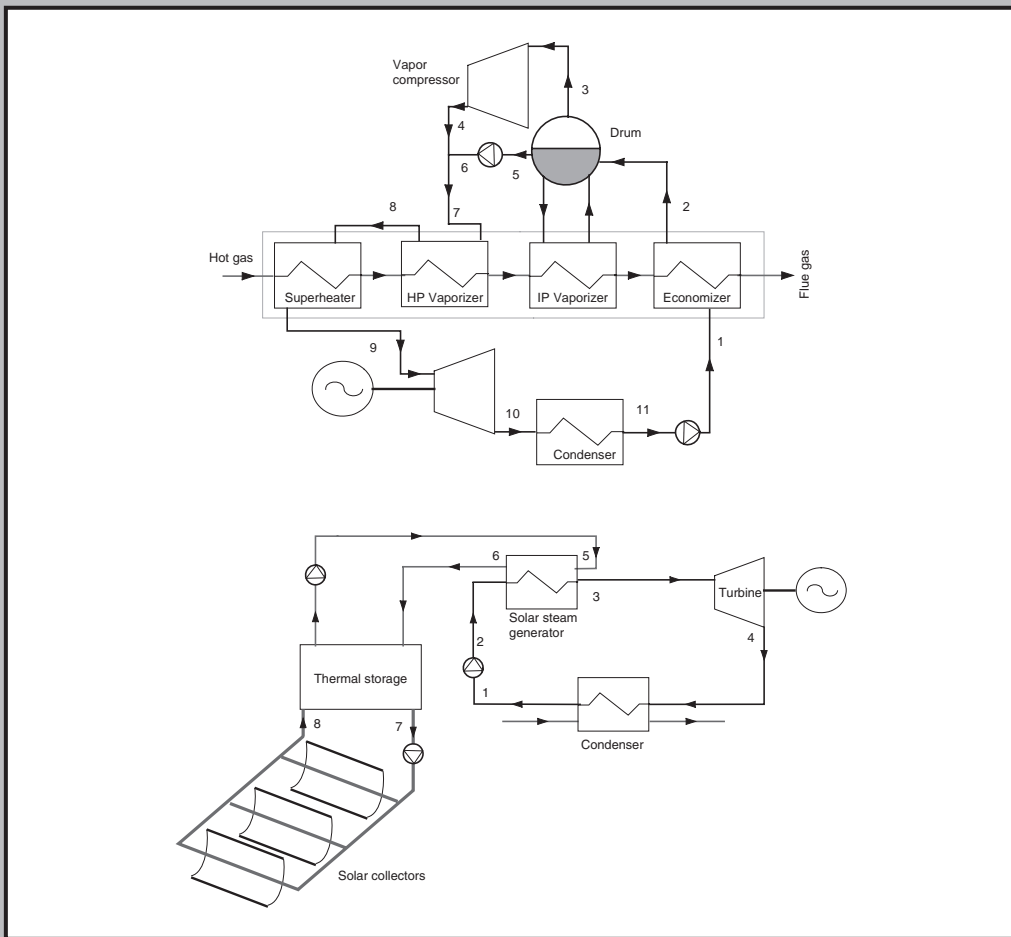
- C. Floudas, I. GROSSMANN *Synthesis of flexible heat exchanger networks for multiperiod operation*, Computers and chemical engineering, Pergamon Press, Oxford, 1986, Vol 10, n° 2, pp. 153–168.
- R. Gicquel, *Méthode d'optimisation systémique basée sur l'intégration thermique par extension de la méthode du pincement : application à la cogénération avec production de vapeur*, Revue Générale de Thermique, tome 34, n° 405, octobre 1995.
- R. Gicquel *Modics, Généralisation de la méthode d'optimisation systémique aux systèmes thermiques avec échangeurs imposés*, Revue Générale de Thermique, tome 35, pp. 423–433, 1996.
- J.P. Gourlia, *La méthode du pincement ou exploitation des diagrammes température/enthalpie*, Notions de base, Revue Générale de Thermique n° 327, Paris, 1989.
- B. Linnhoff, *User Guide on Process Integration for the Efficient Use of Energy*, Pergamon Press, Oxford, 1982.
- B. Linnhoff, E. Hindmarsh, *The pinch design method for heat exchanger networks*, Chemical Engineering Sc., Vol. 38, n° 5, pp. 745–763, 1983.
- B. Linnhoff, *Use pinch analysis to knock down capital costs and emissions*, Chemical Engineering Progress, august 1994, pp. 32–57.
- T. Trivedi, *Pinch Point analysis, The CRC handbook of thermal engineering*, (Edited by F. Kreith), CRC Press, Boca Raton, 2000, ISBN 0-8493-9581-X.

FURTHER READING

- V. R. Dhole, J. Zheng, *Applying combined pinch and exergy analysis to closed cycle gas turbine system design*, ASME COGEN-TURBO, 1993.
- J.P. Gourlia, A. Cavailles, *Expertise de procédés par diagrammes température/enthalpie*, Entropie n°160, 1991.
- I. Grossmann, R. Sargent, *Optimum design of heat exchanger networks*, Computers and chemical engineering, Pergamon Press, Oxford, 1978, Vol 2, pp. 1–7.
- B. Leide, R. Gicquel, *Systemic approach applied to dual pression HRSG*, International Gas Turbine & Aeroengine Congress and Exhibition, Orlando, Florida, 2–5 June 1997.
- B. Linnhoff, V. R. Dhole, *Shaftwork targets for low temperature process design*, Chemical Engineering Sc., Vol. 47, n° 8, pp. 2081–2091, 1992.
- J. Zheng, V. R. Dhole, *Conceptual design of commercial power plants using the combined pinch and exergy approach*, IGTI-Vol. 9, ASME COGEN-TURBO, 1994.

4

Innovative Advanced Cycles, including Low Environmental Impact



This Part completes Part 3 by addressing innovative advanced cycles, including low environmental impact ones,

This page intentionally left blank

External Class Development

Abstract: Based on the experience of its users and the expectations they raised, it appeared desirable to extend the capabilities of the tool so that it would solve problems more difficult than those for which it was originally designed: advanced modeling of certain energy systems was beyond the capabilities of Thermoptim versions released before late 2002, their limits being in two main dimensions:

- first, the area covered by the package: only predefined core components available on the diagram editor palette could be used in energy systems studied. Even if they allowed representation of a very large number of conventional energy technologies, some could not be modeled in Thermoptim, including new systems with low environmental impact. In the same vein, some users had expressed the wish to change models available in the tool by introducing their own equations, which was then impossible;
- secondly the modeling fineness: phenomenological models built certainly allowed one to study thermodynamic cycles of technologies studied, but not to perform specific technological design or to simulate off-design behavior, the latter two issues being much more complex than the first.

These new features are presented in this Chapter (external class development) and in Part 5 (technological design and off-design operation). They are dedicated primarily to confirmed readers wishing to perform advanced modeling. Even if the goal remains to facilitate the study of energy systems, some issues discussed are much more complex than those previously treated.

Keywords: External classes, technological design, external driver.

23.1 GENERAL, EXTERNAL SUBSTANCES

23.1.1 Introducing custom components

The external class mechanism was very briefly introduced in section 6.4 of Part 2 (Thermoptim presentation), without detailed examples, explanations being primarily intended for users. In this chapter, for designers¹, we show how to create simple external classes, giving explanations allowing one to understand their construction principles.

¹ We assume in this chapter that the reader is familiar with the Java language, and do not explain basic programming notions.

In earlier versions of Thermoptim, the only available components could be described as mono-functional since they involve only one form of energy (either mechanical or thermal). This is the case of adiabatic compressors and expansion devices, isenthalpic throttling devices, heat exchangers, combustion chambers etc.

The first three Parts of this book are largely confined to the study of energy technologies involving such mono-functional components. This choice is justified both by the bias to provide a method as simple as possible for beginners, and by the fact that many energy technologies do only involve such components, so that in practice these limitations were largely offset by the simplifications they provide.

However, there are cases where it is desirable to represent more complex multi-functional components. Consider, for example (Figure 18.6.1 of Part 3) the “absorber/solution exchanger/desorber subsystem” of a liquid absorption machine such as that presented in section 18.6 and 20.3 of Part 3: such a cycle involves a pair solvent/solute such as LiBr-H₂O or H₂O-NH₃ (mixtures whose properties are not available in Thermoptim’s core), and requires on the one hand a heat supply at high temperature in the desorber, and on the other hand heat extraction at medium temperature in the absorber).

Because there is a wide variety of multi-functional components, and secondly it is much harder to agree on models representative of their operation than for those of Thermoptim core, it was considered preferable, rather than seeking to include a few in this core, to offer the possibility to extend the package by adding plug-ins that define both the equations and the graphical interface. Written in the Java language but calling if need be on libraries created in other languages, these additional elements are dynamically loaded when starting the software, and appear in its screens as if they were an integral part. They are transparent to the user who can customize Thermoptim by adding his own models as external classes (Java code elements).

A user can extend the software environment by adding his own components, his own substances, defining his own after-processing, controlling the convergence of solving algorithms etc.

While an absorption machine could not be modeled in the earlier versions of the software, it can be done defining three new external classes to represent the pair solvent/solute, the absorber and the desorber (Figure 23.1.1).

The extension mechanism can be used to broaden to process engineering the Thermoptim scope, hitherto limited to nonreactive energy systems (except combustion). It is especially possible with the software to model systems at the interface between these two disciplines corresponding to quite exciting new research issues:

- the need to better control emissions of pollutants leads to integration of more and more operations of sewage treatment in energy conversion facilities (catalytic converters, decarbonation, deNO_x), which results in additional complexity of these devices and the rise of skill needs in process engineering and system integration for energy technologies;
- in parallel, reducing the environmental impact of chemical industries among others leads more and more consumers to seek to reduce their energy consumption. Process engineering itself increasingly requires skills in energy and system integration.

External classes are distributed according to a free software logic (open source) to facilitate their implementation and help build libraries of components reusable and easily customizable if the need arises, by a community as large as possible.

External components are of four types, depending on the number of input and output streams:

- external processes have a single stream as input, and one as output whose substance can be, as appropriate, the same as the input one or another;
- external mixers are connected to multiple inlet streams, usually associated with different substances, and only one at the outlet;
- external dividers are connected to a single inlet stream, and several at the outlet, usually associated with different substances;

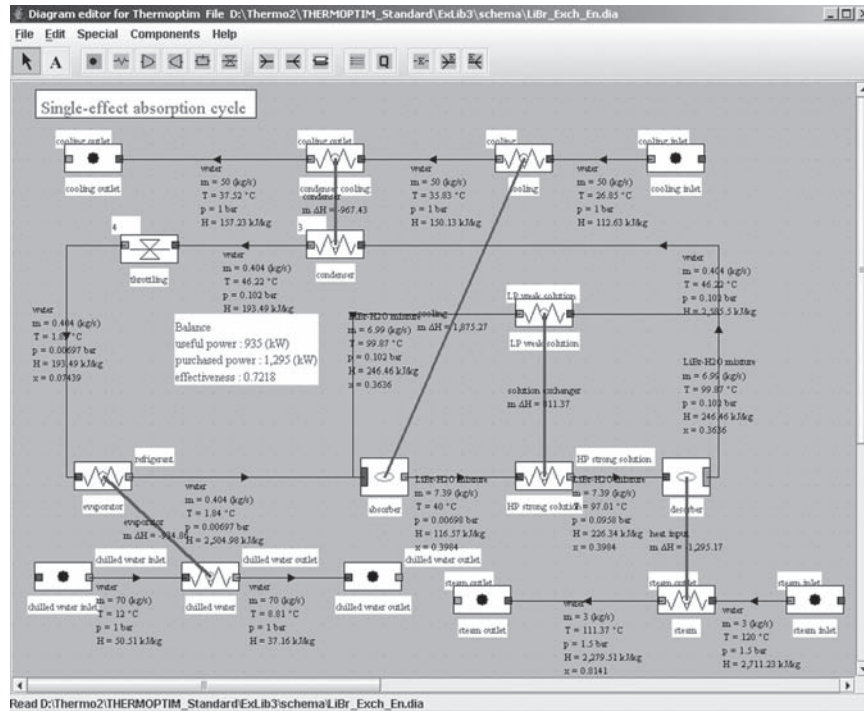


FIGURE 23.1.1

Synoptic view of the absorption cycle

- finally, components connected to multiple streams at inlet as well as at outlet, which form a multipole, are represented by the combination of an external input mixer and an external output divider, connected by a process-point, direct connection between two nodes being not possible in ThermoOptim for reasons of logical consistency.

The model library under constitution has already a score of documented models (solar collector, diffuser, nozzle, absorber and desorber for the lithium bromide-water pair, shift CO reaction, fuel cells, reformer) and will be completed in the next years.

It is obvious that the design of such external classes requires more knowledge of thermodynamics and ThermoOptim software environments than those necessary for simply assembling predefined components. Package documentation specifies rules to follow and provides a number of examples, but cannot go into details of the underlying problem exposed in this book.

PRACTICAL APPLICATION

Java development environment

Without being very difficult, the creation of new classes requires a minimum of external Java programming skills. The examples presented in Volume 3 of the reference manual help you initiate this exercise, and an external class development environment is presented in the ThermoOptim-UNIT portal (<http://www.thermooptim.org/sections/logiciels/thermooptim/ressources/utilisation-conception>).

It allows you to write your classes in Java, compile them and directly test their integration into ThermoOptim.

A Web page explaining how to install and configure this environment has been prepared for you.

In this chapter we restrict ourselves to some indications on the following classes:

- a simple substance (Dowtherm A) and an external mixture (pair LiBr-H₂O);
- a simple external process, to model a flat plate solar collector;
- rules for performing calculations of moist mixtures in external classes;
- rules for performing combustion calculations in external classes;
- two examples of classes involving moist mixtures: a condensing cooling coil and a direct contact cooling tower. These classes involve external nodes;
- a very simple external driver for a Stirling engine;
- the external class manager.

For further details please refer to Volume 3 of ThermoOptim reference manual. Some code excerpts are given below, but it is recommended that you get the complete Java classes available in the ThermoOptim-UNIT portal model library.

23.1.2 Simple substance: example of DowTherm A

It is common that one wishes to use in ThermoOptim a substance whose properties are very simple to model, such as a thermal fluid, not available in the core. We illustrate how to proceed with class DowThermA.java, which represents an oil sold by Dow Chemical, which may in particular serve as thermal fluid for high temperature solar collectors (100–400°C). The substance remains permanently in the liquid state, and calculations are simple: for example that of the enthalpy sole function of temperature, and its reversal.

23.1.2.1 Creation of the class

To create an external substance, just subclass `extThopt.ExtSubstance`.

The very simple constructor initializes molar mass, critical pressure and temperature and the range of validity of the model. Values of parameters used in the properties equations are then set:

```
public DowThermA () {
    //data from FLUIDFILE, Dow Chemical calculation software
    //données extraites de FLUIDFILE, logiciel de calcul de Dow Chemical
    super ();
    type=getType ();
    M=166; PC=31.34; TC=770.15;
    Tmini=288.15; Tmaxi=680;
    chemForm="C12H100 (73.5% vol), C12H10 (26.5% vol)";
    aCv=0.003037892;//valeurs du Cp [kJ/(kg K)], fonction affine Cp=a*t+b avec t=T-273.15
    bCv=1.466457638;//Cp [kJ/(kg K)] values, Cp=a*t+b with t=T-273.15
    aV=-0.430370424;//valeurs du volume [m^3/kg], fonction parabolique inversée V=1/(c*t*t+a*t+b) avec t=
    bV=1041.622415;//volume [m^3/kg] values, reverse parabolic function V=1/(c*t*t+a*t+b) with t=T-273.15
    cV=-0.001179466;
    aVisc=1.080162;//valeurs de la viscosité [10^-5 Pa.s], fonction mu=c*t*t+a*t+b+d/T avec t=T-273.15
    bVisc=-641.5157547;//viscosity [10^-5 Pa.s] values, fonction mu=c*t*t+a*t+b+d/T with t=T-273.15
    cVisc=-7.95033E-04;
    dVisc=234997.5416;
    aCond=-0.00016;//valeurs de la conductivité [W/(m K)], fonction affine lambda=a*t+b avec t=T-273.15
    bCond=0.1419;//conductivity [W/(m K)] values, fonction lambda=a*t+b with t=T-273.15
}
```

Method `getType()` returns the type of substance as it will appear in ThermoOptim screens:

```
public String getType(){
    return "Dowtherm A";
}
```

Method `getClassDescription()` allows to enter a brief description of the class, which will appear in the display screen of external classes (see section 6.4 of Part 2). Give some indications on the model chosen, and if possible refer to more detailed documentation.

```
public String getClassDescription(){
    return "data from FLUIDFILE software by Dow Chemical\n\nauthor : R. Gicquel   march 2006";
}
```

23.1.2.2 Methods for calculating substance properties

Calculations of substance properties can be done as indicated below for enthalpy.

Direct calculation of enthalpy

Calculations of the specific heat capacity, enthalpy and entropy as a function of temperature are based on a polynomial fit (quadratic here) of the specific heat supplied by Dow Chemical in its software FLUIDFILE.

Similarly, the calculation of specific volume is made on the basis of an adjustment by a polynomial of order 3.

```
public double calcH (double T, double P, double x) {
    double V=calcV(T, P,x);
    double TT=T-273.15;
    return bCv*TT+aCv/2.*TT*TT+V*(P-1)*100;
}
```

T-inversion of enthalpy

The inversion of h in T is made by dichotomy:

```
public double getT_from_hP(double $h, double $P){
    double T=Util.dicho_T (this, $h, $P, "calcH", Tmini, Tmaxi, 0.0001);
    return T;
}
```

The calculations are very simple here. If this were to represent a condensable vapor, they would be much more complex. Class LiBrH₂O mixture.java presented below is an example a bit more complicated.

23.1.3 Coupling to a thermodynamic properties server

When the substance that you want to use in ThermoOptim is not as simple as the one we have been studying, writing all the methods for calculating the properties can become a very complex and laborious task. This is particularly true when dealing with mixtures of real fluids.

Considering both that the primary purpose of ThermoOptim is to model energy systems, from simple to complex, rather than being a software package for calculating the thermodynamic properties of substances, and secondly that there is a number of software applications specializing in this type of calculation, we found that the best solution was to combine these two types of environments, and so we have developed an external class sub-mechanism, which allows ThermoOptim to perform calculations by various thermodynamic property servers (TPS). By 2009, the TPSs which have been coupled ThermoOptim are ThermoBlend, NH₃H₂O, and ThermoSoft TEP, developed by the Center for Energy and Processes of École des Mines de Paris, and Refprop distributed by NIST in the U.S.A.

23.1.3.1 Characteristics of external mixtures

The names of pure external substances appear directly in the substance selection list screen where they are used to instantiate classes.

For external mixtures, things are much more complex, because the same external class can be used to define multiple systems, and each system generates as many compositions as the user wants, except of course if it is a pure substance, in which case both mole and mass fractions are equal to 1.

In a file placed in the “mixtures” directory, each class defines all the external systems it offers, which can be modified from ThermoOptim by the user.

Like for compound gases, the list of external mixtures is stored in a file called “mel_ext.txt”, which is updated whenever a new mix is created and is used to initialize the substance selection screen.

To instantiate an external mixture, you need to:

- ensure that the system is well defined in the correct file of folder “mixtures”;
- check that the external class is present in extThopt.zip or extUser.zip;
- create the mixture into the editor from a point screen, then save.

23.1.3.2 Example of external mixture: system LiBr-H₂O

The LiBr-H₂O system is a simple example of external mixture definition. The equations of this mixture were given in section 5.6.8.4 of Part 2.

This mixture, which was modeled in class H2OLiBrMixture.java, is presented in more detail in Volume 3 of the ThermoOptim reference manual.

The constructor does in this case the same initializations as before, and creates in addition Vector vMixtures, which here defines a single system.

Methods allow one to define the class description, the software used, the unit used to define the composition, the proposed system, and the identifier of the class.

The updating of the composition is made by the updateComp() method, and calculating of the substance state by the CalcPropCorps() method, calling the methods that ensure the resolution of equations (5.6.51) to (5.6.53) of Part 2.

THOPT
[CRC_In_14]

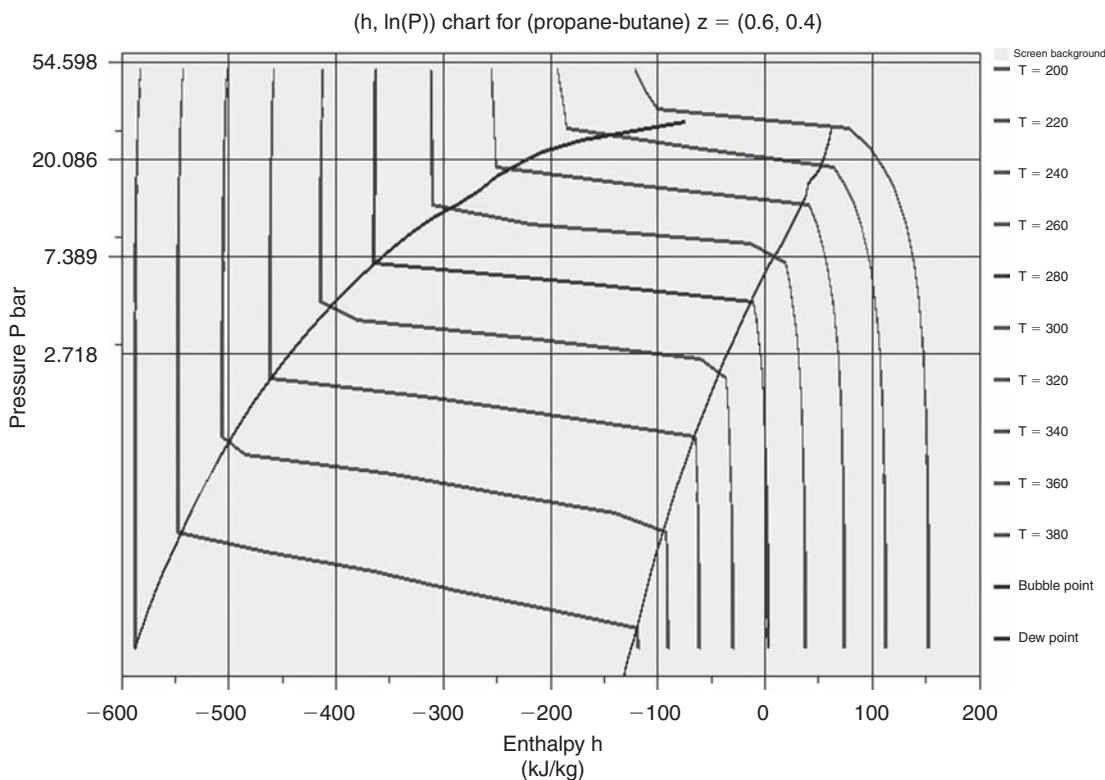


FIGURE 23.1.2

(h, ln(P)) chart for propane-butane system z = (0.6, 0.4)

This external substance is used to model the absorption cycle presented above (Figures 18.6.1 of Part 3 and 23.1.1).

23.1.3.3 Vapor charts for external mixtures

In order to allow one to plot cycles using external mixtures, vapor charts for external mixtures can also be partially plotted in (T, s) and (h, P) coordinates.

The only lines which are displayed are saturation curves as well as either isobars or isotherms depending on the chart (isotherms in Figure 23.1.2 relative to the propane-butane system presented in section 5.6.8 of Part 2).

23.2 FLAT PLATE SOLAR COLLECTORS

A flat plate solar collector² receives a radiative flux of variable intensity (less than about 1200 W/m^2), part of which is reflected and absorbed by the glazing. It is crossed by a fluid that heats up and recovers part of the available power, the rest being lost by heat exchange with the surroundings. The collector performance is characterized by two parameters: a radiative flux transmission coefficient representative of reflection losses and absorption, and a heat exchange coefficient with the outside air.

To be easily comprehensible, the model presented here (SolarCollector.java) is relatively simple in thermodynamic terms, easily calculable with these assumptions. However, it is complicated enough to show clearly the real problems that arise when creating an external component, and solutions to resolve them.

23.2.1 Design of the external component

23.2.1.1 General

Model parameters are:

- the glazing transmittivity τ
- the thermal loss coefficient U ($\text{W/m}^2/\text{K}$)
- the incident solar flux G (W/m^2)
- the collector surface A (m^2)
- the outside temperature T_{out} ($^{\circ}\text{C}$)

The model input data are as follows (provided by other system components):

- the thermal fluid temperature at the collector inlet T_i ($^{\circ}\text{C}$)
- the flow \dot{m} of the thermal fluid (kg/s)

The outputs are:

- the thermal fluid temperature at the collector outlet T_o ($^{\circ}\text{C}$);
- the thermal power received by the thermal fluid Q (W/m^2);
- the collector effectiveness.

23.2.1.2 GUI

A graphical interface for the component can be deduced (Figure 23.2.1). It allows to build the bottom third of the screen, the rest being defined as a Thermoptim standard.

² More detailed explanations on solar collectors are given in chapters 30 and 33 of this Part.

FIGURE 23.2.1

GUI of the external component

Parameters match the first five rows added, the calculation results automatically appear in the sixth row, in the downstream point state and in the field $\dot{m}\Delta H$. The input data is supplied by the upstream process of the system in which is inserted the component: thermal fluid flow and upstream point state.

23.2.1.3 Physical model

With the previous notations, the model equation (established in section 30.2.2) is:

$$Q = \dot{m}C_p(T_o - T_i) = \dot{m}C_p \left(\tau \frac{G}{U} - T_i + T_{out} \right) \left[1 - \exp \left(- \frac{UA}{\dot{m}C_p} \right) \right]$$

Specifically, the sequence of calculations is as follows:

- 1) component update before calculation from the upstream process and point;
- 2) reading of settings on the external component screen;
- 3) calculation of the thermal power into play and the downstream point state;
- 4) update of the external component screen.

Let us now consider the problems encountered in practice at each of these steps.

1) Component update before calculation by loading the upstream process and point

The hard part here is that an external component has no direct access to the variables of the simulator: these quantities are obtained by generic special methods that build Vectors of different structures according to the desired object.

The procedure is not complicated but needs to be respected:

```
String[] args=new String[2];
args[0]="process";//type of the element (see method getProperties(String
args[1]=tfe.getCompName();//name of the process (see method getPropertie
Vector vProp=proj.getProperties(args);
Double f=(Double)vProp.elementAt(3);
double flow=f.doubleValue();
String amont=(String)vProp.elementAt(1);//gets the upstream point name
getPointProperties(amont);//direct parsing of point property vector
Ti=Tpoint;
```

2) Reading of settings on the external component screen

Package `extThopt` provides a number of simple but robust methods for converting in double the String displayed in the `JTextField` controls used in the GUI, and vice versa for displaying double in these fields. They are implemented as static methods of class `extThopt.Util`:

```
P=Util.lit_d(P_value.getText());
A=Util.lit_d(A_value.getText());
tau=Util.lit_d(tau_value.getText());
K=Util.lit_d(K_value.getText());
Tout=Util.lit_d(Tex_value.getText()+273.15;
```

3) Calculation of the thermal power into play and the downstream point state

We begin by estimating the C_p of the thermal fluid in numerically deriving the enthalpy function:

```
double H=Hpoint;
lecorps.CalcPropCorps(Tpoint+1, Ppoint, Xpoint); //this method re
getSubstProperties(nomCorps);
double Cp=(Hsubst-H);
```

We then estimate the value of the outlet temperature in order to determine the thermal power absorbed Q :

```
double DTO=tau*P/K-Ti+Tout;
double T=Ti+(DTO)*(1-Math.exp(-K/1000*A/flow/Cp));
double DT=T-Tpoint;
double Q=Cp*DT*flow;
```

We determine the value of the enthalpy of the downstream point, and then reverse that function to determine the exact value of the outlet temperature (`ExtSubstance` method):

```
double hAval=Q/flow+Hpoint;
Tpoint=lecorps.getT_from_hP(hAval,Ppoint);
getSubstProperties(nomCorps);
Xpoint=Xsubst;
```

4) Update of the external component screen

`Thermoptim` method `setUpPointAval()` allows one to update the downstream point from the values loaded in a `Vector` built here by the method `getProperties()` of `ExtProcess`:

```
tfe.setUpPointAval(getProperties());
```

The value of the collector efficiency is then determined and displayed.

```
eff_value.setText(Util.aff_d(Q/P*1000/A, 4));
```

23.2.1.4 Saving and loading model parameters

It is possible to save in the normal `Thermoptim` project files (and then re-read) the settings of external components using two specific methods:

```
public String saveCompParameters()
public void readCompParameters(String ligne_data)
```

The only constraint is that the entire external component setting must fit into one line, with a format compatible with that used in the core of the package: the various backup fields are separated by tabs.

`extThopt.Util` provides a generic method to attribute to the value of a parameter a code allowing it to be identified:

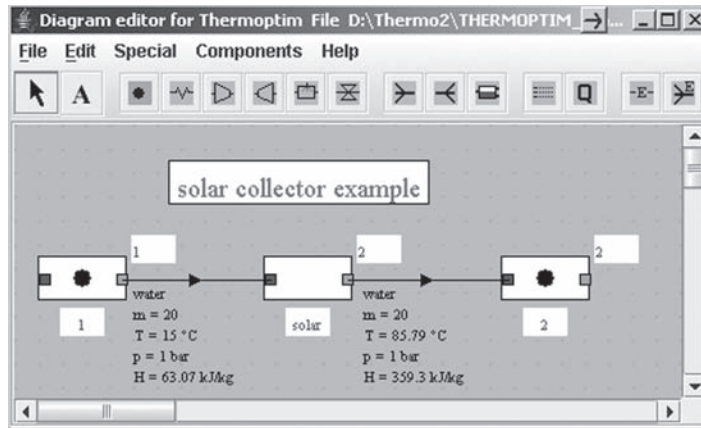


FIGURE 23.2.2
Simulation of a water solar collector

```
public static String extr_value(String ligne_data, String search)
The backup is done in the form "parameter = value" and the search is made in the form:
value = Util.lit_d(Util.extr_value(ligne_data, "parameter"));
```

If the configuration of the component is too complex to be saved in this way, nothing prevents a user from using it to save the name of a specific setting file, and then to re-read this file as he wants.

Examples of use of this class are given in Chapter 30 of this Part and in the ThermoOptim-UNIT portal.

23.3 CALCULATION OF MOIST MIXTURES IN EXTERNAL CLASSES

23.3.1 Introduction

We call a moist mix, and by abuse of language **moist gas**, a mixture of a gas that does not condense, which we call the **dry gas**, and **water** that could condense.

Since its inception, ThermoOptim has functions for calculating properties of moist gases and points, but these are generally used for particular calculations, decoupled from standard thermodynamic cycle calculations, such as for air conditioning treatment (see Chapter 21 of Part 3). It is for this reason that moist processes have no symbol in the diagram editor.

We assume in what follows that the reader is sufficiently familiar with both external class use and moist gas thermodynamics. The definitions, notations and equations are those in section 7.8 of Part 2.

For convenience we use the term **standard** when we refer to the ThermoOptim environment except moist calculations.

The standard ThermoOptim cycle computing environment and that of moist calculations are not directly compatible for two reasons:

- following use in moist calculations, the values of thermodynamic functions are generally referred to the dry gas, whose composition is invariant, whereas the standard calculations performed in ThermoOptim are relative to the actual composition of the gas. The values to which they lead are called specific, to distinguish them from others;
- furthermore, reference temperatures and pressures not being the same in both environments, it is necessary to do conversions when switching from one to another.

However, a number of thermodynamic cycles involve changes in gas moisture, and it was unfortunate not to be able to model them easily with ThermoOptim. That is why the ThermoOptim functions for calculating properties of moist gases and points have been made available from external classes. This section explains how to use them.

A moist gas can be represented in ThermoOptim in two equivalent ways:

- either directly as a compound substance comprising at least two components: H₂O and another gas, pure or compound;
- or as a dry gas of known specific humidity.

The first way has the advantage that the composition of moist gas is available at any time. However, it implies, for the same dry gas, creating a new substance for each value of moist moisture. The second presentation is itself much more concise, since it only uses the invariant gas and the humidity value. This is why it is used by moist gas calculation functions, while the first is the rule in the standard ThermoOptim cycle computing environment.

Let us recall that we call **relative humidity** ϵ the ratio of the partial pressure of water vapor divided by its saturation vapor pressure at the temperature of the mixture, and that, by definition, index dg corresponding to the dry gas, **absolute or specific humidity** w is equal to the ratio of the mass of water contained in a given volume of moist mixture to the mass of dry gas contained in this volume, namely:

$$w = \frac{y_{\text{H}_2\text{O}}}{y_{\text{dg}}} = \frac{M_{\text{H}_2\text{O}}x_{\text{H}_2\text{O}}}{M_{\text{dg}}x_{\text{dg}}} = \frac{18x_{\text{H}_2\text{O}}}{M_{\text{dg}}(1 - x_{\text{H}_2\text{O}})}$$

This relationship allows the calculation of w when we know the moist gas composition.

23.3.2 Methods available in the external classes

Generally, moist gas calculations are made (from external classes) from one point, but a method allows one to directly modify the humidity of a gas. The gas humidity is entered giving either its absolute humidity w or its relative humidity ϵ . Both methods are defined in class ExtProcess, of which derive all external processes and nodes.

Method **updatepoint**("pointName", ...) can do moist calculations while method **getPointProperties**("pointName") recovers in addition to the standard properties (P, T, h, s ...), a point moist properties with the following values: Wpoint for absolute humidity w , Epsipoint for relative humidity ϵ , Qprimepoint for specific enthalpy q' , Tprimepoint for adiabatic temperature t' (°C), Trpoint for dew temperature t_r (°C), VPrimepoint for specific volume v_s , Condpoint for condensates, and M_secpoint for molar mass of dry gas.

23.3.2.1 Search of a point humidity

When the point state has been calculated, w is known and method **getPointproperties**("nomPoint") allows one to access it directly.

When the gas composition is determined by programming, it may be necessary to recalculate w , which can be done by the following formula, fractH2OFuel being $x_{\text{H}_2\text{O}}$:

$$//w = \frac{M_{\text{H}_2\text{O}}x_{\text{H}_2\text{O}}}{M_{\text{dg}}x_{\text{dg}}}$$

```
// / Calculate the gas absolute humidity
double inlet_w=18.01528*fractH2OFuel/fuelM/(1-fractH2OFuel);
```

23.3.2.2 Updating a point moist properties

Method `updatepoint`(String name, boolean updateT, double T, boolean updateP, double P updateX boolean, double x, boolean melHum, String task, double value) is a generic method for update and recalculation of point state variables, which has been generalized to allow for moist calculations.

If boolean melHum is false, the point update is for T, P, or x, depending on whether booleans updateT, updateP updateX are true or false: this is a standard property update without moist calculations.

If boolean melHum is “true”, only moist calculations are made, even if updateT, and updateP updateX are “true”.

These calculations are defined by two parameters **task** and **value**.

task is a String specifying the type of calculations to perform, and **value** a double providing the value of the variable to modify.

1) Calculations without changing the gas composition

The calculations being performed with respect to dry gas, the gas composition is not changed.

Set specific humidity w

If task = “setW and calculate all”, Thermoptim sets w (passed in value) and calculates all moist properties.

When the temperature of a point is high, convergence problems may arise in calculating the wet bulb temperature t' . To circumvent this difficulty, the setting below only calculates specific enthalpy.

If task = “setW and calculate q' ”, Thermoptim sets w (passed in value) and calculates all moist properties except t' .

If task = “calcWsat” Thermoptim calculates w_{sat} and all moist saturation properties except t' .

Set the relative humidity ϵ

If task = “setEpsi” Thermoptim sets ϵ (passed in value).

If task = “setEpsi and calculate”, Thermoptim sets ϵ (passed in value) and calculates all moist properties except t' .

2) Changing the gas composition

2.1 By operating indirectly from a point

Method `updatePoint()` allows to alter the composition of a gas, with the following settings:

If task = “modHum” Thermoptim changes the composition of the gas so that its moisture equals W_{point} (there is then no need to pass a value).

If task = “setGasHum” Thermoptim changes the composition of the gas so that its moisture is equal to w (passed in value).

2.2 By operating directly on the gas

It is also possible to change the humidity of a gas regardless of a point state, using method `updateGasComp()` of `GazIdeal`, accessible by `public void updateGasComposition(Vector Vcomp)` of `Corps`: if the first `Vcomp` element is an Integer of negative value, a particular treatment is made. The absolute humidity passed as third `Vcomp` element is set on the gas.

The example below, from class `BiomassCombustion` shows how to change the composition of a dry gas to match the moist gas whose water mole fraction is `fractH2Ofuel` (see previous section):

```
// Shaping the Vector
Vector vComp=new Vector();
vComp.addElement(new Integer(- 1));
vComp.addElement("setGasHum");
vComp.addElement(Util.aff_d(inlet_w));
// Change the gas composition
NewFuelSubstance.updateGasComposition(vComp);
```

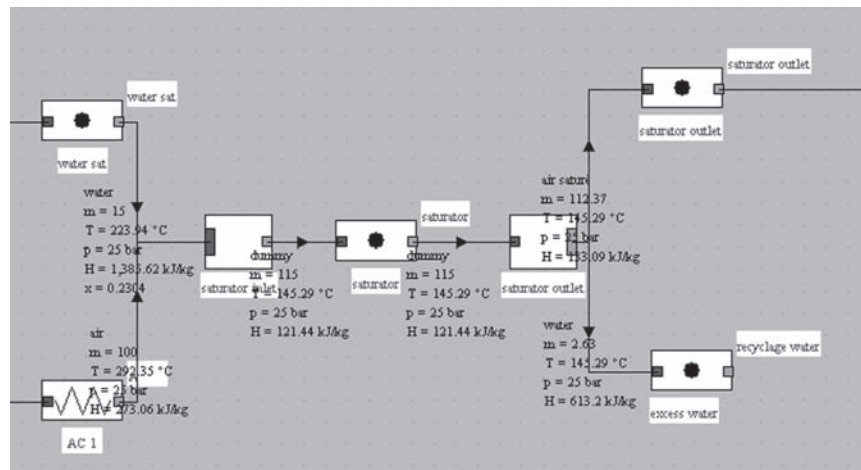


FIGURE 23.3.1

Saturator

23.3.2.3 Usage example: saturator model

In a humid air gas turbine (see section 12.1), the capacity of the machine and the cycle efficiency are increased by humidifying the air in a saturator before entering the combustion chamber. The cycle is quite complex to optimize heat recovery, but the saturation model is relatively simple (Figure 23.3.1): water at a temperature of about 280°C enters the saturator, where it is contacted with a stream of hot (200°C) and relatively dry air leaving the compressor. A portion of the water is vaporized and used to increase the humidity of the air coming out close to being saturated. The remaining water is recycled. It is assumed here that the saturator is adiabatic and that water and air exit at the same temperature.

The class code (Saturator.java) is as follows:

- 1) we begin by getting the incoming gas composition, and we update the composition of the outlet gas, a precaution in case the two dry gases would be different.

```
//Propriétés humides du gaz entrant
//moist properties of the inlet gas
args[0]="process";//type of the element (see method getProperties(String[] args))
args[1]=wq.gasProcess;//name of the process (see method getProperties(String[] args))
Vector vProp=proj.getProperties(args);
String amont=(String)vProp.elementAt(2);//gets the downstream point name
getPointProperties(amont);//direct parsing of point property vector
getSubstProperties(nomCorps);
double M=Msubst;
Vector vComp=lecorps.getGasComposition();
outletGasSubstance.updateGasComposition(vComp);//on met à jour la composition du gaz en sortie
//the outlet gas composition is updated
```

- 2) we calculate the inlet absolute humidity with the definition formula, to avoid, given the high temperature of gas, having to estimate the saturation conditions.

```
//on calcule w inlet par la formule de définition, pour éviter, compte tenu de la
//température élevée du gaz, d'avoir à estimer les conditions de saturation
//w inlet is calculated by the definition formula, in order to avoid to estimate
//saturation conditions due to the high gas temperature
double fractH2O=Util.molarComp(vComp,"H2O");//fraction molaire de H2O
double inlet_w=fractH2O*18.01528/M_secpoint/(1-fractH2O);//(M_H2O)(x_H2O)/(M_gs)/(x_gs)
getPointProperties(amont);
double inletT=Tpoint;
```

- 3) the dry gas flow and the inlet gas specific enthalpy are determined, using methods `updatepoint()` and `getPointProperties()`:

```
//estimation du débit de gaz sec
//estimation of the dry gas flow rate
Double f=(Double)vProp.elementAt(3);
double flow=f.doubleValue();//débit massique de gaz humide / moist gas flow rate
flow_as=flow/(1+inlet_w);//débit massique de gaz sec / dry gas flow rate

updatepoint(wq.gasPoint, false, 0, //T
            false, 0, false, 0, //P,x
            true, "setW and calculate q'", inlet_w);
getPointProperties(wq.gasPoint);
//enthalpie spécifique du gaz entrant dans le saturateur
//specific enthalpy of the gas entering the saturator
qPrimeAmont=QPrimepoint;
```

- 4) At this stage, the upstream moist gas properties are perfectly calculated. We must now determine the saturator exit temperature, solving simultaneously:
- water balance (the flow of water consumed is equal to the product of the dry gas flow by the gas moisture variation);
 - enthalpy balance (the sum of incoming enthalpy flows (specific units for the moist gas) is equal to the sum of outgoing enthalpy flows. Since T_s is unknown, we do a solution search by dichotomy, using generic function `Util.dicho_T()`, which uses `f_dicho()`. The code operates as follows:
 - humidity is passed as input argument, instead of the pressure, otherwise known;
 - we first calculate the enthalpy h_{eau} (T_s) of water at the outlet;
 - we change the gas outlet temperature, then its moisture from the value read on the screen, and we get the values of its absolute humidity and specific enthalpy;
 - we calculate the flow of water left (although we should do a test to make sure it remains positive);
 - we write that the enthalpy lost by the water ends up in the air, and calculate residue `diff`;
 - temperature T_s is determined when `diff = 0`.

```
if (fonc.equals("saturator")){
    double diff;
    double w_dicho=P;
    //enthalpie de l'eau en sortie / outlet water enthalpy
    updatepoint(waterPoint, true, T, //T
                false, 0, false, 0, //P,x
                false, "", 0);
    getPointProperties(waterPoint);//état de l'eau en sortie / outlet water state
    double hEau=Hpoint;

    //enthalpie spécifique et humidité spécifique du gaz en sortie
    //specific enthalpy and moisture of the gas exiting the saturator
    updatepoint(gasPoint, true, T, //T
                false, 0, false, 0, //P,x
                false, "", 0);
    updatepoint(gasPoint, false, 0, //T
                false, 0, false, 0, //P,x
                true, "setEpsi and calculate", Util.lit_d(outletEpsi_value.getText()));
    getPointProperties(gasPoint);//propriétés humides / moist properties
    waterFlow=wq.waterFlow - (Wpoint-w_dicho)*flow_as;//débit d'eau restant / remaining flow rate
    //on écrit que l'enthalpie perdue par l'eau se retrouve dans le gaz
    //we write that the enthalpy lost by water is received by the gas
    diff=wq.waterFlow*wq.waterH-hEau*waterFlow+flow_as*(qPrimeAmont-QPrimepoint);
    return diff;
}
```

5) T_s being determined, we change the composition of moist gas at the outlet:

```
//modification de la composition du gaz / modification of the gas composition
outletT=T;
updatepoint(gasPoint, false, 0, //T
            false, 0, false, 0, //P,x
            true, "modHum", 0);
getPointProperties(aval);
```

6) Consistency checks

Using the values that appear on the diagram of Figure 23.3.1, we can build the apparent saturator balance:

	kW
total inlet enthalpy flow	65,012
total output enthalpy flow	22,570
apparent discrepancy	42,443
difference per kg/s of water consumed	$L_{\text{water}} = 2,547$

Everything happens as if 42.4 MW of heat disappeared but, as shown in the last row of the table, this value corresponds exactly to the enthalpy of vaporization of water in the moist gas, which is not recognized in the values displayed by ThermoOptim given the conventions adopted for ideal gases (zero enthalpy at 25°C and 1 bar).

Obviously, if we sufficiently cooled exhaust gases for the water they contain to condense, this enthalpy would appear again (with the addition of the water formed in the combustion chamber).

23.4 EXTERNAL COMBUSTION

In order for external classes to access combustion calculations available in ThermoOptim, various modifications have been made to the package. They are detailed in Volume 3 of the ThermoOptim reference manual, while combustion setting is presented in Volume 2.

Combustion parameters are exactly the same as that required for combustion calculated in ThermoOptim core, with the proviso that it is possible to set a heat load to be taken into account in calculating the end of combustion temperature. It is also possible to perform preliminary calculations before starting calculations in ThermoOptim. Class BiomassCombustion.java in the model library illustrates how to use these features.

23.4.1 Model of biomass combustion

This section presents briefly the external class BiomassCombustion. This is a simplified model that can simulate different types of biomass combustion, and in which it is possible to vary with some flexibility the composition and fuel moisture and combustion conditions. BiomassCombustion class can be used to simulate both a boiler and a downdraft gasifier.

The main thermodynamic parameters that influence biomass combustion are:

- first, of course, fuel composition;
- second, moisture, which determines the enthalpy required for drying, plays on the gas composition, and finally influences CO_2 dissociation;
- finally, quenching temperature and CO_2 dissociation rate.

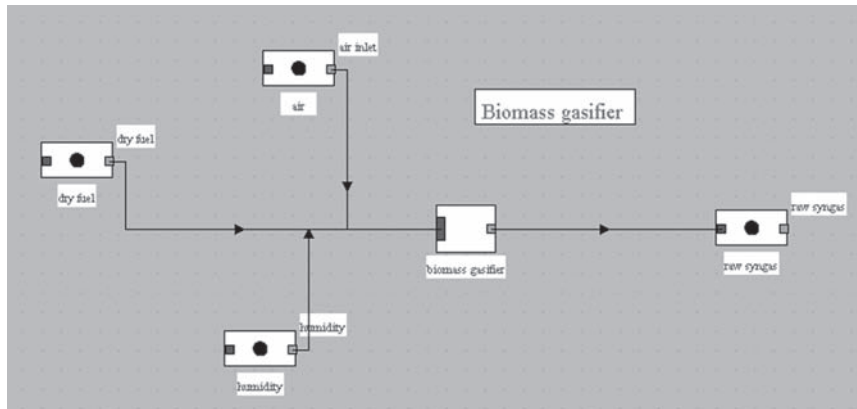

FIGURE 23.4.1

Diagram of the combustion structure

To separate as much as possible the influence of the first two parameters, composition is that of dry fuel, and moisture is taken into account by adding water. Given that overall moisture is not necessarily the one that governs the thermodynamic equilibrium, as part of the steam may not react, for reasons of kinetics or geometry, we introduced an additional parameter, equal to the fraction of water involved in combustion. Physically, this means that a fraction of water is not dissociated: it must be vaporized but its influence on the gas composition is the same as if it were inert.

23.4.1.1 Fuel definition and combustion progress

Fuel definition is made in ThermoOptim as follows (Figure 23.4.1):

- dry gas composition, excluding species not included in ThermoOptim core, is estimated, for example in a spreadsheet, and entered in the form of a compound gas (process-point “dry fuel”);
- species not considered by ThermoOptim core are considered separately: they are entered in the component screen, and are subject to pre-combustion;
- the dry gas is mixed with water (H₂O gas) to form the moist fuel (process-point “humidity”);
- final combustion is calculated by core ThermoOptim functions, which are emulated from the external class (external mixer “biomass combustion”), taking into account pre-combustion and the enthalpy that would have been required to evaporate the water.

The oxidizer (usually air) is itself defined in process-point “air inlet”. Flows involved are also specified in each of the three processes-points entering the external mixer. Their respective ratios allow one to play on fuel moisture and excess air.

23.4.1.2 Example of lack of air combustion (gasifier)

Biomass gasification is partial oxidation of an organic resource, mainly composed of cellulose (C₆H₁₀O₅) to produce synthesis gas. Biomass being generally very wet, oxidation takes place in four stages:

- fuel drying;
- pyrolysis or carbonization (in the absence of oxygen), producing tars and carbon;
- combustion of carbon and oxygen, exothermic reaction drying fuel among others;
- reduction of CO₂, H₂ and water by carbon and tar.

By performing lack of air combustion, we can model a downdraft gasifier (Figure 23.4.1) using class BiomassCombustion. We assumed here that only 50% of fuel moisture takes part in combustion, the rest not participating.

FIGURE 23.4.2

Component biomass gasifier

component name	molar fraction	mass fraction
CO2	0.09095625	0.1780174
H2O	0.2800306	0.2243506
N2	0.3332404	0.4151491
CO	0.1293294	0.1611006
H2	0.1626134	0.01457812
Ar	0.003829836	0.006804206

FIGURE 23.4.3

Composition of raw synthesis gas (LHV: 3.4 MJ/kg)

Figure 23.4.2 shows the component screen allowing one to model biomass combustion. In the case presented, it is assumed that fuel comprises 0.634% ammonia and 10.5% carbon referred to dry mass, that the quenching temperature equals 900°C and that 50% of the moisture is involved in combustion.

As we have said, the input flow-rates of fuel, water and oxidizer obviously play a fundamental role, as their ratios directly influence the synthesis gas composition (Figure 23.4.3).

In this example, fuel moisture is 50% by mass, the flows of the two processes “dry fuel” and “humidity” being equal. Air flow being less than that which would have ensured a stoichiometric combustion (about 7.8 kg/s), combustion occurs in lack of air and the CO₂ dissociation rate is recalculated.

The synthesis gas temperature depends a lot on the heat of reaction, itself a function of oxygen available: if there is very little, it is mainly CO that is produced with few CO₂.

The raw synthesis gas, high humidity, can be washed and partially dried, using class WaterQuench presented in the ThermoOptim-UNIT portal model library.

23.4.1.3 Access to combustion calculations from external classes

So that external classes can access combustion calculations available in ThermoOptim, various modifications were made to the package. In particular, a class called ExternalCombustion, which inherits

directly from Combustion, was added. Accessible from MixerExterne, it allows for combustion calculations in the following manner:

- we start by building Vector vSettings, which includes the three ideal gases involved (oxidizer, fuel, exhaust gases) and all the necessary settings to specify the required calculations;
- the method public void calcExternalCombustion(Vector vSettings) of MixerExterne initiates the combustion, then performs calculations required;
- results are then retrieved by the method public Vector getExternalCombustionResults() of MixerExterne, which returns a Vector comprising the flue gas composition, end of combustion temperature, lambda, energies involved etc.

From external classes (only in external mixers, a combustion chamber being structurally similar to a mixer), access is through the methods of the same name in ExtMixer, with calls like:

```
calcExternalCombustion(vSettings);
Vector results=getExternalCombustionResults();
```

23.4.2 Presentation of the external class

The class is an external mixer (Figure 23.4.1), which receives as input on the one hand water, representing fuel moisture, and on the other hand two gases: the oxidizer, identified by the fact that it contains both oxygen and nitrogen, and fuel, which does not contain both these gases. The main outlet vein is the syngas. Consistency checks are performed on these bases.

The model is somewhat complex given its nature. We limit ourselves here to explain the overall progress of calculations, leaving the reader who wishes further information to refer to the explanations provided in Thermoptim model library.

The calculation procedure is as follows:

1. calculation of ammonia and solid carbon combustion (to simplify things, we have just changed the composition of the oxidizer, making the implicit assumption that it was dry air; we could also have depleted oxygen in the oxidizer and increased fuel H₂O and CO₂ mole fractions);
2. humidification of fuel and calculation of the heat load to be taken into account in the rest of the combustion (referred to 1 kmol of fuel);
3. initialization and calculation of combustion, then recovery of results;
4. update of the outlet gas humidity;
5. update of the mixer (note: in the class, the Houtlet calculation is actually done before step 4 so that the change in composition of synGasSubstance has no influence on its value).

23.5 COOLING COIL WITH CONDENSATION

Section 7.8.4 of Part 2 provides equations allowing one to calculate the cooling with condensation of a moist mixture into contact with a cold coil.

A perfect theoretical cooling in a cooling coil of infinite surface would lead to cool the moist mixture at the coil temperature saturated state. It is customary to characterize a real process taking this cooling as theoretical reference, introducing the cooling coil effectiveness ϵ .

$$\epsilon = \frac{w_2 - w_1}{w_{\text{sat}} - w_1}$$

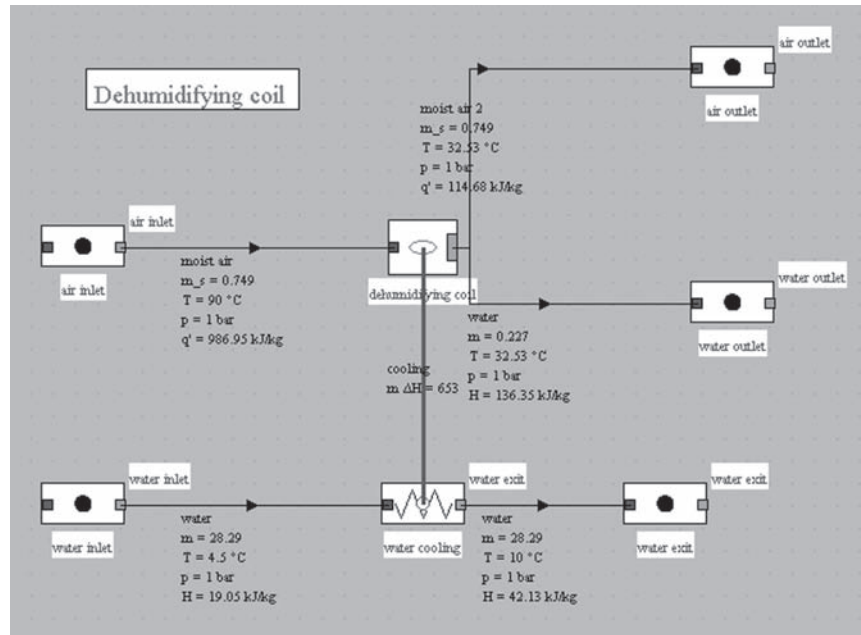


FIGURE 23.5.1

Diagram of component cooling coil with condensation

23.5.1 Modeling a cooling coil with condensation in ThermoOptim

A cooling coil with condensation acts as a divider receiving the humid air coming in and out of which exit two fluids: water and drier air. It is cooled by a fluid, and the thermal coupling can be represented by a thermocoupler. To simplify writing, we talk about air, but this component can cool and condense any moist mixture.

The model structure is given Figure 23.5.1. Here we have chosen in ThermoOptim Global settings screen, the optional display in specific units for moist gas. For air, the flow shown is that of dry gas, which is invariant, and enthalpy h is replaced by the specific enthalpy q' . For water, which is not a moist gas, nothing is changed compared to the usual display.

23.5.1.1 Model of the cooling coil with condensation

Knowing the cooling coil effectiveness ε and its average surface temperature t_s , the calculation of the air outlet state is performed as follows.

We begin by looking for the saturation conditions $w_{\text{sat}}(t_s)$ and $q'(t_s, w_{\text{sat}})$.

We then calculate the moist end conditions in view of effectiveness:

$$w_2 = \varepsilon w_{\text{sat}} + (1 - \varepsilon)w_1$$

$$q'_2 = \varepsilon q'(t_s, w_{\text{sat}}) + (1 - \varepsilon)q'_1$$

We then look for t_2 such as $q'_2 = q'(t_2, w_2)$.

A problem may arise when, in the psychrometric chart, the line from point 1 intersects the saturation curve in two points. Indeed, in this case the point calculated from effectiveness may be in the saturated zone. We speak of early condensation. Two possibilities exist: if we set the downstream point specific humidity w_2 , the end point is then on the saturation curve for $w_{\text{sat}} = w_2$, if we set effectiveness, it is on the saturation curve, for $q'_{\text{sat}} = q'_2$.

If we want to make an exact calculation, the coordinates of the second point of intersection of the line from the upstream point with the saturation curve can be obtained by eliminating ε between the two previous equations, with w_2 and q_2' equal to their saturation values.

One approximate way is to determine temperature $t_{app} = \varepsilon t_{sat} + (1 - \varepsilon)t_1$, and consider it as an estimate of t_2 , then to calculate $w_{sat}(t_{app})$. If $w_2 > w_{sat}(t_{app})$, the point is in the saturated zone. This is the test implemented in the class presented here.

23.5.1.2 Model implementation

The model that we can choose is:

1. the only parameters are firstly the coil effectiveness value ε , read on the screen, and secondly the surface temperature, which we assume to be equal to that of the coolant at the coil entrance;
2. we begin by calculating the inlet moist air properties, and determining the mass flow of dry gas;
3. we calculate the outlet air state at saturation and the final state ("2" in the above equations);
4. the coil outlet temperature is set, and the outlet moist air properties are calculated, which gives the specific and total enthalpy extracted from air;
5. the flow of water transferred by air is determined and the outlet moist air composition is changed;
6. the enthalpy balance provides the thermocoupler load;
7. values downstream of the node are updated.

The component screen is given in Figure 23.5.2 and that of the thermocoupler in Figure 23.5.3.

The mole fraction of water has been divided by about 7 (Figures 23.5.4 and 23.5.5).

23.5.2 Study of the external class DehumidifyingCoil

The study of the external class DehumidifyingCoil allows one to understand how the model has been implemented. As can be seen, six steps are enough to make the calculations:

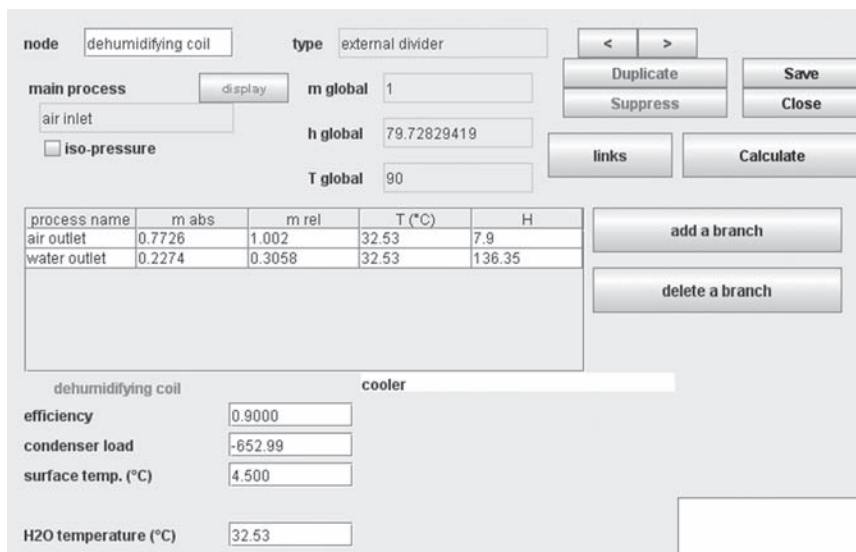


FIGURE 23.5.2

Component screen

- 1) we begin by calculating the inlet moist air properties thanks to generic method updatepoint(), then initializing the dry air flow-rate and the upstream specific enthalpy:

```
//Initialisations relatives à l'état du gaz entrant
//Initializations concerning entering gas
getPointProperties(wetGasPoint);
wInlet=wpoint;
Tinlet=Tpoint;
double test=(inlet_w-wInlet)*(inlet_w-wInlet)/wInlet/wInlet;
if(test>0.0001){
    String msg = "Watch out: the composition of the inlet humid air is not consistent";
    JOptionPane.showMessageDialog(de, msg);
    isBuilt=false;
}
double flow_as=wetGasFlow/(1+Wpoint);//débit massique de gaz sec
//calcul des propriétés humides en entrée du composant
//calculation of moist properties at the component inlet
updatepoint(wetGasPoint, false, 0, //T
            false, 0, false, 0, //P,x
            true, "setW and calculate q'", wInlet);
getPointProperties(wetGasPoint);//direct parsing of point property vector
double qprimeInlet=QPrimepoint;
```

The screenshot shows a software interface for a thermocoupler. It is titled 'cooling' and 'counterflow'. The 'thermal fluid' section is set to 'water cooling' with a 'display' button. The 'process' section is set to 'dehumidifying coil' with a 'display' button and a 'Calculate' button. The 'thermal fluid' parameters are: Ti=4.5, To=10, m=28.28598377, Cp=4.19735793, m ΔH=652.99519068. The 'process' parameters are: Ti=90, To=32.52859497, m=1, Cp=11.36208851, m ΔH=-652.99519068. There are radio buttons for 'calculated' and 'calculated' (selected). A 'pinch method fluid' section has a 'minimum pinch' field set to 0. Other parameters include 'epsilon' (0.672180176), 'UA' (13.17767468), 'R' (0.0956997658), 'NTU' (1.15979335), and 'LMTD' (49.55314247). Buttons for '<', '>', 'Save', 'Suppress', and 'Close' are also visible.

FIGURE 23.5.3

Thermocoupler screen

component name	molar fraction	mass fraction
Ar	0.005845102	0.009295136
O2	0.1363857	0.1737198
N2	0.507225	0.5656051
H2O	0.3505442	0.2513799

FIGURE 23.5.4

Composition of the inlet moist air

component name	molar fraction	mass fraction
Ar	0.008559244	0.01203094
O2	0.1997157	0.2248501
N2	0.7427522	0.7320773
H2O	0.04897291	0.0310416

FIGURE 23.5.5

Composition of the outlet moist air

2) we then initialize the surface temperature:

```
//récupération du nom de la transfo couplée au composant par le thermocoupleu
//gives the name of the process coupled to the component by the thermocoupler
String thcoupl=(String)de.de.getThermoCouplerData("cooler").elementAt(0);
System.out.println(" thermocoupler : "+thcoupl);
if (thcoupl!=null) && (!thcoupl.equals("null")){
String[] args=new String[2];
args[0]="heatEx";
args[1]=thcoupl;
Vector vProp=proj.getProperties(args);
String trsf=(String)vProp.elementAt(0);
System.out.println("hot : "+trsf+" cold : "+(String)vProp.elementAt(1));
args[0]="process";
args[1]=trsf;
vProp=proj.getProperties(args);
String amont=(String)vProp.elementAt(1);
getPointProperties(amont);
//Tpoint contient la valeur de la température d'entrée du fluide de refroidi:
//Tpoint stores the value of thecooling fluid inlet temperature
ts_value.setText(Util.aff_d(Tpoint-273.15,3));
}
double ts=Util.lit_d(ts_value.getText());
```

3) we then calculate the outlet air saturation conditions:

```
//calcul des conditions de saturation pour le gaz sortant
//calculation of saturation conditions for the exiting gas
updatepoint(dryGasPoint, true, ts+273.15, //T
false, 0, false, 0, //P,x
false, "", 0);

updatepoint(dryGasPoint, false, 0, //T
false, 0, false, 0, //P,x
true, "setEpsi and calculate", 1);
getPointProperties(dryGasPoint); //propriétés à la saturation

double wsat_ts=Wpoint;
double qprime_ts=QPrimepoint;
```

4) we calculate the desired end state:

```
//calcul de l'état final recherché
//calculation of the desired final state
w2=epsi*wsat_ts+(1-epsi)*wInlet;
qprime2=epsi*qprime_ts+(1-epsi)*qprimeInlet;
```

5) we seek to know whether the point so determined may be in the saturated zone:

```
//préparation du test sur la zone saturée
//preparation of the test on the saturated zone
double tapp=epsi*ts+(1-epsi)*(Tinlet-273.15);
updatepoint(dryGasPoint, true, tapp+273.15, //T
false, 0, false, 0, //P,x
false, "", 0);

updatepoint(dryGasPoint, false, 0, //T
false, 0, false, 0, //P,x
true, "setEpsi and calculate", 1);
getPointProperties(dryGasPoint); //propriétés à la saturation / saturation pr
double wsat_tapp=Wpoint;
```

- 6) we search the corresponding dry bulb temperature with the generic reverse function Util.dicho (which uses f_dicho):

```

double T=0;
if(w2>wsat_tapp){//Si le point est dans la zone saturée / if the point is in the saturated
    T=Util.dicho_T(this, 0, Pinlet, "qprime2sat", ts+273.15, Tinlet, 0.01);
}
else{//sinon / otherwise
    T=Util.dicho_T(this, 0, Pinlet, "qprime2", ts+273.15, Tinlet, 0.01);
}

public double f_dicho(double T, double P, String fonc){

    if (fonc.equals("qprime2")){//point final hors zone saturée / final point outside satu
        double diff;
        updatepoint(dryGasPoint, true, T, //T
            false, 0, false, 0,//P,x
            false, "", 0);
        updatepoint(dryGasPoint, false, 0, //T
            false, 0, false, 0,//P,x
            true, "setW and calculate q'", w2);

        getPointProperties(dryGasPoint);//propriétés humides / moist properties
        diff=qprime2-QPrimepoint;
        return diff;
    }
    if (fonc.equals("qprime2sat")){//point final saturé / saturated final point
        double diff;
        updatepoint(dryGasPoint, true, T, //T
            false, 0, false, 0,//P,x
            false, "", 0);
        updatepoint(dryGasPoint, false, 0, //T
            false, 0, false, 0,//P,x
            true, "setEpsi and calculate", 1);

        getPointProperties(dryGasPoint);//
        diff=qprime2-QPrimepoint;
        return diff;
    }
    return 0;
}

```

- 7) we modify the outlet moist air composition, and calculate the thermocoupler load and the mass flow of water exiting:

```

//modification de la composition du gaz
//modification of the gas composition
updatepoint(dryGasPoint, false, 0, //T
    false, 0, false, 0,//P,x
    true, "modHum", 0);
//charge du condenseur / condenser load Qprime_inlet
double DeltaQprime=flow_as*qprime2-Qprime_inlet;//enthalpie to
double condLoad=DeltaQprime;

//eau mise en jeu / water put into play
double H2Oflow=(inlet_w-Wpoint)*flow_as;

```

- 8) the node is updated using generic methods.

23.6 COOLING TOWERS

The basics of cooling tower physical modeling having been presented in section 15.8 of Part 3, we will limit ourselves here to demonstrate how an external class can be built using moist gas calculation functions.

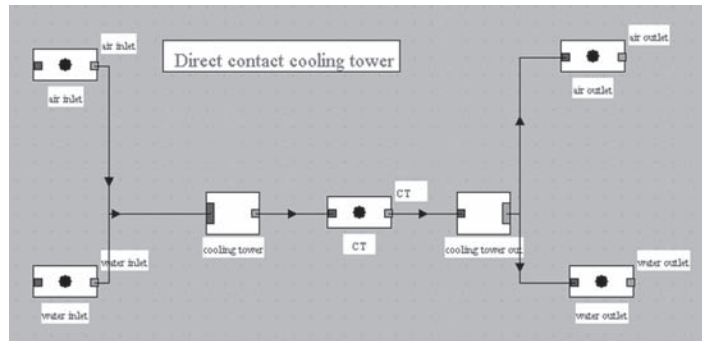

FIGURE 23.6.1

Diagram of the direct contact cooling tower component

23.6.1 Modeling of a direct contact cooling tower in ThermoOptim

A direct contact cooling tower has the distinction of being crossed by two separate streams: air and water, that exchange matter and energy through an interface. It behaves like a quadrupole receiving two input fluid, and of out which come two others (Figure 23.6.1).

23.6.1.1 Model of the direct contact cooling tower

In these conditions, we can reason on the overall enthalpy level knowing the inlet and outlet air side conditions and the inlet ones on the water side: model results are consistent with experimental values and those supplied by manufacturers.

Flow rates of both inlet streams are set by conditions upstream of the component and not recalculated. If water flow is insufficient for its cooling (up to moist bulb temperature of incoming air) to provide air with the enthalpy required, a message warns the user.

Recall that, as usual in calculations of moist functions, values are referred to dry gas, whose composition is invariant, while other calculations in ThermoOptim are relative to the actual gas composition, i.e. are referred to the moist gas. It is therefore necessary to make the corresponding conversions.

Another point to mention is that when you save a point properties, moisture is not taken into account because it is derived from the gas composition. If we desire to save a change in the humidity of the air inlet, we must also change the gas composition from the moist screen calculations of the inlet point.

The model that we can choose, when we know the exit air temperature, is the following:

1. we begin by calculating inlet moist air properties, and determining the dry gas mass flow from that of moist gas; inlet relative humidity ϵ is displayed on the screen;
2. the outlet relative humidity is set equal to 1, and the outlet moist air properties are calculated, which gives the specific and total enthalpy to be brought to air;
3. the flow of water carried by air is determined and the outlet moist air composition is changed;
4. the water enthalpy balance provides its outlet temperature, which must exceed the moist bulb temperature of air entering;
5. values downstream the node are updated;
6. NTU is calculated by integrating the Merkel equation (NTU integrated) established section 15.8.2 of Part 3 and on the basis of the mean logarithmic enthalpies; effectiveness can be deduced from the classical relationship for counter-flow heat exchangers.

The tower is as we said represented by an external mixer connected to an external divider, calculations being made by the latter. Classes are called `DirectCoolingTowerInlet` and `DirectCoolingTower`.

node: cooling tower out type: external divider

main process: CT display: [button] m global: 23.50034099

iso-pressure h global: 88.9706

T global: 27.86992528

process name	m abs	m rel	T (°C)	H
air outlet	10.1996	1.002	27.87	3.09
water outlet	13.3008	0.3058	26.03	109.21

direct cooling tower

NTU value: 1.155 T water out known

inlet rel. humidity: 0.700 epsilon: 0.575 NTU known

$\Delta Q'$: 283.662 UA: 47.419

water involved: 0.09958 R: 0.734

approach (°C): 5.071 LMTD: 4.081

range (°C): 5.066 NTU (integrated): 1.197

FIGURE 23.6.2

Cooling tower component screen

The cooling tower component screen is given in Figure 23.6.2. We wish here to cool 1kg/s of water from 30°C to 25°C. With a rate of 0.9kg/s of air at 18°C and relative humidity equal to 0.5, the exhaust air temperature is 20.1°C and 7.5g/s water are evaporated. The tower capacity is 20.9kW.

On this screen we see two values of NTU. That which is in the editable field is calculated by the approximate formula based on the logarithmic mean differences of enthalpies of saturated air between the tower inlet and outlet, while the one displayed at the bottom is the result of the integration of the Merkel differential equation for a counter-flow tower. It is in principle more accurate, but we can see that their values are close.

WORKED EXAMPLE

Refrigeration Machine Condenser with Cooling Tower

This example corresponds to a R134a refrigeration machine ensuring the production of 200kW of cooling at -12°C , whose condenser is cooled by air at 25°C .

The objective is to compare the performance of the machine depending on whether one uses an air exchanger with a pinch of 16K or a cooling tower, the minimum pinch between water and the refrigerant being below 12K. The result is an increase of COP of about 19% when the cooling tower is used.

It is presented in the portal guidance pages (<http://www.thermoptim.org/sections/enseignement/cours-en-ligne/fiches-guides-td-projets/fiche-sujet-fg6>).



[CRC_we_5]

23.6.1.2 Using external class DirectCoolingTower

Without cooling tower (Figure 23.6.3), with a maximum airflow of 30 kg/s and a pinch of 16K, simulation leads to a COP of 2.15, condenser outlet air temperature equal to 34.7°C and R134a condensation temperature equal to 50.4°C , i.e. condensing pressure of 13.3 bar.

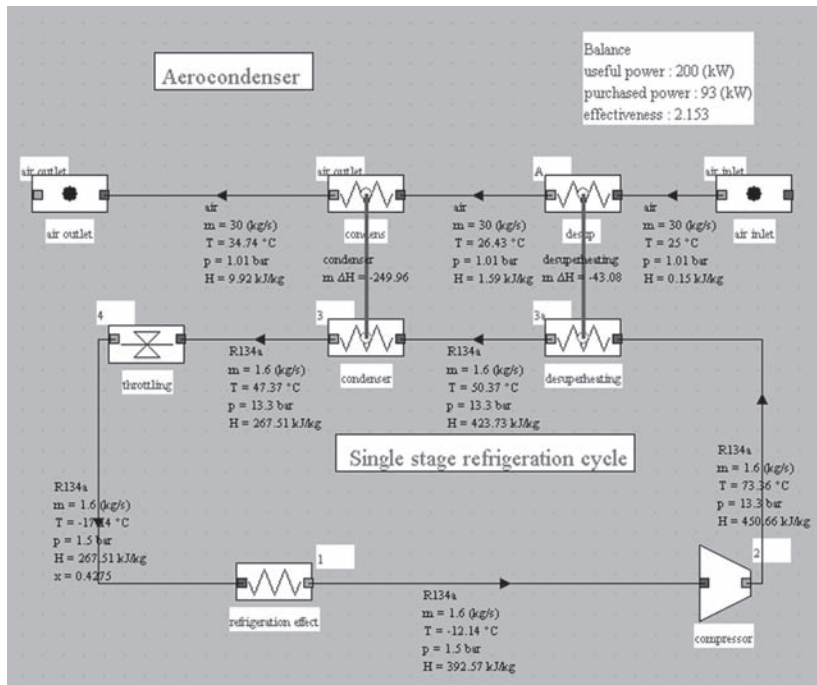


FIGURE 23.6.3
Synoptic view of the system with air exchanger, $\eta_{is} = 0.8$

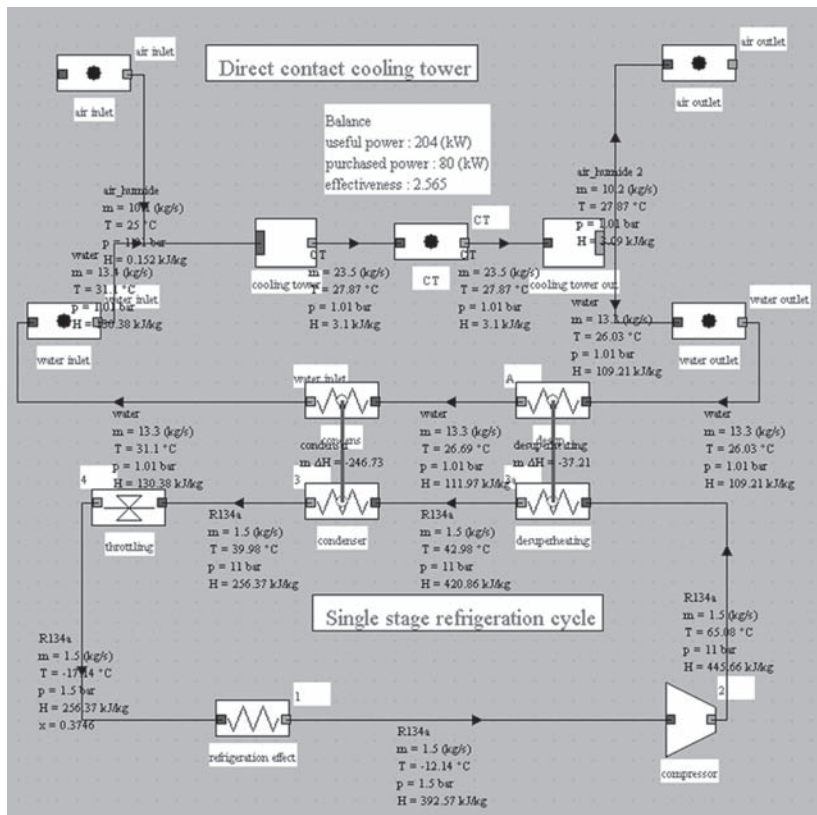


FIGURE 23.6.4
Synoptic view of the facility, $\eta_{is} = 0.8$

The tower settings can in turn (Figure 23.6.4) be done as follows: we set air inlet T and ϵ (here 25°C and 70% RH) and inlet water T (here 31.1°C) and flow (13.4 kg/s). Balancing the condenser and desuperheater gives the power to extract ΔH and the water output temperature (26.03°C). We choose option “Twater out known” and the calculation of the tower provides $T_{air} = 27.89^\circ\text{C}$.

COP without the tower is equal to 2.15 instead of 2.57, representing a decrease of 16%. And yet we have neglected the fan power, air flow passing from 10.1 kg/s to 30 kg/s, or the lower isentropic efficiency, compression ratio passing from 7.33 to 8.87.

In addition, the refrigerant flow must be increased from 1.5 to 1.6 kg/s, due to the increased quality as the end of expansion, which implies a larger displacement, volumetric efficiency dropping too.

Let us consider the compressor isentropic efficiency law:

$$\eta_{is} = 0.893 - 0.004(\tau - 5)^2 - 0.5/(\tau - 0.3)$$

Its value goes from 0.8 to 0.775, bringing the COP decline to 18.7%.

23.6.2 Study of external class DirectCoolingTower

To ensure model consistency (avoiding that the inlet mixer is connected to an inadequate outlet divider), each of the two nodes tries to instantiate the other in its class from the project external components and verifies that both are connected to the same process-point. If the operation fails, a message warns the user that the construction is incorrect. This is checked by methods `setupOutlet()` and `setupInlet()`.

In addition, consistency tests for each node are carried out by method `checkConsistency()` to verify that fluids are appropriately connected: in this case, humid air as well as inlet and outlet water. Refer to Volume 3 of the reference manual for explanations on this point, valid for all external nodes.

The study of external class `DirectCoolingTower` allows one to understand how the model has been implemented. As can be seen, if the outlet air temperature is known, six steps are enough to perform calculations (in other cases, the approach is analogous):

- 1) we begin by calculating the inlet humid air properties thanks to generic method `updatepoint()`, then we initialize the dry air flow-rate and the upstream specific enthalpy:

```
//imposition de w et calcul des propriétés humides
//setting w and moist properties calculation
updatepoint(amont, false, 0, //T
            false, 0, false, 0, //P,x
            true, "setW and calculate all", inlet_w);

getPointProperties(amont);
System.out.println(amont+" w : "+Wpoint+" epsi : "+Epsipoint+" q'
double TprimeAmont=Tprimepoint+273.15;
Double f=(Double)vProp.elementAt(3);
double flow=f.doubleValue();//moist gas mass flow rate / débit ma
flow_as=flow/(1+Wpoint);//dry gas mass flow rate / débit massique
JLabel1.setText("inlet rel. humidity : "+Util.aff_d(Epsipoint,3))
qPrimeAmont=QPrimepoint;//specific enthalpy of the entering air /
```

- 2) we then calculate the moist air properties and deduce the total enthalpy into play:

```
//propriétés humides de l'air sortant
//moist properties of the exiting air
args[0]="process";//type of the element (see method getProperties(String[] args))
args[1]=airProcess;//name of the process (see method getProperties(String[] args))
vProp=proj.getProperties(args);
aval=(String)vProp.elementAt(1);//gets the upstream point name
getPointProperties(aval);
outletT=Tpoint;

epsi=1;
updatepoint(aval, false, 0, //T
            false, 0, false, 0, //P,x
            true, "setEpsi and calculate", epsi);
getPointProperties(aval);

qPrimeAval=QPrimepoint;//specific enthalpy of exiting air / enthalpie spécifique de l'a
DeltaQprime=flow_as*(qPrimeAval-qPrimeAmont);//total enthalpy brought to the air / enth
JLabel13.setText("\u0394Q' : "+Util.aff_d(DeltaQprime,3));
```

- 3) we change the outlet moist air composition, and calculate the mass flow rates exiting:

```
//modification de la composition du gaz
//modification of the gas composition
updatepoint(aval, false, 0, //T
            false, 0, false, 0, //P,x
            true, "modHum", 0);

//bilans massiques air et eau
//air and water mass balance
outletFlow=flow_as*(1+Wpoint);

waterFlow=dcti.waterFlow - (Wpoint-inlet_w)*flow_as;
JLabel14.setText("water involved : "+Util.aff_d((Wpoint-inlet_w)*flow_as,5));
```

- 4) the water enthalpy balance then provides the outlet water temperature:

```
//bilans enthalpique sur l'eau
//water enthalpy balance
args[0]="process";//type of the element (see method getProperties(String[]
args[1]=waterProcess;//name of the process (see method getProperties(String
vProp=proj.getProperties(args);
waterOut=(String)vProp.elementAt(1);//gets the upstream point name
getPointProperties(waterOut);
hAval=dcti.waterH-DeltaQprime/dcti.waterFlow;
getSubstProperties(nomCorps);

waterOutT=lecorps.getT_from_hP(hAval,Ppoint);//water outlet temperature / t
```

T H D P T

[CRC_In_14]

- 5) the node is updated using generic methods described in the reference manual:

```
//mise à jour du lien entre les noeuds externes
//update of the link between the external nodes
args[0]="process";//type of the element (see method getProperties(String[]
args[1]=mainProcess;//name of the process (see method getProperties(String[
vProp=proj.getProperties(args);
String dummy=(String)vProp.elementAt(2);// point name
updatepoint(dummy, true, outletT, //T
            false, 0, false, 0, //P,x
            false, "dummy", 1);
```

```

//mise à jour du noeud en utilisant les méthodes génériques
//update of the node by the generic methods
vTransfo= new Vector[nBranches+1];
vPoints= new Vector[nBranches+1];
setupVector(airProcess, aval, 0, outletFlow, outletT, airP, 0);
setupVector(waterProcess, waterPoint, 1, waterFlow, waterOutT, airP, 0);
setupVector(mainProcess, aval, 2, outletFlow+waterFlow, outletT, airP, 0);
updateDivider(vTransfo,vPoints,outletT,qPrimeAval);

```

- 6) finally, the heat exchanger overall characteristics are estimated:

```

//Calcul du NUT basé sur le Delta H ML
//Calculation of NTU based on Delta H ML
double DqPrimeML=(deltaQprime-deltaQprime0)/(Math.log(deltaQprime/deltaQprime0));
double NUT_ML=4.18*(dcti.waterT-waterOutT)/DqPrimeML;

//Caractéristiques de l'échangeur équivalent
//Characteristics of the equivalent exchanger
double mCpc= DeltaQprime/(dcti.waterT-waterOutT);
double mCpf= DeltaQprime/(outletT-TprimeAmont);
double Tfe=TprimeAmont;
double Tfs=outletT;
double Tce=dcti.waterT;
double Tcs=waterOutT;
double Tfmin=Tfe,Tfmax=Tfs;
if (mCpc>mCpf){
    R=mCpf/mCpc;
    epsilon=epsi_NUT(NUT_ML,R);
    UA=mCpf*NUT_ML;
}
else{
    R=mCpc/mCpf;
    epsilon=epsi_NUT(NUT_ML,R);
    UA=mCpc*NUT_ML;
}
double Delta=(Tce-Tfs)*(Tce-Tfs)-(Tcs-Tfe)*(Tcs-Tfe);
if(Delta<0)Delta=-Delta;//modRG 04/12
if(Delta>1e-6)DTML=(Tce-Tfs+Tfe-Tcs)/(Math.log((Tce-Tfs)/(Tcs-Tfe)));
else DTML=Tce-Tfs;
if(DTML<0)DTML=-DTML;

```

23.7 EXTERNAL DRIVERS

External classes also allow one to control Thermoptim either from another application to guide a user (intelligent tutoring system) or to control code execution (control or regulation, access to thermodynamic libraries). A first example was given in section 12.2.1.10 of Part 3 for modeling a turbojet, but it is especially in Part 5 that external drivers are used because they allow one to find the solutions in off-design studies.

23.7.1 Stirling engine driver

In this section we present the driver which was used to calculate the energy balance of the solar Stirling engine modeled Chapter 14 of Part 3. It is indeed a very simple example which allows this

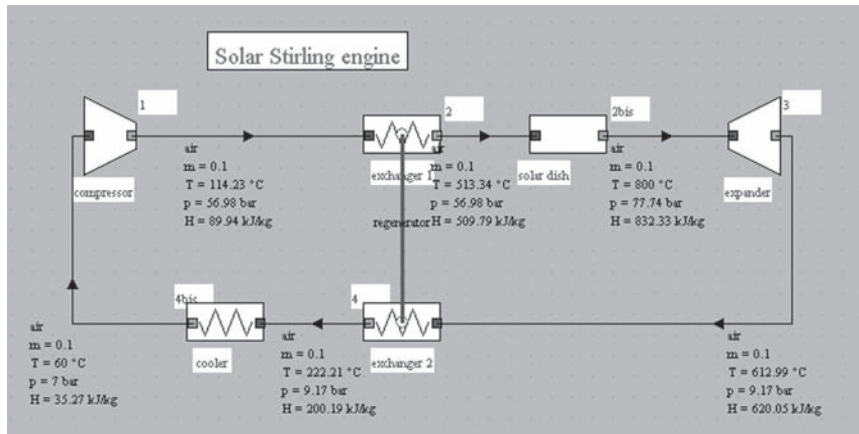


FIGURE 23.7.1
Solar Stirling engine

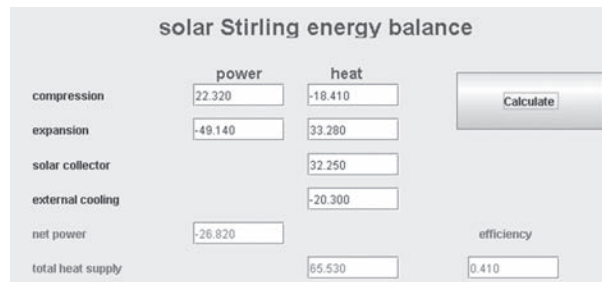


FIGURE 23.7.2
Driver screen

type of external class to be introduced without having to delve into the details of a complex thermodynamic model.

A Stirling engine (Figure 23.7.1) is an engine of a particular type, which works in a closed system, and implements cooled compression and heated expansion, so that the usual ThermoOptim performance indicators cannot be directly used: purchased energy is the sum of heat supplied to the heat source (in this example a solar concentrator) and that provided during expansion.

The objective we assign the driver (StirlingDriver.java) is to provide a table of energies involved in the engine as heat or mechanical power and to calculate the cycle efficiency. Figure 23.7.2 shows the type of screen that you can imagine.

23.7.2 Creation of the class: visual interface

To create an external driver, simply subclass `extThopt`. `ExtPilot`.

The realization of the visual interface is not a particular problem and we do not comment on here.

The constructor must end with a String specifying the code that will nominate the driver in the list of those available: `type = "stirling"`

It is also recommended to document the class:

```
public String getClassDescription(){
    return "pilot for a simple Stirling motor\n\nauthor : R. Gicquel
    february 2008";}
```

23.7.3 Recognition of component names

It is possible to automatically recognize the names of the various components constituting the model, sorting them by type, which makes the driver more generic than if those names are entered as Strings in the code. That is the purpose of methods `init()` and `setupProject()`, which use methods allowing to access the names of the diagram editor components and the list of external classes available (for external process representing the concentration solar collector).

```
public void init(){
    isInitialized=true;
    proj=getProjet();
    setupProject();
    //On récupère la liste et le type des composants présents dans l'éditeur de schémas
    //Retrieves the list and the type of components in the diagram editor
    String[] listComp=proj.getEditorComponentList();
    composant=new String[listComp.length];
    nomComposant=new String[listComp.length];

    //on en extrait les noms des transfos de compression et de détente
    //gets the names of compression et expansion processes
    for(int i=0;i<listComp.length;i++){
        composant[i]=Util.ext_value(listComp[i], "type");
        nomComposant[i]=Util.ext_value(listComp[i], "name");
        if(composant[i].equals("Compression"))compressorName=nomComposant[i];
        if(composant[i].equals("Expansion"))expansionName=nomComposant[i];
    }
    //test de cohérence (des messages d'erreur plus précis seraient souhaitables)
    //consistency test (error messages should be an improvement)
    if(!expansionName.equals("") && !compressorName.equals("")) && isBuilt)isBuilt=true;
    if(isBuilt)setVisible(true);//on n'ouvre le pilote que si sa structure est correcte
    //the driver cannot be open if its structure is wrong

    void setupProject(){
        //on récupère ici l'instance de la transfo externe du capteur solaire
        //Retrieves the instances of the solar collector external class
        Vector vExt=proj.getExternalClassInstances();//Vector contenant les clas:
        int j=0;
        for(int i=0;i<vExt.size();i++){
            Object[] obj=new Object[6];
            obj=(Object[])vExt.elementAt(i);
            ExtProcess ep=(ExtProcess)obj[1];
            if(ep instanceof SolarConcentratorCC){
                collector=(SolarConcentratorCC)ep;
                collectorName=collector.getName();
                j++;
            }
        }
        if(j==1)isBuilt=true;//test de cohérence du pilote par rapport au modèle
        //consistency test (error messages should be an improvement)
```

23.7.4 Calculations and display

Once the names of the various components are identified, one can access their properties using Project method `getProperties()`, which provides all the values needed.

```

void bCalculate_actionPerformed(java.awt.event.ActionEvent event){
    if(!isInitialized) init();
        //the initialization is made during the first call, as the constructor
        //must have no argument because the class is instantiated by the RMI
    String[] args=new String[2];
    args[0]="process";
    args[1]=compressorName;//compression
    Vector vProp=proj.getProperties(args);
    Double f=(Double)vProp.elementAt(4);
    double deltaUcompr=f.doubleValue();//puissance compresseur //compression power
    f=(Double)vProp.elementAt(12);
    double Qcompr=f.doubleValue();//chaleur compresseur //compressor heat
    args[1]=expansionName;//détente //expansion
    vProp=proj.getProperties(args);
    f=(Double)vProp.elementAt(4);
    double deltaUexpan=f.doubleValue();//puissance détente //expansion power
    f=(Double)vProp.elementAt(12);
    double Qexpan=f.doubleValue();//chaleur détente //expansion heat
    args[1]=collectorName;//capteur solaire //solar collector
    vProp=proj.getProperties(args);
    f=(Double)vProp.elementAt(4);
    double solarHeat=f.doubleValue();//chaleur solaire //solar heat

    //calcul des performances globales du moteur et affichages
    //calculates the overall motor energies and displays them on the driver screen
    tauExpan_value.setText(Util.aff_d(deltaUexpan, 3));
    netPower_value.setText(Util.aff_d(deltaUexpan+deltaUcompr, 3));
    tauCompr_value.setText(Util.aff_d(deltaUcompr, 3));
    Q_value.setText(Util.aff_d(Qexpan+solarHeat, 3));
    eta_value.setText(Util.aff_d((-deltaUexpan-deltaUcompr)/(Qexpan+solarHeat), 3));
    expanHeat_value.setText(Util.aff_d(Qexpan, 3));
    comprHeat_value.setText(Util.aff_d(Qcompr, 3));
    solarHeat_value.setText(Util.aff_d(solarHeat, 3));
    extCooling_value.setText(Util.aff_d(-(Qexpan+solarHeat+deltaUexpan+deltaUcompr+Qcompr), 3));

```

As can be seen, the realization of an external driver poses no particular problem. This one is particularly simple, just making energy balances that Thermoptim would calculate wrongly taking into account the specificities of this model. It would for example be quite possible to complicate it slightly, so that it would update the simulator to perform recalculations of the model before building the balance.

23.8 EXTERNAL CLASS MANAGER

Once external classes are developed, they must be integrated into library extUser.zip so they can be automatically recognized in the executable-only version of Thermoptim.

A Thermoptim plugin allows this operation to be performed. Called “External class manager” it shows in its left side (Figure 23.8.1) all classes available in the directory of the class library under development. These classes are arranged by type (substance, external process, external mixers, external dividers, and drivers). On the right side, archive “extUser.zip” content is displayed on the same principle. It is thus possible to easily compare the two sets of classes.

If you select a class in one of the lists, its description appears in the window below, like class Nozzle in Figure 23.8.1. If you make multiple selections, nothing is displayed.

You can transfer a single or multiple selection from the class library (left) to “extUser.zip” archive, clicking on the small central arrow.



You can also delete from the archive “extUser.zip” a single or multiple selection of the right window with the option to save the class in the class library.

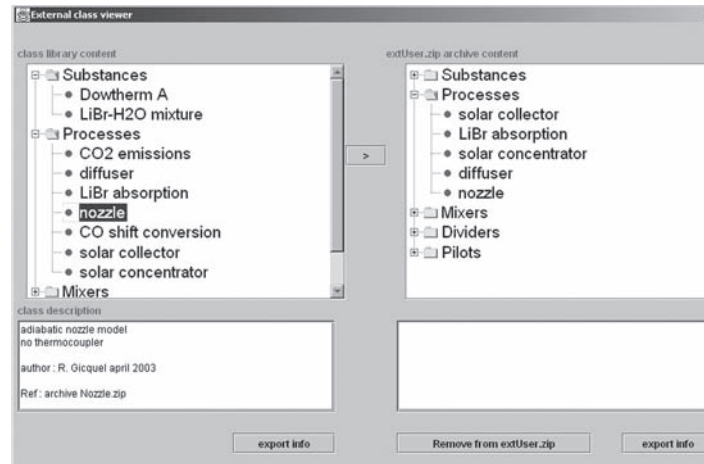


FIGURE 23.8.1
External class manager

During these manipulations, consistency tests are made and messages posted in case of trouble. This plugin facilitates the deployment of external classes.

It is also possible to use a standard compactor such as WinZip, making it add the new class in the archive. To do this, refer to Volume 3 of ThermoOptim reference manual.

This page intentionally left blank

Advanced Gas Turbines Cycles

Abstract: In this chapter, which completes chapters 12 and 17 of Part 3, we present three families of advanced cycles based on the use of gas turbines. In the first, the working fluid is no longer an ideal gas but a mixture a little more complex: the humid air gas turbine cycle takes advantage of the variation of humidity. The second corresponds to the supercritical CO₂ cycle whose interest is to benefit from a compression work in supercritical liquid state much lower than when the working fluid remains in the gaseous state. Its main use considered today is electricity production from high temperature nuclear reactors (HTR, cf. section 29.2.7.2). The third family is four advanced combined cycles. The first three are variants of conventional combined cycle, while the Kalina cycle involves the ammonia-water mixture, which has the advantage of reducing thermal irreversibilities between the gas stream and the working fluid.

Keywords: humid air gas turbine, supercritical CO₂, Kalina, flash, recompression.

24.1 HUMID AIR GAS TURBINE

The humid air gas turbine cycle (HAT) is as shown in Figure 24.1.1. It uses as working fluid system “water–air”, which can significantly improve the capacity and efficiency compared to the simple gas turbine cycle (Mori and al., 1983, Chiesa et al., 1995).

The intake air is compressed (1–4) at about 25 bar with intercooling and post-compression cooling (4–5), to reduce work involved while recovering heat to preheat water.

Air is then introduced into a saturator which it leaves saturated with water. The humid air is preheated in a recuperator (6–7) by exchange with the expanded fumes (9–10), then headed to the combustion chamber, where it serves as an oxidizer to a fuel. Burnt gases are expanded in the turbine (8–9), then cooled in the recuperator prior to preheat water in the economizer before entering the saturator (10–11).

Water that comes in (1e) is heated in the various heat exchangers before being introduced into the saturator (5e).

As in a steam injection gas turbine cycle, water intake increases the mass flow passing through the turbine, which participates in the performance gain.

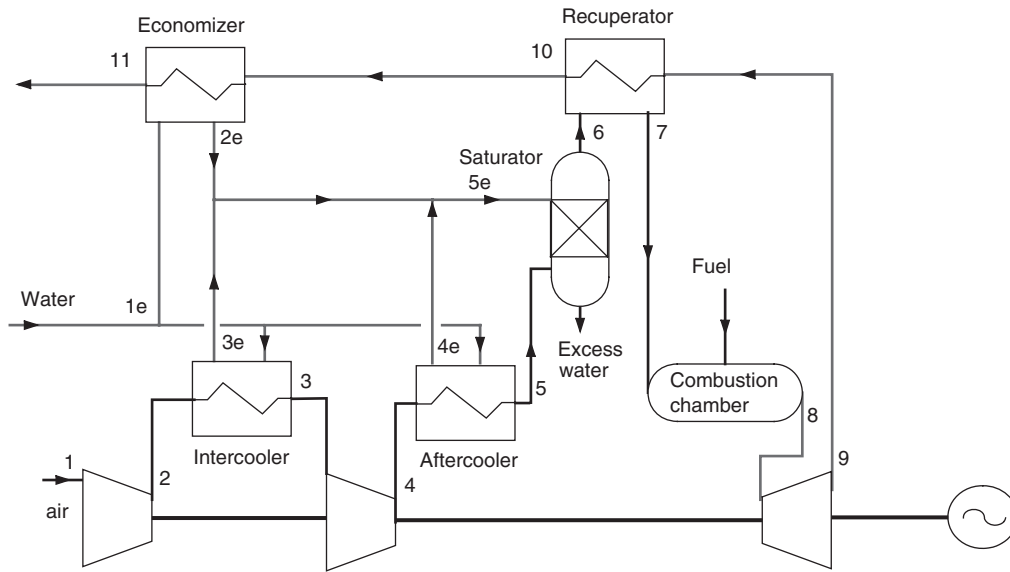


FIGURE 24.1.1
HAT Cycle

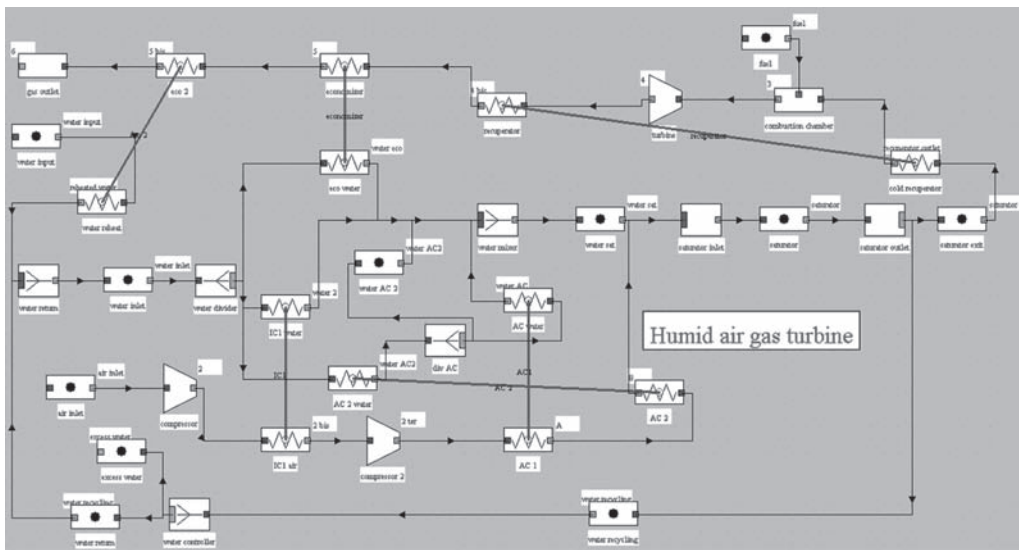


FIGURE 24.1.2
Diagram of the cycle in ThermoOptim

By varying humidity of air leaving the saturator, it is possible to modulate the system capacity. The cycle is much simpler than a combined cycle, and does not require expensive components, so that its capital cost is relatively low (400 U.S. \$/kW for an installed capacity of 300 MW).

Westinghouse (Nakhamkin et al., 1996) has proposed a cycle variant called Cascaded Humidified Advanced Turbine Cycle (CHAT), and announced very high efficiencies (55% to 65% with a compression ratio of 80 and a turbine inlet temperature of 1500°C).

The cycle diagram in ThermoOptim is given Figure 24.1.2. This cycle uses the saturator presented in section 23.3.2.3. Since the amount of makeup water needed is not *a priori* known, we have

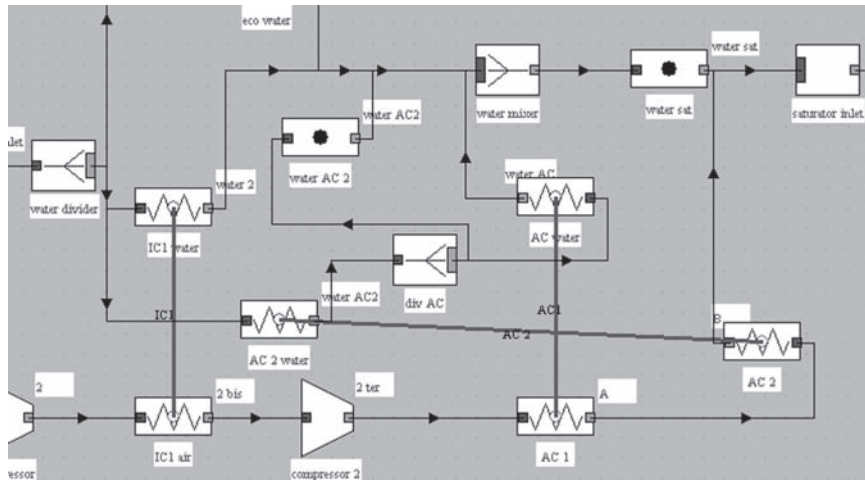


FIGURE 24.1.3

Internal recovery exchangers

node: water divider type: divider

main process: water inlet m global: 30 Duplicate Save

iso-pressure h global: 352.62953101 Suppress Close

T global: 83.28409161 links Calculate

process name	m abs	m rel	T (°C)	H
eco water	4	2	83.28	352.63
IC1 water	20	10	83.28	352.63
AC 2 water	6	3	83.28	352.63

add a branch

delete a branch

flow setting

FIGURE 24.1.4

Water inlet divider

provided a flow of water supply larger than required. At the saturator outlet, a divider allows to separate excess water which is recycled.

Settings are as follows: cycle pressure 25 bar, end of combustion temperature 1250°C. Heat exchanger effectiveness equal to 0.9, except that of the after cooler, which requires a special setting described below.

The overall efficiency is then 58%. These values are relatively close to those provided in the literature: air entering the saturator at 227°C, water entering at 264°C. Exit conditions are here somewhat higher (150°C instead of 120°C). To avoid any temperature crossing in the saturator, T water must be high.

The need to take as much heat as possible on compressed air leads to define a rather complex heat exchanger architecture, especially for the after-cooler (Figure 24.1.3). A counter-flow arrangement is chosen, so that water leaving the divider exchanges with air already cooled. At the outlet of “AC 2 water”, the stream of water is divided into two parts, one providing the vaporization of a portion of the flow, the other being by-passed, otherwise the setting of the heat exchanger oscillates. The choice of the flow of water to vaporize is a bit tricky and must be done by successive approximations, but we thus succeed in cooling appropriately the compressed air.

Settings of the initial water divider also influence the results (Figure 24.1.4). Here the inter-cooler was loaded to cool air well before recompression.

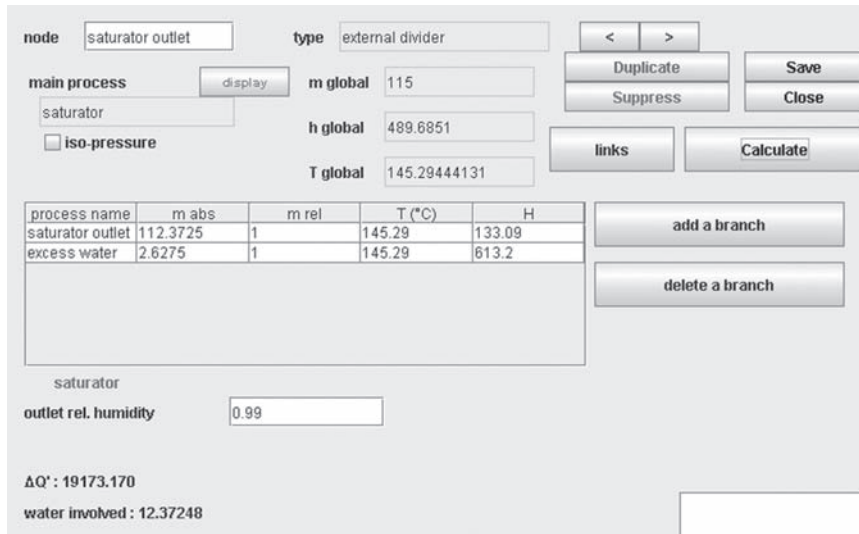


FIGURE 24.1.5

Saturator screen

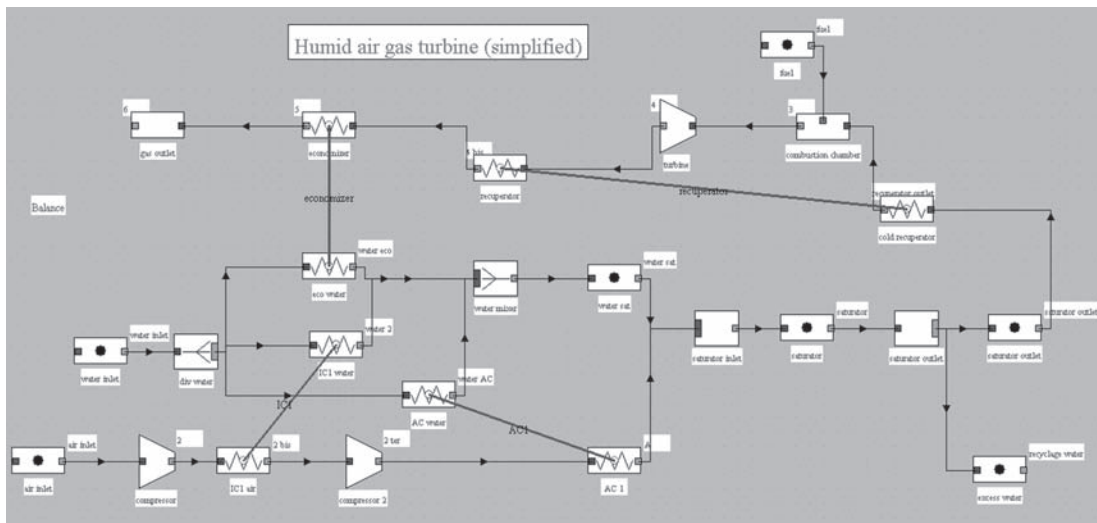


FIGURE 24.1.6

Diagram of the simplified cycle in ThermoOptim

The saturator (Figure 24.1.5) behaves like a moist mixer, and is calculated as such. Class Saturator is presented in section 23.3.2.1.

A simplified model involving just 20 points (19 if we replace process “CO₂ emissions” by a simple process-point), and 20 processes can be constructed (Figures 24.1.6 and 24.1.7). The efficiency is slightly lower (53.4%), but the main elements are there.

There is no recycling of water in excess, and we must therefore seek the minimum flow of water input given parameter values.

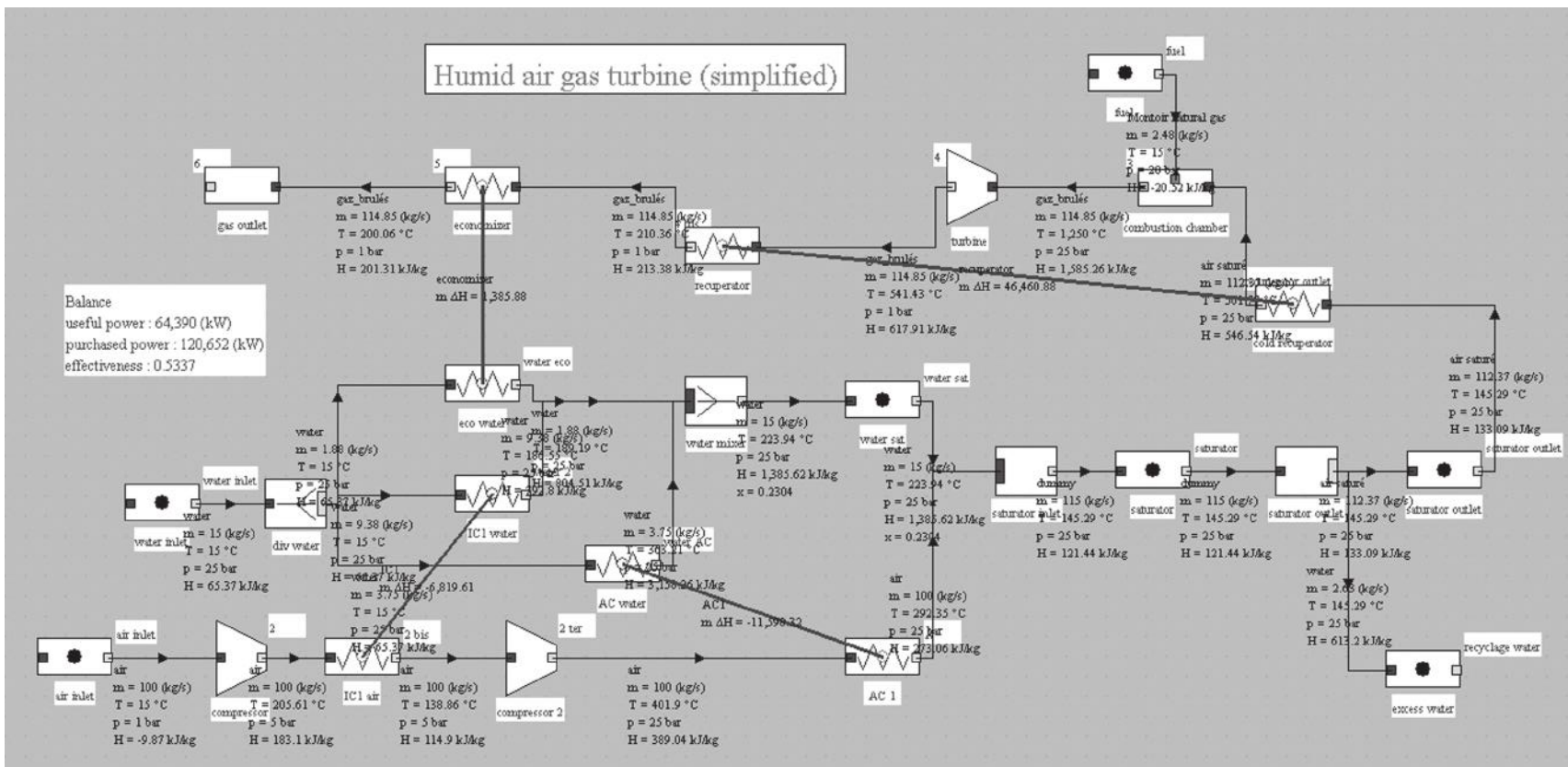


FIGURE 24.1.7
 Synoptic view of the HAT simplified cycle in Theroptim

24.2 SUPERCRITICAL CO₂ CYCLES

MIT has recently worked on cycles using supercritical carbon dioxide, which it considers lead to better performance than others to produce electricity from nuclear reactors at moderate temperatures (see section 29.2.7.2) between 650 and 800°C (Dostal et al., 2003).

Proponents of these cycles argue that efficiencies are, for this temperature range, higher than those of steam cycles and that machines are much more compact.

Let us detail a little, to fix ideas, the magnitudes of the respective sizes of these machines:

- expansion ratio in the turbine is much lower (about 2.6) than that in steam cycles (about 7300). Mass flow rate is however very high (about 3 t/s). Volume flow at the turbine inlet is equal to about 27 m³/s, and 55 m³/s at the outlet. At outlet conditions, assumed to be half the speed of sound (189. 1198. 740) $0.5 = 410$ m/s, this corresponds to a flow area of 0.27 m²;
- for a water steam cycle with extraction and reheats of equivalent capacity, mass flow is 170 kg/s, with at the LP turbine outlet specific volume of 55 m³/kg or a volume flow 170 times greater than for the supercritical CO₂ cycle. At outlet conditions, assumed to be half the speed of sound (462. 1.33. 292) $0.5 = 423$ m/s, this corresponds to a flow area of 45 m²;
- in a 600 MW flame power plant, of which the inlet conditions are 565°C and 163 bar, the main flow is about 500 kg/s. The three LP turbine sections have a exhaust section of 150 m²;
- 1300 MW PWR nuclear power plants have 3 double flow LP turbine sections with a total exhaust area of 112 m², last blades having a height of 1.45 m and a wheel diameter of 5.55 m. To limit the peripheral velocity, their rotation speed is 1500 rpm. The flow through them is only 45% of steam flow at admission because of the different extractions. The turbine length is 56 m (73.5 m with the generator). The HP rotor mass is 83 tons, that of each LP rotor is 218 tons.
- however, if the steam engine turbine is much larger than that of the supercritical CO₂ machine, heat exchangers of the latter are of significant size. On the basis of an exchange coefficient h close to 100 W/m²/K for this gas, the cycle modeled in ThermoOptim (Figure 24.2.4) would involve a 210,000 m² HT regenerator, a 180,000 m² LT regenerator, and a 80,000 m² precooler, not to mention the IHX, while the steam cycle condenser would have an area of tens of thousands of m² only.

Several types of supercritical CO₂ cycles are considered: the simplest is a Brayton cycle with regenerator (Figure 24.2.1) the principal variants involving partial cooling, pre-compression or recompression.

On the thermodynamics, the value of using such a cycle is to benefit from a compression work in supercritical liquid much lower than if the working fluid remains in the gaseous state as in a classic Brayton cycle.

In the following sections, we compare the performance of four variants of these cycles, by considering examples similarly configured.

24.2.1 Simple regeneration cycle

In a 350-MWe supercritical CO₂ **simple regenerative** cycle (Figure 24.2.2), a flow of 3 t/s of CO₂ at 200 bar enters the reactor at a temperature of 330°C and leaves it at 650°C. It is then expanded at the pressure of 77 bar in a turbine. Regeneration takes place between expanded CO₂ and that which enters the reactor. CO₂ then enters the cooler, which it leaves at 32.5°C, before being sucked into the compressor, which brings it at 200 bar.

The efficiency of this cycle remains fairly low, close to 35% with a regenerator of effectiveness 0.9 and polytropic efficiency turbomachinery equals to 0.9.

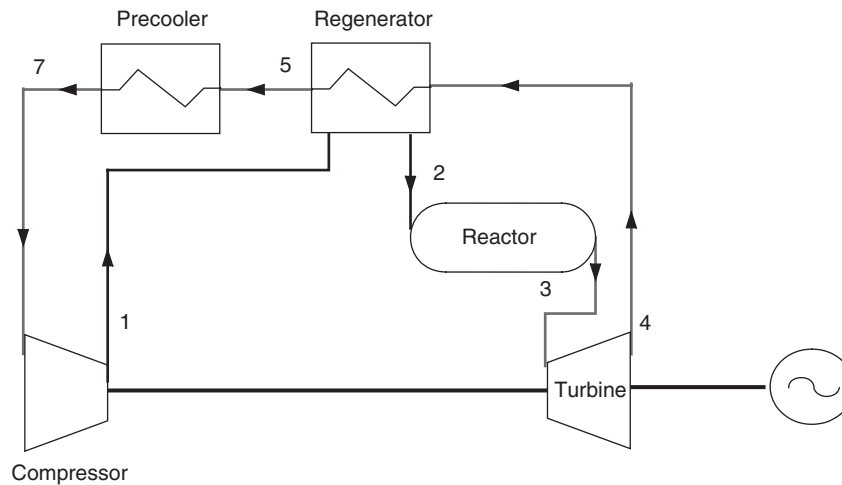


FIGURE 24.2.1

Supercritical CO₂ regenerative cycle

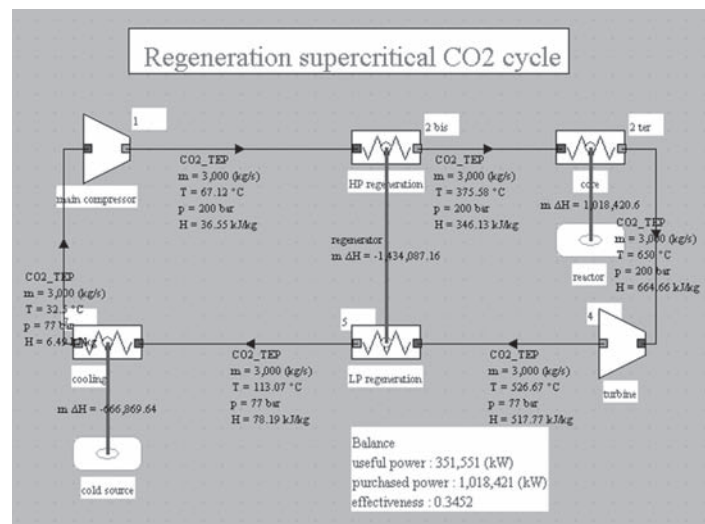


FIGURE 24.2.2

Synoptic view of the supercritical CO₂ regenerative cycle

24.2.2 Pre-compression cycle

A first improvement is to use **pre-compression**. In such a cycle (Figure 24.2.3), compression is two-stage with intercooling. After passing through the high temperature regenerator (4-5), a first compressor compresses CO₂ at about 100 bar (5-10). Pre-compressed CO₂ is cooled in the second low temperature regenerator (10-9), followed by exchange with the cold source (9-7). It is then compressed (7-8) in the main compressor, then heated (8-2) by exchange with the flow exiting the pre-compressor (10-9). A second exchange (2-6) with the flow exiting the turbine allows heating of CO₂ to be continued before entering the reactor.

As shown in Figure 24.2.3, with the same assumptions as before on heat exchanger effectiveness and turbomachinery polytropic efficiency, the capacity of this cycle drops to 300 MW, but its efficiency reaches 39.4%.

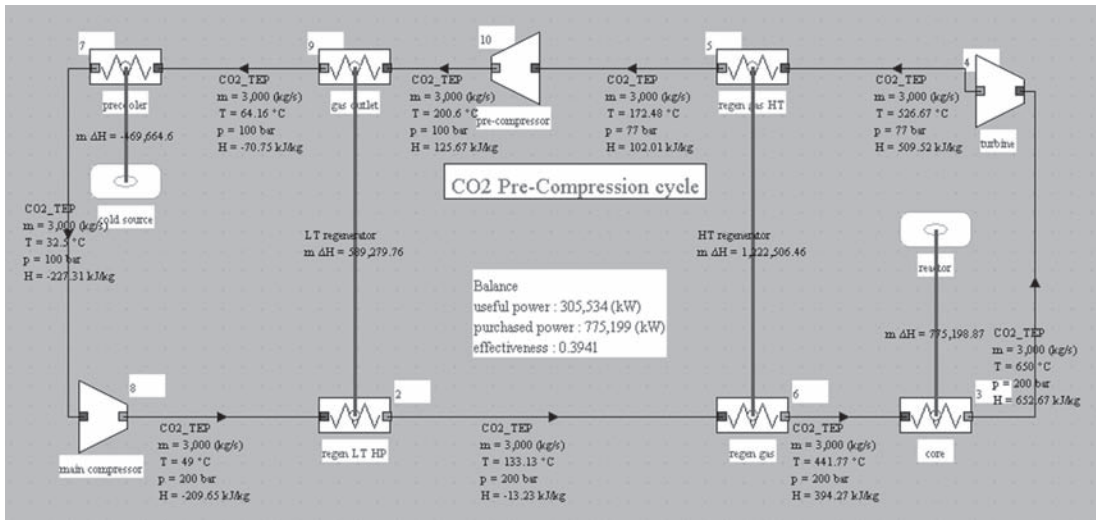


FIGURE 24.2.3
Synoptic view of the supercritical CO₂ pre-compression cycle

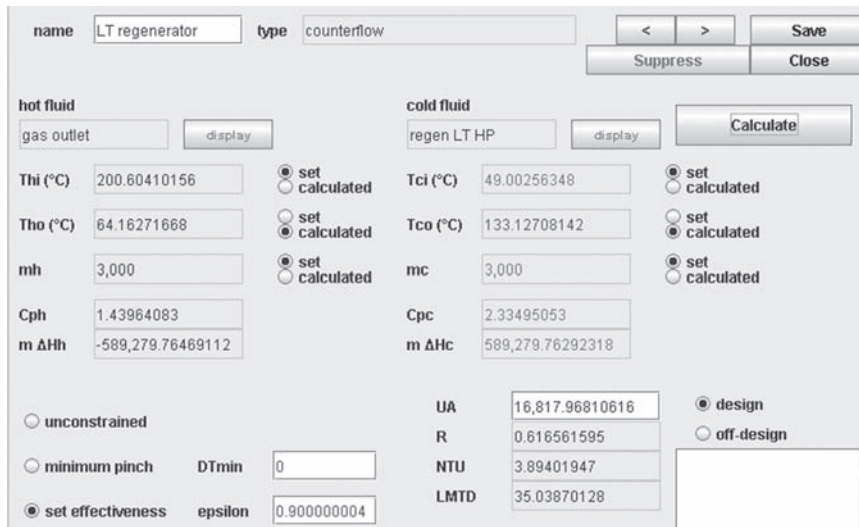


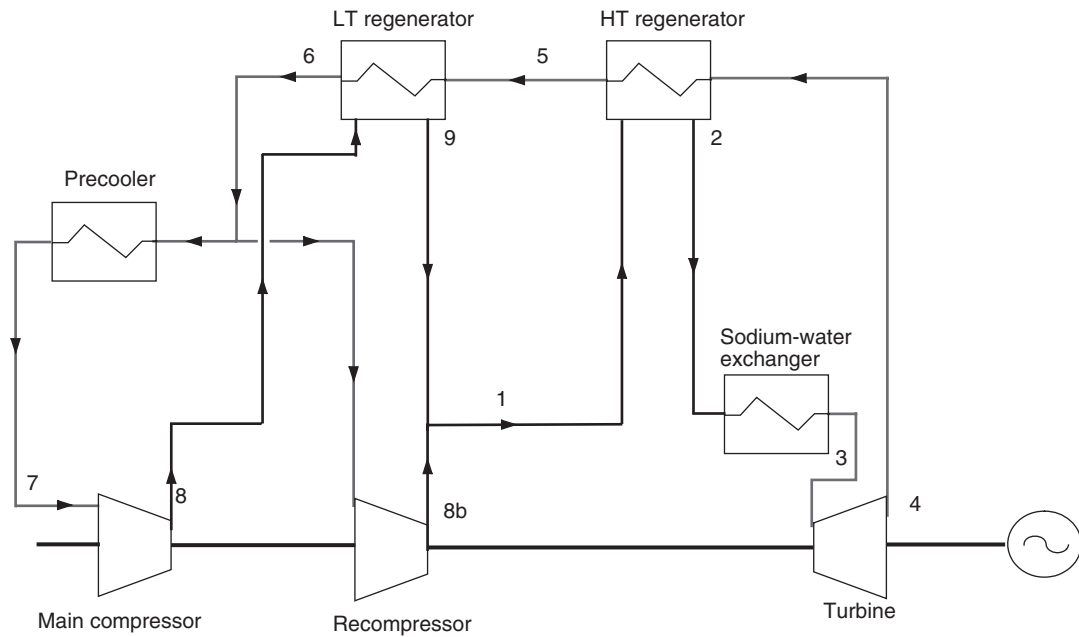
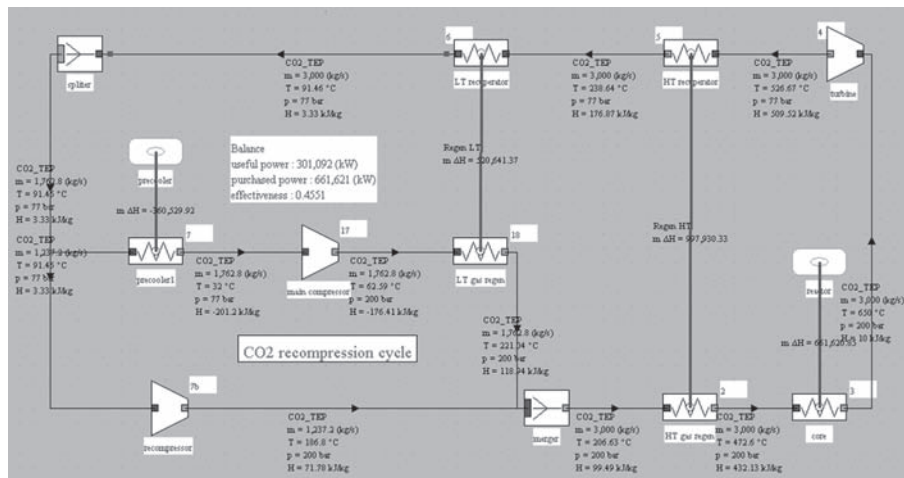
FIGURE 24.2.4
LT regenerator screen

The advantage of this cycle is that when the temperature difference between the two fluids is reduced in the regenerator, the insertion of a pre-compression allows one to increase it, thus promoting regeneration. A problem remains however, as shown in Figure 24.2.4: CO₂ heat capacities of the two fluids becoming very different, the heat exchanger internal irreversibilities increase.

24.2.3 Recompression cycle

In a **recompression** cycle (Figure 24.2.5), compression is two-stage with intermediate cooling of only a portion of the fluid, which allows recycling of a larger amount of heat.

The main flow of CO₂ (3 t/s) leaving the turbine passes through a high temperature regenerator (4-5) and then in a low temperature one (5-6), before being split in two.

**FIGURE 24.2.5**CO₂ supercritical recompression cycle**FIGURE 24.2.6**Synoptic view of the CO₂ supercritical recompression cycle

60% of the flow is cooled in a precooler (6-7), then compressed in the main compressor from 77 to 200 bar (7-8), and heated in the LT regenerator (8-9).

The remaining CO₂ flow is compressed at 200 bar in the recompressor (6-8b), then mixed with another stream exiting the LT regenerator (1), and the total flow is heated in the HT regenerator (1-2) before entering the reactor.

CO₂ exiting the reactor is then expanded in the turbine (3-4), and the cycle is thus closed.

In this case, the reactor inlet temperature is higher, and with the same assumptions as before on the polytropic efficiency of turbomachinery (0.9) and exchanger effectiveness (0.9), the capacity remains close to 300 MWe, and the efficiency exceeds 45% (Figure 24.2.6). Even higher values are hoped for, the order of 50%, with exchanger effectiveness around 95%.

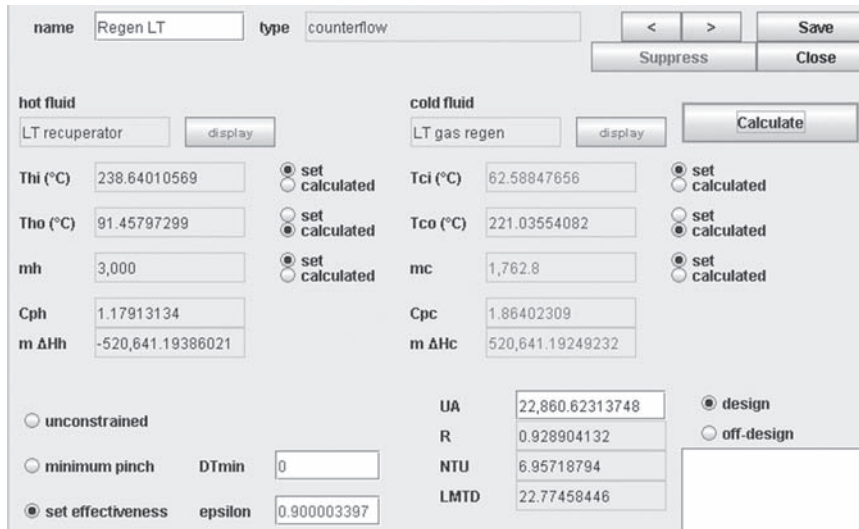


FIGURE 24.2.7
LT regenerator screen

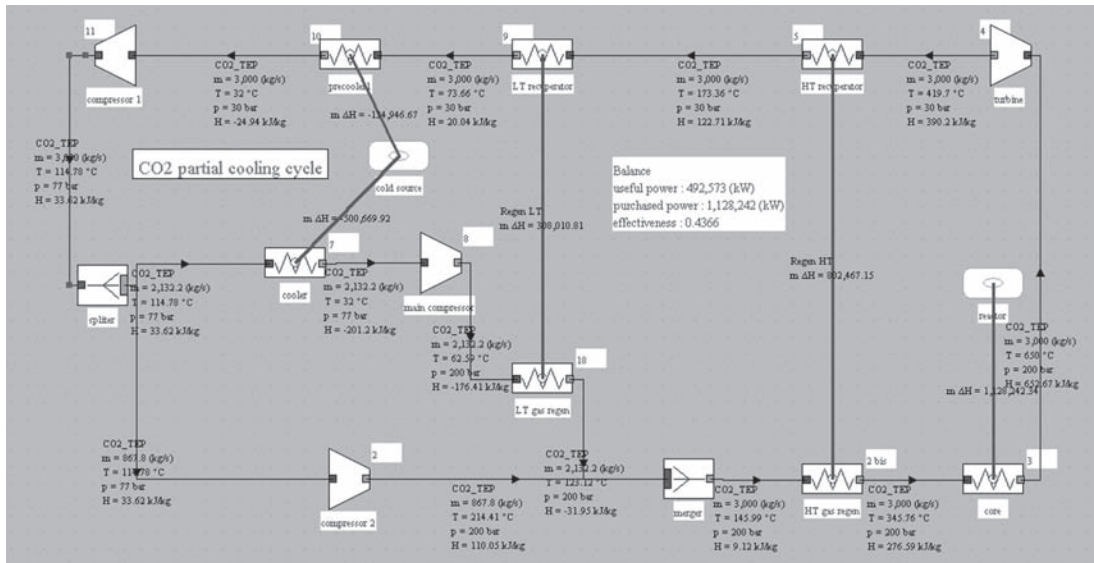


FIGURE 24.2.8
Synoptic view of the partial cooling CO₂ supercritical cycle

The performance improvement is that the LT regenerator is much better balanced in terms of enthalpy than in pre-compression cycle because only a fraction of the flow traverses the high pressure part, thus compensating for the increased thermal capacity of CO₂ in the supercritical region at low temperature, as shown in Figure 24.2.7.

24.2.4 Partial cooling cycle

This cycle is a simplified version of the **partial cooling** cycle (Dostal, 2004), where compression is still two-stage, intercooled with only a portion of the fluid.

After passing through a high temperature regenerator then in a second low temperature one and in a cooler (Figure 24.2.8), a first compressor compresses CO₂ from 30 to 77 bar. The pre-compressed

CO₂ flow-rate is then split into two, one part being cooled by exchange with the cold source, and then compressed in the main compressor and heated in a LT regenerator.

The remaining flow passes through a third compressor to be compressed at 200 bar before being remixed with the stream exiting the LT regenerator, to be heated in the HT regenerator before returning to the reactor compartment. With the same assumptions as before on heat exchanger effectiveness and turbomachinery polytropic efficiency, the efficiency of this cycle is 43.7%, slightly less than the recompression cycle, which is also simpler. Its capacity, however, is much higher (490 MW).

Supercritical CO₂ cycles appear very interesting in thermodynamic terms. The two main technological constraints are the realization of regenerators in the circum-critical zone in particular to avoid any temperature crossing, and that of turbomachinery effective for CO₂, an area where there is no reference. Moreover, these cycles can only work if the CO₂ state at the precooler output is supercritical, which implies a temperature limit of 32°C, which can be difficult to achieve when the cold source is outside air, a river or sea water.

24.3 ADVANCED COMBINED CYCLES

24.3.1 Air combined cycle

In a conventional combined cycle, exhaust gases of a high temperature gas turbine are used as heat source for a steam cycle. In an air combined cycle (Figure 24.3.1), the steam cycle is replaced by a second air gas turbine cycle operating with adequate compression ratio and air flow (Weston, 1993, Najjar, Zammout, 1996). In English we talk about an air bottoming cycle.

The advantage of such a cycle is not to require water cooling, to be less expensive than a conventional combined cycle, and it can be considered if regeneration is impossible.

The hot air leaving the high temperature second cycle can be used in cogeneration.

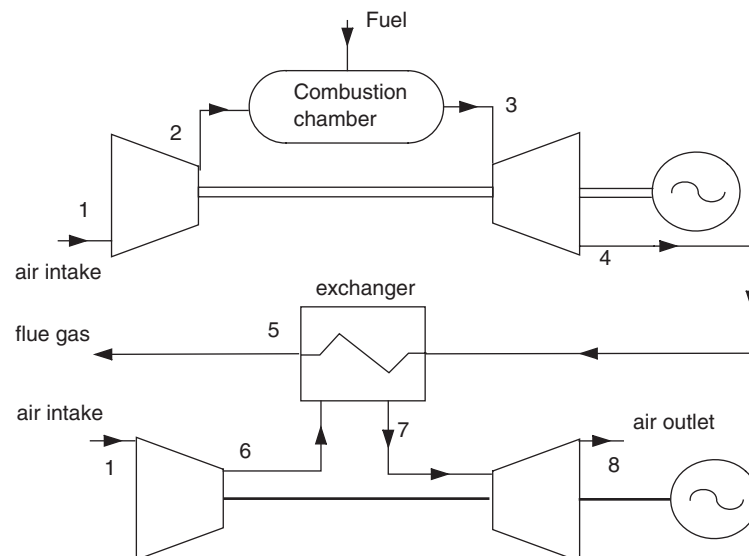


FIGURE 24.3.1

Air combined cycle

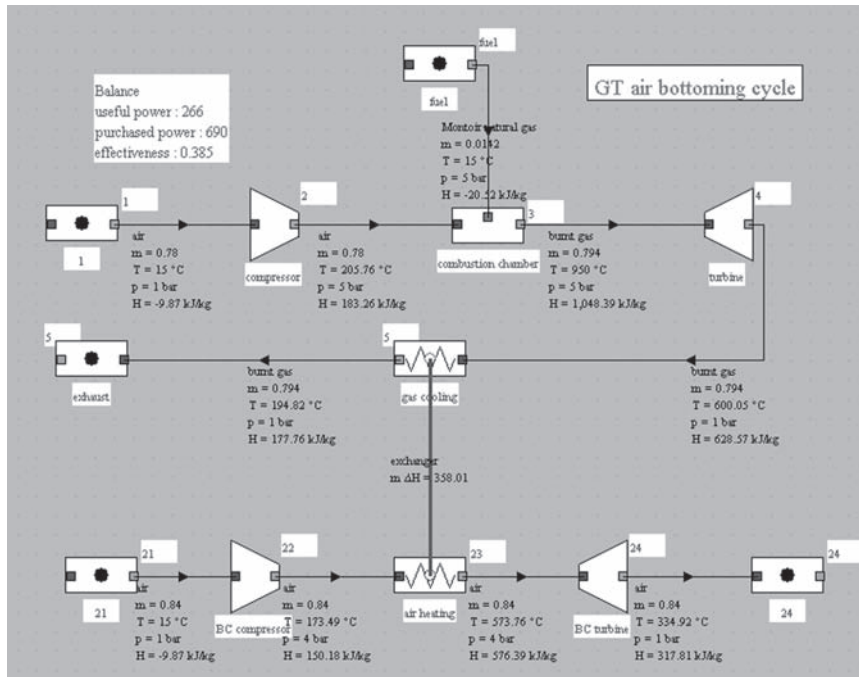


FIGURE 24.3.2
Synoptic view of the air combined cycle

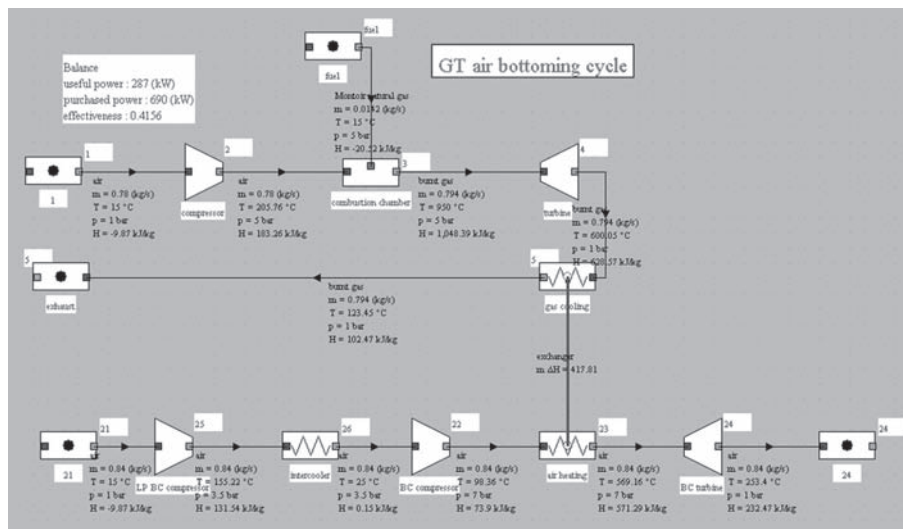
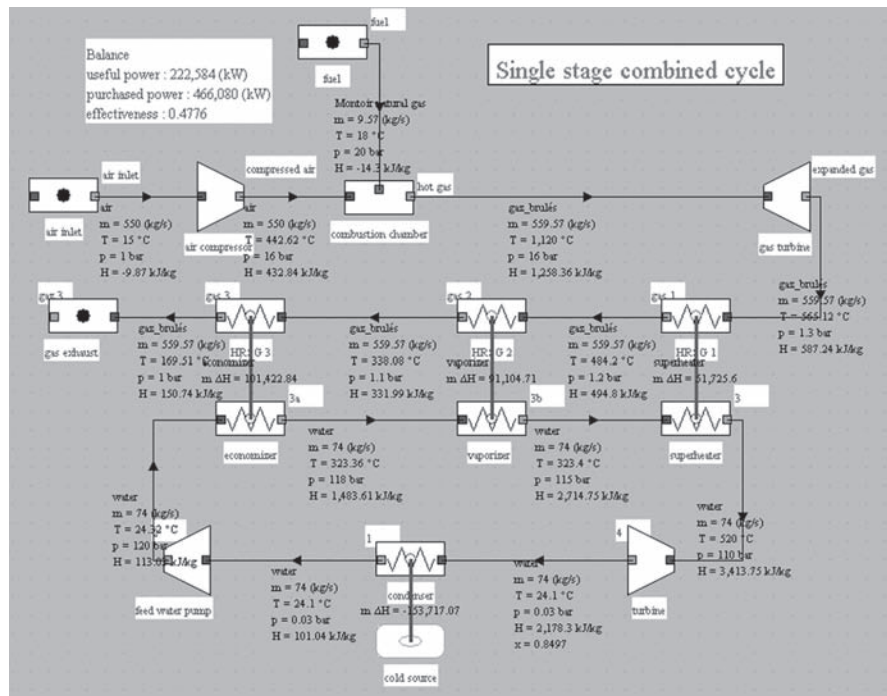


FIGURE 24.3.3
Air combined cycle with intercooler

24.3.1.1 Low compression ratio and low temperature cycle

Let us consider a gas turbine which sucks 0.78 kg/s of air at 15°C and 1 bar. Its compression ratio is equal to 5 and the compression isentropic efficiency is 0.875. At the combustor outlet, turbine inlet temperature is 950°C, and expansion isentropic efficiency is 0.885. It is assumed that fuel is methane.

For the second cycle, we seek the pair (air flow/compression ratio) which leads to the best performance, taking 0.95 as intercooler effectiveness and compressor and turbine polytropic efficiencies of 0.9. The Thermoptim cycle synoptic view is given in Figure 24.3.2.

**FIGURE 24.3.4**

Reference combined cycle

We may also use intermediate cooling, and compare the performance of this cycle to that of a conventional single pressure combined cycle. In this case where the compression ratio is low, a simple regeneration cycle leads to slightly better performance (43.2%).

24.3.1.2 High compression ratio and high temperature cycle

For the remainder of this section, we will consider as base case the single pressure combined cycle studied section 17.3 of Part 3, whose gas turbine has a compression ratio equal to 16, turbine inlet temperature of 1120°C , polytropic efficiency equal approximately to 0.85 for compression, and 0.84 for expansion, and we will take pressure drop of 0.3 bar in the exchanger.

The synoptic view of this combined cycle is given in Figure 24.3.4. Its efficiency is 47.8% and the temperature of the gases leaving the stack is equal to about 170°C .

Taking into account an intermediate cooling for the bottoming cycle, one gets for this new compression ratio an efficiency of nearly 41.6% (Figure 24.3.5), whereas regeneration becomes almost impossible.

The efficiency of this cycle is lower than the reference, but its architecture is much simpler.

24.3.2 Steam flash combined cycle

The performance of a conventional combined cycle depends directly on that of the heat recovery steam generator (HRSG). We have shown in chapters 17 and 22 of Part 3 that a single pressure level does not allow the gas turbine to be sufficiently cooled, and it is desirable to provide two or three pressure levels.

Such technology, however, is restricted to machines of high capacity, for both technical and economic reasons. Technically, it is indeed very difficult to properly control the distribution of the total flow of water or steam between the different circuits. In fact small combined cycles are limited to a single pressure without reheat.

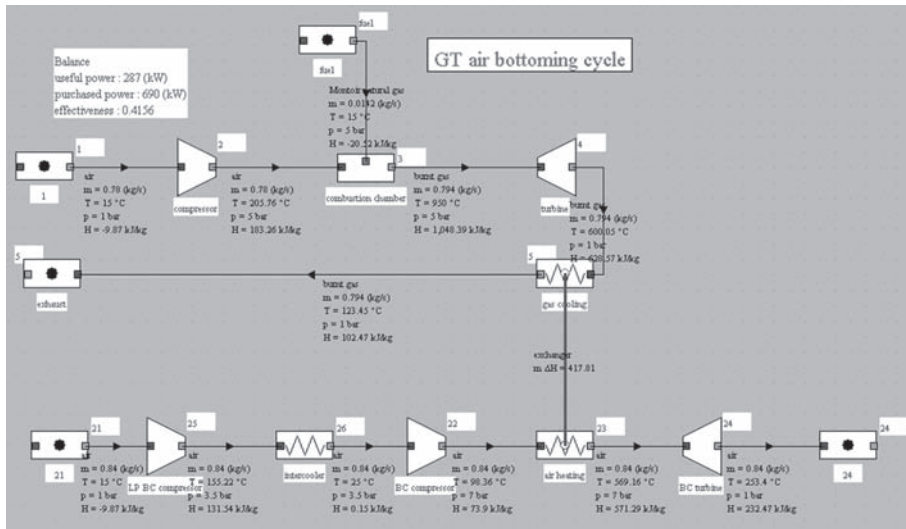


FIGURE 24.3.5
High pressure air combined cycle with intercooler

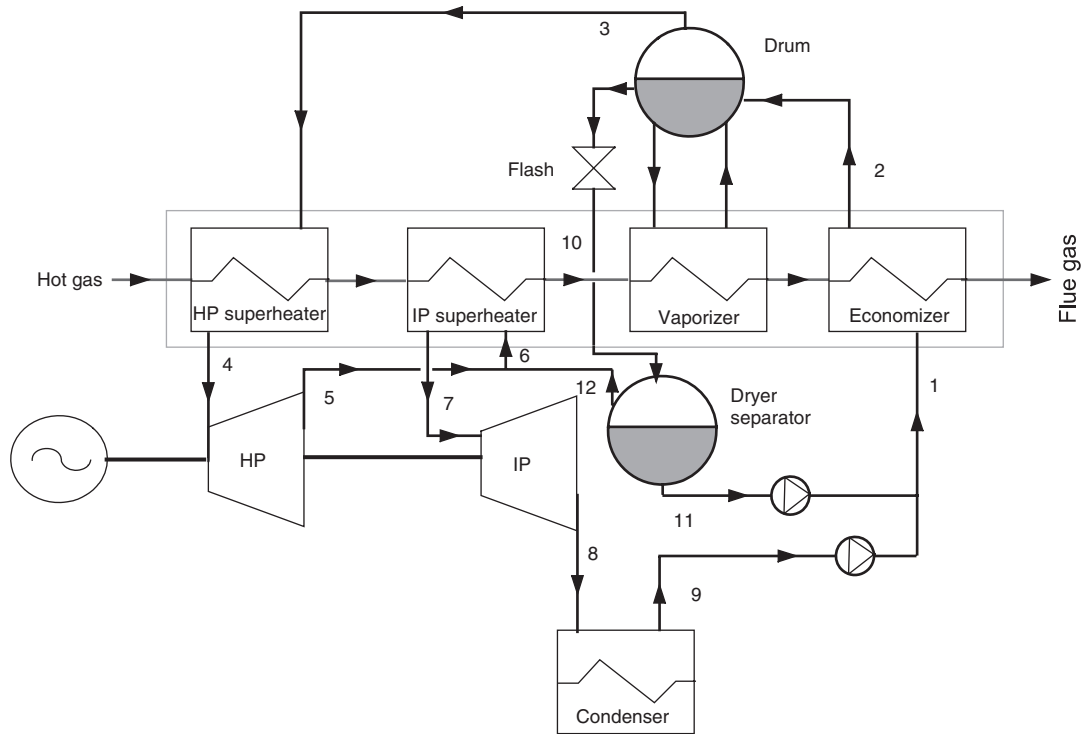


FIGURE 24.3.6
Steam flash combined cycle

To overcome this difficulty, a new steam flash cycle has been proposed (Dechamps, 1994) (Figure 24.3.6). In English we talk about *water flashing bottoming cycle* or WFBC. The advantage of such a cycle is to reduce irreversibilities in the HRSG and be less costly than a combined cycle with several pressure levels.

The total flow of liquid water at HP pressure is vaporized at the corresponding saturation temperature. Much of this flow is then superheated and expanded in a turbine at LP pressure,

while the rest of the flow is expanded in two-phase state at this LP pressure, then the liquid and vapor phases are separated. The two LP steam streams are then remixed before being reheated and expanded in a turbine at the condensation pressure. The liquid flow at LP pressure is recompressed at HP pressure by a pump and mixed with water at the outlet of the recirculation pump located downstream the condenser.

The synoptic view of Figure 24.3.7 shows that the efficiency obtained is 48.3%, as exhaust gases can be cooled at 120°C, which is a small improvement over the reference single pressure combined cycle for which these figures were respectively 47.8% and 170°C.

Composites (see section 22.1.2 of Part 3) for this cycle are given in Figure 24.3.8. They show that the hot fluid is cooled, but the superheating could be increased.

24.3.3 Steam recompression combined cycle

A patent was filed in 1978 by Cheng on a new steam recompression cycle (see Figure 24.3.9). In English we speak of *steam recompression bottoming cycle* or SRBC. The advantage of such a cycle is to reduce irreversibilities in the HRSG and be less costly than a combined cycle with several pressure levels.

The total flow of liquid water leaving the condenser is compressed at LP pressure, then heated at the corresponding saturation temperature. A fraction of this flow is vaporized, then compressed at HP pressure by a compressor, while the rest of the flow is compressed in the liquid state at the same pressure by a pump. Both streams are then remixed before feeding the high pressure evaporator, the superheater and the turbine.

In searching, for steam recompression combined cycle, a set of values (superheating temperature, primary and secondary steam flow rates, IP and HP pressures) that leads to good performance, keeping the same values for HRSG pinches, we get the synoptic view of Figure 24.3.10.

The efficiency is 49%, as the exhaust gas can be cooled to 160°C, which is still a small improvement over the reference single pressure combined cycle.

Composites for this cycle are given in Figure 24.3.11. They show that the hot fluid is cooled less than with the flash steam cycle, but the superheating is better, so that, overall, HRSG irreversibilities are lower.

24.3.4 Kalina cycle

As we discussed in section 17.3 of Part 3, the optimization of a combined cycle is a particularly complex problem that leads to try to minimize irreversibilities stemming from temperature heterogeneity between the two cycles. When the recovery cycle uses a pure substance like water, the existence of a vaporization plateau induces losses that can be reduced only with difficulty by multiplying pressure levels. To overcome this constraint, Kalina has proposed to use as working fluid water-ammonia mixture, which has a large temperature glide (Kalina, 1983, 1984).

An elementary Kalina cycle (Figure 24.3.12) consists of three main elements:

- a recovery steam generator (HRSG);
- a turbine;
- a distillation and condensation system (DCS).

The complexity of the cycle results from two causes:

- to benefit from a significant temperature glide in the temperature range corresponding to the hot gas cooling, the ammonia quality of the mixture should be quite high (typically 50% NH₃, 50% H₂O);
- to be condensed at a temperature above that of the surroundings and at low pressure, the ammonia quality of the mixture should be low (typically 20% NH₃, 80% H₂O).

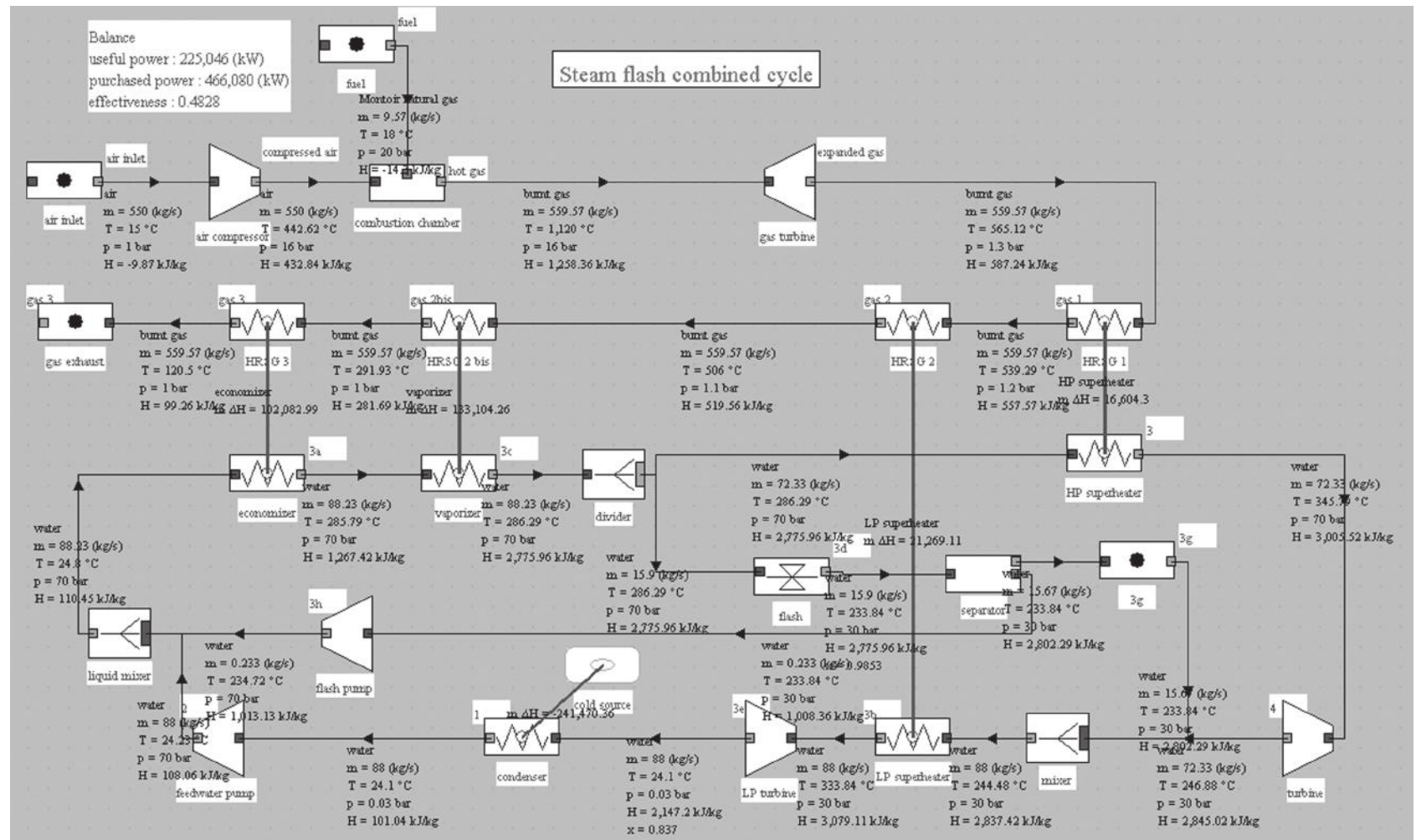


FIGURE 24.3.7

Synoptic view of a steam flash combined cycle

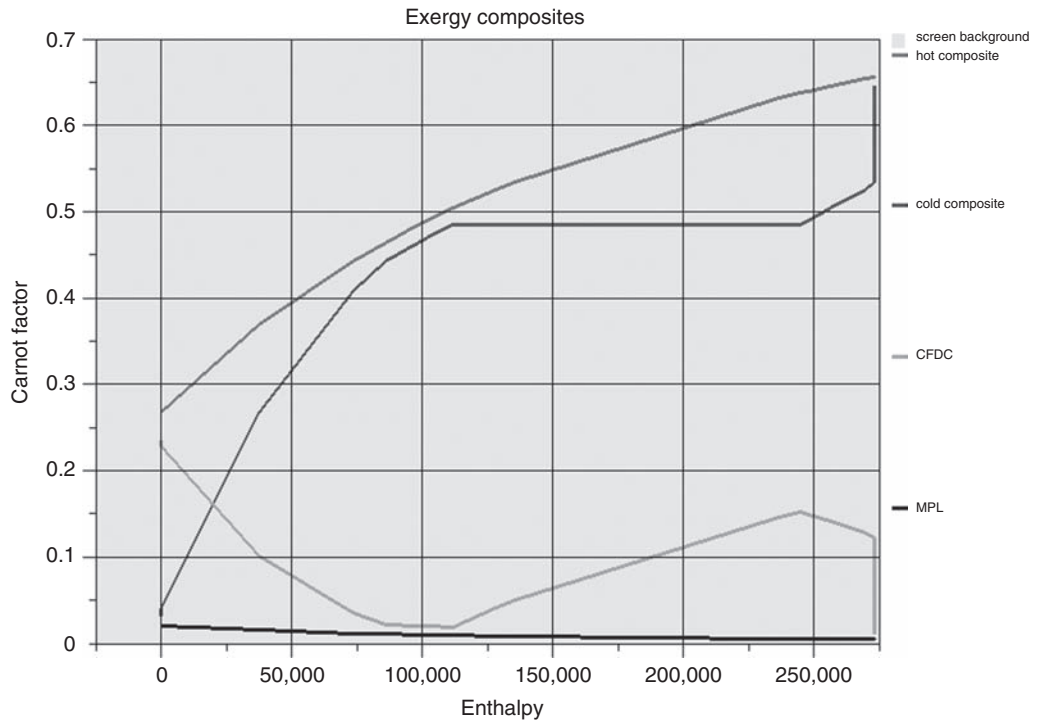


FIGURE 24.3.8
Steam flash combined cycle composites

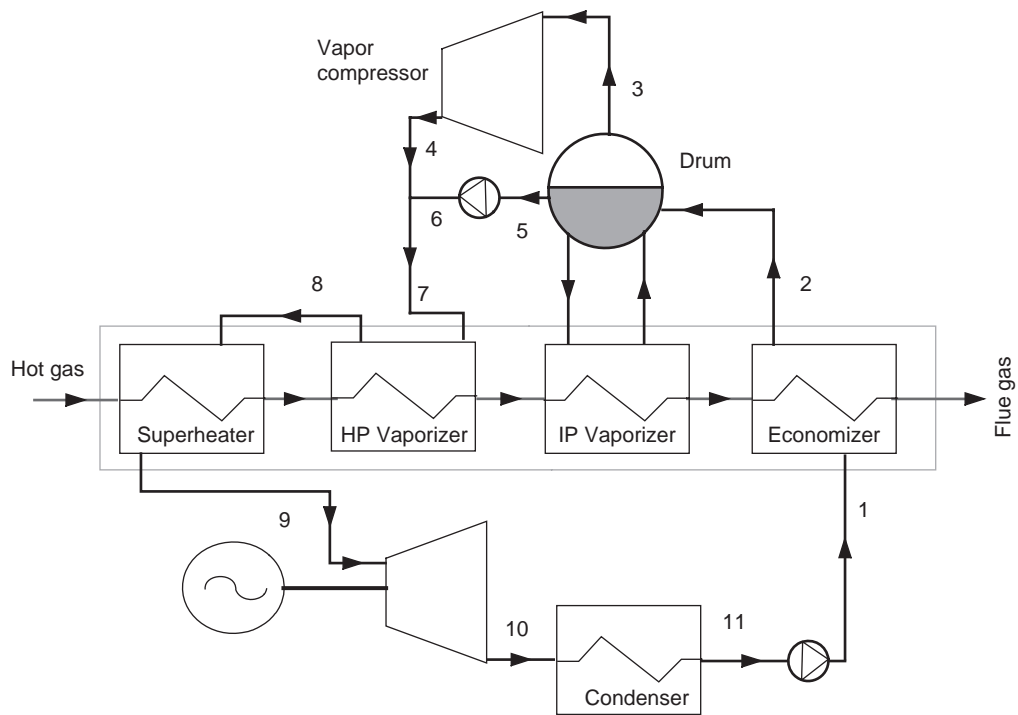


FIGURE 24.3.9
Steam recompression combined cycle

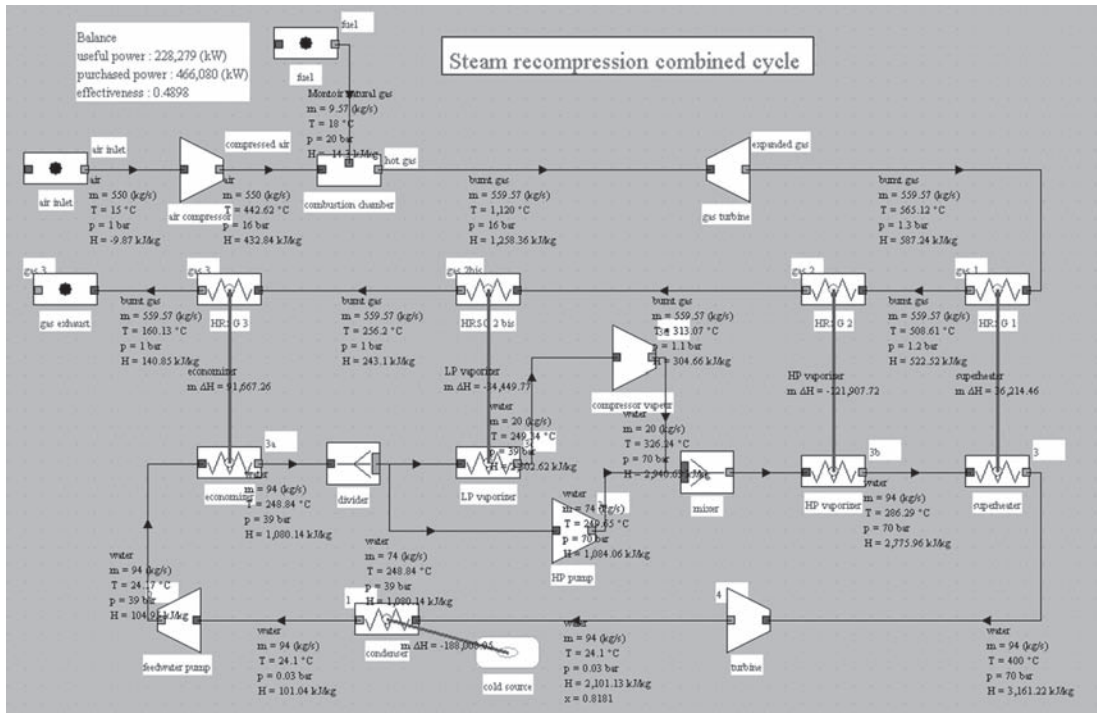


FIGURE 24.3.10
Synoptic view of the steam recombination combined cycle

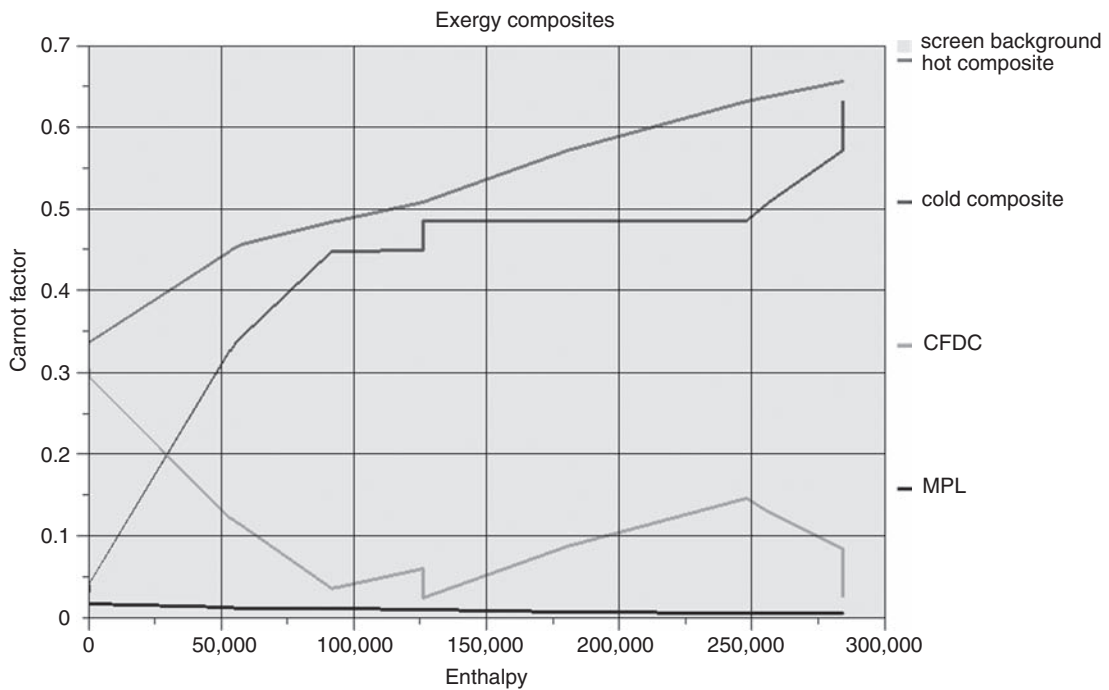
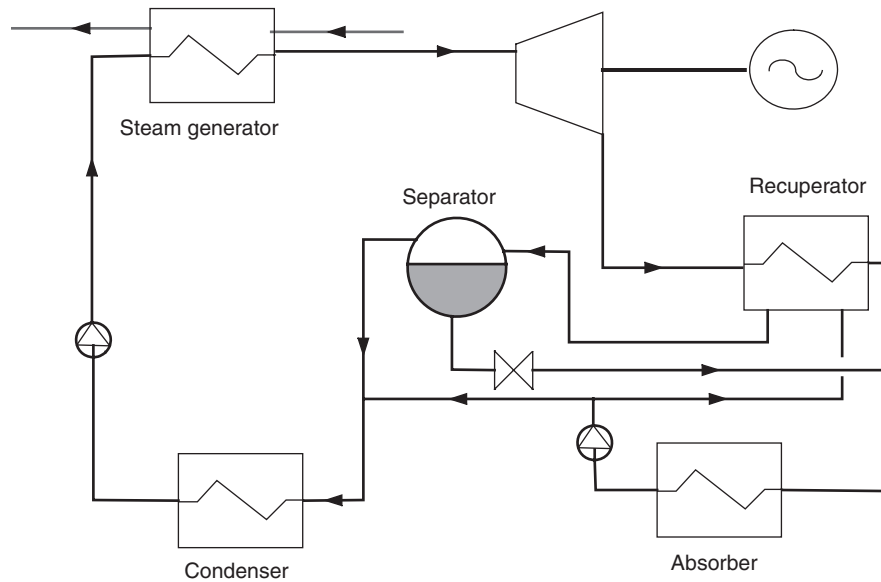
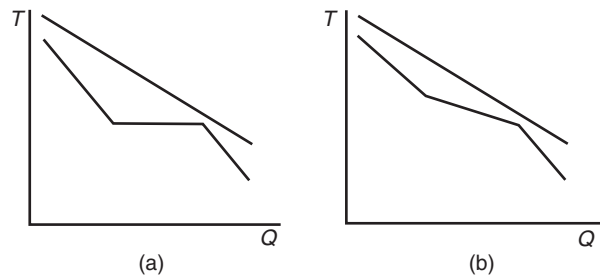


FIGURE 24.3.11
Steam recombination combined cycle composites

**FIGURE 24.3.12**

Kalina cycle

**FIGURE 24.3.13**

Internal irreversibilities in a Hirn (a) and Kalina (b) cycle

The structure of a Kalina cycle is given Figure 24.3.12. It can produce mechanical power from a heat source at variable temperatures, such as effluent or exhaust gas from a gas turbine.

As shown in Figure 24.3.13 (b), the existence of this temperature glide reduces the average difference in temperature between the gas stream cooling in the HRSG and the working fluid as compared to what is happening in a Hirn cycle (Figure 24.3.13(a)). Internal irreversibilities due to the temperature gradient are reduced.

One is therefore led to change the mixture composition between the hot zone (HRSG) and cold zone of the cycle, which is achieved in the DCS.

In the DCS the rich mixture leaving the turbine is cooled in a recuperator, then mixed with a weak solution of NH_3 to raise the condensation temperature. The mixture (basic solution) is condensed in the absorber, recompressed and directed to the recuperator. A portion of the flow is used to dilute the rich solution leaving the separator, while the main stream is distilled at the

component name	molar fraction	mass fraction
ammonia	0.5132229	0.4989364
water	0.4867771	0.5010636

FIGURE 24.3.15

Composition of the working fluid

component name	molar fraction	mass fraction
ammonia	0.1991653	0.1902052
water	0.8008347	0.8097948

FIGURE 24.3.16

Composition of weak liquid

component name	molar fraction	mass fraction
ammonia	0.3097986	0.2977115
water	0.6902014	0.7022885

FIGURE 24.3.17

Composition of the basic mixture

component name	molar fraction	mass fraction
ammonia	0.8823395	0.8762746
water	0.1176605	0.1237254

FIGURE 24.3.18

Composition of rich vapor before mixing

To circumvent this difficulty, we proceed as follows:

- the expanded working fluid ($m = 100 \text{ kg/s}$) is cooled down at 15°C and mixed with a high flow rate ($m = 350 \text{ kg/s}$) of weak liquid (Figure 24.3.16), thus forming the basic mixture (Figure 24.3.17), which is condensed, compressed to 2.1 bar and heated at 70°C ;
- the basic mixture is then distilled, thereby separating the rich vapor (Figure 24.3.18), and weak liquid;
- a fraction of the weak liquid is remixed with the rich vapor to form the working fluid entering the turbine, which should not be too rich in ammonia if we want it to be condensed at room temperature;
- the working fluid is condensed then pressurized and led to the boiler;
- the rest of the weak liquid is cooled and then expanded before being mixed with the working fluid.

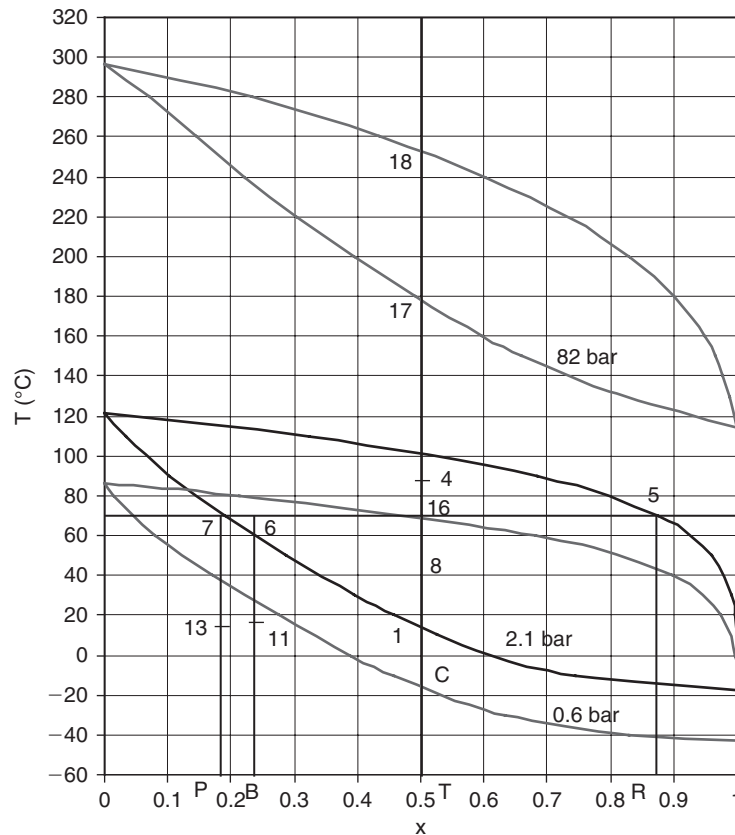
Note that, since the pressure and temperature at the separator inlet are set, the compositions of the weak liquid and rich vapor are independent of the basic mixture, which only affects the distribution of these two fluid flows.

The cycle efficiency approaches 50%, exhaust gases being cooled at 55°C .

Representation of certain points on the ammonia-water mixture isobaric lenses allows one to understand the changes in composition in the Kalina cycle (Figure 24.3.19).

Plotted on this diagram are:

- from bottom to top respectively, the three lenses at 0.6, 2.1 and 82 bar;
- in the form of vertical segments from left to right, respectively, the ammonia compositions of the weak liquid (7-P), basic mixture (6-B), working fluid (18-17-16-T) and rich vapor (5-R).


FIGURE 24.3.19

Water-ammonia isobaric lenses

The working fluid leaves the turbine at point 4, at 0.6 bar. To condense it at this pressure, it should be cooled to point C, i.e. at about -18°C , which is impossible by simple exchange with the surroundings.

The solution is to cool it to point 8, at 40°C and mix it in an absorber with weak liquid subcooled at 15°C (point 13). The mixture leaves the absorber at 19°C with the basic mixture composition, in slightly subcooled liquid state. It can then be compressed to 2.1 bar at the cost of reduced work.

The heated basic mixture enters in state 6 the separator which operates distillation, separating weak liquid (7) and rich vapor (5). A fraction of the weak liquid flow is remixed with the rich vapor to form the working fluid at 2.1 bar (16), which is then condensed in the liquid state (1), thereby allowing to compress it up to 82 bar with a reduced work.

In the steam generator, the working fluid is then heated in the liquid state to point 17 and then vaporized with temperature glide at point 18 and superheated at 532°C (point outside diagram). It is then expanded in the turbine to point 4, closing the cycle.

Figures 24.3.20 and 24.3.21 show the shapes of composites for the Kalina cycle just described. They show that the system can be balanced in terms of enthalpy: heat recovered during the cooling of the expanded steam and the weak liquid is enough to preheat the basic mixture before entering the separator.

Thermal integration of the Kalina cycle is thus relatively simple.

The importance of the temperature glide and its impact on minimizing internal irreversibilities is very clear on these two curves. The Kalina cycle can recover much better the enthalpy available in the exhaust fumes than a conventional steam cycle (El Sayed, Tribus, 1985, Johnsson, Yan, 2001).

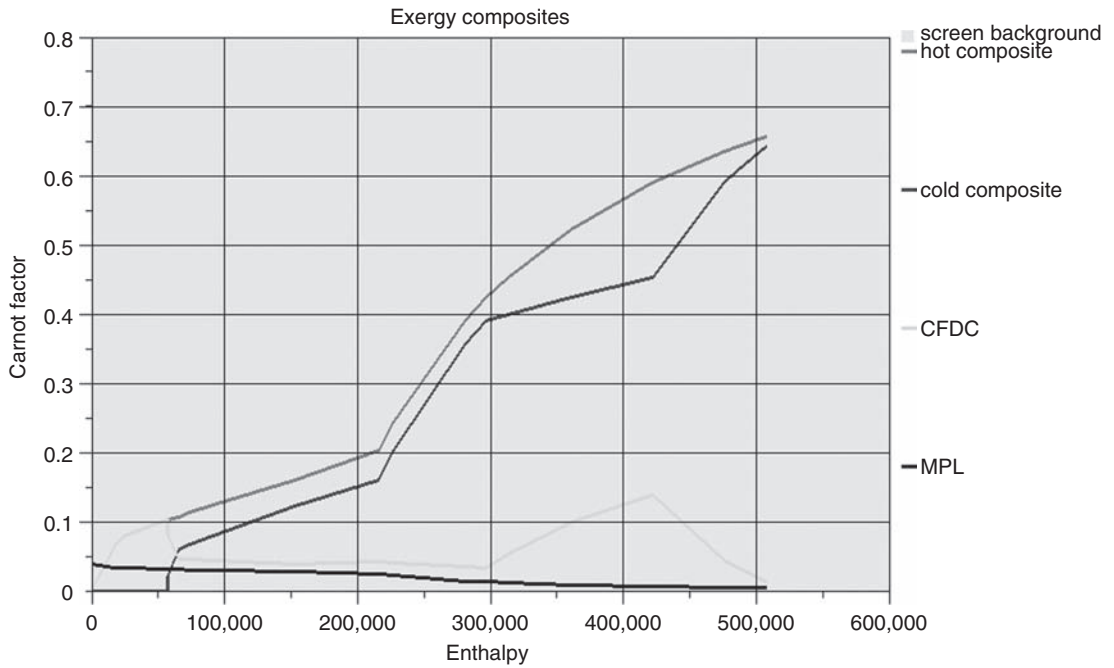


FIGURE 24.3.20
Exergy composites of the Kalina cycle

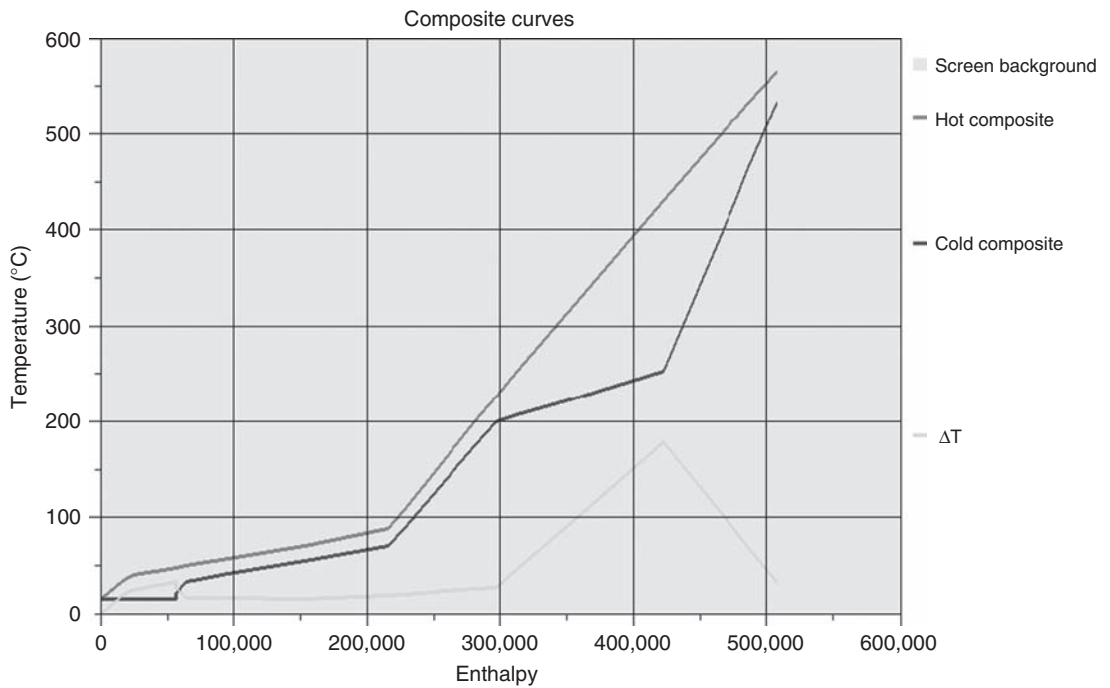


FIGURE 24.3.21
Composites of the Kalina cycle

REFERENCES

- P. Chiesa, G. Lozza, E. Macchi, S. Consonni, *An assessment of the thermodynamic performance of mixed gas-steam cycles: part B—water injected and HAT cycles*, Journal of Engineering for Gas Turbines and Power, vol. 117, pp. 499–508, July 1995.
- T. R. Mori, H. Nakamura, T. Takahashi, and K. Yamamoto, *A Highly Efficient Regenerative Gas Turbine System by New Method of Heat Recovery with Water Injection* Proceedings, 1983 Tokyo International Gas Turbine Congress. Vol. 1, pp. 297–303.
- M. Nakhamkin, E.C. Swensen, J.M. Wilson, G. Gaul, M. Polsky, *The Cascaded humidified advanced turbine (CHAT)*, Journal of Engineering for Gas Turbines and Power, vol. 118, pp. 565–571, July 1996.
- V. Dostal, M.J. Driscoll, P. Hejzlar, N.E. Todreas, *A Supercritical CO₂ Gas Turbine Power Cycle For Next-Generation Nuclear Reactors*, Proc. ICONE-10, Arlington, Virginia, April 14–18, 2003.
- V. Dostal *A Supercritical Carbon Dioxide Cycle For Next-Generation Nuclear Reactors*, PhD thesis, MIT, January 2004.
- P.J. Dechamps, *A Study of Simplified Combined Cycle Schemes with Water Flashing*, Proceedings of the Florence World Energy Research Symposium, FLOWERS'94, Florence, Italy, July 6–8, 1994.
- Y.S.H. Najjar, M.S. Zaamout, *Performance Analysis of Gas Turbine Air-Bottoming Combined System*, Energy Conversion and Management, Vol. 37, pp. 399–403, 1996.
- K.C. Weston, *Dual Gas Turbine Combined Cycles*, Proceedings of the 28th Intersociety Energy Conversion Engineering Conference IECEC'93, Boston, Vol. 1, pp. 955–958, 1993.
- F. Wicks, C. Wagner, *Synthesis and Evaluation of a Combined Cycle with No Steam Nor Cooling Water Requirements*, Proceedings of the 28th Intersociety Energy Conversion Engineering Conference IECEC'93, Boston, Vol. 2, pp. 105–110, 1993.
- D.Y. Cheng, *Pressure-Staged Heat Exchanger*, U.S. Patent 4,072,182, 1978a.
- D.Y. Cheng, *Regenerative Parallel Compound Dual-Fluid Cycle Heat Engine*, U.S. Patent 4,128,994, 1978b.
- Y. M. El-Sayed, M. Tribus, *A Theoretical Comparison of the Rankine and Kalina Cycle*, 1985a, ASME publication AES-Vol. 1.
- A.I. Kalina, *Combined Cycle System with Novel Bottoming Cycle*, Journal of Engineering for Gas Turbines and Power, vol. 106, pp. 737–742, 1984.
- A.I. Kalina, *Combined Cycle System with Novel Bottoming Cycle*, ASME Journal of Engineering for Power, vol. 106, no. 4, Oct. 1984, pp. 737–742 or ASME 84-GT-135, Amsterdam.
- A.I. Kalina, *Combined cycle and waste heat recovery power systems based on a novel thermodynamic energy cycle utilising low temperature heat for power generation*, ASME Paper 83-JPGC-GT-3, 1983.
- M. Johnsson, J. Yan, *Ammonia-water bottoming cycles: a comparison between gas engines and gas diesel engines as prime movers*, Energy, Vol. 26, 2001, pp. 31–44.

Evaporation, Mechanical Vapor Compression, Desalination, Drying by Hot Gas

Abstract: Concentration by evaporation facilities are widely used in industries including food as well as for seawater desalination. The idea is to evaporate the product, the solute being usually nonvolatile. This produces a separation of two components, which allows the concentration to be increased. Desalination is a variant of evaporation, where the valuable output is the vapor evaporated, which is condensed to produce fresh water.

Mechanical vapor compression is often presented as an efficient alternative to heat pump if the cold source is a gas or vapor. The two most conventional mechanical vapor compression (VC) applications being distillation and concentration by evaporation, we deemed it appropriate to address this issue here.

In this chapter, we therefore focus on four issues:

- concentration by evaporation;
- mechanical vapor compression (MVC);
- desalination, including sea water;
- drying by hot gas.

Keywords: evaporation, single-effect, multi-effect, boiling point elevation, ebullioscopic constant, desalination, solute, solvent, multi-stage flash, reverse osmosis, ejector, MED, MVC, MSF, drying.

25.1 EVAPORATION

Evaporation being a major consumer of heat, it is necessary to optimize the design of concentration facilities if we want to get good performance. Thermal integration methods presented in Chapter 22 of Part 3 can find a scope of interest in this area.

25.1.1 Single-effect cycle

In a conventional single-effect evaporation cycle (Figure 25.1.1) a product to concentrate (solute + solvent) is injected into a unit, heated by any heat input Q (steam 4-5). The concentrated product

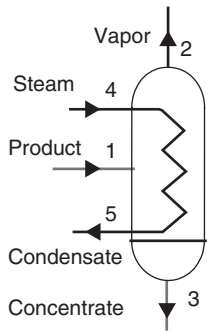


FIGURE 25.1.1
Single-effect evaporation cycle

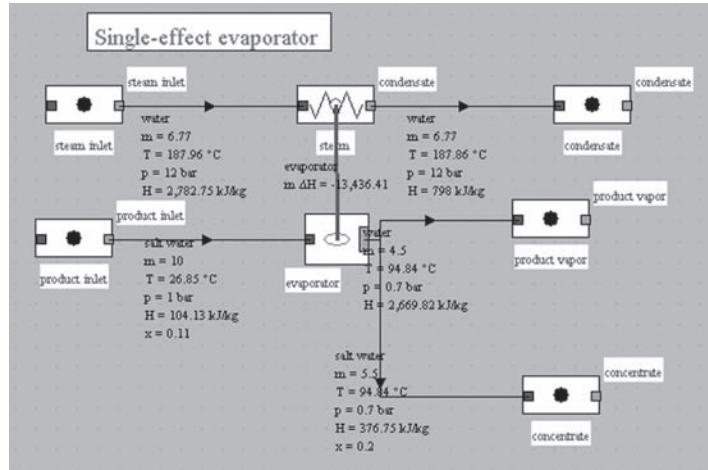


FIGURE 25.1.2
Single-effect evaporator

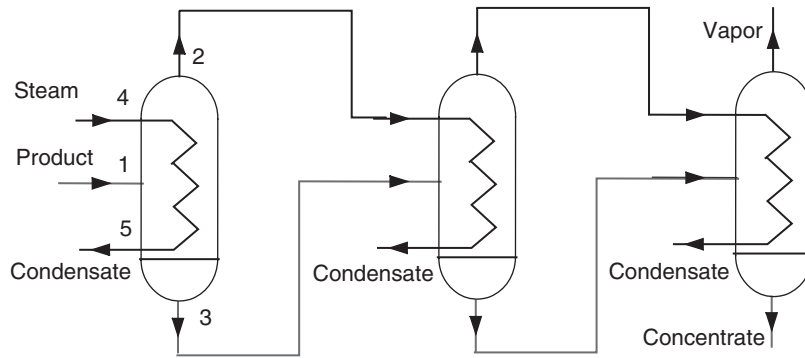


FIGURE 25.1.3
Triple-effect evaporator

is extracted in 3, at the bottom of the unit, while the solvent vapor exits in 2 and is condensed, its enthalpy being lost.

Calling x the mass concentration of solute, equations governing the behavior of this unit are:

$$\text{conservation of the total flow: } \dot{m}_1 = \dot{m}_2 + \dot{m}_3 \quad (25.1.1)$$

$$\text{conservation of solute: } x_1 \dot{m}_1 = x_3 \dot{m}_3 \quad (25.1.2)$$

$$\text{conservation of enthalpy: } h_1 \dot{m}_1 + Q = h_3 \dot{m}_3 + h_2 \dot{m}_2 \quad (25.1.3)$$

Figure 25.1.2 shows the synoptic view of such an evaporator modeled with ThermoOptim by external class EvapoConcentrator.java. In this example, there are 10 kg/s of feed product (salt water) containing 11% solids at 1 bar, that we want to bring to a concentration of 20% at 0.7 bar. It is necessary for this to provide heat in the form of 6.78 kg/s of saturated steam at 12 bar, which is fully condensed.

25.1.2 Multi-effect cycle

In a multi-effect (ME) cycle (Figure 25.1.3), vapor produced is condensed in the evaporator of a second unit operating in series with the previous (the different types of irreversibilities by temperature heterogeneity, pressure drops etc. make it necessary to condense the vapor at a lower pressure and

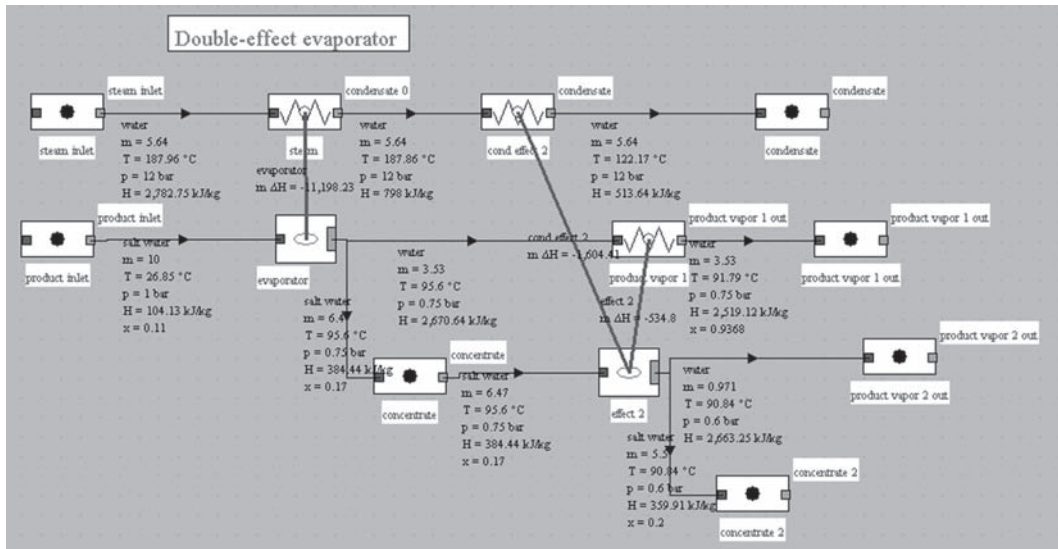


FIGURE 25.1.4

Double-effect evaporator

therefore temperature). A multi-effect concentrator thus allows recovering a portion of the solvent vapor and reduces the operation specific consumption.

Figure 25.1.4 shows the synoptic view obtained for a double effect evaporator operating in conditions close to the previous (the pressure of the concentrate is 0.6 bar instead of 0.7). The flow of live steam, which was equal to 6.7 kg/s for single-effect system, is here 5.65 kg/s thanks to the use of vapor from the first effect for vaporizing part of the second.

In the first case, ratio (steam evaporated)/(heating steam) is 0.66. In the second, it is 0.8.

25.1.3 Boiling point elevation

The saturated vapor pressure of a mixture (solute-solvent) decreases following Raoult's law. It follows that, at given pressure, the boiling point increases slightly compared to that of pure solvent. We call the boiling point elevation this temperature difference ΔT_{eb} . Physically, the presence of the solute impedes the evaporation of the solvent, which may only be made at higher temperature.

It can be shown that ΔT_{eb} is given by the following law:

$$\Delta T_{eb} = ix \frac{K_{eb}}{\rho} \quad (25.1.4)$$

- i is the solute van't Hoff coefficient, representing the number of elementary particles (ions etc.) formed in the solution;
- x is the solute mass concentration;
- K_{eb} is the pure solvent ebullioscopic constant;
- ρ is the solvent density.

Law (25.1.4) indicates that the boiling point elevation is proportional to x . In practice, if we can assume that ρ and K_{eb} are constant, an assumption valid for a small temperature range, it suffices to know some values of the boiling point elevation to identify it as (25.1.5):

$$\Delta T_{eb} = Kx \quad (25.1.5)$$

Class EvapoConcentrator.java used in models of Figures 25.1.2 and 25.1.4 takes into account the boiling point elevation.

25.2 MECHANICAL VAPOR COMPRESSION

In most situations that would be suitable for the use of a heat pump (small temperature difference between a “free” cold source and heat needs), mechanical vapor compression is presented as an efficient alternative if the cold source is a gas or vapor. It is then possible to avoid the evaporator, possibly the condenser, and thus achieve high performance.

Indeed, compression of a vapor (steam or gas in a process) allows its pressure and temperature to be raised, and thus its enthalpy. If the compressed vapor can be recovered either in a process, or in terms of energy, the compression operation can be very attractive economically.

The two most conventional mechanical vapor compression (VC) applications are distillation and concentration by evaporation. It can also be used for recovery of waste heat. However its cycle is then akin to that of a HRSG such as we have discussed in Chapter 15 of Part 3.

25.2.1 Evaporative mechanical vapor compression cycle

In an evaporative mechanical vapor compression cycle (Figure 25.2.1), the idea is to raise the solvent vapor enthalpy level so that it can be directly used to provide heat to the evaporator.

The basic scheme is as in Figure 25.2.1 and its cycle is plotted on the entropy diagram of Figure 25.2.2: in 0, the product to be concentrated is brought in two heat recovery exchangers where it is preheated (0-1) by cooling the concentrated product (1'-7) and condensate (5-6).

In the evaporator, the product to be concentrated is partially evaporated (1-2) by exchange with its own vapor, which condenses (4-5).

At the bottom of the evaporator, the concentrate is extracted in 1', while the solvent vapor exits in 2 to be recompressed in 3, and gain enough enthalpy to be able to serve as cycle hot source. To ensure large heat exchange coefficients (two-phase) in the evaporator, steam is frequently desuperheated from 3 to 4 via a separate heat exchanger, cooled by desuperheating water, even if that requires a steam addition in 4.

The energy interest of the operation is that by providing little additional enthalpy h_{23} (but a mechanical one), it is possible to recover the solvent vapor condensation enthalpy h_{45} . As an indication, if the solvent is water, which has a very high heat of vaporization (almost 10 times that of oil), h_{23} is in practice between 3 and 9% of h_{45} .

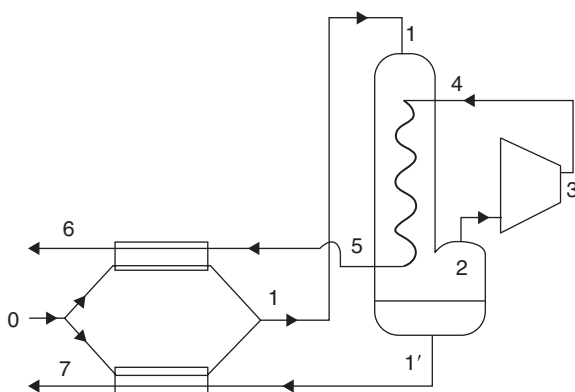


FIGURE 25.2.1
Evaporative mechanical vapor compression cycle

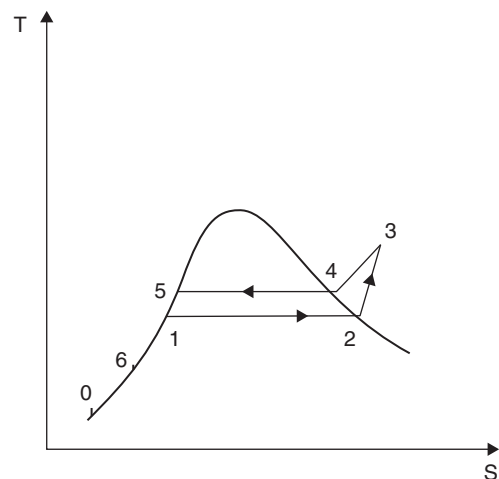


FIGURE 25.2.2
Mechanical vapor compression cycle

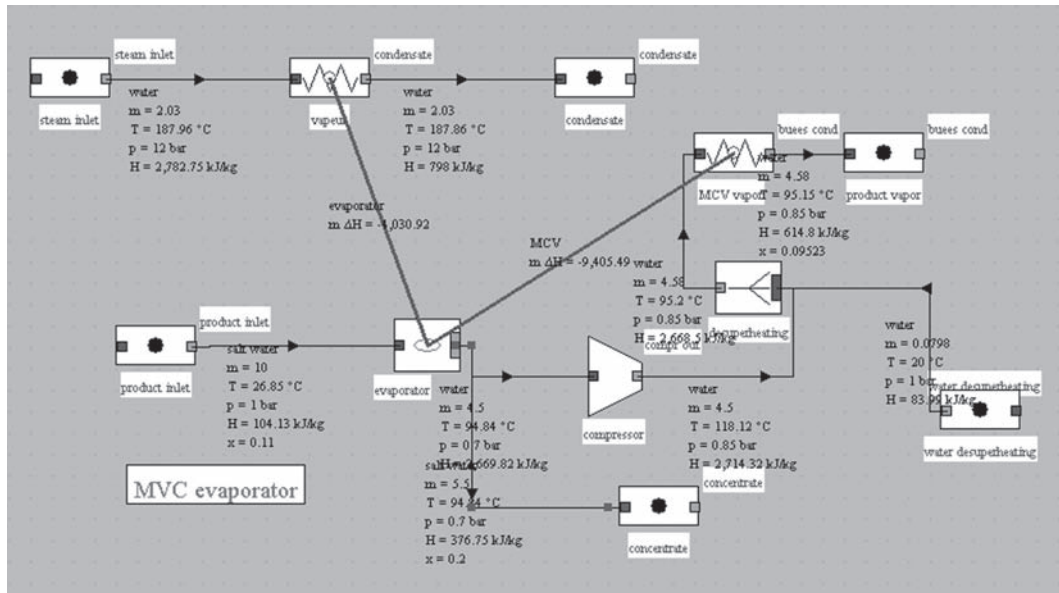


FIGURE 25.2.3
Mechanical vapor compression evaporator

Figure 25.2.3 presents a modification of Figure 25.1.1 single-effect evaporator at which was added a vapor mechanical compression for much of the heat supply. The input steam flow is divided by a factor greater than 3, while the compressor power is only 200 kW. Ratio (steam evaporated)/(heating steam) is 2.2.

25.2.2 Types of compressors used

Evaporators can be combined in series or in parallel, to form multiple-effect mechanical vapor compression evaporators. If evaporators are arranged in parallel, the compressor operates at high flow-rate and low pressure ratio; if they are arranged in series, it works at low flow-rate and high pressure ratio. In the first case, one uses centrifugal or screw compressors, in the second, screw and piston compressors. When the saturation temperature difference to achieve is low ($5\text{--}6^\circ\text{C}$), the pressure difference (about 0.1 bar) can even be supplied by blowers that look like large fans. The latter configuration, which has the advantage of being the most reliable and most flexible, allows, with a speed controller, to modulate within minutes the rate of evaporation from the rated load down to 50% of its value.

In certain situations, if we do not attach too much importance to the compressor isentropic efficiency value, other compression means can be employed: either lobe or liquid ring compressors, or, if steam at high pressure compared to that of the evaporator is available, ejector (or ejecto-compressors), where a steam jet is used to entrain the vapor at the evaporator outlet, and recompress it enough so it can be used as heat source.

25.2.3 Design parameters of a VC

To design and size a VC installation, one must know precise characteristics of the fluid being treated, and in particular, in addition to general thermodynamic data:

- concentrations C_i and C_o at the evaporator inlet and outlet. If the fluid flow at the entrance is \dot{m}_f , the flow of solvent to evaporate is: $\dot{m}_s = \dot{m}_f(1 - C_i/C_o)$;

- the boiling point elevation (see section 25.1.3): depending on the nature of the solute and its final concentration, boiling occurs at a temperature different from that corresponding to the solvent saturation pressure, the gap being up to several tens of degrees Celsius. This elevation depends on the solutions considered. In the case of water, it can lead to increase the compression ratio, and therefore costs;
- thermosensitivity: some products do not stand being processed at too high a temperature or for too long periods of time. This results in specific constraints for processing devices, which it is preferable to take into account in the design phase;
- viscosity can vary significantly from one product to another. It increases with the concentration and decreases with temperature. Its value determines the capacity of circulating pumps;

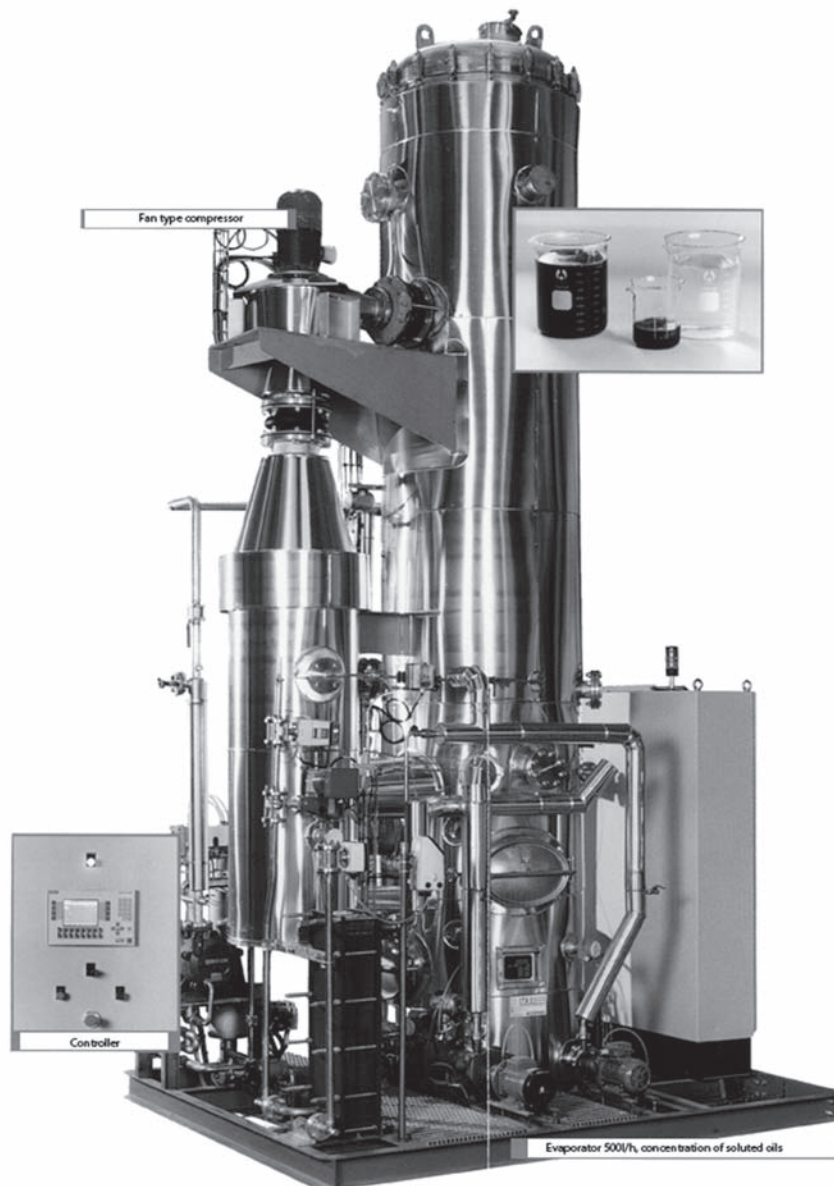


FIGURE 25.2.4
Favier SETREM MVC evaporator

- non-condensable gases drawn or dissolved in the fluid to concentrate reduce heat exchange coefficients. Their extraction can require vacuum pumps, of sometimes important capacity. Careful maintenance of these facilities is crucial for the proper functioning of the whole;
- corrosion: the choice of materials to select, and therefore the cost of various organs is determined by how aggressive are fluids that run through the installation, whether the fluid to treat or cleaning products.

Figure 25.2.4 shows a 500l/h capacity VC evaporator manufactured by company Favier/Setrem SA, used to concentrate soluble oils. The evaporator is of the “falling flow” type, i.e. the solution to concentrate trickles down inside tubes which are heated from the outside by steam. The device characteristics are: weight 4.5 tons, height 5.8 m, width 2.5 m, length 2.95 m.

25.3 DESALINATION

The limitation of freshwater resources in many parts of the world has for centuries led man to seek to produce water from seawater and brackish water. The issue of desalination is similar in many respects to that of the concentration of aqueous solutions we studied in section 25.1, with the proviso that the useful effect is not the same: we focus on distillate and not on concentrate.

In this section, we will simply overview the main desalination techniques now being used commercially, without giving a complete description.

One of the most important parameters to characterize the treated water is its salinity usually expressed in g/l. Its value depends on the sea: 35 g/l for the Atlantic, 50 g/l and more in the Persian Gulf.

25.3.1 Simple effect distillation

The simple distillation is the simplest way to desalinate sea water. It is to vaporize the water by bringing high-temperature heat, then condensing the steam produced.

A single effect desalination cycle can be easily modeled in ThermoOptim with class `EvapoConcentrator.java` (Figure 25.3.1).

In this example, 2 kg/s of seawater of salinity equal to 35 g/l, preheated at 70°C, enter the evaporator to provide 1 kg/s of freshwater. The thermal power involved is 2,513 kW in the absence of losses, and 2,552 kW should be rejected at the condenser to cool the distilled water at 30°C.

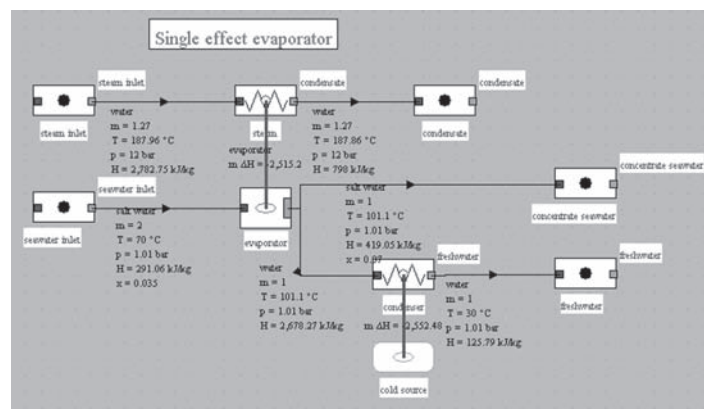


FIGURE 25.3.1

Single effect evaporator

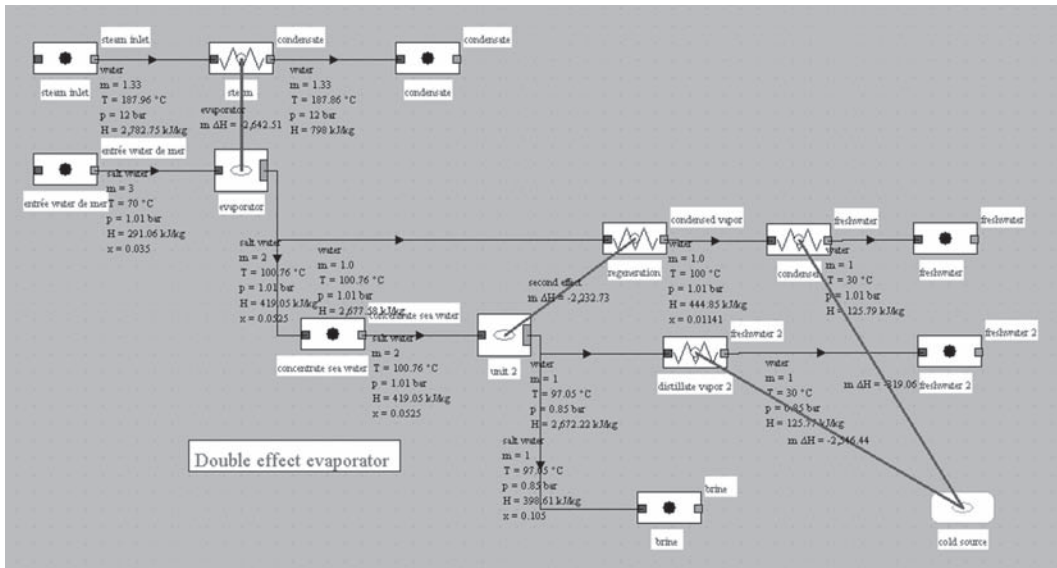


FIGURE 25.3.2
Double effect evaporator

25.3.2 Double effect desalination cycle

In order to recover some of the available enthalpy in the distilled steam, it is possible to arrange several distillation units in cascade. This is called multi-effect cycle. However, increasing the concentration of sea water in the evaporator outlet leads to an increase in evaporation temperature, because of the boiling point elevation, and you have to gradually reduce the pressure in the units.

Figure 25.3.2 shows a double-effect cycle fed with 3 kg/s of seawater, which produces 2 kg/s of distilled water, consuming a thermal power just above the single-effect evaporator (we have neglected the losses and the compression work of the distilled water at the output of the second unit).

The synoptic view of Figure 25.3.2 shows that the steam input required for evaporating 1 kg/s of water is here equal to 0.66kg/s. By adding other units, we gradually improve the performance of the facility.

25.3.3 Mechanical vapor compression desalination cycle

Figure 25.3.3 presents a modification of the simple effect evaporator of figure 25.3.1 with added mechanical compression of steam distilled to ensure most of the heat supply. Heat input is divided by 10, while the compressor power is only 35 kW. Ratio (steam evaporated)/(heating steam) is 9.

25.3.4 Desalination ejector cycle

Another fairly general solution is to utilize the vapor available as motive fluid in an ejector, to entrain the steam distilled exiting the last unit of a multiple-effect cycle, allowing to recompress it and to use it to provide the evaporator with heat needs. The analysis of ejectors is made in section 7.9.3 of Part 2.

Figure 25.3.4 shows the architecture of such a cycle. The motive steam flow is significantly greater than for a VC facility, but the cost of the ejector is much lower than that of a compressor.

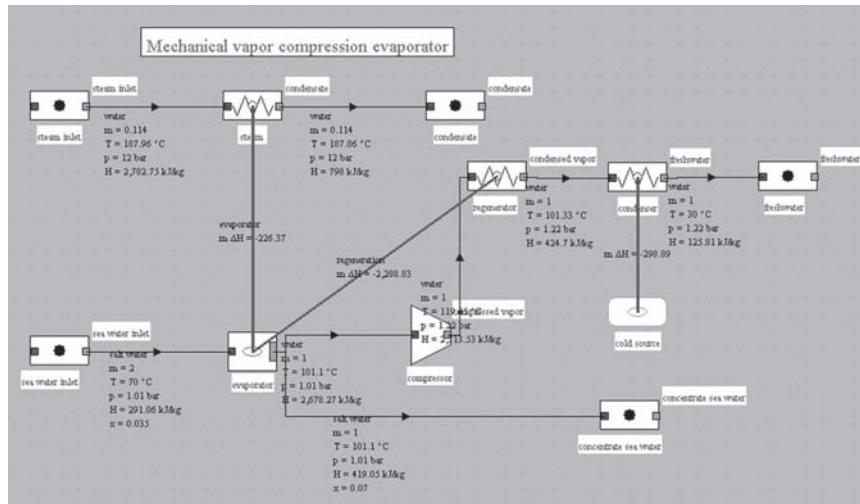


FIGURE 25.3.3
Mechanical vapor compression evaporator

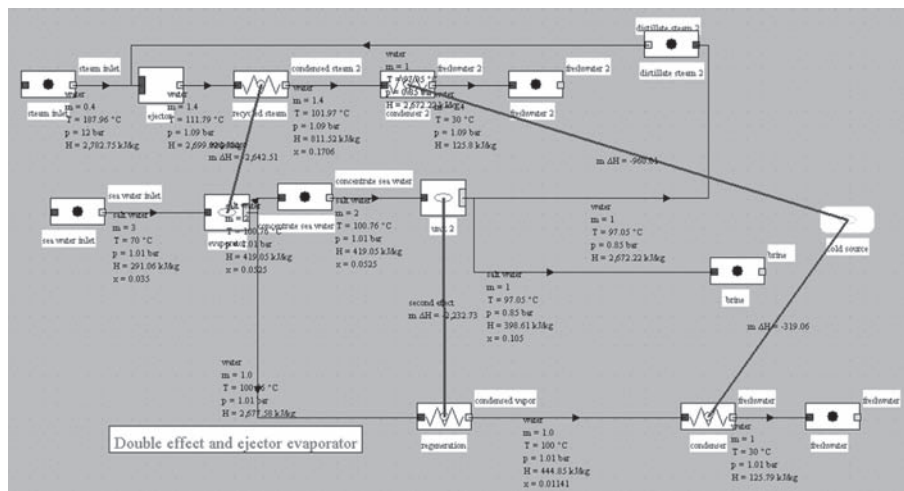


FIGURE 25.3.4
Ejector evaporator

25.3.5 Multi-stage flash desalination cycle

In a multi-stage flash (MSF) cycle, seawater is preheated by heat exchange with distilled steam. To reduce the temperature differences between the two fluids, a counter-flow arrangement is used, with several chambers (stages) in series as shown in Figure 25.3.5 (Nior, 2000). In each stage, salt water is expanded by flash, vaporizing it partially.

Seawater at low temperature warms in the lowest pressure chamber, then passes into the next stage and so on. A high temperature heat input is supplied by live steam.

The warm seawater is expanded in the first stage, the distilled steam generated being condensed as described above. The salt concentrated residue is then routed to the next stage at lower pressure, and so on.

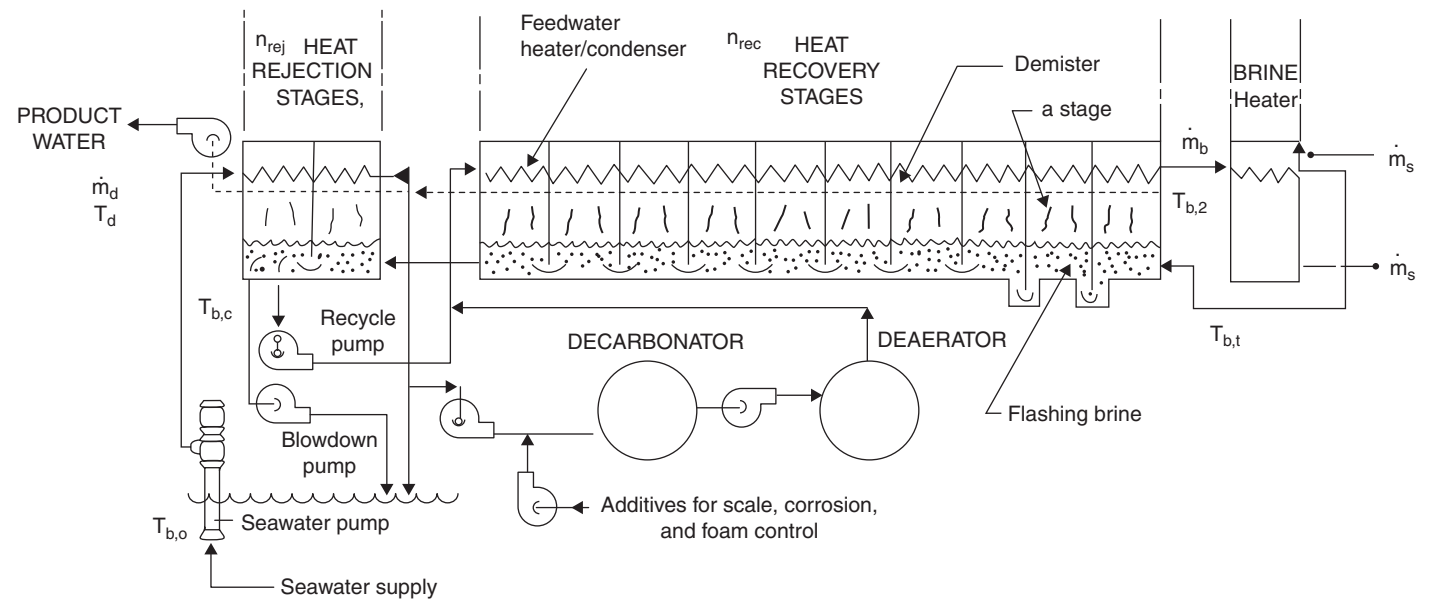


FIGURE 25.3.5

Multi-stage flash desalination system, Extract from (Lior, 2000), with permission

PRACTICAL APPLICATION

External class FlashBrine

The external class FlashBrine.java has been set up in order to allow you to make multi-stage flash desalination models. It is presented in the Thermoptim portal model library (<http://www.thermoptim.org/logiciels/thermoptim/modelotheque/modele-chbre-flash>).

The flash chamber acts as a divider receiving as input salt water, and from which exit two fluids, water vapor and the concentrated solution. The chamber being adiabatic, the enthalpy of vaporization is taken from the aqueous solution, whose temperature drops.

The synoptic view of Figure 25.3.6 shows that the steam input required for evaporating 1 kg/s of water is here equal to 0.54 kg/s.

25.3.6 Reverse osmosis desalination

Let us consider two media consisting of two mixtures of the same pair solvent-solute but of different concentration, and separated by a semipermeable membrane. Experience shows that:

- if the two media are at the same pressure, a solvent transfer called **osmosis** takes place;
- if you apply some pressure, called osmotic pressure π , to the most concentrated medium, this transfer can be canceled;
- if pressure is greater than π , the solvent migrates from the more concentrated solution to the other: this is called **reverse osmosis** (RO).

Desalination plants using reverse osmosis operate on this principle (Figure 25.3.7): by applying a pressure higher than osmotic pressure of salt water in a chamber equipped with a semipermeable membrane, it is possible to collect on the other side of the membrane a solution of very low salinity, called the permeate.

Figure 25.3.8 (Nior, 2000) shows the cutaway of a spiral wound type reverse osmosis module which appears externally as a cylinder of about 1 m long and 20 cm in diameter: the flat semipermeable membrane is spirally wound around the tube-manifold, enclosing a fine polyester mesh through which passes permeate, forming a stack sealed by glue on three sides. Outside this envelope, water to desalinate flows through a spacer.

The energy consumed is only the compression work of the initial solution, and is therefore much lower than that brought into play (as heat) in most devices that we have studied so far.

The van't Hoff law (25.3.1) states that the osmotic pressure exerted by the solute is equal to the pressure it would have exercised in the perfect gas state in the same volume and at the same temperature. If the solute is dissociated as ions, osmotic pressure is multiplied by the number of ions present.

$$\pi = n_i XRT \quad (25.3.1)$$

For seawater, the magnitude of π is 25 to 30 bar.

ΔP being the pressure difference across the membrane, we can show that the flow of solvent through the membrane J_e is given by (25.3.2).

$$J_e = A(\Delta P - \Delta\pi) \quad (25.3.2)$$

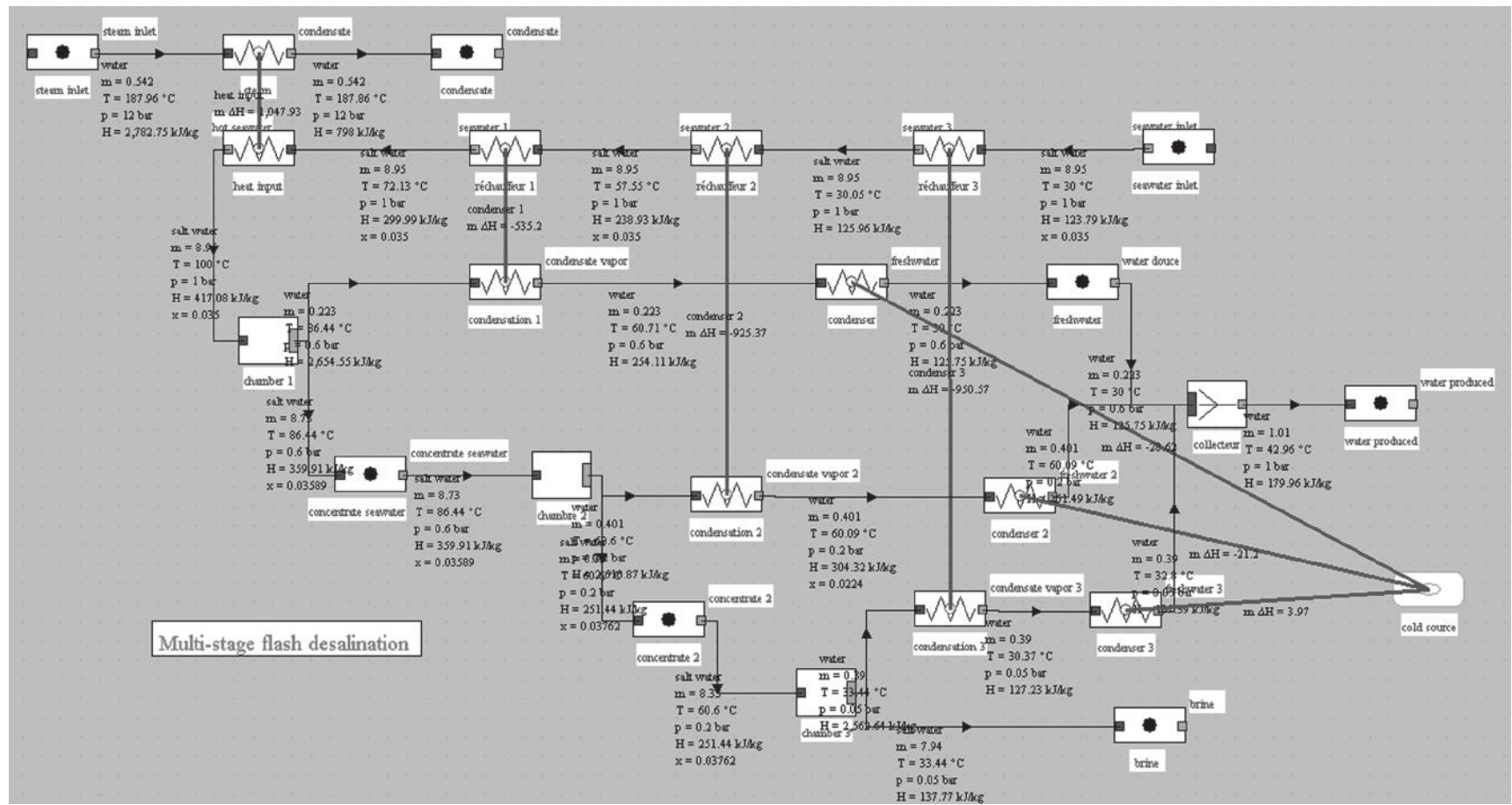
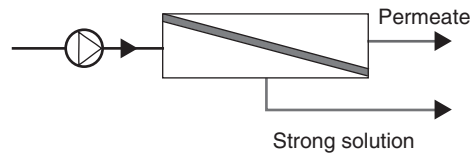
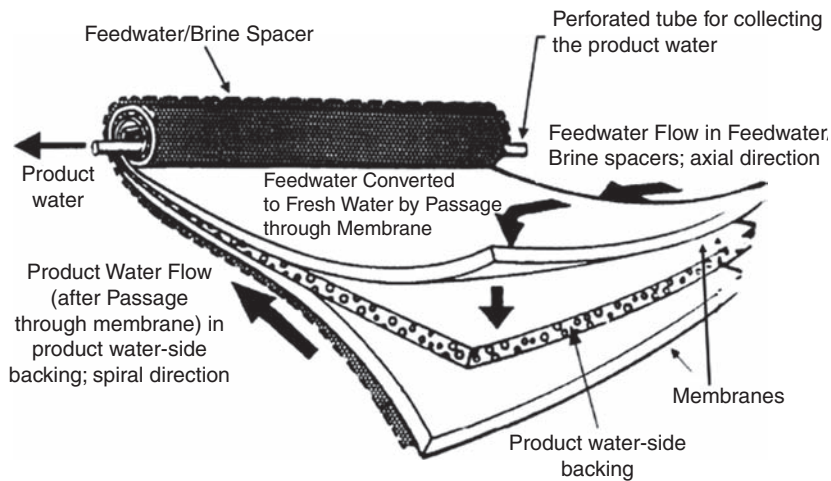


FIGURE 25.3.6

Multi-stage flash desalination cycle

**FIGURE 25.3.7**

Reverse osmosis unit

**FIGURE 25.3.8**

Spiral-wound reverse osmosis module (Documentation Dow Chemical), Extract from (Lior, 2000), with permission

A is called water permeability of the membrane. It is a characteristic parameter of the membrane, which depends on temperature according to an Arrhenius type law (25.3.3).

$$A = A_0 \exp \left[\frac{E}{R} \left(\frac{1}{298} - \frac{1}{T} \right) \right] \quad (25.3.3)$$

Even if there is a preferential transfer of the solvent, a small fraction of the solute also crosses the membrane. The flow of solute J_s is given by (25.3.4). It is proportional to the concentration difference.

$$J_s = B \Delta X \quad (25.3.4)$$

B is called the salt permeability of the membrane. This parameter depends on the membrane but not the temperature.

We call conversion rate the ratio of flow through the membrane to the feed flow-rate, and retention rate the ratio of the concentration difference between the initial solution and permeate to the initial solution concentration.

Figures 25.3.9 and 25.3.10 show the ThermoOptim diagram and component screen allowing one to model a Dow Chemical FilmTech SW30-4040 membrane of the type presented in Figure 25.3.8, used to desalinate sea water. The values of A and B were estimated from the manufacturer's documentation. The component is modeled by external class ReverseOsmosis.java.

The compression power to produce 1 kg/s of fresh water is equal to 63.3 kW, or nearly twice that required by mechanical vapor compression. However, it is possible to recover some of that power by expanding the concentrate in a turbine connected to the compressor.

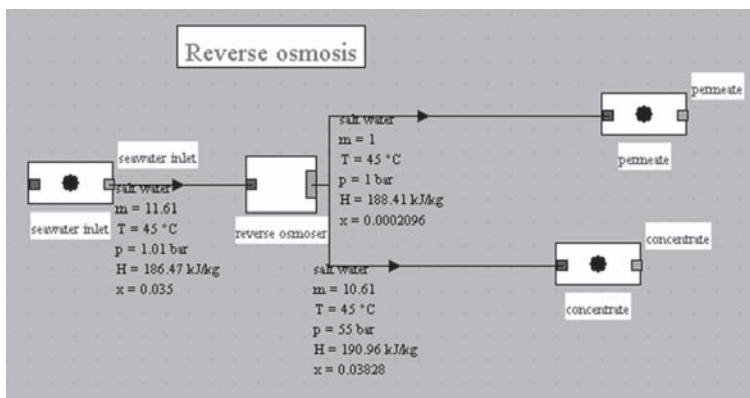


FIGURE 25.3.9
Thermoptm diagram of a reverse osmosis unit

node: reverse osmoser type: external divider

main process: seawater inlet iso-pressure:

m global: 11.61 h global: 186.46828898 T global: 45

process name	m abs	m rel	T (°C)	H
concentrate	10.6097	0	45	190.96
permeate	1.0003	0.223	45	188.41

ReverseOsmosis

High pressure (bar): 55 Compression power: 63.29

membrane surface m2 s/kg: 7.4 Retention rate: 0.9941

A0 (*10000): 3.25

B (*10000): 0.67

Inlet concentration: 0.03500

Permeate concentration: 0.00021

FIGURE 25.3.10
Reverse osmosis component screen

25.4 DRYING BY HOT GAS

In section 25.1 we introduced evaporation concentration facilities. Drying by hot gas is to evaporate the product by increasing the absolute humidity of the gas. There is thus also a separation of the solvent and solute which increases the concentration.

The hot gas must be clean enough to be placed in direct contact with the product to concentrate. It is generally air or gas turbine exhaust gases.

A particularly simple model allows us to get an idea of how such a facility works: it confines itself to establishing the mass and energy balances, assuming firstly that the fraction of the product flow which is extracted is known, and secondly, that only the hot gas provides the enthalpy corresponding to the evaporated water, taking into account heat loss from the component as a percentage of that value. Flow rates of both inlet streams are set by conditions upstream of the component and not recalculated. If the gas (here air) flow is insufficient for allowing its cooling to saturation to evaporate the water involved, a message warns the user.

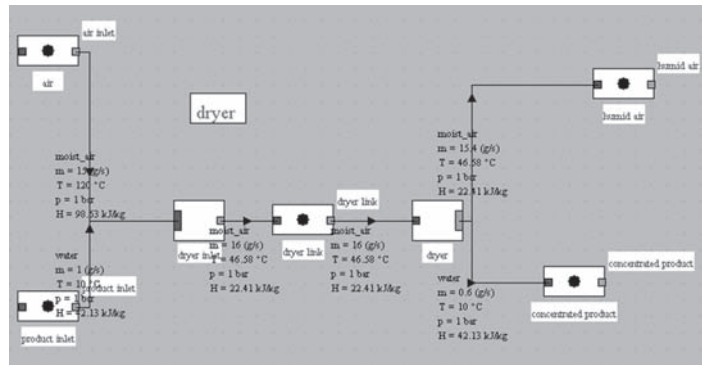


FIGURE 25.4.1

Diagram of component “dryer”

point		LINKS		
point	humid air			
substance	moist_air	display	Duplicate	Save
	<input type="checkbox"/> external mixture	Suppress	Close	
Open system (T,P,h)		Closed system (T,v,u)		Water vapor/gas mixtures
	set w	set epsi		
set the gas humidity		specific values (relative to 1 kg of dry gas)		
w (kg/kg)	0.0342168298	q' (kJ/kg)	135.2558	
epsi	0.501916645	v (m ³ /kg)	0.9684496	
condensation	0	t' (°C)	35.8547	
p (bar)	1	tr (°C)	33.643	
T (°C)	46.57714844			

FIGURE 25.4.2

Exit point screen

The model we can choose is:

1. the only parameters are the fraction of the flow of product evaporated and the percentage of losses;
2. we first calculate the absolute humidity of the incoming gas, and determine the mass flow of dry gas from that of moist gas;
3. absolute humidity w at the outlet is determined, and we iterate on the outlet air temperature, which allows us to calculate the specific enthalpy. When the variation of air specific enthalpy is equal to that required to evaporate water, the solution is found (we neglect here the variation of sensible heat of water involved);
4. the composition of the outlet moist gas is changed;
5. values downstream of the node are updated.

Such a component can be easily implemented in ThermoOptim as an external class, using moist properties calculation functions which are presented in section 23.3.

Figure 25.4.1 shows the ThermoOptim synoptic view of such a device (external classes `DryerInlet.java` and `DryerOutlet.java`): a rate of 15 kg/s of hot and very dry air ($\varepsilon < 0.6\%$) at 120°C is blown on a product stream of 1 kg/s at 10°C. 40% of the water contained in the product evaporates increasing cooling air moisture. At the component outlet, air thermodynamic state is given in Figure 25.4.2: temperature of 47.7°C, relative humidity of 47.5%.

This air can then optionally be cooled and condensed then recycled if necessary.

REFERENCES

- J. F. Reynaud, *Concentration par évaporation et recompression mécanique de vapeur*, Ed. Eyrolles, Paris, 1984.
- P. Danis, *Dessalement de l'eau de mer*, Article J2700, Techniques de l'Ingénieur, Paris.
- R. Leleu, *Evaporation*, Article J2320, Techniques de l'Ingénieur, Paris.
- N. Lior, *Water desalination*, *The CRC handbook of thermal engineering*, (Edited by F. Kreith), CRC Press, Boca Raton, 2000, ISBN 0-8493-9581-X.
- A. Maurel, *Dessalement de l'eau de mer et des eaux saumâtres*, 2^{ème} édition, Ed. Tec et Doc, Paris, 2006.
- F. B. Petlyuk, *Distillation Theory and its Application to Optimal Design of Separation Units*, Cambridge Series in Chemical Engineering, Cambridge University Press, 2004, ISBN 0-521-82092-8
- M. E. Williams, A Review of Reverse Osmosis Theory, [Online] Available from: http://www.eetcorp.com/heapm/RO_TheoryE.pdf

Cryogenic Cycles

Abstract: The term cryogenics is used to describe methods of refrigeration at very low temperatures (typically below 125 K), and distinguish them from ordinary refrigeration cycles. Many of these methods relate to the liquefaction of gases known as permanent, like air, natural gas, hydrogen or helium.

Cryogenics is the field of engineering that focuses on systems operating at very low temperature, which poses special problems, particularly in terms of fluids and materials.

Refrigeration and cryogenic liquefaction cycles involve combinations of para-isothermal compressions, cooling, thermal regeneration, and isenthalpic or adiabatic expansion of fluids.

There are four major families of cryogenic thermodynamic processes:

- isenthalpic expansion Joule-Thomson processes;
- isentropic expansion reverse Brayton cycles;
- mixed processes involving isenthalpic and isentropic expansion (Claude cycle);
- conventional or integrated cascades.

It is possible to model with Thermoptim some cryogenic cycles, but the exercise is often difficult because the fluid properties are rarely defined for the entire temperature range considered. You will find in this section some examples of liquefaction cycles for methane and nitrogen, and a reverse Brayton helium refrigeration cycle at very low temperatures. These examples are drawn from the documents cited in the bibliography, particularly from the 3,600J leaflet of Techniques de l'Ingénieur, by P. Petit.

Keywords: cryogenics, liquefaction, regeneration, throttling, flash, Linde, Claude, reverse Brayton, incorporated cascade.

26.1 JOULE-THOMSON ISENTHALPIC EXPANSION PROCESS

We illustrate this process by some examples of cycles for liquefying natural gas and form Liquefied Natural Gas (LNG), considered here as pure methane.

26.1.1 Basic cycle

This first example is adapted from the exercise proposed by (Sandler, 1999) p. 129.

To liquefy natural gas methane taken at 1 bar and 280 K is compressed to 100 bar and then cooled to 210 K (it is assumed in this example that a refrigeration cycle is available for that).

Isentropic compression is assumed, but the very high compression ratio requires the use of several compressors (3 in this example) with intermediate cooling at 280 K. Intermediate pressures are equal to 5 and 25 bar.

The gas cooled at 210 K is isenthalpically expanded from 100 bar to 1 bar, and gas and liquid phases separated. As shown in the diagram in Figure 26.1.1, the methane enters in the upper left, and liquid and gaseous fractions exit in the bottom right.

With the settings chosen, the synoptic view is given in Figure 26.1.2.

The compression work required per kilogram of methane sucked is 798.5 kJ, and 0.179 kg of liquid methane is produced, which corresponds to a work of 4.46 MJ per kilogram of liquefied methane.

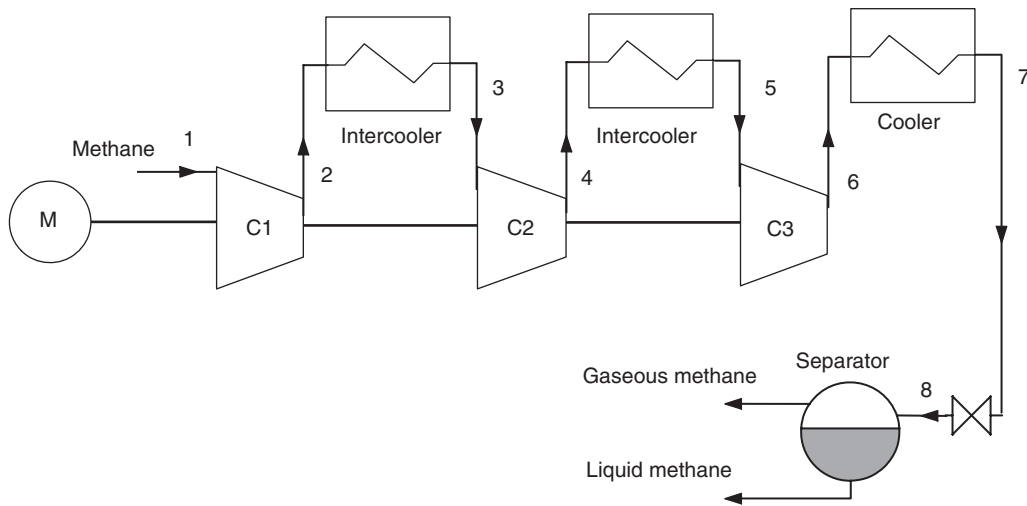


FIGURE 26.1.1
Simple liquefaction cycle

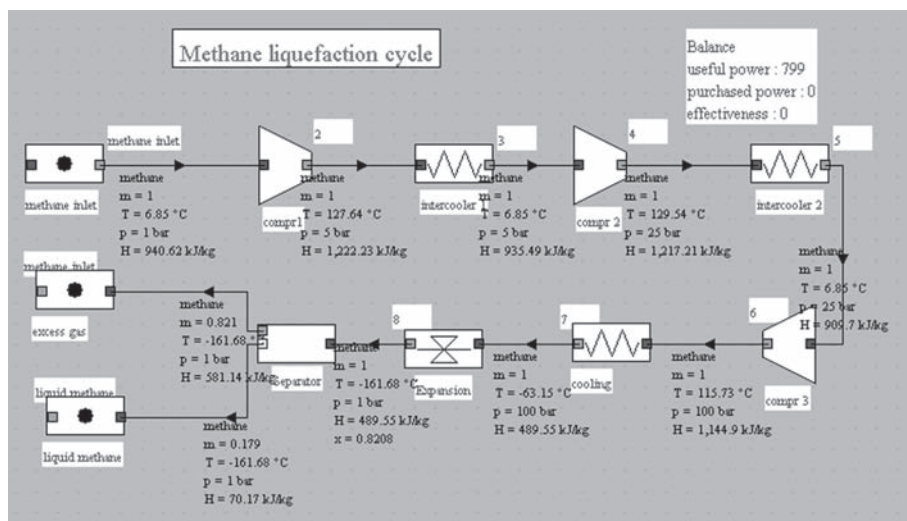


FIGURE 26.1.2
Synoptic view of the facility

pjlwstk|402064|1435602006

26.1.2 Linde cycle

The Linde cycle (Figure 26.1.3) improves the previous on two points:

- gaseous methane is recycled after isenthalpic expansion;
- we introduce a heat exchanger between the gaseous methane and methane out of the cooler in order to cool the compressed gas not at 210 K but at 191 K.

For these new conditions the compression work per kilogram of liquefied methane becomes equal to 1.91 MJ, i.e. just 43% of the previous one.

The calculation of this cycle requires some caution, given the sensitivity of the balance of the heat exchanger to flow variations set by the separator.

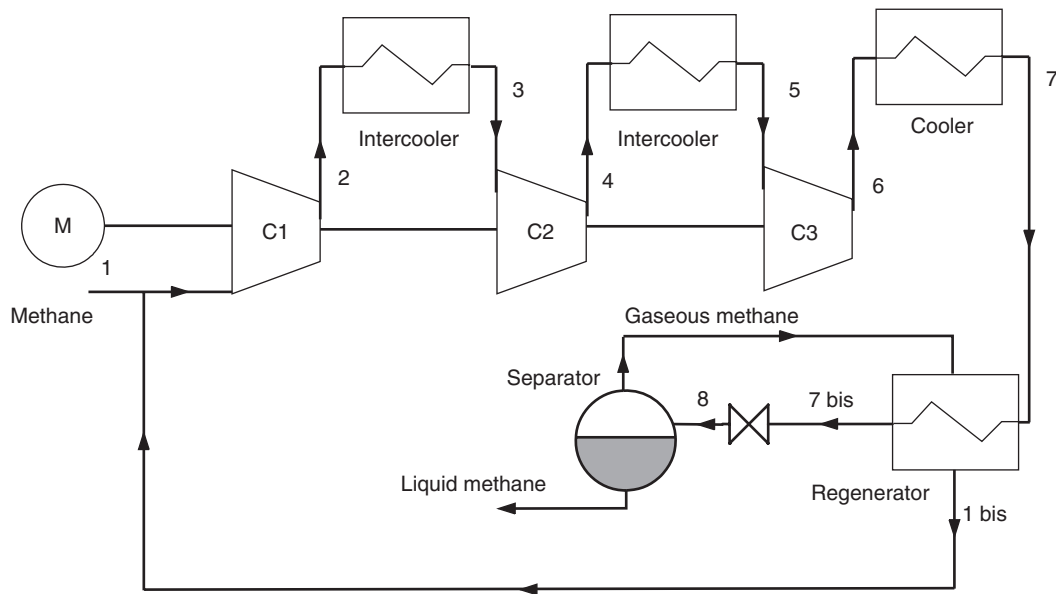


FIGURE 26.1.3

Linde cycle

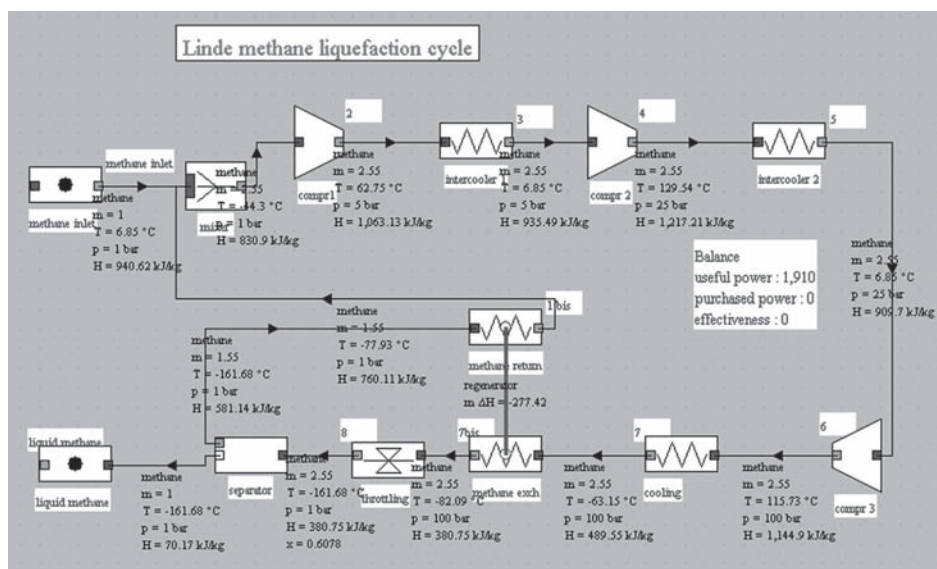


FIGURE 26.1.4

Synoptic view of the Linde cycle

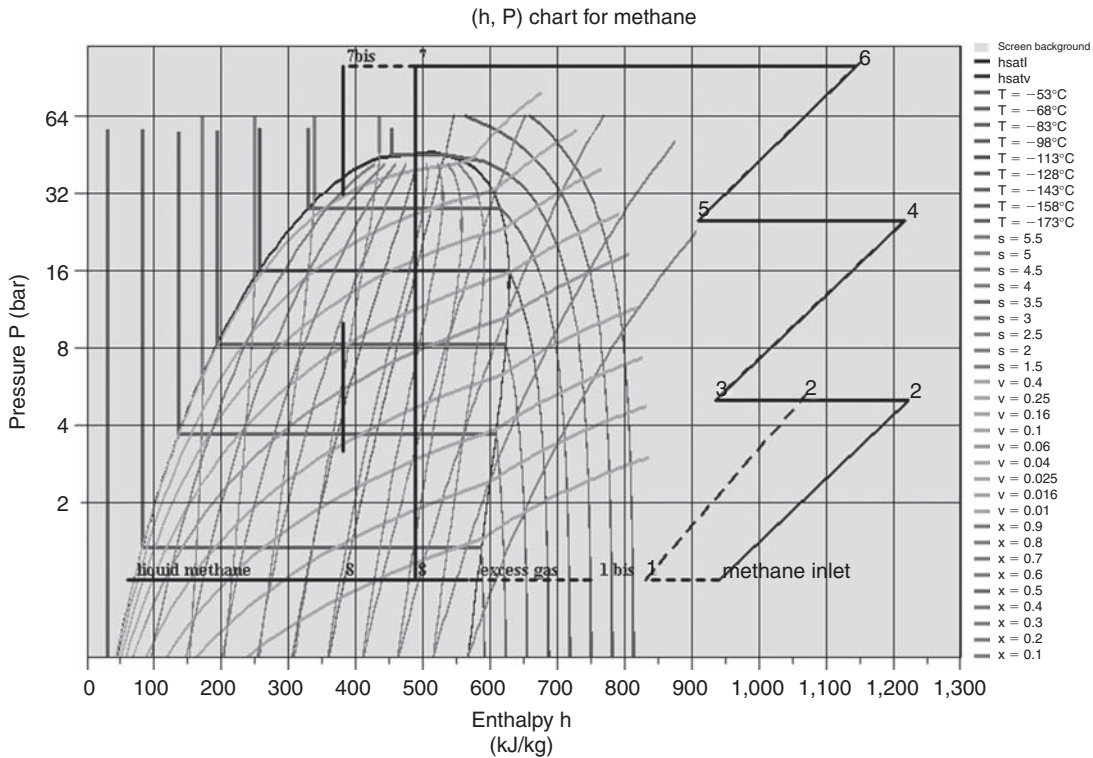


FIGURE 26.1.5

Linde cycle in dashed line, and basic cycle in continuous line, in a (h, ln(P)) chart

The solution we found was to set the flow rate in the first intercooler, then to recalculate the entire project by recalculating in addition the regenerator repeatedly. A stable solution could then be found, but it led to an inaccurate flow recirculation at the beginning. The correct rate value to set was obtained by successive iterations.

The performance gain comes mainly from the decrease of the expansion valve inlet temperature, which reduces the exit quality and thus increases the flow of the liquid phase. Moreover, the decrease in temperature at the inlet of the first compressor reduces the compressor work, but this effect is less important than the first.

The plot of both cycles in (h, ln(P)) and entropy diagrams (Figures 26.1.5 and 26.1.6) illustrates the benefits of the second: the leftward shift of point 7 in 7bis in the Linde cycle more than doubles liquid quality at the valve outlet (point 8).

26.1.3 Linde cycles for nitrogen liquefaction

As air is not modeled in ThermoOptim as condensable, we will consider here the liquefaction of nitrogen.

Gaseous nitrogen at 1 bar and 280 K is compressed at 200 bar (cooled compression at 50°C), then cooled at 280 K.

Nitrogen is then cooled in a heat exchanger with the non-liquefied part, allowing it to reach a temperature of about -110°C. It is then isenthalpically expanded at 1 bar, thereby about 8% is liquefied.

The liquid fraction is extracted, and the remainder in the form of saturated vapor is recycled in the regenerator and mixed with atmospheric nitrogen at 280 K, which closes the cycle.

The performance of this machine is small, about 5.7 MJ/kg, but the cycle can be modeled without difficulty in ThermoOptim (Figure 26.1.7).

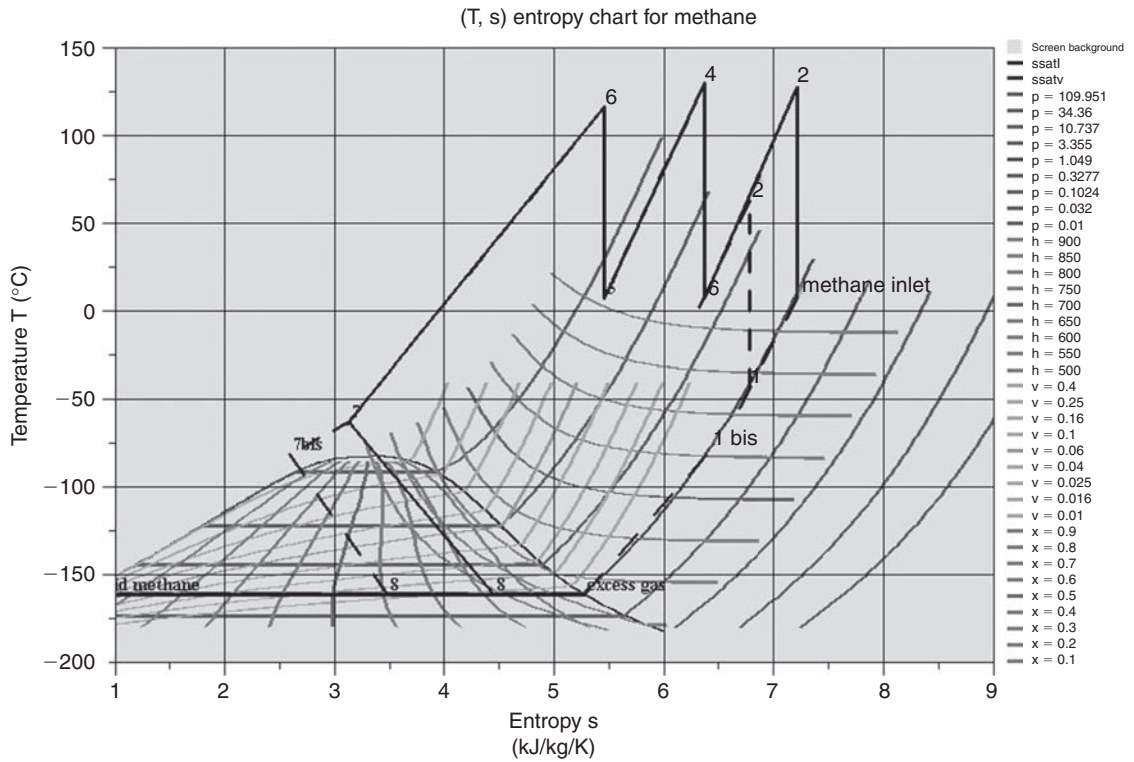


FIGURE 26.1.6
Linde cycle in dashed line, and basic cycle in continuous line, in a (T, s) chart

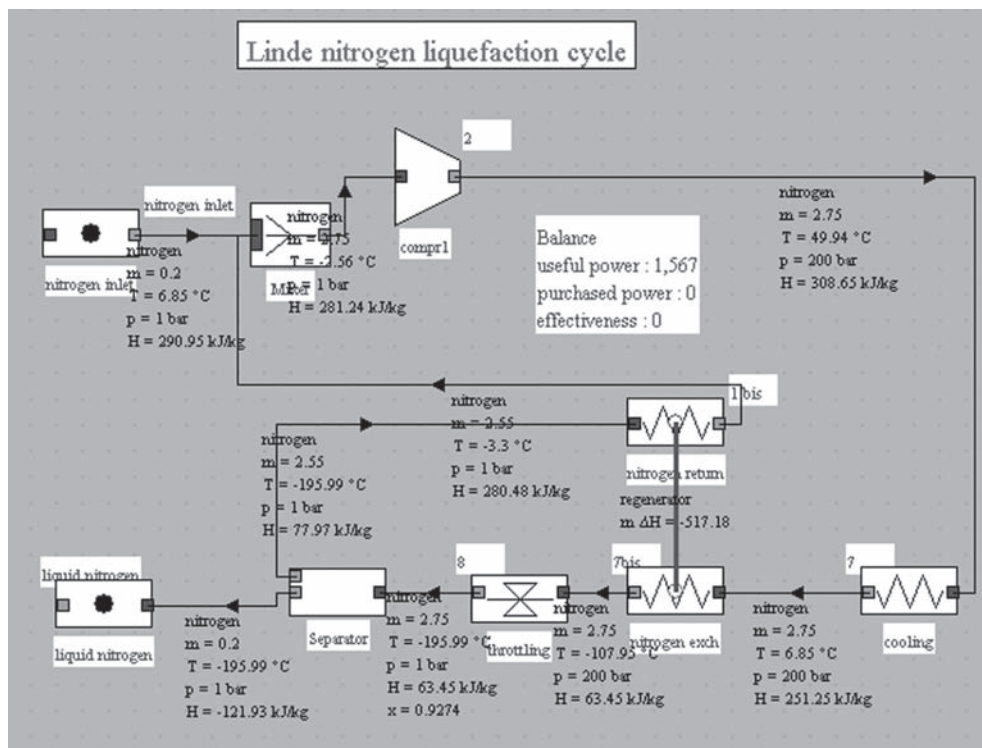


FIGURE 26.1.7
Synoptic view of nitrogen Linde cycle

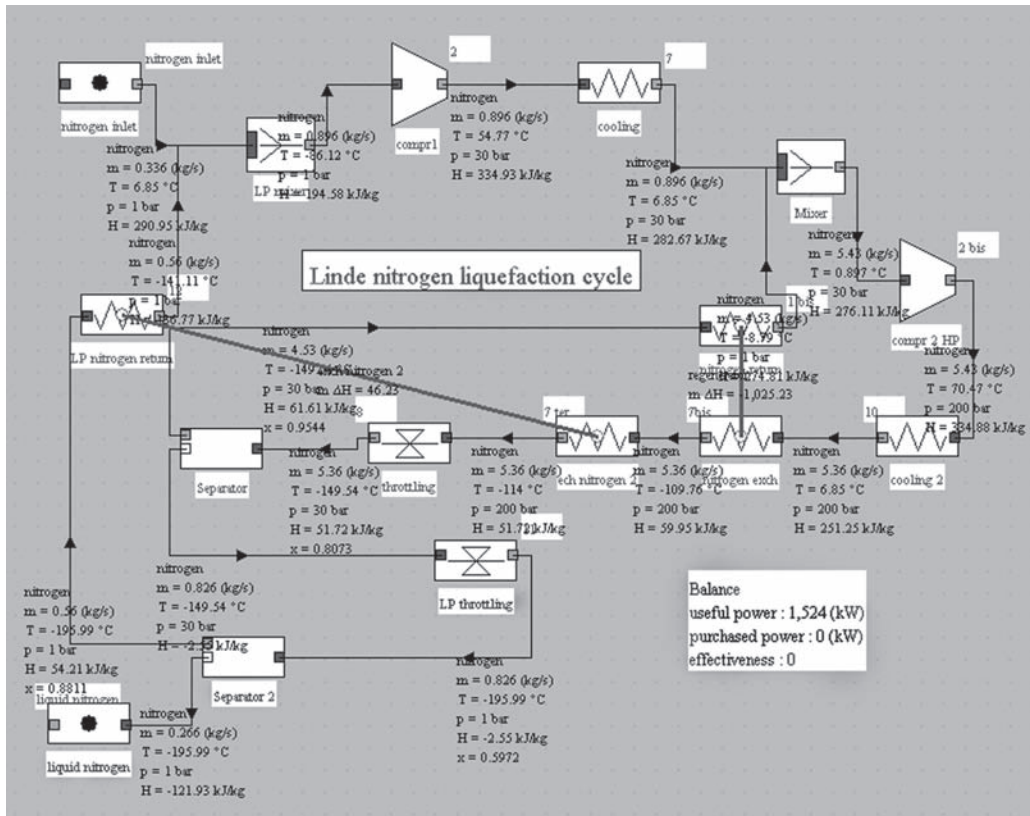


FIGURE 26.1.8
Synoptic view of two-stage nitrogen Linde cycle

It can be improved by a double expansion cycle, but the setting is much more difficult to obtain because instabilities can occur in flow-rates, because of the role played by the phase separators (Figure 26.1.8).

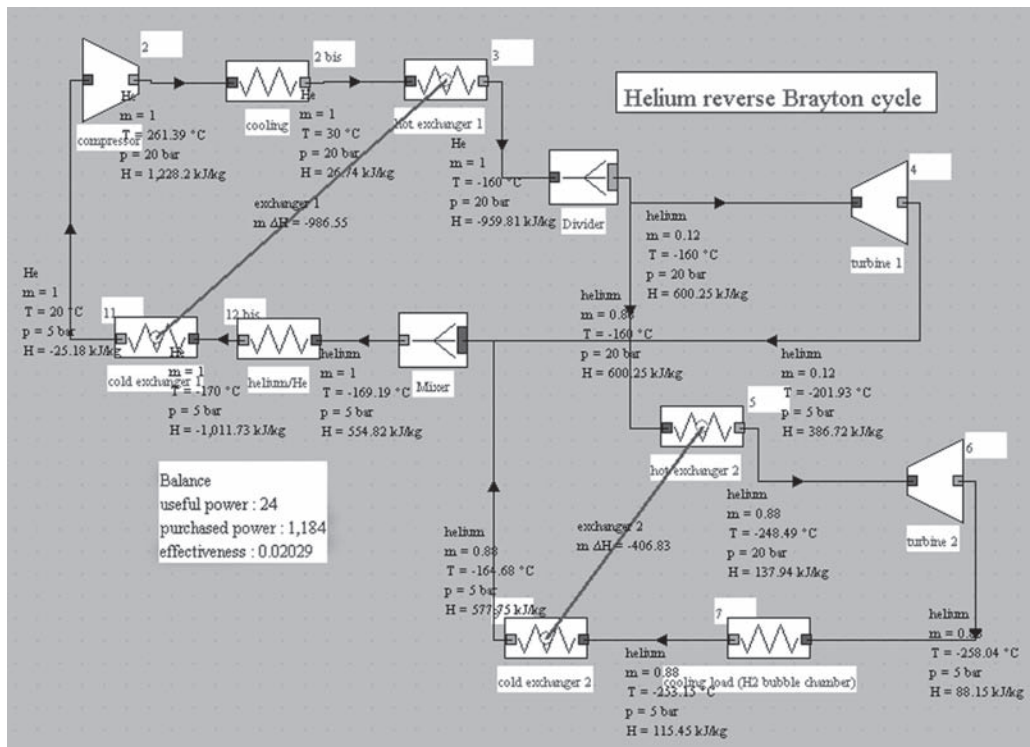
26.2 REVERSE BRAYTON CYCLE

The reverse Brayton cycle has been presented in section 19.6.4 of Part 3, which we recommend you to refer to for details.

This cycle can be used for cryogenic applications. For example, Figure 26.2.1 shows the block diagram obtained for example 3.2.1 by B. Petit, relative to a plant for producing cooling below 20 K to refrigerate a liquid hydrogen bubble chamber.

In this cycle, helium is compressed to 20 bar, then cooled to 30°C before being divided into two streams which are expanded in parallel, the main stream following a conventional reverse Brayton cycle, while the secondary contributes to cooling the total flow.

Note that in this example, point 12a temperature must be forced by hand, equal to that of point 12, because of the need to change the substance, the helium vapor being defined in Thermoptim only for $T < 200$ K.

**FIGURE 26.2.1**

Synoptic view of the helium reverse Brayton cycle

26.3 MIXED PROCESSES: CLAUDE CYCLE

The Linde cycle uses isenthalpic expansion which has two drawbacks: firstly the expansion work is lost, and secondly cooling cannot be achieved if the fluid thermodynamic state is such that the Joule Thomson expansion leads to a temperature lowering.

Claude has proposed a cycle that involves a turbine and an expansion valve and has the peculiarity that the plant operates with a single fluid compressed at a single pressure level, as shown in Figure 26.3.1.

The advantage of this cycle is that the compression ratio can be significantly lower than in the case of the Linde cycle. One difficulty is that the expansion machine cannot operate with good efficiency if the fluid remains in the vapor zone or keeps a high quality. The originality of the Claude cycle is to combine isentropic expansion in the turbine, and isenthalpic expansion only in expansion leading to the gas liquefaction.

The beginning of the cycle is the same as that of Linde: compression of gas to liquefy, then cooling to about room temperature (1–3). The gas then passes through a regenerator which allows it to cool at about -105°C (3–4). The flow is then divided, about 15% being expanded in a turbine (4–8). The main flow passes through a second regenerator of which it is released at very low temperature (4–12). It undergoes isenthalpic expansion (12–5) and the liquid phase is extracted. The vapor is mixed with the flow exiting the turbine, and serves as a coolant in the second regenerator (10–11), then in the first (11–7) before being recycled by mixing with the gas entering the cycle.

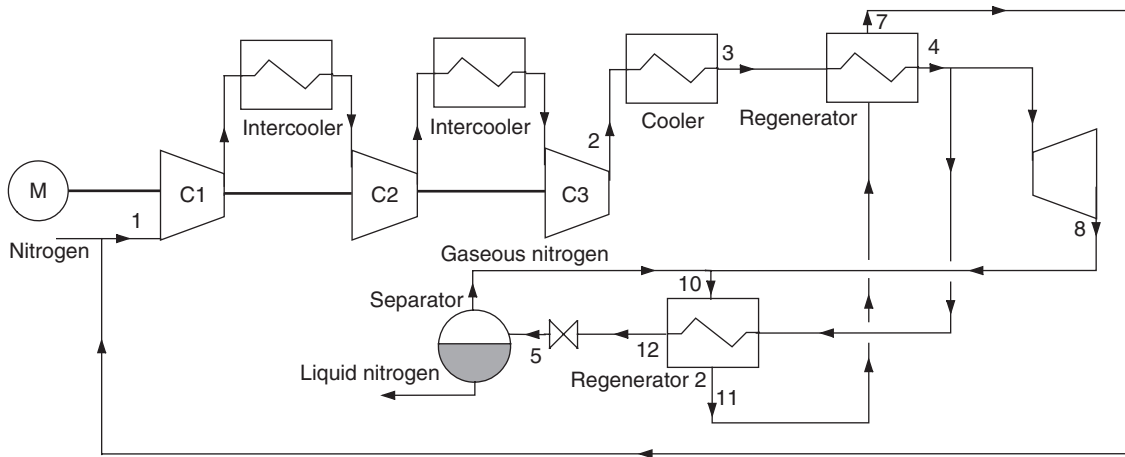


FIGURE 26.3.1
Sketch of the Claude cycle

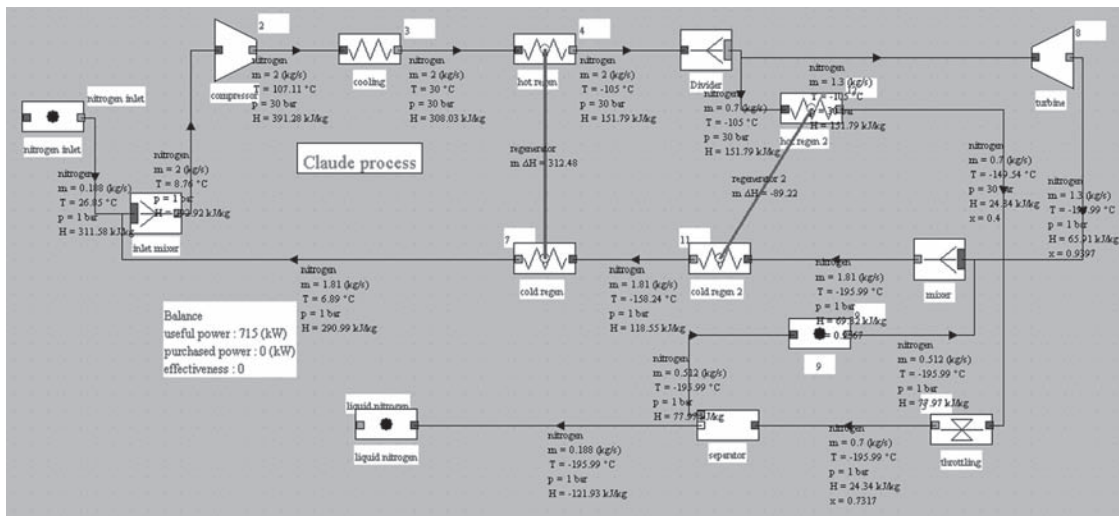


FIGURE 26.3.2
Synoptic view of the Claude cycle

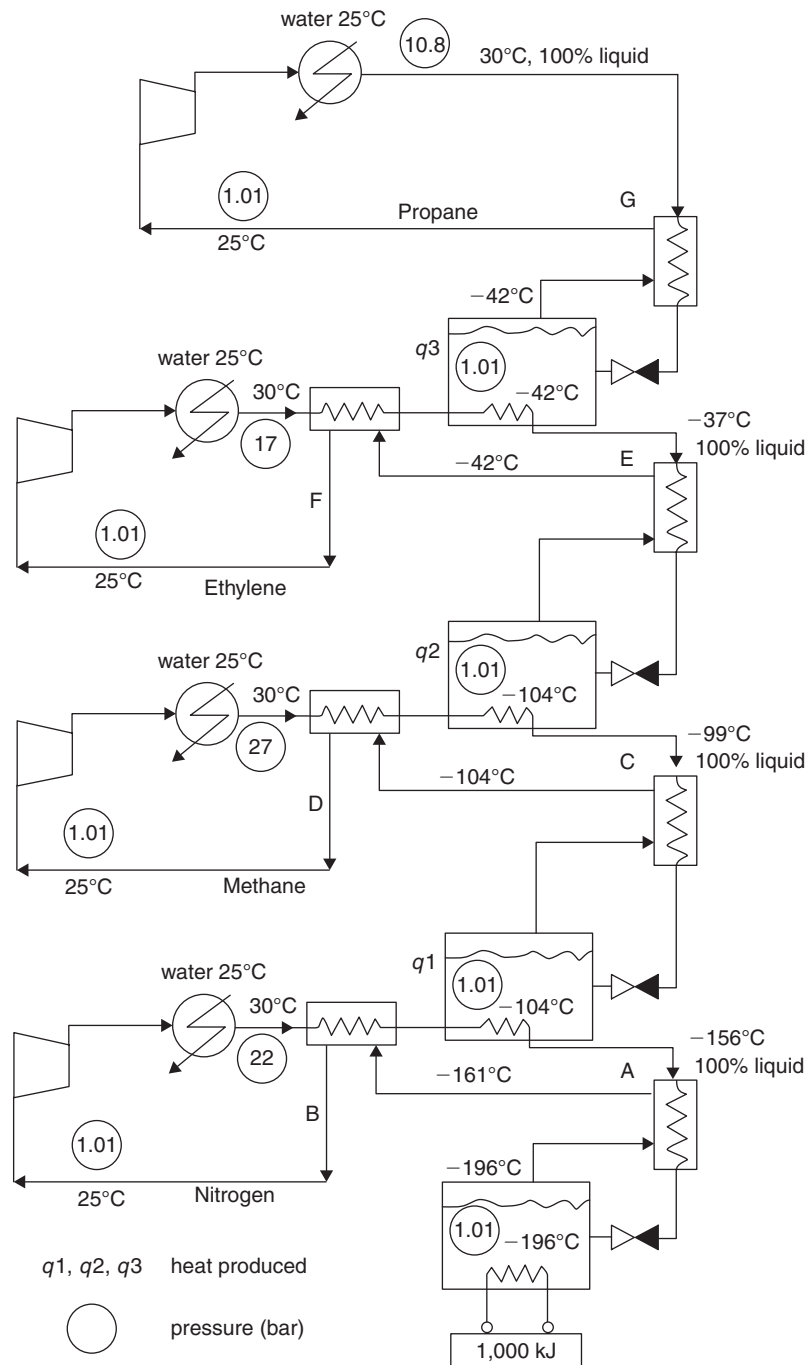
This cycle can be modeled with ThermoOptim. Inspired by the example 3.2.2.2 by B. Petit presented in the Techniques de l'Ingénieur, we obtain the block diagram in Figure 26.3.2. The compression power is about 3.8 MJ/kg.

The Claude cycle has been used in many air liquefying facilities.

26.4 CASCADE CYCLES

It is also possible to use cascading refrigeration cycles, the evaporator of one of them serving as a condenser to another and so on (Figure 26.4.1). The various cooling circuits are then independent from the hydraulic, but thermally coupled by their evaporative condensers.

An alternative, widely used nowadays in the liquefaction of natural gas, is to use a so-called incorporated cascade, using a single working fluid consisting of a mixture of methane, ethane, propane, butane and pentane.

**FIGURE 26.4.1**

Classical cascade (after B. Petit) Copyright Techniques de l'Ingénieur, Génie Energétique

REFERENCES

Ashrae, *Cryogenics*, ch. 38, Fundamentals Handbook (SI), 2002.

R.F. Barron, *Cryogenic systems, The CRC handbook of thermal engineering*, (Edited by F. Kreith), CRC Press, Boca Raton, 2000, ISBN 0-8493-9581-X.

- T. Flynn, *Cryogenic Engineering*, Second Edition, Revised and Expanded, CRC Press, Boca Raton, 2004, ISBN 9780824753672
- J.-Cl. Boissin, G. Gistau, B. Hébral, P. Pelloux-Gervais, A. Ravex, P. Seyfert, *Cryogénie: mise en œuvre des basses températures*, Techniques de l'Ingénieur, Traité Génie énergétique, B 2 382.
- A. Bui, B. Hébral, F. Kircher, Y. Laumond, M. Locatelli, J. Verdier, *Cryogénie: propriétés physiques aux basses températures*, Techniques de l'Ingénieur, Traité Génie énergétique, B 2 380.
- M. Feidt, *Production de froid et revalorisation de la chaleur: machines cryogéniques*, Techniques de l'Ingénieur, Traité Génie énergétique, BE 8 097.
- B. Hébral, *Cryogénie*, Techniques de l'Ingénieur, Traité Génie énergétique, B 2 380a.
- P. Petit, *Séparation et liquéfaction des gaz*, Techniques de l'Ingénieur, J 3600.
- S. Sandler, *Chemical and Engineering Thermodynamics* 3ème édition, J. Wiley editors, 1999.

Electrochemical Converters

Abstract: Electrolysis is an old and well known process: an electrolyzer performs an electrochemical reaction that produces hydrogen and oxygen from water through electricity consumption by an endothermic reaction.

A fuel cell performs the reverse electrochemical reaction: hydrogen and oxygen react to produce electricity and water while releasing heat.

The heart of the cell consists of two electrodes, the anode and cathode, separated by an electrolyte.

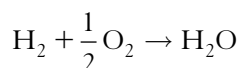
If the fuel used is pure hydrogen, the fuel cell has only byproduct of water: such a generator is particularly clean, which explains the growing interest in this technology.

In this chapter we will study these two types of electrochemical converters: fuel cells and electrolyzers, gradually building several cell models, and only one for the electrolyzer.

Keywords: Electrolyzer, fuel cell, stack, anode, cathode, fuel use, reforming, SOFC, PEMFC, AFC, PAFC, MCFC.

27.1 FUEL CELLS

A fuel cell performs the reverse electrochemical reaction of electrolysis according to reaction:



Thus we see that if the fuel used is pure hydrogen, the fuel cell only byproduct is water: this is a particularly clean generator.

The heart of the cell consists of two electrodes, the anode and cathode, separated by an electrolyte.

In some cells, such as solid oxide fuel cells (SOFC), oxide ions O^{2-} migrate from the cathode to the anode where water is produced, and in others like proton exchange membrane fuel cells (PEMFC), cations H_3O^+ (hydrated protons H^+) migrate from the anode to the cathode.

The stack behaves as a quadrupole: In Figure 27.1.1, which represents a cell stack, hydrogen enters in the top left of the stack, combines at the anode with ions O^{2-} to form water, and exits in the lower left, enriched in water, while air enters in the top right and exits in the bottom right depleted in oxygen.

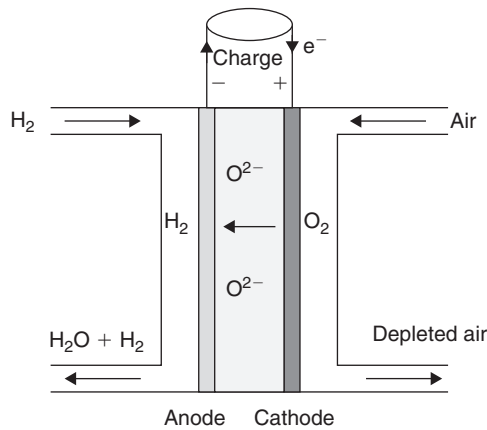


FIGURE 27.1.1
Solid Oxide Fuel Cell

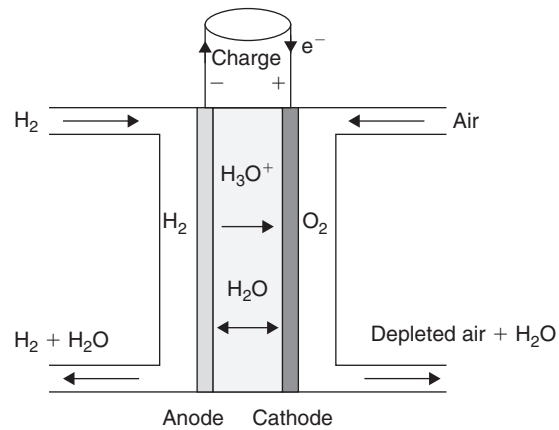
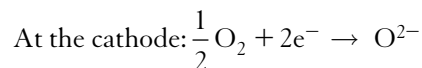
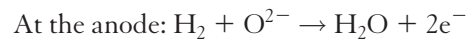


FIGURE 27.1.2
Proton Exchange Membrane Fuel Cell

A SOFC works at very high temperatures (between 600 and 1,000°C), so that water at the outlet is in gaseous form.

Both reactions that take place are:

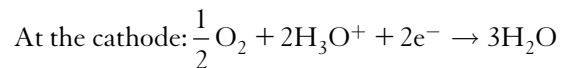


In a proton exchange membrane cell (PEMFC), hydrated protons H_3O^+ migrate from the anode to the cathode, where water is produced.

In Figure 27.1.2, which represents a cell stack, hydrogen enters in the top left of the stack, combines at the anode with water to form cations, and exits in the lower left, while the air enters in the top right and exits at the bottom right, oxygen-depleted and water-enriched.

A PEMFC works at low temperature (between 80 and 120°C), so that water is in liquid form at the outlet.

Both reactions that take place are:



In reality, this fuel cell works only if the membrane is wetted on both sides, and is permeable to water. Water balance is governed by two phenomena: a portion of the water goes through the membrane from the anode to the cathode under the effect of electro-osmosis, driven by protons, while a part crosses in the other direction by diffusion due to concentration difference between the two sides of the membrane.

The operation of a fuel cell can be characterized by two parameters:

- the rate of fuel use τ , which represents the fraction of fuel that reacts;
- the energy efficiency ε , ratio of electric output to the flow of enthalpy put into play by reaction $\text{H}_2 + \frac{1}{2}\text{O}_2 \rightarrow \text{H}_2\text{O}$, under standard temperature and pressure conditions (25°C, 1 atm). ε is close to 50% in practice.

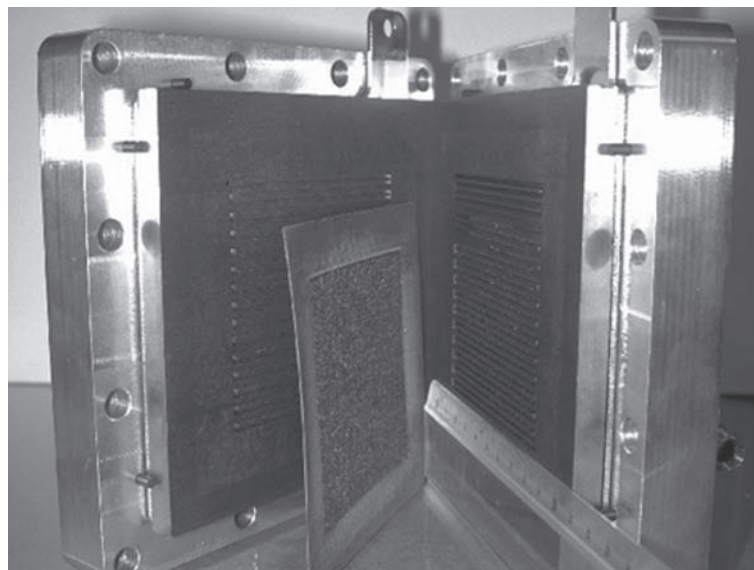


FIGURE 27.1.3

Internal view of a single cell PEMFC (Copyright CEP Mines-ParisTech)

Each cell theoretically implements a 1.23 V voltage, but in practice the open circuit voltage barely exceeds 1 V, and the operating voltage is around 0.7 V.

Figure 27.1.3 shows the internal content of a single cell PEMFC test bench allowing one to assess fuel cells of 50 cm² active surface (7.1 cm × 7.1 cm).

In the middle is the Membrane Electrode Assembly MEA, with on both sides graphite bipolar plates through which flow hydrogen and air.

The plate width is about 1 cm. Electric collectors are placed on the side opposite the MEA. Structural end-plates allow one to maintain the various parts in place.

To get high voltages, it is therefore necessary to set many cells in series. Commonly known as a stack of cells it is in practice limited to 100 or 200.

Current densities are generally between 0.1 and 1 A/cm².

For large intensities, it is necessary to increase the cell surface, but there are limits, because it is difficult to supply gas uniformly on large areas.

There are several types of fuel cells, usually classified according to the nature of their electrolyte:

- AFC (**Alkaline Fuel Cell**) uses potash as electrolyte. Developed for space, this type of cell is used in all inhabited spaceflight at NASA, is entirely satisfactory and is cheap, but suffers from the need not operate in the absence of CO₂ produced today by reforming. Its operating temperature is 80°C;
- PEMFC (**Proton Exchange Membrane Fuel Cell**) uses, as we have seen, a proton exchange membrane electrolyte. It seems today one of the most promising and is the subject of the largest development efforts and thereby supplants AFC. It has great potential for many applications in all capacity ranges from watts to megawatts. Its main drawback is cost, but cost reductions are hoped for in the short term. Its operating temperature is 80°C;
- PAFC (**Phosphoric Acid Fuel Cell**) uses phosphoric acid as electrolyte. Marketed by U.S. company ONSI Corp. for several years, it is especially interesting in CHP in light of its operating temperature of 200°C;
- MCFC (**Molten Carbonate Fuel Cell**) uses molten carbonate as electrolyte. Operating at high temperature (650°C), ionic transport is performed by ions CO₃²⁻. It has the advantage of being directly fed with a synthesis gas, and can be integrated in high performance complex cycles in combination with gas turbines;

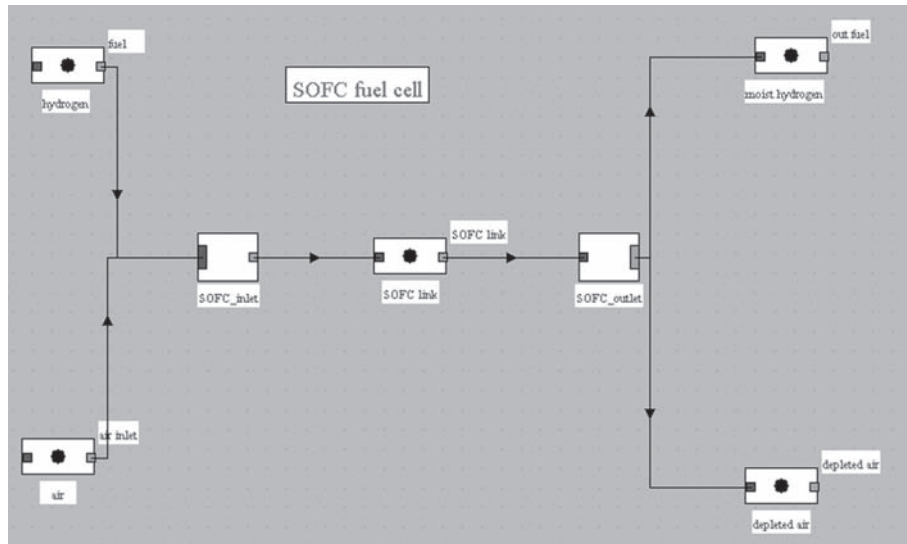


FIGURE 27.1.4
SOFC component screen

- SOFC (**Solid Oxide Fuel Cell**) uses a solid oxide (ZrO_2) doped with small amounts of calcium oxide and yttrium oxide. Its main advantage is being able to consume carbon monoxide. Operating at high temperature (600 to $1,000^\circ C$), it can also be integrated with combined cycle gas turbines, as we shall show in section 27.1.4.

27.1.1 SOFC modeling

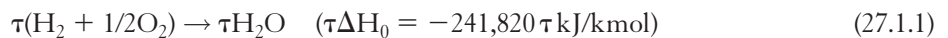
In Thermoptim, the model structure is given Figure 27.1.4.

27.1.1.1 Cell model

The first model we develop is very simple: rate of hydrogen τ and energy efficiency ϵ are assumed known.

At the anode, only a fraction τ is transformed in the cell, the rest emerging from it. Typically, $\tau = 0.5$. The overall reaction giving the outlet species is written:

For the part used:



For the unused part:



We get therefore at the anode outlet:



$\tau\Delta H_0$ represents the theoretical energy put into play by the conversion of the part used. A fraction ϵ of this energy is converted directly into electricity, and $(1 - \epsilon)$ is transformed into heat.

FIGURE 27.1.5

SOFC component screen

component name	molar fraction	mass fraction
N2	0.781	0.7555302
Ar	0.009	0.01241636
O2	0.21	0.2320534

FIGURE 27.1.6

Air entering the cell, flow rate 120 g/s

Moreover oxygen is withdrawn from the oxidizer air at the cathode. λ representing the flow of incoming air, we get:

$$\text{Intake air:} \quad \lambda(\text{O}_2 + 3.76 \text{ N}_2) \quad (27.1.4)$$

$$\text{Depleted air exiting:} \quad (\lambda - \tau/2)\text{O}_2 + 3.76\lambda\text{N}_2 \quad (27.1.5)$$

The model retained is the following:

1. species composition is given by solving equations (27.1.1) to (27.1.5): one determines hydrogen and air inlet molar flows, which provides the value of λ , from which we deduce molar flows at the outlet, τ and ε values being known;
2. heat released by fraction $\tau(1 - \varepsilon)$ of the fuel is used to provide energy to heat gases.

\dot{m}_{mol} being the molar flow of hydrogen, enthalpy released is equal to $\dot{m}_{\text{mol}}\tau\Delta H_0$. It is split between electricity $\dot{m}_{\text{mol}}\varepsilon\tau\Delta H_0$, and energy to heat gases $\dot{m}_{\text{mol}}\tau(1 - \varepsilon)\Delta H_0$.

In Thermoptim, the cell is represented by an external mixer connected to an external divider (classes SOFCinlet.java and SOFCoutlet.java), the calculations being made by the latter.

The SOFC component screen is given in Figure 27.1.5. Input data labels are displayed in blue, and it was assumed that gases enter the cell at 500°C.

It is a cylindrical stack technology such as that developed by Westinghouse, corresponding to a 100 kWe system, where $\tau = 0.48$ and $\varepsilon = 0.44$.

component name	molar fraction	mass fraction
H2	0.52	0.1081169
H2O	0.48	0.8918831

FIGURE 27.1.7

Humidified hydrogen at the outlet, flow rate 19.24 g/s, LHV: 11,230 kJ/kg

component name	molar fraction	mass fraction
N2	0.8824047	0.8654283
Ar	0.01016856	0.01422242
O2	0.1074267	0.1203493

FIGURE 27.1.8

Air depleted in O₂ flow-rate 104.76 g/s

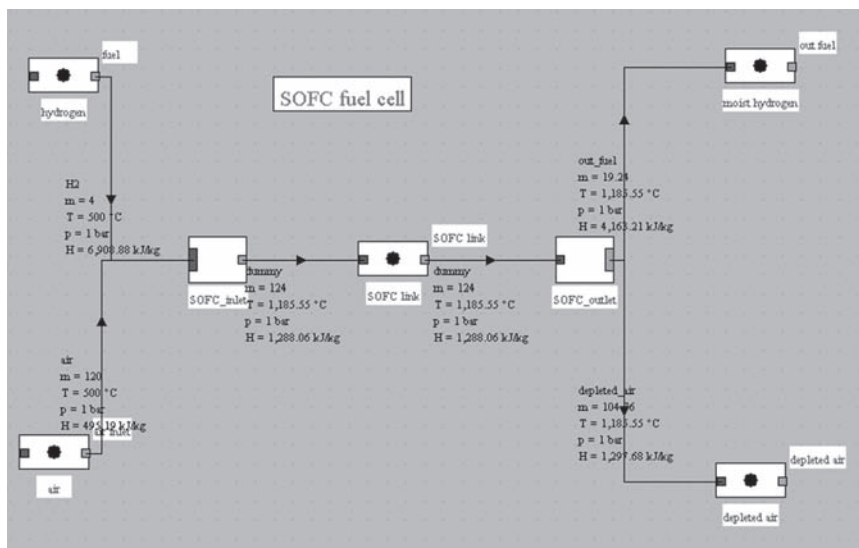


FIGURE 27.1.9

Synoptic view of the SOFC

27.1.1.2 Results of the simple model

With the following settings corresponding to Figures 27.1.5 and 27.1.9 (4 g/s of hydrogen and 120 g/s of air entering the cell at 1 bar and 500°C), gas compositions obtained are given in Figures 27.1.6, 27.1.7 and 27.1.8.

27.1.2 Improving the cell model

In this second model we assume that rate of hydrogen use τ and energy efficiency ϵ are determined from an electric model (classes SOFCH2ElecInlet.java and SOFCH2ElecOutlet.java).

To calculate the cell voltage V_{cell} knowing the intensity and the active surface (Figure 27.1.10), various models have been proposed. We retain that which was developed at the Center for Energy and Processes of École des Mines de Paris (Hubert, 2005). Its equation is:

$$V_{cell}(J) = E + \frac{b}{\ln(J/J_d) - 2} + \left(\frac{b}{4J_d} - \Delta \right) J \tag{27.1.6}$$

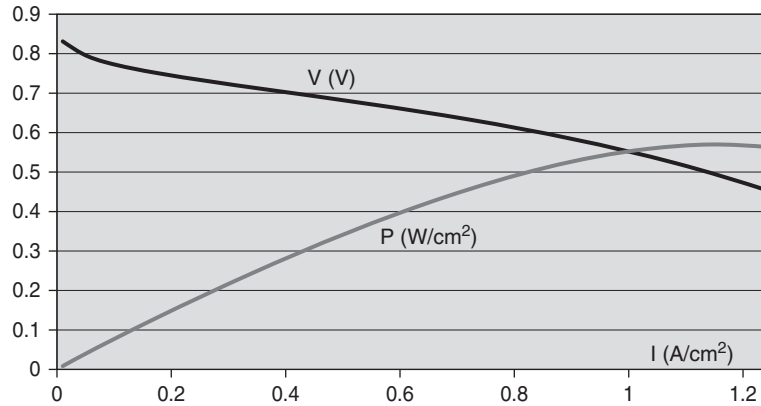


FIGURE 27.1.10

Polarization curve of the cell

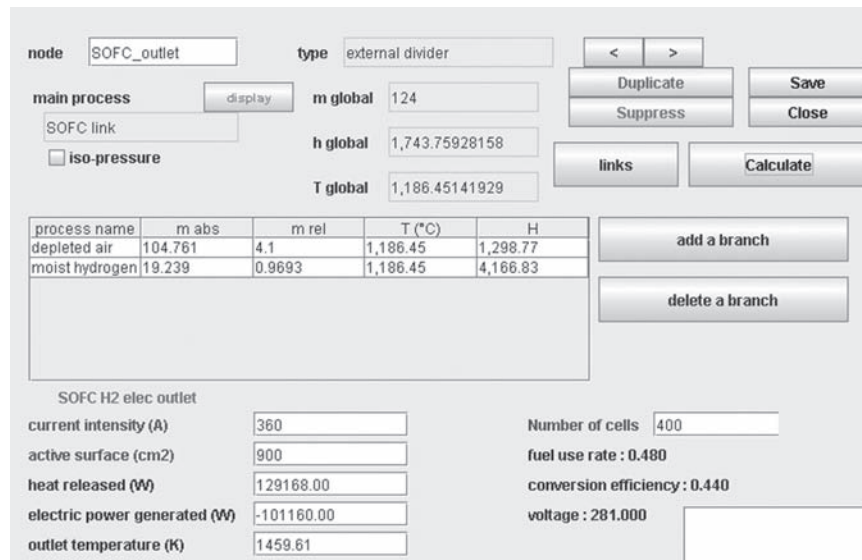


FIGURE 27.1.11

SOFC component screen

where $J = I/A$ is the current intensity (intensity divided by the active area A), in A/cm^2 .

E , J_d , b and Δ are four parameters *a priori* dependent on the cell temperature and the hydrogen pressure. They can be considered constant as a first approximation, but the influence of temperature and partial pressure of H_2 on each parameter can also be taken into account if necessary.

Knowing V_{cell} , it is possible to simply calculate the cell capacity:

$$P_{elec} = V_{cell} I N_{cell}$$

The rate of hydrogen use is assumed to be proportional to the current density J , which corresponds in first approximation to what happens in practice: the fraction of hydrogen consumed is zero in a physically open circuit, and increases when the output current increases. We choose the following law: $\tau = 1.2J$.

New model parameters are: number of cells N_{cell} , current intensity sought I , and active surface of a cell A . The model calculates τ and ε as well as output voltage V .

The SOFC component screen is given in Figure 27.1.11, input data labels being displayed in blue (it was assumed that the gases enter the cell at $500^\circ C$).

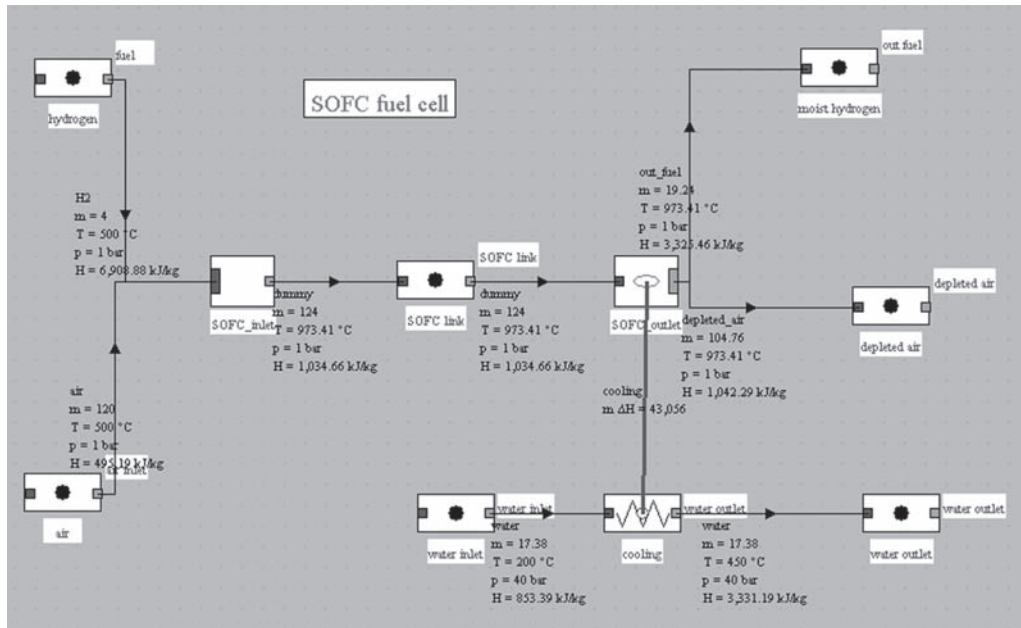


FIGURE 27.1.12
Synoptic view of the SOFC with thermocoupler

It is a cylindrical stack technology such as that developed by Westinghouse, each cell having a diameter of 19 mm and a length of 1.5 m, an area of 900 cm², leading to an intensity of 360 mA with a current density of 400 mA/cm².

Calculation results for a set of 400 cells, corresponding to a 100 kWe system are given below: $\tau = 0.48$, $\varepsilon = 0.44$, $V = 281$ V. In terms of electrical power and heat, this model leads to the same values as the simple model developed previously.

27.1.3 Model with a thermocoupler

The third model is an extension of the previous one, which assumes that the fuel cell is cooled by water at 40 bar, its temperature rising from 200°C (liquid) to 450°C (steam).

Stack cooling is modeled by a thermocoupler connected to the outlet divider.

We assume in this model that a third of the heat in the stack is recovered by steam cooling, the rest being used to heat gases that enter the fuel cell. The thermocoupler setting is explained below.

Figures 27.1.12 to 27.1.14 show model changes (classes SOFCH2ThermoInlet.java and SOFCH2ThermoOutlet.java). With the new assumptions, the thermocoupler allows us to heat 17.4 g/s of water at 40 bar from 200°C to 450°C.

27.1.4 Coupling SOFC fuel cell with a gas turbine

It is possible to model the coupling of a SOFC fuel cell with a gas turbine. The diagram is given in Figure 27.1.15.

Air and hydrogen are initially at 15°C and 1 bar. Their respective flow rates are 300 g/s and 4 g/s (we have greatly increased the airflow to on the one hand have enough oxygen in the depleted air to burn all the residual hydrogen at the stack output, and secondly to limit the turbine inlet temperature at a reasonable value).

node: SOFC_outlet type: external divider

main process: SOFC link m global: 124 h global: 1,396.53348665 T global: 973.40525354

iso-pressure

process name	m abs	m rel	T (°C)	H
depleted air	104.761	4.1	973.41	1,042.29
moist hydrogen	19.239	0.9693	973.41	3,325.46

SOFC H2 thermo outlet SOFC cooler

current intensity (A): 360 Number of cells: 400

active surface (cm²): 900 fuel use rate: 0.480

heat released (W): 86112.00 conversion efficiency: 0.440

electric power generated (W): -101160.00 voltage: 281.000

outlet temperature (K): 1246.56

FIGURE 27.1.13

SOFC component screen

name: cooling type: counterflow

thermal fluid: cooling process: SOFC_outlet

Ti: 200 To: 450 m: 17.37666416 Cp: 9.91122305 m ΔH: 43,055.99857134

Ti: 500 To: 973.40525354 m: 124 Cp: 90.94955801 m ΔH: -43,055.99857134

calculated calculated pinch method fluid

calculate exchange minimum pinch: 0

epsilon: 0.833333333

UA: 311.12949506 R: 0.0152711372 NTU: 1.80653977 LMTD: 264.134107

FIGURE 27.1.14

Thermocoupler screen

Air and hydrogen are compressed at 20 bar by compressors of isentropic efficiency 0.85, then preheated before entering the cell by exchange with gas leaving the anode and cathode. 43 kW heat is provided by the cell to produce steam at 40 bar and 500°C.

Depleted air and humidified hydrogen are then burnt in the combustion chamber and flue gases expanded in the turbine of isentropic efficiency 0.9.

Figure 27.1.15 shows the synoptic view of the facility for such a simulation.

While the cell efficiency is only equal to 44%, the electrical efficiency of this facility is already equal to 45.4%, and in addition 43 kW of steam and approximately 180 thermal kW are available in the exhaust gas exiting the turbine at about 600°C.

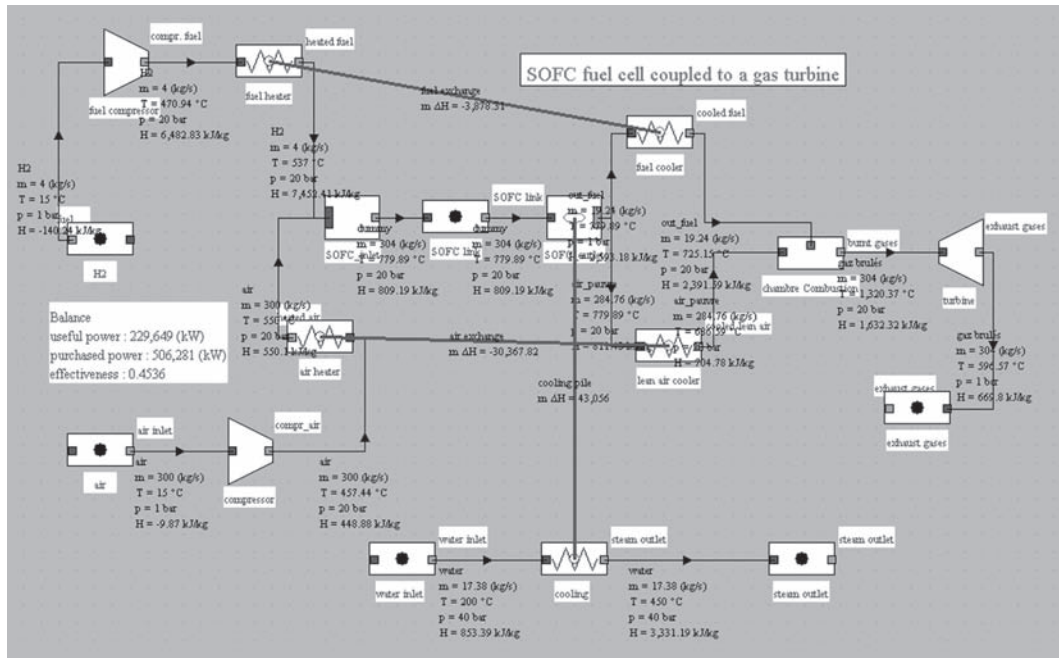


FIGURE 27.1.15
Synoptic view of the plant

The available cogeneration power is equal to 230 kWe, plus 223 kW thermal energy at a cost of 506 kW. The overall efficiency is therefore equal to 89.5%.

27.1.5 Change in the model to replace H₂ by CH₄

The models we have developed so far only allowed for pure hydrogen as fuel. In reality, it is very rare that one has hydrogen, which must be produced from another fuel. This is called reforming.

The basic equation for reforming a fuel such as methane, is:



Reforming converts fuel into hydrogen, but requires water and heat supply, and produces carbon monoxide, which is a poison for some fuel cells such as PEMFC, where it is then necessary to also convert CO.

Note that one advantage of SOFC technology is that it tolerates the presence of CO well, while in other cases a shift reaction is necessary to convert it into CO₂. The energy efficiency of the whole is improved.

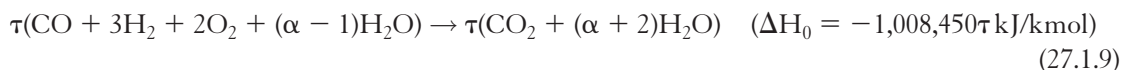
Let us call α the molar ratio of water and methane flows (α must be greater than 1 so that all methane can be processed).

At the anode, given the high operating temperature of SOFC, we can consider that the whole fuel is converted by the cracking reaction:



Then, only a fraction τ (rate of fuel use) is transformed in the cell, the rest coming out of it. The overall reaction giving the output species is written:

For the part used:



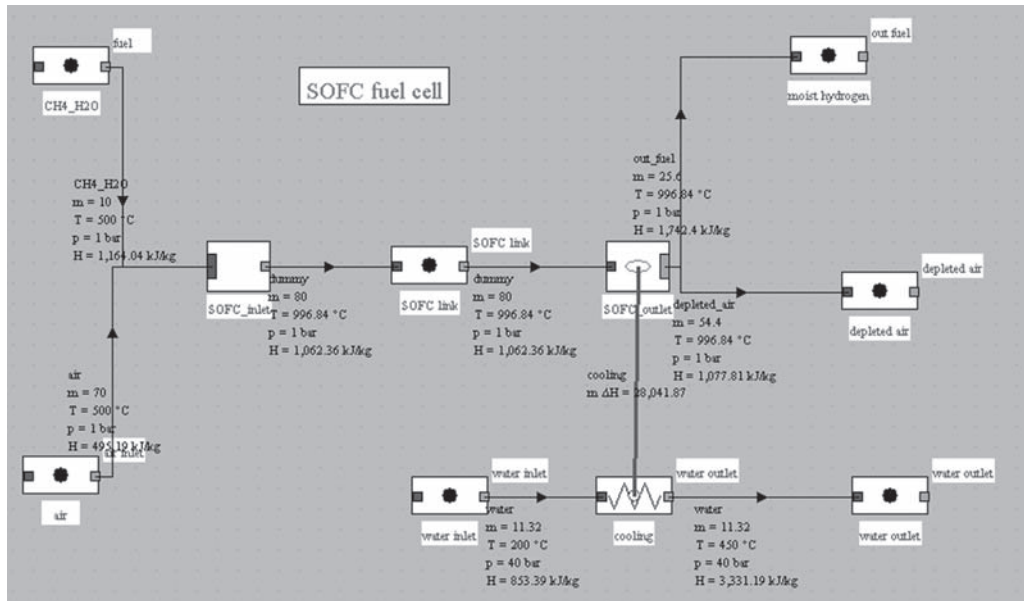


FIGURE 27.1.16

Synoptic view of the SOFC cell

Heat of reaction ΔH_0 is calculated here by considering that water remains in the gaseous state due to the temperature (LHV).

For the unused part:

$$(1 - \tau)(\text{CO} + 3\text{H}_2 + (\alpha - 1)\text{H}_2\text{O}) \quad (27.1.10)$$

We therefore get at the anode outlet:

$$(1 - \tau)\text{CO} + \tau\text{CO}_2 + 3(1 - \tau)\text{H}_2 + (3\tau + \alpha - 1)\text{H}_2\text{O} \quad (27.1.11)$$

Of the amount used, a fraction ε is directly converted into electricity, and $(1 - \varepsilon)$ is transformed into heat (some of which is used for steam cracking).

Moreover, λ being a parameter representing the incoming air, oxygen is removed from the oxidizer air at the cathode:

$$\text{Intake air:} \quad \lambda(\text{O}_2 + 3.76\text{N}_2) \quad (27.1.12)$$

$$\text{Depleted air exiting:} \quad (\lambda - 2\tau)\text{O}_2 + 3.76\lambda\text{N}_2 \quad (27.1.13)$$

The model retained is the following (classes SOFCCH4inlet.java and SOFCCH4outlet.java):

- species composition is given by solving the equations above: we determine the molar flow rates of fuel and humidified air at the inlet, which provides values for α and λ , we deduce the molar flow at the output, the values of τ and ε being read on the screen;
- heat released by fraction $\tau(1 - \varepsilon)$ of the fuel is used to provide the energy needed to heat gas and by steam cracking.

The enthalpy released is equal to $\tau\Delta H_0$. It is divided into electricity ($\varepsilon\tau\Delta H_0$), and heat required for steam cracking (ΔH_v) and heating of gas ($\tau(1 - \varepsilon)\Delta H_0 - \Delta H_v$).

Figure 27.1.16 shows the synoptic view of the fuel cell. The settings used are similar to that of the hydrogen-powered cell model: inlet gas temperature 500°C, flow rate 10 g/s for fuel, and 80 g/s for air.

Figure 27.1.17 shows the upstream mixer screen where appear the settings of the electric model, the fuel utilization rate and the fraction of the thermal power extracted by the thermocoupler.

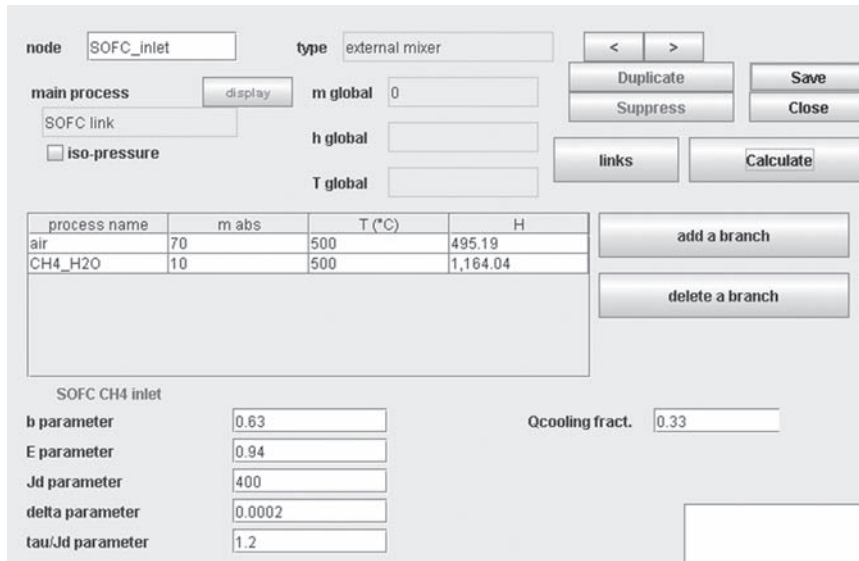


FIGURE 27.1.17
Screen of the mixer upstream of the SOFC

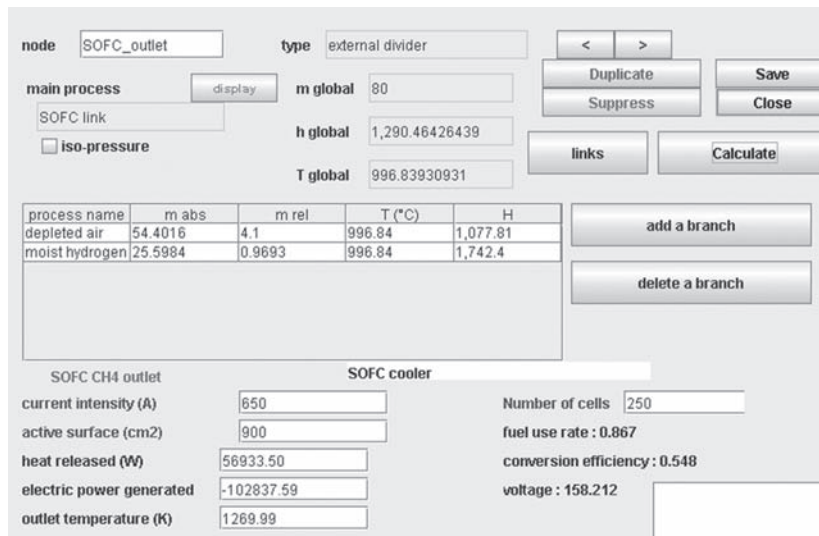


FIGURE 27.1.18
SOFC component screen

WORKED EXAMPLE

Diapason Sessions on Fuel Cells

A series of sessions (S61En to S65En) has been prepared to enable students to become familiar with the operation and modeling of fuel cells.

In session S61En, we study a SOFC fuel cell, fueled by pure hydrogen, using the simple two parameters model. In session S62En, the previous model is progressively refined, first by taking into account the equation of polarization of the cell and then introducing a cooling of the stack. Finally, an exercise shows how to couple the battery to a gas turbine to form an installation of high efficiency cogeneration.

In session S63En we see how to modify the previously established models to replace hydrogen with a fuel such as methane. Session S64En deals with reforming, and session S65En models a PEMFC fuel cell.



component name	molar fraction	mass fraction
H2O	0.52	0.5488451
CH4 ` methane	0.48	0.4511549

FIGURE 27.1.19

Fuel, flow-rate 10 g/s, LHV: 22,562 kJ/kg

component name	molar fraction	mass fraction
N2	0.781	0.7555302
Ar	0.009	0.01241636
O2	0.21	0.2320534

FIGURE 27.1.20

Air, flow-rate 80 g/s

component name	molar fraction	mass fraction
CO	0.03265306	0.0410301
CO2	0.2122449	0.4190309
H2	0.09795918	0.008858684
H2O	0.6571429	0.5310803

FIGURE 27.1.21

Fuel at the outlet, flow-rate 25.6 g/s, LHV: 1,477 kJ/kg

component name	molar fraction	mass fraction
N2	0.9782662	0.9721497
Ar	0.01127323	0.01597628
O2	0.01046053	0.01187401

FIGURE 27.1.22O₂-depleted air, flow-rate 64.4 g/s

The SOFC component screen is shown in Figure 27.1.18. We have taken a fuel utilization rate of almost 85%, corresponding to the figure announced by Siemens and Westinghouse for this type of cell operating with natural gas.

The gas compositions that are obtained are given in Figures 27.1.19 to 27.1.22.

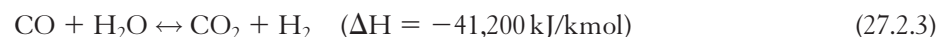
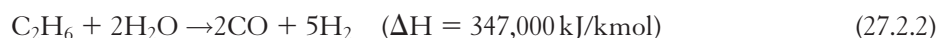
27.2 REFORMING

In the SOFC, we have taken into account reforming by a simple equation, but for other cases such as PEMFC, it is necessary to perform the reforming through a specific component before entering the cell. That is what we study in this section.

27.2.1 Modeling of a reformer in Thermoptim

For simplicity, we assume in this example that natural gas contains only methane, ethane, carbon dioxide and nitrogen. Taking into account other reactive or inert components poses no particular problem, if one assumes that the other reactants react completely as ethane.

The reformer receives humidified natural gas, which reacts according to the three reactions: (procédure)



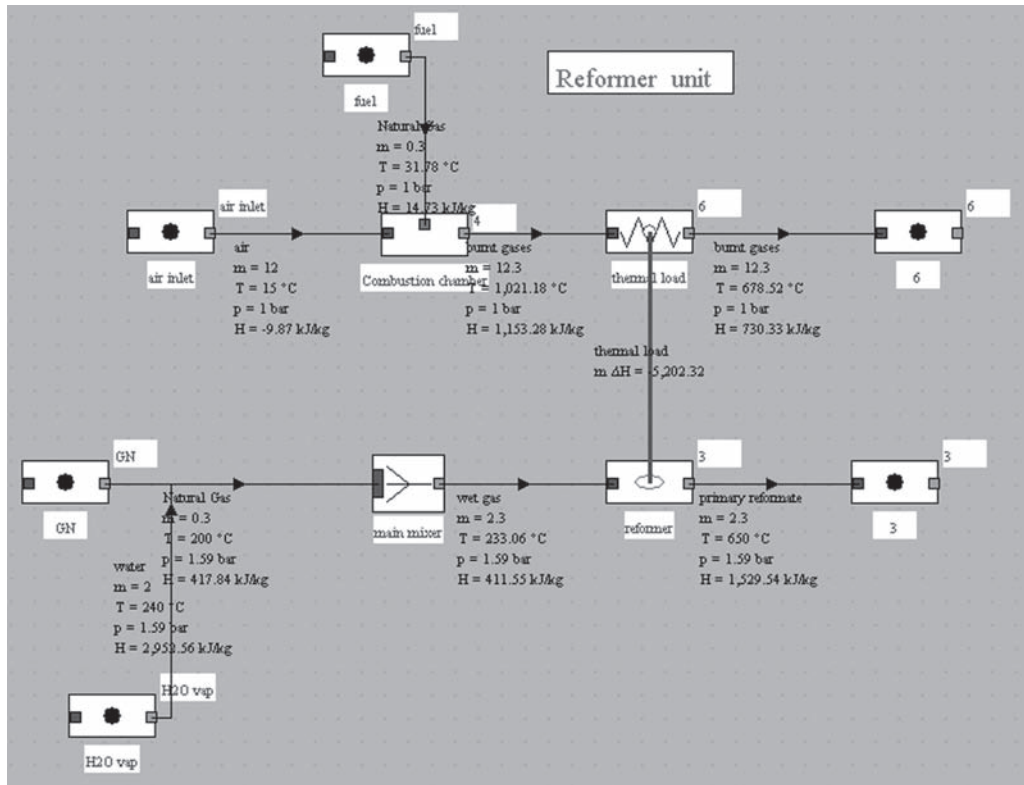

FIGURE 27.2.1

Diagram of the reformer

Ethane reaction can be considered complete, while the other two are in equilibrium, their constants being given by:

$$\ln(K_{p1a}) = 31.0152 - \frac{28,357.7}{T} + \frac{610,573}{T^2} \quad (27.2.4)$$

$$\ln(K_{p2}) = 3.57414 + \frac{3,642.48}{T} + \frac{292,593}{T^2} \quad (27.2.5)$$

Calling F° the molar flow of natural gas, x the molar flow of CO from reaction (27.2.1), y the molar flow rate of CO_2 from (27.2.3), $w/2$ the molar flow of CO from reaction (27.2.2), and a and d the mole fractions of CH_4 and CO_2 in the natural gas, and SC the number of moles of H_2O per mole of natural gas, we can write:

$$\begin{aligned} F_{\text{CO}} &= x + 2w - y \\ F_{\text{CO}_2} &= y + d \cdot F^\circ \\ F_{\text{H}_2} &= 3x + 5w + y \\ F_{\text{CH}_4} &= a \cdot F^\circ - x \\ F_{\text{H}_2\text{O}} &= SC \cdot F^\circ - x - 2w - y \\ F_{\text{tot}} &= (1 + SC) \cdot F^\circ + 2x + 4w \\ K_{p1a}(T) &= P^2 \cdot (F_{\text{H}_2}^3 \cdot F_{\text{CO}}) / (F_{\text{CH}_4} \cdot F_{\text{H}_2\text{O}} \cdot F_{\text{tot}}^2) \end{aligned} \quad (27.2.6)$$

$$K_{p2}(T) = (F_{\text{CO}_2} \cdot F_{\text{H}_2}) / (F_{\text{CO}} \cdot F_{\text{H}_2\text{O}}) \quad (27.2.7)$$

The screenshot shows a software interface for a reformer component. At the top, 'process' is set to 'reformer' and 'type' is 'external'. There are navigation buttons '<', '>', 'Save', 'links', 'Suppress', and 'Close'. Below this, 'energy type' is 'other', 'set flow' is unchecked, and 'flow rate' is 2.3. System options include 'closed system' (unchecked) and 'open system' (checked). 'inlet point' is 2, with a 'display' button. 'm Δh' is 2,571.37, with a 'Calculate' button. Inlet properties: T (°C) 233.06, P (bar) 1.59, h (kJ/kg) 411.55, quality 1. The process is labeled 'CH4 reformer' with 'Tcr (°C)' set to 650.000. Outlet properties: T (°C) 650, P (bar) 1.59, h (kJ/kg) 1,529.54, quality 1. 'outlet point' is 3, with a 'display' button. A coordinate string 'F° : 0.01736 SC : 6.40 y : 0.01257 x : 0.01542' is shown. At the bottom, there is a 'thermal load' input field.

FIGURE 27.2.2

Screen of the reformer component

The two equilibrium equations (27.2.6) and (27.2.7) form a nonlinear system difficult to solve. However, it can be noted that reaction (27.2.7) is a quadratic form in x and y , which allows one of these two variables to be formally expressed as the solution of an equation of the second degree of the other.

If x is expressed in terms of y this way and that the value obtained is reinjected into the other equation, we obtain an implicit formulation in y , which can easily be solved numerically. Only one of the two solutions of the quadratic equation must be chosen, and equation y has only one real positive solution. The search range of its value is not easy to find, especially because of the existence of a singularity in the function, corresponding to the zero of F_{CH_4} .

x being an increasing function of y , one solution is to seek an upper interval bound y_{max} by solving equation $y = f(aF^\circ)$ solution of (27.2.7). The lower bound can be chosen proportionally to y_{max} : $y_{\text{min}} = 0.9y_{\text{max}}$. The solution of (27.2.6) is then easily obtained by dichotomy between these two bounds.

The model that can be retained under these conditions is as follows:

- species composition is given by solving the equations above: from the molar flow of humidified fuel input, we determine the compositions and molar flow rates of different species at the outlet, the only parameter to consider being the reactor temperature;
- the heat required by the reaction can then be calculated and set by a thermocoupler;
- this heat is supplied by a combustion chamber located directly upstream of the thermocoupler.

In Thermoptim, the reformer is represented by an external process connected to a thermocoupler. Its class is Reformer.java.

The screens of the reformer component and its thermocoupler are given in Figures 27.2.2 and 27.2.3.

Inlet flows are determined by components located upstream of the process and the combustion chamber. As they are expressed in mass units, the molar flow rate F° , the value of SC and the values of x and y are displayed on the process screen.

The thermal power supplied by the thermocoupler is determined by the process.

FIGURE 27.2.3

Thermocoupler screen

component name	molar fraction	mass fraction
CH4 ` méthane	0.1243921	0.1113837
C2H6 ` éthane	0.008112529	0.01361569
CO2	0.001352088	0.003321271
N2	0.001352088	0.002114077
H2O	0.8647912	0.8695652

FIGURE 27.2.4

Humidified natural gas, LH: 6,217 kJ/kg

component name	molar fraction	mass fraction
CO	0.03018695	0.06006241
CO2	0.07799918	0.2438392
H2	0.3919335	0.05612304
CH4 ` méthane	0.003366579	0.003836472
H2O	0.4954514	0.6340248
N2	0.001062407	0.002114077

FIGURE 27.2.5

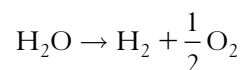
Primary reformate, LHV: 7,531 kJ/kg

27.2.2 Results

Gas compositions that are obtained are given in Figures 27.2.4 and 27.2.5.

27.3 ELECTROLYSERS

An electrolyzer performs an electrochemical reaction that produces the hydrogen and oxygen from water through electricity consumption by the endothermic reaction:



An electrolyzer is composed of two electrodes, the anode and cathode, separated by an electrolyte.

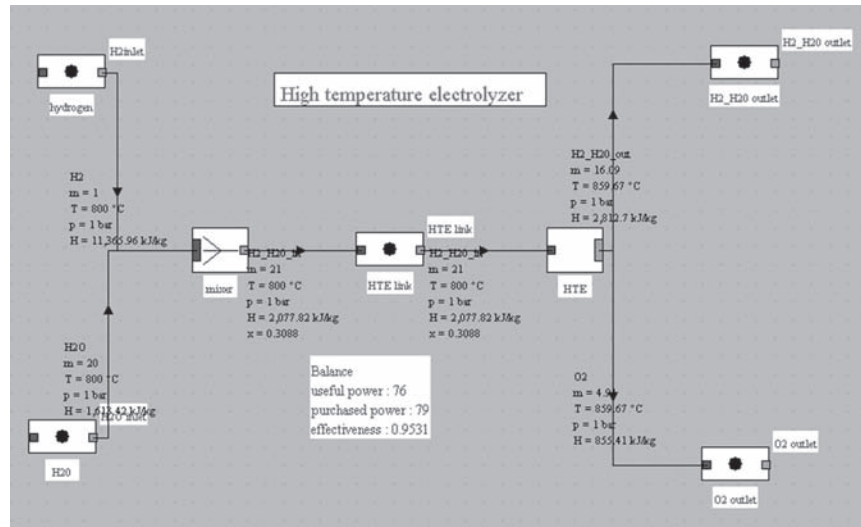


FIGURE 27.3.1

Diagram of EHT component with upstream and downstream connections

27.3.1 Modeling of a high temperature electrolyser in ThermoOptim

A high temperature electrolyzer receives a water and hydrogen mixture. It releases two fluids: oxygen and the initial mixture enriched in hydrogen.

A ThermoOptim model must involve a conventional mixer in input and an external divider in output, the two being connected by a process-point playing a passive role. The model structure is given in Figure 27.3.1.

The model we develop (classes EHT.java and EHToutlet.java) is very simple: it takes as parameters the molar fraction of hydrogen at the outlet α or the electricity supplied ΔH , and the “efficiency” in kWh/Nm³, which expresses the amount of electricity to provide for electrolyzing 1 Nm³ of hydrogen.

The balance of species is easy to establish. Electricity provided electrolyzes water and produces hydrogen and oxygen, and is partly converted into heat which raises the temperature of the device.

Two calculation methods are possible:

- either determine ΔH knowing α and the efficiency in kWh/Nm³;
- or determine a knowing ΔH and the efficiency in kWh/Nm³.

In the first mode, the calculation is as follows: the model determines the inlet molar fraction and molar flow rate from the external divider main flow, deduces the molar flow of hydrogen electrolyzed and establishes its balance.

Let us call β the inlet mole fraction of hydrogen, and \dot{m}_{mol} the inlet total molar flow rate.

The molar flow of hydrogen electrolyzed \dot{m}_{H_2} is:

$$\dot{m}_{\text{H}_2} = (\alpha - \beta)\dot{m}_{\text{mol}}$$

The composition of the mixture $[\text{H}_2]/[\text{H}_2\text{O}]$ being known, its molecular weight can be determined. As its molar flow rate is equal to the inlet molar flow rate, the mass flow is known.

The molar flow-rate of oxygen is $\dot{m}_{\text{H}_2}/2$. Its mass flow rate is deduced directly.

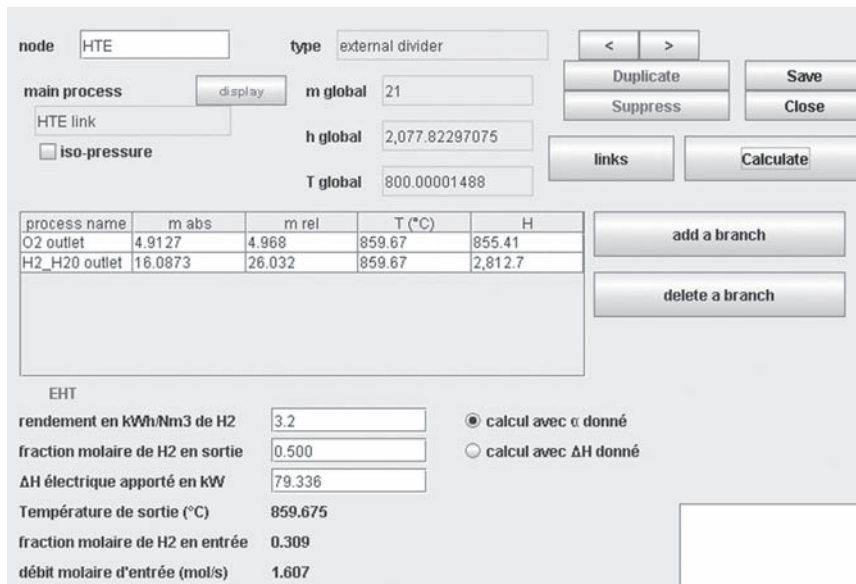


FIGURE 27.3.2

Screen of EHT component

component name	molar fraction	mass fraction
H2	0.3088358	0.04761905
H2O	0.6911642	0.952381

FIGURE 27.3.3

Humidified hydrogen at inlet, flow-rate 21 g/s, LHV: 5,712 kJ/kg

component name	molar fraction	mass fraction
H2	0.5	0.1006372
H2O	0.5	0.8993628

FIGURE 27.3.4

Humidified hydrogen at outlet, flow-rate 16.09 g/s, LHV: 12,072 kJ/kg

The “efficiency” in kWh/Nm³ allows us to calculate the amount of electricity to be supplied, ΔH, by:

$$\Delta H = \dot{m}_{H_2} M_{H_2} \frac{3,600}{1,000 \cdot 0.08988}$$

ΔH₀ being the theoretical heat of reaction (246 kJ/mol), heat released is:

$$Q = \Delta H - \dot{m}_{mol} \Delta H_0$$

In the second mode, the sequence of calculations is slightly modified: knowing ΔH, \dot{m}_{H_2} can be determined. We deduce α. Q is determined in the same way.

27.3.2 Results

With the settings above (1 g/s hydrogen and 20 g/s of water at the electrolyzer inlet), gas compositions obtained are given in Figures 27.3.3 and 27.3.4.

This model can be used to represent an electrolyzer integrated into a system, and particularly to study the thermal integration of the process, in order to minimize the external heat input.

REFERENCES

- D. Candusso, R. Glises, D. Hissel, J.-M. Kauffmann, M.-C. Pera, *Piles à combustible PEMFC et SOFC: Description et gestion du système*, Techniques de l'Ingénieur, Traité Génie énergétique, BE 8 595.
- D. Candusso, R. Glises, D. Hissel, J.-M. Kauffmann, M.-C. Pera, *Piles à combustible PEMFC et SOFC: Transferts de chaleur et de masse*, Techniques de l'Ingénieur, Traité Génie énergétique, BE 8 596.
- Ch.-E. Hubert, *Etude du fonctionnement et optimisation de la conception d'un système pile à combustible PEM exploité en cogénération dans le bâtiment*, Thèse de Doctorat, École des Mines de Paris, 2005.
- F. Werkoff, A. Marechal, F. Pra, *Technico-economic study on the production of hydrogen by high-temperature steam electrolysis*.
- CEA, *Nouvelles technologies de l'énergie*. Rapport d'activités, 2001–2003. Document Internet: www cea fr.
- G. Hoogers, Ed. *Fuel Cell Technology Handbook*, Second Edition, CRC Press, Boca Raton, 2002, ISBN 9780849308772.
- B. Viswanathan, M. Aulice Scibioh, *Fuel Cells: Principles and Applications*, CRC Press, Boca Raton, 2008, ISBN 9781420060287.
- S. Kuai, J. Meng, Eds, *Electrolysis: Theory, Types and Applications*, Chemistry Research and Applications, Nova Science Publishers, 2010, ISBN 978-1-60876-619-2.

This page intentionally left blank

Global Warming and Capture and Sequestration of CO₂

Abstract: In this chapter, we discuss a subject that until recently seemed to be utopian, and which now appears to be technically and economically feasible in the short term: capture and sequestration of carbon dioxide emitted by large energy or industrial facilities.

The subject being vast and rapidly evolving, we first make a general presentation, largely based on publications of the IPCC. In a second step, we illustrate some possible technical solutions by showing how they can be modeled with Thermoptim. These are examples that we have studied in recent years. We do not claim to give a comprehensive overview of different possibilities, which would in any case be impossible in the scope of this book. We are just trying to show the reader the types of models that can be considered with a rather easily accessible tool such as Thermoptim.

Keywords: Capture, sequestration, carbon dioxide, global warming, oxycombustion, CCS, steam reforming, gasification, shift CO, IGCC, anti-sublimation, cascade, CO₂ absorption, methanol, regeneration, AZEP, Chemical Looping Combustion, Graz, Matiant.

28.1 PROBLEM DATA

Global warming has recently become a major environmental issue, which has been the subject of national policies and international negotiations for more than fifteen years. The UN Convention on Climate Change (1992) and the Kyoto conference (1997) attest to the global awareness of the need to control anthropogenic greenhouse gas emissions, the most important of which is carbon dioxide (CO₂).

In a context of sustained economic growth, where 85% of energy needs are provided by fossil fuels, current forecasts predict a doubling of current CO₂ emissions by 2050 if nothing changes, which is an emission of 50 billion tonnes per year, whereas stabilization of the atmosphere around 550 ppm CO₂ would require a halving of emissions as of 1990. In the light of current economic and technological constraints, the latter objective is certainly a real **global challenge of unprecedented proportions**.

Technological solutions that we are now considering are of three complementary levels:

- Firstly, wherever possible, improve energy efficiencies by rational use of energy;
- Second, develop national energy mix so that it depends much less on fuel with high carbon content (that is to say, expanding the share of natural gas), and using carbon-free technologies (nuclear, solar, wind etc.);
- develop technology adoptable at industrial scale capable of capturing and storing CO₂ produced by conventional fossil fuel technologies.

This axis, which is the subject of this chapter, is being explored by many research laboratories and manufacturers.

Since the industrial revolution, which marks the beginning of the significant use of fossil fuels, an almost exponential rise in CO₂ concentrations in the atmosphere has been observed, this increase being highly correlated with an increase in average temperatures at the earth surface. CO₂ being a major greenhouse gas (it represents three quarters of the current global warming increase), we cannot deny the significant part due to human activities (anthropogenic) in these developments.

The concentration of CO₂ in the atmosphere in 2000 was approximately 370 ppm, corresponding to emissions of 23.5 Gt of CO₂ per year, these emissions being still on the increase (1.4% on average globally from 1990 to 1998 with strong regional disparity, from -4.6% for economies in transition (former Soviet countries) to about 5% for Asia-Pacific). In its summary report of 2001, the IPCC has studied various scenarios of CO₂ concentrations in the atmosphere, according to several socio-economic assumptions. The main results lead to predictions of temperature increases of 1.4 to 5.8 degrees Celsius by 2100, associated with a rise in sea level of 9 cm to about 1 m on average.

Even if the consequences of such climatic changes are poorly known, they were enough to cause the creation of global negotiation structures. The Kyoto Protocol and the United Nations Convention Framework on Climate Change assert the need to reduce global emissions of greenhouse gases in order to stabilize the concentration in the atmosphere and mitigate the impact of climate change. These statements are accompanied by quantitative binding reduction targets: countries known as Annex B (mostly OECD, the U.S. excluded) are committed to reduce emissions by 5% in 2008–2012 compared to the 1990 levels, growth forecast for the same emissions being around 20% if no action was taken.

However, although the need to reduce emissions of greenhouse gases appears to be recognized by the implementation of national and international public policy, the major difficulty is the strong link between CO₂ emissions and economic growth. All developed economies in fact consume much energy, and particularly fossil fuels.

Two indicators of policy performance can be used:

- the energy intensity of the economy (energy consumption/GDP);
- the carbon intensity of energy (CO₂ emissions/energy consumed).

They are used to characterize the types of mitigation measures, knowing that a set of measures is needed to build an effective and economically acceptable policy.

28.2 CARBON CAPTURE AND STORAGE

28.2.1 Introduction

Carbon capture and storage (CCS) is, as its name implies, to recover CO₂ from combustion of carbonaceous materials (mainly fossil fuels but also biomass) for injection underground at high-pressure in adequate geological formations, and store it in the long term. This is a mitigation measure to reduce the carbon intensity of energy that could be described as a “measure of second order”

since the amount of carbon is not reduced at source, in terms of fuel, but at the output: we do not limit the amount of CO₂ emitted, but avoid its release into the atmosphere.

We can identify two *a priori* advantages of this measure:

- First, it is a source of flexibility in the short term. Indeed, the known fossil fuel resources are 5 times the amount of carbon released into the atmosphere by human activities since 1860. Restrictions on the use of this fuel will not stem from any constraint on resources, whatever the uncertainties on the technological developments needed to exploit unconventional sources, and geopolitical aspects. In addition, if any decision or political incentive to abandon this type of fuel is put in place, a “reaction time” of actors and technologies must be taken into account. The IPCC estimates that, whatever the scenarios, fossil fuels will remain the main source of energy until 2020. CCS would modulate these unavoidable emissions, and make technological adaptations cheaper: you continue to use fossil fuels, but their impact is less in terms of CO₂ emissions. This short term benefit is that which has been extensively studied and evaluated, especially by the IPCC special report given in the references;
- combined with other technological advances, CCS would provide a much greater potential for reducing emissions: it could well afford to produce from fossil fuels new clean non-fossil energy carriers, such as hydrogen. Its scope would be greatly expanded.

An important argument in favor of CCS is that its feasibility is almost established. CO₂ emissions must first be trapped or caught in a gas stream often mixed (there are approximately 15% of CO₂ in the gas exiting a power plant for example). Almost pure and high pressure CO₂ must then be transported to its storage location, where it must be injected into geologic or ocean formations with characteristics appropriate to sequester it in the long term.

For each of these steps, there are now several technical solutions at various degrees of technological maturity, but on the whole they have been demonstrated and commercialized in other fields. Most of these solutions are tightly controlled by the oil and gas industry, which has some experience in particular in the transport of gas under pressure, and expertise in geological layers. If you enter into a little more detail, the trapping step is technically the less developed today (at the demonstration stage only), and awaiting the most progress.

Three solutions, to which we shall return later, are now envisaged to achieve it: post-combustion capture, pre-combustion capture, and oxycombustion, the latter being the least mature. You can add the recovery of almost pure CO₂ produced by certain industries. Transportation from the production site to storage site could be mainly done by pipeline, with possible use of tankers, but does not pose new problems in relation to current transport of various gases and fuel products made by the oil and gas industry.

Geological storage is itself considered mainly in old oil or gas reservoirs, in saline aquifers in deep formations, or in coalfields difficult to exploit. These formations are indeed regarded as offering the best guarantees in terms of permeability and ability to retain and/or fix the gas under pressure. Three industrial projects already exist: Sleipner in the North Sea, Weyburn in Australia, and In Salah in Algeria, to store from 1 to 3 Mt of CO₂ per year. Pressurized CO₂ injection is used in some cases by the oil industry for enhanced oil recovery. Ocean storage, based on the principle of dissolving CO₂ in water at great depths, is a proposal still under research. The potential seems immense, but the risks for ecosystems (dissolved CO₂ acidifies water) and climate regulation in the long term are still largely unknown, suggesting the greatest caution. In terms of storage capacity, the ratings provide between 1,685 and 11,100 Gt of CO₂ (without ocean storage), but the various models show that this is not a limiting factor.

Before detailing the various CCS techniques and progress that can be expected, let us point out the main obstacles still existing to their implementation on a large scale:

- The first limitation concerns storage, and uncertainties related to leaks. Occasional leaks during transport for example, represent a danger for some local people living nearby, but not a real

problem on a large scale. The difficulty comes from more diffuse leaks, but over a long period, once the CO₂ is stored: to what extent can we consider that CO₂ storage in a geological formation is a permanent storage, particularly in relation to the time scale of climate change;

- environmental risks associated with CCS are also poorly understood. We know for example that certain possible processes or technologies, such as post-combustion capture, require use of organic solvents: how will these solvents be produced and recycled, and in what quantities;
- Finally, many legal matters are still pending.

CCS is an interesting option for mitigation. It should be attainable at a cost “economically and socially acceptable”, since it is not asking for a reconsideration of consumption levels. However, its cost is not zero, because it leads to additional energy consumption. CO₂ capture is mainly of value in the large emitters represented by power plants using coal or gas and for certain industries such as iron, steel, cement or heavy chemicals. It is much more expensive and difficult to extract CO₂ from small or mobile sources.

28.2.2 Capture strategies

As we have said, there are three main systems for capturing CO₂:

- Post-combustion capture;
- Pre-combustion capture;
- capture by oxycombustion.

Each of these systems involves a step of gas separation. The separations achieved vary by trapping systems but share some separation techniques of which there are four major families: cryogenics, use of solvents, membranes or solid adsorbents.

28.2.1.1 Post-combustion capture

Post-combustion capture refers to the separation of CO₂ from gases emitted burning fossil fuels or biomass. Instead of rejecting directly into the air combustion fumes, gases are processed to extract CO₂ which is compressed, transported and stored. The remaining gas is then released into the atmosphere. The separation technique commonly used involves chemical or physical absorption. One method announced the most promising is absorption in refrigerated ammonia, in which Alstom is currently investing heavily (chilled ammonia process or CAP).

But other methods also exist. In section 28.3.1 we present capture by anti-sublimation of CO₂.

Beyond the existing industrial applications, post-combustion capture would especially apply to existing oil, coal or gas power plants including pulverized coal or natural gas combined cycles.

28.2.1.2 Pre-combustion capture

A pre-combustion capture method is typically composed of two stages. Some already exists at small scale.

The first step generates a mixture of carbon monoxide (CO) and hydrogen from the primary fuel. Two reactions are possible:

- steam reforming;
- partial oxidation or gasification.

The second step is a conversion step which converts CO to CO₂ using water gas reaction (see section 28.3.2).

Finally, CO₂ is extracted from the mixture CO₂/H₂, whose initial concentration is 15 to 60% and pressure 20 to 70 bar. CO₂ can then be stored. Note now that pre-combustion capture has a

significant energy cost, because of the need to convert to CO₂ all the CO produced during the first stage, and this before entering the combustion chamber. Part of the initial fuel LHV is lost.

Two applications are possible for pre-combustion:

- production of fuel (H₂) with virtually no carbon. Hydrogen need not be pure, but the less carbon the fuel product contains, the less its combustion produces CO₂;
- decrease in the carbon content of fuels. For example, coal has a low H/C. Using pre-combustion, we can produce fuel with a larger ratio and sequester corresponding carbon released as CO₂. The subsequent use of the fuel obtained releases far less CO₂.

28.2.1.3 Oxyfuel capture

This technology is to achieve combustion in pure oxygen or a mixture of oxygen and recycled gas rich in CO₂ or water. Thus, gases produced by combustion are composed mainly of water, CO₂ and excess oxygen for complete combustion. To implement such a combustion, oxygen must be separated from nitrogen, the main component of air.

We will give more detail on this technique in section 28.3.3.

28.3 TECHNIQUES IMPLEMENTED

In this section, we list most CO₂ capture technologies currently being considered, but detail only a few:

- Post-combustion technique patented and developed by D. Clodic, Center for Energy and Processes of École des Mines de Paris, known as capture by CO₂ anti-sublimation;
- a technique applicable to the case of energy facilities in which the oxidizer is air. This is pre-combustion capture involving shift conversion and absorption in methanol, the latter technique being fairly representative of other methods by sorption used in post-combustion;
- some oxycombustion techniques, where the oxidizer consists of pure oxygen and a mixture of H₂O and CO₂.

28.3.1 Post-combustion techniques

Conventionally, CO₂ capture must be performed at the outlet of power plants, on a gas already expanded, cool and highly diluted.

Techniques implemented, fairly standard, are essentially:

- chemical or physical absorption in liquid absorbents such as amines or methanol, an example being given in the next section;
- physical adsorption on solids (zeolites, silicas, activated carbons), few promising for CO₂ capture;
- membrane separation;
- methods based on low temperature refrigeration as anti-sublimation capture, which we will develop by way of example, drawing on the PhD thesis of M. Younes (confidential until 2013).

28.3.1.1 Overview of anti-sublimation capture process

Capture process by anti-sublimation can be divided into three phases:

- **water condensation**, which is to cool combustion gases from their initial temperature to about 0°C. A full dehumidification is necessary to prevent formation of plugs;
- **refrigeration cascade**, separate or integrated, which cools the gas from about 0°C to CO₂ frosting temperature at atmospheric pressure;
- **CO₂ capture**, including frosting and defrosting CO₂ and then storing it.

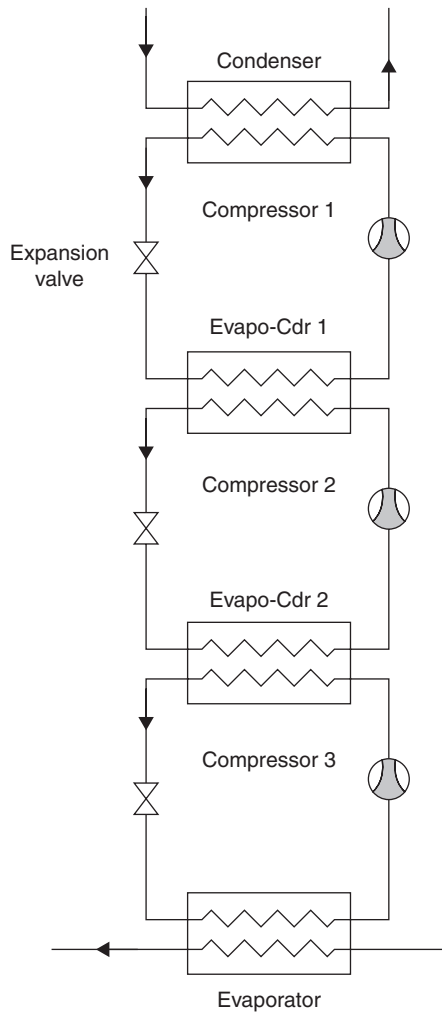


FIGURE 28.3.1
Three stage separated cascade

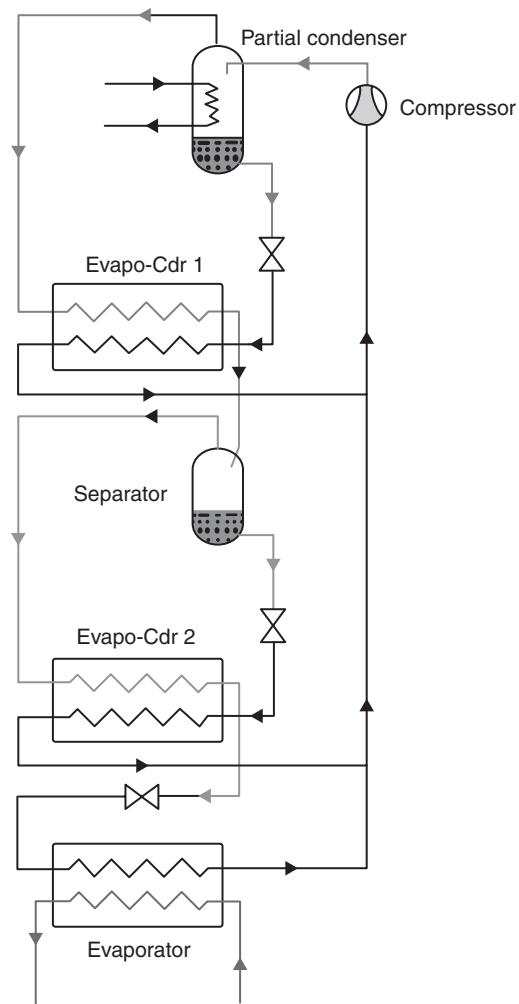


FIGURE 28.3.2
Three stage integrated cascade

The first phase, which aims at dehumidifying combustion gases as completely as possible, is not specific to the anti-sublimation process. Necessary for most capture techniques, it poses no particular problem on a technical level, but is reflected mostly by an energy penalty, which varies depending on flue gas dew point. We do not specifically detail it here.

28.3.1.2 Refrigeration cascade

The refrigeration cascade is the key element of the process. Its importance stems from the fact that the evaporation temperature it should achieve depends on both the volume concentration of CO_2 in the flue gas, and the percentage of CO_2 that we want to capture.

At partial pressure of 13.7 kPa (13.7% CO_2 by volume in gas), CO_2 frosting temperature is about 173 K (-100°C), but it drops to 152 K (-121°C) if one wishes to extract 90% CO_2 .

If we consider that the cascade condensing temperature must generally be above 20°C , corresponding to a total temperature difference of about 140°C , that it is of course impossible to achieve with simple refrigeration cycles.

Partial pressure of CO_2 in the flue gas being lower than the triple point, gas cooling leads directly to CO_2 frosting, which then is deposited in solid form on the surface of the heat exchanger without

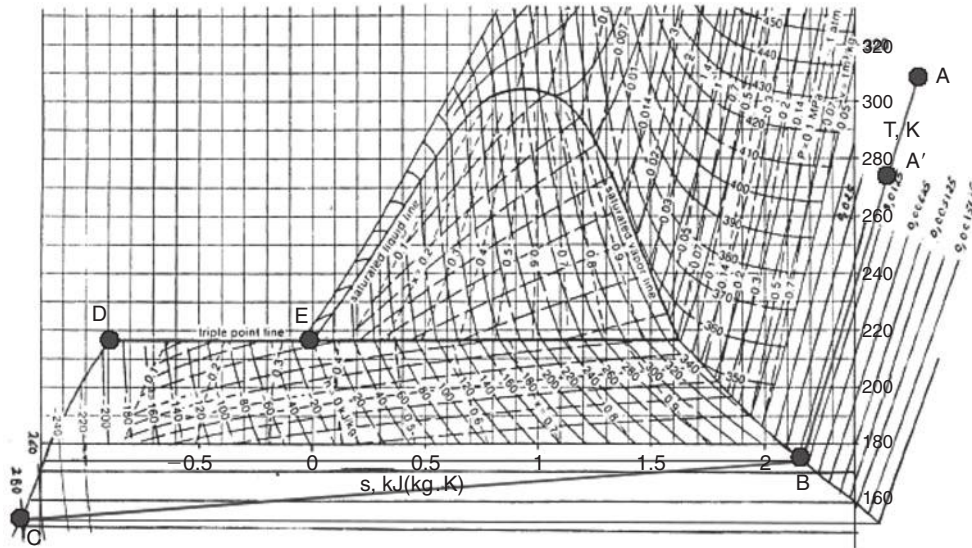


FIGURE 28.3.3

Cycle in the entropy chart

passing through the condensation phase in the liquid state. This is the reverse of sublimation we discussed in section 5.6.1 of Part 2. It is called anti-sublimation and gives its name to the process.

The cascade can be separated (Figure 28.3.1), that is to say consisting of a series of separate refrigeration cycles (3–5), coupled by evaporative condensers, or integrated (Figure 28.3.2). In the latter case, a mixture of 3 to 5 fluids passes in the entire circuit, and undergoes successive distillations which change its composition and determine the variable boiling temperatures.

Whatever the type of cascade chosen, the number of stages and the refrigerant choice is an optimization problem relatively complex to conduct, particularly if all technical and economic constraints are taken into account.

28.3.1.3 Representation of the cycle in the entropy diagram

Let us consider a stream of CO₂ of 10% volume concentration, treated by the process, with capture efficiency of 90%. At the output CO₂ concentration is 1%. CO₂ frosting begins at -103.1°C and ends at -121.9°C .

The CO₂ frosting cycle is represented on the CO₂ entropy diagram of Figure 28.3.3.

Combustion gases are first cooled at room temperature by exchange with air or water. Then, we start by cooling gas at about 0°C , which condenses much of the water (A'). Gases are then cooled to point B by exchanging on the one hand with treated gases (CO₂ free) before they are released in the atmosphere (regeneration), and secondly with the low temperature evaporator. CO₂ anti-sublimation takes place in this variable temperature heat exchanger, until point C. The frosting evaporator is then disconnected from the gas circuit to allow a hot refrigerant to pass through, forcing frosted CO₂ to sublime. Since the evaporator is an enclosed vessel, CO₂ pressure rises until it reaches the triple point (close to point D). At that time, the rest of the CO₂ starts to melt producing a two-phase mixture (E).

Line AB represents the cooling of combustion gases to CO₂ frosting temperature. Line BC is CO₂ frosting and capture. Line CD represents CO₂ sublimation energy recovery, while line DE represents the recovery of CO₂ fusion energy.

component name	molar fraction	mass fraction
N2	0.7537621	0.725
CO2	0.1237526	0.187
O2	0.02548511	0.028
H2O	0.09700014	0.06

FIGURE 28.3.4

Composition of flue gas

28.3.1.4 Energies involved in the capture

To estimate the energy needed to cool combustion gases at CO₂ frosting temperature, it can be decomposed into three components:

- that which allows moist combustion gases to dehumidify;
- that needed to cool the smoke from room temperature to CO₂ frosting temperature;
- that which must be extracted to ensure frosting of CO₂ in the gas.

As we said, the second can be obtained by regeneration, heating gas treated before discharge into the atmosphere.

The energy required to dehumidify the gas depends on its composition (which we assume given Figure 28.3.4, corresponding to a coal-fired power plant), their initial temperature and dew point: for a dew point of about 40°C this energy is 135.4 kJ/kg gas, and for 20°C, 42.2 kJ/kg.

The energy corresponding to CO₂ frosting can, in the above conditions be evaluated at about 138 kJ/kg gas.

28.3.1.5 Modeling in ThermoOptim a separate three-stage cascade

We limited our ThermoOptim modeling to part of the process: a separate three-stage cascade. It involves the following refrigerants: polypropylene (R1270), ethane (R170) and tetrafluoromethane CF₄ (R14). Fluid properties are calculated with ThermoBlend, a thermodynamic property server developed at the Center for Energy and Processes of École des Mines de Paris.

Such a cascade being a simple combination of vapor compression cycles in series, the following assumptions were chosen for each of them and their interactions:

- refrigerant is superheated by 7 K at the evaporator outlet, subcooled by 1 K at the condenser outlet;
- in evaporative condensers the saturation temperature difference of the two fluids is about 3 K;
- isentropic efficiency of compressors is assumed equal to 0.8. It would be possible to refine it by retaining a law like the one presented in section 7.2.1.5 of Part 2 (equation 7.2.7).

This simplified model was set in a plausible manner, but the choice of intermediate pressures has not been optimized. It shows that the energy penalty of capture (without water condensing) is equal to 271 kJ/kg of flue gas.

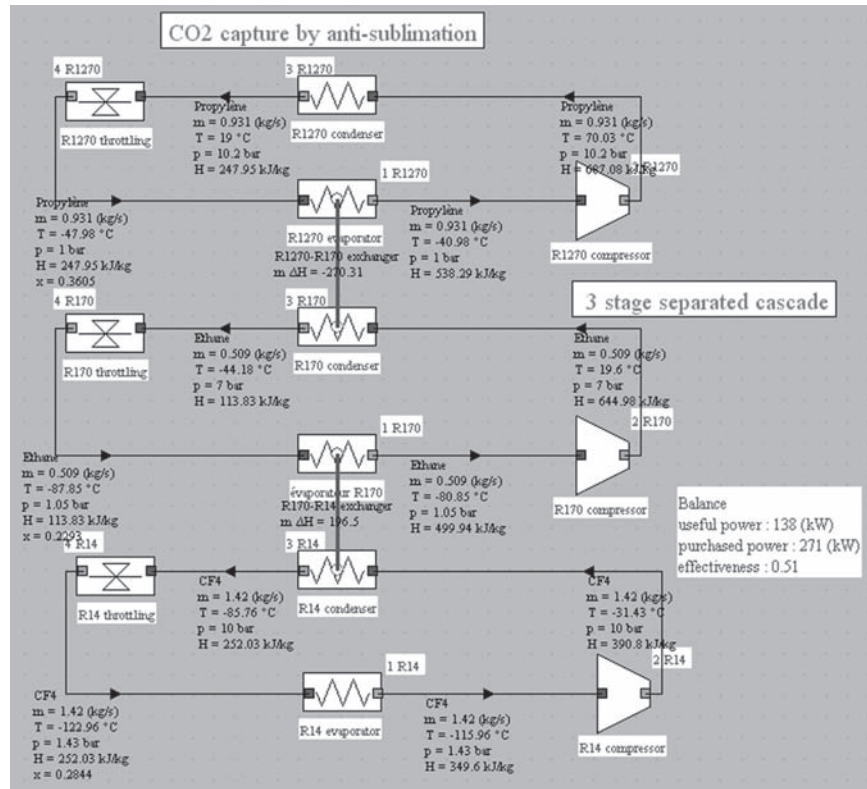
An integrated cascade should lead to better performance.

Based on the fume composition given Figure 28.3.4, and taking a steam cycle efficiency equal to 45%, the penalty calculated with this simplified model is a little more than 20% of electricity generation, which corresponds to an efficiency decrease of 9 percentage points, while it is estimated to be between 4 and 8 in (Eide et al. 2005).

28.3.2 Pre-combustion techniques

In pre-combustion processes the fuel is decarbonized before entering the combustion chamber.

We give here an example of CO₂ capture by absorption in methanol for a 325 MWe coal integrated gasification combined cycle (IGCC), which was the subject in 2002 of a research work in Integrated Research Program PRI CO₂ of French CNRS.

**FIGURE 28.3.5**

Synoptic view of the separate three-stage cascade

We show how a pre-combustion capture can be implemented and then we consider its impact on the overall performance of the power plant. The capture process has the effect firstly of inducing consumption of auxiliary heat and electricity, and secondly to reduce the fuel LHV at the inlet of the combustion chamber compared to synthesis gas.

Let us recall (Part 3, section 16.2.2.4), that IGCC plants are highly complex, involving a large number of heat exchangers, and may operate with different fuels at different times of their operation.

The great advantage of this technology is to reduce emissions of gaseous pollutants well below current standards and strongly reduce solid waste, while resulting in excellent efficiency (45%).

Its main drawback is its capital and operating cost, which is today estimated at 25% higher than that of a oil or pulverized coal plants with flue gas treatment.

In an IGCC (Figure 28.3.6), coal is converted to syngas in a gasifier. This gas is then washed and purified before being used as fuel in a combustion turbine (i.e. a gas turbine), whose effluent is cooled in a recovery boiler or steam generator (HRSG).

In an IGCC without CO₂ capture, the synthesis gas containing as fuel CO + H₂ (Figure 28.3.7) is burned in the combustion turbine, which provides a CO₂ + H₂O mixture considerably diluted in nitrogen.

An alternative is to convert CO to CO₂ before combustion. It can then be removed from this concentrate and under pressure mixture, which provides fuel to the turbine consisting essentially of hydrogen.

By working this way, we can benefit from the pressure of synthesis gas and its lower dilution. This requires the CO₂ capture process to be placed between modules "Cooling and eparation" and "Combustion turbine" of Figure 28.3.6.

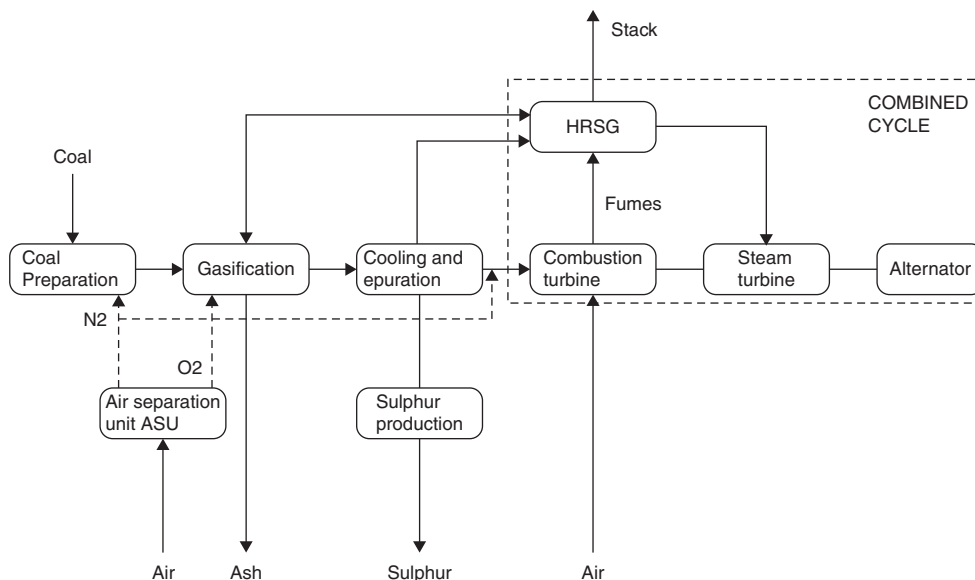


FIGURE 28.3.6
Sketch of an IGCC

component name	molar fraction	mass fraction
CO	0.543	0.6833846
H2	0.2	0.0181151
CO2	0.034	0.06723174
H2O	0.11	0.08903889
N2	0.113	0.1422297

FIGURE 28.3.7
Composition of the clean syngas

In this section we show how to model all these processes in ThermoOptim, assuming a CO₂ separation by physical absorption in methanol. Once constructed, the model allows us to study the impact of the capture device on the overall performance of the power plant.

28.3.2.1 CO conversion reaction

The clean synthetic gas, at a pressure of about 23 bar, typically has a composition similar to that given Figure 28.3.7.

To capture CO₂ before combustion, CO, which represents the largest mole fraction of the syngas, must be converted. This conversion is done according to the equilibrium reaction (28.3.1), equimolar and therefore not influenced by pressure.



This reaction shows that, at stoichiometry, a mole of H₂O is required per mole of CO, whereas in the synthesis gas there is about 0.2. So we must begin by moistening the clean gas to form a moist synthesis gas.

In ThermoOptim we have represented that humidification by a simple mixer between the flow of dry gas and an appropriate flow of steam that we assumed to be both at 23 bar and 340°C.

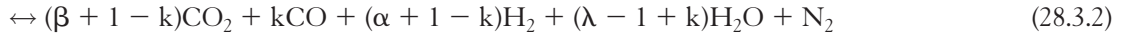
Under these conditions, the moist synthesis gas composition is given Figure 28.3.8 (so that the CO conversion reaction is as complete as possible, we operate with an excess of water close to 10%).

On entering the CO unit conversion, moist syngas contains not only reactants but also products (CO₂ and H₂) and N₂ which is inert. The actual reaction may be written as (28.3.2).

component name	molar fraction	mass fraction
H ₂ O	0.40435	0.3493135
CO	0.3634134	0.4881318
H ₂	0.1338539	0.01293936
CO ₂	0.02275517	0.04802267
N ₂	0.07562747	0.1015926

FIGURE 28.3.8

Composition of moist synthesis gas



We established a model for this reaction assuming it is in equilibrium, the equilibrium constant being given by equation (28.3.3).

Between 500 K and 1000 K with an accuracy of about 0.5%, K_p is given by equation (28.3.3), which has the advantage that it can be reversed without any particular problem: it is a second degree equation in $1/T$.

$$\ln(K_p) = -3.69088 + \frac{3,710.59}{T} + \frac{292,593}{T^2} \quad (28.3.3)$$

Reaction (28.3.1) involving a constant number of moles, equilibrium is independent of pressure and depends only on temperature. According to the law of mass action, we have here:

$$K_p = \frac{[\text{CO}_2][\text{H}_2]}{[\text{CO}][\text{H}_2\text{O}]} = \frac{(\beta + 1 - k)(\alpha + 1 - k)}{(\lambda - 1 + k)k} \quad (28.3.4)$$

Knowing α , β , λ and T , that is to say K_p , k is also given by a quadratic equation.

In practice, however, T , K_p and k are the solution of a system of three equations with three unknowns, unfortunately not linear. The first two are (28.3.3) and (28.3.4), while the third (28.3.5) is the reactor enthalpy balance: heat released by the reaction is used to heat the reactants and products, up to temperature T .

To express this, we must calculate the composition of the reaction products and the adiabatic temperature at the end of reaction.

T_{ad} is obtained by writing the reaction energy balance for 1 kmol of fuel.

The enthalpy of products is equal to that of reactants plus heat released during the reaction. Total mass flow is conserved. Heat released is used to heat the product at temperature T_{ad} .

We can possibly introduce an additional term to account for reactor losses: thermal efficiency η_{th} . In these conditions, we no longer speak of end of reaction adiabatic temperature, but rather of end of reaction temperature T_{react} .

The enthalpy equation is then:

$$\dot{m}h_2(T_{\text{react}}) = \dot{m}h_1 + Q\eta_{\text{react}}\eta_{\text{th}} \quad (28.3.5)$$

T_{react} can be obtained by inversion of the enthalpy function.

$Q\eta_{\text{react}}$ is easily calculated from reaction (28.3.1) or (28.3.2):

$$Q\eta_{\text{react}} = -\Delta H_r = (1 - k)h_{\text{fCO}} + (1 - k)h_{\text{fH}_2\text{O}} - (1 - k)h_{\text{fCO}_2}$$

$$Q\eta_{\text{react}} = 41,170 (1 - k) \text{ kJ/kmol of CO}$$

The ThermoOptim component is an external process available in the ThermoOptim-UNIT portal model library (class ShiftCO.java).

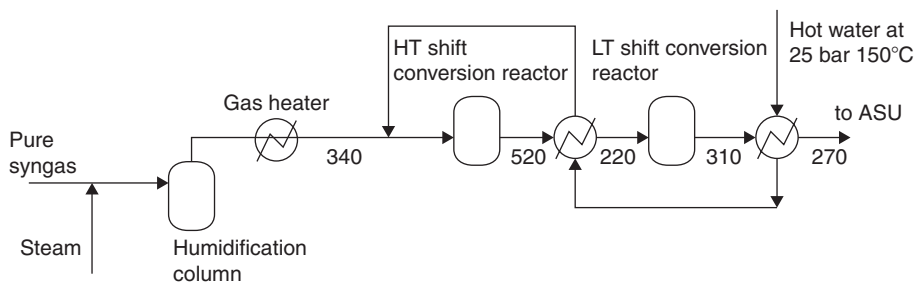


FIGURE 28.3.9
Diagram of the overall conversion unit

component name	molar fraction	mass fraction
CO	0.04794129	0.06435771
H2	0.4513904	0.04361024
CO2	0.3398304	0.7167755
H2O	0.08489655	0.07329977
N2	0.07594142	0.1019568

FIGURE 28.3.10
Composition of converted syngas

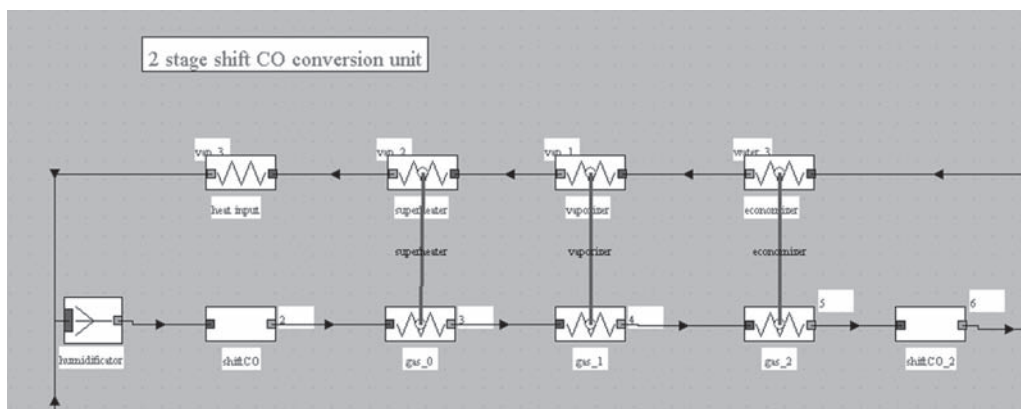


FIGURE 28.3.11
Diagram of the conversion unit

Shift reaction is an exothermic reaction quite strongly influenced by temperature. To convert a large portion of CO, we operate in several stages with cooling exchangers between reactors.

Considering the sketch of the two-reactor conversion unit given in Figure 28.3.9, the converted gas final composition is given Figure 28.3.10.

The Thermoptim diagram of the two-reactor conversion unit is given in Figure 28.3.11.

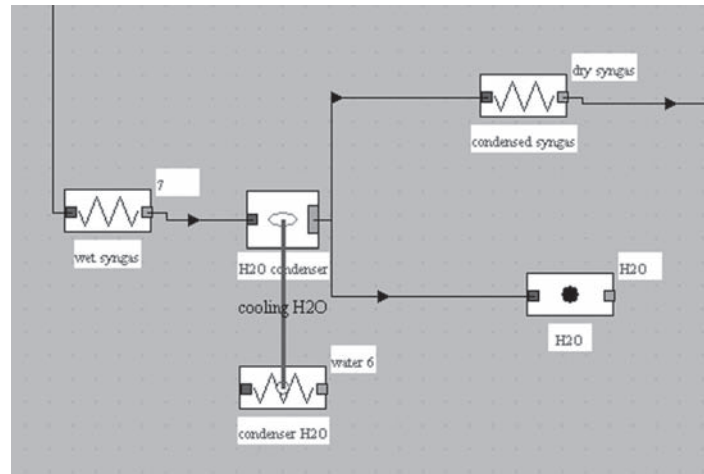
The model uses twice the external component modeling the reactor, under the names “shiftCO” and “shiftCO_2. Other elements are standard components of Thermoptim core.

Comparisons with Aspen (REQUIL) show a good agreement.

In the whole unit to be studied further, the shift reaction will involve three reactors.

28.3.2.2 Condensation of converted gas

λ being greater than 1, the converted gas always contains water at the shift conversion output. It turns out that methanol preferentially absorbs water, which leads to blowdown and an

**FIGURE 28.3.12**

Converted gas condensing model

component name	molar fraction	mass fraction
H2O	0.000688846	0.0005894046
CO	0.02767684	0.0368202
H2	0.5048089	0.04833281
CO2	0.3858417	0.8065085
N2	0.0809837	0.1077491

FIGURE 28.3.13

Composition of dehydrated converted syngas

injection of pure solvent. To reduce the costs associated with these operations, we must condense the converted gas water before introducing it into the absorption column. Since we must in addition cool the converted gas from 240°C to about -30°C, condensation occurs on cooling.

The model we develop here is that presented in section 7.8.4.1 of Part 2. The only parameters are firstly the coil effectiveness σ , and secondly the surface temperature.

An external divider is sufficient to represent this component modeled by class DehumidifyingCoil presented section 23.5.2: the main vein receives the converted gas, while the two output streams correspond to the dry synthesis gas and extracted water. The model also involves a cooling thermocoupler (Figure 28.3.12).

Calculation is as follows: the molar fraction of residual H₂O is determined from σ , then the mass flow of water extracted at 30°C is determined, and the mass and enthalpy balances allow the flows exiting the component and its thermal load to be determined. Figure 28.3.13 provides the composition of dehydrated gas.

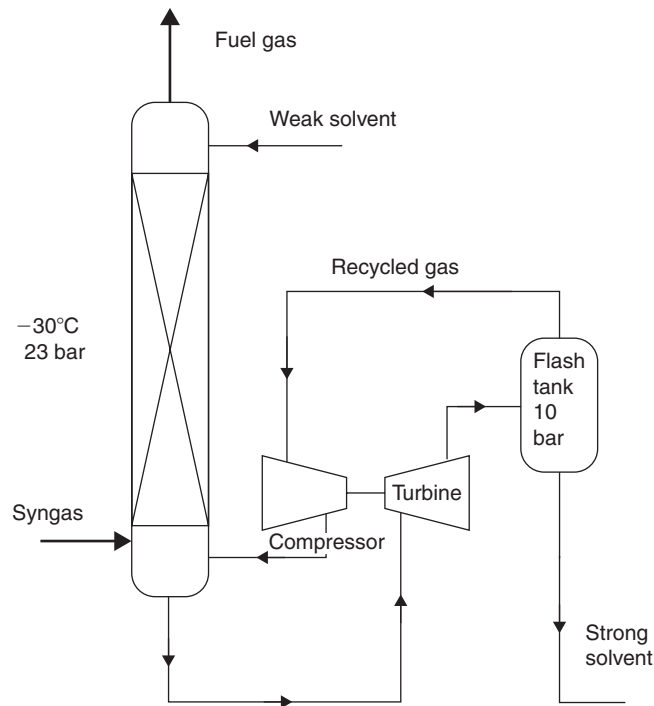
28.3.2.3 CO₂ absorption

The CO₂ absorption in the methanol Thermoptim model is keyed to that established under Aspen Plus by C. Descamps¹.

Given the differences in saturating pressures of the various gases making up the converted gas, CO₂ is absorbed preferentially.

The cooled and dried synthesis gas enters in the left side of the absorption column (Figure 28.3.14), where it dabbles in the solvent at a pressure of 23 bar. Given the low temperature and high pressure, solubility in methanol is high, even to the point that it also absorbs hydrogen.

¹ Cathy DESCAMPS, PhD thesis, June 1st 2004, Étude de la capture du CO₂ par absorption physique dans les systèmes de production d'électricité basés sur la gazéification du charbon intégrée à un cycle combiné.


FIGURE 28.3.14

 Absorption of CO_2 in methanol

To recover it, the enriched solvent is then expanded at 10 bar, a turbine allowing some mechanical energy to be recovered. At the top of the flash tank, the hydrogen-rich gas portion is recycled, a compressor bringing it to 23 bar, and a heat exchanger cooling it to -30°C .

The rich solvent is recovered at the bottom of flash drum, and the low-carbon synthesis gas exits at the top of column.

The mass balance of the absorber is rigorously established in the following manner:

- residual water (this is a very small fraction) is fully absorbed in the solvent;
- nitrogen and carbon monoxide exit completely on top;
- about 99% of hydrogen is recovered on top of the column, the rest being absorbed into the solvent;
- most CO_2 is absorbed in the solvent.

We call ε the CO_2 separation rate. This is the model key parameter, which determines:

- the solvent flow;
- CO_2 temperature at the column output;
- cooling and compression capacities.

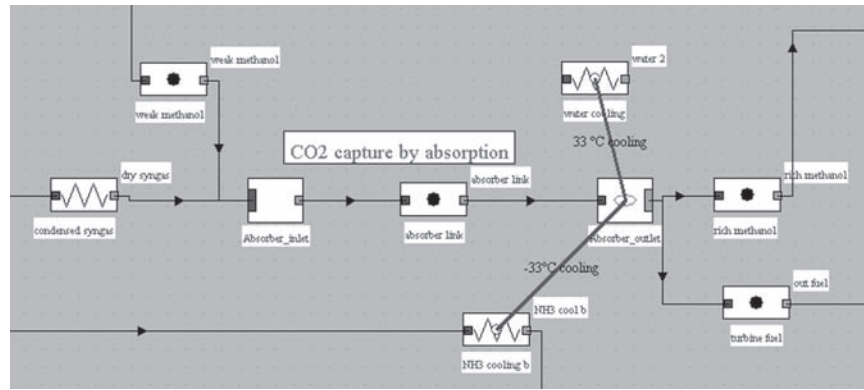
Based on the results obtained in ASPEN Plus, a number of simplifying assumptions were used: converted water and hydrogen are neglected, as well as the fraction of CO_2 contained in the methanol weak solution. In addition, the properties of methanol/ CO_2 mixture are considered equal to those of pure methanol. These points could be refined if necessary.

Under these conditions, treatment performed for one mole of CO_2 is given by equation (28.3.6):



If we call $x_{0\text{CO}_2}$ the initial molar fraction of CO_2 per mole of total gas to be treated, we get:

$$\varepsilon x_{0\text{CO}_2} \text{ of } \text{CO}_2 \text{ separated and } (1 - \varepsilon x_{0\text{CO}_2}) \text{ of fuel gas}$$

**FIGURE 28.3.15**Structure of CO₂ absorption model

In the fuel gas, mole fractions become:

$$x_{i \text{ out}} = \frac{x_{i \text{ in}}}{1 - \varepsilon x_{0\text{CO}_2}}$$

$$x_{\text{CO}_2 \text{ out}} = \frac{(1 - \varepsilon)x_{0\text{CO}_2}}{1 - \varepsilon x_{0\text{CO}_2}}$$

Molar mass of gas to be treated being M_{inlet} , total molar flow rate is: $\frac{\dot{m}}{M_{\text{inlet}}}$

The molar flow rate of separated CO₂ is: $\varepsilon x_{0\text{CO}_2} \frac{\dot{m}}{M_{\text{inlet}}}$

and its mass flow: $\varepsilon x_{0\text{CO}_2} \frac{\dot{m} M_{\text{CO}_2}}{M_{\text{inlet}}}$

Mass flow of fuel gas is then $\dot{m} \left(1 - \varepsilon x_{0\text{CO}_2} \frac{M_{\text{CO}_2}}{M_{\text{inlet}}} \right)$

Separated CO₂ is absorbed by methanol. In Thermoptim, the methanol/CO₂ mixture is modeled by class CO2Methanol.java. It is characterized by its mass fraction, ratio of CO₂ mass flow to total mass flow (methanol + CO₂), the CO₂ mass fraction being associated in the point screen to the usual quality x .

Moreover, with the solvent completely dehydrating the treated gas, water disappears from the residual fuel gas.

The absorption unit model has been developed as external classes. Since it uses several fluid veins (two input and two output), the solution adopted was to represent it by two external nodes whose computation is synchronized (Figure 28.3.15).

The input external mixer (MethanolAbsorInlet.java) role is to receive the composition and thermodynamic state of the dry synthesis gas and weak methanol. It initializes the calculation input parameters, which is carried out in the output external divider (MethanolAbsorOutlet.java) that initializes parameters needed, and then performs its calculations and updates the two output streams, which correspond to CO₂-enriched methanol and fuel gas for combustion turbine (Fig. 28.3.16).

process name	m abs	m rel	T (°C)	H
rich methanol	353.2344	353.2344	-12	650.58
turbine fuel	17.9876	17.9876	-26.78	-169.74

FIGURE 28.3.16

CO₂ absorption component screen

The model involves firstly compression work and secondly two thermocouplers (as shown in the diagram), one representing cooling at 33°C by simple utilities, and the other cooling at -30°C, requiring a refrigeration cycle.

Knowing the dry syngas flow rate (and thus CO₂ entering), and separation rate ϵ , the model determines the flow of weak methanol, and the flow and composition of fuel gas. The temperature of the fuel gas, thermocoupler loads and compression work are estimated from regressions calibrated on the ASPEN Plus model.

28.3.2.4 Regeneration of methanol

The methanol regeneration ThermoOptim model (MethanolRegen.java) is keyed to that established under Aspen Plus by C. Descamps.

The rich solvent is flashed in a first column, where some CO₂ is desorbed (Figure 28.3.17). The rest is directed to a regeneration column where heat input and low pressure allow the remaining CO₂ to desorb. A certain amount of solvent being carried with the gas at the column head, a separation device allows it to be retrieved. A pump is used to recompress the weak solvent.

Based on the results obtained in ASPEN Plus, a number of simplifying assumptions were made:

- only CO₂ absorbed is taken into account (water and hydrogen are neglected);
- regeneration is supposed complete (weak solution is pure methanol);
- the model characteristic parameter is as before ϵ , CO₂ separation rate in the absorber, which can be determined knowing the rich solution CO₂ mass fraction.

An external divider is used to represent this model: the main vein (rich solution flow) provides the parameters needed (CO₂ mass fraction, total flow), then it makes its calculations and updates the two output streams, corresponding to CO₂-depleted methanol and extracted CO₂.

As shown in the diagrams of Figures 28.3.13 and 28.3.14, the model involves firstly a weak solution compression work, and secondly two thermocouplers, one representing heat input at a temperature at least 10°C above the column bottom (reboiler) and the other cooling at -30°C.

CO₂ temperature, thermocoupler loads and compression work are estimated from regressions calibrated on the ASPEN Plus model.

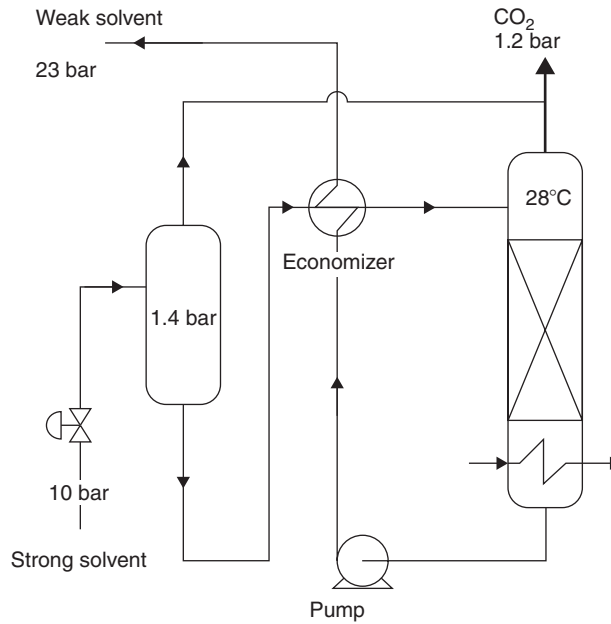


FIGURE 28.3.17
Regeneration of methanol

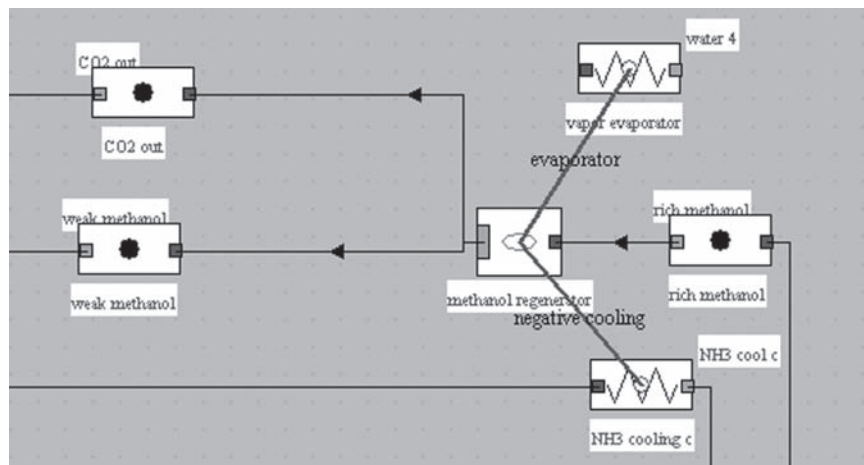


FIGURE 28.3.18
Methanol regeneration model structure

Figure 28.3.15 shows the global CO₂ capture model obtained by combining the three units as described above (condensation of gas converted, absorption, methanol regeneration).

28.3.2.5 Overall architecture, coupling with the rest of the IGCC

Once available the components representing CO conversion units, condensation of water contained in the converted gas after the shift reaction, CO₂ absorption and methanol regeneration, it becomes possible to test their integration and look at their thermal and mechanical energy requirements. It is also necessary to introduce a refrigeration cycle to extract the various thermal loads at -30°C .

The overall architecture without heat exchangers is given Figure 28.3.21. In pinch studies (please refer to Chapter 22 of Part 3 for an overview of the pinch method), it is often best to start by not

node: methanol regenerator type: external divider

main process: display m global: 353.23438527

rich methanol: h global: 229,805.46881979

iso-pressure T global: -12

process name	m abs	m rel	T (°C)	H
weak methanol	305.5052	305.5052	-24.15	622.35
CO2 out	47.7291	47.7291	-28.99	-43.89

Buttons: Duplicate, Suppress, Save, Close, Calculate, add a branch, delete a branch

methanol regenerator boiling heat

efficiency: 0.89 -30 °C methanol condenser

condenser load: -1092.91

boiler heat: 2173.40

compression power: 1663.49

CO2 temperature (°C): -28.84

FIGURE 28.3.19

Methanol regeneration component screen

taking into account the hot and cold utilities in order not to predetermine them: you can only size them when the other exchangers have been placed, and the internal regeneration maximized. By working this way, we obtain the composites of Figure 28.3.22, which show that the system is globally adiabatic, except for the cooling requirements for negative temperatures, which require the use of a refrigeration machine, shown in Figure 28.3.22 for the part corresponding to thermocouples for the absorption column and the regenerator.

For the rest, an exchange can be made between the dry syngas cooling at the absorption column inlet and the fuel gas heating at the outlet of this column, and possibly that of CO₂ at the regenerator outlet, but this exchange is not enough to completely cool the dry syngas.

The refrigeration cycle shown in Figure 28.3.21 is incomplete. If one uses CO₂ for partial cooling of the dry syngas, CO₂ compression work increases: a parametric study would be needed to find the best solution.

Importantly, if the system is globally adiabatic, the exchanger network is far from simple. This includes thoroughly checking that it can be built without too complex technological constraints.

The loss on LHV, which comes from the need to convert CO to CO₂ is about 14%.

Mechanical energy needed to compress CO₂ for the purposes of the absorption column and the regenerator, as well as for the refrigeration cycle, is close to 17.5 MW.

The overall loss on the cycle efficiency under these conditions is of the order of 18–20%.

28.3.3 Oxycombustion techniques

To conduct an oxyfuel combustion is to replace by pure oxygen the usual oxidizer, namely air, a mixture mainly of oxygen and nitrogen (respectively 21% and 78% by volume). Oxy-fuel technology allows at the same time to get fumes composed almost exclusively of water and carbon dioxide, and to drastically reduce emissions of nitrogen oxides. These are technologies already used in industry, including glass and steel.

The separation of CO₂ and H₂O is then easily done by simple water condensation, and the absence of nitrogen allows in addition NO_x emissions and the volume of smoke to be greatly reduced.

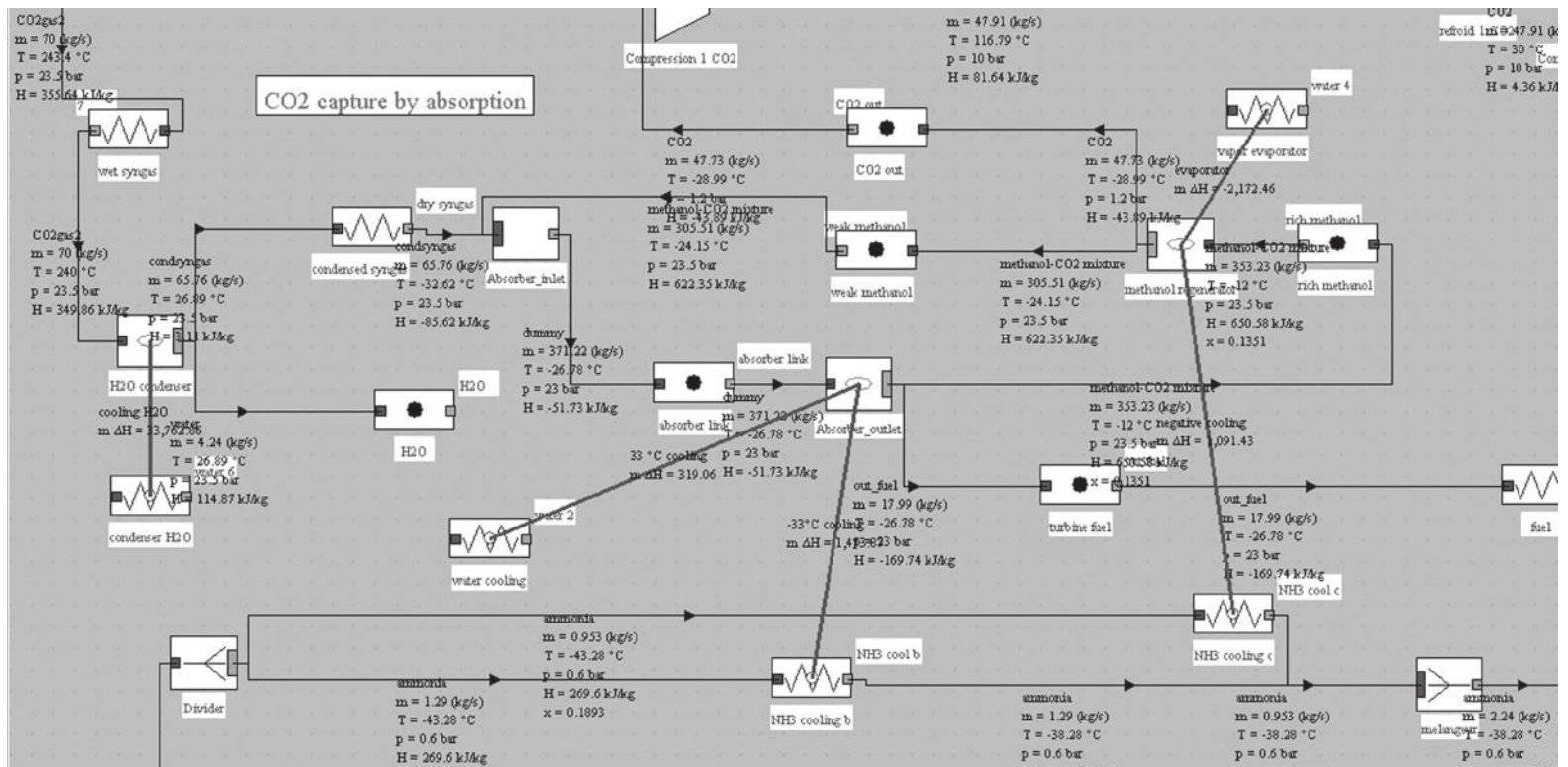


FIGURE 28.3.20
Coupling of the three units (converted gas condensation, absorption, methanol regeneration)

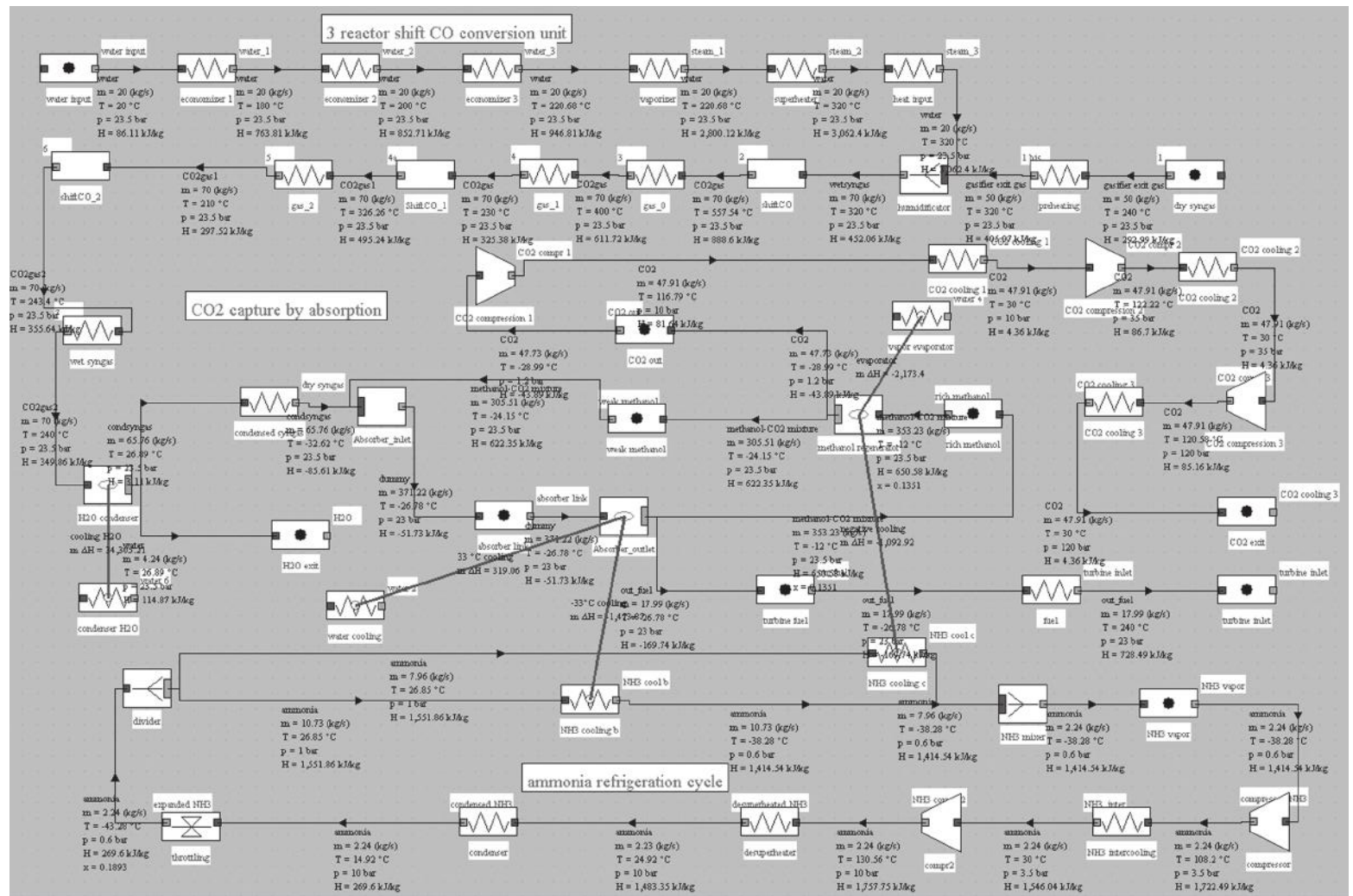


FIGURE 28.3.2I

Overall architecture without exchangers other than thermocouples

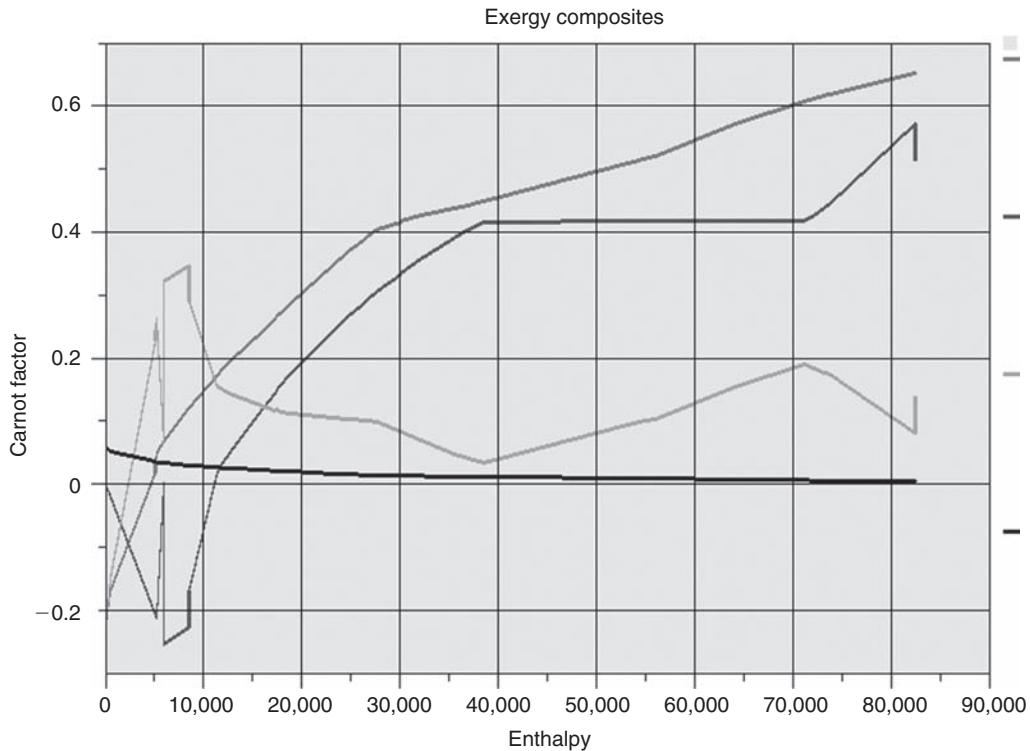


FIGURE 28.3.22

Composites of the overall architecture, without utilities

Despite these advantages, these technologies have so far hardly been used for electricity generation, given the difficulties and costs involved in the production of oxygen. Several technical solutions exist, but the more developed today, called the Air Separation Unit, is to separate oxygen and nitrogen from air by cryogenic operation both costly and energy consuming.

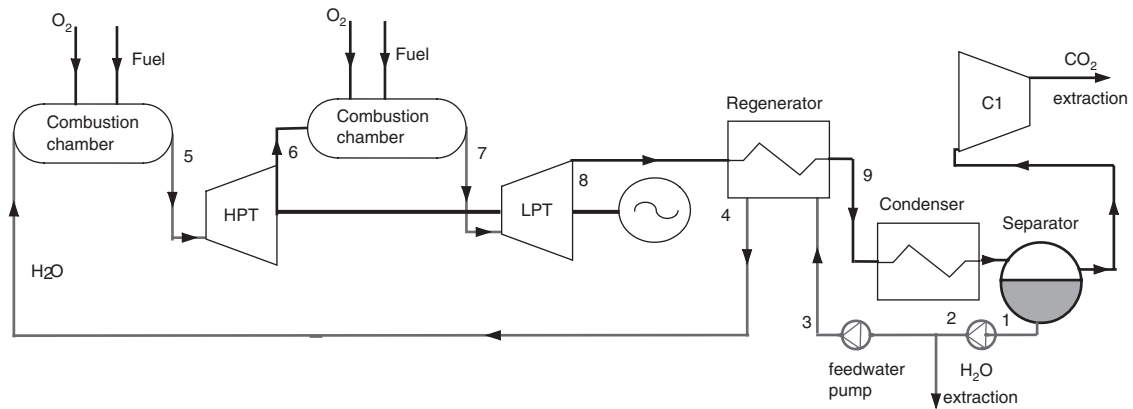
Four oxycombustion devices using this separation technique have been recently proposed: cycles called “Water Cycle”, Matiant, “Oxyfuel” and Graz. Their principle is to use as oxidizer a gas containing on the one hand oxygen, and secondly a mixture of CO₂ and H₂O in different proportions depending on the case. Under these conditions flue gas thermophysical properties are similar to those encountered in a gas turbine whose oxidizer is air, which allows the use of existing high performance expansion turbines without the need to make further technological developments.

The four cycles are distinguished by their configurations, close to regeneration GT for the first two, a combined cycle for the third and more original for the Graz one, whose gas and steam cycles are integrated directly rather than simply juxtaposed.

This process based on separation of the external air into oxygen and nitrogen is not the only one, and innovations are being considered in the form of internal separation cycles such as those based on use of:

- membranes permeable to oxygen (AZEP cycle);
- or transport of oxygen by chemical carrier by making, in the presence of air, a metal oxide which is then reduced before combustion (this is called Chemical Looping Combustion (CLC)).

All of these cycles but two (Water cycle, Matiant) involve both gas turbines and steam turbines. Their diagrams are given in the following sections, and two synoptic views in Figures 28.3.30 and 28.3.31, the other being available in the portal. Water extraction is modeled by class DehumidifyingCoil.java presented in section 23.5.2.


FIGURE 28.3.23

Water cycle

28.3.3.1 Water cycle

In this regeneration cycle (Figure 28.3.23), the oxidizer of the first combustion chamber is a mixture of O_2 and H_2O , and expansion is sequential with intermediate reheat.

At the condenser inlet (9), we get fumes containing O_2 and H_2O at a pressure of 0.1 bar. They are cooled by an external heat sink at a temperature low enough for almost all water to be condensed. The condensed water (1) is compressed at 4 bar (2), and the surplus to 125 kg/s is extracted from the cycle. At the separator outlet, the gas is composed mainly of extracted CO_2 .

Liquid water is compressed at 83 bar (3) before it enters the regenerator (actually a steam generator), which it exits in the state of saturated liquid at $300^\circ C$ (4).

Water is mixed with pure oxygen (about 33 kg/s), the mixture being used as oxidizer in a first combustion chamber (stoichiometric) whose fuel is methane, the end of combustion temperature being at about $900\text{--}1000^\circ C$ (5).

In modeling, one must be careful that it is impossible to mix oxygen with liquid water to form steam, because we do not have enough enthalpy in oxygen for the water vaporization. In reality, this energy is drawn from the available heat in the combustion chamber. We may either, as shown in Thermoptim diagram of Figure 28.3.30, build a thermocoupler between the combustion chamber and the “vaporizer” process or model the whole as a combustion process followed by an exchange process designed to vaporize the water before mixing with oxygen.

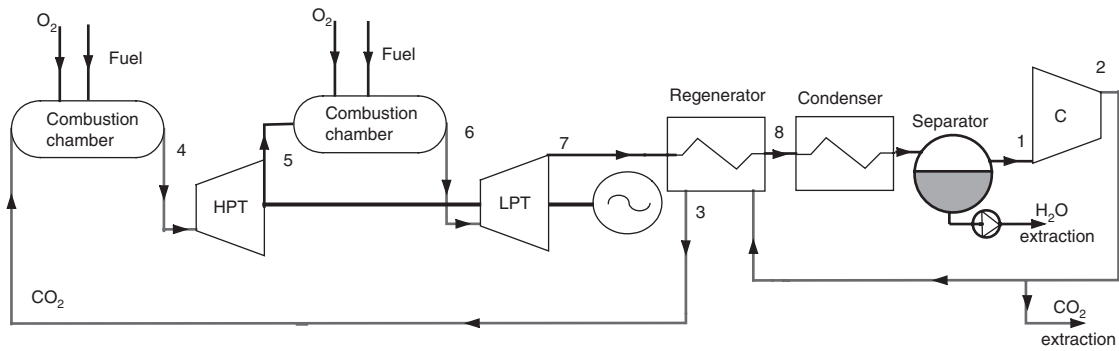
The burnt gases are expanded in a high pressure turbine at the pressure of 8.3 bar (6), then mixed with pure oxygen (about 25 kg/s). This mixture is then used as an oxidizer in a second combustion chamber, also stoichiometric, whose fuel is methane, the end of combustion temperature being 1200 to $1300^\circ C$ (7). The fumes are expanded in a low pressure turbine at the pressure of 0.1 bar (8), then cooled in the steam generator, thus closing the cycle.

The Thermoptim synoptic view of such a cycle is given in Figure 28.3.30. It leads to the following performance: capacity 437 MW, 59.5% gross efficiency.

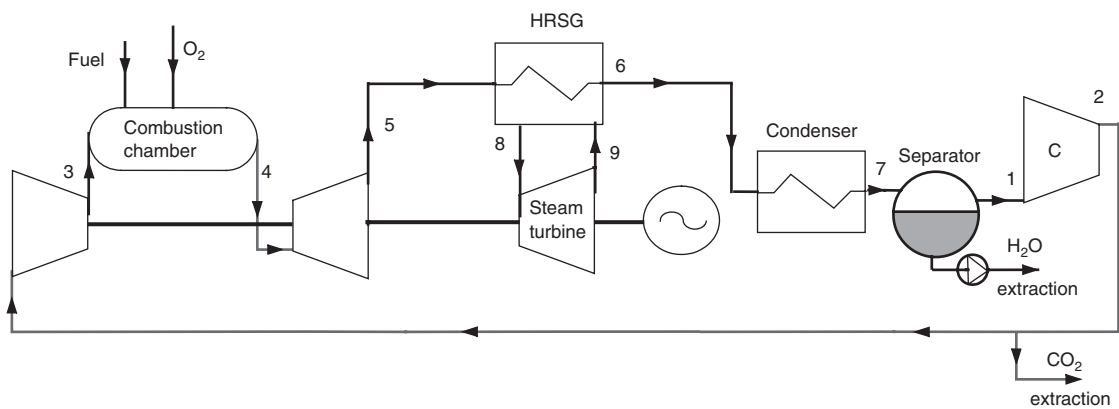
28.3.3.2 Matiant cycle

In this regeneration cycle (Figure 28.3.24), whose architecture is very similar to the previous one (Mathieu, Nihart, 1999), the oxidizer of the first combustion chamber is a mixture of O_2 and CO_2 , and expansion is sequential with intermediate reheat.

At point 1, a gas composed mainly of CO_2 , at a pressure we assume initially equal to 1 bar, is compressed at the pressure of 110 bar (2) in a four-stage compressor with intermediate cooling at $30^\circ C$.

**FIGURE 28.3.24**

Matiant cycle

**FIGURE 28.3.25**

Oxy-fuel cycle

A fraction of CO₂ is then extracted, the remaining flow, equal to 50 kg/s, being heated in a regenerator (3), before being mixed with pure oxygen (about 2.5 kg/s). This mixture is then used as an oxidizer in a first combustion whose fuel is methane, the temperature at the end of combustion being equal to 1300°C (4).

The burnt gases are expanded in a high pressure turbine at a pressure of 40 bar, then mixed with oxygen (about 5 kg/s). This mixture (5) is then used as an oxidizer in a second combustion chamber where the fuel is methane, the temperature at the end of combustion being equal to 1300°C (6). The fumes are expanded in a low pressure turbine at the pressure of 1 bar (point 7), then cooled in the regenerator to point 8.

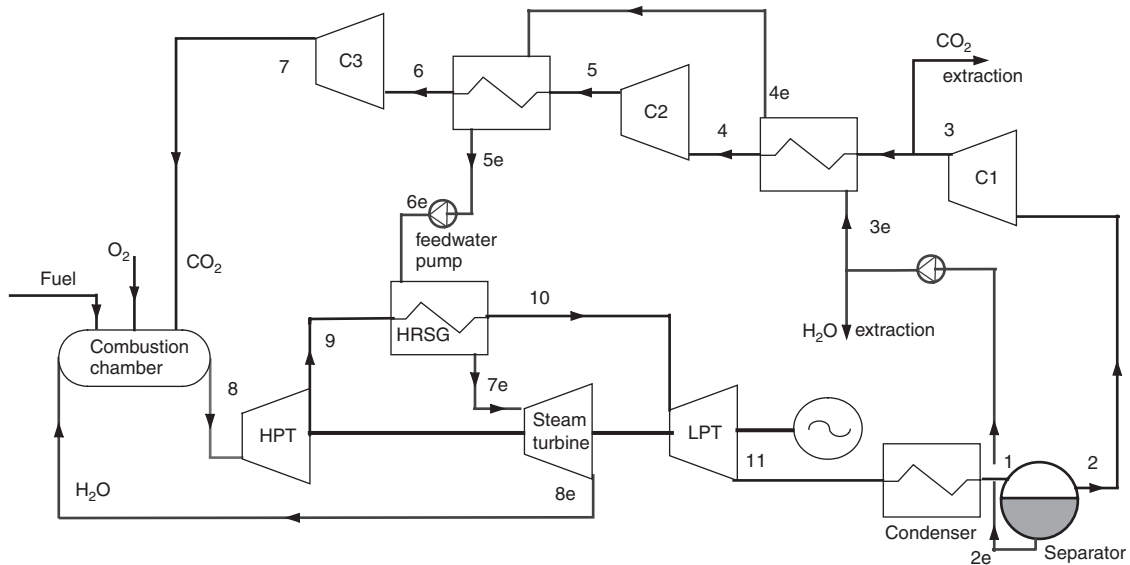
They are then cooled by an external heat sink at a temperature low enough for almost all water to be condensed. The condensed water is extracted from the cycle, while the residual gas enters the multi-stage compressor, closing the cycle.

The Thermoptim model of such a cycle leads to the following performance: 47.8 MW capacity, gross efficiency 56.5%.

28.3.3.3 Oxy-fuel cycle

In this combined cycle (Figure 28.3.25), the oxidizer is a mixture of O₂ and CO₂.

At the condenser inlet (6), we get fumes containing CO₂ and H₂O at a pressure of 1 bar. They are cooled by an external heat sink at a temperature low enough for almost all water to be condensed (7). The condensed water is extracted from the cycle.


FIGURE 28.3.26

Graz cycle

At the condenser outlet, a fraction of the gas composed mainly of CO_2 is extracted (2), the remaining flow, equal to 35 kg/s in this example being compressed at the pressure of 40 bar in a compressor (2–3) before being mixed with pure oxygen (about 4.4 kg/s). This mixture is then used as an oxidizer in a stoichiometric combustion chamber (3–4) whose fuel is methane, the temperature at the end of combustion being about 1350°C.

Fumes are expanded at 1 bar in a turbine (4–5), then cooled in a recovery steam generator (5–6) before entering the condenser, thus closing the cycle.

A steam cycle, working between pressures of 0.03 bar and 150 bar and 530°C, involving a water flow of 10 kg/s, is coupled to the previous cycle to form a combined cycle. In the diagram of Figure 28.3.25, a simplified steam cycle is represented as a HRSG and the turbine pump and condenser are not shown nor oxygen and fuel compressors.

The Thermoptim synoptic view of such a cycle is given in Figure 28.3.31. It leads to the following performance: 33.55 MW capacity, 60.7% gross efficiency.

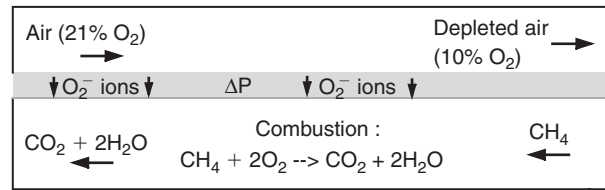
28.3.3.4 Graz cycle

In this cycle (Figure 28.3.26), the oxidizer is a mixture of O_2 , CO_2 and H_2O , the latter two gases being mixed in the combustion chamber inlet, and then separated after expansion, each following a particular sub-cycle (Heitmair & Jericha, 2003).

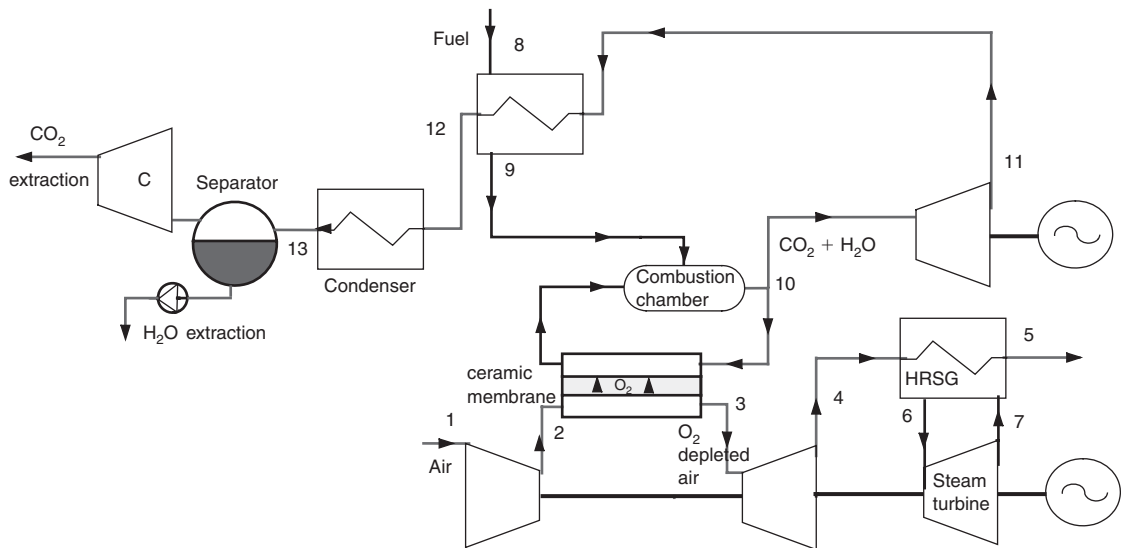
At the condenser inlet (11), we get fumes containing CO_2 and H_2O . They are cooled by an external heat sink at a temperature low enough for almost all water to be condensed. The condensed water is compressed at 12 bar (2e–3e), and the surplus to 110 kg/s is extracted from the cycle.

At the outlet of the separator (2), gas composed mainly of CO_2 at a pressure of 0.25 bar, is compressed (2–7) at the pressure of 40 bar in a three-stage compressor with intermediate cooling (C_1 , C_2 and C_3). A fraction of CO_2 is extracted from C_2 , the remaining flow being equal to 200 kg/s. The intermediate cooling is by exchange with liquid water, which is compressed at 180 bar (5e–6e) before it enters the recovery steam generator (HRSG on the diagram), which it exits superheated at 560°C (7e).

The gas at the outlet of C_3 (7) is mixed with pure oxygen (about 0.5 kg/s) and steam from turbine “Steam turbine”, the mixture being used as oxidizer in the combustion chamber (stoichiometric) whose fuel is methane, the end of combustion temperature being equal to 1328°C (8).

**FIGURE 28.3.27**

Schematic of the MIEC membrane

**FIGURE 28.3.28**

AZEP cycle

Burnt gases are expanded in a high pressure turbine (8–9) at the pressure of 1 bar and then cooled in the recovery steam generator (9–10). They are finally expanded in a low pressure turbine (10–11) at the pressure of 0.25 bar and then cooled in the condenser, thus closing the cycle.

The ThermoOptim model of such a cycle leads to the following performance: 396 MW capacity, 56.4% gross efficiency.

28.3.3.5 AZEP cycle

The AZEP cycle (Sundkvist) (Advanced Zero Emission Process) is a combined cycle involving internal separation of air through a membrane (Figures 28.3.27 and 28.3.28).

Air is sucked into the compressor of a modified gas turbine, where the combustion chamber is replaced by a chamber with two compartments separated by a ceramic membrane permeable to oxygen (Mixed Ionic-Electronic Conducting Membrane MIEC). In one of the chambers, air is depleted in oxygen because of the difference in oxygen partial pressures between the two media. In the other, this oxygen acts as oxidizer for combustion of fuel in the presence of an inert gas that is but a recirculation of exhaust gases, composed mainly of CO₂ and H₂O, plus inert gases if the fuel contains some.

At high temperatures (above 700°C), the ceramic membrane (Figure 28.3.27) is a mixed ionic and electronic conductor, through which pass simultaneously O₂⁻ ions and electrons, oxygen being adsorbed on the surface.

Depleted air is expanded in a turbine (3–4), then used as a heat source (4–5) for a steam cycle (see Figure 28.3.28, the pump and condenser not being shown in figure so as not to overload). The part

of the flue gas not recirculated is expanded in a turbine (10–11), then cooled (11–12) either to pre-heat the fuel (8–9) or as a hot source for the steam cycle, before being condensed for water extraction (12–13). Remaining CO₂ can then be captured. The part of flue gas that is recirculated is first cooled slightly by preheating air.

Much of the gas leaving the combustion chamber is recycled, in particular so that the average molar fraction of oxygen in the oxidizer is low enough that oxygen can pass through the membrane. Exchangers around the ceramic membrane have not been shown.

Although this is not the only possible solution, the steam generator can be split into two parts, one heated by the depleted air and the other by the flue gases.

WORKED EXAMPLE Modeling of an Advanced Zero Emission Power cycle

The project objective is to study one AZEP cycle of innovative power generation using oxy-combustion, and show how it can realistically be modeled with ThermoOptim. It is presented in the portal guidance pages (<http://www.thermoOptim.org/sections/enseignement/cours-en-ligne/fiches-guides-td-projets/fiche-sujet-fg7>).

This cycle uses classes MIEC_Inlet.java and MIEC.java modeling a ceramic membrane permeable to oxygen (Mixed Ionic-Electronic Conducting Membrane MIEC).

This work is the result of a collaboration between the CEP, Mines ParisTech (R. Gicquel) and the EPFL LENI (D. Favrat, F. Marechal).



[CRC_we_11]

The ThermoOptim model of such a cycle leads to the following performance: 403 MW capacity, gross efficiency 59%.

28.3.3.6 CLC cycle

The general principle of the CLC (Chemical Looping Combustion) cycle (J. Wolf, 2004) is close to the AZEP cycle: this is still a combined cycle, but air separation is accomplished through a chemical reaction allowing oxygen to be preferentially attached (Figure 28.3.29).

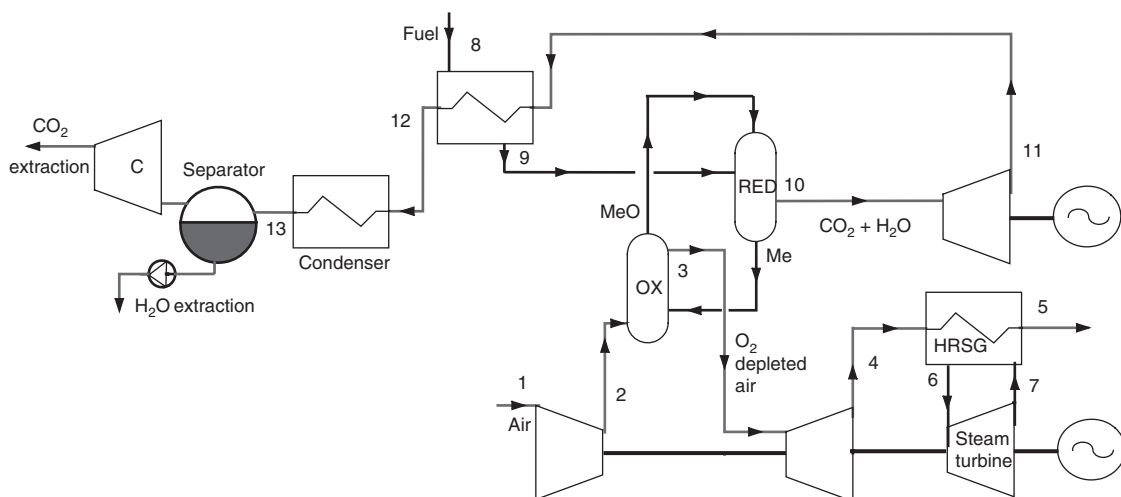


FIGURE 28.3.29

CLC cycle

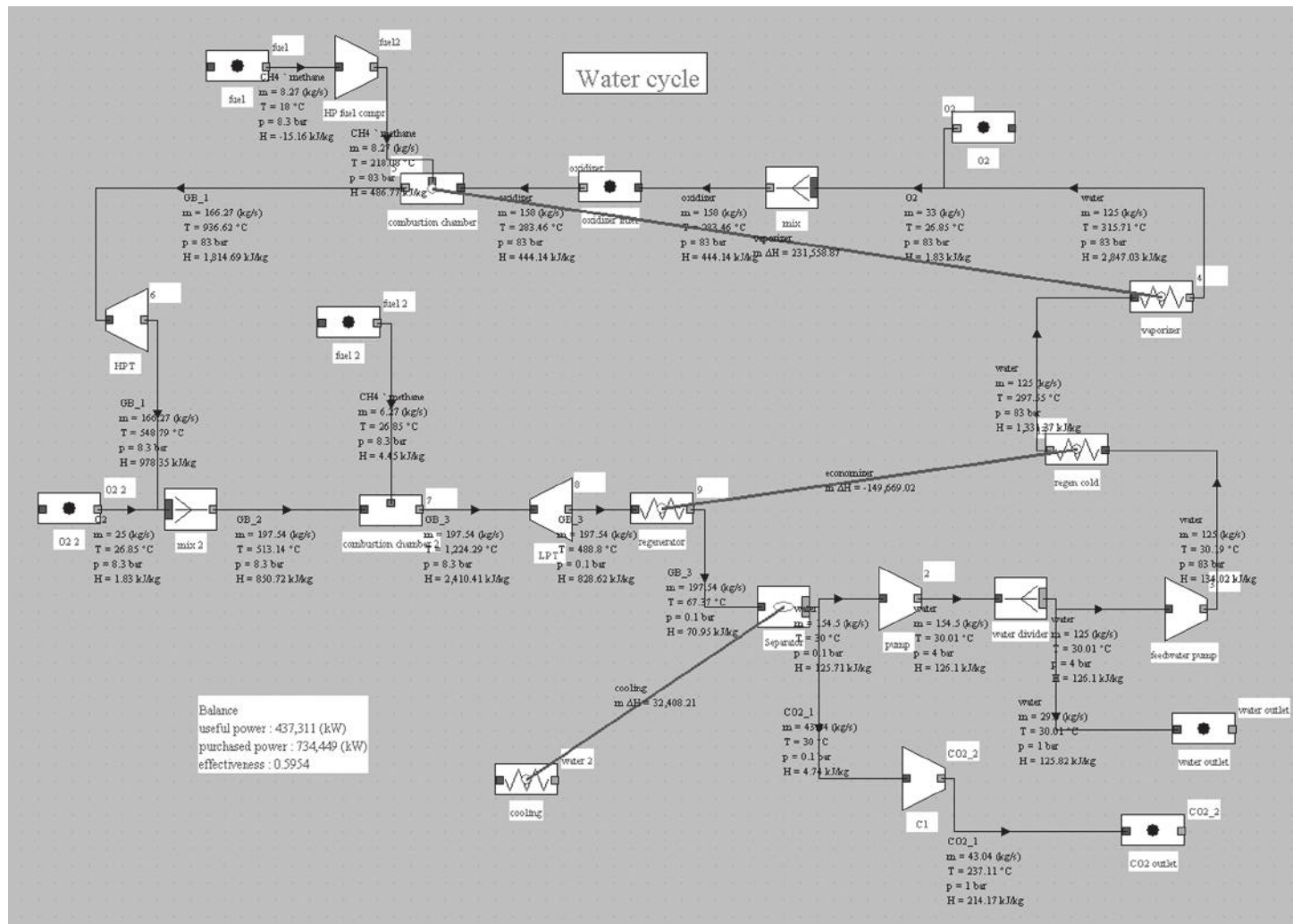


FIGURE 28.3.30
 Synoptic view of the WaterCycle

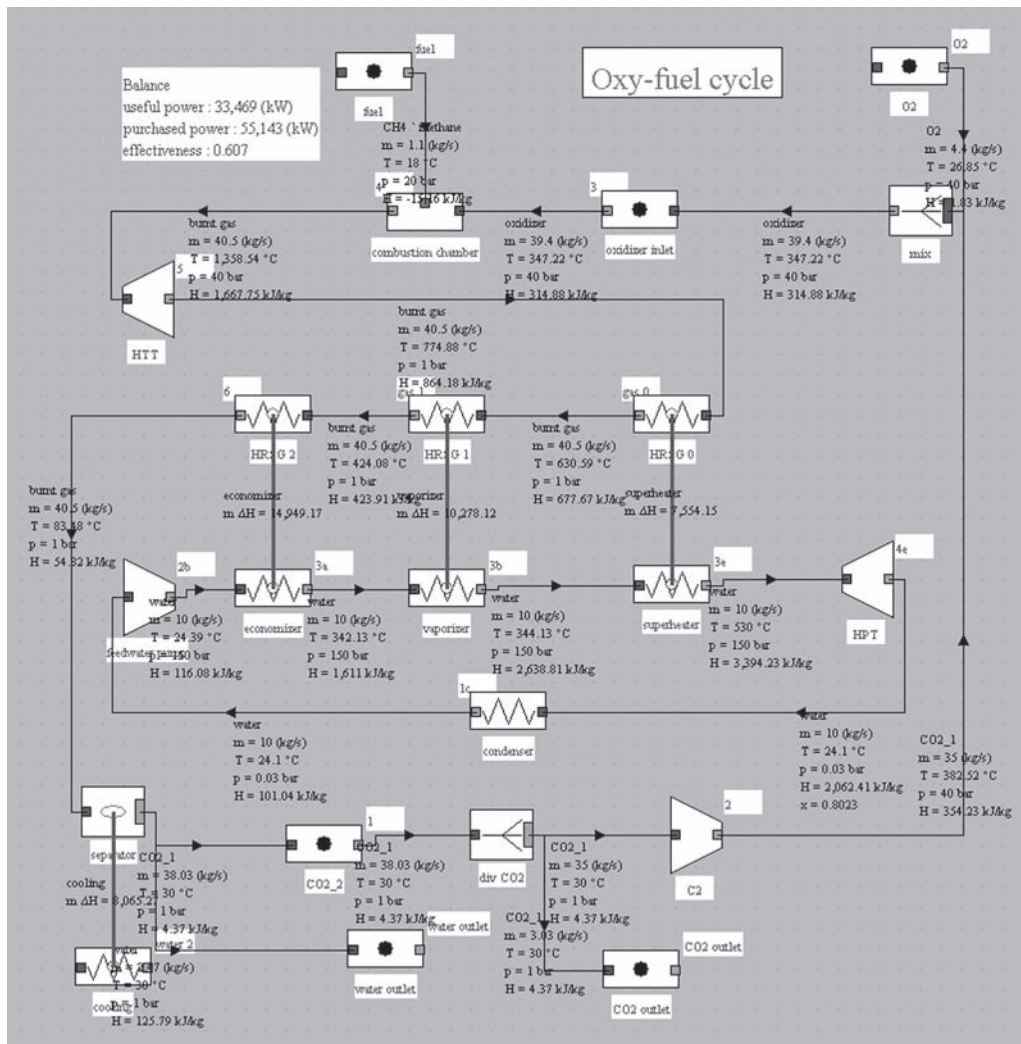


FIGURE 28.3.31
Synoptic view of the Oxyfuel cycle

Air (about 50 kg/s) is compressed (1–2) between 15 and 20 bar by the compressor of a modified gas turbine, whose combustion chamber is replaced by a chamber with two compartments between which circulates a metal oxide such as NiO, thanks to a circulating fluidized bed. In one of the chambers, air is depleted in oxygen (2–3) due to oxidation of the metal. In the other, the oxide is reduced and the oxygen released burns with a fuel (9–10).

The depleted air (mole fraction of oxygen of about 0.14) is expanded in a turbine (3–4), then used as a heat source (4–5) for a steam cycle (6–7). The exhaust gases are also expanded in a turbine (10–11) and then used as heat source (11–12) on the one hand to preheat the fuel (8–9), and on the other hand (not shown in figure so as not to overload it) as hot source for the steam cycle, before being condensed for water extraction. The remaining CO₂ can then be captured.

Although this is not the only possible solution, the steam generator can be divided into two parts, one heated by the depleted air and the other by the flue gases with a reheat.

The Thermoptim model of such a cycle using classes CLCReactorInlet.java and CLCReactor.java leads to the following performance: 378 MW capacity, gross efficiency 53.28%.

TABLE 28.3.1

(Capacities in kW)	OxyFuel	Water cycle	Graz	Matiant
Gross capacity	33,469	437,311	395,819	47,800
Purchased capacity	55,143	734,449	701,815	84,363
Gross efficiency	60.7%	59.54%	56.40%	56.66%
O ₂ flow-rate	4.4	58	56.1	7.5
O ₂ power	5,874	77,430	74,894	10,013
Net capacity	27,595	359,881	320,926	37,788
Net efficiency	50.04%	49%	45.73%	44.79%
Efficiency reduction	10.65%	10.54%	10.67%	11.87%

28.3.3.7 Estimate of oxygen separation work

Many oxyfuel cycles require oxygen as oxidizer. As mentioned, the excellent performance of these cycles has to be tempered by the “cost” of separating oxygen from air.

To estimate this cost, we will make the simplifying assumption that the power required to produce oxygen is equal to that required to condense the gas, which is calculated as the theoretical power corresponding to the condensation of the flow of pure substance, divided by a carefully chosen exergy efficiency. This method is of course debatable, but it is much closer to reality than the consideration of the minimum separation power alone, which is simply equal to exergy lost during the mixing of air constituents.

We proceed on the basis of a rate of 1 kg/s of oxygen. To separate the air, we must operate in three phases:

- we begin by cooling it to the boiling point of oxygen at atmospheric pressure, 85 K;
- oxygen is condensed and separated from nitrogen;
- oxygen and nitrogen are separately heated to room temperature.

For simplicity, we can assume that the thermal power required to cool air is almost equal to that corresponding to heat separated gases, so we can perform internal regeneration between these two gas streams. The only power input is then that corresponding to the condensation of oxygen, i.e. 211 kW.

If this thermal power was produced in a perfect reverse Carnot engine, its efficiency would be equal to $85/(300 - 85) = 0.395$. The mechanical power of a perfect machine allowing 1 kg/s of oxygen at 85 K to condense is then equal to $211/0.395 = 534$ kW.

The various examples of refrigeration machines discussed in Chapter 19 of Part 3 have exergy efficiencies between 25 and 42%. We use here an exergy efficiency value of 40% for our simplified air separation unit. Under these conditions, the power required to separate 1 kg/s of oxygen is equal to $534/0.4 = 1,335$ kW, or a work of 1,335 kJ/kg of O₂.

This estimate allows us to correct performance of the cycles we studied previously to determine their net capacities and efficiencies, given in Table 28.3.1. The reduction in efficiency is from 10.5 to about 12 points.

REFERENCES

- O. Bolland, H. M. Kvamsdal, J. C. Boden, *A thermodynamic comparison of the oxy-fuel power cycles water-cycle, graz-cycle and matiant-cycle*, Power generation and sustainable development (Liège, 8–9 October 2001), pp. 293–298.

- L.I. Eide, M. Anheden, A. Lyngfelt, C. Abanades, M. Younes, D. Clodic, A.A. Bill, P.H.M. Feron, A. Rojey and F. Giroudière, *Novel Capture Processes*, Oil & Gas Science and Technology – Rev. IFP, Vol. 60 (2005), No. 3, pp. 497–508.
- H. M. Kvamsdal, O. Maurstad, K. Jordal, and O. Bolland, *Benchmarking of gas-turbine cycles with CO₂ capture*, GHGT-7, Vancouver, 2004.
- F. Heitmeir, H. Jericha, *Graz cycle – An optimized power plant concept for CO₂ retention*, First International Conference on Industrial Gas Turbine Technologies, Brussels – 10/11 July 2003
- P. Mathieu, R. Nihart, *Zero-emission MATIANT cycle*, International Gas Turbine and Aeroengine Congress and Exhibition, Stockholm, Sweden, 1999, vol. 121, No. 1, pp. 116–120.
- J. Wolf, *CO₂ Mitigation in Advanced Power Cycles – Chemical Looping Combustion and Steam-Based Gasification*, Doctoral Thesis 2004, KTH – Royal Institute of Technology, Department of Chemical Engineering and Technology Energy Processes, SE-100 44 Stockholm, Sweden.
- S. G. Sundkvist, Å. Klang, M. Sjödin, K. Wilhelmsen, K. Åsen, A. Tintinelli, S. Mccahey, H. Ye, *AZEP, gas turbine combined cycle power plants – thermal optimisation and lca analysis*, [Online] Available from: <http://uregina.ca/ghgt7/PDF/papers/peer/079.pdf>
- IPCC Special Report on Carbon dioxide Capture and Storage, Summary for Policymakers, A Special Report of Working Group III of the Intergovernmental Panel on Climate Change, [Online] Available from: http://www.ipcc.ch/pdf/special-reports/srccs/srccs_summaryforpolicymakers.pdf

Future Nuclear Reactors

Abstract: It is customary to consider that the evolution of nuclear reactors took place in several generations. The first, called Generation I, saw in France the development of natural uranium graphite gas systems (GCR), with completion of 9 reactors, with efficiency close to 29%. From 1969 it was replaced by Generation II, corresponding to Pressurized Water Reactor (PWRs), of better efficiency (33%) developed under US Westinghouse license, which we discussed in detail in section 16.3 of Part 3. Generation III is a simple evolution of the previous, with some improvements in terms of efficiency (35%), but especially an even safer design. New reactors in progress (European Pressurized Reactor EPR) belong to this generation. Generation IV reactors currently under investigation share a common feature compared to pressurized water reactors (PWR): a significant increase of the cooling fluid maximum temperature.

Given the subject of this book, which concerns mainly the study of thermodynamic cycles, we begin by presenting the reactors coupled to Hirn or Rankine cycles, then we address those involving gas Brayton cycles.

In this chapter we expand our previous analyses of thermodynamic nuclear energy conversion by presenting the main types of cycles that are considered to be used in future nuclear reactors.

Keywords: fast neutrons, thermal neutrons, supercritical water, lead cooled, sodium cooled, molten salt reactors, pebble bed, combined cycle, cogeneration, HTR, VHTR, GFR, SFR, LFR, MSR, SCWR, PBMR, GT-MHR,

29.1 INTRODUCTION

Although PWR technology is today the most developed on the industrial side, future nuclear reactor projects mainly concern other systems, and correspond to concepts already studied in the years 1960–1970, often abandoned because of development difficulties or disappointing economic performance.

The aim is twofold: first to overcome technological obstacles encountered at that time, and secondly to achieve viable economic and technical performance, with better adaptation to sustainable development criteria.

For this, a number of qualitative leaps are to be made:

- The first is security: it is to develop inherently safe reactors, i.e. for which there is no possibility of core fusion due to chain reaction and loss of control;

- Second, these reactors should not produce highly active and long term radioactive waste or produce only a limited amount relative to reactors currently in operation, so as to reduce or eliminate the end of cycle problems. An alternative would be the development of reactors burning waste from other systems;
- The third qualitative leap concerns size and modularity: the capacity of new reactors should be about a hundred MWe to be adaptable to all types of networks. Note however that this target is not new but has been postponed, economies of scale favoring high capacities;
- Fourth, the innovative reactors should be versatile and lend themselves to different applications, such as cogeneration of electricity and heat at medium or high temperature, desalination of seawater or production of hydrogen from water;
- Finally, higher efficiencies, including conversion of nuclear fuel, is a prime criterion, both to save on cost per kWh, but also to improve all ratios (waste/kWh, water consumption/kWh etc.): we should be able to produce 50 times more electricity with the same amount of uranium etc.

Since the early 1990s, different types of projects have emerged, taking into account to varying degrees the objectives outlined above. Among these projects, we will describe on the one hand, those for high temperature gas-cooled reactors, entitled PBMR (Pebble Bed Modular Reactor) and GT-MHR (Gas Turbine Modular Helium-cooled Reactor), and secondly those put up from 2001 following the initiative of the United States Department of Energy (DOE), called *Generation IV Nuclear Energy Systems Initiative*, which has managed to unite around it a group of nuclear research organizations from 10 countries in a loose cooperation called the GIF (*Generation IV International Forum*). It is to study systems that could be the fourth generation of reactors, after those in use or planned in the short term (EPR), and deployable by 2030.

The notion of generations of reactors has been introduced to distinguish the main developments that marked the history of civilian nuclear reactors:

- first generation corresponds to the first prototypes built mainly in the U.S. until the late 50s. It saw in France the development of natural uranium graphite gas systems (GCR), with completion of 9 reactors, efficiency close to 29%;
- second generation, from 1960 to 1995, marks the first phase of commercialization of nuclear power plants, with three main systems: light water reactors (BWR Boiling Water Reactors), pressurized water reactors (PWR, efficiency about 33%), and heavy water (in Canada). Most operational plants are currently second generation;
- third generation has the main objective to increase plant safety, accidents at Three Mile Island in the United States, Chernobyl in the USSR and Fukushima in Japan having shown the major risks associated with certain units of second generation. The EPR (European Pressurized Reactor) reactor is a third generation. Its performance is slightly higher: 35%;
- it is increased efficiencies which primarily justifies the value of the work on the fourth generation reactors, including the great innovation which is to design the reactor with the cycle that goes with it and optimize the whole, which allows sustainability issues to be properly handled.

After studying in detail a hundred reactor types, the GIF has selected in September 2002 six concepts on which efforts of its members will focus:

- supercritical water reactors (SCWR);
- very high temperature reactors (HTR and VHTR);
- gas cooled fast neutron reactors (GFR);
- sodium cooled fast neutron reactors (SFR);
- lead cooled fast neutron reactors (LFR);
- molten salt reactors (MSR).

Among these six options, a major interest is given to gas-cooled systems.

Let us recall that there are two main categories of reactors, depending on the neutron energy put into play: fast neutron reactors and slow neutron reactors.

- we call “fast neutrons” neutrons produced by fission reactions before they are slowed by a large number of shocks. Their energy is about 0.1 MeV to 2 or 3 MeV. These neutrons are able to split, thus destroying not only nuclei known to be fissile but also actinides, which are nuclei heavier than uranium accumulating in the reactor fuel. If you wish to burn effectively this radioactive waste, fast neutrons are required. We say that fast reactors operate as breeders, which means they produce more plutonium-239 fuel than they consume: fuel becomes inexhaustible;
- we call “slow neutrons” or “thermal neutrons” neutrons slowed by a large number of shocks, usually in a medium called a moderator. Their energy is of the order of one electron volt or a fraction of electron volt, i.e. 6 orders of magnitude smaller than that of fast neutrons. They can only split a small number of nuclei: uranium 235 (the only one existing in nature), plutonium 239 and uranium-233 produced in the reactors. Such reactors are almost all the existing fleet.

Let us specify, in addition to what has been said, that we call “epithermal neutrons” neutrons with an energy intermediate between the two previous modes. This type of spectrum occurs in the molten salt reactors which will be discussed in section 29.3.6.

29.2 REACTORS COUPLED TO HIRN CYCLES

29.2.1 Sodium cooled fast neutron reactors

Two variants of sodium cooled fast neutron reactors are considered, differing according to capacity (150–500 MWe for one, 500–1500 MWe for the other) and fuel. In both cases, a primary cooling loop is provided, the working fluid differing from the coolant. The core outlet temperature is about 550°C.

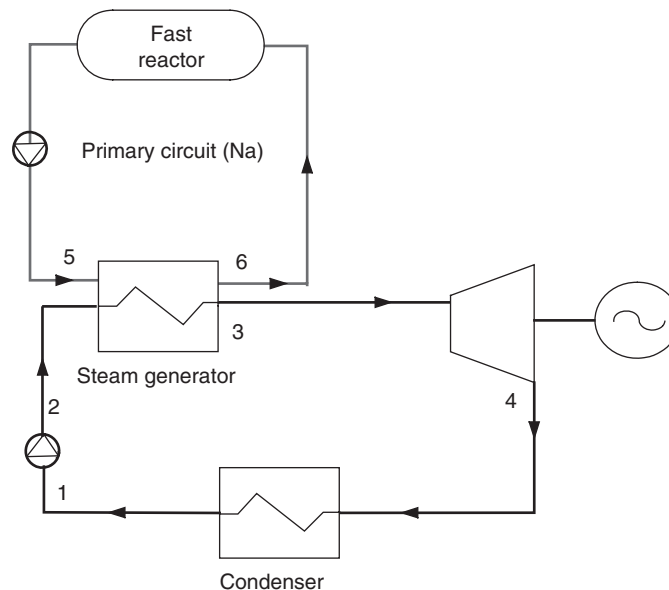
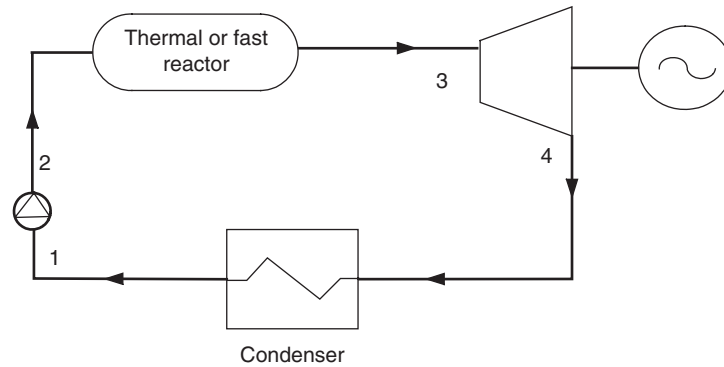


FIGURE 29.2.1

Sodium cooled fast neutron reactor

**FIGURE 29.2.2**

Supercritical water reactor

These reactors are designed to valorize high-level waste, particularly plutonium and other actinides, but they can also use fissile and fertile fuel, with a much higher efficiency than PWRs (see section 16.3 of Part 3).

29.2.2 Supercritical water reactors

The principle of supercritical cycles has been exposed in section 16.1.6 of Part 3. The cycle used by the GIF reaches an efficiency of 45%, with a turbine inlet temperature from 510 to 550°C and a pressure of 250 bar. Two versions of the reactor are considered, one for thermal neutrons, and one for fast neutrons.

While in PWRs and sodium-cooled fast neutron reactors, it is necessary to provide a primary cooling circuit mainly due to the steam change of state, it could be deleted in this type of supercritical cycle, the working fluid being also the reactor coolant, which would significantly simplify the system (Figure 29.2.2).

The reference capacity of such a reactor would be 1,700 MWe. Note that opinions on the actual feasibility of such a reactor are fairly mixed.

Figure 29.2.3 shows the synoptic view of a supercritical cycle with two reheats at 550°C, maximum pressure 280 bar. Its efficiency is about 44%.

29.3 REACTORS COUPLED TO BRAYTON CYCLES

High-temperature reactors that were studied in the years 1960–1970, including Germany and the United States, had the following characteristics:

- fuel was packaged in the form of nuclei of oxide or carbide of uranium, plutonium or thorium, coated with pyrolytic carbon and silicon carbide supposed to prevent fission products from escaping from fuel spheres;
- helium was considered as gas coolant in order to reach temperatures of around 800°C for a high thermodynamic efficiency of 40%;
- reactors were generally of the slow neutron type with graphite as moderator.

One of the advantages of these reactors is to significantly exceed temperature levels to which those using water are limited, which allows high conversion efficiencies to be considered.

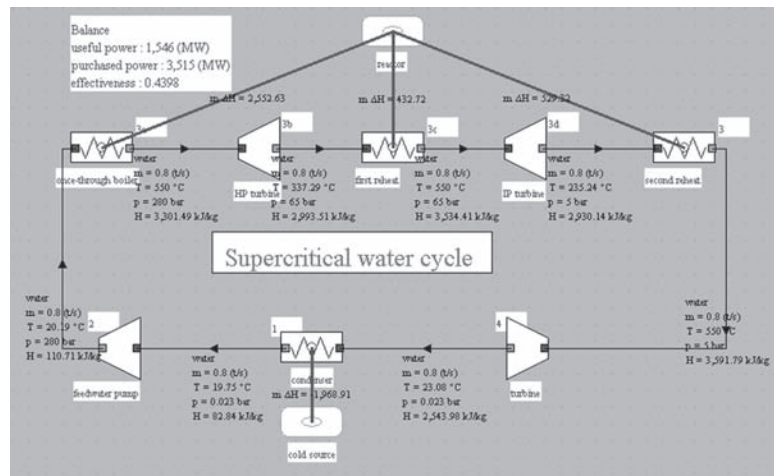


FIGURE 29.2.3

Synoptic view of a supercritical water cycle

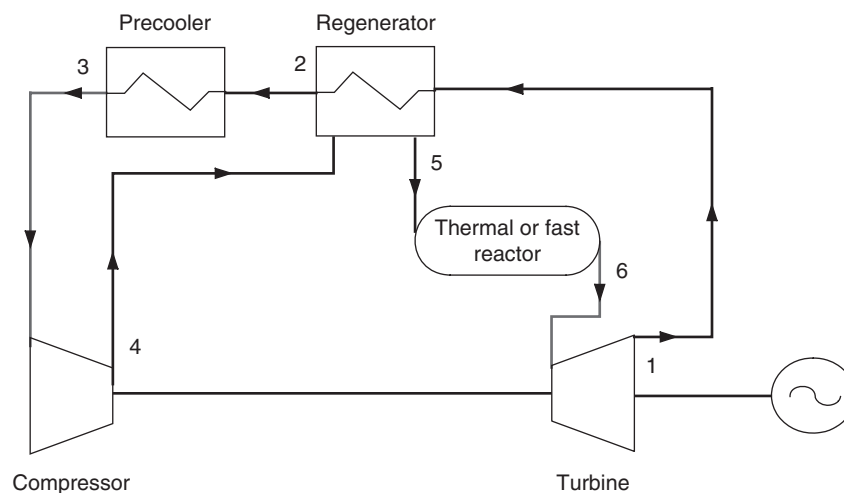


FIGURE 29.3.1

Gas-cooled reactor

Their design concept is shown in Figure 29.3.1, in case the reactor cooling is provided by the working fluid.

29.3.1 Small capacity modular reactor PBMR

PBMR (Pebble Bed Modular Reactor, Figure 29.3.2) reactors are high temperature thermal neutron reactors with an output of 100MW using pebbles of weakly enriched uranium fuel embedded in carbon (which plays the role of moderator) and using helium as coolant.

In the example shown in Figure 29.3.3, a rate of 140 kg/s of helium is compressed to 70 bar (1), enters a regenerator, which it exits at 514°C (2) before cooling the reactor core which it exits at 900°C (3) and at 67.4 bar. This flow is expanded in a HP turbine (3–4) used to drive the HP compressor, before entering a second IP turbine (4–5), equilibrated with the LP compressor.

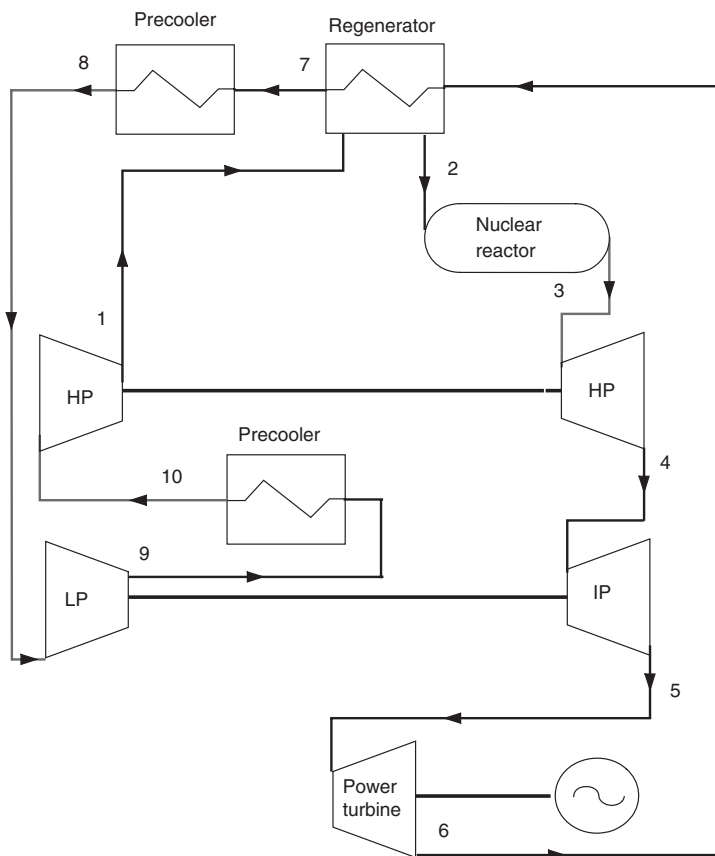


FIGURE 29.3.2
PBMR reactor

Helium is then expanded at 26 bar and 559°C in the LP turbine (5–6), which produces useful power. The cycle is closed by two step helium cooling (regeneration (6–7) and then cooling at about 28°C (7–8)), followed by a two-stage compression (8–9) and (9–1) with intermediate cooling (9–10). In this example, turbomachinery polytropic efficiency and regenerator effectiveness are assumed equal to 0.9.

PBMR cycles theoretically have an excellent efficiency, close to 48%, as shown in Figure 29.3.3. However, their industrial production is hampered by various technological difficulties, particularly in terms of on-site review of the fuel, which means that real efficiencies are actually much lower.

In addition, there is currently no high efficiency helium turbomachinery. Launched in South Africa in the early 1990s this concept was abandoned in 2002.

29.3.2 GT-MHR reactors

Studied by an international consortium led by General Atomics (USA), GT-MHR (*Gas Turbine Modular Helium cooled Reactor*) reactor is a modular thermal neutron reactor (300 MW units), helium-cooled, high-temperature, which can use various fuels (plutonium or enriched natural uranium, thorium) packed in silicon carbide beads. Differences between GT-MHR and PBMR are numerous, although they are both high-temperature helium cooled reactors.

The GT-MHR capacity is 300 MW, a compromise between the requirement of intrinsic safety, which involves reduced capacity, and economic competitiveness which requires economies of scale.

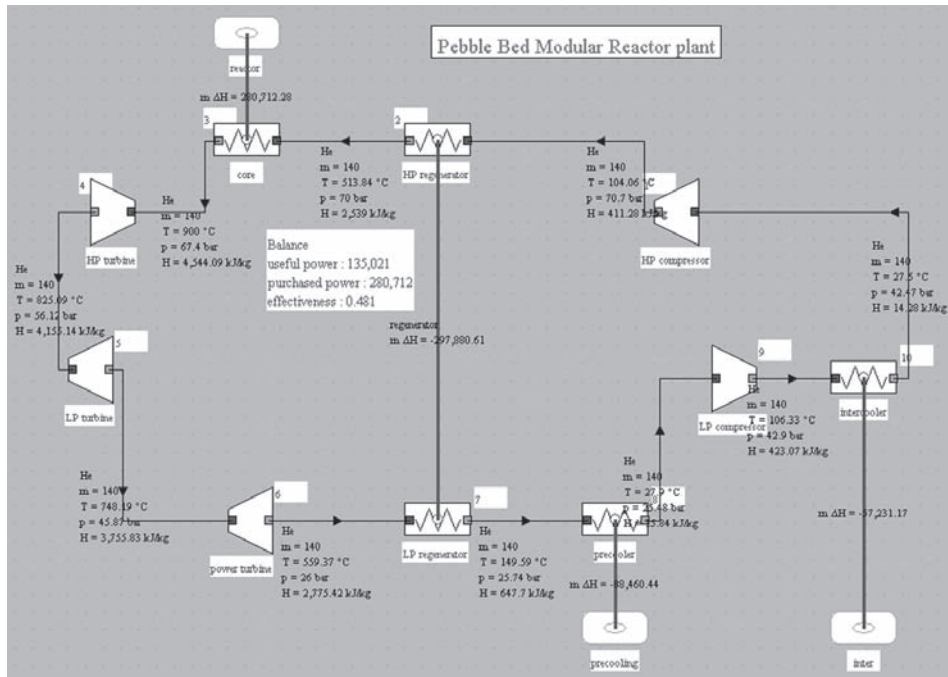


FIGURE 29.3.3

Small capacity PBMR modular reactor

As fuel, GT-MHR uses the same principle as PBMR, beads coated with millimeter fuel refractory beads by TRISO process. However, instead of being agglomerated in the form of pebbles, the balls are in the form of small cylinders of a few centimeters in height, the cylinders themselves being formed into fuel elements in graphite prismatic shape. This method allows a better knowledge of the location of the fuel and yields a higher unit power than for the PBMR. It also reduces by a factor of 5 to 10 the pressure drop in the reactor.

To control the chain reaction, the GT-MHR has control rods which may be supplemented by an injection system by gravity of boron particles. Moreover, in case of damage on these two active systems, designers made sure that the reactor can cool itself through a heat transfer by conduction to the tank walls, themselves water circulated. Finally, the concrete structure is supposed to absorb heat and transmit it by conduction in the surrounding basement, the reactor being buried. The GT-MHR developers ensure that fuel temperature remains below 1,600°C temperature limit for stability of materials used for making millimeter beads, including in case of reactor depressurization. GT-MHR is supposed to achieve a thermal efficiency of 48%. The refueling outages are scheduled every 18 months, with replacement of half the fuel elements.

29.3.3 Very high temperature reactors

Very high temperature reactor VHTR is in line with modular reactors type GT-MHR (thermal neutrons). It is distinguished by a much higher temperature, since the temperature of the coolant gas is expected to reach 1,000 to 1,100°C.

VHTR reactor fuel is designed along the same lines as that of high temperature reactors, with a package in the form of millimeter beads agglomerated as cylinders inserted in fuel elements. VHTR should use helium as coolant, the temperature of gases leaving the reactor vessel reaching 1000°C. A VHTR priority is that it can burn its fuel with a much higher efficiency than current reactors.

With high thermodynamic efficiency, VHTR would have a unit capacity of 600 MWe. VHTR was originally intended to burn essentially a mixture of highly enriched uranium and thorium. The objective today is explicitly that this reactor can not only burn low-enriched uranium, but also incinerate plutonium and plutonium mixed with some minor actinides. Contested by some experts, this capability would allow a resumption of PWR waste.

The goal of the proponents of very high temperature reactors is not only to cover the needs of power generation, but also to advance the technology of refractories, which will be useful for the development of other systems and finally to open new markets for nuclear power. For electricity production, efficiencies achieved with as high operating temperatures would be above 50%, which is significantly higher than those of existing PWRs (33%), which should lead to competitive production costs.

However, to successfully make them work, many technological problems must be solved, particularly the development of materials capable of withstanding very high temperatures. The know-how for the development of high temperature reactors would then be useful to that of gas-cooled fast reactor GFR.

New markets opened by VHTR should be multiple. Many industrial processes are indeed performed at high temperature: production of cement, glass, steel, coal gasification and thermochemistry.

However, given the inertia of industrial processes and hopes for developing alternative fuels for transportation, the main VHTR application would be hydrogen production.

29.3.4 Gas cooled fast neutron reactors

Gas cooled fast neutron reactors are somehow variants of GT-MHR or VHTR, where the thermal neutron core is replaced by a fast neutron core. The reference capacity is 288 MWe, with a turbine inlet temperature of 850°C. The cooling gas is typically helium, and, as we shall see in section 29.3.7 many thermodynamic cycles are possible, from direct cycles where helium that cools the core is directly expanded in the turbine, which avoids the intermediate heat exchanger IHX and improves performance up to combined cycles, through innovative cycles type supercritical CO₂.

29.3.5 Lead cooled fast reactors

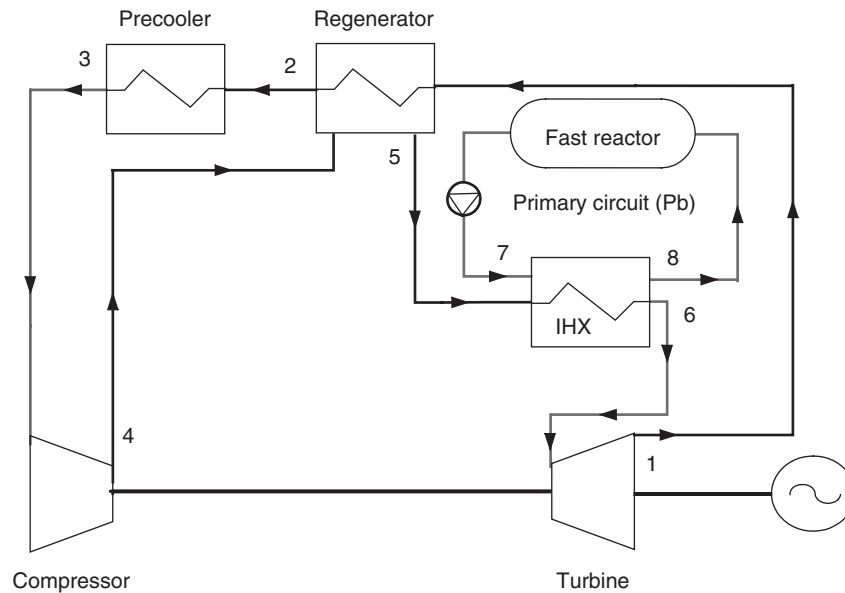
Fast neutron reactors cooled by lead (or lead-bismuth eutectic) are variations from Russian submarine reactors (Figure 29.3.4). Their reference capacity is thus low, between 120 and 400 MWe, and the tank outlet temperature is between 550 and 800°C, allowing us to consider a gas thermodynamic cycle (e.g. He or CO₂).

29.3.6 Molten salt reactors

Although regarded as potentially very attractive in the long term, molten salt epithermal neutron reactors are not currently a priority for the GIF.

One of their characteristics is to have a homogeneous core and a fuel flow in the cooling circuit, fuel acting also as thermal fluid. If corrosion problems are solved one day, their value is to minimize radioactive waste and mitigate proliferation risks. They are indeed characterized by the possibility of an online processing of spent fuel, with a small chemical unit, which processes all the salt every ten days.

The proposed reference capacity is 1,000 MWe, with a core outlet temperature between 700 and 800°C, allowing use of high temperature gas thermodynamic cycles. Their diagram is similar to

**FIGURE 29.3.4**

Lead cooled fast reactor

Figure 29.3.4, with a two-stage primary circuit to prevent molten salts from directly interacting with the working fluid.

29.3.7 Thermodynamic cycles of high temperature reactors

In the previous sections, we briefly introduced the various types of future nuclear reactors envisaged, especially in the Generation IV project. The 6 systems studied by the GIF differ more by the type of neutron involved (slow or fast) or by the type of core cooling envisaged than by the temperature level and thus the thermodynamic cycles that can be associated with them. In this section, we summarize what has been said of gas cycles in the previous pages, and we introduce two new types of cycles that have good potential for high temperature reactors.

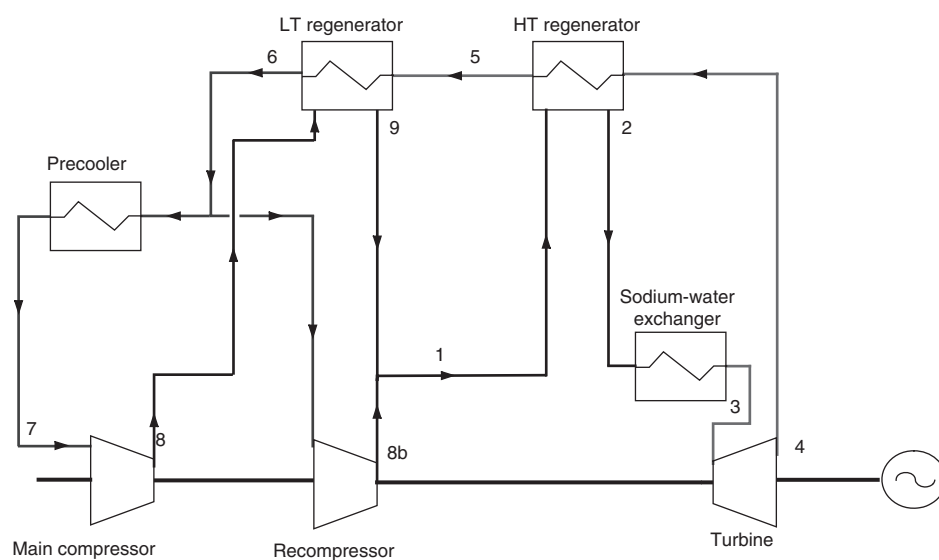
29.3.7.1 Brayton cycles

The simple helium Brayton cycle used for the PBMR reactor (Figure 29.3.2) leads on the paper to excellent efficiencies (48%), but there is currently no adequate industrial turbomachinery, and it will take many years to develop it.

An alternative is then to use helium as the core coolant, and another gas as working fluid, especially a mixture of nitrogen and helium, whose thermodynamic properties are relatively close to those of air for which industrial technology is well controlled. This solution however requires the introduction of an intercooler IHX (this is called indirect Brayton cycle), whose manufacture is not simple, even if it is under control, and introduces irreversibilities which lower the overall efficiency.

29.3.7.2 Supercritical CO₂ cycles

MIT has recently worked on cycles using supercritical carbon dioxide, which it considers lead to better performance than others at moderate reactor temperatures between 650 and 800°C (Dostal et al., 2003).


FIGURE 29.3.5

 Recompression supercritical CO₂ cycle

Proponents of these cycles argue that efficiencies are, for this temperature range, higher than those of steam cycles and that machines are much more compact.

On the thermodynamics, the value of using such a cycle is to benefit from a compression work in supercritical liquid much lower than if the working fluid remains in the gaseous state as a Brayton classic cycle.

Several types of supercritical CO₂ cycles were presented in section 24.2 of this Part, to which you should refer for details. Figure 29.3.5 shows a diagram of a recompression cycle, and Figure 29.3.6 its synoptic view.

Supercritical CO₂ cycles appear very interesting in thermodynamics terms. The two main technological constraints are the realization of regenerators in the circum-critical zone in particular to avoid any temperature cross, and that of efficient turbomachinery for CO₂, an area where there is no reference. Moreover, these cycles can only work if the CO₂ state at the precooler outlet is supercritical, which implies a temperature limit of 32°C, which can be difficult to achieve when the cold source is outside air, a river or sea water

29.3.7.3 HTR combined cycles

The GT-MHR reactor is the result of optimization work performed by General Atomics in 1985. Since 2000, Areva, which is involved in this work, changed the basic concept (helium Brayton cycle) so as to make the design easier and the adaptation to cogeneration more immediate (Gauthier et al., Gosset et al., 2005).

Considerations governing the selection of cycles are numerous. Obviously, intrinsic cycle efficiency is fundamental, but technological feasibility is not less. This has led Areva to choose for HTR-VHTR a combined cycle using a helium-nitrogen mixture (20–80 wt%) instead of pure helium, because of the considerable experience gained over several decades in air gas turbines.

In 2002, Areva optimized with Thermoptim a combined cycle associated with a HTR (Figure 29.3.7). Variations of this cycle can provide superheated steam at 110 bar using water at 120°C for some cogeneration applications, for capacities from 50 to 300 MW. The efficiency announced by Areva in electricity production is only 47%, but the objective is actually 50%, without any particular

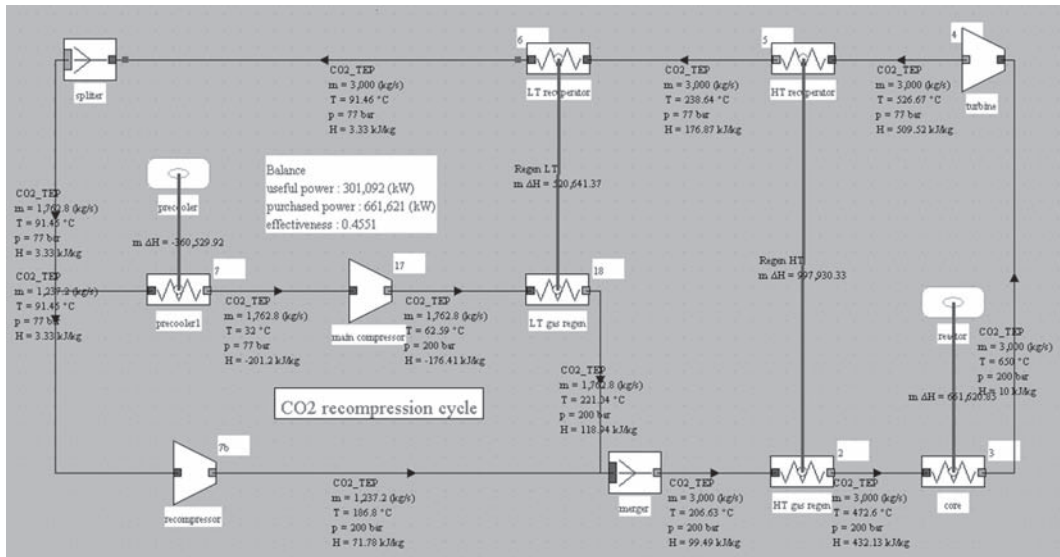


FIGURE 29.3.6
Synoptic view of the supercritical recompression CO₂ cycle

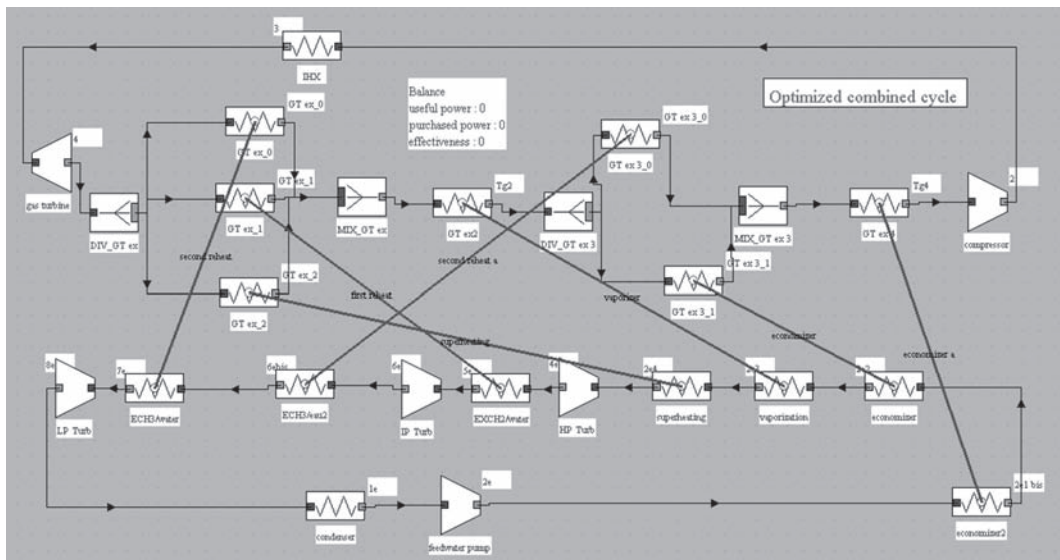
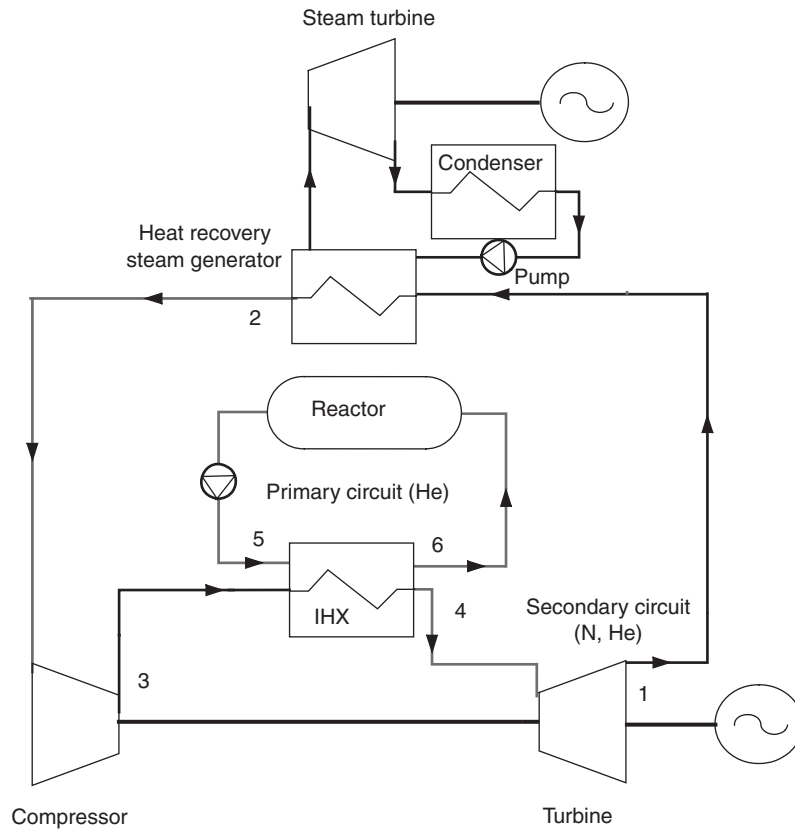


FIGURE 29.3.7
Optimized combined cycle

technological development except the IHX intercooler, the Mitsubishi company committing itself of making all turbomachinery (gas and steam) on the basis of current knowledge.

The gas circuit (a mixture of helium and nitrogen) is composed of a heat exchanger IHX that allows the transfer of energy from the coolant fluid (helium) warmed in the nuclear reactor core. A temperature difference of about 50°C between the hot fluid inlet and of cold fluid outlet is desirable to maintain the surface of this exchanger in a range of reasonable values.


FIGURE 29.3.8

Combined cycle optimized by Areva with ThermoOptim

Before passing through the exchanger IHX, the gas is first compressed by a compressor at a pressure between 55 and 70 bar, the latter value of 70 bar being a maximum value for reasons of strength of materials. At the exchanger outlet, the gas is expanded at about 40 bar in a turbine and exits at still relatively high temperature (about 600°C). It is then cooled in a heat exchanger, and redirected to the compressor. The thermodynamic cycle selected utilizes the enthalpy available in this exchanger to operate a steam cycle and thereby obtain a combined cycle.

Gas temperature at the IHX heat exchanger inlet (thus at the compressor outlet) is 300°C and pressure 55 bar. Gas temperature at the IHX exchanger outlet is 800°C and pressure 55 bar. This results from a temperature differential of 50°C selected on the IHX exchanger.

The proposed steam circuit consists of three successive turbines (high, intermediate and low pressure). Superheated steam available at the entrance of the HP turbine goes through an economizer that heats the liquid, a vaporizer that vaporizes it and a superheater. Two reheats are provided at the entrance of the IP and LP turbines.

Variations of this cycle adapted to CHP have also been optimized by Areva with ThermoOptim (Figure 29.3.8).

To illustrate the usefulness of this type of cycle, let us start again from the example of PBMR helium cycle of Figure 29.3.2, and build for this case a dual pressure combined cycle (120 and 10 bar, with HP and LP superheating at 500 and 300°C). The synopsis of this optimized cycle, given in Figure 29.3.9, shows that the efficiency rises from 48 to 52.5%. The architecture is different from that of Figure 29.3.7, being slightly simpler.

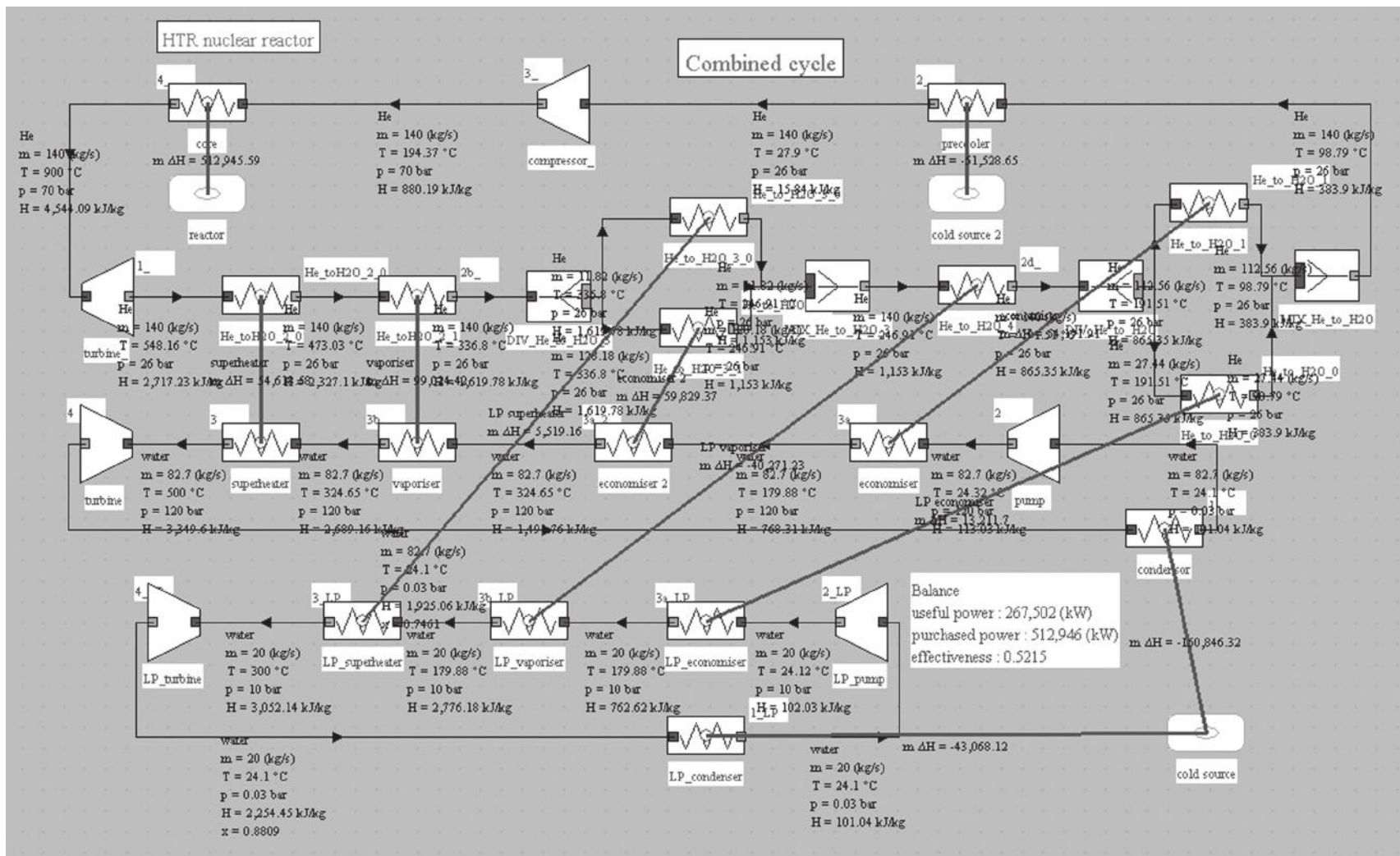


FIGURE 29.3.9
 Combined cycle coupled to a helium Brayton cycle

TABLE 29.4.1
OPTIONS FOR THE FUTURE NUCLEAR REACTORS

	T (°C)	P (MWe)	cooling	neutrons	thermo cycle
SFR	550	500–1500	indirect	fast	steam/super-crit.
SCWR	550	1700	direct	th. or fast	supercritical steam
HTR	900	100–600	dir/indir.	thermal	gas, CO ₂ , CC
VHTR	1100	600	dir/indir.	thermal	gas, CO ₂ , CC
GFR	850	300	dir/indir.	fast	gas, CO ₂ , CC
LFR	550–800	100–400	indirect	fast	gas, CO ₂ , CC
MSR	700–800	1000	indirect	thermal	gas, CO ₂ , CC

29.4 SUMMARY

Thermodynamic cycles to be used in future nuclear reactors should have much higher efficiencies than PWR, thanks to the increased working fluid temperature. It is too early to know, among the major cycles considered (supercritical water, Brayton helium, supercritical CO₂, combined cycle), those which will prove the best. The answer depends on many parameters, and primarily the type of reactor that will be the safest and most economical.

Table 29.4.1 summarizes the main options that exist today with regard to future nuclear reactors (HTR here is essentially GT-MHR, close to PBMR as we have seen).

REFERENCES

- V. Dostal, M.J. Driscoll, P. Hejzlar, N.E. Todreas, *A Supercritical CO₂ Gas Turbine Power Cycle For Next-Generation Nuclear Reactors*, Proc. ICONE-10, Arlington, Virginia, April 14–18, 2003.
- V. Dostal, *A Supercritical Carbon Dioxide Cycle For Next-Generation Nuclear Reactors*, PhD thesis, MIT, January 2004.
- J. C. Gauthier, M. Lecomte, PH. Billot, *The Framatome-anp near term HTR concept and its longer term development perspective*, 13th International Conference on Nuclear Engineering, Beijing, China, May 16–20, 2005
- J. Gosset, R. Gicquel, M. Lecomte, D. Queiros-conde, Optimal design of the structure and settings of nuclear HTR thermodynamic cycles, *International Journal of Thermal Sciences*, 44, 2005, pp. 1169–1179
- P. Pradel, *La R&D sur les filières nucléaires actuelles et futures : enjeux et perspectives*, Réalités Industrielles, Annales des Mines, ISSN 1148.7941, Fev. 2007, pp. 23–30.
- P. F. Peterson, *Multiple-reheat Brayton cycles for nuclear power conversion with molten coolants*, *Nuclear Technology*, Vol. 144, Numbre 3, Dec. 2003, pp. 279–288.
- T. Schulenberg, H. Wider, M. A. Fütterer, *Electricity Production in Nuclear Power Plants – Rankine vs. Brayton Cycles*, ANS/ENS International Winter Meeting (Global 2003), nov. 2003, New Orleans La, USA.

Solar Thermodynamic Cycles

Abstract: This chapter deals with the conversion of solar energy into electricity. It begins by introducing technical and economical problems, focusing on the specific terms that they induce thermodynamically and on available technologies for solar radiation collection, including concentration. Thermal models are proposed for solar collectors. We then present the main conversion cycles considered and provide some examples, on the one hand of ThermoOptim models of external components required, and on the other hand of models of solar cycles that can be implemented. It does not however address the consideration of the variability of the resource, which is the subject of Chapter 33.

Keywords: Flat plate, parabolic trough, parabolic dish, Fresnel, power tower, Stirling, effectiveness, SEGS, ISCCS.

30.1 DIRECT CONVERSION OF SOLAR ENERGY

30.1.1 Introduction

Presumably promising to be a significant development in the medium to long term, most solar energy conversion technologies are not yet mature enough to compete with conventional energy on a large scale, although this situation could evolve fairly rapidly in the future.

Technical constraints are mainly threefold:

- power density available is relatively low, which means large areas of collectors and high material costs;
- source variability is high: solar energy fluctuates a lot, which requires often complex control systems;
- need to store: being an energy-flow, storage is required for most applications, which poses a problem because today we do not know how to store energy in good conditions.

Economic constraints are twofold:

- high capital cost. Even when properly managed, technologies are relatively expensive in investment, while their operating costs are generally low;
- need for a back-up. In case of source unavailability, another energy is often required, imposing additional costs, sometimes significant.

By contrast, emissions of pollutants are zero in operation, which is an undeniable asset for sustainable development.

Solar energy comes from thermonuclear reactions that occur within the sun, causing the emission of high power electromagnetic radiation, appearing much like a blackbody at 5,800 K.

Outside the atmosphere, the radiation received by the earth varies depending on time of the year between 1,350 and 1,450 W/m². It is then partially reflected and absorbed by the atmosphere, so that the radiation received at ground level has a direct part and a diffuse part, the total ranging from 200 W/m² (overcast) to about 1,000 W/m² (zenith clear sky). The energy received by a given surface depends on its tilt and orientation and local climatic conditions. Solar radiation atlases at ground level are issued by national and international meteorological services in the form of maps and charts, on paper or computer.

Direct conversion of solar radiation is in three main ways:

- thermal, the only mentioned in this chapter;
- by photoelectric effect;
- photosynthesis.

30.1.2 Thermal conversion of solar energy

Thermal conversion of solar energy is to intercept the incident photons on an absorbing material, whose temperature increases.

Several methods of capture are possible:

- **passive solar housing.** For space heating and cooling applications, it is possible to design the architecture of buildings so that they optimize naturally (or passively) the use of the solar resource, without using fluid flow and capture and storage auxiliary devices. The advantage of passive solar design of buildings is that it can lead to substantial energy savings with low incremental costs;
- **flat plate collectors** generally use the greenhouse effect to minimize heat loss from the absorber. Indeed, the glass is transparent to visible radiation, and therefore lets through the incident solar energy, but opaque to infrared radiation, which has the effect of trapping heat. According to the technology used, the operating temperatures of flat plate collectors vary from 40°C to 120°C (vacuum collectors). Figure 30.1.1 shows the sectional view of a collector. The absorber consists of a metal plate on which are welded pipes in which circulates the thermal fluid. Heat losses to the front of the collector are reduced by one or more glazings (2 on the figure) and those to the rear by insulation;
- **concentration collectors.** To reach temperatures above about 120°C, it is necessary to concentrate the solar radiation by suitable sets of reflective elements (mirrors) or lenses (usually Fresnel). The main constraint, apart from the higher device cost, is the tracking system intended to follow the sun in its course. A series of concentrators has been proposed and developed (Figures 30.1.2 to 30.1.5).

To thermodynamically convert solar radiation into electricity with a good efficiency, it is generally necessary to concentrate it, otherwise heat losses of absorptive surfaces are very high and the collector effectiveness low.

It is customary to characterize concentration collectors by their concentration factor C , ratio of the collector surface to that receiving the concentrated solar flux.

The experience of the last thirty years shows that four main technologies are used in practice to concentrate solar radiation in technical and economically viable conditions:

- parabolic trough PT ($C \approx 40\text{--}80$, Figure 30.1.2), which are cylinders of parabolic cross section, that concentrate sunlight onto a straight tube;
- concentrating linear Fresnel reflectors CLFR ($C \approx 30$, Figure 30.1.3): these use narrow rectangular plate mirrors to concentrate sunlight onto a fixed absorber consisting of a series of parallel tubes;

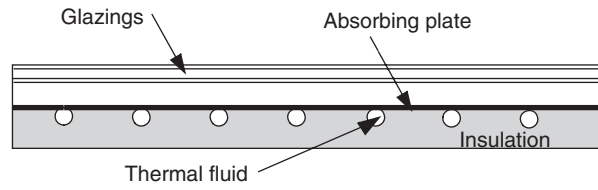


FIGURE 30.1.1
Flat plate collector section

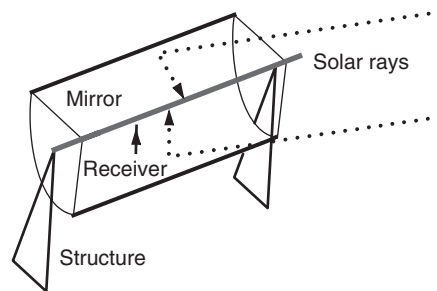


FIGURE 30.1.2
Parabolic trough

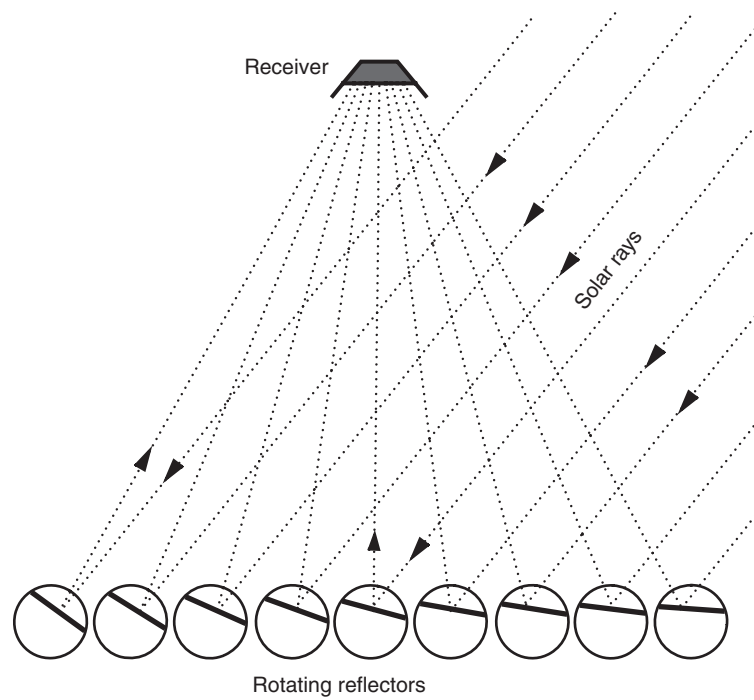


FIGURE 30.1.3
Concentrating linear Fresnel reflector

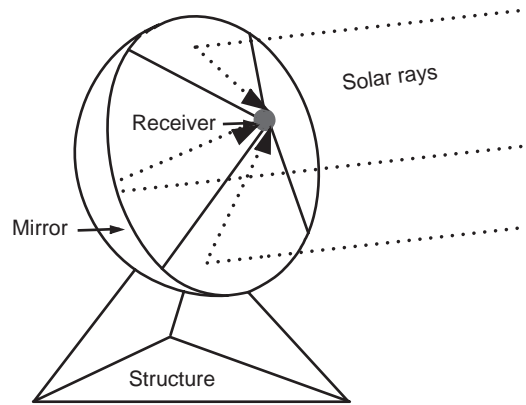


FIGURE 30.1.4
Dish collector

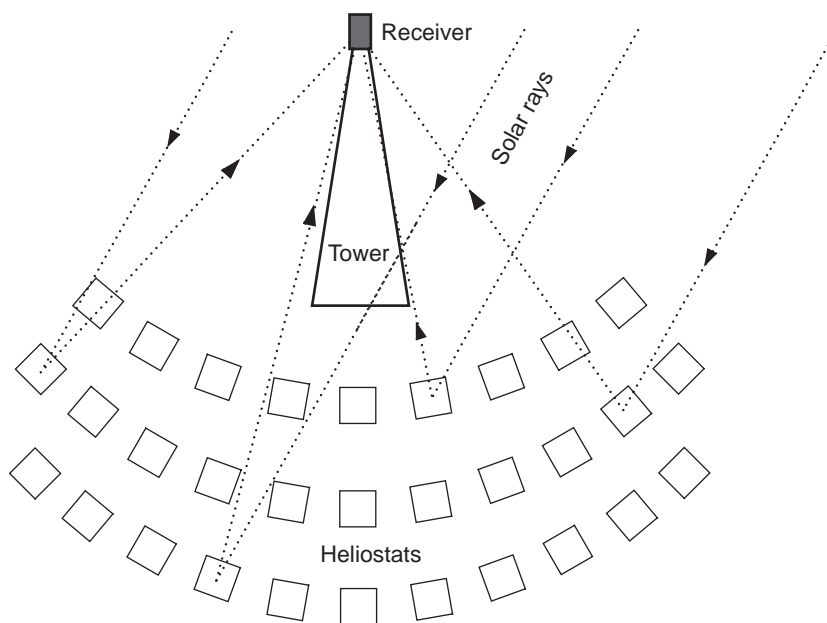


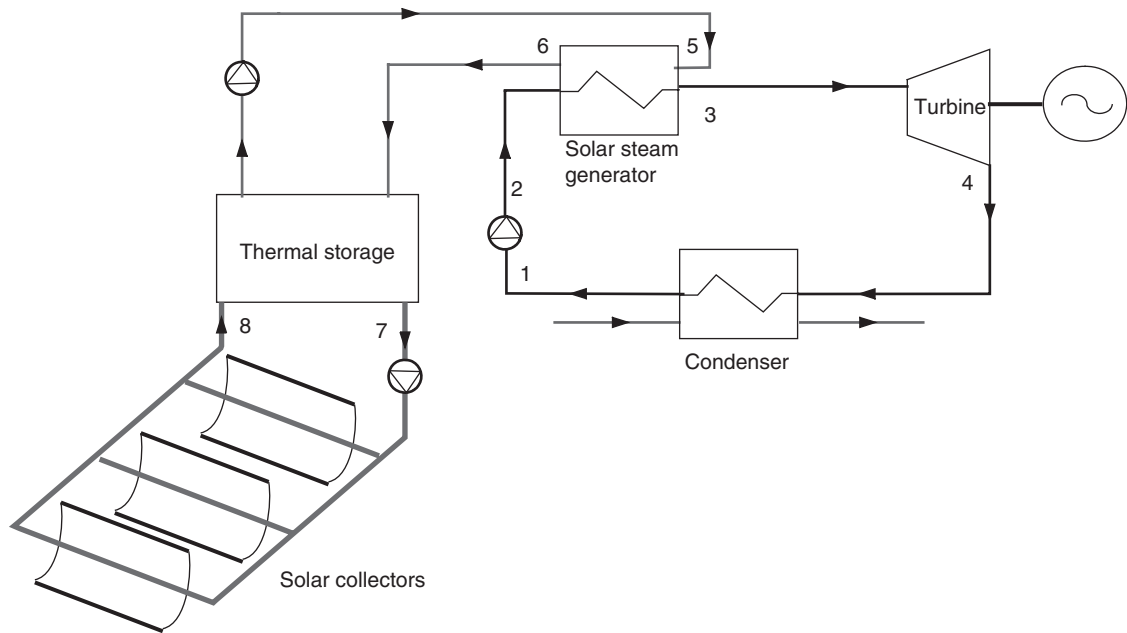
FIGURE 30.1.5
Central or power tower

- parabolic dish PD ($C \approx 1,000\text{--}2,500$, Figure 30.1.4), where the reflector is a paraboloid of revolution;
- power towers PT or central tower plants ($C \approx 200\text{--}700$, Figure 30.1.5), in which thousands of tracking reflectors, called heliostats, redirect incoming solar radiation to an absorber at the top of a tower, allowing achievement of both high concentrations and high radiation fluxes.

The first two technologies only require to track the sun in one direction, but concentration, and thus collector temperature is lower (400°C). The other two require a double tracking movement, but can reach much higher temperatures ($750\text{--}1000^\circ\text{C}$).

30.1.2 Thermodynamic cycles considered

Electro-power solar energy systems are relatively complex and include at least one collection circuit, an energy distribution circuit, storage and various control systems (Figure 30.1.6). In these, both the

**FIGURE 30.1.6**

Schematic diagram of an electro-solar plant

load (demand) and availabilities vary continuously, leading to methodological difficulties that will be discussed in Chapter 33.

Four thermodynamic cycles are now mostly considered for conversion to electricity:

- Hirn (or Rankine) cycle for PT, CLFR and CT;
- Brayton cycle for PD (micro GT) and CT (hot air cycles);
- Stirling cycle for PD;
- combined cycle, combining the first two, for PT or CLFR (ISCCS).

We discuss them in sections 30.4 to 30.6, after presenting solar collector models we will use.

30.2 PERFORMANCE OF SOLAR COLLECTORS

Flat plate solar collectors differ depending on the type of coverage: unglazed (swimming pools), single or double glazing, vacuum, anti-emissivity coatings. Their transmittivity τ depends on this coverage. Because the effectiveness of solar collectors drops with temperature, it is preferable to operate at temperatures as low as possible given the intended use.

30.2.1 Low temperature solar collectors

For space heating, a very good solution (but one limited to new housing), is to use a direct solar floor, in which hot water circulates through a solar floor heating device at about 23°C in winter, and is used to make hot water in summer. This system can provide 40–70% of heating needs. It requires a specific design of the floor (heavy, up to 30 cm thick, high inertia, which allows a temperature shift from 5 to 10 h). Per 100 m^2 housing, the heating floor is 45 to 70 m^2 , and the collector surface 8 to 15 m^2 .

There are three main types of solar water heaters:

- integrated storage, standard-size piece, factory assembled, driven by hot water, the tank being placed above the collector;

- compact, the tank being close to the collector, but distinct, with a primary circuit generally anti-freeze, operating by thermosyphon, sized (collector area, volume of tank) as needed;
- separate elements (the collector is far from storage, primary circuit anti-freeze, operating by thermosyphon or forced circulation).

30.2.2 Low temperature flat plate solar collector model

A flat plate solar collector model has been briefly presented in section 23.2 to illustrate the design of an external process. We will now justify this model.

The solar flux received by the collector goes generally through a glazing intended to isolate the absorbing surface. Reflection, transmission through the glazing and absorption result in optical losses, characterized by an overall transmittivity τ .

The absorber heats up and loses heat to the outside essentially by radiation and convection. This heat exchange can be characterized by a thermal loss coefficient U . A thermal fluid cools the absorber, taking useful heat that is then transferred or converted for different uses.

Based on this brief analysis, it is possible to produce a model whose parameters are:

- glazing transmittivity τ ;
- thermal loss coefficient U ($\text{W}/\text{m}^2/\text{K}$);
- incident solar flux G (W/m^2);
- collector surface A (m^2);
- outside temperature T_{out} ($^{\circ}\text{C}$).

The heat balance of a small slice of collector length dx is: the power carried out by the fluid $\dot{m}C_p dT$ is equal to the radiation received reduced by optical losses $\tau GA/L dx$, less the collector heat loss $U(T - T_{\text{out}})A/L dx$, which is also written:

$$\dot{m}C_p dT = [\tau G - U(T - T_{\text{out}})]A/L dx \quad (30.2.1)$$

This is a differential equation that integrates seamlessly and leads to:

$$Q = \dot{m}C_p(T_o - T_i) = \dot{m}C_p \left(\tau \frac{G}{U} - T_i + T_{\text{out}} \right) \left[1 - \exp \left(- \frac{UA}{\dot{m}C_p} \right) \right] \quad (30.2.2)$$

Equation (30.2.2) is valid whatever the value of the flow. However, it can be replaced by a simplified formula when the flow is high enough that it can be assumed that the temperature varies almost linearly between the inlet and outlet of the collector. We write then that the losses are proportional to the average temperature T_m , itself equal to half the sum of inlet and outlet temperatures:

$$Q = \dot{m}C_p A [\tau G - U(T_m - T_{\text{out}})] \quad (30.2.3)$$

These are the models proposed in Thermoptim model library.

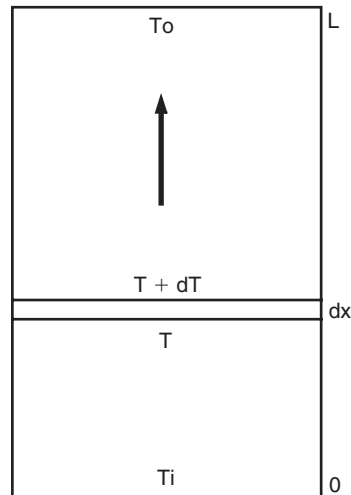
Two calculation methods are possible: to determine the outlet point state knowing the collector surface, or determine this surface knowing the outlet point state.

The model input data are as follows (provided by other system components):

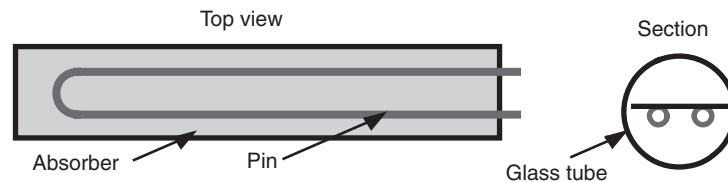
- the thermal fluid temperature at the collector inlet T_i ($^{\circ}\text{C}$);
- the flow \dot{m} of the thermal fluid (kg/s).

The outputs are:

- the thermal fluid temperature at the collector outlet T_o ($^{\circ}\text{C}$);
- the thermal power received by the thermal fluid Q (W/m^2);
- the collector effectiveness.

**FIGURE 30.2.1**

Flat plate solar collector model

**FIGURE 30.2.2**

Vacuum collector module

30.2.3 High temperature solar collectors

The low temperature flat plate collectors we just presented do not allow electricity to be produced with acceptable efficiencies. It is desirable to approach or exceed 100°C to consider thermodynamic conversion of solar energy.

It is therefore possible to use flat plate solar collectors provided that their absorber is very well thermally insulated, which implies both an anti-emissivity treatment and good convective insulation.

Vacuum tube collectors are now seriously considered a solution for that (Figure 30.2.2). These collectors are usually made up of modules comprising a U-shaped pin of small diameter (of the order of 1 cm) provided with fins and inserted into a glass tube of large diameter (about 1 dm). The coolant circulates inside the pin. Such modules are placed to form parallel flat plate collectors.

30.2.4 Modeling high temperature concentration collectors

The solar collector model presented above is based on two assumptions that we will refine in this section:

- first, we assumed that losses are proportional to the temperature difference between the thermal fluid and the surroundings;
- second the absorber section is assumed to be equal to that of the collector.

The new model is a variation of the above, adapted to represent high temperature concentration collectors.

The solar flux received by the collector is first reflected on the concentrator mirrors and goes then through the glazing material thermally insulating the receiver where it is absorbed by a suitable

surface. In high concentration collectors, only the direct component of solar radiation can be directed to the receiver, as the diffuse component cannot be concentrated.

The loss coefficient U can often be decomposed into a constant term and a term proportional to the temperature difference between absorber and ambient air: $U = U_0 + U_1(T_m - T_{out})$. τ is a function of radiation angle of incidence, mirror reflectivity, absorber absorptivity and transmittance of the glazing protecting the absorber.

With the previous notations, and assuming a linear distribution of temperatures in the collector (the assumption is only valid if the flow is not too low, which is often the case in practice) the model equation is as follows, T_m being the average absorber temperature, and S_c and S_a being respectively the collector and absorber surfaces:

$$Q = \dot{m}C_p(T_o - T_i) = \tau EsS_c - S_a(U_0 + U_1(T_m - T_{out}))(T_m - T_{out}) \quad (30.2.4)$$

It would be possible to generalize relation (30.2.1) to obtain the differential equation of the high temperature collector, but its integration would be a bit more difficult (it requires factorization of the degree 2 polynomial in T).

Table 30.2.1 gives values of coefficients valid for three types of concentrating collectors, among which are the two parabolic troughs used in Luz SEGS power plants presented in section 30.3.

The characteristics of the Luz 3 parabolic trough are as follows: area 235 m^2 , width 5 m, length 48 m, receiver consisting of a steel tube 70 mm in diameter covered with a cermet selective coating and surrounded by a vacuum glass tube (with pressure of the order of 0.013 Pa). The absorption coefficient of the selective coating is equal to 0.96 with respect to direct radiation, and its emissivity at 350°C is 0.19. Mirrors are made of glass panels, hot shaped, silvered on their posterior surface and protected against external damage. Collectors track the sun by rotating around a north-south axis thanks to hydraulic control.

TABLE 30.2.1
CONCENTRATION COLLECTOR PARAMETERS

	Luz 2	Luz 3	Trough	Fresnel
τ	0.737	0.8	0.7	0.66
S_c/S_a	22.6	26.1	500	20
U_0	-0.0223	-0.0725	0.21	-0.031
U_1	0.000803	0.00089	0.000134	0.00061

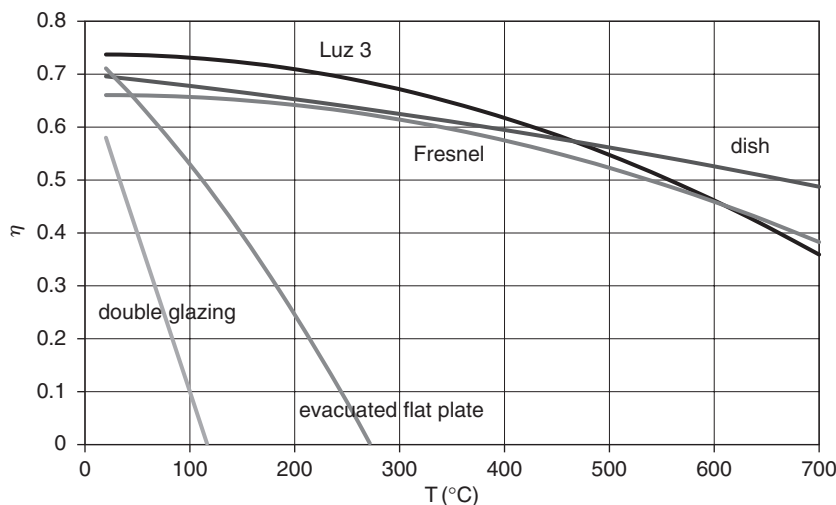


FIGURE 30.2.3
High temperature collector effectiveness

Figure 30.2.3 compares the effectiveness of different solar collectors, depending on the temperature difference between the absorber and the surroundings for an irradiation of $1,000 \text{ W/m}^2$. It illustrates the value of concentration, but also shows that vacuum tube collectors, which do not require device tracking, remain attractive to just above 100°C .

30.3 PARABOLIC TROUGH PLANTS

Technology today considered the most mature is parabolic troughs (PT), thanks to the experience in California's Mojave Desert, where 9 plants have been operational since 1984. Their capacity ranges between 14 and 80 MW, totaling 354 MW. These plants, called Solar Electric Generating Systems (SEGS) were built by the Luz company under an agreement with Southern California Edison Company benefiting from the Public Utility Regulatory Policies Act (PURPA). The particularly appealing electricity sale financial conditions of this agreement being no longer available for new plants, their development stopped since the late 80s.

In SEGS plants (Figure 30.1.4), the steam gets its heat from a thermal oil heated (at a maximum temperature of 393°C) by a field of parabolic trough solar collectors. Superheating temperature under these conditions is limited to 371°C and steam pressure at 100 bar. Moreover, these plants being used in hot, sunny areas, the condensing temperature is relatively high (42°C , a pressure close of 0.082 bar).

Note that concentrating linear Fresnel reflectors (CLFR) operate at temperatures close to parabolic troughs, so that they could also be used in SEGS plants.

30.3.1 Optimization of the collector temperature

To optimize the cycle, a compromise must be found between the superheating temperature and effectiveness of solar collection. The latter is a decreasing function of the average temperature in the collector, while the maximum exergy of water vapor is an increasing function of steam temperature (Figure 15.2.2 of Part 3).

Under the conditions of the SEGS plants, a simple model can show that the optimum temperature of operation is about 400°C and 100 bar, which corresponds precisely to the choice made for these plants (Figure 30.3.1).

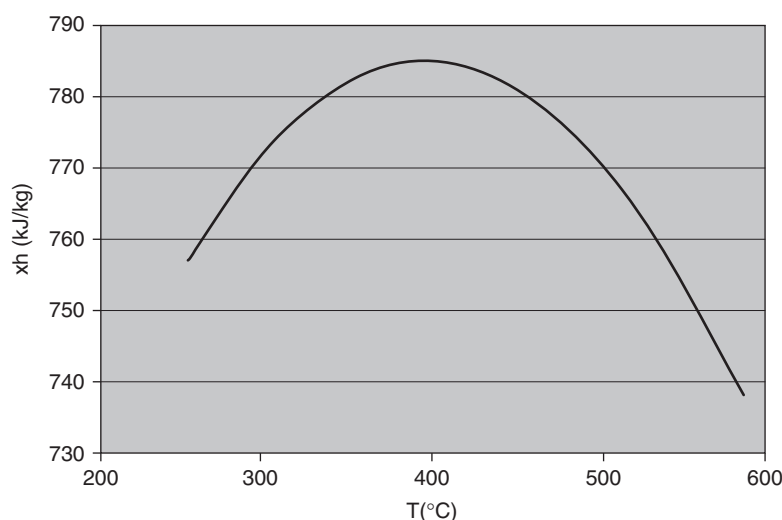


FIGURE 30.3.1

Optimal operation temperature

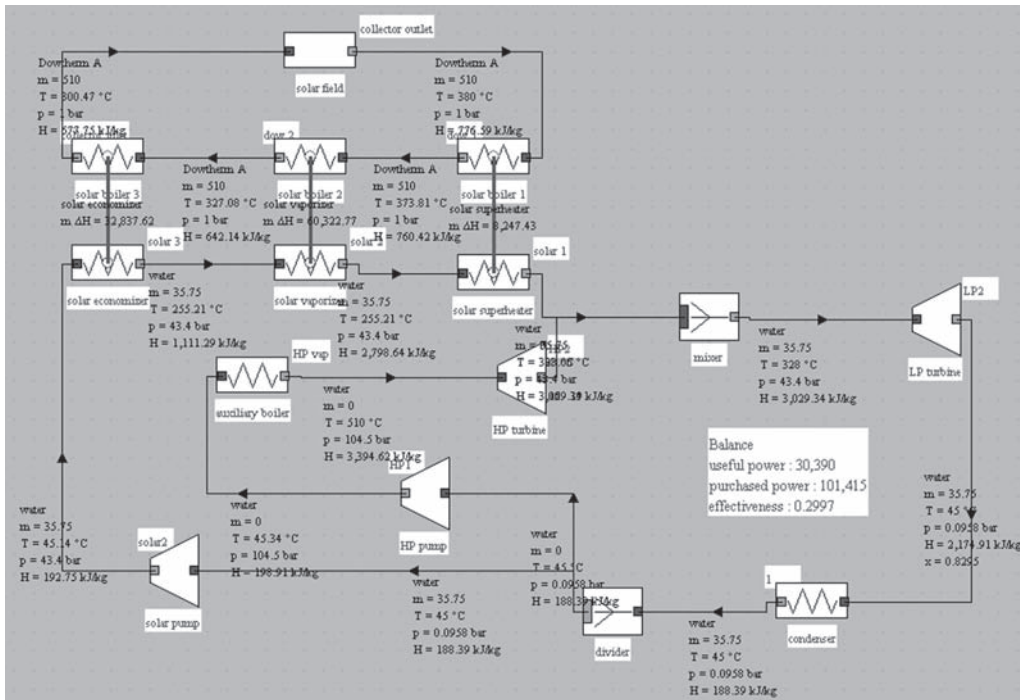


FIGURE 30.3.2
SEGS 3 plant with collector field and back-up

The temperature level is relatively low in comparison with conventional power plants, and efficiency without extraction is about 33%.

30.3.2 Plant model

To increase the plant capacity, and especially to enable it to function in the absence of sunshine, a back-up is often expected. When the auxiliary boiler runs continuously, the plant is also known as hybrid system, a concept which will be discussed later.

We also know that it is often possible to improve the efficiency of a steam cycle by conducting an internal regeneration through a series of extractions. The gain in efficiency is obtained by reducing irreversibilities taking place when heat at low temperature in the economizer is provided by the source at high temperature. The more efficient the basic cycle, the less important is the relative effect of extraction. In the case of SEGS plants, optimization of extractions achieves an efficiency of about 37.5%, an improvement of 11% (see Figure 30.3.3).

WORKED EXAMPLE

Modeling of a SEGS solar plant

The modeling of a SEGS solar power plant is presented in a guidance page of the Thermoptim-UNIT portal (<http://www.thermoptim.org/sections/enseignement/cours-en-ligne/fiches-guides-td-projets/fiche-sujet-fg1>).

It allows you to study the operation of solar power plants and shows how they can be realistically modeled with Thermoptim. The solar collector is type SEGS developed by the company Luz. The cycle is as a simple variant of a Rankine cycle, where the boiler is replaced by a steam generator in which the thermal fluid is heated by the field of collectors.

The model uses two external classes, “solar concentrator” and “Dowtherm A”.



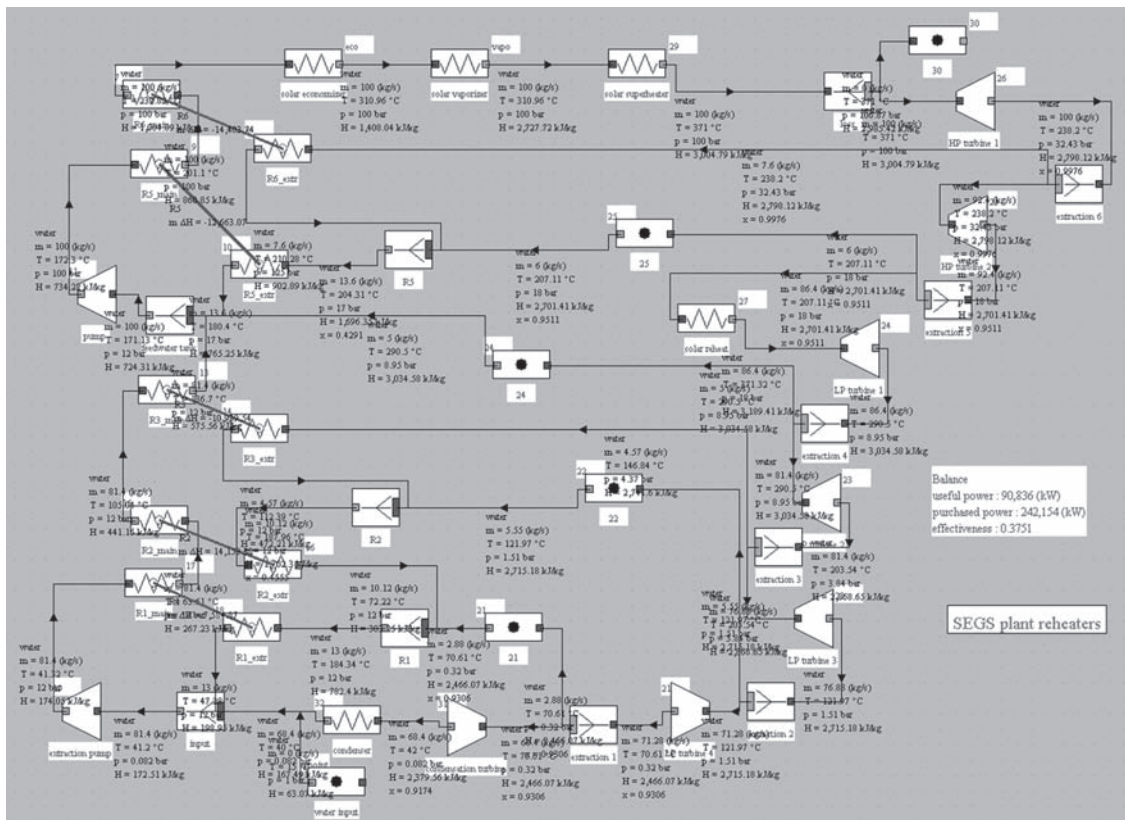


FIGURE 30.3

Detailed model of the SEGS IX plant

30.4 PARABOLIC DISH SYSTEMS

Parabolic dish systems are those that achieve the highest concentrations, and thus allow the use of high temperature cycles, the most efficient. However the constraints of accurate tracking of the sun and mechanical resistance, including effects of wind, just limit their size, and thus their capacity. Technologically, few machines are available, the pair high temperature and low capacity occurring only rarely.

Two technologies are competing here: micro-turbines operating with the Brayton cycle, and Stirling engines.

The latter, which lead to the best theoretical efficiency, but often to much lower actual efficiencies, have the advantage of being mainly suited for small capacities, unlike gas turbines, whose speed increases with inverse of the capacity.

In both cases, a back-up is normally used to compensate for the momentary lack of solar radiation due to a passing cloud.

As we showed in Chapter 14 of Part 3, it is possible to model a Stirling cycle in Thermoptim, but the gap between theoretical and practical performance being important, the confidence one can have in this model is relatively limited. For a Stirling engine using a heated expansion, we must include heat supplied during the expansion in the energy balance, as explained in section 23.7 (Figure 30.4.1).

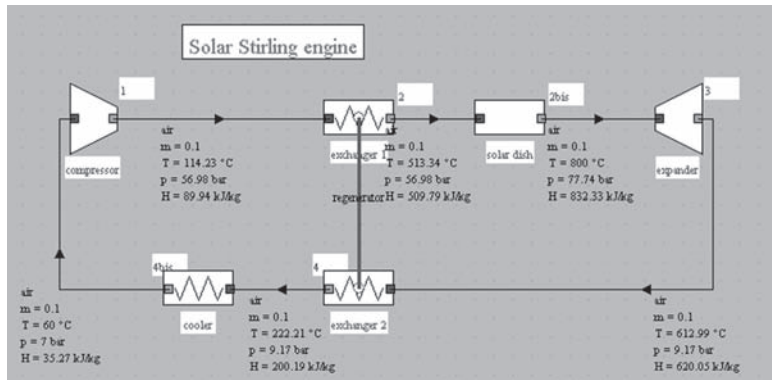


FIGURE 30.4.1
Solar Stirling engine

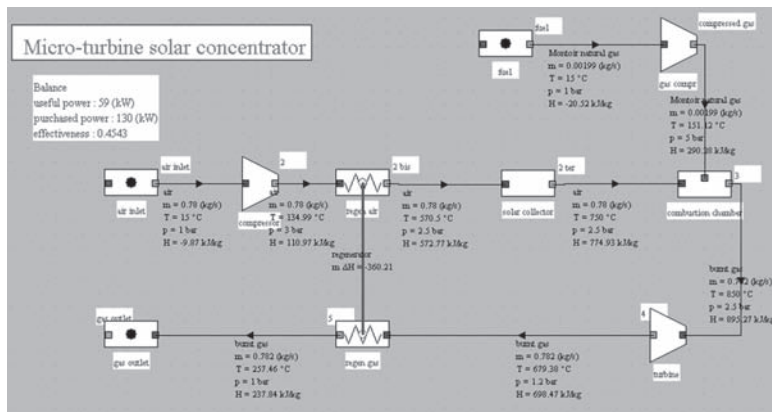


FIGURE 30.4.2
Micro-turbine solar concentrator

Figure 30.4.2 shows a micro-turbine solar concentrator cycle: the solar hot-air receiver is located upstream of the combustion chamber of a micro-turbine, thereby reducing fuel consumption, and leading to high efficiency (43% by taking into account the solar heat in the purchased energy).

30.5 POWER TOWERS

Two types of thermodynamic cycles are used: either a steam cycle at about 520°C and 100 bar, with a reheat, or a hot air Brayton cycle. A number of experimental plants were constructed over the last thirty years (Themis in France, Solar One and Two at Brastow California, CESA in Almeria, Spain, Eurelios).

Given the very high temperatures reached in the absorber, it is difficult to find an organic fluid resistant enough, and molten salt are used, which can optionally be stored to decouple the capture of solar radiation from its use, allowing thus the plant to operate during cloudy periods or at night.

Figure 30.5.1 shows, far left, the Solar One power tower, and at the center, a parabolic dish Stirling system of about 90 m^2 opening.

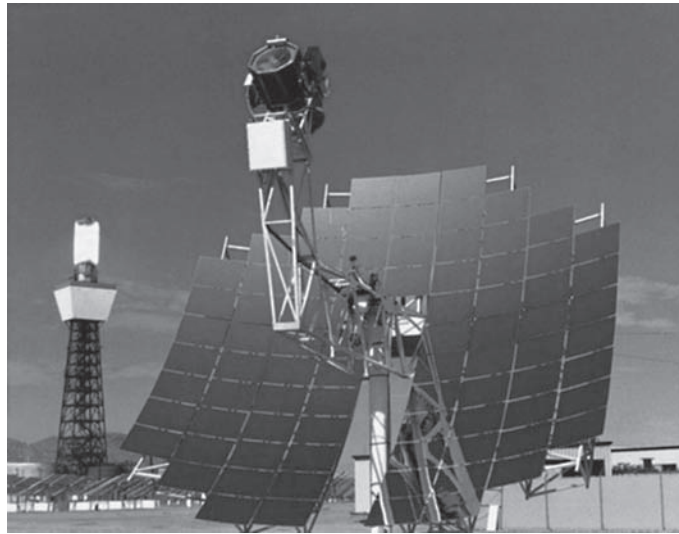


FIGURE 30.5.1

Parabolic dish Stirling engine in the foreground and power tower in the left background (Copyright Sandia Laboratories)

30.6 HYBRID SYSTEMS

The concept of hybrid solar power plant is an extension of that of solar power plant with back-up in which we could ultimately say that it is the sun which is supplemental to conventional thermal power plants. We will see that this reversal of roles, which may seem *a priori* surprising, has a number of advantages, technically, economically and environmentally.

Concentration solar collectors provide heat at a substantially constant temperature, as the heating in the absorber must remain limited to a few tens of degrees. In hybrid systems, this ensures the vaporization of steam with minimal exergy loss.

It turns out that the most efficient thermal power plants are today combined cycles, which combine a gas turbine with a steam power plant.

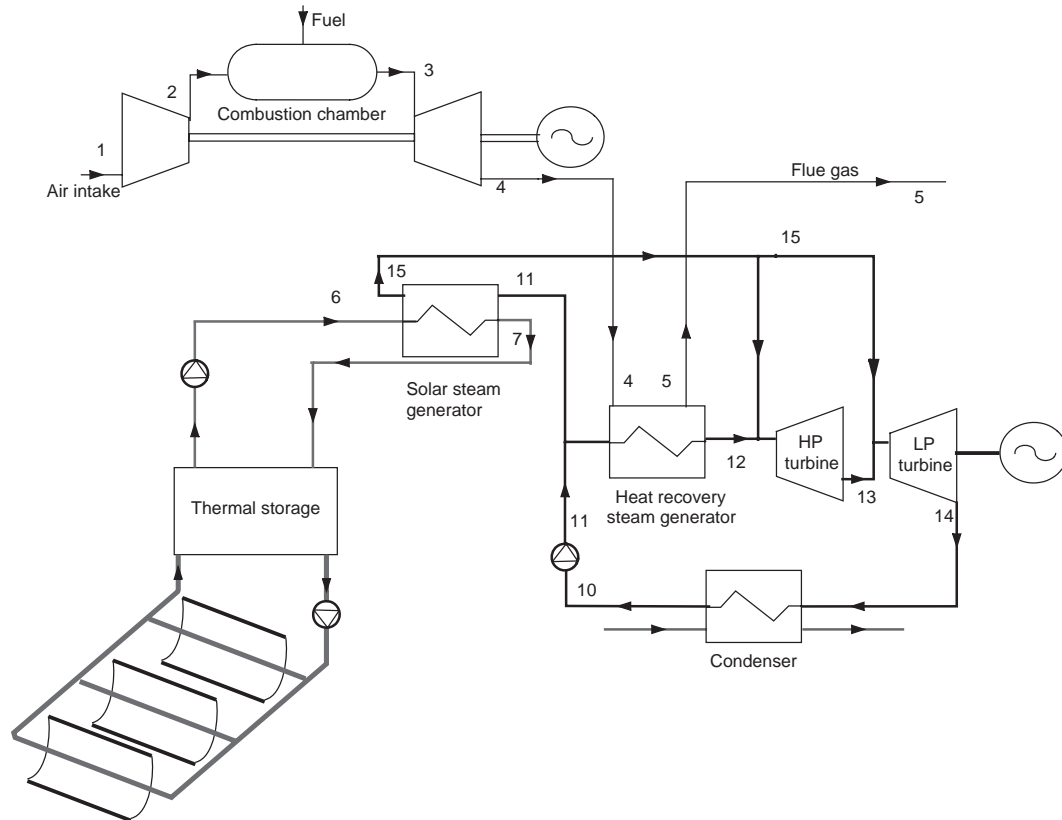
As we have shown in sections 15.6.4 and 17.3 of Part 3, optimization of the heat exchanger that provides the coupling between these two machines is made difficult precisely because of the pressurized water vaporization plateau. Ensuring that vaporization in a field of solar collectors can significantly reduce the system irreversibility, and thus achieve excellent efficiencies.

In hybrid-type solar power plants, known as Integrated Solar Combined Cycle System (ISCCS) (see Figure 30.6.1), steam cycles receive part of the heat from a thermal oil heated by a solar field of parabolic troughs of Luz type, and the other from the exhaust of a gas turbine.

An additional interest of hybrid systems is to allow turbines to operate even if there is no sun. The availability rate of the plant is then much higher than in solar mode only. Losses due to collector field reheating in the morning are greatly reduced and solar efficiency increases.

A major constraint is that operating in hybrid mode should not reduce performance in classic mode, otherwise the overall annual balance may be negative. Thus, some ISCCS plants only provide a very small sun share, in the order of 5 to 10% on the year, the technical and economic optimum being at this level.

Several options are possible in terms of system configuration. The two main options for using solar heat are to produce steam at high pressure (11-15-12 on Figure 30.6.1) or low pressure (11-15-13). Each has advantages and disadvantages, but the first is the most efficient, the exergy of the steam produced by the solar collector field being higher.


FIGURE 30.6.1

Example of ISCC solar plant

In terms of engineering design, ISCC plants pose multiple problems very interesting to study: how best to include solar thermal input, how to size the heat exchangers so that they can adapt to daytime functioning in ISCC and single combined-cycle at night etc.

REFERENCES

- M. Kane, *Intégration et optimisation thermoéconomique & environnologique de centrales solaires hybrides*, Thèse de doctorat, École Polytechnique Fédérale de Lausanne, 2002.
- E. A. Demeo, *Solar-Thermal Electric Power*, 2003 Status Update, EPRI report, February 2003.
- J. A. Duffie, W. A. Beckman, *Solar engineering of thermal processes*, John Wiley and sons, New York, 1980.
- A. Ferrière, *Centrales solaires thermodynamiques*, Techniques de l'Ingénieur, Traité Génie énergétique, BE 8 903.
- R. Gicquel, *Behavior of plane solar collectors under transient conditions*. International Chemical Engineering, Vol. 19, n° 1, January 1979.
- A. Rabl, *Active solar collectors and their applications*, Oxford University Press, New York, 1985.
- K. J. Riffelmann, D. Krüge, R. Pitz-paal, *Solar thermal plants, Power and process heat*, DZLR. Bechtel Corporation, *ISCCS Study Integrated Solar Combined Cycle System*, Report for the National Renewable Energy Laboratory, 1998.
- Status of Thermal Solar Electric Technology*, EPRI Report, December 1989.
- Renewable Energy Technical Assessment Guide*, EPRI Report, December 2002.

Other than Solar NRE Cycles

Abstract: Renewable energy sources, as the name suggests, are distinguished from other energy sources in that they are in the form of flow rather than stock. Provided by the sun, wind, earth and sea, they are practically inexhaustible. It is customary to denote them as new and renewable energies (NRE), although some of them have been used for centuries, because it is only recently that they are considered for production of commercial energy.

Presumably promising to be a significant development in the medium to long term, a number of NRE conversion technologies are not yet mature enough to compete with conventional energy on a large scale, although this situation could evolve fairly rapidly in the future.

In this chapter we will examine thermodynamic cycles for NRE conversion other than those where the heat source is direct solar energy, which were discussed in the previous chapter. We will successively discuss solar ponds, ocean thermal energy conversion, geothermal energy, and biomass combustion.

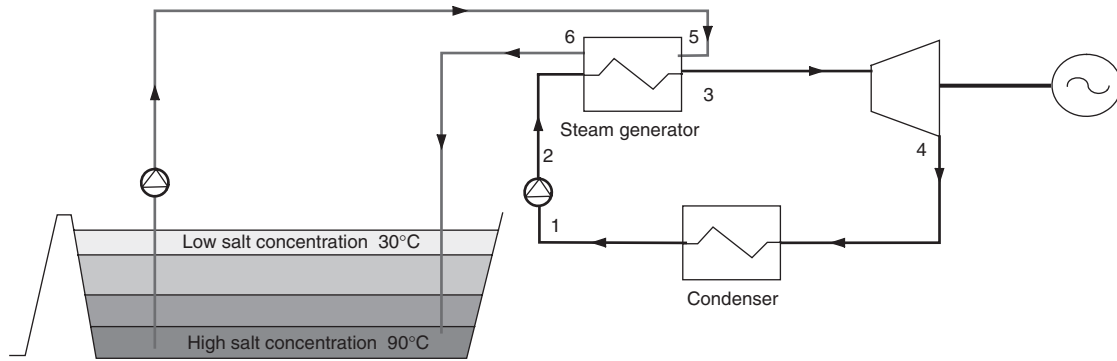
Keywords: new and renewable energies, solar ponds, ocean thermal energy conversion, geothermal energy, biomass combustion, NRE, OTEC, Uehara, Kalina, direct-steam, flash, binary, combined cycle, pyrolysis, gasification, fluidized bed, downdraft, updraft.

31.1 SOLAR PONDS

Inverse gradient solar ponds are collectors of a particular type. They are reservoirs of salt water (NaCl or MgCl_2) with an area of several thousand m^2 , whose bottom is covered with an absorbent surface. To avoid the internal convection and heat loss that result, the pond is divided vertically into three zones:

- a thin surface region at low salt concentration (1 g/cm^3), at almost homogeneous temperature, stirred by wind and convection;
- a zone of 1 m–1.5 m, increasing salt concentration with depth, the salt gradient preventing the onset of convection;
- a 2 to 4 m high lower zone of homogeneous and very high salt concentration ($>1.3 \text{ g/cm}^3$, and sometimes saturated) which stores solar heat.

Such a configuration allows a surface temperature close to that of the atmosphere (25°C), while the bottom of the pond reaches 90°C or more. Heat losses are reduced.


FIGURE 31.1.1

Solar pond

Inverse gradient solar pond applications are numerous: space heating, absorption refrigeration, power generation through a thermodynamic closed vapor cycle.

In the latter case, hot water is pumped and used to evaporate a working fluid, which follows a motor cycle and is condensed by exchange with ambient air, for example in an air-coil.

Although technically valid, the concept of an inverse gradient solar pond is not economically viable, which explains why prototypes built in Israel (a solar pond of 20 ha producing 5 MW worked in Israel until 1989) and USA (the University of Texas at El Paso pond has an area of 3000 m² of 70 kWe capacity) are no longer exploited.

It is possible to model such a cycle with Thermoptim and calculate its efficiency, then build up its exergy balance. We can especially look among available thermodynamic fluids (ammonia, butane, propane, R134a), for the one that leads to the best performance.

In what follows, the hot water flow is equal to 12 kg/s, its temperature is 90°C and the cold water temperature is 25°C.

31.1.1 Analysis of the problem

We have to study a vapor cycle which is a little special, whose hot source is at relatively low temperature (90°C), and cold source at about 25°C. Its architecture is entirely conventional: it leads to the diagram of Figure 31.1.2.

We assume here that the working fluid is ammonia. The pump can be considered isentropic, but not the turbine, whose isentropic efficiency can by example be taken equal to 0.9.

To design heat exchangers, it is necessary to set the values of minimum temperature differences between the fluids, that is to say, pinches. The lower they are, the better the thermodynamic cycle, but also the larger will be the exchange surfaces.

For temperature differences between the cycle and hot and cold sources, we choose pinches as low as possible: 10°C for superheating (gas-liquid exchange), 11°C at the economizer outlet (liquid-liquid exchange), 8°C at the condenser outlet (liquid/two-phase mixture exchange).

The need to have a sufficient temperature difference between the hot source and the working fluid makes us select a superheating temperature of 80°C and a vaporization temperature of 72.5°C, i.e. a high pressure of 35 bar.

For similar reasons, the condensation temperature of ammonia is 36°C, which corresponds to a pressure of 14 bar.

The hot water flow-rate is given but not that of the working fluid. We must start with an estimate value, which is then modified so that the pinch at the economizer outlet is equal to 11°C as

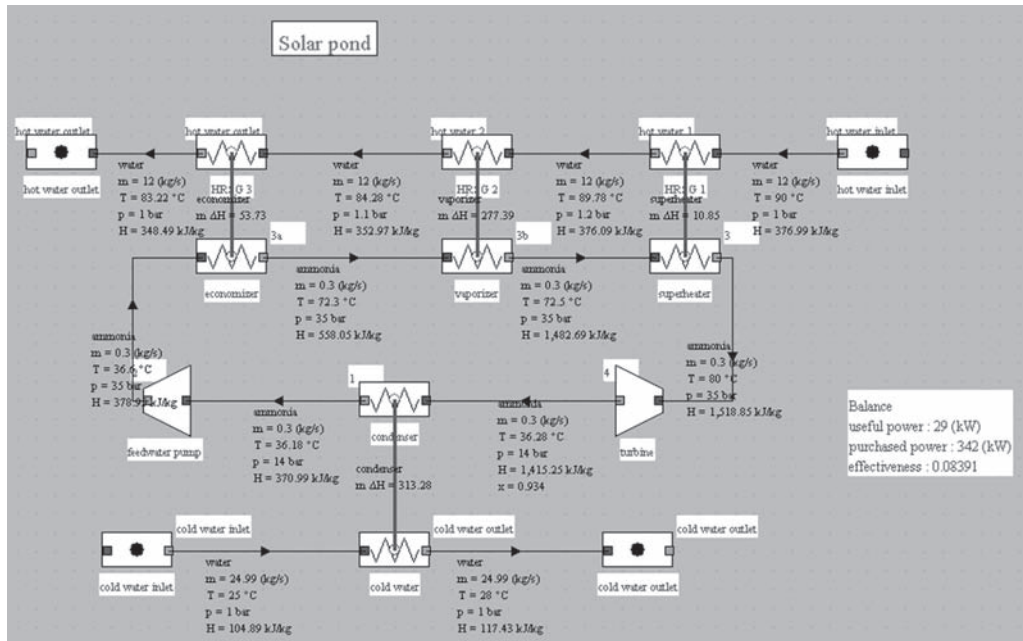


FIGURE 31.1.2

Synoptic view of the plant

chosen. Once this value obtained (about 0.3 kg/s), the flow of cooling water can be directly determined by exchanger “condenser” if we set its outlet temperature (e.g. 28°C). We find about 25 kg/s.

With these parameters, the results are displayed on the synoptic view of Figure 31.1.2: electrical power of about 29 kW, and low efficiency of 8.4%, which is mainly due to the small temperature difference between sources.

31.1.2 Plot of the cycle in the entropy chart

The cycle can easily be represented in thermodynamic charts, including entropy, as in Figure 31.1.3.

31.1.3 Exergy balance

The exergy balance of the ammonia cycle can be built without any particular difficulty, considering that the environment temperature is 25°C, and 90°C for the hot source. The results obtained are given in Figure 31.1.4.

What is most remarkable is that exergy efficiency is very high (47%), while energy efficiency is very low: this means that, although the difference in temperatures of sources is low, the performance of the facility is quite good.

31.1.4 Auxiliary consumption

An estimate of solar pond pumping losses leads to a pumping power close to 200 W for the hot brine, and 300 W for the cold brine, considering a piping length of 100 m and a diameter of 0.1 m. As for the pressure drops in the exchangers, they can be very low (about ten watts).

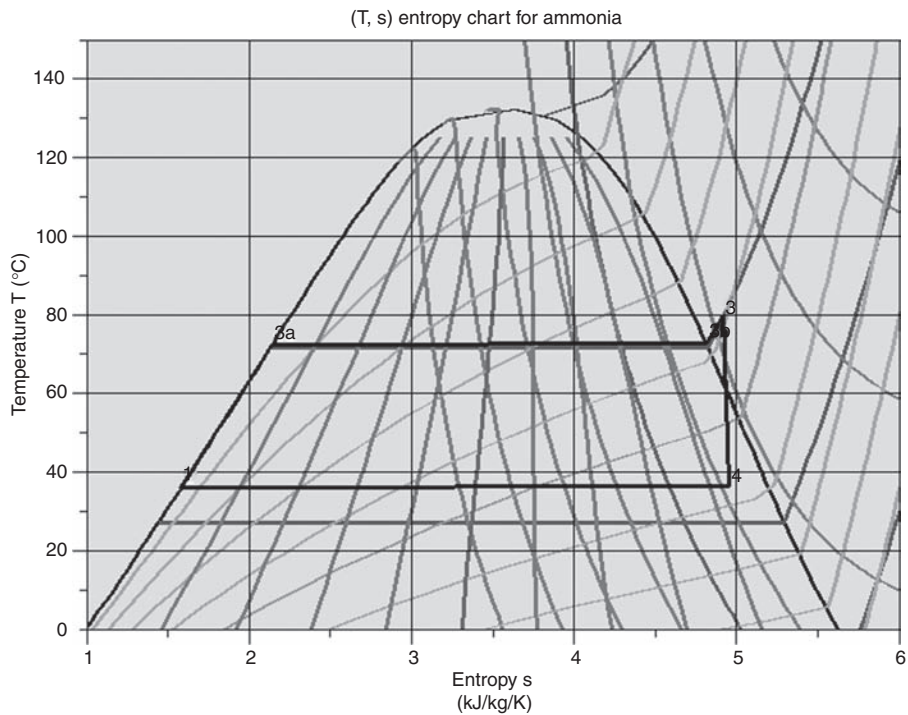


FIGURE 31.1.3
Cycle in the entropy chart

enthalpy balance				exergy balance				
component	dh	τ	Q	Tk	dxq	dxh	dxhi	% overall losses
condenser	-313		-313	298.15	0	-12	12	36%
superheater	11		11	363.15	2	2	0	1%
vaporizer	277		277	363.15	50	38	12	36%
economizer	54		54	363.15	10	4	6	18%
feedwater pump	2	2				2	0	0%
turbine	-31	-31				-34	3	10%
cycle	0	-29	29			0	33	100%
				$\sigma(xq+)$		61		
				$\sigma(\tau+)$		0.00		
energy efficiency		8.39%	exergy efficiency			46.82%		

FIGURE 31.1.4
Exergy balance

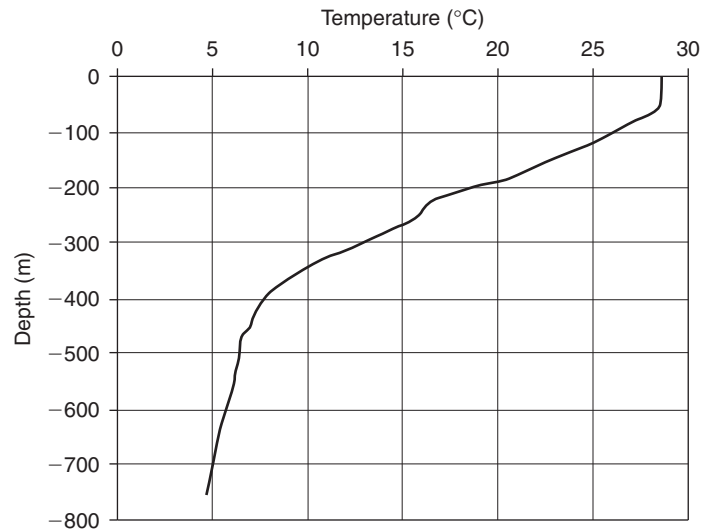
31.2 OCEAN THERMAL ENERGY CONVERSION (OTEC)

OTEC means Ocean Thermal Energy Conversion; its equivalent in French is Energie Thermique des Mers (ETM). OTEC cycles are designed to generate electricity in warm tropical waters using the temperature difference between water at the surface (26–28°C) and in depth (4–6°C), from 1000 m (Figure 31.2.1).

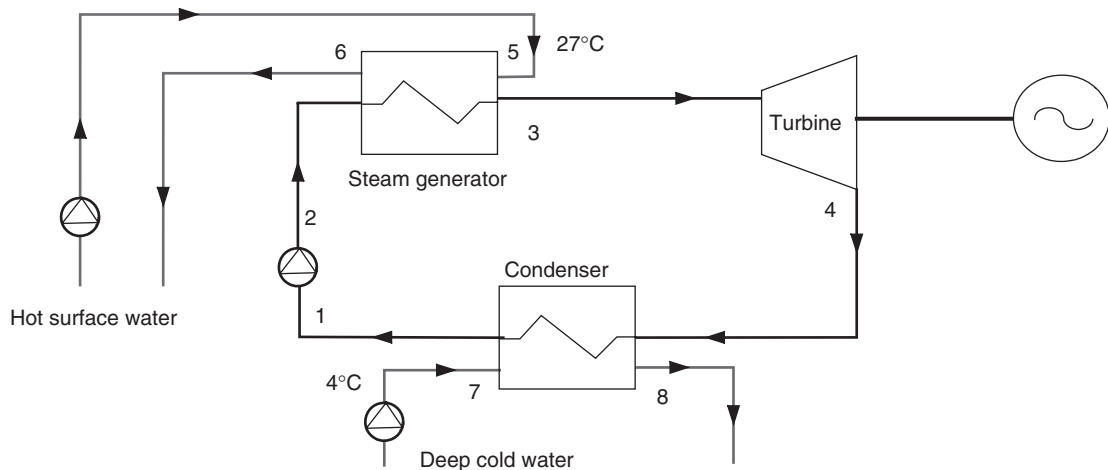
Two main types of cycles are used: closed cycles and open cycles, invented by two French, respectively Jacques d’Arsonval in 1881 and Georges Claude in 1940, who proceeded to a first experiment.

In all cases, the need to convey very high water flow rates and pump cold water at great depth induces significant auxiliary consumption. Optimization of an OTEC cycle is imperative to take into account those values.

Although technically valid, OTEC cycles are not yet economically viable. Prototypes of various capacities have been realized or are being considered, including in Hawaii and Tahiti.

**FIGURE 31.2.1**

Ocean thermal gradient

**FIGURE 31.2.2**

OTEC closed cycle

31.2.1 OTEC closed cycle

Closed cycles use hot water at about 27°C to evaporate a liquid that boils at a very low temperature, such as ammonia or an organic fluid. The vapor produced drives a turbine, then is condensed by heat exchange with cold water at about 4°C from deeper layers of the ocean.

The thermodynamic cycle is similar to the one we have studied in section 31.1.1 for solar ponds: an intermediate Hirn or Rankine cycle, whose modeling in Thermoptim poses no particular problem. The sizing of heat exchangers is of course even more critical given the very small temperature difference between hot and cold sources. Pinch values should be as low as possible while remaining realistic.

Obviously, if one seeks to compare the performance of cycles using different fluids, pinch values should be roughly the same.

A possible Thermoptim model of this cycle is given in Figure 31.2.3.

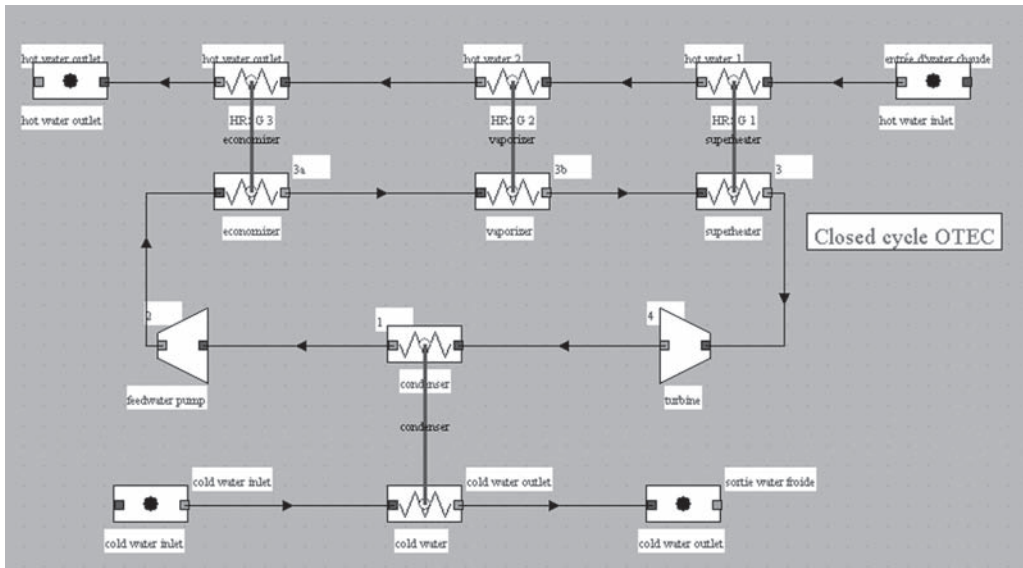


FIGURE 31.2.3
 OTEC closed cycle Thermoptim diagram

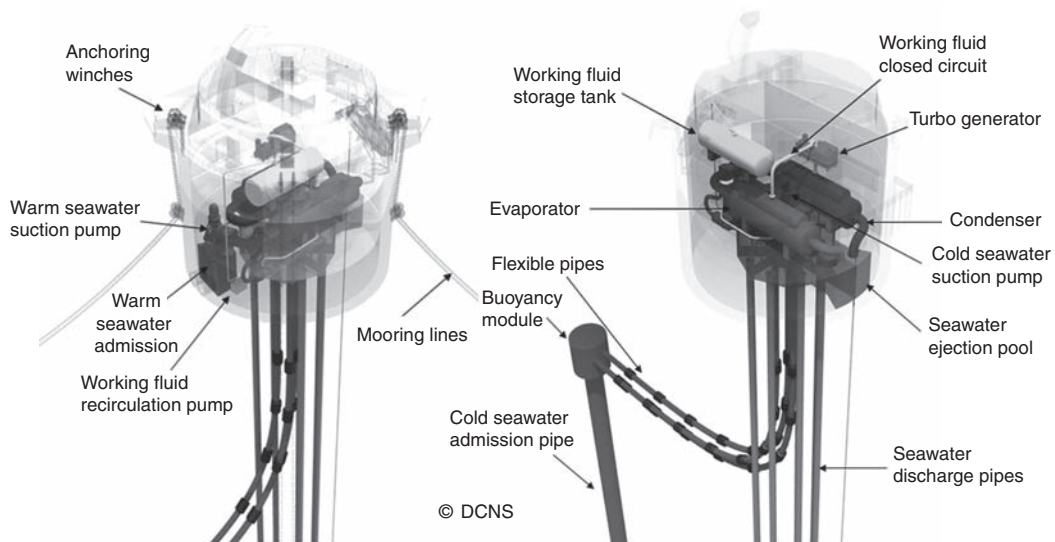


FIGURE 31.2.4
 Artist view of an OTEC plant (Documentation DCNS)

The hot water flow-rate is here equal to 27,000kg/s, its temperature 26°C and the cold water temperature 4°C.

All other values must be determined, justifying the assumptions made (thermodynamic properties of salt water will be taken equal to that of pure water).

You may check that although the OTEC closed cycle efficiency is low, its exergy efficiency may be correct.

Figure 31.2.4 presents an artist's view of an OTEC plant such as that being developed by DCNS, a prototype of which is considered in La Reunion Island (Fr). The transparent superstructure would

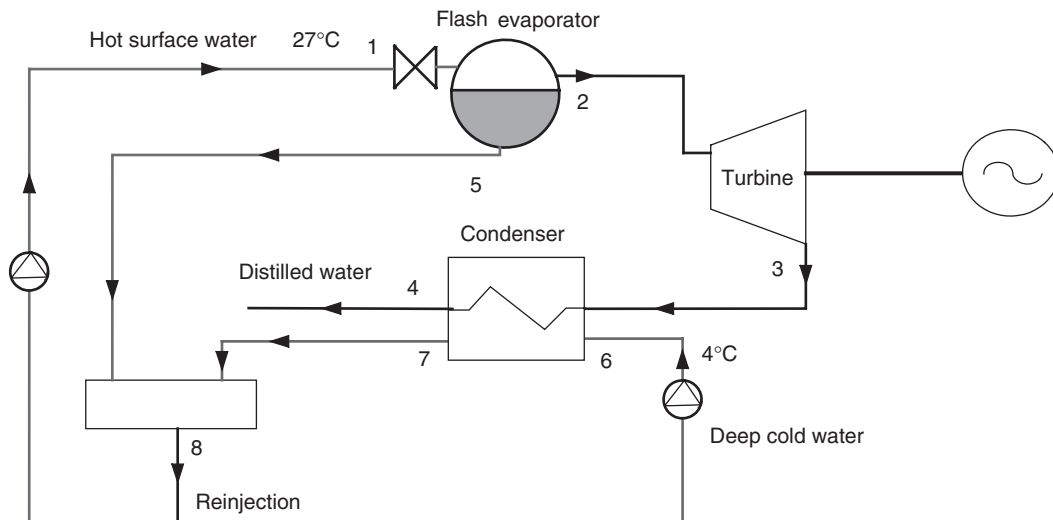


FIGURE 31.2.5

OTEC single flash open cycle

be floating on the sea, anchored by mooring lines. The image shows the different elements of the plant as well as the cold seawater admission pipes and the discharge pipes.

31.2.2 OTEC open cycle

In open cycles, warm water at about 26°C is expanded in a low-pressure chamber (called flash), which allows to evaporate a small fraction (around 5%). The steam produced drives a turbine and is condensed in a low pressure chamber by heat exchange with cold water at about 4°C from deeper layers of the ocean. The condensate is virtually pure water, which can be used for food.

The open cycle thus has the advantage of producing both electricity and fresh water, but the very low expansion ratio involves using very large turbines.

Figure 31.2.5 shows the cycle operation. It involves five elements: a flash evaporator, a turbine, a condenser, a basin for collecting used sea water, and a vacuum pump.

Hot water is pumped at the surface and brought to a certain height (1), then it is injected into the evaporator in which there is a slight depression determined by the height of the water column between the evaporator and the collection basin. Because of the pressure difference, water undergoes an isenthalpic throttling (flash) and a small fraction is vaporized (2), then headed to the turbine (2-3).

In the condenser pressure is lower than in the evaporator, thanks to the vacuum pump and the height of the water column between the condenser and the collection tank. The turbine expands the steam produced in the evaporator, producing mechanical power. The steam is then condensed (3-4) by exchange with cold water, producing fresh water.

The hot and cold water mixed in the collection basin (8) are fed back into the sea at a depth of sixty meters.

It is possible to model such a cycle with Thermoptim, to calculate its efficiency, then to build its exergy balance, and estimate the magnitudes of the system sizes (exchange surfaces, flow sections etc.), not forgetting to take into account the pumping power, *a priori* not negligible.

The synoptic view obtained for a cycle involving a little more than 6t/s of surface water is given in Figure 31.2.6. It leads to production of 28 kg/s of potable water and a capacity of 1,300 kW.

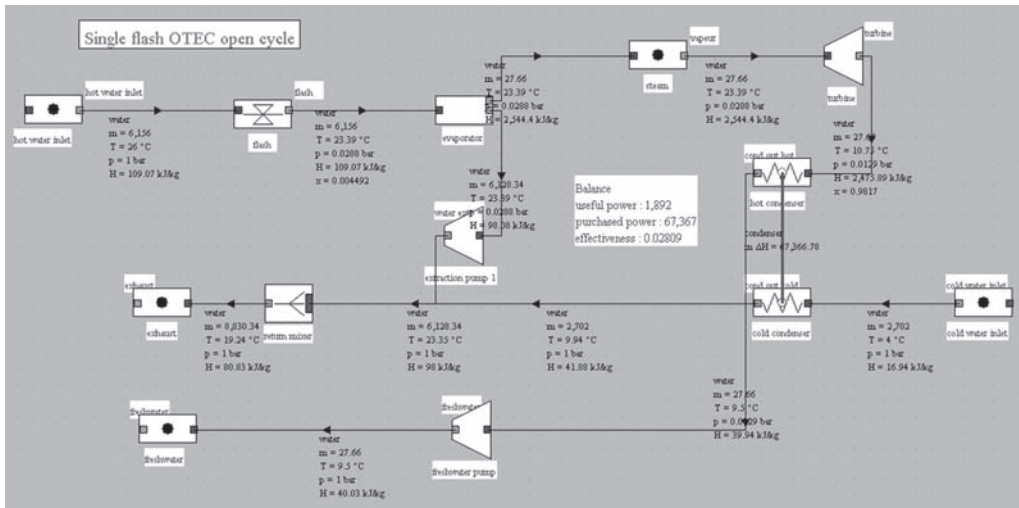


FIGURE 31.2.6
 Synoptic view of a single flash OTEC open cycle

It is also possible to model a more complex cycle with double flash, which would be a little more efficient and produce more fresh water.

31.2.3 Uehara cycle

In order to maximize a power generation cycle using ocean thermal energy, Uehara (1999) has developed a new cycle that he says is an improvement of the Kalina cycle studied in section 24.3.4, whose main feature is to simplify the composition change of the ammonia-water mixture by using a staged expansion with extraction (Figure 31.2.7).

As for the Kalina cycle, the interest of this cycle is to replace evaporation and condensation of the working fluid at constant temperature by changes with temperature glide, thus reducing system irreversibilities.

In this cycle, an ammonia rich mixture is heated in an economizer (4-5a) and an evaporator (5a-5) and exits in the two-phase state. The vapor (6) and liquid (7) phases are then separated, the first being expanded at an intermediate pressure in a turbine (6-11).

Part of this expanded stream is recirculated at medium pressure, then cooled (11-12) by exchange with the basic mixture (13-14), with which it is mixed to form the working fluid, which is then delivered under pressure (15-3).

The main flow exiting the HP turbine is expanded at low pressure in a second turbine (11-10) then led to an absorber where it is mixed with the liquid fraction (7) leaving the separator and precooled (7-8) in the regenerator by exchange with the working fluid leaving the rich pump (3-4), then expanded at low pressure (8-9).

At the absorber outlet, the basic mixture obtained is condensed before being compressed at the intermediate pressure (2-13).

Modeling of such a cycle in Thermoptim leads to a synoptic view of the type in Figure 31.2.8.

In our view, the main interest of this cycle is that it better valorizes the cold water from depths than a conventional closed cycle in which pumping takes a significant fraction of the power produced (10-15%): for the same water discharge temperature the working fluid may be cooled at lower temperature due to the temperature glide of the water-ammonia mixture.

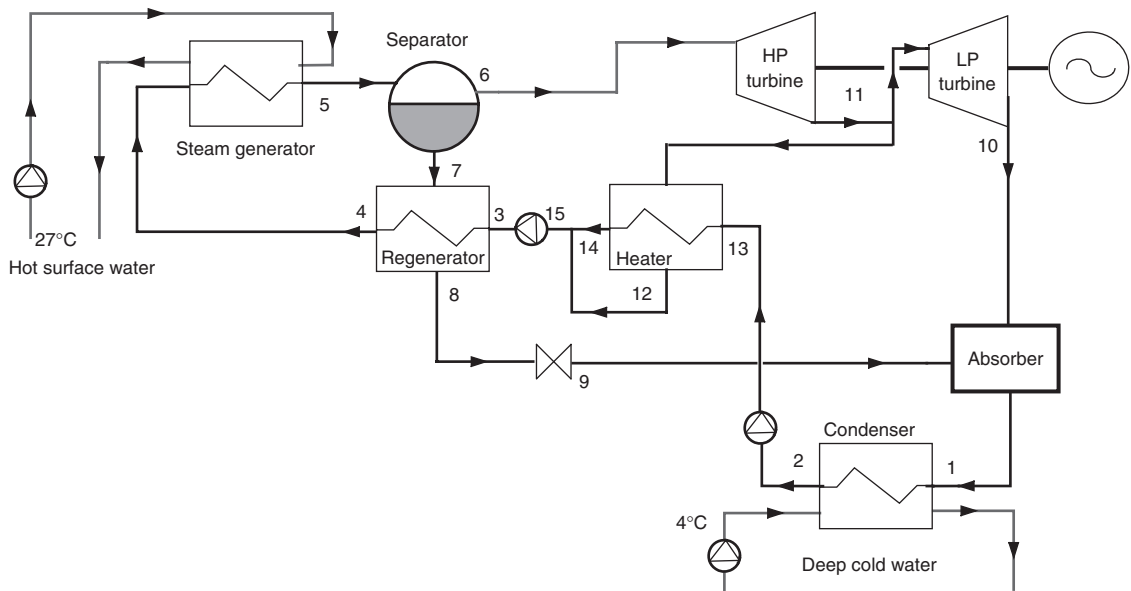


FIGURE 31.2.7

Uehara cycle

name: condenser		type: counterflow		Save	
hot fluid: condenser		cold fluid: cold water		Calculate	
Tce (°C)	11.16473984	<input checked="" type="radio"/> set	<input type="radio"/> calculated	Tfe (°C)	4
Tcs (°C)	9.48473	<input checked="" type="radio"/> set	<input type="radio"/> calculated	Tfs (°C)	10
mc	92.83677191	<input checked="" type="radio"/> set	<input type="radio"/> calculated	mf	2,151.27134035
Cpc	347.4140727			Cpf	4.19790708
m ΔHc	-54,185.02309074			m ΔHf	54,185.02309074
<input checked="" type="radio"/> unconstrained	UA		19,434.78365556	<input checked="" type="radio"/> design	
<input type="radio"/> minimum pinch	DTmin	0	R	0.28000164	
<input type="radio"/> set effectiveness	epsilon	0.837434455	NTU	2.15204673	
		LMTD	2.78804354		

FIGURE 31.2.8

Synoptic view of a Uehara cycle

Everything happens at that level in the cycle condenser, the use of ammonia-water mixture allowing the working fluid to be cooled much more than if it were a pure substance. In the example in Figure 31.2.9 (pinch of 1.1°C and pumped cold water heating from 4 to 10°C), the working fluid is cooled below the discharge seawater temperature, which does not allow an OTEC cycle of the type in Figure 31.2.3. It follows that the model of Figure 31.2.7 has a cycle efficiency of 3.2% while the equivalent closed-cycle would not exceed 3%, representing an improvement of about 10%.

FIGURE 31.2.9

Condenser screen

31.3 GEOTHERMAL CYCLES

Geothermal energy comes from the gradual temperature increase as one penetrates deeper into the earth's crust, either because of the natural gradient ($3^{\circ}\text{C}/100\text{m}$, with an average flux of $60\text{mW}/\text{m}^2$), or because of geophysical singularities (high temperature natural geothermal reservoirs of porous rock).

It is customary to distinguish three broad categories of reservoirs, according to their temperature levels:

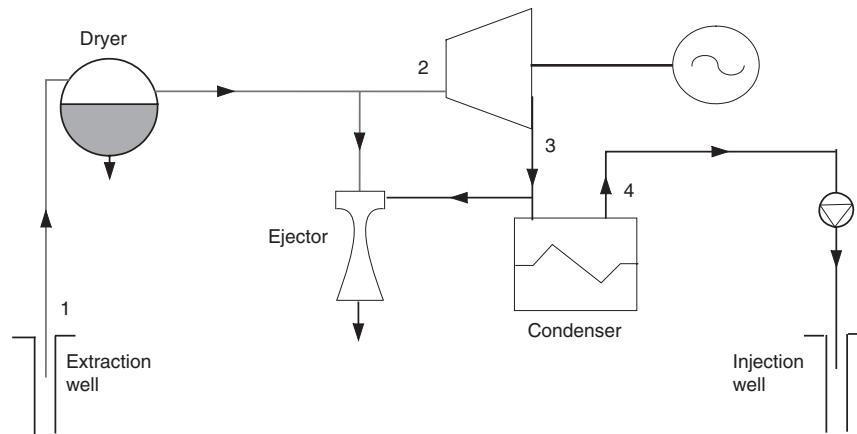
- high temperature ($>220^{\circ}\text{C}$);
- intermediate temperature ($100\text{--}200^{\circ}\text{C}$);
- low temperature ($50\text{--}100^{\circ}\text{C}$).

In the first case, the geothermal fluid can be essentially composed of water or steam, in the other two it is water, optionally under pressure. A special feature of geothermal fluid is that it is never pure water: it also includes many impurities, corrosive salts (the concentration limit for an operation to be possible is equal to $1.5\text{mol}/\text{kg}$) and non-condensable gas (NCG) in varying amounts ($0.1\text{--}10\%$). We shall see that this feature imposes constraints on thermodynamic cycles that can be used.

For environmental reasons, the geothermal fluid should generally be reinjected into the reservoir after use, but it is not always the case.

The thermodynamic conversion of geothermal energy uses four main techniques:

- plants called “direct-steam” can be used if the geothermal fluid is superheated steam that can be directly expanded in a turbine. Historically, this type of plant was first implemented in Larderello in Italy since 1904;
- flash vaporization power plants can exploit sites where geothermal fluid is in the form of pressurized liquid or liquid-vapor mixture. Today it is the type of plant most used. Geothermal fluid begins by being expanded in a chamber at pressure lower than that of the well, thereby vaporizing a portion, which is then expanded in a turbine;
- systems known as binary use a secondary working fluid, which follows a closed Hirn or Rankine cycle, the boiler being a heat exchanger with the geothermal fluid;
- fluid mixture systems, such as Kalina cycle, a variant of binary systems where the working fluid is no longer pure but consists of two fluids to achieve a temperature glide during vaporization.

**FIGURE 31.3.1**

Direct-steam plant

Mixed or combined cycles can use both a direct or flash system and a binary system. In what follows, we present these different cycles modeled in Thermoptim.

Immediately note a small feature of some of these models: in a geothermal cycle calculating purchased energy is not always immediate, since the geothermal fluid (which will be treated as water) is most often distributed in several streams, reinjected or not. We can therefore rarely directly estimate the enthalpy it provides. When this happens, it is preferable not to declare in Thermoptim a process as “purchased energy”, and simply compare cycles on the basis of mechanical power produced.

To estimate an efficiency on a comparable basis, we may consider as a reference a cycle that would allow the entire geothermal fluid to be reinjected at a temperature of 50°C. We will talk then of reference efficiency.

Note that temperature and pressure levels of the geothermal fluid considered in the examples that follow are not necessarily the same, leading us to temper these comparisons.

31.3.1 Direct-steam plants

Direct-steam cycle is very close to that of Hirn or Rankine. The main difference comes from the need to extract the NCG in order to condense water at the turbine outlet, which allows the steam to be expanded at pressure below the ambient. Depending on circumstances, the extraction is done using an ejector driven by geothermal steam, or a compressor coupled to the turbine.

Generally, the condenser cooling is provided by a cooling tower whose makeup water may be taken from the condensate itself.

As mentioned above, this type of plant requires the existence of dry steam in production wells, which is exceptional: the only known sites that have this property are Larderello in Italy and the Geysers in NW California.

The synoptic view of such a cycle is given in Figure 31.3.2. We considered available 111 kg/s of steam at 5.5 bar and 204°C, which represents approximately a 50°C superheating. This steam is expanded at 0.123 bar, 50°C and then condensed and recompressed before reinjection. In this case, the mechanical power produced is 57.3 MW, the cycle efficiency being 20.9%.

31.3.2 Simple flash plant

Generally, the well contains a low quality (below 0.5) liquid-vapor mixture, which cannot be sent directly to the turbine.

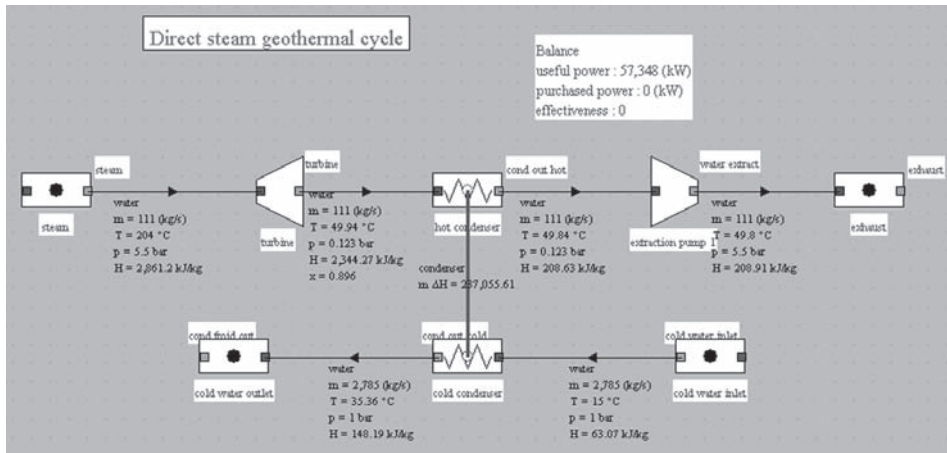


FIGURE 31.3.2
 Synoptic view of a direct steam geothermal cycle

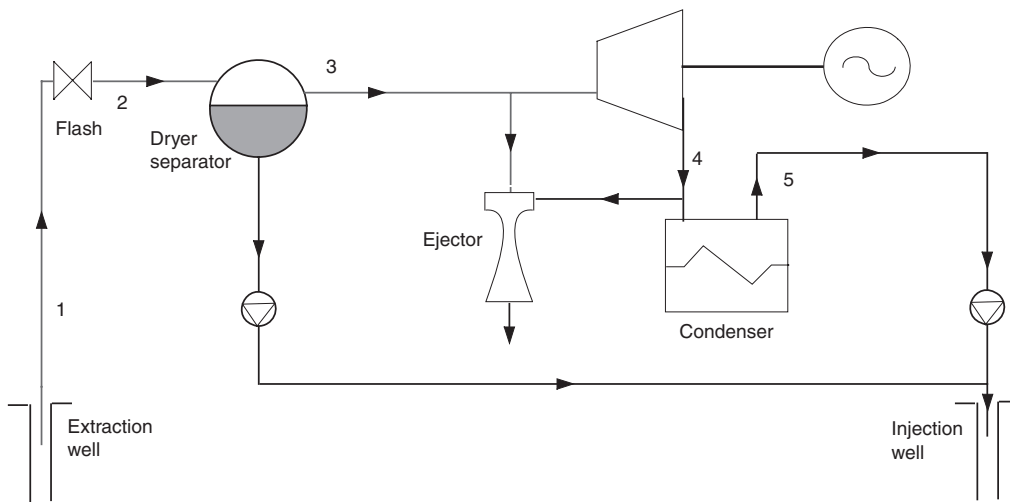


FIGURE 31.3.3
 Single flash plant

If the initial pressure is sufficient, a solution is to partially expand the mixture in order to vaporize a portion, which is then sent to the turbine, while the liquid fraction is reinjected.

As in the case of direct-steam plant, the vapor phase typically contains a significant amount of NCG to be extracted if we want to condense water at the turbine outlet.

Note that steam through the turbine is distilled water which can sometimes be valorized notably as drinking water.

Figure 31.3.4 shows the synoptic view of such a cycle modeled in ThermoOptim. We assumed that we had 760 kg/s of hot water in the saturated liquid state at 230°C and 28 bar.

This water undergoes a flash at 6 bar, leading to a 0.15 quality. The liquid and vapor phases are then separated, the first being recompressed before reinjection, whereas the latter is expanded at the pressure of 0.123 bar (50°C) and then condensed. The mechanical power produced is 57 MW and efficiency 9.6%.

Note that the pressure at which the flash is performed (6 bar) has not been optimized. The condensing pressure and temperature are relatively high because of noncondensable gases present in the geothermal fluid.

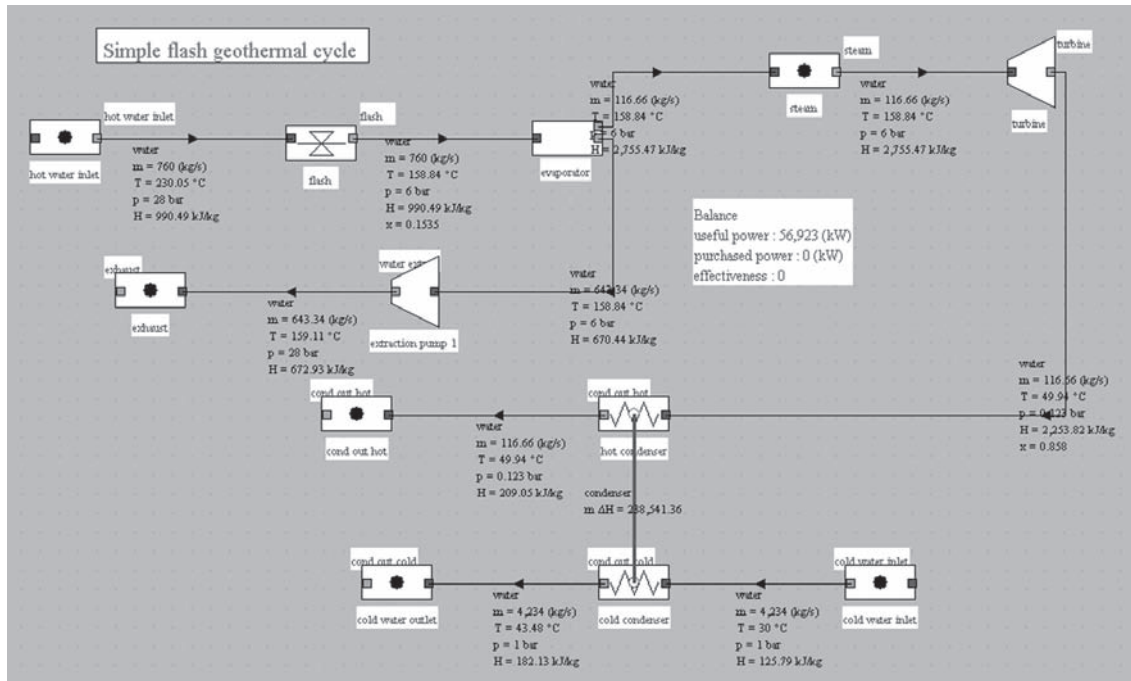


FIGURE 31.3.4
Synoptic view of a single flash geothermal cycle

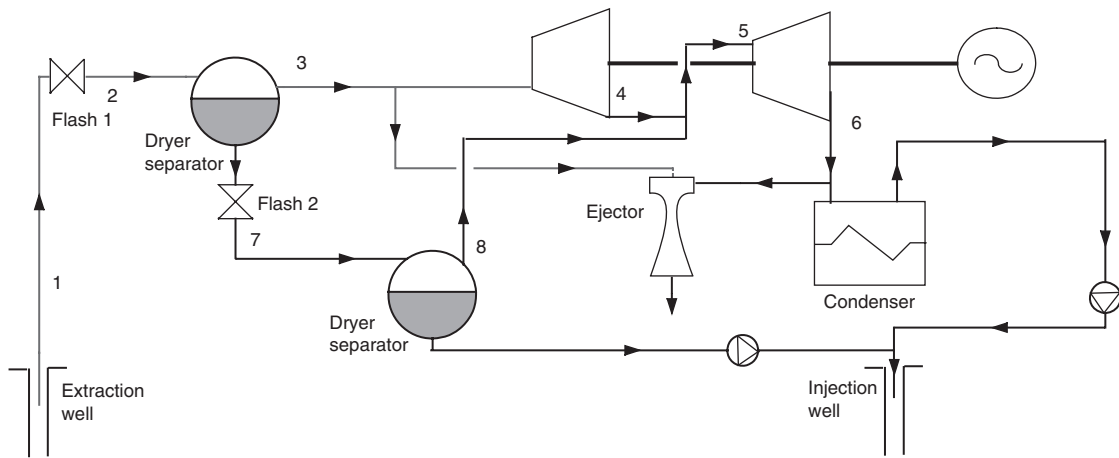


FIGURE 31.3.5
Double flash plant

31.3.3 Double flash plant

In some cases, if the pressure at the well outlet is sufficient, it is possible to achieve a double flash, which allows steam to be obtained at two different pressure levels and increases plant performance.

Theoretically, we could thus increase the number of flashes, but technological and economic constraints limit them in practice to 2.

As shown in the synoptic view of Figure 31.3.6, the liquid stream, which in the previous cycle was recompressed and re-injected, undergoes this time a second flash at a pressure of 0.931 bar, which leads to a 0.115 quality.

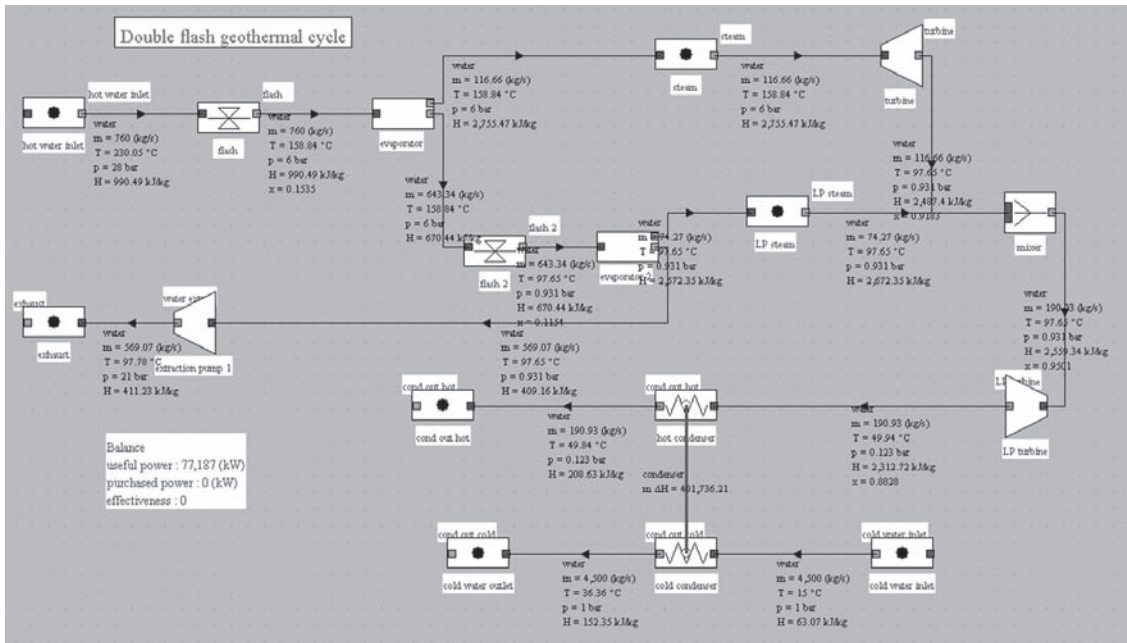


FIGURE 31.3.6
Synoptic view of a double flash geothermal cycle

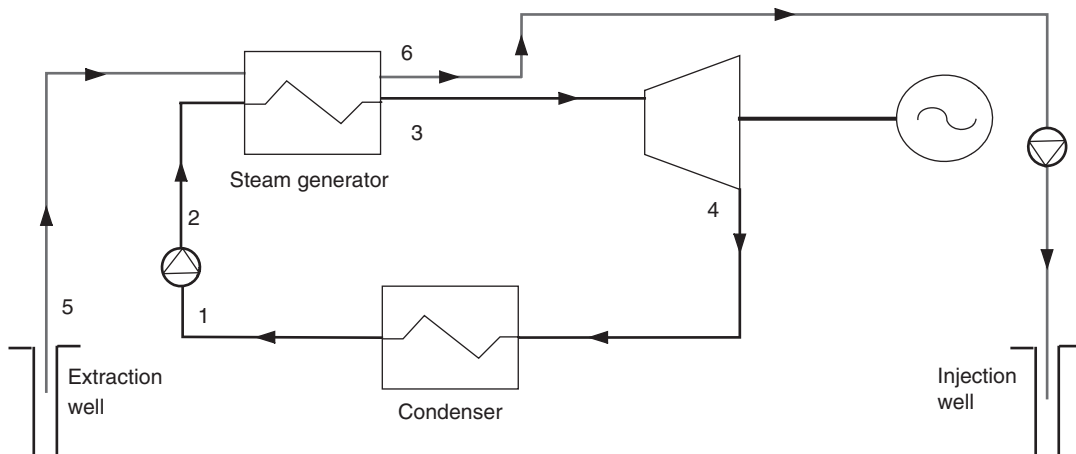


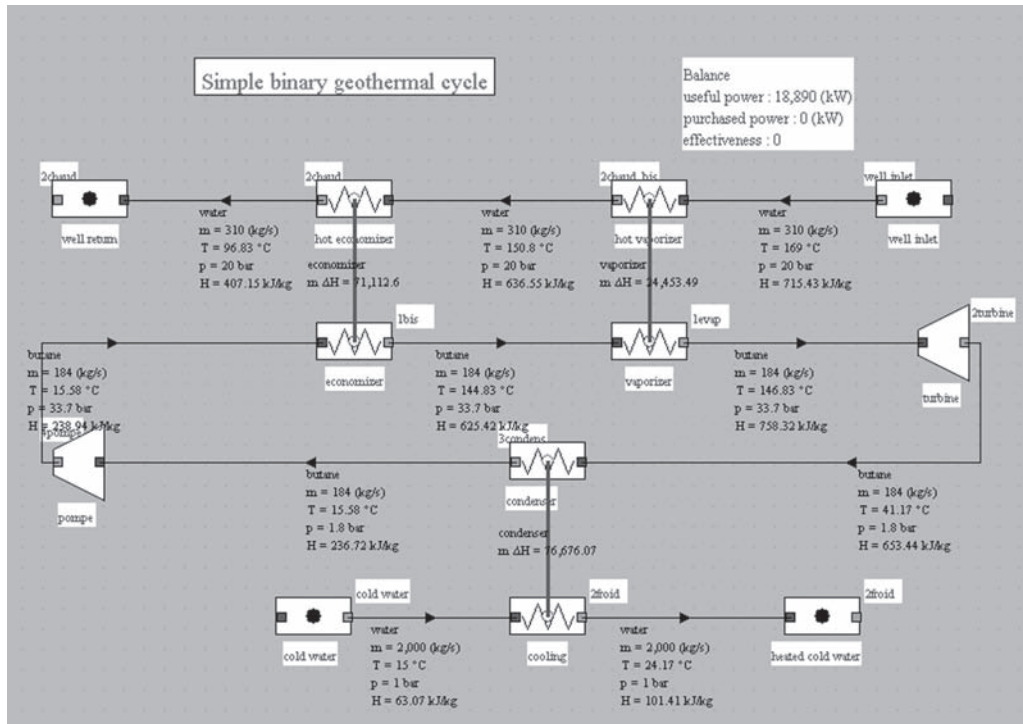
FIGURE 31.3.7
Binary cycle

The liquid phase is recompressed and reinjected, while the vapor is mixed with the steam flow from the first flash expanded at the same pressure. The whole is then expanded at the condenser pressure in a LP turbine. Mechanical power produced rises from 57 to 77 MW, representing an increase of 35%. Efficiency becomes 13%.

Here too the flash pressures (6 and 0.931 bar) have not been optimized.

31.3.4 Binary cycle plants

When the temperature or pressure at the well outlet is low, it becomes impossible to make use of direct-steam or flash cycles. We then use a second working fluid, which follows a closed Hirn or Rankine cycle (with or without superheating).

**FIGURE 31.3.8**

Synoptic view of a butane binary geothermal cycle

The geothermal fluid then transfers its heat to the fluid before being reinjected.

A cooling tower ensures condensation of the working fluid, whose choice depends on many considerations, technological, economic and environmental. Since this is often an organic fluid, it is customary to speak of Organic Rankine Cycle (ORC).

Figure 31.3.8 shows the synoptic view of such a cycle modeled in ThermoOptim. We assumed we had 310 kg/s of hot water in the subcooled liquid state at a temperature of 169°C and pressure of 20 bar.

This water is used to vaporize with a very low superheating (2°C) butane, which is then expanded in a turbine and condensed in an entirely conventional Hirn cycle. The mechanical power produced here is 18.9 MW, and the efficiency 12%.

The condensation pressure and temperature of butane may be here lower than for the geothermal fluid in flash cycles because of the absence of noncondensable gases in the second cycle.

Like any Hirn cycle, this cycle can be improved by judiciously introducing reheats and/or extractions.

31.3.5 Kalina cycle

The Kalina cycle, which was presented in detailed manner in section 25.4, uses as working fluid system “water – ammonia”, which has an important temperature glide.

The Kalina cycle replaces the ORC cycle of the previous example.

Given the temperature glide, irreversibilities in heat exchanger between the geothermal fluid and the working fluid are reduced, and geothermal heat better used. Compared to the binary cycle, mechanical power produced rises from 19 to 23.5 MW, and the efficiency reaches 18.9%.

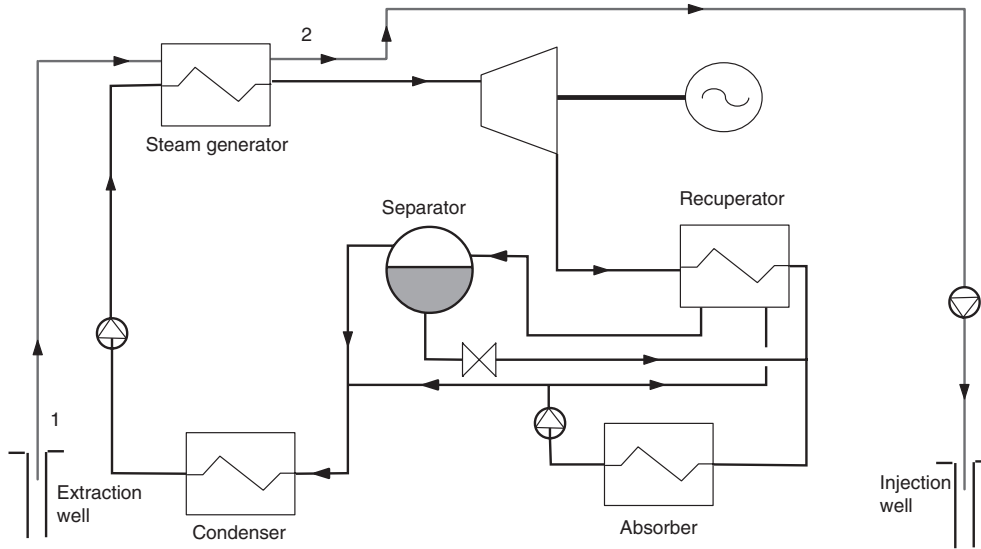


FIGURE 31.3.9
Kalina geothermal cycle

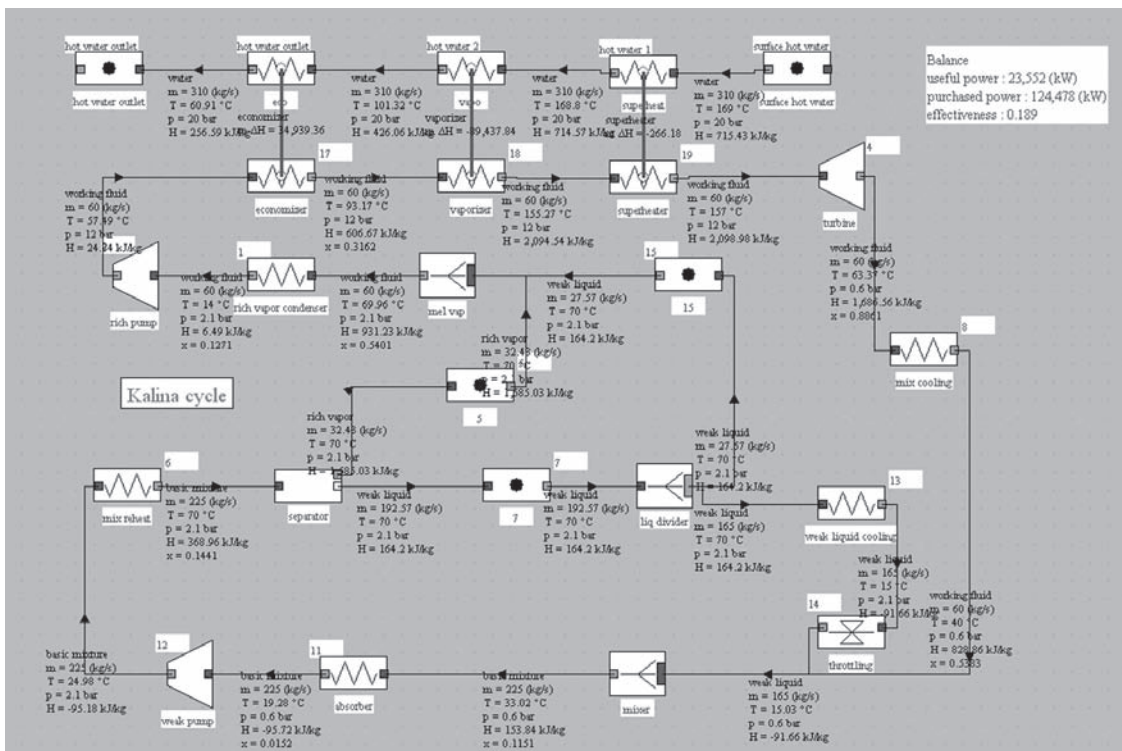


FIGURE 31.3.10
Synoptic view of a Kalina geothermal cycle

31.3.6 Combined cycles

As we have seen, one of the constraints encountered in condensation of direct-steam or flash cycles is the need to extract NCG, resulting in significant parasitic energy consumption.

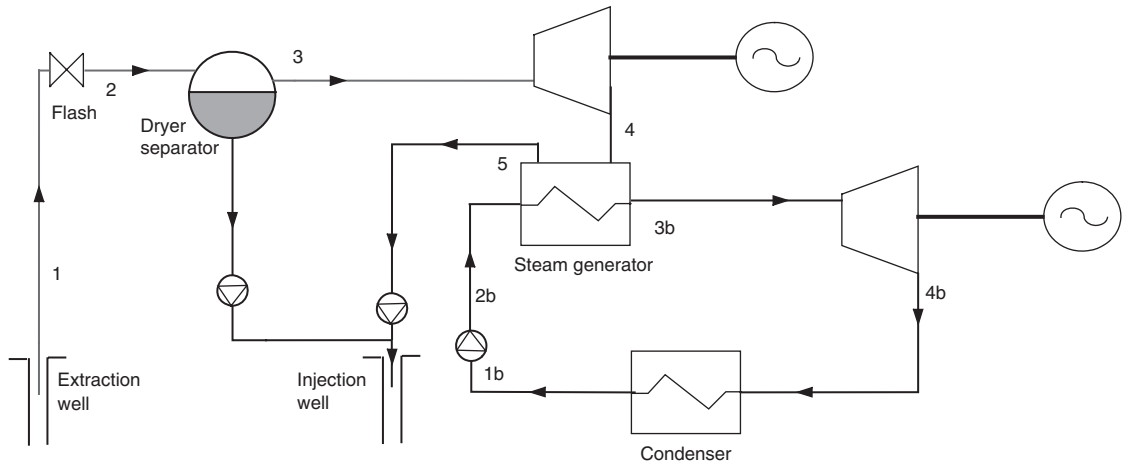


FIGURE 31.3.11
Combined cycle

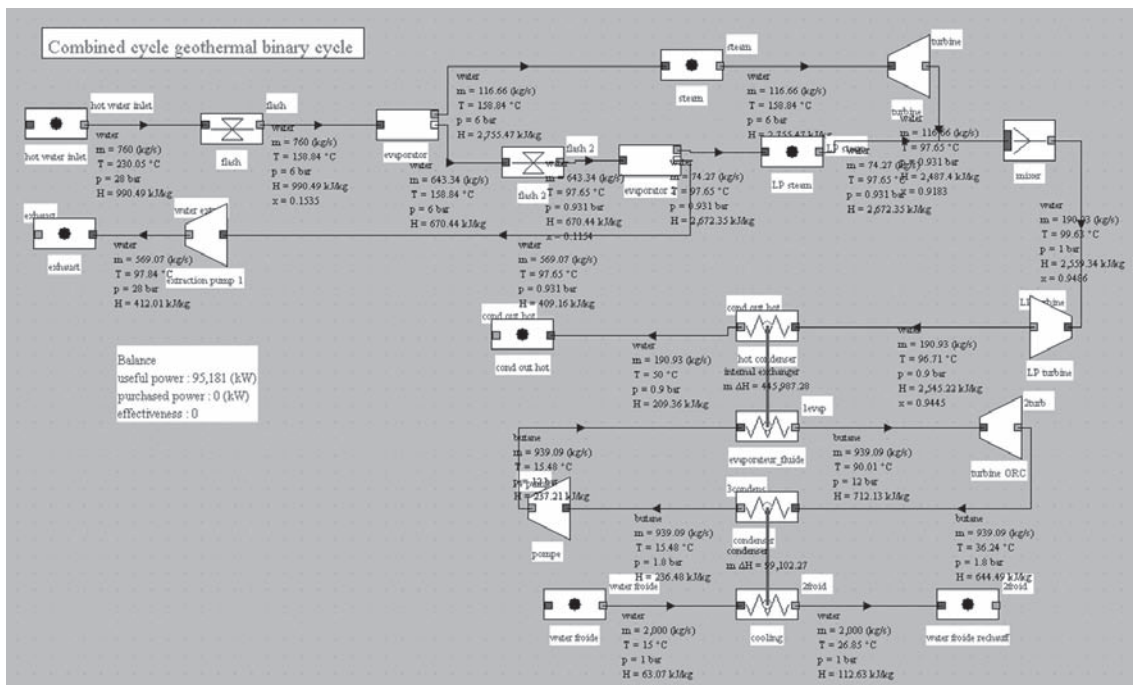


FIGURE 31.3.12
Synoptic view of a geothermal combined cycle

An alternative is to use a combined cycle, combining direct-steam or flash cycle with an ORC, the steam leaving the turbine being at a pressure higher than atmospheric, and being cooled in the boiler of the second cycle.

Let us for example consider the case of the double-flash cycle studied previously, the steam being expanded this time at only 0.9 bar instead of 0.123 bar and then cooled at 50°C in a heat exchanger used as vapor generator for a butane Hirn cycle.

This gives the combined cycle in figure 31.3.12: mechanical power increases from 77 to 95 MW and efficiency from 13 to 16.1%.

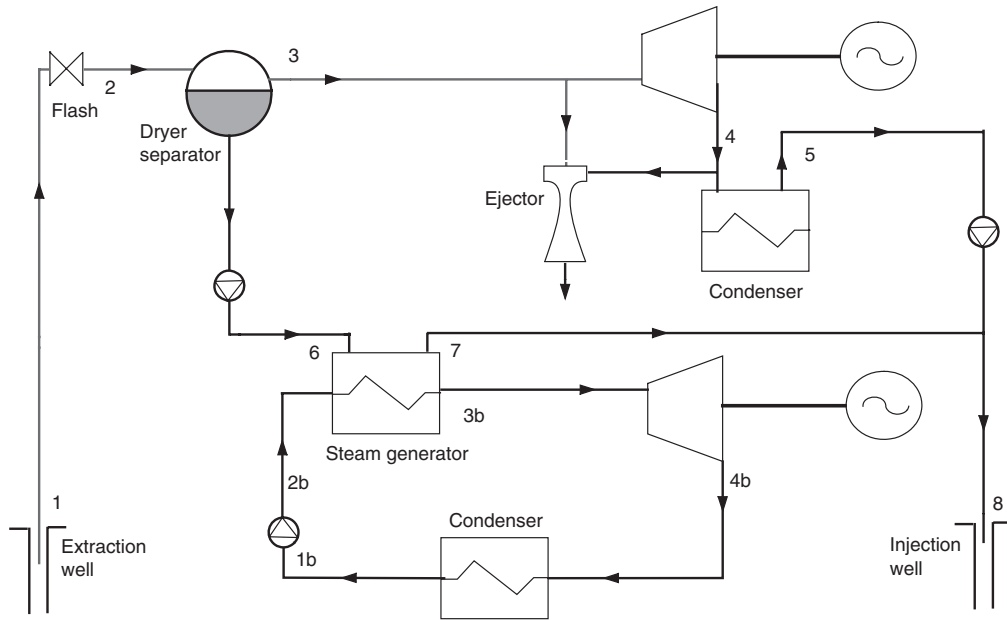


FIGURE 31.3.13
Mixed cycle

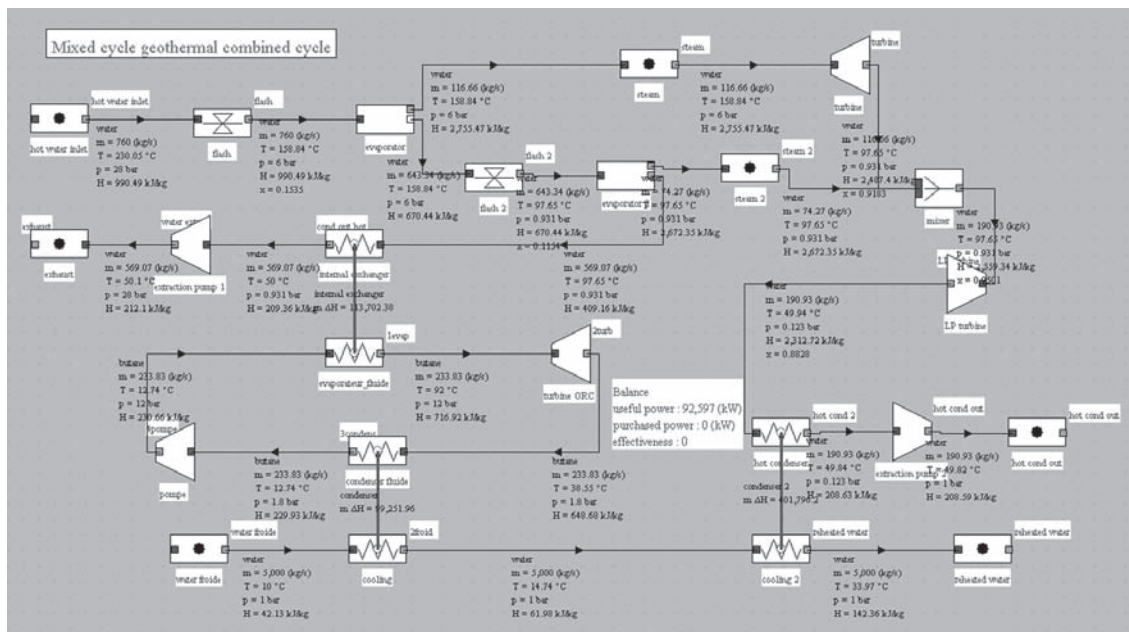


FIGURE 31.3.14
Synoptic view of a geothermal mixed cycle

31.3.7 Mixed cycle

One major drawback of flash cycles is that they exploit only a small share of the total flow of geothermal fluid, the one corresponding to the vapor fraction after the flash, the liquid fraction being reinjected.

Mixed cycles valorize the geothermal fluid, using the liquid fraction to provide the energy necessary for an ORC cycle.

One can thus obtain a total efficiency well above that of a flash cycle. Of course, if the topping cycle of a combined cycle is the flash type, it is possible to associate a second ORC cycle of the mixed type.

Let us consider again the double flash cycle studied in section 31.3.3, and add a butane Hirn cycle, no longer on the circuit of expanded steam, but this time on the circuit before reinjection of geothermal fluid. The diagram of Figure 31.3.14 shows the result: mechanical power produced increases from 77 to 94 MW and efficiency from 13 to 15.8%. The gain is somewhat lower than that obtained in the combined cycle, but already quite significant. Note that it would indeed be quite possible to add this butane cycle on the combined cycle, which would improve performance.

31.4 USE OF BIOMASS ENERGY

In this section, after a brief presentation of the main biomass energy conversion systems, including thermochemical processes, we give some details on gasification, and then introduce an external class that models different types of combustion of this fuel type.

31.4.1 Introduction

We call biomass all organic materials, mainly of vegetable origin, natural or cultivated, land or sea, produced by chlorophyll conversion of solar energy, fossil fuels excluded.

Biomass is mainly composed of lignin ($C_{40}H_{44}O_6$) (25%) and carbohydrate $C_n(H_2O)_m$ (cellulose $C_6H_{10}O_5$ and hemicellulose) (75%).

Biomass can be converted in energy by three main categories of processes:

- biochemical conversion: digestion, hydrolysis and fermentation;
- chemical conversion (esterification);
- thermochemical conversion: combustion, co-combustion, pyrolysis and gasification.

Biochemical conversion comprises two main types: anaerobic digestion and aerobic digestion.

In the first case, which occurs in the absence of oxygen, there is production of a “biogas”, consisting mainly of methane (50–65%), CO_2 (30–35%) and other gases. Reactions take place at temperatures between 20 and 70°C. The basic reaction is:



In the second case, there is production of more CO_2 and H_2O .

Thermochemical conversion is divided into combustion and co-combustion (excess air), gasification (lack of air) and pyrolysis (in the absence of air).

Combustion is the oldest and probably most used conversion mode for both domestic and industrial uses. Its efficiency is good insofar as the fuel is rich in structured carbohydrates (cellulose and lignin), and especially dry enough (humidity below 35%).

Co-combustion is to simultaneously burn a fossil fuel, usually coal, and biomass (up to 15%) to reduce, in an existing boiler, the amount of initial fuel.

We call the C/N ratio the ratio of the amounts of carbon and nitrogen in biomass. It varies from 10 to about 100. Pyrolysis allows conversion of relatively dry biomass (humidity below 10%) of C/N ratio greater than 30, in various high LHV fuels, storable, gaseous, liquid and solid (charcoal). It takes place at temperatures between 400 and 800°C, and can be done in several modes: slow pyrolysis or char (solid product only), conventional pyrolysis at moderate temperature (600°C) (1/3 gas, 1/3

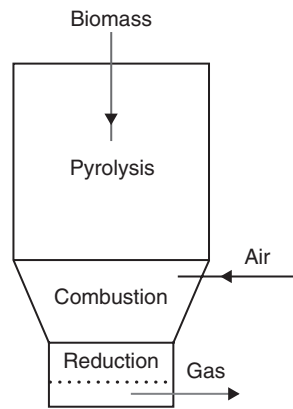


FIGURE 31.4.1
Parallel-flow downdraft gasifier

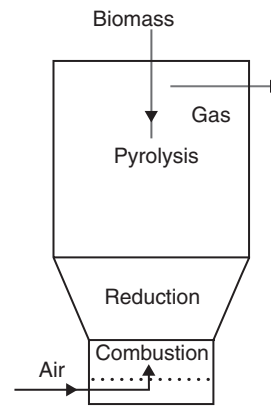


FIGURE 31.4.2
Counter-flow updraft gasifier

liquid, 1/3 solid), fast pyrolysis at 500–600°C, which takes place in about one second (70–80% of liquid), flash pyrolysis at over 700°C and in less than one second (more than 80% of liquid).

Gasification of biomass is obtained by performing combustion with lack of air in schematically two main stages: pyrolysis producing gas, liquid and solid phases, followed by the gasification itself of the last two phases.

In a gasifier, the fuel begins by being dried and is then pyrolyzed, these two steps being endothermic. The gaseous products are then burned at high temperature, releasing heat, a part of which is used by the previous two steps. The exhaust gases are then put into contact with the solid phase after pyrolysis and with water from the drying, which causes a reduction reaction which leads to the formation of a synthesis gas rich in CO and H₂, whose LHV is approximately 70 to 75% of that of the original biomass.

Several gasification processes exist:

- fixed bed systems, which consist of two main technologies, the parallel-flow gasifiers (downdraft), and the counter-flow (updraft);
- fluidized bed systems, which consist of three categories depending on the fluidization speed, dense, circulating and entrained fluidized beds.

The first match small or medium facilities, and the latter large ones. The advantages and disadvantages of these systems are given below (van de Steene et al., 2003).

31.4.1.1 Parallel-flow gasifiers (downdraft)

Of simple design and construction (Figure 31.4.1), these devices have a high conversion efficiency, and are very well suited for certain fuels, that they convert into a relatively clean gas. Their maintenance cost is however high (wear). The fuel should be uniform, low humidity and significant size. The capacity is very limited (350kWe), and ash fusion may happen in the reactor grid, which locks the device.

31.4.1.2 Counter-flow gasifiers (updraft)

These gasifiers are also simple in design and construction (Figure 31.4.2), and have high conversion efficiency, but are unsuitable for producing electricity. However, they are more flexible with respect to raw material moisture. Gases highly loaded in tar exit at low temperature, with condensation risk.

31.4.1.3 Dense fluidized bed gasifier

Since the 70s, we looked for combustion processes which can significantly reduce pollutant emissions during combustion of low quality fuels.

Fluidized bed technology involves (cf. Section 16.2.2.2 of Part 3) blowing a gas vertically beneath a layer of solid particles of suitable size. At a certain gas velocity, the particles are raised and the layer swells, creating a suspended medium whose behavior is similar to a fluid: it is said that the bed is fluidized. If the gas velocity increases, the particles are mixed and transported: the bed becomes turbulent.

The technology of dense fluidized bed gasifiers, characterized by high reaction rates and good solid/gas contact, allows temperatures to be controlled well. Of relatively simple and operational construction, they are not limited in size, although their economically optimal capacity exceeds 20 MW. Treatment in the catalytic bed is possible, tar is moderate to high, and particles are high. Entrainment losses of carbon in ash limit their performance. Fuel must be low humidity (<20%), be packaged in the form of small pieces, combustion being sensitive to their distribution in the bed.

31.4.1.4 Circulating fluidized bed gasifier

These high conversion efficiency devices provide good temperature and reaction speed control. They have a high tolerance for fuel (type, size), although the best performance is achieved with small particle size and low humidity (<20%). Tar in the gases is moderate, but particles are high.

As dense fluidized beds, they are not limited in size, although their economically optimal capacity exceeds 20 MW, and entrainment losses of carbon in ash limit their efficiency.

31.4.1.5 Entrained fluidized bed gasifier

These high conversion efficiency gasifiers ensure good gas-solid contact. Their high temperature operation produces gas of quality but low LHV, clean with little tar, and leads to vitrification of ashes. However, the cost of biomass preparation is high and the types of fuels limited. The capacity of these plants is large (>50 MWe).

31.4.2 Modeling thermochemical conversion

This section presents a simplified model that can simulate different types of biomass combustion, and in which it is possible to vary with considerable flexibility fuel composition and moisture and combustion conditions. The external class in which it is implemented, called BiomassCombustion, can be used to simulate both a boiler or a parallel-flow gasifier.

This model is quite simplified compared to those currently being studied in research laboratories, particularly in its representation of pyrolysis (Vijeu et al., 2005). Its main interest is to allow Thermoptim users to approach the study of thermochemical biomass conversion and the insertion of gasifiers or combustors into complete systems.

To simplify the writing of the model, we took advantage of using the combustion calculation functions already present in Thermoptim (see section 23.4), just adding equations corresponding to reactions that the software does not take into account.

On the thermodynamics, the main parameters that influence biomass combustion are:

- first, of course, fuel composition;
- second, moisture, which firstly determines enthalpy required for drying, on the other hand plays on gas composition, and finally influences CO₂ dissociation;
- finally, quenching temperature and CO₂ dissociation rate.

To separate as much as possible the influence of these first two parameters, composition is that of dry fuel, and moisture is taken into account by adding water. Given that the overall moisture is not necessarily the one that governs the thermodynamic equilibrium, as part of the steam may not react, for reasons of kinetics or geometry, we introduced an additional parameter, equal to the fraction of water involved in combustion. Physically, this means that a fraction of the water is not

TABLE 31.4.2

	[CO]	[H ₂]	[CH ₄]	[CO ₂]	[N ₂]	LHV MJ/m ³ N
Charcoal	28–31	5–10	1–2	1–2	55–60	4.6–5.6
12% moist wood	17–22	16–20	2–3	10–15	50–55	5–5.85
Wheat straw	14–17	17–19	–	11–14		4.5
Typical estimate	19–15	15–20	3–5	10–15	40–50	4–6

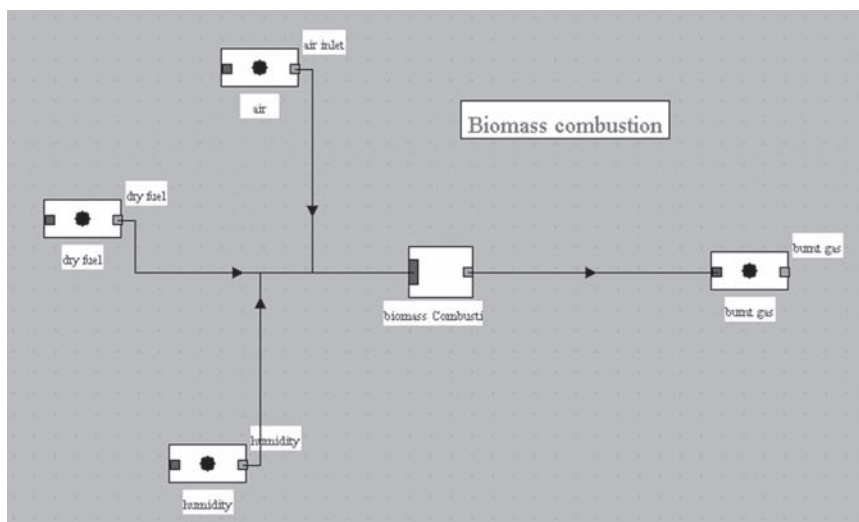

FIGURE 31.4.3

Diagram of the combustion structure

dissociated: it must be vaporized but its influence on the composition of the gas is the same as if it were inert.

The biomass composition varies widely depending on its origin and humidity. However, we can retain values close to 25% lignin (C₄₀H₄₄O₆) and 75% carbohydrates C_n(H₂O)_m (cellulose C₆H₁₀O₅ and hemicellulose).

An estimate of the synthesis gas composition and its LHV (values referred to the dry gas) is given in Table 31.4.2.

31.4.2.1 Definition of fuel and progress of combustion

Fuel definition is made in ThermoOptim as follows (Figure 31.4.3):

- dry gas composition, excluding species not included in ThermoOptim core, is estimated, for example in a spreadsheet, and entered in the form of a compound gas (process-point “dry fuel”);
- species not considered by ThermoOptim core are considered separately: they are entered in the component screen, and are subject to pre-combustion;
- dry gas is mixed with water (H₂O gas) to form moist fuel (process-point “humidity”);
- final combustion is calculated by core ThermoOptim functions, which are emulated from the external class (external mixer “biomass Combustion”), taking into account pre-combustion and enthalpy that would have been required to evaporate water.

The oxidant (usually air) is itself defined in process-point “air inlet”. Flows involved are also specified in each of the three process-points entering the external mixer. Their respective ratios allow the system to adjust the fuel moisture and excess air.

node: biomass Combustion type: external mixer

main process: burnt gas display: [button] m global: 12.639175

iso-pressure h global: 1,735.66729509 T global: 1,327.31926737

process name	m abs	T (°C)	H
air	10	20	-4.86
dry fuel	1.25	20	-6.58
humidity	1.25	20	83.99

biomass combustion

NH3 (% dry mass): 0.634

C solid (% dry mass): 10.5

quench T (°C): 900

CO2 diss. rate: 0.0500

H2O in combustion (%): 100.0

lambda: 1.22896

FIGURE 31.4.4

Biomass combustion component

component name	molar fraction	mass fraction
O2	0.01374655	0.01641626
H2	0.1041061	0.007832275
C2H6 ` éthane	0.1096048	0.1230014
CO2	0.2733782	0.4490144
CO	0.2348086	0.2454598
CH4 ` méthane	0.2643558	0.1582759

FIGURE 31.4.5

Composition of dry gas (LHV: 17.2 MJ/kg)

component name	molar fraction	mass fraction
CO2	0.1180614	0.1892233
H2O	0.2398588	0.1573671
O2	0.03282001	0.03824633
N2	0.5864343	0.5982773
CO	0.006213756	0.006338563
H2	0.009859662	0.0007238424
Ar	0.006752062	0.009823597

FIGURE 31.4.6

Composition of smoke (LHV: 0.15 MJ/kg)

31.4.2.2 Example of lack of air combustion (gasifier)

An example of lack of air combustion has been presented in section 23.4.1.2 to which you should refer for details. It shows how external class BiomassCombustion can be used for modeling a parallel-flow gasifier.

31.4.2.3 Example of combustion in excess air

In this example simulating a boiler burning biomass, combustion is performed in excess air.

Figure 31.4.4 shows the component screen allowing to model biomass combustion. In the case presented, we as previously assume that fuel comprises 0.634% ammonia and 10.5% carbon by dry mass and that quenching temperature is equal to 900°C. We assume however that all the moisture is involved in combustion, and CO₂ dissociation rate is 0.05, while its value was previously calculated.

A rate of 1.25 g/s of dry fuel, composition given Figure 31.4.5, humidity 50% by weight (water flow of 1.25 g/s) is burned with 10 g/s of dry air, leading to air factor $\lambda = 1.23$. Exhaust gas composition is given figure 31.4.6.

In Figure 31.4.4, in addition to values for exhaust gases (flow, temperature, enthalpy), magnitudes displayed are air factor λ and CO₂ dissociation rate (if $\lambda > 1$ it is an entry otherwise it is recalculated).

REFERENCES

- La géothermie, une énergie d'avenir*, Georama n° 12, journal d'information du BRGM, juin 2004.
- S. P. Babu, *Observations on the current status of biomass gasification, prepared for task 33, Gasification of biomass*, 2005.
- P. Bombarda, E. Macchi, *Optimum cycles for geothermal power plants*, Proceedings World Geothermal Congress 2000, Kyushu-Tohoku, Japan, June 10, 2000.
- R. Dipippo, *Small geothermal power plants: design, performance and economics*, GHC Bulletin, June 1999.
- R. Dipippo, *Second law assesment of binary plants generating power from low-temperature geothermal fluids*, Geothermics 33, pp. 565–586, 2004.
- K. W. Kwant, H. Knoef, *Status of gasification in countries participating in the IEA and GasNet activity*, 2004.
- Ph. Laplaige, J. Lemale, *Géothermie*, Techniques de l'Ingénieur, Traité Génie énergétique, BE 8 590v2.
- L. Van de steene, G. Philippe, *Le point sur la gazéification de la biomasse*, Bois-Energie n°1, 2003.
- H. Uehara, et al. (1999), "The Experimental Research on Ocean Thermal Energy Conversion using the Uehara Cycle", Proceedings of the International OTEC/DOWA Conference '99, Imari, Japan, pp. 132–141.
- R. Vije, L. Gerun, J. Bellettre, M. Tazerout, Z. Younsi, C. Castelain, *Modèle thermochimique bidimensionnel de pyrolyse de la biomasse*, International Congress on the Renewable Energies and the Environment – CERE, 24–26. mars 2005, Sousse, Tunisie, 8 p.

Heat and Compressed Air Storage

Abstract: This chapter, which deals with temporal energy management, must address energy storage, although this issue is not strictly speaking in the field of thermodynamics applied to energy systems.

We begin this chapter with a methodological section to illustrate these problems, then we focus our presentation on some storage systems which are either already widely used, especially for cooling, or still being considered and studied.

Our purpose being to study energy systems, we will not detail the technological aspects of thermal and air storage, referring readers to the literature. Note that we are only interested here in high capacity storage.

Keywords: Peak, off-peak power consumption, thermal storage, pneumatic storage, compressed air storage, CAES, phase change material, gas turbine, heat pump.

32.1 INTRODUCTION

Energy is generally very difficult to store, except in the form of fuels, including liquids. In particular, we do not know how to store in economic conditions large amounts of electricity, forcing power plant fleet managers to adjust their production to meet demand that fluctuates greatly, both daily or seasonally. This way of working however has its limits and has a cost, so that electricity prices vary widely depending on the time (Figure 32.1.1).

Several systems have been proposed to move off-peak power consumption in production during peak hours, such as compressing air when electricity is cheap, and expanding air in a turbine when it is expensive. The association of such a compressed air storage with thermal storage can improve system performance.

Thermal energy storage can be done in several ways:

- sensible heat: water, synthetic oils, pressurized steam, molten salts without phase change, ceramics, concrete etc.;
- latent heat: solid-liquid, liquid-vapor, solid-vapor or solid-solid phase transition for a variety of materials (water, paraffin, salts, metals etc.);
- thermochemical form through endo/exothermic chemical reactions, adsorption, absorption.

Pneumatic storage is compressing gas in the storage phase, then expanding it during the retrieval phase. The gas most often considered for this is air.

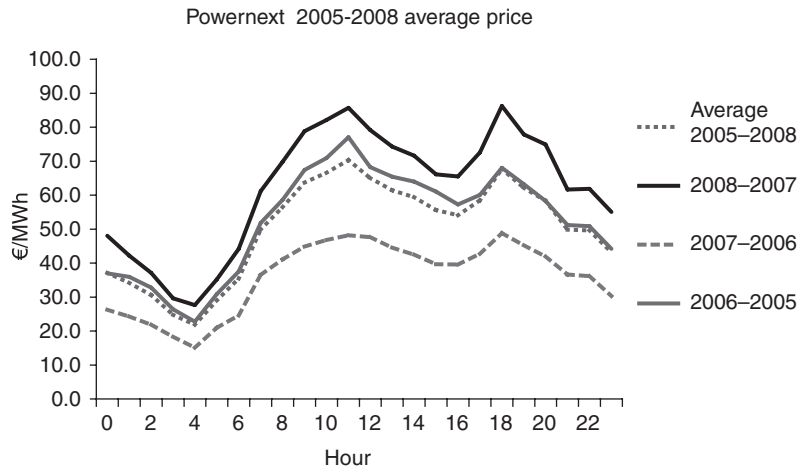


FIGURE 32.1.1

Changes in the average price of electricity during the day, Doc. Poweo

Both forms of storage can be combined to achieve better performance.

Almost always, thermal or air storage effectiveness is relatively low, so the use of such storage is generally justified in two cases:

- when resource is variable and not synchronized with needs. This is typically the case for solar installations;
- when the energy price varies greatly from one period to another. It may be interesting to store off-peak for release during peak hours.

In any case, during the retrieval phase, thermal or pneumatic storage systems do not restore energy in exactly the same state (in the thermodynamic sense of the word) as during the storage phase. Exergy losses are reflected by lower temperature and pressure; it is important to assess them if you want to be able to determine the functioning of the entire system. However, transfer functions between the stored energy and the energy removed from storage are often poorly known.

32.2 METHODOLOGICAL ASPECTS

The introduction of storage in a thermodynamic system poses a number of methodological difficulties. As might be expected, the storage-release operation induces losses, but their assessment can rarely be accomplished by a simple effectiveness that would be equal to the ratio of energy released to energy stored: the energy quality generally drops, and also depends on how the storage is made.

Let us consider a simple storage tank by sensible heat of a liquid thermal fluid (water, oil etc.). The modeling of such storage is usually done by considering two limiting cases, called “perfectly mixed storage” and “plug flow”. In the first case, we assume that at any time the temperature is uniform throughout the tank, set at the average value depending on its temperature before injection of fluid and on the amount of fluid added, whereas in the latter case, it is assumed that there is a perfect layering in the tank between the fluid initially present and the fluid stored (with the assumption that hot fluid is injected in the upper part of the tank).

Moreover, one can consider tank heat losses to the outside, usually assumed to be proportional to its surface and the temperature difference between the stored fluid and outside temperature.

It is clear that these two cases correspond to extreme situations, the first leading to exergy losses much larger than the second. The reality is certainly between the two: some mixing exists, but can be

minimized by taking technically-sound measures. It is thus possible, when you have a large storage tank, to design it in the form of modules connected to each other. Each module can then be considered mixed, while a very good stratification exists between different modules at different temperatures.

In pneumatic storage, a compressor fills a storage chamber by injecting a gas whose pressure and temperature vary depending on the storage state, because only the assumption of a perfectly mixed medium may be used. Compressor performance and thus energy cost of the operation also depend directly on technological characteristics and storage conditions. In release mode, pressure and temperature drop, also according to complex laws. Section 38.2.4 of Part 5 provides an example of modeling a simple system of this type.

To simulate in a plausible manner the operation of such facilities we must be able to correctly model not only the storage itself, but also how the rest of the system adapts to the temporal evolution of its condition. As shown in Part 5 dedicated to the technological design and off-design regime, models we must be able to build are much more complex than those we have seen so far.

32.3 COLD STORAGE IN PHASE CHANGE NODULES

We begin by presenting an example of latent heat system storage called STL, marketed by Company Cristopia (www.cristopia.com).

STL consists of a tank filled with a heat transfer fluid and nodules containing a phase change material whose melting point can be chosen between -33°C and 27°C . Approximately 60% of the volume of the tank is occupied by the nodules and the remaining 40% by the heat transfer fluid (ethylene glycol or brine). The number of nodules in a system determines both the total energy stored in the STL and heat exchanged between nodules and heat transfer fluid during charge and discharge.

Since industrial refrigeration systems must produce cooling energy with often very important loads for short durations (corresponding to production cycles), STL have many advantages such as significant reduction of cooling capacity installed (up to 70%), use of electrical energy at the lowest rates for savings, and management of refrigeration according to actual needs.

Figure 12.1.33 of Part 3 shows how such a storage device may be coupled to a gas turbine to cool the inlet air.

Performance of gas turbines being very sensitive to intake air temperature, it may indeed be advantageous to cool the air in an artificial way, using a compression refrigeration cycle. This is particularly the case in hot countries where power needs are time varying, and where the peak call is often due to air conditioning needs during the hottest hours. In such circumstances it may be economically attractive to produce ice during off-peak hours and use this ice as a cold source to cool the GT intake air during peak hours. The machine efficiency is slightly improved, but its capacity is substantially increased.

The example in Figure 12.1.33 of Part 3 is a gas turbine where the air, sucked at 30°C , is cooled at 1°C . The gain in efficiency is 1 point, but capacity is increased by 12.5%.

32.4 PROJECT SETHER (ELECTRICITY STORAGE AS HIGH TEMPERATURE HEAT)

Saipem Company has patented a storage method called THESE (Thermal Energy Storage of Electricity) which implements heat regenerators filled with refractory materials which store energy, and heat engines (turbines and compressors) used for energy conversion.

The storage method is based on innovative technology, which combines a heat pump during storage phase and heat conversion thanks to gas turbine cycles (Figures 32.4.1 and 32.4.2).

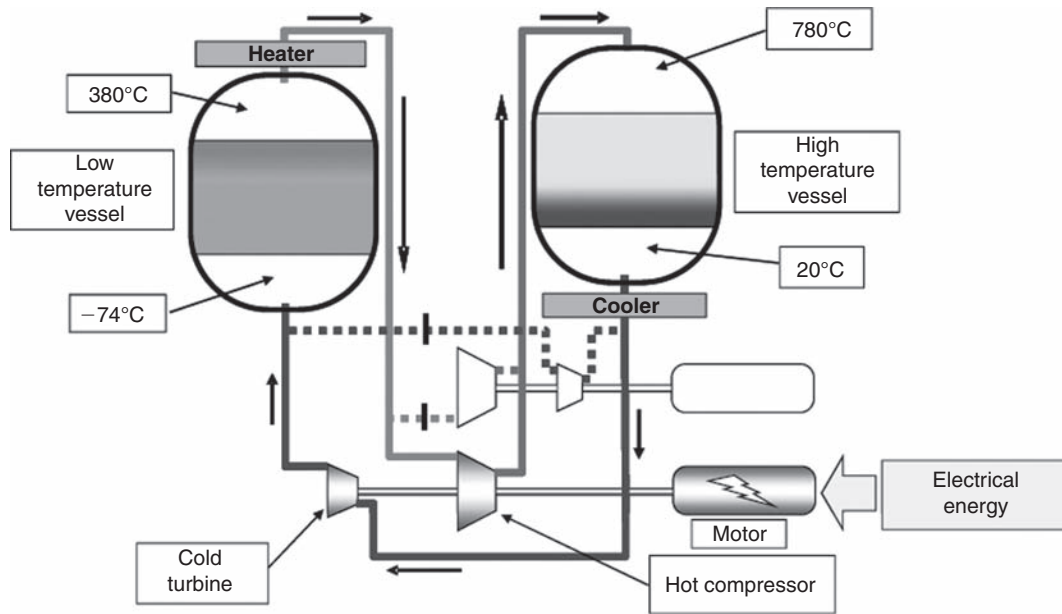


FIGURE 32.4.1
Storage phase (Doc. Saipem)

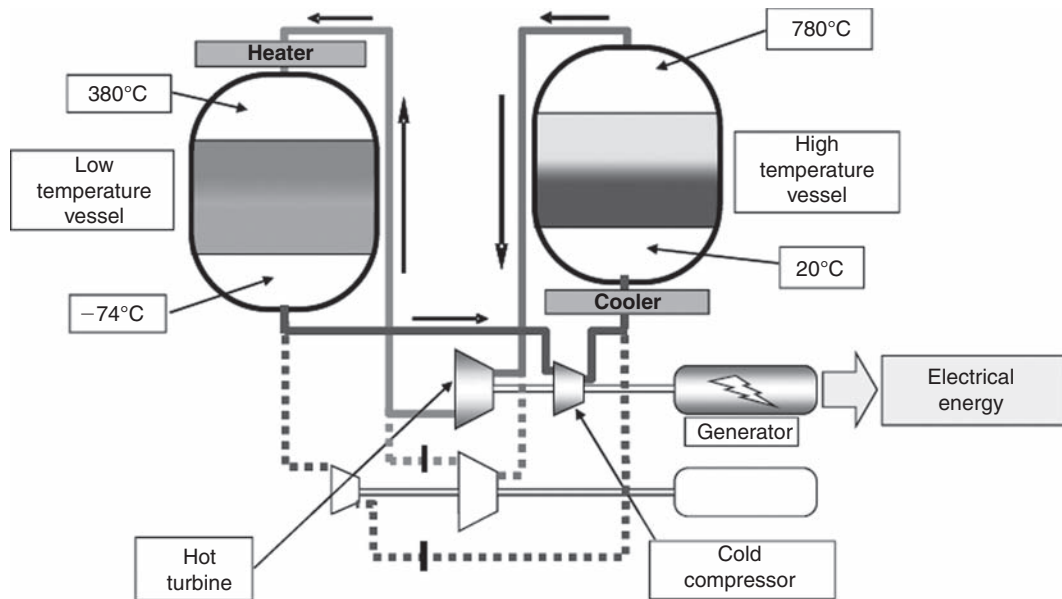


FIGURE 32.4.2
Release phase (Doc. Saipem)

The energy storage process includes the following steps:

- during the storage phase electricity is used to drive a heat pump that transfers heat from one vessel to another at higher temperature;
- during the release phase, heat is turned back into mechanical energy by a heat engine.

Figure 32.4.1 shows a simplified diagram of the system in storage mode. As you can see, each vessel must be as much stratified as possible.

The facility includes two pressurized vessels interconnected by the heat pump:

- the low temperature vessel (LTV) has a solid bed with a certain porosity to allow passage of a gas. The top of the bed is at high temperature T_2 (380°C) while the bottom is cold $T_3 = -74^\circ\text{C}$. This is the low-pressure vessel;
- the high temperature vessel (HTV) is similar, except that the temperature of the top of the bed is at even higher temperature T_1 (780°C) and the bottom at a temperature close to room temperature (20°C). This is the high pressure vessel;
- the heat pump consists of a compressor and an expansion turbine. Gas flows through the system in a closed loop.

During the storage period material in the LTV vessel cools gradually. The thermal front between the layers at T_2 and those at T_3 rises gradually. However, during most of this phase, gas continues to leave at the top of the bed at temperature T_2 .

The phenomenon occurs symmetrically in the HTV vessel in which the thermal front descends.

Figure 32.4.2 shows the operation during release. The vessels are then connected by a heat engine (turbine-compressor) that makes use of heat between temperatures T_1 and T_2 and drives a generator. The gas is still flowing in a closed loop.

Preliminary studies have shown that an overall efficiency of 70% can be obtained with these conditions.

32.5 COMPRESSED AIR STORAGE DEVICES

Several compressed air storage systems for electricity have been proposed in recent years.

32.5.1 CAES (Compressed Air Energy Storage) concept

The best known is called CAES (Compressed Air Energy Storage, Figure 32.5.1) or its variant AACAES (Advanced Adiabatic CAES). It requires large underground caverns, which is possible only in places where geology is favorable (deep salt domes for example, or highly permeable deep aquifers) rarely

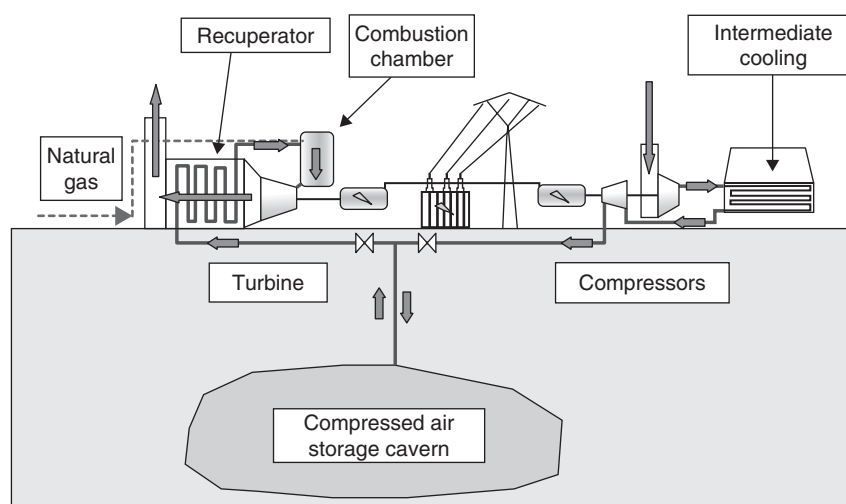


FIGURE 32.5.1

Compressed Air Energy Storage (Doc. Saipem)

located in appropriate areas. Moreover, except for AACAES, this technology requires combustion of natural gas during release.

In such a device (Nakhamin, Daniel, 2007), air is stored under pressure during peak hours in a cave of large volume. In production mode, this air is used as an oxidizer in a gas turbine, substantially reducing the compression work, which, as we saw in Chapter 12 of Part 3, represents 60–70% of the work produced by the turbine in classic GT cycle. The available capacity can be tripled compared to operation without storage.

Two CAES pilot plants have been constructed, one in 1974 in Hundorf, Germany, and the other in 1991 in McIntosh, Alabama (USA). The latter, more powerful than the first, uses 0.7 kWh of electricity and 1.32 kWh of heat as a gas to produce 1 kWh.

The aim of AACAES (Bullough et al, 2004) is to associate thermal storage to pneumatic storage, inserting a regenerator to cool hot compressed air before it is stored, and reheat it at the time of release, so that it can be directly expanded, without fuel input.

32.5.2 Peaker concept of Electricite de Marseille Company

The Electricity de Marseille Company (EdM) patented a few years ago a device called Peaker, which is similar to AACAES, except that pneumatic storage would be done in sets of concentric spheres to ensure their mechanical strength when under pressure. In addition, this system is akin to an isotherm compression involving a staged compression with intermediate cooling and staged expansion with intermediate reheats.

The Peaker works coupled with a gas turbine which valorizes flue gas escaping at about 550°C. Exchangers can recover the energy they contain, in order to store it (as heat), and reuse it to preheat air from the storage device before entering the turbine during peak hours.

We modeled such a system with Thermoptim. If one considers that the available thermal power at the GT outlet is recovered for storage with a heat exchanger of effectiveness equal to 0.8, the power transmitted to storage (at a temperature above 150°C) represents 62% the total available.

Let us consider a storage sphere at 58 bar, where air is heated at about 210–220°C (depending on the heat exchanger balance) before expansion, assuming it is stored at 50°C (conservative assumption corresponding to compression of air at 15°C with three intermediate coolings).

The results of Figure 32.5.2 show an overall effectiveness equal to 2.32, which must, given that the storage phase lasts 12 h and that of release 5 h, be divided by $12/5 = 2.4$, This corresponds to an overall electrical effectiveness of 96.7% (electricity produced divided by electricity consumption).

The thermal power to provide for this heating is that of the four heaters Figure 32.5.2, i.e. $3.17 + 2.38 + 2.26 + 2.23 = 10$ MW heat, and this for 5 h, 50 MWh heat per sphere. Assuming (rather weak) heat storage efficiency of 60%, this represents 83 MWh to provide the storage with, or 35 minutes of gas turbine operation. For 10 storage spheres, the GT running time would be a little less than 6 h.

32.5.3 Hydropneumatic energy storage HPES

As we have seen, the use of isothermal processes allows good efficiencies to be obtained. Using an isothermal cycle at room temperature has the advantage of not requiring storage of heat, eliminating losses and allowing for indefinite storage.

This basic idea has been studied at the École Polytechnique Fédérale de Lausanne (EPFL) and led to the concept of “Oleo-Pneumatic Battery” or BOP (Batterie Oléo-Pneumatique in French). Initial studies were conducted with oil hydraulic circuit and small capacity storage devices.

Another approach, proposed by Ph. Lefevre formerly with EDF, whom we thank for allowing us to include in this section excerpts from one of his publications (Brunet, 2009), has resulted from the

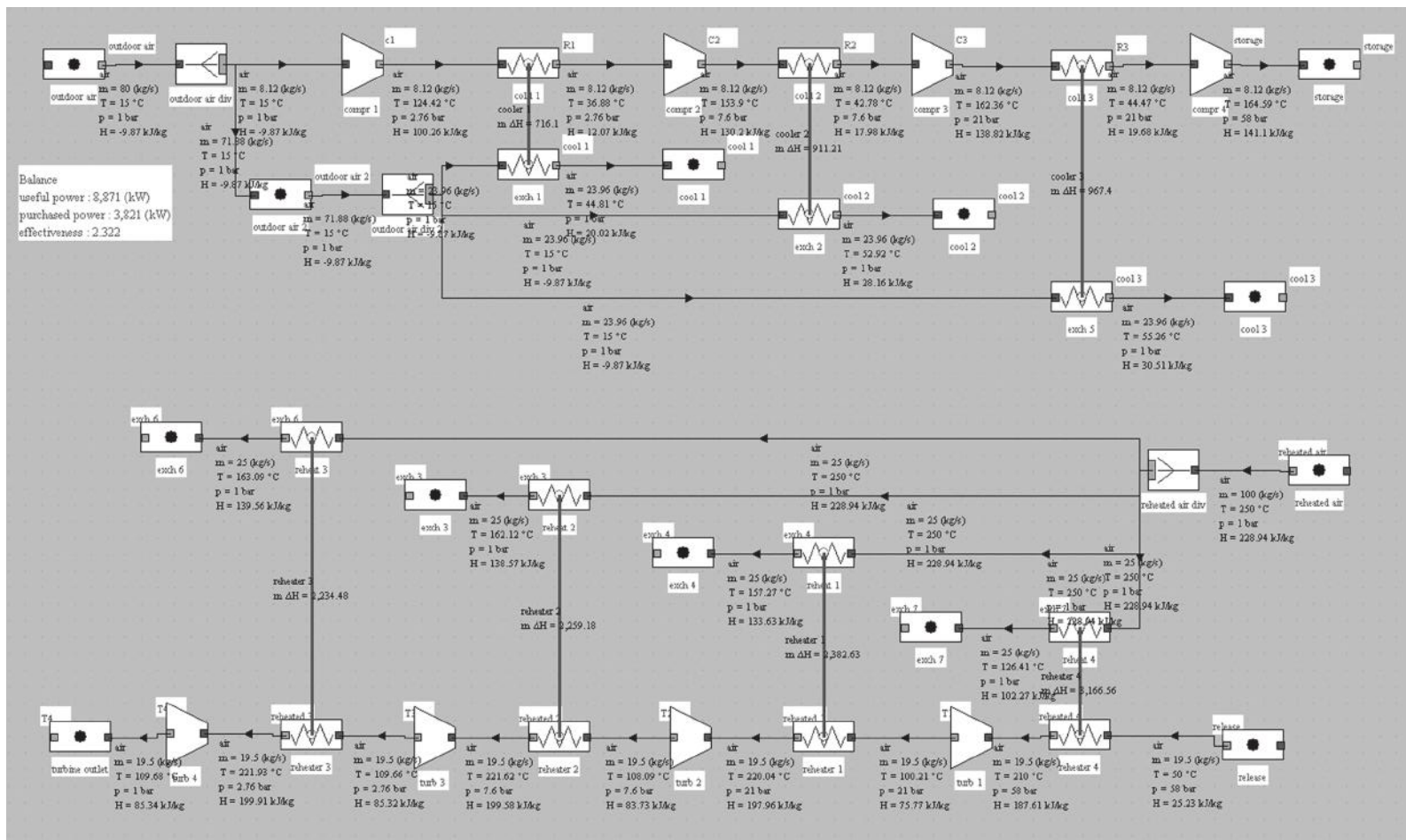


FIGURE 32.5.2
Synoptic view of an EdM Peaker

observation that the only effective means we have to store large capacities of energy, is still pumping water in a reservoir at altitude, the gravitational potential energy of the water being then used.

Knowing that the atmospheric pressure is equivalent to a water height of 10 m, the extrapolation is simple: instead of pumping water to a height of 300 m, why not submit it to a pressure of 30 bar, or even higher?

The convergence of both ideas led to the concept of large water hydraulic accumulators, with a limited water flow at pumps to operate continuously in an isothermal process mode. Water from this point of view has an important advantage: its heat capacity is very high compared to that of air, which allows operation at a stable temperature, both in compression and expansion. This is called Hydro Pneumatic Energy Storage HPES.

HPES storage is therefore nothing else than the modern and large-scale development of an old concept: that of the hydraulic accumulator, or hydraulic piston. For this application, a hydraulic piston consists of a closed tank partially filled with water, above which there is an air pocket. Water is injected slowly using a hydraulic pump, which raises the level in the tank and compresses air. Conversely, the pressure of the air pocket is transmitted to the water that restores energy by operating a hydraulic motor.

This simple device has many advantages:

- choosing a low flow-rate relative to total filling volume, we can make slow compression and expansion;
- water, an excellent heat transfer fluid, is in constant contact with air, thereby transferring heat between them. Moreover, as the specific heat of water is much higher than that of air, this leads to relatively small changes in water temperature;
- conditions are well satisfied that we may have high efficiency isothermal processes;

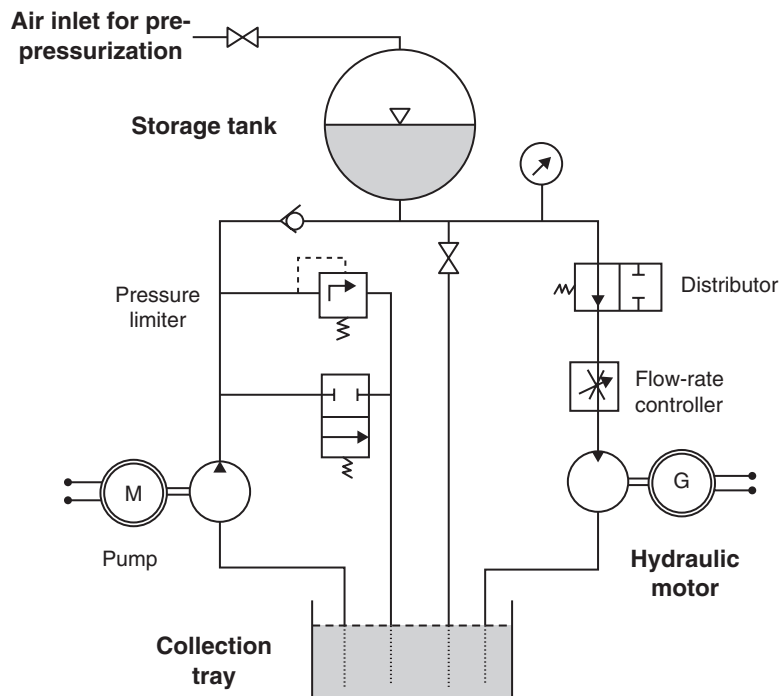


FIGURE 32.5.3

Hydro Pneumatic Energy Storage, after Ph. Lefevre

- efficiencies of hydraulic pumps and motors (volumetric) are significantly higher than those of compressors and air engines: for some technologies and optimal operating conditions, they are approaching 95%.

Overall cycle efficiency about 75% seems realistic.

After some investigation, it appeared that the use of standard pipeline tubes would be the easiest way to produce tanks of large volume, enduring high pressure, at an acceptable price: we now carry flammable gas in subsea pipelines hundreds of miles at a pressure of up to 400 bar.

We can show that with this concept, it is possible to store 1 kWh per cubic meter of reservoir and hectobar of maximum pressure. For example, with containers that support 300 bar, you can store 3 kWh per cubic meter. This energy density is modest, but compares favorably with pumping electric storage, in which 1 kWh requires one cubic meter of water to be carried 500 meters up.

Specifically:

- in a pumping-storage station (station de pompage-turbinage STEP in French) at 250 m altitude, to store 1 MWh, you must pump 2,000 m³ of water;
- with a hydraulic system at 250 bar, 1 MWh of storage would require pumping 200 m³ of water in a tube volume of 500 m³.

REFERENCES

- Ph. Lefèvre, A. Rufer, Stockage hydropneumatique, in Y. Brunet, Technologies du stockage d'énergie, Hermès Science, Lavoisier 2009.
- P. Odru. Le stockage de l'énergie, Dunod, Idées 2010.
- Energy Storage. A key technology for decentralised power, power quality and clean transport*, European Commission, Report EUR 19978, 2001, ISBN 92-894-1561-4
- Survey of Thermal Storage for Parabolic Trough Power Plants*, Pilkington Solar International GmbH, September 2000, contract report NREL/SR-550-27925, Cologne, Germany.
- C. Bullough, C. Gatzen, C. Jakiel, M. Koller, A. Nowi, S. Zunft, *Advanced Adiabatic Compressed Air Energy Storage for the Integration of Wind Energy*, Proceedings of the European Wind Energy Conference, EWEC 2004, 22–25 November 2004, London UK
- F. Dinter, M. Geyer and R. Tamme (Eds.), *Thermal Energy Storage for Commercial Applications*, Springer-Verlag, New York, 1990.
- J.-P. Dumas, *Stockage du froid par chaleur latente*, Techniques de l'Ingénieur, Traité Génie énergétique, BE 9 775.
- M. Nakhamkin, C. Daniel, *Available Compressed Air Energy Storage (CAES) Plant Concepts*, Power-Gen Conference, New Orleans, Dec. 2007.

This page intentionally left blank

Calculation of Thermodynamic Solar Installations

Abstract: We presented in Chapter 30 the main thermodynamic cycles used to produce solar electricity. Here we discuss an issue so far not addressed: how can we, given the variation of the solar resource, calculate the performance of such a facility over a long period.

We thus present the basic methodology for estimating solar radiation received by a collector, whatever its orientation and tilt. We then show the advantage of a form of data presentation that emphasizes the phenomena of thresholds and nonlinearity: cumulative frequency curves (CFC) of solar irradiation received by a receiving surface. We finally present the general principles governing the development of electro-solar plant hourly simulation software and give some indications on how simplified design methods can be defined.

Keywords: solar radiation, sunshine duration, pyranometer, astronomical equations, cumulative frequency curves, simulation, usability curves.

33.1 SPECIFIC SOLAR PROBLEMS

Solar facilities, even the most simple, are relatively complex and include at least one collection circuit, an energy distribution circuit, storage and various control systems (Figure 30.1.6). In these, both the load (demand) and availabilities vary continuously. The working principle of solar thermal collectors is explained in Chapter 30.

When trying to calculate the energy balance of a solar installation the main problems often stem from the variation of solar radiation. Indeed, analysis of the behavior of solar collectors, or system to which they are associated, can highlight different operating regimes that depend on incident solar radiation, transition from one regime to another being triggered by certain critical values called radiation thresholds.

When radiation intensity varies greatly, as is usually the case, the whole system frequently changes operation mode. In these circumstances it is not possible to determine *a priori* an average behavior of the entire facility that could be used to size it.

To calculate the energy balance of a solar system, it is necessary to have maximum information on the distribution of incoming solar power. Thus, one of the first problems to be solved is to correctly estimate the **radiation received by solar collectors**.

In order to take into account accurately the variation of the resource and the interactions of the different solar system components, most accurate methods rely on **simulation programs** (often called hourly, cf. section 33.4), which calculate, for time steps generally of several minutes, plant performance, starting from the hourly radiation measured by national weather services.

For example, Figure 33.1.1 shows the hourly simulation of the electricity production P_e of a thermodynamic solar plant over a period of four days, and variations of solar radiation G received by 1 m^2 of solar collector, outside temperature $T_{\text{out}} (\times 40)$ and storage tank volume V_s . This figure shows that electricity production is not proportional to the sunlight received. It depends on many factors, such as tank volume, T_{out} , existing control system etc.

Hourly simulation has the advantage of being very precise and can be adapted to each particular case, but it also has several drawbacks:

- it requires a good knowledge of simulation environments, which is beyond the reach of many solar energy users;
- it calls for the development of calculation programs expensive to make and use;
- it requires large data files.

For all these reasons, many researchers have attempted to develop **simplified calculation methods**, easy to use, even if their accuracy or generality is somewhat reduced.

For this it is necessary to summarize in one way or another solar radiation weather data. The first idea that comes to mind is to use the **average values** published by national weather services.

However, they are established so that **information on the power thresholds is lost**, and their use can lead to large errors.

Some authors also proposed to set reference days, or typical days, during which the operation of the facility could be simulated. In this case, the difficulty lies in the selection criteria for typical days, and you never know how much you can rely on them.

The analysis of meteorological data required for calculations, and our fine simulation experience led us to choose a form of data presentation that emphasizes the phenomena of thresholds and nonlinearity: **cumulative frequency curves (CFC) of solar irradiation** received by a collecting surface. Based on work done in the 80s at the Centre for Energy Studies of the École des Mines de Paris (Gicquel, 1977, Bourges et al. 1990), the value of these curves and how to build and use them are explained below.

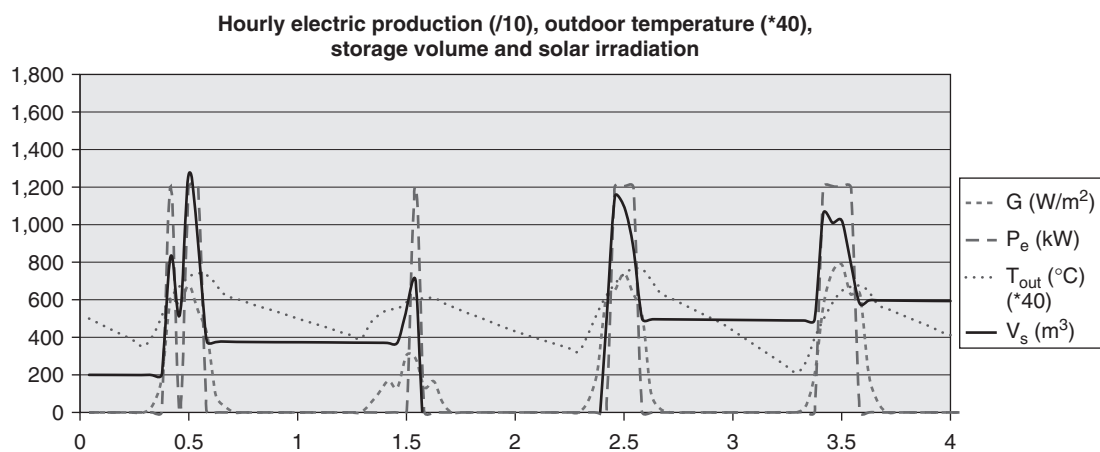


FIGURE 33.1.1

Climatic data and output of an electro-solar plant

33.2 ESTIMATION OF THE SOLAR RADIATION RECEIVED BY A SOLAR COLLECTOR

In this section we will try to present the basic methodology for estimating solar radiation received by a collector, without making a complete statement of solar climatology, which is outside the scope of this book.

Solar energy comes from thermonuclear reactions that occur within the sun, causing the emission of high power electromagnetic radiation, appearing much like a blackbody at 5,800 K.

Outside the atmosphere, the radiation received by the earth varies depending on time of the year between 1,350 and 1,450 W/m². It is then partially reflected and absorbed by the atmosphere, so that radiation received at ground level has a direct part I and a diffuse part D, the total G ranging from 200 W/m² (overcast) to about 1,000 W/m² (zenith clear sky). The energy received by a given surface depends on its tilt and orientation and local climatic conditions (Figure 33.2.1).

Total irradiation G received by a solar collector can be decomposed into a direct component I cos(i) and a diffuse component D, which is often viewed as independent of the tilt, whereas strictly it is not. In some cases¹ it is desirable to consider a direct component of radiation reflected by surfaces surrounding the collector. We then introduce the concept of albedo.

Solar radiation atlases at ground level are issued by national and international meteorological services in the form of maps and charts, on paper or computer. They are based on measures carried out daily in weather station networks, mainly for two values:

- sunshine duration, which is the period during which the direct radiation remains above a certain value internationally accepted. There are two readings per day, one for the morning, one for the afternoon. The unit used is the tenth of an hour of sunshine duration, and the measurement device is called a sunshine recorder;
- global horizontal radiation noted Gh, which is the energy received in a given time by a horizontal surface, from the sun and sky in the form of radiation of short wavelength. The hourly measurements are expressed in J/cm², the measuring device being called pyranometer.

To interpolate between the network stations, it is now common to use satellite data.

Furthermore, some stations are exceptionally equipped with pyranometer fitted with a visor strip that hides the direct component of radiation, thus allowing diffuse radiation to be measured.

The sunshine duration not being an energy measurement, to determine radiation received by a collector, there are usually only records of hourly global horizontal radiation Gh. It is therefore necessary to have methods as reliable as possible to separate direct and diffuse components of Gh,

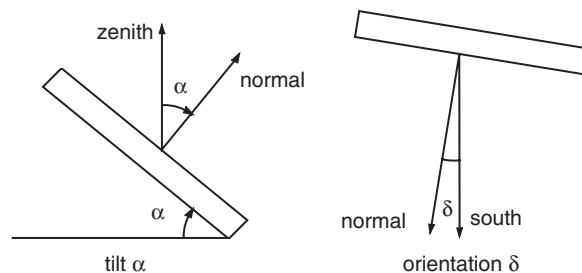


FIGURE 33.2.1

Tilt and orientation of a solar collector

¹ For example for a collector facing south on a seafront or in front of a snowy field.

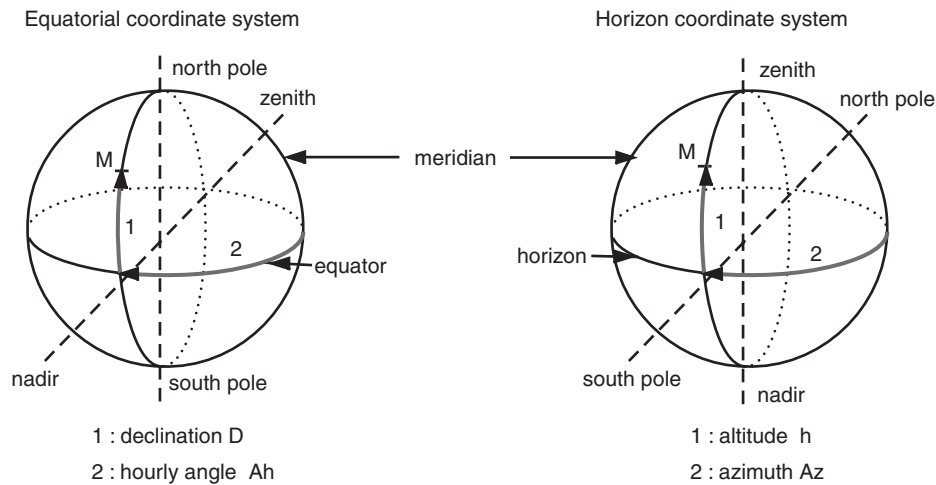


FIGURE 33.2.2

Coordinate systems for spherical trigonometry

methods generally based on statistical correlations validated from records of stations where Gh and D are measured simultaneously.

One both simple and reliable way is to correlate ratio D/Gh to Gh/G₀, an indicator representing the ratio of global radiation received on Earth to global radiation outside the atmosphere, which has the great advantage of being determined on the sole basis of astronomical data. Such correlations (33.2.1) are called Liu and Jordan type, named after the scientists who have proposed them in the early 60s (for daily and not hourly values at that time).

$$D/Gh = aGh/G_0 + b \tag{33.2.1}$$

The values of a and b in equation (33.2.1) depend naturally on the location considered, and even the season if you want to be very accurate. Similar correlations can be established with other indicators, including the sunshine duration, but we will only present in detail in this section that corresponding to equation (33.2.1), and provide a small Excel macro allowing perform these calculations.

The establishment of astronomical equations requires the definition of two cartesian coordinate systems (Figure 33.2.2):

- equatorial coordinates, whose axes are given by the poles and the equator plane, the meridian of the place being taken as the origin. The daily astronomical tables of the sun are given in this reference;
- horizontal coordinates, whose axes are given by the vertical location and the horizon plane, the first meridian of the place being taken as the origin. It is the only coordinate system simple to use locally to measure the inclination and the solar orientation, as defined by angles α and δ.

In Table 33.2.1, we find indicated successively notations used for angles 1 and 2 of Figure 33.2.2 in both coordinate systems.

The calculation shows that i and h are related by the following equations:

$$\sin dn = \sin \varphi \cos \alpha - \sin \alpha \cos \varphi \cos \delta \tag{33.2.2}$$

$$\sin an = \sin \delta \sin \alpha / \cos dn \tag{33.2.3}$$

$$\sin h = \sin \varphi \sin D + \cos \varphi \cos D \cos Ah \tag{33.2.4}$$

$$\cos i = \sin dn \sin D - \cos dn \cos D \cos (Ah - an) \tag{33.2.5}$$

The hourly angle is easily determined: it is 15 degrees per hour.

TABLE 33.2.1

	Equatorial coordinates	Horizontal coordinates
Sun	Declination D	Altitude h
	Hourly angle Ah	Azimuth Az
Zenith	Latitude φ	Origin (o)
	Origin (o)	Origin (o)
Normal to collector	dn	Tilt α
	an	Orientation versus south δ
Angle of incidence of solar radiation	i	i

The value of declination D is easily obtained by (33.2.7) when you know the day of the year considered j. With

$$\Gamma = 2\pi(j - 1)/365 \quad (33.2.6)$$

$$D = (0.006918 - 0.399912 \cos \Gamma + 0.070257 \sin \Gamma - 0.006758 \cos 2\Gamma + 0.000907 \sin 2\Gamma - 0.002697 \cos 3\Gamma + 0.00148 \sin 3\Gamma) \quad (33.2.7)$$

The value of the solar constant outside the atmosphere is given by (33.2.8).

$$I_0 = 1367(1.00110 + 0.034221 \cos \Gamma + 0.001280 \sin \Gamma + 0.000719 \cos 2\Gamma + 0.000077 \sin 2\Gamma) \quad (33.2.8)$$

All these relations allow to calculate I_0 , an, dn, then h and I for any time.

Correlation (33.2.1) gives D and I knowing G_h and $G_0 = I_0 \sin h$. Irradiation G received by the collector is then given by (33.2.9):

$$G = I \cos i + D \quad (33.2.9)$$

It is thus possible to determine the solar radiation received, hour by hour, for a fixed solar collector, whatever its orientation δ and tilt α . If it is a concentration collector, the diffuse part can be neglected, and if the collector is equipped with a sun tracking device, the values of α and δ must be recalculated at each time step (a double-tracking should ensure a normal incidence of sunlight).

PRACTICAL APPLICATION

Excel macro allowing perform solar radiation calculations

An Excel macro has been prepared on the basis of the equations presented in this section. It can be downloaded from the ThermoOptim portal (http://www.thermooptim.org/sections/base-methodologique/simulation-systemes/calcul-installations/downloadFile/attachedFile_f0/CalculsSolaires.xls?nocache=1262751514.1). You may download it and use it at your convenience for estimating solar radiation received at any time by a surface of given orientation and tilt.



[CRC_Pa_9]

33.3 CUMULATIVE FREQUENCY CURVES OF IRRADIATION

As we have indicated, the analysis of meteorological data required for calculations, and our experience of fine simulations, led us to choose a form of data presentation that emphasizes the phenomena of thresholds and nonlinearity: **cumulative frequency curves (CFCs) of solar radiation** received by a collecting surface.

33.3.1 Curve construction

These curves (see Figure 33.3.1) are obtained as follows: one considers the historical file of hourly measurements corresponding to a given period (usually one month): solar irradiation G (averaged over one hour) may take values ranging from 0 to $1,200 \text{ W/m}^2$. We divide this interval into M classes of equal width (25 W/m^2 if $M = 48$). We then sort the hourly values to establish a table of absolute frequencies $N(I)$, I varying from 1 to M , which gives the number of hours in the period when solar irradiation was between the bounds of class I .

N_{days} being the number of days in the period, we then obtain the cumulative frequency table $n_h(I)$ by expression:

$$n_h(I) = \sum_{j=1}^M \frac{N(j)}{N_{\text{days}}}$$

This leads to table $G(I)$ which contains the values of lower bounds of the various classes.

Cumulative frequency curves therefore read as follows: we have in the abscissa the number of hours n_h (reduced to one day), during which solar irradiation has exceeded the value read in the ordinate.

For example, in Figure 33.3.1, in Ajaccio in July, the threshold of 600 W/m^2 was exceeded on average 6 hours per day on a horizontal plane. The x-intercept corresponds to the average day duration for the period. The area bounded by the curve and the axes is none other than the daily average energy received over this period.

These diagrams can be plotted, of course, for different receiving surface orientations and tilts.

33.3.2 Curve smoothing

Once the cumulative frequency curve obtained, it is possible to smooth the histogram by different families of curves depending on the uses that we want to make of them.

Based on work done in the 80s at the Centre for Energy Studies of École des Mines de Paris, the best representation of these curves is explained below.

CFCs are expressed relative to reduced variables:

$x = n_h/d_d$, number of hours referred to day duration

$y = G/G_{\text{max}}$, solar radiation received referred to maximum radiation

$x = f_0(y) + A_1f_1(y) + A_2f_2(y) + A_3f_3(y) + A_4f_4(y) + A_5f_5(y) + A_6f_6(y) + A_7f_7(y) + A_8f_8(y)$

The 6 or 8 A_i , depending on the precision that we seek, can be tabulated for different locations and different inclinations.

f_i are orthogonal polynomials defined as follows:

$$f_0 = (1 - y)$$

$$f_1 = y(1 - y)30^{0.5}$$

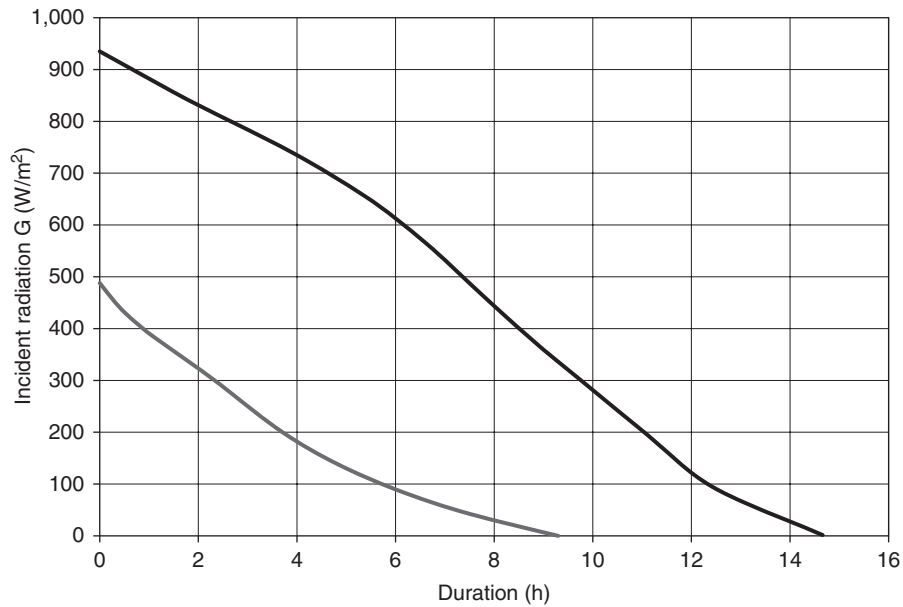
$$f_2 = y(1 - y)(-1 + 2y)210^{0.5}$$

$$f_3 = y(1 - y)(9 - 42y + 42y^2)10^{0.5}$$

$$f_4 = y(1 - y)(-1 + 8y - 18y^2 + 12y^3)2310^{0.5}$$

$$f_5 = y(1 - y)(2 - 24y + 90y^2 - 132y^3 + 66y^4)1365^{0.5}$$

$$f_6 = y(1 - y)(-18 + 300y - 1650y^2 + 3960y^3 - 4290y^4 + 1716y^5)35^{0.5}$$

**FIGURE 33.3.1**

Ajaccio CFCs, on a horizontal plane in January and July

$$f_7 = y(1 - y)(6 - 132y + 990y^2 - 3432y^3 + 6006y^4 - 5148y^5 + 1716y^6)595^{0.5}$$

$$f_8 = y(1 - y)(-6 + 168y - 1638y^2 + 7644y^3 - 19110y^4 + 26208y^5 - 18564y^6 + 5304y^7)1045^{0.5}$$

H being the average daily energy received, the area subtended by the CFC is:

$$\nu = \frac{H}{d_d G_{\max}} = (0.5 + A_1(5/6)^{0.5} + A_3 0.1^{0.5} + A_5(13/420)^{0.5} + A_7(17/1260)^{0.5}) d_d G_{\max}$$

You just need to know d_d , G_{\max} , H and values of the 6 A_i to reconstitute a CFC.

33.3.3 Estimation of CFCs from empirical formulas

When you do not have the values of coefficients A_i involved in the expressions giving the CFC, it is possible to reconstruct these curves from empirical correlations connecting A_i with ν :

$$A_1 = -0.42297 + 0.16183\nu + 2.48691\nu^2 - 2.23697\nu^3$$

$$A_2 = 0.34623 - 1.47635\nu + 1.83694\nu^2$$

$$A_3 = -0.2789 + 1.91022\nu - 4.77807\nu^2 + 4.11137\nu^3$$

$$A_4 = 0.18865 - 1.36236\nu + 3.37632\nu^2 - 2.75771\nu^3$$

$$A_5 = -0.11845 + 0.98872\nu - 2.77182\nu^2 + 2.53303\nu^3$$

$$A_6 = 0.06968 - 0.60008\nu + 1.73839\nu^2 - 1.65775\nu^3$$

The accuracy of such estimates being limited, 6 polynomials suffice.

You can find in the literature on solar climatology various correlations to estimate H and G_{\max} , and day duration is given by $d_d = 1/w \text{Arcos}(-\text{tg } \varphi / \text{tg } D)$, with $w = 7.5$ if the angles are expressed in degrees, and $w = 2\pi/24$ when expressed in radians.

33.3.4 Interpolation on tilt

CFC parameter values are given for 0° , 30° , 45° , 60° and 90° . For a different slope, linear interpolation is sufficient for A_i . For H and G_{\max} , it is recommended to use a polynomial of degree 4 (same coefficients for H and G_{\max}):

$$Y_0 = H(45)$$

$$Y_1 = H(90) - H(0)$$

$$Y_2 = H(90) + H(0)$$

$$Y_3 = H(60) - H(30)$$

$$Y_4 = H(60) + H(30)$$

$$a = Y_0$$

$$b = \frac{27Y_3 - Y_1}{48}$$

$$d = \frac{Y_1 - 3Y_3}{48}$$

$$e = \frac{16Y_0 + Y_2 - 9Y_4}{144}$$

$$c = Y_4/2 - a - e$$

$$z = \frac{s - 45}{15} \quad s, \text{ inclination in degrees of the plane considered}$$

$$H(s) = a + bz + cz^2 + dz^3 + ez^4$$

33.4 HOURLY SIMULATION MODELS

We present in this section the general principles governing the development of electro-solar plant hourly simulation software.

Generally, systems with solar collectors do not behave as simply as it sounds, because of interactions between their components (collection, storage, distribution, free inputs, etc.) In particular, if it is possible to define unambiguously energy available at the outlet of a collector alone, the use of this concept becomes more delicate when it is integrated into a system: for the energy actually supplied by the system we can talk of useful energy.

That is why hourly (or sub-hourly) simulation methods are tools well suited for studying this type of installation.

As mentioned in previous sections, meteorological data input is usually outdoor temperature and horizontal global radiation G_h at the location.

Hourly values are most often derived from databases provided by national meteorological services or servers as SoDa². These values are used to determine G , radiation received by a surface of any tilt α and orientation δ , as explained in section 33.2. Knowing the layout of the collector field and its surface, it is possible to determine the incident solar power. Thermal power supplied by the collectors can be deduced if one knows their operating temperatures and their characteristics (see section 30.2).

This power is carried out by the fluid passing through the collectors, and directed to the storage tank, whose volume V_{stock} varies depending on the inputs and uses to feed the boiler steam cycle.

² <http://www.soda-is.com/fr/index.html>.

A possible model is to consider that the storage volume being limited by value V_{\max} , the power plant remains stopped as long as V_{stock} remains below a lower limit V_{\min} , and we simply store heat available if the solar radiation is sufficient for that. When the volume of stored fluid is greater than V_{\min} , the plant starts and continues to operate as long as $V_{\text{stock}} > 0$.

When the storage is full and the turbine in operation, and there is a surplus of solar power, the excess is discharged to the outside.

As we have seen in Section 32.2, we can take into account storage thermal losses proportional to its surface and the difference between its temperature and the ambient air.

Such a simulation tool, which can be implemented in a spreadsheet, leads to results such as those presented in Figure 33.1.1.

This model is very simplified since it does not take into account the heating of the collector field in the morning (more precisely, it does not take it into account explicitly, but the collector heats up as the sun remains below the positive efficiency threshold).

In this model, we do not take into account the initial heating of the solar boiler, and we assume that the inlet and outlet collector temperatures remain constant as long as the field produces heat, which implicitly assumes the existence of a very efficient flow control. It is possible to refine these assumptions, establishing a fine model of the collector field and of the flow management strategy actually implemented.

The thermodynamic cycle efficiency can be assumed constant or variable depending on the one hand on the condensation conditions, which often depend on ambient temperature, and secondly on temperature and flow of the fluid entering the boiler. If one wishes to know the performance of the thermodynamic cycle when its boundary conditions vary, it is necessary to model it in off-design mode, as explained in Part 5: the steam cycle case study treated in section 5.2 provides an example of the type of model that should be built.

33.5 SIMPLIFIED DESIGN METHODS

33.5.1 Principle of methods

In the study of solar thermal conversion, we are led to focus on phenomena of threshold (start, transition between operating modes etc.) and nonlinearity of efficiency as a function of radiation. The solar resource is therefore characterized by the cumulative frequency curve.

For collectors of a given type characterized by their optical factor τ and thermal conductance U (see Section 30.2.2), control being set (values of the differential, mass flow), the amount of heat that we can recover, at best, only depends on the fluid inlet temperature (T_i) in collectors. We call it “Energy available at temperature T_i ” and we denote it $Q(T_i)$.

The easiest way to calculate it is to admit that during each hour, the steady state corresponding to the average hourly radiation and the outdoor temperature is established: stop, steady pulse or steady operation without pump stop. It is a linear function of the surface of the CFC below the threshold.

We call usable energy the area between the curve itself and the operating threshold. It can also be determined analytically based on CFC formulations, to provide usability curves presented below.

33.5.2 Usability curves

If the reduced threshold value of a solar system is y_s , solar energy available is given by:

$$g(y_s) = \int_{y_s}^1 f(t) dt \quad (33.5.1)$$

It is thus possible to express g as:

$$g(y) = g_0(y) + A_1g_1(y) + A_2g_2(y) + A_3g_3(y) + A_4g_4(y) + A_5g_5(y) + A_6g_6(y) + A_7g_7(y) + A_8g_8(y)$$

with

$$g_0 = 0.5(1 - y)^2 (1 - y)$$

$$g_1 = (2y + 1)(1 - y)^2(5/6)^{0.5}$$

$$g_2 = y^2(1 - y)^2(105/2)^{0.5}$$

$$g_3 = (1 - y)^2(1 + 2y - 42y^2 + 84y^3)(1/10)^{0.5}$$

$$g_4 = y^2(1 - y)^2(1 - 4y + 4y^2)(1155/2)^{0.5}$$

$$g_5 = (1 - y)^2(1 + 2y - 207y^2 + 1404y^3 - 2970y^4 + 1980y^5) (13/420)^{0.5}$$

$$g_6 = y^2(1 - y)^2(18 - 176y + 605y^2 - 858y^3 + 429y^4)(35/4)^{0.5}$$

$$g_7 = (1 - y)^2(1 + 2y - 627y^2 + 8404y^3 - 41470y^4 + 94380y^5 - 100100y^6 + 40040y^7)/210(595)^{0.5}$$

$$g_8 = y^2(1 - y)^2(30 - 520y + 3445y^2 - 11154y^3 + 18837y^4 - 15912y^5 + 5304y^6)(10.45)^{0.5}$$

This curve, known as usability (Figure 33.5.1), reads very easily: the daily energy available H on a horizontal plane in Ajaccio above threshold 200 W/m^2 , is equal to $4,500 \text{ Wh/m}^2$ in July and 600 Wh/m^2 in January. These values fall to $1,010 \text{ Wh/m}^2$ for threshold 500 W/m^2 in July and 0 in January.

It is thus possible for different thresholds, to determine energy available during the year (Figure 33.5.2).

The calculation of the collector output is done by multiplying this energy by optical factor τ , and subtracting heat losses, equal to the product of the difference $(T_i - T_{out})$ by U and the number of hours of operation. The threshold varying according to T_{out} , we must first determine the threshold value for each month, taking as value of the average outdoor temperature T_{out} the daytime one, as solar collectors do not operate at night.

Knowing usability curves, it is possible to determine the energy available at the desired temperature T_i .

This energy is indeed equal to the sum of several terms:

- usable energy as given by curves of Figure 33.5.1, multiplied by the optical factor τ of solar collectors;

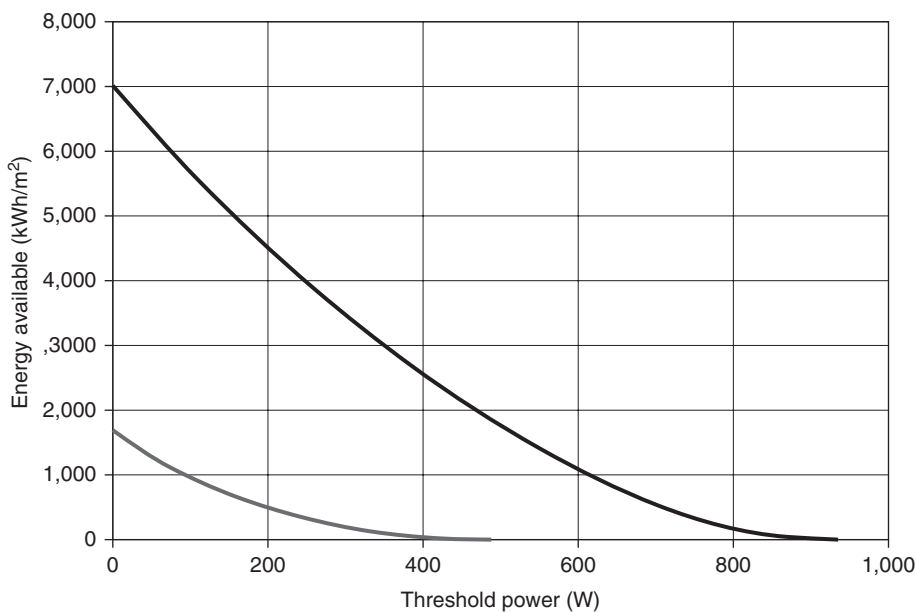


FIGURE 33.5.1

Energy available in Ajaccio, on a horizontal plane in January and July

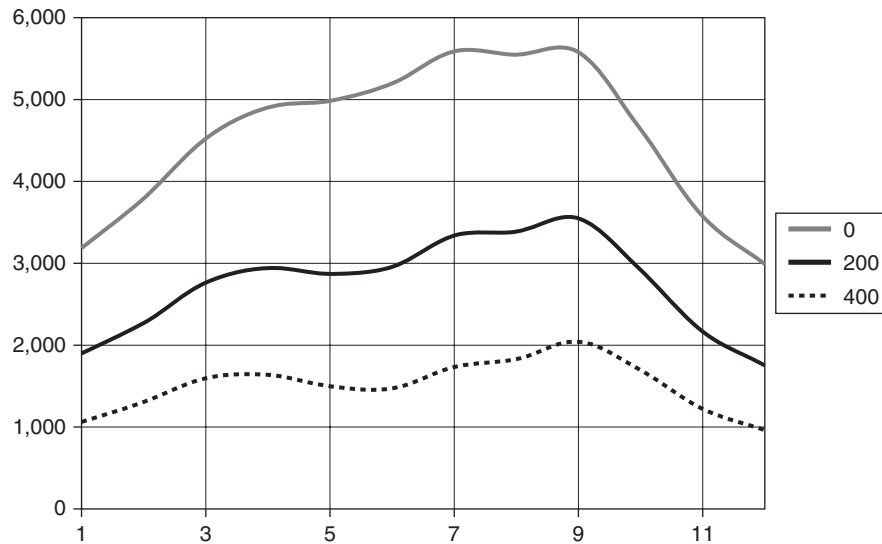


FIGURE 33.5.2

Monthly energy use in Ajaccio, 60°, depending on the threshold

- energy threshold, multiplied by the number of hours above the threshold and τ ;
- heat losses, counted negatively, multiplied by the number of hours above the threshold.

The first two terms correspond to the whole irradiation received by the collectors, reduced by the optical factor, and the third to heat loss. It turns out that the sum of the two latter is nil, so that only the first has to be taken into account.

In a solar power plant, all the power produced by thermal collectors is not converted into electricity, because of:

- the need to store that energy when it is available, until the stored heat is sufficient so that the power plant operates stabilized, which implies some storage losses;
- storage capacity, which is necessarily limited, so that at certain periods in summer, solar heat can be a surplus, which induces additional specific losses during this period.

We can consider a storage effectiveness constant for the first of these terms, and depending on the radiation received and the storage volume for the second. Simplified methods being unable to calculate the influence of these losses, they often include correction terms based on hourly simulation software which allow them to be estimated with reasonable accuracy.

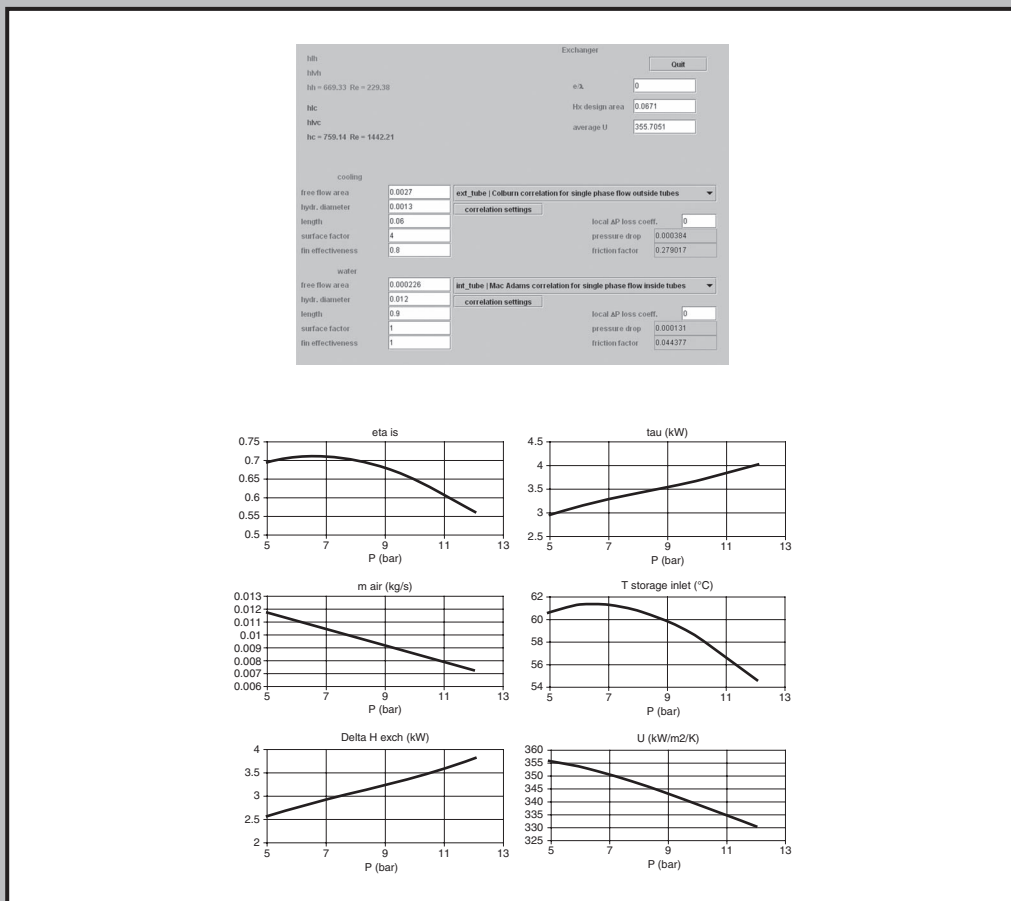
REFERENCES

- J. Adnot, B. Bourges, D. Campana, R. Gicquel, *Utilisation des courbes de fréquences cumulées de l'irradiation solaire pour le calcul des installations solaires*. In: Climatologie solaire. Ed. CNRS, Paris, 1979.
- J. Adnot, R. Gicquel, *Réflexion sur la régulation des installations de conversion thermique de l'énergie solaire*. Communication présentée à la rencontre internationale de la COMPLES, Hambourg 1978.
- B. Bourges, R. Gicquel, D. Schmoll, *Contribution à l'étude du comportement des capteurs plans en régime transitoire*, Revue internationale d'héliotechnique – 1er semestre 1978.
- B. Bourges, *European simplified methods for active solar system design*, ISBN: 0792317165, Kluwer academic publishers, Dordrecht, The Netherlands, 1991.

- ESRA *European Solar Radiation Atlas*, 2000. Fourth edition, includ. CD-ROM. Edited by J. Greif, K. Scharmer. Scientific advisors: R. Dogniaux, J. K. Page. Authors: L. Wald, M. Albuisson, G. Czeplak, B. Bourges, R. Aguiar, H. Lund, A. Joukoff, U. Terzenbach, H. G. Beyer, E. P. Borisenko. Published for the Commission of the European Communities by Presses de l'Ecole, Ecole des Mines de Paris, France, France
- R. Gicquel, *Méthode pour évaluer l'énergie solaire fournie par un insolateur plan*. Revue Générale de Thermique, n° 164–165, août-septembre 1975.
- R. Gicquel, *Method for evaluating the solar energy provided by a flat insulator*. International Chemical Engineering, Vol. 17, n° 4, October 1977.
- R. Gicquel, *Présentation statistique des données relatives à l'ensoleillement*. Revue Internationale d'Héliotechnique – 1er semestre 1977.
- R. Gicquel, *Cumulated frequencies Diagrams*, Energie Solaire: conversion et applications. CNRS 1977 (Cargèse).
- F. Kasten, H.J. Golchert, *Atlas Européen du Rayonnement Solaire* Grosschen, 1980
- S. Klein, W. Beckman, J. Duffie, *A design procedure for solar heating systems* Solar Energy, vol. 18, p. 113, 1976.
- B. Y. H. Liu, R. C. Jordan, *The interrelationship and characteristics distribution of direct, diffuse, and total solar radiation*. Solar Energy 4: 1–19. 1960.
- B. Y. H. Liu, R. C. Jordan, *A rational procedure for predicting the long term average performance of flat plate solar energy collectors*, Solar Energy, Vol. 7, p. 53, 1965.
- J. F. Orgil, K. G. T. Hollands, *Correlation equation for hourly diffuse radiation on a horizontal surface*. Solar Energy 19: 357–359. 1977.
- Ch. Perrin de Brichambaut, G. Lamboley, *Le rayonnement solaire au sol et ses mesures* Cahier AFEDES n° 1, 2ème édition, 1974.
- W. Spencer, *Fouries series representation of the position of the Sun*, Search 2 (5), 172. 1971.
- Swanson, Boehm, *Calculation of long term solar collector heating system performance* Solar Energy, vol. 19, p. 129, 1977.

5

Technological Design and Off-design Operation



Part 5 deals with ThermoOptim extensions that have been introduced to conduct technological design and off-design operation studies.

This page intentionally left blank

Technological Design and Off-design Operation, Model Reduction

Abstract: Until 2003, the fineness of component models used in Thermoptim was limited: phenomenological models built certainly allowed one to study the thermodynamic cycle of the technology under consideration, but not to perform a specific technological design nor to simulate off-design behavior; the latter two problems being much more complex than the first.

In this chapter, we present in a comprehensive manner technological design and off-design simulation problems in explaining a concrete example, that of a simple refrigeration cycle. In subsequent chapters, we will deepen the issue by proposing models for key components of the Thermoptim core. The final chapter (38) will be devoted to a few case studies.

We begin by explaining the problems posed by technological design of the main components used in a refrigerator (heat exchangers, compressor), then we give the calculation principles of its off-design operation, whose detailed study will be subject of section 38.4. Finally we give some indications on how reduced models can be deduced from simulation results.

Keywords: technological design, off-design simulation, modeling, external driver, model reduction.

34.1 INTRODUCTION

To address technological design and off-design simulation, we have been led to **distinguish two levels in models:**

- **phenomenological models**, these were implemented initially in Thermoptim only to give access to the calculation of thermodynamic cycles, irrespective of the choice of a particular component technology;
- **technological design and off-design simulation models** not only provide the same results as the previous ones, but in addition allow the user to geometrically design the various components and once the technological design is achieved, to study the behavior of the system outside the operating conditions for which it has been sized.

Such models are for example necessary when one wants to evaluate the performance of an existing facility, operated under conditions different from those for which it was designed. This audit issue (particularly with a view to proposing improvements) is of interest to a growing number of organizations, industrial and others.

Off-design analysis of energy systems poses many problems much more difficult to resolve than those we faced when we merely studied thermodynamic cycles in terms purely phenomenological at rated point, independently of technology choices¹.

Let us make clear that what we call off-design analysis corresponds to the stabilized operation of a facility for operating conditions other than those for which it has been designed: it is not to study the fast transient caused by control actuators.

We do not focus on dynamic changes in very short timescales, for which our models are not suitable. We assume that time constants of regulators that control the systems studied are much shorter than those of components themselves. For example, we consider that the characteristic time of a refrigerator expansion valve is small (about one minute) as compared to that of the condenser or evaporator (about ten minutes). This assumption allows us to neglect the transient behavior during off-design analysis of these two exchangers.

Let us consider for example a simple refrigeration cycle, very easily modeled with Thermoptim phenomenological version (Figure 34.1.1). To set up such a model, the user sets the values of flow rate, evaporation and condensation pressure as well as compressor isentropic efficiency, but needs specify neither the exchange surfaces brought into play, nor the type of compressor used (piston, scroll, centrifugal etc.). Thermoptim allows us to calculate the thermodynamic state of all points of the cycle and the energies involved.

For the model to make a real technological design, we must also specify as precisely as possible the type and physical dimensions of the various components used. In the case of a refrigera-

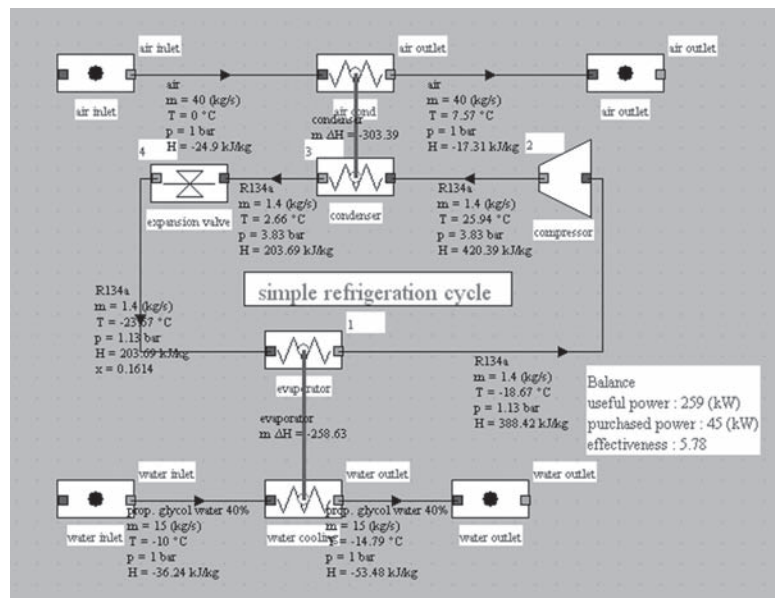


FIGURE 34.1.1

Refrigeration cycle model

¹The results presented in this section have received support in 2003–2005 of the French Programme de Recherche Interdisciplinaire 2.9 Varitherm, ACI Energie.

tion machine, you have to choose a type of compressor, for example in a list of devices available on the market. If it is a displacement machine, you should at least provide its swept volume and the volumetric and isentropic efficiency laws depending on compression ratio and rotation speed. For heat exchangers, we must first choose the flow pattern (plate, shell and tube, etc.) and then calculate the exchange surfaces, which involves determining internal heat exchange coefficients, and therefore dimensionless numbers governing thermal transfer between the fluids involved and the walls (Reynolds, Prandtl and Nusselt numbers).

Many values, which were set exogenously in the phenomenological model, then depend on the initial design and adaptation of the machine to operating conditions.

By making these technology choices, the user indirectly determines some parameters on which he could previously play freely. For example, in the case of a displacement compressor, flow is not necessarily exactly the one that was desired: it depends on the swept volume, compression ratio, suction specific volume, volumetric efficiency, rotation speed etc.

For a **simulation in off-design mode** to be realistically feasible, you must be able not only to make the technological design of each component, but also to characterize the interactions between components due to their adaptation to new operating conditions.

For example, the condenser and desuperheater of a refrigerating machine do in fact form a single exchanger, whose total area is known (Figure 7.8.6 of Part 2). The adaptation of the exchanger to changes in its boundary conditions therefore requires a coupled calculation much more complex than the two separate parts.

Moreover, new systemic constraints appear: in the example above, the pressure levels are set by the thermal equilibrium of two phase-change heat exchangers, the evaporator and the condenser, which determine the saturation temperatures. As for the compressor, it sets the refrigerant volume flow (depending on its rotation speed and compression ratio that determine its volumetric efficiency), and therefore the mass-flow (depending on the specific volume of refrigerant at suction). The main parameters of the refrigeration machine, namely the pressure levels and flow-rate are determined by several strongly coupled components whose calculation cannot be done independently.

Phenomenological models implemented in Thermoptim are inadequate to address these two issues. To do so, it is necessary:

- firstly to refine the internal representation of the various components so that their thermodynamic properties can be calculated in terms of technological parameters and conditions of use. Technological design screens have precisely this function;
- secondly to define and implement algorithms to calculate the complete system to account for coupling between components much stronger than before, the entire system adapting to its boundary conditions. The solution to this has been to implement these algorithms in external drivers, which take control on the software automatic recalculation mechanism.

34.2 COMPONENT TECHNOLOGICAL DESIGN

Component technological design requires to refine phenomenological models used in the Thermoptim core, supplemented to reflect mechanisms operating in off-design, if any.

To perform technological design, we have introduced new screens, complementary to those that perform phenomenological modeling. They can be activated by the button “tech. design” placed in the usual screens of the different components.

These new screens allow you to define the geometric characteristics representative of the different technologies used and the parameters necessary to calculate them. For a given component, they obviously depend on the type of technology used.

In this section we briefly introduce models allowing one to realize the technological design of a refrigeration cycle, then we will show how such a cycle can be designed in practice.

34.2.1 Heat exchangers

The most significant changes relate to heat exchangers, as earlier versions of Thermoptim only determine the UA value, which is the product of the overall heat exchange coefficient U by the exchanger surface A, the two terms not being evaluated separately. To design a heat exchanger, i.e. calculate its surface, one must first choose a geometric configuration, and second compute U, which depends on that configuration, fluid thermophysical properties and operating conditions.

Let us recall that although the approach we have adopted in Thermoptim is unconventional, it has proved quite fruitful for the study of complex systems: a heat exchanger ensures the coupling between two “exchange” processes, one representing the hot fluid which is cooled, and the other the cold fluid which warms up. It follows that the definition of the exchanger flow patterns and geometry is made at the process level, and not globally.

34.2.1.1 Calculation method

The method for calculating heat exchangers in off-design operation is based on the NTU method. When we know the two inlet temperatures and flow rates, an exchanger can be represented by a quadrupole, whose generalized matrix formulation can be expressed in various ways, depending on temperatures known (see Chapter 8 of Part 2).

Formulation (8.2.20) corresponds to the case where the inlet temperatures of both fluids are known, and equation (8.2.22) where the inlet and outlet temperatures of the cold fluid are known (if these are those of the hot fluid, simply invert the matrix C).

$$\begin{pmatrix} T_{ho} \\ T_{co} \end{pmatrix} = \begin{pmatrix} 1 - \varepsilon_h & \varepsilon_h \\ \varepsilon_c & 1 - \varepsilon_c \end{pmatrix} \begin{pmatrix} T_{hi} \\ T_{ci} \end{pmatrix} = \mathbf{A} \begin{pmatrix} T_{hi} \\ T_{ci} \end{pmatrix} \quad (8.2.20)$$

$$\begin{pmatrix} T_{ho} \\ T_{hi} \end{pmatrix} = \begin{pmatrix} \frac{1 - \varepsilon_h}{\varepsilon_c} & 1 - \frac{1 - \varepsilon_h}{\varepsilon_c} \\ \frac{1}{\varepsilon_c} & 1 - \frac{1}{\varepsilon_c} \end{pmatrix} \begin{pmatrix} T_{co} \\ T_{ci} \end{pmatrix} = \mathbf{C} \begin{pmatrix} T_{co} \\ T_{ci} \end{pmatrix} \quad (8.2.22)$$

The notations used in these equations are:

$$\varepsilon_h = \inf \left(\varepsilon, \frac{(\dot{m}c_p)_c}{(\dot{m}c_p)_h} \varepsilon \right) \quad \text{and} \quad \varepsilon_c = \inf \left(\varepsilon, \frac{(\dot{m}c_p)_h}{(\dot{m}c_p)_c} \varepsilon \right)$$

Furthermore:

$$NTU = \frac{UA}{(\dot{m} \cdot c_p)_{\min}}$$

$$R = \frac{(\dot{m}c_p)_{\min}}{(\dot{m}c_p)_{\max}} \leq 1$$

$$\varepsilon = f(NTU, R, \text{flow pattern})$$

In design mode, the calculation of a heat exchanger is done in three steps:

- knowing the inlet and outlet temperatures and flows of both fluids, we first determine effectiveness ε , and we deduce UA by the NTU method;
- U is then estimated by correlations depending on the exchanger flow pattern and geometry;
- calculation of area A is deduced immediately: $A = UA/U$.

In off-design mode, if we know the inlet temperatures and flow rates of both fluids, the area A of the exchanger and its geometry (flow patterns and technological parameters), calculation is done in three steps:

- determining U by correlations depending on the exchanger flow pattern and geometry (see Chapter 2);
- calculating UA , product of U and A , and then NTU;
- determining effectiveness ε of the exchanger by the NTU method, and calculating the hot and cold fluid outlet temperatures, equations (8.2.20) and (8.2.22) allowing to determine how the heat exchanger adapts to the operating conditions set.

Knowing T_{hi} , T_{ci} , m_h , m_c and U , it is possible with (8.2.20) to calculate R and NTU to deduce ε and determine outlet temperatures T_{co} and T_{ho} .

Knowing T_{ci} , T_{co} , m_h , m_c and U , it is possible with (8.2.22) to calculate R and NTU to deduce ε , and determine temperatures T_{ho} and T_{hi} .

34.2.1.2 Multizone heat exchangers

The calculation of multizone heat exchangers is more complex than simple ones, but it relies on the same principle. Let us consider the case of the condenser of the refrigeration machine whose temperature/enthalpy diagram is shown in Figure 34.2.1.

The refrigerant leaving the compressor is first desuperheated ($T_{hi}-T_{hv}$), then it is condensed at constant temperature, and then slightly subcooled ($T_{hl}-T_{ho}$). In this case, the calculation must be completed for each zone, the surface of the heat exchanger being the sum of the three zone areas. Obviously, the heat transfer coefficients are very different in these three areas.

In off-design mode, the total area remains constant, but its distribution among the three areas varies. A precise calculation is therefore requested to seek the solution that corresponds to the same total area and meets all other thermal and thermodynamic constraints.

You should refer to section 35.2.5 for detailed explanations on how to operate.

34.2.1.3 Geometric setting

The geometric setting of heat exchangers is a difficult subject. Here we just introduce quantities used, without discussing the reasons for their choice.

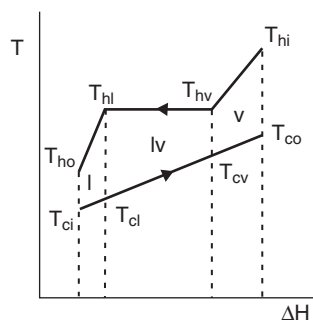


FIGURE 34.2.1

Temperature/enthalpy diagram

condenser			
free flow area	0.004	cond Shah correlation for condensation inside pipes	
hydr. diameter	0.01	correlation settings	
length	2	local ΔP loss coeff.	0
surface factor	1	pressure drop	0.074431
fin effectiveness	1	friction factor	0.026653

FIGURE 34.2.2

Condenser technological design screen

In order to calculate heat transfer coefficients and pressure drops, two geometrical quantities are particularly important besides the exchanger surface: section A_c devoted to the fluid flow, and hydraulic diameter d_h . When fluid heat exchange coefficients are very different, various devices such as fins can be used to compensate for the difference between their values. This is called extended surfaces, which can be characterized by a surface factor f and a fin effectiveness η_0 .

These four parameters are those which have been chosen in ThermoOptim to characterize heat transfer in each fluid. The length of the exchanger is also used for certain calculations such as pressure drops.

In the heat exchanger technological design screen (figure 34.2.2), the following conventions are adopted:

- type configuration (here, “cond”) is selected in a combo;
- “free flow area” represents the flow area A_c ;
- “hydr. diameter” is the usual hydraulic diameter d_h ;
- “length” is the exchanger length (used for calculating the boiling number Bo and pressure drops, not yet implemented in the two-phase case);
- “surface factor” is the surface factor f for large surfaces;
- “fin effectiveness” is the fin effectiveness η_0 ;

34.2.1.4 Correlations for calculating the heat exchange coefficients

A major difficulty is the calculation of the overall exchange coefficient U , which depends on both fluid heat transfer coefficients h , by general formula (34.2.1), which is simply a variant of equation (8.1.7) of Part 2. Many correlations have been proposed in the literature, and choosing the one best suited is not always obvious.

$$\frac{1}{U_c A_c} = \frac{1}{A_c \eta_{0,c} h_c} + \frac{e}{A \lambda} + \frac{1}{A_f \eta_{0,f} h_f} \quad (34.2.1)$$

Chapter 35 we explain options available in ThermoOptim and present in Table 35.4.1 the main configurations proposed.

34.2.2 Displacement compressors

We limit our presentation in this section to the case of displacement compressors, dynamic compressors being presented in Chapter 37.

A displacement compressor is geometrically defined by its swept volume, and its technological parameters allow one to calculate its volumetric and isentropic efficiencies, according to its rotation speed and conditions of suction and discharge. You should refer to Chapter 36 for a detailed presentation of the subject.

Models implemented in ThermoOptim are based on the assumption that the behavior of volumetric compressors can be represented with reasonable accuracy by two parameters: volumetric efficiency which characterizes the actual swept volume (36.1.1), and classical isentropic efficiency η_s (36.1.2).

$$\lambda = \alpha_0 - \alpha_1 \frac{P_{\text{ref}}}{P_{\text{asp}}} \quad (36.1.1)$$

$$\eta_s = K_1 + K_2 \cdot \left(\frac{P_{\text{ref}}}{P_{\text{asp}}} - R_1 \right)^2 + \frac{K_3}{\frac{P_{\text{ref}}}{P_{\text{asp}}} - R_2} \quad (36.1.2)$$

Calculation of a compressor is made as follows:

- isentropic and volumetric efficiencies are calculated from equations (36.1.1) and (36.1.2);
- if we know rotation speed, swept volume and volumetric efficiency, volumetric flow can be calculated as:

$$\dot{V} = \frac{\lambda N V_s}{60} \quad (36.2.2)$$

- knowing the suction volume v , we deduce mass flow:

$$\dot{m} = \frac{\dot{V}}{v} = \frac{\lambda N V_s}{60v}$$

In design mode, the rotation speed or the swept volume required to provide the desired flow is determined. Calculation is done taking into account the inlet and outlet pressures, and the flow value entered in the compressor flow field.

In off-design mode, the compression ratio allows one to determine λ and η_s , which sets the compressor flow and outlet temperature. The sequence of calculations is as follows:

1. knowing the inlet and outlet conditions, compression ratio $P_{\text{ref}}/P_{\text{asp}}$ and suction volume v are updated;
2. the volumetric and isentropic efficiencies λ and η_s and the actual flow are calculated knowing the rotation speed N ;
3. the flow volume \dot{V} is deduced by (36.2.2);
4. the compressor sets $\dot{M} = v\dot{V}$ and spreads this value to connected components;
5. the useful work can then be calculated knowing isentropic efficiency η_s .

34.2.3 Expansion valves

The technological design of expansion valves is taken into account in a simplified way, because we consider that their dynamics are much faster than that of other cycle components, and therefore they act as regulators. The only parameter introduced at this level is the superheating value.

34.2.4 Practical example: design of a cycle

Suppose we want to size a refrigeration cycle to provide a cooling capacity of 250 kW for an outside temperature of 0 °C, the temperature of the brine being equal to -10 °C at the evaporator inlet.

For this cycle (Figure 34.1.1), the cold fluid is 40% by volume propylene glycol, available among the external substances. Evaporation temperature must of course be lower than the brine, about -23°C , i.e. a pressure of 1.15 bar for R134a.

It is assumed that the compressor isentropic efficiency is 0.8.

Evaporation superheating ΔT_{surch} is 5 K, which for a coolant flow of 1.35 kg/s sets the cooling capacity at about 250 kW. With a brine flow of 15 kg/s, this leads to a cooling of 4.6°C .

For condenser, air temperature is 0°C and its flow rate 40 kg/s. Condensing temperature is estimated at 11.8°C , with a subcooling ΔT_{ssrefr} of 5 K, which corresponds to a condensation pressure of about 3.8 bar. The COP of the machine is in these conditions 5.88.

The sizing is done in two separate steps, the first is the classic setting of the cycle in Thermoptim, while the second is made from the technological screens.

We assume, for simplicity, that the cycle Thermoptim model has already been built. Otherwise, we would first build it then the method would be the same. This refrigeration cycle is similar to those presented Chapter 19 of Part 3, the main difference being that the condenser is modeled by a single exchanger, desuperheating not being dissociated from the condensation itself.

34.2.4.1 Creating technological screens

We will show in the examples in Chapter 38 how to create technological screens by building drivers, which requires a minimum of programming.

As discussed in section 34.3, this work is imperative when you want to perform off-design calculations, because it is then necessary to take control of Thermoptim recalculation engine. However, when we simply want to make the technological design of a project that implements components of the Thermoptim core, it is possible to automatically create technological screens using the generic driver that we will briefly present, which avoids having to program one.

Open the Thermoptim project, and load the generic driver by choosing from among the list of drivers, the one whose title is “generic techno design driver”, then click “Set the technological design screens” (Figure 34.2.3). The list of components for which there are technological screens is displayed in the table with their name, type and name of the technological screen class instantiated by default: VolumCompr for the compressor, and TechnoHx for both exchangers.

In this example, this initial setting is suitable for the compressor, but not for heat exchangers: the condenser should be modeled by class TechnoCondensor, and the evaporator by TechnoEvaporator.

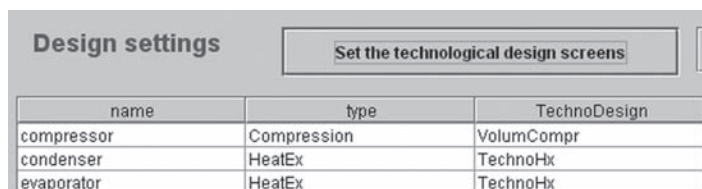
To change a component TechnoDesign class, select its line and double-click. A message asks you to confirm your choice, then displays a list of available classes. Choose the one you want and confirm.

After modifying the two heat exchanger classes, you get the screen shown in Figure 34.2.4.

You can then access the screens of these technological components either from their own screens (“tech. design” button) or from the upper part of a global window that opens from the simulator screen by typing Ctrl T (Figure 34.2.5).

34.2.4.2 Sizing components

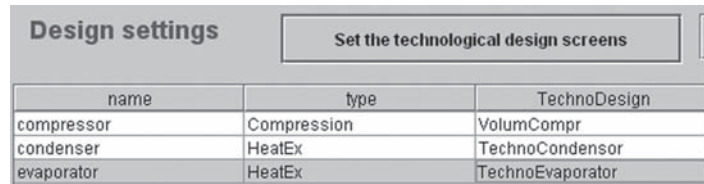
Technological screens being created, you can proceed to set and design the different components. This step must be done carefully, because it involves making a series of choices about internal



name	type	TechnoDesign
compressor	Compression	VolumCompr
condenser	HeatEx	TechnoHx
evaporator	HeatEx	TechnoHx

FIGURE 34.2.3

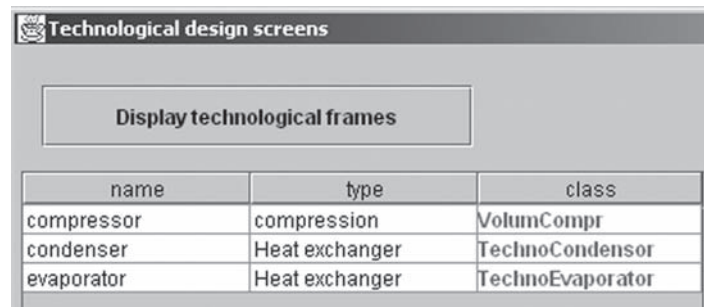
Generic driver screen (default initialization)



name	type	TechnoDesign
compressor	Compression	VolumCompr
condenser	HeatEx	TechnoCondensor
evaporator	HeatEx	TechnoEvaporator

FIGURE 34.2.4

Generic driver screen after selection



name	type	class
compressor	compression	VolumCompr
condenser	Heat exchanger	TechnoCondensor
evaporator	Heat exchanger	TechnoEvaporator

FIGURE 34.2.5

Technological screen window

configurations, geometrical dimensions etc. Some clarification on this point is given in this section, but you should refer to Chapters 35 and 36 for more details.

We consider that the evaporator is of shell and tube type. Start by choosing the type of configuration: “evap” for evaporation inside the tubes for the “evaporator” (refrigerant), and “ext tube” for the brine, with the settings of the screen in Figure 34.2.6 (on the water side we considered a free flow area of 0.015 m^2 and a hydraulic diameter of 1 cm, and refrigerant side a free flow area of 0.3 dm^2 and a hydraulic diameter of 1 cm, with a tube length of 6 m).

For the condenser, first choose the type of configuration: “cond” for condensation inside the tubes for the “condenser” (refrigerant), and “air coil” for air, with the settings of screen in Figure 34.2.7 (we considered air side a fluid free flow area of 0.5 m^2 and a hydraulic diameter of 0.5 cm with an extended surface factor of 20 and a length of 0.4 m, and refrigerant side a free flow area of 0.4 dm^2 and a hydraulic diameter of 1 cm, with a tube length of 2 m).

We now size the compressor from its technological screen (Figure 34.2.8). For the time being we do not detail the setting, which will be explained in Chapter 36. Let us just say that we must provide on the one hand the swept volume or displacement V_s , and secondly the values of the parameters involved in volumetric and isentropic efficiency equations.

To achieve the design once the technological screens are set, return to the driver screen, select the three rows in the table, and click “Design the selected components” below the table to start the design. The results are displayed in the technological screens: exchange surface of 12.2 m^2 for the evaporator and 99 m^2 for the condenser, rotation speed of 848 rpm for the compressor.

Various computational results are displayed in the technological screens, like the values of Re and local exchange coefficients for heat exchangers, and those of the isentropic and volumetric efficiencies for the compressor.

34.2.4.3 Recalculation of the whole cycle

Once the sizing of components is done, we get only an estimate of the actual state of the refrigerating machine, and it is necessary to recalculate the entire cycle, to reflect more accurately the interactions within the system.

h_{lh} = 2756.59 Re = 408.03
 h_{Mh} = 2824.99 Re = 441.77
 h_{vh} = 2899.20 Re = 480.73

h_{lc} = 1015.85 Re = 24849.00
h_{lvc} = 8815.23 Re = 24843.28
 h_{vc} = 549.34 Re = 395166.61

evaporator

e/λ

Hx design area

water cooling

free flow area	<input style="width: 80px;" type="text" value="0.015"/>	ext_tube Colburn correlation for single phase flow outside tubes ▼	
hydr. diameter	<input style="width: 80px;" type="text" value="0.01"/>	<input type="button" value="correlation settings"/>	
length	<input style="width: 80px;" type="text" value="6"/>		local ΔP loss coeff. <input style="width: 80px;" type="text" value="0"/>
surface factor	<input style="width: 80px;" type="text" value="1"/>		pressure drop <input style="width: 80px;" type="text" value="0.414377"/>
fin effectiveness	<input style="width: 80px;" type="text" value="1"/>		friction factor <input style="width: 80px;" type="text" value="0.144874"/>

evaporator

free flow area	<input style="width: 80px;" type="text" value="0.003"/>	evap Gungor Winterton correlation for evaporation inside tubes and a... ▼	
hydr. diameter	<input style="width: 80px;" type="text" value="0.01"/>	<input type="button" value="correlation settings"/>	
length	<input style="width: 80px;" type="text" value="6"/>		local ΔP loss coeff. <input style="width: 80px;" type="text" value="0"/>
surface factor	<input style="width: 80px;" type="text" value="1"/>		pressure drop <input style="width: 80px;" type="text" value="1.400869"/>
fin effectiveness	<input style="width: 80px;" type="text" value="1"/>		friction factor <input style="width: 80px;" type="text" value="0.026667"/>

FIGURE 34.2.6
Heat exchanger technological design screen

h_{lh} = 856.45 Re = 24395.09
 h_{Mh} = 2199.52 Re = 24917.86
 h_{vh} = 487.64 Re = 258093.19

h_{lc} = 10871.52 Re = 23328.63
h_{lvc} = 10905.89 Re = 23103.95
 h_{vc} = 10941.73 Re = 22873.63

condenser

e/λ

Hx design area

condenser

free flow area	<input style="width: 80px;" type="text" value="0.004"/>	cond Shah correlation for condensation inside pipes ▼	
hydr. diameter	<input style="width: 80px;" type="text" value="0.01"/>	<input type="button" value="correlation settings"/>	
length	<input style="width: 80px;" type="text" value="2"/>		local ΔP loss coeff. <input style="width: 80px;" type="text" value="0"/>
surface factor	<input style="width: 80px;" type="text" value="1"/>		pressure drop <input style="width: 80px;" type="text" value="0.074431"/>
fin effectiveness	<input style="width: 80px;" type="text" value="1"/>		friction factor <input style="width: 80px;" type="text" value="0.026653"/>

air cond

free flow area	<input style="width: 80px;" type="text" value="0.5"/>	air_coil Morisot correlation for air coil flow outside tubes ▼	
hydr. diameter	<input style="width: 80px;" type="text" value="0.005"/>	<input type="button" value="correlation settings"/>	
length	<input style="width: 80px;" type="text" value="0.4"/>		local ΔP loss coeff. <input style="width: 80px;" type="text" value="0"/>
surface factor	<input style="width: 80px;" type="text" value="20"/>		pressure drop <input style="width: 80px;" type="text" value="0.054248"/>
fin effectiveness	<input style="width: 80px;" type="text" value="0.4"/>		friction factor <input style="width: 80px;" type="text" value="0.027021"/>

FIGURE 34.2.7
Condenser technological design screen

VolumCompr < >

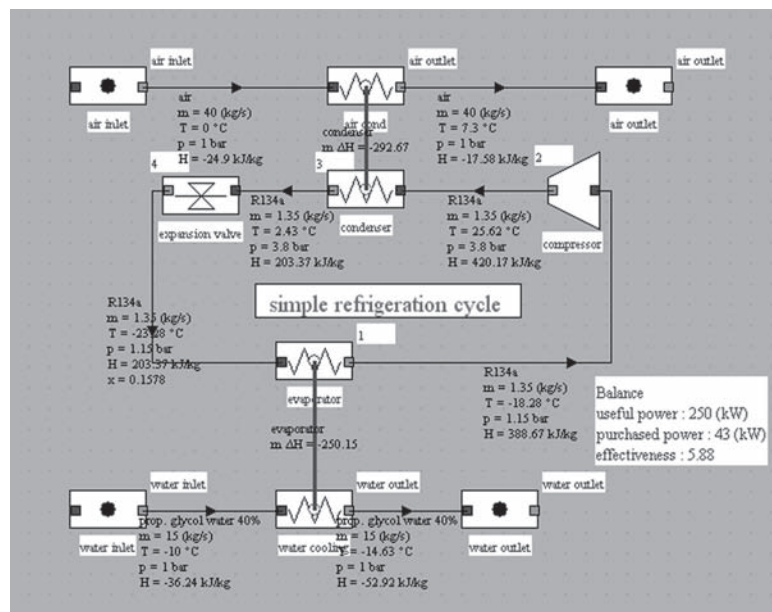
compressor Quit

a0 vol efficiency	0.96
alpha vol. efficiency	0.038
K1	0.81
K2	0.0038
K3	-0.152
R1	7
R2	1.236
rotation speed	848.06383780 <input type="radio"/> Calculate N
Vs	0.0199 <input type="radio"/> Calculate Vs <input checked="" type="radio"/> Calculate m

isentropic efficiency	0.7884113
flow rate	1.3500000
volumetric efficiency	0.8344348

FIGURE 34.2.8

Compressor technological design screen

**FIGURE 34.2.9**

Recalculated synoptic view of refrigeration cycle

Moreover, previous calculations allow to size the various components, but nothing says that the technological choice is exactly consistent with the results of the model: heat exchangers will be chosen from the range given by the manufacturer, so that their surface be as close as possible to the desired value, but probably slightly different. The compressor rotation speed will not necessarily be the one that the calculation provided: this depends on the speed control system available.

It is therefore necessary to enter the actual technological values, and recalculate, in off-design mode as explained in the next section, the performance of the machine for selected settings. The cycle is then slightly modified.

Let us for example, suppose that the compressor rotation speed is chosen equal to 900 rpm. The recalculation of the cycle leads to very slight changes: the flow rate increases slightly, the condensing pressure becomes 3.83 bar, the evaporation pressure 1.127 bar, and the isentropic efficiency drops by 12%. The COP is 5.7, and the cooling capacity 259 kilowatts. Figure 34.2.9 shows the result.

34.3 OFF-DESIGN CALCULATIONS

In this section we present the principles for calculating the off-design operation of a refrigerator. After recalling how Thermoptim calculates the various components of a system, we introduce the specific off-design problems.

Historically, we started to implement a solution method where the various components altered independently of each other flows and pressures of the cycle, but this first method proved very unstable, and the “off-design” Thermoptim development version remained unfinished for several years. At the time, the algorithms were implemented in the package core, and therefore not modifiable by users.

We have subsequently completely reconsidered our approach with two objectives: firstly to guide the search for the solution by coordinating recalculations of the various components, and also to outsource the off-design algorithms so that users can alter them if they wish.

The solution was to implement the main algorithms in **external drivers**² using technological design screens built themselves as external classes. This second method yields the same results as the first for the cases where it converged, and especially is much more robust and generic.

The cases we have treated have shown that there are two major additional challenges:

- The first concerns the development of physical phenomena equations. The behavior of the different components, which may be far from simple, must be analyzed carefully and correctly modeled. We propose in this book and in the examples posted on the Thermoptim-Unit portal a number of models, but they are not the only ones possible, and we have not covered all interesting cases;
- The second corresponds to the resolution, usually numerical, of the model equations, which requires on the one hand to find a suitable algorithm, and secondly to initialize it properly.

Our intention being primarily focused on applied thermodynamics, we mainly concentrated on the first difficulty. Numerical tools that we offer make use of libraries either included in Thermoptim, to perform simple searches by dichotomy, or generic, like minPack, which is a set of classes allowing the user to make nonlinear optimization, in particular to seek the solution of systems of equations.

In what follows, after a brief reminder of how the Thermoptim core manages recalculations, we illustrate our approach by showing how the case of the refrigeration cycle can be solved in off-design mode, and we provide the results obtained for the refrigerator sized in the previous section.

Let us recall that what we call off-design regime is the steady state operation of a facility for operating conditions other than those for which it has been designed, and not resulting in fast transient such as control actuators. We do not focus on dynamic changes at very short timescales, for which our models are not suitable.

34.3.1 Principle of computing coupled systems in Thermoptim

Calculate off-design operation of an energy technology consisting of several coupled components amounts to solving a system of equations which is usually highly non-linear.

²An overall presentation of external drivers is given Section 23.7 of Part 4, and concrete examples of implementation for off-design calculations are provided in Chapter 38.

Each component involving up to several tens of equations, it is common that a full project includes a few hundred. To solve them, it is possible to use powerful solvers, but this assumes that one can obtain an explicit formulation of these equations. In practical terms, the problem is then essentially to ensure the consistency of equations expressing the coupling between components. Without an appropriate environment, the task can be very complex and very difficult to secure.

Thermoptim has the advantage of facilitating the description of the technology studied thanks to its diagram editor, which ensures consistency of coupling between components. However, it does not in its current version formally express the equations that come into play: they are solved numerically by each component.

The Thermoptim simulator calculates step by step the various elements of a project. This is a sequential method of calculation, which differs from other modeling environments (matrix) in which all equations of the problem are solved simultaneously. This manner of proceeding has the advantage that it is much easier to calculate successively the elements one by one than solving the entire system at once. However, it induces two problems: first it may be necessary to iterate the calculations a number of times to find the right solution, especially if the system is coupled, and secondly, for a project a little complex, the question arises in what order calculations should be performed. To solve this latter problem, a set of algorithms was developed. Called Thermoptim automatic recalculation engine, it is a key element of the package. A particular screen can be displayed if desired to follow recalculation steps, and thus ensure the relevance of modeling.

The automatic recalculation engine, however, is only able to calculate phenomenological models, in which the couplings between components are much simpler than when one wants to study the system in off-design mode. It was therefore necessary to supplement it with appropriate algorithms, the use of **external drivers** appearing to be the best solution.

For a simulation in off-design mode to be realistically feasible, we must indeed be able not only to make the technological sizing of each component, but also to take into account interactions between components due to their adaptation to the new operating conditions.

To illustrate this point, consider the equations governing the behavior of the refrigerator presented section 34.1.

34.3.2 Off-design equations of the refrigerator

The evaporation temperature is set by the evaporator heat balance, which depends mainly on the one hand on the coolant temperature T_f and flow-rate (brine in this example), and secondly on the refrigerant flow.

$$Q_e = \dot{m}(h(T_e + \Delta T_{\text{surch}}, P_e) - h(T_c - \Delta T_{\text{ssrefr}}, P_c)) = U_e A_e \Delta T_{\text{ml}_{ef}} \quad (34.3.1)$$

It should be noted that the exchange coefficient U_e also depends on many parameters, including temperature and flow of fluids through the exchanger, so that solving this equation is particularly complex.

Similarly to what we presented for the evaporator, the condensation temperature is determined by the condenser thermal balance, which depends mainly on the one hand on the cooling air temperature and flow rate, on the other hand on refrigerant flow, and finally on the condenser outlet temperature.

The latter depends on the compression ratio and isentropic efficiency of the compressor itself also depending on this ratio.

$$Q_c = \tau + Q_e = U_c A_c \Delta T_{\text{ml}_{ac}} \quad (34.3.2)$$

The balance of the compressor expresses that the compression work is equal to the product of mass flow by the isentropic compression work, divided by the isentropic efficiency. It also depends on several variables and is given by:

$$\tau = \dot{m} \frac{\Delta h_s(T_e, P_e, P_c)}{\eta_s(P_c/P_e)} \quad (34.3.3)$$

These three variables are connected by (34.3.4), which is nothing but the expression of the first law.

$$Q_c = \tau + Q_e \quad (34.3.4)$$

The search for a triplet (coolant flow, evaporation temperature, condensation temperature) corresponds to that of solving a set of relatively complex nonlinear equations.

The solution we have adopted is to code an external driver that provides the resolution of this system of equations and updates Thermoptim once it has determined that triplet. A solution using the minPack library will be presented in section 38.4.

34.3.3 After processing of simulation results

When performing off-design simulations, each setting leads to a new result, which can be saved in a specific project file. This generates a set of files with the same structure which we must then be able to exploit.

PRACTICAL APPLICATION

Excel macro for after-processing of Thermoptim files



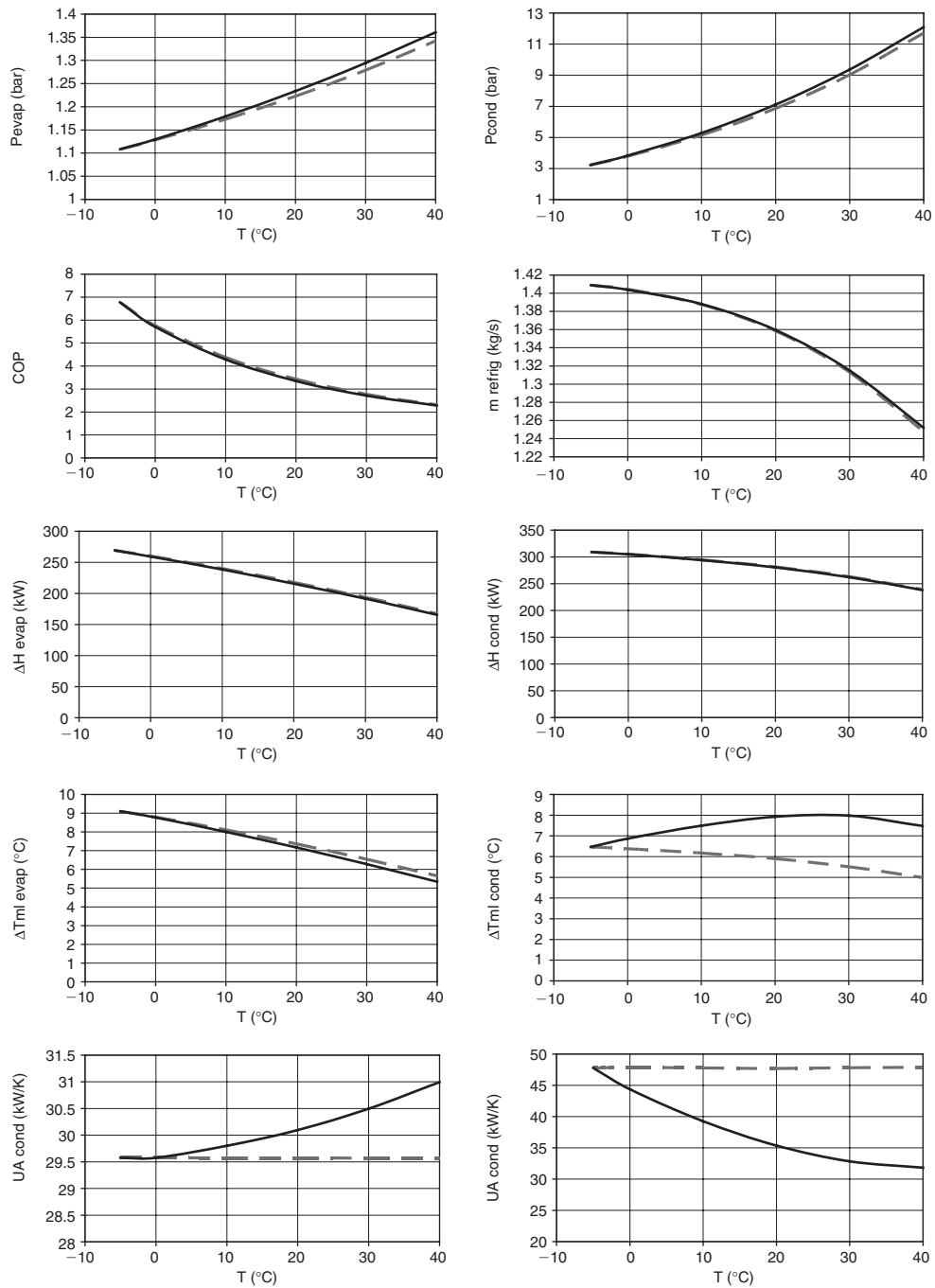
[CRC_pa_11,
CRC_In_18]

An Excel macro for after-processing Thermoptim has been designed to facilitate the exploitation of sets of simulated project files.

Presented in Volume 1 of the software reference manual, it can be downloaded from the Thermoptim portal (<http://www.thermoptim.org/sections/logiciels/thermoptim/ressources/macro-excel-post>). You may download it and use it at your convenience.

An Excel spreadsheet containing a macro has been specifically developed for this. Its instructions for use are given Volume 1 of the reference manual of the software. The principle is as follows:

- Save each new simulation in a separate project file;
- Once all the states sought obtained, open the Excel spreadsheet, and remove all sheets other than “macro” and “graph”;
- Open Windows Explorer in the project directory, select all the project files you want, and drag them into the spreadsheet window. Excel opens them all in different windows;
- Go to sheet “macro” of the spreadsheet, and click “Load Project”, which automatically performs the loading of files into new sheets in the workbook. However, you have no control over the order in which sheets will be placed, and you may need to reorder them by hand;
- back in sheet “macro”, update the table of values to be extracted from the result sheets, changing the labels in column A to fit your desires, and entering column B the cell number corresponding to each value. Finally, enter in B4 the number of values to be extracted;
- click “extract”. The macro updates sheet “graph” by extracting from result files values you want to monitor. If applicable, remove from this sheet values that may still exist from another study;
- use spreadsheet functions to calculate further values if you wish, and to draw graphics you want.

**FIGURE 34.3.1**Effect of U variation (dashed: without, continuously: with)

34.3.4 Effect of change in UA

It is interesting to evaluate the influence on the results of taking into account the variation of heat exchange coefficients in heat exchangers. Figure 34.3.1, where we plotted the evolution of different indicators, depending on outside temperature, shows the gap between them, depending on whether or not one takes into account the variation of U as a function of temperature and flow. Both cases are set in the same way for an outside temperature of -5°C .

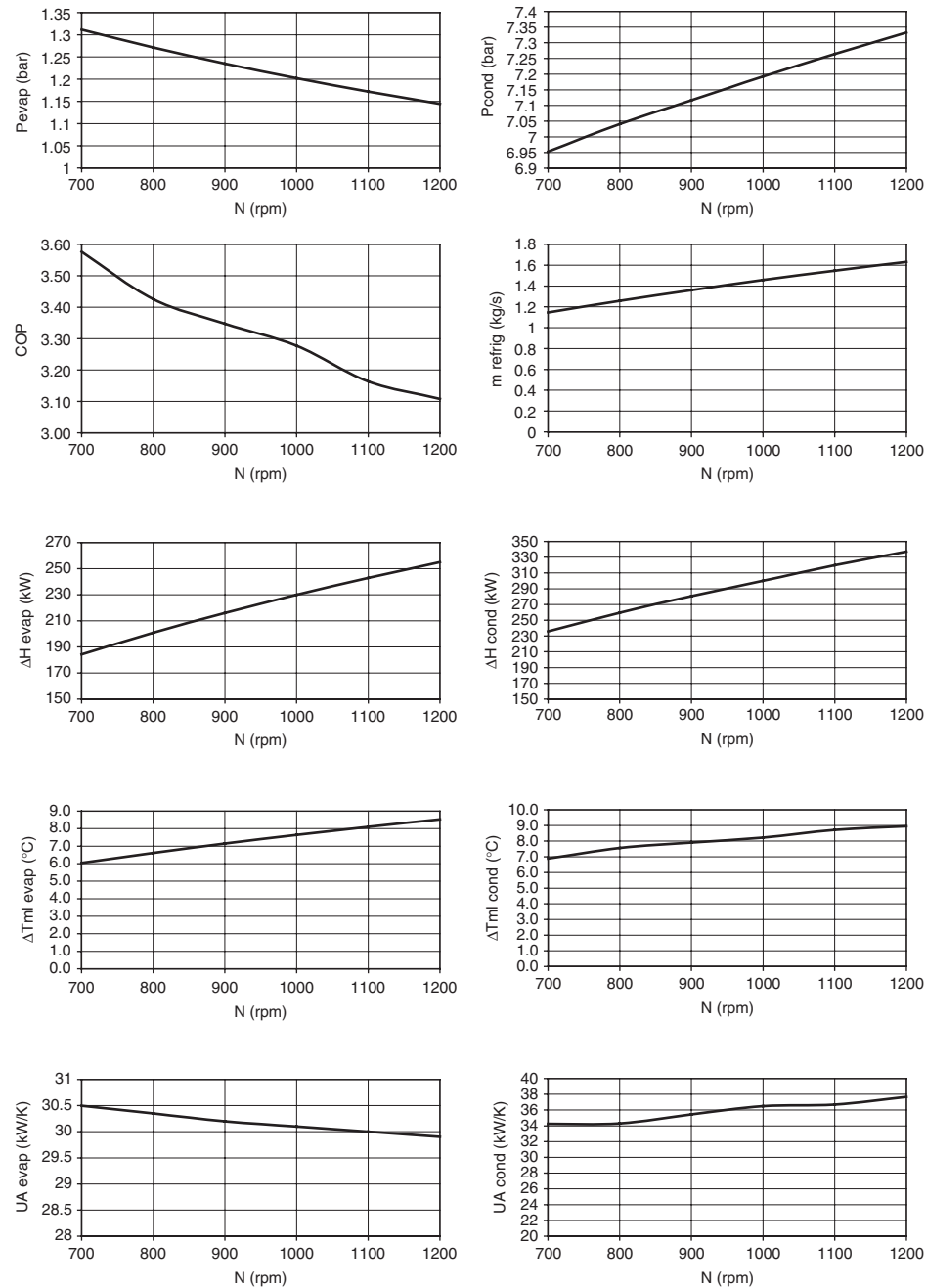


FIGURE 34.3.2

Effect of rotation speed

In the case that we studied, this influence is almost undetectable on the variation of COP, and remains low on the condensing pressure P_{cond} and cooling capacity ΔH_{evap} . It is apparent on the refrigerant flow and becomes especially important for parameters relating to heat exchangers, including condenser ΔT_{ml} .

The last two graphs show the evolution of UA, which is far from negligible, which fully justifies seeking to take into account the influence of heat exchange coefficients in off-design models.

Note the variation of the condenser logarithmic mean temperature difference, which is far from being linear when one takes into account the variation of U.

Figure 34.3.2 shows the shape of results when the speed of the compressor varies.

The comparison between these two cases shows several differences in behavior, such as between the refrigerant flow and the COP. The latter decreases in both cases, while the flow decreases in the first and increases in the second, thus showing the difficulty in predicting the evolution laws for even a cycle as simple as this.

The results obtained show that, particularly for refrigerators involving multi-zone exchangers, the off-design laws of evolution are not simple, and do not amount to a power function of flow. This arises because the total area available for heat exchange is divided into two-phase and vapor zones, in which the heat exchange coefficients are very different.

It is also noteworthy that the changes are typically relatively simple, while the underlying models are very complex. It is tempting in these circumstances to try and find simplified models (e.g. polynomial laws) equivalent to the knowledge model.

There is a real challenge in terms of model reduction. We will show in the next section how that can be done.

34.4 DEVELOPMENT OF SIMPLIFIED MODELS OF SYSTEMS STUDIED

Thermoptim is a modeling environment which allows one to easily represent and calculate with great precision energy systems which can be very complex.

Based on detailed phenomenological or technological equations, it is very versatile but has the inherent limitations of knowledge models: computation times may be quite long, especially for off-design operation analyses.

Therefore, when you need to make a very large number of simulations, for example because you study over a long period the behavior of a system subject to variable boundary conditions (load, storage etc.), Thermoptim may become inappropriate because it is too heavy and too slow.

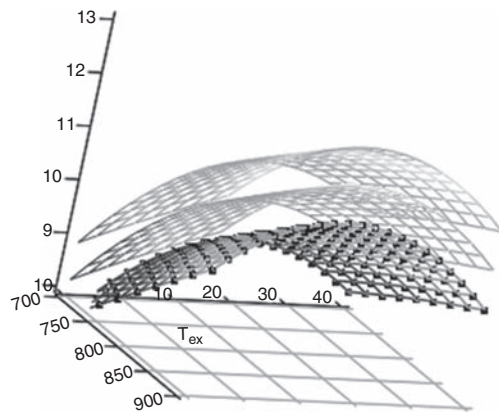
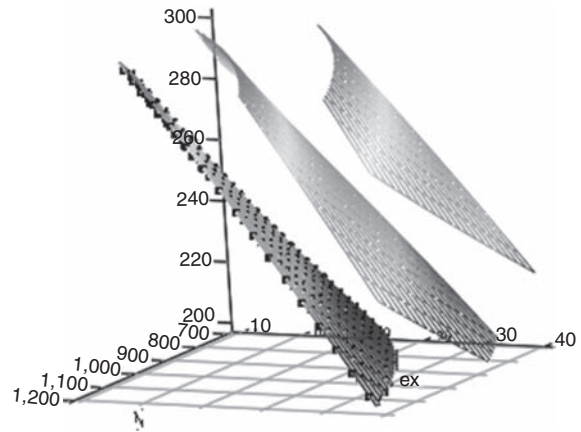
34.4.1 Model reduction principle

To circumvent this difficulty, we may use techniques known as model reduction, which aim to develop simplified empirical models providing results equivalent to knowledge models from which they are derived. Model reduction can sometimes be done directly when the mathematical properties of the knowledge model allow, but it is pretty rare. Most of the time simplified models are obtained numerically using parameter identification methods.

The operating principle is as follows:

- we first perform a sufficient number of simulations with the knowledge model for different sets of its input variables, and tables or files are saved with these sets of values and outputs;
- we select an *a priori* mathematical form of the simplified model we want to test (of course it must have the same input variables as those used for simulations). The choice of this mathematical form is guided by experience and by various considerations, including in particular the kind of results and graphs linking the input and output variables;
- the simplified model parameters are estimated by minimizing the difference between results it provides and those obtained with the knowledge model for different sets of input variables selected.

When the simplified model is expressed linearly with respect to simple functions of its parameters, these can be directly determined by least square regressions. Otherwise, it is necessary to use nonlinear optimization algorithms.

**FIGURE 34.4.1** ΔT_{ml_cond} condenser**FIGURE 34.4.2**

Cooling capacity

The quality of the model crucially depends on two elements:

- its structure, which must be as consistent as possible with digital sets of variables and reference results;
- information contained in the sets of variables selected, which must be sufficiently rich and discriminating against model entries so that parameters can be estimated unambiguously. This includes taking care that inputs are not correlated with each other, otherwise the identified model can become inaccurate for other values of input variables.

34.4.2 Model reduction example

We give below some guidance about how very accurate scale models may be developed from a Thermoptim project such as the refrigeration cycle studied in off-design mode. Results presented here show that it can be represented faithfully by polynomial models of order 2 in a wide range of its input variables (as the model reduction was done on a variant, values are not exactly the same as those given in sections 34.3 and 38.4).

Figures 34.3.1 and 34.3.2 were drawn with Excel, which allows for very easy adjustment of trendlines. For example, the condenser log-mean temperature difference ΔT_{ml_cond} can be represented by quadratic relationships with respect to the outside air temperature T_{ex} or the compressor rotation speed N .

The correlation coefficients being excellent, a quadratic in two variables of the following type is possible:

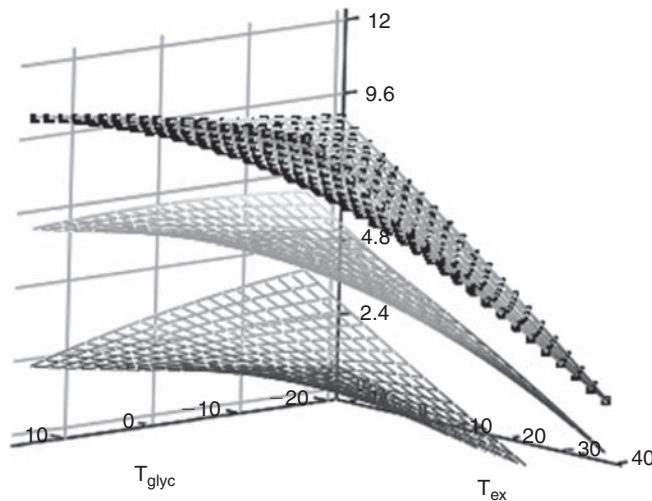
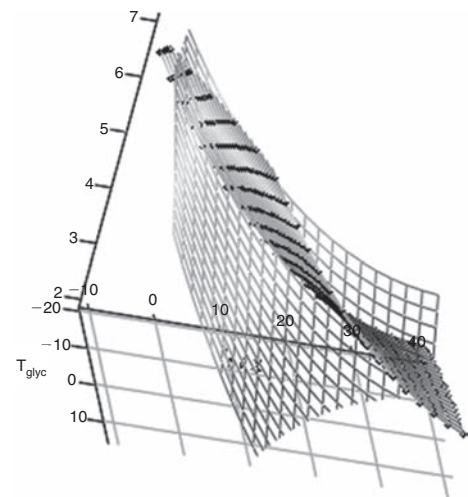
$$\Delta T_{ml_cond} = aT_{ex}^2 + bN^2 + cT_{ex}N + dT_{ex} + eN + f$$

The result is very good too, so that one can hope to fit a generalized quadratic relation for several input variables: outside air temperature T_{ex} , compressor rotation speed N , brine temperature T_{glyc} , and superheating DT_{sur} .

From 45 well-chosen simulations, it was possible to identify a quadratic form covering intervals $[-5, 45]$ for T_{ex} , $[-15, 15]$ for T_{glyc} , $[770, 1170]$ for N , $[1, 12]$ for DT_{sur} , with a correlation coefficient $r^2 = 0.998$.

In the same way, one can express by similar equations and with similar accuracy, cooling capacity, compressor power, refrigerant flow etc.

Figures 34.4.1 and 34.4.2 show the shapes of surfaces obtained by setting two of the four independent variables. In both cases, the temperature of the brine T_{glyc} is -10°C for the bottom surface, and -5°C and 0°C for others.

**FIGURE 34.4.3** ΔT_{ml} evaporator**FIGURE 34.4.4**

COP

As can be seen, the model identified from 45 points is then used to explore a relatively large area, and this much more efficiently than using Thermoptim. Of course, these curves are valid only for the selected project and the technological parameters chosen: what is gained in flexibility of use is lost in genericity.

Figure 34.4.3 shows the evaporator log-mean temperature difference $\Delta T_{ml_{evap}}$ for three values of superheating DT_{sur} : 4, 8 and 12°C, from top to bottom. It shows that for this example the sensitivity of the model in this area is rather strong, and that superheating must be limited otherwise $\Delta T_{ml_{evap}}$ becomes too low.

Figure 34.4.4 shows the COP trend as a function of T_{ex} and T_{glyc} for two values of the rotation speed: 870 (surface with black dots) and 1170 rpm.

For simplicity, we also selected a quadratic form for the COP, but it would have been strictly preferable to recalculate it as the ratio of cooling capacity to compression power, the latter two being represented by our model. The reader can easily verify that, given the mathematical form of the model used, the two surfaces intersect in a plane parallel to the axis OZ.

Another example will be given in section 38.2.4: the Thermoptim model of an air piston compressor allows one to calculate the filling of a compressed air storage of given volume at variable pressure, thanks to polynomial fits of the results it provides.

34.5 METHODOLOGICAL DIFFICULTIES

When attempting to perform off-design calculations, one is faced with a number of methodological difficulties. These include:

- have relevant technological models, both at component level and for their interaction. For this, as we have seen, two main methods of approach can be adopted: either a purely digital fit, if there is one that is satisfactory, or keep an approach as physical as possible. As appropriate, one or the other choice will be made;
- obtain experimental data usable. Experience shows that this can be a very big job;

- set models of components selected, that is to say, identifying the parameters of these models. This is probably one of the main difficulties of the whole (see Chapters 35 to 38);
- have a reference modeling environment sufficiently powerful, able to simulate different configurations encountered in practice. As we have seen, Thermoptim responds to some extent to those specifications;
- whenever possible, develop simplified models from the reference tool (data analysis, model reduction etc.).

In subsequent chapters, we will describe these difficulties, first for the various components, and then for the examples to be presented.

We have just mentioned that two of the main methodological difficulties are obtaining exploitable data and experimental model parameterization of components selected. A necessary condition is to have reliable test benches, which represents a considerable investment, both materially and in human terms. We express our deep appreciation to the institutions that have agreed to make available to us data from their test benches for our work (Laborelec, Trane-EDF and Cemagref).

REFERENCES

- Rapport du Programme de Recherche Interdisciplinaire 2.9 Varitherm, ACI Energie, 2003–2005* (http://energie.cnrs.ensma.fr/Rapport_activites_2002-2006/RAPPORT%20FINAL/PR2.9.pdf).
- R. Gicquel, P. Riviere, R. Zmeureanu, *Enseignement de la thermodynamique appliquée problématique d'une nouvelle approche pédagogique par simulation et essais de machines frigorifiques ou pompes à chaleur*, 7ème Colloque Interuniversitaire franco-québécois sur la thermique des systèmes, 23–25 Mai 2005, Saint-Malo.
- J.M. Gordon, K.Ch. Ng, *Cool thermodynamics: the engineering and physics of predictive, diagnostic and optimization methods for cooling systems*, Cambridge International Science Publishing, Cambridge, 2000.
- I. Guitari, P. Haberschill, A. Lallemand *Modélisation dynamique d'une pompe à chaleur fonctionnant au CO₂*, 12ème JITH, Tanger, Maroc, 15–17 nov. 2005.

Technological Design and Off-design Behavior of Heat Exchangers

Abstract: The purpose of this chapter is to explain how to model and set heat exchangers so that they can be sized and calculated in off-design mode. It complements Chapter 8 of Part 2 which provides all the background for simple heat exchanger calculations in energy systems.

Not particularly complicated, it uses non-trivial thermal engineering concepts, as we recall in this chapter, but supposes that the reader has a basic culture in the discipline. If this is not the case, it is preferable that you refer to a good thermal engineering textbook. The notations are those of Chapter 8 of Part 2.

Keywords: heat exchanger, heat transfer coefficient, thermal resistance, NTU, pinch, shell and tube, air coils, plate, Reynolds, Nusselt, Prandtl, correlation, evaporator, condenser, pressure drop, identification.

35.1 INTRODUCTION

35.1.1 General

Let us recall that the NTU method, used in the Thermoptim phenomenological version, provides only the product UA of the global exchange coefficient by the surface of the exchanger, without the two terms being evaluated separately.

To size the heat exchanger, i.e. calculate its surface, one must on the one hand choose its geometry, and secondly calculate the overall exchange coefficient U , which depends on the configuration and fluid thermophysical properties.

As we stated in Part 2, there is actually a very important qualitative leap between the basic arithmetic of balancing the heat exchanger and what we call its technological design.

As we have seen, two main methods of approach can be adopted: either a purely digital fit, if there is one that is satisfactory, or keep an approach as physical as possible. This last choice has been made here.

The approach we adopted in Thermoptim is unconventional, but it is consistent with other approaches used in heat exchangers, and it proves quite fruitful for the study of complex systems.

35.1.2 Reminders on the NTU method

We begin with a brief review of the NTU method, which is an excerpt from section 8.2.1 of Part 2 (the equation numbers are those in that Part).

By definition, NTU is defined as the ratio of the UA product to the minimum heat capacity rate.

$$NTU = \frac{UA}{(\dot{m} \cdot c_p)_{\min}} \quad (8.2.1)$$

We call R the ratio (less than 1) of heat capacity rates:

$$R = \frac{(\dot{m}c_p)_{\min}}{(\dot{m}c_p)_{\max}} \leq 1 \quad (8.2.2)$$

and ε the **effectiveness of the exchanger**, defined as the ratio of the heat flux actually transferred to the maximum possible flux:

$$\varepsilon = \frac{\phi}{\phi_{\max}} \quad (8.2.3)$$

We can show that ϕ_{\max} , that would be obtained for a counter-flow heat exchanger of infinite length, is:

$$\phi_{\max} = (\dot{m}c_p)_{\min} \Delta T_i$$

ΔT_i is the difference between inlet temperatures of both fluids.

ΔT_{\max} and ΔT_{\min} being the temperature differences within each of the two fluids and not between them, we have:

$$\phi = (\dot{m}c_p)_{\min} \Delta T_{\max} = (\dot{m}c_p)_{\max} \Delta T_{\min} \quad (8.2.4)$$

We get:

$$\varepsilon = \frac{\Delta T_{\max}}{\Delta T_i} \quad (8.2.5)$$

Since $\phi = UA \Delta T_{ml} = (\dot{m}c_p)_{\min} \Delta T_{\max} = (\dot{m}c_p)_{\max} \Delta T_{\min}$

$$NTU = \frac{UA}{\dot{m}c_{p\min}} = \frac{\Delta T_{\max}}{\Delta T_{ml}}$$

With these definitions, it is possible to show that there is a general relation of type:

$$\varepsilon = f(NTU, R, \text{flow pattern}) \quad (8.2.7)$$

In practice, it suffices to have a set of relationships corresponding to flow patterns representative of exchangers studied, and the design of a heat exchanger is made on the basis on the one hand of balance equations (8.2.4) and on the other hand of the internal equation (8.2.7).

In **design mode**, if we know the flow of both fluids, their inlet temperatures and the heat flux transferred, the procedure is as follows:

- we start by determining the outlet temperatures of fluids from equation (8.2.4);
- we deduce the fluid heat capacity rates $\dot{m}c_p$ and their ratio R;
- the effectiveness ε is calculated from equation (8.2.5);

- the value of NTU is determined from the appropriate (NTU, ϵ) relationship;
- UA is calculated from equation (8.2.1).

In **off-design mode**, if you know UA, (8.2.1) gives the value of NTU, and you can determine ϵ from the appropriate (NTU, ϵ) relationship. Equation (8.2.5) allows you to calculate heat transferred.

In both cases, the enthalpy balance provides the outlet temperatures.

In practice, we do not know UA but A. However, we can often consider that U varies only in the second order, and seek an approximate solution by considering U constant, then recalculate its value for new operating conditions, and iterate until a reasonable accuracy is obtained. It is particularly necessary to operate this way when the exchanger is multi-zone, because only the total area is known, not its distribution among different areas.

As explained section 8.3.6 of Part 2, the phenomenological heat exchanger screen “off-design” calculation mode allows one to calculate in a simplified manner off-design operation. In this case, the software considers that the four input variables of the exchanger are set. No correction is made on the exchange coefficients ($U = \text{Const.}$), but it is possible to modify by hand the UA value in the exchanger screen.

Generally however, this calculation mode is not satisfactory: the heat exchange coefficients must be recalculated iteratively and the off-design behavior is determined thanks to an external driver.

Several examples using both calculation modes are given in Chapter 38.

35.2 MODELING OF HEAT TRANSFER

The overall heat transfer coefficient U depends on the distribution of thermal resistances in the exchanger. If the exchange surfaces are equal for both fluids:

$$\frac{1}{U} = \frac{1}{h_h} + \frac{e}{\lambda} + \frac{1}{h_c} \quad (35.2.1)$$

The values of convection coefficients h_h and h_c are based on fluid thermophysical properties and exchange configurations, convective regimes being strongly dependent on the flow velocity.

They can be obtained from correlations giving the value of Nusselt number $Nu = hd_h/\lambda$, depending on Reynolds $Re = \rho C d_h/\mu$ and Prandtl $Pr = \mu c_p/\lambda$ numbers.

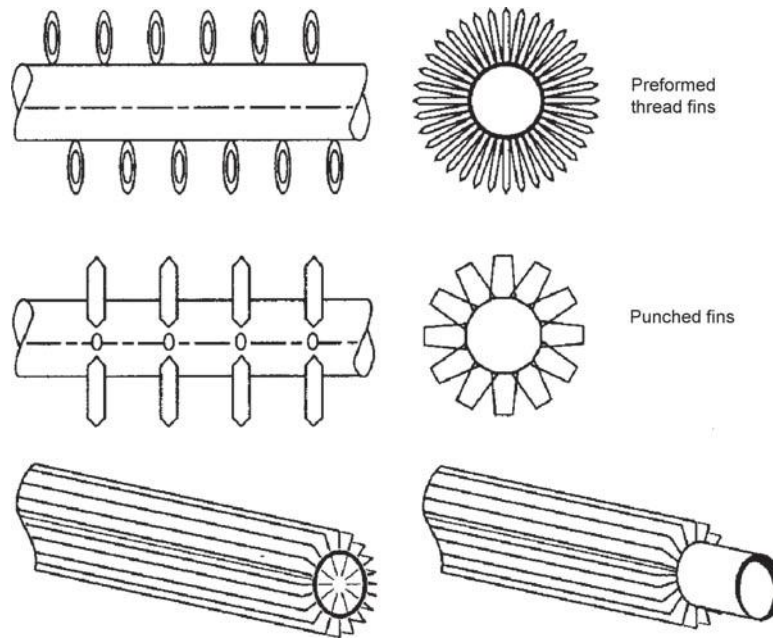
In implementations proposed in Thermoptim, we take into account the thermal resistance of the wall (as well as that of the fins if they exist), and calling S_h and S_c the total exchange areas of hot and cold sides, we relate these two surfaces to a common reference (or primary) surface S or A, called exchanger surface. For this, we introduce two “surface factors” f_h and f_c , such as $S_h = f_h A$, and $S_c = f_c A$. If there are no extended surfaces, $f_h = f_c = 1$.

The calculation of U is ultimately done by:

$$\frac{1}{U} = \frac{d_{hh}}{\lambda_h Nu_h} + \frac{e}{\lambda} + \frac{d_{hc}}{\lambda_c Nu_c}$$

35.2.1 Extended surfaces

If there are extended surfaces, one takes as a reference surface that without extended surfaces, and calculates a surface factor greater than 1 for the other (Figure 35.2.1). Taking into account


FIGURE 35.2.1

 Extended Surfaces (From *Techniques de l'Ingénieur – Génie énergétique*)

the existence of fins, $\eta_{0,h}$ and $\eta_{0,c}$ being the overall effectiveness of fins hot and cold sides, we have:

$$\frac{1}{U_h A_h} = \frac{1}{A_h \eta_{0,h} h_h} + \frac{e}{A_w \lambda} + \frac{1}{A_c \eta_{0,c} h_c} \quad (35.2.2)$$

with A_h and A_c total exchange areas warm and cold sides, A_w exchanger wall surface, and $\eta_{0,h}$ and $\eta_{0,c}$ overall fin effectiveness on warm and cold sides (see section 8.1.3).

There is also a cold side global exchange coefficient U_c , with of course:

$$U_c A_c = U_h A_h$$

35.2.2 Calculation of Reynolds and Prandtl numbers

$Re = \rho C d_h / \mu$ can be expressed directly from fluid mass flow, fluid free flow area A_c , and mass velocity $G = \rho C$.

Since $\dot{m} = G A_c$

$$Re = \frac{G d_h}{\mu} = \frac{\dot{m} d_h}{\mu A_c} \quad (35.2.3)$$

Knowing mass flow, you have to give the free flow area A_c and the hydraulic diameter d_h .

For gases, the Prandtl number varies slightly depending on temperature and remains between 0.7 and 0.75. It can therefore be considered constant without committing an error. For liquids, it is imperative to consider temperature in the computation of Pr. This is obviously what is done in Thermoptim, where thermophysical properties of substances are calculated accurately.

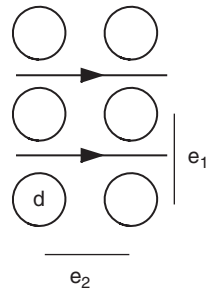


FIGURE 35.2.2
Arrangement in line

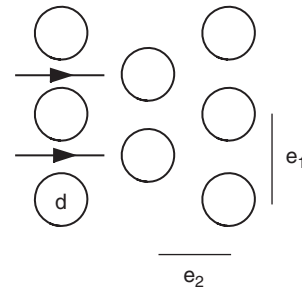


FIGURE 35.2.3
Staggered arrangement

35.2.3 Calculation of the Nusselt number

The Nusselt number is almost always given by the following equation:

$$\text{Nu} = C_1 \text{Re}^a \text{Pr}^b (\mu/\mu_p)^c \quad (35.2.4)$$

where C_1 , a , b , and c are constants. Coefficients C_1 , a and b vary depending on configurations encountered, and the additional term to account for variations in viscosity is often neglected.

The viscosity correction is made at the wall temperature. However, it is not calculated in Thermoptim. Initially, the solution is to estimate it as being equal to the average temperature of both fluids, but this is only valid in first approximation, and in the case of a multizone heat exchanger, this can lead to discrepancies.

In general, the Reynolds number exponent is between 0.5 and 0.8, and that of the Prandtl number between 0.33 and 0.4. You can find in the literature values of correlations for very special finned geometries.

The flow regime has a significant influence on the value of Nu . Where Re is less than 2,000, the regime is laminar, and if Re is greater than 5,000, it is turbulent, with a transition zone, these boundaries not being perfectly stable.

For established laminar flow, $\text{Nu} = \text{Const}$, the value being between 4 and 8 or so, depending on the shape of the tube and the heat exchange mode (constant temperature or flux).

35.2.3.1 Inside tubes

Inside tubes, the formula most used is that of Mac Adams and Dittus-Boettler:

$$\text{Nu} = 0.023 \text{Re}^{0.8} \text{Pr}^{0.4} \quad (35.2.5)$$

35.2.3.2 Flow perpendicular to tubes

For flows perpendicular to tubes, the arrangement of tubes influences the exchange coefficients, and several formulas exist, such as Colburn:

$$\text{Nu} = 0.33 \text{KpKrRe}^{0.6} \text{Pr}^{0.33} \quad (35.2.6)$$

Coefficients Kp and Kr depend on the arrangement and relative values of e_1 , e_2 and d (Kp of the number of rows, and Kr of the network geometry and Re). At first, not to overcomplicate things, we have neglected the influence of these two terms in external classes provided with Thermoptim, taking them both equal to 1.

35.2.3.3 Finned coils

For finned coils, predictive correlations are relatively complex. However ultimately, things are simplified, and it can be shown that simple relationships such as (35.2.7) can be used.

$$h = \text{K}_1 \text{Re}^{0.77} = \text{K}_2 G^{0.77} = \text{K}_3 V^{0.77} \quad (35.2.7)$$

Just identify coefficient K based on the parameter chosen to obtain a simple relationship characterizing heat exchange air side.

35.2.3.4 Two-phase exchange

For two-phase exchange, things are much more complicated. Most accurate methods take into account several zones depending on the vapor quality and a related quantity, called void fraction. Some correlations calculate h from an implicit relationship, while others prevent this complication.

In correlations used for two-phase exchange, Nusselt is often calculated as the product of a liquid Nusselt by an amplification factor, Nu_{liq} being calculated from the MacAdams correlation, valid inside a tube. It is a legitimate question whether this calculation remains valid for other types of heat exchangers including plate heat exchangers. Can we especially recalculate Nu_{liq} for the configuration chosen, and keep the amplification factor? As discussed below, the tests suggest not.

formulation for condensation outside horizontal tubes

We selected correlation given by W. Levy, section 1.2.2 of article B1540 from Techniques de l'Ingénieur:

$$Nu = \frac{3.022d_h}{\lambda} \left[\frac{\lambda^3 H \rho^3 g}{d_h \mu \Delta \theta} \right]^{0.25} \quad (35.2.8)$$

formulation for condensation in tubes

We selected correlation of Shah (1979), modified by Bivens (1994):

$$Nu = Nu_{10} F = 0.023 Re_{10}^{0.8} Pr_{10}^{0.4} \left[(1-x)^{0.8} + \frac{3.8x^{0.76}(1-x)^{0.04}}{\left(\frac{P}{P_c}\right)^{0.38}} \right]$$

$$Nu = Nu_{Shah} [0.78738 + 6187.89G^{-2}]$$

In this expression, the calculation of Nu_{10} must be done with the total mass flow \dot{m} .

This relationship is applied by averaging the F factor in the range of variation of x , which simply asks to calculate average values for the integrated functions of x . The following equation was identified numerically to obtain a simple expression of F averaged:

$$\int x^{0.76}(1-x)^{0.04} dx = -0.0155x^3 + 0.1669x^2 + 0.1083x - 0.0065$$

$$\int (1-x)^{0.8} dx = -0.5555556(1-x)^{1.8}$$

Formulation for the evaporation in tubes

We selected the Gungor and Winterton correlation (1987):

$$Nu = Nu_{liq} F$$

$$Nu = 0.023 Re_{liq}^{0.8} Pr_{liq}^{0.4} \left[\left(1 + 3000 Bo^{0.86} + 1.12 \left(\frac{x}{1-x} \right)^{0.75} \left(\frac{v_v}{v_l} \right)^{0.41} \right) \right]$$

In this expression, the calculation of Nu_{liq} must be done with the liquid phase flow alone $(1-x)\dot{m}$.

This relationship is applied by averaging the F factor in the variation range of x , taking into account the flow of the liquid phase alone. The following equation was identified numerically to obtain a simple expression of F averaged:

$$\int \left(\frac{x}{1-x} \right)^{0.75} (1-x)^{0.8} dx = 0.0079x^4 - 0.131x^3 + 0.6128x^2 + 0.0651x - 0.0054$$

$$\int (1-x)^{0.8} dx = -0.5555556 (1-x)^{1.8}$$

The expression of Bo, boiling number is given below in general, then for a tube, q_{th} being the flux density, A_{ext} the outer surface and G the mass velocity:

$$Bo = \frac{q_{th}}{GL_v}, \text{ which can be approximated as follows for a tube:}$$

$$Bo = \frac{mL_v}{A_{ext}} \frac{1}{GL_v} = \frac{GA_c L_v}{A_{ext}} \frac{1}{GL_v} = \frac{A_c}{A_{ext}} = \frac{d_h}{4L}$$

35.2.3.5 plate heat exchangers

For plate heat exchangers, exponent b is almost always $1/3$ and c 0.14 for Muley and Manglik (1999) and 0.17 for Kumar (1984).

For chevron of angles $\leq 30^\circ$ Kumar (1984) gives 0.348 for C_1 and 0.663 for a . Alfa Laval provides $C_1 = 0.142$, $a = 0.72$, $b = 0.37$ and $c = 0.108$ for the A20 exchanger. Manglik and Muley (1999) propose a more complex formula for chevron angles $\beta = 90 - \alpha$ from 30° to 60° , and surface factors μ from 1 to 1.5 for $Re > 10^3$.

$$Nu = [0.2668 - 0.006967\beta + 7.244 \times 10^{-5}\beta^2] \times [20.78 - 50.84\mu + 41.16\mu^2 - 10.51\mu^3] \\ \times Re^{[0.728 + 0.0543 \sin[(\pi\beta/45) + 3.7]]} Pr^{1/3} (\eta/\eta_w)^{0.14}$$

Figure 35.2.4 shows the importance of the influence of the correlation used on Nu value as a function of Re for $Pr = 0.7$. Correlations used are listed hereafter.

- inside tubes (Mac Adams): $Nu = 0.023Re^{0.8}Pr^{0.4}$
- outside tubes (Colburn): $Nu = 0.33Re^{0.6}Pr^{0.33}$
- plate with viscosity correction: $Nu = 0.2Re^{0.674}Pr^{0.33}(\mu/\mu_p)^{0.14}$

Figures 35.2.4 and 35.2.5 show the influence of correlation parameters on the Nusselt number, and on the exchange coefficients.

As expected, we note that the correlation for the plate heat exchanger leads to U values larger than those of Mac Adams and Colburn. However, it is not the only one to be proposed (Ayub, 2003).

35.2.4 Calculation of multi-zone exchangers

The calculation of U by $1/U = d_{hh}/(\lambda_h Nu_h) + \epsilon/\lambda + d_{hc}/(\lambda_c Nu_c)$ is only valid for a simple exchanger, through which flow two fluids with constant thermophysical properties.

For multizone exchangers such as evaporators and condensers for refrigeration machines, the calculation of U is more difficult, because the overall exchanger is actually a heat exchanger in series

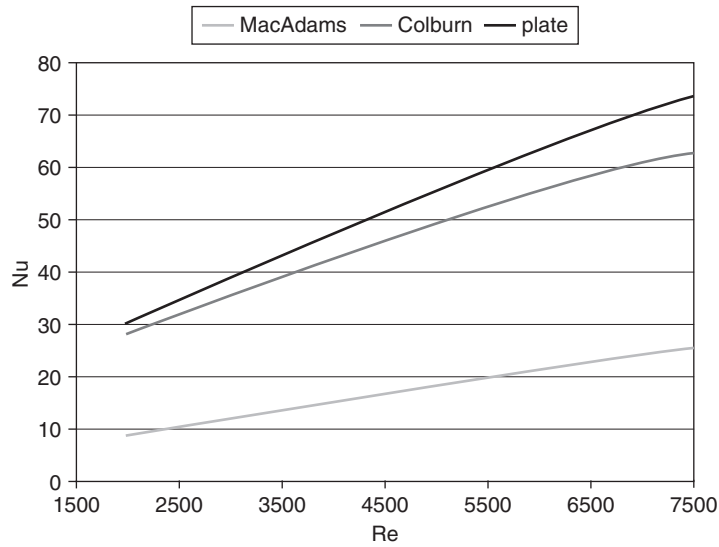


FIGURE 35.2.4
Correlations used

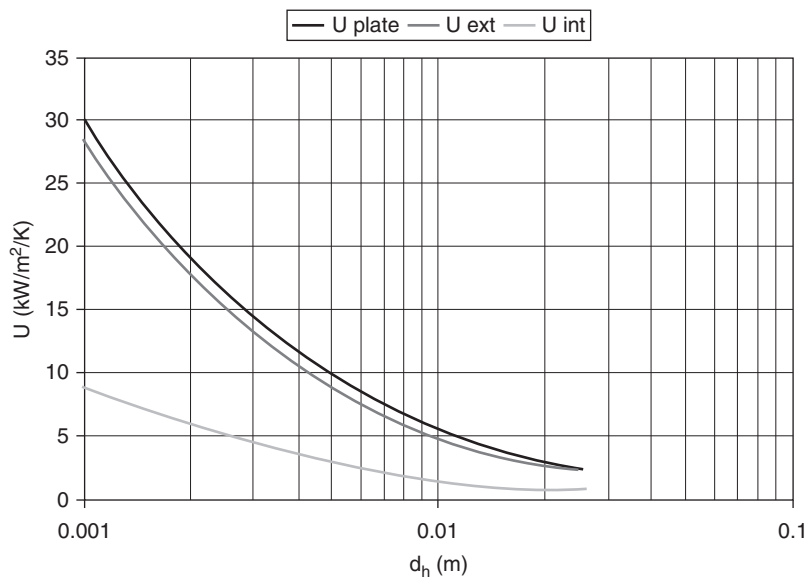


FIGURE 35.2.5
Effect of dh on U

or series-parallel because of the linkages between the three sub exchangers-liquid (l), liquid-vapor (lv) and vapor (v), which share the total area of the exchanger. Only the total area being known, it is necessary to compute simultaneously the three parts of the exchanger to find the solution.

Additivity rules that apply are the following: the total area A is the sum of the surfaces of different zones, and the total flux exchanged ϕ is the sum of fluxes exchanged in the different zones.

For multizone exchangers, the calculation must be conducted in several iterations since UA and NTU must be determined for each zone. Convergence problems may occur.

Several cases must be considered:

- the hot fluid is two phase and the cold fluid sensible heat;
- the cold fluid is two phase and the hot fluid sensible heat;
- both cold and hot fluids are two phase.

35.2.4.1 Equations for evaporators

two phase cold fluid and hot fluid sensible heat

The equations are as follows (Figure 35.2.6):

$$\begin{aligned} m_h C_{p_h} (T_{hi} - T_{hv}) &= m_c C_{p_{cv}} (T_{co} - T_{cv}) \\ m_h C_{p_h} (T_{hv} - T_{hl}) &= m_c C_{p_{clv}} (T_{cv} - T_{cl}) = m_c L_c \\ m_h C_{p_h} (T_{hl} - T_{ho}) &= m_c C_{p_{cl}} (T_{cl} - T_{ci}) \end{aligned}$$

Relations giving epsilon and R are then:

$$\begin{aligned} \epsilon_v &= \frac{T_{co} - T_{cv}}{T_{hi} - T_{cv}} & R_v &= \frac{m_c C_{p_{cv}}}{m_h C_{p_h}} \\ \epsilon_{lv} &= \frac{T_{hv} - T_{hl}}{T_{hv} - T_{ci}} & R_{lv} &= \frac{m_h C_{p_h}}{m_c C_{p_{clv}}} \\ \epsilon_l &= \frac{T_{cl} - T_{ci}}{T_{hl} - T_{ci}} & R_l &= \frac{m_c C_{p_{cl}}}{m_h C_{p_h}} \end{aligned}$$

If the fluid enters in two-phase state in the evaporator, the equations are slightly different.

35.2.4.2 Equations for condensers

Two phase hot fluid and cold fluid sensible heat

The equations are as follows (Figure 35.2.7):

$$\begin{aligned} m_h C_{p_{hv}} (T_{hi} - T_{hv}) &= m_c C_{p_c} (T_{co} - T_{cv}) \\ m_h C_{p_{hlv}} (T_{hv} - T_{hl}) &= m_c C_{p_c} (T_{cv} - T_{cl}) = m_h L_h \\ m_h C_{p_{hl}} (T_{hl} - T_{ho}) &= m_c C_{p_c} (T_{cl} - T_{ci}) \end{aligned}$$

Relations giving epsilon and R are then:

$$\begin{aligned} \epsilon_v &= \frac{T_{hi} - T_{hv}}{T_{hi} - T_{cv}} & R_v &= \frac{m_h C_{p_{hv}}}{m_c C_{p_c}} \\ \epsilon_{lv} &= \frac{T_{cv} - T_{cl}}{T_{hv} - T_{cl}} & R_{lv} &= \frac{m_c C_{p_c}}{m_h C_{p_{hlv}}} \\ \epsilon_l &= \frac{T_{hv} - T_{ho}}{T_{hv} - T_{ci}} & R_l &= \frac{m_h C_{p_{hl}}}{m_c C_{p_c}} \end{aligned}$$

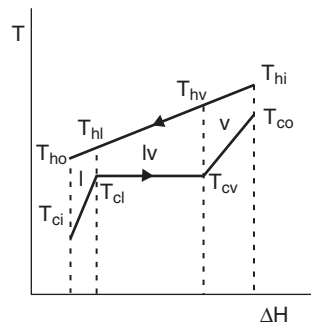


FIGURE 35.2.6

Evaporator temperature/enthalpy diagram

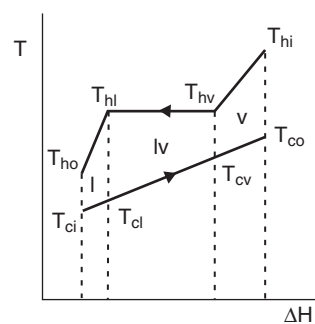


FIGURE 35.2.7

Condenser temperature/enthalpy diagram

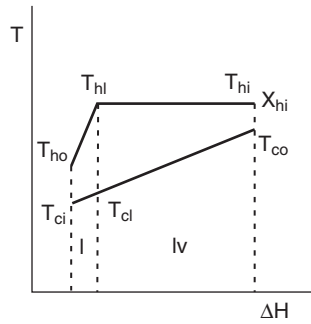


FIGURE 35.2.8
Condenser temperature/enthalpy diagram

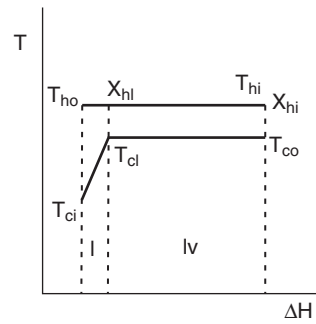


FIGURE 35.2.9
Evapo-condenser temperature/enthalpy diagram

35.2.4.3 Equations for two-phase inlet condensers

Two phase hot fluid and cold fluid sensible heat

The equations are as follows (Figure 35.2.8):

$$m_h C_{p_{hlv}}(T_{hi} - T_{hl}) = m_c C_{p_c}(T_{co} - T_{cl}) = m_h L_h x_{hi}$$

$$m_h C_{p_{hl}}(T_{hl} - T_{ho}) = m_c C_{p_c}(T_{cl} - T_{ci})$$

Relations giving epsilon and R are then:

$$\varepsilon_{lv} = \frac{T_{co} - T_{cl}}{T_{hi} - T_{ci}} \quad R_{lv} = \frac{m_c C_{p_c}}{m_h C_{p_{hlv}}}$$

$$\varepsilon_l = \frac{T_{hi} - T_{ho}}{T_{hi} - T_{ci}} \quad R_l = \frac{m_h C_{p_{hl}}}{m_c C_{p_c}}$$

35.2.4.4 Equations for condensers-two-phase inlet evaporators

Two phase hot fluid and cold fluid sensible heat

Assuming that the cold fluid exits in the saturated vapor state, the equations are as follows (Figure 35.2.9):

$$m_h L_h (x_{hi} - x_{hl}) = m_c L_c$$

$$m_h L_h x_{hl} = m_c C_{p_c}(T_{cv} - T_{ci})$$

For part lv, notions of epsilon and R lose their meaning, and we have:

$$m_c L_c = U_{lv} A_{lv} (T_{hv} - T_{cv})$$

which provides A_{lv} in design mode. Note that if the liquid zone is small compared to the lv zone, this relationship very simply gives the difference of saturation temperatures of both fluids.

For part l, relationships giving epsilon and R are:

$$\varepsilon_l = \frac{T_{cv} - T_{ci}}{T_{hv} - T_{ci}} \quad R_l = \frac{m_c C_{p_{ci}}}{m_h C_{p_{hlv}}}$$

with $m_h C_{p_{hlv}}(T_{hi} - T_{ho}) = m_h L_h$

These equations allow one to find the two saturation temperatures that meet both the constraint on equal fluid state change plateaus and the thermal constraint related to the exchange surface.

35.2.4.5 Sizing and off-design calculations

In each case, we deduce for each sub-exchanger NTU and UA from relations $NTU = f(\varepsilon, R, \text{flow pattern})$ and from $NTU = UA/(\dot{m} \cdot c_p)_{\min}$. If U is known, we get A.

When sizing, we determine the three surfaces A_1 , A_{1v} and A_v .

Knowing all temperatures and heat capacity rates, we can estimate the values of ε and R for each zone, deduce the UA_j , and hence A_j . A is equal to their sum.

In off-design mode, the general algorithm for finding the solution is implemented as a driver, and depends on the problem.

The sequence of calculations can then be:

- for an evaporator, the value of superheating ΔT_0 is usually assumed known. T_{co} , T_{ho} and T_{hv} are recalculated, which allows one to estimate the values of ε and R for each zone, then deduce the UA_j , and hence A_j ;
- for a condenser, the surface area A_1 corresponding to the liquid subcooling is usually assumed known. We begin by recalculating T_{ho} for sub-cooling, then recalculate T_{co} , T_{cl} and T_{cv} , which allows us to estimate the values of ε and R for each zone, then deduce the UA_j , and hence A_j .

35.2.4.6 Outstanding issues for off-design operation

The issues addressed in this study correspond to a refrigerator but could easily be applied to other devices.

In design mode, we start from a thermodynamic state known and we seek to identify a set of parameters characteristic of the components. We know then superheating, subcooling, and possible pressure drops.

In off-design operation these values are not known, and we try to estimate them realistically. On the basis of experimental data that we have treated, we propose some ideas, but they are only partial.

For superheating, we usually assume a constant value set by the expansion valve. This assumption would require to be substantiated, but it has the advantage of simplicity.

For subcooling, a hypothesis is to consider that the wetted surface of the condenser is constant. If you wish to be more precise, and experimental data are available, you can try to identify the value of sub-cooling by a linear or quadratic law with respect to control variables used (evaporation and condensation temperatures, compressor rotation speed, compression ratio etc.).

One can also directly estimate the wetted surface of the condenser, which is directly compatible with the Thermoptim calculation method.

35.3 PRESSURE DROP CALCULATION

35.3.1 Gas or liquid state pressure drop

C being the fluid velocity and v the specific volume, the so-called regular or linear pressure drop is generally expressed in the form of:

$$\Delta P = f \frac{C^2}{2} \frac{L}{vd_h}$$

f is the friction coefficient, given by correlations depending on the geometry as for heat exchange coefficients, and function of the relative roughness RR. For an initial rapid assessment, f can be taken approximately equal to 0.02 for a smooth tube.

Referred to the mass flow rate, for a total free flow area equal to A_c , pressure drop is equal to:

$$\Delta P = f \frac{(\dot{m}v)^2}{2Ac^2} \frac{L}{vd_h} = f_v \frac{\dot{m}^2}{2Ac^2} \frac{L}{d_h} \quad (35.3.1)$$

The calculation of pressure drop in turbulent flow can be made from a relation of the type $\Delta P = 4fG^2L v_m/2d_h$ where f is the friction coefficient, given by correlations based on Re .

In laminar flow, pressure drop is proportional to flow rate and fluid viscosity: $f = 64/Re$.

For smooth tubes, f is given by Blasius formula ($f = 0.316Re^{-0.25}$) if $Re < 30,000$, or by formula $(0.0032 + 0.221Re^{-0.237})$ for higher values of Re .

For rough tubes in turbulent flow ($Re > 2,100$) the friction coefficient is given by Colebrook equation:

$$\frac{1}{\sqrt{f}} = -0.868589 \ln \left[\frac{RR}{3.71} + \frac{2.51}{Re\sqrt{f}} \right] \quad (35.3.2)$$

$$RR = \frac{\varepsilon}{D} \quad \varepsilon = \text{absolute roughness of the tube}$$

We can show that this implicit equation f can be approximated by:

$$\frac{1}{\sqrt{f}} = -0.78173 \ln \left[\left[\frac{RR}{3.71} \right]^{1.1} + \frac{6.9}{Re} \right] \quad (35.3.3)$$

35.3.2 Two-phase pressure drop

In the two-phase system, pressure drop calculation can be very complex, not least because we must first determine the lengths of the exchanger various zones.

In the liquid-vapor equilibrium zone, we used the approximate formula for nuclear steam generators proposed by Gallori and Herre, adjusted to take account of a nonzero quality at the inlet (Techniques de l'Ingénieur, BN 3050).

$$\Delta P_{\text{diff}} = \varphi \Delta P_{\text{liq}}$$

$$\varphi = \left[1 + |x_o - x_i| \left(\frac{\rho_l}{\rho_v} - 1 \right) \right] \left[1 + |x_o - x_i| \left(\frac{\mu_l}{\mu_v} - 1 \right) \right]^{-0.2} \quad (35.3.4)$$

The pressure drop is thus calculated from the saturated liquid state using this enhancement factor φ .

Taking pressure drop in multizone evaporators into account requires some care: if we assume that pressure drop takes place during evaporation, the temperature at the end of evaporation is lower than that at the exchanger inlet, so that the heat capacity rate must be negative, leading to a miscalculation of the exchanger by the NTU method. The calculation is performed assuming that the pressure drop takes place after the outlet, as shown in Figure 35.3.1. Superheating is calculated using the outlet pressure, and vaporization with that at the exchanger inlet.

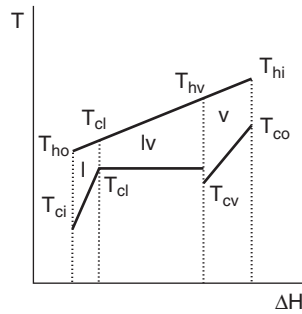


FIGURE 35.3.1
Evaporator with pressure drop

35.4 HEAT EXCHANGER TECHNOLOGICAL SCREEN

35.4.1 Heat exchanger technological screen

The heat exchanger technological screen contains in its lower left part two zones for the “exchange” processes.

In order to calculate heat transfer coefficients and pressure drops, two geometrical quantities are particularly important besides the surface of the exchanger: the section A_c devoted to the fluid flow, and the hydraulic diameter d_h . When the fluid heat exchange coefficients are very different, various devices such as fins can be used to compensate for the difference between their values. This is called extended surfaces, which can be characterized by a surface factor f and a fin effectiveness η_0 .

These four parameters are those which have been chosen in Thermoptim to characterize heat transfer in each fluid. The length of the exchanger is also used for certain calculations such as pressure drops.

In the heat exchanger technological design screen (Figure 35.4.1), the following conventions are adopted:

- type configuration (here, “cond”) is selected in a combo;
- “free flow area” represents the flow area A_c ;
- “hydr. diameter” is the usual hydraulic diameter d_h ;
- “length” is the length of the exchanger (used for calculating the boiling number Bo and the pressure drops, not yet implemented in the two-phase case);
- “surface factor” is the surface factor f for large surfaces;
- “fin effectiveness” is the fin effectiveness η_0 ;

The values of technological design parameters must be entered for both fluids, having chosen for each one the flow pattern in the list (“cond” and “air_coil” in Figure 35.4.1).

When calculations are made, the values of h and Re are displayed in the upper left for each phase of each fluid, and the exchange surface appears beneath the field dedicated to thermal resistance. Values are displayed in red for the hot fluid and blue for the cold fluid.

35.4.2 Correlations used in Thermoptim

The external classes provided with Thermoptim propose several exchange configurations for each fluid. Parameter values are provided by default, but can be modified using the screens shown below. It is also very easy to add new configurations by subclassing those proposed.

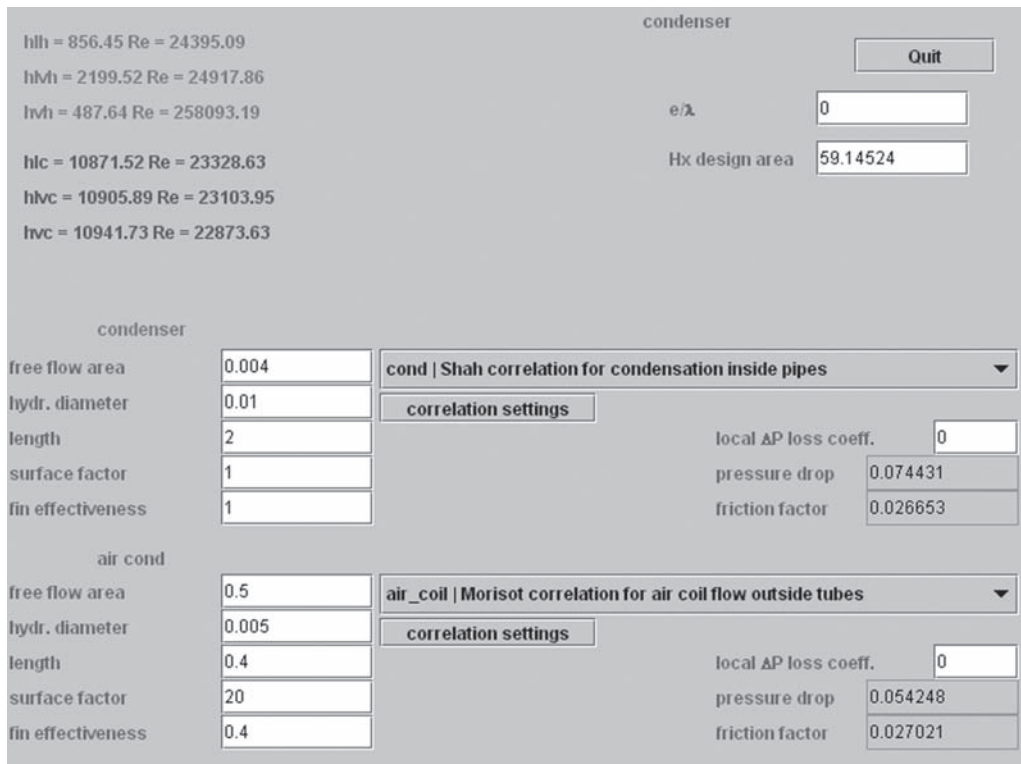


FIGURE 35.4.1
Condenser technological design screen

TABLE 35.4.1

	TYPE	CORRELATION	TYPE OF FLUID
"int_tube"	inside tubes	Mac Adams	single-phase
"ext_tube"	outside tubes	Colburn (Dittus Boettler)	single-phase
"cond"	condensation	Shah/Bivens	two-phase
"cond_ext_hor"	horiz. cond. ext. tubes	BI540 T/I	two-phase
"evap"	evaporation	Gungor Winterton	two-phase
"air_coil"	air coil	Morisot ¹	air
"cool_tower"	evaporative cooling	Colburn	moist air
"flooded"	flooded	generic	two-phase
"plate"	plate	generic	single-phase

Take care that changes of Nusselt correlation parameters must be made very carefully, otherwise results may be erroneous. These are digital fitting parameters whose physical meaning is far from clear. They cannot be estimated based on simple geometric considerations.

Table 35.4.1 summarizes the main configurations proposed, indicating their type, correlations used and the type of fluid to which they correspond.

A screen accessible by a small button called "correlation settings" placed in the exchanger technological design screen allows the user, for each fluid, to determine or change the values of correlations used for the calculation (Figure 35.4.2).

¹ Olivier MORISOT, thèse de Doctorat, 27 janvier 2000, Modèle de batterie froide à eau glacée adapté à la maîtrise des consommations d'énergie en conception de bâtiments climatisés et en conduite d'installations.

FIGURE 35.4.2

Correlation setting screen

Clicking “Load Settings”, you load the current values, and clicking “Save settings” you force the values you entered on the screen.

35.5 MODEL PARAMETER ESTIMATION

The model used being as we said a physical model, and not purely digital, except for correlations giving Nu, its parameters can be directly estimated from the geometric data available or identified from experimental data. A detailed example of determining their values for a simple case will be presented in section 38.2.1.

35.5.1 Direct setting from geometric data

The exchanger geometric description depends on its configuration, which can be quite complex.

By definition, hydraulic diameter d_h is equal to the ratio of 4 times the fluid flow area to the wetted perimeter p : $d_h = 4A_c/p$ (if there are insulated walls, the heat exchange perimeter must be considered).

Caution: in the following, expressions are sometimes given for a mesh, and sometimes for the entire section.

35.5.1.1 Flow outside tubes

The following example relating to flow outside tubes, parallel to tubes, illustrates this feature (Figure 35.5.1). For a mesh, calling e_1 and e_2 the vertical and horizontal pitches:

$$A_c = e_1 e_2 - \pi d^2/4$$

To calculate the wetted perimeter, do not include straight portions that do not participate in exchange:

$$p = 4(\pi d/4) = \pi d$$

$$d_h = 4A_c/p = (4e_1 e_2/\pi d) - d$$

For the entire section, these results remain valid if the number of tubes is large enough. Otherwise, it may be necessary to make corrections to account for edge effects.

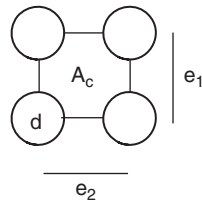


FIGURE 35.5.1
Outside of tubes

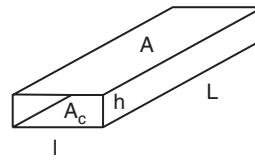


FIGURE 35.5.2
Rectangular section

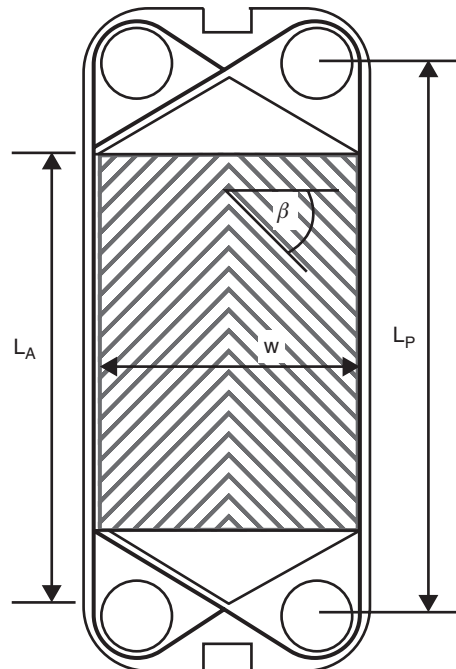


FIGURE 35.5.3
Plate heat exchanger

35.5.1.2 Rectangular section

Assuming that on a fluid side the flow section can be assimilated to a rectangle of dimensions l and h (Figure 35.5.2), we get:

$$\begin{aligned} A &= Ll & A_c &= hl \\ p &= 2(l+h) \\ d_h &= 4A_c/p = 2A_c/(l+h) = 2hl/(l+h) \end{aligned}$$

In the general case, things are much more complex, but knowing A , A_c and d_h is enough in practice to characterize the exchange for a fluid.

35.5.1.3 Case of plate heat exchangers

In plate heat exchangers (Figure 35.5.3), the geometry of each face can sometimes be likened in first approximation to a rectangular section and the above formulas apply. If you know the internal details of the corrugations, a more precise calculation can be performed. The profiles are generally symmetric, but it is not always the case.

Estimation techniques of A_c and d_h can be found in the literature for some specific configurations, including tube bundles.

Depending on circumstances, the reference length is L_p or L_A (see Figure 35.5.3). The average gap between plates, b , is equal to the pitch, p , minus the thickness of plates, t .

$$b = p - t$$

The free flow area for both fluids, A_c , is:

$$A_c = bw/2$$

Corrugation surface amplification factor

The equivalent diameter of a channel d_e , used for calculating the Reynolds number, must be based on actual flow area and not projected section, which leads to defining an amplification factor, μ , ratio of developed length to projected length, which varies from 1.1 to 1.25 with a typical average of 1.17 (Kumar, 1984).

Knowing that the area is generally developed in a single dimension, the ratio of developed and projected surfaces is the same as that of their lengths.

If corrugations are sinusoidal, calling a the half-height of the sinusoid, μ is given by:

$$\frac{\int_0^{2\pi} \sqrt{1 + a^2(\sin(t))^2} dt}{2\pi}$$

h/l being the ratio of the corrugation height to its pitch (4/7.8 in Figure 35.5.4), this relationship can be replaced by the approximate formula (Figure 35.5.4):

$$\mu = 0.9075e^{(0.9576 h/l)}$$

Channel length

If we know the corrugation pitch p_c , the width of plates c , and the chevron angle α (complementary to angle β) (Figure 35.5.5), we can determine the number of channels per plate:

$$c = a \sin \alpha$$

$$b = a \cos \alpha$$

$$b = c \cot \alpha$$

$$h = b \sin \alpha = c \cos \alpha$$

The number of channels per plate is $N_c = h/p_c = c \cos \alpha/p_c$.

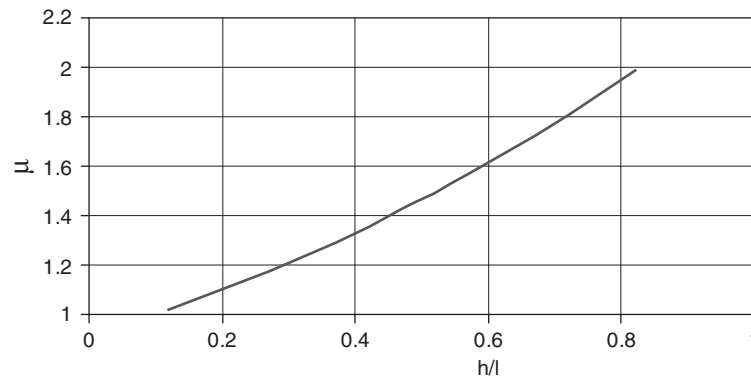


FIGURE 35.5.4

Corrugation surface amplification factor

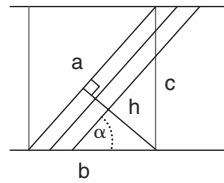
**FIGURE 35.5.5**

Plate exchanger

If we know the number of plates N_p and the number of channels per plate N_c , we can determine the average channel length L by relation $A = N_p N_c p / 2L$, or by making the simplifying assumption $p = \pi d_h$: $A = N_p N_c \pi d_h / 2L$.

Factor 2 appears because each plate has two sides and the exchange area to consider is that of a single face.

Moreover, the exchange surface is equal to the product of the number of plates by their width c and useful length L_u :

$$A = N_p c L_u$$

We therefore have $N_c \pi d_h / 2L = c L_u$

Hydraulic diameter

Hydraulic diameter is given by $d_h = 4A_c / P_w$.

where $P_w = 2(b + w)$ which gives:

$$d_h = \frac{4bw}{2(b+w)}$$

As b is very small compared to w , $d_h = 2b/\mu$

It is common that one does not take into account the amplification factor μ . In this case, $d_h = 2b$.

35.5.1.4 Case of shell and tube exchangers

For standard shell and tube configurations, the fluid free flow is about one-quarter the shell diameter D_c .

Calling B the spacing of the baffles, e_1 the pitch perpendicular to flow, and w the smallest space between two tubes ($w = e_1 - d$), the free flow area between two tubes is equal to wB and the total section depends on the number of tubes to be considered. At the center of the shell:

$$A_c = wBDc/e_1$$

The wetted perimeter between two tubes is $p = 2(w + B)$, and the hydraulic diameter $d_h = B2w/(w + B)$.

35.5.2 Identification of exchanger parameters

In practice, we rarely know enough about the internal geometry of the exchanger to estimate accurately the parameters we have just presented. Moreover, given the multiplicity of proposed correlations for heat exchangers, including plate (Ayub, 2003), it is difficult to rely on literature to know which to choose and how to set the values of geometric parameters characteristics of the exchanger. A second approach is to identify the parameters of the exchanger from experimental data. To

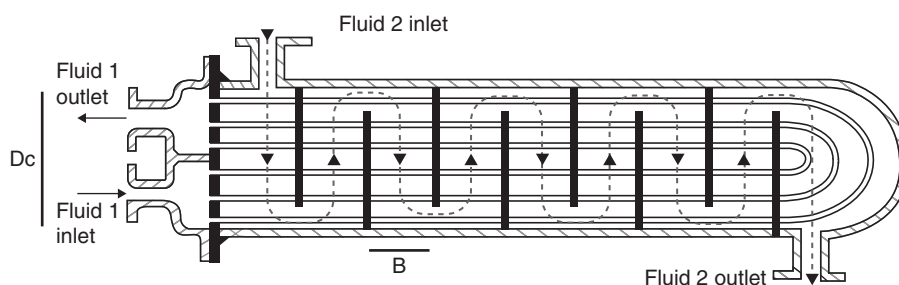


FIGURE 35.5.6

Cross section of a shell and tube exchanger

facilitate this, specific features have been implemented in Thermoptim to help conduct a series of sizing calculation of area A by varying A_c and d_h for a set of project files corresponding to test points. They are presented in Chapter 38.

Note that it is sometimes difficult to initialize the setting of a multizone exchanger. We must first study in detail the exchanger geometric configuration, on the one hand to deduce the best choice among the configurations available in Thermoptim and on the other hand to approximate values of the parameters required. The setting is performed by introducing for each fluid geometric characteristics and values of correlation coefficients used.

To define the accuracy of model parameter estimation, it is necessary to give a criterion. One can for example choose the scattering of the design surface calculated for different measurement points. We then compare all simulations conducted for selected sets of parameters, which leads to perform multiple simulations. To facilitate this, a special mechanism was introduced in Thermoptim. It is presented in Chapter 38.

REFERENCES

- Z. H. Ayub, *Plate heat exchanger literature survey and new heat transfer and pressure drop correlations for refrigerant evaporators*, *Heat Transfer Engineering*, 24(5), 3–16, 2003.
- D.B. bivens, A. Yokozeki, *Heat transfer coefficients and transport properties for alternative refrigerants*, Int. Refrigeration Conference Proceedings, Purdue University, pp. 299–304, 1994.
- O. Garcia-valadares, *Review of in-tube condensation heat transfer correlations for smooth and microfin tubes*, *Heat Transfer Engineering*, 24(4), 6–24, 2003.
- K. E. Gungor, R. H. S. Winterton, *Simplified general correlation for saturated flow boiling and comparisons of correlations with data*, *Chemical Engineering research and design*, vol 65, mars 1987
- F. P. Incropera, D. P. Dewitt, T. L. Bergman, *Fundamentals of Heat and Mass Transfer*, Wiley, 6th Edition, 2007.
- Ch. Herer, D. Gallori, *Thermohydraulique des réacteurs à eau sous pression*, Techniques de l'Ingénieur, BN 3050.
- S. Kakac, H. Liu, *Heat exchangers, Selection, rating, and thermal design*, 2nd edition, CRC Press, Boca Raton, 2002, ISBN 0-8493-0902-6.
- W. M. Kays, A. L. London, *Compact Heat Exchangers*, Mac Graw Hill, 1984.
- H. Kumar, *The plate heat exchanger: construction and design*, First UK National Conference on Heat Transfer, July 1984, I Chem E Symposium Series, No. 86, 1275–1288.
- M. Lallemand, *Transferts en changement de phase: ébullition convective*, Techniques de l'Ingénieur, Traité Génie énergétique, BE 8 236.
- W. Levy, *Condenseurs par surface dans les centrales thermiques*, Techniques de l'Ingénieur B1540.

- A. Muley, R. M. Manglik, *Experimental study of turbulent flow heat transfer and pressure drop in a plate heat exchanger with chevron plates*, *Trans of the ASME, Journal of Heat Transfer*, **121**, 110–117, 1999.
- E. A. D. Saunders, *Heat Exchangers: Selection, Design and Construction*, Longman Scientific and Technical, Harlow, Essex, 1988.
- R. K. Shah, K. J. Bell, *Heat exchangers, The CRC handbook of thermal engineering*, (Edited by F. Kreith), CRC Press, Boca Raton, 2000, ISBN 0-8493-9581-X.
- M. M. Shah, *A general correlation for heat transfer during film condensation inside pipes*, *Int. Journal of Heat and Mass Transfer*, vol. 22, p. 547–556, 1979.

Modeling and Setting of Displacement Compressors

Abstract: In this chapter we focus on off-design modeling of displacement compressors. The study of dynamic compressors, pumps and fans has been merged with that of turbines in Chapter 37.

The models of displacement compressors we propose are based on the assumption that their behavior can be represented with reasonable accuracy by their volumetric efficiency and classical isentropic efficiency. Typical laws allowing one to represent these two parameters are given and we discuss problems related to their identification which can cause many difficulties, because of the very few experimental data available in practice and uncertainty about them.

Keywords: volumetric efficiency, isentropic efficiency, compression, displacement compressor, dead space, swept volume.

36.1 BEHAVIOR MODELS

Models implemented in ThermoOptim are extensions of those described in section 7.2 of Part 2. As we have seen, two main methods of approach can be adopted: either a purely digital fit, if there is one that is satisfactory, or keep to an approach as physical as possible. The first choice was made here.

Models of displacement compressors are based on the assumption that their behavior can be represented with reasonable accuracy by two parameters: volumetric efficiency λ which characterizes the actual swept volume, and classical isentropic efficiency η_s .

Let us recall that volumetric efficiency is not an efficiency in the classic sense: it appears in the numerator of the expression of work per cycle and not in the denominator, as it reflects the fact that, the actual swept volume being only a fraction of the total displacement, the work is lower than that theoretically corresponding to the displacement.

Analysis and experimentation have shown that λ can be written as follows (Conan, 1988), the two biggest losses being in first place β_3 , then β_1 :

$$\lambda = 1 - (\beta_1 + \beta_2 + \beta_3 + \beta_4 + \beta_5)$$

$\beta_1 = \varepsilon((P_2/P_1)^{1/\gamma} - 1)$ is the loss due to dead space.

β_2 : loss due to pressure drop in the intake and discharge manifolds;

β_3 : losses due to wall effects (thermal shunt);

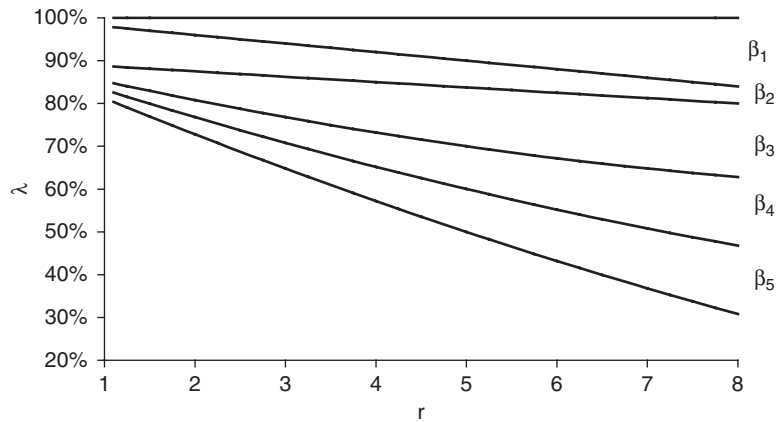


FIGURE 36.1.1
Volumetric efficiency function of compression ratio

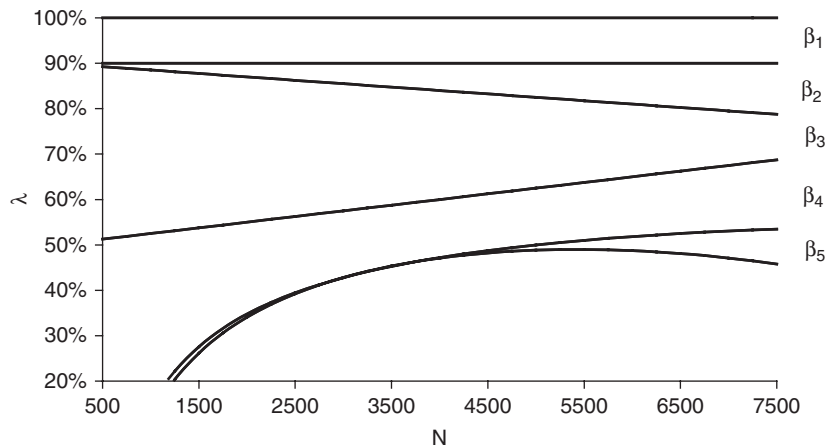


FIGURE 36.1.2
Volumetric efficiency function of rotation speed

β_4 : losses by leakage (at the piston rings and valves);
 β_5 : loss due to pressure drop in the inlet and outlet valves.

There is a limit compression ratio r_{max} beyond which the compressor no longer provides any fluid flow. Physically, this means that at the end of expansion, mass contained in the dead space at pressure P_1 occupies the entire volume of the cylinder, so that the compressor can no longer suck the upstream gas.

Equation $\lambda > 0$ allows us to express this condition. Limited to its first term, it gives:

$$r_{max} = \frac{P_2}{P_1} < \left(1 + \frac{1}{\epsilon}\right)^\gamma$$

The set of all losses combine to give volumetric efficiency laws of variation with respect to compression ratio and to rotation speed which look like in Figures 36.1.1 and 36.1.2.

At constant compression ratio, they show an optimum at fairly high speed. Indeed, at low speeds, wall effects (β_3) and leakage (β_4) are relatively large, and drop when speed increases. However, at high speed, pressure drop in collectors (β_2) and especially valves (β_5) plays an increasing role.

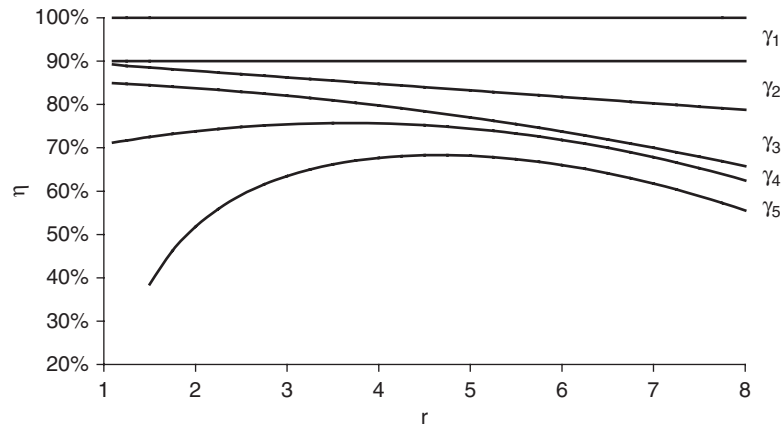


FIGURE 36.1.3

Isentropic efficiency function of compression ratio

Three sources of losses linked to the previous ones mainly affect compression efficiency, which can be written:

$$\eta = 1 - (\gamma_1 + \gamma_2 + \gamma_3 + \gamma_4 + \gamma_5)$$

- wall effects (γ_3) are very disadvantageous because they greatly increase the compression work by deforming the isentropic;
- losses due to valves (γ_5) come next, followed by default leakage losses (γ_4).

At a given speed, the shape of the compression efficiency law as a function of the compression ratio is given in Figure 36.1.3. It shows the existence of a maximum at compression ratios rather low (3 to 5). At a given compression ratio, when speed varies, compression efficiency goes by a maximum close to that of volumetric efficiency.

All of these phenomena are extremely complex to model, so we usually just adjust numerical models to represent the behavior of displacement compressors.

36.1.1 Operation at rated speed and full load

At rated speed, the equations that we used are extensions of those which have been proposed in Part 2 (7.2.6 and 7.2.7) for adiabatic displacement compressors¹. We show later how to adapt these models to the case of cooled compressors. Depending on compression ratio, these two characteristics are given by equations (36.1.1) and (36.1.2 and 2a):

$$\lambda = \alpha_0 - \alpha_1 \frac{P_{\text{ref}}}{P_{\text{asp}}} \quad (36.1.1)$$

Typically, for reciprocating compressors α_0 is close to 0.95, and α_1 of 0.038, and for screw compressors α_0 is close to 0.9, and α_1 of 0.008.

¹ We wish to thank Prof. J. Lebrun of University of Liège for his advice on this subject.

For isentropic efficiency, we propose two equations, roughly equivalent, the first using five parameters, and the second three.

$$\eta_s = K_1 + K_2 \cdot \left(\frac{P_{\text{ref}}}{P_{\text{asp}}} - R_1 \right)^2 + \frac{K_3}{\frac{P_{\text{ref}}}{P_{\text{asp}}} - R_2} \quad (36.1.2)$$

For the first, typical values of parameters are, for piston as well as for screw compressors, K_1 close to 0.8, K_2 to 0.0037, K_3 to -0.16 , R_1 to 7 and R_2 to 1.2.

Note that, although positive values of K_2 are acceptable, they lead to an increase of η_s for high values of compression ratio, which is physically questionable.

The second equation, of type $y = a + bx + cx^2$, is very easy to identify.

$$\eta_s = K_1 + K_2 \cdot \frac{P_{\text{asp}}}{P_{\text{ref}}} + K_3 \cdot \left(\frac{P_{\text{asp}}}{P_{\text{ref}}} \right)^2 \quad (36.1.2a)$$

Note that it is expressed linearly as a function of the inverse of compression ratio and its square. Its parameters have the advantage of having a physical sense, since it can be rewritten as follows (36.1.4).

$$\eta_s = \eta_{\text{lim}} + (\eta_{\text{max}} - \eta_{\text{lim}}) \cdot \left(2 \left[\tau_{\text{max}} \frac{P_{\text{asp}}}{P_{\text{ref}}} \right] - \left[\tau_{\text{max}} \frac{P_{\text{asp}}}{P_{\text{ref}}} \right]^2 \right)$$

η_{lim} is the asymptotic value of isentropic efficiency for high compression ratios, and η_{max} the maximum efficiency obtained for a compression ratio equal to τ_{max} .

Knowing K_1 , K_2 and K_3 , we get very easily these values:

$$\eta_{\text{lim}} = K_1$$

$$\eta_{\text{max}} = K_1 - \frac{K_2^2}{4K_3}$$

$$\tau_{\text{max}} = -2 \frac{K_3}{K_2}$$

Figure 36.1.4 is $\eta_{\text{lim}} = 0.6$, $\eta_{\text{max}} = 0.8$, $\tau_{\text{max}} = 3$.

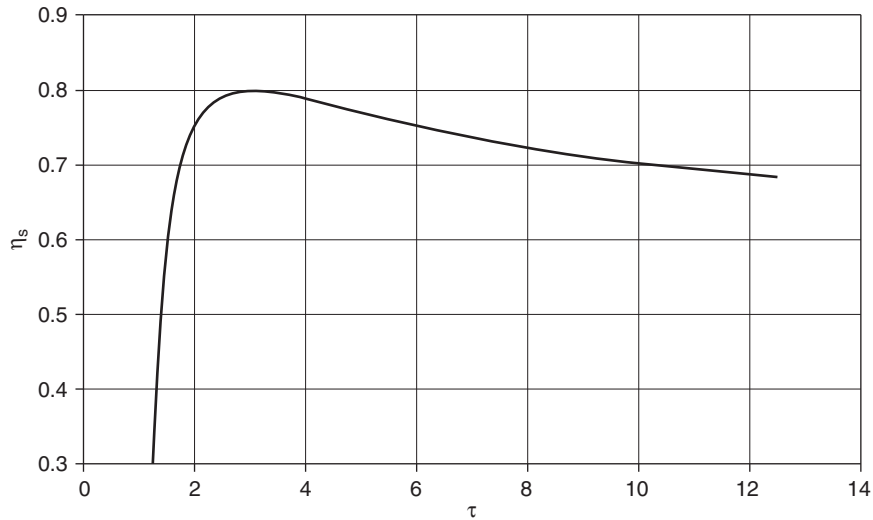
The estimation of K_1 from physical parameters is straightforward:

$$K_1 = \eta_{\text{lim}}$$

$$K_2 = \frac{\tau_{\text{max}}}{2} (\eta_{\text{max}} - \eta_{\text{lim}})$$

$$K_3 = -\frac{\tau_{\text{max}}}{4} (\eta_{\text{max}} - \eta_{\text{lim}})$$

Unlike (36.1.2), (36.1.2a) cannot grow when compression ratio tends to infinity. However, a blind identification on a relatively small number of grouped points can lead to negative parameter values, which of course has no physical meaning. So if the number of points is limited, it may be desirable to manually adjust the equation in the form (36.1.2).

**FIGURE 36.1.4**

Three-parameter equation

Although both models are much less detailed than others, comparisons with existing reciprocating compressors usually give satisfactory results. If this is not the case, it is also possible to use a polynomial model. The model choice depends primarily on available data, the range of values of compression ratio or rotation speed we seek to cover, and desired accuracy.

N being the rotation speed (rpm), and $V_{s,fl}$ the volume swept by the cylinders at full load, the volumetric flow rate at full load is given by (36.1.3):

$$\dot{V} = \lambda \frac{N}{60} V_{s,fl} \quad (36.1.3)$$

36.1.2 Operation at partial load and speed

Partial load operation of a displacement compressor can be modeled simply by introducing into the calculation of volumetric and isentropic efficiencies a multiplier which is more or less a simple function of partial load factor X_{pl} , itself defined as the ratio of the volume swept at partial load to the volume swept at full load:

$$\lambda_{pl} = X_{pl} \lambda_f \quad (36.1.4)$$

$$\eta_{s,pl} = \eta_{s,fl} \cdot \left[1 - \left(0.682 \cdot e^{-3.96 \cdot X_{pl}} \right) \right] \quad (36.1.5)$$

The influence of the rotation speed can in turn be taken into account by a simple law of type (36.1.6).

$$\eta_{s,rpm_2} = \eta_{s,rpm_1} \cdot \left[\frac{rpm_1}{rpm_2} \right]^m \quad (36.1.6)$$

Exponent m value depends on compressors: it may, as appropriate, be positive or negative. Everything depends on the (implicit or explicit) constructor choice: whether to favor the compressor efficiency at rated or reduced speed. A positive value of m indicates a better efficiency at reduced speed.

We draw the reader's attention to the fact that there may be ambiguity in the definition of the partial load factor, depending on whether one looks at the influence of speed or that of a cylinder bypass. For our part, we reserve X_{pl} for the second case, and are content to speak of variable speed for the first.

The indications given in this section are tentative: they have not been sufficiently validated on experimental data to be considered final. They have not yet been implemented in external classes on technological design and off-design operation provided with Thermoptim.

36.2 PRACTICAL MODELING PROBLEMS

36.2.1 TECHNOLOGICAL SCREEN OF DISPLACEMENT COMPRESSORS

The screen of Figure 36.2.1 is the five parameter isentropic efficiency model. For other models, screens are slightly different: fields R_1 and R_2 are absent for the three parameter model.

The blue fields on the left side of the compressor technological screen allow you to enter the compressor characteristics: the two volumetric efficiency parameters α_0 and α_1 , the five isentropic efficiency parameters K_1 , K_2 , K_3 , R_1 and R_2 , the reference speed (for which the five parameters were determined), the swept volume at full load V_s (m^3), and finally a coefficient to estimate a possible cooling power, and the number of devices used.

The fields on the right side of the screen show calculated values of isentropic efficiency, mass flow and volumetric efficiency.

For screw compressors, the speed is set and cannot be changed.

In this screen, the compressor is assumed to be adiabatic. If it is cooled, which is sometimes necessary to limit the fluid discharge temperature, we must take into account the thermal power extracted, which can be done as follows, which is a little schematic, but corresponds to a case we have treated. The external class can easily be subclassed to implement another algorithm.

The state of fluid leaving the compressor is first calculated as if the machine was adiabatic and the heat load is applied at constant output pressure, which shifts the value of the temperature.

The thermal load is considered equal to the product of a coefficient ($K_{NonAdiab}$) by the difference between the isentropic outlet temperature and 290 K:

$$Q = K_{NonAdiab} (T_s - 290) \quad (36.2.1)$$

Two possibilities exist depending on whether the heat load is known or not:

- If yes, the value of the thermal load is entered in a field of the screen;
- Otherwise, heat load is estimated by (36.2.1).

FIGURE 36.2.1

Technological design screen of a compressor

If Q_{NonAdiab} or K_{NonAdiab} is negative, the compressor is cooled, otherwise it is heated (which of course has no technological or thermodynamical interest).

36.2.3 Identification of compressor parameters

The identification of the compressor parameters can cause many difficulties, because of the very few experimental data available in practice and uncertainty about them.

The problem is further complicated when the compressor is cooled, because you must either measure the cooling power Q , or estimate it.

The methodology comprises ten stages: we first identify λ , then Q , then η at rated speed, and end up with η at partial speed or load. It would be quite possible to apply this methodology to data from catalogs or software published by manufacturers.

36.2.4 Calculation in design mode

In design mode, the rotation speed or the swept volume required to provide the desired flow is determined. Calculation is done taking into account the inlet and outlet pressures, and the flow value entered in the compressor flow field.

36.2.5 Calculation in off-design mode

In off-design mode, the compression ratio allows to determine λ and η_s , which sets the compressor flow and outlet temperature. The sequence of calculations is as follows:

1. knowing the inlet and outlet conditions, compression ratio $P_{\text{ref}}/P_{\text{asp}}$ and suction volume v_{su} are updated;
2. volumetric and isentropic efficiencies λ and η_s and actual flow are calculated knowing rotation speed N ;
3. flow volume \dot{V} is deduced by (36.1.3);
4. the compressor sets $\dot{M} = v_{\text{su}}\dot{V}$ and spreads this value to connected components;
5. useful work can then be calculated knowing the isentropic efficiency η_s .

36.2.6 Fixed V_i screw compressors

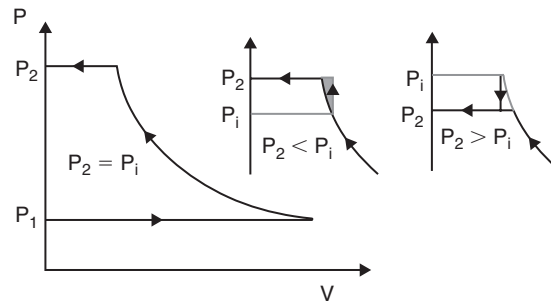
As explained in section 7.2.2 of Part 2, a specific characteristic of fixed V_i screw compressors (and spiral) is the possibility of an under-or over-compression if the internal pressure ratio π differs from the constructive π_i .

The inadequacy of the compressor pressure results in losses as shown in Figure 36.2.2. If the constructive pressure P_i is known, calculation can be performed as follows, τ_{is} being the isentropic work between P_1 and P_i , and τ_{ref} the reference work for an internal isentropic compression:

$$\begin{aligned} \text{if } P_2 > P_i & \quad \tau_{\text{ref}} = \tau_{\text{is}} + (P_2 - P_i)v_1/V_i \\ \text{if } P_2 < P_i & \quad \tau_{\text{ref}} = \tau_{\text{is}} - (P_i - P_2)v_1/V_i \end{aligned}$$

In all cases, the ‘‘isentropic’’ compression work is equal to the real isentropic work between P_1 and P_i , plus the transfer work between P_i and P_2 :

$$\tau_{\text{ref}} = \tau_{\text{is}} + (P_2 - P_i)v_1/V_i \quad (36.2.1)$$

**FIGURE 36.2.2**

Adaptation of the pressure for fixed V_i screw compressors

The actual useful work is then given by:

$$\tau = \tau_{\text{ref}}/\eta_s. \quad (36.2.2)$$

To calculate P_i , it suffices to determine the intersection of isentrope $s = s_1$ and isovolume $v = v_1/V_i$.

REFERENCES

- M. Bernier, B. Bourret, *Pumping Energy and Variable Frequency Drives*, ASHRAE Journal, December 1999.
- R. Cohen, E. Groll, W. H. Harden, K. E. Hickman D. K. Mistry, E. Muir, *Compressors, The CRC handbook of thermal engineering*, (Edited by F. Kreith), CRC Press, Boca Raton, 2000, ISBN 0-8493-9581-X.
- J. G. Conan, *Réfrigération Industrielle*, Eyrolles, Paris 1988.
- T. Giampaolo, *Compressor handbook, Principles and practice*, The Fairmont Press, Lilburn, CRC Press, Boca Raton, 2010, ISBN 0-88173-615-5.
- F. Trebilcock, J. Lebrun, E. Winandy, *Reciprocating and screw compressors simulation through polynomial expressions*, University of Liège, October 2002.

Modeling and Setting of Dynamic Compressors and Turbines

Abstract: In this section, we present different models that can be used to represent the off-design behavior of turbomachinery, mainly turbines and dynamic compressors, but also pumps and fans.

It is important to note that this is a very difficult subject, on which there are few books or reference publications, and so one on which there is no real consensus approach in the scientific community and engineering departments.

We present different models that seem relevant, and that we have at least partially implemented in the examples which are given either in Chapter 38 or in the ThermoOptim-UNIT portal. We therefore have no claim to be exhaustive, and we limit our ambition to guide the reader in the discovery of this issue, so he can if he wants start building his own models.

The off-design study of turbomachinery is in fact much more complex than that of displacement compressors, given the flows that take place in these components.

Two main approaches are generally used for this:

- either consider how the velocity triangle is deformed due to the change in operating conditions of the machine;
- or use similarity laws and experimental performance maps of the machine to find its new operating point.

So far, for the sake of simplicity, we limited developments relating to the thermodynamics of turbomachinery. We will now deepen our analysis by making some additions to what has been presented in Chapter 7 of Part 2.

Keywords: compression, expansion, isentropic efficiency, turbomachinery, compressor, turbine, performance maps, off-design, Stodola, Baumann, cone rule, centrifugal, axial, velocity triangle, Euler, degree of reaction, impulse turbines, reaction turbines, nozzle, efficiency island, similarity, flow factor, enthalpy factor, pump, fan.

37.1 SUPPLEMENTS ON TURBOMACHINERY

37.1.1 Analysis of the velocity triangle

We presented in section 7.3.2.4 of Part 2 the Euler relationship, which links the enthalpy change and thus the useful work to the velocity profile in turbomachinery. In this section we will complete this presentation with a more detailed analysis of equations for flows in turbomachinery, especially those corresponding to velocity triangle. This analysis is necessary if we are to understand the physical phenomena that govern turbomachinery off-design behavior.

In general, the Euler relationship is written:

$$\tau = \overline{U}_2 \overline{C}_{t2} - \overline{U}_1 \overline{C}_{t1}$$

C_t being the tangential component of absolute velocity C : $C_t = C \cos \alpha$.

If the fluid enters the wheel radially, the Euler relation is simplified and written as:

$$\tau = \overline{U}_2 \overline{C}_{t2}$$

or: $\tau = UC_t$, leaving indices and vector notations for ease of writing.

Moreover, the velocity triangle gives in the case of a turbine (Figure 37.1.1):

$$C_t = w \cos \beta - U$$

Since $w = C_r / \sin \beta$, we have $C_t = Cr \cotg \beta - U$

For a compressor, we would have:

$$C_t = U + w \cos \beta$$

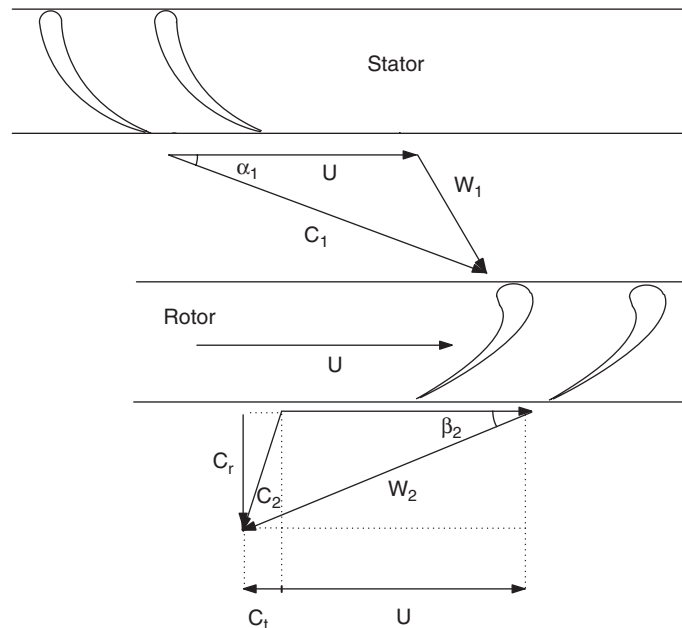


FIGURE 37.1.1
Turbine velocity triangle

And

$$C_t = U + C_r \cotg \beta$$

or:

$$\frac{C_t}{U} = 1 + \frac{C_r}{U} \cotg \beta \quad (37.1.1)$$

This relationship can also be written:

$$\frac{\tau}{U^2} = 1 + \frac{C_r}{U} \cotg \beta \quad (37.1.2)$$

Yet τ/U^2 is precisely the power factor μ defined in section 7.3.3 of Part 2, if τ is positive (compressors), and its opposite if τ is negative (turbines). We assume temporarily, in order not to overburden the presentation, that τ is positive.

In addition, C_r/U can be expressed in terms of volume flow \dot{V} :

$$\frac{\pi D e}{v} C_r = \dot{m} \quad \dot{V} = \dot{m} v = \pi D e C_r$$

With $\delta = \dot{V}/UD^2$, we get:

$$\mu = 1 + \delta \frac{D}{\pi e} \cotg \beta \quad (37.1.3)$$

The relation (37.1.3) binding μ and δ is very general because it is derived immediately from the velocity triangle. It must be verified, as (37.1.1) or (37.1.2), for all types of turbomachinery.

μ , the power factor, is the work that is put into play in a turbomachinery stage. δ is called the flow coefficient. It is representative, up to a factor, of the ratio between the flow velocity and the circumferential velocity. These two are Rateau coefficients introduced in section 7.3.3 of Part 2, which are directly involved in the study of the turbomachinery similarity.

For a wheel of given shape, the Rateau coefficients perfectly determine the flow in the wheel:

$$\cotg \beta = \frac{\pi e(\mu - 1)}{\delta D} \quad \text{and} \quad C_t = \mu U$$

The shape of the velocity triangle is characterized by these coefficients and the geometric characteristics of the wheel. For example, consider the case $\mu = 1$.

We have $\beta = \pi/2$ and $C_t = U$

The output triangle is right-angled.

37.1.2 Degree of reaction of one stage

The energy balance of a stage that we built in section 7.3 of Part 2 has shown that the enthalpy change is partly in the rotor, and partly in the diffuser. We call the degree of reaction ε the fraction of the enthalpy change that takes place in the rotor. With the previous notations, we have:

$$\varepsilon = \frac{h_2 - h_1}{h_r - h_1} = \frac{h_2 - h_1}{\Delta h} \quad \text{By definition, } \varepsilon \text{ is between 0 and 1.}$$

In a dynamic compressor stage $0.5 \leq \varepsilon \leq 1$ is commonly obtained. The lower limit ($\varepsilon = 0.5$) is approximated in axial dynamic compressors. As for the upper limit (pure reaction: $\varepsilon = 1$), it is reached in the case of a single stage machine whose diffuser is nonexistent or of negligible effectiveness.

In a turbine stage, pure reaction is impossible. Two limiting cases frequently arise:

- **impulse turbines**, in which $\varepsilon = 0$: any expansion of the fluid is then carried out in fixed blades or nozzles, at the inlet of the wheel, and the rotor inlet and outlet pressures are equal;
- **reaction turbines**, where $\varepsilon = 0.5$: the expansion is then evenly distributed between the nozzle and the wheel.

We can relate the **Rateau coefficients to the degree of reaction**:

By definition, we have:

$$\varepsilon = \frac{h_2 - h_1}{h_r - h_1} = \frac{h_2 - h_1}{\Delta h}$$

$$\varepsilon = 1 - \frac{h_r - h_2}{\Delta h} = 1 - \frac{h_r - h_2}{\tau}$$

If we neglect the kinetic energy at the diffuser outlet,

$$h_r - h_2 = \frac{1}{2} C_2^2 = \frac{1}{2} (C_{t2}^2 + C_{r2}^2)$$

By showing the power factor μ , we get:

$$\varepsilon = 1 - \frac{h_r - h_2}{\mu U^2} = 1 - \frac{C_{t2}^2 + C_{r2}^2}{2\mu U^2} \quad (37.1.4)$$

Each of the squares of the velocities can be expressed in terms of the Rateau coefficients.

All calculations done, we get:

$$2(1 - \varepsilon)\mu = \mu^2 + \frac{1}{\pi^2} \left(\frac{D}{e} \right)^2 \delta^2$$

Generally, the ratio C_r/U of flow velocity to circumferential velocity is low, between 0.1 and 0.2. We can neglect its square, and (37.1.4) simplifies to:

$$\varepsilon = 1 - \frac{\mu}{2}$$

Thus the radial exit vane ($\mu = 1$) has a degree of reaction close to 0.5.

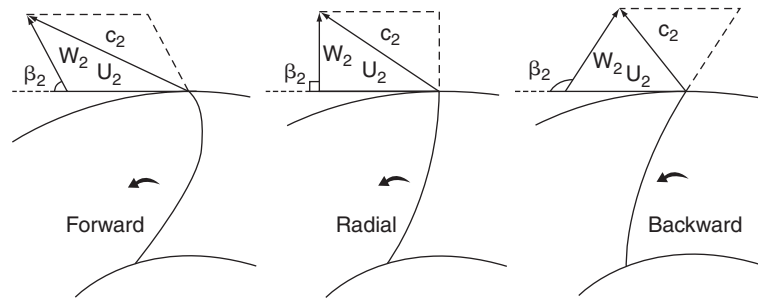
37.1.3 Theoretical characteristics of turbomachinery

Let us come back to the general equation (37.1.3) and study its form for various turbomachinery.

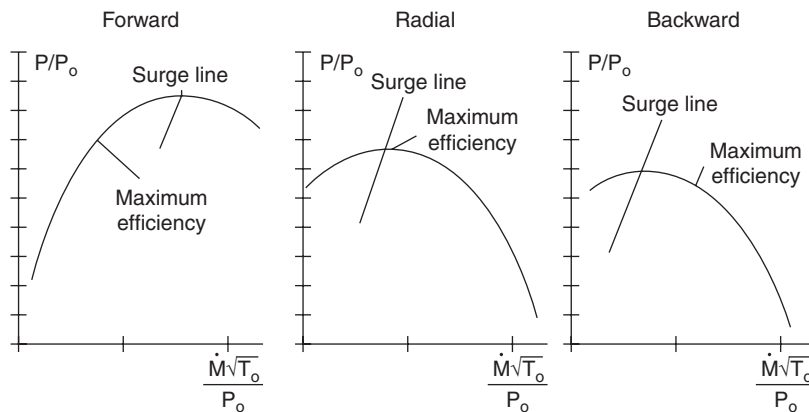
37.1.3.1 Centrifugal compressors

In the case of centrifugal compressors, the velocity triangle can be arbitrary, as β_2 can take values above or below $\pi/2$. Three types of blades may exist (Figure 37.1.2):

$$\beta_2 < \pi/2 \text{ blade lying forward } \varepsilon < 0.5 \quad \mu > 1$$

**FIGURE 37.1.2**

Velocity triangles of centrifugal compressors

**FIGURE 37.1.3**

Influence of exit angle on surge

The velocity at the impeller outlet is very large, which allows a high compression ratio, but on condition that the diffuser is very effective. We must therefore use a vaned diffuser, whose efficiency drops when operating conditions deviate from the rated conditions. Moreover, the point of best efficiency of these compressors is in the surge zone, which makes them unstable.

$$\beta_2 = \pi/2 \text{ radial exit vane } \varepsilon = 0.5 \quad \mu = 1$$

The velocity at the impeller outlet is still important, and so it is best to use a vaned diffuser. Moreover, the point of best efficiency is at the limit of the surge zone, so that the stability of radial vane compressors remains low.

$$\beta_2 > \pi/2 \text{ blade lying back } \varepsilon > 0.5 \quad \mu < 1$$

The velocity at the impeller outlet is much lower than in the previous cases, so that a vaneless diffuser should be perfect. Moreover, the point of best efficiency is outside the surge zone, so that these lying-back blade compressors are much more stable than others. If we desire to have an operating range as wide as possible, these compressors are better suited than others.

Equation (37.1.3) results in a diagram (δ, μ) by a straight line whose slope is positive for $\beta_2 < \pi/2$, zero for $\beta_2 = \pi/2$, and negative for $\beta_2 > \pi/2$.

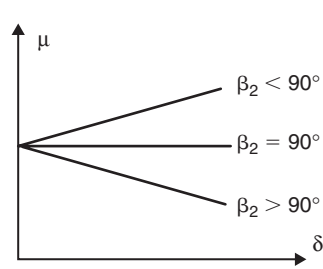


FIGURE 37.1.4
Centrifugal compressor

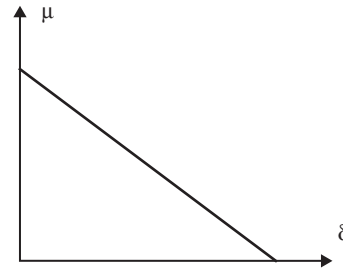


FIGURE 37.1.5
Axial Compressor

The intercept is 1, and its slope depends only on geometry (Figure 37.1.4).

37.1.3.2 Axial compressors

In the case of axial compressors, the velocity triangle is such that $\beta_2 > \pi/2$, due to conservation of flow velocity and circumferential velocity. In practice, we do not use β , but $\pi - \beta$, and equation (37.1.3) becomes:

$$\mu = 1 - \delta \frac{D}{\pi e} \cotg \beta \quad (37.1.5)$$

The line always has a negative slope, of intercept 1. Its slope only depends here on the geometry (Figure 37.1.5). μ is always below 1, meaning that the compression ratio achievable in an axial turbocharger is pretty low.

37.1.3.3 Turbines

In the case of turbines, the useful work τ is negative, so μ must be replaced by its opposite $-\mu$ in equation (37.1.3).

For the same reason as in the case of axial compressors, the velocity triangle is such that $\beta_2 > \pi/2$, β_2 is also replaced by $\pi - \beta_2$. Moreover, the assumption $U_1 C_{t1} = 0$ is no longer valid in turbines (Figure 37.1.1), and equation (37.1.3) becomes:

$$-\mu = 1 - \delta \frac{D}{\pi e} (\cotg \alpha_1 + \cotg \beta_2)$$

or:

$$\mu = \delta \frac{D}{\pi e} (\cotg \alpha_1 + \cotg \beta_2) - 1 \quad (37.1.6)$$

The line has a positive slope and an intercept equal to -1 . Its slope depends only on geometry (Figure 37.1.6).

37.1.4 Real characteristics of turbomachinery

37.1.4.1 Form of real compressor performance map

The characteristics that were highlighted in the previous section are theoretical lines, valid for perfect flows.

As we noted earlier, thermodynamics proves powerless to date to theoretically determine the differences due to irreversibilities. For this it is necessary to use fluid mechanics.

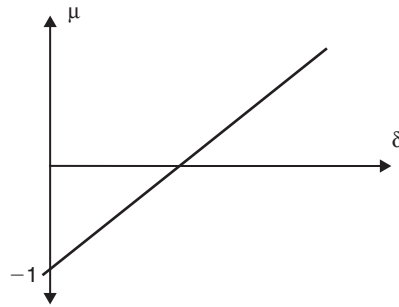


FIGURE 37.1.6
Turbine

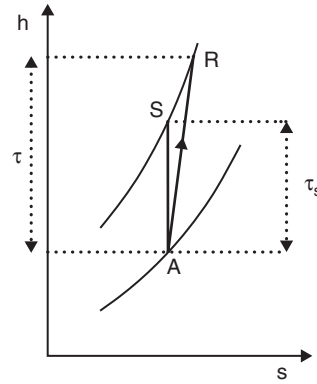


FIGURE 37.1.7
Mollier (h, s) chart

This allows us to know the shape of losses due to friction and shocks in the flow. This suggests the look of actual characteristics.

On the Mollier (h, s) chart, the theoretical compression results in a vertical AS, and the actual process in a curve AR, which can often be approximated by a polytropic (Figure 37.1.7).

We therefore define a factor $\mu_s = \tau_s/U^2$ which is lower than μ , the ratio μ_s/μ being the internal isentropic efficiency η_{int} .

For each flow-rate value, and thus δ , there is a value of μ corresponding to work spent, and a value of μ_s corresponding to the useful compression effect.

The curve $\mu_s = f(\delta)$ is called the performance curve of the compression stage.

37.1.4.2 Qualitative analysis of losses

Friction losses

In turbomachinery stage channels, flow is always turbulent, due to very high speeds reached by the fluid and discontinuities corresponding to the passage of the moving blades.

Experimental fluid mechanics tells us that in such flows, enthalpy losses are proportional to the square of velocity. In dimensionless variables, this results into a law like this:

$$\Delta\mu_f = -k_f\delta^2$$

We must therefore subtract from the theoretical line of heights a parabolic quantity $k_f\delta^2$.

Shock losses

The wheel blades are drawn for a design operation flow-rate, for which fluid lines pass through the impeller with minimum possible impact. When operating conditions deviate from this regime, shock losses are inevitable, as shown by fixed β_1 and β_2 velocity triangle. Fluid mechanics tells us here that shocks have the effect of creating losses proportional to the square of the difference between the actual flow and the design flow-rate. In dimensionless variables, corresponding loss is of the form:

$$\Delta\mu_{ch} = -k_{ch}(\delta - \delta_0)^2$$

If the diffuser is vanned, the same phenomenon occurs, whereas if it is vaneless shock losses do not occur. So it is better, if machines are working in a wide flow range, to adopt vaneless diffusers, while vanned devices can contribute more effectively to the recovery of kinetic energy when the flow-rate variation range is narrow.

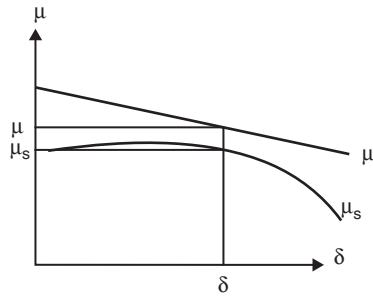


FIGURE 37.1.8
Real performance curve

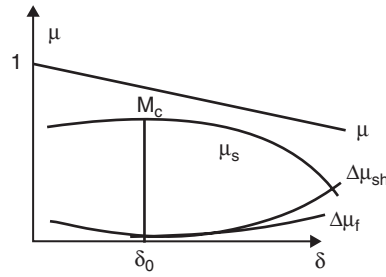


FIGURE 37.1.9
Losses due to friction and shock

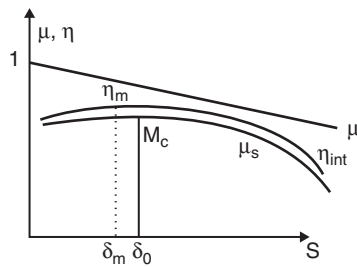


FIGURE 37.1.10
Real performance curve

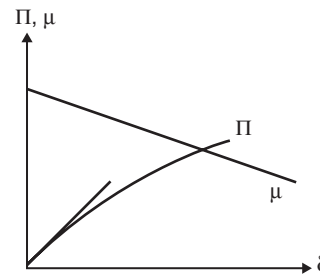


FIGURE 37.1.11
Internal power

Summary

By bringing together all the above results on one graph in the plane (δ, μ) , we can plot point by point the curve giving the power factor μ_s , by subtracting from the theoretical line the two parabolas representing losses. The resulting curve is the real performance curve (Figure 37.1.10).

We can also plot point by point the internal isentropic efficiency η_{int} curve, which is the ratio, for a value of δ , of the ordinate of the actual characteristic to that of the theoretical line.

The maximum efficiency is obtained for a value δ_m slightly less than rated δ_0 , due to the shape of loss laws.

We can also plot the internal power P_{int} curve (i.e. the real power minus mechanical losses). We introduce a dimensionless variable for this:

$$\Pi = \frac{vP_{int}}{U^3D^2} \quad \text{We find: } \Pi = \mu\delta$$

The above analysis is however incomplete in that it neglects mechanical losses and internal leaks, which have the effect of recirculating some of the fluid.

We often prefer for a given type of equipment, reasoning about macroscopic quantities rather than reduced variables such as Rateau coefficients.

So instead of working in the (δ, μ) plane, we retain the (μ, H) or the (μ, r) plane, H being the head, and r the compression ratio. We then plot the performance map for different rotation speeds N .

Two homologous points, i.e. of the same (δ, μ) are on a vertical axis parabola, since for fixed μ and δ we have:

$$\frac{\dot{m}'}{\dot{m}} = \frac{U'}{U} = \frac{N'}{N}$$

$$\frac{H'}{H} = \frac{U'^2}{U^2} - \frac{N'^2}{N^2}$$

In particular, the peaks of the different features are arranged on a parabola.

According to this analysis, iso-efficiency curves should be parabolas with vertex 0. In fact, given the interference phenomena at very low and very high speeds, as well as leakage and mechanical losses, they are closed curves, and the name of efficiency island is sometimes given to the chart prepared by experiment.

The developments we have just made on velocity triangle speeds and characteristics analytically justify the look of turbomachinery performance maps, that we briefly presented in section 7.3.3 of Part 2, and that we will deepen further in the rest of this chapter.

They also show the limits of off-design modeling based on the analysis of velocity triangle deformation, which cannot take into account losses by shock and friction. The approach based on similarity rules and machine performance maps allows us to do it and is therefore in our view more accurate.

37.1.5 Factors of similarity

In section 7.3.3 of Part 2, we have also introduced, in addition to Rateau coefficients μ and δ two dimensionless magnitudes widely used in the Anglo-Saxon literature, particularly interesting for the study of turbomachinery: **flow factor** φ and **enthalpy factor** ψ .

By definition (equations (7.3.18) and (7.3.19) of Part 2):

$$\varphi = \frac{(M_a)_c}{(M_a)_u} = \frac{4\dot{m}\sqrt{rT_a}}{\pi D^2 P_a \sqrt{\gamma}} \frac{60\sqrt{\gamma r T_a}}{\pi D N} = \frac{240\dot{m}r T_a}{\pi^2 D^3 P_a N} = \frac{240}{\pi} \delta = \frac{240\dot{V}}{\pi^2 D^3 N} \div \frac{\theta}{(M_a)_u}$$

$$\psi = \frac{|\Delta h_s|}{1/2U^2} = 2\mu = \frac{7,200 |\Delta h_s|}{\pi^2 D^2 N^2} = \frac{\Omega}{(M_a)_u^2}$$

For the design and representation of the performance of turbomachinery, one can also use reduced performance maps defined by a combination of similarity factors φ and ψ . Moreover, given the importance of off-design operation are introduced Mach numbers of flow, usually the wheel Mach number $(Ma)_u$.

Among the most used reduced performance map we have:

– the power factor Λ :

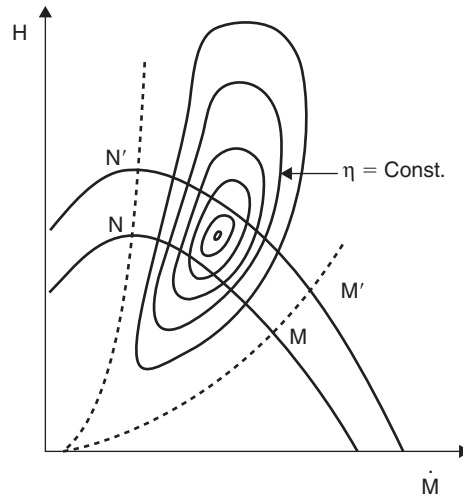
$$\Lambda = \varphi \cdot \psi = \frac{8}{\pi^4} \frac{\dot{V} |\Delta h_{ts}|}{N^3 D^5} \quad (37.1.7)$$

– the specific diameter of the machine Δ :

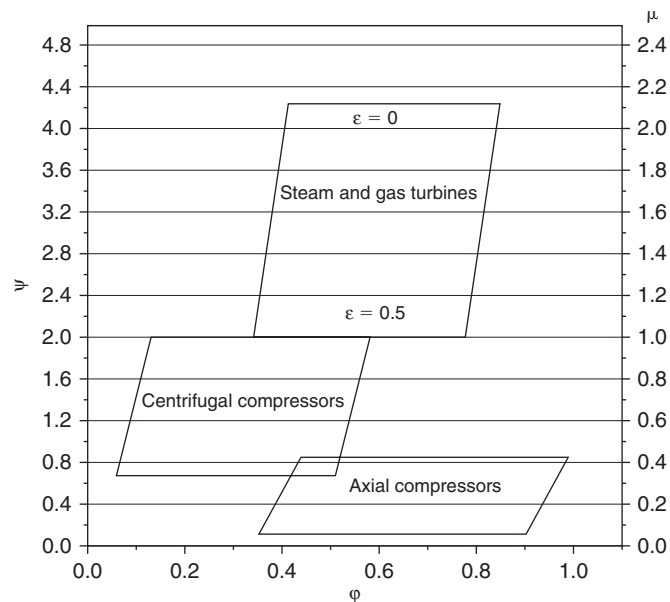
$$\Delta = \frac{\psi^{1/4}}{\varphi^{1/2}} \quad (37.1.8)$$

– the specific speed σ :

$$\sigma = \frac{\varphi^{1/2}}{\psi^{3/4}} \quad (37.1.9)$$


FIGURE 37.1.12

Performance map


FIGURE 37.1.13

Similarity and turbomachinery stage

Combining (37.1.7) and (37.1.8) with equations (7.3.18) and (7.3.19) of Part 2, we can also express these last two quantities depending on the performance map of the machine:

$$\Delta = 1.054D \frac{|\Delta h_s|^{1/4}}{\dot{V}^{1/2}} \quad (37.1.10)$$

$$\sigma = 2.108N \frac{\dot{V}^{1/2}}{|\Delta h_s|^{3/4}} \quad (37.1.11)$$

Similarity factors are often useful to guide the design of turbomachinery. Technological constraints induce that, depending on values of similarity factors, choice is limited: for a given flow factor, the enthalpy factor or Rateau coefficient of a turbomachinery stage can be obtained from charts of the type shown Figure 37.1.13.

Indeed, part of the interest of the similarity theory comes from the fact that, in off-design operation, actual machines are such that, because of the constructive possibilities, the ranges of variation of characteristic factors are relatively narrow.

Besides their applications for the selection of machines, these similarity factors prove also very interesting for studying the off-design behavior of a dynamic compressor, as we shall see.

37.2 PUMPS AND FANS

The mechanical and thermodynamic study of flows in pumps and fans is to a very large extent similar to that of dynamic compressors that was presented in section 7.3.3 of Part 2, but with an important simplification: for them it is perfectly legitimate to assume that the **fluid is incompressible**.

In particular, the expression giving ψ is considerably simplified, because $\Delta h_s = v\Delta P$ or $\Delta h_s = \Delta P/\rho$. For a pump, the data provided is generally the head H , and g being the acceleration due to gravity, $\Delta h_s = gH$.

Let us recall that similarity factors are always defined at a factor of proportionality. Those we have identified for turbines and dynamic compressors were developed by referring them to Mach numbers, which are not expected to be used in the case of pumps and fans. Therefore, their expressions given in the literature are generally different.

Similarity factors φ , ψ , Δ and σ introduced in section 37.1.5 are very useful for studying the turbomachinery off-design behavior. It is possible to plot the performance map either with φ as abscissa and ψ as ordinate or σ as abscissa and Δ as ordinate. Figure 37.2.1 shows the performance map of a Gebhardt RZR 315 fan as provided by the manufacturer, giving, according to the intake flow, first the pressure supplied and also the efficiency at three speeds (1600, 2400 and 3200 rpm).

When expressed in reduced coordinates in the (φ, ψ) and (φ, η) coordinate systems, they overlap perfectly as shown Figure 37.2.2.

This simplicity is also found for pumps, for which manufacturers generally provide a single set of performance maps, including, depending on intake flow, first pressure supplied and second efficiency.

Figure 37.2.3 shows the performance map of a Grundfos centrifugal pump (model LP 100-200/183 rotating at 2940 rpm).

By expressing them in reduced variables in the (φ, ψ) and (φ, Λ) coordinate systems, the power factor being representative of the efficiency, we obtain those in Figure 37.2.4, which eliminates the need for speed data.

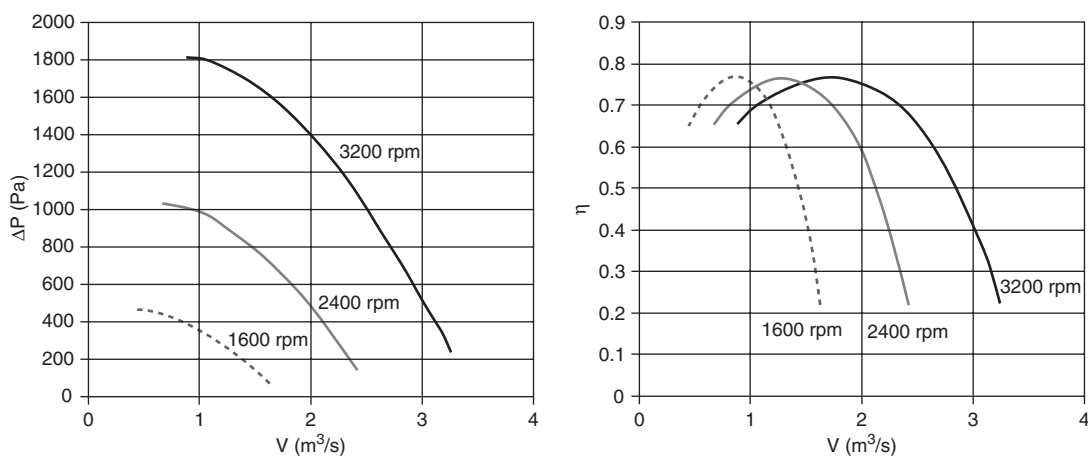


FIGURE 37.2.1

Performance map of a fan

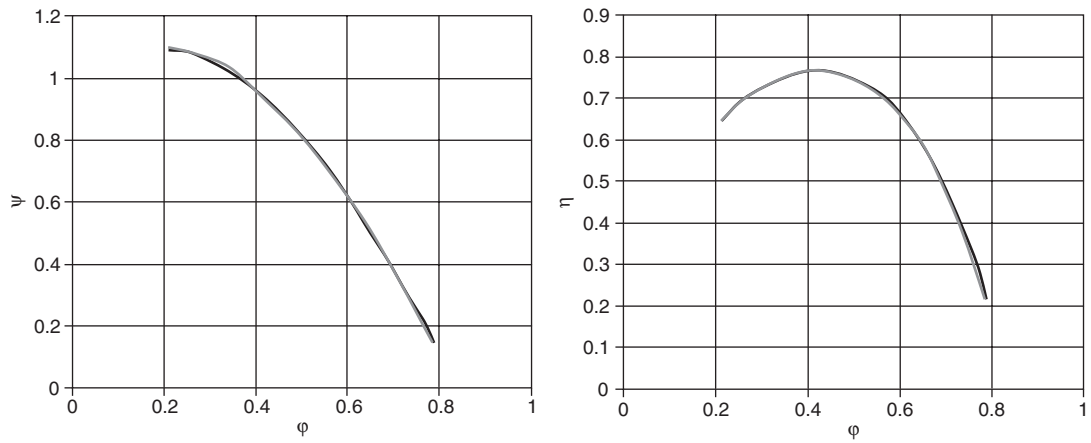


FIGURE 37.2.2
Reduced performance map of a fan

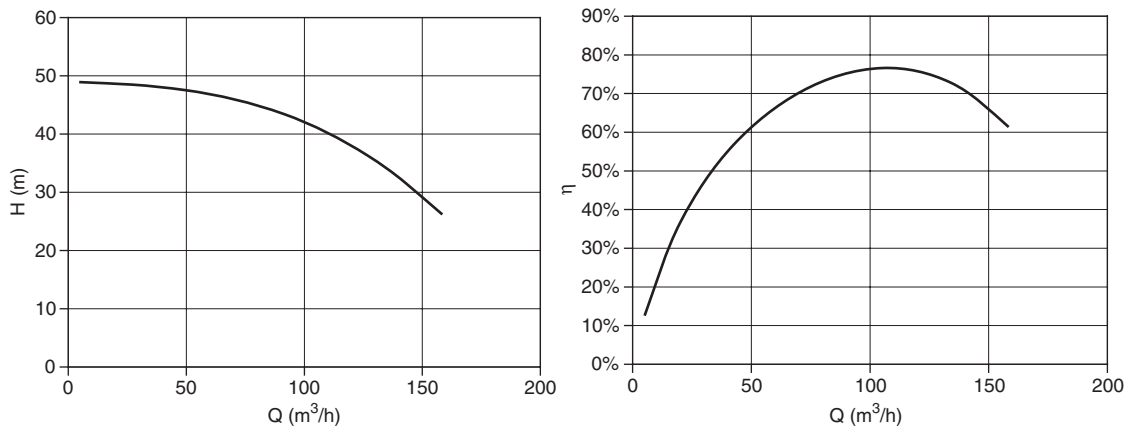


FIGURE 37.2.3
Absolute performance map of a centrifugal pump

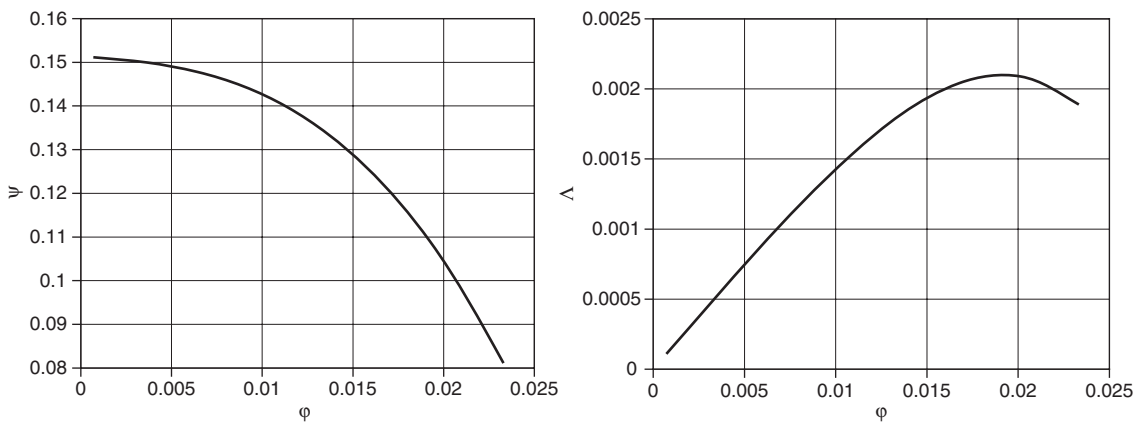


FIGURE 37.2.4
Performance map of a centrifugal pump

The performance map of **positive displacement pumps** are generally drawn in a frame where the abscissa is the height and the ordinate the flow or efficiency. They have the form of lines of low slope.

These developments explain why the fan or pump off-design modeling can be made by simply providing the two curves giving, depending on the flow factor φ , enthalpy factor ψ and efficiency η or power factor Λ . Such curves can be approximated by polynomials of order 2-4, as appropriate.

As we have seen, reduced performance maps of pumps and fans are relatively simple. It is not the same with those of dynamic compressors and turbines, which we now study.

37.3 DYNAMIC COMPRESSORS

37.3.1 Performance maps of dynamic compressors

Models of dynamic compressors that we will consider here are based on those in section 7.3.3 of Part 2. These numerical models are generally expressed relative to the similarity factors presented in section 37.1.5.

In practice, performance maps are usually established for constant values of the corrected rotation speed N_c , and are expressed relative to the corrected flow \dot{m} :

$$N_c = \frac{N}{\sqrt{T_a}}; \quad \dot{m}_c = \frac{\dot{m}\sqrt{T_a}}{P_a}; \quad \frac{P_r}{P_a} = f(\dot{m}_c); \quad \eta_s = f\left(\frac{P_r}{P_a}\right) \quad \text{or} \quad f(\dot{m}_c)$$

Curves of equal efficiency can be directly plotted on charts: $P_r/P_a = f(\dot{m}_c)$.

Sometimes, curves are presented in relation to reference values of the corrected mass flow rate or corrected speed.

For dynamic compressors (Figures 37.3.1 to 37.3.3) the corrected mass flow is used as abscissa. In the ordinate, we plot the pressure ratio or isentropic efficiency. The corrected rotation speed is still the parameter.

The corrected rotation speed strongly influences the performance of dynamic compressors. This is easily explained by considering that in such a machine, energy is transmitted to the fluid by the rotor in the form of kinetic energy. At most, this energy is $1/2 U^2$, that is to say, is proportional to N^2 . It is therefore natural that the sensitivity of these machines to regime change is dramatic.

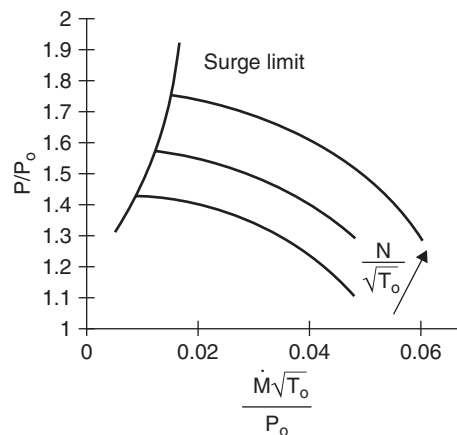


FIGURE 37.3.1

Dynamic compressor performance map

Axial compressors

The compression ratio per stage that can provide axial compressors (Figure 37.3.2) is relatively low, generally between 1.2 and 2.

Centrifugal compressors

Performance maps of centrifugal compressors (Figure 37.3.3) are steeper than those of axial compressors, making them more stable.

Due to the acceleration that the fluid receives during passage through the rotor, the compression ratio per stage they can provide is far more important, between 2.5 and 9.

The analysis of these performance maps shows that for the isentropic efficiency, the effect of speed essentially results in a shift of the curves along the abscissa axis. For the pressure ratio, there is additional amplification along the axis of ordinates.

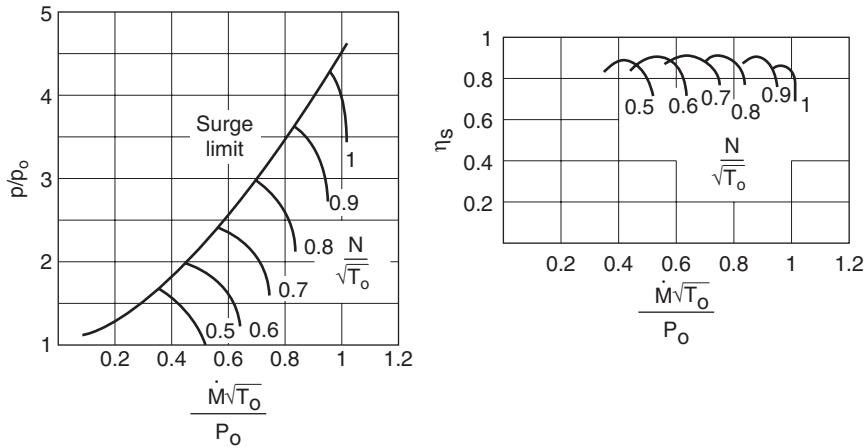


FIGURE 37.3.2

Performance map of an axial compressor

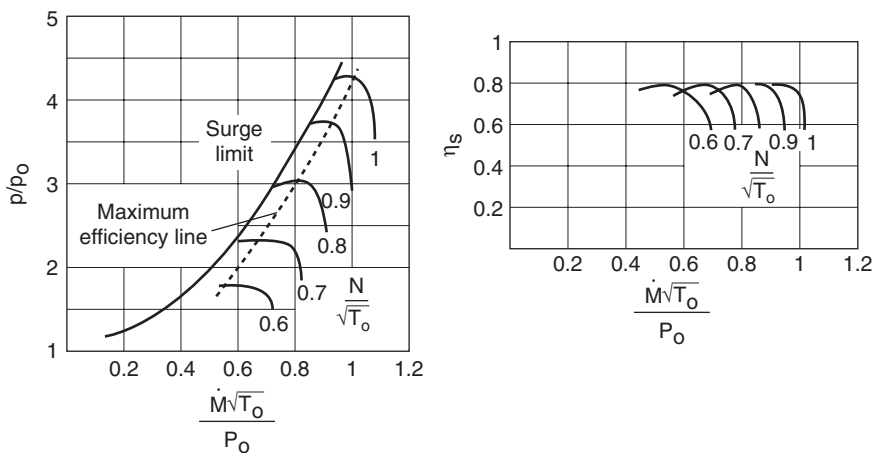


FIGURE 37.3.3

Performance map of a centrifugal compressor

It is also common to use in the ordinate, not the compression ratio, but a coefficient Ω proportional to isentropic work Δh_s , and in the abscissa a coefficient θ proportional to corrected mass flow \dot{m}_c . You shift from one coordinate system to another relatively easily.

$$\Omega = \frac{\Delta h_s}{C_s^2} \quad \theta = \frac{\dot{V}}{C_s D^2}$$

For example, Figure 37.3.4 provides the performance map of an industrial centrifugal compressor in a (θ, Ω) coordinate system, lines in bold representing iso-speeds, Mach number, and thin lines iso-efficiencies.

37.3.2 Analysis of performance maps of dynamic compressors

Figure 37.3.5 shows the reduced performance map, in the (φ, ψ) and (φ, η) coordinate systems, of the industrial centrifugal compressor of Figure 37.3.4.

Iso-speed curves are much more clustered than in Figure 37.3.4, but the differences between them remain important, especially for efficiencies at extreme speeds: it is far from the simplicity highlighted in the pump and fan study.

However, as shown in Figure 37.3.6, the dispersion of the power-flow performance map is drastically reduced when using the (θ, Δ) coordinate system.

The performance map of Figure 37.3.6 can be approximated with reasonable accuracy by a cubic or a power function: $\Delta = a\theta^b$ with $a = 2$ and $b = -0.61$, the regression coefficient r^2 being equal to 0.966.

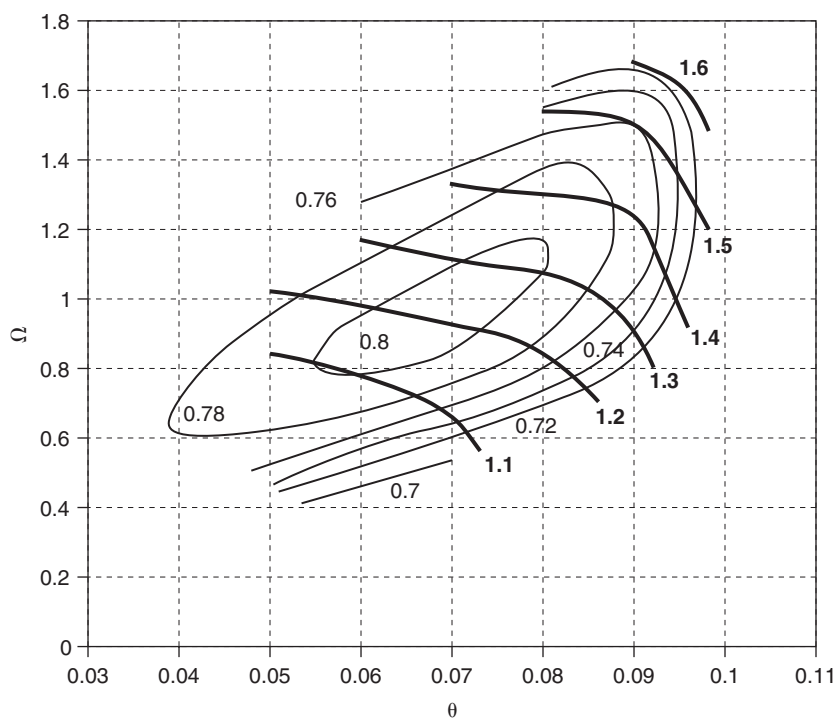


FIGURE 37.3.4

Performance map of an industrial centrifugal compressor

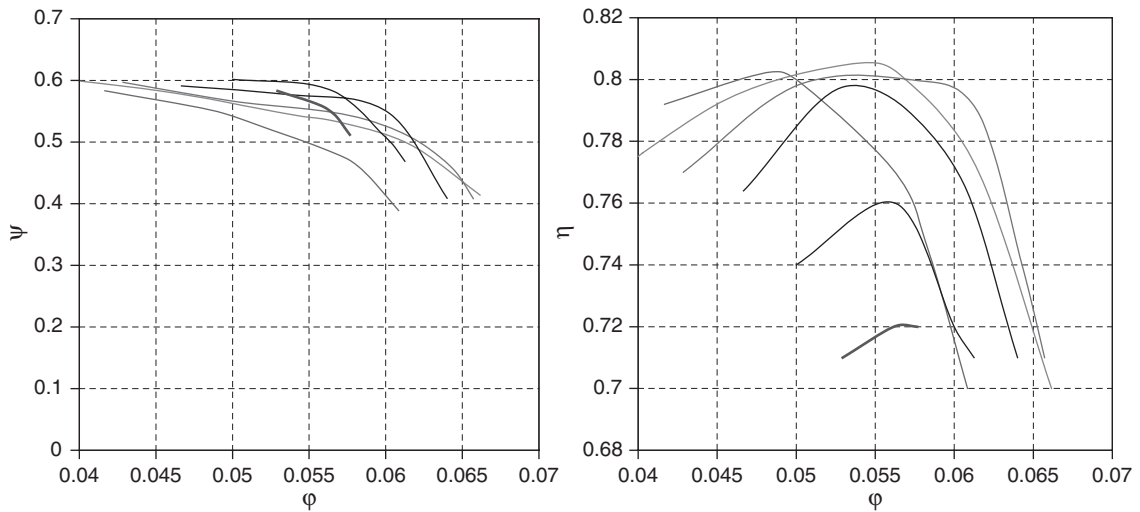


FIGURE 37.3.5
Centrifugal compressor reduced performance map

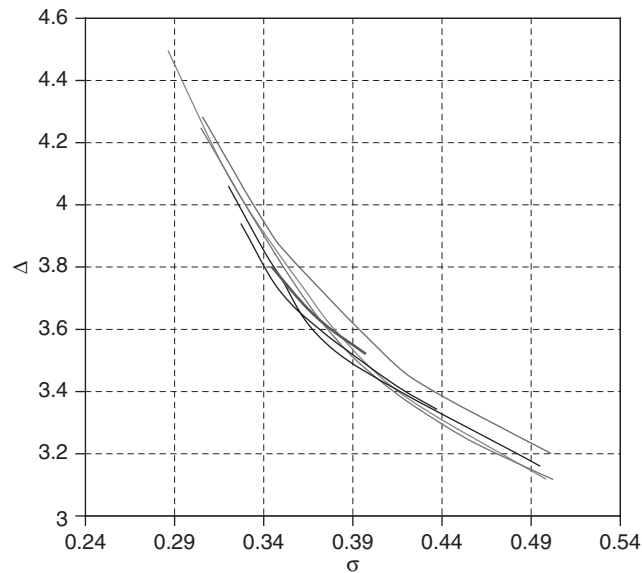


FIGURE 37.3.6
Performance map in the (θ, Δ) coordinate system

This provides a simple relationship between Δ and σ , which can be used both in design (determination of the diameter of the wheel), and to study off-design operation. If you have a compressor efficiency map, you can either search for the pair (speed, diameter) that maximizes efficiency, or determine efficiency if you know the speed.

These results, drawn here for a particular compressor, are quite general, as shown in the figures below, drawn for different axial and centrifugal compressors.

Figure 37.3.7 is the centrifugal compressor cell used by M. Pluviose to illustrate some of the exercises suggested in his book (Pluviose, 1988), and Figure 37.3.8 the centrifugal compressor presented by Conan on page 240 of his book (Conan, 1988).

Figures 37.3.9 to 37.3.11 correspond to axial compressors used in jet engines or gas turbines, the first two representing the same compressor.

In all cases, representation in the (θ, Δ) coordinate system allows us to group the cloud of data points. This is particularly remarkable in the case of Figure 37.3.9. However, the dispersion is not completely reduced, and only detailed adjustments allow the curves to be digitalized.

The conclusions we can draw for our purposes are the following: if one has a precise mapping of the dynamic compressor, such as that of Figure 37.3.4, it is much better to use it because shapes of efficiency islands can vary significantly with speed. When there are only a few experimental points, one can seek an approximate law of the type that can be identified in the (θ, Δ) coordinate system.

Examination of all these curves shows that, even if the efficiency islands are very interesting visually and allow an engineer to see the machine operation areas, it is much easier to build computer models using two sets of performance maps, one dedicated to the pressure ratio or ψ , and the other to the machine isentropic efficiency η .

If we choose to use the complete map, various methodological problems may arise, including the fact that the iso-speed curves can be either very steep (Figure 37.3.2), or very flat (Figure 37.3.3).

The interested reader can refer to (Kurzke, 1996) for complementary explanations.

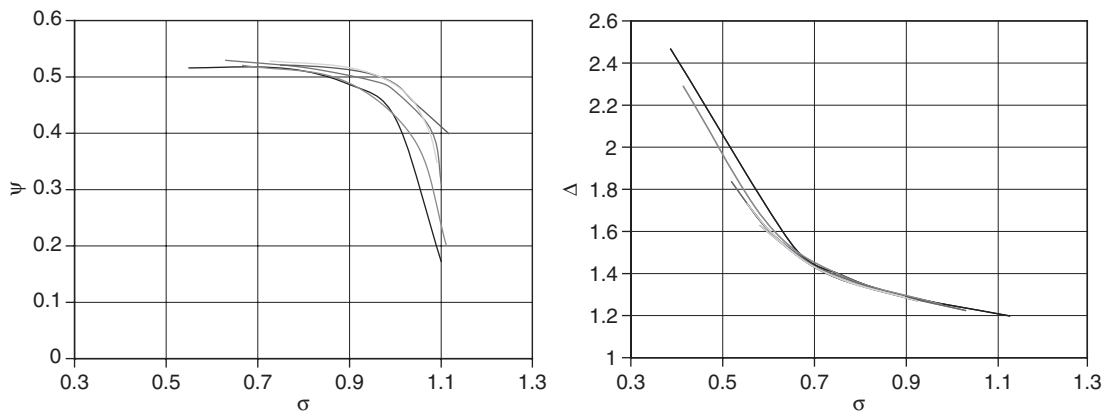


FIGURE 37.3.7

Performance map of a centrifugal compressor cell

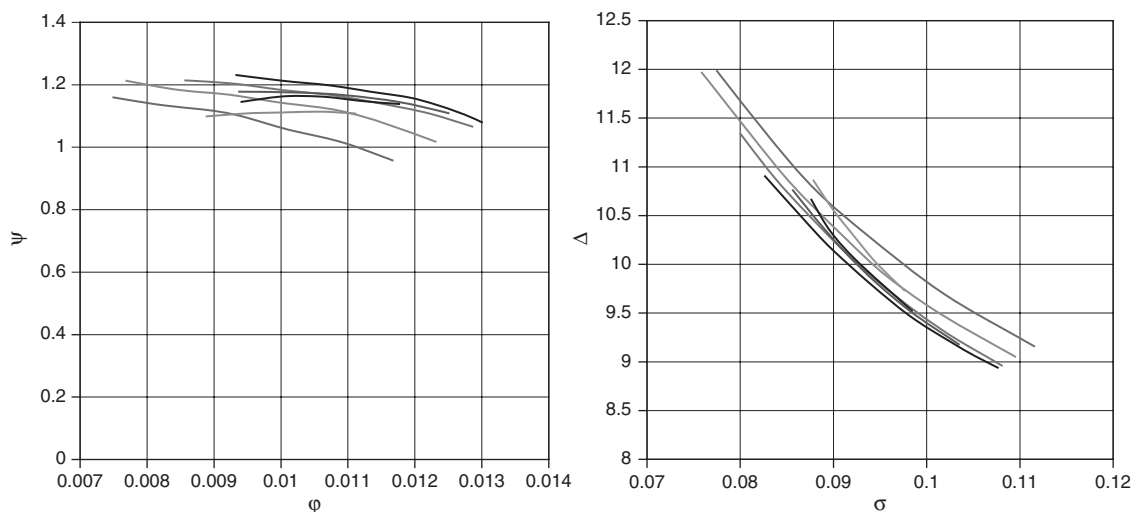


FIGURE 37.3.8

Performance map of a centrifugal compressor

Fan Rotor J.Propulsion 1992 Page 200

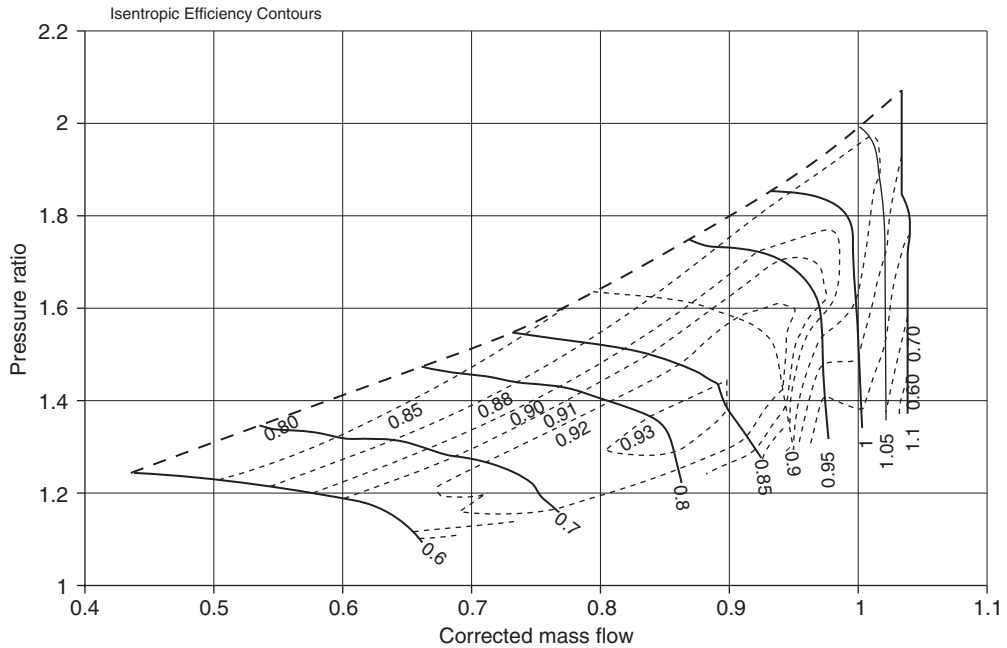


FIGURE 37.3.9

Reduced performance map of an axial compressor, according to the calculator GasTurb by J. Kurzke (www.gasturb.de)

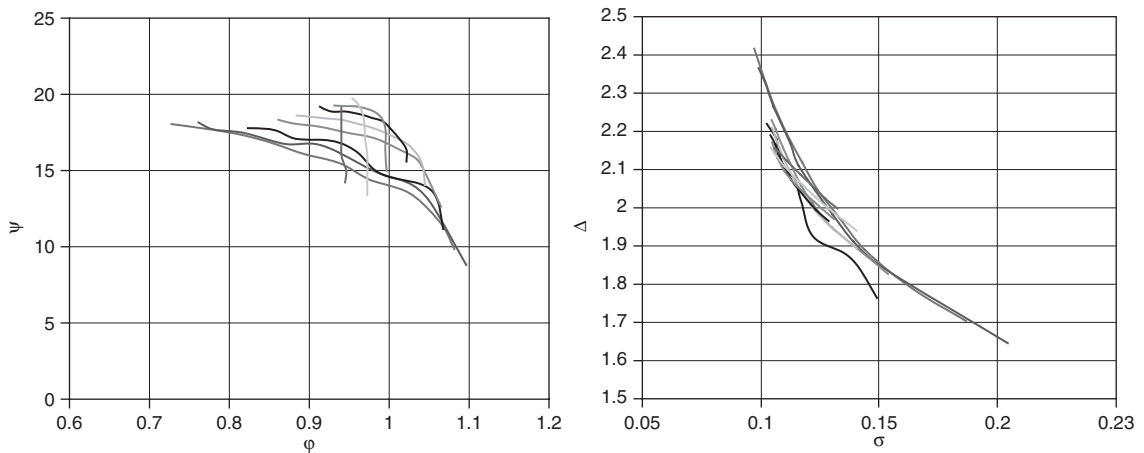
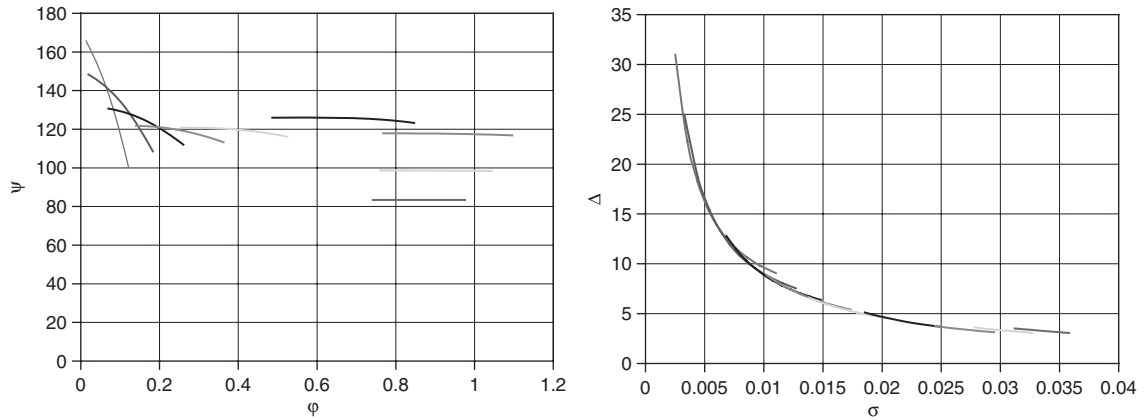


FIGURE 37.3.10

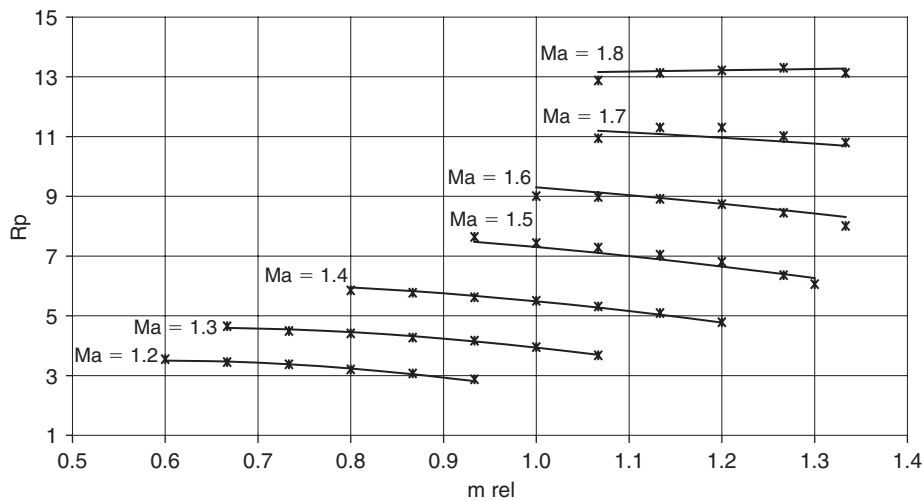
Performance map of an axial compressor

The digitization of detailed performance maps is an exercise that needs to be done carefully if they are to be reproduced accurately. Given the wide operating range of dynamic compressors, it is particularly preferable to normalize all curves so that they are evenly adjusted. Several techniques are presented in the literature (Kurzke, 1996), (El Gammal, 1991), (Tirnovan et al, 2008).

Figure 37.3.12 shows the results we can obtain with a 6 parameter model: initial performance maps (those of Figure 37.3.8) are represented by asterisks and curves adjustment in continuous dark.

**FIGURE 37.3.11**

Reduced performance map of an axial compressor

**FIGURE 37.3.12**

Reconstituted performance map

PRACTICAL APPLICATION**Application for Digitalizing Performance Maps**

To facilitate the digitization of curves, we created a small application that lets you view a previously scanned chart, then easily record points of interest. It can be downloaded from the Thermoptim portal (<http://www.thermoptim.org/sections/logiciels/thermoptim/ressources/utilitaire>). You may download it and use it at your convenience.

It allows you to display on a screen a chart image previously scanned, then to easily identify with the mouse the curve points that interest you.

**[CRC_pa_10]**

The adjustment is given by a degree 3 polynomial function of corrected flow and compression ratio, whose parameters are quadratic polynomials of Mach number. The equation is: $y = a_1 + a_2y(x + 1/x + y)$, with $a_i = \alpha_i + \beta_i Ma + \gamma_i Ma^2$.

The isentropic efficiency can also be similarly represented, an adjustment by a cosine function of the type: $y = a_1 \cos(a_2 x + a_3 x^2)$ leading however to a better estimate (Figure 37.3.13).

37.3.3 Technological screen of dynamic compressors

In the jet engine example that will be presented in Chapter 38, we opted for the representation that was justified in section 37.2 for pumps and fans, but remains simplified for dynamic compressors. We assumed that a single curve was enough to represent the performance map in the (φ, ψ) coordinate system, and another in the (φ, η) coordinate system, as shown in Figure 37.3.14.

Relating these performance maps to corrected flow and replacing ψ by the compression ratio, they take the shape of Figure 37.3.15.

Although it is simplified, this way of working allows for a first likely modeling of the behavior of a dynamic compressor.

The corresponding technological screen is given in Figure 37.3.16. It uses a series of coefficients describing the two performance maps, explained in more detail Chapter 38.

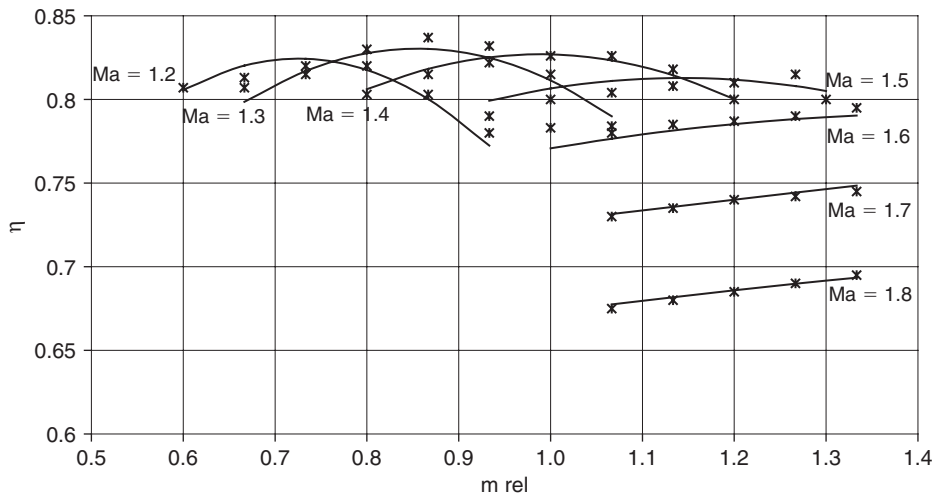


FIGURE 37.3.13
Reconstituted performance map (cosine function)

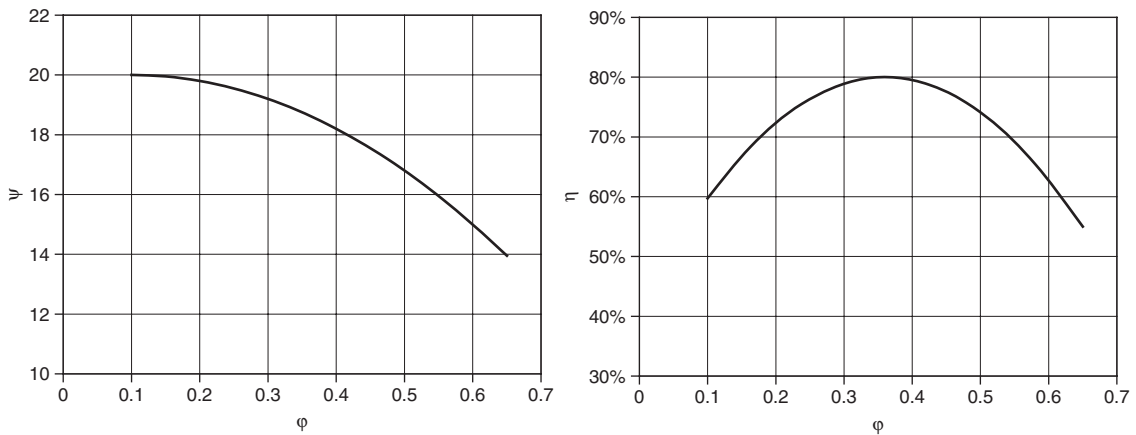


FIGURE 37.3.14
Simplified reduced performance map

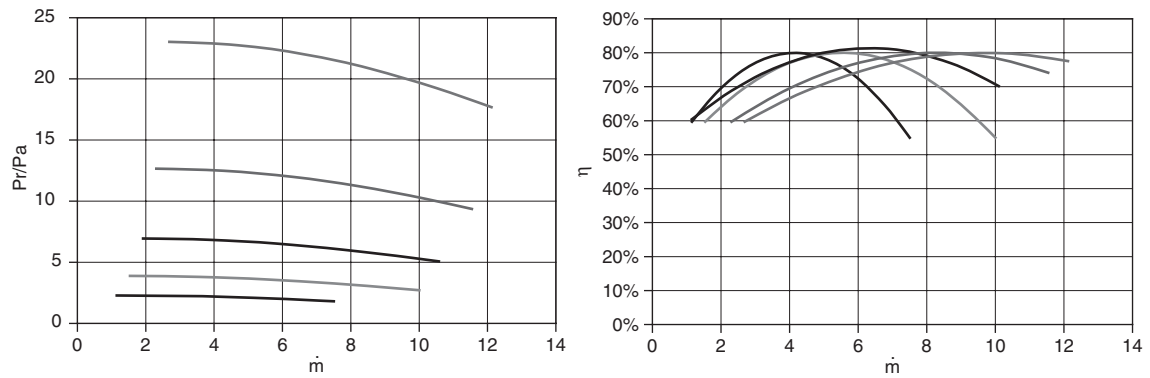


FIGURE 37.3.15

Corresponding performance map

generic turbocompressor		compressor	
Kc	20	isentropic efficiency	0.6000
diameter	1.7	reduced flow Rate	0.2115
psi Max	1.01	flow rate	139.8085
psi coefficient	-1		
phi psi max	0.1		
eta max	0.85		
eta coefficient	-25		
phi eta max	0.38		

FIGURE 37.3.16

Simplified dynamic compressor technological screen

The parameters to define are:

- K_c , compressor characteristic (equation (38.5.2));
- compressor diameter;
- ψ is represented by a branch of a parabola, defined (equation (38.5.3)) by ψ_{\max} , maximum value, ψ_{coeff} , and $\varphi\psi_{\max}$, abscissa of the maximum corrected flow $m\dot{c}$;
- η is also represented by a branch of a parabola, defined by η_{\max} , maximum value, η_{coeff} , and $\varphi\eta_{\max}$, abscissa of the maximum corrected flow $m\dot{c}$.

The calculated values of isentropic efficiency, reduced flow and mass flow appear on the right of the screen.

37.4 TURBINES

Turbine models that we will consider here are based on those described in section 7.5 of Part 2. Very often, models chosen are based on the assumption that the behavior of adiabatic turbine can be represented with reasonable accuracy by two parameters: the classic isentropic efficiency η_s , and a magnitude K_0 called cone or Stodola constant, which characterizes the design flow.

If one searches the literature on turbine off-design modeling, almost all approaches are indeed based on the Stodola and Baumann rules.

The ASHRAE Toolkit (Bourdhoux, 1993) holds the following assumptions:

- either the flow is considered choked in the turbine, the isentropic efficiency being assumed constant: $\dot{m}\sqrt{T/P} = \text{const.}$;
- or the turbine is represented as a Laval nozzle without adiabatic diffuser, and modeled from the Euler relationship and the velocity triangle. The blade orientation angle and the nozzle section should then be provided. The isentropic efficiency is calculated in this case. This way of working is similar to how we have chosen to take into account residual velocity losses as explained section 37.4.5.

37.4.1 Performance maps of turbines

For turbines (Figure 7.5.4 of Part 2) it is conventionally the pressure ratio which is used as abscissa. As ordinate, we find the corrected mass flow or isentropic efficiency of the machine. Of course it is also possible to use the same coordinate system as for dynamic compressors. The curve parameter is still the corrected rotation speed, which plays a secondary role.

We can see the flexibility of turbines to adapt to various operating conditions: efficiency tends to deteriorate only when we want to dramatically reduce the pressure ratio or the speed.

This flexibility is particularly due to the flow stability in the blades due to the gradient of pressure therein. But what is most remarkable is the stability of the flow for high pressure ratios, which comes from the supersonic regime which takes place in part at least of the machine (the flow is choked at the place where the speed of sound is reached).

The limiting value reached by the flow, when the pressure ratio exceeds the critical ratio, is called the critical flow. It is proportional to the throat section, which is obviously independent of the rotation speed, which explains the weak influence of this parameter.

Figure 37.4.1 gives the appearance of an aircraft turbine performance map, for different rotation speeds in the usual dynamic compressor coordinate system. It shows that the influence of this parameter cannot be neglected if one wants to be accurate. Since the useful area of the performance map is very small, we can represent them using as abscissa the product of corrected mass flow and velocity, leading to the plots in Figure 37.4.2.

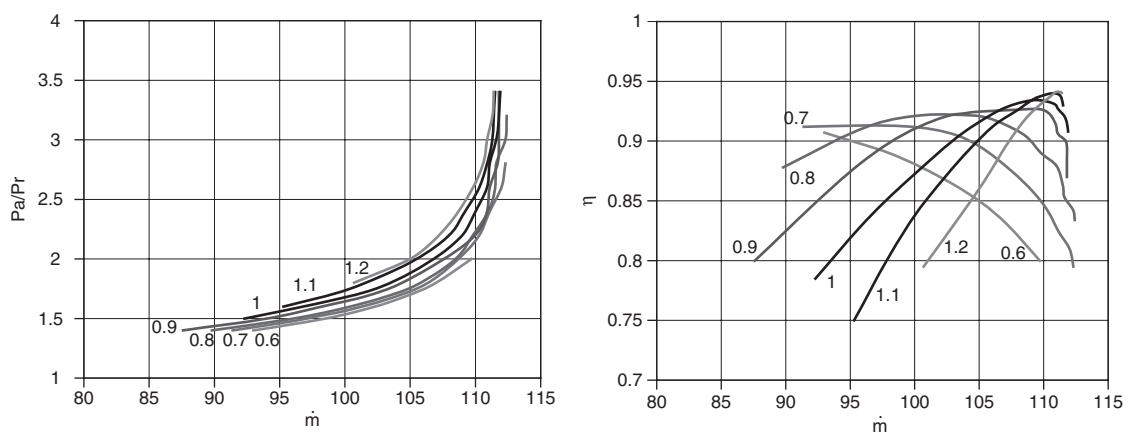


FIGURE 37.4.1

Performance map of aircraft turbine

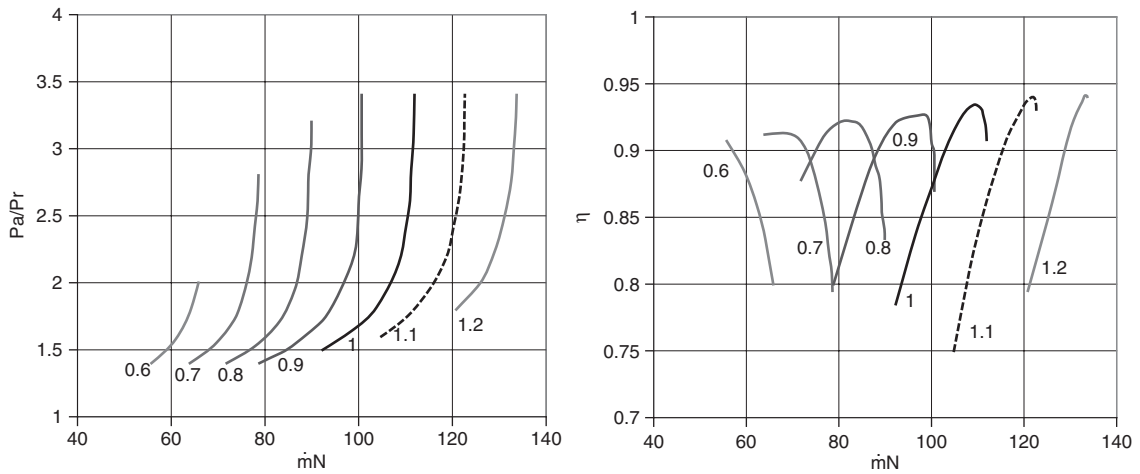


FIGURE 37.4.2

Modified performance map of aircraft turbine

37.4.2 Isentropic efficiency law

For isentropic efficiency, the shape of performance map in Figures 37.4.1 and 37.4.2 shows that a polynomial representation of curves versus flow can provide good accuracy. It is also possible to retain an equation based on the expansion ratio which is very easy to identify of type $y = a + bx + cx^2$, analogous to the positive displacement compressor law (3.1.2).

$$\eta_s = K_1 + K_2 \cdot \frac{P_r}{P_a} + K_3 \cdot \left(\frac{P_r}{P_a} \right)^2 \quad (37.4.1)$$

Note that it is expressed linearly as a function of the inverse of the expansion ratio and its square. Its parameters have the advantage of having a physical sense, since it can be rewritten as follows (37.4.2).

$$\eta_s = \eta_{\text{lim}} + (\eta_{\text{max}} - \eta_{\text{lim}}) \cdot \left(2 \left[\tau_{\text{max}} \frac{P_r}{P_a} \right] - \left[\tau_{\text{max}} \frac{P_r}{P_a} \right]^2 \right) \quad (37.4.2)$$

η_{lim} is the asymptotic value of isentropic efficiency for high expansion ratios, and η_{max} the maximum efficiency obtained for an expansion ratio equal to τ_{max} .

Knowing K_1 , K_2 and K_3 , we get very easily these values:

$$\eta_{\text{lim}} = K_1$$

$$\eta_{\text{max}} = K_1 - \frac{K_2^2}{4K_3}$$

$$\tau_{\text{max}} = -2 \frac{K_3}{K_2}$$

Figure 37.4.3 is $\eta_{\text{lim}} = 0.6$, $\eta_{\text{max}} = 0.8$, $\tau_{\text{max}} = 3$.

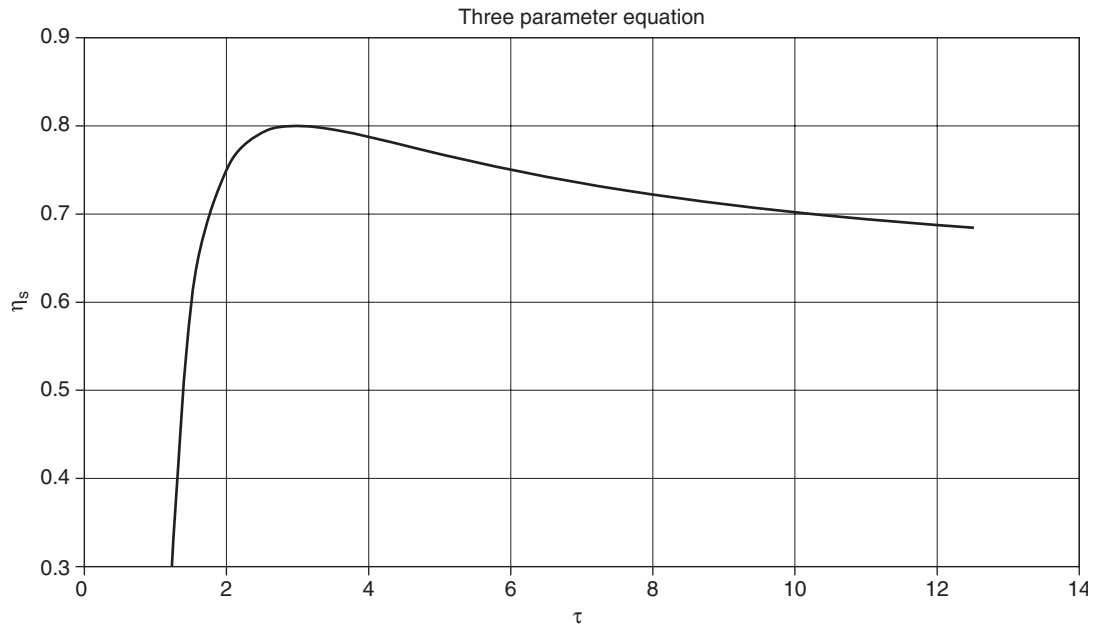


FIGURE 37.4.3
Three-parameter equation

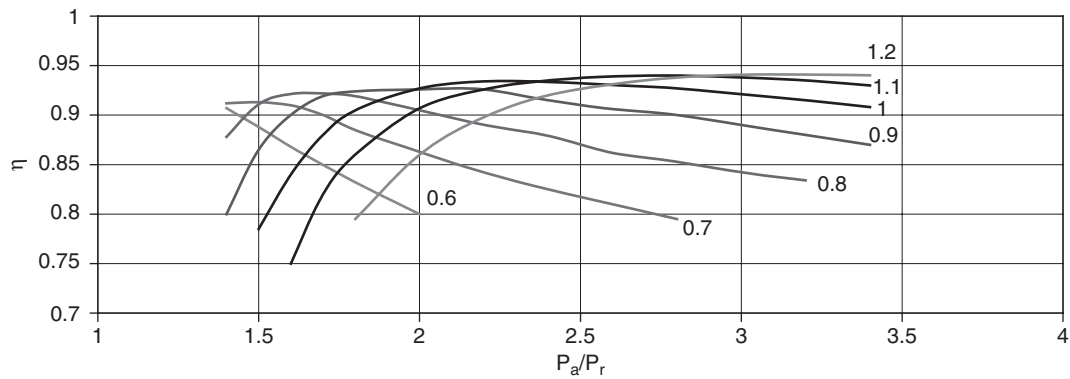


FIGURE 37.4.4
Aircraft turbine isentropic efficiency

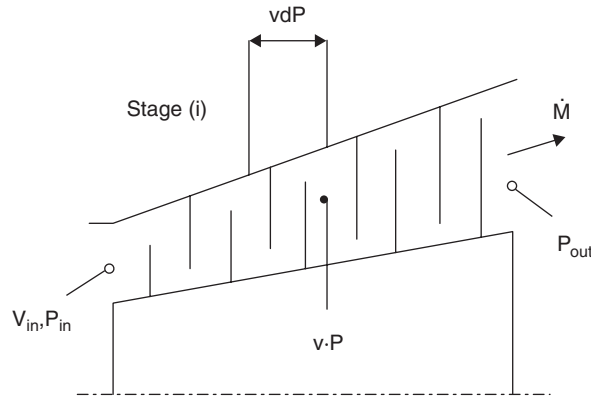
The estimation of K_1 from the physical parameters is straightforward:

$$K_1 = \eta_{lim}$$

$$K_2 = \frac{\tau_{max}}{2} (\eta_{max} - \eta_{lim})$$

$$K_3 = -\frac{\tau_{max}}{4} (\eta_{max} - \eta_{lim})$$

This law depends on the rotation speed N , η_{lim} being generally an increasing function of it, as is well illustrated in Figure 37.4.4, which shows the plot of the isentropic efficiency of the aircraft turbine described above, according to the expansion ratio.

**FIGURE 37.4.5**

Multi-stage turbine, after (Kane, 2002)

37.4.3 Stodola's cone rule

As discussed in section 7.3.3 of Part 2, manufacturers design turbines respecting similarity rules for the different stages: their flow factor φ and enthalpy factor ψ can generally be considered constant for a given turbine.

With the notations of Part 2:

- flow factor φ is the ratio of the two Mach numbers representative of flows in the machines, $(Ma)_c$ and $(Ma)_u$ i.e. C_f/U , C_f and U being respectively the flow and circumferential velocities;
- enthalpy factor ψ is $2|\Delta h_s|/U^2$.

Moreover, the equation providing the flow rate can be obtained for a multi-stage turbine (Figure 37.4.5) reasoning as follows (Kane, 2002).

The continuity equation is written, A_i being the outlet section of stage i :

$$\dot{m} = \frac{A_i C_f}{v} \quad (37.4.3)$$

$$\dot{m} = \frac{A_i U \varphi}{v} \quad (37.4.4)$$

$$\dot{m} = \frac{A_i \varphi \sqrt{2|\Delta h_s|}}{v \sqrt{\psi}} \quad (37.4.5)$$

Assuming a polytropic process, $|\Delta h_s|$ can be replaced by $v dP/\eta_p$. Raising the two members to the square, (37.4.5) can be rewritten as:

$$\frac{\psi}{2} \left[\frac{\dot{m}}{\varphi A_i} \right]^2 = \frac{dP}{\eta_p v} \quad (37.4.6)$$

This equation is integrated over the entire length of the turbine, and provides:

$$\sum_i \frac{\psi}{2} \left[\frac{\dot{m}}{\varphi A_i} \right]^2 = \frac{P_{in} v_{in}^k}{\eta_p} \int_{P_{in}}^{P_{out}} P^{1/k} dP \quad (37.4.7)$$

Stodola's cone rule is only valid as long as the flow remains below a limit value, which is reached when sonic conditions are established in the stator nozzle throat.

For a turbine stage, the critical ratio is given (for isentropic) by equation (37.4.13). For n stages, it is raised to the power n .

$$\frac{P_{in}}{P_{out}} = \left[\frac{2}{\gamma + 1} \right]^{(\gamma+1)/2(\gamma-1)} \quad (37.4.13)$$

Stodola's cone rule applies generally quite well when the turbine is running at constant speed and with an inlet temperature which varies little. When the speed varies significantly, experimental results generally show that its influence on the characteristics cannot be neglected (Figure 37.4.1), so that if one wants to be accurate, it should be taken into account, using a turbine mapping. When the inlet requirements differ significantly from those for which K_0 was determined, Stodola's cone rule should be used with caution.

Figure 37.4.7 shows the shape of a radial turbine performance map based on test results provided by Rogers and Colin (1966), for different speeds, as a percentage of design rotation speed. The influence of speed for low flows is rather sensitive.

Identification of constant K_0 leads to a value close to 0.89, but low-flow reconstructions may lead to errors of almost 20%.

37.4.4 Baumann rule

Let us recall the Baumann rule presented in section 15.7.3 of Part 3, which takes into account the efficiency degradation of a turbine operating in a humid zone.

Relationship (15.7.1) provides the isentropic efficiency of a humid stage η_{hum} , α being the Baumann coefficient, close to 1, and η_{dry} the isentropic efficiency for dry steam.

$$\frac{\eta_{hum}}{\eta_{dry}} = 1 - \alpha(1 - x) \quad (15.7.1)$$

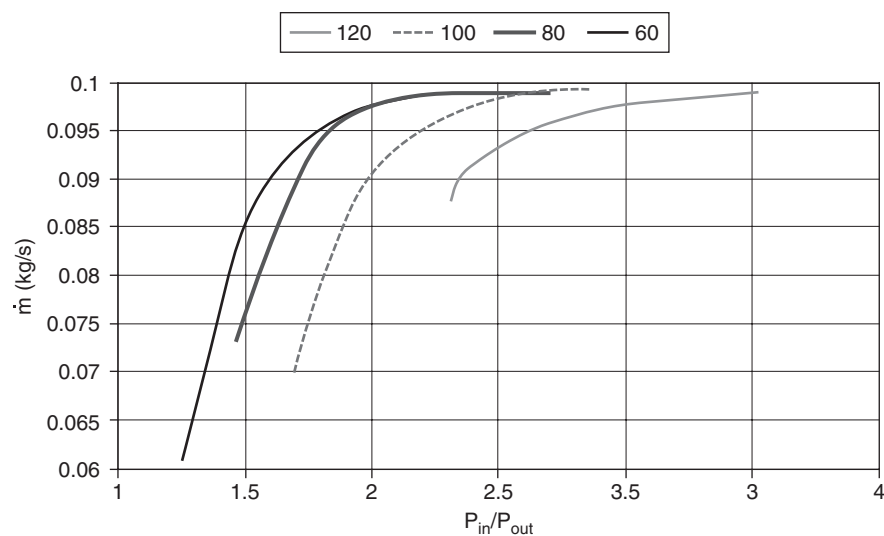


FIGURE 37.4.7

Performance map of a radial turbine

FIGURE 37.4.8

Turbine technological design screen

It is clear that the calculations of x and η_{hum} are related and cannot be made independently. We can however note that in the vapor-liquid equilibrium zone, enthalpy of fluid leaving the turbine is a linear function of x , which allows us to write:

$$\Delta H_{\text{is}} = H_a - H_{\text{is}} = H_a - (H_l + x_{\text{is}}L_0)$$

$$\Delta H_{\text{real}} = H_a - H_r = H_a - (H_l + xL_0)$$

$$\eta_{\text{hum}} = \frac{\Delta H_{\text{real}}}{\Delta H_{\text{is}}} = \eta_{\text{dry}}(1 - \alpha(1 - x))$$

$$\eta_{\text{hum}} = \frac{H_a - (H_l + xL_0)}{\Delta H_{\text{is}}} = \eta_{\text{dry}}(1 - \alpha(1 - x)) \quad (37.4.14)$$

(37.4.14) is a first-degree equation in x which is solved easily and avoids iterative calculations.

When the expansion takes place partly in the dry vapor zone and partly in the wet steam zone, the rule of Baumann is to be taken into account only in the latter. One way to do this is to replace x in equation (37.4.14) by the ratio of the enthalpy drop in the humid zone to the total enthalpy drop.

37.4.5 Loss by residual velocity

When the downstream pressure drops, for a given free flow area, the flow velocity increases, so that the kinetic energy lost may not be negligible. Physically, this means that some of the available power is not recovered on the turbine shaft, and is converted downstream in heat. The corresponding loss assessment can be made on the basis of the velocity triangle, which assumes the downstream flow section is known, also the circumferential speed U and outlet angle β . In the equation below, C_2 represents the flow velocity C_f with our usual notation.

These losses are equal to $C_2^2/2$, with (Figure 37.1.1):

$$C_t = C_r \cotg \beta - U$$

$$C_2^2 = C_r^2 + C_t^2 = C_r^2 + (C_r \cotg \beta - U)^2$$

In practical terms, if one does not want to modify the isentropic efficiency expression, the calculation of residual velocity losses (RVL) can be performed as follows.

- we first determine the turbine outlet conditions in the absence of RVL;
- knowledge of the specific volume and the exhaust section lets us know C_r and so RVL;
- work done by the turbine is equal to that in the absence of RVL minus RVL. Knowing the isentropic work (in the absence of RVL because we assume the machine is perfect), we deduce a new value of isentropic efficiency;
- recalculation of the turbine with this isentropic efficiency value gives the exit point state taking into account RVL.

37.4.6 Technological screen of turbines

The screen of Figure 37.4.8 is the turbine model presented above.

The meaning of the fields is as follows:

- Stodola constant is K_0 , the Stodola coefficient. If “choked turbine” is checked, the flow is considered choked, and the formula used is (37.4.12). Otherwise, it is (37.4.11);
- when η is represented by a 3 parameter equation, eta max is the maximum value, eta lim the limit for very high expansion rates, and tau max abscissa of the maximum. If the first two values are equal, the isentropic efficiency is constant;
- alpha Baumann is coefficient α of equation (37.4.14);
- rotation speed is the turbine rotation speed;
- for calculating residual velocity losses, the outlet section and the turbine diameter as well as the outlet angle β must be provided.

The values of the isentropic efficiency, mass flow rate and expansion ratio appear on the right of the screen.

37.4.8 Identification of turbine parameters

The identification of turbine parameters generally poses many difficulties because very few experimental data are available in practice and there is uncertainty about them. It is more fitting to use *a priori* laws based on physical phenomena than accurately identifying very accurate models.

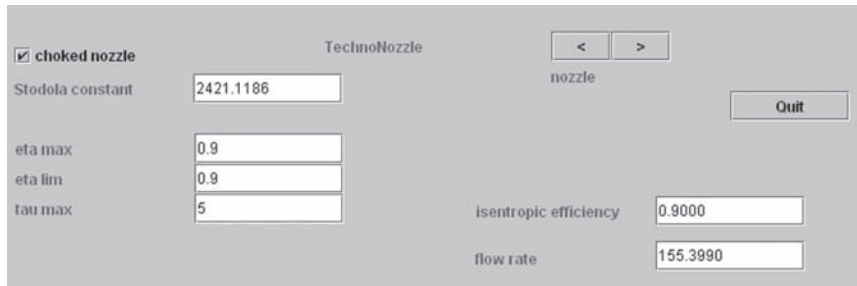
In particular, when the exit point of the turbine is two-phase, we usually do not know its exact quality, which poses a real problem.

37.5 NOZZLES

We made a presentation of the thermodynamics of nozzles in section 7.9.1 of Part 2. In off-design mode, a nozzle can be modeled similarly to a turbine, and characterized by Stodola constant and isentropic efficiency.

So we implemented a nozzle model derived from that of a turbine, whose screen is given in Figure 37.5.1. It will be used in section 38.5 on the adaptation of a turbojet aircraft.

Ideally, the study of the impact on isentropic efficiency of adaptation conditions of the output section in choked regime should be done.

**FIGURE 37.5.1**

Nozzle technological design screen

REFERENCES

- R. F. Boehm, *Pumps and fans, The CRC handbook of thermal engineering*, (Edited by F. Kreith), CRC Press, Boca Raton, 2000, ISBN 0-8493-9581-X.
- J.P. Bourdouxhe, M. Grodent, J.J. Lebrun, C. Saavedra, K. Silva, *A toolkit for primary HVAC system, energy calculations*. Draft prepared for ASHRAE TC 4.7. University of Liège. Belgium, 1993.
- R. Cohen, E. Groll, W. H. Harden, K. E. Hickman D. K. Mistry, E. Muir, *Compressors, The CRC handbook of thermal engineering*, (Edited by F. KREITH), CRC Press, Boca Raton, 2000, ISBN 0-8493-9581-X.
- J.G. Conan, *Réfrigération industrielle*, Eyrolles, Paris, 1988.
- A. M. El-Gammal, *An Algorithm and Criteria for Compressor Characteristics Real Time Modeling and Approximation*, Transactions of the ASME, Vol. 113, JANUARY 1991, 112–118
- A. F. El-Sayed, *Aircraft propulsion and gas turbine engines*, CRC Press, Boca Raton, 2008, ISBN 978-0-8493-9196-5.
- T. Giampaolo, *Compressor handbook, Principles and practice*, The Fairmont Press, Lilburn, CRC Press, Boca Raton, 2010, ISBN 0-88173-615-5
- M. Kane, *Intégration et optimisation thermoéconomique et environnomicque de centrals solaires hybrides*, These de Doctorat, Ecole Polytechnique Fédérale de Lausanne, 2002.
- J. Kurzke, *How to Get Component Maps for Aircraft Gas Turbine Performance Calculations*, ASME 96-GT-164 (1996).
- J.-M. Méricoux, *Ventilateurs Compresseurs: Aspects technologiques*, Techniques de l'Ingénieur, Génie mécanique, BM 4 501
- M. Pluviose, *Similitude des Turbomachines à fluide compressible*, Techniques de l'Ingénieur, Génie mécanique, BM 4 680
- M. Pluviose, *Turbomachines hydrauliques et thermiques – Exercices commentés*, Eyrolles, Paris, 1988.
- Rogers, Colin, *Efficiency and performance characteristics of radial turbines*, SAE Paper 660754, 1966
- R. Tîrnovan, S. Giurgea, A. Miraoui, M. Cirrincione, *Surrogate modelling of compressor characteristics for fuel-cell applications*, Applied Energy, 85 (2008) 394–403.
- M. Vincent de paul, *Turbines à fluide compressible: Conception et fonctionnement*, Techniques de l'Ingénieur, Génie mécanique, BM 4560
- M. Vincent de Paul, *Turbines à fluide compressible: Pertes et moyens de les réduire*, Techniques de l'Ingénieur, Génie mécanique, BM 4561
- L. Vivier, *Turbines à vapeur et à gaz*, Ed. Albin Michel, Paris, 1965.
- M. de Vlamincq, P. Wauters, *Thermodynamique et Turbines*, CIACO, Louvain-la-Neuve, 1988.

Case Studies

Abstract: In this chapter, we present some case studies about technological design and off-design operation. Our goal is first and foremost, as we indicated in the general introduction of this book, to show the way for users who wish to develop their own models. Even if we tried to retain models and settings as realistic as possible, the choices we made cannot be considered fully validated. In particular, the sensitivity analyses which are provided should only be considered as indicative: the values given depend on the settings chosen and on equations selected. Numerical tools that we offer use either specific ThermoOptim classes to perform simple searches by dichotomy, or generic libraries, like minPack, which allows one to make nonlinear optimization, and in particular to seek the solution of systems of equations.

We focus mainly on modeling assumptions and the achievement of the drivers as well as the presentation of results. We suggest you refer to Volume 4 of ThermoOptim reference manual for details on computer implementation of external technological design classes for the various components that come into play in these examples.

In any case, as external classes are distributed as open-source code, they may be customized quite easily to match any specific requirement.

Keywords: compression, expansion, combustion, piston compressor, compressed air storage, refrigerating machine.

38.1 INTRODUCTION

We will explore four complementary cases of increasing difficulty:

- The first is that of an air piston compressor, exchanger cooled, which loads a compressed air storage of given volume. It helps to familiarize the user with the creation of a driver and to study off-design operation of a simple system. We present first the model of the exchanger alone, then the cooled compressor;
- The second corresponds to a simplified steam power plant (without extraction or reheat). It involves a turbine and two heat exchangers, and in particular allows one to study the evolution of the cycle performance when vary the temperature of cooling water, the maximum pressure or superheating temperature. It is solved numerically by a simple dichotomy;
- The third is that which was used in Chapter 34 to present the problems of technological design and off-design operation. It is a refrigerating machine involving a displacement compressor, a

thermostatic valve and two two-phase heat exchangers, whose pressures vary with external conditions. The resolution is performed using minPack;

- The fourth is a two-shaft turbojet. It allows one to study the adaptation of the machine to coupled changes of speed and turbine inlet temperature. It involves a diffuser, a dynamic compressor, a combustion chamber, a turbine and a nozzle.

38.2 COMPRESSOR FILLING A STORAGE OF COMPRESSED AIR

38.2.1 Modeling of the heat exchanger

Let us consider a tube and fin heat exchanger cooling approximately 0.0117 kg/s of air leaving a compressor at 5 bar and 275°C with a flow rate of 0.02 kg/s of cold water passing through a coil of two parallel tubes.

The tube diameter is 15 mm, thickness 1.5 mm. The spacing between fins is 3 mm.

The exchanger can be easily modeled in Thermoptim.

To size the heat exchanger, we set an efficiency of 0.84.

Using the Thermoptim technological design screens, it is possible to calculate the overall heat transfer coefficient and to derive the area needed to transmit the desired heat capacity.

This requires first determining the hydraulic diameter d_h and the free flow areas of both fluids.

For inside tubes, d_h is given, and calculation of A_c is very simple: it is equal to the product of the number of tubes by the unit section.

For outside tubes, calculations are somewhat more complicated. d_h is equal to 4 times the flow area divided by the wetted perimeter (see Section 38.5.1). A_c is the cross sectional area available to the air.

We assumed that fins multiplied by 4 the exchange surface, with an effectiveness equal to 0.8.

WORKED EXAMPLE

Practical Design of a Heat Exchanger

The precise determination of the tube and fin air-water heat exchanger settings is explained in a breadcrumb thread in the Thermoptim-UNIT portal (<http://www.thermoptim.org/sections/enseignement/pedagogie/fils-d-ariane/filechangeur>).

It allows you to calculate the parameters (free flow area, hydraulic diameter, surface factor) necessary to assess the U value and size the heat exchanger.

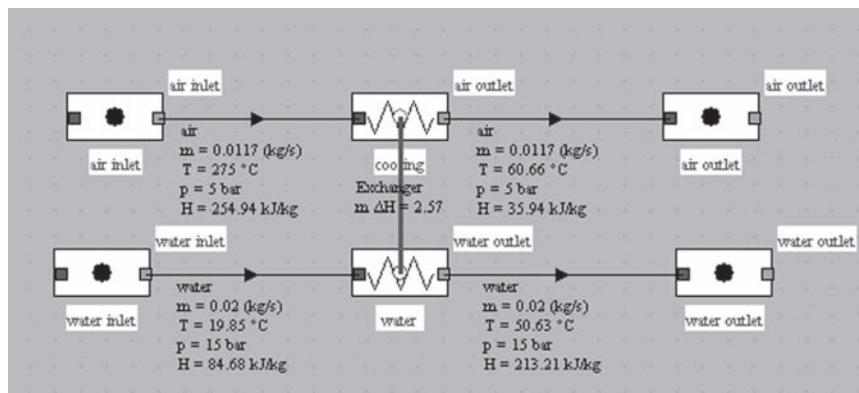


FIGURE 38.2.1

Synoptic view of the example

name: Exchanger type: counterflow

hot fluid: cooling cold fluid: water

Thi (°C): 275 Tci (°C): 19.85

Tho (°C): 60.66190053 Tco (°C): 50.63216961

mh: 0.0117378 mc: 0.02

Cph: 1.02174975 Cpc: 4.17543185

m ΔHh: 0 m ΔHc: 0

UA: 0.0238677556

R: 0.143615016

NTU: 1.99012491

LMTD: 0

epsilon: 0.840047421

FIGURE 38.2.2

Exchanger screen

Exchanger

Quit

hlh
hMh
hlh = 669.33 Re = 229.38

hlc
hlvc
hc = 759.14 Re = 1442.21

cooling

free flow area: 0.0027

hydr. diameter: 0.0013

length: 0.06

surface factor: 4

fin effectiveness: 0.8

ext_tube | Colburn correlation for single phase flow outside tubes

correlation settings

local ΔP loss coeff.: 0

pressure drop: 0.000384

friction factor: 0.279017

water

free flow area: 0.000226

hydr. diameter: 0.012

length: 0.9

surface factor: 1

fin effectiveness: 1

int_tube | Mac Adams correlation for single phase flow inside tubes

correlation settings

local ΔP loss coeff.: 0

pressure drop: 0.000131

friction factor: 0.044377

e/λ: 0

Hx design area: 0.0671

average U: 355.7051

FIGURE 38.2.3

Technological design screen

Once determined, they must be entered in the exchanger technological design screen (Figure 38.2.3).

To create the technological screen of this exchanger, we could use the generic driver presented section 34.2.4, but to illustrate the creation of a driver on a simple example, we will build ourselves a little specific driver, as a first step in developing that of the cooled compressor presented Section 38.2.3.

Once the technological screen is created, we can calculate the exchange area needed, which is here equal to 0.067 m^2 , exchange coefficients being $669 \text{ W/m}^2/\text{K}$ air side and $759 \text{ W/m}^2/\text{K}$ water side, the whole leading to an overall coefficient of $355.7 \text{ W/m}^2/\text{K}$.

The heat exchanger will ultimately consist of two tubes of 90 cm in length arranged in coils on 3 sheets and passing through 540 iron plates 2 cm square, with a total area of 0.31 m², separated from each other by 3 mm.

38.2.2 Design of the driver

The driver class is called AirExchangerDriver. Its graphical interface being simple and classic, we do not elaborate here.

38.2.2.1 Initializations

For the name of the exchanger, one can either enter it directly in the code or use Project method getHxList(), but it has the disadvantage of requiring that the diagram associated with the project is opened.

For the other initializations we use PointThopt instances, which are like clones of the core ThermoOptim points, which allow for easy access to their values. Four of these objects are instantiated, representing the inlets and outlets of both fluids. Here we have their names entered in the code, but it would be possible to recognize them automatically.

```
//initializations for the simulation
//watch out: the names of points and components must be correct, otherwise an error will
hxName="Exchanger";
hotUpstream=new PointThopt(proj,"air inlet");
hotDownstream=new PointThopt(proj,"air outlet");
coldUpstream=new PointThopt(proj,"water inlet");
coldDownstream=new PointThopt(proj,"water outlet");
```

The technological screen is then instantiated and placed in Vector vTechno for ThermoOptim core to recognize it:

```
//instantiation of the TechnoDesign in the external class
technoExchanger=new TechnoHx(proj, hxName, hotUpstream, hotDownstream, coldUpstream,
addTechnoVector(technoExchanger);

//initialization of the TechnoDesign in ThermoOptim
setupTechnoDesigns(vTechno);
```

The last line initializes the TechnoDesign when opening an existing project file or initially loading the driver. Without it, it does not appear in the TechnoDesign list of the technological and simulation screen.

```
if(!hxName.equals("")){//initialization of the heat exchanger
    args=new String[2];
    args[0]="heatEx";
    args[1]=hxName;
    vProp=proj.getProperties(args);
    Double f=(Double)vProp.elementAt(15);
    UAech=f.doubleValue();

    hotUpstream.getProperties();
    hotDownstream.getProperties();
    coldUpstream.getProperties();
    coldDownstream.getProperties();

    //TechnoDesign initializations
    technoExchanger.UA=UAech;
    technoExchanger.makeDesign();

    //display
    U_value.setText(Util.aff_d(technoExchanger.getU(),4));
    UAech_value.setText(Util.aff_d(UAech,4));
    AechReel=Util.lit_d(technoExchanger.ADesign_value.getText());
    AcalculatedEch_value.setText(Util.aff_d(AechReel,4));
}
```

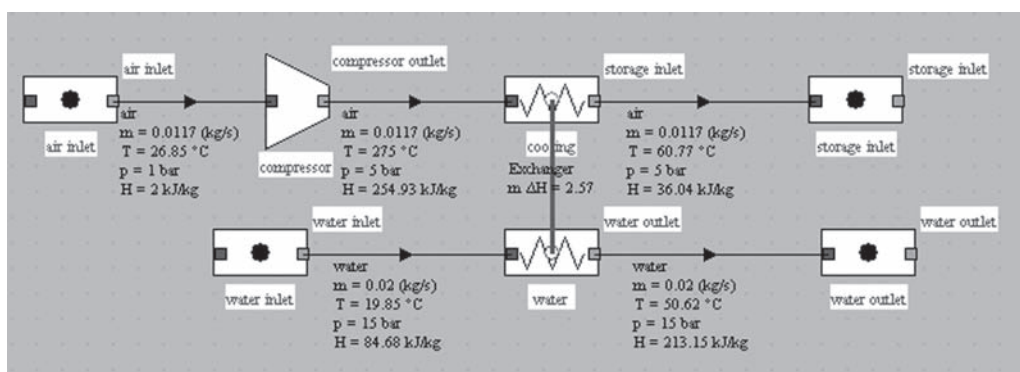


FIGURE 38.2.4

Cooled compressor example

FIGURE 38.2.5

Compressor technological design screen

38.2.2.2 Calculations

The calculations here are very simple, as shown in the code above: using Project method `getProperties()`, we get the values of UA and ΔH . The exchanger is then sized by method `makeDesign()` and the results are displayed on the screen.

38.2.3 Analysis of the cooled compressor

To illustrate the ThermoOptim ability to perform off-design calculations, we will study the behavior of an air piston compressor filling a compressed air storage of given volume at variable pressure. The compressed air is cooled before storage by a water exchanger of the type that was presented in the previous section.

The system can easily be modeled in ThermoOptim and leads to a diagram of the type of Figure 38.2.4, which differs from that studied in the previous example by adding the compressor.

The compressor model is that which is presented section 36.1.1 of this Part. Its volumetric and isentropic efficiencies are given by equations (36.1.1) and (36.1.2). Its technological design screen is given in Figure 38.2.5. That of the heat exchanger is similar to the previous.

38.2.3.1 Results

Once the driver is realized (the screen will be presented in the next section, Figure 38.2.7), it is very easy to vary the compression ratio to obtain the evolutions of the main variables when the tank pressure varies. Simply save the project file under a different name after each simulation, then load these files into the macro and extract the relevant values.

Figure 38.2.6 shows, depending on the storage pressure, changes in the compressor isentropic efficiency η_s , work consumed, intake air flow, temperature of air entering the tank, load of the exchanger and heat transfer coefficient U .

WORKED EXAMPLE Modeling of the Cooled Compressor



[CRC_we_14,
CRC_In_18]

The modeling of the air cooled compressor is explained in a breadcrumb thread in the ThermoOptim-UNIT portal (<http://www.thermoOptim.org/sections/enseignement/pedagogie/fils-d-ariane/fil-compr-volum>).

It allows you to simulate the cooled compressor which can be exploited with the Excel ThermoOptim simulation file post-processing macro presented in Chapter 34 and Volume I of the reference manual.

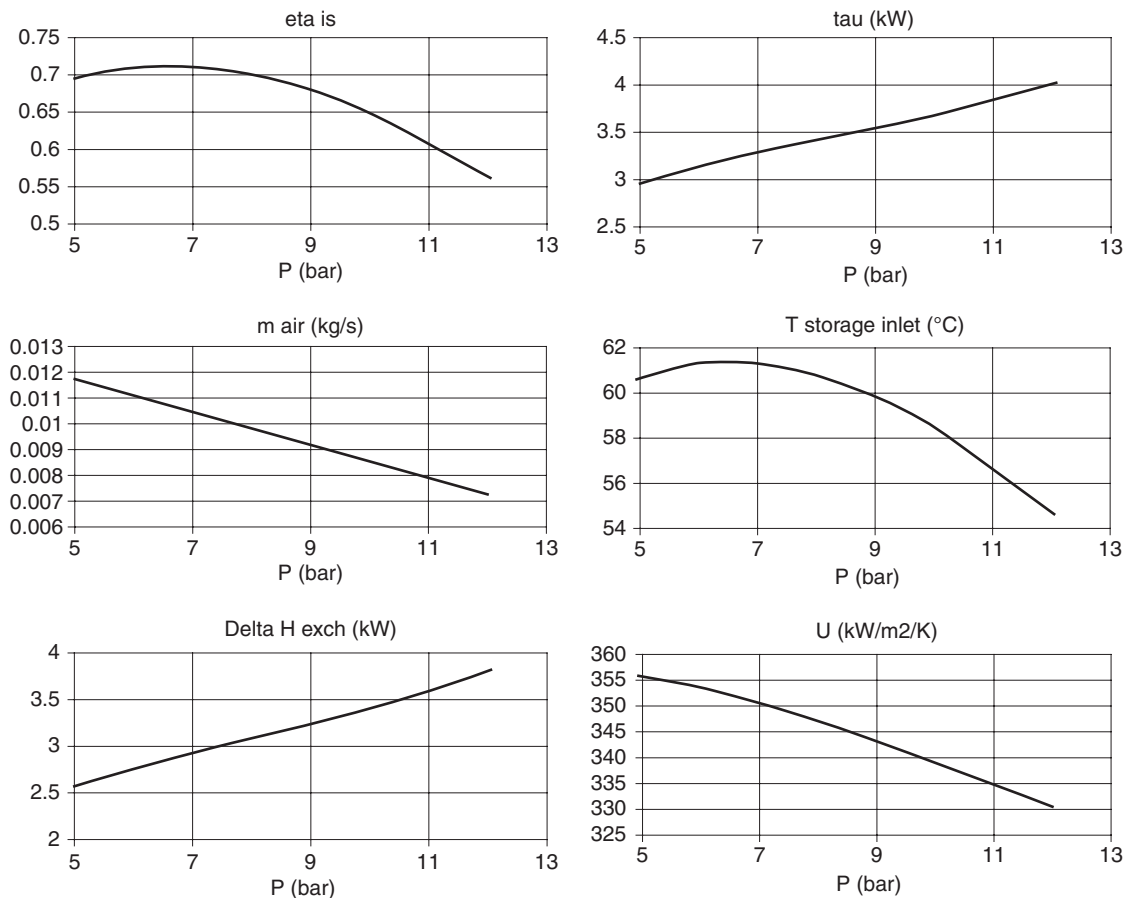


FIGURE 38.2.6

Simulation results

FIGURE 38.2.7

Driver screen

Between 5 and 12 bar, η_s and U vary by 22% and 7%. As the curves are in some cases far from linear, overly simplistic approaches are not sufficient, which demonstrates the usefulness of our approach.

38.2.3.2 Driver design

The driver class is called `VsCompressorDriver`. Its graphical interface being simple and classic, we do not elaborate here.

The driver screen is shown in Figure 38.2.7.

To achieve the relevant class, we take the exchanger driver class, and complete it on two points:

- first by instantiating and initializing the compressor technological screen, analogous to that of the exchanger;
- secondly, by introducing a “Calculate” button, and setting calculations and changes of the simulator configuration that should be performed when the downstream pressure is varied.

Initializations

During initialization, after both `PointThopt` and `TechnoDesign` have been constructed, the displacement of the compressor allowing one to obtain the desired flow can be determined based on the technological screen settings.

```
//initializations for the simulation
//watch out: the names of points and components must be correct, otherwise an error w
hxName="Exchanger";
compressorName="compressor";
hotDownstream=new PointThopt(proj,"storage inlet");
hotUpstream=new PointThopt(proj,"compressor outlet");
comprUpstream=new PointThopt(proj,"air inlet");
coldUpstream=new PointThopt(proj,"water inlet");
coldDownstream=new PointThopt(proj,"water outlet");

//instantiation of the TechnoDesign in the external classes
technoExchanger=new TechnoHx(proj, hxName, hotUpstream, hotDownstream, coldUpstream,
addTechnoVector(technoExchanger);
technoCompr=new VolumCompr(proj, compressorName, comprUpstream, hotUpstream);
addTechnoVector(technoCompr);

//initialization of the TechnoDesign in Thermoptim
setupTechnoDesigns(vTechno);
```

Calculations

The calculations are made as follows;

- start by updating the pressure at the compressor outlet;
- calculate its volumetric and isentropic efficiencies;

- recalculate the compressor and downstream process, knowing that being parameterized as isobaric it spreads the new pressure;
- update the exchanger inlets and outlets and then recalculate it in off-design mode after determining the new values of U and UA;
- update the simulator and recalculate the project several times to ensure the stabilization of values.

This example illustrates even better than the previous how PointThopt can be used to communicate between the driver and the simulator. The syntax of updates is much more readable than using only Project methods `getProperties()` and `updatePoint()`.

The calculation of the compressor is made using the two methods `getRisentr()` and `getLambdaVol()` introduced previously. Method `updateprocess()` modifies the compressor flow and isentropic efficiency and then recalculates. Point downstream, called here “hotUpstream” because it corresponds to the upstream of the exchanger hot fluid is then updated.

```
void bCalc_actionPerformed(java.awt.event.ActionEvent event)
{
    Vs=Util.lit_d(Vs_value.getText());//reads the compressor swept volume
    technoCompr.setVs(Vs);
    Preservoir=Util.lit_d(P_value.getText());
    double UA_ech=Util.lit_d(UAech_value.getText());

    hotUpstream.P=Preservoir;// updates the compressor outlet pressure
    hotUpstream.update(!UPDATE_T,UPDATE_P,!UPDATE_X);
    hotUpstream.getProperties();

    massFlow=technoCompr.getMassFlow(comprUpstream.V);
    double eta_is=technoCompr.getRisentr();// calculates compressor isentropic efficiency
    lambdaVol=technoCompr.getLambdaVol();

    //recalculates the compressor and the downstream process
    updateprocess(compressorName, "Compression",RECALCULATE,IS_SET_FLOW, UPDATE_FLOW, mass:
    hotUpstream.getProperties();
    updateprocess("refroidissement", "Exchange",RECALCULATE,IS_SET_FLOW, UPDATE_FLOW, mass:
    updateprocess("entree air", "Exchange",RECALCULATE,IS_SET_FLOW, UPDATE_FLOW, massFlow,

    hotUpstream.getProperties();//updates heat exchanger inlets and outlets
    hotDownstream.getProperties();
    coldUpstream.getProperties();
    coldDownstream.getProperties();
}
```

The calculation of the heat exchanger is made as follows: we make a first calculation using method `updateHx()` by setting the value of UA read on the screen, UA_ech (the exchanger is set for an off-design calculation, so that the UA value is taken into account). This calculation is used to initialize the exchanger for the new operating conditions.

We then use method `makeDesign()` of `TechnoDesign`, which updates the value of U. The real UA is obtained by multiplying the new U by the initial A value (`AechReel`), which allows to correctly recalculate the exchanger.

```
//calculates the heat exchanger (several iterations)
for(int i=0;i<5;i++){
    updateHx(hxName, RECALCULATE, UPDATE_UA, UA_ech, !UPDATE_EPSI, 0, !UPDATE_DTMIN, 0, UF
    coldDownstream.getProperties();
    hotDownstream.getProperties();

    technoExchanger.UA=UA_ech;//calculates U
    technoExchanger.makeDesign();
    double U=technoExchanger.getU();

    UAech=U*AechReel/1000;//updates UA and recalculates the heat exchanger
    UAech_value.setText(Util.aff_d(UAech,4));
    updateHx(hxName, RECALCULATE, UPDATE_UA, UAech, !UPDATE_EPSI, 0, !UPDATE_DTMIN, 0, UPI
}
```

```

coldDownstream.getProperties();
hotDownstream.getProperties();
U_value.setText(Util.aff_d(U,4));
UA_ech=UAech;
}

//updates the simulator and displays
for(int j=0;j<3;j++){proj.calcThopt();
flow_value.setText(Util.aff_d(massFlow,4));
eta_is_value.setText(Util.aff_d(eta_is,4));
lambdaVol_value.setText(Util.aff_d(lambdaVol,4));
AcalculatedEch_value.setText(technoExchanger.ADesign_value.getText());
}

```

Since U depends on the average temperatures of fluids, and therefore on those of output, we iterate five times the calculations to ensure proper stabilization, resetting each time UA_{ech} .

38.2.4 Use of the model to simulate the filling of a compressed air storage

Results in Figure 38.2.6 can be used to simulate the filling of a compressed air storage. For this, we develop a second model, solved with Excel, with the following equations:

- mass M of air contained in storage is equal to the initial mass plus the integral of the flow;
- internal energy U is equal to initial internal energy plus the integral of the product of the flow by the enthalpy of the air leaving the cooler, less the integral of losses by convection with ambient air;
- storage temperature is inferred from its internal energy;
- pressure is determined by the ideal gas law.

The look of the results is given Figure 38.2.8, for a half m^3 storage (diameter 80 cm, length 1 m) fed by a compressor of displacement $V_s = 0.55$ l. The pressure and temperature in storage, its mass and the workload of the compressor are displayed versus time in seconds.

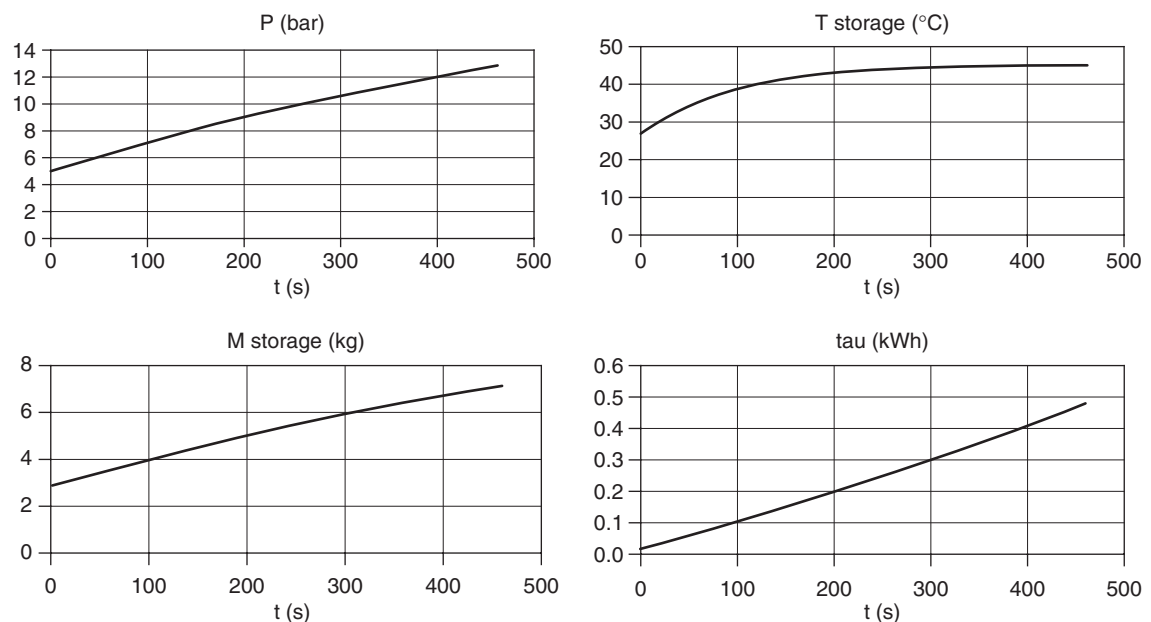


FIGURE 38.2.8

Filling of the compressed air storage

WORKED EXAMPLE

Filling of the Compressed Air Storage

The modeling of the compressed air storage filling is presented in the ThermoOptim-UNIT portal (<http://www.thermoOptim.org/sections/enseignement/pedagogie/fils-dariane/fil-compr-volum>).

It allows you to use previous simulations of the cooled compressor to model the filling of the compressed air storage, making polynomial regressions from previous ThermoOptim simulations in order to express the flow and enthalpy of the stored air.

This is an example of a simplified model which can be derived from a ThermoOptim knowledge model, as explained in Section 34.4.2.

This simplified model provides the equations constituting the dynamic compressed air storage model.

38.3 STEAM POWER PLANT

This section introduces external class SimpleSteamPlantDriver which is used as a steam power plant driver to perform the study of its off-design operation.

38.3.1 Introduction, results

Figure 38.3.1 shows a synoptic view of the steam power plant model which we wish to drive.

This is a 600 MW flame plant cooled by river water. Technological settings that were selected here for both exchangers were conducted in a manner analogous to that described Section 38.2.1. For vaporization, we consider that water flows inside tubes and retain the Gungor and Winterton correlation. For condensation, we consider that the steam circulates outside the tubes and choose the correlation proposed by W. Levy (Techniques de l'Ingénieur B1540) (see section 35.2.4.4).

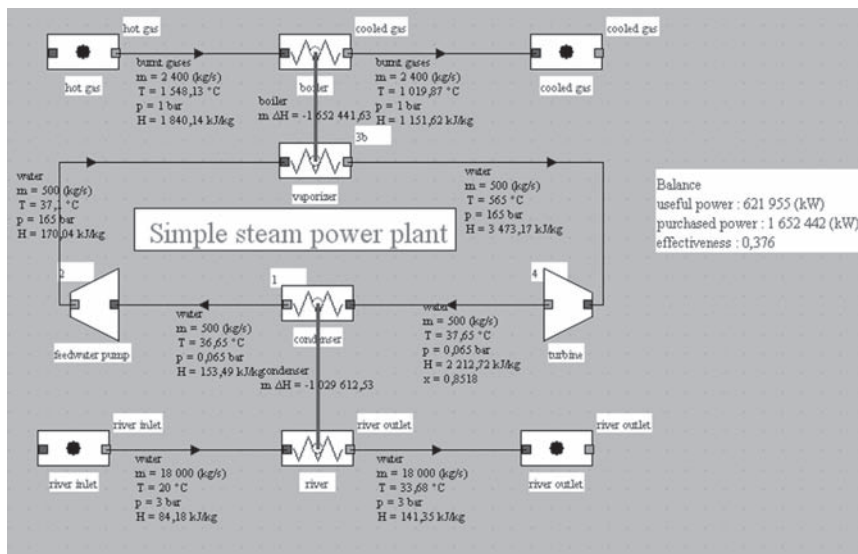


FIGURE 38.3.1

Steam power plant model

The problem to solve is the following (we have assumed that the pressure and temperature of the steam boiler outlet were known, defined in the driver screen).

The steam mass flow is given by formula (37.4.11), K being the Stodola constant:

$$T_{in} \frac{\dot{m}^2}{K^2} = P_{in}^2 - P_{out}^2 \quad (37.4.11)$$

The condensing temperature is set by the condenser thermal balance, which depends mainly on the one hand on the temperature and flow of cooling water, secondly on the steam flow, and finally on the condenser inlet temperature.

The latter depends on the expansion ratio and turbine isentropic efficiency, that we consider constant here for simplicity.

$$Q_c = \tau + Q_b = U_c A_c \Delta T_{ml_cond}$$

It should be noted that exchange coefficient U_c also depends on many parameters, including temperature and flow of fluids through the exchanger and the distribution of areas between the condensation zone and the sub-cooling, so that the resolution of this equation is particularly complex. Please refer to Chapter 35 for details on how to operate.

The turbine balance also depends on many parameters. It is given by:

$$\tau = \dot{m} \eta_s(P_b, P_c) \Delta h_s(T_b, P_b, P_c)$$

Finally, the boiler heat balance sets the value of hot gas outlet temperature.

Looking for a pair (steam flow, temperature of condensation) corresponds to solving a set of relatively complex nonlinear equations.

The algorithm determines the load of the boiler assumed to be controlled at selected temperature and pressure, deduces that of the condenser after having determined the power produced by the turbine, and seeks the residual of the condenser heat balance, which serves as a convergence criterion when iteration is performed by varying the condensation pressure.

The strong coupling between fluid thermophysical properties and U value make it very difficult to directly search the exact solution of this set of equations, all the more so that exchangers are multi-zone, which does not allow one to change their UA as easily as we did in the previous case study (see Section 38.2.3.2). Since our primary objective is not to make the numerical analysis but just to find a way to reach the solution, we present in this section a resolution guided by hand: it is the user who changes in the driver screen (Figure 38.3.2) values of the two exchanger UA s, before performing a calculation. Based on the results obtained, the user changes the values he had previously entered, and stops when the values of exchange surfaces calculated correspond to those selected.

WORKED EXAMPLE

Off-Design Driver for a Steam Power Plant

This worked example generalizes the model presented in this section and shows how to solve the set of 4 coupled equations obtained when the UA values are included in the variables.

The code of the Java class `MinPackSteamPlantDriver` is explained in a programming note in the Thermoptim-UNIT portal (<http://www.thermoptim.org/sections/logiciels/thermoptim/modelotheque/pilote-vapeur>).

Design settings		Initial settings	
evaporator UA	1681.1108	condenser UA	116326.3139
set boiler area	7500	set condenser area	48000.0000
calculated boiler area	7449.60447	calculated condenser area	48245.00244
Stodola constant	87.7300	high pressure	165.0000
water temperature (°C)	20.0000	max temperature (°C)	565.0000

FIGURE 38.3.2

Driver screen

Simulation results		Calculate	
low pressure	0.0651	DeltaH boiler	1659747.8365
DeltaH cond	1029307.7246	turbine power	-630440.1119
flow rate	500.0014	Efficiency	0.3799

FIGURE 38.3.3

Simulation results

To calculate an operating point, we must first initialize calculations by clicking the button “Initial settings”, which shows:

- values of UA for the evaporator and the condenser;
- desired values for exchange surfaces;
- values calculated for exchange surfaces;
- turbine Stodola constant;
- steam evaporation pressure;
- temperature of the water used to cool the condenser;
- superheating temperature.

If you change the editable values, they are those which are taken into account in calculations. Once a simulation is made, the results are displayed (Figure 38.3.3), and it is best to save the project file by renaming it wisely in order to further exploit multiple simulations, for example through the Excel after-treatment macro.

Figure 38.3.4 shows the results provided by the model when the temperature of the cold source varies from 5 to 40°C. The shape of the cycle efficiency curve is due to the inclusion of residual velocity losses (see Section 37.4.5), the turbine in this example being optimized for operation with a cooling temperature of 20°C. When the temperature drops, the residual velocity losses offset gains due to lower condensing temperature.

Figure 38.3.5 shows results obtained when varying the evaporation pressure, 30 to 185 bar. We call this type of regulation the sliding pressure setting (see Section 15.7.2.2 of Part 3). The steam flow is itself quasi-proportional to the evaporation pressure, the influence of the downstream pressure being very low (see equation 37.4.11).

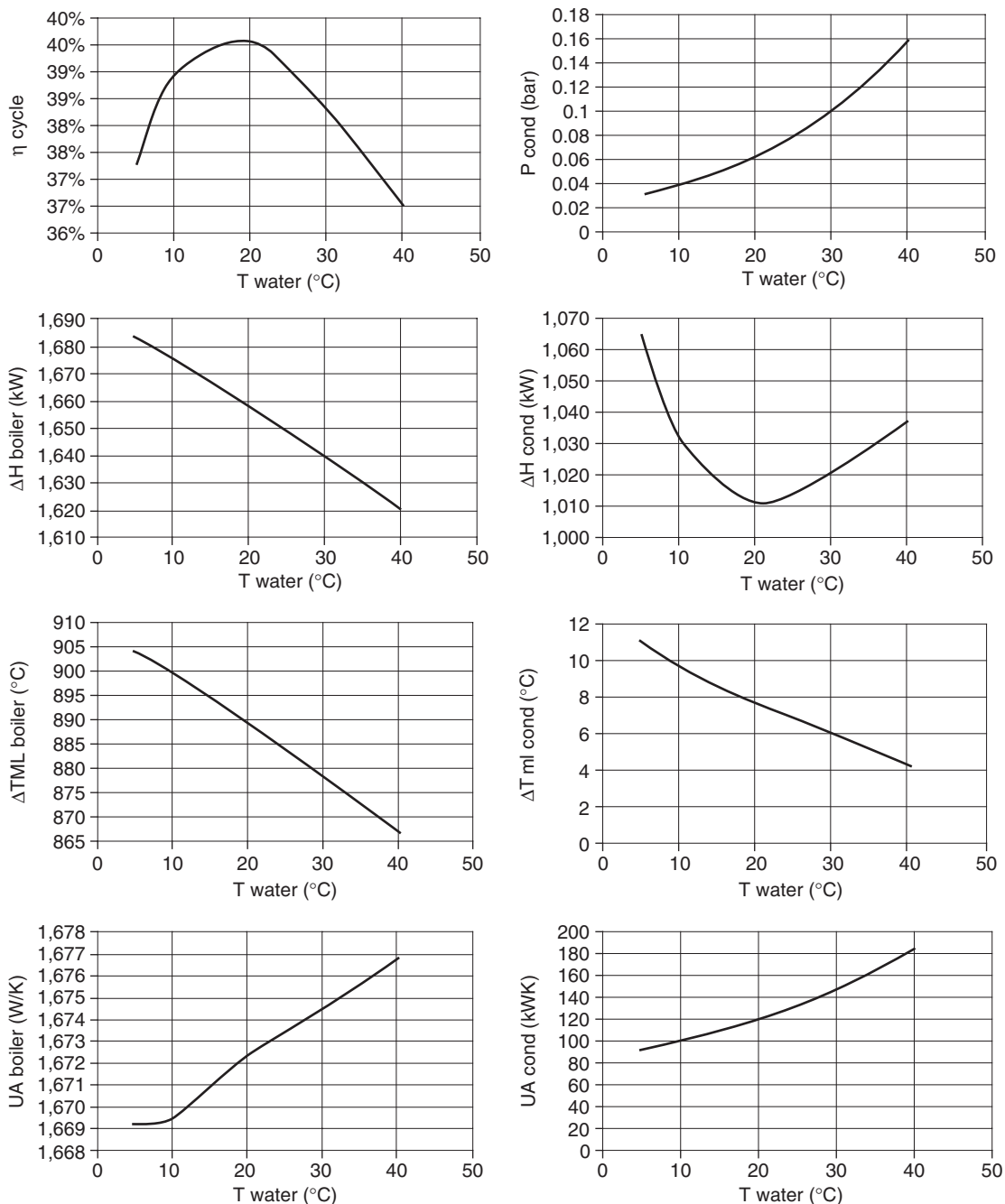


FIGURE 38.3.4
Effect of cooling water temperature

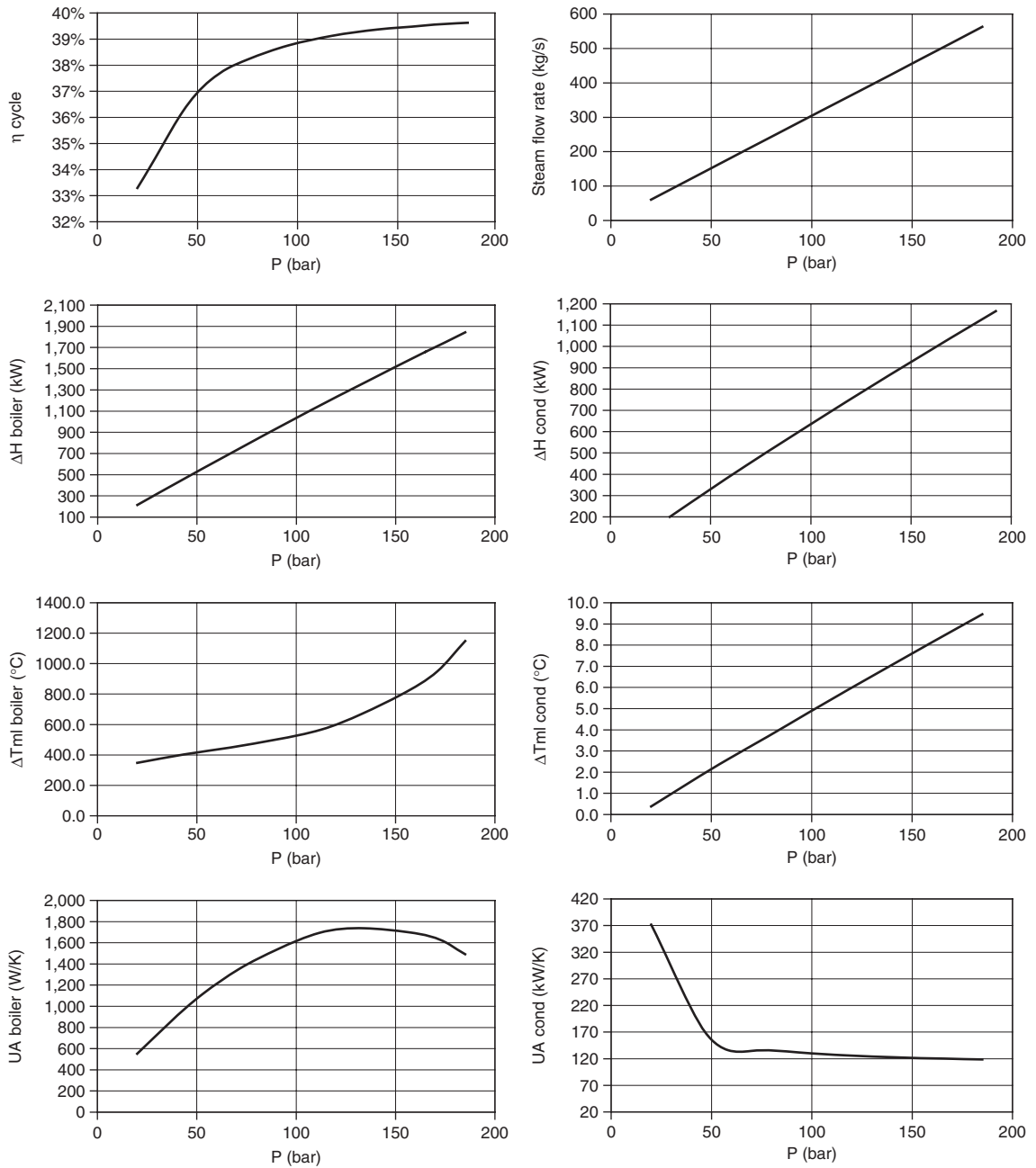


FIGURE 38.3.5
Effect of evaporation pressure

38.4 REFRIGERATION MACHINE

The refrigerating machine on which we focus in this section corresponds to that used to illustrate the introduction of this Part, in Chapter 34.

38.4.1 Introduction, results

Figure 38.4.1 shows a synoptic view of the refrigerator model we wish to drive.

Figure 38.4.2 displays the driver that we have built to coordinate the calculations of the various components. It allows one to change the input variables such as compressor rotation speed or outside air temperature.

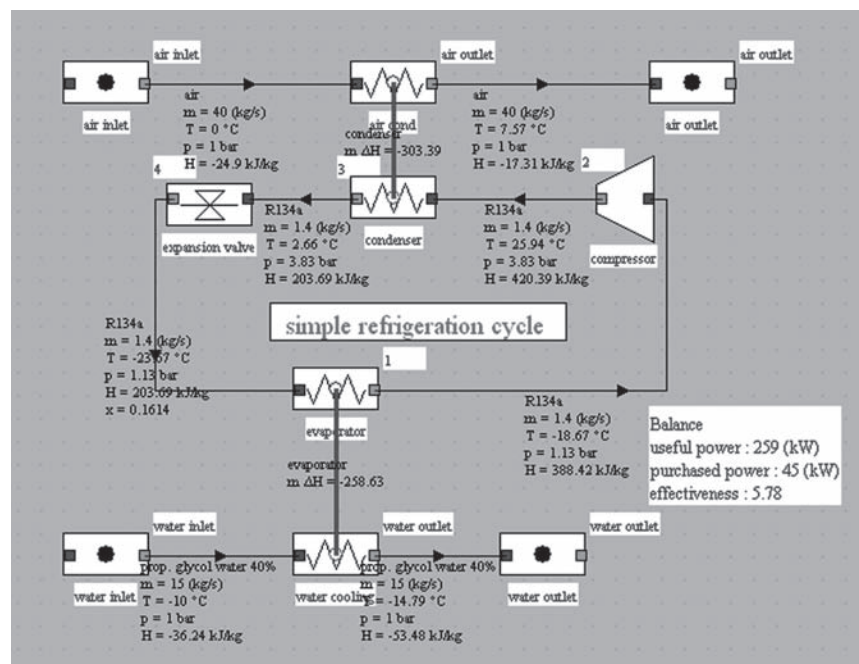


FIGURE 38.4.1

Model of refrigeration cycle

Design settings		Initial settings	
evaporator UA	29.3726	condenser UA	36.9071
set evaporator area	12.23	set condenser area	59.14
calculated evaporator area	12.12379	calculated A Cond	59.44030
Rotation speed	900	air temperature (°C)	0

FIGURE 38.4.2

Driver screen

To calculate an operating point, we must first initialize calculations by clicking button “Initial settings”, which shows:

- compressor rotation speed corresponding to the simulator flow;
- UA values for the evaporator and condenser;
- temperature of the air used to cool the condenser;
- heat rates of fluids in the two exchangers.

If you change values in the left of the screen, they are those which are taken into account in calculations.

Figure 38.4.3 shows the simulation results when varying the temperature of the cooling air, for the settings of technological screens selected section 34.2.5.1.

38.4.2 Principle of resolution

Unlike other examples, we will not discuss here the code of the Java class `RefrigDriverMinPack`, referring the reader to a programming note on the Thermoptim-UNIT portal. We will only explain the principle of resolution that was adopted and has the advantage of being generic. The problem we are trying to solve is the following:

$V_{s,fl}$, being the displacement, the refrigerant volumetric flow is given by equation (38.4.1):

$$\dot{V} = \lambda \frac{N}{60} V_{s,fl} \quad (38.4.1)$$

with λ volumetric efficiency, given by (38.4.2):

$$\lambda = \alpha_0 - \alpha_1 \frac{P_{ref}}{P_{asp}} \quad (38.4.2)$$

The mass flow rate depends thus on the specific volume at the suction and compression ratio.

The evaporation temperature is set by the evaporator heat balance, which depends mainly on the one hand on the temperature and flow of coolant (brine water here), and secondly on the refrigerant flow. Equation (38.4.3) provides the exchanger overall balance, but in reality it is an evaporator with a two-phase part and a slight superheating, so that it has to be modeled as multi-zone, knowing that only the total area is known, the boundary between the two areas varying according to the conditions of use (see Section 35.2.4).

$$Q_e = \dot{m}(h_v(T_i) - h_l(T_c)) = UA_{evap}(T_e - T_c) = U_e A_e (T_e - T_c) \quad (38.4.3)$$

It should be noted that the exchange coefficient U_e also depends on many parameters, including temperature and flow of fluids through the exchanger, so that solving this equation is particularly complex. Assuming the value of U_e known, it can be made as indicated below.

WORKED EXAMPLE

Off-design Driver for a Refrigeration Machine

The code of the Java class `RefrigDriverMinPack`, which allows one to study the off-design behavior of a refrigeration machine, is explained in a programming note in the Thermoptim-UNIT portal (<http://www.thermoptim.org/sections/logiciels/thermoptim/documentation/pilote-pourcycle>).

It is based on a principle of resolution similar to that explained in this section, with the proviso that pressure drops and the refrigerant charge are taken into account. The practical implementation of the model is presented in details.

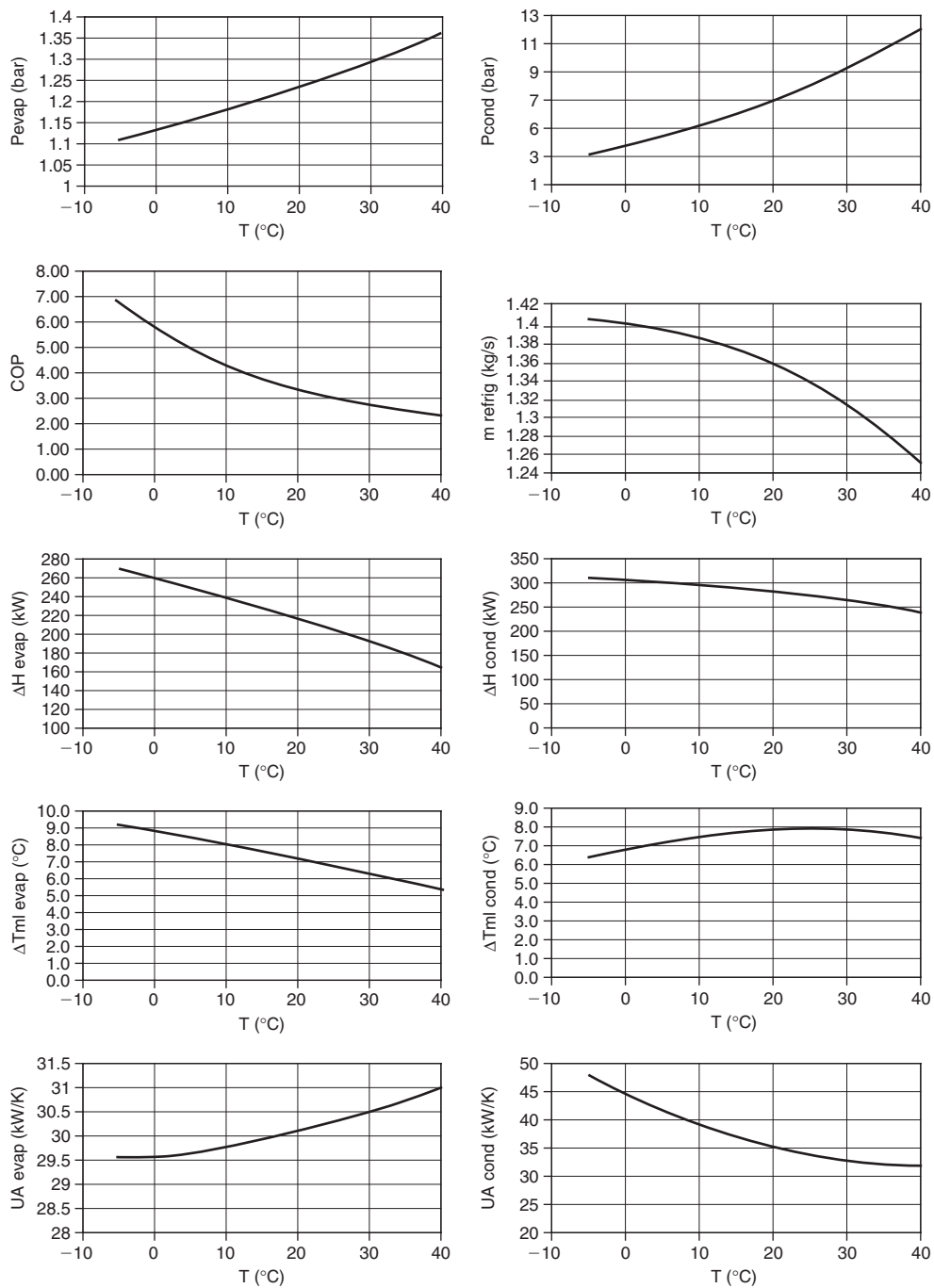


FIGURE 38.4.3
Effect of outside air temperature

The balance of the compressor also depends on many parameters:

$$\tau = \dot{m} \frac{\Delta h_s(T_c, P_{ref})}{\eta_s(T_c, P_{ref})} \quad (38.4.4)$$

Similarly to the evaporator, the condensation temperature is set by thermal equilibrium of the condenser, which depends mainly on the one hand on the temperature and flow of cooling air, on the other hand on refrigerant flow, and finally on the condenser outlet temperature.

The latter depends on the compression ratio and compressor isentropic efficiency, itself also depending on this ratio.

Equation (38.4.5) provides the overall balance of the condenser, but as it includes a desuperheater, with a two-phase part and a slight sub-cooling, it has actually to be modeled as three zone knowing that only the total area is known, the boundaries between the zones varying according to usage conditions.

$$Q_c = \tau + Q_e = UA_{cond}(T_c - T_a) = U_c A_c (T_c - T_a) \quad (38.4.5)$$

The search for a triplet (refrigerant flow, evaporation temperature, condensation temperature) corresponds to that of solving a set of relatively complex nonlinear equations. The interest of the external driver is that it is able to implement an algorithm for solving the set of equations (38.4.1) to (38.4.5), to which must be added all those necessary to determine the thermophysical properties of fluids and values of heat exchange coefficients.

The solution we have adopted is to set an external driver that provides the resolution of this system of equations and updates Thermoptim once that triplet is determined.

According to the remark made earlier about the difficulties of calculating U , it uses two nested algorithms, one searching for a solution at UA constant for the two exchangers, one amending U according to the solution found previously.

We use the method of Marquardt-Levenberg with algorithms developed in Fortran as the min-Pack 1 package, and translated in Java. This method combines the Gauss-Newton method and gradient descent. Its main interest is to be very robust and to only require an approximate solution as initialization.

Its implementation in Java is done using an interface called `optimization.Lmdif_fcn`, which forces the calling class (in this case our driver) to have a function called `fcn()`.

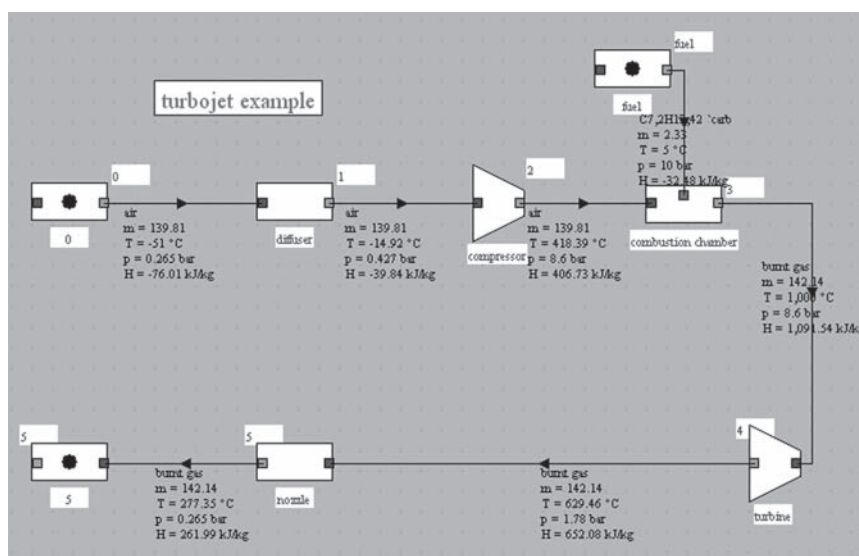
This function `fcn()` receives as key arguments a vector (array `x[n]`) containing the variables and a vector (array `fvec[m]`) referring to residues of the functions we seek to set to zero. Their number may exceed that of variables, but in our case it is the same.

The vector of variables here is the following: `Tcond=x[1]`; `Tevap=x[2]`; `massFlow=x[3]`. The three `fvec` methods are functions `resEvap()`, and `resCond()` and `resFlow()` returning these residuals. To estimate the residuals, we must begin by updating Thermoptim variables corresponding to vector `x`, and secondly we calculate the other variables.

38.5 SINGLE FLOW TURBOJET

Our final case study deals with a single flow jet engine. We have already presented such an engine section 12.2.1.9 of Part 3, and discussed section 7.9.1 and 7.9.2 of Part 2 the nozzle and diffuser components that are necessary to model it.

Figure 38.5.1 presents a synoptic view of the jet engine model that we wish to calculate. It involves an inlet diffuser for creating a dynamic pressure at compressor inlet when the aircraft is in flight, a gas generator comprising a compressor, a combustion chamber and a turbine, and finally a nozzle that propels the aircraft.

**FIGURE 38.5.1**

Simulation results, flight at Mach 0.9

Remember that with such a model, in the absence of an external driver, we must proceed as follows to compute an operating point:

- enter in the diffuser screen values of external conditions, that is to say the aircraft speed (m/s), outdoor pressure and temperature;
- enter in the nozzle screen the value of the ambient pressure;
- set the calculation of compression ratio;
- enter the turbine inlet temperature in the combustion chamber screen;
- recalculate the entire project with these settings;
- recover in the diffuser and nozzle screens the speed values of the plane C_0 and exhaust gas flow C_5 as well as the flow sucked \dot{m}_0 and rejected \dot{m}_5 to calculate the thrust and specific consumption per unit thrust.

We must then assess outside Thermoptim, e.g. in a spreadsheet, the thrust, specific thrust, consumption per unit of thrust, which are respectively $F = \dot{m}_0 C_0 - \dot{m}_5 C_5$, F/\dot{m}_0 and \dot{m}_c/F , ($\dot{m}_c = \dot{m}_5 - \dot{m}_0$ being the mass flow of fuel consumed).

Such a sequence of operations is tedious to repeat when you want to do sensitivity studies, and has in addition serious risks of error. The completion of a driver being perfectly justified in this case, we have presented a very simple one in section 12.2.1.10 of Part 3. It just changes project initialization parameters then restarts calculations and display values of F/\dot{m}_0 and \dot{m}_c/F .

The model we will now consider is much finer: it takes into account the performance maps of the compressor, turbine and nozzle as they were considered in Chapter 37 to determine, for a given turbine inlet temperature, a set of values of flow through the machine, compression ratio and compressor and turbine rotation speeds that is consistent with flight conditions (in the first model, these values were set exogenously by the user).

38.5.1 Introduction, results

In a real machine indeed, adapting the machine requires that the compression ratio and flow-rate are determined by the compressor and turbine characteristics.

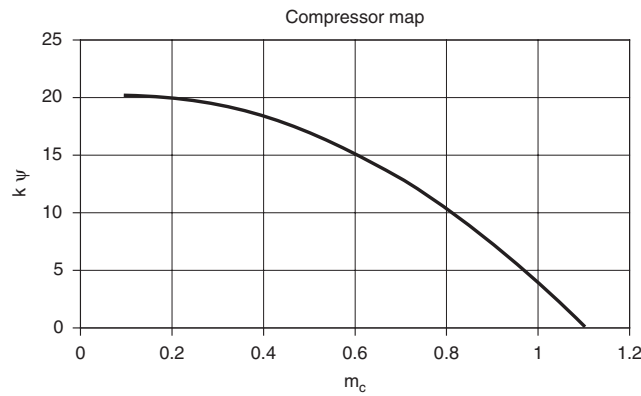


FIGURE 38.5.2
Compressor characteristics

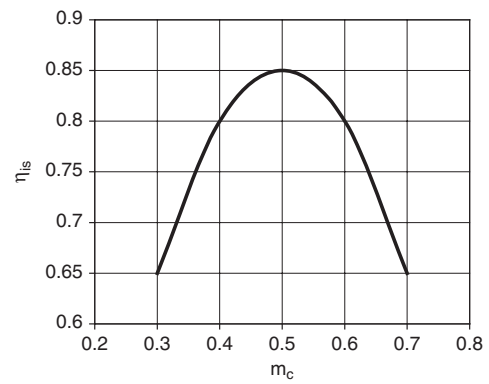


FIGURE 38.5.3
Isentropic efficiency compressor characteristics

A driver a little more elaborate than the previous one may take into account these characteristics as follows.

Flow into the turbine and the nozzle is considered choked, so that $\dot{m}\sqrt{T_3}/P_3 = K_t$ and $\dot{m}\sqrt{T_4}/P_4 = K_n$. The values of the two Stodola constants are determined on the basis of the reference point and entered into the driver screen.

These relationships therefore set the flow rate through the turbine and nozzle. To get the one that passes through the compressor, just subtract the fuel flow.

Compressor characteristics are assumed to have the appearance of Figure 38.5.2, given by a simple parabola, set in the technological screen of the compressor (see section 37.3.4). In these characteristics, the ordinate and abscissa are proportional to similarity factors ψ and φ .

The horizontal axis is $mc = \dot{m}T_1/K_cNP_1$ i.e. the flow coefficient φ divided by a value entered in the driver screen.

Knowing the flow rate, provided by the turbine characteristics, the conditions upstream of the compressor determined by the diffuser, and finally the rotation speed, the compression ratio can be determined by inverting expression (7.1. 4) of Part 2 giving the isentropic work.

$$\tau_s = C_p T_a \left[\left(\frac{P_r}{P_a} \right)^{(\gamma-1)/\gamma} - 1 \right] \quad (7.1.4)$$

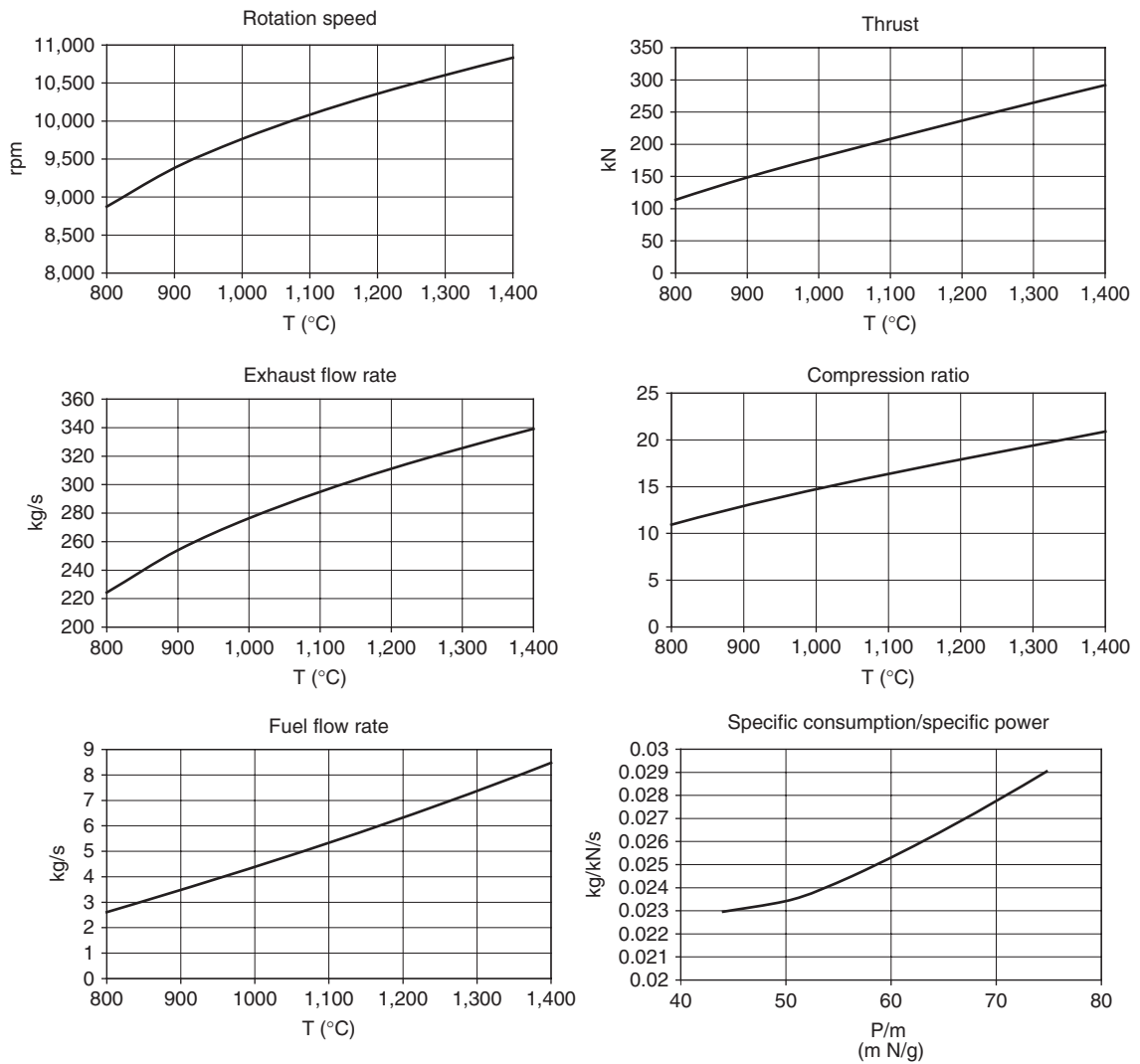
The evolution of the compressor isentropic efficiency is itself given by a law of the type given Figure 38.5.3, again a simple parabola, lower bounded by 0.6.

Watch out: given what has been said compression must be “adiabatic” calculated in “isentropic” mode and not “polytropic”. Moreover, the setting is done by changing the downstream point pressure, which requires that the compression is performed with a ratio “calculated” and not “set”.

To find a solution consistent with the characteristics of the turbine and compressor, we look for a triplet (rotation speed, flow, compressor outlet pressure P_3) which verifies the following set of equations:

$$\text{turbine characteristics } \dot{m} = \frac{K_t P_3}{\sqrt{T_3}} \quad (38.5.1)$$

$$\text{reduced corrected compressor flow } m_c = \frac{\dot{m} T_1}{K_c N P_1} \quad (38.5.2)$$

**FIGURE 38.5.4**

Model results (takeoff at Mach = 0.25)

$$\text{reduced compressor charact } \psi = \psi_{\text{coeff}}(m_c - \varphi\psi_{\text{max}})^2 + \psi_{\text{max}} \quad (38.5.3)$$

$$\text{definition of power factor } \frac{\psi N^2}{T_1} = K \left[\left(\frac{P_3}{P_1} \right)^{(\gamma-1)/\gamma} - 1 \right] \quad (38.5.4)$$

$$\text{nozzle characteristics } \frac{\dot{m}\sqrt{T_4}}{P_4} = K_n \quad (38.5.5)$$

The value of K in equation (38.5.4) is given by (38.5.6), D being the compressor diameter.

$$K = \frac{2C_p}{(\pi D/60)^2} \quad (38.5.6)$$

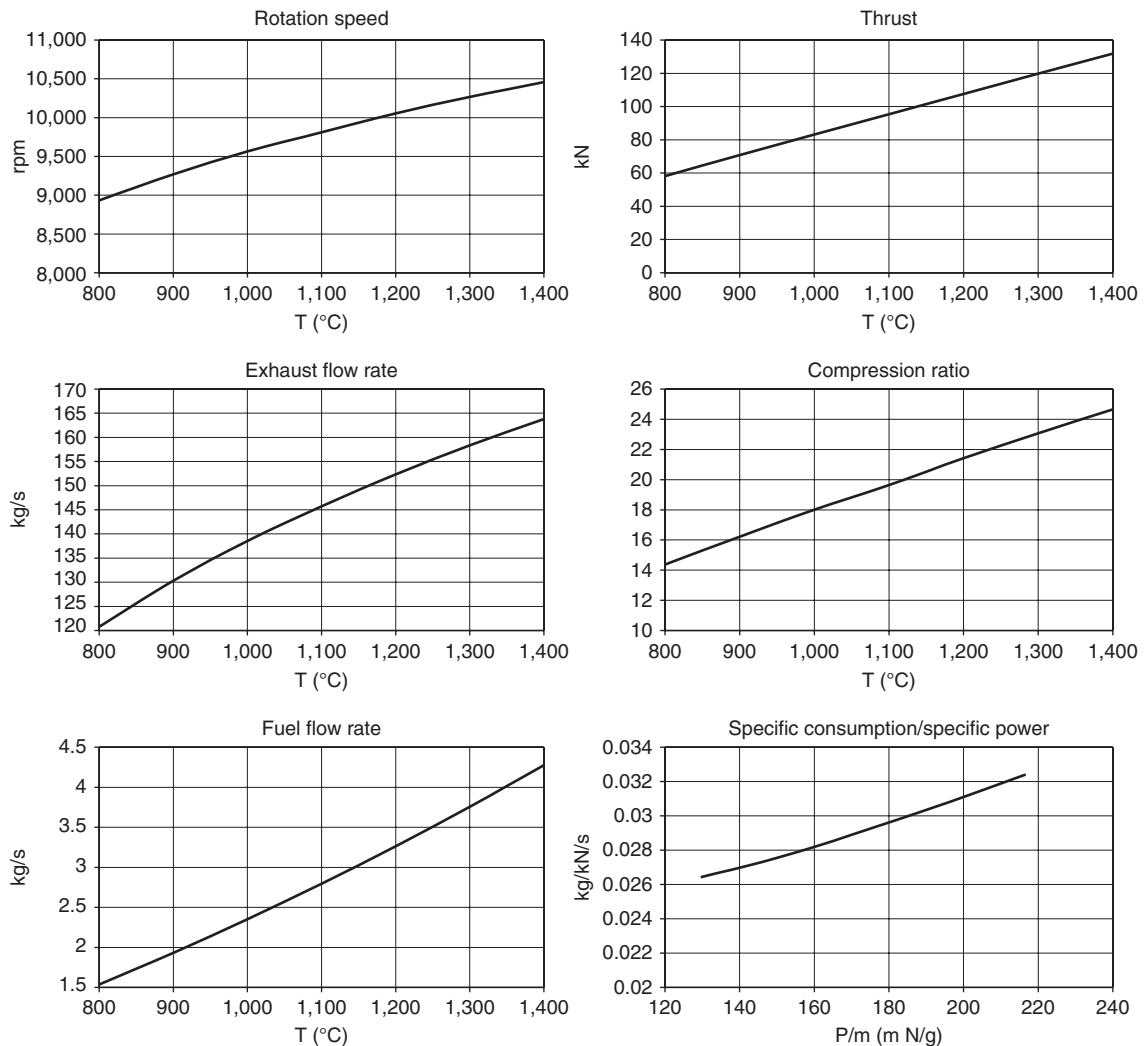


FIGURE 38.5.5
Results of the model (flight at Mach = 0.9, altitude 10,000 m)

Substituting in (38.5.2) \dot{m} by its expression from (38.5.1), then $m\dot{c}$ in (38.5.3), and finally ψ in (38.5.4), we obtain a polynomial expression implicit in P_3 , which once solved, provides \dot{m} .

Then just look for N satisfying all these equations, and update the flow-rates in the different components and change the compressor outlet pressure, and finally recalculate the project.

Once treated with the Excel post-processing macro, the results obtained are of the type of Figures 38.5.4 and 38.5.5, which demonstrate, for takeoff and for operation in altitude, at cruising speed, performance depending on the turbine inlet temperature, except for specific consumption, which depends on the specific power.

The influence of turbine inlet temperature on the engine performance, including rotation speed, is very sensitive. While rotation speeds are close, the engine power, fuel consumption and the flow through it are not at all the same.

As we stated Chapter 37, the compressor model that we used in this example is rather simplistic, for enthalpy factor as for isentropic efficiency. Ideally, we should have considered detailed performance maps.

Exterior conditions			
plane mach number	<input type="text" value="0.9"/>		
ambient pressure (bar)	<input type="text" value="0.265"/>		
ambient temperature (K)	<input type="text" value="222.15"/>		
<input type="button" value="Calculate"/>			
Single compression ratio calculation			
turbine constant Kt	<input type="text" value="650"/>	compressor constant Kc	<input type="text" value="20"/>
nozzle constant Kn	<input type="text" value="2400"/>	turbine inlet temp. (°C)	<input type="text" value="1000"/>
specific thrust	<input type="text" value="0.607"/>	Rotation speed (rpm)	<input type="text" value="9835.35"/>
specific fuel consumption	<input type="text" value="0.02750"/>		

FIGURE 38.5.6

Driver screen

38.5.2 Presentation of the external class

The external class model is presented in details in the ThermoOptim model library. The principle of calculation is the following.

For each value of the turbine inlet temperature, the driver initiates a search for a solution by iterating on the motor rotation speed and the turbine inlet pressure, trying each time to verify the characteristics of the three turbomachinery.

Once convergence is obtained, the ThermoOptim project is fully updated and recalculated, and main results are displayed in the driver screen (Figure 38.5.6).

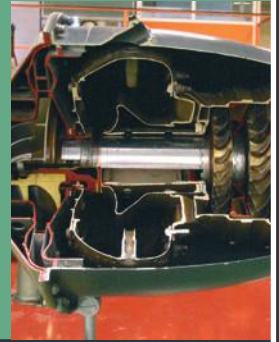
This page intentionally left blank

"An encouraging and stylish manifesto of a new teaching practice of engineering thermodynamics. It opens the doors to creativity, a major requirement for our energy future."

Alain Lambotte, Competence and Training Center, Electricity Utility, Belgium

"A comprehensive book with an almost encyclopedic coverage of the equipment and systems involved in power production, refrigeration, and air-conditioning. One that engineers will keep on their desks for ready reference and study."

John W. Mitchell, Prof. Em. of Mechanical Engineering, University of Wisconsin-Madison, USA



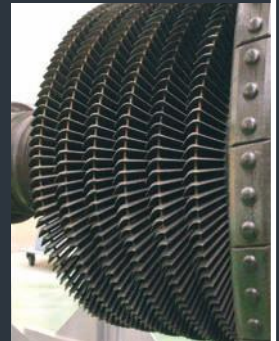
Considered as particularly difficult by generations of students and engineers, thermodynamics applied to energy systems can now be taught with an original instruction method. **Energy Systems** applies a completely different approach to the calculation, application and theory of multiple energy conversion technologies. It aims to create the reader's foundation for understanding and applying the design principles to all kinds of energy cycles, including renewable energy. Proven to be simpler and more reflective than existing methods, it deals with energy system modeling, instead of the thermodynamic foundations, as the primary objective. Although its style is drastically different from other textbooks, no concession is done to coverage: with encouraging pace, the complete range from basic thermodynamics to the most advanced energy systems is addressed.



The accompanying **Thermoptim™** portal presents the software and manuals (in English and French) to solve over 200 examples, and programming and design tools for exercises of all levels of complexity. The reader is explained how to build appropriate models to bridge the technological reality with the theoretical basis of energy engineering. Offering quick overviews through e-learning modules moreover, the portal is user-friendly and enables to quickly become fully operational. Students can freely download the **Thermoptim™** modeling software demo version (in seven languages) and extended options are available to lecturers. A professional edition is also available and has been adopted by many companies and research institutes worldwide - www.thermoptim.org



This volume is intended for courses in applied thermodynamics, energy systems, energy conversion and thermal engineering to senior undergraduate and graduate-level students in mechanical, energy, chemical and petroleum engineering and in related fields. Students should already have taken a first-year course in thermodynamics. The refreshing approach and exceptionally rich coverage also make this book a great reference tool for researchers and professionals. Contains International Units (SI).



Dr Renaud Gicquel is Professor at the École des Mines de Paris (Mines ParisTech), France. He has a special passion for the combination of thermodynamics and energy-powered system education with modern information technology tools. He has developed various software packages to facilitate the teaching and commercial use of applied thermodynamics and the simulation of energy systems.